MULTICOMPONENT SYNTHESIS OF NEW HETEROCYCLIC COMPOUNDS AND THEIR BIOLOGICAL EVALUATION

THESIS SUBMITTED TO
NATIONAL INSTITUTE OF TECHNOLOGY
WARANGAL

FOR THE DEGREE OF
DOCTOR OF PHILOSOPHY
IN CHEMISTRY

BY

CHEDUPAKA RAJU
(Roll No. 716191)

DEPARTMENT OF CHEMISTRY
NATIONAL INSTITUTE OF TECHNOLOGY-WARANGAL
WARANGAL-506 004, TELANGANA, INDIA

JANUARY, 2023

DEDICATED TO MY...
BELOVED FAMILY AND MY SUPERVISOR

Dr. V. Rajeswar Rao
Professor, Former Dean R & C
Department of chemistry

National Institute of Technology
Warangal-506004
Telangana, India.
Mobile: 91-9912186430
Email: rajeswarnitw@gmail.com
vrajesw@yahoo.com

CERTIFICATE

This is to certify that the research work presented in this thesis entitled **"Multicomponent Synthesis of New Heterocyclic Compounds and their Biological Evaluation"** submitted by **Mr. Chedupaka Raju** for the award of the degree of **Doctor of Philosophy in Chemistry**, National Institute of Technology, Warangal (Telangana), under my guidance and supervision. This work has not been submitted earlier either in part or in full for any degree or diploma to this or any other university.

(Prof. V. Rajeswar Rao)

DECLARATION

I hereby declare that the research work presented in this thesis entitled **"Multicomponent Synthesis of New Heterocyclic Compounds and their Biological Evaluation"** has been carried out by me under the supervision of **Prof. V. Rajeswar Rao**, Department of Chemistry, National Institute of Technology Warangal. I declare that this work is original and has not been submitted in part or full, for any degree or diploma to this or any other university.

Date: 11-01-2023

Place: Warangal

(Raju Chedupaka)
(Roll No. 716191)

ACKNOWLEDGEMENTS

In this journey of research work, I come across several people who helped and traveled with me to achieve this ambition of my life. Therefore, for this achievement of mine, I should express my sincere gratitude and appreciation towards those persons who unconditionally supported, helped, and encouraged me in all situations.

I am highly thankful to Almighty for blessings me and giving me strength, energy, and patience to overcome all the difficulties and reach this ambition.

It gives me immense pleasure and delights to express my profound sense of gratitude to my teacher and research guide **Prof. V. Rajeswar Rao**, former Dean, R & C, Department of Chemistry, National Institute of Technology, Warangal for his inspiring and valuable guidance. His unfailing attention, unmitigated encouragement, and cooperation have helped me in attaining my goal. It would have been impossible to achieve this goal without his able support and valuable advice. I consider myself extremely fortunate that he has given me a decisive tune, a significant acceleration to my career. I will be thankful to him throughout my lifetime.

I am greatly indebted to ***Prof. N. V. Ramana Rao***, Director, National Institute of Technology, Warangal allowing me to submit my research work in the form of a thesis. I express my gratitude to ***Prof. T. Srinivasa Rao*** and ***Prof. G. R. C. Reddy***, former Directors, of the National Institute of Technology, Warangal for allowing me to carry out the research work.

My special words of thanks to ***Prof. D. Kashinath*** Head, Department of Chemistry and ***Prof. Vishnu Shanker, Prof. P. V. Srilakshmi*****, and** ***Prof. K. V. Gobi*** former Heads, of the Department of Chemistry, National Institute of Technology, Warangal for their valuable advice, help, and support.

I express my sincere thanks to Doctoral Scrutiny Committee (DSC) members, ***Prof. P. V. Srilakshmi*****, *Dr. B. Srinivas,*** Department of Chemistry, and ***Prof. J. V. Ramana Murthy*** Department of Mathematics for their support and encouragement.

I am highly thankful to the Ministry of Education (MoE), the government of India, for their financial assistance in the form of a fellowship.

I am very much grateful to work with my colleagues and organic research labmates. My sincere thanks to Dr. V. Krishnaish, Dr. M. Srikanth, Dr. A. Varun, Dr. J. Parameshwara Chary, Dr.

K. Sujatha and Mr. P. Venkatesham for their support and encouragement throughout my Ph.D. and thesis would not have come to a successful completion, without the help of these members. Also, I am thankful to CRIF (Central Research Instrument Facility), NIT Warangal for their support to characterize the synthesized compounds. My special thanks to K. Narasimha, K. Venkanna, Venu (NMR instrument operators), and B. Srinu (ESI-HRMS operator). And also thanks to the non-teaching and technical supporting staff of the chemistry department for their help at every time needed.

I sincerely express my deep sense of gratitude to Prof. B. Venkatappa Rao, Prof. G. V. P. Chandramouli, Prof. I. Ajitkumar Reddy, Prof. P. Nageswar Rao, Prof. K. Laxma Reddy, Prof. A. Ramachandraiah, Dr. Venkatathri Narayan, Dr. Santhoosh Penta, Dr. Raghu Chitta, Dr. S. Nagarajan, Dr. C. Jugun Prakash, Dr. Ravinder Pawar, Dr. M. Raghasudha, Dr. Mukhul Pradan, Dr. Rajesh Khanna, Dr. V. Rajesh Kumar, and for their fruitful suggestions and encouragement.

I express my sincere thanks to Dr. G. Kiran Kumar, anti-diabetic activity, computational studies, and ADME properties, Department of Pharmaceutical Chemistry, Anurag University Hyderabad, and Dr. Perugu Shyam, Assistant Professor, Biotechnology Department, NIT Warangal for evaluating the antimicrobial activity.

I am very much grateful to Dr. Anwitha, Post-doc fellow, University of Hyderabad, Department of Biotechnology and Bioinformatics, School of Life Sciences, Hyderabad for screening the anti-cancer activity studies and Dr. Amruthavalli, Associate Professor, Botany& Biotechnology Department, Acharya Nagarjuna University, Guntur, Andrapradesh for screening the anti-bacterial activity studies.

As Dr. Abdul Kalam said that " One best book is equal to a hundred good friends, but one good friend is equal to a library" I am so fortunate to get a couple of good friends in my life like Dr. K. Vimal Kumar, P. Soumya, Dr. P. Sathish, Mr. G. Sripal Reddy, Mr. K. Sampath, Mr. A. Naveen Kuamr, Mr. R. Arun, Mr. M. Venkanna, Mr. K. Krishna and Dr. R. Venkatesh all many others from my childhood to Ph.D. days. I always enjoyed their company and they are my strength in many things in my life.

I would like to thank my M. Sc friends in NIT Warangal like, G. Soujanya, K. Shilpana, SK. Shabhana, D. Divyasree, D. Rajesh Babu, M. Suneel, K. Raghu, K. Vinod, and Nandakishore Krishna for their moral support and constant encouragement.

It gives me great pleasure to express my gratitude to my colleagues and friends Dr. Venkata Bharat Nishtala, Dr. G. Ramesh, P. Babji, R. Hithavani, Dr. T. Sanjay, Dr. P. Vinay, Dr. M. Venkanna, Mr. T. Dhanunjay Rao, Dr. N. Satyanarayana, Dr. A. Bhargava Sai, Mr. K. Vijendar reddy, Dr. V. Sunil Kumar, Dr. Ch. Suman, Dr. S. Suresh, Dr. K. Shekar, Dr. G. Ambedhkar, Dr. K. Satish, G. Sivaparvathi, Mr. G. Srinath, M. Sireesha. T. Shireesha, Mr. Subhir, Mr. Akash, Mr. Vijay, Mr. Avinash, Mr. Apurba, Mr. Arokya Raj, Shashi Sree, Mr. Vara Prasad, Mr. A. Chandra Mohan, and Mr. Thirupathi for their good cooperation and for creating a nice atmosphere in and outside the laboratory and their encouragement and help during my research period.

I express my gratitude to Mr. D. Anantha Ramakrishna, Junior lecturer in Physics, Mr. M. Mahender, Junior lecturer in History, and Mr. M. Sathya Narayana, Junior lecturer in Botany for their continuous support and valuable suggestions.

My family is always a source of great inspiration and moral support for me in perceiving my education. My heart always goes to thank the god of almighty for giving me a such wonderful family. I take this great opportunity to express my deep sense of gratitude to my beloved parents Yakaiah **(**Father), and Sathemma (Mother), for their tons of blessings, love, caring, encouragement, unconditional support, and sacrifice. I find no words to express my feelings for my dearest three siblings Mr. Ch. Vijay Kumar (elder brother), Mrs. Ch. Mamatha (Sister-in-law), Mahendra-Maheshwari (younger sisters-twins) brother-in-laws Mr. A. Mahender, Mr. K. Ranjith, Grandparents Rajamma-Maraiah, Grand parents-in-law, Lakshmi-Venkataiah for their blessings.

I would never forget the motivational, inspiring, enthusiastic behavior and unconditional love, of Mr. V. Upender (Father-in-law), Mrs. V. Anitha (Mother-in-law), and Mr. V. Mukesh Varma (brother-in-law) for their support.

Charunya Sri, Abhiram (Brother Daughter, and son), Nephew: Yougeshwar, Anirudh, Vikram, Virat, and Arjun who with all their patience, prayers, and faith in the Almighty, waited all these long years to see me reaching this stage. Their blessings and care always gave me new fevour and gusto to do something more with perfection.

Finally, it is a great privilege to thank my dearest wife, Prathyusha without her endless patience and unconditional love, and continuous support during my Ph.D. tenure, it would not have been possible for me to be where I am present. At this important moment, it is my honor to acknowledge and thank all who directly or indirectly helped me to make this thesis real.

(Raju Chedupaka)

Table of contents

CHAPTER-I

A brief review on multi-component condensation reactions and their applications in the synthesis of biologically active compounds

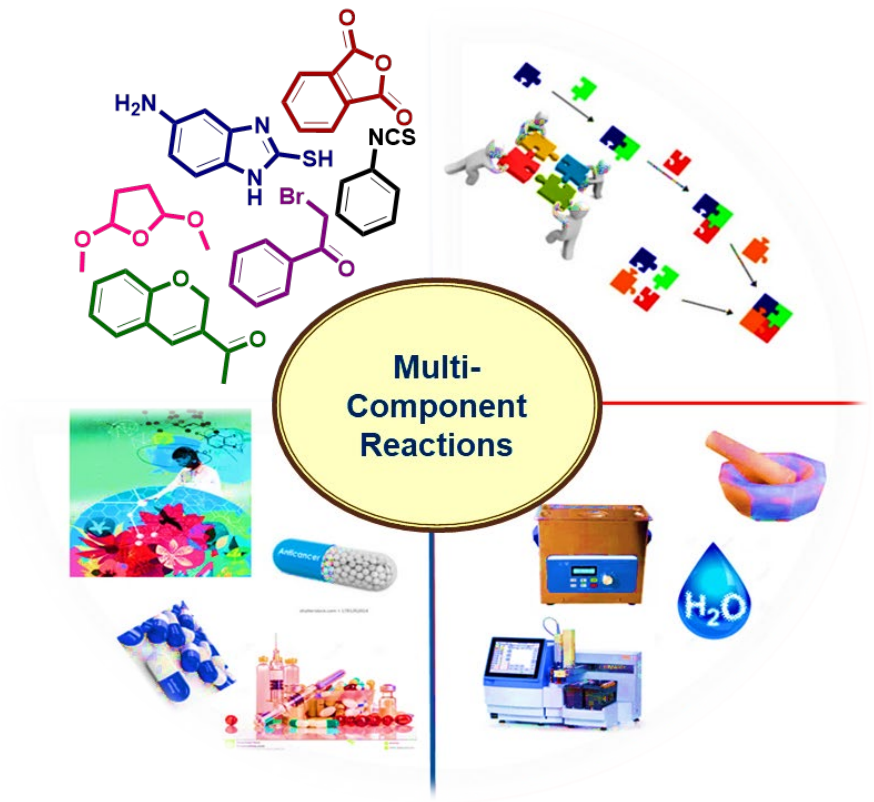

CHAPTER-I

A brief review on multi-component reactions and their applications in the synthesis of biologically active compounds.

Synthetic organic chemistry has always been a frontier area of research due to its impact on the materials and biological sciences. The scientific community thrilling to develop some efficient methodologies, novel reactions, and processes that will lead to the synthesis of desired target molecules and their derivatives with ease. It is not only a tool for obtaining compounds that can be utilized for understanding biological functions or behaviour of materials but it also leads to the creation of novel drugs or drug-like candidates and of new materials with interesting properties.

In general, the targets are usually made *via* an elaborate chain of separate reaction steps that takes longer time to complete, and when that process is extended to large-scale or industrial, it becomes environmentally, economically, and energetically non-viable.

These environmental and economic concerns have increased in the potential and economic world and the last one or two decades because the quality of life is strongly dependent on a clean environment. Chemists can put all the ingredients together at the beginning. This type of reaction has always been a part of organic synthesis, which is called a “one pot-reaction or multicomponent reaction” meaning “chemical conversions consisting of several sequential transformations are brought about in one reaction step. This approach is not only selective but also highly efficient, saving time, energy, and raw materials and adds chemists aim to use the mildest possible conditions, ideally at ambient temperature, atmospheric pressure, an environmentally safe solvent, and a non-toxic catalyst.

A multicomponent reaction (MCR) is a process in which three or more easily accessible components are combined in a single reaction vessel to give a final product displaying features of all inputs and they offer greater possibilities for molecular diversity with a minimum of synthetic time and effort. MCRs can be divided into two groups, (i) Domino reactions and (ii) consecutive reactions. Domino reactions also called tandem, sequential, interactive, zipper, or cascade reactions, are a type of process in which two reactions happens one after other because of the functionality created when a reactive intermediate forms a bond or breaks apart. In consecutive reactions, another reagent mediator or catalyst is added after the first reaction without isolation of the first formed product.

Over many decades, ubiquitous sweat has been paid towards the disquisition of green chemical methodologies both in industry and academia. Also, hazardous, impulsive, and poisonous organic solvents are constantly replaced by either the use of solvent-free [1], water-medium [2], microwave irradiated [3], or multicomponent reactions [4-7] (MCRs).

Multi-component Reactions:

Nowadays MCRs have been widely used in the area of organic synthesis [8], medicinal chemistry [9–11], natural product synthesis [12,13], polymer chemistry [14–18], agro chemistry [19,20], and combinatorial chemistry [21,22].

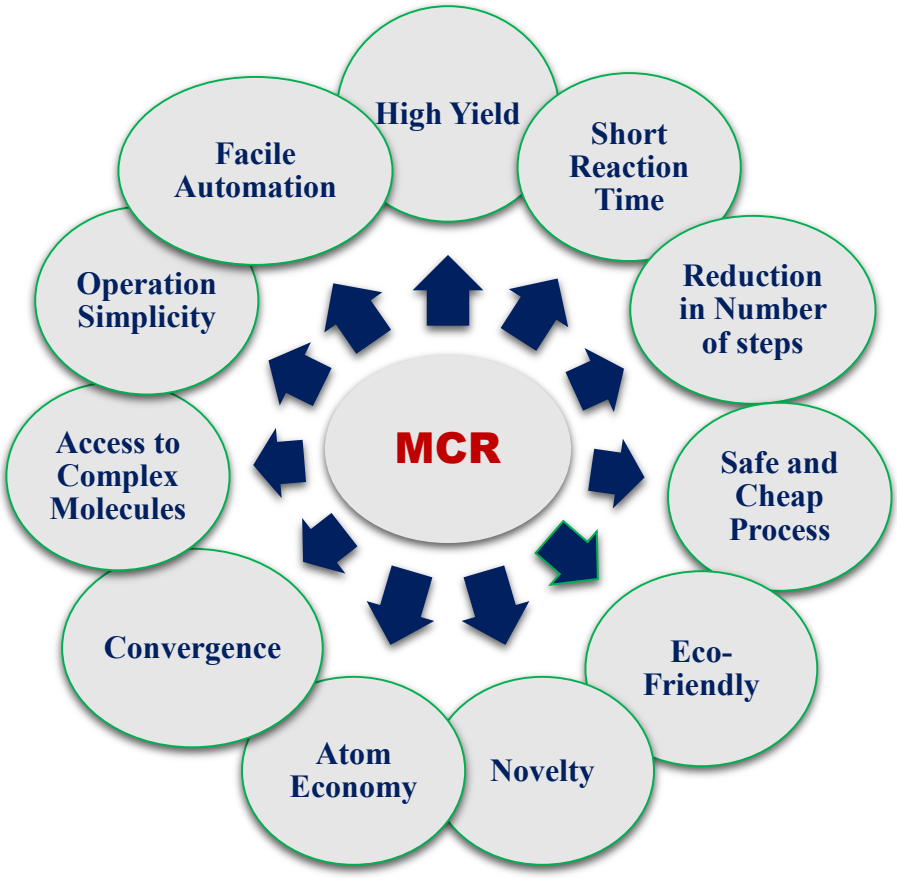

Figure 1.1

1.1. History of multi-component reactions:

The following reactions are some examples of the principal multi-component reactions based on named organic reactions.

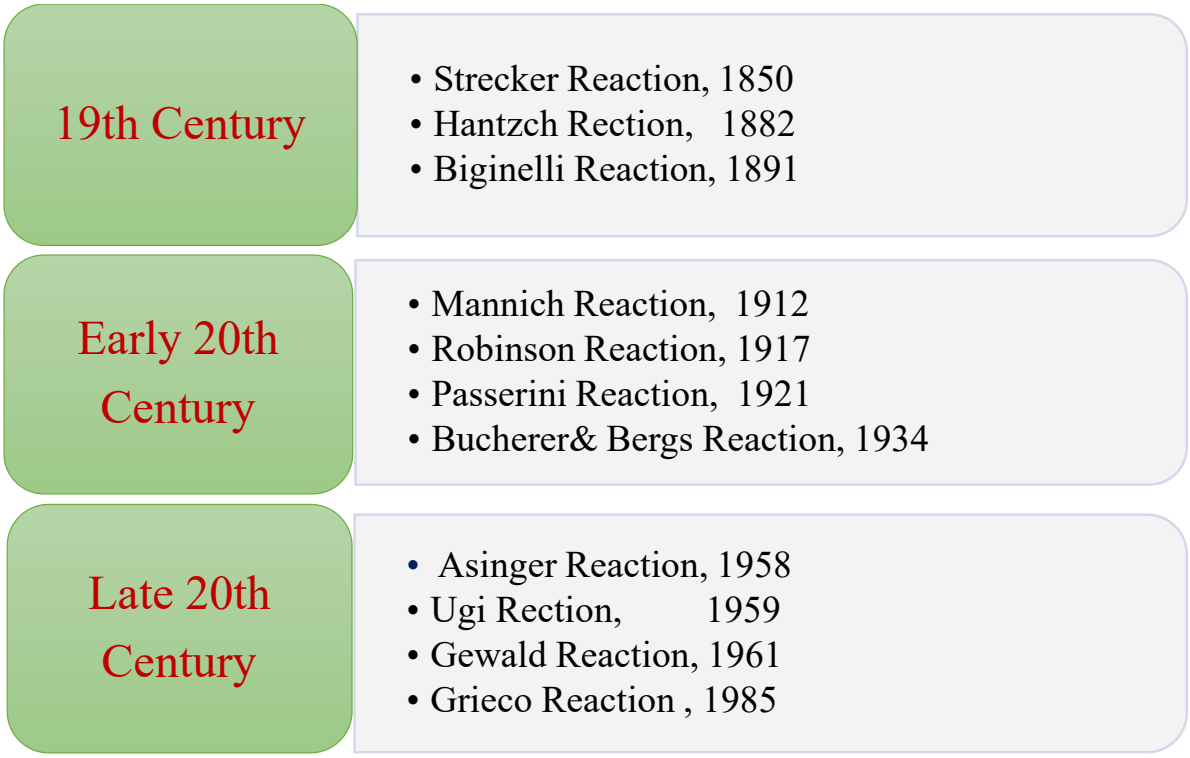

Figure 1.2

The multi-component reaction itself occurs in nature in the evolution procedure [23]. RNA and DNA purine bases i.e., adenines are formed by a multi-component reaction approach *via* the condensation reaction of HCN, which is catalysed by ammonia (Scheme 1.1).

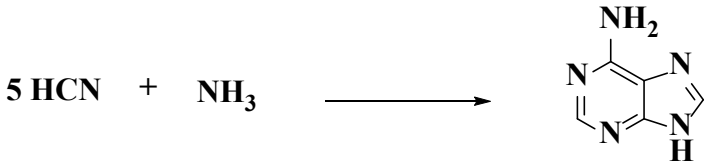

Scheme 1.1

Strecker's synthesis

The first report on multi-component reactions was disclosed by Strecker [24] in 1850. Strecker synthesized α – amino nitriles *via* a one-pot, a three-component reaction by using ammonia, aldehyde, and hydrogen cyanide as starting materials (Scheme 1.2).

Scheme 1.2

Biginelli reaction

An Italian chemist, Biginelli [25] established a multi-component reaction for the synthesis of dihydropyrimidines. These dihydropyrimidine compounds were reported by a one-pot, three-component reaction of various aldehydes, urea, and β–keto esters in presence of ethanol under reflux conditions using an acid catalyst (Scheme 1.3).

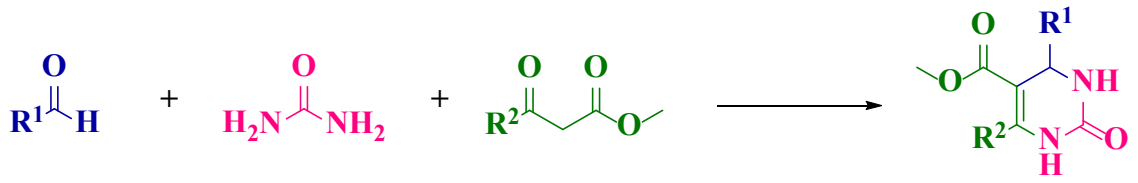

Scheme 1.3

Mannich reaction

Carl Mannich [26] explored a multi-component condensation reaction of aldehyde and amine with carbonyl compounds having active methylene groups to generate the corresponding scaffolds (Scheme 1.4).

Scheme 1.4

Passerini reaction

Passerini [27] reported the first isocyanides-based one-pot, multi-component reaction. He reported the synthesis of α-acyloxy carbamides by reaction of isocyanides, carbonyl compounds, and carboxylic acids (Scheme 1.5).

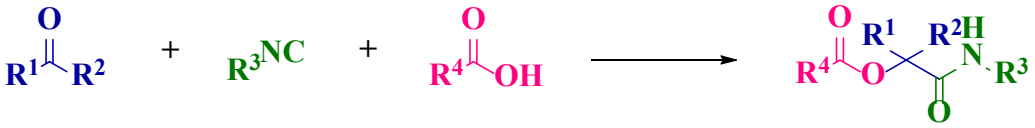

Scheme 1.5

Ugi reaction

A series of α-acylamino amides were reported by Ivar Karl Ugi [28] *via* one-pot, four-component reaction using aldehydes/ketones, amines, isonitriles, and carboxylic acids (Scheme 1.6). This reaction is enormously described and applied in modern organic synthesis.

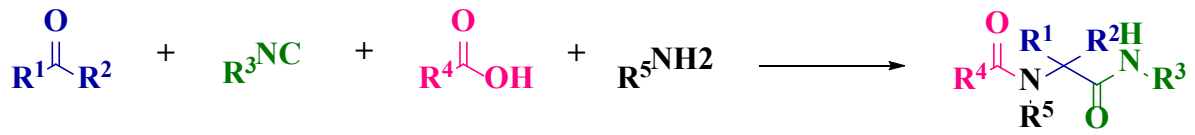

Scheme 1.6

Petasis reaction

Petasis [29] developed one-pot, three-component synthesis of substituted amines by the condensation of carbonyl compounds amines and vinyl or aryl boronic acids to form substituted amines (Scheme 1.7).

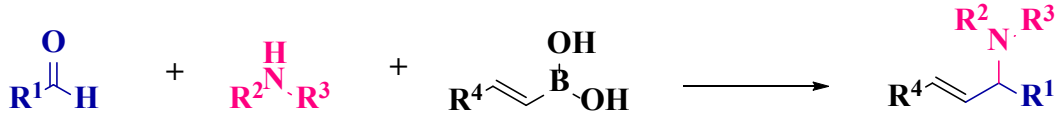

Scheme 1.7

Orru reaction

Orru [30] explored one of the most significant multi-component reaction to synthesize 2-imidazolines by the condensation reaction of amine, an aldehyde, and α-acidic isocyanides (Scheme 1.8).

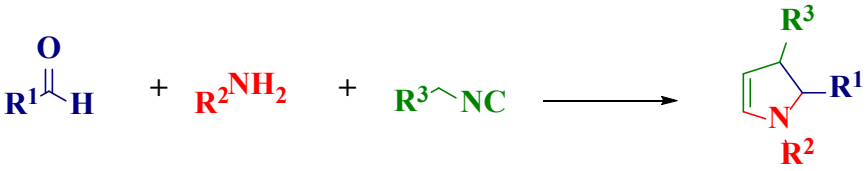

Scheme 1.8

Laurent and Gerhardt multicomponent reaction

Laurent and Gerhardt [31] reported the multi-component reaction of "benzoyl azotid". At firstly benzaldehyde in the presence of hydrogen cyanide and ammonia produced α-amino benzyl cyanide. Further, the reaction mixture was added by another mole of benzaldehyde to produce the anil of benzyl cyanide i.e. "benzoyl azotid" (Scheme 1.9).

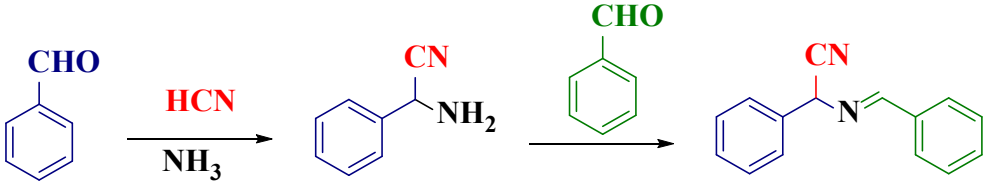

Scheme 1.9

Radziszewski imidazole synthesis

Radziszewski [32] explored a one-pot, four-component reaction for the synthesis of substituted imidazoles. In this reaction, the starting materials are 1,2-dicarbonyl compounds, formaldehyde, primary amine, and ammonia were used to produce the substituted imidazole's (Scheme 1.10).

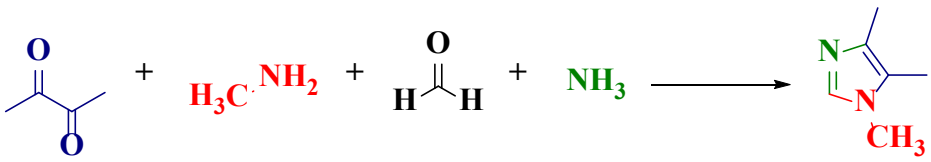

Scheme 1.10

Hantzsch dihydropyridine synthesis

Hantzsch [33] reported a four-component reaction for the synthesis of substituted 1,4-dihydropyridines *via* cyclo-condensation reaction using ethyl acetoacetate, ammonium acetate, and aldehyde (Scheme 1.11).

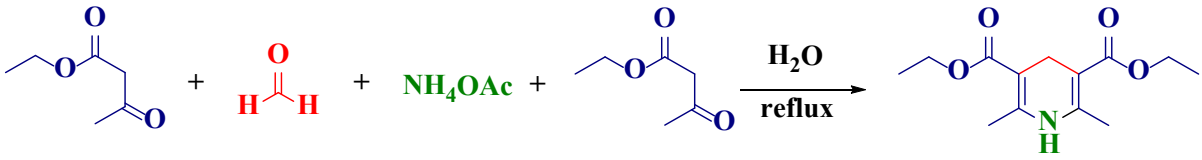

Scheme 1.11

Hantzsch pyrrole synthesis

Hantzsch [34] reported a one-pot, three-component reaction for the synthesis of pyrroles by the reaction of β–keto esters with α-halo β – keto esters and primary amines (Scheme 1.12).

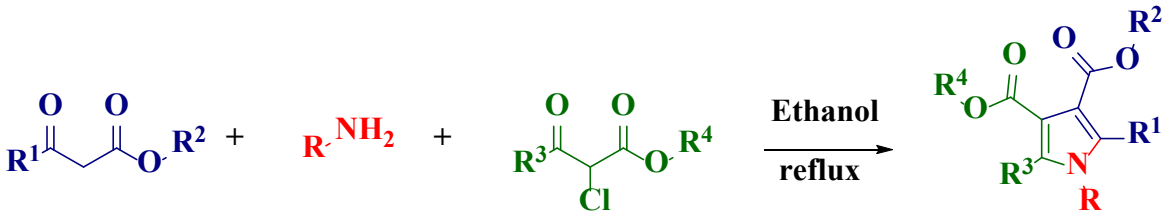

Scheme 1.12

Bucherer Berg's hydantoin synthesis

Bucherer and Bergs [35] established one of the most important four-component reaction method for the synthesis of hydantoin *via* cyclo condensation of carbonyl compounds, hydrogen cyanide, ammonia, and carbon dioxide (Scheme 1.13).

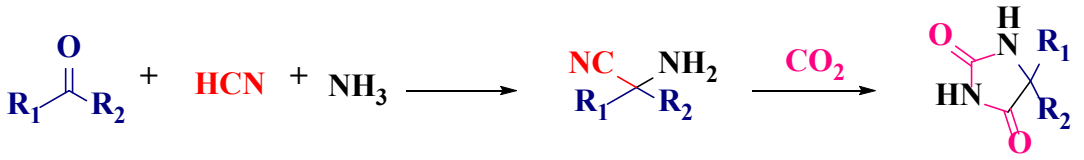

Scheme 1.13

Asinger reaction

Asinger [36] developed a one-pot, four-component method for the synthesis of thiazolines by using a multicomponent reaction approach. Here, thiazolines are synthesized from α-halogenated carbonyl compounds, ammonia, and sodium hydrosulphide (Scheme 1.14).

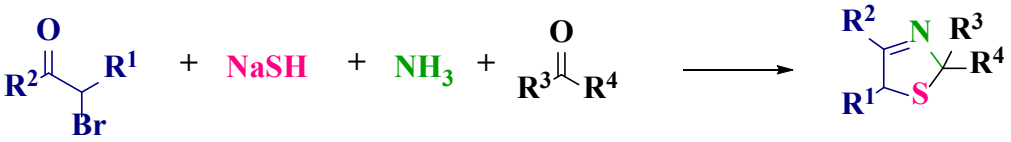

Scheme 1.14

Gewald reaction

Karl Gewald [37] developed an efficient, one-pot, three-component reaction approach for the synthesis of poly substituted 2- amino thiophenes. These title compounds were synthesized by a reaction of α-methylene carbonyl compounds, elemental sulphur, and α-cyano esters in presence of a base (Scheme 1.15).

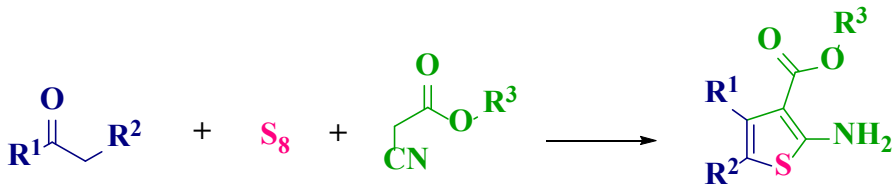

Scheme 1.15

Grieco synthesis (three components) of tetrahydro quinolines

Grieco [38] reported a three-component reaction approach for the synthesis of tetra hydro quinolones using amines, aldehydes, and cyclopentadiene *via* cyclo addition reaction in presence of trifluoroacetic acid (Scheme 1.16).

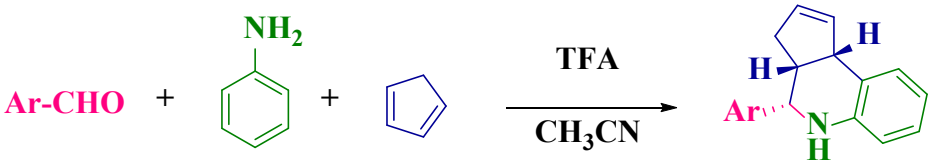

Scheme 1.16

Povarov three-component reaction

Povarov [39] developed a three-component reaction approach for the synthesis of tetra hydro quinolones. At first anilines and benzaldehydes undergo a condensation reaction, and the intermediate Schiff bases react with Lewis acid-like boron trifluoride to activate imine for electrophilic addition of the activated alkene. The reaction step forms an oxonium ion which then reacts with the aromatic ring in a classical electrophilic aromatic substitution. Two additional elimination reactions lead to the formation of tetra hydro quinolone structure (Scheme 1.17).

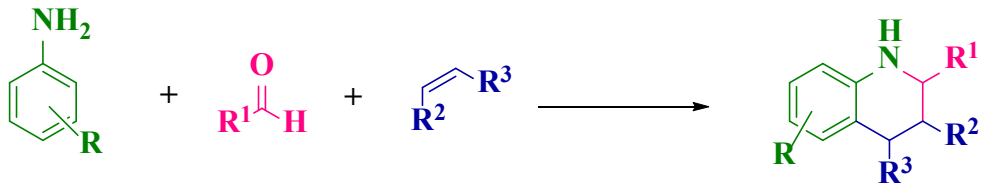

Scheme 1.17

Betti three-component reaction

Betti [40] established a three-component reaction approach for the synthesis of α-amino benzyl phenols. In this reaction primary aromatic amines and aldehydes form imines, further, this intermediate reacts with phenol to form α-amino benzyl phenol derivatives (Scheme 1.18).

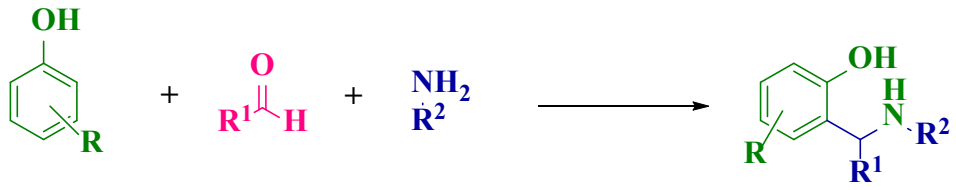

Scheme 1.18

1.2. Classifications of multi-component reactions

Multi-component reactions can be classified into several types as follows

- Based on the reactants involved in the synthesis i.e. three-component, four-component, and five-component reactions, etc.
- Based on the functional groups on the reactant molecules as follows.

1. Imine-based multi-component reactions.
2. Isocyanide-based multi-component reactions.

Number of well-established multi-component reactions were related to the imine based multi-component reactions. In this type of reaction, the products encompassing the imine functional group were produced by the condensation of carbonyl functional group scaffolds with amines. Whereas, in second method the isocyanide based reactants are the starting material for the reactions elaborated in isocyanide established multi component reactions.

- Based on the reaction kinetic paths i.e. reversible or irreversible, based on isolabilty and reactivity of the products.

Type-I: In this type, starting materials used for the reaction, reaction intermediates, and the final products are in equilibrium with each other. These reactions are thermodynamically controlled reactions because the yield and isolability of the reaction depend on the thermodynamics of the reaction (Scheme 1.19).

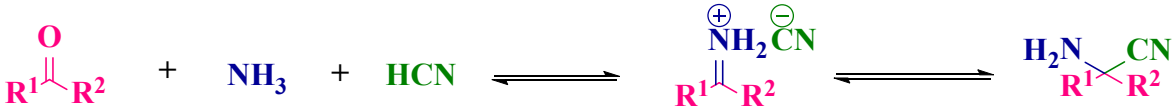

Scheme 1.19

Type-II: In these reactions, equilibrium exists among substrates and reaction intermediates. The reaction is completed by an irreversible step between the intermediate and the final product (Scheme 1.20).

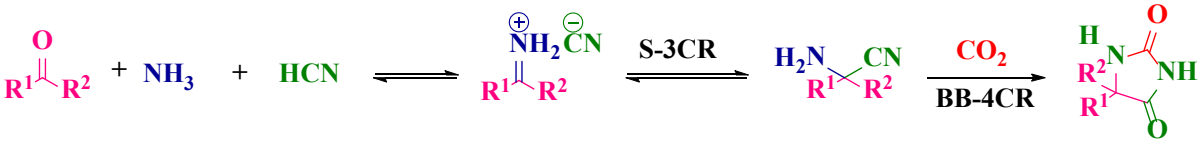

Scheme 1.20

Type-III: In these types of reactions one product is formed by all sub-reactions encompassing irreversible steps (Scheme 1.21).

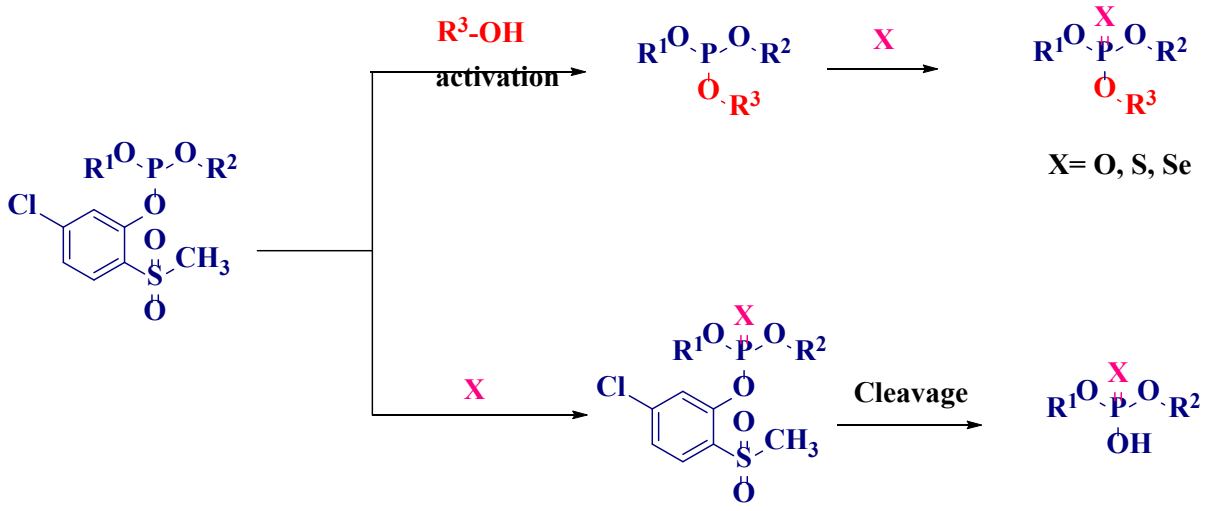

Scheme 1.21

1.3. Different approaches in MCRs

There are various approaches established other than normal conventional methods to solve the purification problems, minimize the reaction time, improve the product yields, and to develop easier workup techniques, etc.

Solid Phase MCRs

Yanira Mendez [41] *et al*. have reported a four-component condensation reaction approach for the synthesis of small ring heterocycles by solid phase synthesis. For example, the Ugi-azide one-pot, four-component reaction of amine, aldehyde, followed by the addition of isocyanide and trimethylsilyl azide provides a tetrazole-peptidomimetics (Scheme 1.22). it can serve as an inhibitor of *Escherichia Coli* M1-aminopeptidase.

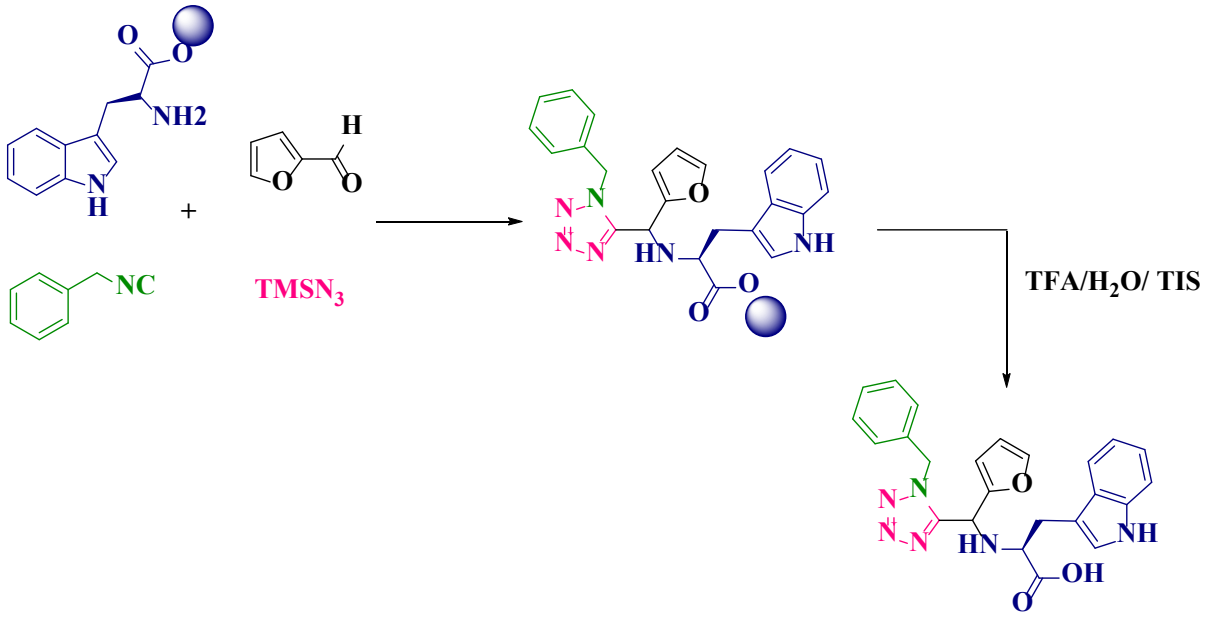

Scheme 1.22

Aqueous medium MCRs

Menezes [42] *et al.* reported an efficient and aqueous mediated multi-component reaction approach for the synthesis of SQXO derivatives using *o*-phenylenediamine, aldehydes, and sodium pyruvate in 20% aqueous acetic acid containing sodium acetate provided the title products in good yields (Scheme 1.23).

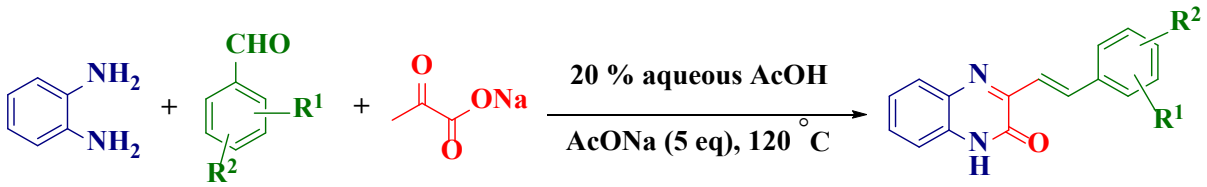

Scheme 1.23

Solvent-free MCRs

Singh [43] *et al.* established one of the most important regioselective approach for synthesis of 5,6-dihydro- 4*H*-thiopyrans *via* one-pot, three-component domino coupling *α, β*- unsaturated aldehydes, *β*-oxodithioesters and cyclic aliphatic secondary amines under solvent free and catalyst-free conditions at room temperature provided good yields (Scheme 1.24).

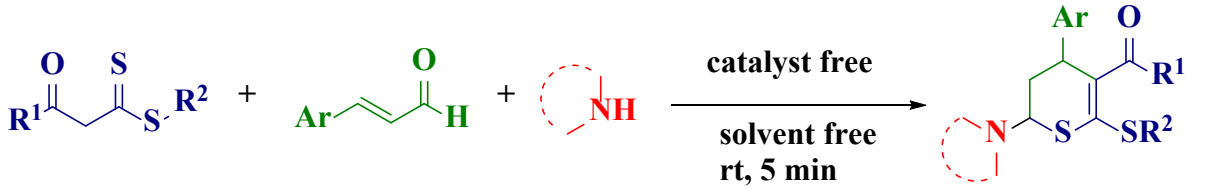

Scheme 1.24

Microwave irradiated MCRs

Rao [44] *et al.* reported an efficient, one-pot, three-component synthesis of coumarin-based thiazoles using thiocarbohydrazide, various aldehydes, and 3-(2-bromo) acetyl coumarins using a catalytic amount of acetic acid and ethanol under microwave-irradiated condition (Scheme 1.25).

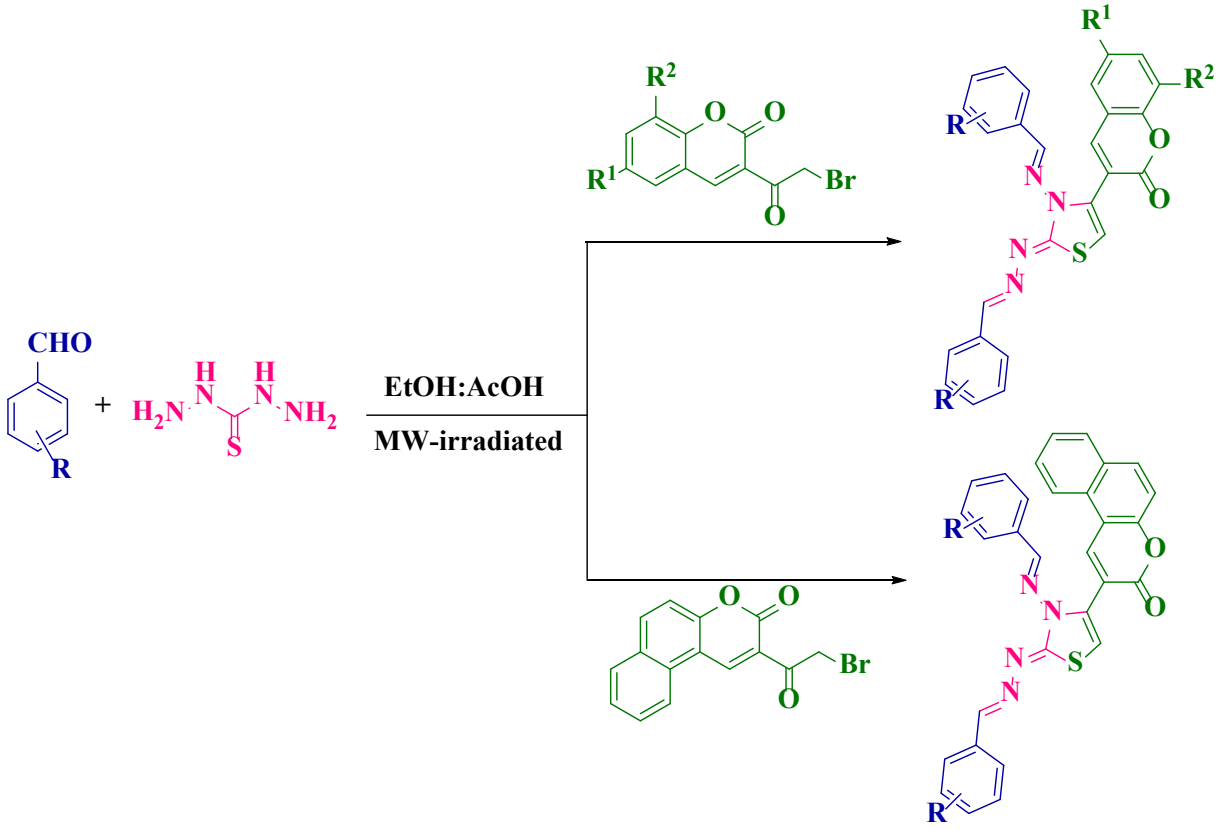

Scheme 1.25

Ultrasonic MCRs

Pasha [45] *et al.* explored copper (I) catalyzed a one-pot, four-component reaction approach for the synthesis of N-substituted 1,4-dihydropyridine derivatives using aldehydes, dialkylacetylenedicarboxylate, malononitrile, and substituted anilines in water as green solvent under ultrasonic irradiation condition provided good yields (Scheme 1.26).

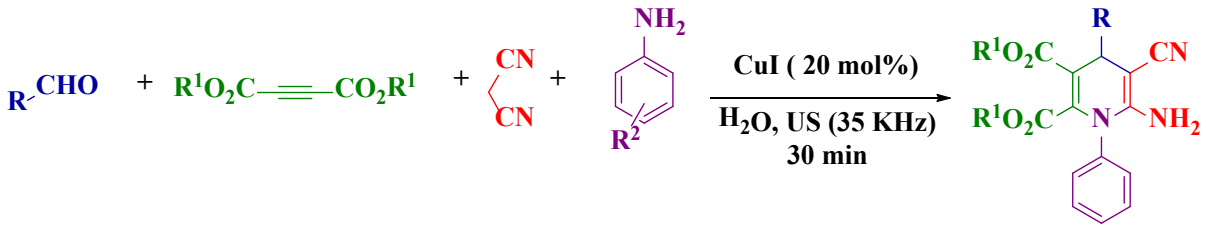

Scheme 1.26

1.4. Applications of multi-component reactions

Applications in natural product synthesis

Number of natural products were widely used in medicinal chemistry. Because of their limited availability, it is important to synthesize these natural products with good yields. In this regard,

multi-component reactions play a vital role in the synthesis of natural products. The following are some instances of the role of MCRs in the synthesis of natural products.

Cannabinols are the natural products that are used as CNS (central nervous system) G-protein agonists. In their synthesis, 6*H*-dibenzo[*b*, *d*]pyranone is recognized as one of the intermediates. Bodwell [46] and co-workers established an efficient multi-component reaction approach for the synthesis of 6*H*-dibenzo[*b*,*d*]pyranone (Scheme 1.27).

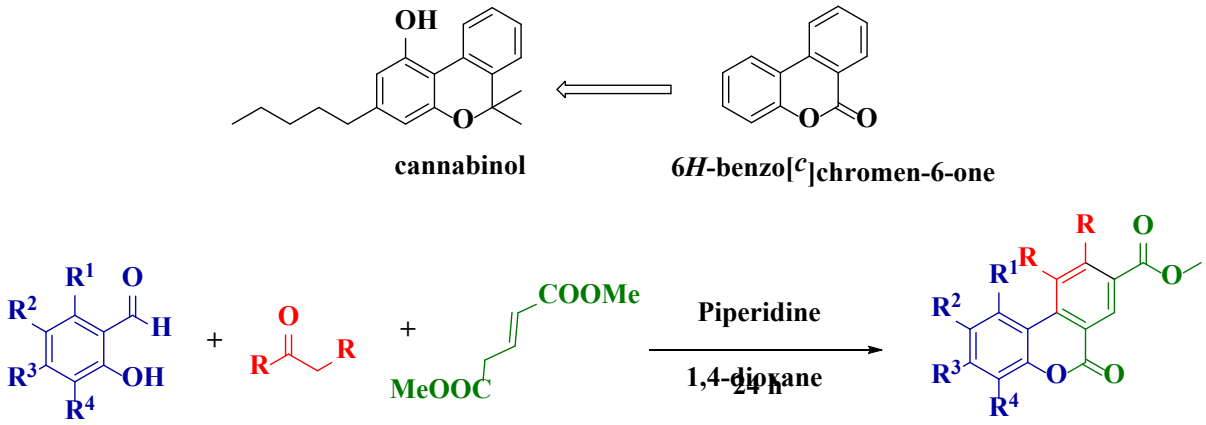

Scheme 1.27

Dysidea frondosa is a marine sponge; from this marine sponge marine sesquiterpenoid Frondosin B is isolated. It behaves as an interleukin-8 receptor antagonist. On account of its medicinal significance, most of the natural product chemists have been motivated to synthesize the Frondosin-B. Hence, Chaplin and Flynn [47] established a multi-component reaction approach by using substituted alkyne, 2-bromophenol, and bromoenone by palladium catalysis to produce the benzofuran analogue (Scheme 1.28).

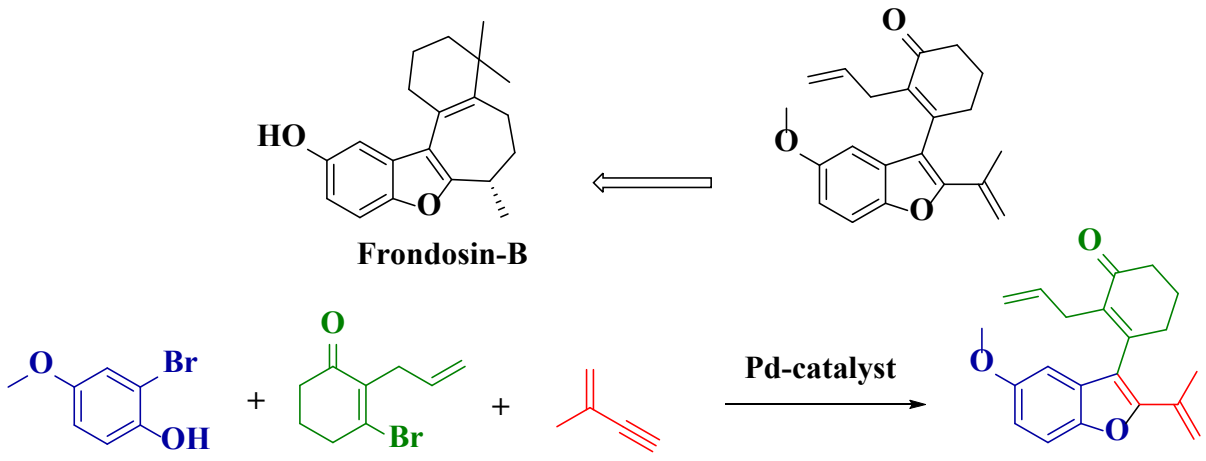

Scheme 1.28

Martinelline is isolated from *Martinella iquitosensis* vine roots and used as a natural nonpeptidic bradykinin B2 receptor antagonist. The alkaloid comprises hexahydropyrrolo[3,2-*c*]quinoline as prime moiety with three pendant isoprenyl-derived guanidine structures. Powell [48] and a co-worker established multi-component Povarov approach to synthesize Martinelline precursor (Scheme 1.29).

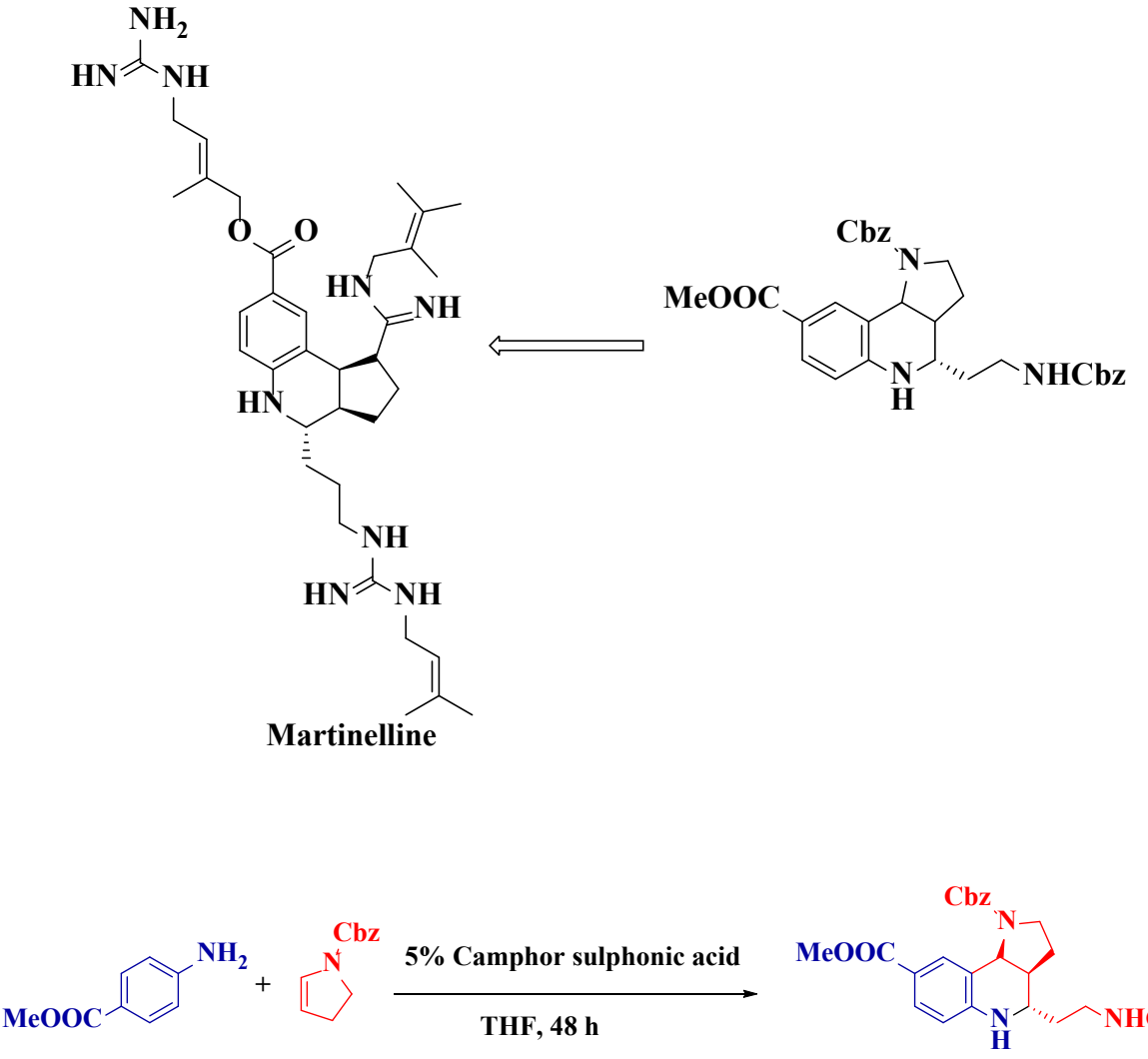

Scheme 1.29

Justicidine E is a naturally obtaining Lignan type of aryl naphthalene lactone ring moieties. Anastas [49] *et al.* established a one-pot, multi-component reaction for Justicidine E. which was synthesized from 5-(3-chloroprop-1-yn-1-yl)benzo[*d*][1,3]dioxole, 5-ethynylbenzo[*d*][1,3]dioxole and carbon dioxide (Scheme 1.30).

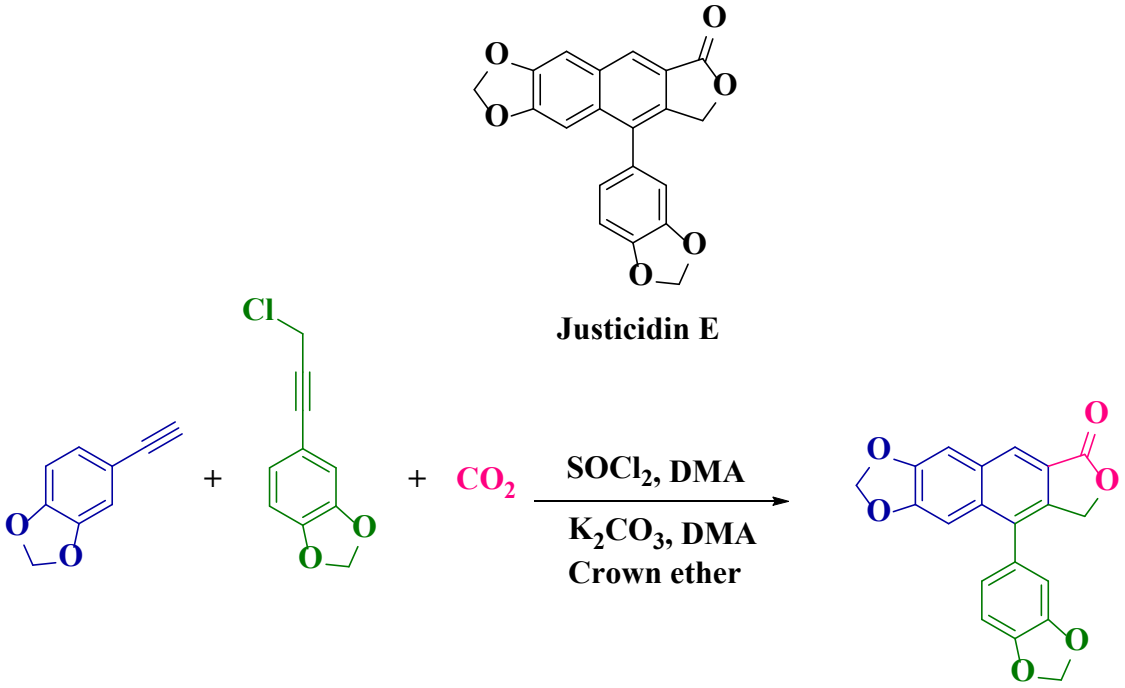

Scheme 1.30

Multi-component reaction applications in the synthesis of drugs

Multi-component reactions are considered a powerful modern synthetic organic tool because they are used for the synthesis of a library of compounds and drug-like moieties. For example, they are efficient protocols to synthesize well-known drugs such as penicillin analogue, Crixivan, bicalutamide, and (S)-clopidogrel, etc.

Synthesis of Penicillin analogues *via* Asinger and Ugi multi-component reaction

Ugi established a multi-component reaction for the synthesis of penicillin [50] analogues by coupling Asinger and Ugi reaction (Scheme 1.31).

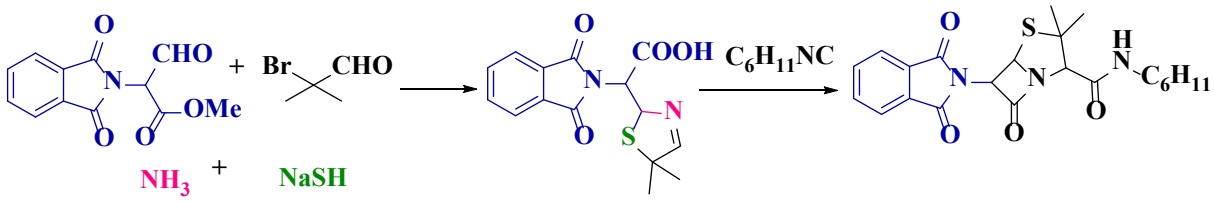

Scheme 1.31

Synthesis of HIV-protease inhibitor Crixivan intermediate (piperazine intermediate)

Rossen [51] *et al*. established an efficient synthetic approach for the synthesis of Crixivan intermediate. This piperazine intermediate was synthesized from *tert*-butyl propyl carbamate, *tert*-butylisocyanide, di-chloroacetaldehyde, and formic acid by Ugi multicomponent reaction (Scheme 1.32).

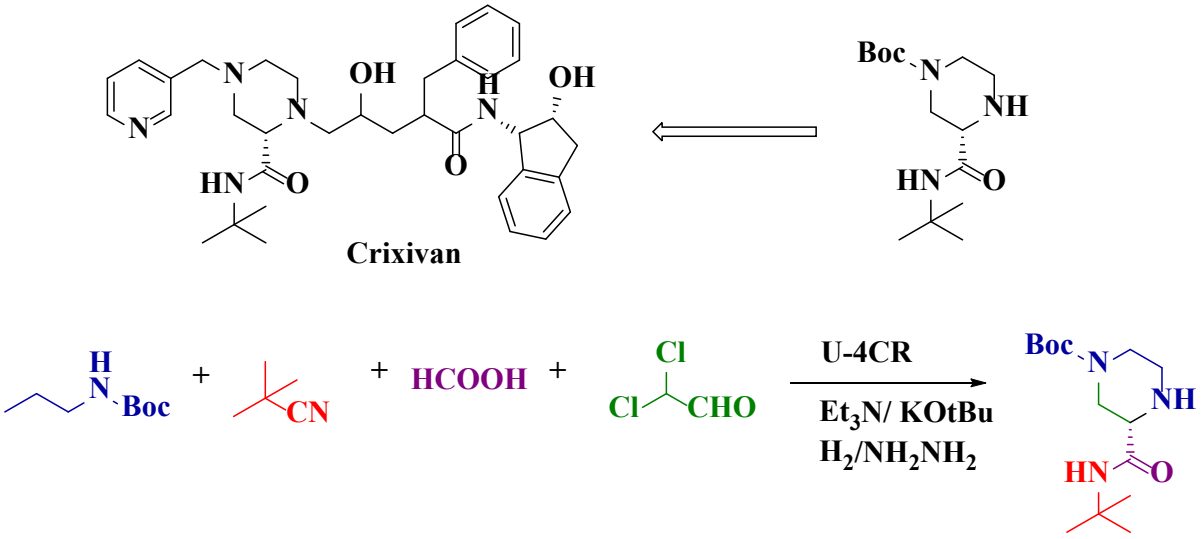

Scheme 1.32

Synthesis of the anti-malarial drug *via* Ugi multi-component reaction

Chibale [52] *et al.* developed an efficient method for the synthesis of an anti-malarial drug (lactam). The lactam was synthesized using diamines, 4-oxobutyric acid, and cyclohexyl isocyanide using Ugi multi-component reaction (Scheme 1.33).

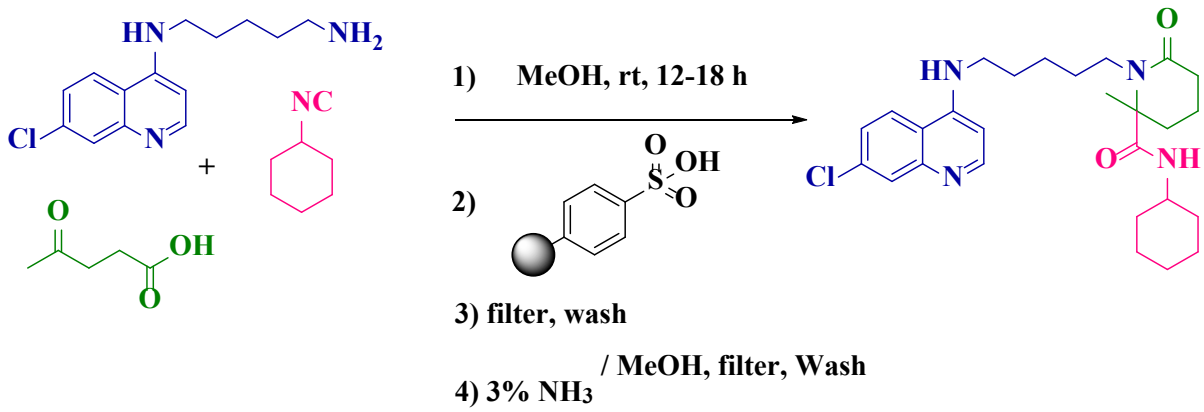

Scheme 1.33

Synthesis of an enzyme inhibitor (calpain) *via* Passerini multi-component reaction

An efficient method for the synthesis of an enzyme inhibitor (calpain) intermediate i.e. dipeptide moiety has been developed. The dipeptide moiety was synthesized using Boc protected amino aldehyde, an isonitrile, and a suitably protected amino acid using Passerini multicomponent reaction [53] (Scheme 1.34).

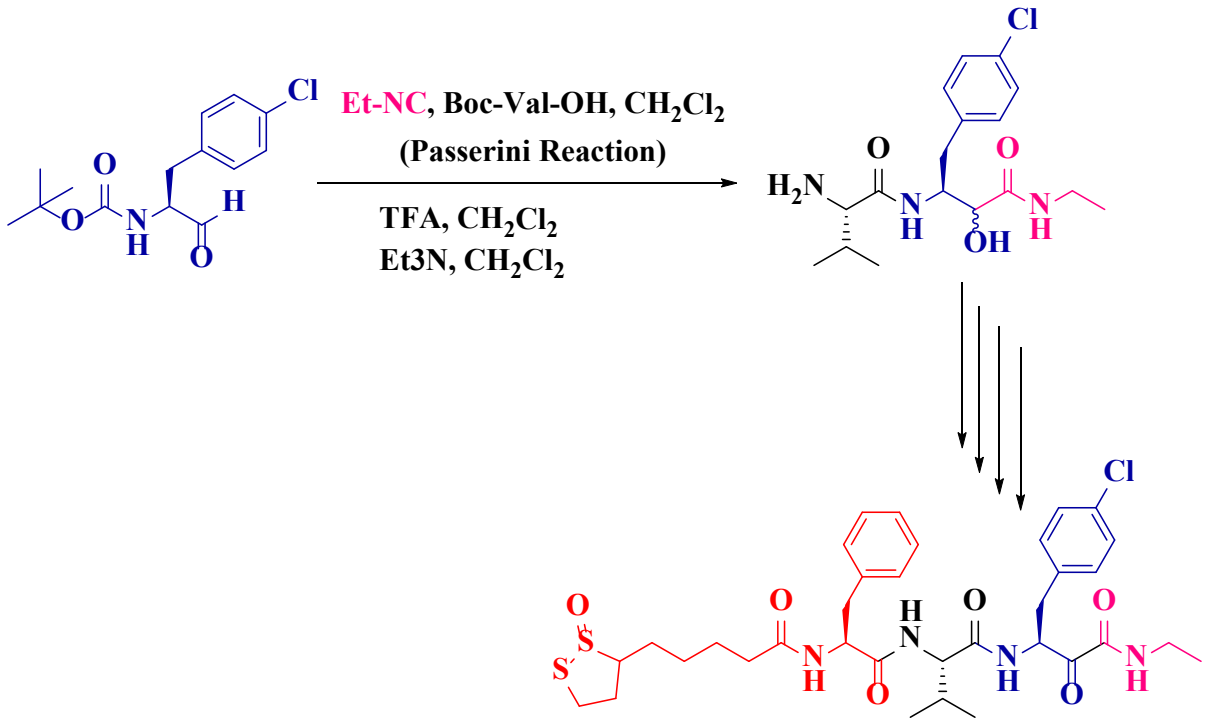

Scheme 1.34

Synthesis of the anti-cancer drug *via* multiple multi-component reactions

An efficient method for the synthesis of a new generation of highly cytotoxic tubulin analogues (tubugis) was developed. The tubulin moieties are among the most potent artificial anti-cancer agents ever invented and manifest the first example of a target-oriented synthesis method using multiple multi-component reactions [54]. In this Ugi- Nenajdenko, Passerine-Domiling, three-component reactions, and Ugi 4 component reactions were used (Scheme 1.35).

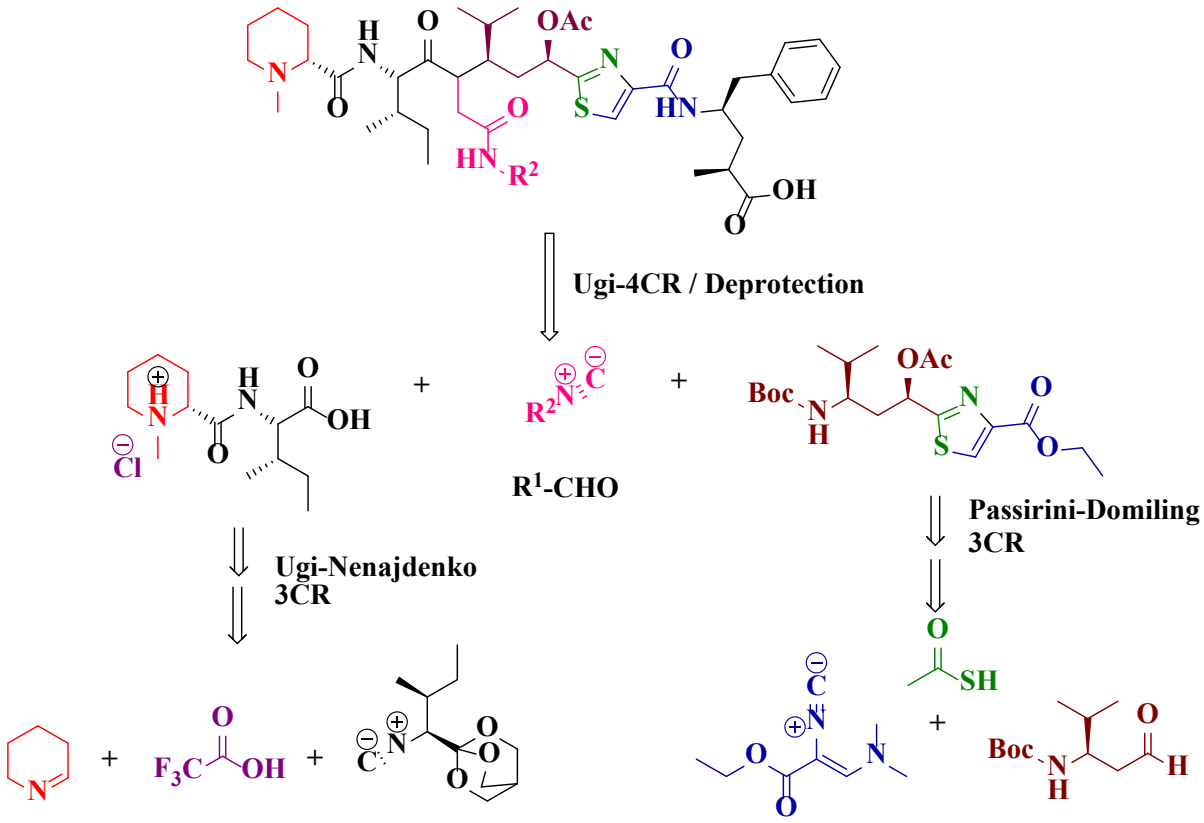

Scheme 1.35

1.5. Chemistry of benzimidazoles

Heterocyclic chemistry is one of the most important topics in modern organic chemistry, because of its widespread applications in various domains [55-58]. In particular, among the heterocyclic pharmacophores, the benzimidazole ring system is quite common and contains a phenyl ring fused to an imidazole ring as depicted in figure 1.23.

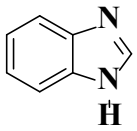

Figure 1.23

1.6. History of benimidazoles

Benzimidazole is a six-membered bicyclic heteroaromatic compound in which the benzene ring is fused to the 4- and 5th positions of the imidazole ring. Historically, the first benzimidazole was prepared by Hoebrecker [59] in 1872 of 2, 5- and 2, 6-dimethylbenzimidazole by ring closure reaction of benzene-1,2-diamine derivatives [60] and more interest in the area of benzimidazole based chemistry was developed in the 1950s, when 5,6-dimethyl-1-(a-Dribofuranosyl) benzimidazole was found as an integral part of the structure

of vitamin B12. Moreover, in 1882, Radziszewski reported the first synthesis of highly substituted imidazoles by condensing 1, 2-diketones with different aldehydes in the presence of ammonia [61].

1.7. Nature of benzimidazoles

Benzimidazole ring contains two nitrogen atoms at the one and third position of imidazole ring with amphoteric, i.e., possessing both acidic and basic characteristics. These rings exist in two equivalent tautomeric forms, in which the hydrogen atom can be located on either of the two nitrogen atoms (Figure 1.24). Furthermore, the electron-rich nitrogen heterocycles could not only readily accept or donate protons but also form diverse weak interactions easily.

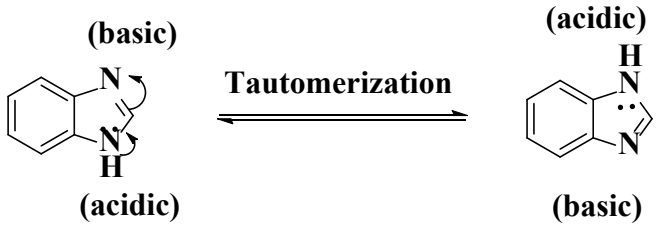

Figure 1.24

1.8. Biological applications of benzimidazoles

Benzimidazole derivatives have revolutionized the medicine discovery process through their different range of pharmaceutical applications, which makes this compound a necessary anchor for the invention of new remedial agents. Therefore, the remedial eventuality of benzimidazole and affiliated medicines has attracted modern organic researchers to design and develop more potent derivations with a wide range of pharmaceutical potentials. Owing to the immense synthetic value and extended bioactivities displayed by benzimidazoles and their derivations, efforts have been made from time to time to produce libraries of these compounds.

These act as structural isosteres of naturally occurring nucleotides. Notably, the benzimidazoles substituted at 2 and 5 or 6 positions are useful for the development of novel medicinal compounds in the pharmaceutical fields. For instance, benzimidazole drugs like rabeprazole and omeprazole act as proton pump inhibitors (treatment of stomach ulcers) thiabendazole and albendazole are anthelmintic drugs used to inhibition of tubulin polymerization. Therefore, with the high prevalence of benzimidazole importance within medicinal and various domains there has been considerable interest in developing efficient approaches for their synthesis. The synthetic benzimidazole scaffolds are also known to exhibit extended biological activities including antimicrobial agents [62-65], anti-cancer [66-68], antifungal agents [69,70], antidiabetic agents [71], anti-inflammatory agents [72,73], anti-Alzheimers [74], antagonists [75], anti-parasitic agents [76], and anti-tublin [77].

Kankala [78] ***et al***. Synthesized a facile catalytic method for the regioselective synthesis of 2,5-di-substituted-isoxazole bounds to benzimidazoles *via* catalytic nitrile oxide-alkyne 1,3-dipolar cycloaddition (**figure 1.25**). Further, these compounds were screened for their *in-vivo* analgesic and anti-inflammatory activity. Herein, pentazocine and Diclofenac are the standard drugs.

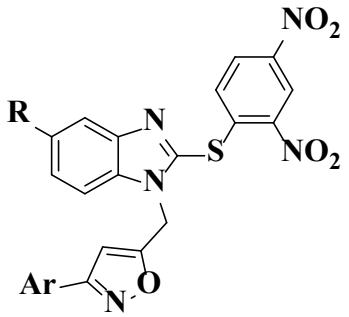

45

Figure 1.25

Mostafa. M. Ramla [79] ***et al***. reported a novel series of 2-(1-benzyl-2-methyl-1*H*-benzimidazol-5ylimino)-3-(substituted-thiazolidin-4-one or 3-(2-methyl-1*H*-benzimidazol-5-yl)-2-substituted-thiazolidin-4-one derivatives. Further, these scaffolds were screened for their *in-vitro* inhibitory activity against the Epstein-Barr Virus Early Antigen (EBV-EA). Among the tested compounds the following were shown potent activity (**Figure 1.26**).

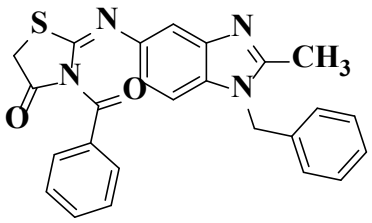

Figure 1.26

Cruz-Gonzalez [80] ***et al***. Carried out the microwave-assisted synthesis of 2-mercapto benzimidazoles and its alkylated derivatives by using various 1,2-diamino benzenes, carbon disulfide, and various alkyl/aralkyl halides in ethanol-NaOH (**Figure 1.27**).

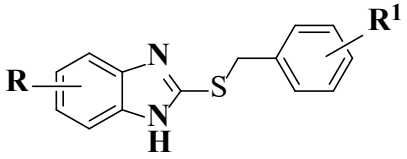

Figure 1.27

Abdel-Aziz [81] *et al.* synthesized a series of novel 2-(benzimidazol-2-yl)thio)-1-aryl ethan-1-one derivatives by using 1,2-amino benzenes, carbon disulfide, and α-Bromo acetophenones in glacial acetic acid and a catalytic amount of sulphuric acid. Further, these scaffolds were screened for their *in-vitro* anti-proliferative activity against colon HT-29 cancer cell lines. The following compound shows potent activity (**Figure 1.28).**

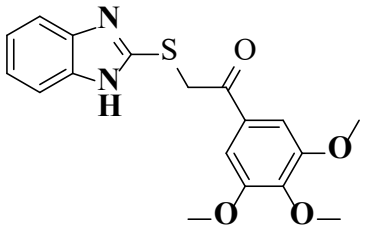

Figure 1.28

Malladi [82] *et al.* reported diversity-oriented, one-pot, synthesis novel imidazo[4, ′5′] benzo[e][1,4]thiazepinones and benzo[*d*]imidazolyl thiazolidines *via* cyclization method by using 5-amino-2-mercapto benzimidazole, various substituted aromatic aldehydes and thioglycolic acid in dry toluene and a catalytic amount of *p*-TSA under reflux. Further, these compounds were screened for their *in-vitro* anti-microbial and anti-inflammatory activity (**Figure 1.29**).

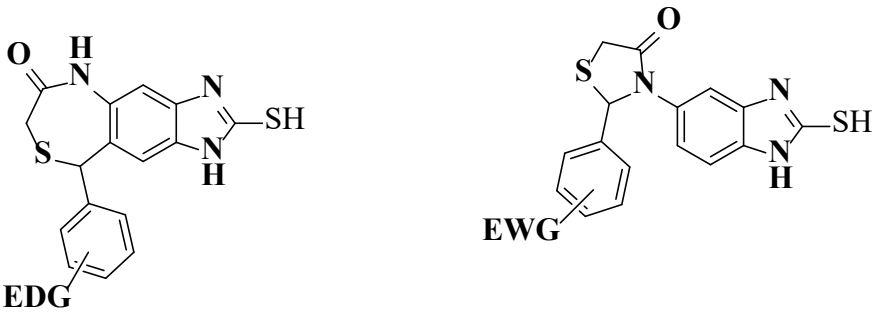

EDG: Electron donating groups **EWG: Electron withdrwaing groups**

Figure 1.29

Kumar [83] *et al*. reported, a facile one-pot, synthesis of 2-substituted benzylsulfanyl -1*H*-benzimidazoles by using 2-mercapto benzimidazole and various aralkyl halides in acetone/ potassium carbonate gave good to excellent yields. Further, these compounds were screened for their *in-vitro* anti-microbial activities against *B. Subtilis, E. Coli, P. aeruginosa, C. Albicans,* and *A. niger,* and all the synthesized compounds showed moderate to good activity (**Figure 1.29).**

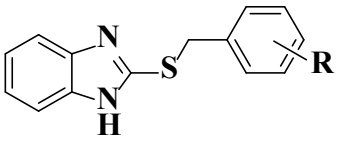

Figure 1.30

Madsen [84] ***et al.*** synthesized 2-(benzimidazol-2-yl-thio)-1-(3,4-di-hydroxyphenyl)-1-ethanone derivatives by using 2-mercapto benzimidazole, 2-bromo-1-(3,4-di-hydroxyphenyl) ethanones in MeCN gave good yields. Further, these scaffolds were screened for thei*r in-vitro* non-peptide competitive human-glucagon receptor antagonist activity. All the compounds were shown potent activity (**Figure 1.31**).

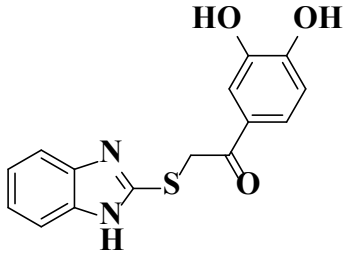

Figure 1.31

Dong [85] ***et al***. described a convenient, efficient, and one-pot, green protocol for the synthesis of 2-benzyl/ 2-allyl substituted thiobenzoazoles in water by using 2-aminothiophenols, 2-aminophenols, and1,2-phenylene diamines with tetramethyl thiuram disulfide [TMTD] gave mercapto benzoheterocycles. And these subsequently react with various benzyl or allyl halides in water/ potassium carbonate giving good to excellent yields (**Figure 1.32**).

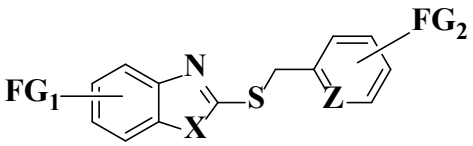

X= S, O, NH
Z= C, O, N

Figure 1.32

Anisetti [86] ***et al.*** reported an efficient novel one-pot synthesis of 2-mercapto-1,5-dihydrospiro[imidazo[4',5':4,5]benzo[1,2-*e*][1,4]thiazepine-9,3'-indoline] derivatives by using 5-amino-2-mercapto benzimidazole, various isatins, and thioglycolic acid in CH_3CN, and a catalytic amount of *p*-TSA gave good to excellent yields. Further, these scaffolds were screened for their *in-vitro* anti-microbial, anti-inflammatory, and antioxidant activities. And all the compounds exhibited potent activity (**Figure 1.33**).

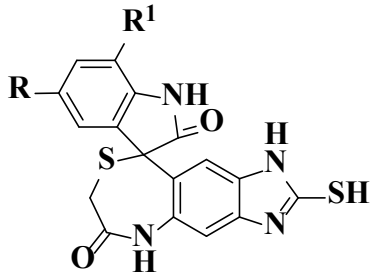

Figure 1.33

Malladi [87] ***et al.*** have described a series of novel benzimidazolyl pyrano[2,3-*d*] [1,3]thiazolo carbonitriles *via* Michael addition using 5-amino-2-mercapto benzimidazole, various aromatic aldehydes, mercaptoacetic acid and 2-(phenyl methylene) malononitrile gave good to excellent yields. Further, all the synthesized scaffolds were screened for their *in-vitro* anti-inflammatory and anti-oxidant activity. All the synthesized compounds were shown potent activity against the standard drugs (**Figure1.34**).

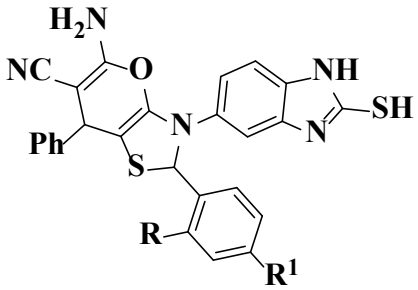

Figure 1.34

Aims and objectives of the research work

1. To develop efficient, environmentally benign, facile methods for the synthesis of biologically potent molecules.
2. To evaluate the biological activities of newly synthesized heterocycle compounds.

The present work covers the synthesis of benzimidazole-linked heterocyclic compounds and their biological activity studies. The target heterocyclic compounds were synthesized by using easily and readily available starting materials such as 5-amino-2-mercaptobenzimidazole, 2,5-dimethoxytetrahydrofuran, alkyl or aralkyl halides, phenacyl bromides, ammonium isothiocyanate, phenylisothiocyanate's, hydrazine hydrate, and 3-acetyl coumarins.

Chapter-I describes the introduction to multi-component reactions and the chemistry of benzimidazoles.

Chapter-II deals with the synthesis of benzimidazole-linked pyrrole derivatives by the MCR approach and their molecular docking studies.

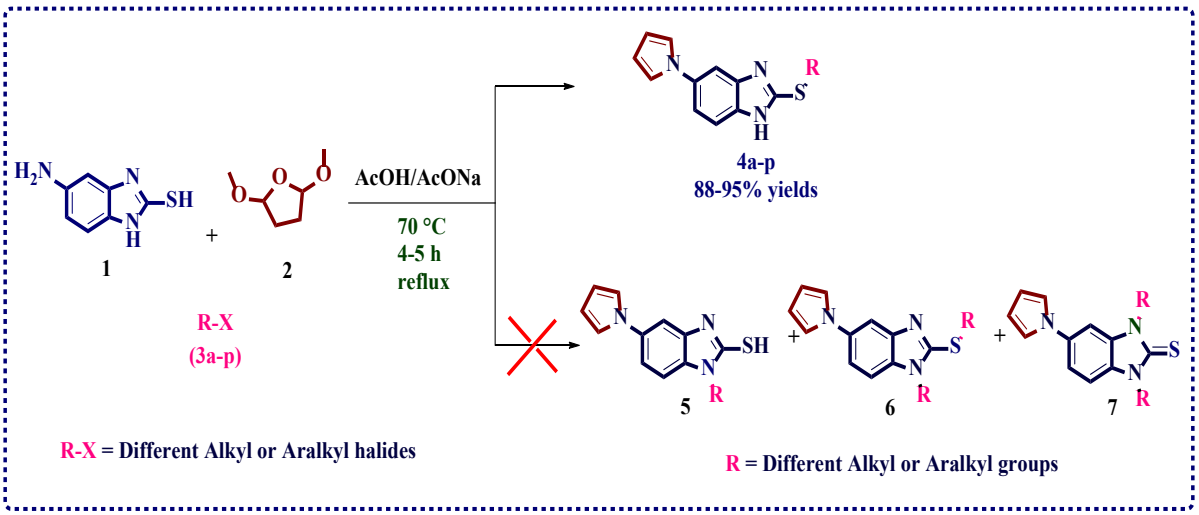

Chapter III portrays the one-pot synthesis of thioalkylated benzimidazole-based 4-substituted mercaptoimidazole molecular hybrids *via* a multi-component approach and their DFT mechanical studies.

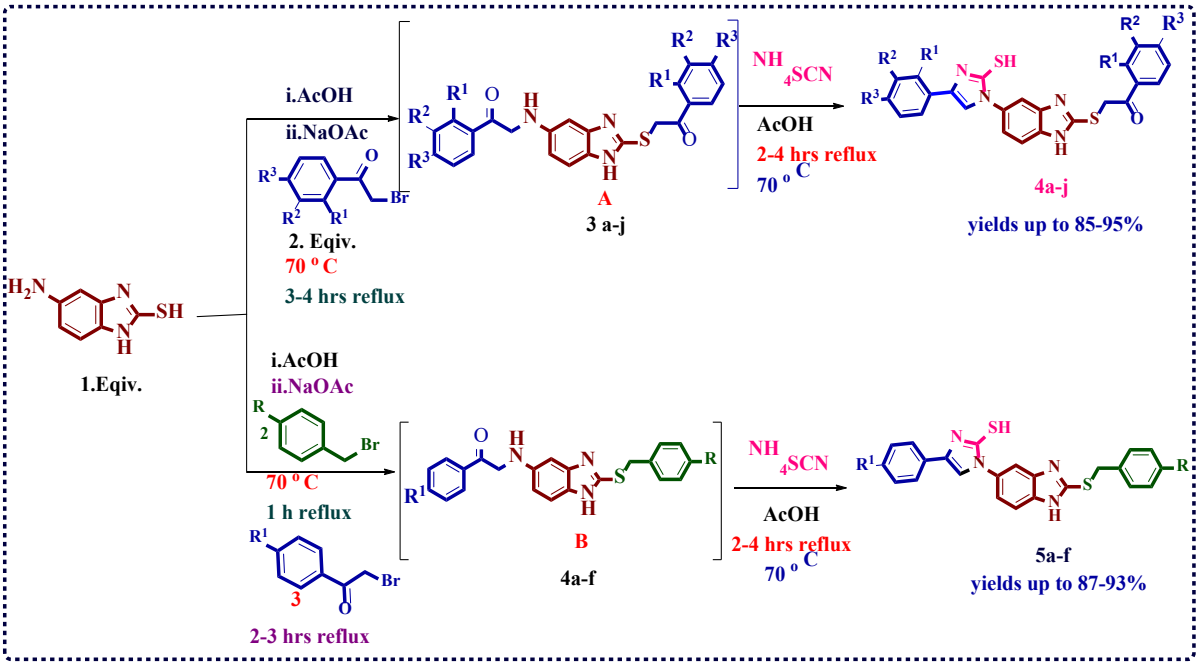

Chapter IV is divided into three sections.

Chapter IVA reports the polyethylene glycol-mediated three-component synthesis of benzimidazole-based thiazoles as α-glucosidase inhibitors. Design, synthesis, molecular modelling and ADME studies.

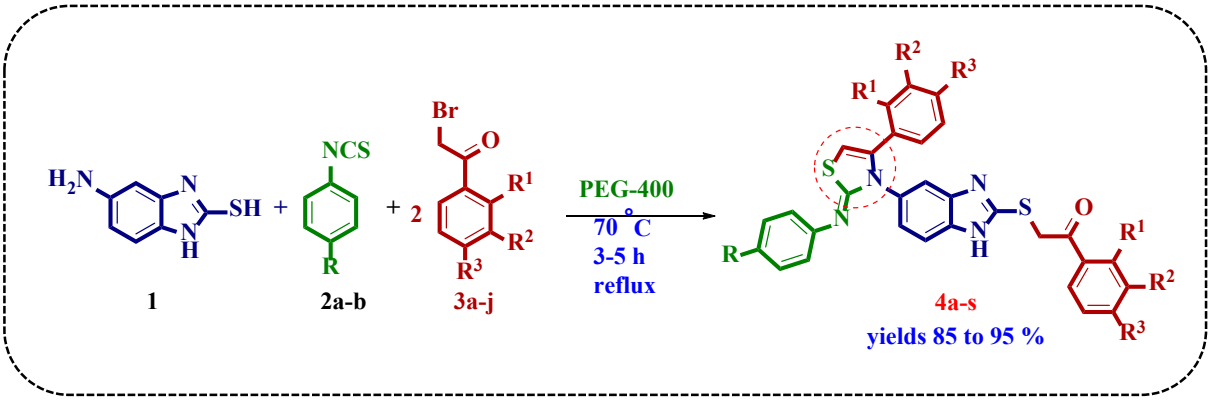

Chapter IVB explains a facile, pseudo-four-component synthesis of novel thiazolyl-benzimidazoles *via a* multi-component approach and their biological evaluation.

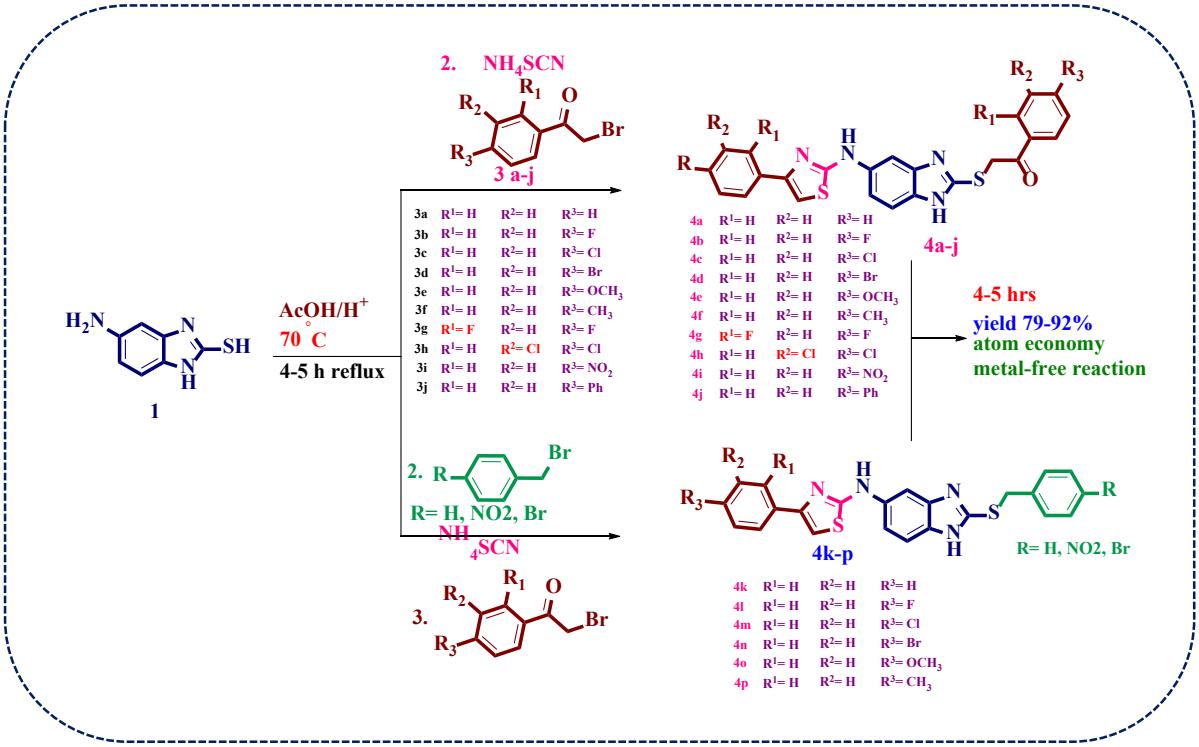

Chapter IVC described a facile, four-component synthesis of coumarin-based thiazoles *via* a multi-component approach and their anti-cancer activity.

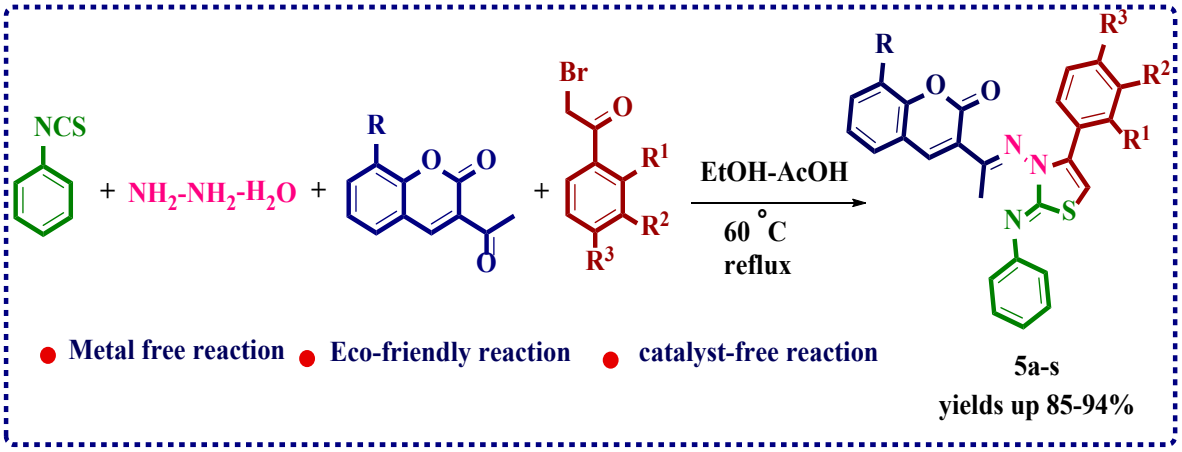

Chapter V comprises a synthesis of novel benzimidazole-based isoindoline-1,3-dione compounds and benzo[4,5]imidazoles and their antibacterial activity.

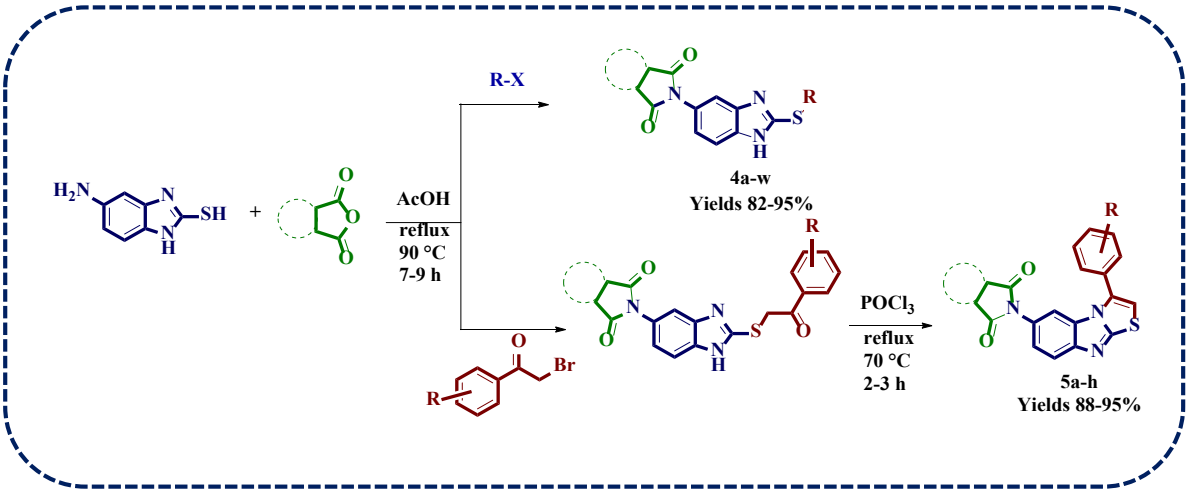

The current research program was undertaken to build new heterocyclic structural modification moieties on benzimidazoles and to evaluate their biological activities like anti-bacterial, anti-diabetic and anti-cancer activities. In this direction, we have designed and synthesized novel building blocks of benzimidazoles. The summary of our present study on 5-amino-2-mercapto-benzimidazole has been shown in the following figure.

Summary of the present work

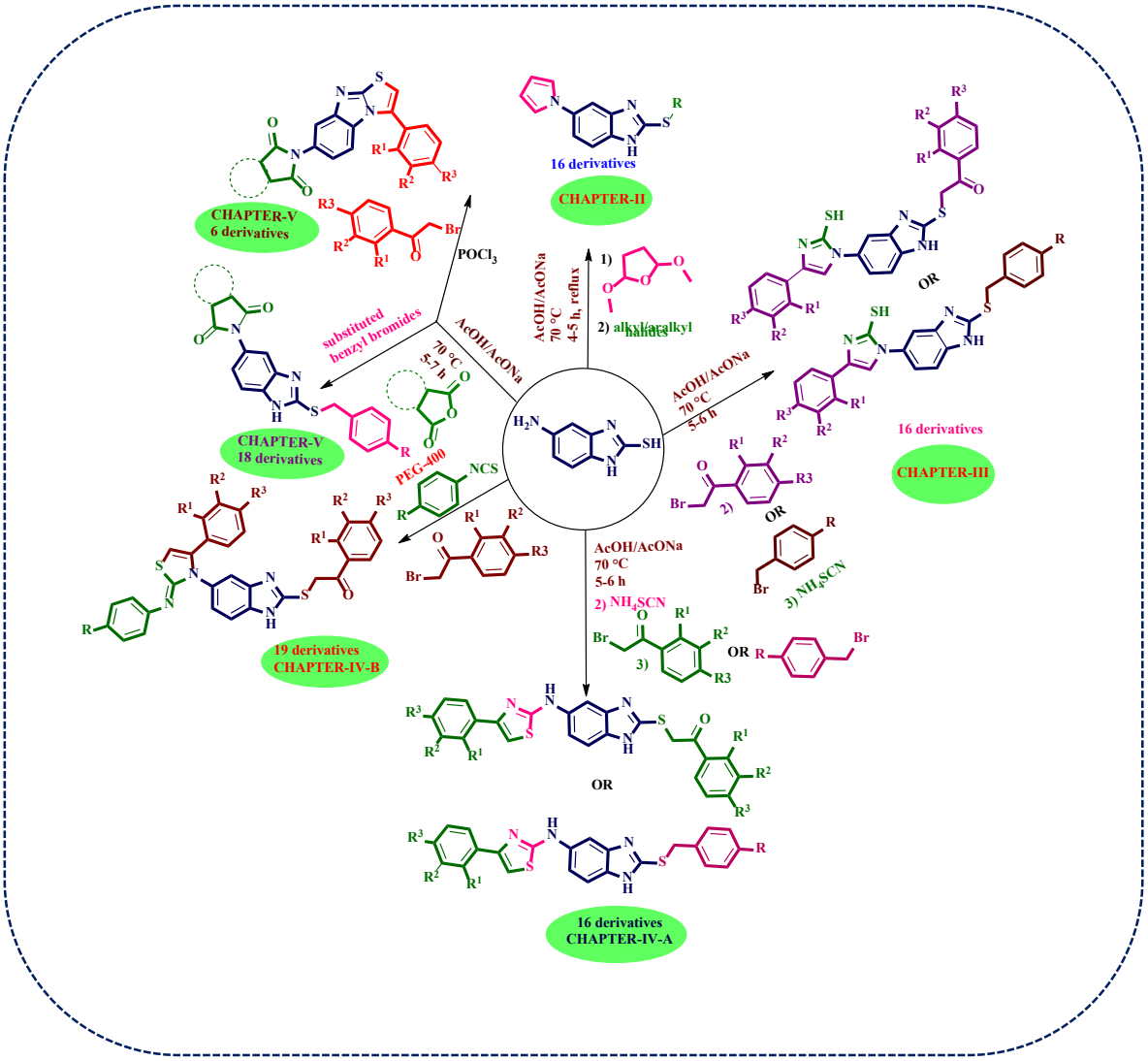

References

1. Walsh, P. J.; Li, H.; Anaya de Parrodi, C. *Chem. Rev.* **2007**, *107*, 2503–2545.
2. Maya, V.; Raj, M.; Singh, V. K. *Org. Lett.* **2007,** *9*, 2593–2595.
3. Mamidala, S.; Peddi, S. R.; Aravilli, R. K.; Jilloju, P. C.; Manga, V.; Vedula, R. R. *J. Mol. Struct.* **2021***,* 1225 .
4. Vila, C.; Rueping, M. *Green Chem.* **2013,** *15,* 2056–2059.
5. Chedupaka, R.; Papisetti, V.; Sangolkar, A. A.; Vedula, R. R. *Polycycl. Aromat. Compd.* **2021,** 1–15.
6. Jilloju, P.C.; Shyam, P.; Raju, C.; Vedula, R.R. *Polycycl. Aromat. Compd.* **2021**.
7. Vaarla, K.; Vishwapathi, V.; Vermeire, K.; Vedula, R. R.; Kulkarni, C. V. *J. Mol. Struct.* **2022**, *1249*, 131662.
8. Gu, Y. *Green Chem.* **2012**, *14*, 2091-2128.
9. Ruijter, E.; Orru, R. V. A. *Drug Discov. Today Technol.* **2013**, *10*, e15–e20.
10. Hulme, C.; Gore, V. *Curr. Med. Chem.* **2003**, *10*, 51–80.
11. Akritopoulou-Zanze, I. *Curr. Opin. Chem. Biol.* **2008**, *12*, 324–331.
12. Ulaczyk-Lesanko, A.; Hall, D. G. *Curr. Opin. Chem. Biol.* **2005**, *9*, 266–276.
13. Touré, B. B.; Hall, D. G. *Chem. Rev.* **2009**, *109*, 4439–4486.
14. Kakuchi, R. *Angew. Chemie Int. Ed.* **2014**, *53*, 46–48.
15. Zhang, Z.; Tan, Z.-B.; Hong, C.-Y.; Wu, D.-C.; You, Y.-Z. *Polym. Chem.* **2016**, *7*, 1468–1474.
16. Dong, R.; Chen, Q.; Cai, X.; Zhang, Q.; Liu, Z. *Polym. Chem.* **2020**, *11*, 5200–5206.
17. Zhang, J.; Zhang, M.; Du, F.-S.; Li, Z.-C. *Macromolecules* **2016**, *49*, 2592–2600.
18. Yang, L.; Zhang, Z.; Cheng, B.; You, Y.; Wu, D.; Hong, C. *Sci. China Chem.* **2015**, *58*, 1734–1740.
19. Jabusch, T. W.; Tjeerdema, R. S. *J. Agric. Food Chem.* **2006**, *54*, 5962–5967.
20. Gonzalez, M. A.; DGorman, D. B.; Hamilton, C. T.; Roth, G. A. *Org. Process Res. Dev.* **2008**, *12*, 301–303.
21. Sumesh, R. V.; Muthu, M.; Almansour, A. I.; Suresh Kumar, R.; Arumugam, N.; Athimoolam, S.; Jeya Yasmi Prabha, E. A.; Kumar, R. R. *ACS Comb. Sci.* **2016**, *18*, 262–270.
22. Kim, Y.-S.; Kwak, S. H.; Gong, Y.-D. *ACS Comb. Sci.* **2015**, *17*, 365–373.
23. Miller, S.L. *Science (80-).* **1953**, *117*, 528–529.
24. Strecker, A. *Ann. der Chemie und Pharm.* **1850**, *75*, 27–45.

25. Biginelli, P. *Berichte der Dtsch. Chem. Gesellschaft* **1891**, *24*, 1317–1319.
26. Mannich, C.; Krösche, W. *Arch. Pharm. (Weinheim).* **1912**, *250*, 647–667.
27. Passerini, M. *Gazz. Chim. Ital.* **1921**, *51*, 126–129.
28. IUgi, I.; R. Meyr, R. *Angew. Chemie* **1958**, *70*, 702–703.
29. Petasis, N. A.; Akritopoulou, I. *Tetrahedron Lett.* **1993**, *34*, 583–586.
30. Bon, R. S.; Hong, C.; Bouma, M. J.; Schmitz, R. F.; de Kanter, F J. J.; Lutz, M.; Spek, A. L.; Orru, R. V. A. *Org. Lett.* **2003**, *5*, 3759–3762.
31. Laurent, A.; Gerhardt, *Ann. der Pharm.* **1838**, *28*, 265–269.
32. Radziszewski, B. *Berichte der Dtsch. Chem. Gesellschaft* **1882**, *15*, 1493–1496.
33. Hantzsch, A. *Justus Liebig's Ann. der Chemie* **1882**, *215*, 1–82.
34. Hantzsch, A. *Berichte der Dtsch. Chem. Gesellschaft* **1890**, *23*, 1474–1476.
35. Bucherer, H. T.; Steiner, W. *J. fuer Prakt. Chemie* **1934**, *140*, 291–316.
36. Asinger, F. *Angew. Chemie* **1956**, *68*, 413–413.
37. Gewald, K.; Schinke, E.; Böttcher, H. *Chem. Ber.* **1966**, *99*, 94–100.
38. Larsen, S. D.; Grieco, P. A. *J. Am. Chem. Soc.* **1985**, *107*, 1768–1769.
39. Povarov, L S. *Russ. Chem. Rev.* **1967**, *36*, 656–670.
40. Cardellicchio, C.; Capozzi, M. A. M.; Naso, F. *Tetrahedron: Asymmetry* **2010**, *21*, 507–517.
41. Méndez, Y.; De Armas, G.; Pérez, I.; Rojas, T.; Valdés-Tresanco, M. E.; Izquierdo, M.; Alonso del Rivero, M.; Álvarez-Ginarte, Y.M.; Valiente, P.A.; Soto, C. et al., *Eur. J. Med. Chem.* **2019**, *163*, 481–499.
42. da Costa, E. P.; Coelho, S. E.; de Oliveira, A. H.; Araújo, R. M.; Cavalcanti, L. N.; Domingos, J. B.; Menezes, F. G. *Tetrahedron Lett.* **2018**, *59*, 3961–3964.
43. Koley, S.; Chowdhury, S.; Chanda, T.; Ramulu, B. J.; Singh, M. S. *Tetrahedron* **2013**, *69*, 8013–8018.
44. Mamidala, S.; Peddi, S. R.; Aravilli, R. K.; Jilloju, P. C.; Manga, V.; Vedula. R. R. *J. Mol. Struct.* **2021**, 1225, 129114.
45. Tabassum, S.; Govindaraju, S.; Khan R. R.; Pasha. M. A. *RSC Adv.,* **2016**, 6, 29802.
46. Nandaluru, P. R.; Bodwell, G. J. *Org. Lett.* **2012**, *14*, 310–313.
47. Chaplin, J. H.; Flynn, B. L. *Chem. Commun.* **2001**, *1*, 1594–1595.
48. Powell, D. A.; Batey, R. A. *Org. Lett.* **2002**, *4*, 2913–2916.
49. Foley, P.; Eghbali, N.; Anastas, P. T. *J. Nat. Prod.* **2010**, *73*, 811–813.
50. Ugi, I.; Wischhöfer, E. *Chem. Ber.* **1962**, *95*, 136–140.

51. Rossen, K.; Pye, P. J.; DiMichele, L. M.; Volante, R. P.; Reider, P. J. *Tetrahedron Lett.* **1998**, *39*, 6823–6826.
52. Musonda, C. C.; Gut, J.; Rosenthal, P. J.; Yardley, V.; R. Carvalho de Souza, R. C.; Chibale, K. *Bioorg. Med. Chem.* **2006**, *14*, 5605–5615.
53. Ramiro, E. *Guix d'infantil, núm.* **2011**, *60*, 33–36.
54. Slobbe, P.; Ruijter, E.; Orru, R. V. A. *Medchemcomm.* **2012**, *3*, 1189.
55. Liao, J.; Wang, J.; Liu, Z.; Ye Z. *ACS Appl. Energy Mater.* **2019**, *2,* 6732-6740.
56. Zhang, F. M.; Dong, L. Z.; Qin, J. S. *et al*. *J. Am. Chem. Soc.* **2017**, *139*, 6183-6189.
57. Padhy, A. K.; Chetia, B.; Mishra, S.; Pati, A.; Iyer P. K. *Tetrahedron Lett*. **2010**, *51*, 2751-2753.
58. Ng, V. W. L,; Tan, J. P. K.; Leong, J.; Voo, Z. X.; Hedrick, J. L.; Yang, Y. Y. *Macromolecules*. **2014**, *47*, 1285-1291.
59. Hobrecker, F.; Ber.**1872,** *6,* 920-923.
60. Stringer, A.; Wright, M. A. *Pest. Sci*. **1976**, *7,* 459–464.
61. Radziszewski, B. *Chem. Ber.* **1882**, *15,* 1493-1496.
62. Sun, H.; Ansari, MF.; Fang, B.; Zhou, C. H. *J. Agric. Food. Chem*. **2021**, *69*, 7831-7840.
63. Malasala, S.; Ahmad, M. N.; Akunuri, R.; *et al*. *Eur. J. Med. Chem.* **2021**, *212*, 112996. Dokla, E. M. E.; Abutaleb, N. S.; Milik, S. N.; *et al*. *Eur. J. Med. Chem.* **2020,** *186*, 111850.
64. Dokla, E. M. E.; Abutaleb, N. S.; Milik, S. N.; *et al*. *Eur J Med Chem.* **2020**, *186*, 111850.
65. Desai, N. C.; Shihory, N. R.; Kotadiya, G. M.; Desai, P. *Eur. J. Med. Chem*. **2014**, *82*, 480-489.
66. Cheong, J. E.; Zaffagni, M.; Chung, I.; *et al*. *Eur. J. Med. Chem.* **2018**, *144*, 372-385.
67. Ali, I.; Lone, M. N.; Aboul-Enein, H. Y. *Med. Chem. Comm*. **2017**, *8*, 1742-1773.
68. Refaat, H. M. *Eur. J. Med. Chem*. **2010**, *45*, 2949-2956.
69. Bai Y, Bin.; Zhang, A. L.; Tang, J. J.; Gao, J. M. *J. Agric. Food. Chem*. **2013**, *61*, 2789-2795.
70. Yang, W-C.; Li, J.; Li, J.; Chen, Q.; Yang, G-F. *Bioorg. Med. Chem. Lett*. 2012, *22*, 1455-1458.
71. Akande, A. A.; Salar, U.; Khan, K. M.; *et al*. *ACS Omega*. **2021**, *6*, 22726–22739.
72. Sharma, R.; Bali, A.; Chaudhari, B. B. *Bioorg. Med. Chem. Lett*. **2017**, *27*, 3007-3013.
73. Chen, G.; Liu, Z.; Zhang, Y.; *et al*. *ACS Med. Chem. Lett*. **2013**, *4*, 69-74.

74. Cornec, A. S.; Monti, L.; Kovalevich, J.; *et al*. *J. Med. Chem.* **2017**, *60*, 5120-5145.
75. Cheng, D.; Han, D.; Gao, W.; *et al*. *Bioorganic. Med. Chem. Lett*. **2012**, *22*, 6573-6576.
76. Leshabane, M.; Dziwornu, G. A.; Coertzen, D.; *et al*. *ACS Infect. Dis.* **2021**, *7*, 1945-1955.
77. Xiao, M.; Ahn, S.; Wang, J.; *et al*. *J. Med. Chem.* **2013**, *56*, 3318-3329.
78. Kankala, S.; Kankala, R. K.; Gundepaka, P.; Thota, N.; Nerella, S.; Gangula, M. R.; Guguloth, H.; Kagga, M.; Vadde, R.; Vasam, C. S. *Bioorg. Med. Chem. Lett.* **2013**, *23* (5), 1306–1309.
79. Ramla, M. M.; Omar, M. A.; Tokuda, H.; El-Diwani, H. I. *Bioorganic Med. Chem.* **2007**, *15* (19), 6489–6496.
80. Cruz-Gonzalez, D. Y.; González-Olvera, R.; Angeles-Beltrán, D.; Negrón-Silva, G. E.; Santillan, R. *Synth.* **2013**, *45* (23), 3281–3287.
81. Abdel-Aziz, H. A.; Ghabbour, H. A.; Eldehna, W. M.; Al-Rashood, S. T. A.; Al-Rashood, K. A.; Fun, H.-K.; Al-Tahhan, M.; Al-Dhfyan, A. *Eur. J. Med. Chem.* **2015**, *104*, 1–10.
82. Saini, R.; Malladi, S. R.; Dharavath, N. *J. Heterocycl. Chem.* **2018**, *55* (7), 1579–1588.
83. Kumar, R. V.; Gopal, K. R.; Seshu Kumar, K. V. S. R. *J. Heterocycl. Chem.* **2005**, *42*, 1405–1408.
84. Madsen, P.; Knudsen, L. B.; Wiberg, F. C.; Carr, R. D. *Receptor.* **1998**, 5150–5157.
85. Zhang, S. B.; Liu, X.; Gao, M. Y.; Dong, Z. B. *J. Org. Chem.* **2018**, *83* , 14933–14941.
86. Anisetti, R.; Srinivas Reddy, M. *J. Sulfur Chem.* **2012**, *33*, 363–372.
87. Malladi, S. R.; Anisetti, R.; Rao, P. R. *Indian J. Pharm. Sci.* **2014**, *76*, 510–518.

CHAPTER-II

Synthesis of benzimidazole linked pyrrole derivatives by MCR approach and their molecular docking studies

CHAPTER-II

SYNTHESIS OF BENZIMIDAZOLE LINKED PYRROLE DERIVATIVES BY MCR APPROACH AND THEIR MOLECULAR DOCKING STUDIES

2.1. Introduction

Nitrogen heterocycles are of special interest because they constitute an important class of natural and synthetic products, many of them which exhibit useful biological activities. The synthesis of nitrogen-containing heterocyclic compounds and their derivatives plays an important role in organic chemistry as they frequently exhibit therapeutic and pharmacological properties. They have emerged as an integral backbone of several existing drugs. Studies reveal that the incorporation of a pyrrole moiety into various heterocyclic ring systems results in useful molecules from the pharmacological point of view [1-3].

Pyrrole is a major class of five-membered heteroaromatic cyclic compounds containing nitrogen hetero atoms in the cyclic ring system with molecular formula C_4H_5N. Pyrrole manifests different resonance structures by the delocalization of nitrogen lone pairs of electrons in the ring system (**Figure 2.1**). Due to the delocalization of lone pair of electrons on nitrogen, the basicity of pyrrole showed lower than amines and other aromatic compounds containing pyridine moiety.

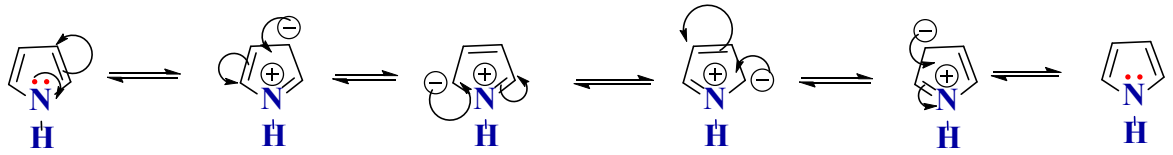

Figure 2.1. Different resonance forms of pyrrole

Moreover, the –NH, and –CH protons of pyrrole moiety exhibit a moderately acidic nature and they can be deprotonated by strong bases and which makes the pyrrole ring a nucleophile. Pyrroles are contemplated as a cyclic scaffold of 1,4- di carbonyl compounds with primary amines. This fundamental moiety is present in a large number of chemical, therapeutic agents, and natural products as well as in bio-molecular structures like hemoglobin, chlorophyll, myoglobin, vitamin B12, cytochromes, and bile pigments like bilirubin and biliverdin. etc. Since it was first detected by F.F. Runge in 1834 as a constituent of coal tar. Further, in 1857 it was isolated from the pyrolysate of bone. Its name pyrrole originated from the Greek word ‘pyrrols’ meaning fiery from its reaction imparting red colour to wood when moistened with HCl. Haemin was the first pyrrole-containing molecule, which is synthesized by E. Fisher in 1929. Furthermore, developing synthetic methodologies towards the construction of pyrrole

scaffolds is always of considerable interest to synthetic chemists and has led to several classical methods like Hantzsch pyrrole synthesis [4], Knorr pyrrole synthesis [5], Paal-Knorr pyrrole synthesis [6], Van-Luesen reaction [7], Barton-Zard reaction [8] , and Piloty-Robinson synthesis [9], etc. As well known, the Paal-Knorr pyrrole synthesis is one of the most commonly used methods for the construction of polysubstituted pyrrole by utilizing 1,4 dicarbonyl compound and primary amines.

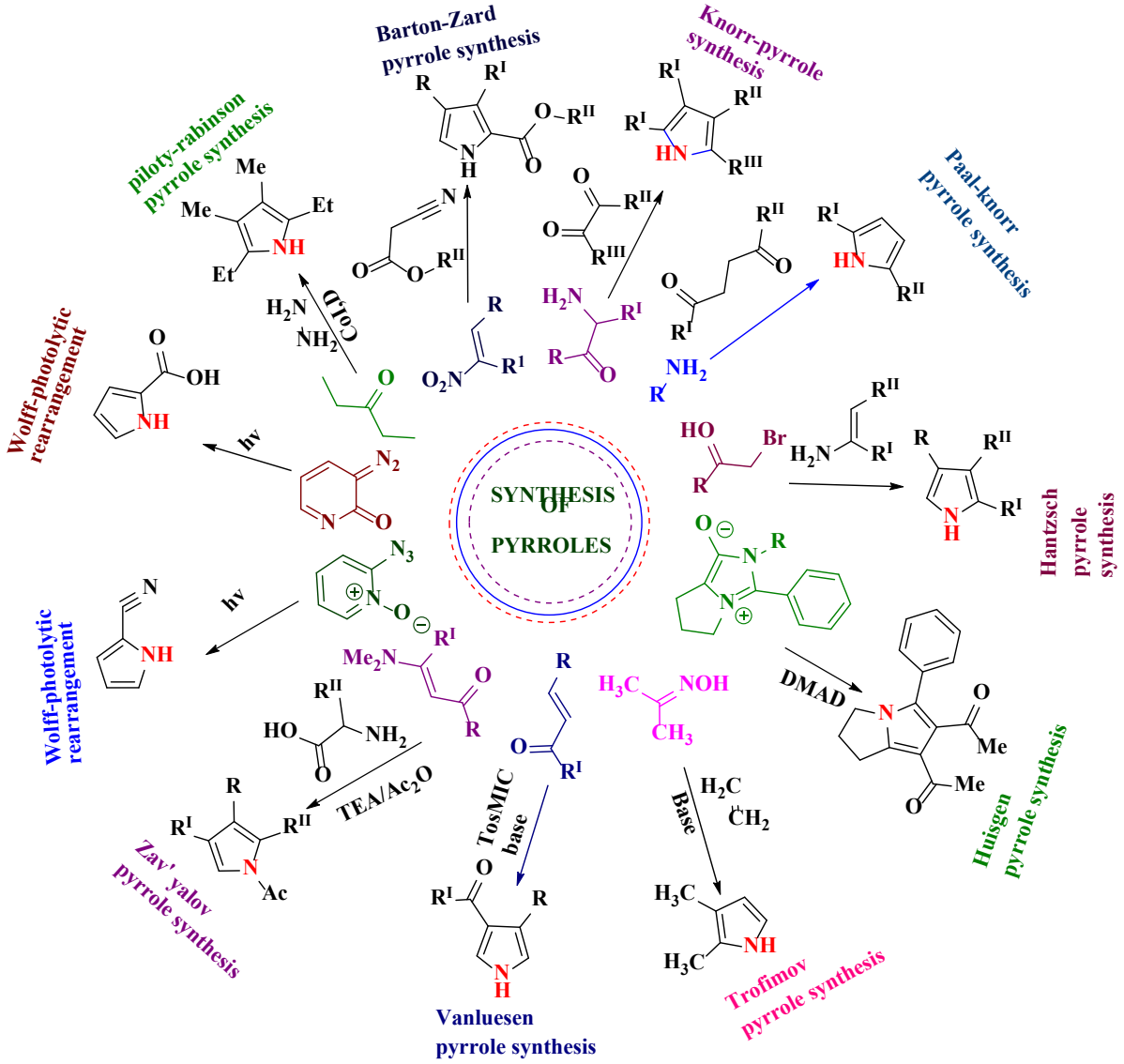

Figure 2.2. An overview of Different methods for the synthesis of the pyrrole molecule

A wide variety of biologically active compounds have pyrrole as a core pharmacophore unit and several drug molecules contain pyrrole as a principle unit as depicted in **Figure 2.3**. Pyrrole moiety has attracted a profound interest due to their anti-oxidant [10,11], anti-inflammatory [12-14], anti-cancer [15-19], anti-depressant [20], anti-virus [21], anti-hypertensive [22], anti-malarial [23], anti-diabetic [24], anti-microbial [25-27], HMG-CoA reductase inhibitors [28], CB_2 receptor

antagonists [29], also used as co-oxygenase inhibitors [30-31], JAK-2 inhibitors [32] also used in the application of bio-sensors [33] and neuroprotective agents [34]. Pyrroles are also used as corrosion inhibitors [35] and as a solvent for resins [36]. Some of the biologically active drugs containing pyrrole units are listed in **Figure 2.2**.

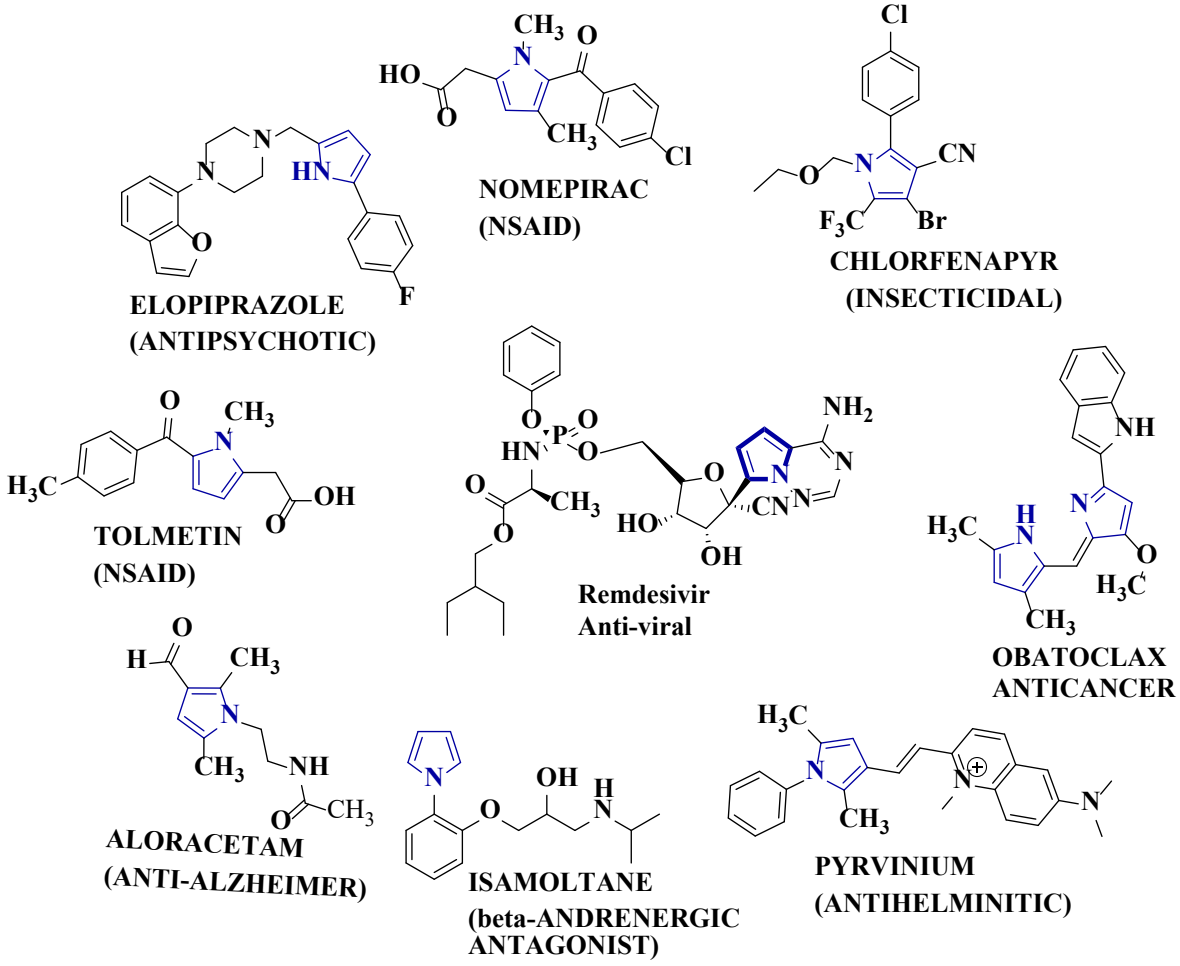

Figure 2.3. Marketing drugs containing pyrrole moiety

Hantzsch [37] ***et al.*** reported the first multi-component synthesis of pyrroles from an equimolar mixture of chloroacetone, and acetoacetic ester under reflux in concentrated aqueous ammonia.

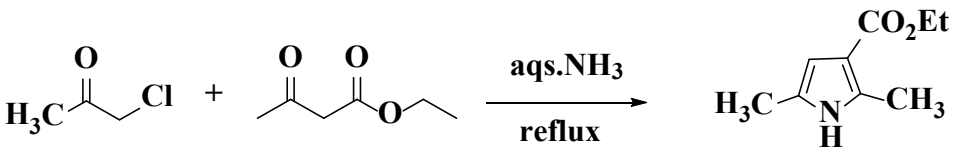

Scheme 2.1. The first multi-component pyrrole synthesis

Liu [38] ***et al.*** described a new approach for the synthesis of pyrrole derivatives based on this hit compound. Further, they synthesized compounds and were evaluated for *in-vitro* studies

against ClpP1P2 peptidase and anti-tubercular activities were explored. Among the tested compounds some of the compounds exhibited $MtbH_{37}$ Ra.

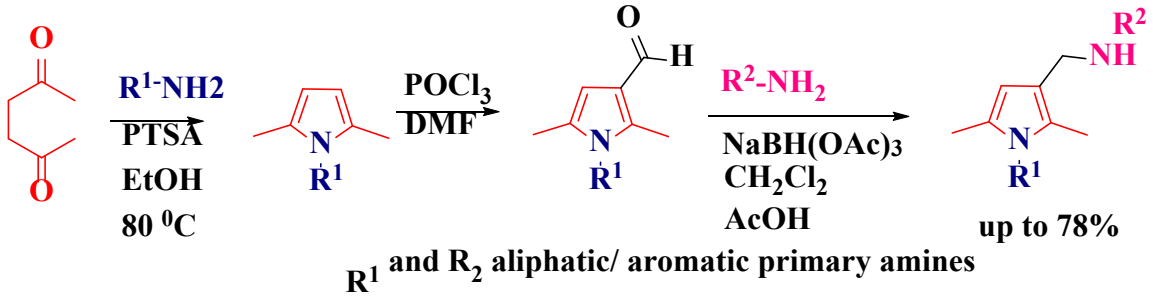

Scheme 2.2a. 2,3,5-Trisubstituted pyrrole compounds

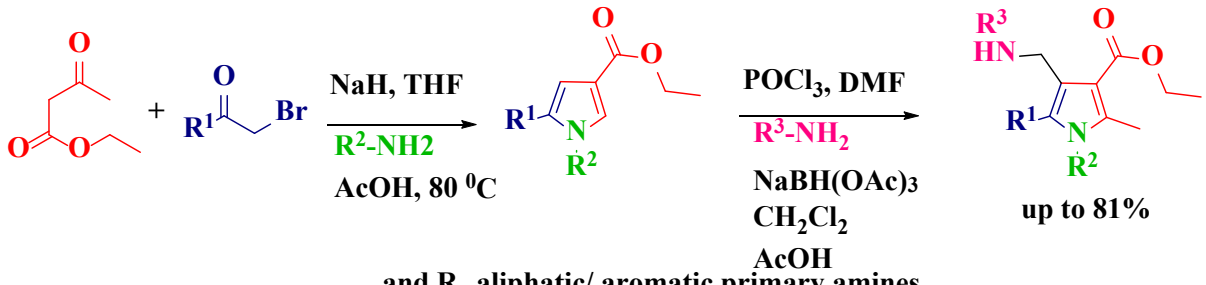

Scheme 2.2b. Tetra substituted pyrrole compounds

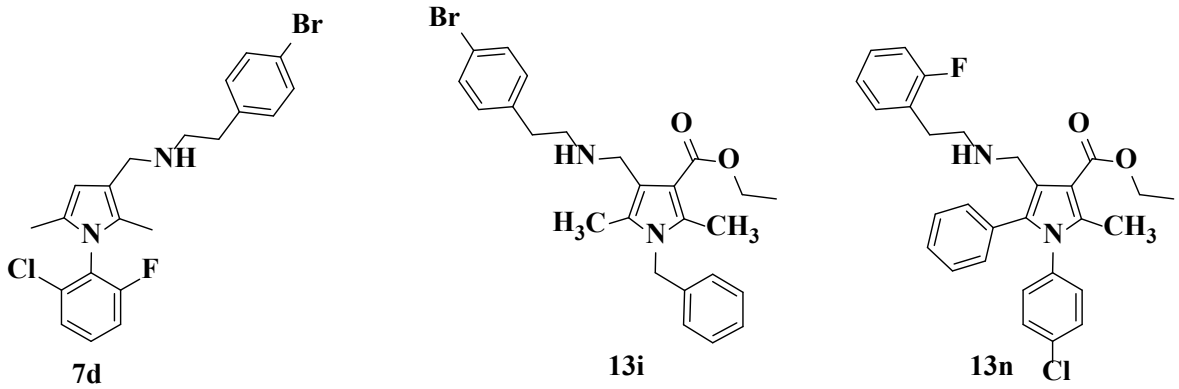

Figure 2.4. Biologically potent compounds

Bortolozzi [39] ***et al***. reported a new series of pyrrole moiety interposed between the two aryl rings by a palladium-mediated coupling approach and evaluated for their anti-proliferative activity against the CA-4 resistant HT-29 cells. Among the tested compounds some of them showed maximal anti-proliferative activity.

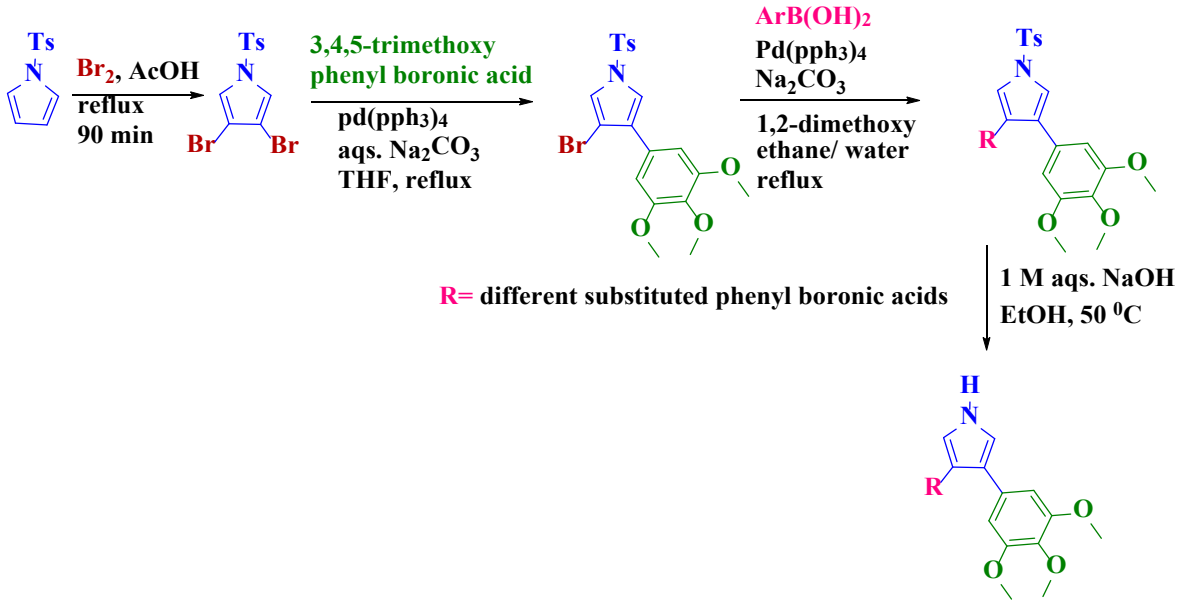

Scheme 2.3. 2,4-di aryl interposed pyrrole derivatives

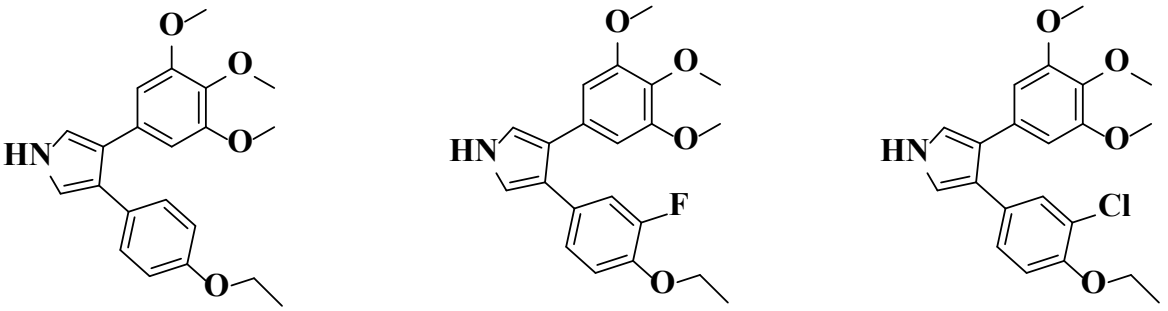

11i **11j** **11k**

Figure 2.5. Compounds showed anti-proliferative activity

Pagadala [40] ***et al.*** reported an efficient method for the synthesis of novel tetra-substituted pyrrolyl-N-acetic acid and acetamide scaffolds through the coupling of 1,4-di-ketones with different substituted amino acids following Paal-Knorr's approach. For this reaction, 1,4-di-ketones were prepared through the hydroacylation of α, β- unsaturated ketones with aromatic or heterocyclic aldehydes in ethanol using 20 mol% of bis-thiazolium salt in the presence of triethyl amine. Furthermore, the synthesized compounds were evaluated for anti-mycobacterial activity against *mycobacterium smegmatis* and *mycobacterium tuberculosis* strain H37Rv. Compounds **5n, 5q,** and **5r** showed excellent activity.

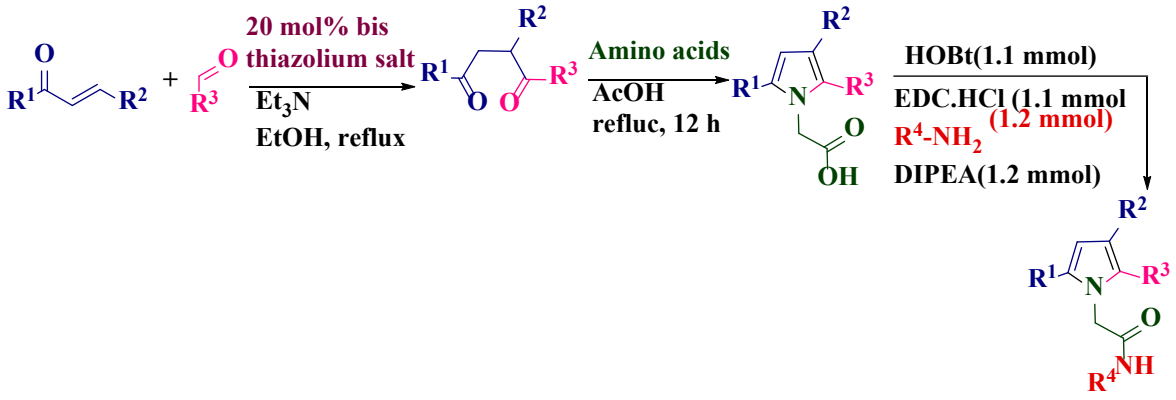

Scheme 2.4. Synthesis of tetra-substituted pyrrolyl-N-acetic acid and acetamide scaffolds

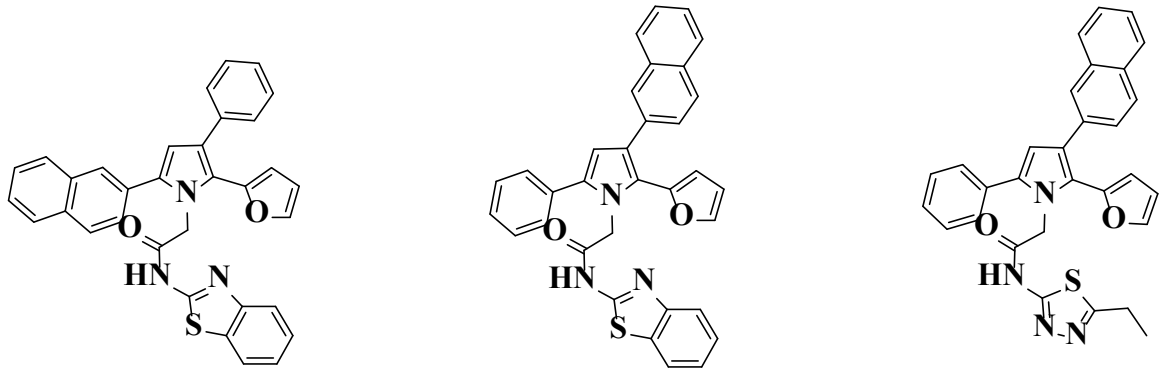

5n **5q** **5r**

Figure 2.7. Anti-mycobacterial compounds

Zhao [41] ***et al.*** developed an efficient one-pot reaction for the synthesis of tetra-substituted pyrroles through an intra-inter molecular reaction of strained azirines with 1,3-di carbonyl compounds involving nucleophilic addition to the C=N bond and ring opening of the aziridine ring through nickel- catalyzed [3+2] cycloaddition.

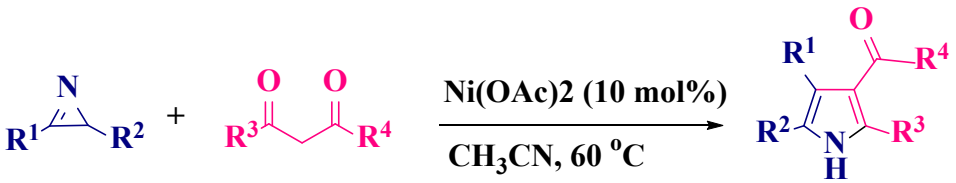

up to 98% yield

Scheme 2.5. Transition-metal catalyzed synthesis of pyrroles from 2*H*- azirines

Nageswar [42] ***et al*** synthesized an efficient, simple, economically viable, and environmentally friendly methodology for the synthesis of N-substituted pyrroles in excellent yields from

appropriate amounts of different substituted aromatic amines and 2,5-dimethoxytetrahydrofuran *via* Paal-Knorr's reaction method under neat reaction conditions.

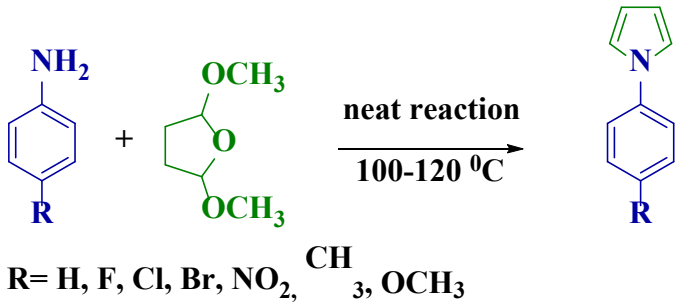

Scheme 2.6. One-pot synthesis of N-substituted pyrroles under catalyst and solvent-free conditions

Sarkar [43] ***et al.*** has been reported an efficient, one-pot, three components, Fe(III) catalyzed coupling synthesis of tri and tetra substituted N-aryl pyrroles *via* tandem amination/ Michael/ cycloisomerization reaction. The title compounds were synthesized from acetylacetone, β-nitro styrene, and different substituted aromatic primary amines in anhydrous $FeCl_3$ and nitromethane as solvent giving the title compounds with good yields scheme (2.13).

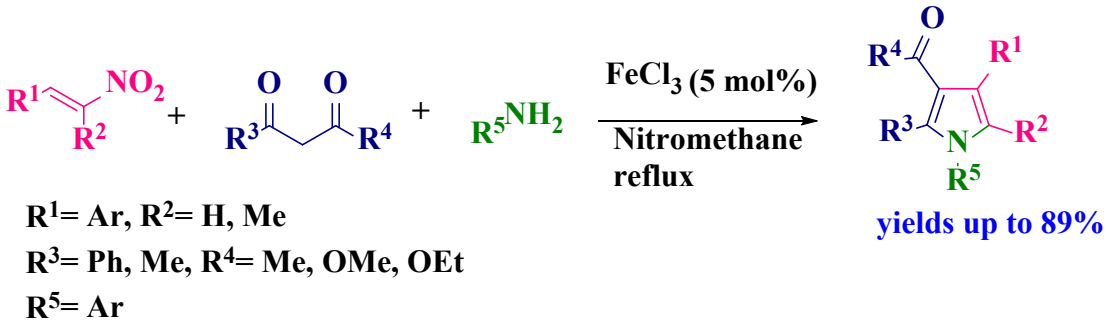

Scheme 2.7. One-pot three-component synthesis of tri and tetra substituted *N*-aryl pyrroles

Balu Atar [44] ***et al.*** synthesized a series of new tetra-substituted pyrroles derivatives *via* greener and one-pot three components coupling reactions. The title compounds were synthesized using primary amines, di-alkyl acetylene dicarboxylate, and β-nitro styrene using imidazolium Bronsted acidic ionic liquids as a catalyst as well as solvent (scheme-2.12).

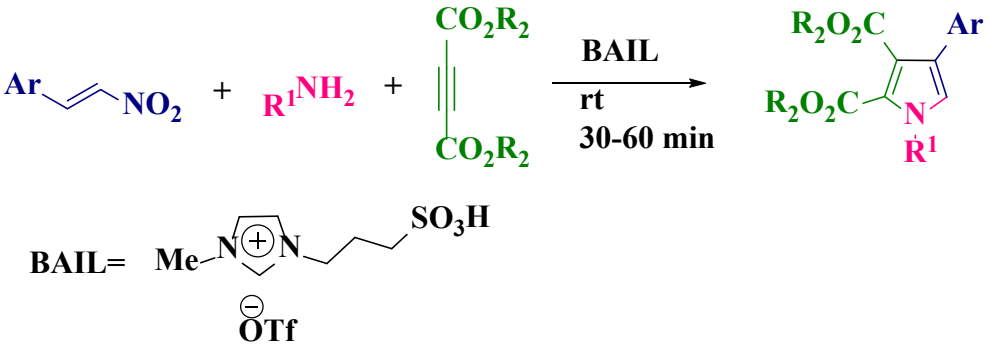

Scheme 2.8. One-pot three-component synthesis of tetra substituted N-substituted pyrroles

Das [45] ***et al.*** reported a one-pot three-component synthesis of pyrroles from primary amines, 2,4-pentanedione, and 3(2-Bromo acetyl) coumarin gave good to excellent yields in 15% of alum and a mixture of PEG-400 and water in 3:2 ratios.

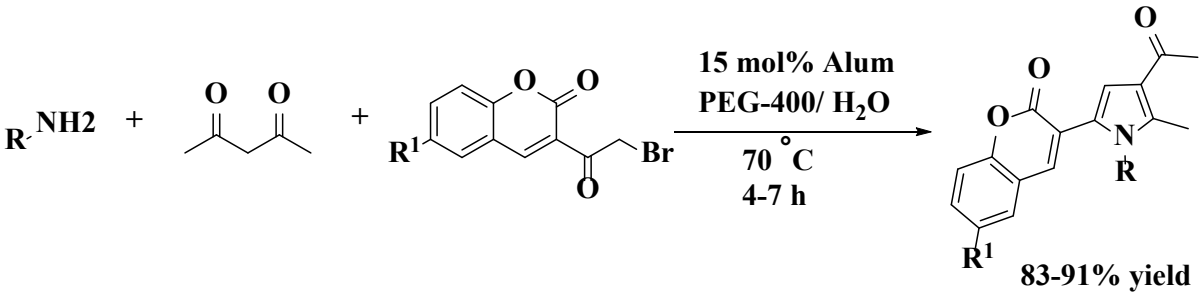

Scheme 2.9. Alum-promoted one-pot three-component pyrrole synthesis in polyethylene glycol-water

Meshram [46] ***et al.*** synthesized a one-pot three-component base catalyzed tetra substituted pyrroles by using α-Bromo acetophenones, 2,4-pentanedione, and primary amines in presence of organic base DABCO (1,4-diazobicyclo [2,2,2] octane as the catalyst and water as the reaction medium.

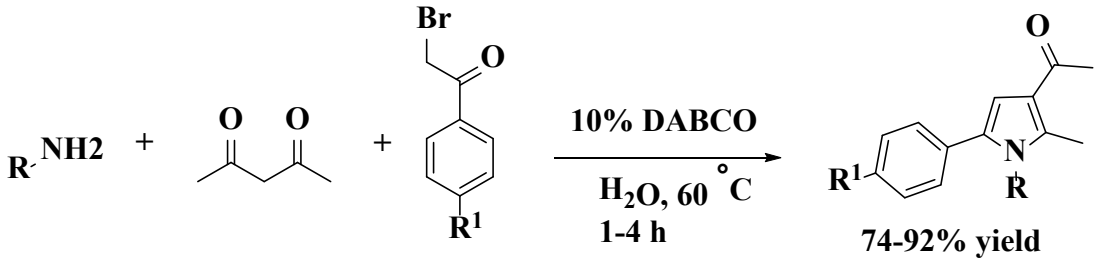

Scheme 2.10. One-pot three-component base catalyzed pyrrole synthesis in water

Trivedi [47] and co-workers developed a catalyst and solvent-free one-pot three-component reaction for the regioselective synthesis of poly-substituted pyrroles using β-hydroxy ketones, ammonium acetate, and 1,3-di-carbonyl compounds.

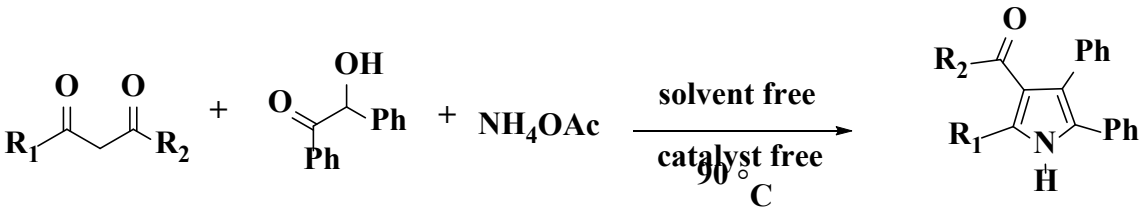

Scheme 2.11. One-pot three-component synthesis of 2,3,4,5 tetra substituted pyrroles

Wang and Dömling [48] *et al.* an efficient one-pot three-component synthesis of 2-amino-5-keto aryl pyrrole scaffolds by using a mixture of N-protected α-amino acetophenones, aromatic aldehydes, and malononitrile, cyano acetic acid or cyanoacetamide in trifluoroethanol as solvent and triethylamine as a base under reflux to give a good yield of the product.

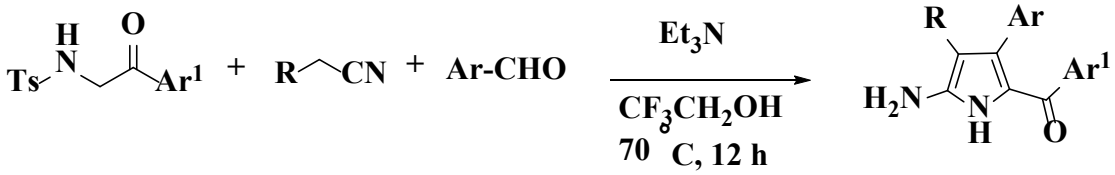

Scheme 2.12. Dömling's one-pot three-component synthesis of 2-acyl pyrroles

Lei [49] and co-workers synthesized polysubstituted pyrroles from primary amines, aldehydes, or ketones by the electro-oxidative annulation method.

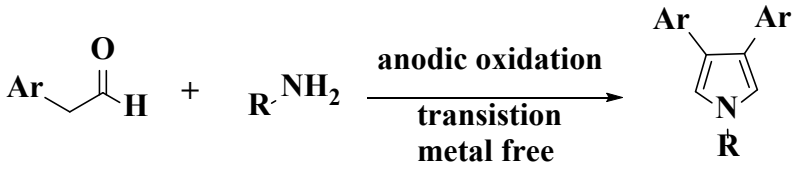

Scheme 2.13. One-pot electrochemical synthesis of pyrrole derivatives

Wang [50] *et al.* reported a one-pot four-component synthesis of 1,2,3,5-tetrasubstituted pyrroles by using primary amines, ethyl glyoxylate, and two equivalents of 2-bromoacetophenones in presence of acetonitrile as solvent and pyridine as a base catalyst. This formation involves the creation of four bonds by the assembly of [2+1+1+1] atom fragments.

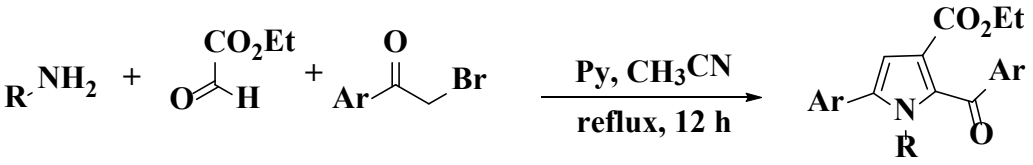

Scheme 2.14. One-pot four-component synthesis of 2-acyl pyrroles

Tran [51] ***et al.*** developed a green and efficient method for the synthesis of N-substituted pyrroles using primary amines, and acetonyl acetone in deep eutectic solvent ([CholineCl] $[ZnCl_2]_3$) under ultrasound irradiation method gave yields up to 99% in a short reaction time.

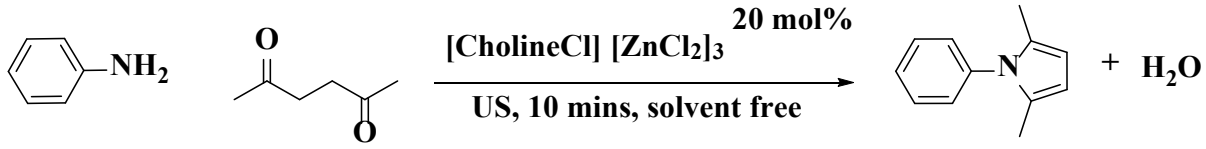

Scheme 2.15. One-pot synthesis of N-substituted pyrroles

Kim [52] ***et al.*** developed indium-mediated, reductive heterocyclization of di-nitrobenzene with 1,4-diketones in presence of indium-acetic acid and resulted in the formation of 2,5-di-substituted pyrroles.

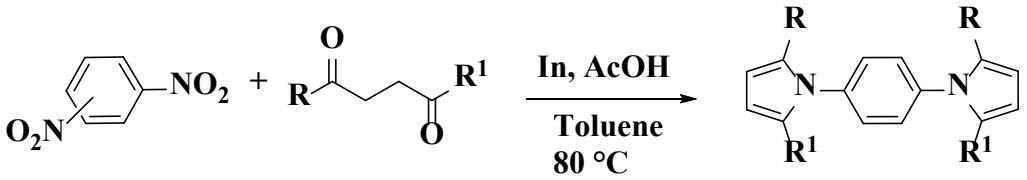

Scheme 2.16. One-pot indium-mediated reductive synthesis of pyrroles

Konkala [53] ***et al.*** has been developed an elegant, mild, and straightforward reaction method for the synthesis of poly-functional pyrroles *via* a one-pot four-component method using aromatic aldehydes, primary amines, 2,4-diketones, and nitro alkanes in β-cyclodextrins as a catalyst in the aqueous medium.

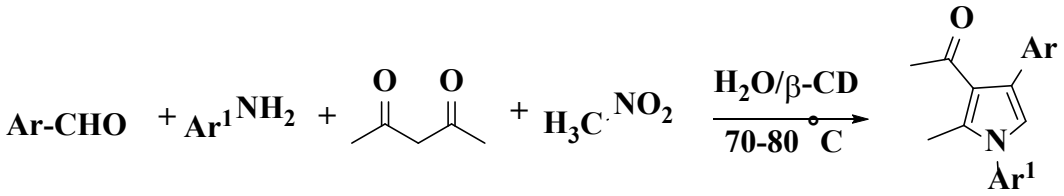

Scheme 2.17. One-pot four-component synthesis of pyrroles

Naeimi [54] and co-workers synthesized various N-substituted pyrroles by using primary amines and 2,5-dimethoxy tetrahydrofuran in water and multi-walled carbon nanotubes (MWCNTs) as a catalyst.

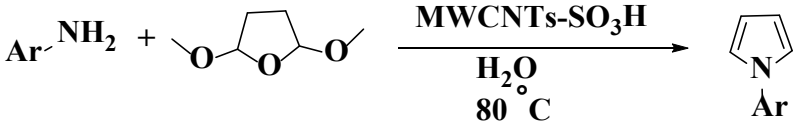

Scheme 2.18. One-pot synthesis of various N-aryl pyrroles

Goyal [55] *et al.* has been developed a zirconocene dichloride catalyzed one-pot three-component synthesis of pyrroles using primary amines, β-di carbonyl compounds, and nitro alkenes through the nitroalkane-enamine process in ethanol as solvent.

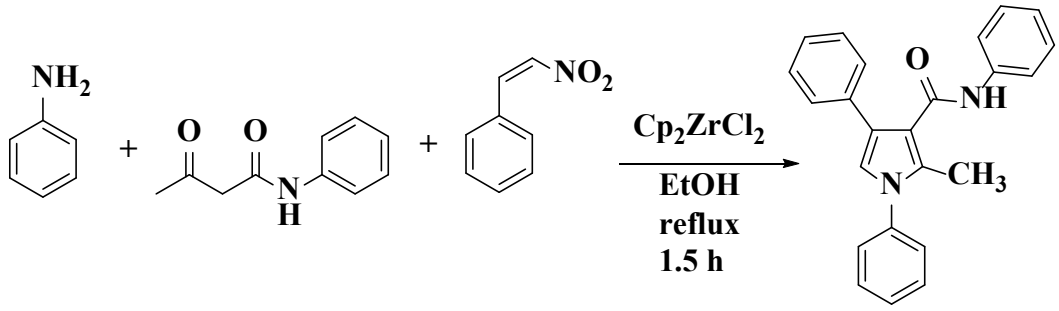

Scheme 2.19. Cp_2ZrCl2 catalyzed one-pot three-component synthesis of *N*-substituted pyrroles

Zhang [56] *et al.* synthesized N-substituted pyrroles from nitro compounds and 2,5 hexadione via one-pot synthesis using heterogeneous cobalt Co-Nx/C-800-AT as a catalyst followed by Paal-knorr condensation process. In this reaction, formic acid acts as both catalysts and served as a hydrogen donor for nitro to amine transformation.

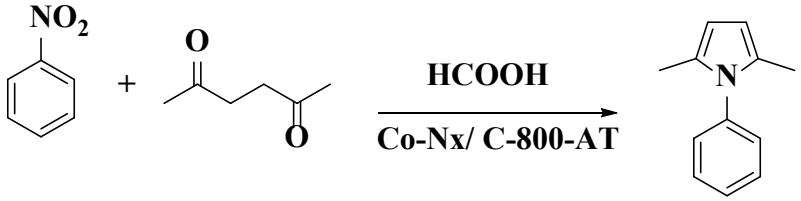

Scheme 2.20. One-pot hetero-cyclization of nitro-compounds to pyrroles

Mendes [57] *et al.* synthesized 1,2,3,4 tetra substituted pyrroles *via* a one-pot four-component reaction using aromatic aldehydes, nitro alkanes, 2,4-diketones, and primary amines in presence of ionic liquid $[NMPH]CH_3SO_3$ as green reaction medium.

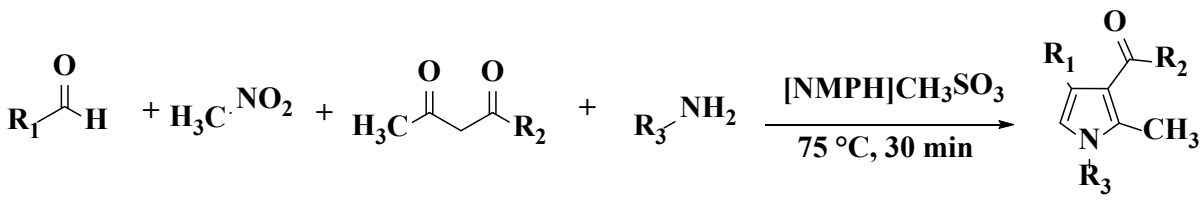

Scheme 2.21. One-pot four-component synthesis of tetra-substituted pyrroles

Xu [58] ***et al.*** developed a one-pot three-component copper/manganese co-catalyzed hetrocyclization of aryl amines with styrene and acetone via Paal-Knorr type of condensation to give 2-methyl 1,5-diaromatic-1*H*-pyrroles.

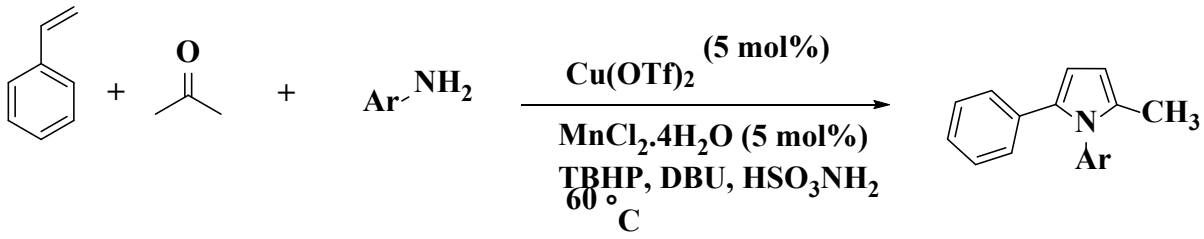

Scheme 2.22. One-pot three-component synthesis of 2-methyl-1,5-di aromatic 1*H*-pyrrole

Bharate [59] ***et al***. has been reported an efficient and eco-friendly one-pot four-component clay-catalyzed synthesis of functionalized pyrroles from amines, aldehydes, 1,3-dicarbonyl compounds, and nitro alkanes in good yields.

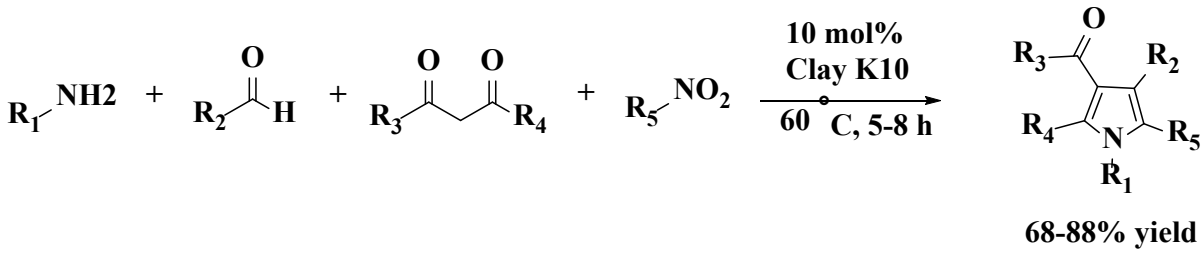

Scheme 2.23. One-pot four-component montmorillonite clay catalyzed synthesis of pyrroles

2.2. Present work

Because of the importance of pyrroles and benzimidazole moieties and their biological activities, we have taken up the synthesis of synthesis of 2-alkyl thio-5-(1*H*-pyrrol-1-yl)-1*H*-benzo[*d*]imidazoles.

2.2.1. Starting materials: In this chapter, the synthesis of new pyrrole and thioether scaffolds was described. The starting materials for the synthesis of the target compounds are 5-amino-2-

mercaptobenzimidazole, 2,5-di-methoxytetrahydrofuran, and different substituted alkyl/aralkyl halides. All these compounds were procured from commercial sources.

2.3. Synthesis of pyrrole derivatives

The synthesis of thioalkylated benzimidazole-linked pyrrole analogues was carried as outlined in **Scheme 2.1.** The title compounds (4a-p) were synthesized by a combination of 5-amino-2-mercaptobenzimidazole (**1**), 2,5-dimethoxytetrahydrofuran (**2**), and substituted aralkyl/ aliphatic halides (**3**) in presence of glacial acetic acid as solvent and fused sodium acetate as a base at 70 ºC gives with good to excellent yields.

The current part explains the synthesis of S-alkylated/aryl alkylated benzimidazole–linked pyrrole **(4a-p)** derivatives by a one-step three-component process. The specialty of this reaction is the simultaneous formation of two N-C and one C-S bond are formed. The experimental procedure involves heating an equimolar amount of 5-amino-2-mercaptobenzimidazole, 2,5 dimethoxytetrahydrofuran, and alkyl/aryl alkyl halides in acetic acid and sodium acetate.

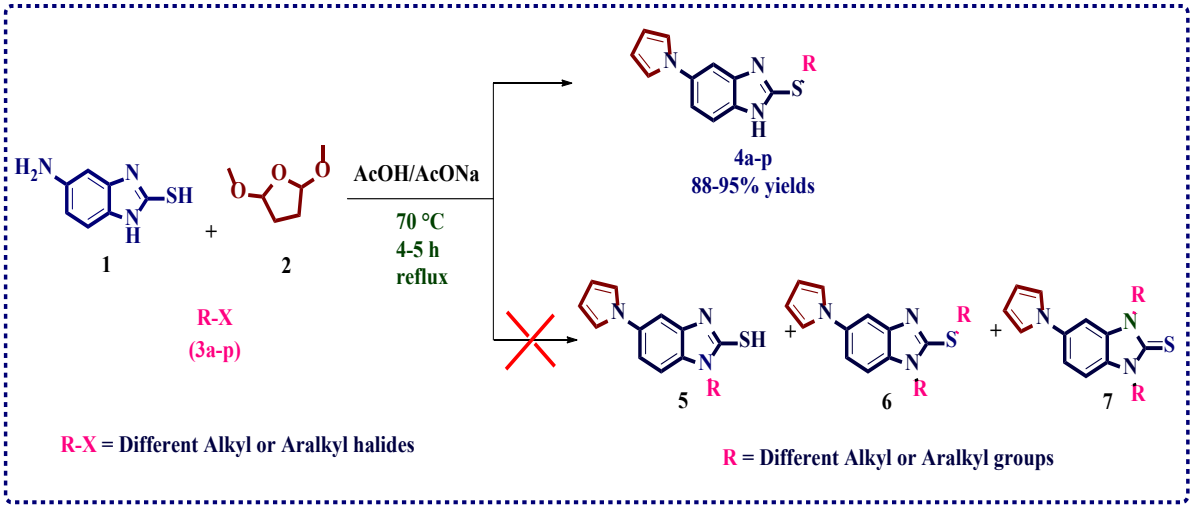

Scheme 2.1. Synthesis of 2-(alkyl/ aralkythio-5-(1*H*-pyrrol-1-yl)-1*H*-benzo[*d*]imidazoles (**4a-p**)

2.4. Results and discussion

To find the optimized conditions for the above three-component reaction, the test reaction was carried out with 5-amino-2-mercaptobenzimidazole (1.0 mmol), 2,5-dimethoxy tetrahydrofuran (1.0 mmol), and alkyl/aryl alkyl halides (1.0 mmol) as starting materials in different solvents like H_2O, CH_3CN, DMF, Toulene, MeOH, EtOH, and acetic acid respectively at temperature 60 °C (**Table 2.1**). Among the tested solvents acetic acid was found to be the best solvent in the terms of yield and time. Among the tested conditions **(Table 2.1 entries 1-14)** it was found that the best results have been obtained when the reaction was

conducted in acetic acid and sodium acetate at 70 °C **(Table 2.1, entry-12)**. Furthermore, there is no improvisation in terms of product yield beyond 70 °C **(Table 2.1, entries 13-14**) rise in reaction temperature and amount of base from 1.0 mmol to 1.5 mmol. Hence in the present methodology, we have used acetic acid and sodium acetate as an optimized reaction condition with lower time and the highest conversion rate with a yield of 90% obtained at 70 °C **(Table 2.1, entry-12)**.

[a]Table 2.1. Optimization of the solvent and base for the synthesis of 4a *via* a three-component reaction.

Entry	Solvent	Solvent/ Base	Temp (°C)	Time (h)	Yield[b] (%)
1	H_2O	-	60	24	NR
2	CH_3CN	-	60	20	Trace
3	DMF	-	60	17	18
4	Toulene	-	60	24	NR
5	MeOH	-	60	14	25
6	MeOH	AcOH (1.0mL)	60	12	37
7	EtOH	-	60	13	42
8	EtOH	AcOH (1.0 ml)	60	11	50
9	EtOH	AcOH (1.5 mL)	60	10	55
10	AcOH	-	60	8	65
11	AcOH	NaOAc (1.0 mmol)	60	6	80
12	**AcOH**	**NaOAc(1.0 mmol)**	**70**	**5**	**90**
13	AcOH	NaOAc (1.5 mmol)	70	5	70
14	AcOH	NaOAc (1.0 mmol)	reflux	5	62

[a]*Reaction conditions*: **1** (1.0 mmol), **2** (1.0 mmol), sodium acetate (1.0 mmol), **3a** (1.0 mmol), solvent (2 mL) refluxing conditions for 5h. [b]isolated yield.

By utilizing the above optimistic conditions, the designed compounds (**4a-p)** were synthesized in good to excellent yields. The first step involves classical Paal-Knorr pyrrole synthesis to give an intermediate containing a pyrrole ring. This intermediate further reacts with different substituted alkyl/ aryl alkyl halides to provide final products **(4a-p).** This is a regioselective S-alkylation.

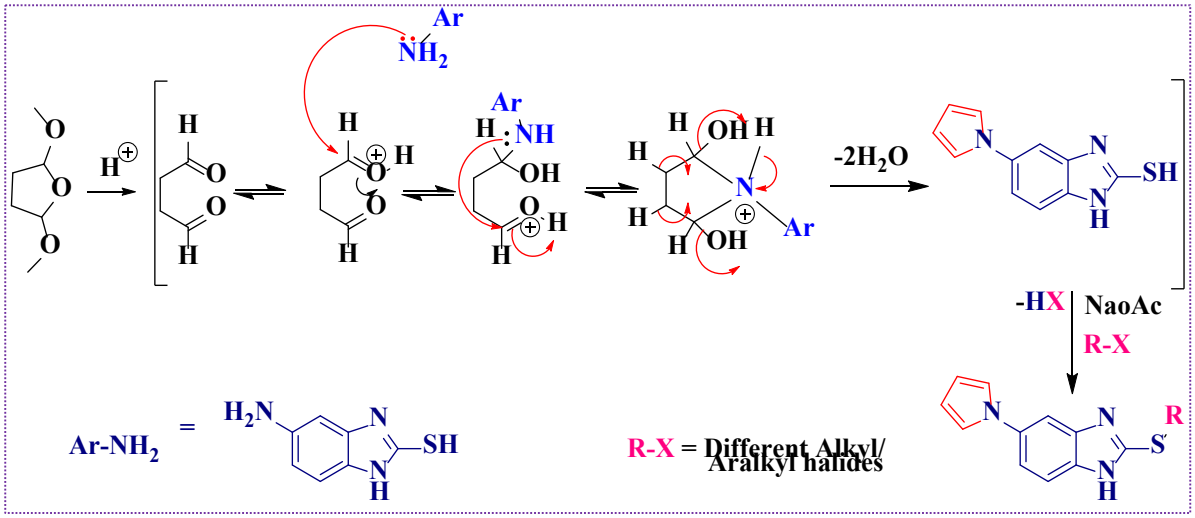

Scheme 2.1. Plausible reaction mechanism for the synthesis of compounds 4a-p

The alkylation of intermediate with different alkyl/ aryl alkyl halides may results in different types of products, like S-alkylated or N-alkylated or a mixture of both depending on reaction conditions. But, in the present investigation, no mixture of products is formed (as evidenced by TLC). Due to the high nucleophilicity of the thiol group S-alkylated / aryl alkylated products were formed in preference over N-alkylated products.

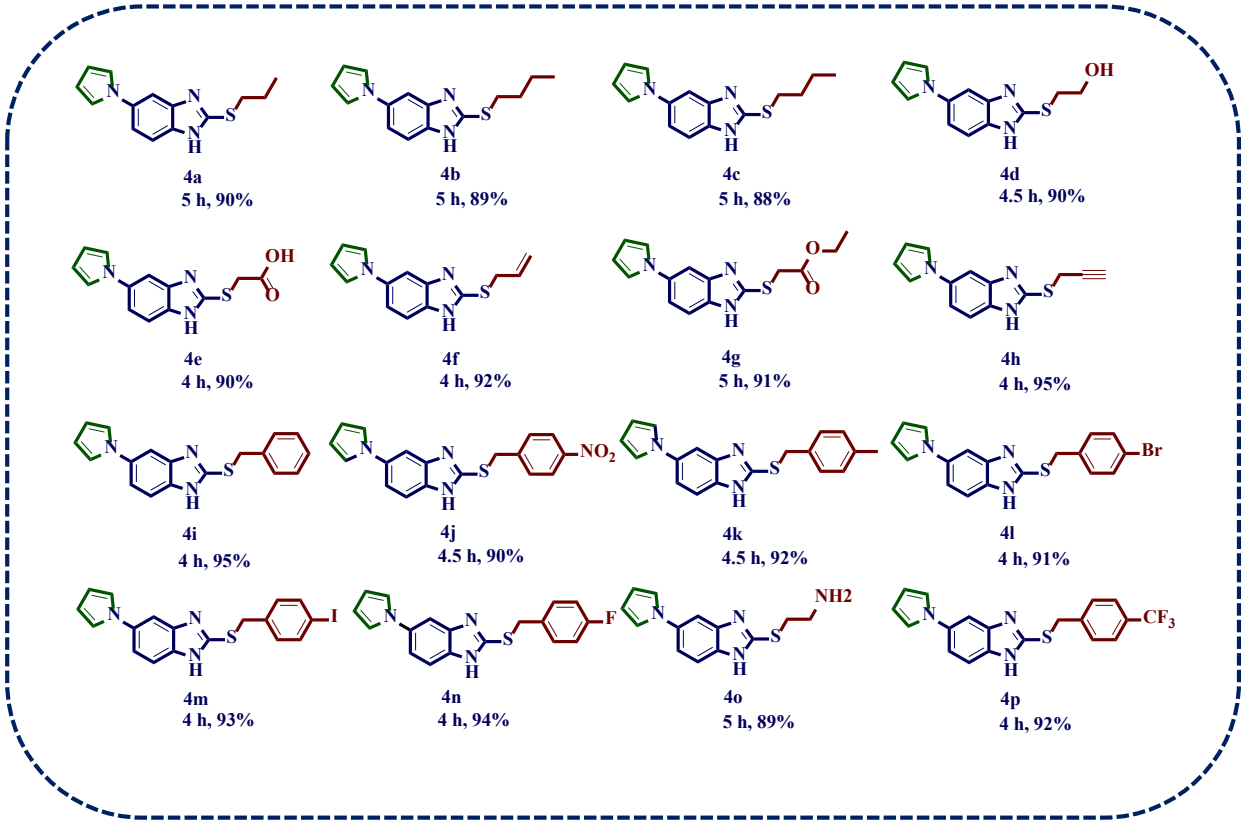

Figure 2.2. Scope of substrates

The formation of S-alkylated products was confirmed by their spectral data. All the newly synthesized compounds were characterized by their physical, analytical, and spectral data. The IR spectrum of compound **4a** showed characteristic bands at 3338, 2949, and 1631 cm^{-1} due to NH, C-H, and C=N stretching frequencies respectively. The ^{1}H-NMR spectrum of compound **4a** showed two singlets at 12.65 and 3.27 δ ppm indicating the presence of NH and S-CH_2-protons.^{13}C-NMR spectrum of compound, **4a** showed characteristic peaks at 35.3 and 169.5 δ ppm indicating the presence of aliphatic carbon and presence of N=C-S carbon respectively. The ESI-HRMS spectrum of compound **4a** gave the molecular ion peak at 258.1020 $[M+H]^+$.

2.5. Molecular Docking Studies

The X-ray crystallographic structure of *αβ*-tubulin (receptor protein) which is complexed with DAMA-colchicine was obtained from the protein data bank (PDB ID: 1SA0). To facilitate docking simulation on the receptor protein, DAMA-colchicine was removed and polar hydrogens were added. A grid box generated at 118.484, 89.709, and 6.950 of sizes 90,90, and 90 was utilized while performing the molecular docking simulations. Molecular docking simulation was performed using Auto Dock Vina [60] with an effectiveness value set to 16. To test the reproducibility of the docking pose, the molecule is redocked at the same active site and the root mean square deviation (RMSD) of the two poses was estimated. The minimum distance between the molecule and interacting amino acid was determined using Protein-Ligand Interaction Profiler (PLIP). Further, the nature of interactions along with the interacting residues (amino acids) of the protein with the molecule is visualized using the same PLIP [61]. The Visual Molecular Dynamics (VMD) program was utilized to generate the graphical images [62].

Microtubules are one of the most prominent choices among the targets used for the treatment of cancer due to their crucial role during cell division. Microtubules are the cytoskeletal structure of tubulin that forms mitotic spindles *via* a reversible process called dynamic instability which plays a vital role in chromosomal segregation and signaling during mitosis [63-68]. Therefore, attention has been paid to investigating the *anti-tubulin* property of the synthesized compounds. To probe the *anti-tubulin* properties of the synthesized compounds, a molecular docking simulation has been performed and the inhibitory activity is predicted based on the best docking score.

In silico molecular docking simulation was performed to scrutinize the *anti-tubulin* properties of the synthesized compounds. The *anti-tubulin* properties of the molecules are predicted based on their binding affinity values at the active site of the receptor protein. The lower binding affinity value indicates the better affinity of the molecule towards the protein. The binding affinity values (kcal/mol) of these compounds along with Root Mean Square Deviation (RMSD) between two docked poses at the active site are tabulated in **Table 2**.2 **Figure 2.3** illustrates the docked pose of **4j** and **4p** at the active site of the receptor protein (1SA0).

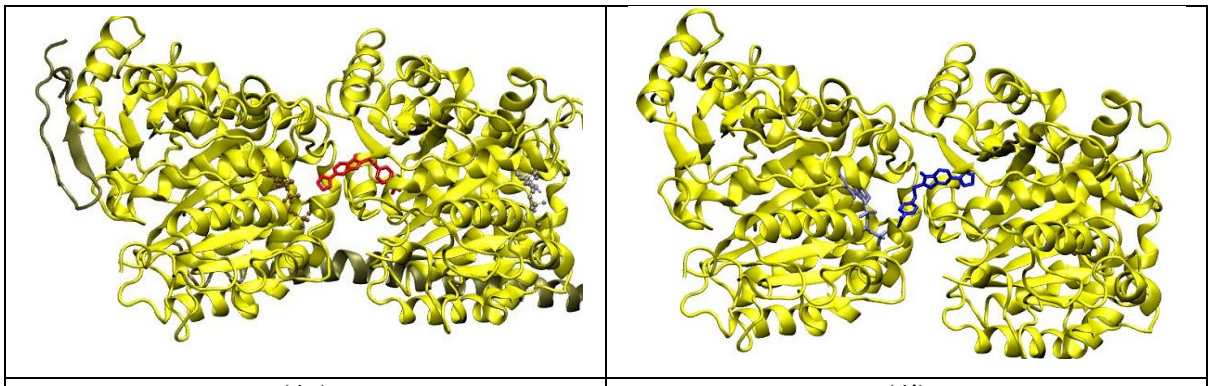

(4p)	(4j)

Figure 2.3. The docked position of the compounds at the active site of the receptor protein

It can be seen from **Table 2.2** that the lowest binding affinity value is found to be -8.9 and -8.3 kcal/mol for **4p** and **4j** respectively. Therefore, these are the best *anti-tubulin* agents among the molecules considered in the present investigation. Close analysis of the docking results reveals that alkyl substitution **(4a and 4b),** shows a high value of binding affinity. It is further found to increase for **4c** which may be attributed to the increase in the carbon chain length in the substitution. Further, it is observed that the affinity value decreases with an increase in the polarity of the substitution **(4d, 4e, and 4g).** Moreover, it is worth mentioning that among the compounds considered in the present investigation, the best binding value is found to be for the benzyl group substitutions. Furthermore, it is worth noting that the value is further found to decrease with the presence of the electron-withdrawing group at the benzyl ring **(4j and 4p).**

To study the effect of pyrrole substitution in the compound on the binding affinity at the active site, the pyrrole group was removed from the structure of **4p** and the molecule is then indicated as **A**. The binding affinity value of **A** is also calculated and given in **Table 2.2**. The binding affinity value obtained for **A** is -8.0 kcal/mol which is comparatively -0.9 kcal/mol more than found for **4p**. This is a clear indication that the binding affinity with the receptor protein decreases in absence of a pyrrole ring.

Table 2.2. Binding Affinity (kcal/mol) and Root Mean Square Deviation (RMSD) of the Compounds at the Active Site of the Receptor Protein (1SA0)

S. No.	compound	Binding affinity (kcal/mol)	RMSD
1	4a	-6.7	3.09
2	4b	-6.7	1.24
3	4c	-6.6	0.58
4	4d	-7.3	1.32
5	4e	-7.4	0.59
6	4f	-6.6	0.73
7	4g	-7.2	0.52
8	4h	-6.7	1.19
9	4i	-7.8	0.85
10	4j	-8.3	0.89
11	4k	-8.1	0.62
12	4l	-7.7	0.38
13	4m	-7.9	0.87
14	4n	-7.9	1.20
15	4o	-6.9	0.51
16	4p	-8.9	0.86
17	A	-8.0	0.86

To validate the reproducibility of the binding pose at the active site of the receptor protein, the root mean square deviation was evaluated and the results are given in **Table 2.2**. The lower root mean square deviation between the two poses demonstrates the reproducibility of the two docked conformers. The two docked poses of **4j** and **4p** at the active site are shown in **Figure 2.4**.

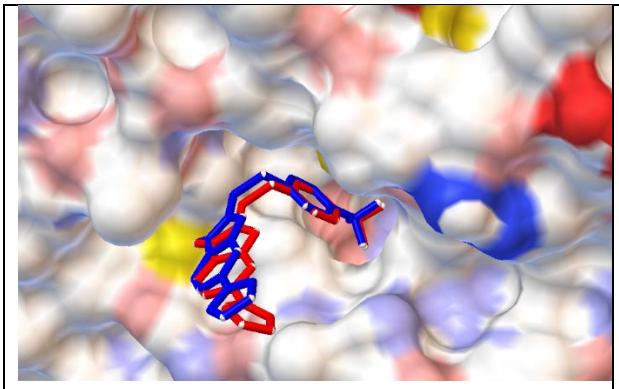

(4p)

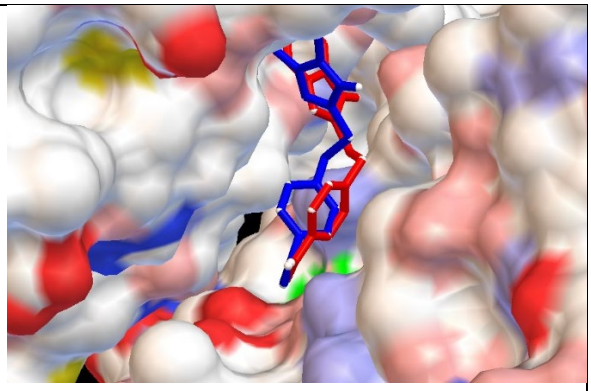

(4j)

Figure 2.4. The two docked poses of the compounds at the active site indicate the reproducibility of the docking conformer

The amino acid residues which are found to interact with the compound at the active site of the protein are given in **Table 2.3**. The value given in the parenthesis indicates the minimum distance between the compound with its residual interacting amino acid. The amino acid residues involved in hydrophobic interactions with the compounds are given in the third column. The amino acid residues which are involved in H-bonding, salt bridge, and π-cationic interactions are listed in column four of the same **Table 2.3**. The type of interaction is also mentioned in the parenthesis.

It can be seen from **Table 2.3** that **4p** shows only hydrophobic interactions at the active site of the receptor protein. The interacting amino acids are ALA180A (3.57), LEU248B (3.79), ALA250B (3.64), LEU255B (3.52), LEU255B (3.42), and ILE378B (3.76). The compound **4j** is found to interact at the active site involving both hydrophobic and π-cationic interactions. LEU248B (3.98), LYS254B (3.74), ALA316B (3.68), VAL318B (3.14), LYS352B (3.71), ALA354B (3.57), and ILE378B (3.81) shows hydrophobic interactions while LYS254B (3.91) shows π-cationic interactions.

Table 2.3. Interacting Amino Acids Residues at the Active Site of the Protein

S. No.	Compound	Amino acids involved in hydrophobic interactions	Other interacting amino acids
1	4a	LEU248B (3.55), LYS254B (3.86), ASN258B (3.72)	LEU284B (2.39), LYS254B (2.91) (H-bonding)
2	4b	ALA180A (3.57), VAL181A (3.67), Lys254B (3.77), ASN258B (3.74), ALA316B (3.64), LYS352B (3.60),	

		LYS352B (3.67)	
3	4c	LEU248B (3.80), LEU248B (3.95), LYS254B (3.67), LYS352B (3.84)	ALA250B (3.59) (H-bonding)
4	4d	VAL181A (3.58), LYS254B (3.73), ASN258B (3.76), ALA316B (3.63), LYS352B (3.68), LYS352 (3.71)	ASN101A (2.44), GLY144A (2.46), THR179A (2.51) (H-bonding)
5	4e	ALA180A (3.84), LYS254B (3.84), ASN258B (3.78), LYS352B (3.84)	ASN101A (2.40), ASN249B (2.63) (H-bonding) LYS254 (3.0) (SALT BRIDGE)
6	4f	ALA180A (3.83), LYS254B (3.58), ASN258B (3.86), LYS352B (3.74)	ASN101A (3.13) (H-bonding)
7	4g	VAL181A (3.72), LYS254B (3.83), ASN258B (3.65), ALA316B (3.54), LYS352B (3.60)	ASN101A (3.11), ASN249B (2.46) (H-bonding) LYS254B (3.75) (SALT BRIDGE)
8	4h	ALA180A (3.98), ASN258B (3.92), ALA316B (3.90), LYS352B (3.82), LYS352B (3.95)	ASN101A (2.28) (H-bonding)
9	4i	VAL181A (3.73), TYR224A (3.74), LEU248B (3.76), LYS254B (3.69), ASN258B (3.80), ALA316B (3.80), LYS352B (3.80), LYS352B (3.61)	
10	4j	LEU248B (3.98), LYS254B (3.74), ALA316B (3.68), VAL318B (3.14), LYS352B (3.71), ALA354B (3.57), ILE378B (3.81)	LYS254B (3.91) (π-cationic)
11	4k	LEU248B (3.83), LEU248B (3.75), ALA250B (3.50), LEU255B (3.45), LEU255B (3.43), ILE378B (3.90)	LYS254B (3.76) (π-cationic)
12	4l	VAL181A (3.69), TYR224A (3.85), LYS254B (3.59), ASN258B (3.94), ALA316B (3.94), LYS352B (3.65)	ASN101A (3.12) (H-bonding)

13	4m	VAL181A (3.75), LEU248B (3.84), LYS254B (3.77), ASN258B (3.64), ALA316B (3.57), LYS352B (3.64)	ASN101A (2.95) (H-bonding)
14	4n	LEU248B (3.63), ALA250B (3.89), LEU255B (3.80), ALA316B (3.69), VAL318B (3.76), ILE378B (3.66)	
15	4o	VAL181A (3.89), LYS254B (3.47), ASN258B (3.74), ALA316B (3.83), LYS352B (3.67)	ASN101A (2.76), GLY144A (2.72) (H-bonding)
16	4p	ALA180A (3.57), LEU248B (3.79), ALA250B (3.64), LEU255B (3.52), LEU255B (3.42), ILE378B (3.76)	
17	A	ASN258B (3.57), ALA316B (3.74), VAL318B (3.66), LYS352B (3.80), ALA354B (3.79)	ASN258B (2.85), VAL315B (2.96) (H-bonding)

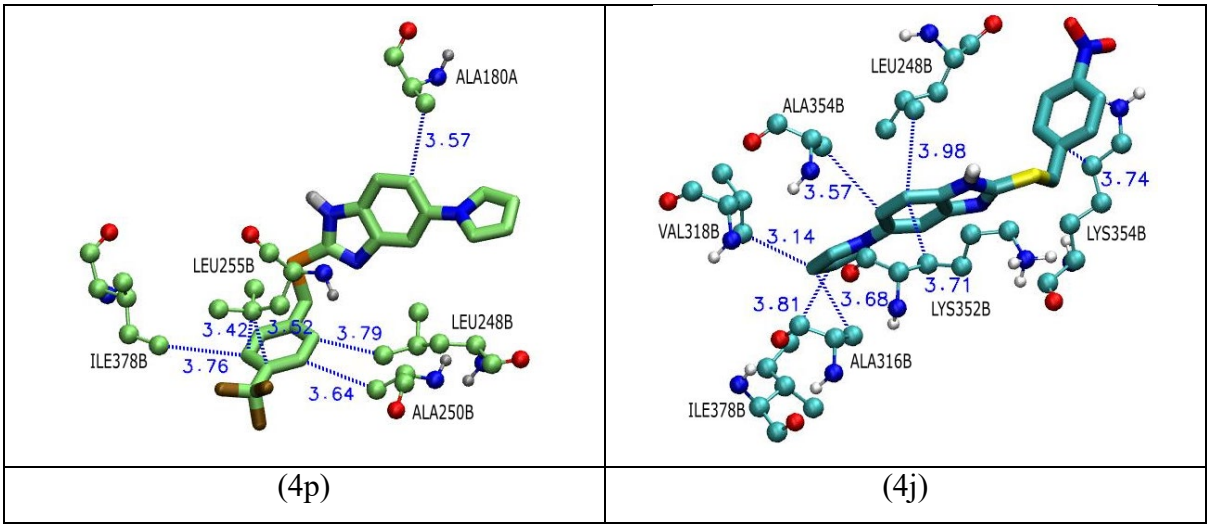

(4p) (4j)

Figure 2.5 Interacting amino acids at the active site of the protein with the compounds.

2.6. Conclusion

In summary, we have synthesized 2-alkyl/aryl alkyl thio-5-pyrrolyl-benzimidazole scaffolds *via* a novel, facile one-pot three-component approach using acetic acid and sodium acetate as a reaction medium with good to excellent yields. The usefulness of this reaction is that it involves easy workup, shorter reaction time, broad substrate scope, and column-free purification of the products. Further, *in silico* molecular docking studies were carried out against the colchicine binding site of α*β*-tubulin with newly synthesized compounds. Among all the compounds **4j** and **4p** exhibited good docking interactions.

2.7. Experimental section

General procedure for the synthesis of **2-(Propylthio)-5-(1*H*-pyrrol-1-yl)-1*H*-benzo[*d*]imidazole compounds (4a-p)**

A mixture of 5-amino-2-marcaptobenzimidazole **1** (1.0 mmol), 2,5-dimethoxy tetrahydrofuran **2** (1.0 mmol) was refluxed in 2 mL of acetic acid for about 3 h by monitoring TLC (EtOAc: n-hexane, 80:20). After completion of the reaction, to the reaction mixture different substituted alkyl/ aryl alkyl halides **3** (1.0 mmol) and anhydrous sodium acetate (1 mmol) was added. The reaction mixture was refluxed for another 2-3 h. After completion of the reaction, the reaction mixture was cooled to room temperature and poured into crushed ice and the precipitated product was filtered. The crude product was dried and recrystallized from ethanol.

2.8. Characterization data of products

2-(Propylthio)-5-(1*H*-pyrrol-1-yl)-1*H*-benzo[*d*]imidazole (4a).

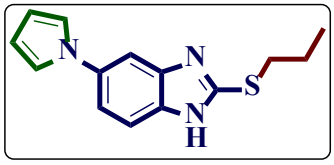

White solid; yield: 90%; mp: 272-274ºC; FT-IR (KBr, cm^{-1}): 3338 (NH), 2949 (C-H), 1631 (C=N), 1464 (C=C); ^{1}H NMR (400 MHz, DMSO-d_6 δ ppm) 1.01 (t, 3H, *J*=7.2 Hz), 1.71-1.80 (m,2H), 3.27 (t, 2H, *J*= 6.8 Hz), 6.25 (unresolvable singlet, 2H, Ar-H) 7.31 (unresolvable singlet, 2H, Ar-H) ,7.55-7.73 (m, 2H, Ar-H) 7.96 (s, 1H, Ar-H), 12.64 (brs, 1H, NH), ^{13}C NMR (100 MHz, DMSO- d_6) δ: 14.9, 24.8, 35.3, 101.7, 110.7, 115.3, 120.0, 130.6, 133.5, 136.2, 169.5; ESI-HRMS (*m/z*): Calcd. for $C_{14}H_{16}N_3S$ $[M+H]^+$: 258.1059, found: 258.1020. Elem. Anal. : C, 65.34; H, 5.88; N, 16.33; S, 12.46; found: C, 65.30; H, 5.83; N, 16.38; S, 12.40.

2-(Butyllthio)-5-(1*H*-pyrrol-1-yl)-1*H*-benzo[*d*]imidazole (4b).

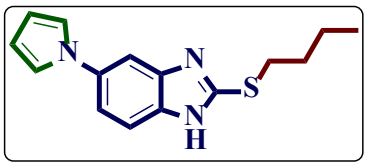

White solid; yield: 89%, mp 280-282 ºC, FT-IR (KBr, cm^{-1}): 3390 (NH), 2962 (C-H), 1464 (C=C), 1619 (C=N); ^{1}H-NMR (400 MHz, $CDCl_3$+DMSO-d_6 δ ppm): 0.89 (t, *J*=2.4 Hz, 3H) 1.20-1.22 (m, 2H), 1.40 – 1.47 (m, 2H), 1.70 (t, *J*=5.2 Hz, 2H), 6.20 (t, *J*=2.4 Hz, 2H, Ar-H), 7.07 (t, *J*=2.4 Hz 2H, Ar-H), 7.14-7.16 (m, 2H, Ar-H), 8.02 (s, 1H, Ar-H), 12.48 (s, 1H, NH); ^{13}C NMR (100 MHz, DMSO-d_6) δ; 14.4, 22.6, 29.5, 31.8, 101.8, 110.7, 115.3, 120.0, 130.6, 133.5, 136.2 , 169.5; ESI-HRMS: *m/z* Calcd. for $C_{15}H_{18}N_3S$ $[M+H]^+$; 272.1216, found: 272.1217. Elem. Anal. : C,66.39; H,6.31; N,15.48; S,11.81; found: C, 66.35; H, 6.35; N, 15.55; S, 11.85.

2-(Pentyltyllthio)-5-(1*H*-pyrrol-1-yl)-1*H*-benzo[*d*]imidazole (4c).

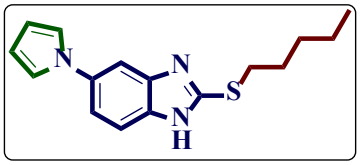

White solid; yield: 85%; mp: 289-291ºC; FT-IR (KBr, cm^{-1}): 3137 (NH), 2962 (C-H), 1619 (C=N),1464 (C=C); ^{1}H-NMR (400 MHz, DMSO-d_6 δ ppm): 0.85 (t, *J* = 1.6 Hz, 3H) 1.15-1.25 (m, 6H aliphatic), 4.02 (t, *J*= 6.8 Hz, 2H, S-CH_2 protons), 6.24 (unresolvable singlet, 2H, Ar-H), 7.16-7.21 (m, 2H, Ar-H), 7.28-7.32 (m, 3H, Ar-H) 12.66 (brs, 1H, -NH), ^{13}C-NMR (100

MHz, DMSO-d_6 δ ppm); 13.9, 21.7, 31.4, 31.8, 101.8, 110.7, 114.8, 115.3, 120.0, 130.6, 133.5, 135.4, 136.1, 169.5; ESI-HRMS *m/z* Calcd. for $C_{16}H_{20}N_3S$ $[M+H]^+$: 286.1312, found: 286.1392; Elem. Anal. C,67.33; H,6.71; N,14.72; S,11.23; found: C,67.38; H,6.74; N,14.76; S,11.28.

((5-(1*H*-pyrrol-1-yl)-1*H*-benzo[*d*]imidazole-2-yl) thio) ethan-1-ol (4d).

Brown solid; yield: 91%; mp: 166-168ºC; FT-IR (KBr, cm^{-1}): 3349 (OH), 2938 (C-H),1627 (C=N),1460 (C=C); ^{1}H-NMR (400 MHz, DMSO-d_6 δ ppm): 4.06 (t, *J* = 7.2 Hz, 2H), 4.39 (t, *J* = 7.2 Hz, 2H), 5.76 (br s, 1H, OH), 6.26 (d, *J*=9.6 Hz, 2H, Ar-H), 7.34 (t, *J*=2.4 Hz, 2H, Ar-H), 7.47-7.52 (m, 2H, Ar-H), 7.64 (s,1H, Ar-H), 12.50 (brs,1H, NH); ESI-HRMS *m/z* Calcd. for $C_{13}H_{14}N_3OS$ $[M+H]^+$: 260.0852, found: 260.0848; Elem. Anal.: C, 60.21; H,5.05; N,16.20; S,12.36; found: C,60.25; H,5.09; N,16.24; S,12.31.

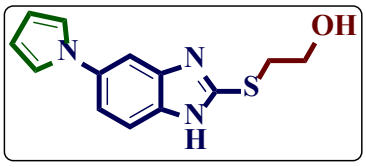

((5-(1*H*-pyrrol-1-yl)-1*H*-benzo[*d*]imidazole-2-yl) thio) acetic acid (4e).

Brown solid; yield: 90%; mp: 180-182 ºC; FT-IR (KBr, cm^{-1}): 3357 (COOH), 3078 (NH), 2936(C-H), 1591 (C=N), 1455 (C=C); ^{1}H-NMR (400 MHz, $CDCl_3$ δ ppm): 3.11 (s, 2H, S-CH_2), 6.20 (t, *J*= 2.4 Hz, 2H, Ar-H), 6.97 (t, *J*=2.0 Hz, 2H, Ar-H), 7.09-7.10 (m, 2H, Ar-H), 7.63 (s, 1H, Ar-H), 12.31 (brs, 1H, NH proton), 12.35 (brs 1H, OH); ^{13}C NMR (100 MHz, DMSO-d_6) δ ; 34.2, 110.4, 114.9, 118.1, 120.0, 135.5, 151.0, 155.1, 170.2; ESI-HRMS: *m/z* Calcd. for $C_{13}H_{12}N_3O_2S$ $[M+H]^+$; 274.0645, found: 274.0643; Elem. Anal. C,57.13; H,4.06; N,15.37; S,11.73; found: C,57.16; H,4.00; N,15.31; S,11.77.

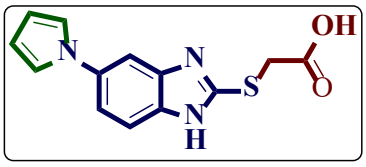

2-(Allylthio)-5-(1*H*-pyrrol-1-yl)-1*H*-benzo[*d*]imidazole (4f).

white solid; yield: 92%; mp: 150-152ºC; FT-IR (KBr, cm^{-1}): 3439 (NH), 2948 (C-H), 1628 (C=N),1444 (C=C); ^{1}H-NMR (400 MHz, DMSO-d_6 δ ppm): 3.99 (d, *J* = 6.4 Hz, 2H, S-CH_2), 5.12 (d H_A, *J* = 9.6 Hz, 1H, H_A, H_x), 5.33 (d, H_B *J* = 17.2 Hz, 1H, H_B, H_X), 5.97-6.06 (m, 1H,

H_X proton), 6.25 (unresolvable singlet, 2H, Ar-H), 7.31-7.57 (m, 4H, Ar-H),7.70 (s, 1H, Ar-H), 12.70 (brs, 1H, NH); ^{13}C NMR (100 MHz, DMSO-d_6) δ: 34.4. 110.4, 115.0, 118.7, 120.1, 134.2, 135.5, 151.2,162.8;

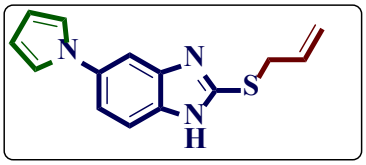

ESI- HRMS *m/z* Calcd. for $C_{14}H_{14}N_3S$ $[M+H]^+$; 256.0903, found: 256.0300; Elem. Anal., C,65.86; H,5.13; N,16.46; S,12.56; found: C,65.90; H,5.19; N,16.50; S,12.51.

Ethyl 2-((5-(1*H*-pyrrol-1-yl)-1*H*-benzo[*d*]imidazol-2-yl) thio) acetate (4g).

white solid; yield: 91%; mp 144-146 ºC; FT-IR (KBr, cm^{-1}): 3440 (NH), 2938 (C-H), 1713 (C=O, ester (1622 (C=N), 1431 (C=C); ^{1}H-NMR (400 MHz, $CDCl_3$ δ ppm): 1.15 (t, *J*=8.4 Hz, 3H), 3.67 (s, 2H), 5.69 (q, 2H),

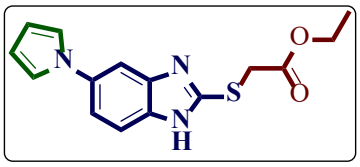

6.05 (unresolvable singlet, 2H, Ar-H), 6.77 (unresolvable singlet, 2H, Ar-H), 6.98 (d, *J*=7.6 Hz, 2H, Ar-H), 7.28 (s, 1H, Ar-H), 8.33 (brs, 1H, NH); ^{13}C NMR (100 MHz, DMSO-d_6) δ: 14.5 (aliphatic-C), 33.8, 61.6, 110.4, 114.9, 120.1, 135.5, 150.7, 151.5, 169.0, 170.3; ESI-HRMS *m/z* Calcd. For $C_{15}H_{16}N_3O_2S$ $[M+H]^+$: 302.0958, found: 302.0959: Elem. Anal., C,59.78; H,5.02; N,13.94; S,10.64; found: C,59.74; H,5.07; N,14.00; S,10.69.

2-(Prop-2-ynylthio)-5-(1*H*-pyrrol-1-yl)-1*H*-benzo[*d*]imidazole (4h).

White solid; yield: 95%; mp: 156-158 ºC; FT-IR (KBr, cm^{-1}): 3439 (NH), 3276 (C-H), 1628 (C=N), 1479(C=C); ^{1}H-NMR (400 MHz, $CDCl_3$ δ ppm): 2.15 (s, 1H, ≡CH), 2.38 (brs, 1H, NH), 3.96 (s, 2H, S-CH_2), 6.12

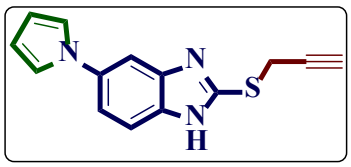

(unresolvable singlet, 2H, Ar-H), 6.89 (unresolvable singlet, 2H, Ar-H), 7.07 (d, *J*=7.2 Hz, 1H, Ar-H), 7.33-7.36 (m, 2H, Ar-H); ^{13}C-NMR (100 MHz, $CDCl_3$+DMSO-d_6) δ: 20.5, 73.72, 79.5, 106.1, 110.3, 114.9, 115.5, 119.9, 135.9, 137.8, 140.0, 149.9; ESI-HRMS *m/z* Calcd. for $C_{14}H_{12}N_3S$ $[M+H]^+$: 254.0746, found: 254.1774; Elem. Anal. C, 66.38; H, 4.38; N, 16.59; S, 12.66; found: C, 66.35; H, 4.32; N, 16.64; S, 12.61.

2-(Benzylthio)-5-(1*H*-pyrrol-1-yl)-1*H*-benzo[*d*]imidazole (4i).

Brown solid; yield:95%; mp: 135-137 ºC; FT-IR (KBr, cm^{-1}): 3405 (NH), 2900 (C-H), 1619 (C=N), 1494 (C=C); ^{1}H-NMR (400 MHz, DMSO-d_6 δ ppm): 4.58 (s, 2H, S-CH_2), 6.25 (unresolvable singlet, 2H, Ar-H), 7.24-7.32 (m, 7H, Ar-H), 7.45-7.47 (m, 3H, Ar-H), 12.73 (brs, 1H, NH); ^{13}C-NMR (100MHz, DMSO-d_6) δ: 36.8, 104.8, 111.1, 117.4 , 120.2, 128.4, 129.2, 129.4, 136.5, 137.4, 151.0 ; ESI-HRMS *m/z* Calcd. for $C_{18}H_{16}N_3S$ $[M+H]^+$: 306.1059, found: 306.1087; Elem. Anal. C,70.79; H, 4.95; N, 13.76; S, 10.50; found: C,70.73; H, 4.90; N, 13.80; S, 10.42.

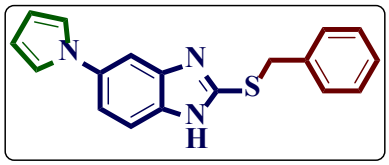

2-((4-Nitrobenzyl) thio)-5-(1*H*-pyrrol-1-yl)-1*H*-benzo[*d*]imidazole (4j).

Brown solid; yield: 95%; mp: 155-157 ºC; FT-IR (KBr, cm^{-1}): 3313 (NH), 2937 (C-H), 1628 (C=N), 1444 (C=C); ^{1}H-NMR (400 MHz, DMSO-d_6 δ ppm): 4.73 (s, 2H, S-CH_2), 6.25 (t, *J*=2.0 Hz, 2H, Ar-H), 7.32 (t, *J*=2.0 Hz, 2H, Ar-H), 7.36-7.39 (m, 2H, Ar-H), 7.52 (s, 1H, Ar-H), 7.54 (brs, 1H, -NH), 7.74 (d, *J* = 8.8 Hz, 2H, Ar-H), 8.18 (d, *J* = 8.8 Hz, 2H, Ar-H); ^{13}C-NMR (100 MHz, DMSO-d_6) δ: 35.0, 105.6 , 110.6 ,114.9, 115.8, 120.1, 124.1, 130.6, 136, 146.2, 147.2 , 150.6; ESI-HRMS *m/z* Calcd. For. $C_{18}H_{15}N_4O_2S$ $[M+H]^+$: 351.0910, found: 351.0917; Elem. Anal. C, 61.70; H, 4.03; N, 15.99; S, 9.15; found: C, 61.75; H, 4.04; N, 15.92; S, 9.11.

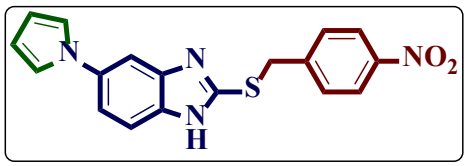

2-((4-Methylbenzyl) thio)-5-(1*H*-pyrrol-1-yl)-1*H*-benzo[*d*]imidazole (4k).

Brown solid; yield 92%; mp: 188-190 ºC; FT-IR (KBr, cm^{-1}): 3367 (NH), 2920 (C-H), 1628(C=N), 1422 (C=C); ^{1}H-NMR (400 MHz, DMSO-d_6 ppm): 2.27 (s, 3H -CH_3), 4.56 (s, 2H, S-CH_2), 6.26 (t, 2H, *J*= 2.0 Hz, Ar-H), 7.13 (d, 2H, *J*=7.6 Hz, Ar-H), 7.33-7.35 (m, 4H, Ar-H), 7.36-7.39 (m, 2H Ar-H),7.52 (brs, 1H, -NH-proton), 7.61 (s, 1H, Ar-H); ^{13}C-NMR (100 MHz, DMSO-d_6) δ: 21.2, 35.7, 110.5, 115.4, 120.1, 129.2, 129.6, 134.6, 135.8, 137.2, 151.5; ESI-HRMS *m/z* Calcd.

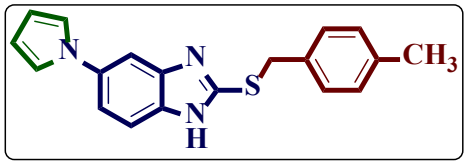

for $C_{19}H_{18}N_3S$ $[M+H]^+$: 320.1216, found: 320.1220; Elem. Anal. C, 71.44; H, 5.36; N, 13.16; S, 10.04; found: C, 71.40; H, 5.40; N, 13.12; S, 10.10.

2-((4-Bromobenzyl) thio)-5-(1*H*-pyrrol-1-yl)-1*H*-benzo[*d*]imidazole (4l).

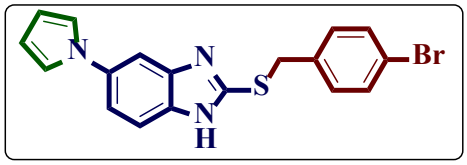

Brown solid; yield: 91%; mp: 168-170 ºC: FT-IR (KBr, cm^{-1}): 3345 (NH), 2936 (C-H), 1628(C=N), 1423 (C=C); ^{1}H-NMR (400 MHz, $CDCl_3$+DMSO-d_6 δ ppm): 4.67 (s, 2H, S-CH_2); 6.22 (t, 2H, *J*=2.0 Hz, Ar-H), 7.19 (t, 2H, *J*= 2.0 Hz, Ar-H), 7.46 (d, 1H, *J*= 8.8 Hz, Ar-H), 7.50 (brs, 1H, -NH), 7.60-7.65 (m, 2H, Ar-H),7.72 (d, 2H, *J*= 8.4 Hz, Ar-H), 8.09-8.02 (m,1H, Ar-H), 8.17 (s, 1H, Ar-H); ^{13}C-NMR (100 MHz, DMSO-d_6) δ: 35.0, 105.9, 110.3, 114.7, 120.1, 130.0, 131.5, 131.6, 135.2, 137.4, 137.7, 138.4, 151.8; ESI-HRMS *m/z* Calcd. for $C_{18}H_{15}Br\ N_3S$ $[M+H]^+$: 384.0165, found: 384.0165; Elem. Anal., C, 56.26; H, 3.67; N,10.93; S, 8.34; found: C, 56.22; H, 3.64; N,10.89; S, 8.38.

2-((4-Iodobenzyl) thio)-5-(1*H*-pyrrol-1-yl)-1*H*-benzo[*d*]imidazole (4m).

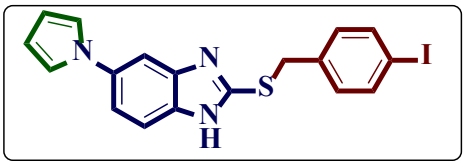

white solid: yield: 93%, mp: 174-176 ºC; FT-IR (KBr, cm^{-1}): 3345 (NH), 2899 (C-H), 1628 (C=N), 1423 (C=C); ^{1}H-NMR (400 MHz, $CDCl_3$+DMSO-d_6 δ ppm): 4.47 (s, 2H, S-CH_2), 6.20 (unresolvable singlet, 2H, Ar-H), 7.12 (unresolvable singlet, 2H, Ar-H), 7.17-7.22 (m, 3H, Ar-H) 7.42 (brs, 1H) 7.54-7.59 (m, 4H, Ar-H); ^{13}C NMR (100 MHz, DMSO-d_6) δ: 35.0, 93.7, 105.9, 110.3, 114.7, 120.1, 130.0, 131.5, 131.6, 135.2, 137.4, 137.7, 138.4, 151.9; ESI-HRMS *m/z* Calcd. for $C_{18}H_{14}I\ N_3S$ $[M]^+$: 430.9953, found: 430.0958; Anal.; C, 50.13; H, 3.27; N,9.74; S, 7.43; found: C, 50.16; H, 3.30; N,9.78; S, 7.40.

2-((4-Fluorobenzyl) thio)-5-(1*H*-pyrrol-1-yl)-1*H*-benzo[*d*]imidazole (4n).

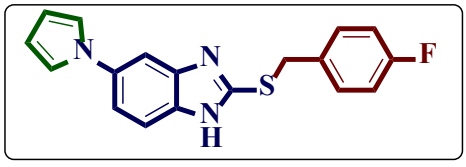

White solid; yield: 94%; mp: 145-147 ºC; FT-IR (KBr, cm^{-1}): 3317 (NH), 2936 (C-H), 1629 (C=N), 1482 (C=C); ^{1}H-NMR (400 MHz, DMSO-d_6 δ ppm): 4.71 (s,

2H, S-CH_2), 6.29 (t, 2H, *J*= 2.0 Hz, Ar-H), 7.30-7.36 (m, 4H Ar-H), 7.42 (t, 2H, *J*= 2.0 Hz, Ar-H), 7.57-7.60 (m, 2H Ar-H), 7.67 (s, 1H, Ar-H), 7.73 (brs, 1H, NH); ^{13}C-NMR (100 MHz, DMSO-d_6) δ: 34.7, 110.4, 115.0, 120.1, 123.9, 124.0, 128.5, 130.5, 135.5, 146.8, 147.0, 147.1, 149.8, 151.0; ESI-HRMS *m/z* Calcd. for $C_{18}H_{15}F\,N_3S$ $[M+H]^+$: 324.0965, found: 324.0965; Elem. Anal., C, 66.85; H, 4.36; N, 12.99; S, 9.91; found: C, 66.89; H, 4.40; N, 12.95; S, 9.96.

2-((5-(1*H*-pyrrol-1-yl)-1*H*-benzo[*d*]imidazol-2-yl) thio) ethan-1-amine (4o).

Brown solid; yield: 89%; mp: 167-169 ºC; FT-IR (KBr, cm^{-1}): 3372 (NH), 2961 (C-H), 1634 (C=N), 1465 (C=C); ^{1}H-NMR (400 MHz, $CDCl_3$+DMSO-d_6 δ ppm): 3.04 (t, *J*=6.0 Hz, 2H), 3.38 (t, *J*=5.6 Hz, 2H), 3.76 (s, 2H, -NH_2 protons), 6.22-6.26 (m, 2H, Ar-H), 7.02-7.29 (m, 2H, Ar-H), 7.17-7.20 (m, 2H, Ar-H), 7.45 (brs, 1H, Ar-H),7.82 (s, 1H, Ar-H); ^{13}C-NMR (100 MHz, DMSO-d_6) δ: 30.0, 36.6, 101.7, 110.5, 110.7, 114.9, 115.3, 120.0, 130.6, 133.5, 136.1, 169.4; ESI-HRMS *m/z* Calcd. for $C_{13}H_{15}N_4S$ $[M+H]^+$: 259.1012, found: 259.1039; Elem. Anal. C,60.44; H, 5.46; N,21.69; S,12.41; found: C, 60.40; H, 5.50; N,21.65; S,12.45.

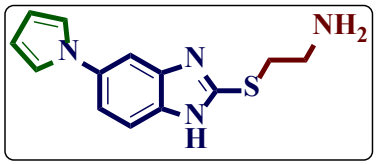

5-(1*H*-pyrrol-1-yl)- 2-((4-trifluoromethyl) benzyl) thio)-1*H*-benzo[*d*]imidazole (4p).

Brown solid; yield: 94%; mp: 160-162 ºC; FT-IR (KBr, cm^{-1}): 3334 (NH), 2939 (C-H), 1629 (C=N), 1479 (C=C); ^{1}H-NMR (400 MHz, DMSO-d_6 δ ppm): 5.25 (s, 2H S-CH_2), 6.28 (unresolvable singlet, 2H, Ar-H), 7.39 (unresolvable singlet, 2H, Ar-H), 7.46 (t, 2H, *J*= 8.4 Hz, Ar-H),7.52 (d, *J* = 8.8 Hz, 1H, Ar-H), 7.62 (d, *J*= 8.8 Hz, 1H, Ar-H), 7.67 (s, 1H, Ar-H), 8.16 (d, *J*=6.8 Hz, 2H, Ar-H), 8.33 (brs, 1H, -NH proton); ^{13}C-NMR (100 MHz, DMSO-d_6) δ: 34.9, 110.4, 120.1, 125.8, 125.8, 128.2, 128.5, 130.1, 130.6, 143.4, 151.0; ESI-HRMS *m/z*: 374.0938 $[M+H]^+$; Anal. Calcd. for $C_{20}H_{18}F_3N_3S$, C, 61.84; H, 4.41; N,10.82; S,8.25. found: C, 61.88; H, 4.45; N,10.86; S,8.20.

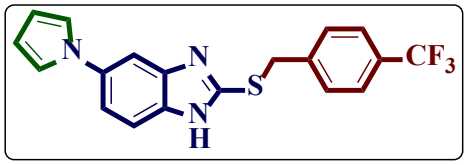

2.9. Spectra

^{1}H-NMR Spectrum of compound 4a (DMSO-d_6, 400MHz):

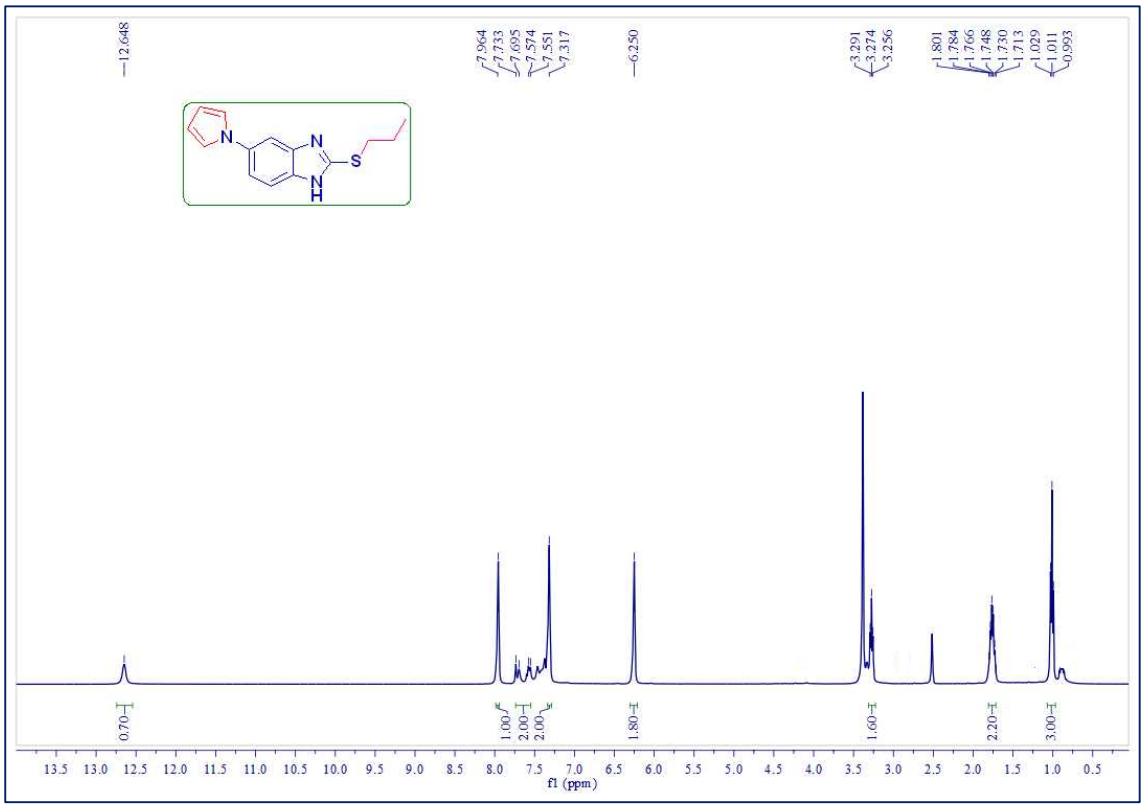

^{13}C-NMR Spectrum of compound 4a (DMSO-d_6, 100MHz):

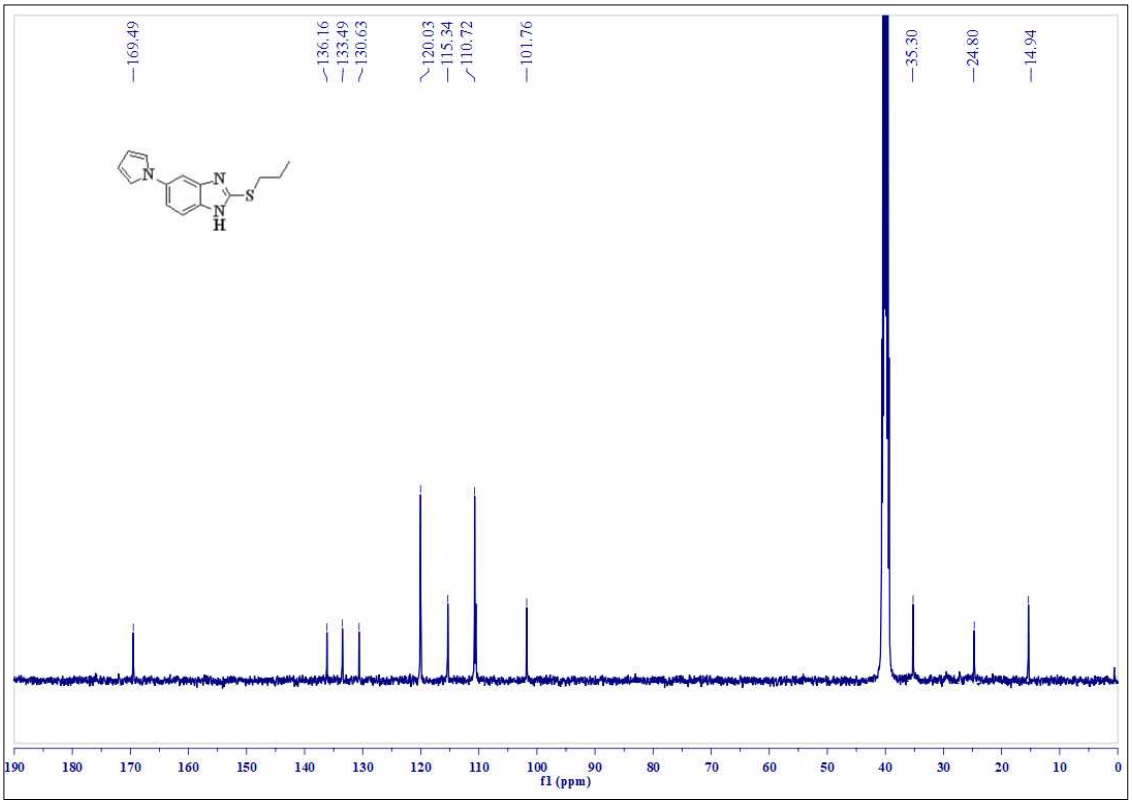

Mass spectrum of compound 4a:

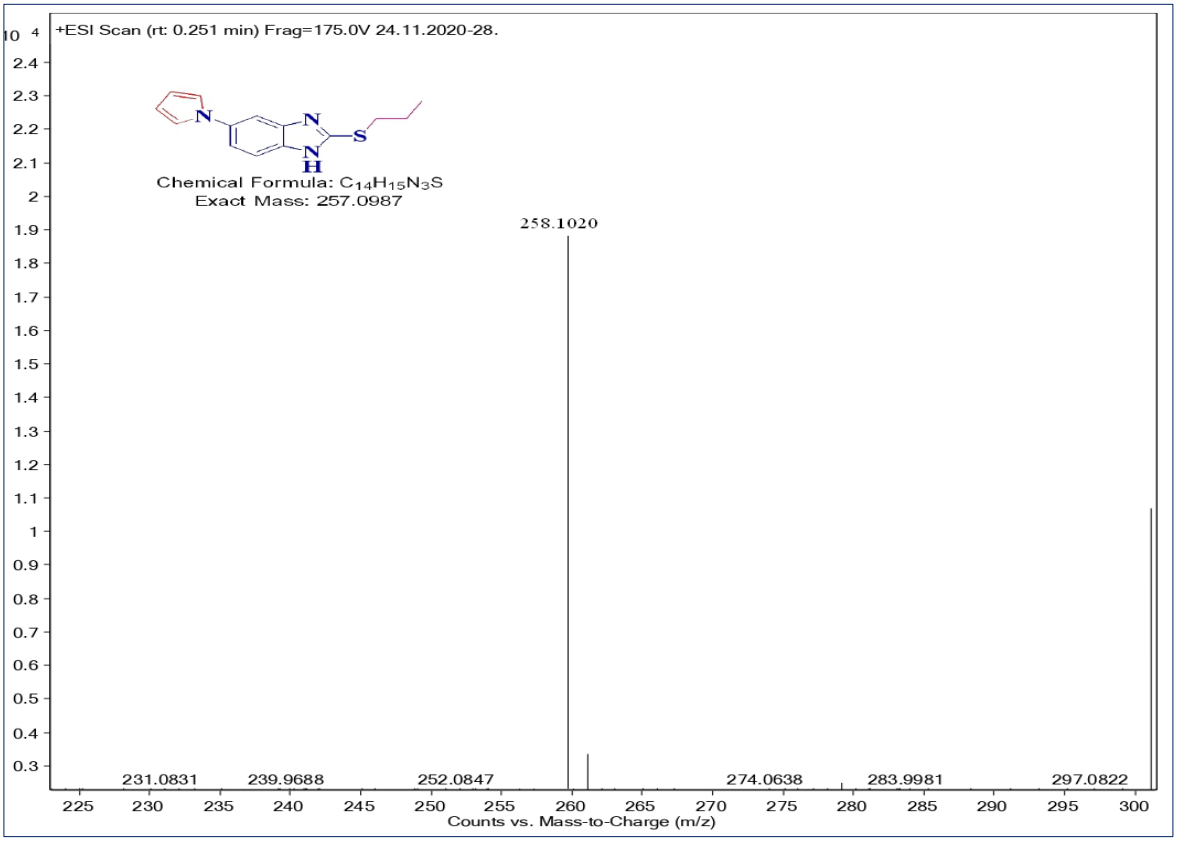

^{1}H-NMR Spectrum of compound 4b ($CDCl_3$+DMSO-d_6, 400MHz):

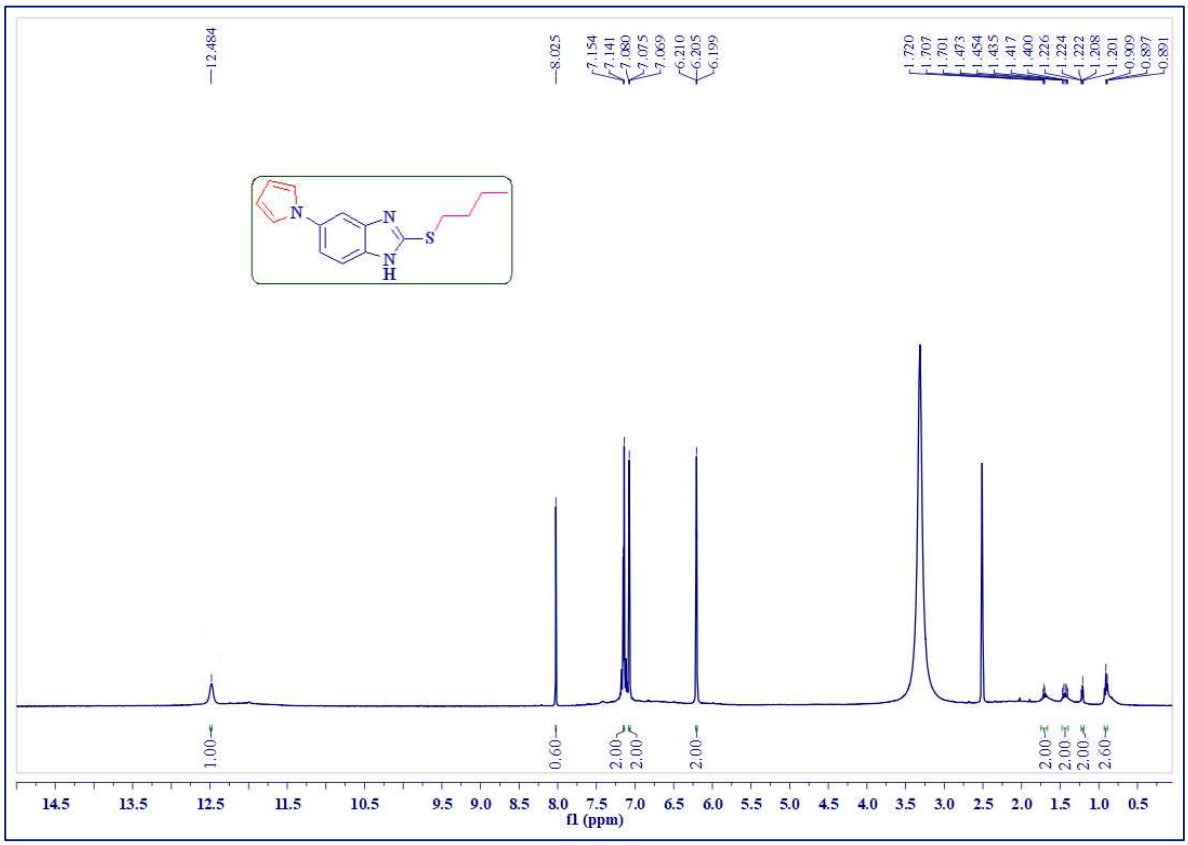

^{13}C-NMR Spectrum of compound 4b (DMSO-d_6, 100MHz):

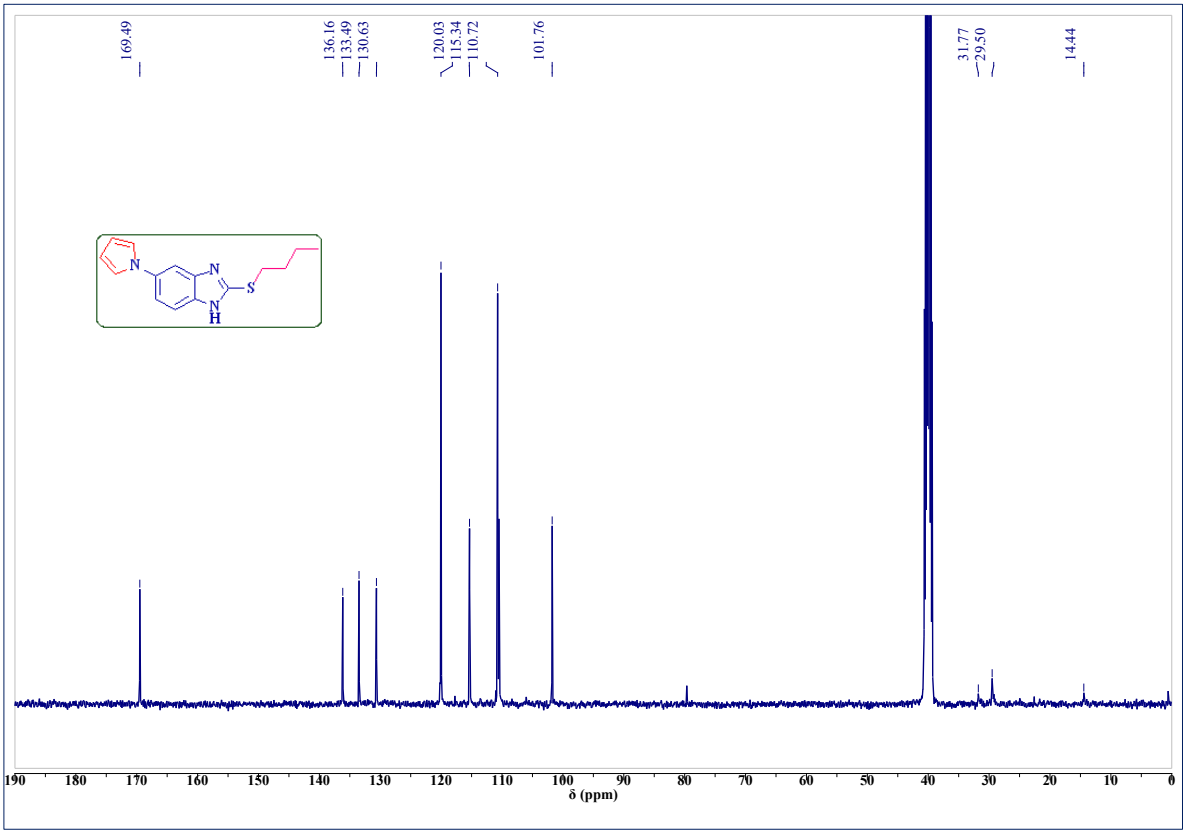

Mass spectrum of compound 4b:

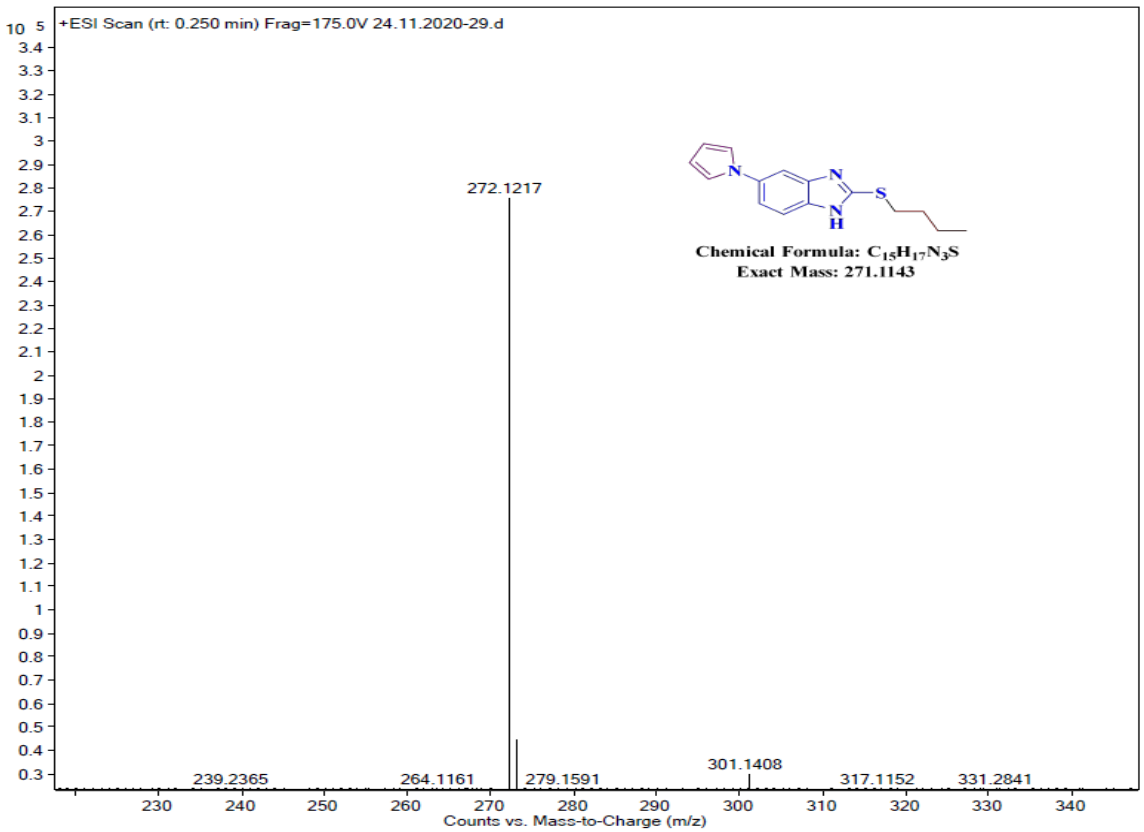

^{1}H-NMR Spectrum of compound 4c (DMSO-d$_6$, 400MHz):

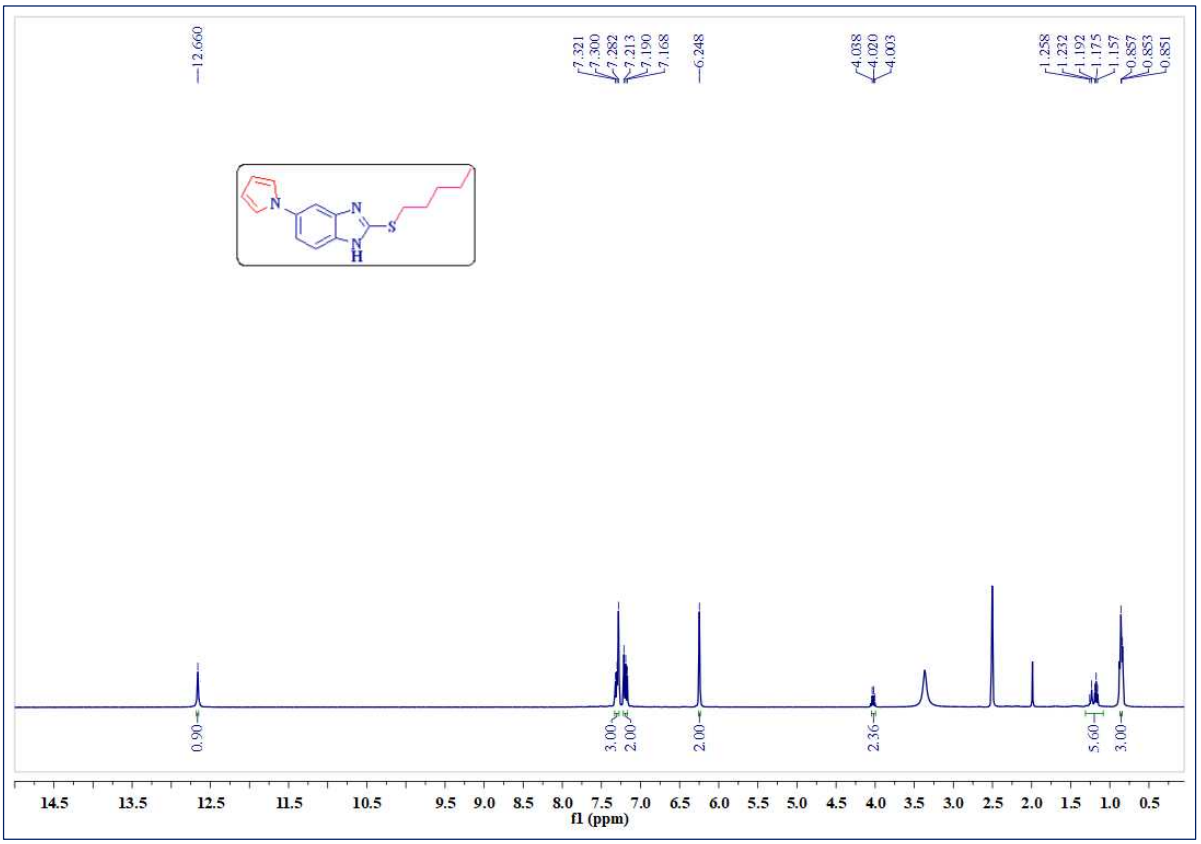

^{13}C-NMR Spectrum of compound 4c (DMSO-*d$_6$*, 100MHz):

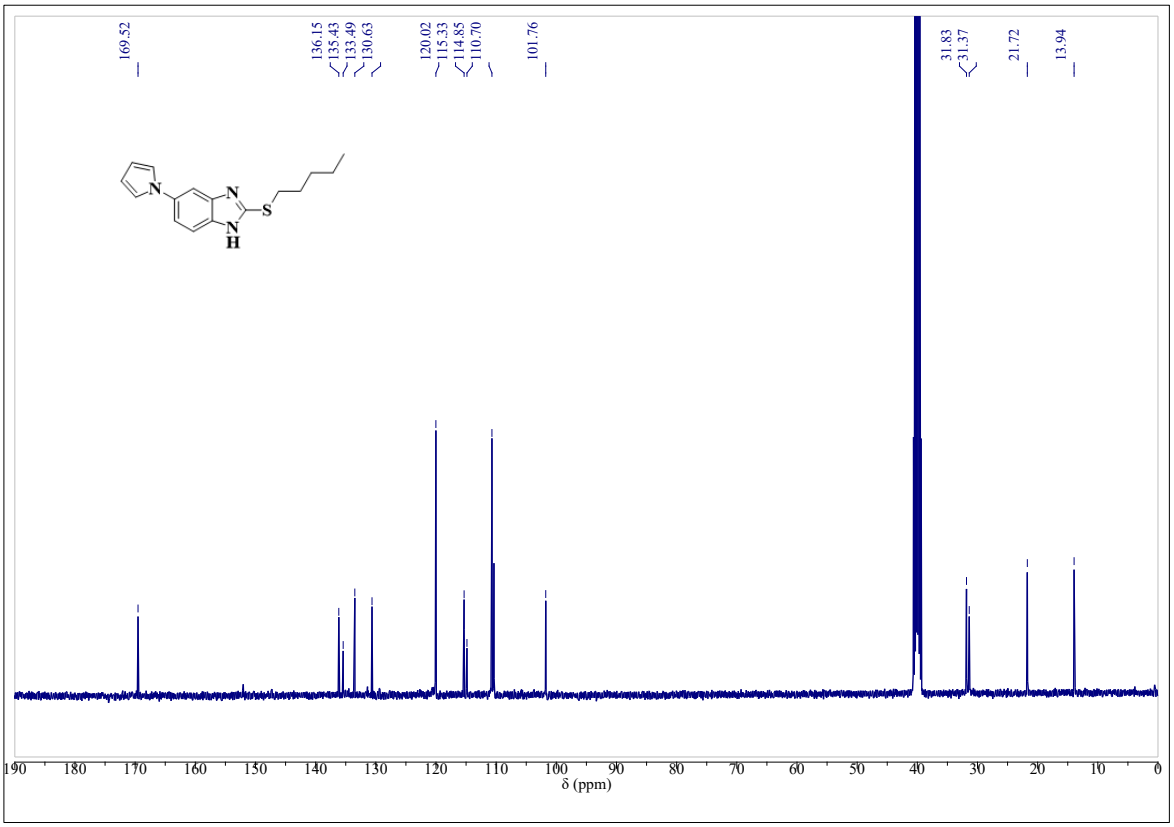

Mass Spectrum of compound 4c:

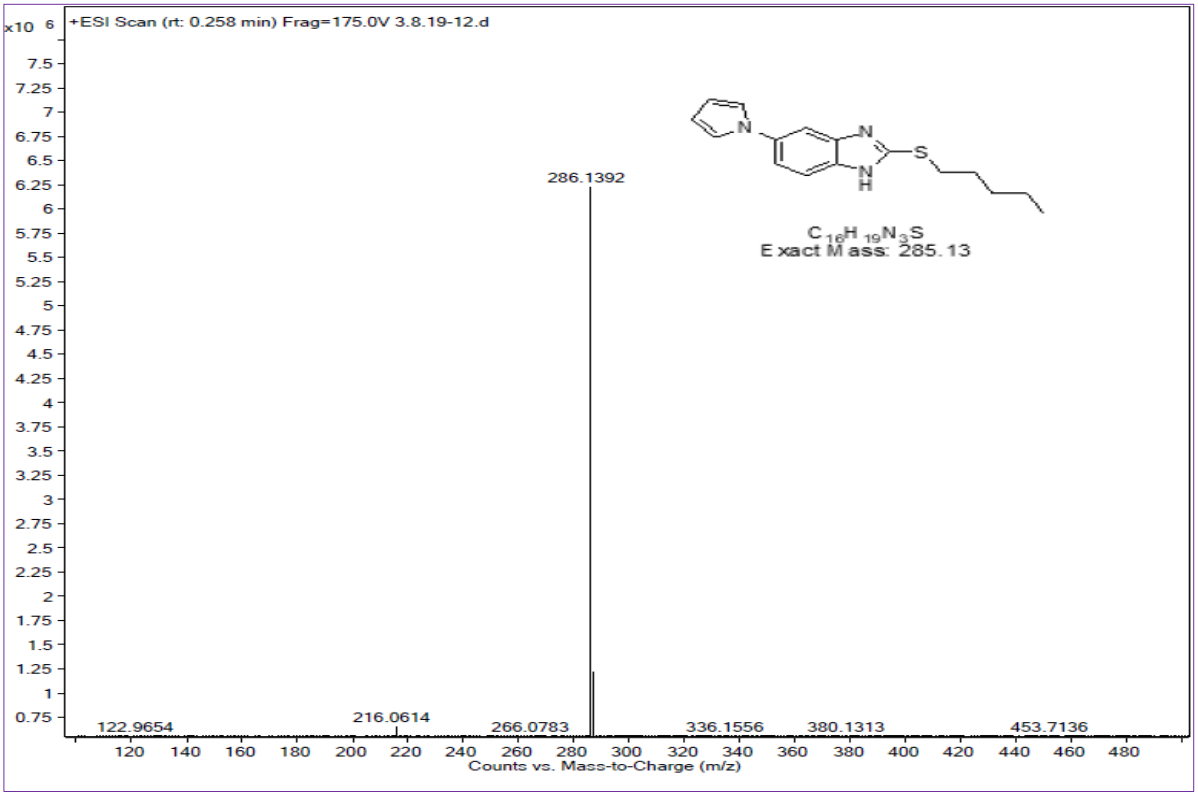

^{1}H-NMR Spectrum of compound 4d (DMSO-*d*$_6$, 400MHz):

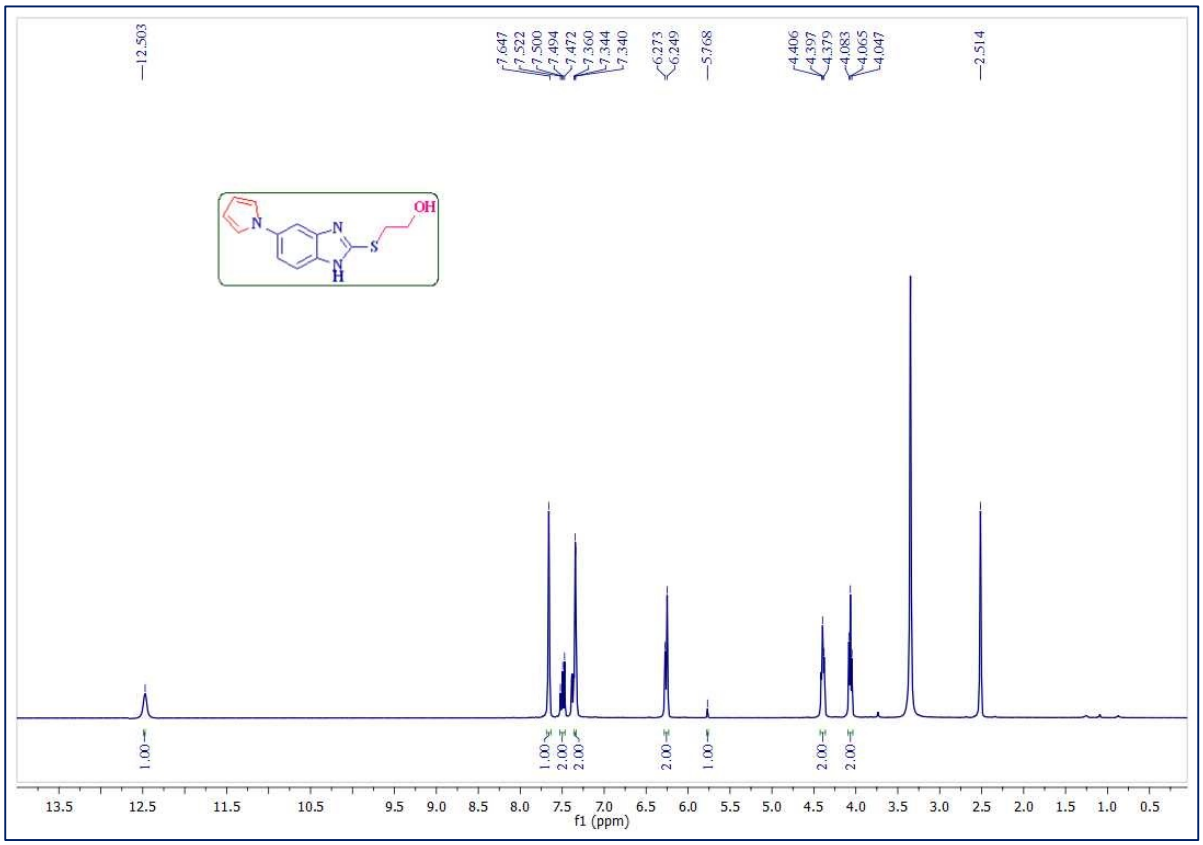

Mass Spectrum of compound 4d:

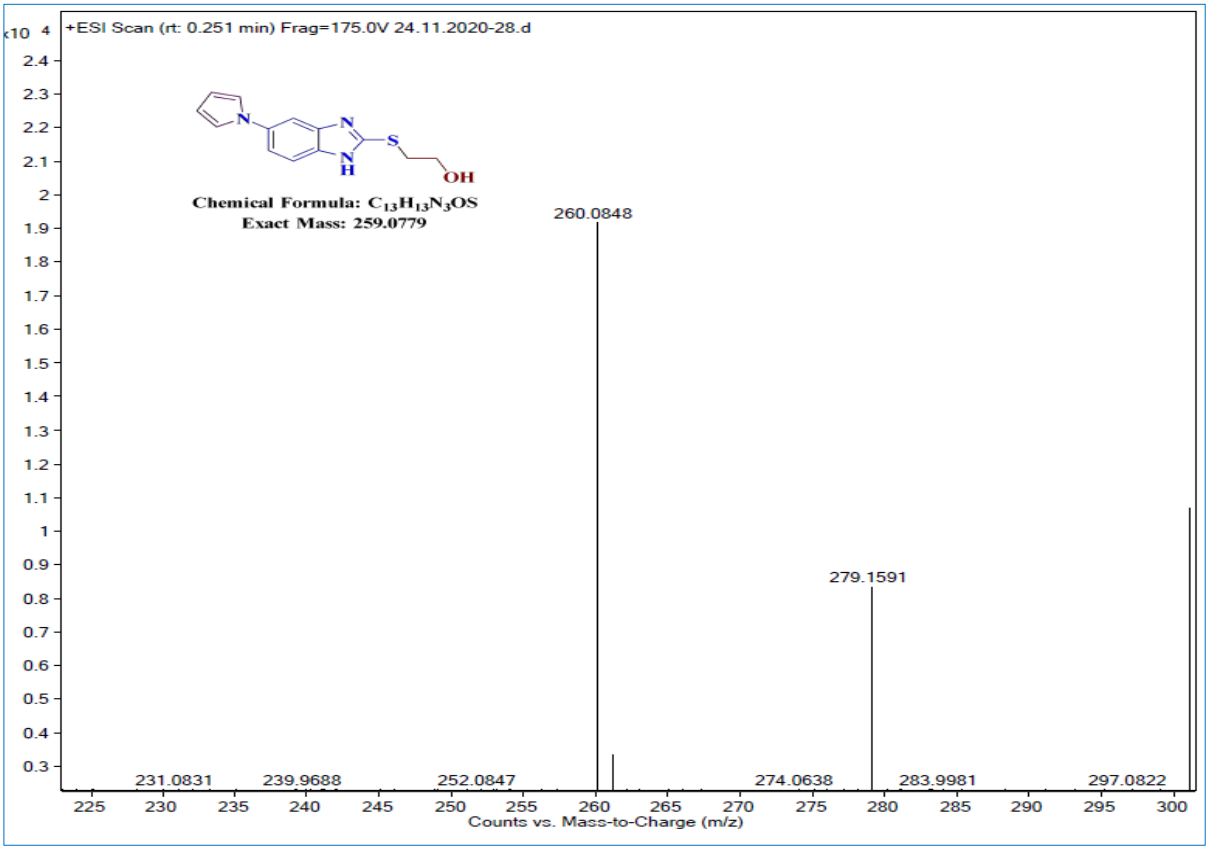

^{1}H-NMR Spectrum of compound 4e ($CDCl_3$+DMSO-d_6, 400MHz):

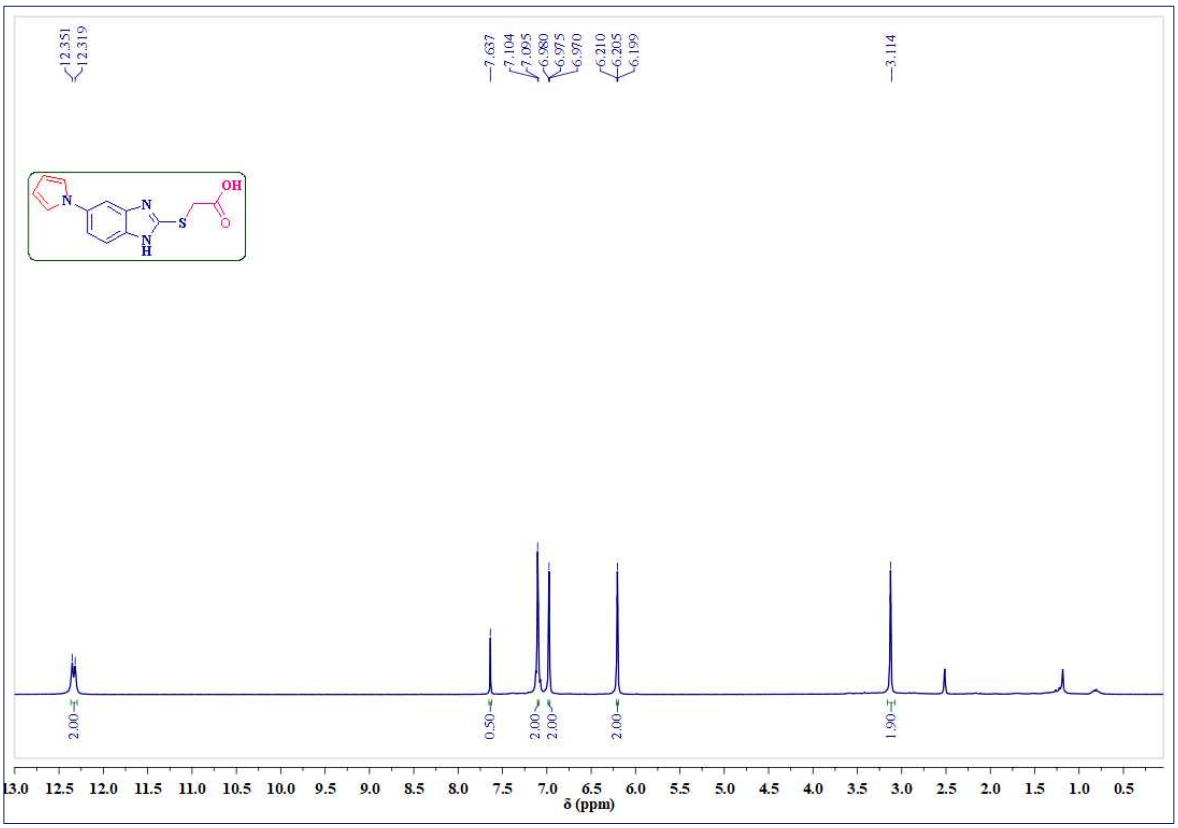

^{13}C-NMR Spectrum of compound 4e (DMSO-d_6, 100MHz):

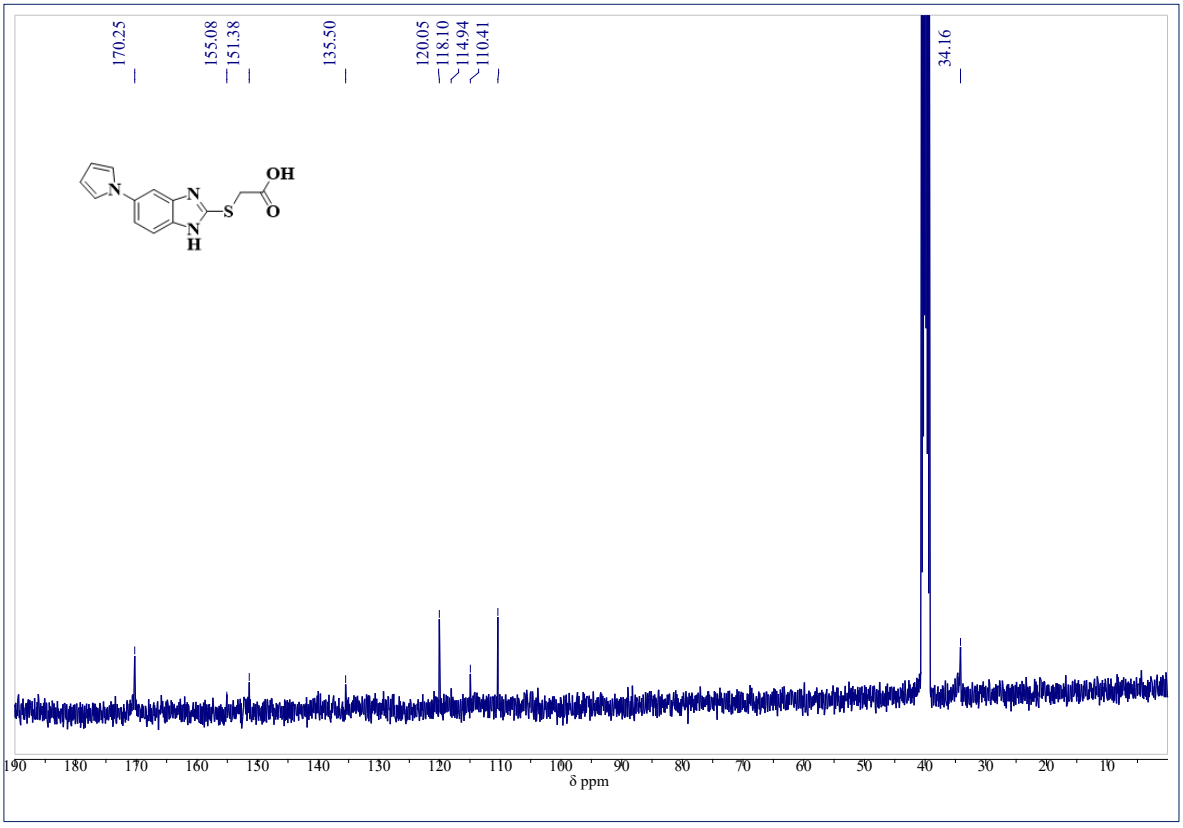

Mass spectrum of compound 4e:

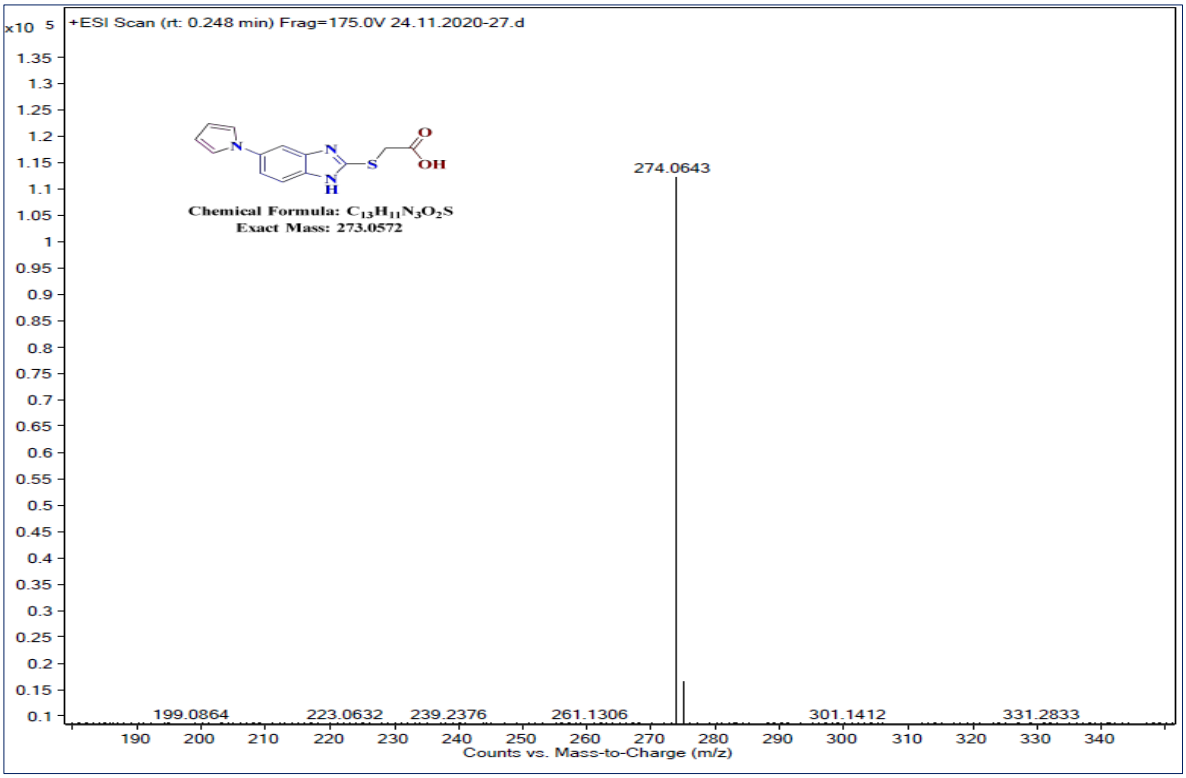

^{1}H-NMR Spectrum of compound 4f (DMSO-*d*$_{6}$, 400MHz):

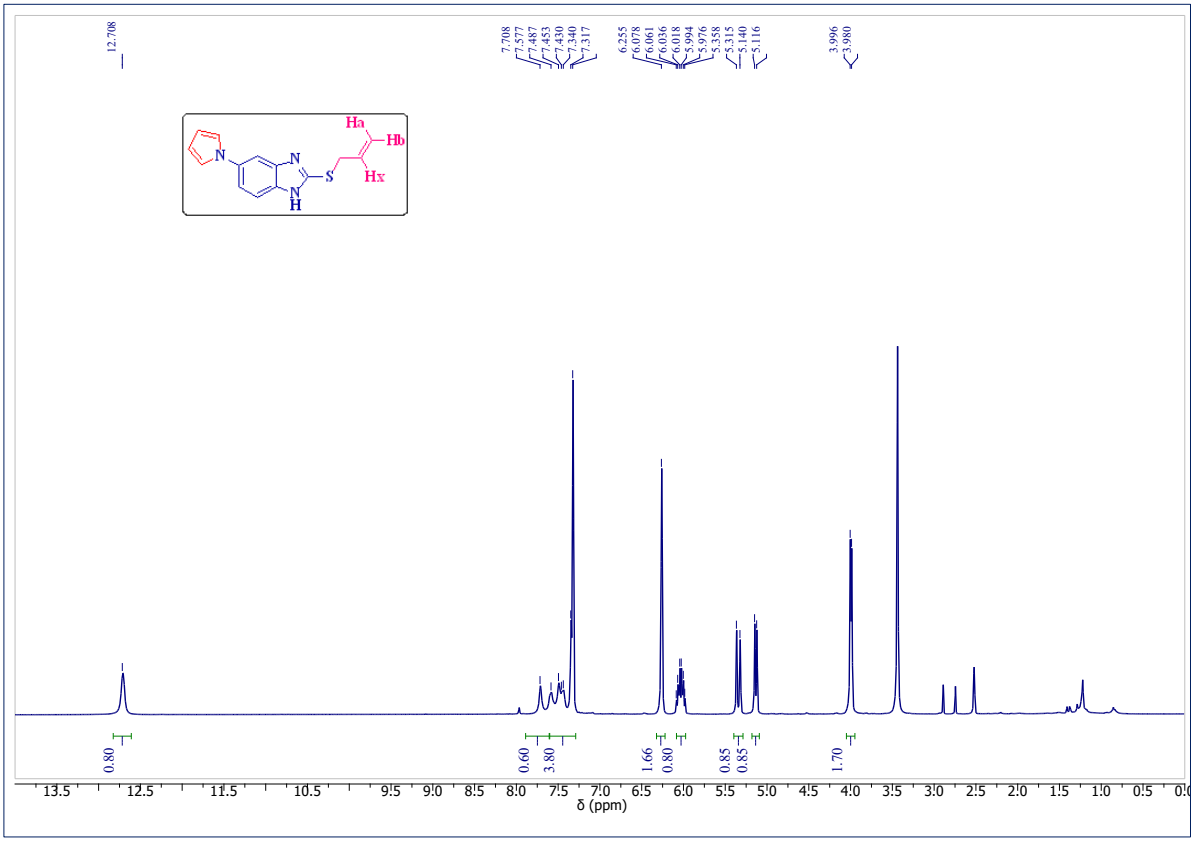

^{13}C-NMR Spectrum of compound 4f (DMSO-*d*$_{6}$, 100MHz):

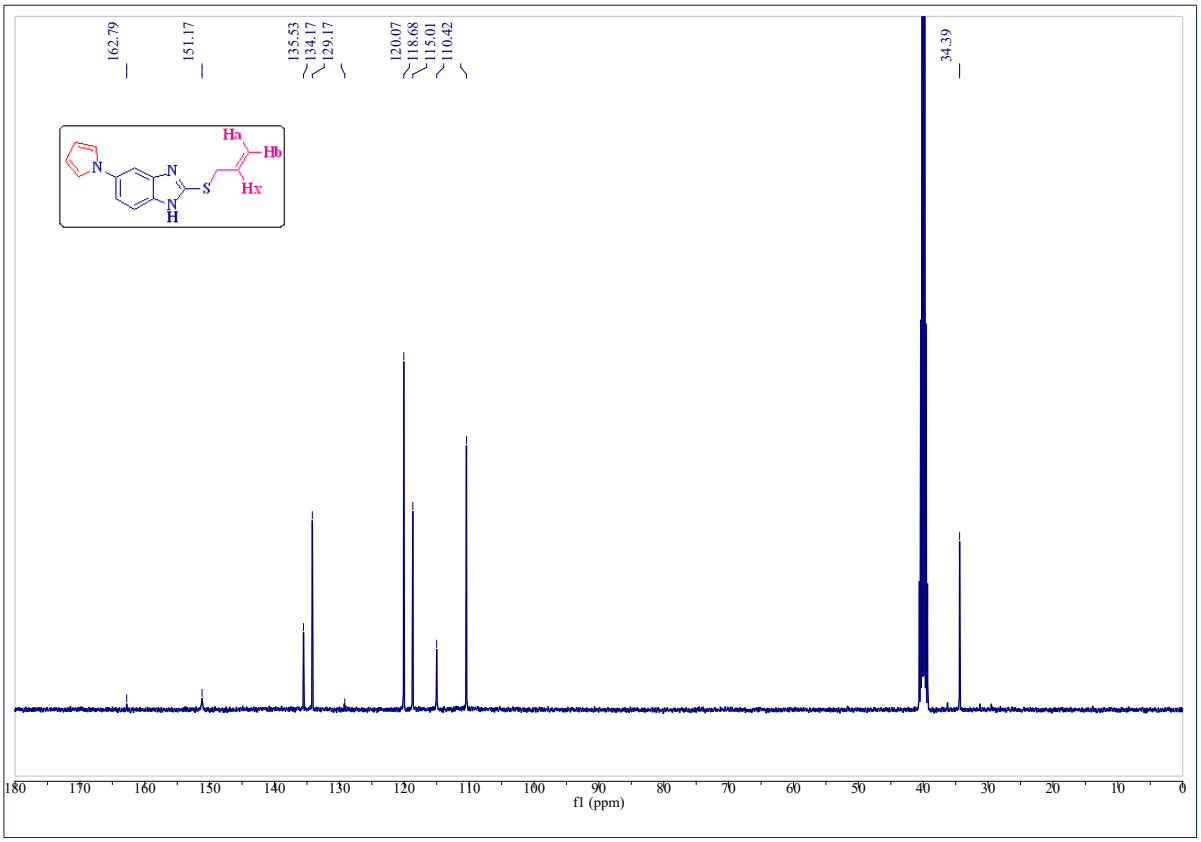

Mass spectrum of compound 4f:

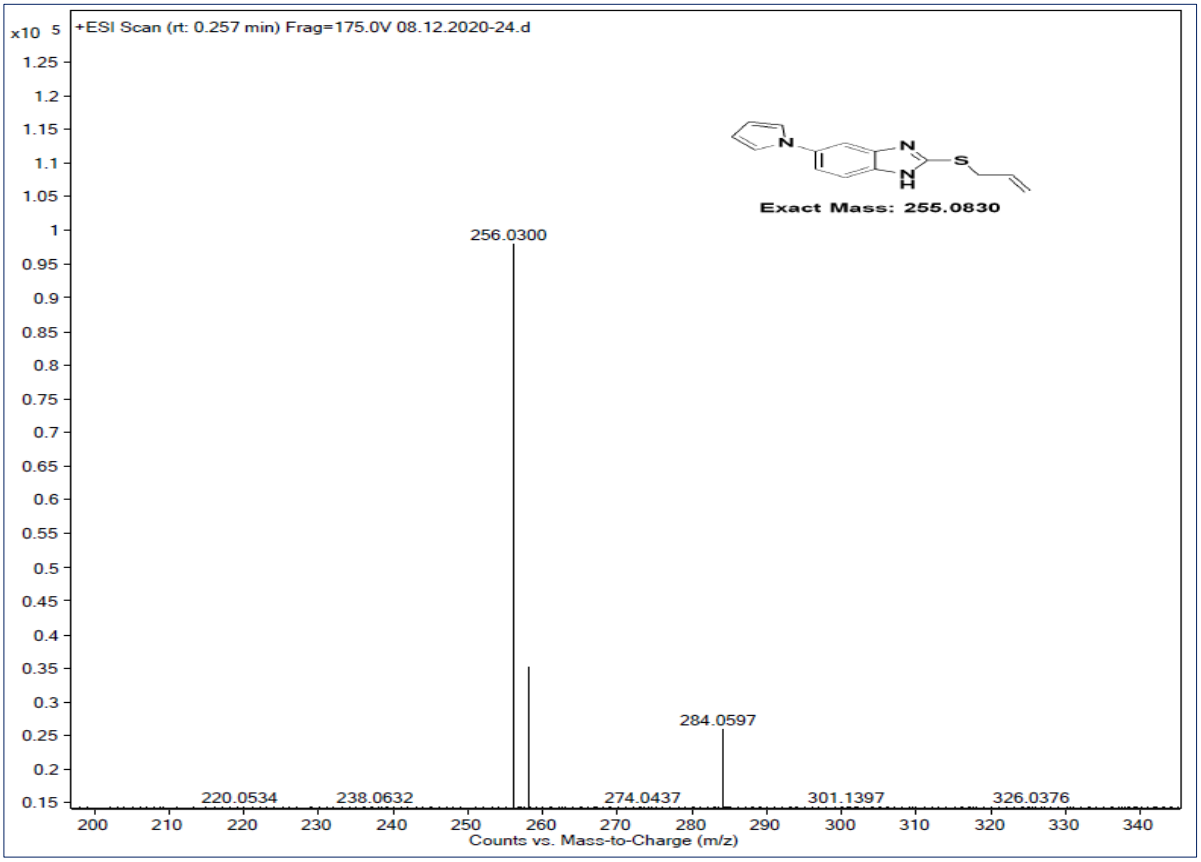

^{1}H-NMR Spectrum of compound 4g ($CDCl_3$, 400MHz):

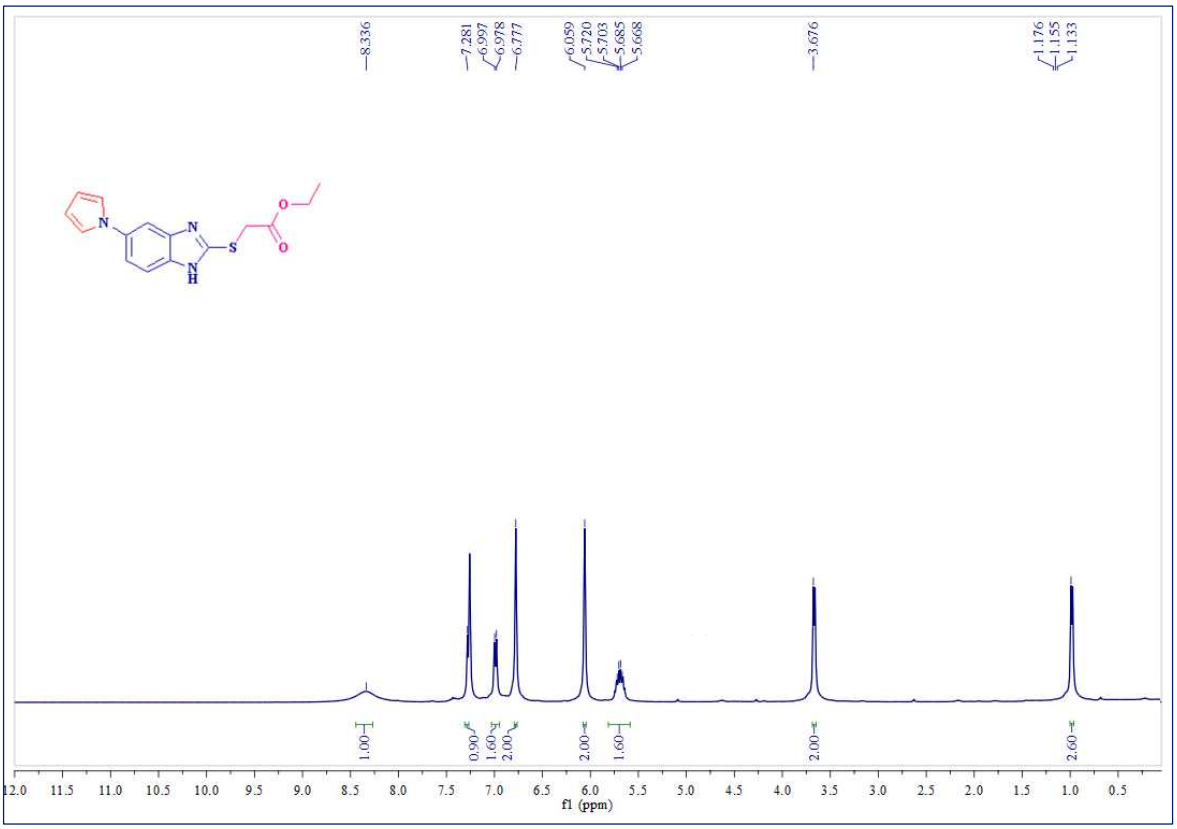

^{13}C NMR Spectrum of compound 4g (DMSO-*d*$_6$, 100MHz):

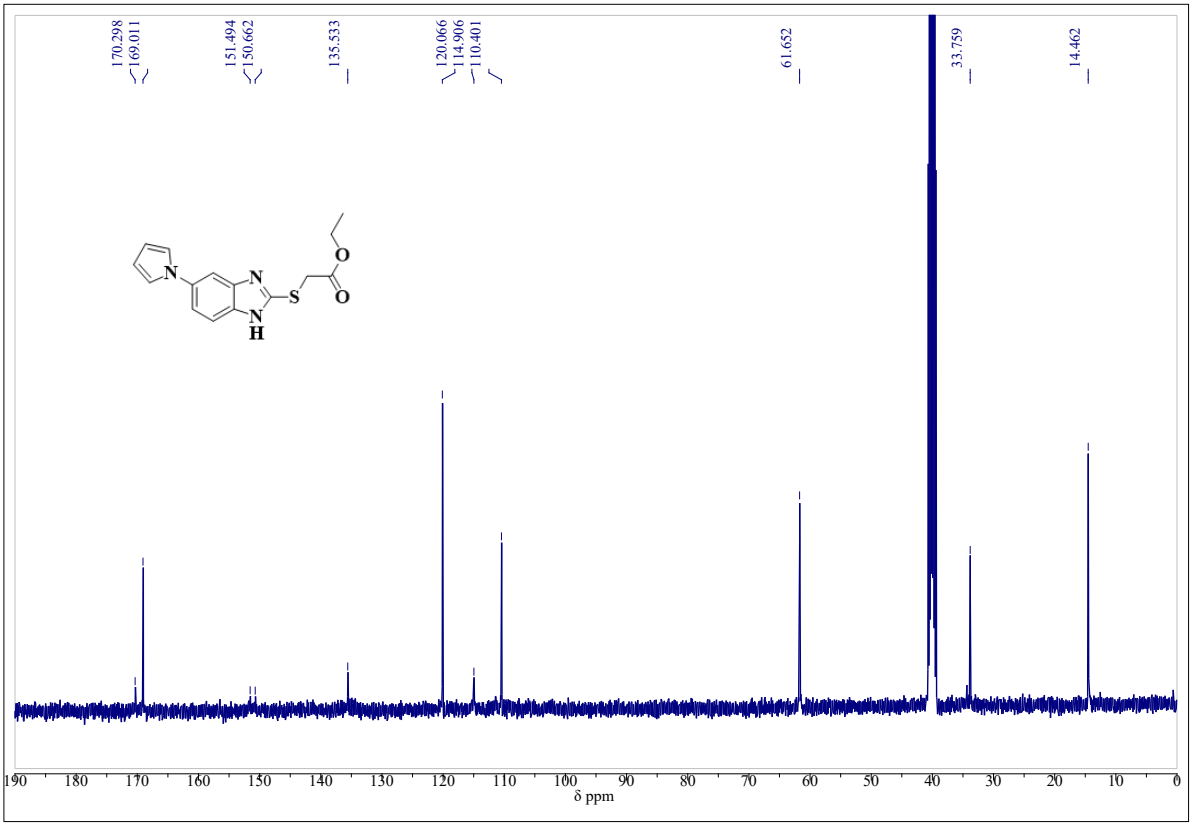

Mass spectrum of compound 4g:

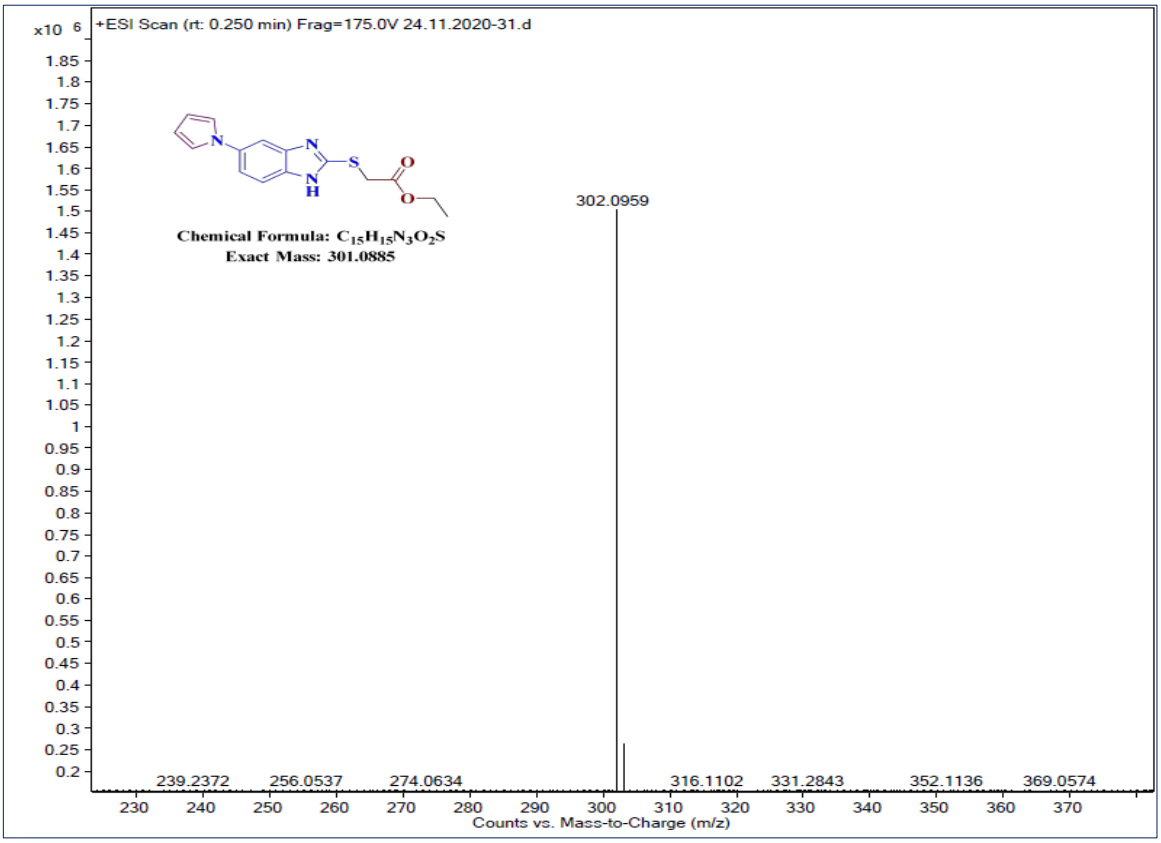

^{1}H-NMR Spectrum of compound 4h ($CDCl_3$+DMSO-d_6, 400MHz):

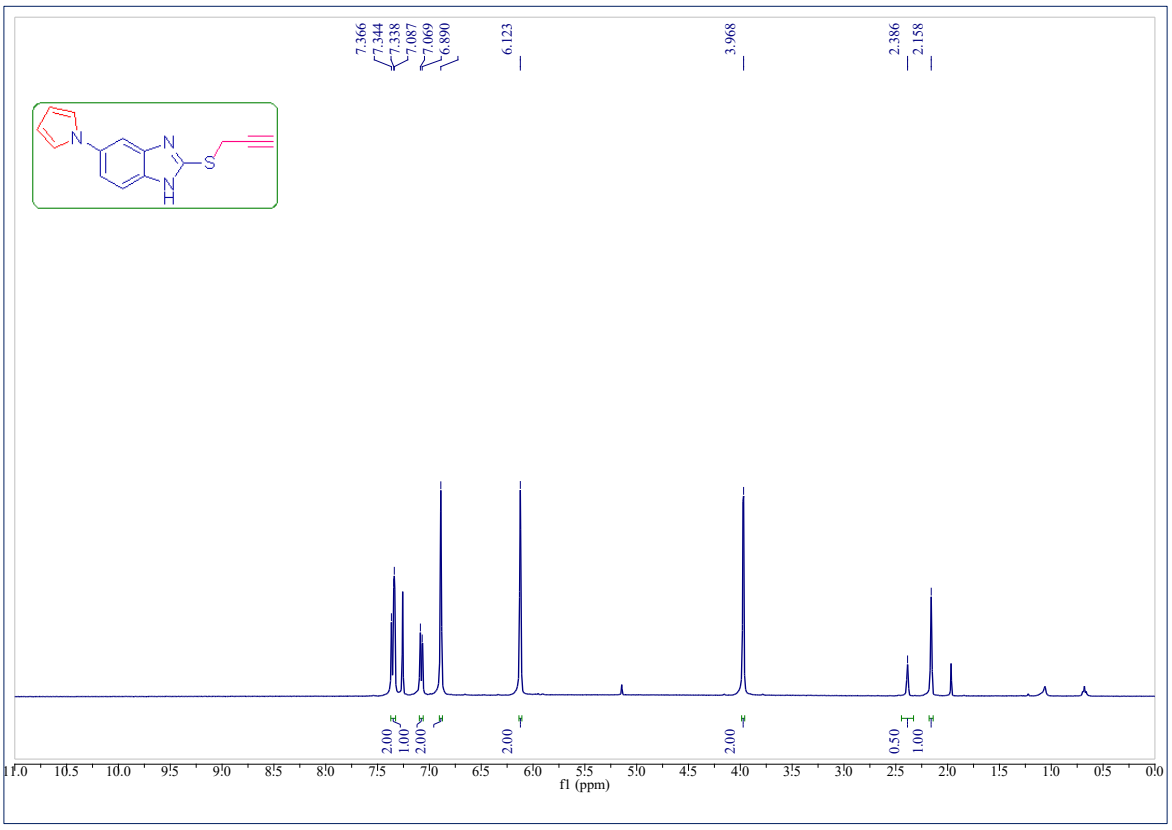

^{13}C NMR Spectrum of compound 4h (DMSO-d_6, 100MHz):

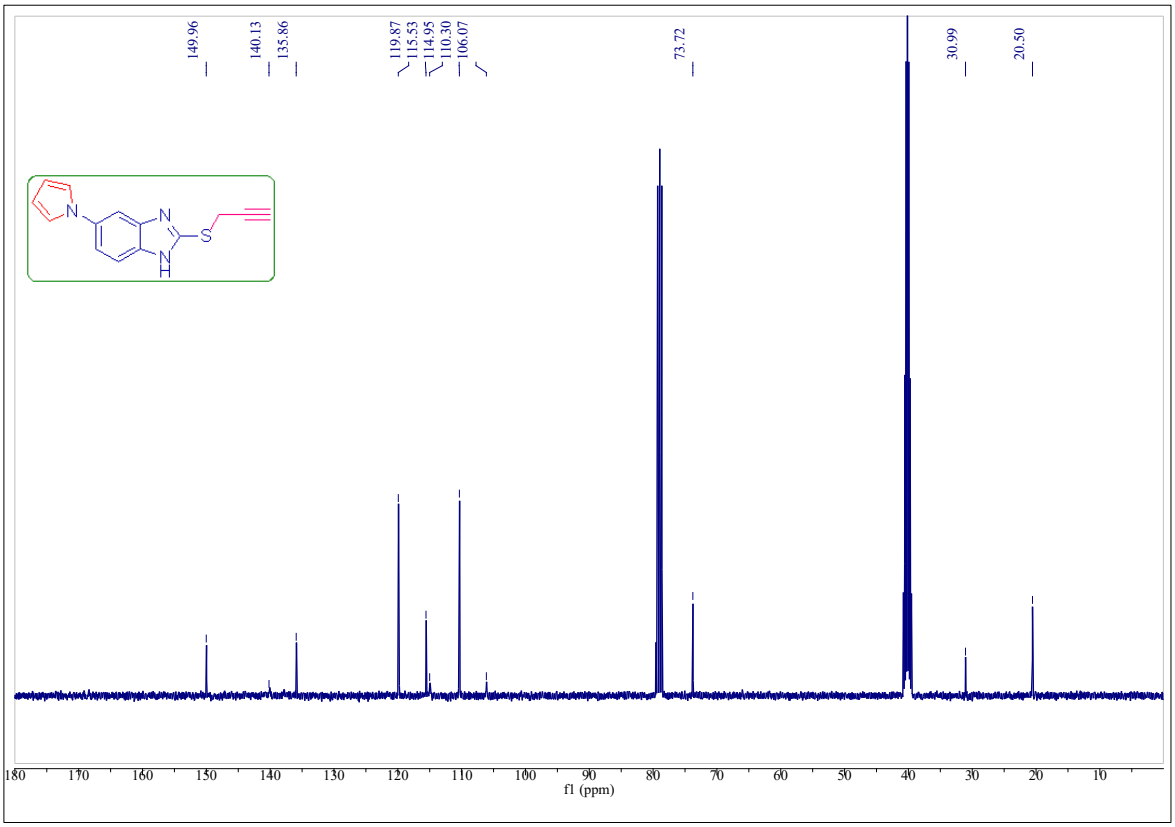

Mass spectrum of compound 4h:

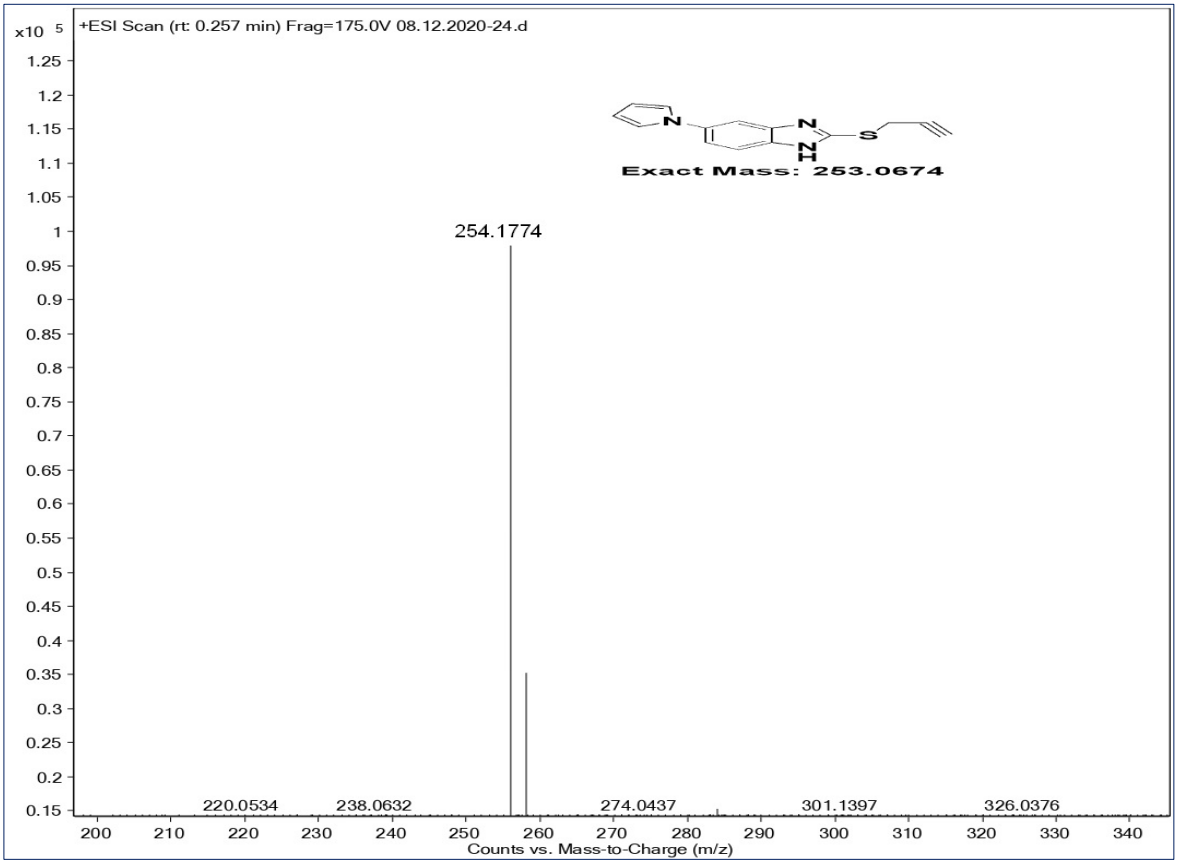

^{1}H-NMR Spectrum of compound 4i (DMSO-d_6, 400MHz):

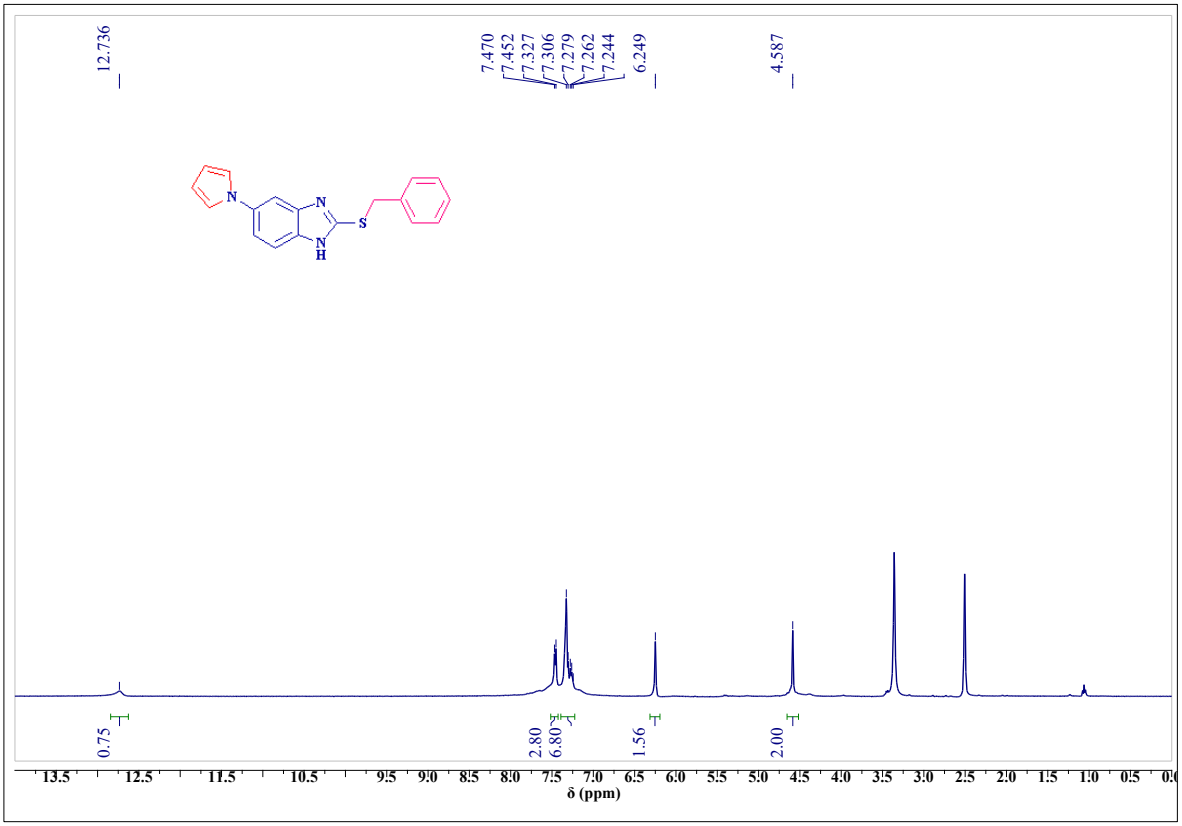

^{13}C-NMR Spectrum of compound 4i (DMSO-*d*$_6$, 100MHz):

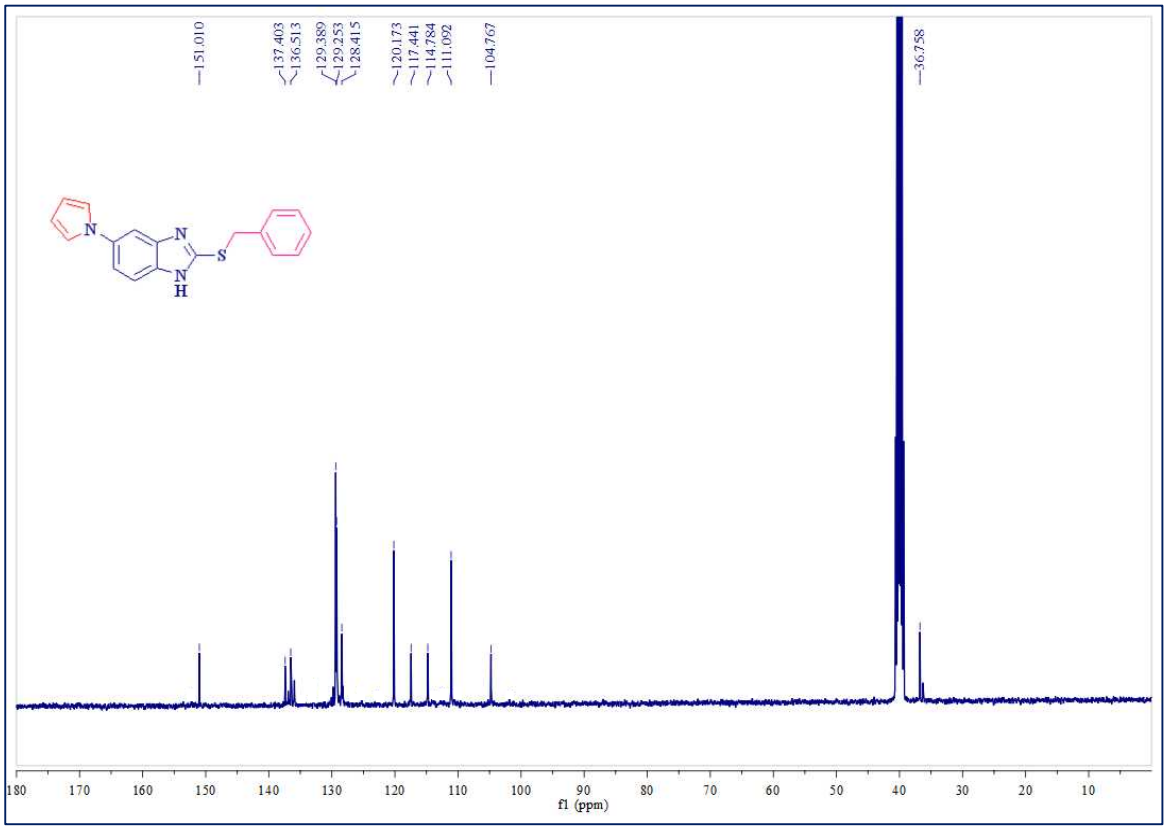

Mass spectrum of compound 4i:

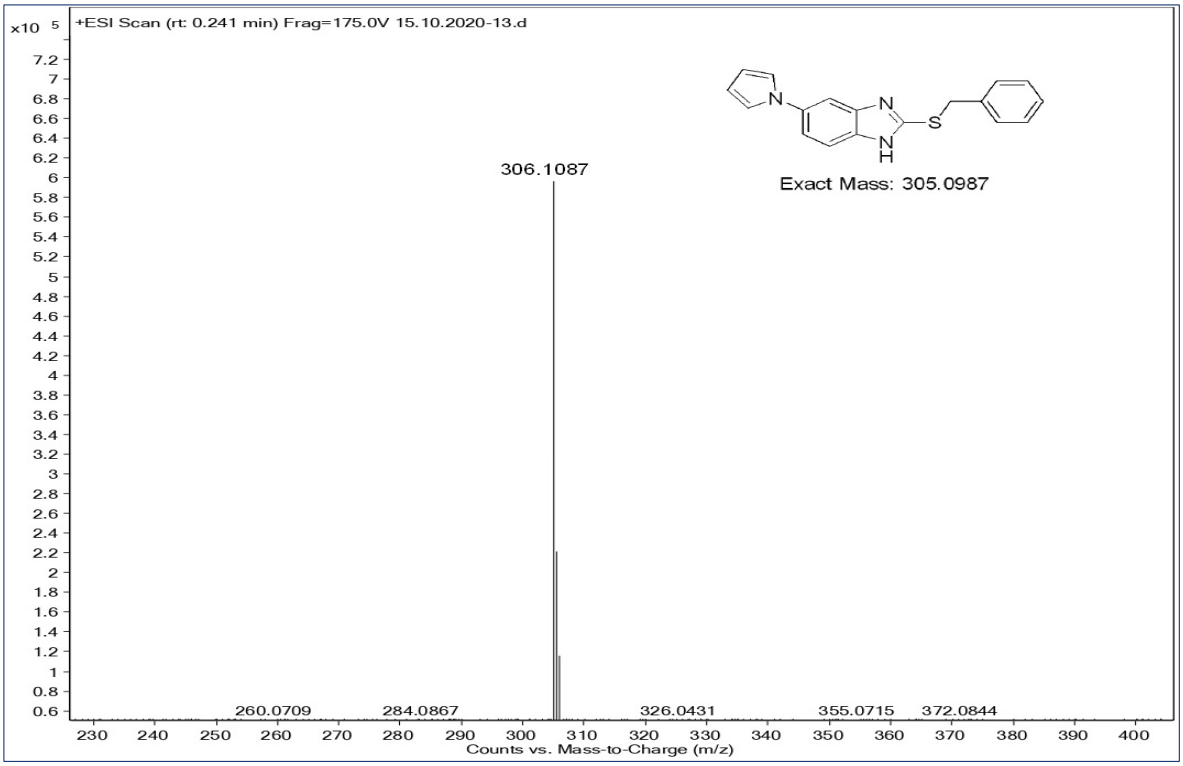

^{1}H-NMR Spectrum of compound 4j (DMSO-*d*$_6$, 400MHz):

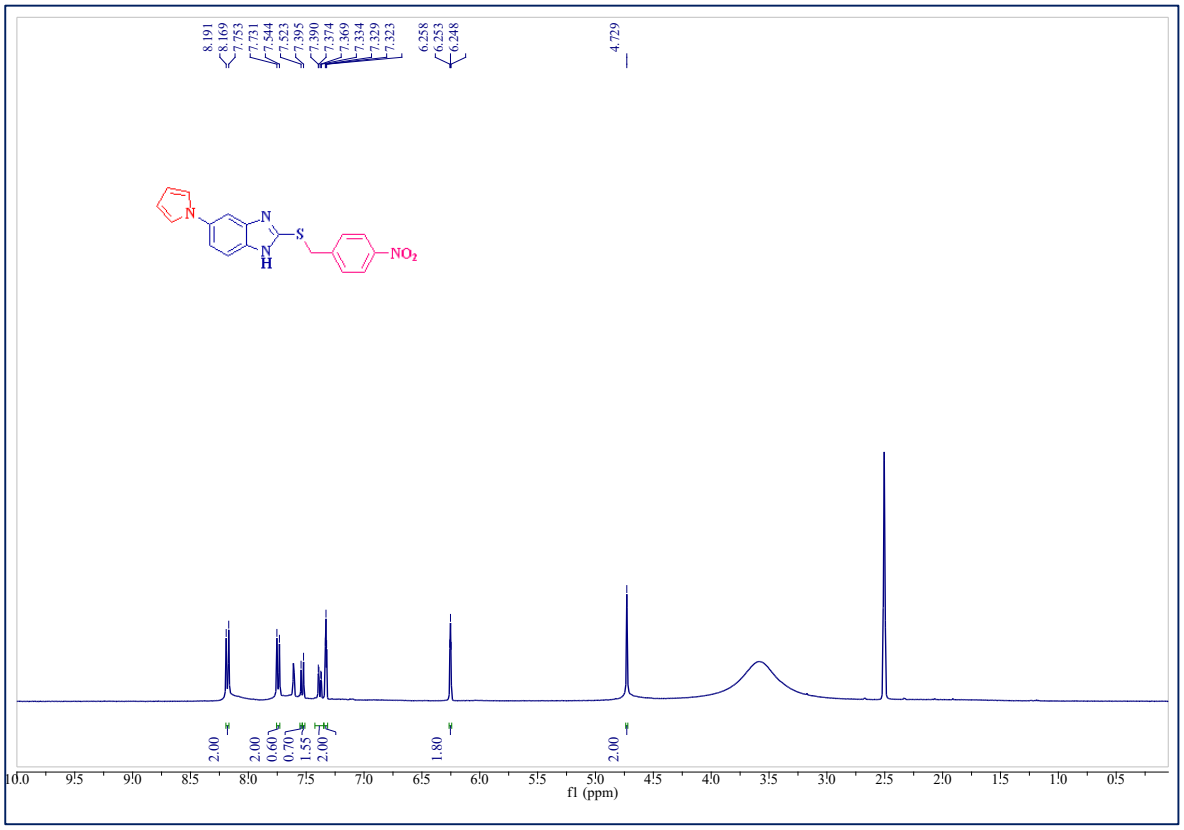

^{13}C NMR Spectrum of compound 4j (DMSO-*d*$_6$, 100MHz):

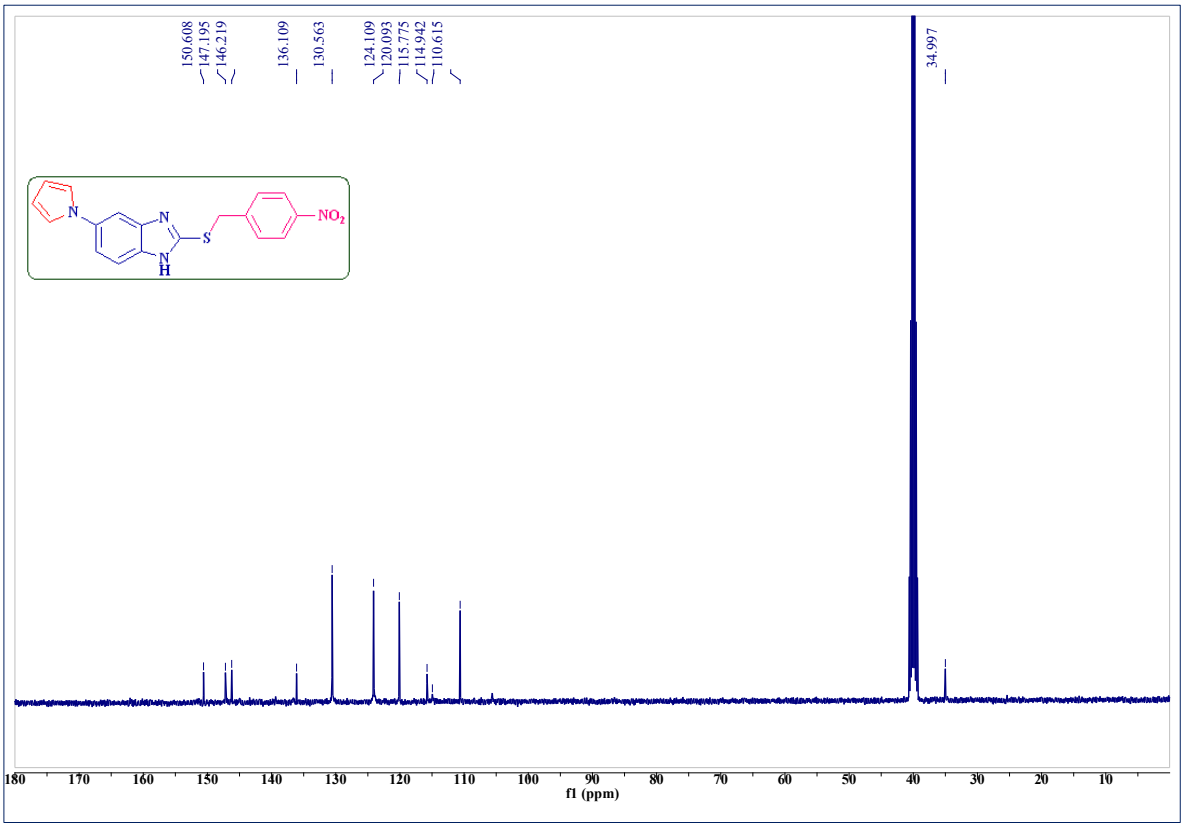

Mass spectrum of compound 4j:

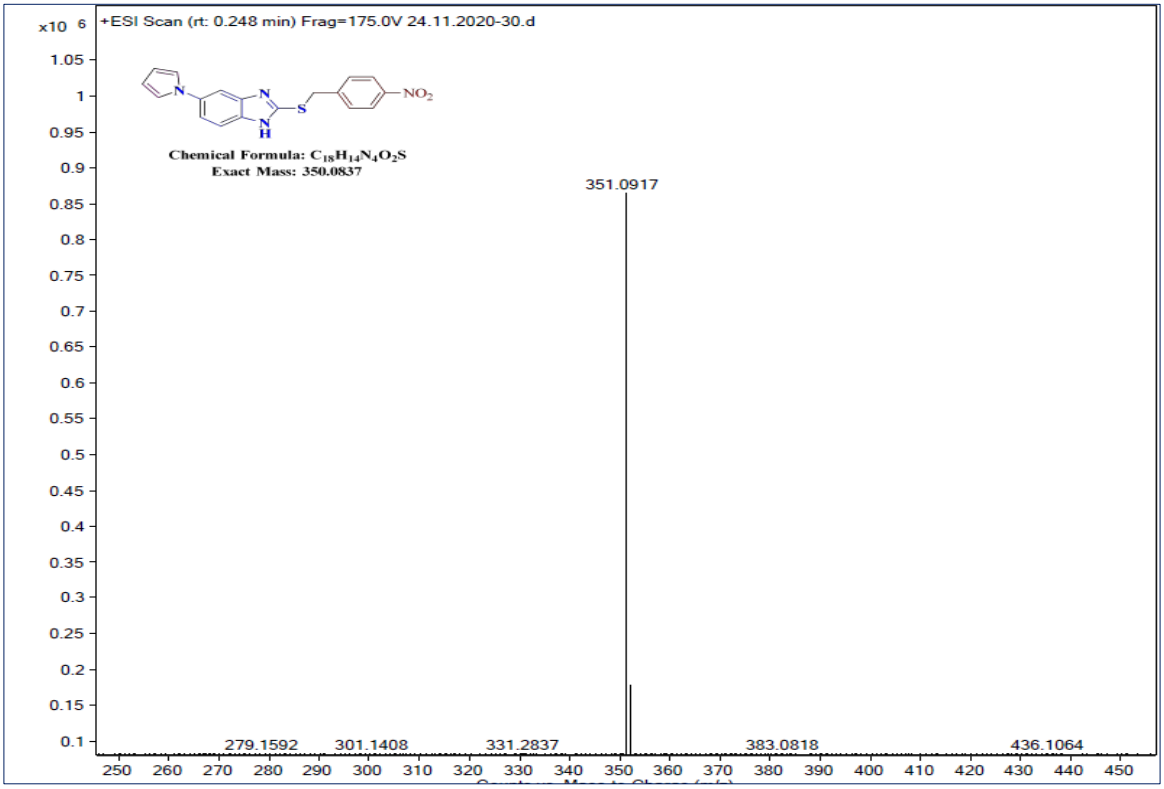

^{1}H-NMR Spectrum of compound 4k (DMSO-d_6, 400MHz):

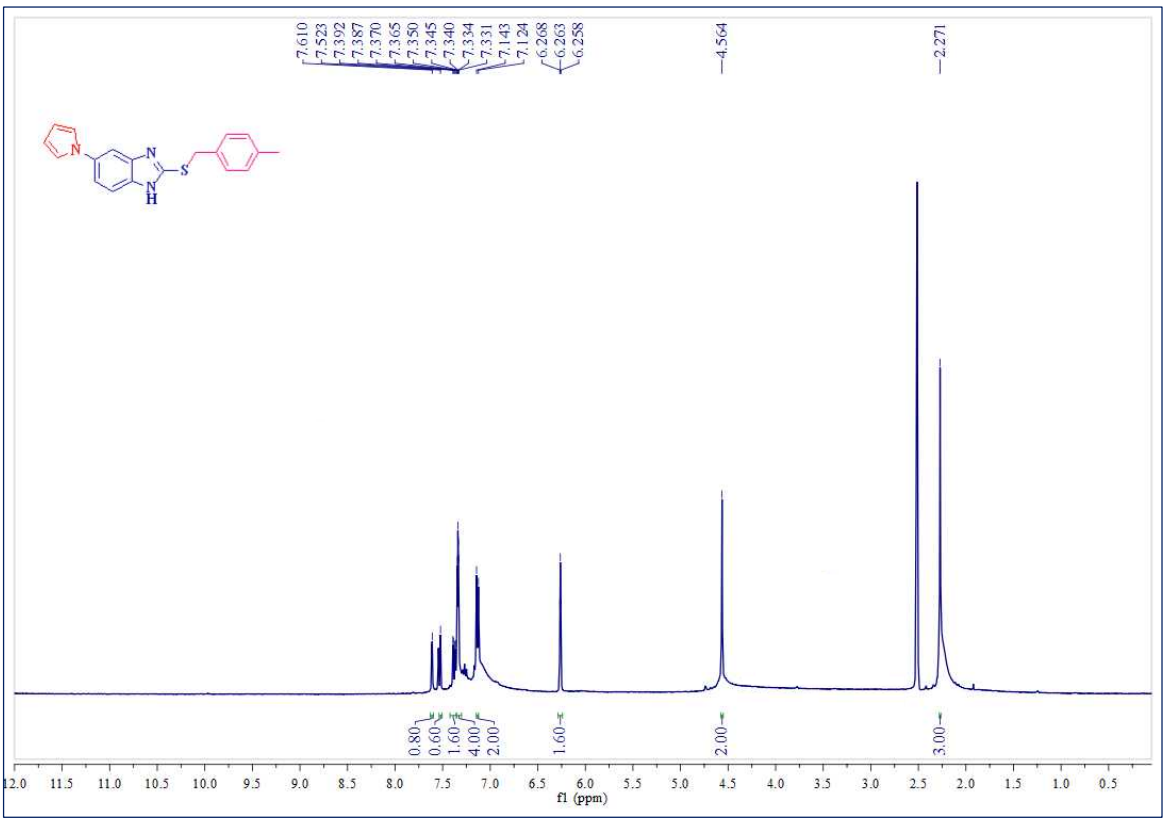

^{13}C-NMR Spectrum of compound 4k (DMSO-d_6, 100MHz):

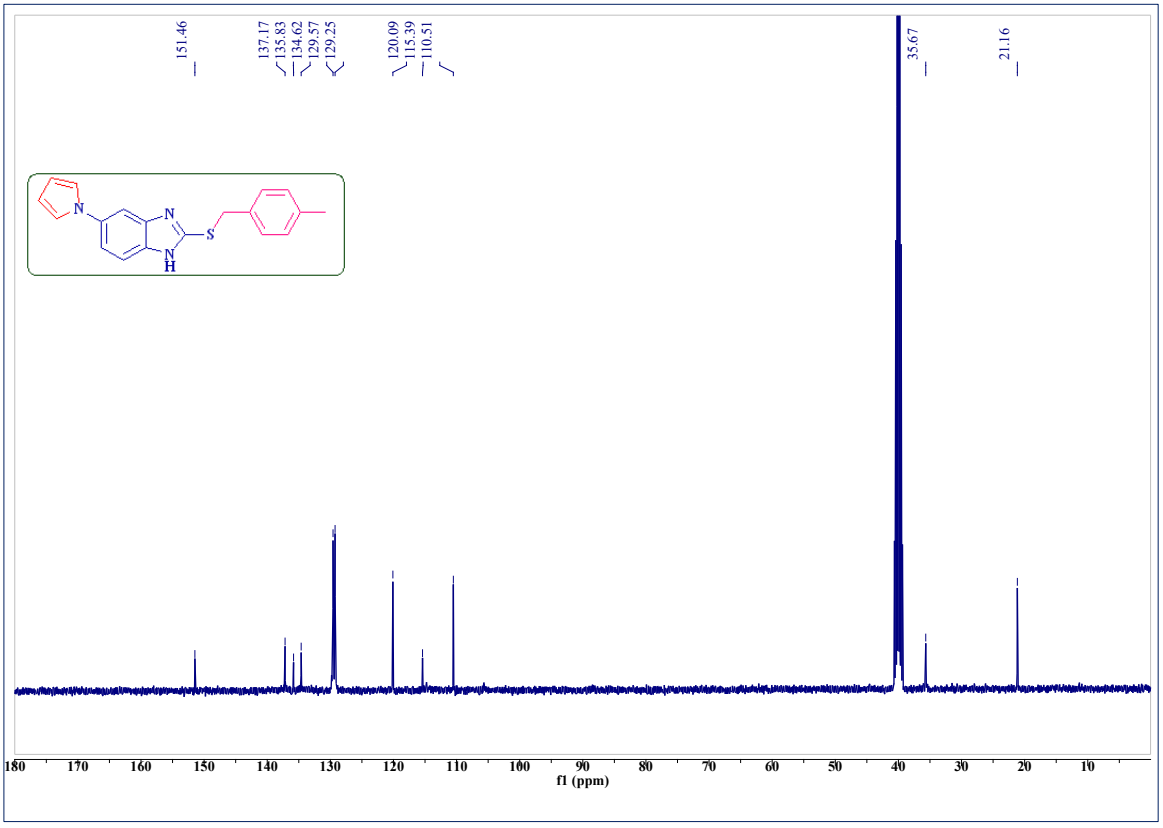

Mass spectrum of compound 4k:

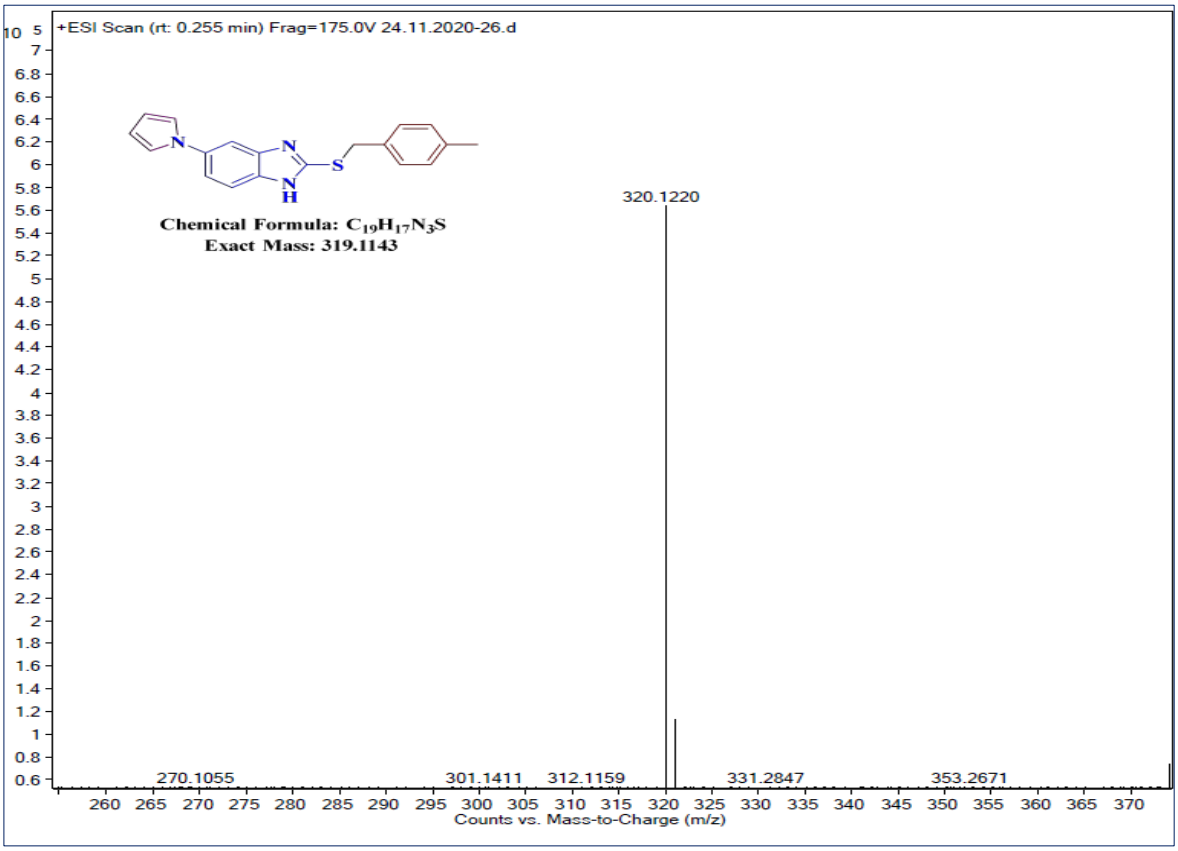

^{1}H-NMR Spectrum of compound 4l (CDCl$_3$+DMSO-*d*$_6$, 400MHz):

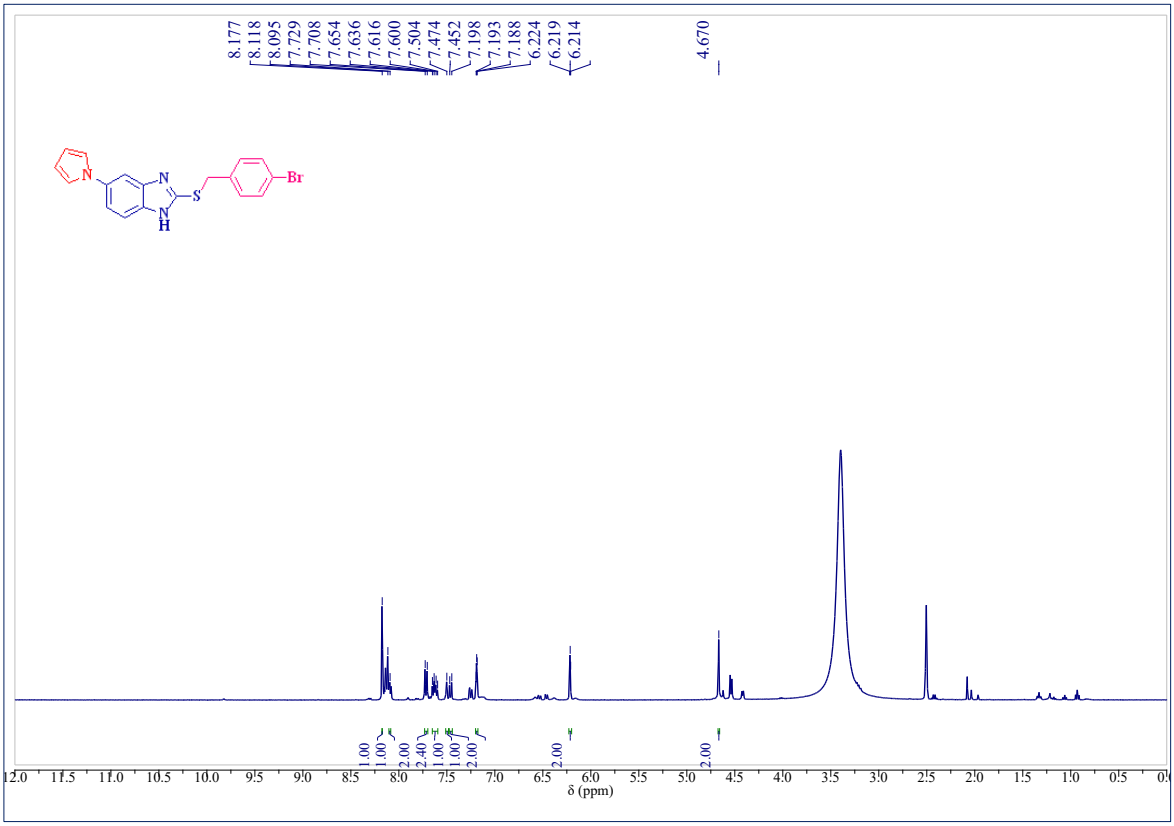

^{13}C-NMR Spectrum of compound 4l (DMSO-*d*$_6$, 100MHz):

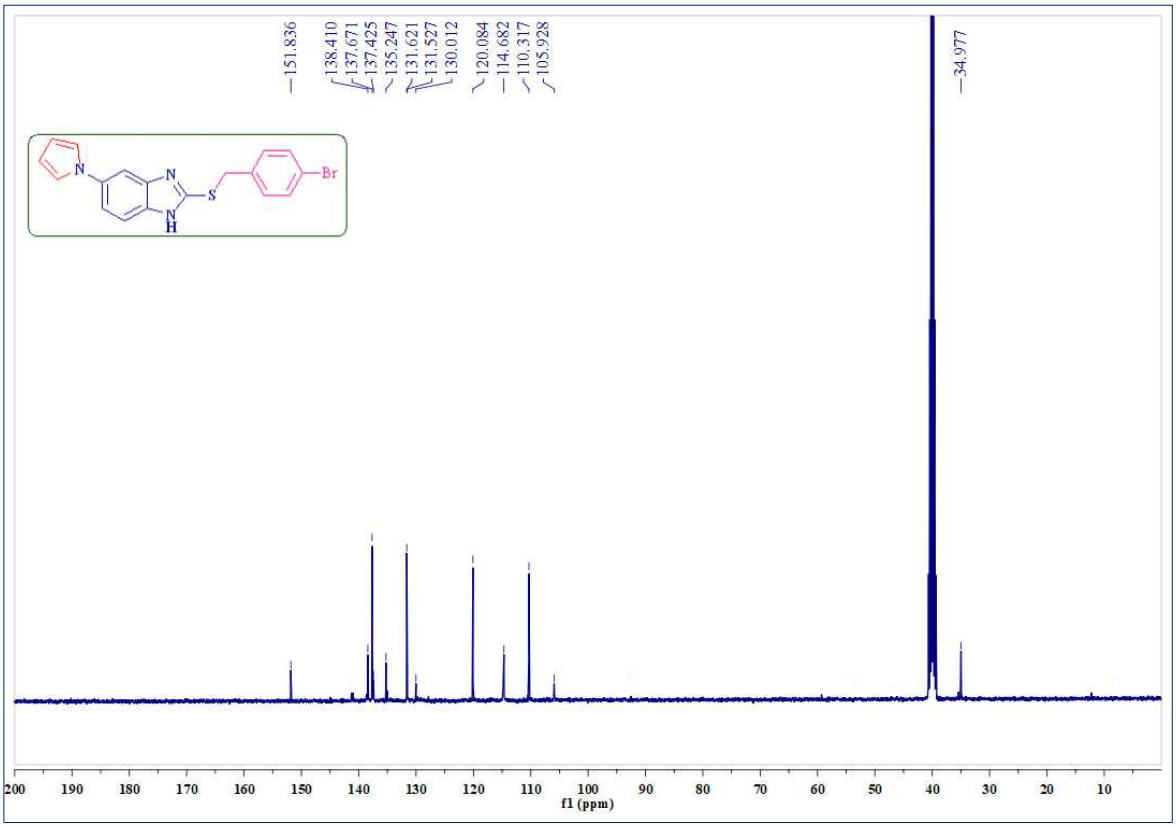

Mass spectrum of compound 4l:

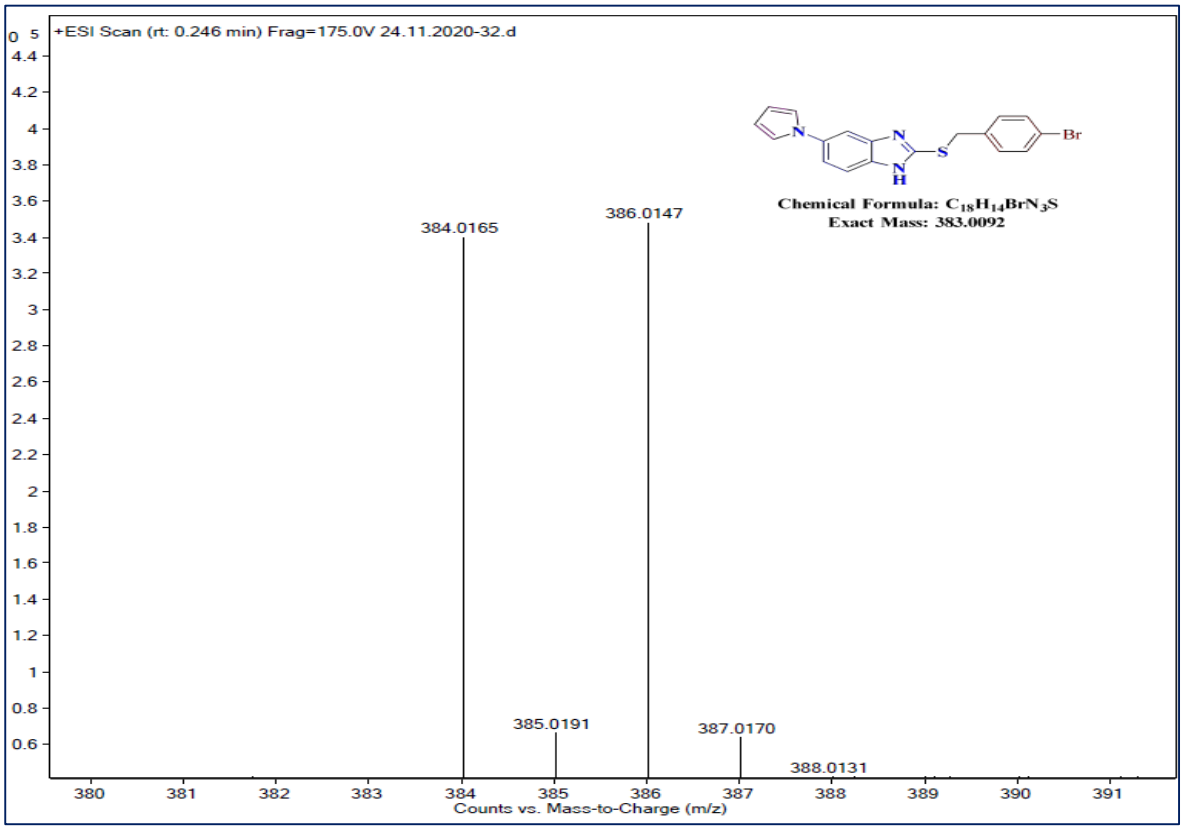

^{1}H-NMR Spectrum of compound 4m ($CDCl_3$+DMSO-d_6, 400MHz):

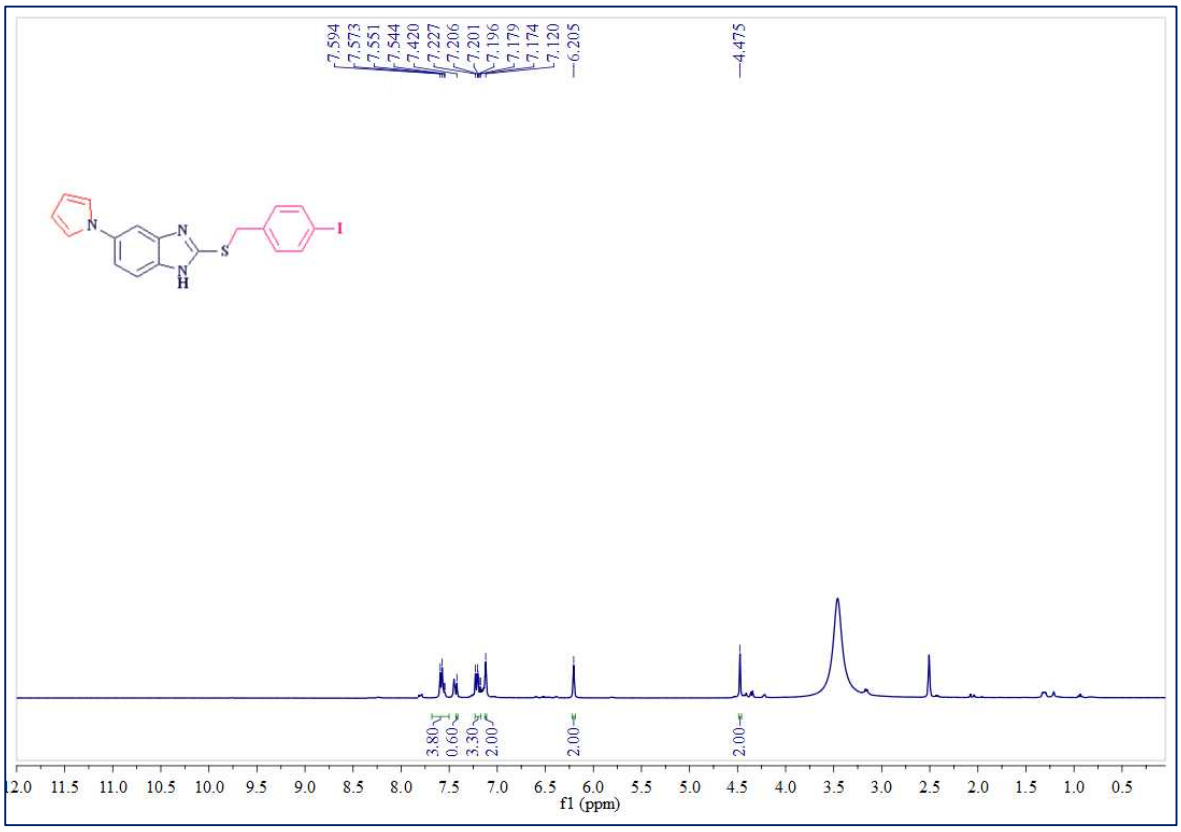

^{13}C-NMR Spectrum of compound 4m (DMSO-d_6, 100MHz):

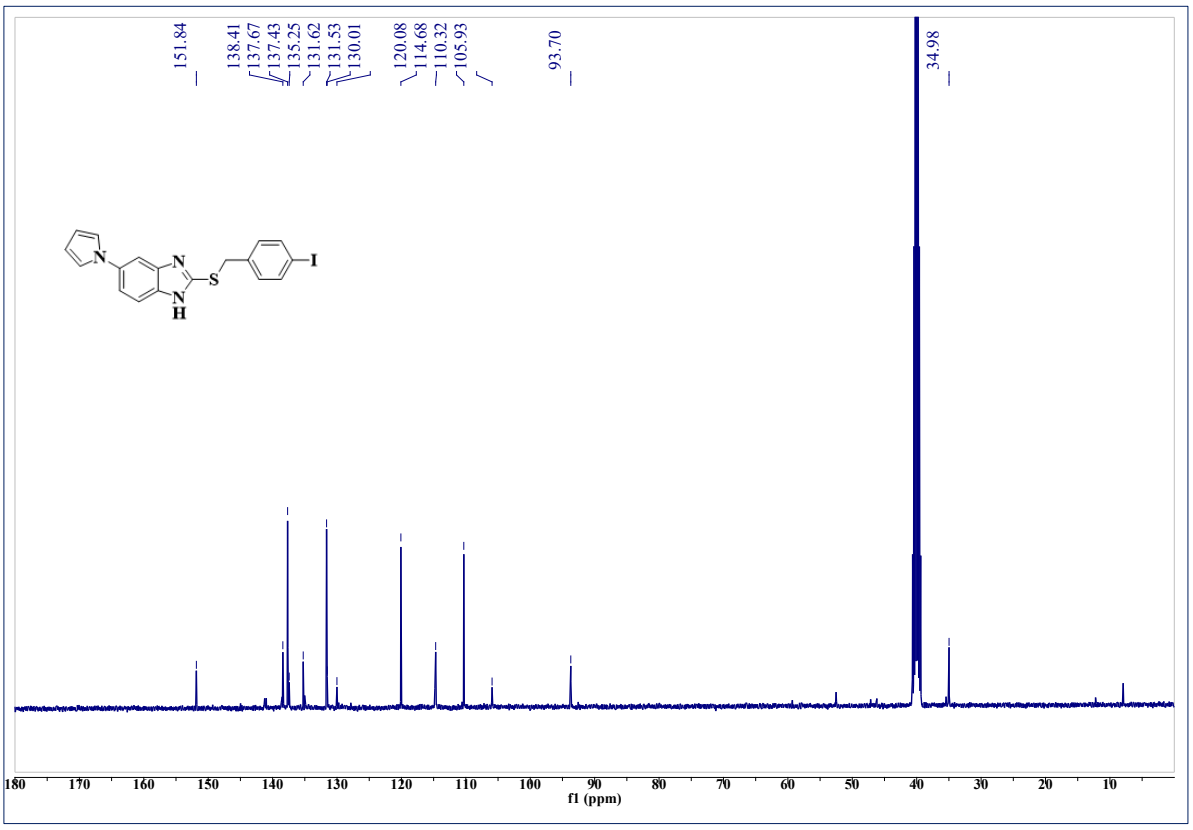

Mass spectrum of compound 4m:

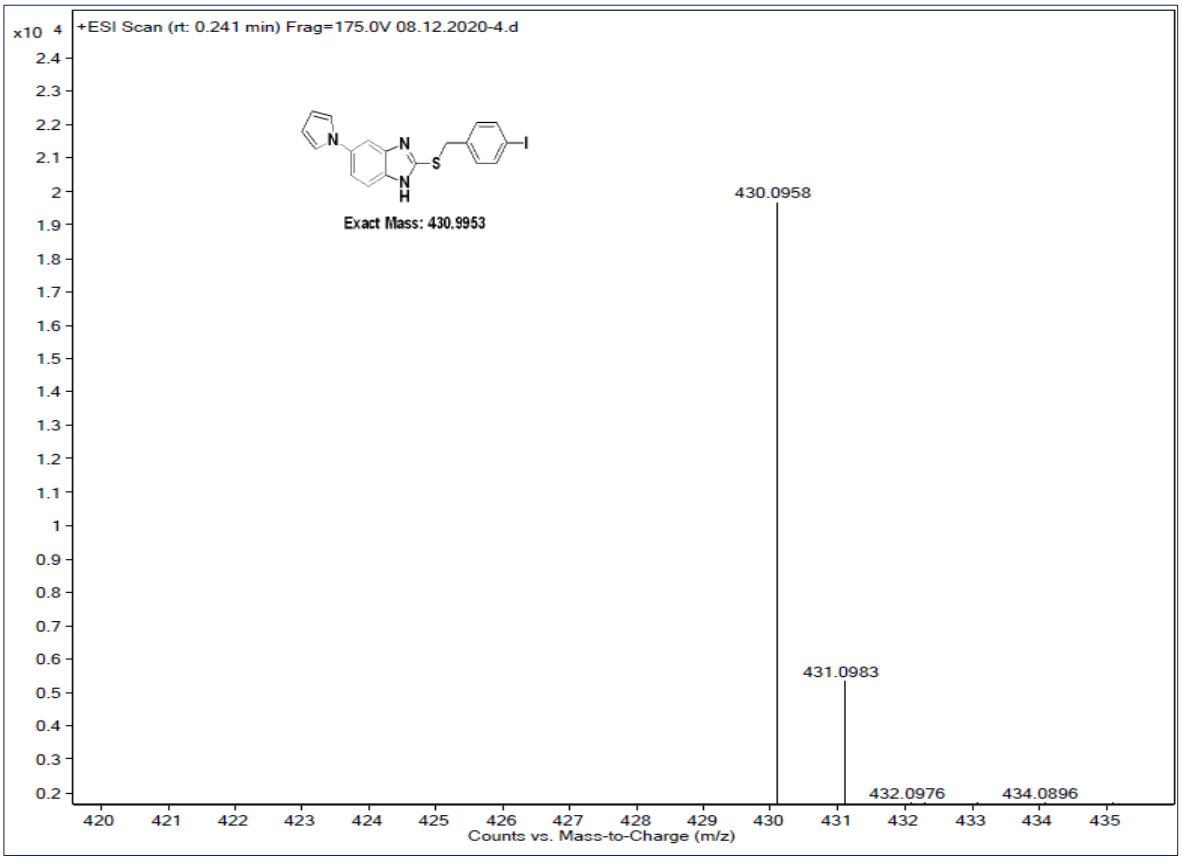

^{1}H-NMR Spectrum of compound 4n ($CDCl_3$+DMSO-d_6, 400MHz):

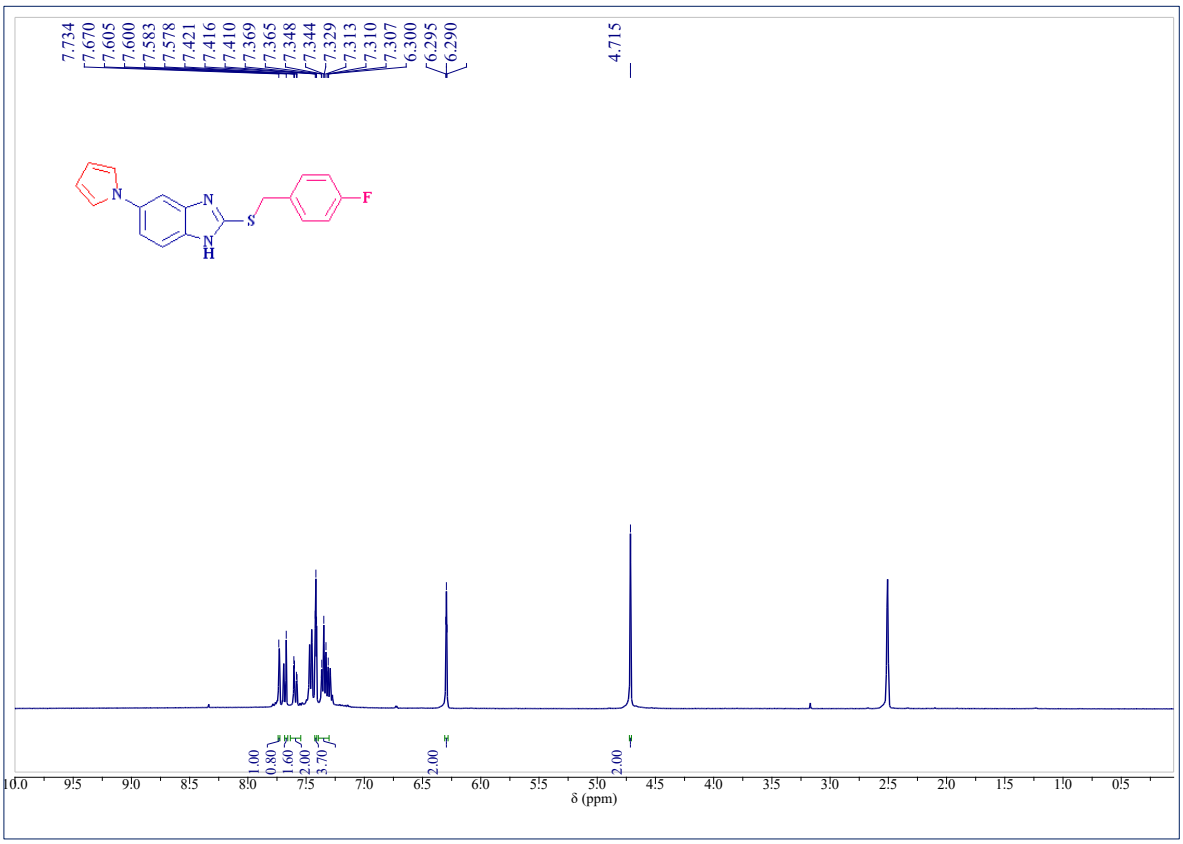

^{13}C-NMR Spectrum of compound 4n (DMSO-d_6, 100MHz):

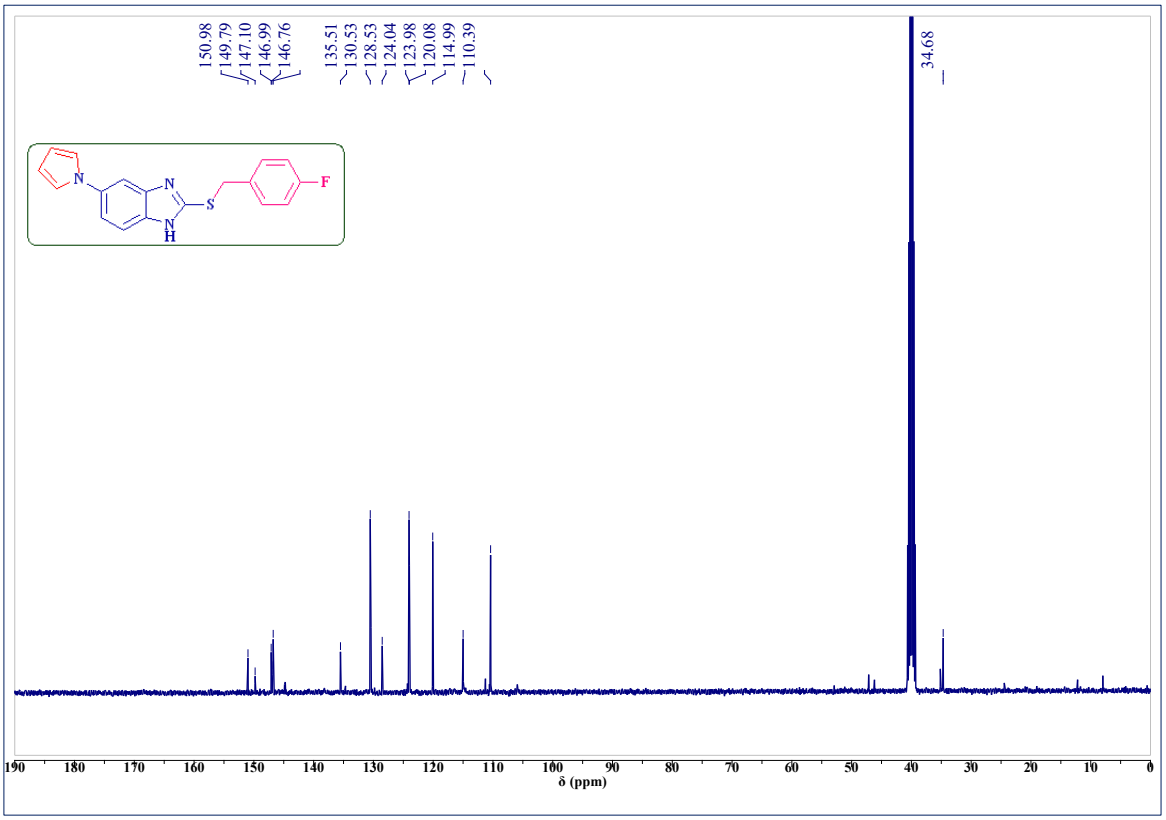

Mass spectrum of compound 5n

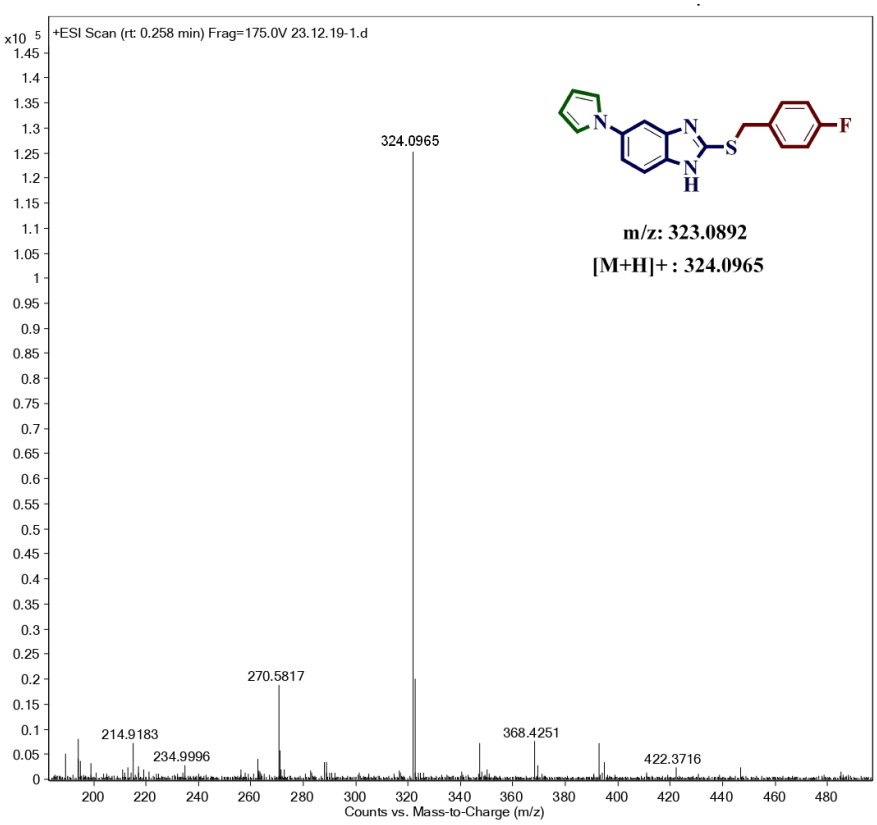

^{1}H-NMR Spectrum of compound 5o ($CDCl_3$+DMSO-d_6, 400MHz):

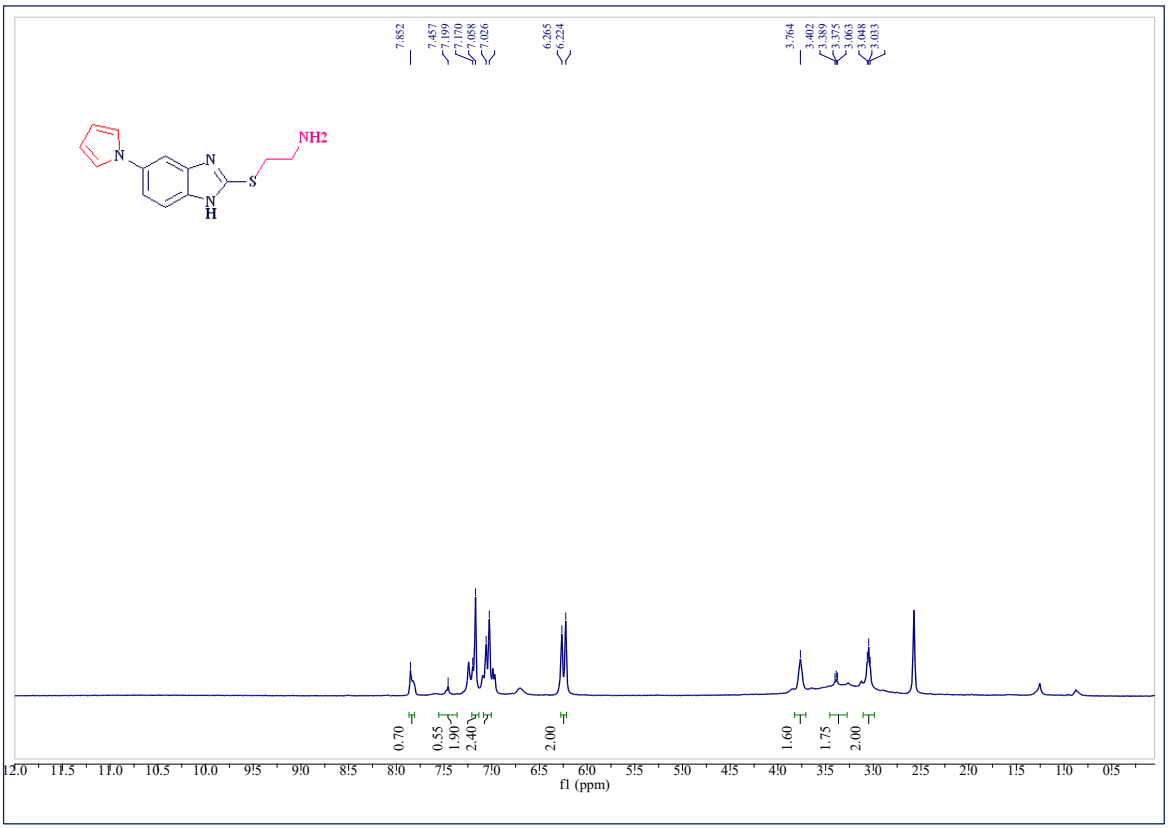

^{13}C-NMR Spectrum of compound 4o (DMSO-d_6, 100MHz):

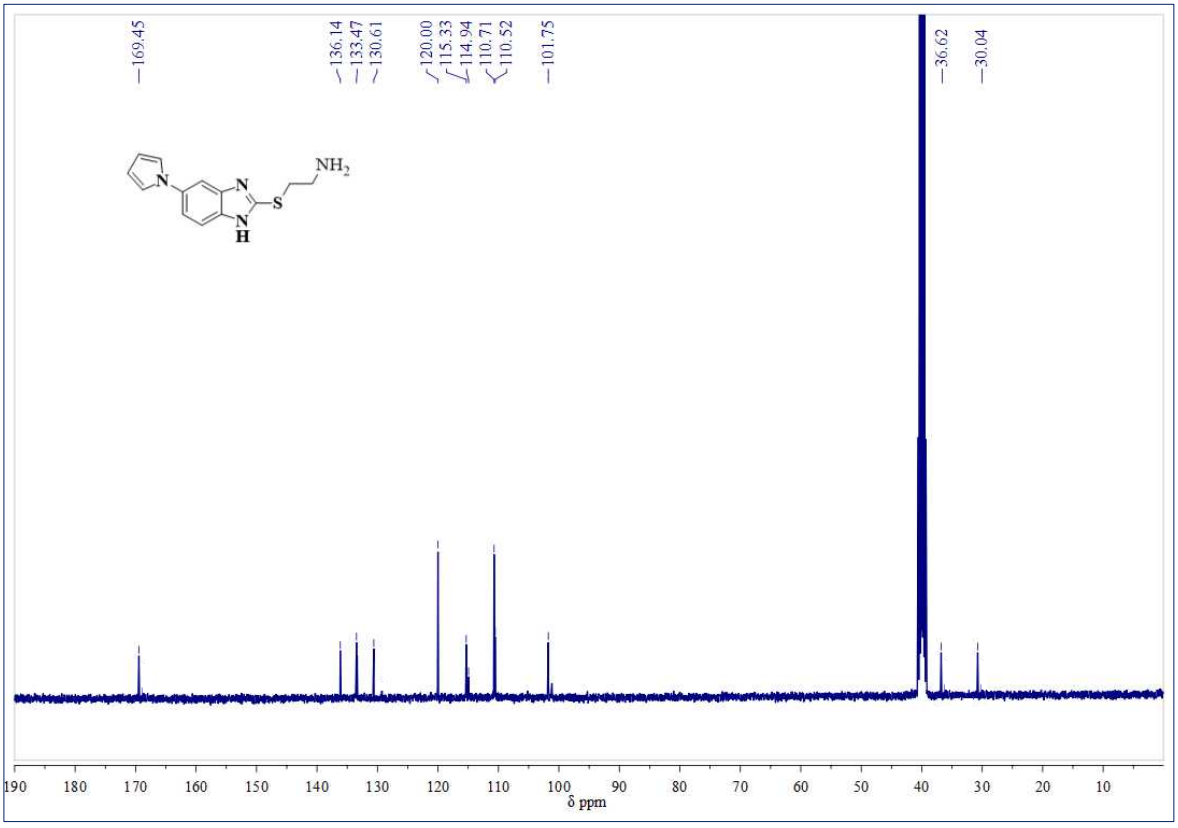

Mass spectrum of compound 4o:

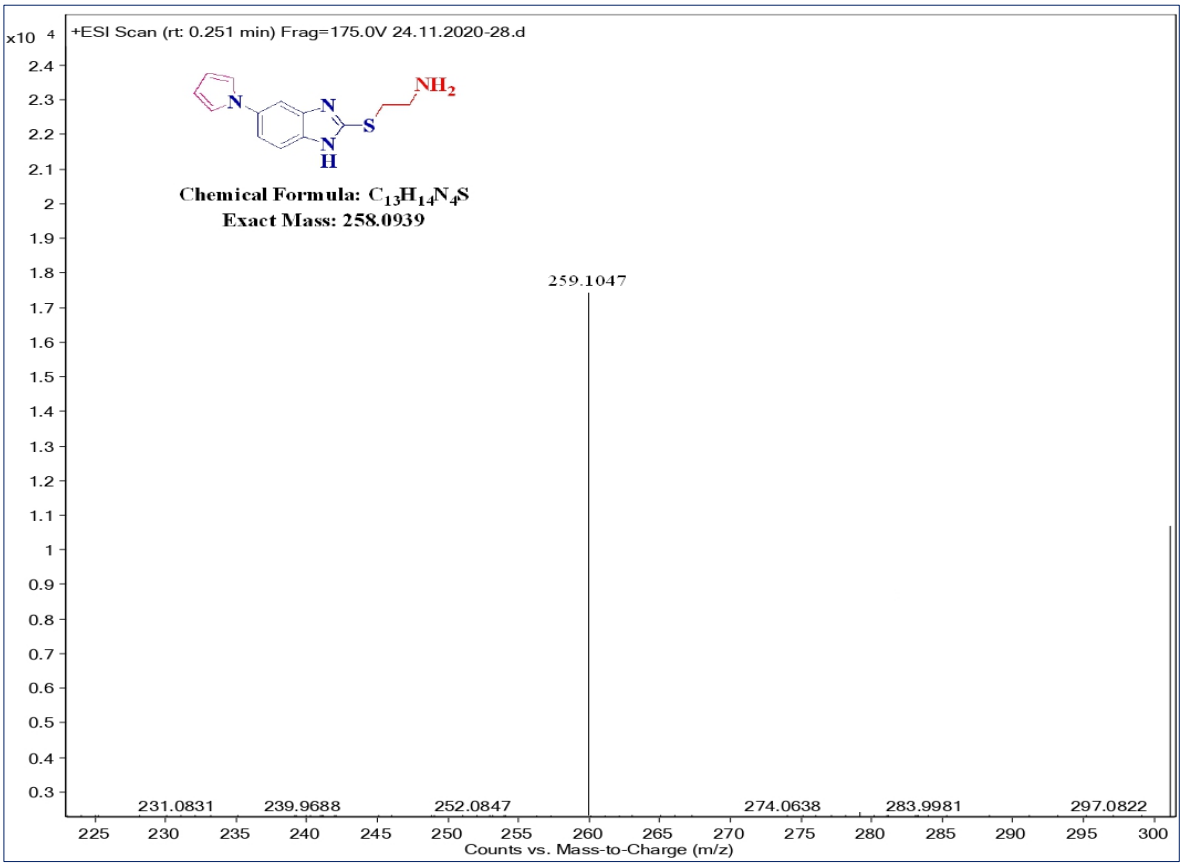

^{1}H-NMR Spectrum of compound 4p ($CDCl_3$+DMSO-d_6, 400MHz):

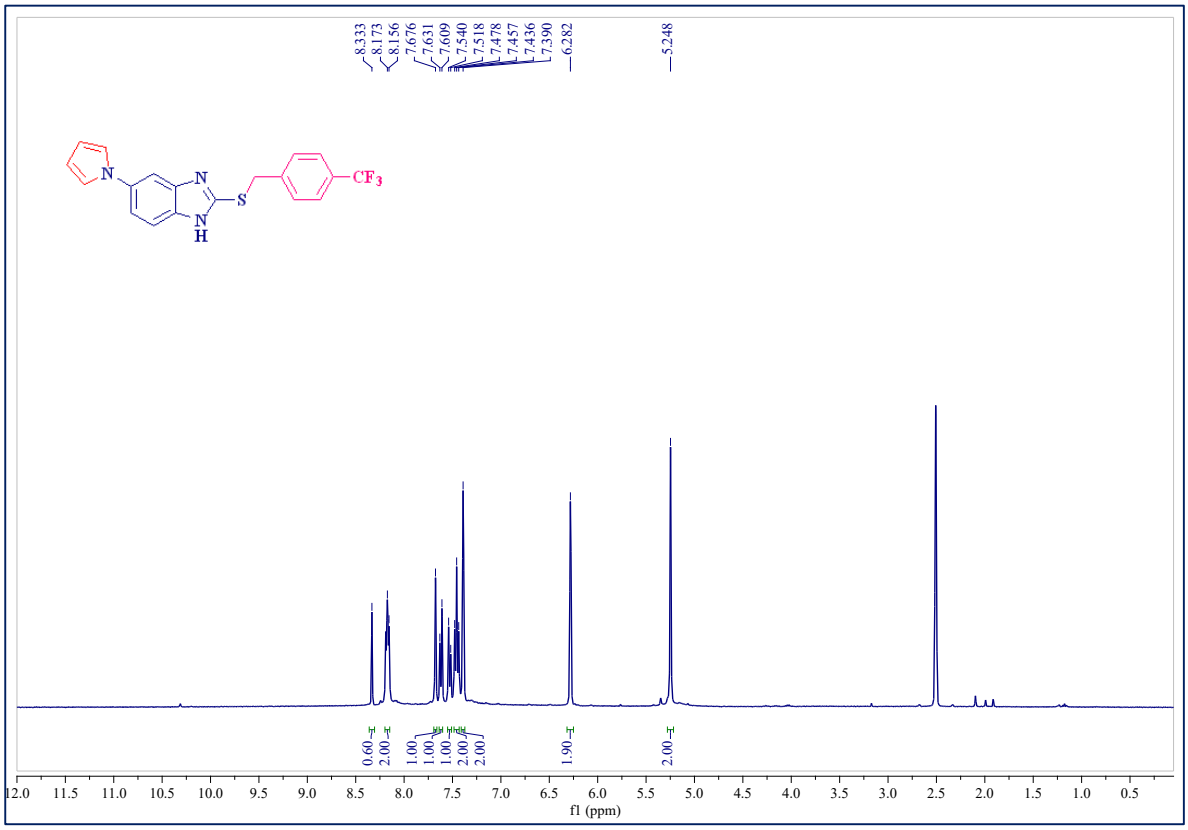

^{13}C-NMR Spectrum of compound 4p (DMSO-d_6, 100MHz):

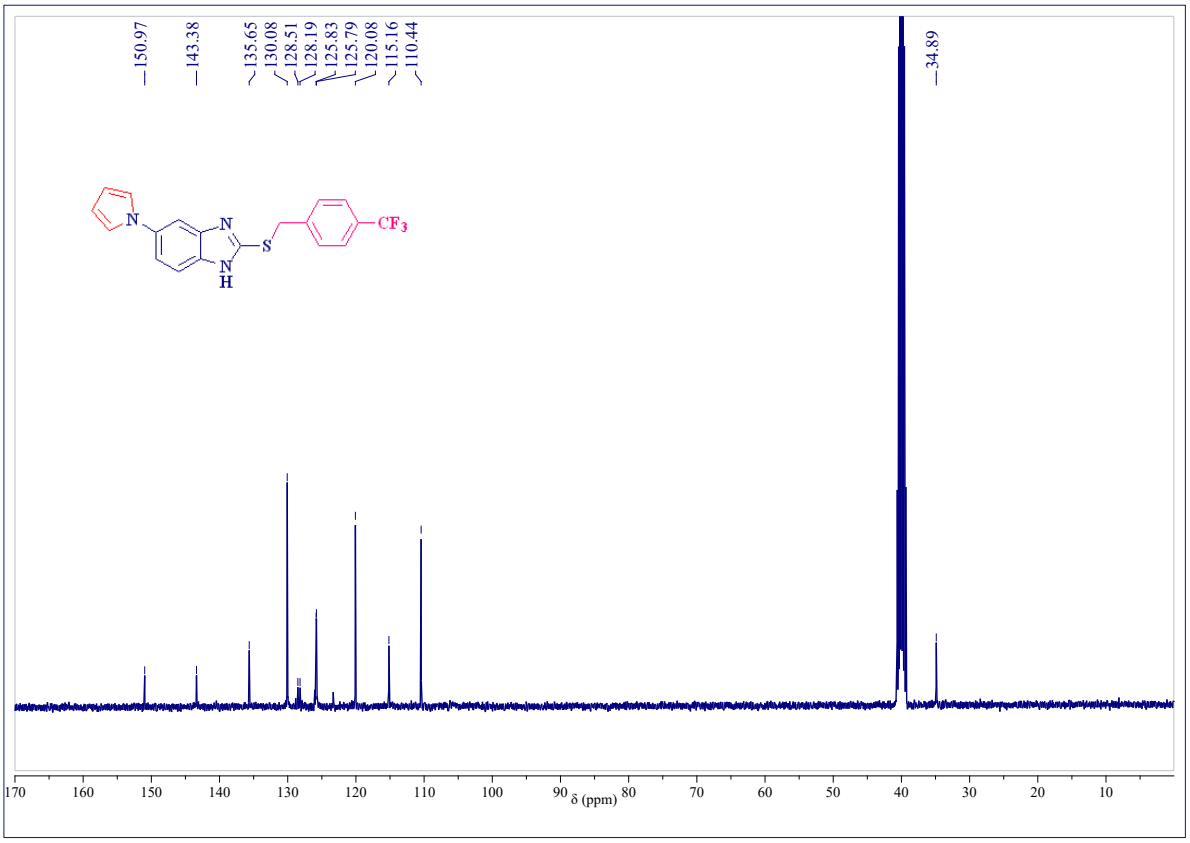

Mass spectrum of compound 4p:

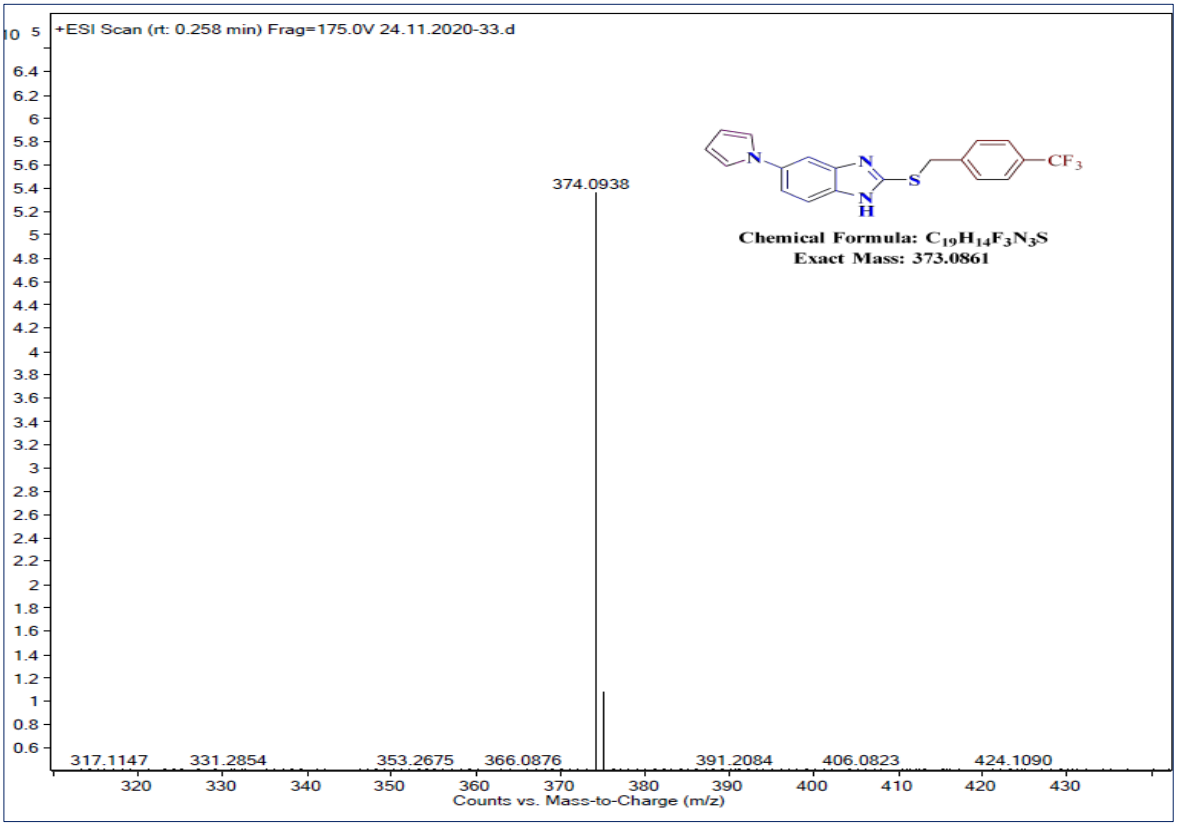

2.10. References

1. Dervan, P. B.; Edelson, B. S. *Curr. Opin. Struct. Biol.* **2003**, *13*, 284–299.
2. Hariharan, A.; Kumar, S.; Alagar, M.; Dinakaran, K.; Subramanian, K. *Polym. Bull.* **2018**, *75*, 93–107.
3. Khan, S. A.; Asiri, A. M.; Al-Dies, A. A. M.; Osman, O. I.; Asad, M.; Zayed, M. E. M. *J. Photochem. Photobiol. A Chem.* **2018**, *364*, 390–399.
4. (a) Hantzsch, A.; *Chem. Ber*. **1890**, 23, 1474–1476; (b) Feist, F. *Chem. Ber*. **1902**, 35, 1537.
5. Corwin, A. H. *Heterocyclic Compounds*, **1950**, ch. 6, vol. 1.
6. (a) Paal, C.; *Chem. Ber*. **1884**, 17, 2756–2767; (b) Knorr, L. *Chem. Ber*. **1884**, 17, 2863.
7. Oldenziel, O.H.; Van Leusen, D. and Van Leusen, A.M. *J. Org. Chem*. **1977**, 42, 3114.
8. Li, J. J.; *Heterocyclic Chemistry in Drug Discovery*, New York, Wiley, **2013**.
9. (a) Piloty, O. *Chem. Ber*. **1910**, 43, 489; (b) Robinson, G.M.; Robinson, R. *J. Chem*. *Soc*. *Trans*. **1918**, 113, 639.
10. Mallikarjuna Reddy, G.; Camilo, A.; *Bioorg. Chem.* **2021**, *106*.
11. Kundu, T.; Pramanik, A. *Bioorg. Chem.* **2020**, *98*, 103734.
12. Xu, X.-T.; Mou, X.-Q.; Xi, Q.-M.; Liu, W.-T.; Liu, W.-F.; Sheng, Z.-J.; Zheng, X.; Zhang, K.; Du, Z.-Y.; Zhao, S.-Q.; Wang, S.-H. *Bioorg. Med. Chem. Lett.* **2016**, *26*, 5334–5339.
13. Biava, M.; Porretta, G. C.; Poce, G.; Battilocchio, C.; Alfonso, S.; Rovini, M.; Valenti, S.; Giorgi, G.; Calderone, V.; Martelli, A.; Testai, L.; Sautebin, L.; Rossi, A.; Papa, G.; Ghelardini, C.; Di Cesare Mannelli, L.; Giordani, A.; Anzellotti, P.; Bruno, A.; Patrignani, P.; Anzini, M. *J. Med. Chem.* **2011**, *54*, 7759–7771.
14. Biava, M.; Porretta, G. C.; Poce, G.; Battilocchio, C.; Manetti, F.; Botta, M.; Forli, S.; Sautebin, L.; Rossi, A.; Pergola, C.; Ghelardini, C.; Galeotti, N.; Makovec, F.; Giordani, A.; Anzellotti, P.; Patrignani, P.; Anzini, M. *J. Med. Chem.* **2010**, *53*, 723–733.
15. Rasal, N. K.; Sonawane, R. B.; Jagtap, S. V. *Bioorg. Chem.* **2020**, *97*, 1–8.
16. La Regina, G.; Bai, R.; Coluccia, A.; Famiglini, V.; Pelliccia, S.; Passacantilli, S.; Mazzoccoli, C.; Ruggieri, V.; Sisinni, L.; Bolognesi, A.; Rensen, W. M.; Miele, A.; Nalli, M.; Alfonsi, R.; Di Marcotullio, L.; Gulino, A.; Brancale, A.; Novellino, E.; Dondio, G.; Vultaggio, S.; Varasi, M.; Mercurio, C.; Hamel, E.; Lavia, P.; Silvestri, R. *J. Med. Chem.* **2014**, *57* (15), 6531–6552.

17. Bavadi, M.; Niknam, K.; Shahraki, O. *J. Mol. Struct.* **2017**, *1146*, 242–253.
18. Puxeddu, M.; Shen, H.; Bai, R.; Coluccia, A.; Bufano, M.; Nalli, M.; Sebastiani, J.; Brancaccio, D.; Da Pozzo, E.; Tremolanti, C.; Martini, C.; Orlando, V.; Biagioni, S.; Sinicropi, M. S.; Ceramella, J.; Iacopetta, D.; Coluccia, A. M. L.; Hamel, E.; Liu, T.; Silvestri, R.; La Regina, G. *Eur. J. Med. Chem.* **2021**, *221*.
19. Li, Z.; Luo, M.; Cai, B.; Haroon-Ur-Rashid; Huang, M.; Jiang, J.; Wang, L.; Wu, L. *Eur. J. Med. Chem.* **2018**, *157*, 665–682.
20. Kang, S. Y.; Park, E.-J.; Park, W.-K.; Kim, H. J.; Choi, G.; Jung, M. E.; Seo, H. J.; Kim, M. J.; Pae, A. N.; Kim, J.; Lee, J. *Bioorg. Med. Chem.* **2010**, *18*, 6156–6169.
21. Teixeira, C.; Barbault, F.; Rebehmed, J.; Liu, K.; Xie, L.; Lu, H.; Jiang, S.; Fan, B.; Maurel, F. *Bioorg. Med. Chem.* **2008**, *16*, 3039–3048.
22. Demirayak, S.; Karaburun, A. C.; Beis, R. *Eur. J. Med. Chem.* **2004**, *39*, 1089–1095.
23. Diaz, C. A.; Allocco, J.; Powles, M. A.; Yeung, L.; Donald, R. G. K.; Anderson, J. W.; Liberator, P. A. *Mol. Biochem. Parasitol.* **2006**, *146*, 78–88.
24. Li, Z.; Pan, M.; Su, X.; Dai, Y.; Fu, M.; Cai, X.; Shi, W.; Huang, W.; Qian, H. *Bioorg. Med. Chem.* **2016**, *24*, 1981–1987.
25. Lakhrissi, Y.; Rbaa, M.; Tuzun, B.; Hichar, A.; Anouar, E. H.; Ounine, K.; Almalki, F.; Hadda, T. Ben; Zarrouk, A.; Lakhrissi, B. *J. Mol. Struct.* **2022**, *1259*, 132683.
26. Masci, D.; Hind, C.; Islam, M. K.; Toscani, A.; Clifford, M.; Coluccia, A.; Conforti, I.; Touitou, M.; Memdouh, S.; Wei, X.; La Regina, G.; Silvestri, R.; Sutton, J. M.; Castagnolo, D. *Eur. J. Med. Chem.* **2019**, *178*, 500–514.
27. Wang, M. Z.; Xu, H.; Liu, T. W.; Feng, Q.; Yu, S. J.; Wang, S. H.; Li, Z. M. *Eur. J. Med. Chem.* **2011**, *46*, 1463–1472.
28. Bratton, L. D.; Auerbach, B.; Choi, C.; Dillon, L.; Hanselman, J. C.; Larsen, S. D.; Lu, G.; Olsen, K.; Pfefferkorn, J. A.; Robertson, A.; Sekerke, C.; Trivedi, B. K.; Unangst, P. C. *Bioorg. Med. Chem.* **2007**, *15*, 5576–5589.
29. Ragusa, G.; Gómez-Cañas, M.; Morales, P.; Hurst, D. P.; Deligia, F.; Pazos, R.; Pinna, G. A.; Fernández-Ruiz, J.; Goya, P.; Reggio, P. H.; Jagerovic, N.; García-Arencibia, M.; Murineddu, G. *Eur. J. Med. Chem.* **2015**, *101*, 651–667.
30. Redzicka, A.; Szczukowski, Ł.; Kochel, A.; Wiatrak, B.; Gębczak, K.; Czyżnikowska, Ż. *Bioorg. Med. Chem.* **2019**, *27*, 3918–3928.
31. Biava, M.; Porretta, G. C.; Poce, G.; Supino, S.; Forli, S.; Rovini, M.; Cappelli, A.; Manetti, F.; Botta, M.; Sautebin, L.; Rossi, A.; Pergola, C.; Ghelardini, C.; Vivoli, E.; Makovec, F.; Anzellotti, P.; Patrignani, P.; Anzini, M. *J. Med. Chem.* **2007**, *50*, 5403–

5411.

32. Brasca, M. G.; Nesi, M.; Avanzi, N.; Ballinari, D.; Bandiera, T.; Bertrand, J.; Bindi, S.; Canevari, G.; Carenzi, D.; Casero, D.; Ceriani, L.; Ciomei, M.; Cirla, A.; Colombo, M.; Cribioli, S.; Cristiani, C.; Della Vedova, F.; Fachin, G.; Fasolini, M.; Felder, E. R.; Galvani, A.; Isacchi, A.; Mirizzi, D.; Motto, I.; Panzeri, A.; Pesenti, E.; Vianello, P.; Gnocchi, P.; Donati, D. *Bioorg. Med. Chem.* **2014**, *22*, 4998–5012.
33. Premkumar, R.; Hussain, S.; Koyambo-Konzapa, S.-J.; Jayram, N. D.; Mathavan, T.; Benial, A. M. F. *J. Mol. Struct.* **2021**, *1236*, 130272.
34. Aiello, A.; Esposito, M. D.; Fattorusso, E.; Menna, M.; Tsuruta, H.; Gulder, A. M.; Perovic, S.; Mu, W. E. G.; Bringmann, G. Daminin, T. *Tetrahedron,* **2005**, *61*, 7266–7270.
35. Johnston, V.; Wiest, M. M.; Tallman, D. E.; Bierwagen, G. P.; Wallace, G. G. *Prog. Org. Coat.* **2001**, *43*, 149–157.
36. Kałędkowski, A.; Trochimczuk, A. W. *React. Funct. Polym.* **2006**, *66*, 740–746.
37. Hantzsch, *Biomed. Engineer. Res*. **1890,** *23*, 1474-1476.
38. Liu, P.; Yang, Y.; Ju, Y.; Tang, Y.; Sang, Z.; Chen, L.; Yang, T.; An, Q.; Zhang, T.; Luo, Y. *Bioorg. Chem.* **2018**, *80*, 422–432.
39. Romagnoli, R.; Oliva, P.; Salvador, M. K.; Manfredini, S.; Padroni, C.; Brancale, A.; Ferla, S.; Hamel, E.; Ronca, R.; Maccarinelli, F.; Rruga, F.; Mariotto, E.; Viola, G.; Bortolozzi, R. *Eur. J. Med. Chem.* **2021**, *214*.
40. Pagadala, L. R.; Mukkara, L. D.; Singireddi, S.; Singh, A.; Thummaluru, V. R.; Jagarlamudi, P. S.; Guttala, R. S.; Perumal, Y.; Dharmarajan, S.; Upadhyayula, S. M.; Ummanni, R.; Basireddy, V. S. R.; Ravirala, N. *Eur. J. Med. Chem.* **2014**, *84*, 118–126.
41. Zhao, M. N.; Ning, G. W.; Yang, D. S.; Gao, P.; Fan, M. J.; Zhao, L. F. *Tetrahedron Lett.* **2020**, *61*, 8–12.
42. Ramesh, K.; Murthy, S. N.; Nageswar, Y. V. D. *Synth. Commun.* **2012**, *42* , 2471–2477.
43. Sarkar, S.; Bera, K.; Maiti, S.; Biswas, S.; Jana, U. *Synth. Commun.* **2013**, *43*, 1563–1570.
44. Balu Atar, A.; Han, E.; Sohn, D. H.; Kang, J. *Synth. Commun.* **2019**, *49* (9), 1181–1192.
45. Pal, G.; Paul, S.; Das, A. R. *Synth.* **2013**, *45*, 1191–1200.
46. Meshram, H. M.; Madhu Babu, B.; Santosh Kumar, G.; Thakur, P. B.; Bangade, V. M. *Tetrahedron Lett.* **2013**, *54*, 2296–2302.
47. Bhat, S. I.; Trivedi, D. R. *Tetrahedron Lett.* **2013**, *54*, 5577–5582.

48. Wang, K.; Dömling, A. *Chem. Biol. Drug Des.* **2010**, *75*, 277–283.
49. Gao, X.; Wang, P.; Wang, Q.; Chen, J.; Lei, A. *Green Chem.* **2019**, *21* (18), 4941–4945.
50. Lin, X.; Mao, Z.; Dai, X.; Lu, P.; Wang, Y. *Chem. Commun.* **2011**, *47* (23), 6620–6622.
51. Truong Nguyen, H.; Nguyen Chau, D. K.; Tran, P. H. *New J. Chem.* **2017**, *41*, 12481–12489.
52. Kim, B. H.; Bae, S.; Go, A.; Lee, H.; Gong, C.; Lee, B. M. *Org. Biomol. Chem.* **2015**, *14*, 265–276.
53. Konkala, K.; Chowrasia, R.; Manjari, P. S.; Domingues, N. L. C.; Katla, R. *RSC Adv.* **2016**, *6*, 43339–43344.
54. Naeimi, H.; Dadaei, M. *RSC Adv.* **2015**, *5*, 76221–76228.
55. Goyal, S.; Patel, J. K.; Gangar, M.; Kumar, K.; Nair, V. A. *RSC Adv.* **2015**, *5*, 3187–3195.
56. Gong, Z.; Lei, Y.; Zhou, P.; Zhang, Z. *New J. Chem.* **2017**, *41*, 10613–10618.
57. Pachechne, L. A.; Pereira, V. F.; Martins, G. M.; Martendal, E.; Xavier, F. R.; Mendes, S. R. *Tetrahedron Lett.* **2019**, *60*, 151043.
58. Xu, C.; Han, Y.; Chen, S.; Xu, D.; Zhang, B.; Shan, Z.; Du, S.; Xu, L.; Gong, P. *Tetrahedron Lett.* **2018**, *59*, 260–263.
59. Bharate, J. B.; Sharma, R.; Aravinda, S.; Gupta, V. K.; Singh, B.; Bharate, S. B.; Vishwakarma, R. A. *RSC Adv.* **2013**, *3*, 21736–21742.
60. Allouche, A. *J. Comput. Chem.* **2012**, *32,* 174-182.
61. Salentin, S.; Schreiber, S.; Haupt, V. J.; Adasme, M. F.; Schroeder, M. *Nucleic Acids Res.* **2015**, *43*, W443-W47.
62. Humphrey, W.; Dalke, A.; Schulten, K. *J. Mol. Graph.* **1996,** *14*, 33-38.
63. Da, C.; Mooberry, S. L.; Gupton, J. T.; Kellogg, G. E. *J. Med. Chem.* **2013**, 56, 7382-7395.
64. Da, C.; Telang, N.; Hall K, K. *Med. chem. comm.* **2013**, *4,* 417-421. Ravelli, R. B. G.; Gigant, B.; Curmi, P. A. *Nature.* **2004***, 428,* 198-202.
65. Ravelli, R. B. G.; Gigant, B.; Curmi, P. A. Nature. **2004**, *428*, 198-202.

66. La Regina, G.; Bai, R.; Coluccia, A.; Famiglini, V.; Pelliccia, S.; Passacantilli, S.; Mazzoccoli, C.; Ruggieri, V.; Sisinni, L.; Bolognesi, A.; Rensen, W. M.; Miele, A.; Nalli, M.; Alfonsi, R.; Di Marcotullio, L.; Gulino, A.; Brancale, A.; Novellino, E.;. Dondio, G; Vultaggio, S. ; Varasi, M.; Mercurio, C.; Hamel, E.; Lavia, P. ; Silvestri, R. *J. Med. Chem.* **2014**, *57*, 6531-6552.

67. Da, C.; Telang, N.; Barelli, P. *ACS Med. Chem. Lett.* **2012**, *3,* 53-57.

68. Tripati, A.; Fornabaio, M.; Kellogg, G.E.; Gupton, J. T.; Gewirtz, D. A.; Yeudall, W. A. ; Vega, N. E.; Mooberry, S. L. *Bioorg. & Med. Chem.* **2008***, 16,* 2235-2242.

CHAPTER-III

One-pot synthesis of thioalkylated benzimidazole-based 4-substituted mercaptoimidazole molecular hybrids *via* multi-component approach

CHAPTER-III

One-pot synthesis of thioalkylated benzimidazole-based 4-substituted mercaptoimidazole molecular hybrids *via a* multi-component approach

3.0. Introduction

Aromatic heterocyclic scaffolds are extremely distributed in the environment and are essential to life [1-5]. Among the various heterocyclic compounds, imidazoles are the most pivotal and privileged heterocyclic aromatic nitrogen-containing heterocyclic compounds with molecular formula $C_3H_4N_2$. These three carbons and two nitrogen atoms are set at 1st and 3rd position with pyrrole and pyridine type of annular nitrogen. The possible isomeric structures with that molecular formula are depicted in **Figure 3.1** and different resonance forms of imidazole are depicted in **Figure 3.2**. Historically, imidazole was first named as gluoxaline (first synthesized from glyoxal and ammonia). These derivatives are broadly present in biologically active natural products [6-8] such as histamine, vitamin B_{12}, biotin, histidine, nucleic acids, and alkaloids. Additionally, numerous synthetic drugs, frequently prescribed medicines, such as cimetidine (Tagamet), ketoconazole, etomidate (amidate), and clotrimazole drugs are the component of imidazole scaffolds **Figure 3.3**. These heterocycles are also known to exhibit biological activities such as anti-fungal [9], anti-cancer [10-12], anti-bacterial [13,14], and anti-inflammatory [15] agents. Moreover, these derivatives are also used as functional material [16,17], N-heterocyclic carbenes [18] in organometallic catalysis, vital structural blocks in the synthesis of several biologically active scaffolds [19,20], and also used as ionic liquids [21] green chemistry.

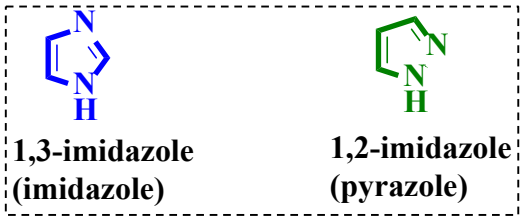

Figure 3.1. Isomeric structures of imidazoles

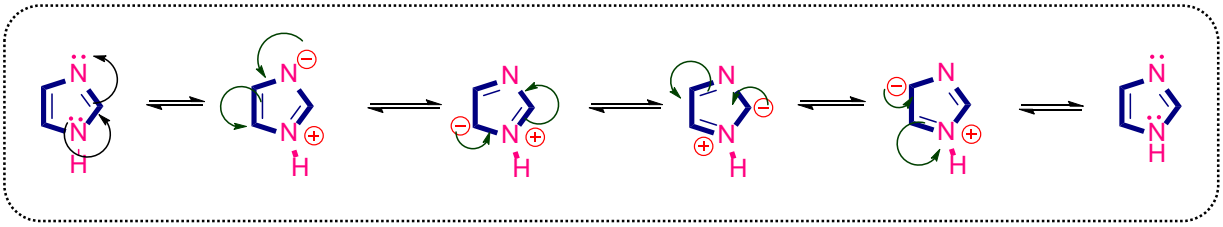

Figure 3.2. Different resonance structures of imidazole

Appropriately the imidazoles and their derivatives are extensively used as JAK (Janus Associated Kinase) inhibitors [22], glucagon receptors [23], Axl Kinase Inhibitors [24], fluorescent probes [25,26], TGR5 receptor antagonists [27].

A vast number of molecules containing imidazole skeletons have shown prominent biological and pharmaceutical applications as depicted in **Figure 3.3**. Owing to the immense synthetic impotence and the broad range of bioactivities exhibited by these derivatives efforts have been made from time to time to innovate libraries of these compounds. Therefore, imidazole's have received much attention from the researcher's point of view.

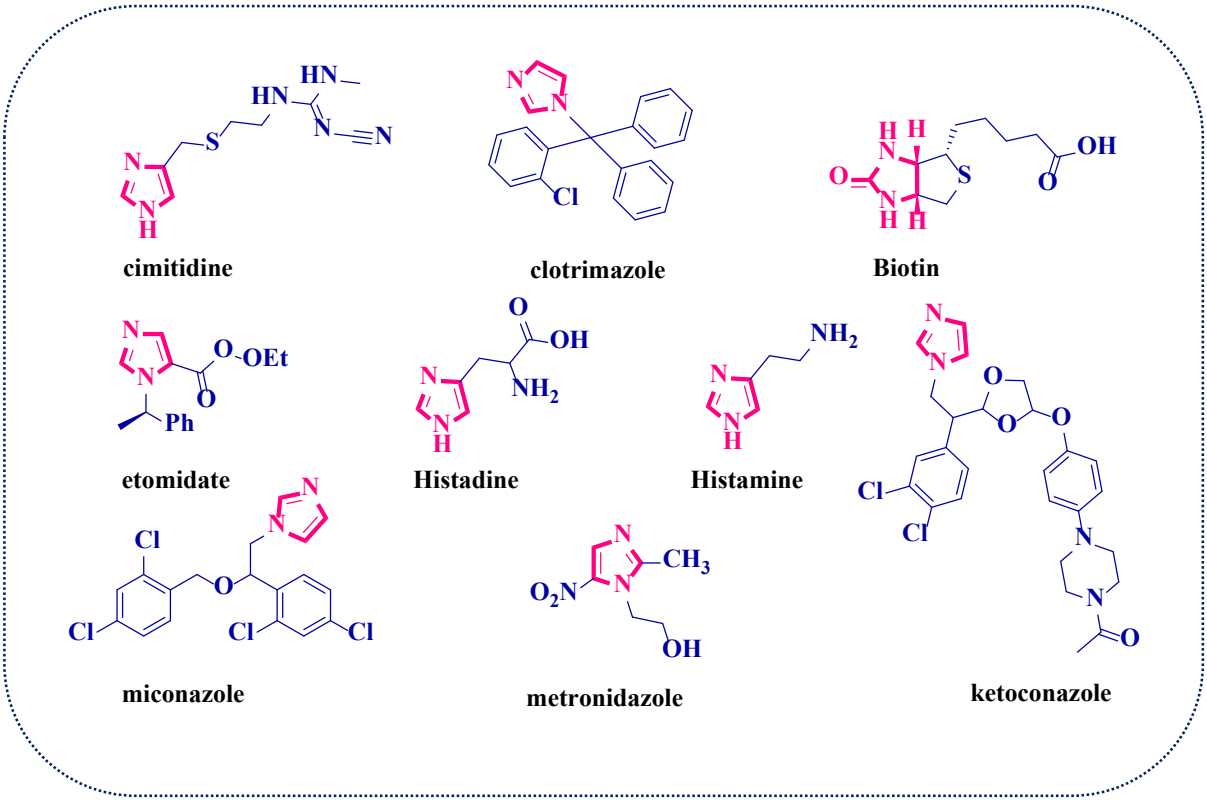

Figure 3.3. Selected structures of some natural and pharmaceutical compounds containing imidazole motifs

Gupta [28] ***et al.*** synthesized a series of novel 1,4-diaryl-2-mercaptoimidazoles *via* a one-pot solid phase reaction. The title compounds were synthesized by using starting materials like different substituted anilines, and phenacyl bromides in presence of K_2CO_3/Na_2CO_3 to yield α-anilinoacetophenones, which on subsequent cyclization in presence of KSCN and p-TSA gave the titled compounds with excellent yields.

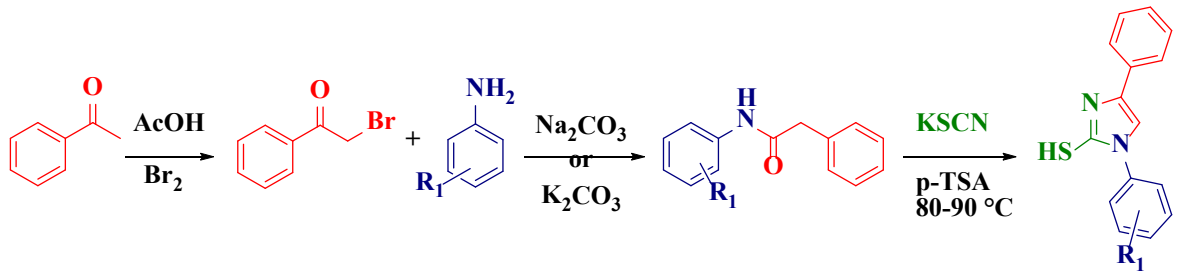

Scheme 3.1. One-pot solid phase synthesis of 1,4-diaryl-2-mercaptoimidazole derivatives

Naureen [29] ***et al.*** reported a series of novel tri-arylimidazoles containing 2-aryl indoles moiety *via* a one-pot four-component reaction method. The title compounds were synthesized from substituted-2-arylindole-3-carbaldehyde, benzil, substituted anilines, and ammonium acetate in acetic acid under reflux conditions for about 5-6 h. Further, the synthesized compounds screened for their *in-vitro* α-glucosidase inhibitory activity. Among the tested compounds **4j** showed more potent inhibitory activity (**Figure3.1**).

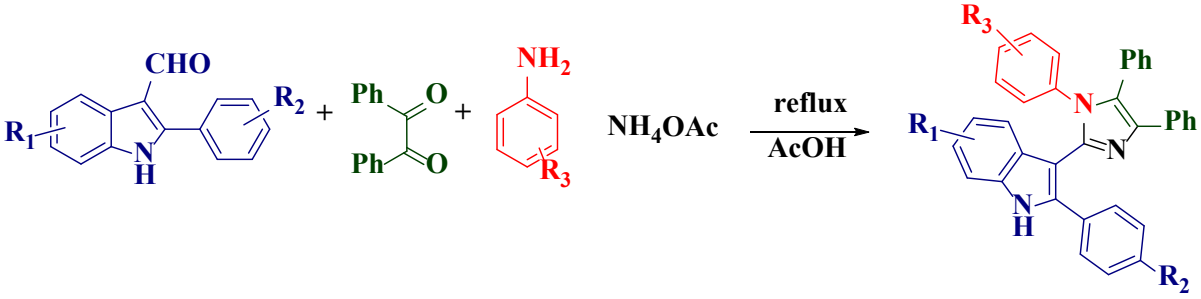

Scheme 3.2. Synthesis of tri-aryl indoline imidazole derivatives *via the* one-pot four-component method

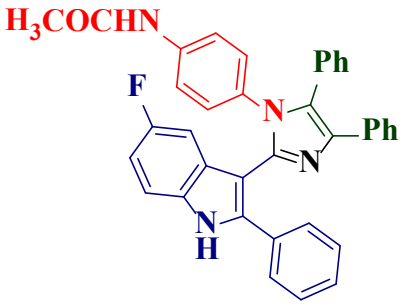

4j

Figure 3.1. Biologically active compound

Alanthadka [30] ***et al.*** reported a novel one-pot, solvent-free synthesis of substituted imidazoles. The title compounds were synthesized by using substituted aryl methyl ketones and different benzyl amines *via* N-heterocyclic carbene (NHC) catalysis.

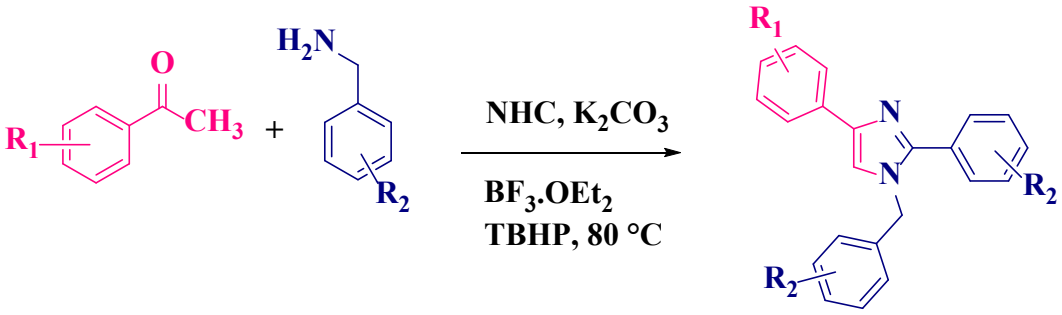

Scheme 3.3. One-pot solvent-free synthesis of substituted imidazoles

Banerji [31] ***et al.*** reported a series of tri and tetra-substituted imidazole derivatives *via a* one-pot iodine-catalyzed ariel oxidation method in water. The title compounds were synthesized from easily available starting materials like benzil/ benzoin and the corresponding amine followed by a catalytic amount of iodine in water giving 1,2,4,5-tetra substituted imidazole. The benzil or benzoin substituted aromatic aldehydes and ammonium acetate with the same reaction condition gave tri-substituted imidazoles with good to excellent yields. Further, the title compounds were subjected to fluorescence properties and among the tested, some of the compounds like **8e** and **8f** showed excellent fluorescence properties (**Figure 3.2**).

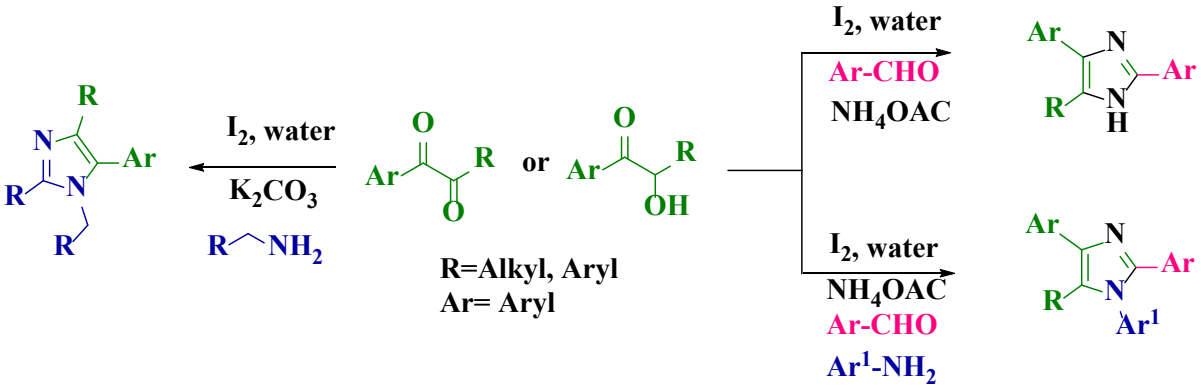

Scheme 3.4. One-pot iodine catalyzed tri and tetra substituted imidazole derivatives

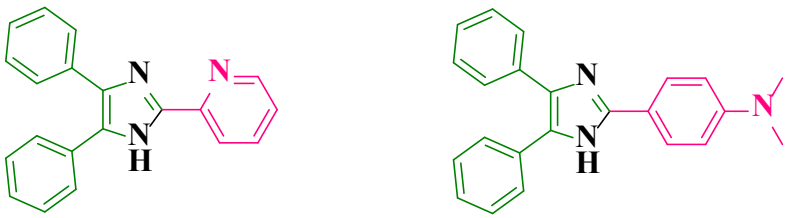

8e **8f**

Figure 3.2. Fluorescence active compounds.

Vedula [32] ***et al.*** synthesized a novel series of tri-substituted coumarin-based imidazole derivatives *via a* one-pot, three-component reaction method. The title compounds were synthesized from α-amino ketones, excess ammonium thiocyanate and different substituted 3-(2-bromoacetyl)-2*H*-chromen-2-one in acetic acid. Further, these titled compounds were screened for their anti-bacterial activity against Gram-negative bacteria *Escherichia Coli.* Among the tested compounds, compound **4a** showed good anti-bacterial activity (**Figure 3.3**).

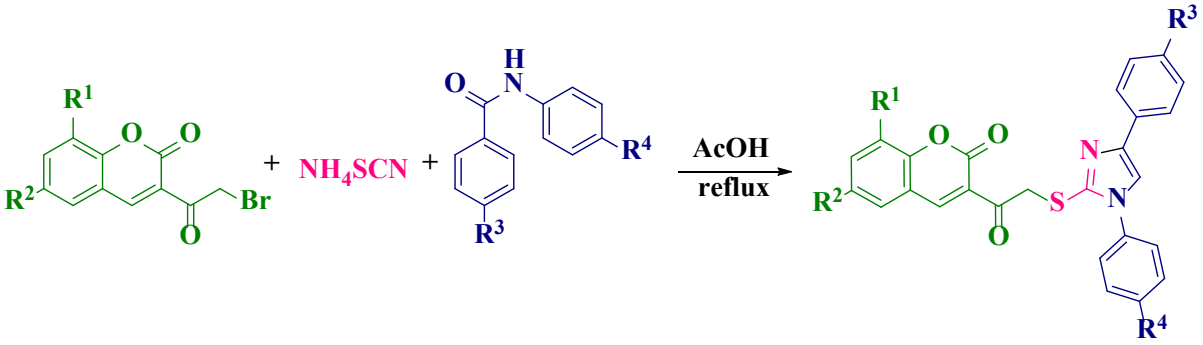

Scheme 3.5. One-pot three-component synthesis of coumarin-based thiazole derivatives

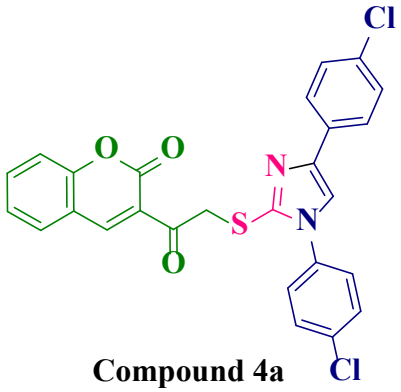

Compound 4a

Figure 3.3. Biologically active compound

Wang [33] ***et al.*** reported a new series of 4-aryl-2-benzoyl imidazole derivatives. The title compounds were synthesized from different substituted 3,4,5-trimethoxy phenyl glyoxal hydrate, aryl glyoxal hydrate, and ammonium acetate in ethanol. Further, the synthesized compounds were screened for their *in-vitro* anti-cancer activity against eight cancer lines including multi-drug resistant cancer cell lines. Among the tested compounds, compound **12a** showed excellent *in-vitro* anti-cancer activity with low nanomolar IC_{50} values (**Figure 3.4**).

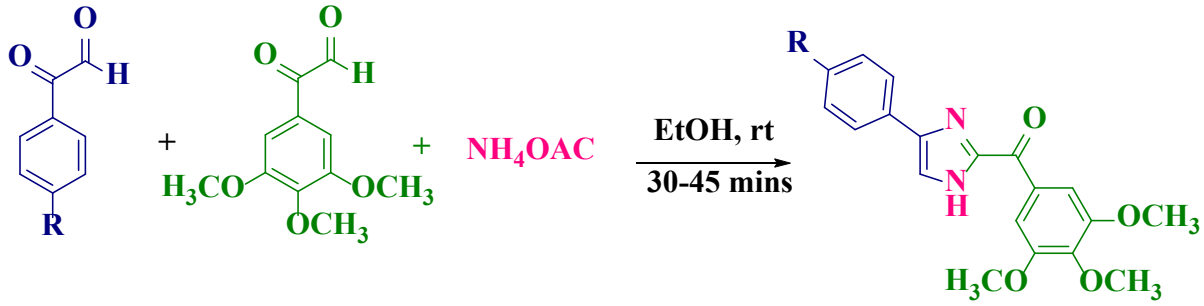

Scheme 3.6. Synthesis of 4-aryl-2-benzoyl imidazole derivatives

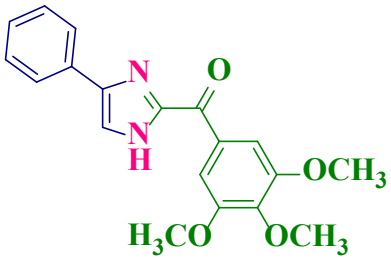

compound 12a

Figure 3.4. Biologically active compound

Aggarwal[34] ***et al.*** synthesized 1,4-diaryl-2-mercaptoimidazole *via* a solvent-free, one-pot, green synthesis method. These compounds were synthesized from easily available starting materials like α-tosyloxyacetophenones, and anilines afford α-anilinoacetophenones, which further undergo cyclization in presence of acid catalyst PTSA *in situ* manner with KSCN to give final products in excellent yields.

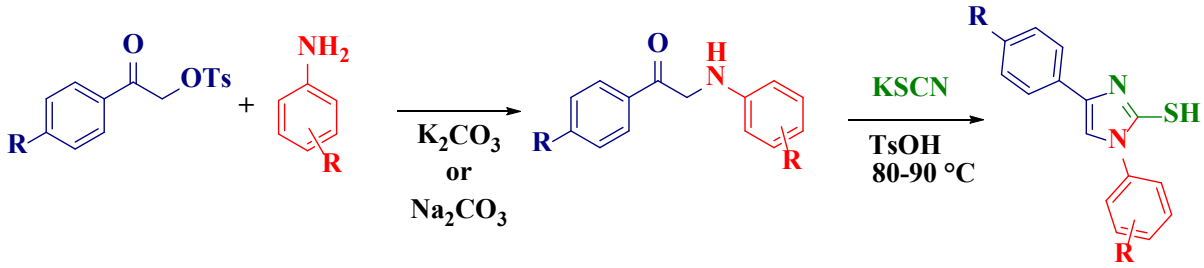

Scheme 3.7. One-pot synthesis of 1,4-diaryl mercaptoimidazole derivatives

Wang[35] ***et al.*** developed an efficient, one-pot, three-component, Ag-catalysed reaction method for the synthesis of functionalized imidazole derivatives. The title compounds were synthesized from various amidines, ynals phenols, alcohols, or water providing moderate to good yields with high regioselectivities.

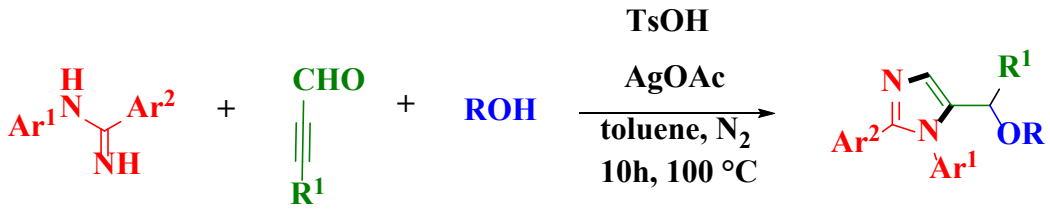

Scheme 3.8. One-pot three-component synthesis of functionalized imidazoles

Baidya [36] ***et al.*** developed a novel, one-pot synthesis of α-aminoketones through the aromatic nitroso aldol reaction with silyl enol ether and disilane backbone in presence of Brønsted acid. Further, these α-amino ketones react with ammonium thiocyanate in presence of acid catalyst p-TSOH giving polysubstituted mercaptoimidazoles, on further alkylation gave fully substituted imidazole derivatives in high yields.

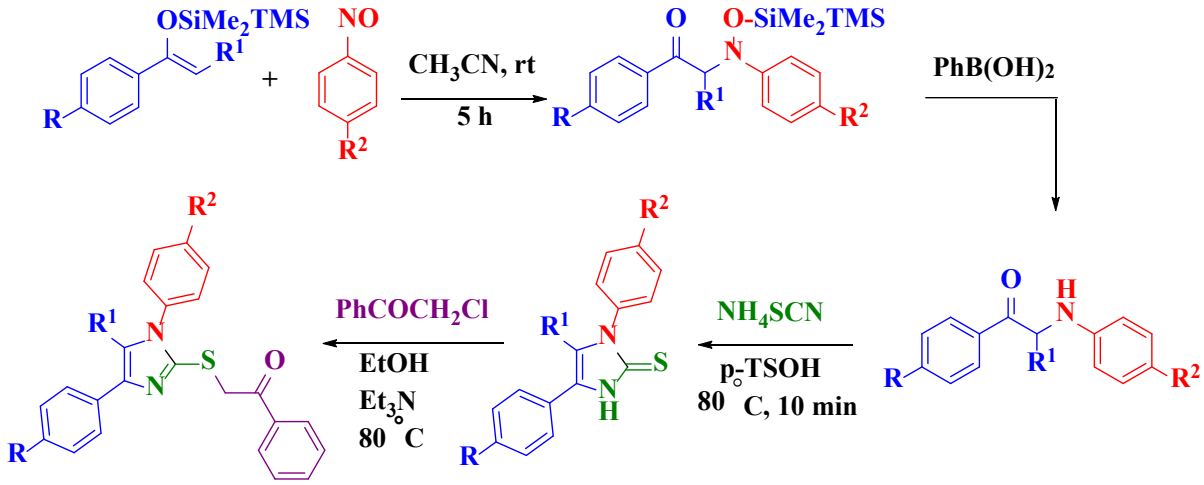

Scheme 3.9. One-pot synthesis of polysubstituted mercaptoimidazole derivatives

Radziszewski [37] ***et al.*** synthesized a series of novel, 2,4,5-triphenyl 1*H*-imidazoles *via* a one-pot three-component reaction. The title compounds were synthesized from commercially available starting materials, benzil, benzaldehyde, and with an excess of ammonia gave title compounds.

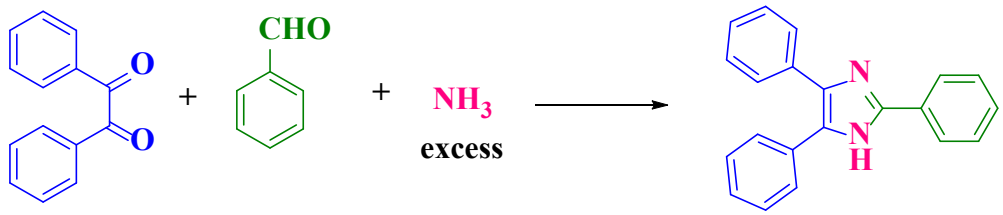

Scheme 3.10. One-pot, three-component synthesis of 2,4,5-tri-substituted imidazoles.

Drefahal [38] ***et al.*** synthesized a series of 1-substituted-2,4,5-triphenyl 1*H*-imidazole derivatives *via* a one-pot four-component reaction method. The title compounds were synthesized from commercially available starting materials like benzil, benzaldehyde, primary amines, and excess ammonia.

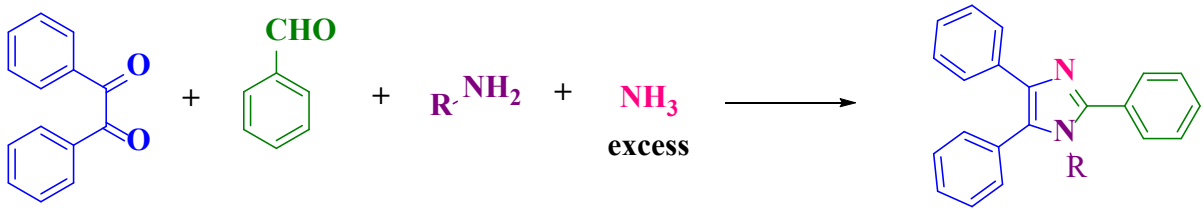

Scheme 3.11. One-pot, four-component synthesis of tetra-substituted imidazole derivatives

Shafeel [39] ***et al.*** synthesized a novel series of 4-aryl-5-(3,4,5-trimetoxyphenyl)-2-alkylthio-1*H*-imidazolederivatives. The title compounds were synthesized from the starting material like various benzoins with an excess of ammonium thiocyanate in n-butanol yielding the required 4,5-disubstituted-1*H*-imidazole 2(3*H*) thiones. These compounds were alkylated using various alkyl iodides in a basic medium to produce titled compounds. Further, the final compounds were screened for further cytotoxic activity against four various cell lines HT-29, MCF-7, NIH-3T3, and AGS. Among the tested scaffolds, the compound **6g** showed potent cytotoxic activity (**Figure 3.5**).

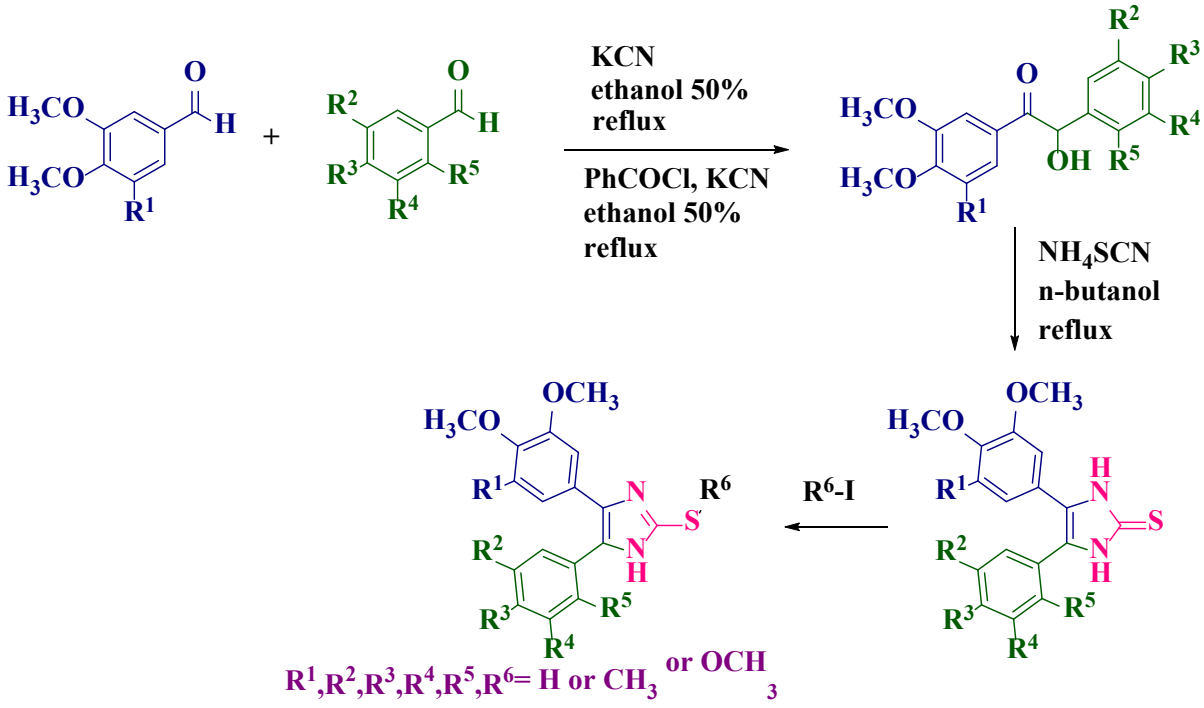

Scheme 3.12. Synthesis of polysubstituted mercaptoimidazole derivatives

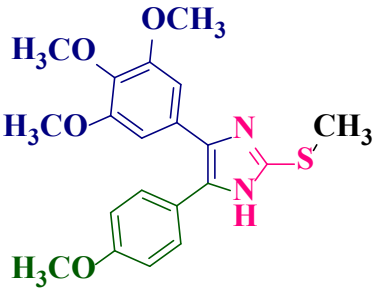

compound 6g

Figure 3.5. Biologically potent compound

Wang [40] ***et al.*** developed an acid-promoted, metal-free construction of tri and tetra-substituted imidazole derivatives *via* a multi-component reaction. The title compounds were synthesized with various internal alkynes, aldehydes, and anilines or ammonium acetate.

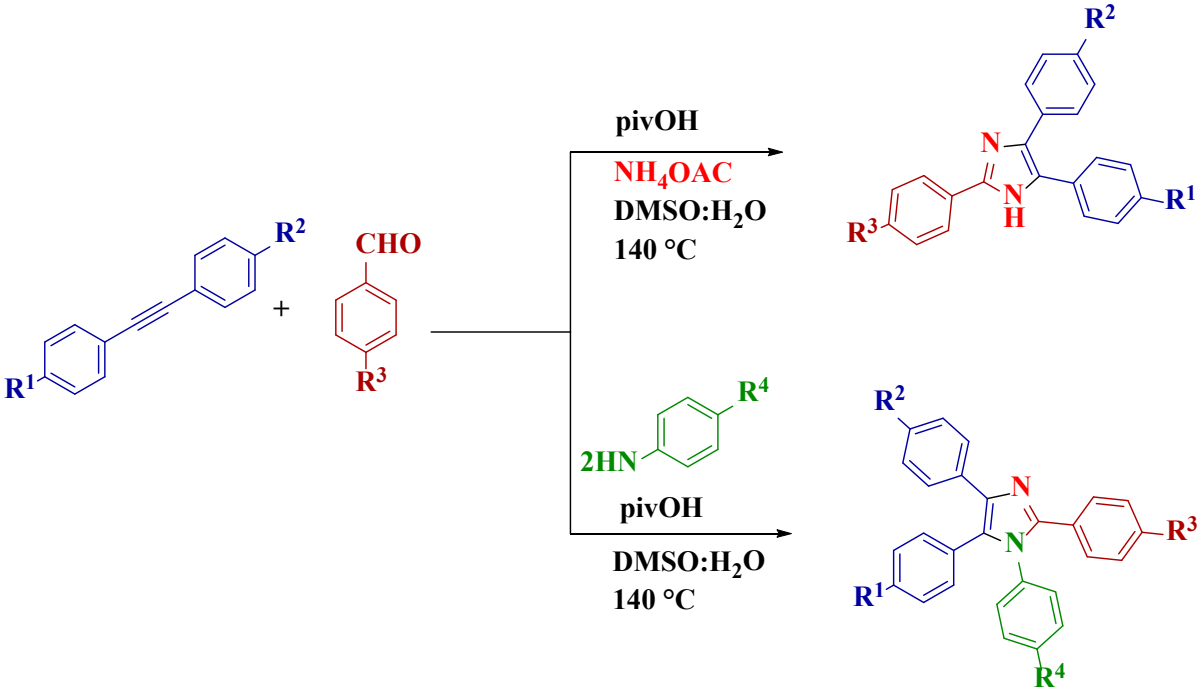

Scheme 3.13. One-pot synthesis of tri-and tetra substituted imidazoles

Zhang [41] ***et al.*** reported novel one-pot synthesis of 2-(2-azaaryl) imidazole derivatives via an efficient three-component domino [3+1+1] heterocyclization. The title compounds were synthesized by using azaaryl amidines with aromatic aldehydes and were conducted using K_2CO_3 under the microwave-assisted condition to form polysubstituted imidazoles.

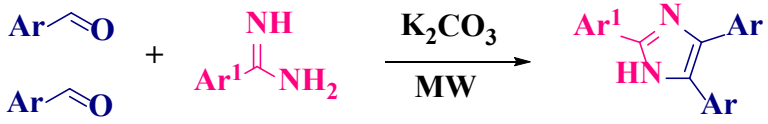

Scheme 3.14. One-pot three-component synthesis of polysubstituted imidazoles

3. 1. Present work

In line with our interest, considering the importance of imidazole and benzimidazole moieties and prompted by the mentioned previous literature, we aimed for an update and extension of its usefulness focusing on the synthesis of mercaptoimidazole derivatives *via* the MCR approach.

3.2. Starting materials

In this present chapter, the synthesis of new mercaptoimidazole hybrids was described. The starting materials required for the synthesis of the target compounds are, 5-amino-2-mercapto-benzimidazole, various substituted phenacyl bromides, and ammonium thiocyanate. All the chemicals were procured from commercial sources.

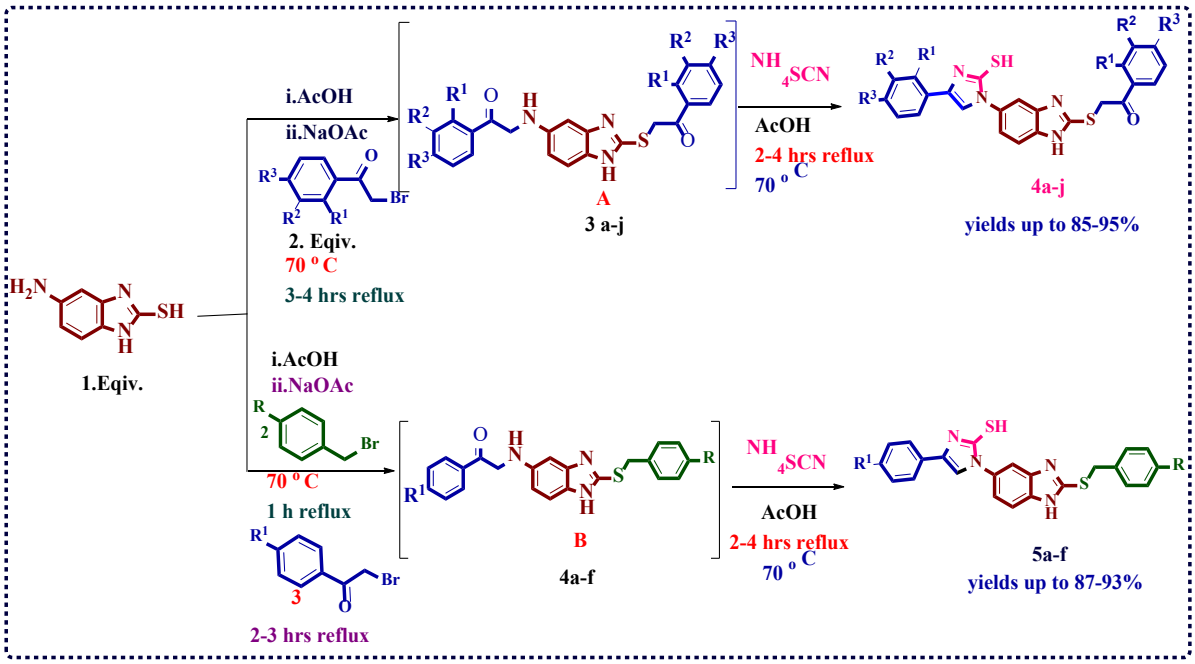

Scheme 3.1. Synthesis of mercaptoimidazoles *via* one-pot pseudo-four component reaction.

3.3. Synthesis of mercaptoimidazoles

The synthesis of mercaptoimidazole scaffolds was carried out as outlined in **Scheme 3.1.** The title mercaptoimidazoles were synthesized by a reaction of 5-amino-2-mercaptobenzimidazole (1), phenacyl bromides (2), and ammonium thiocyanate (3) (1:2:1) in glacial acetic acid and fused sodium acetate provides good to excellent yields.

3.4. Results and discussion

The conditions required for the synthesis of imidazole derivatives are shown in **Table 3.1.** To optimize the reaction conditions for the synthesis of title compounds we have investigated the

Table 3.1. Optimized reaction conditions.4aa

Entry	Solvent	Base	Temp (°C)	Time (h)	Yield (%)
1	H_2O	-	rt	24	NR
2	H_2O	-	60	24	NR
3	CH_3CN	-	60	24	trace
4	Dioxane	-	60	24	NR
5	DMSO	-	60	22	17
6	DMF	-	60	21	21
7	Toluene	-	60	24	NR
8	Methanol	-	60	20	25
9	Ethanol	-	60	18	38
10	Ethanol	Et_3N (1.0 mmol)	60	12	trace
11	Ethanol	NaOH (1.0 mmol)	60	12	40
12	Ethanol	KOH (1.0 mmol)	60	12	42
13	Ethanol	Na_2CO_3 (1.0 mmol)	60	12	45
14	Ethanol	K_2CO_3 (1.0 mmol)	60	12	47
15	AcOH	-	60	12	60
16	AcOH	piperidine (1.0mmol)	60	10	trace
17	AcOH	AcONa (1.0 mmol)	60	10	75
18	AcOH	AcONa (1.5 mmol)	60	10	80
19	AcOH	AcONa (2.0 mmol)	60	9	85
20	**AcOH**	**AcONa (2.0 mmol)**	**70**	**8**	**90**
21	AcOH	AcONa (2.0 mmol)	80	8	60
22	AcOH	AcONa (2.0 mmol)	reflux	8	52

[a]*Reaction conditions*: 5-amino-2-marcaptobenzimidazole (**1.0 mmol**), phenacyl bromide (**2.0 mmol**), ammonium thiocyanate (**1.0 mmol**), solvent (2 mL), [b]Isolated yields.

reaction 5-amino-2-mercapto-benzimidazole (1.0 mmol), phenacyl bromide (2.0 mmol), and ammonium thiocyanate (1.0 mmol) in water at room temperature for 24 hours stirring, but there

is no reaction. To our surprise, there is no reaction even at 60 °C under this condition. Then, we screened the reaction in various aprotic solvents like CH_3CN, dioxane, DMSO, DMF, and toluene (**Table 3.1, entries 3-7)** where the reaction did not proceed or the yields of the products obtained are low. Then we carried out the same reaction in protic solvents like methanol, ethanol, and acetic acid (**Table 3.1, entries, 8,9, and 15)**. Fortunately, the reaction was smooth in acetic acid and gave the title compounds with the still-low yield at 60 °C **(Table 3.1, entry 15).** Further, the reaction was optimized in the terms of base. Here, we tried with different organic and inorganic bases (**Table 3.1, entries 10-14, and 16),** unfortunately, the yields were found to be poor, and took more time to complete the reaction. Finally, we tried fused sodium acetate (**1.0 mmol**) in acetic acid. It was observed from the optimized reaction conditions that when fused sodium acetate was used, the yields were found to be improved at 60 °C (**Table 3.1, entry 17)**. Further, the reaction was optimized in the terms of the amount of base and reaction temperature. A change in the yield was observed when the amount of base was increased. **Table 3.1** indicates the best results were obtained when the reaction was performed using 2.0 mmol of fused sodium acetate as a base at 70 °C in acetic acid (**Table 3.1, entry 20**). However, there is no further improvisation of product yield beyond the 70 °C rise in reaction temperature (**Table 3.1, entries 21-22)**. After optimization of the reaction conditions, we studied this reaction with a variety of electron-rich phenacyl and electron-deficient phenacyl/ benzyl bromides. In this study, we found that when electron-withdrawing groups are present on phenacyl (90-95%) or benzyl (90%) bromides, they gave high yields of the products when compared with electron-releasing groups on phenacyl or benzyl bromides (89%) **Table 3.1**.

The synthesized scaffold structures **(4a-j)** and **(5a-f)** were established based on their physical and analytical data. The infrared spectra of synthesized compounds **4a-j** and **5a-f** exhibited the presence of amine(-NH), carbonyl (-C=O), and imine (C=N) functional groups appears in the region of 3449-3345cm^{-1},1666-1685 cm^{-1}, and 1599-1634 cm^{-1} respectively. The ^{1}H-NMR spectra showed characteristic resonance peaks for –SH, imidazole C5-proton, and S-CH2-protons appeared at 10.25-13.15 δ ppm, 7.39-8.47 δ ppm, and 5.09-5.37 δ ppm respectively. The ^{13}C-NMR spectra also confirm the synthesized compounds **(4a-j)** and **(5a-f)** structures with characteristic resonance peaks of carbonyl carbon, imidazole C5-carbon, and aliphatic carbon (S-CH_2-carbon) appeared at δ_C 189.2-192.8 δ ppm, 105.1-112.3 δ ppm, and 34.5-44.9 δ ppm respectively. The ESI-HRMS spectra of all the synthesized compounds are shown $[M+H]^+$ as base peak.

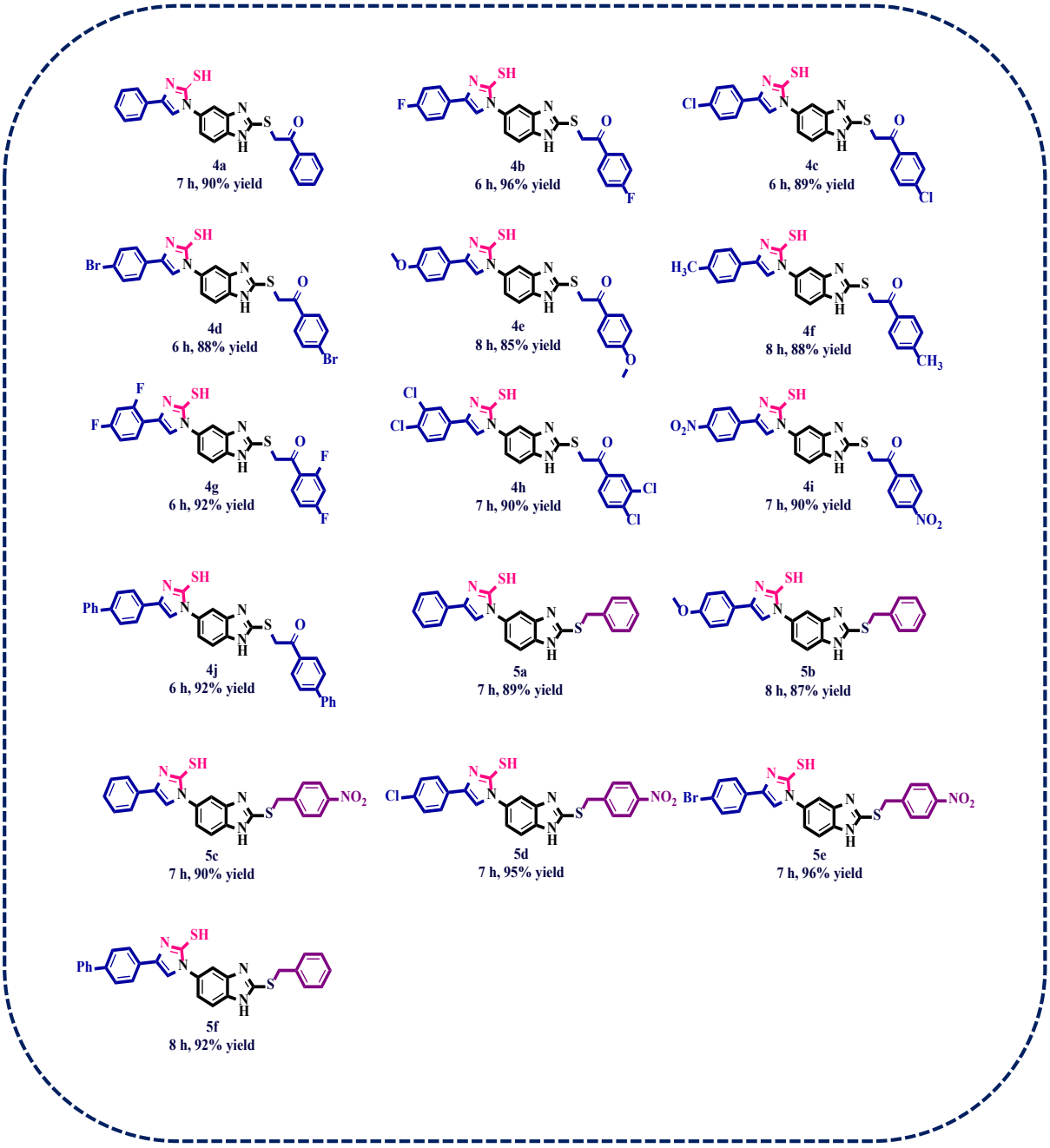

Figure 3.2. Scope of substrates.

The plausible reaction mechanism for the formation of title compounds is shown in **scheme 3.2** by the reaction of 5-amino-2-mercaptobenzimidazole (1.0 mole), with two moles of phenacyl bromides in presence of acetic acid and fused sodium acetate to give intermediate 'A' followed by subsequent reaction with NH_4SCN. In this process initially, the thiol and amino groups displace the bromine atoms of phenacyl bromides to give intermediate '**A**' with the elimination of two equivalents of hydrobromic acid. The intermediate '**A**' further reacts with NH_4SCN to form the intermediates II, III, IV, and V. Further the intermediate V rearranged to

titled mercaptoimidazolyl phenacylthio benzimidazole derivatives. The mechanistic path for the above synthesis was confirmed by DFT studies.

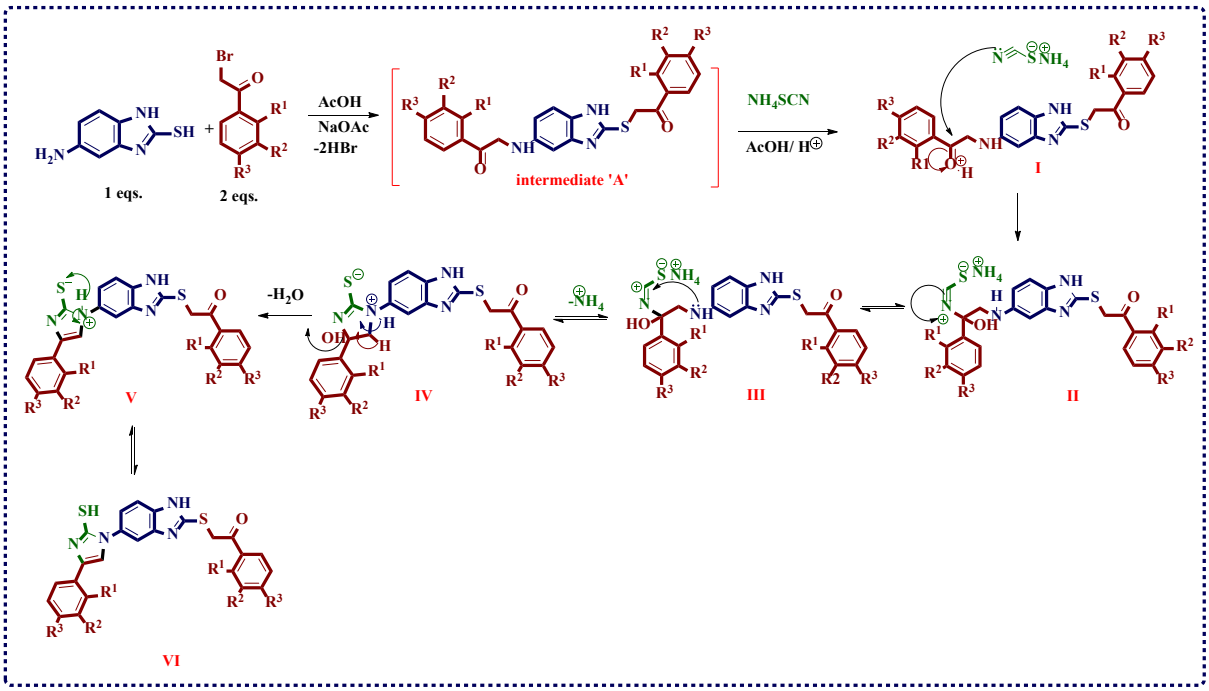

Scheme 3.2. Plausible reaction mechanism for the formation of mercaptoimidazolyl phenacyl thio benzimidazoles.

3.5. Density Functional Theory (DFT) Computational details and Calculations

The geometries of all the point structures were fully optimized without any geometrical/symmetrical constraints using the ωb97xd method employing a 6-31G* basis set [42] The nature of the critical point structures was characterized as local minima and as first-order saddle points by the frequency calculations at the same level of theory. The TSs were confirmed by the existence of a characteristic single imaginary frequency with displacement vectors in the direction of bond formation (breaking). All the density functional theory (DFT) based calculations performed in the present investigation were carried out using Gaussian16 [43].

The density functional theory calculations have been performed to probe the energetics for the synthesized substituted mercaptoimidazole scaffolds. In the course of calculations, all the geometries of the point structures were fully optimized. The relative energy profile of the reaction is shown in **Figure 3.1** along with important geometries of TSs which include the important geometrical parameters.

It is interesting to note that the ammonium thiocyanate (rearranged product of thiourea), which is an active moiety for proceeding with the reaction. It has been found that in the TS1, the calculated N–C distance (N atom of the ammonium thiocyanate and C atom of carbonyl group of the reactant) is 1.73 Å. The calculated C–O and O–H distances are 1.33 and 0.98 Å, respectively. The similar N–C, C–O, and O–H distances in **II** are found to be 1.47, 1.38, and 0.97 Å, respectively. TS2 indicates the transition state for the cyclization reaction to give the five-membered ring structure. The calculated N–C distance involved in the formation cyclic ring is 2.08 Å in TS2 and the corresponding distance in structure IV is found to be 1.72 Å.

The relative energy of TS1 is significantly smaller when compared with the starting materials. Typically, the calculated relative energy value is -33.11 kcal/mol. Thus, it is worth mentioning that the conversion of I to II is a barrier-less reaction. Calculated energetics of conversion of I to II clearly emphasizes that the former converts readily to later in the presence of ammonium thiocyanate. The low energy barrier may be attributed to the additional non-covalent

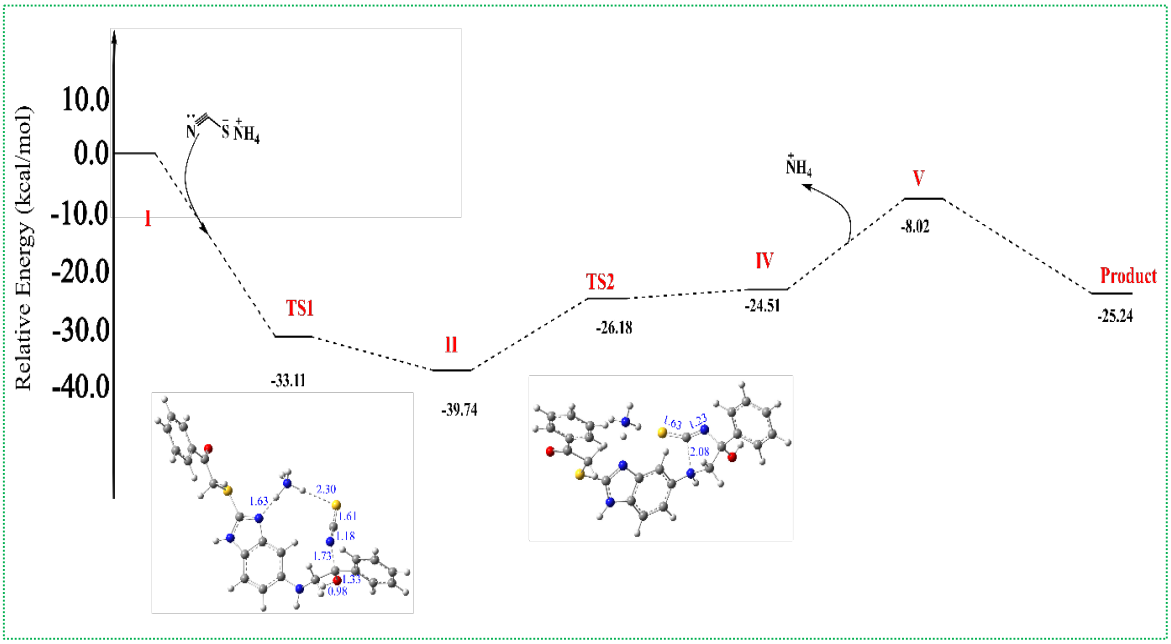

Figure 3.1. Relative energy profile for the synthesis of substituted imidazole.

interactions involved due to the presence of NH_4^+ ion as shown in **Figure 3.1**. The intermediate II is further stabilized by -6.63 kcal/mol as compared to that of TS1. It can be noticed that 13.56 kcal/mol of activation energy is required for the cyclization of II to give a five-membered cyclic ring. The cyclization reaction of II to give intermediate IV is an endoergic reaction. The increment in the energy of IV is may be attributed to the repulsive steric factors and ring strain. The removal of ammonium ion from IV requires the energy of 16.49 kcal/mol to give

intermediate V and therefore, the removal of ammonium ion from IV is also endothermic. It may be due to the dissociation of charged species from the polar moiety. The intermediate V undergoes intramolecular dehydration and rearrangement to give the desired product. The desired product is thermodynamically more stable than the reactants. Furthermore, the intramolecular dehydration and rearrangement taking place from V are minor reactions involving proton transfer, therefore in this investigation, only product formation from intermediate V is discussed. Overall, the reaction is exothermic and the initiation of the reaction is barrier-less.

3.6. Conclusion

In conclusion, we have synthesized thioalkylated benzimidazole-tethered 4-substituted mercaptoimidazole molecular hybrids *via* a novel, facile one-pot three/ four-component approach using acetic acid and fused sodium acetate as a reaction medium with good to excellent yields. The usefulness of this reaction is that it involves easy workup, shorter reaction time, broad substrate scope, and column-free purification of the products. Further DFT calculations were performed to gain insight into the reaction mechanism.

3.7. Experimental section

3.7.1. General procedure for the synthesis **of 2-((5-(2-Mercapto-4-phenyl-1*H*-imidazol-1-yl)-1*H*-benzo[*d*]imidazol-2-yl)thio)-1-phenylethan-1-one (4a-j)**

A mixture of 5-amino-2-marcaptobenzimidazole (1.0 mmol), different substituted phenacyl bromides (2.0 mmol), and fused sodium acetate (2.0 mmol) was taken in a round bottom flask and the reaction mixture was refluxed in acetic acid (2 ml) at 70 $^{\circ}$C for 4 h to give intermediate '**A**' and this intermediate (without isolation) was further reacted with ammonium thiocyanate **3** (1.0 mmol) under reflux condition for about 4 h. After completion of the reaction (checked through TLC, 50:50, n-hexane: EtOAc), the reaction mixture was cooled to room temperature and placed in ice-cold water. The solid separated was filtered, washed with water, dried, and recrystallized from ethanol.

3.6.2. General procedure for the synthesis of **1-(2-(Benzylthio)-1*H*-benzo[*d*]imidazol-5-yl)-4-phenyl-1*H*-imidazole-2-thiol (5a-f)**

A mixture of 5-amino-2-marcaptobenzimidazole (1.0 mmol), different substituted benzyl bromides (0.1187 g, 1.0 mmol), and fused sodium acetate (0.82g, 1.0 mmol) was taken in a round bottom flask and the reaction mixture was refluxed in acetic acid (2 ml) at 70 ^{0}C for 1 h. To this reaction mixture again 1.0 mmol of fused sodium acetate and phenacyl bromide (0.1990 g, 1.0 mmol) was added and refluxed for another 3h to give intermediate 2-((2-(benzylthio)-

1*H*-benzo[*d*]imidazol-5-yl)amino)-1-phenylethan-1-one and this intermediate (without isolation) was further reacted with ammonium thiocyanate 1.0 mmol. After completion of the reaction (checked through TLC, 50:50, n-hexane: EtOAc), the reaction mixture was cooled to room temperature and placed in ice-cold water. The solid separated was filtered, washed with water, dried, and recrystallized from ethanol.

3.8. Characterization data of products

2-((5-(2-Mercapto-4-phenyl-1*H*-imidazol-1-yl)-1*H*-benzo[*d*]imidazol-2-yl)thio)-1-phenylethan-1-one. **4a**

White solid: yield: 90%, mp: 254-256 °C; FT-IR (KBr, cm^{-1}): 3406 (NH), 1685 (C=O), 1624 (C=N); **^{1}H-NMR** (400 MHz, $CDCl_3$+DMSO-d_6 δ ppm):13.00 (s, 1H, SH), 8.11 (d, *J* = 7.2 Hz, 2H, Ar-H), 7.97 (s, 1H, imidazole proton), 7.69-7.75 (m, 5H, Ar-H), 7.58-7.60 (m,3H, Ar-H), 7.29-7.43 (m, 3H, Ar-H,), 5.37 (s, 2H, S-CH_2 protons), 1.25 (brs, 1H); **^{13}C NMR** (100 MHz, $CDCl_3$+DMSO-d_6) δ:192.1, 152.5, 135.1, 134.4, 129.2, 128.9, 128.7, 128.2, 128.0, 124.8, 123.1, 116.1, 113.6, 111.5, 41.7; ESI-HRMS: *m/z* Calcd for $C_{24}H_{19}N_4OS_2$ $[M+H]^+$ 443.1000: found: 443.1940.

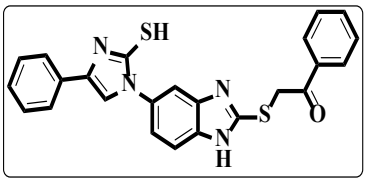

1-(4-Fluorophenyl)-2-((5-(4-(4-fluorophenyl)-2-mercapto-1*H*-imidazol-1-yl)-1*H*-benzo[*d*]imidazol-2-yl)thio)ethan-1-one. **4b**

White solid: yield: 96%, mp: 249-251 °C; FT-IR (KBr, cm^{-1}): 3449 (NH), 1678 (C=O), 1634 (C=N); **^{1}H NMR** (400 MHz, DMSO-d_6 δ ppm): 12.99 (s, 1H, SH), 8.19-8.16 (m, 2H, Ar-H), 7.91 (s, 1H, imidazole proton), 7.90 (s, 1H, Ar-H), 7.84-7.80 (m, 2H, Ar-H), 7.66 (d, *J* = 8.4 Hz, 1H, Ar-H), 7.53 (d, *J* = 8.4 Hz, 1H, Ar-H), 7.45 (t, *J* = 8.8 Hz, 2H), 7.30 (t, *J* = 8.8 Hz, 2H), 5.24 (s, 2H, S-CH_2-protons); **^{13}C NMR** (100 MHz, DMSO-d_6) δ ppm: ^{13}C NMR (100 MHz, DMSO-d_6) δ 191.6, 167.2, 164.7, 163.3, 160.9, 152.5, 132.2, 132.1, 126.9, 126.9, 124.9, 122.6, 120.9, 116.6, 116.5, 116.4, 116.3, 113.8, 111.8, 109.7, 41.2; ESI-HRMS: *m/z* Calcd for $C_{24}H_{17}F_2N_4OS_2$ $[M+H]^+$ 479.0812. Found: 479.1784.

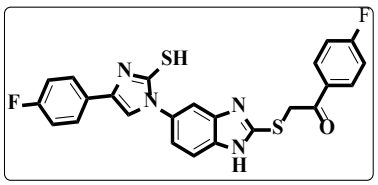

1-(4-Chlorophenyl)-2-((5-(4-(4-chlorophenyl)-2-mercapto-1*H*-imidazol-1-yl)-1*H*-benzo[*d*]imidazol-2-yl)thio)ethan-1-one. **4c**

White solid: yield: 89%, mp: 208-210 °C; FT-IR (KBr, cm^{-1}): 3397 (NH), 1677(C=O), 1625 (C=N); **^{1}H NMR** (400 MHz, $CDCl_3$+DMSO-d_6 δ ppm): 13.00 (s, 1H, SH), 8.09 (d, *J* = 8.8 Hz, 2H, Ar-H), 8.02 (s, 1H, Ar-H), 7.98 (s, 1H, imidazole proton), 7.73 (d, *J* = 8.8 Hz, 2H Ar-H), 7.65 (d, *J* = 5.6 Hz, 2H, Ar-H), 7.57 (d, *J* = 8.4 Hz, 2H, Ar-H), 7.39 (d, *J* = 8.4 Hz, 2H, Ar-H), 5.24 (s, 2H, S-CH2- protons), 1.25 (brs, 1H, NH); **^{13}C NMR** (100 MHz, DMSO-d_6) δ; 192.3, 152.3, 139.4, 134.3, 132.7, 130.9, 130.7, 129.5, 129.3, 129.1, 127.2, 126.4, 122.0, 117.5, 113.8, 112.0, 109.7, 108.1, 35.4. ESI-HRMS: *m/z* Calcd for $C_{24}H_{17}Cl_2N_4OS_2$ $[M+H]^+$ 511.0221, found: 511.1175.

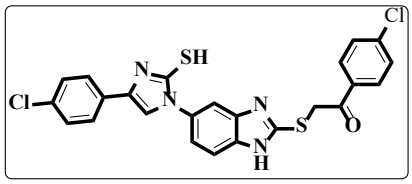

1-(4-Bromophenyl)-2-((5-(4-(4-bromophenyl)-2-mercapto-1*H*-imidazol-1-yl)-1*H*-benzo[*d*]imidazol-2-yl)thio)ethan-1-one. **4d**

White solid: yield: 88%, mp: 214-216 °C; FT-IR (KBr, cm^{-1}): 3372 (NH), 1676 (C=O), 1621 (C=N); **^{1}H NMR** (400 MHz, $CDCl_3$+DMSO-d_6 δ ppm) 12.99 (s, 1H, SH), 8.01 (d, *J* = 8.4 Hz, 2H, Ar-H), 7.98 (d, *J* = 1.6 Hz, 1H, Ar-H), 7.75 (s, 1H, imidazole proton), 7.73 – 7.66 (m, 4H, Ar-H), 7.64 (s, 1H, Ar-H), 7.57 (d, *J* = 2.0 Hz, 2H, Ar-H), 7.54 (d, *J* = 8.4 Hz, 2H, Ar-H), 5.20 (s, 2H, S-CH_2), 1.25 (s, 1H); **^{13}C NMR** (100 MHz, $CDCl_3$+DMSO-d_6) δ; 191.6, 152.2, 134.1, 132.3, 132.0, 130.6, 128.9, 127.2, 126.5, 122.5, 121.4, 116.5, 113.6, 111.6, 41.2; ESI-HRMS: *m/z* Calcd for $C_{24}H_{18}Br_2N_4OS_2$ [M+2] 601.9268, found : 601.0272.

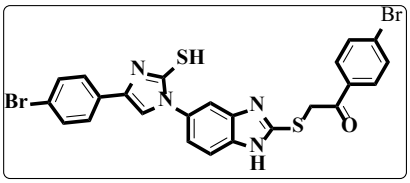

2-((5-(2-Mercapto-4-(4-methoxyphenyl)-1*H*-imidazol-1-yl)-1*H*-benzo[*d*]imidazol-2-yl) thio)-1-(4-methoxyphenyl) ethan-1-one. 4e

White solid: yield: 85%, mp: 257-259 °C; FT-IR (KBr, cm^{-1}): 3355 (NH), 1671 (C=O), 1599 (C=N); **^{1}H NMR** (400 MHz, DMSO-d_6 δ ppm): 12.82 (s, 1H, SH), 8.07 (d, *J* = 8.8 Hz, 2H, Ar-H), 7.82 (s, 1H, imidazole proton), 7.73-7.70 (m, 3H, Ar-H), 7.58 (d, *J* = 8.8 Hz, 1H, Ar-H), 7.44 (d, *J* = 8.8 Hz, 1H, Ar-H), 7.11 (d, *J* = 8.8 Hz, 2H, Ar-H), 7.00 (d, *J* = 9.2 Hz, 2H, Ar-H), 5.11 (s, 2H, S-CH_2-protons), 3.88 (s, 3H, -OCH_3-protons), 3.79 (s, 3H, -OCH_3-protons); **^{13}C NMR** (100 MHz, DMSO-d_6) δ: 191.5, 164.3, 152.3, 137.0, 134.9, 131.4, 129.2, 128.2, 118.3, 114.7, 114.6, 107.6, 56.2, 40.7; ESI-HRMS: *m/z* Calcd for $C_{26}H_{23}N_4O_3S_2$ $[M+H]^+$ 503.1212, found: 503.1243.

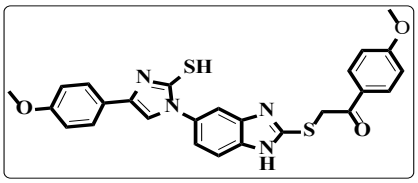

2-((5-(2-Mercapto-4-(*p*-tolyl)-1*H*-imidazol-1-yl)-1*H*-benzo[*d*]imidazol-2-yl)thio)-1-(p-tolyl)ethan-1-one. 4f

White solid: yield: 88%, mp: 277-279 °C; FT-IR (KBr, cm^{-1}): 3426 (NH), 1676 (C=O), 1631 (C=N); **^{1}H NMR** (400 MHz, DMSO-d_6 δ ppm): 13.01 (s, 1H, SH proton), 7.97-7.99 (m, Ar-H, 4H), 7.58-7.60 (m, Ar-H, 2H), 7.47 (s, 1H, imidazole proton), 7.40-7.42 (m, 4H, Ar-H), 7.17-7.19 (m, 2H, Ar-H), 5.19 (s, 2H, S-CH_2-protons), 2.42 (s, 6H, -CH_3 protons); ^{13}C NMR (100 MHz, DMSO-d_6 δ ppm); **^{13}C NMR** (100 MHz, DMSO-d_6) δ:192.5, 152.5, 145.2, 136.2, 134.7, 132.9, 130.2, 129.9, 129.1, 118.9, 116.8, 114.7, 112.9, 107.9, 55.4, 41.3, 21.8; ESI-HRMS: *m/z* Calcd for $C_{26}H_{23}N_4OS_2$ $[M+H]^+$ 471.1313, found: 471.2277.

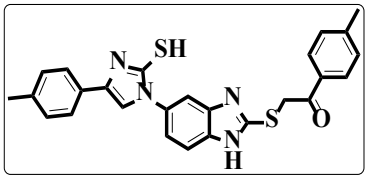

1-(2,4-Difluorophenyl)-2-((5-(4-(2,4-difluorophenyl)-2-mercapto-1*H*-imidazol-1-yl)-1*H*-benzo[*d*]imidazol-2-yl) thio)ethan-1-one. 4g

White solid: yield: 92%, mp: 223-225 °C; FT-IR (KBr, cm^{-1}); 3397 (NH), 1678 (C=O), 1625 (C=N); **^{1}H NMR** (400 MHz, DMSO- d_6 δ ppm): 10.70 (s, 1H, SH), 8.47 (s, 1H, imidazole proton), 8.21-8.28 (m,1H, Ar-H), 8.05-8.10 (m, 1H, Ar-H), 7.59 (d, 1H, *J* = 8.8 Hz, Ar-H), 7.52 (t, 1H, *J* = 9.4 Hz, Ar-H), 7.44 (d, *J* = 8.8 Hz, 1H, Ar-H), 7.23 – 7.41 (m, 4H, Ar-H), 7.20 (t, *J* = 8.4 Hz, 1H, Ar-H), 5.23 (s, 2H, S-CH_2-protons); **^{13}C NMR** (100 MHz, DMSO-d_6) δ: 189.2, 164.0, 163.9, 162.7, 148.8, 143.3, 139.1, 134.3, 133.6, 131.6, 128.5, 120.9, 116.1, 114.1, 113.2, 112.9, 112.5, 108.0, 105.9, 100.4, 44.5; ESI-HRMS: *m/z* Anal Calcd for $C_{24}H_{15}F_4N_4OS_2$ $[M+H]^+$ 515.0623, found: 515.0616.

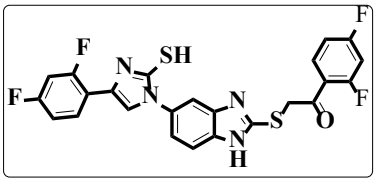

1-(3,4-Dichlorophenyl)-2-((5-(4-(3,4-dichlorophenyl)-2-mercapto-1*H*- imidazol-1-yl)-1*H*-benzo[*d*]imidazol-2-yl)thio)ethan-1-one. 4h

White solid: yield: 90%, mp: 219-221 °C; FT-IR (KBr, cm^{-1}): 3397 (NH), 1673(C=O), 1622 (C=N); **^{1}H NMR** (400 MHz, DMSO- d_6 δ ppm): 13.01 (s, 1H), 8.11 (d, 2H, *J* = 8.4 Hz, Ar-H), 7.95 (s, 1H, imidazole proton), 7.85 (s, 1H, Ar-H), 7.80 (d, 2H, *J* = 8.4 Hz, Ar-H), 7.69 (d, 2H, *J* = 8.4 Hz, Ar-H), 7.62 (d, 1H, *J* = 8.4 Hz, Ar-H), 7.51 (d, 2H, *J* = 8.4 Hz, Ar-H), 5.19 (s, 2H, S-CH2-protons); **^{13}C NMR** (100 MHz, DMSO-d_6) δ: 191.2, 151.3, 138.3, 133.2, 132.5, 131.6, 129.8, 128.4, 128.4, 128.0, 125.3, 121.0, 116.6, 112.7, 110.9, 108.6, 107.0, 39.9; ESI-HRMS: *m/z* Calcd for $C_{24}H_{16}Cl_4N_4OS_2$ [M+2] 579.9520, found: 579.1554.

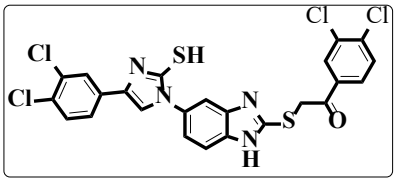

2-((5-(2-Mercapto-4-(4-nitrophenyl)-1*H*-imidazol-1-yl)-1*H*-benzo[*d*]imidazol-2-yl) thio)-1-(4-nitrophenyl)ethan-1-one. 4i

Brown solid: yield: 90%, mp: 275-277 °C; FT-IR (KBr, cm^{-1}): 3362 (NH), 1678 (C=O), 1629 (C=N); **^{1}H NMR** (400 MHz, $CDCl_3$+DMSO- d_6 δ ppm): 13.15 (s, 1H, SH), 8.37 (d, J = 9.2 Hz, 2H), 8.32 (d, J = 8.8 Hz, 2H), 8.23 (d, J = 9.2 Hz, 2H), 7.97 (d, J = 8.8 Hz, 2H), 7.94 (s, 1H, imidazole proton), 7.86 (d, J = 2.0 Hz, 1H), 7.78 (d, J = 2.0 Hz, 1H), 7.55 (s, 1H, Ar-H), 7.53 (s, 1H, Ar-H), 7.39 (d, J = 6.4 Hz, 1H, Ar-H), 5.09 (s, 2H, S-CH_2-protons); **^{13}C NMR** (100 MHz, $CDCl_3$+DMSO-d_6) δ: 192.5, 164.6, 151.5, 150.5, 146.4, 140.3, 134.3, 132.3, 130.0, 127.0, 124.9, 124.4, 124.0, 120.6, 119.4, 113.8, 112.3, 44.9; ESI-HRMS: *m/z* Calcd for $C_{24}H_{17}N_6O_5S_2$ $[M+H]^+$ 533.0702, found: 533.1707.

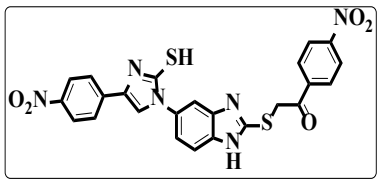

1-([1, 1' –Biphenyl]-4-yl)-2-((5-(4-([1, 1' –biphenyl]-4-yl)-2-mercapto-1*H*-imidazol-1-yl)-1*H*-benzo[*d*]imidazol-2-yl) thio) ethan-1-one. 4j

Light yellow solid: yield: 92%, mp: 251-253 °C; FT-IR (KBr, cm^{-1}): 3393 (NH), 1668 (C=O), 1631 (C=N); **^{1}H NMR** (400 MHz, DMSO-d_6 δ ppm): 13.00 (s, 1H, SH), 12.75 (s, 1H, NH), 8.16 (d, J = 8.0 Hz, 2H, Ar-H), 7.90-7.92 (m, 3H, Ar-H), 7.78-7.80 (m, 5H Ar-H), 7.52-7.55 (m, 5H, Ar-H), 7.45 – 7.48 (m, 4H), 7.39 (s, 1H, imidazole proton), 7.11 (d, J = 8.8 Hz, 2H), 5.18 (s, 2H, S-CH_2-protons); **^{13}C NMR** (100 MHz, DMSO-d_6) δ: 192.8, 152.1, 146.0, 145.8, 139.1, 137.9, 135.6, 134.3, 133.9, 133.7, 129.8, 129.6, 129.1, 128.9, 127.5, 117.8, 114.7, 107.6, 41.9; ESI-HRMS: *m/z* Calcd for $C_{36}H_{27}N_4OS_2$ $[M+H]^+$ 595.1626, found: 595.1648.

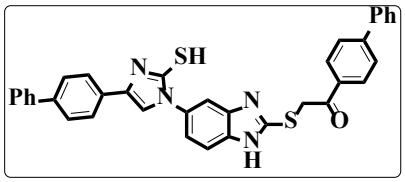

1-(2-(Benzylthio)-1*H*-benzo[*d*]imidazol-5-yl)-4-phenyl-1*H*-imidazole-2-thiol. 5a

White solid: yield: 89%, mp: 172-174 °C; FT-IR (KBr, cm^{-1}): 3345 (NH), 1628 (C=N), 1423 (C=C); **^{1}H NMR** (400 MHz, $CDCl_3$+DMSO-d_6 δ ppm): 12.65 (s, 1H, SH), 8.15 (s, 1H, Ar-H), 8.06 (d, 2H, J = 7.6 Hz), 7.16 (d, 1H, J = 7.7 Hz), 7.48-7.57 (m, 4H, Ar-H), 7.40 (s, 1H, Ar-H), 7.17 – 7.31 (m, 5H, Ar-H), 7.09 (d, 1H, J = 6.8 Hz, Ar-H), 5.19 (s, 2H, S-CH_2- protons); **^{13}C NMR** (100 MHz, $CDCl_3$+DMSO-d_6) δ: 171.6, 151.5, 135.6, 135.4, 135.1, 134.4, 134.0, 132.0, 131.4, 129.3, 129.2, 128.9, 121.7, 119.6, 114.7, 108.4, 36.1; ESI-HRMS: *m/z* Calcd for $C_{23}H_{19}N_4S_2$ $[M+H]^+$ 415.1051, found: 415.1054.

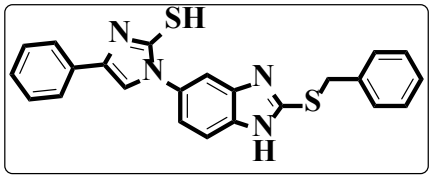

1-(2-(Benzylthio)-1*H*-benzo[*d*]imidazol-5-yl)-4-(4-methoxyphenyl)-1*H*-imidazole-2-thiol. 5b

White solid: yield: 87%, mp: 176-178 °C; FT-IR (KBr, cm^{-1}): 3376 (NH), 1666 (C=O), 1634 (C=N); **^{1}H NMR** (400 MHz, $CDCl_3$+DMSO- d_6 δ ppm):12.41 (s, 1H, SH), 10.25 (s, 1H, NH), 8.15-8.19 (m, 1H, Ar-H), 8.11 (s, 1H, Ar-H), 8.03 (d, J = 7.6 Hz, 2H), 7.42-7.57 (m, 5H, Ar-H), 7.31 (d, J = 7.6 Hz, 1H), 7.10 (d, J = 7.2 Hz, 1H), 7.05 (d, J = 8.4 Hz, 2H), 5.26 (s, 2H, S-CH_2-protons), 3.9 (s, 3H,-OCH_3); **^{13}C NMR** (100 MHz, $CDCl_3$+DMSO d_6) δ: 170.1, 164.4, 152.4, 133.1, 132.5, 131.3, 129.2, 129.0, 128.2, 127.9, 126.0, 117.4, 114.4, 110.3, 107.8, 105.1, 55.9, 41.7; ESI-HRMS: *m/z* Calcd for $C_{24}H_{21}N_4OS_2$ $[M+H]^+$ 445.1157, found: 445.1181.

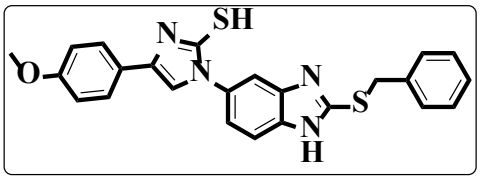

1-(2-((4-Nitrobenzyl)thio)-1*H*-benzo[*d*]imidazol-5-yl)-4-phenyl-1*H*-imidazole-2-thiol. 5c

White solid: yield: 90%, mp: 146-148 °C; FT-IR (KBr, cm^{-1}): 3372 (NH), 1621 (C=N); **^{1}H NMR** (400 MHz, DMSO- d_6 δ ppm): 13.00(1H, SH), 8.10 (s, 1H, Ar-H), 8.06 (d, J = 7.2 Hz, 2H), 7.65-7.72 (m, Ar-H, 2H), 7.59 (s, 1H, imidazole proton), 7.51-7.57 (m, 5H), 7.24 (dd, J = 8.4, 2.0 Hz, 2H, Ar-H), 5.23 (s, 2H, S-CH_2-protons), 1.21 (brs, 1H); ESI-HRMS: *m/z* Calcd for $C_{23}H_{18}N_5O_2S_2$ $[M+H]^+$ 460.0902, found: 460.0940.

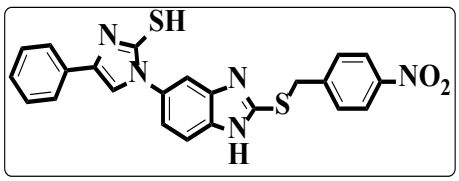

4-(4-Chlorophenyl)-1-(2-((4-nitrobenzyl) thio)-1*H*-benzo[*d*]imidazol-5-yl) 1*H*-imidazole-2-thiol. 5d

White solid: yield: 95%, mp: 155-157 °C; FT-IR (KBr, cm^{-1}): 3372 (NH), 1622 (C=N); **^{1}H NMR** (400 MHz, DMSO-d_6 δ ppm): 10.55 (s, 1H, SH), 8.33 (s, 1H, NH), 8.10 (d, J = 7.6 Hz, 2H), 8.00 (d, J = 7.2 Hz, 2H), 7.75 (d, 2H, J= 6.8 Hz Ar-H), 7.67 (s, 1H, imidazole proton), 7.60 – 7.64 (m, 3H),7.56 (d, 2H, J= 7.6 Hz Ar-H), 5.45 (s, 2H, S-CH_2-proton); **^{13}C NMR** (100 MHz, DMSO d_6) δ: 170.2, 152.9, 147.1, 146.4, 140.1, 134.8, 131.6, 130.6, 128.9, 128.3, 127.2, 124.0, 122.0, 105.9, 34.5; ESI-HRMS: *m/z* Calcd for $C_{23}H_{17}ClN_5O_2S_2$ $[M+H]^+$ 494.0512, found: 494.0562.

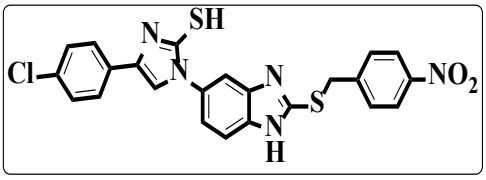

4-(4-Bromophenyl)-1-(2-((4-nitrobenzyl) thio)-1*H*-benzo[*d*]imidazol- 5-yl) 1*H*-imidazole-2-thiol. 5e

Pale yellow solid: yield: 96%, mp: 167-169 °C; FT-IR (KBr, cm^{-1}): 3359 (NH), 1621 (C=N); 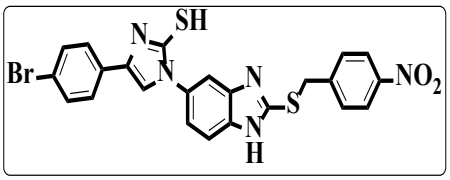

^{1}H NMR (400 MHz, DMSO- d_6 δ ppm) 10.25 (s, 1H, SH), 8.07-8.09 (m, 4H, Ar-H), 8.01 (s, 1H, imidazole proton), 7.73 (d, 1H, *J*=7.6 Hz Ar-H), 7.60-7.64 (m, 4H, Ar-H), 7.43 (d, 2H, *J* = 8.8 Hz, Ar-H), 5.33 (s, 2H, S-CH_2-protons); **^{13}C NMR** (100 MHz, DMSO d_6) δ: 170.3, 152.9, 147.1, 146.4, 140.2, 132.5, 131.8, 130.6, 128.6, 127.2, 124.0, 123.6, 122.0, 105.9, 34.5; ESI-HRMS: *m/z* Calcd for $C_{23}H_{17}BrN_5O_2S_2$ $[M+H]^+$; 538. 0007, found: 538.0041.

4-([1, 1' –Biphenyl]-4-yl)-1-(2-(benzylthio)-1*H*-benzo[*d*]imidazol-5-yl)-1*H*-imidazole-2-thiol. 5f

Brown solid: yield: 92%, mp: 175-177 °C; FT-IR (KBr, cm^{-1}): 3369 (NH), 1633 (C=N), 1423; 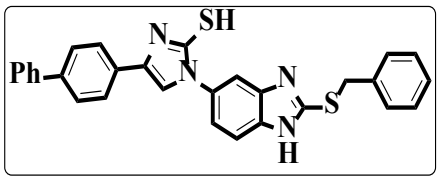

^{1}H NMR (400 MHz, $CDCl_3$+DMSO- d_6 δ ppm): 10.09 (s, 1H, SH), 9.89 (brs, 1H, NH), 8.37 (s, 1H, Ar-H), 8.18 (d, *J* = 8.4 Hz, 2H), 7.93 (s, 1H, imidazole proton), 7.82 (d, 2H, *J* = 8.8 Hz, Ar-H), 7.70 (d, 2H, *J* = 8.0 Hz, Ar-H), 7.58-7.55 (m, 3H, Ar-H), 7.51 – 7.49 (m, 3H, Ar-H), 7.44 (d, 1H, *J* = 7.2 Hz, Ar-H), 7.33 (t, 2H, *J*= 8.0 Hz, Ar-H), 7.14 (d, 1H, *J* = 7.6 Hz, 1H), 5.37 (s, 2H, S-CH_2-protons); **^{13}C NMR** (100 MHz, $CDCl_3$+DMSO d_6) δ: 170.14, 152.3, 151.6, 136.1, 134.2, 134.0, 133.1, 132.5, 129.9, 129.6, 129.4, 129.3, 129.0, 128.2, 127.4, 127.0, 126.1, 118.9, 117.5, 114.6, 110.4, 107.9, 105.1, 36.8; ESI-HRMS: *m/z* Calcd for $C_{29}H_{23}N_4S_2$ $[M+H]^+$ 491.1364, found: 491.1382.

3.9. Spectra

^{1}H-NMR Spectrum of compound 4a in ($CDCl_3$+DMSO-d_6 400 MHz):

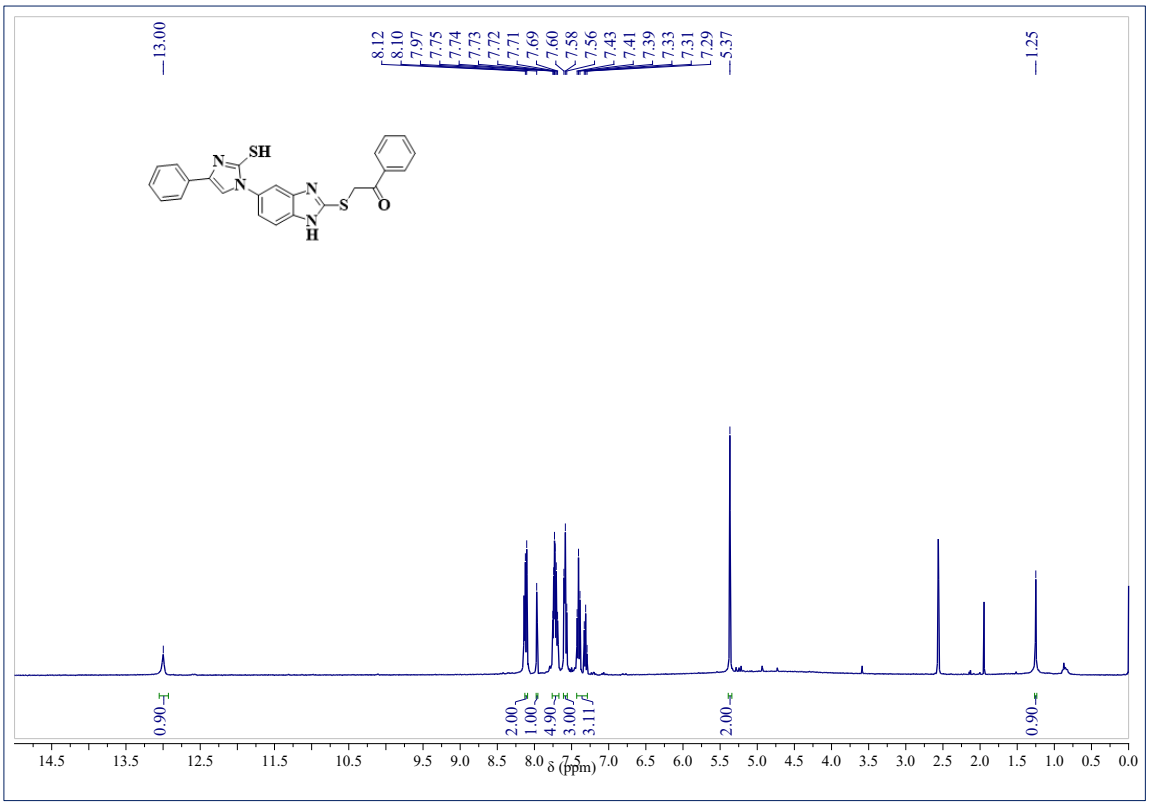

^{13}C-NMR spectrum of compound 4a in ($CDCl_3$+DMSO-d_6, 100 MHz):

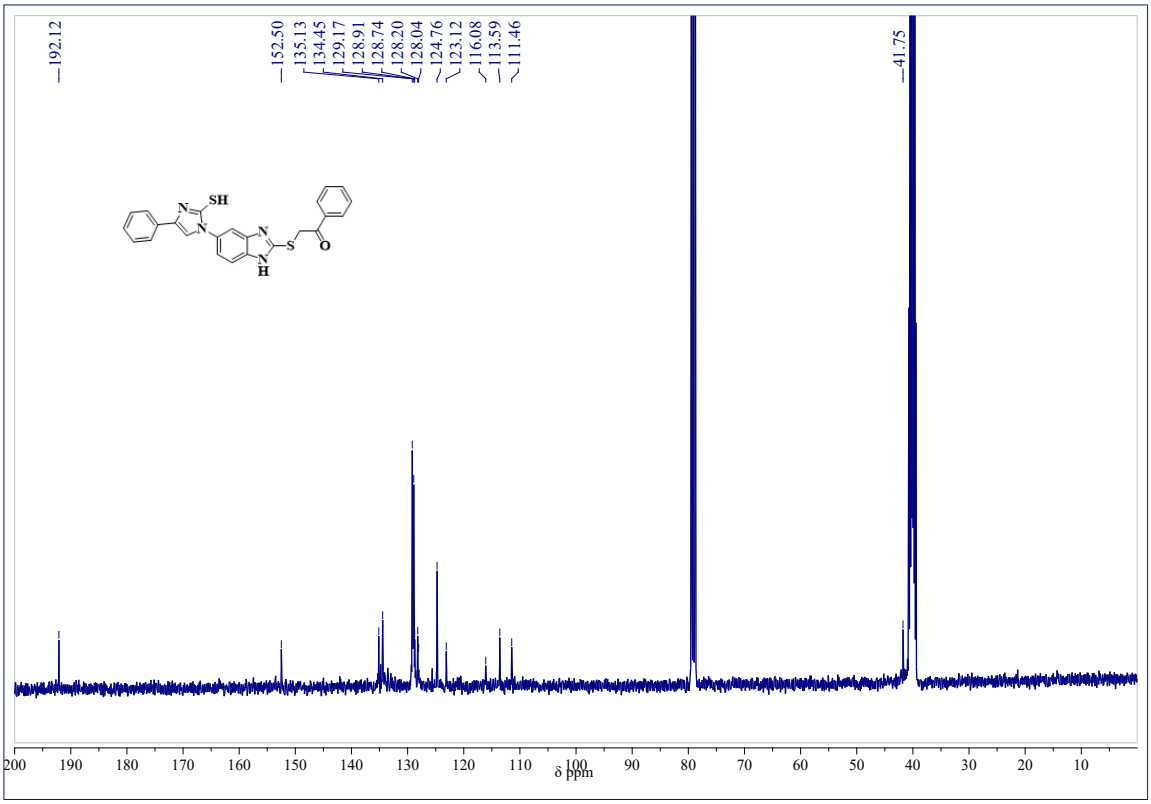

Mass spectrum of compound 4a:

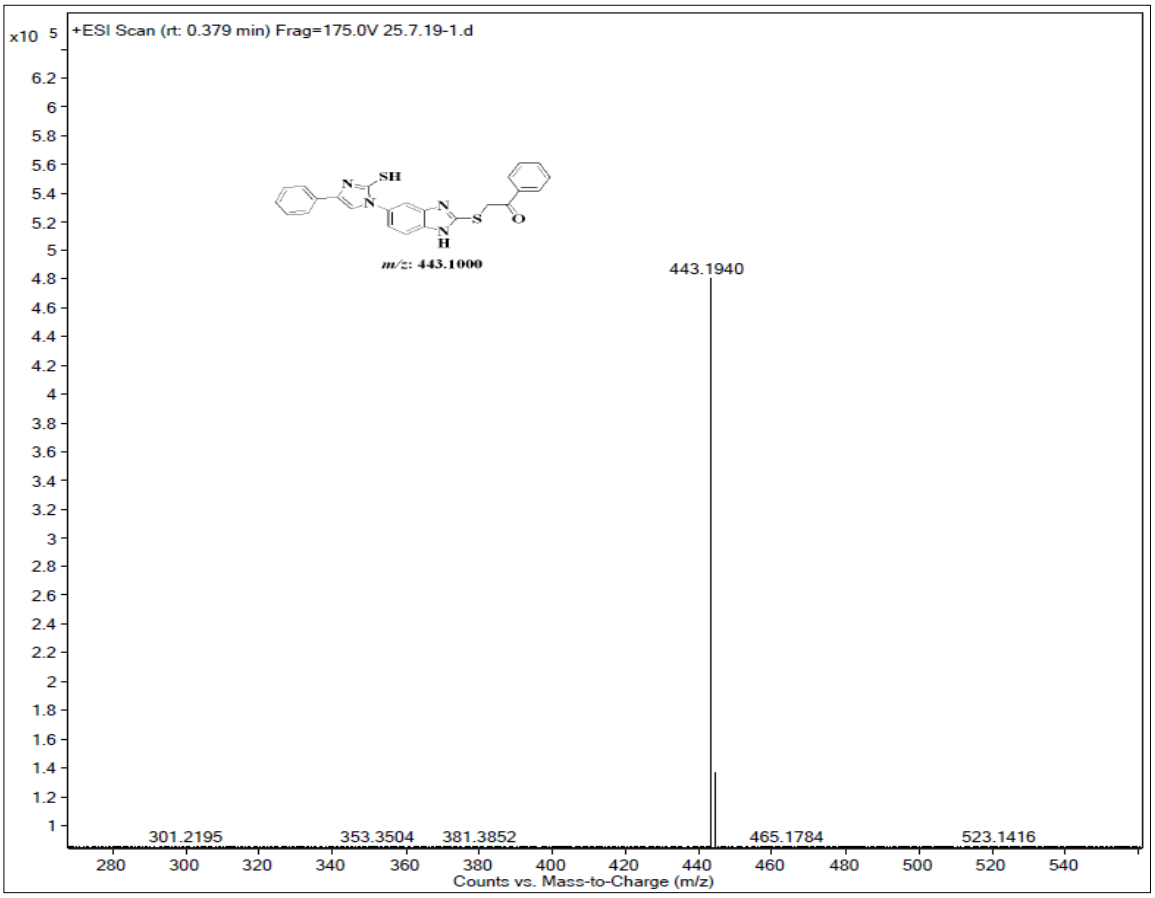

^{1}H-NMR Spectrum of compound 4b in (DMSO-d_6 400 MHz):

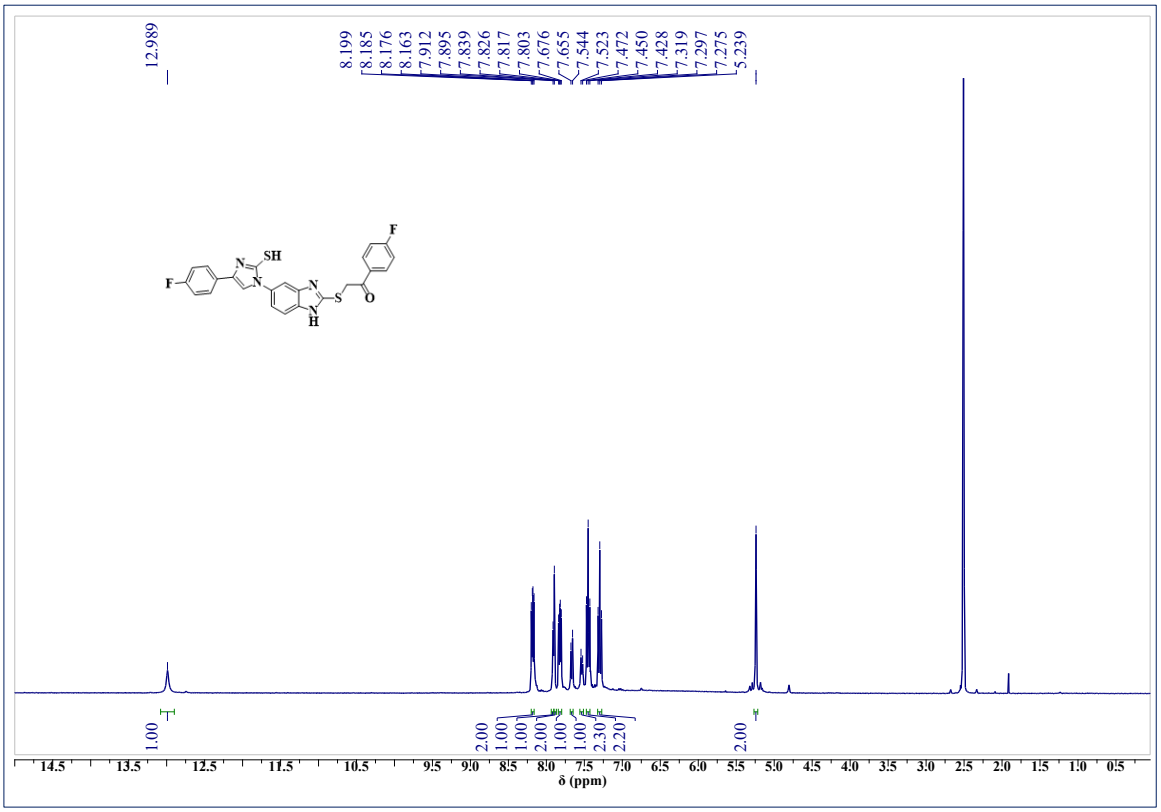

^{13}C-NMR Spectrum of 4b in (DMSO-d_6 100 MHz):

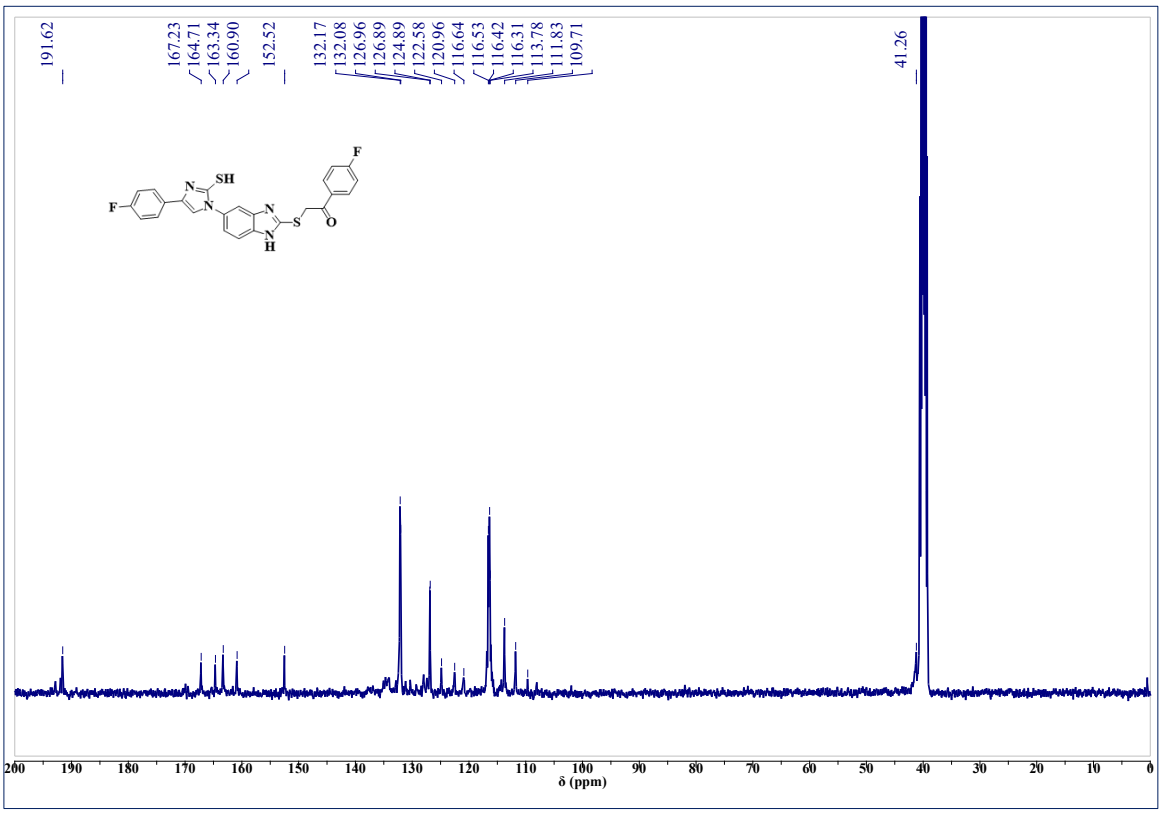

Mass spectrum of compound 4b

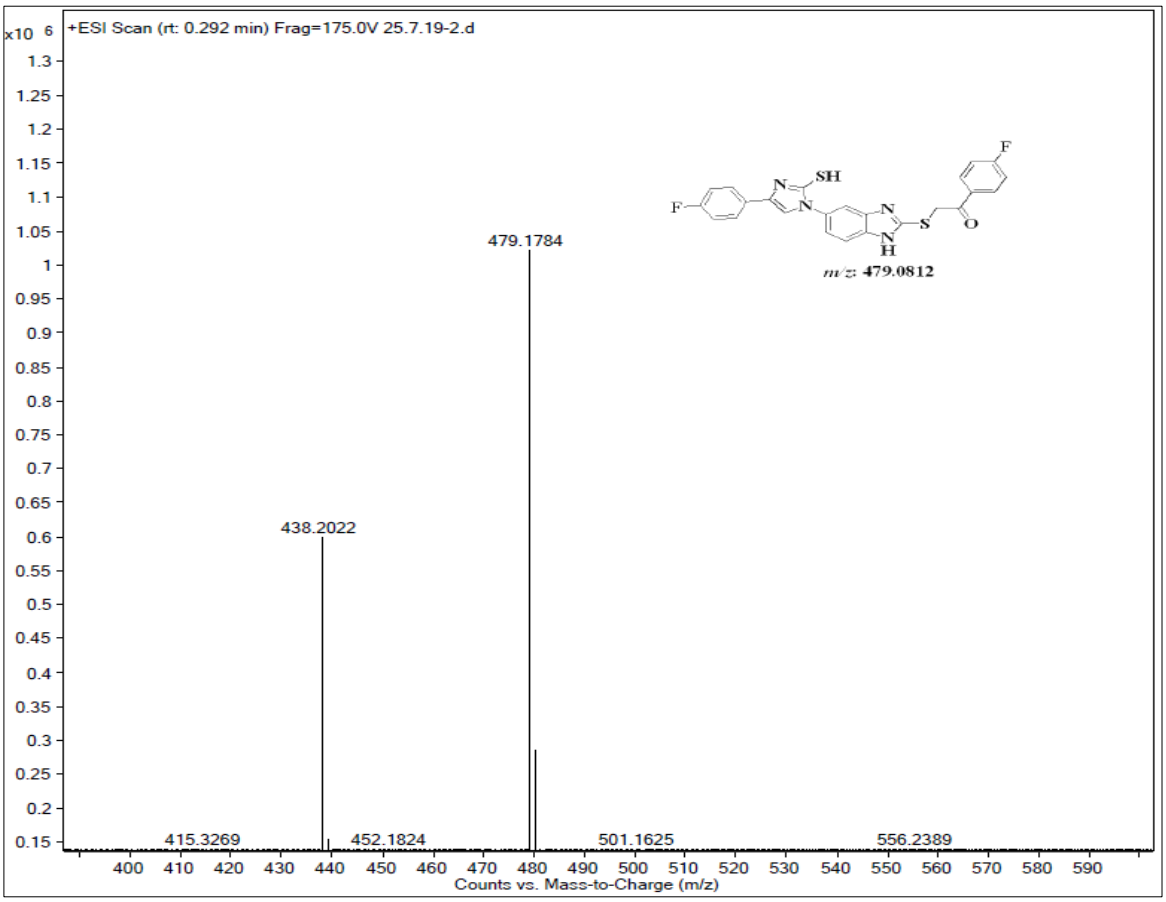

^{1}H-NMR Spectrum of compound 4c in ($CDCl_3$+DMSO-d_6, 400 MHz):

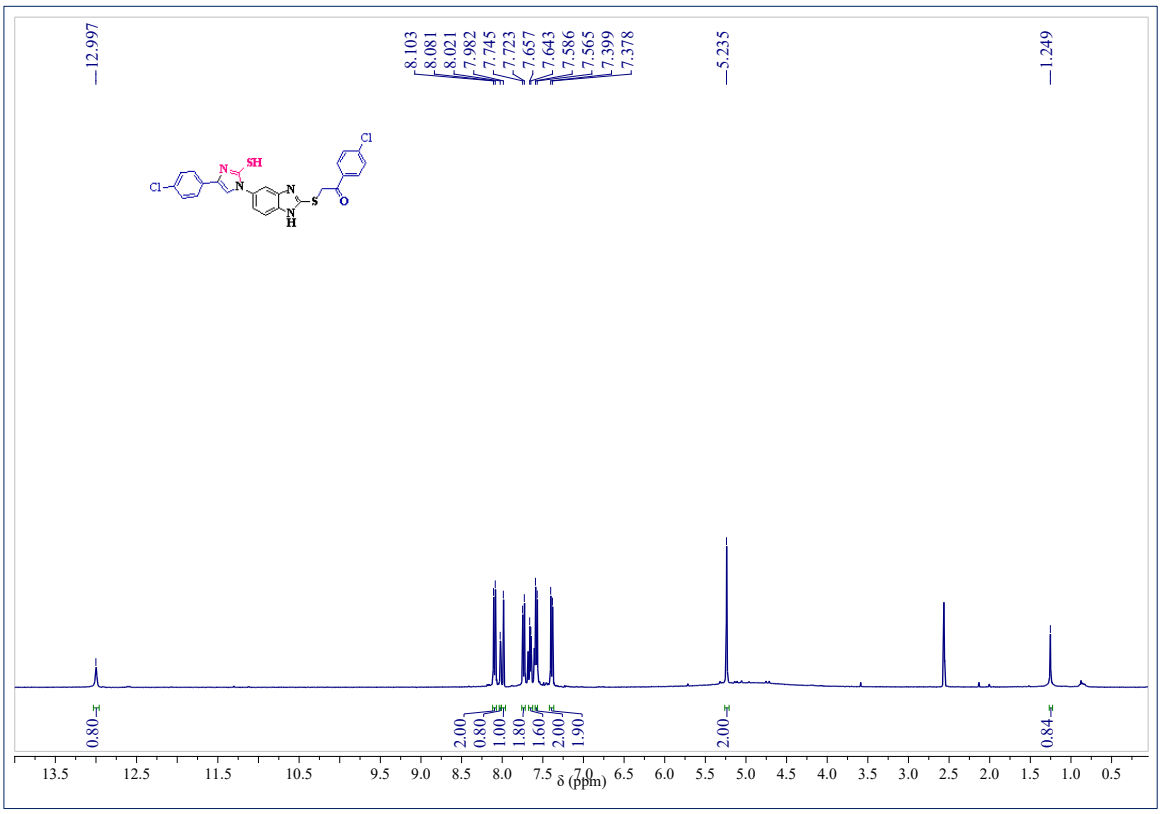

^{13}C-NMR Spectrum of compound 4c in (DMSO-d_6, 100 MHz):

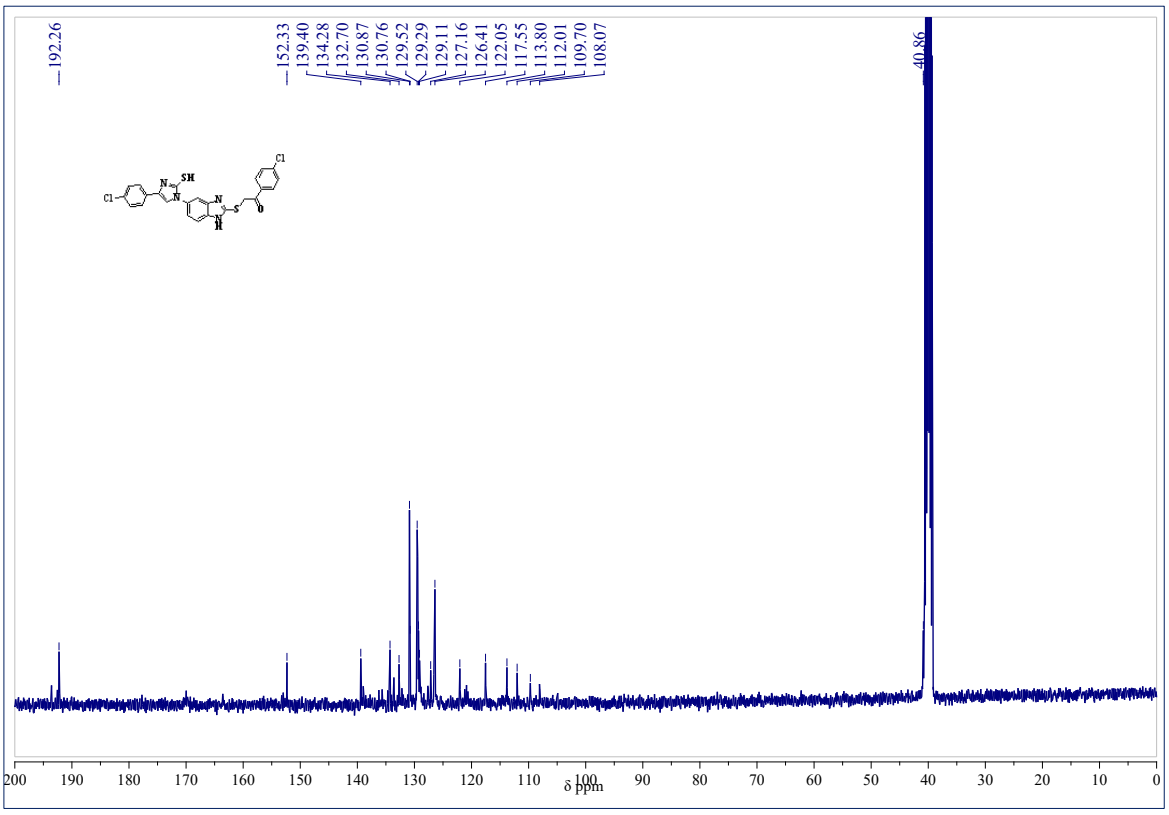

Mass spectrum of compound 4c

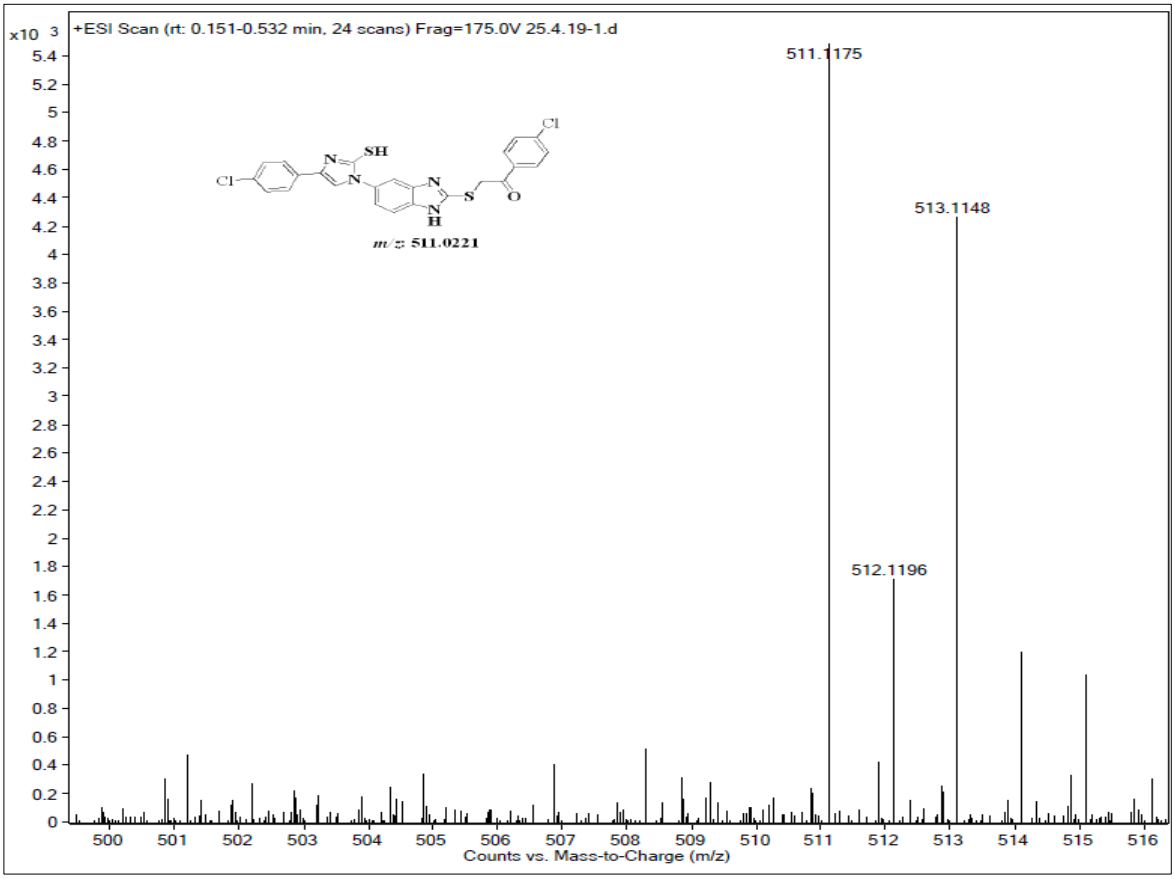

^{1}H-NMR Spectrum of compound 4d in ($CDCl_3$+DMSO-d_6, 400 MHz):

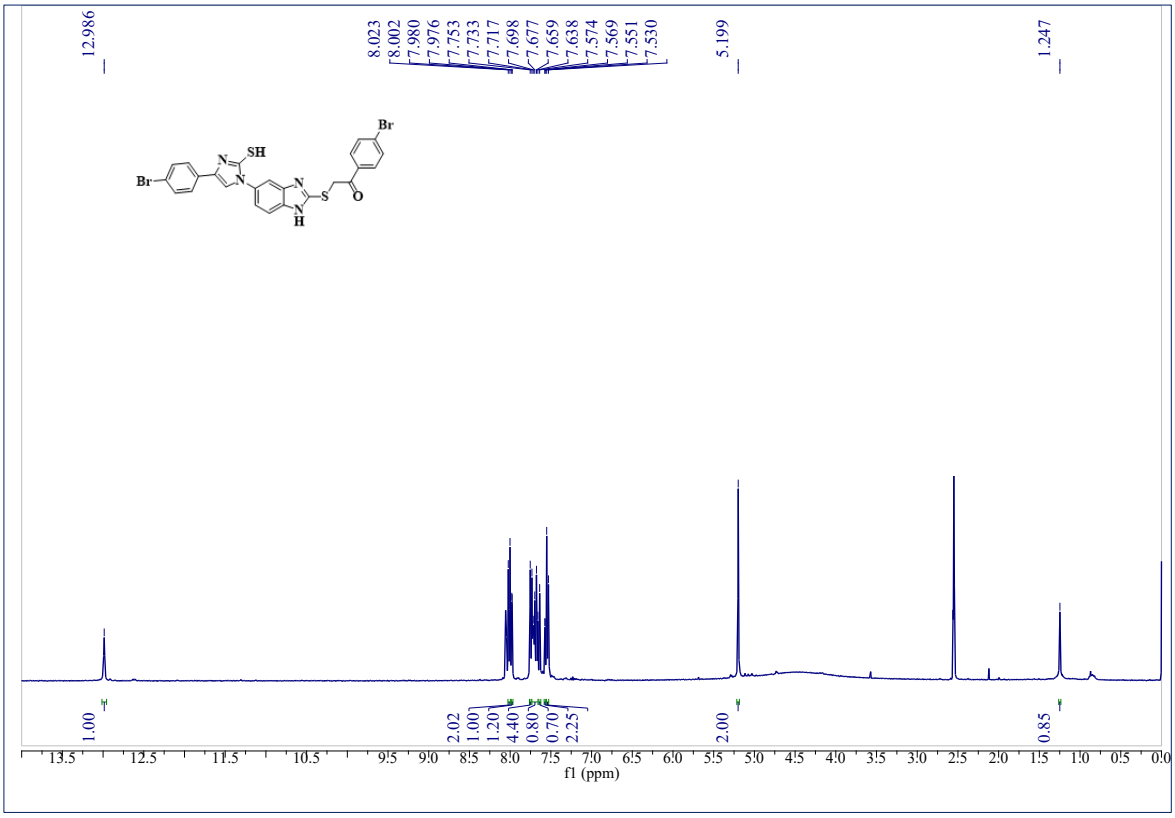

^{13}C-NMR Spectrum of compound 4d (CDCl$_3$+DMSO-d_6, 100 MHz):

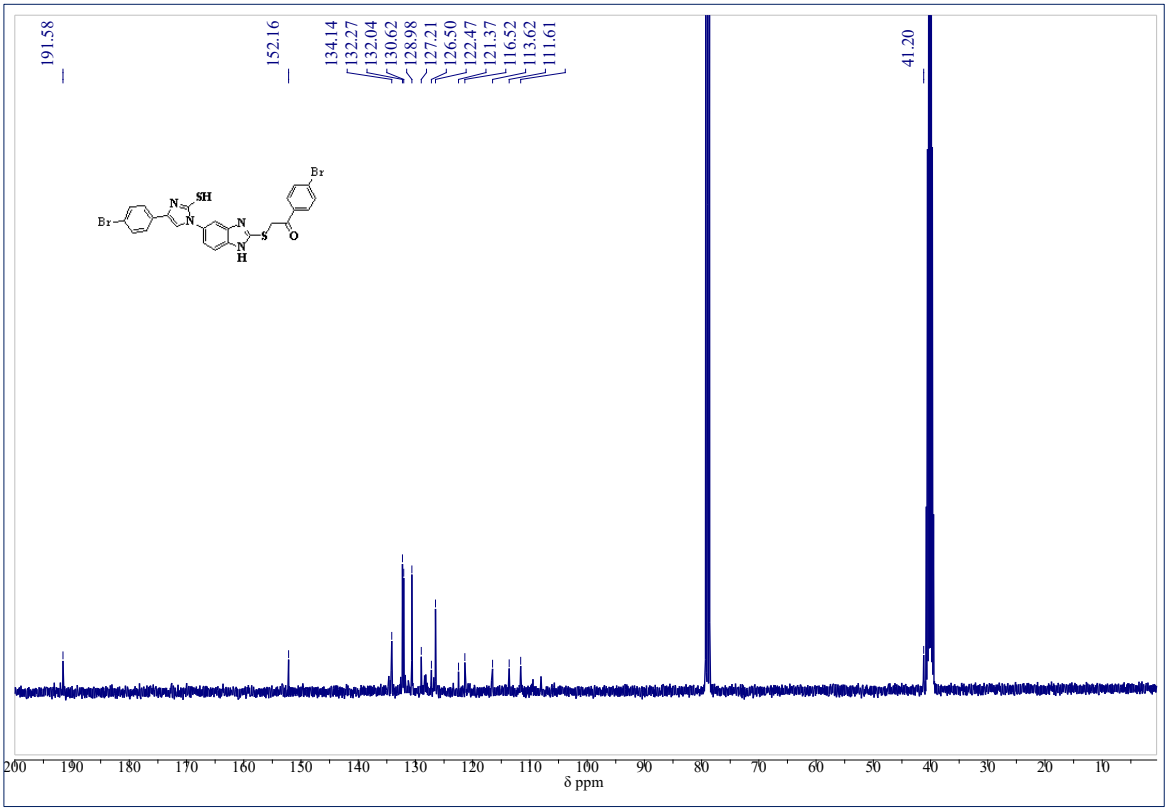

Mass spectrum of compound 4d

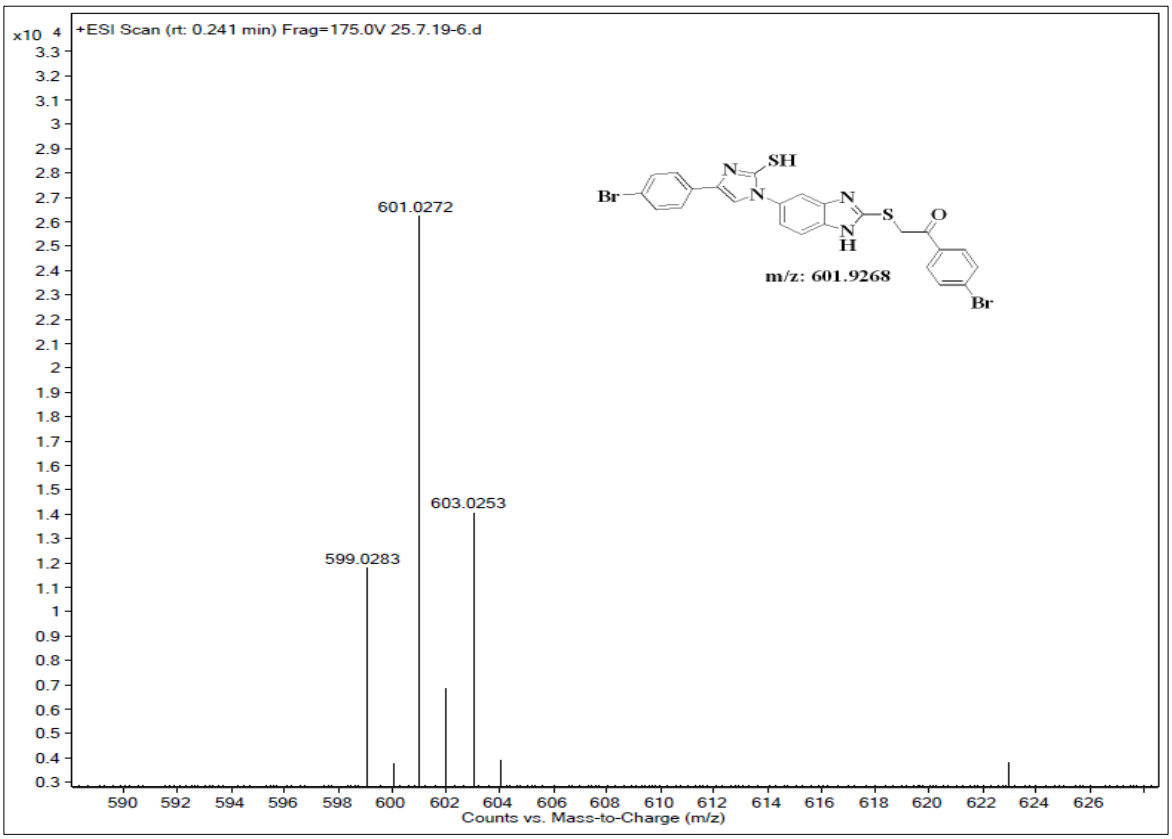

^{1}H-NMR Spectrum of compound 4e in (DMSO-d_6, 400 MHz):

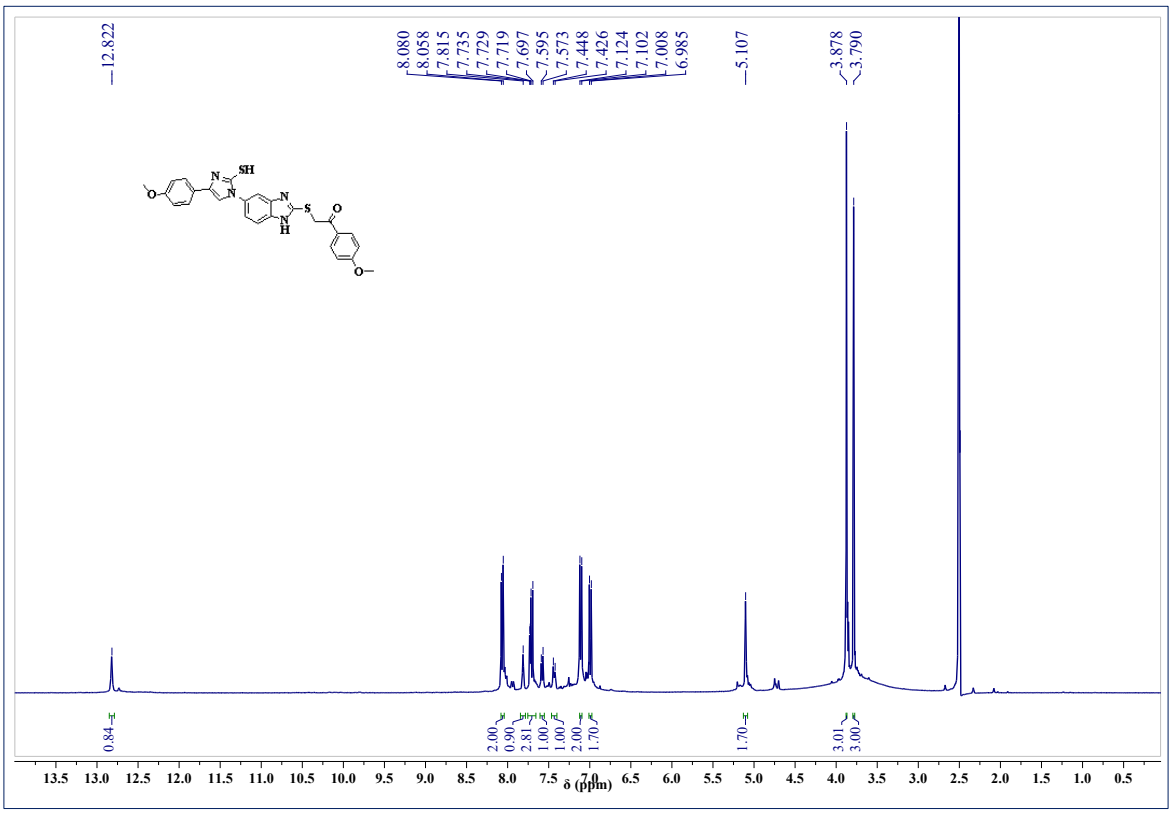

^{13}C-NMR Spectrum of compound 4e in (DMSO-d_6, 100 MHz):

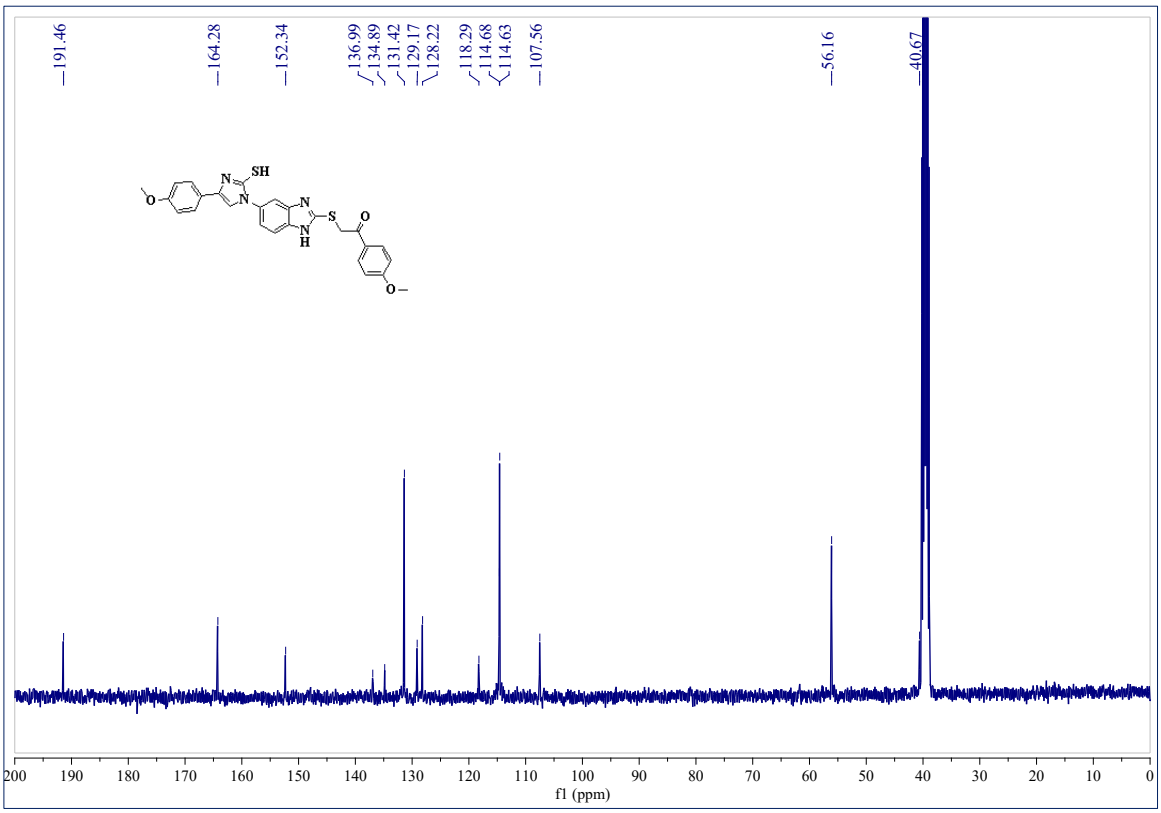

Mass spectrum of compound 4e

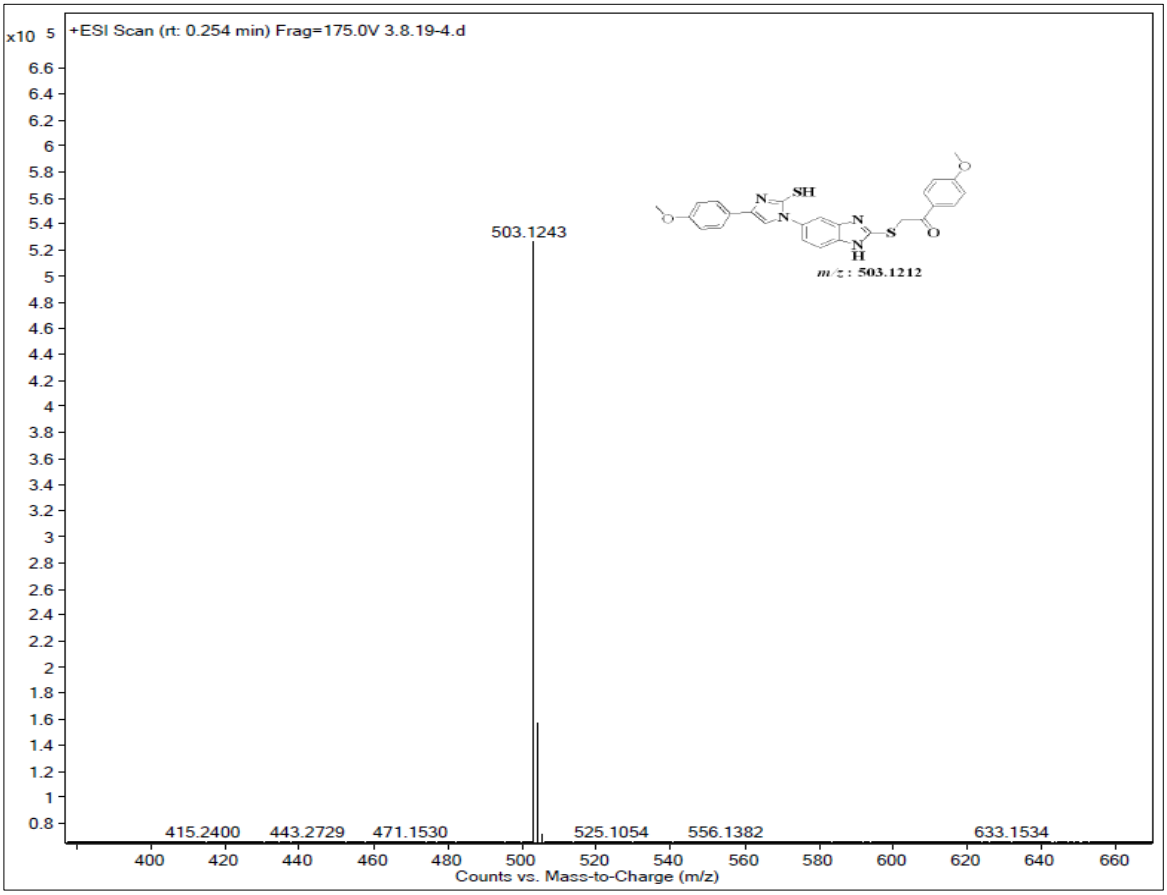

^{1}H-NMR Spectrum of compound 4f in (DMSO-d_6, 400 MHz):

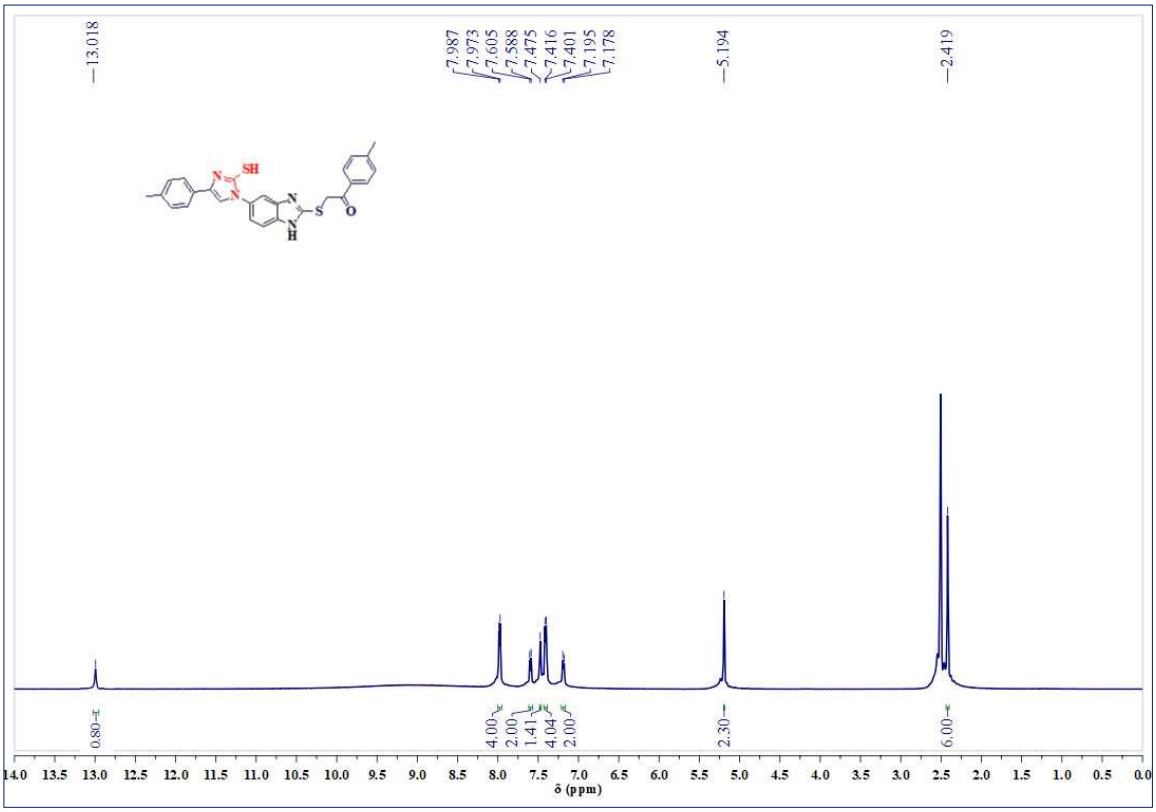

^{13}C-NMR Spectrum of compound 4f ($CDCl_3$+DMSO-d_6, 100 MHz):

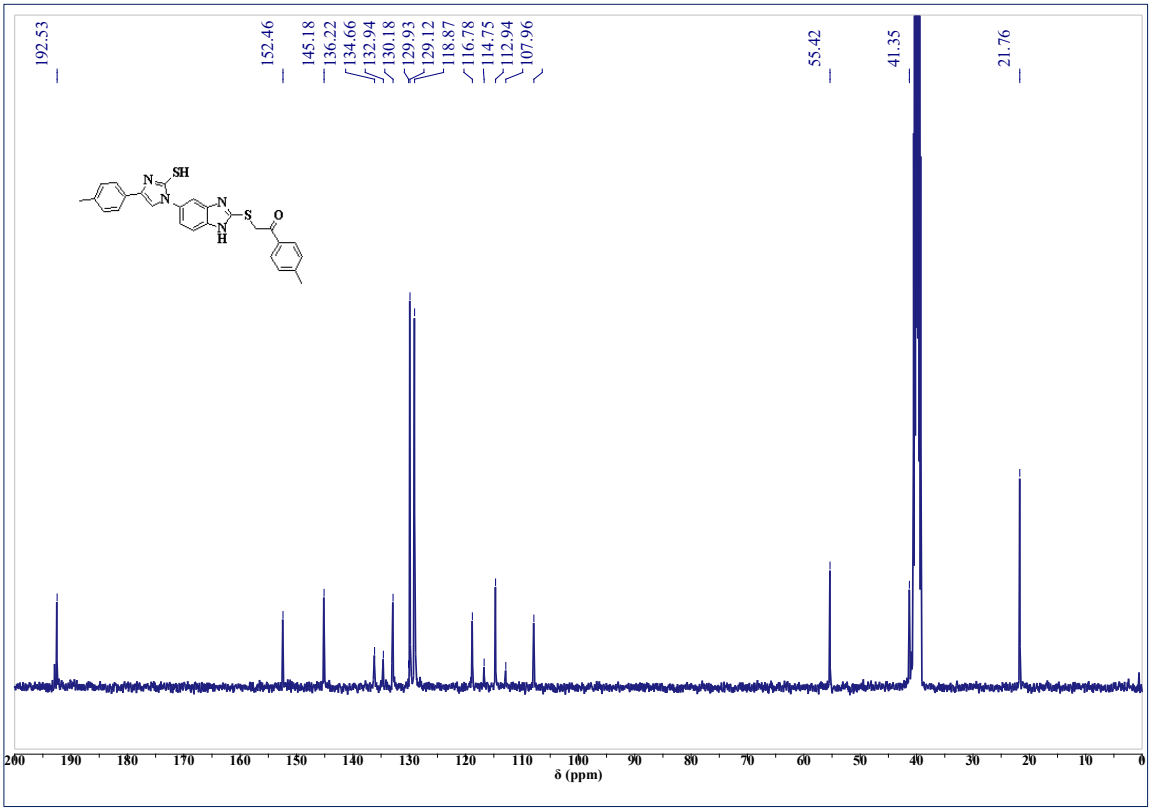

Mass spectrum of compound 4f

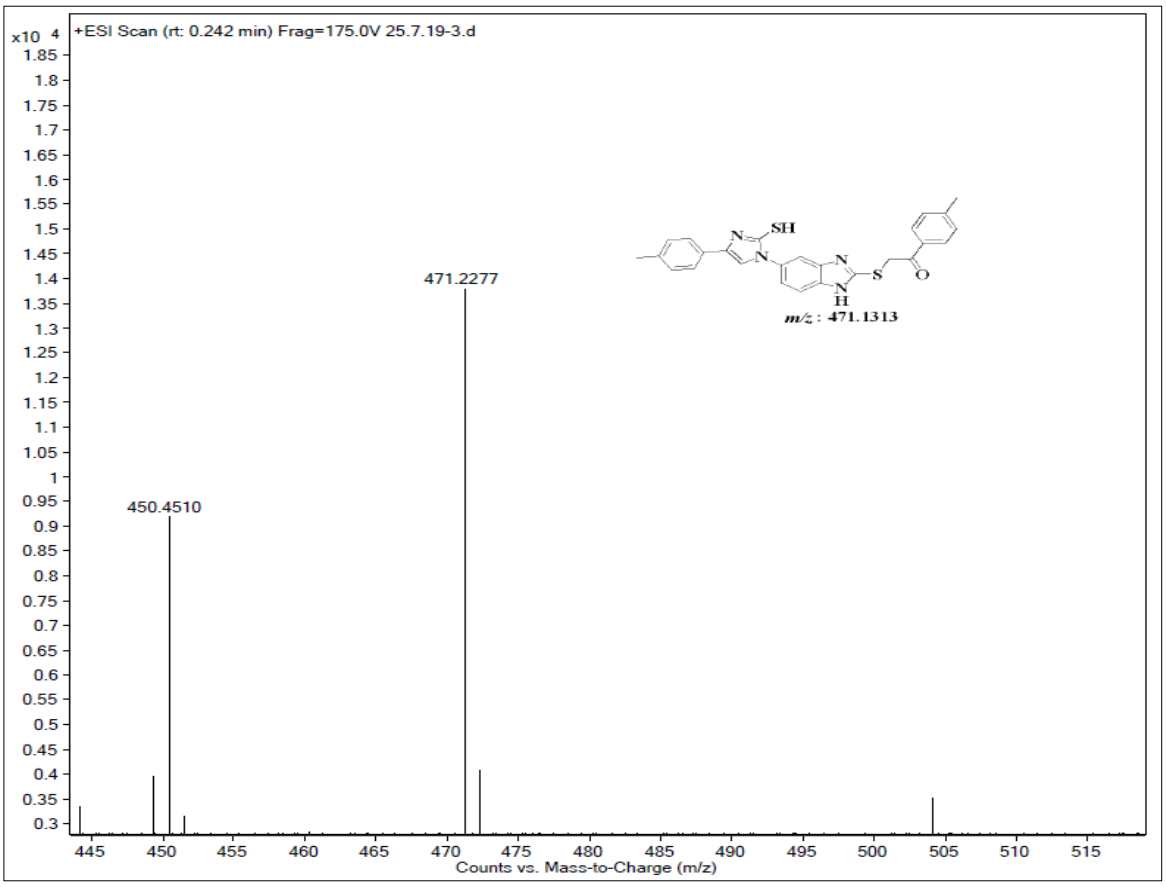

^{1}H-NMR spectrum of compound 4g in (DMSO-d_6, 400 MHz):

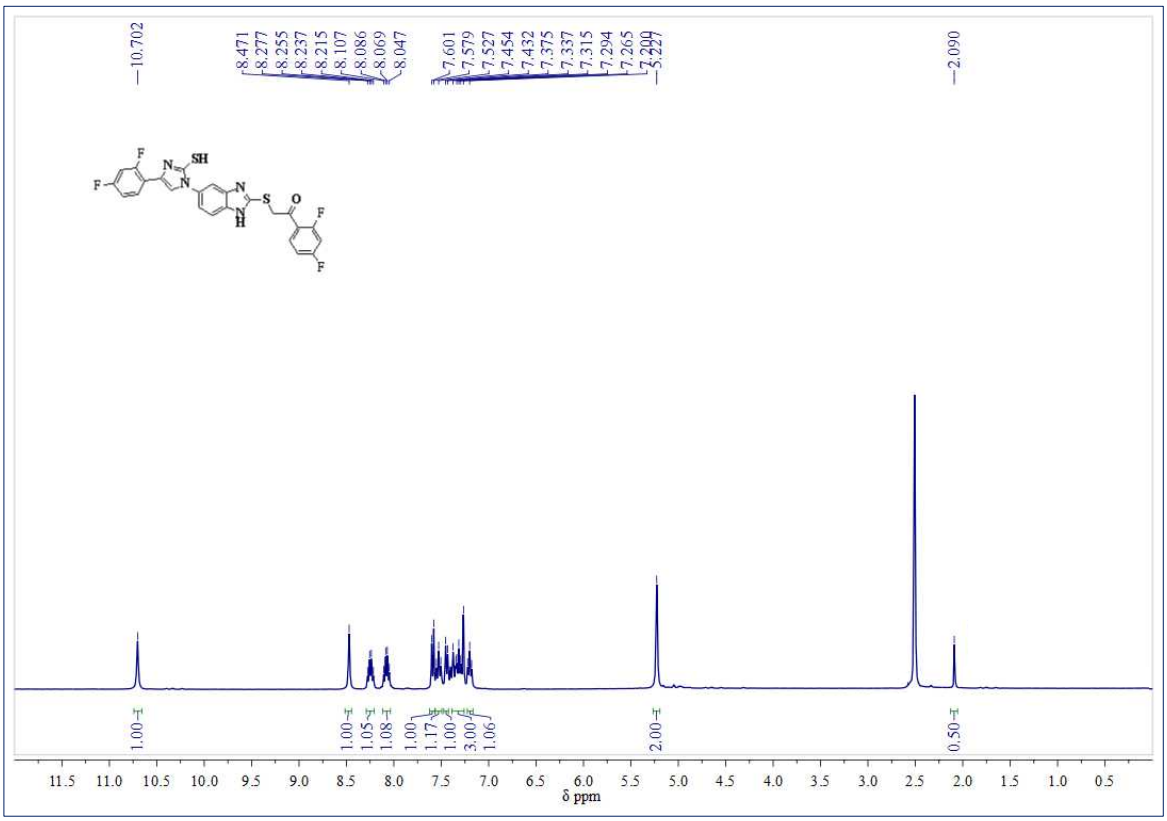

^{13}C-NMR Spectrum of compound 4g in (DMSO-d_6, 100 MHz):

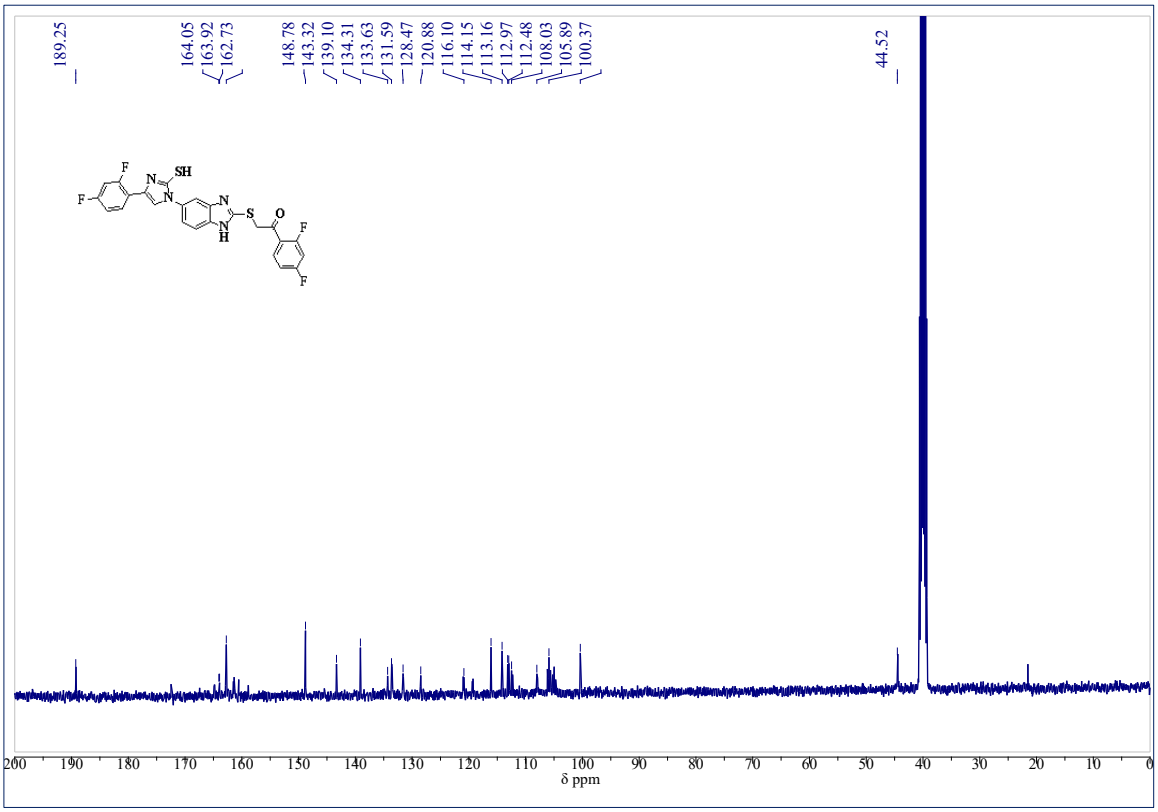

Mass spectrum of compound 4g

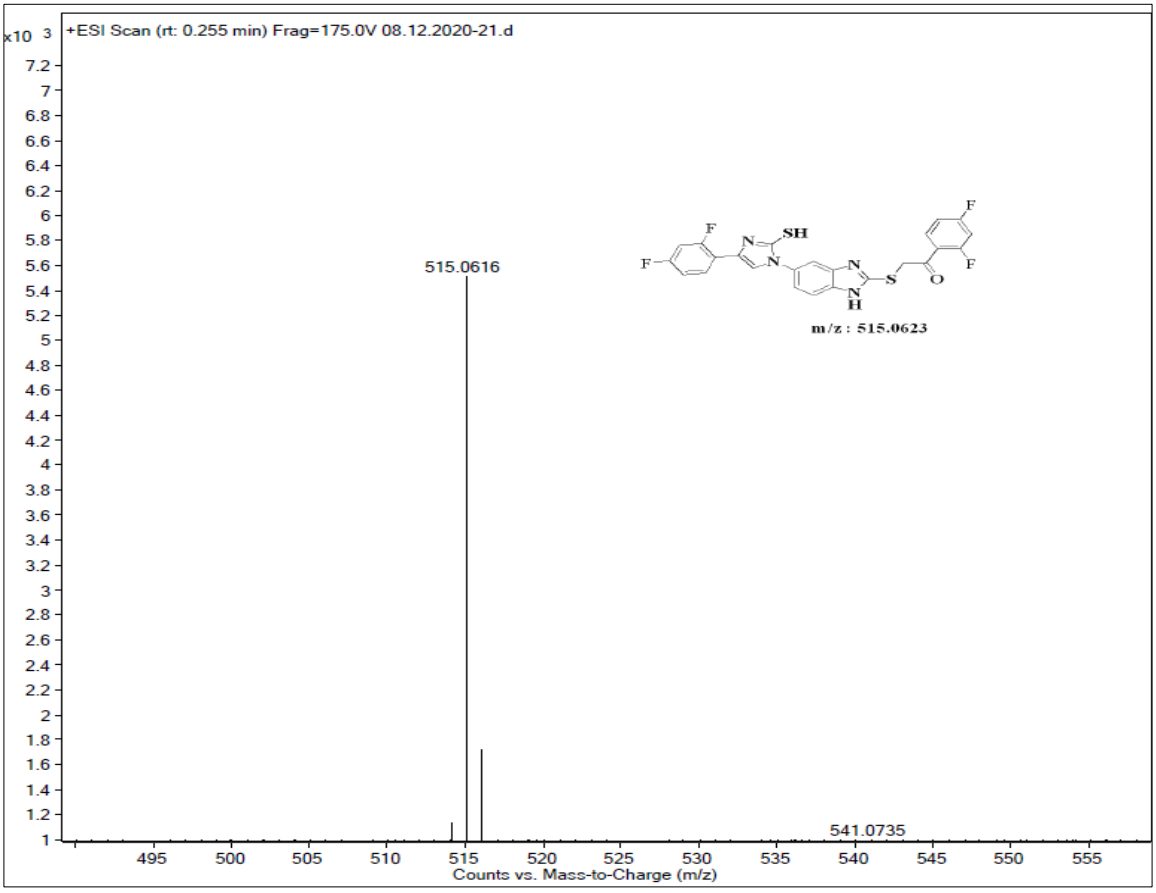

^{1}H-NMR Spectrum of compound 4h in (DMSO-d_6, 400 MHz):

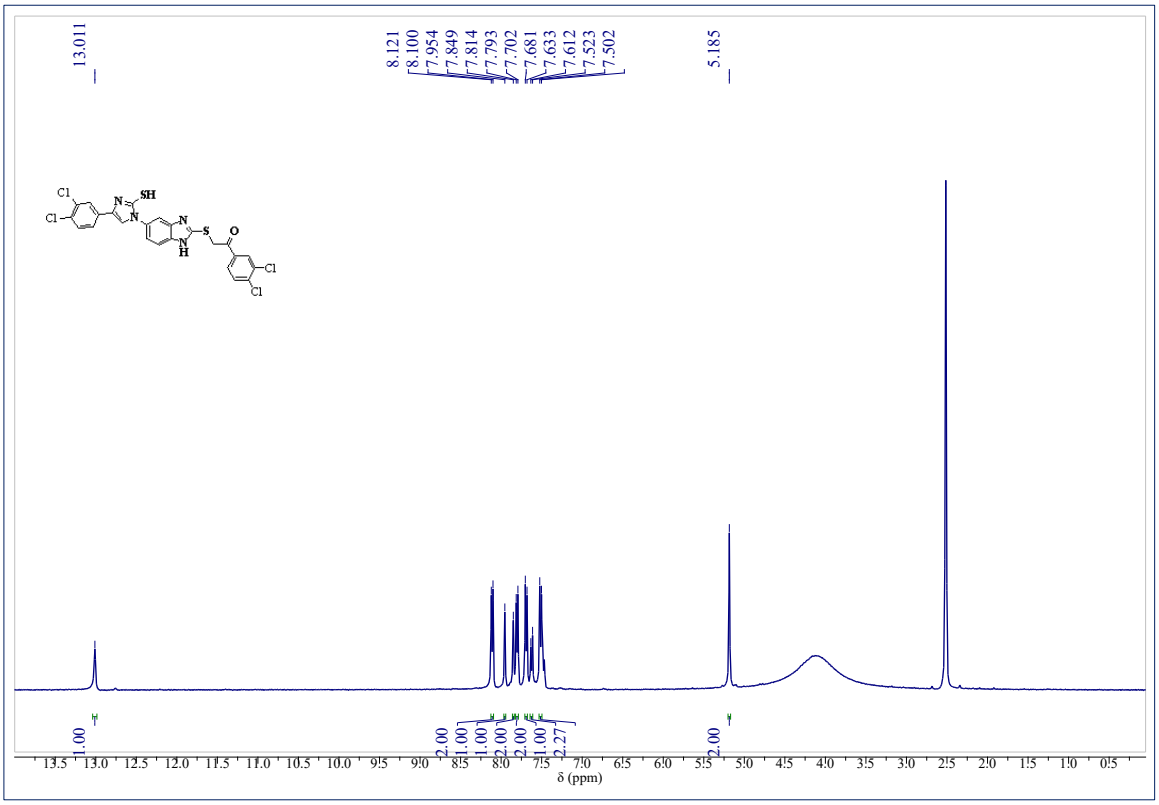

^{13}C-NMR Spectrum of compound 4h in (DMSO-d_6, 100 MHz):

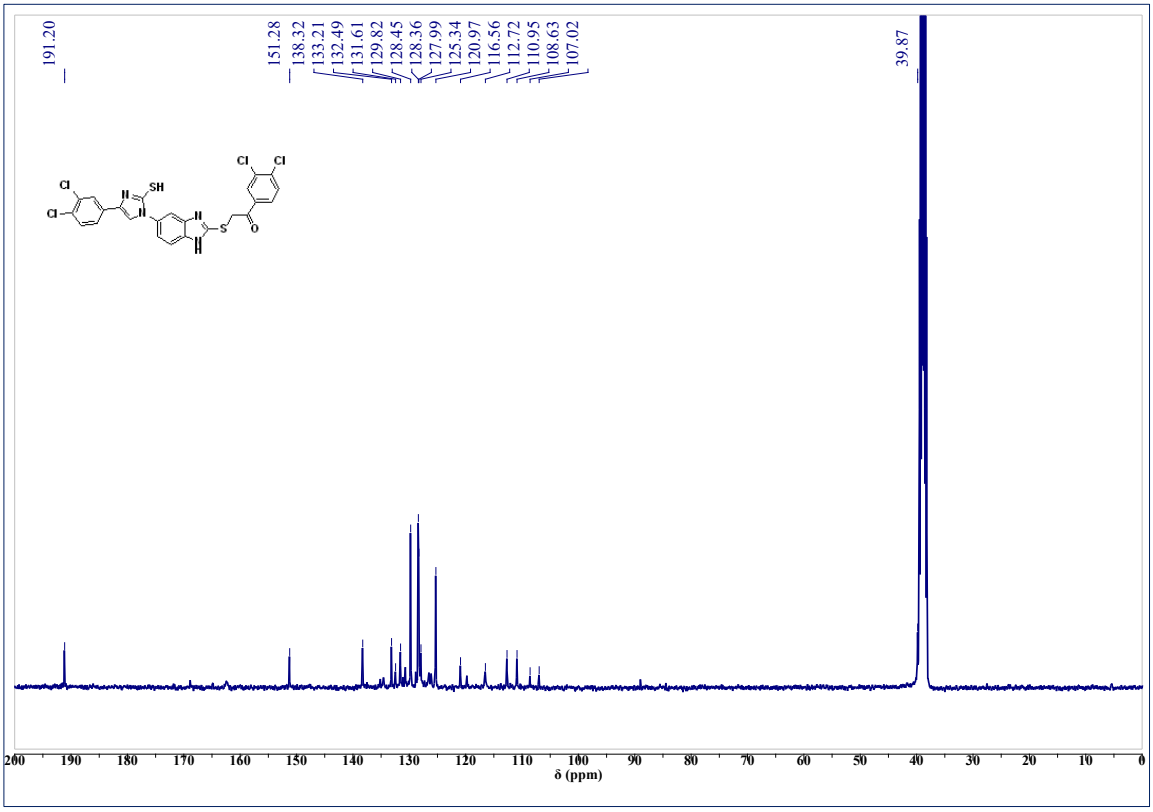

Mass spectrum of compound 4h

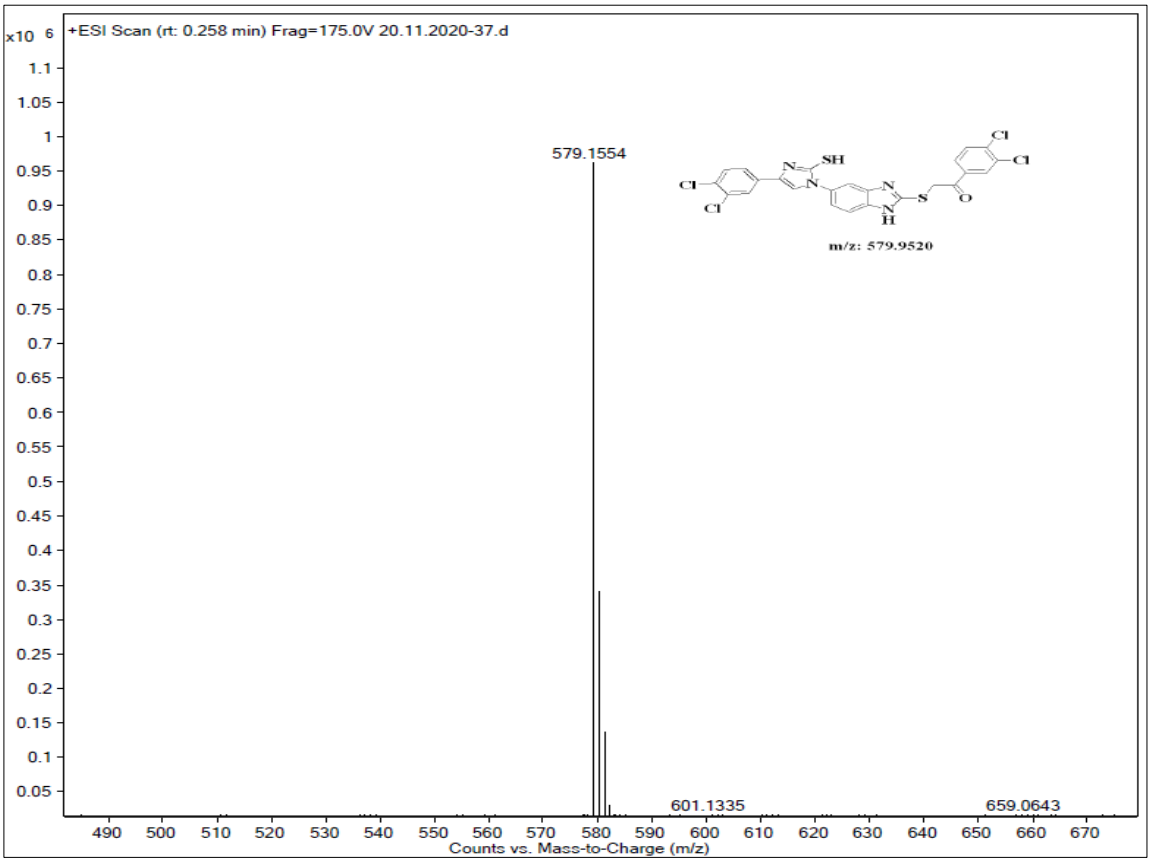

^{1}H-NMR spectrum of compound 4i in ($CDCl_3$+DMSO-d_6, 400 MHz):

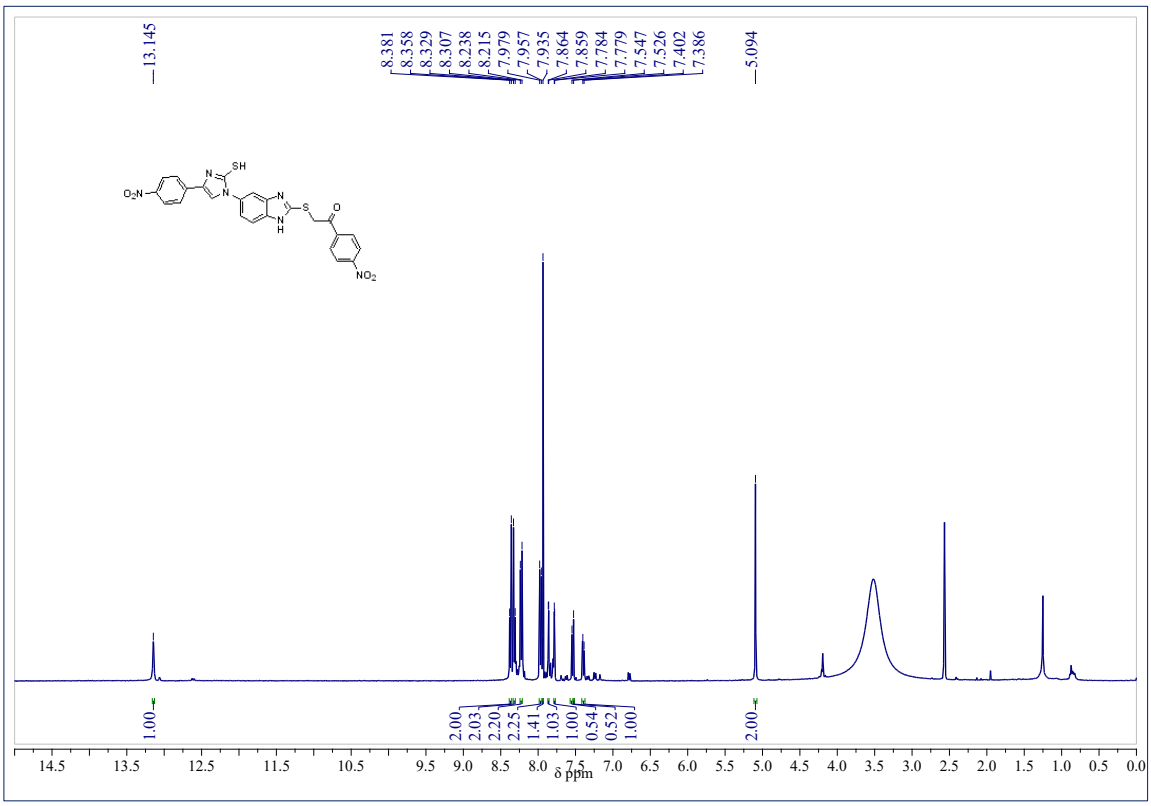

^{13}C-NMR spectrum of compound 4i in ($CDCl_3$+DMSO-d_6, 100 MHz):

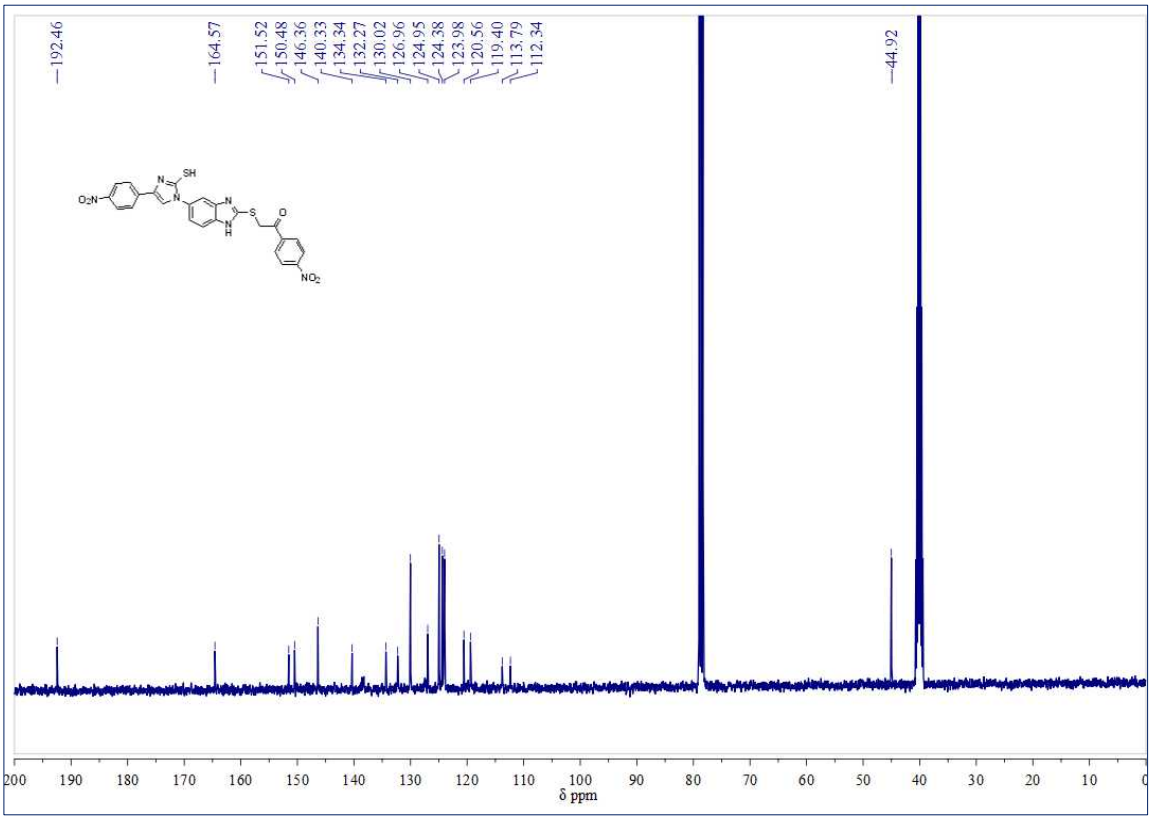

Mass spectrum of compound 4i

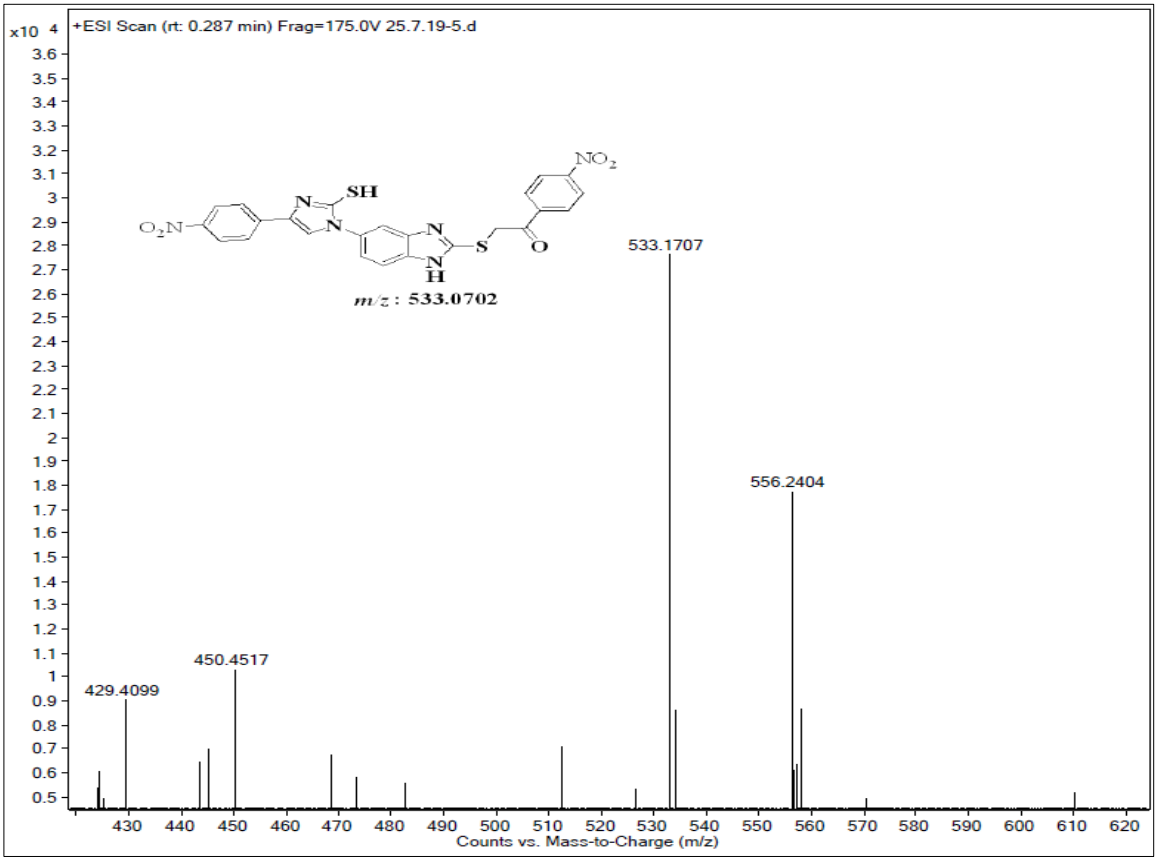

^{1}H-NMR Spectrum of compound 4j in (DMSO-d_6, 400 MHz):

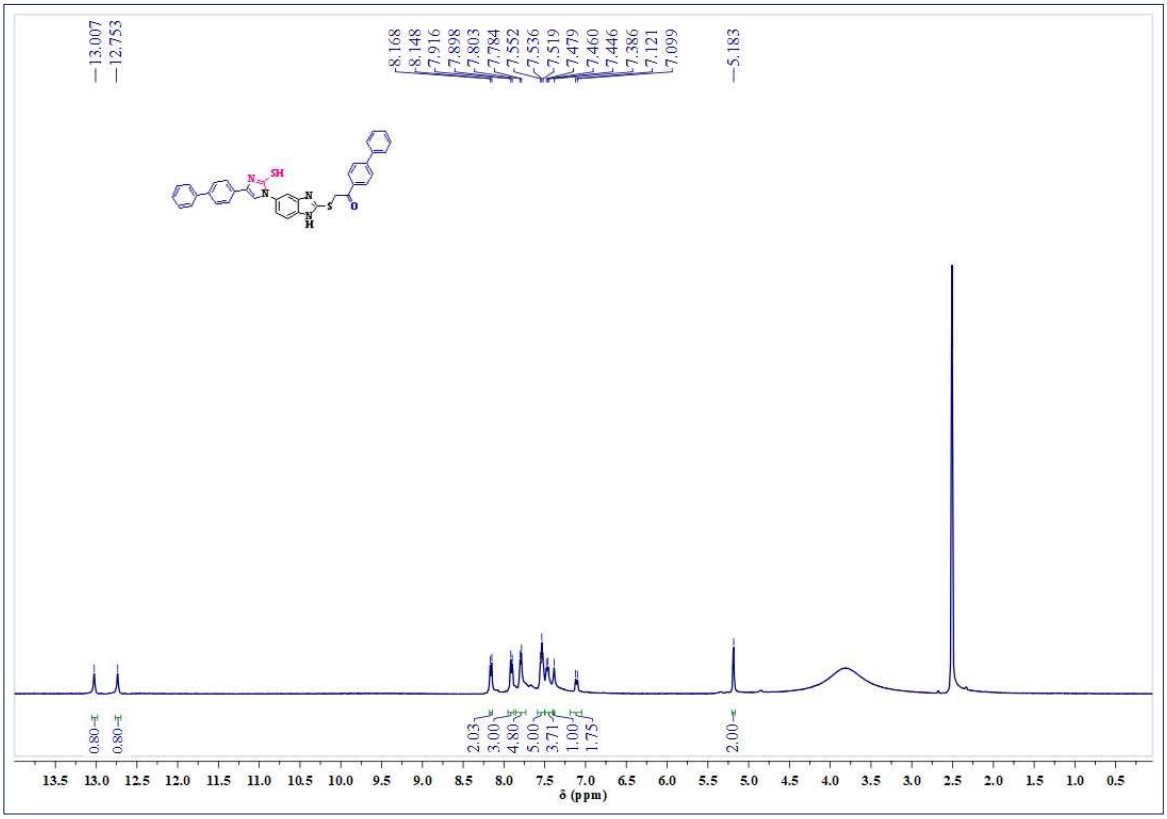

^{13}C-NMR spectrum of compound 4j in (DMSO-d_6, 100 MHz):

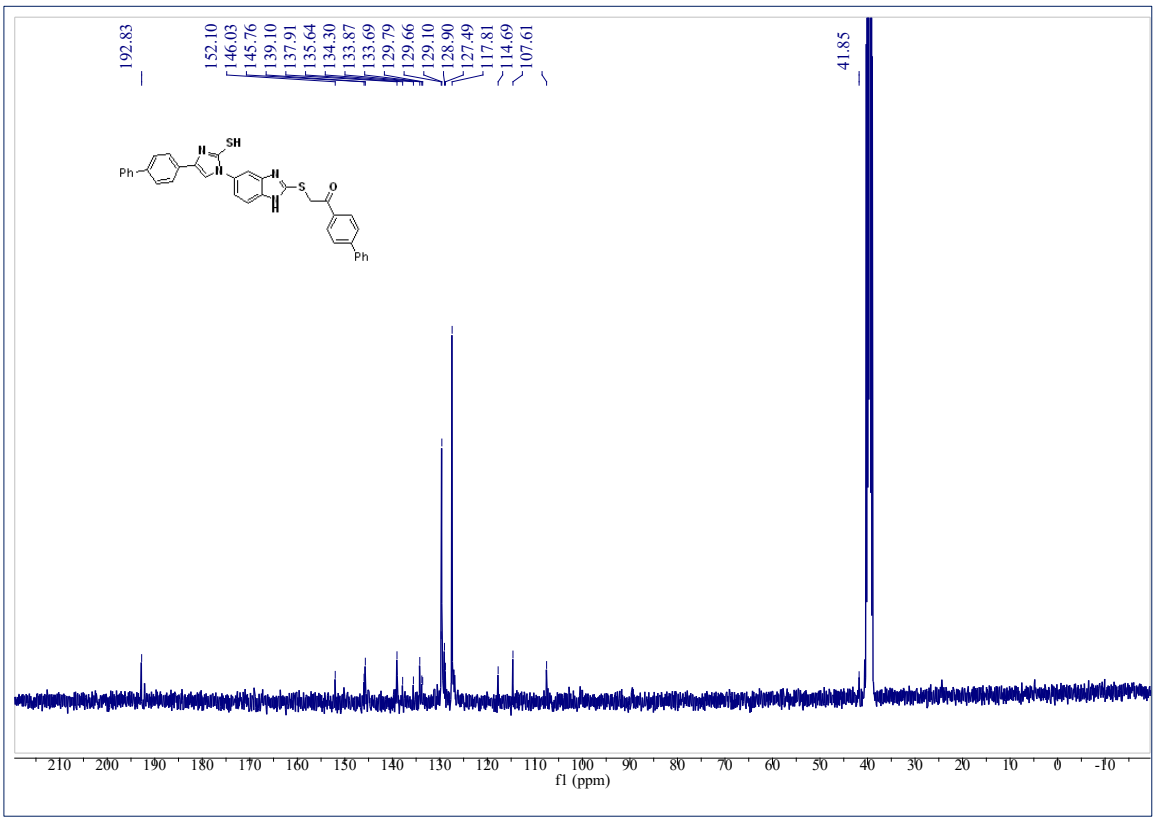

Mass spectrum of compound 4j

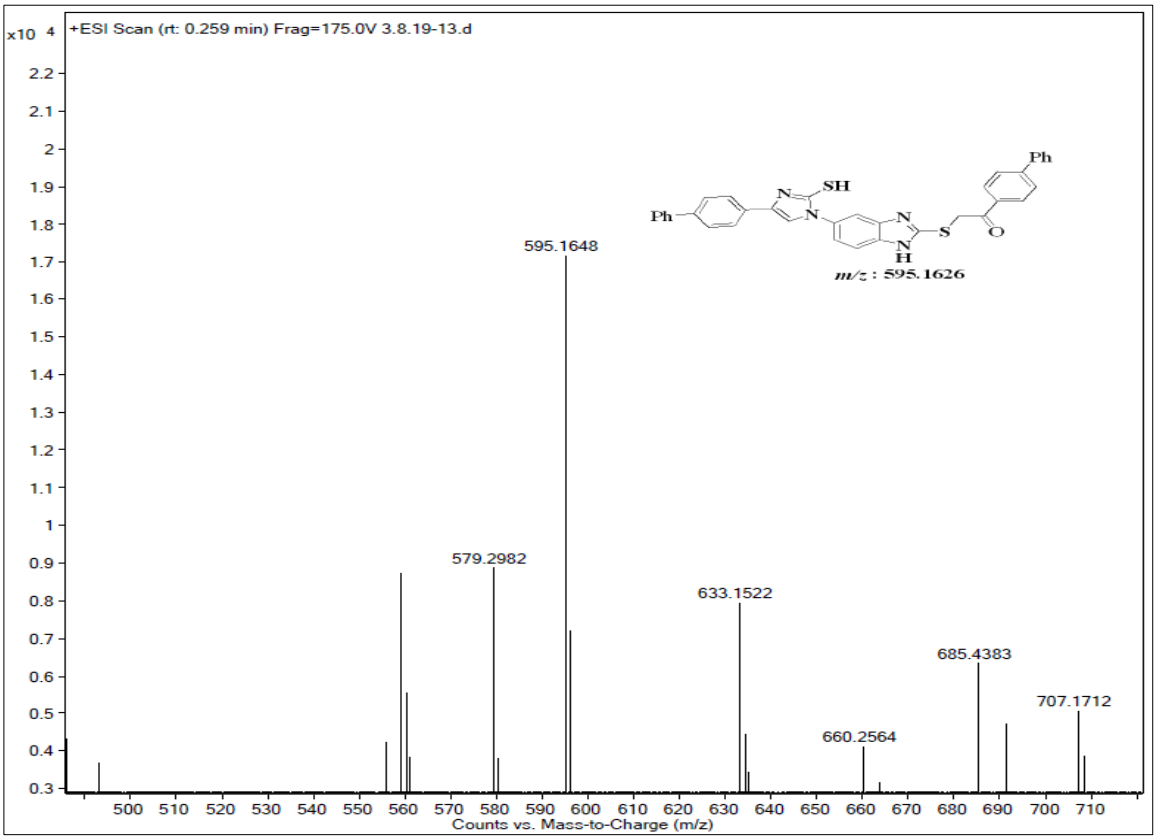

^{1}H-NMR Spectrum of compound 5a in ($CDCl_3$+DMSO-d_6, 400 MHz):

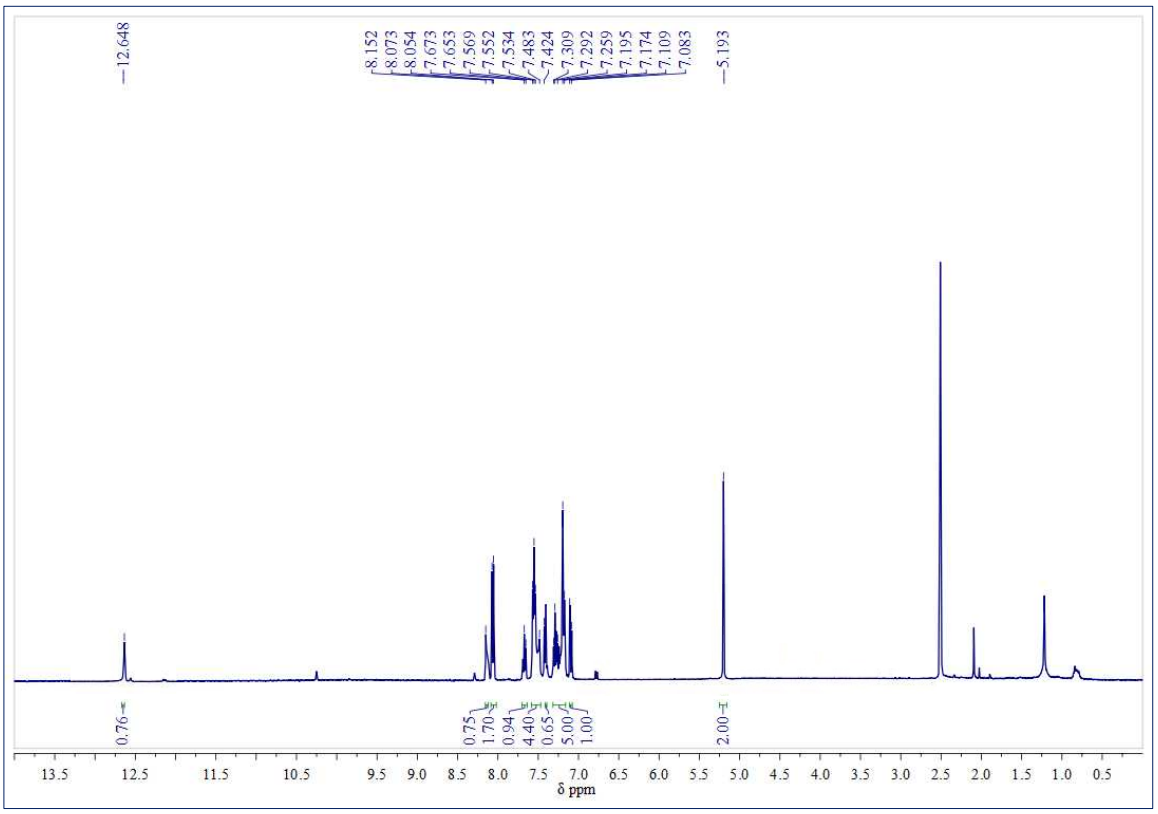

^{13}C-NMR spectrum of compound 5a in ($CDCl_3$+DMSO-d_6, 100 MHz):

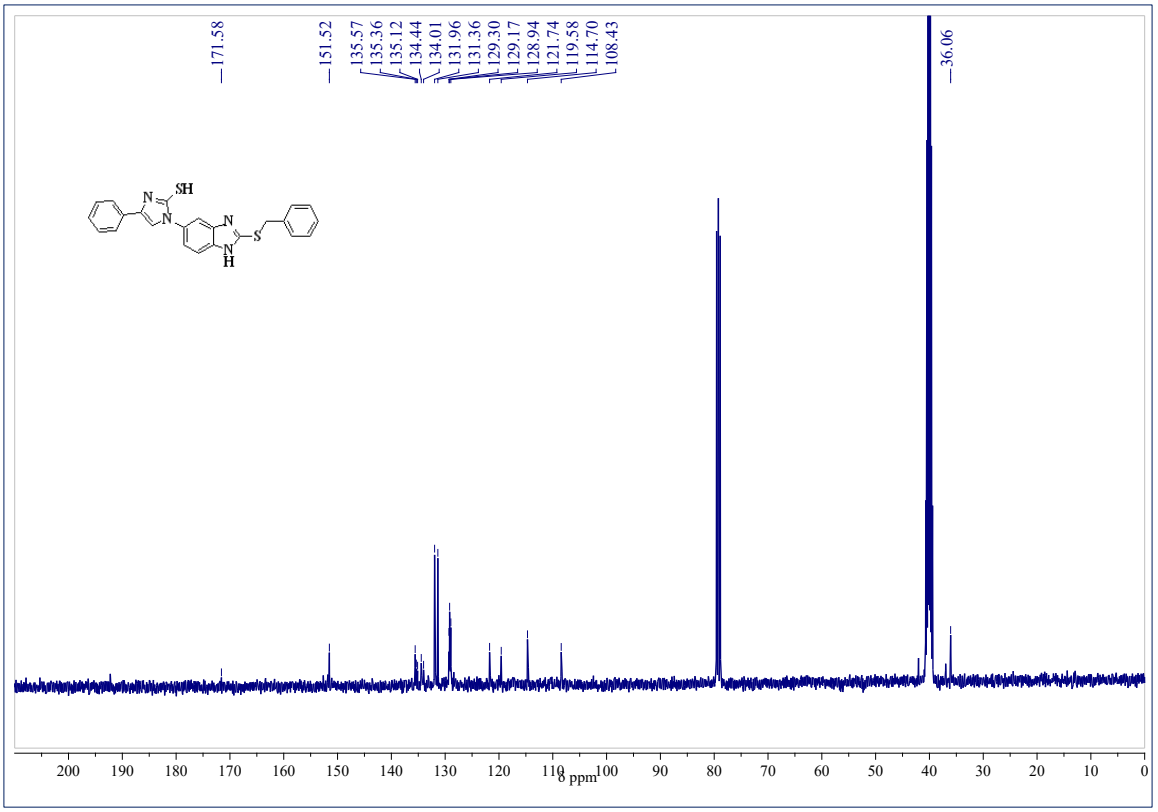

Mass spectrum of compound 5a

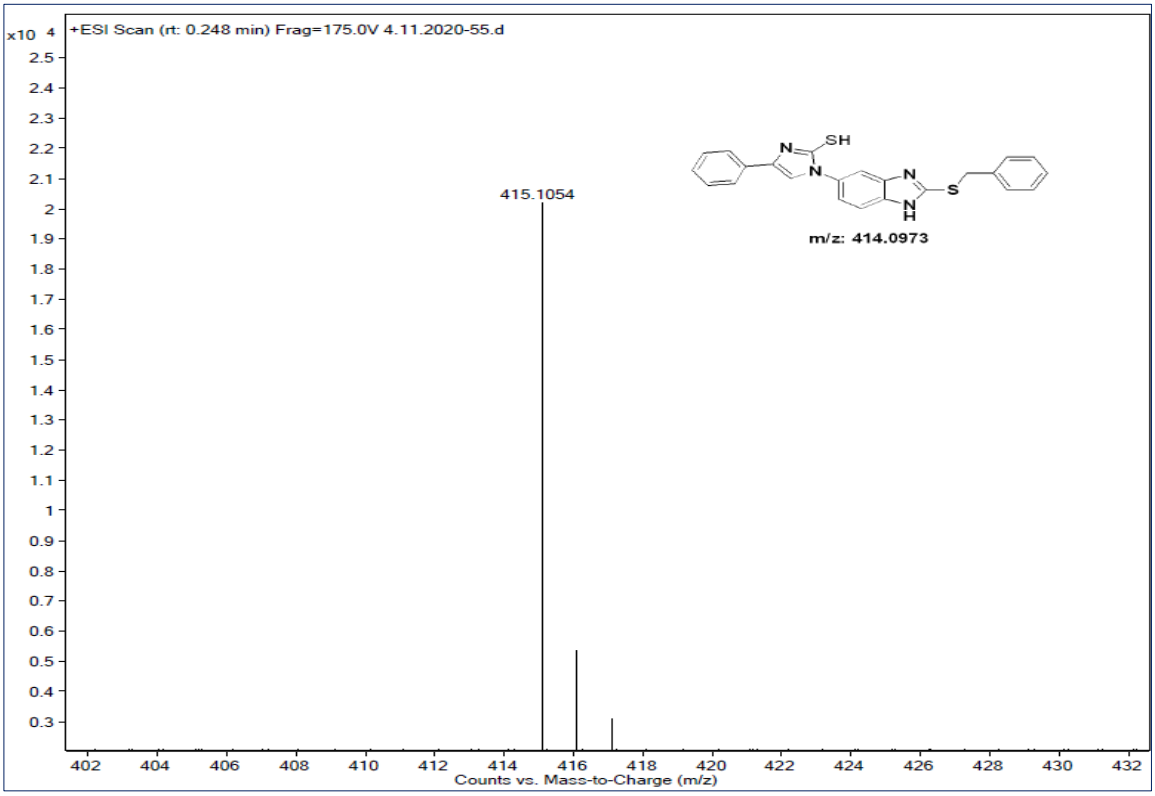

^{1}H-NMR spectrum of compound 5b in ($CDCl_3$+DMSO-d_6, 400 MHz):

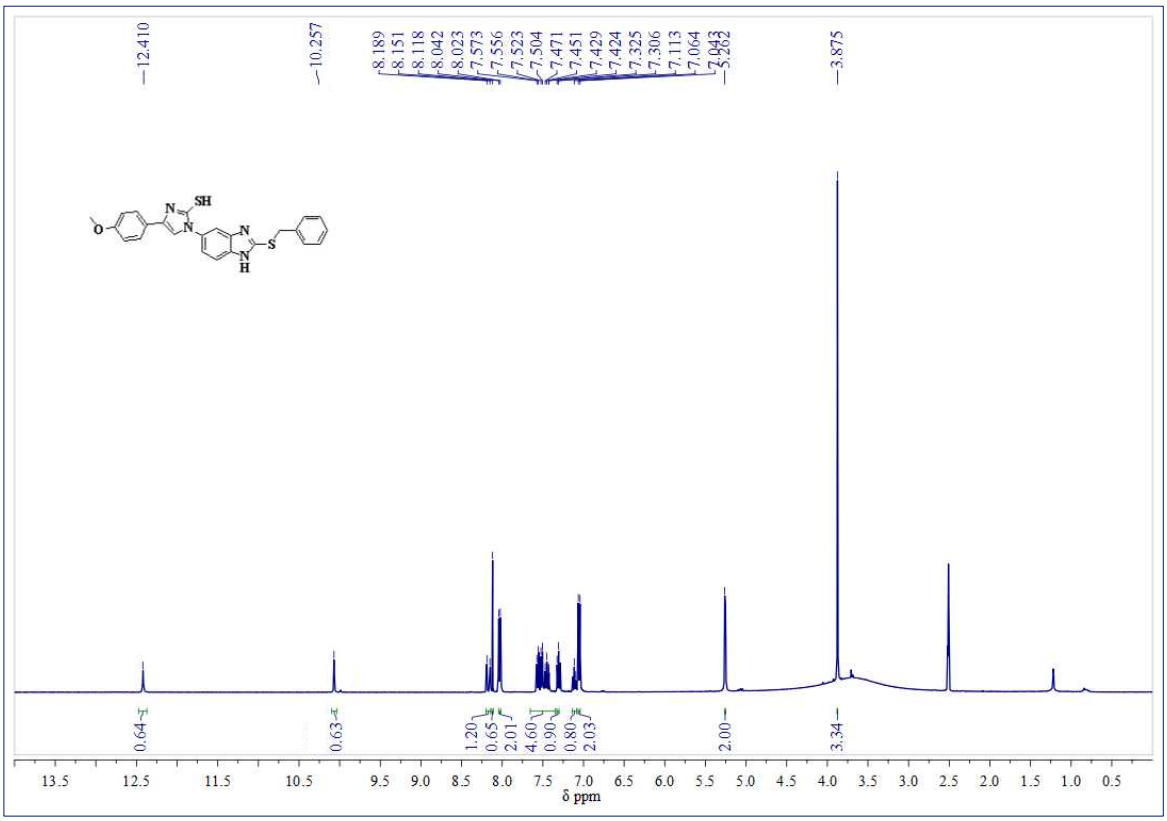

^{13}C-NMR Spectrum of compound 5b (CDCl$_3$+DMSO-d_6, 100 MHz):

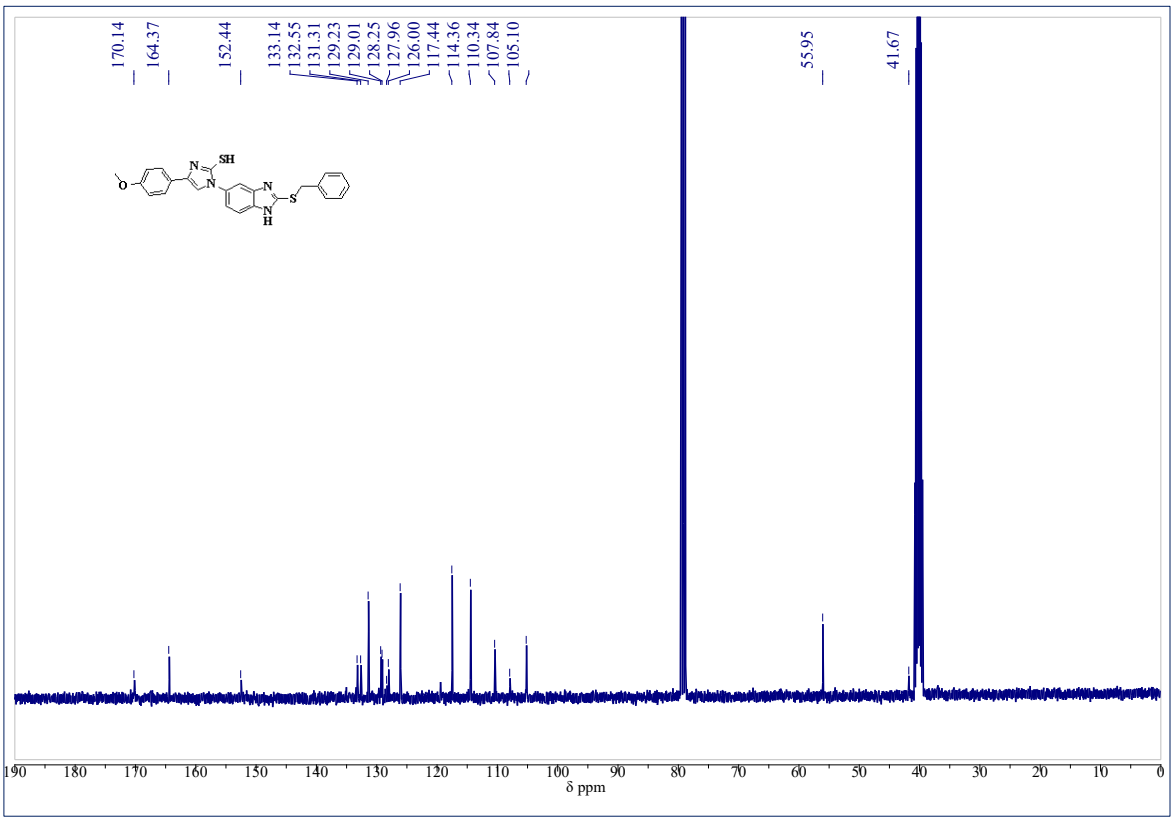

Mass spectrum of compound 5b

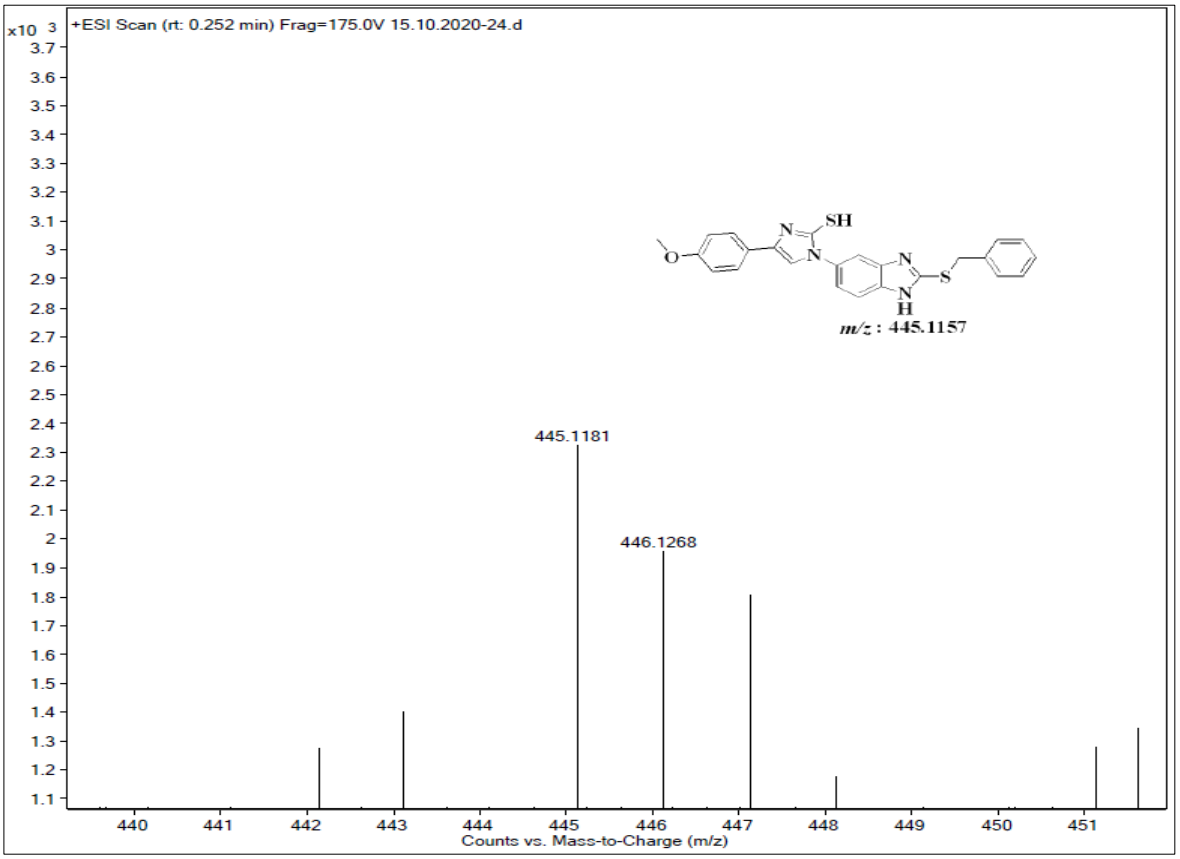

^{1}H-NMR Spectrum of compound 5c in (DMSO-d_6, 400 MHz):

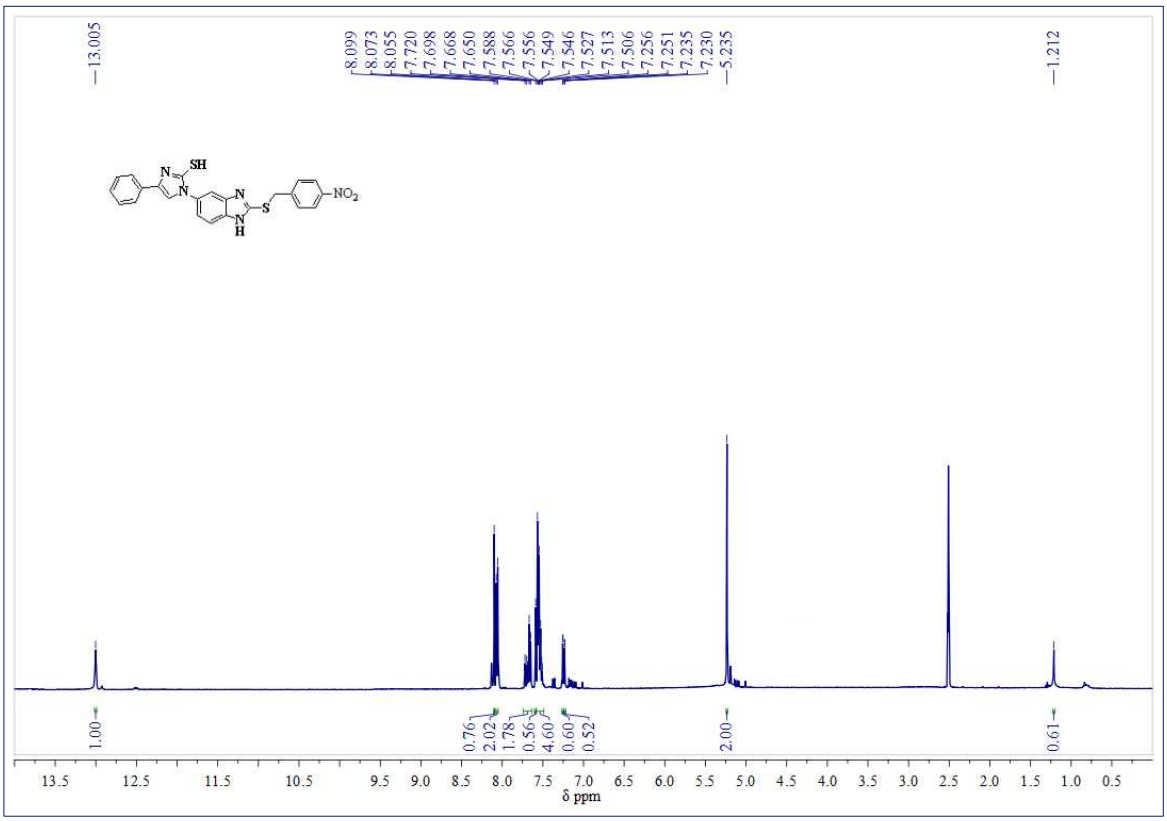

Mass spectrum of compound 5c

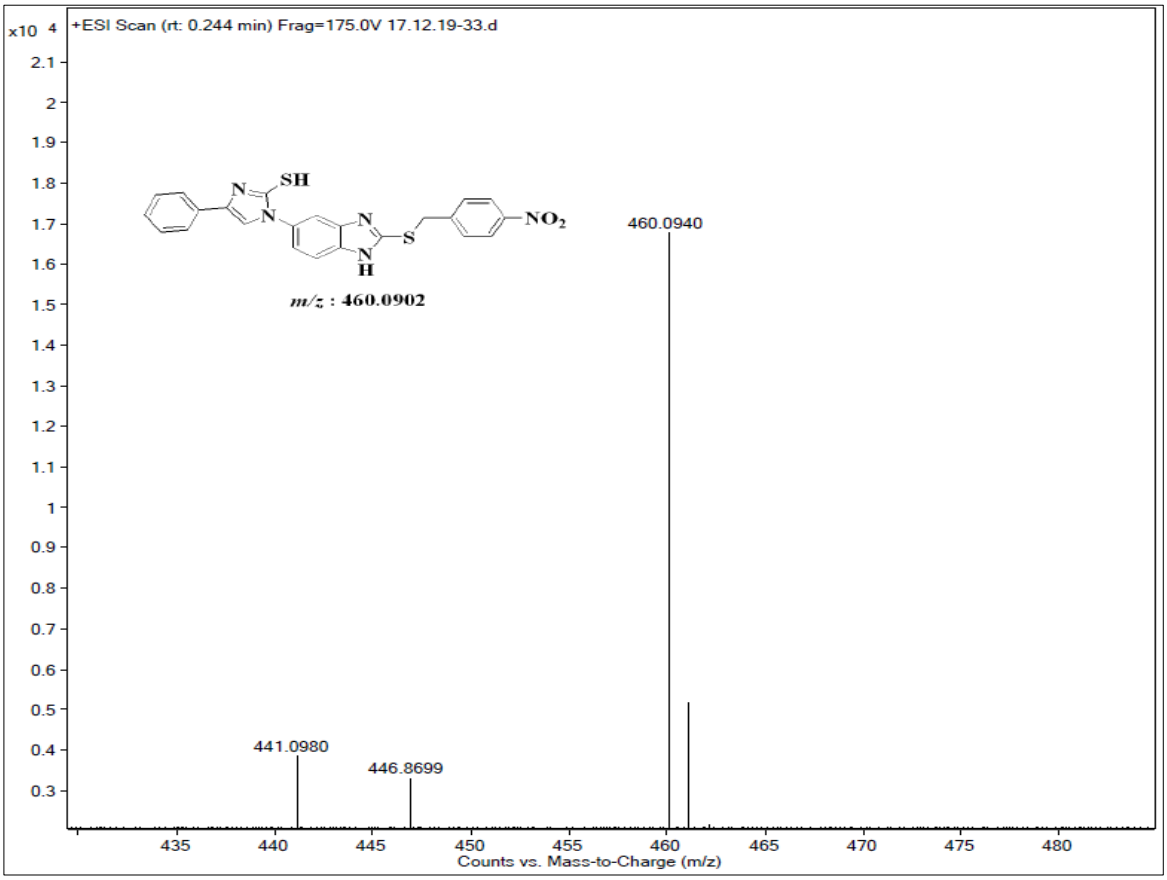

^{1}H-NMR Spectrum of compound 5d in (DMSO-d_6, 400 MHz):

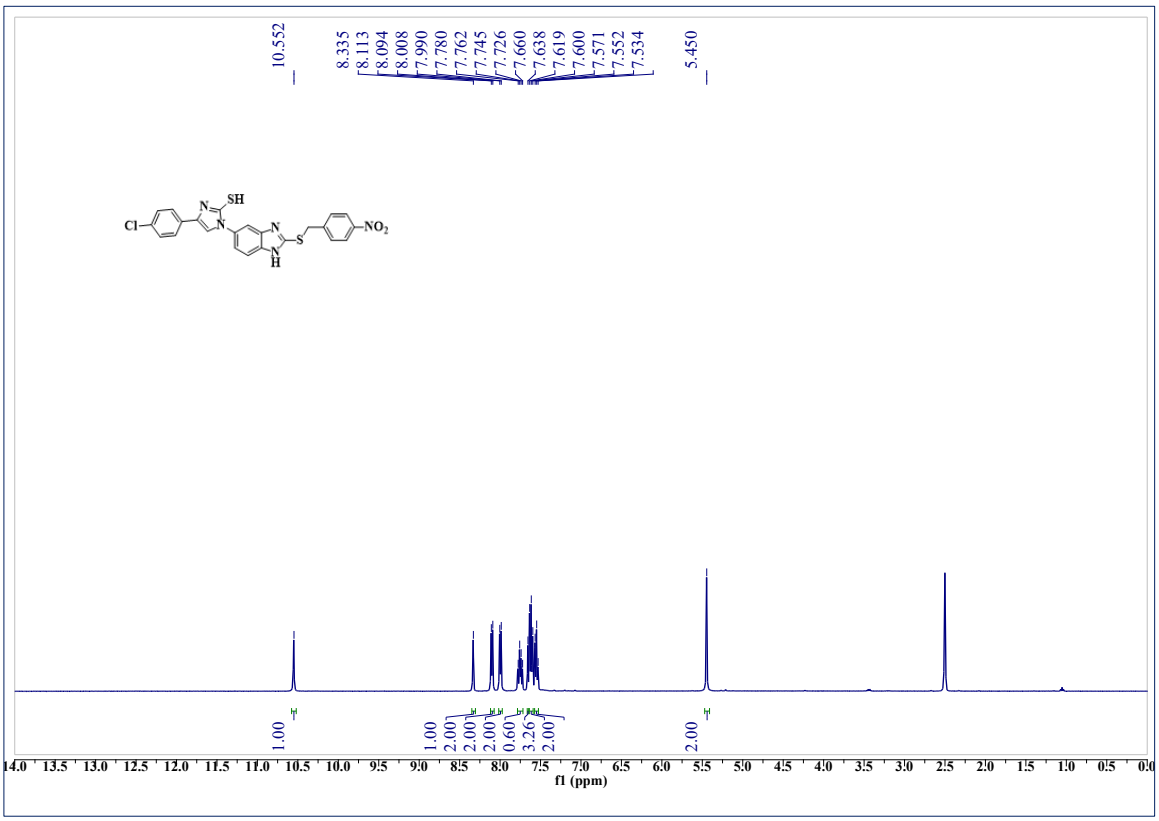

^{13}C-NMR Spectrum of compound 5d in (DMSO-d_6, 100 MHz):

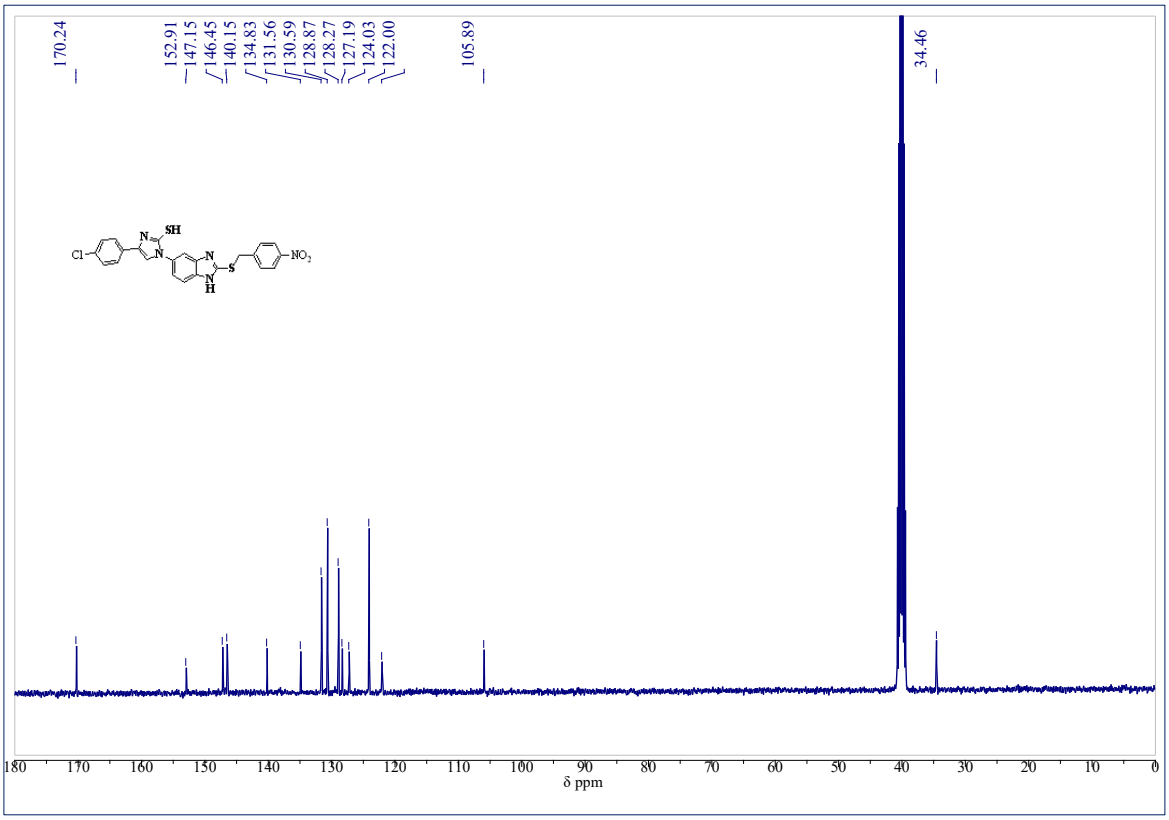

Mass spectrum of compound 5d

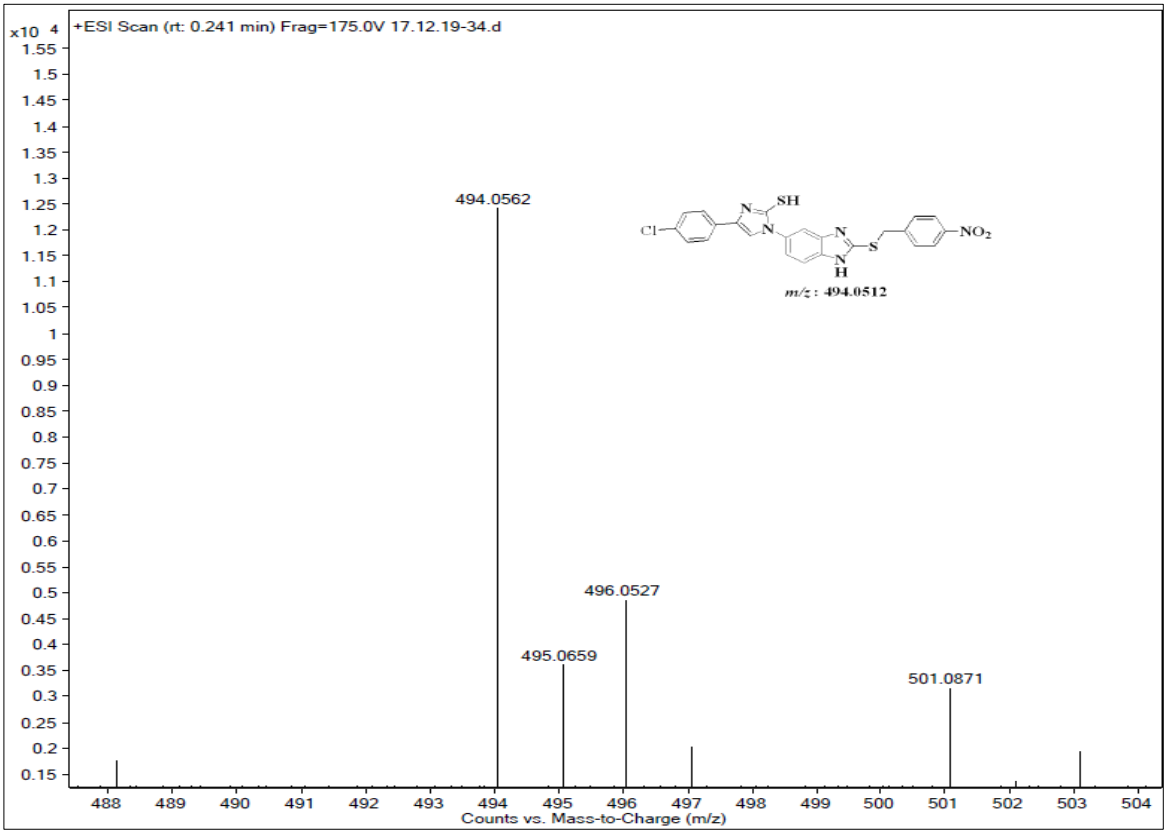

^{1}H-NMR spectrum of compound 5e (DMSO-d_6, 400 MHz):

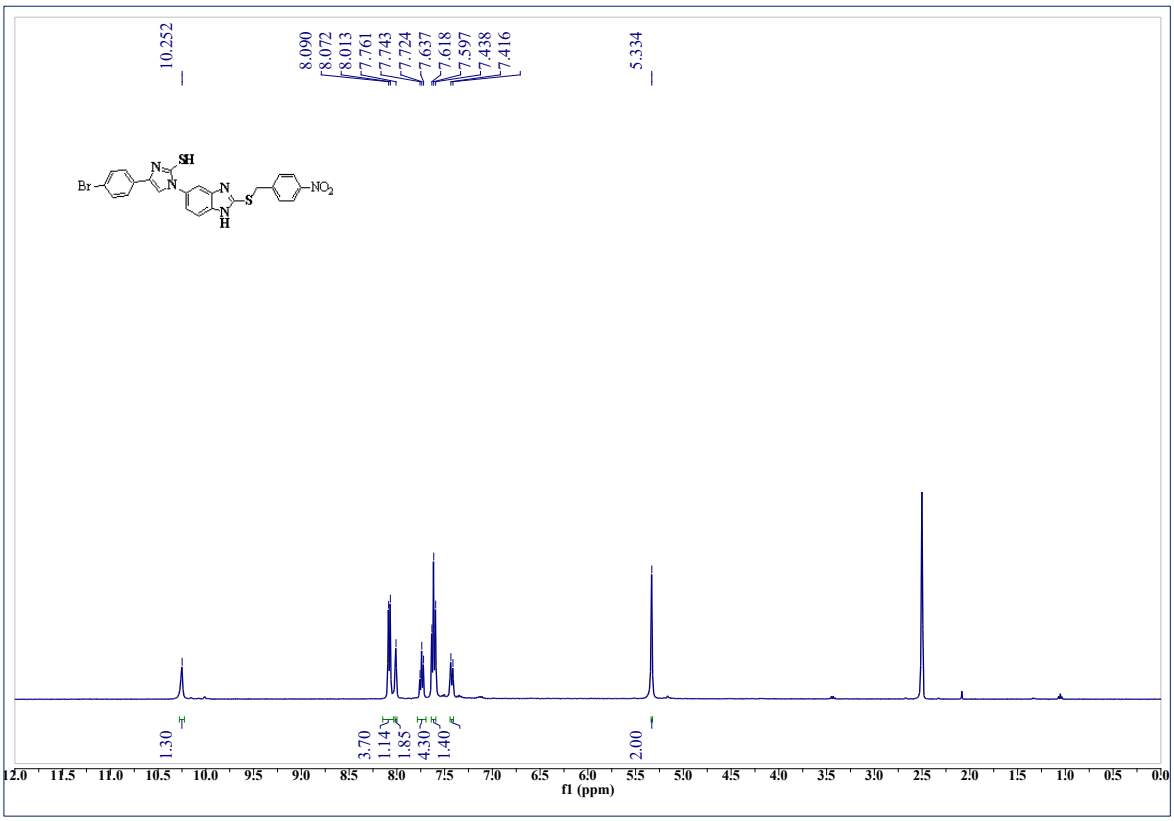

^{13}C-NMR Spectrum of compound 5e in (DMSO-d_6, 100 MHz):

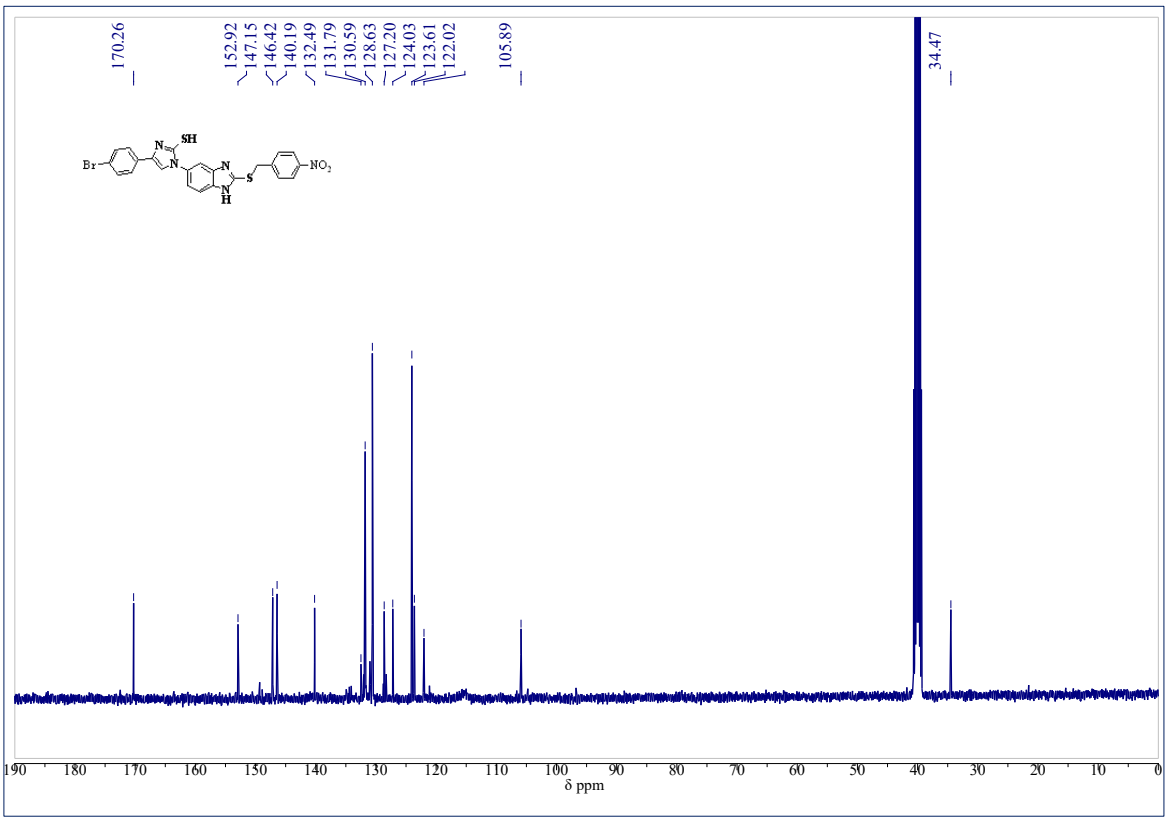

Mass spectrum of compound 5e

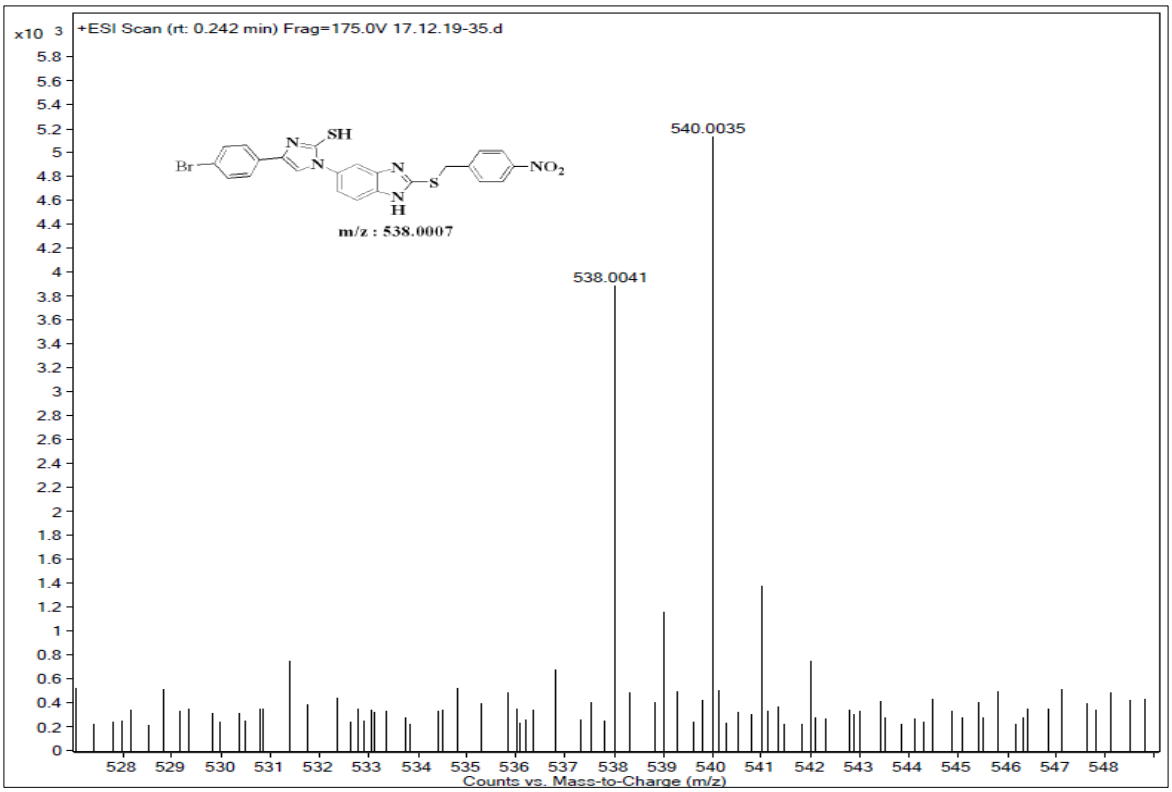

^{1}H-NMR Spectrum of compound 5f (CDCl$_3$+DMSO-d_6, 400 MHz):

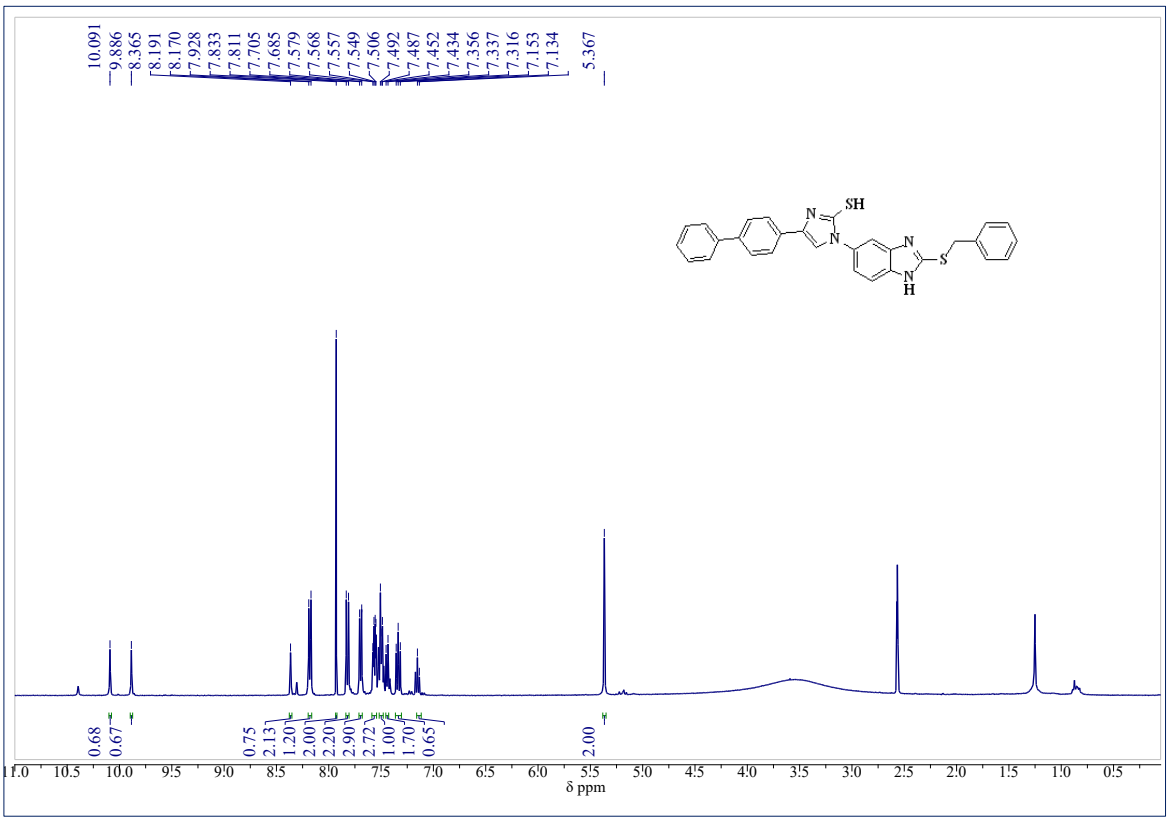

^{13}C-NMR spectrum of compound 5f (CDCl$_3$+DMSO-d_6, 100 MHz):

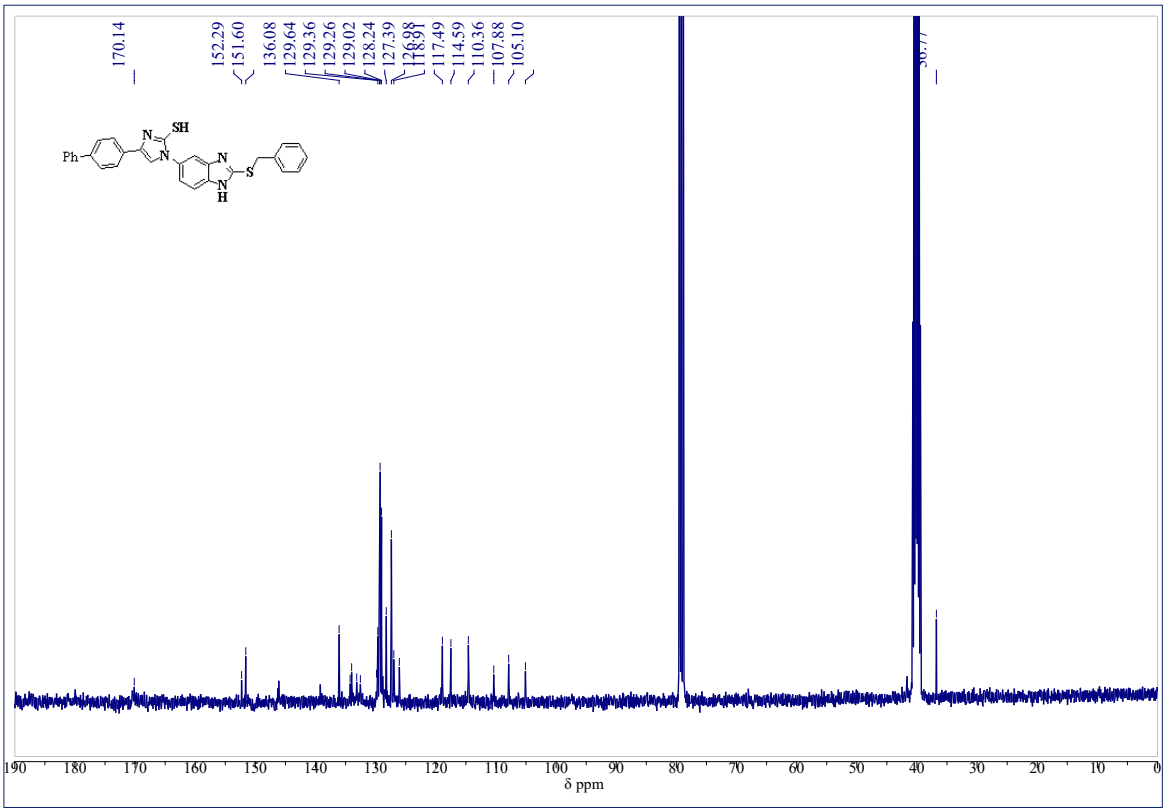

Mass spectrum of compound 5f

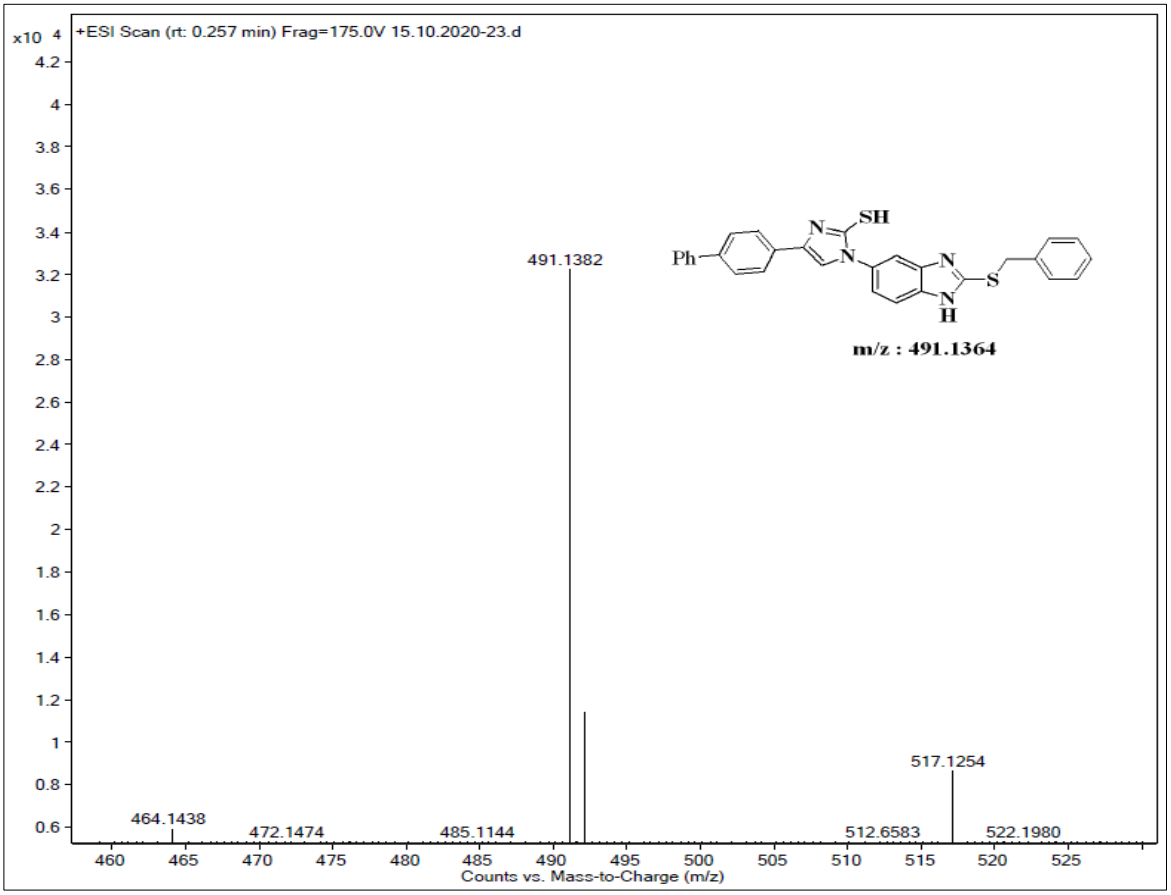

3.10. References

1. Dervan, P. B.; Edelson, B. S. *Curr. Opin. Struct. Biol.* **2003**, *13*, 284–299.
2. Ng, V. W. L.; Tan, J. P. K.; Leong, J.; Voo, Z. X.; Hedrick, J. L.; Yang, Y. Y. *Macromolecules.* **2014**, *47*, 1285–1291.
3. Hariharan, A.; Kumar, S.; Alagar, M.; Dinakaran, K.; Subramanian, K. *Polym. Bull.* **2018**, *75*, 93–107.
4. Khan, S. A.; Asiri, A. M.; Al-Dies, A. A. M.; Osman, O. I.; Asad, M.; Zayed, M. E. M. *J. Photochem. Photobiol. A Chem.* **2018**, *364*, 390–399.
5. Jang, J.; Sim, Y.; Kang, seokwoo; Shin, D.; Park, M.; Kay, K. Y.; Park, J. *Mol. Cryst. Liq. Cryst.* **2019**, *687*, 14–20.
6. Newman, D. J.; Cragg, G. M. *J. Nat. Prod.* **2007**, *70* (3), 461–477. https://doi.org/10.1021/np068054v.
7. Jin, Z. *Nat. Prod. Rep.* **2011**, *28*, 1143–1191.
8. O'Malley, D. P.; Li, K.; Maue, M.; Zografos, A. L.; Baran, P. S. *Chemtracts.* **2008**, *21*, 300–301.
9. Yang, W.-C.; Li, J.; Li, J.; Chen, Q.; Yang, G.-F. *Bioorg. Med. Chem. Lett.* **2012**, *22*, 1455–1458.
10. Cheong, J. E.; Zaffagni, M.; Chung, I.; Xu, Y.; Wang, Y.; Jernigan, F. E.; Zetter, B. R.; Sun, L. *Eur. J. Med. Chem.* **2018**, *144*, 372–385.
11. Alkahtani, H. M.; Abbas, A. Y.; Wang, S. *Bioorganic Med. Chem. Lett.* **2012**, *22*, 1317–1321.
12. Xiao, M.; Ahn, S.; Wang, J.; Chen, J.; Miller, D. D.; Dalton, J. T.; Li, W. *J. Med. Chem.* **2013**, *56*, 3318–3329.
13. Vijesh, A. M.; Isloor, A. M.; Telkar, S.; Peethambar, S. K.; Rai, S.; Isloor, N. *Eur. J. Med. Chem.* **2011**, *46*, 3531–3536.
14. Wen, S.-Q.; Jeyakkumar, P.; Avula, S. R.; Zhang, L.; Zhou, C.-H. *Bioorg. Med. Chem. Lett.* **2016**, *26*, 2768–2773.
15. dos Santos Nascimento, M. V. P.; Mattar Munhoz, A. C.; De Campos Facchin, B. M.; Fratoni, E.; Rossa, T. A.; Mandolesi Sá, M.; Campa, C. C.; Ciraolo, E.; Hirsch, E.; Dalmarco, E. M. *Biomed. Pharmacother.* **2019**, *111*, 1399–1407.
16. Dhanunjayarao, K.; Mukundam, V.; Ranga Naidu Chinta, R. V.; Venkatasubbaiah, K. *J. Organomet. Chem.* **2018**, *865*, 234–238.
17. Dong, Y.; Qian, J.; Liu, Y.; Zhu, N.; Xu, B.; Ho, C. L.; Tian, W.; Wong, W. Y. *New J.*

Chem. **2019**, *43*, 1844–1850.

18. Chiarotto, I.; Feeney, M. M. M.; Feroci, M.; Inesi, A. *Electrochim. Acta* **2009**, *54*, 1638–1644.
19. Bey, E.; Marchais-Oberwinkler, S.; Kruchten, P.; Frotscher, M.; Werth, R.; Oster, A.; Algül, O.; Neugebauer, A.; Hartmann, R. W. *Bioorg. Med. Chem.* **2008**, *16*, 6423–6435.
20. Congiu, C.; Cocco, M. T.; Onnis, V. *Bioorg. Med. Chem. Lett.* **2008**, *18*, 989–993.
21. Chowdhury, S.; Mohan, R. S.; Scott, J. L. *Tetrahedron.* **2007**, *63*, 2363–2389.
22. Su, Q.; Ioannidis, S.; Chuaqui, C.; Almeida, L.; Alimzhanov, M.; Bebernitz, G.; Bell, K.; Block, M.; Howard, T.; Huang, S.; Huszar, D.; Read, J. A.; Rivard Costa, C.; Shi, J.; Su, M.; Ye, M.; Zinda, M. *J. Med. Chem.* **2014**, *57*, 144–158.
23. de Laszlo, S. E.; Hacker, C.; Li, B.; Kim, D.; MacCoss, M.; Mantlo, N.; Pivnichny, J. V.; Colwell, L.; Koch, G. E.; Cascieri, M. A.; Hagmann, W. K. *Bioorg. Med. Chem. Lett.* **1999**, *9*, 641–646.
24. Keung, W.; Boloor, A.; Brown, J.; Kiryanov, A.; Gangloff, A.; Lawson, J. D.; Skene, R.; Hoffman, I.; Atienza, J.; Kahana, J.; De Jong, R.; Farrell, P.; Balakrishna, D.; Halkowycz, P. *Bioorganic Med. Chem. Lett.* **2017**, *27*, 1099–1104.
25. Uslu, A.; Tümay, S. O.; Şenocak, A.; Yuksel, F.; Özcan, E.; Yeşilot, S. *Dalt. Trans.* **2017**, *46*, 9140–9156.
26. Wang, X.; Wang, D.; Guo, Y.; Yang, C.; Iqbal, A.; Liu, W.; Qin, W.; Yan, D.; Guo, H. *Dalt. Trans.* **2015**, *44*, 5547–5554.
27. Zhang, X.; Sui, Z.; Kauffman, J.; Hou, C.; Chen, C.; Du, F.; Kirchner, T.; Liang, Y.; Johnson, D.; Murray, W. V.; Demarest, K. *Bioorg. Med. Chem. Lett.* **2017**, *27*, 1760–1764.
28. Gupta, G. K.; Saini, V.; Khare, R.; Kumar, V. *Med. Chem. Res.* **2014**, *23*, 4209–4220.
29. Naureen, S.; Chaudhry, F.; Munawar, M. A.; Ashraf, M.; Hamid, S.; Khan, M. A. *Bioorg. Chem.* **2018**, *76*, 365–369.
30. Alanthadka, A.; Elango, S. D.; Thangavel, P.; Subbiah, N.; Vellaisamy, S.; Chockalingam, U. M. *Catal. Commun.* **2019**, *125*, 26–31.
31. Adhikary, S.; Majumder, L.; Pakrashy, S.; Srinath, R.; Mukherjee, K.; Mandal, C.; Banerji, B.; Banerji, B. *ACS Omega* **2020**, *5*, 14394–14407.
32. Ramagiri, R. K.; Thupurani, M. K.; Vedula, R. R. *J. Heterocycl. Chem.* **2014**, n/a–n/a.
33. Xiao, M.; Ahn, S.; Wang, J.; Chen, J.; Miller, D. D.; Dalton, J. T.; Li, W. *J. Med. Chem.* **2013**, *56*, 3318–3329.

34. Aggarwal, R.; Kumar, R.; Kumar, V. *J. Sulfur Chem.* **2007**, *28*, 617–623.
35. Wang, C.; Wang, E.; Chen, W.; Zhang, L.; Zhan, H.; Wu, Y.; Cao, H. *J. Org. Chem.* **2017**, *82*, 9144–9153.
36. Ramakrishna, I.; Sahoo, H.; Baidya, M. *Chem. Commun.* **2016**, *52* (15), 3215–3218.
37. a) Heinrich, D. *Der. Chemie.* **1858**, *107*,199 −208. b) Radziszewski, B. *Ber Dtsch Chem Ges.* **1882**, *15*, 2706−2708.
38. Drefahl, G.; Herma, H. *Chem. Ber.* **1960**, 93, 486– 492.
39. Assadieskandar, A.; Amini, M.; Ostad, S. N.; Riazi, G. H.; Cheraghi-Shavi, T.; Shafiei, B.; Shafiee, A. *Bioorg. Med. Chem.* **2013**, *21*, 2703–2709.
40. Chen, C. Y.; Hu, W. P.; Yan, P. C.; Senadi, G. C.; Wang, J. J. *Org. Lett.* **2013**, *15*, 6116–6119.
41. Zhang, X. J.; Fan, W.; Fu, L. P.; Jiang, B.; Tu, S. J. *Res. Chem. Intermed.* **2015**, *41*, 773–783.
42. Chai, J.-D.; Head-Gordon, M. *Phys. Chem. Chem. Phys.* **2008**, *10*, 6615.
43. Frisch, M. J.; Trucks, G. W.; Schlegel, H. B.; Scuseria, G. E, Robb, M. A.; Cheeseman, J.R.; Scalmani, G.; Barone, V.; Petersson, G. A.; Nakatsuji, H. *et al.* **2016**, *Gaussian, Inc., Wallingford CT.*

CHAPTER-IV (Section-A)

Polyethylene glycol mediated, three-component synthesis of thiazolyl-benzimidazoles as potent α-glucosidase inhibitors: Design, synthesis, molecular modelling, and ADME studies

CHAPTER-IVA

Polyethylene glycol mediated three-component synthesis of thiazolyl-benzimidazoles as potent α-glucosidase inhibitors: Design, synthesis, molecular modelling, and ADME studies

4A.0. Introduction

Heterocycles occupy a predominant position in all types of agrochemicals, veterinary products, and materials, and are frequently used in the drug development process [1]. Thus, thiazoles are considered one of the most important and privileged structural motifs and are often found in several natural products like vitamin B1(thiamine) and penicillin. Due to their immense impotence and wide range of bio-activities, the present study was made towards thiazole synthesis. Fortunately, synthetic thiazoles are also used in the drug discovery process [2] and are also found in many marketed drugs as potent inhibitors (**Figure 4A.1**). For instance, thiazole core unit-containing substances often show a large number of bio-activities like anti-bacterial [3], anti-fungal [4], anti-cancer [5], and anti-diabetic [6]. In addition, thiazole derivatives are also found application in functional materials [7], as synthetic intermediates [8], as CDK inhibitors [9], as liquid crystals for ferroelectric display [10], and as cosmetic sunscreens [11].

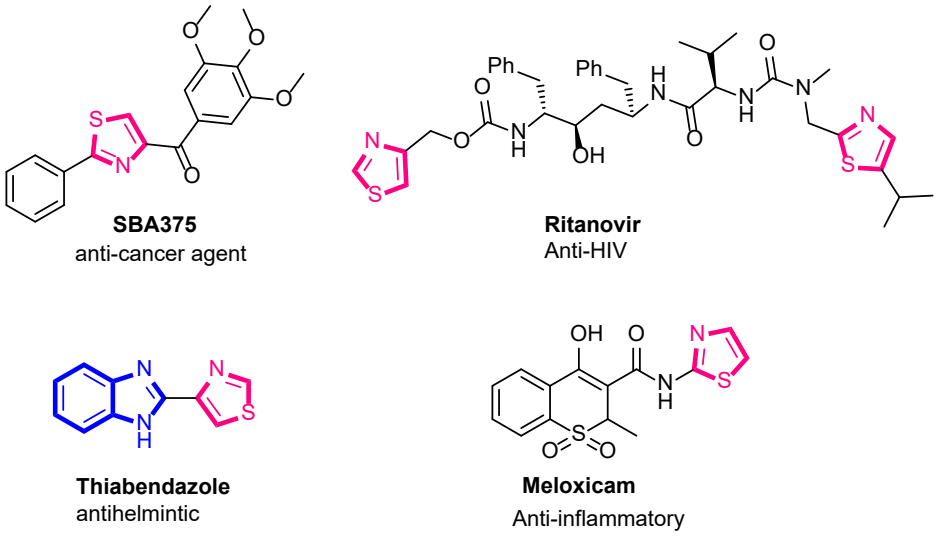

Figure 4A.1. Following are marketed drugs with thiazole core unit

The following is a compact review of the literature on the synthesis of thiazoles.

Vedula [12] ***et al.*** reported a new series of one-pot three-component synthesis of coumarinyl-based thiazoles from appropriate amounts of thiocarbohydrazide, substituted aromatic aldehydes, and different substituted 2-bromoacetophenones in ethanol and a catalytic amount

of glacial acetic acid under microwave condition provides good to excellent yields (**Scheme 4.1**). Moreover, the synthesized composites further screened *in-vitro* cytotoxicity activity against Gram-positive spheroid firmicute. Among the tested compounds, compound **4e** showed good anti-bacterial activity (**Figure 4A.1**).

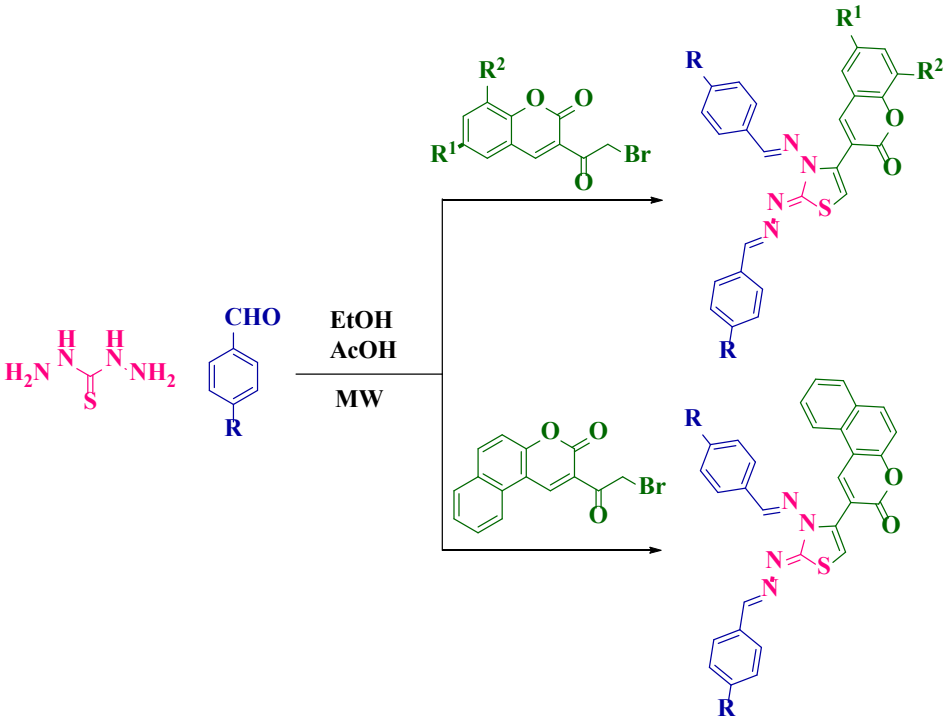

Scheme 4A.1. One-pot three-component coumarin based-thiazoles

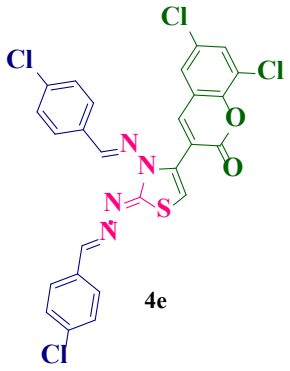

Figure 4A.1. Biologically potent compound

Meshram [13] ***et al.*** developed a simple and eco-friendly one-pot, the three-component procedure for the synthesis of pyrazolyl-thiazoles using various (E)-N, N-dimethyl-3-phenylprop-1-en-1-amines, thiosemicarbazide and substituted 2-bromoacetophenones in presence of sulfamic acid as green catalyst in water (**scheme 4A.2**). Further, the synthesized scaffolds were evaluated for *in-vitro* cytotoxic activity against three human cancer cell lines

A549, MCF-7, and HeLa. Among the tested compounds, compounds **4b, 4c,** and **4e** (**Figure 4A.2**) showed considerable cytotoxic activity with an IC_{50}<5 µM.

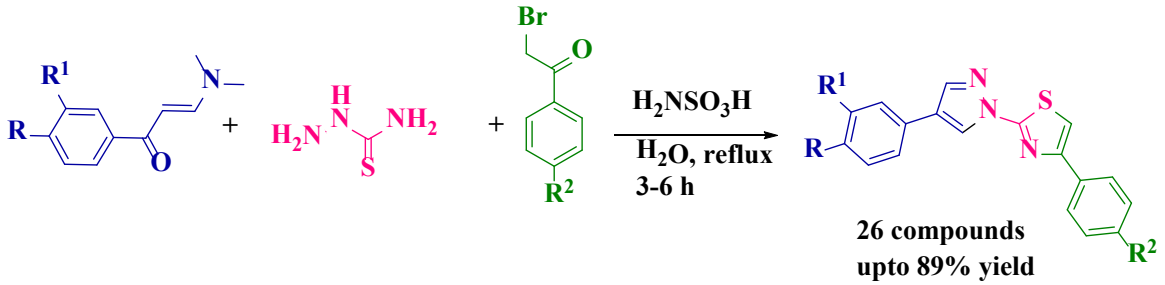

Scheme 4A.2. One pot, three-component synthesis of pyrazolyl-thiazoles

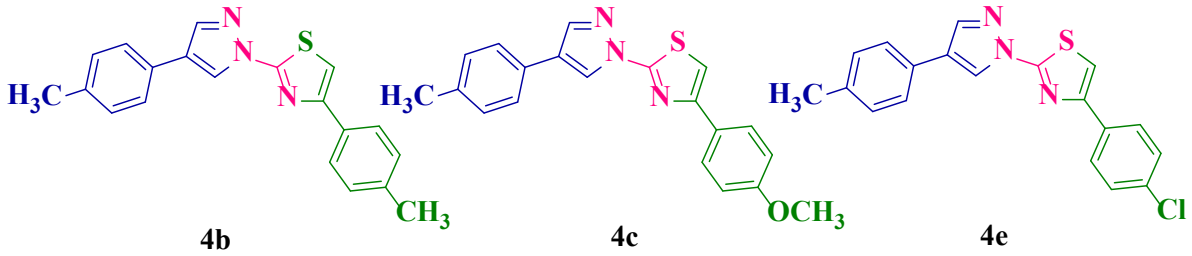

Figure 4A.2. Biolological active pyrazolyl-thiazole composites

Mamidala [14] ***et al.*** has been reported a novel one-pot three-component microwave-assisted procedure for the synthesis of pyrozolo-thiazoles using thiosemicarbazide, 3-(furan-2-yl)-1-(pyridin-2-yl)prop-2- en-1-one and 1-(pyridin-2-yl)-3-(thiophen-2-yl)prop-2-en-1-one with substituted 2-bromoacetophenones in NaOH and ethanol as solvent provides good to excellent yields (**Scheme 4A.3**). Moreover, the synthesized scaffolds were evaluated for their *in-vitro* cytotoxic activity against four human cancer cell lines, A549, HeLa, SK-N-SH, and DU-145. Among the tested, compounds **4h** has shown excellent *in-vitro* cytotoxic activity against HeLa with IC_{50} values 9.97 ± 0.05 µM. Similarly, compounds **4c,** and **4j** exhibit moderate anti-cancer activity with IC_{50} values of 19.78 ±0.03 µM, and 15.61 ± 0.06 µM respectively **(Figure 4A.4).**

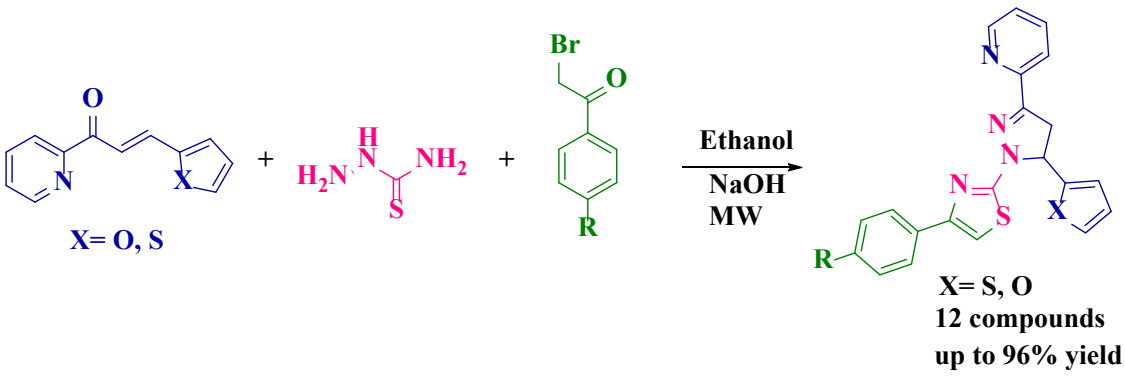

Scheme 4A.3. One-pot three-component synthesis of pyrazolo-thiazole derivatives

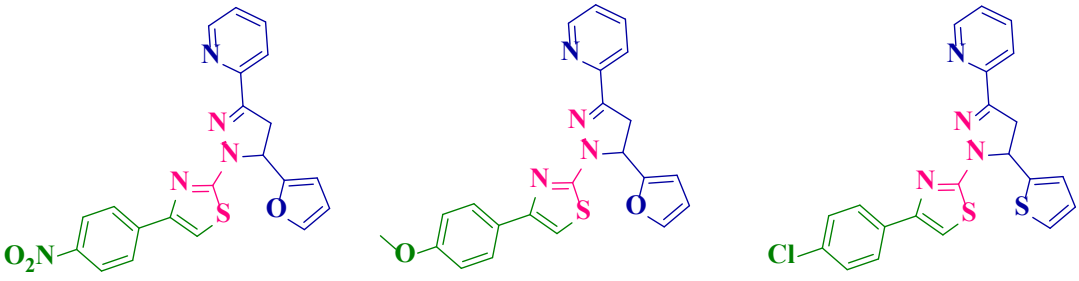

4h **4c** **4j**

Figure 4A.4. Biological potent pyarazolo-thiazole compounds

Gondru [15] ***et al.*** reported 1,2,3 triazolo-thiazole molecular hybrids *via* multicomponent reaction method using 4-((1-(4-methoxyphenyl)-1*H*-1,2,3-triazol-4-yl)methoxy)benzaldehyde, thiosemicarbazide and substituted 2-bromoacetophenones in methanol and a catalytic amount of acetic acid (**Scheme 4A.5)**. Moreover, the synthesized derivatives were further screened for their *in-vitro* antimicrobial and biofilm studies. Among the tested scaffolds, compounds **8i, 8k,** and **8l** showed promising antimicrobial activity with IC_{50} values of 6.6 µM, 16.6 µM, and 15.9 µM respectively against *Bacillus subtilis* MTCC 121, and compounds **8k** and **8l** exhibit inhibitory activity against *Staphylococcus aureus MTCC* 96 with IC_{50} values 13.5 and 12.0µM respectively (**Figure 4A.5**).

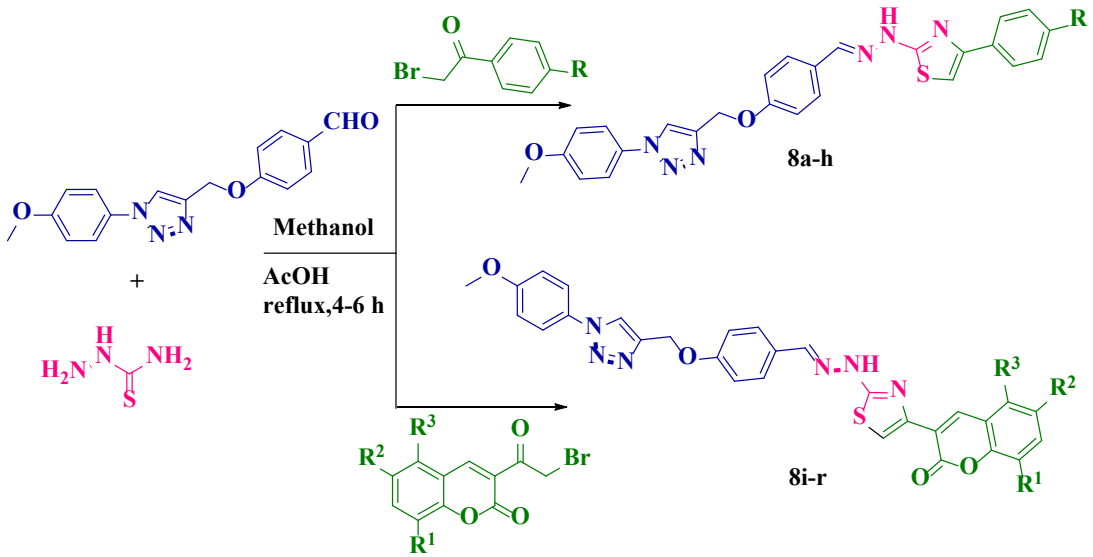

Scheme 4A.5. Multi-component synthesis of triazolo-thiazole molecular hybrids

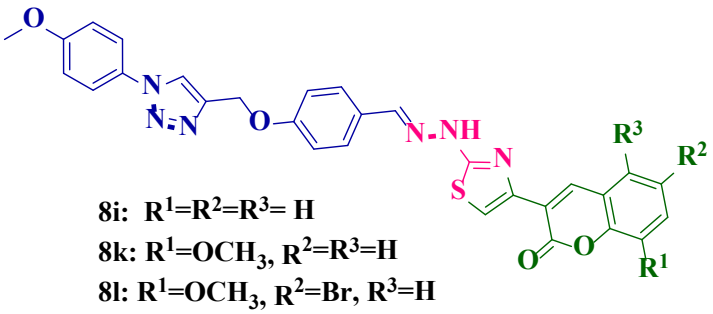

Figure 4A.5. Biologically active triazole-thiazole derivatives

Vedula [16] ***et al.*** reported a one-pot, efficient, novel, inexpensive synthetic procedure for the synthesis of (*E*)-ethyl2-(2-((*E*)-2-(1-(4-methyl-2-(phenylamino) thiazol-5yl)ethylidene)hydrazinyl)-4-oxothiazol-5(4*H*)-ylidene)acetates *via* one-pot, five component reaction using various substituted anilines, 3-chloropentane-2,4-dione, ammonium thiocyanate, thiosemicarbazide, and dialkylacetylene dicarboxylate in PEG-400 as green and recyclable solvent provides good to excellent yields (**Scheme 4A.6**).

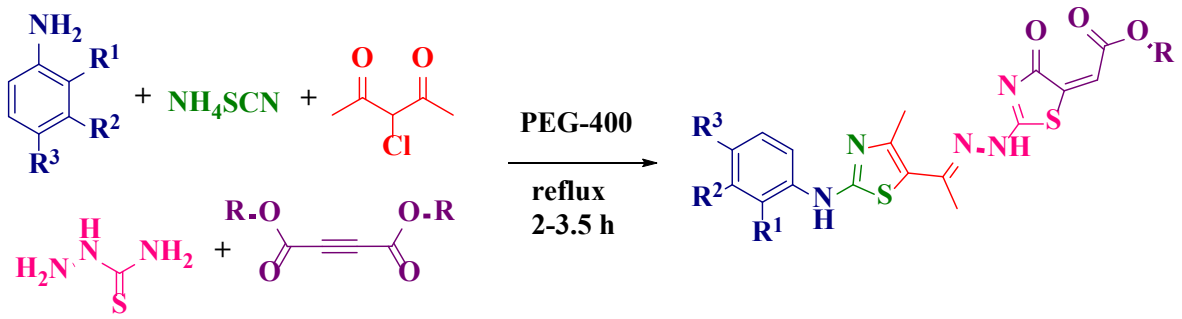

Scheme 4A.6. One-pot five-component synthesis of thiazole derivatives

Sreejalakshmi [17] ***et al.*** developed a series of novel 4-hydarzinothiazole composites *via* a sequential one-pot four-component reaction approach. The title compounds were synthesized using aminoguanidine, carbonyl compounds, isothiocyanates, and α-halo carbonyl compounds with excellent yields (**Scheme 4A.7**). Moreover, the synthesized compounds were further screened for their *in-vitro* anti-cancer activity against six human cancer cell lines MCF-7, SW620, A549, HL60, SK-MEL-2, and OVCAR-3. Compounds **2b** and **4b** exhibit good activity against MCF-7, and compound **3b** shows good activity against A549 (**Figure 4A.6**).

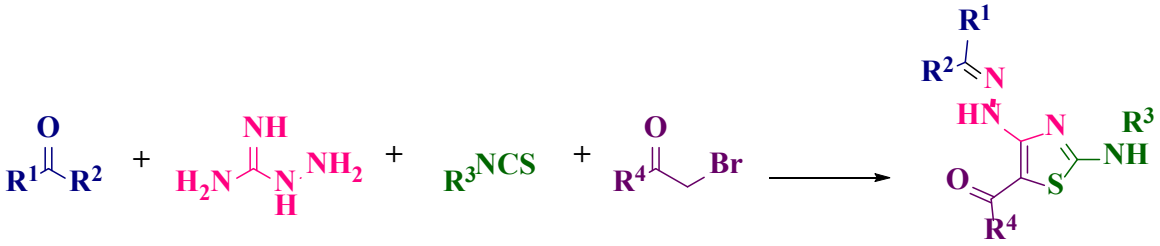

Scheme 4A.7. One-pot four-component synthesis of thiazoles

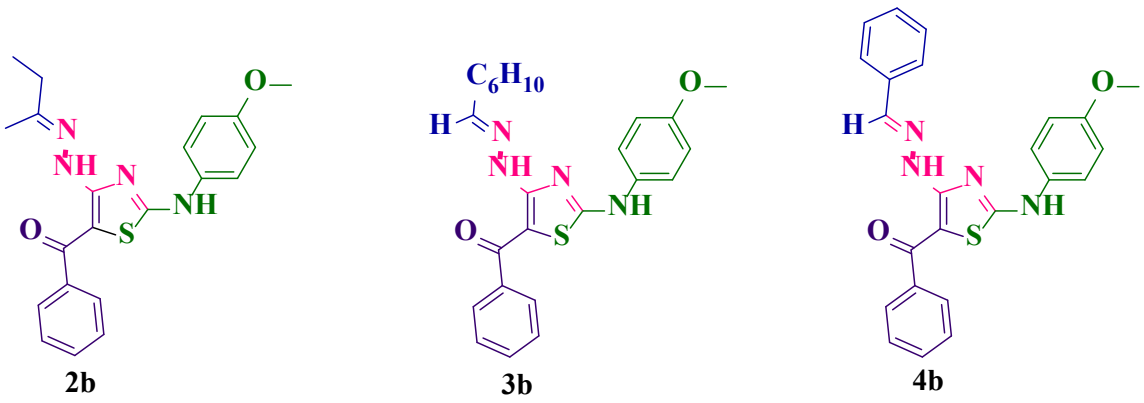

Figure 4A.6. Biologically active scaffolds

Costa and co-workers [18] have developed a series of fused thiazolo[5,4-d]thiazoles (TzTz) and thiazolo[5,4-c]isoquinolines (TzIQ) or mixtures of TzTz and TzIQ. To synthesize titled compounds dithooxamide and 2-halosubstituted benzaldehydes were used. The use of lanthanum(III) triflate as the catalyst favours the formation of TzIQ (**Scheme 4A.8**).

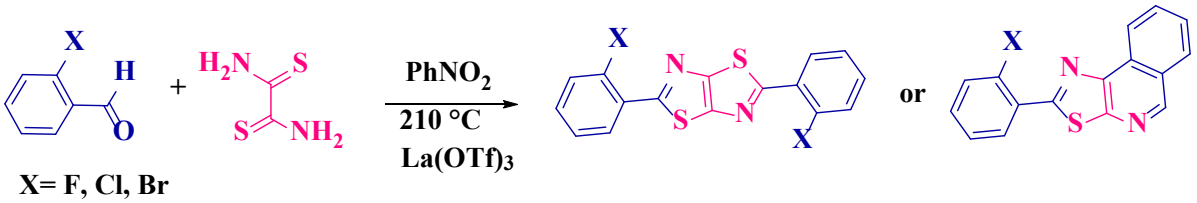

Scheme 4A.8. Synthesis of fused thiazolo-thiazole and thiazolo-isoquinoline derivatives

Choudhury [19] ***et al.*** synthesized a series of novel 2,4-diphenyl 1,3-thiazole-linked barbituric acid analogues *via* a multi-component reaction method. The title compounds were synthesized using readily available starting materials i.e. arylglyoxal, barbituric acid, and aryl thioamides in presence of 3-4 drops of water, and LAG (liquid-assisted grinding) provide titled composites with good to excellent yields. Similarly, same-titled compounds were also prepared by involving aryl nitriles, ammonium sulphide, arylglyoxal, and barbituric acid in a water medium was developed (**Scheme 4A.9**). Further studied the photophysical properties of titled compounds. The compound **4l** showed the highest quantum yield of 0.660 (**Figure 4A.7**).

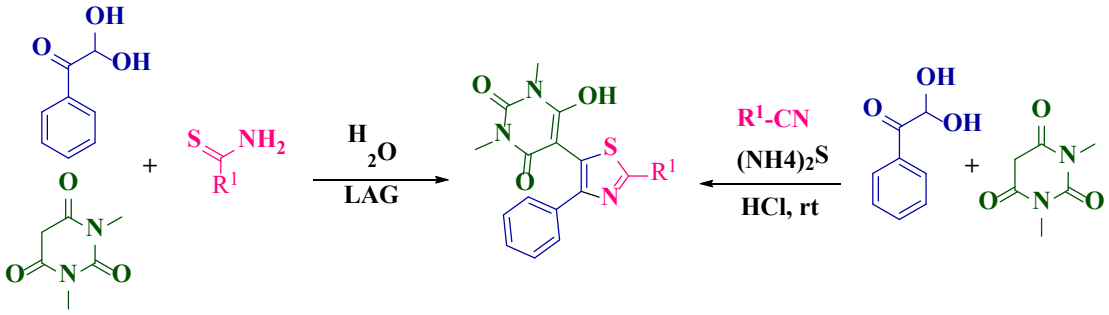

Scheme 4A.9. Tri-substituted thiazolo barbituric acid compounds

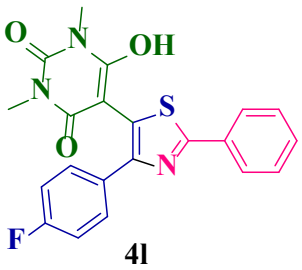

4l

Figure 4A.7

Saroha [20] **and Khurana** developed an efficient method for the regioselective synthesis of 2,4,5-tri-substituted thiazole compounds by MCR method using thiosemicarbazide, aldehyde/ketone/isatins, followed by addition of araylglyoxal and active methylene containing compounds/ C-H activated acids in ethanol and catalytic amounts of glacial acetic acid provide good to excellent yields (**Scheme 4A.10**)

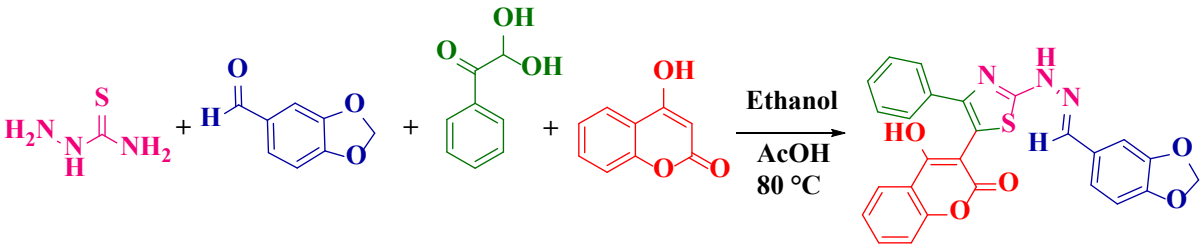

Scheme 4A.10. One-pot four-component synthesis of 2,4,5 tri-substituted thiazole scaffolds

Peng and *co-workers* [21] reported a novel one-pot synthesis of imidazo[1,2-*c*]thiazoles through a Pd-catalysed cascade by cyclization using isonitriles and thioamides provides good to excellent yields (**Scheme 4A.11**). Moreover, the titled compounds screened for *in-vitro* antitumor activity against HepG2. Compound **3c** showed excellent activity with IC_{50} values of 7.06±0.68μM (**Figure 4A.8**).

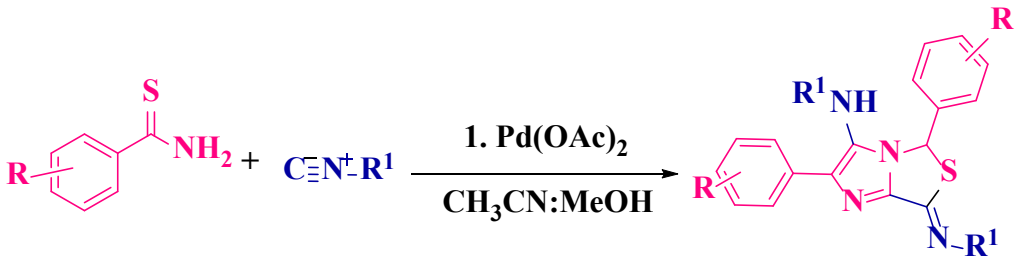

Scheme 4A.11. Pd-catalysed imidazolo-thiazole compounds

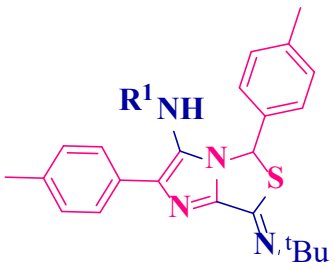

3c

Figure 4A.8

Yang [22] ***et al.*** developed a one-pot, facile, and efficient protocol to synthesize the 2,5-disubstituted thiazoles composites from chromone derivatives and thioamides in ethanol solvent and KOH as a base followed by Michael addition/ intramolecular cycloaddition process provides excellent yields (**scheme 4A.12**).

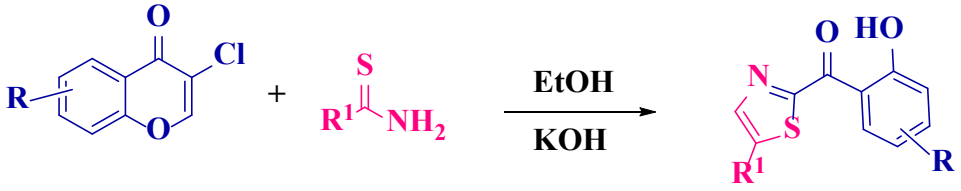

Scheme 4A.12. One-pot synthesis of 2,5 disubstituted thiazole derivatives

Deng [23] ***et al.*** described a new, one-pot, Brønsted acid-catalyzed synthesis of di-substituted thiazoles from benzyl amines, acetophenones, and sulphur powder in isonicotinic acid media that provides good to excellent yields under metal-free conditions (**Scheme-4A.13**).

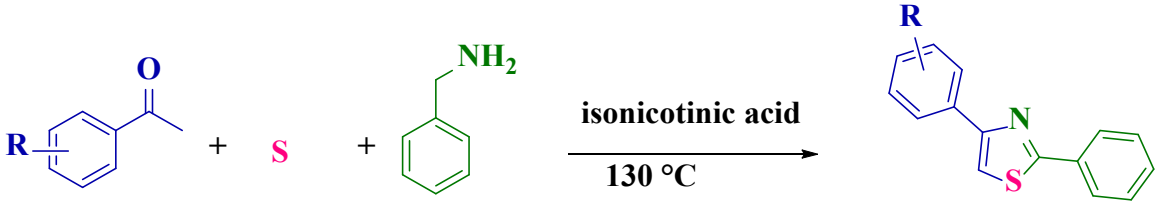

Scheme 4A.13. Brønsted acid catalyzed 2,4-disubstituted thiazole derivatives

Vaarla [24] ***et al.*** developed a novel, efficient, one-pot, three-component synthetic procedure for the synthesis of alkyl-4-oxo-coumarinyl-ethylidine-hydrazono-thaizolidin-5-yl-diene-acetate compounds by using different substituted 3-acetyl coumarins, thiosemecarzide and dialkyl acetylenedicarboxylates in acetic acid solvent (**Scheme 4A.15**). Moreover, the titled compounds were further screened for their *in-vitro* antiviral activity against different human viruses. The compound **IV-19** showed potent activity (**Figure 4A.9**).

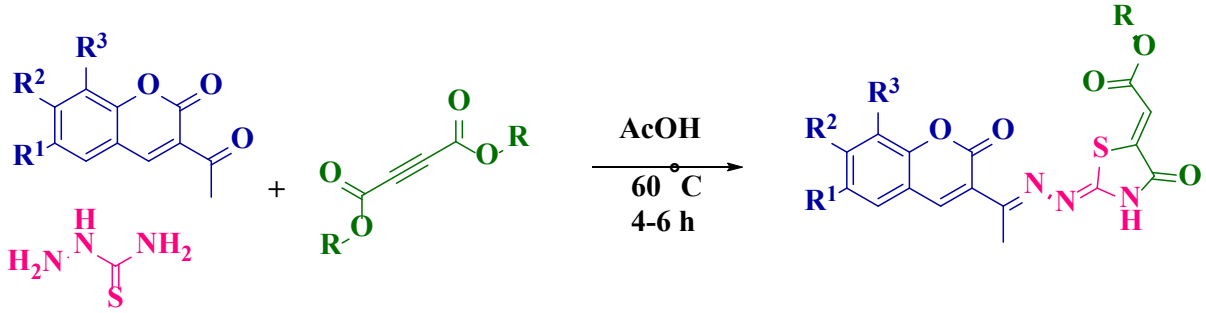

Scheme 4A.15. One-pot three-component synthesis of coumarinyl-hydrazono-thiazolodines acetate derivatives

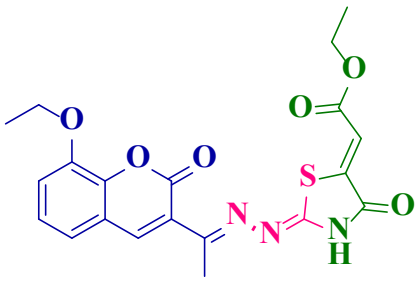

compound-IV-19

Figure 4A.9. Biologically active compound

Ramagiri [25] **and *co*-workers** reported a simple, one-pot, three-component synthesis of 3-(3-phenyl-2-(phenylimino)-2,3-dihydrothiazol-4-yl)-2*H*-chromen-2-one derivatives by using 3-(2-bromoacetyl) chromen-2-one, various substituted primary amines and phenyl isothiocyanates in DMF. (**Scheme 4A.16**).

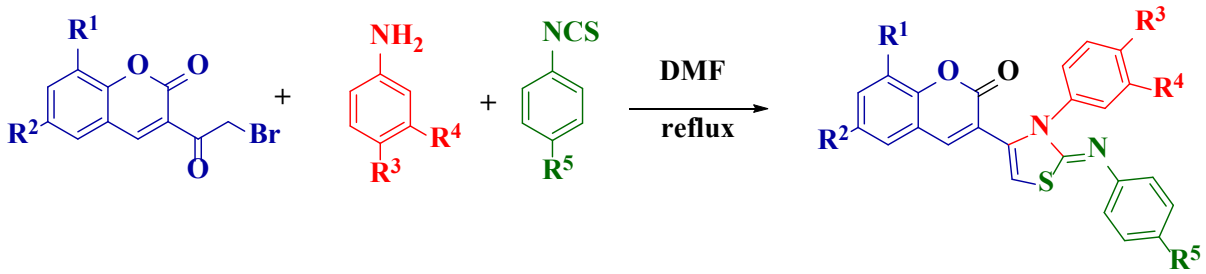

Scheme 4.16. One-pot three-component synthesis of 2,3,4-trisubstituted thiazoles

Vedula [26] ***et al.*** synthesized a series of novel coumarin-based thiazolyl-pyarazolo-carbaldehyde derivatives *via a* one-pot three-component reaction using various substituted 3-(2-bromoacetyl)coumarins, thiosemicarbazide and substituted acetophenones followed by Vilsmeier-Haack reaction condition (**Scheme 4A.17**). Moreover, the titled compounds were screened for their *in-vitro* cytotoxic activity against human cancer cell lines and antibacterial

activity. Among the tested, compounds **4m,** and **4n** exhibit significant anticancer activity against HeLa cell lines (**Figure 4A.10**).

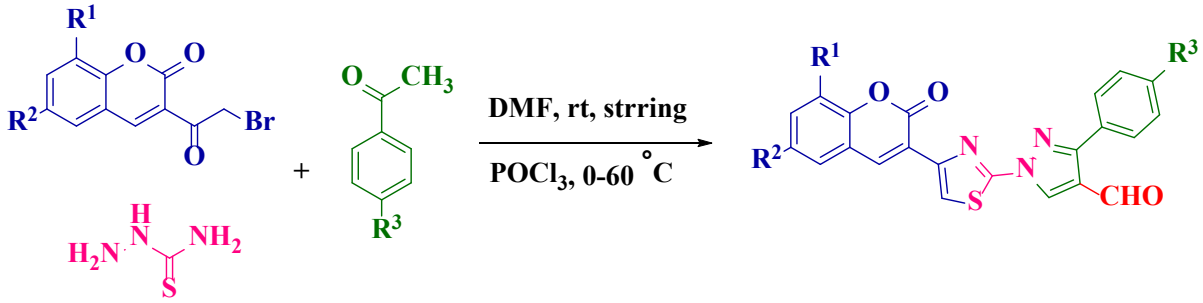

Scheme 4A.17. One-pot three-component synthesis of coumarin-based thiazolyl-pyrazolo-carbaldehyde derivatives

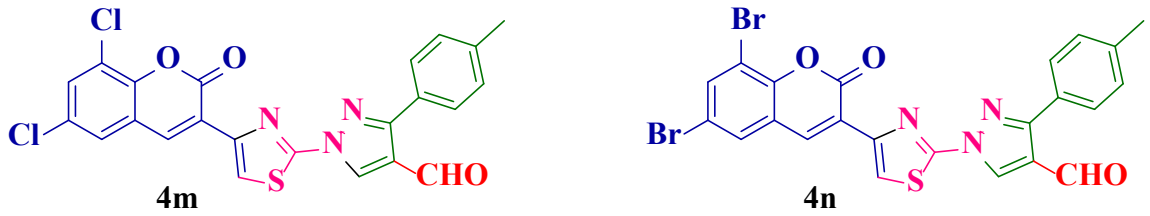

Figure 4A.10. Biologically active scaffolds

4A.1. Present work

4A.1.1. Starting Materials

In this present work, the synthesis of novel thiazole-based benzimidazole **(4a-s)** derivatives were described. The starting materials required for the synthesis of the target compounds were 5-amino-2-mercaptobenzimidazole, phenyl isothiocyanate, and substituted 2-bromoacetophenones. All the starting materials were procured from commercial sources.

4A.2. Synthesis of Thiazoles

The synthesis of target thiazole analogues was carried out as outlined in Scheme 4A.1. These compounds (**4a-s**) were synthesized by a reaction of 5-amino-2-mercaptobenzimidazole (**1**), phenyl isothiocyanate (**2**) and phenacyl bromides (**3**) (**1:1:2**) in PEG-400. The yields of products are good.

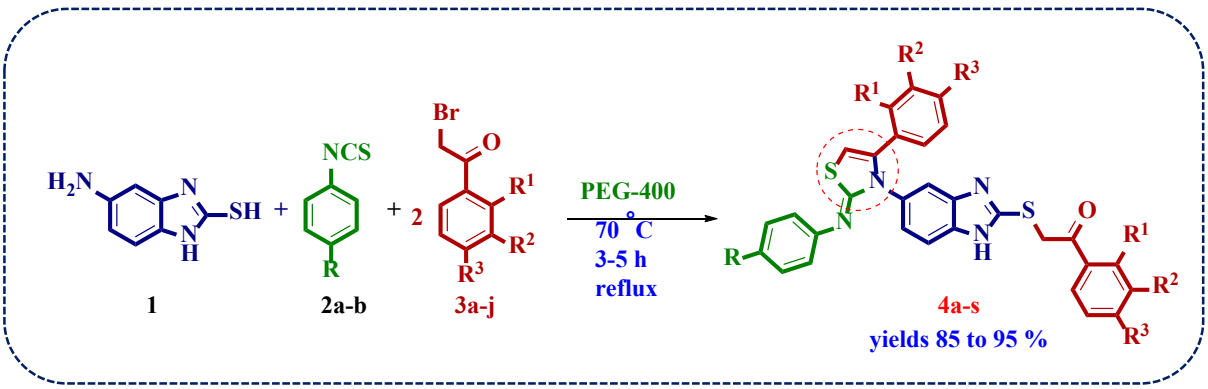

Scheme 4A.1. Synthesis of thiazole derivatives *via* one-pot three component reaction.

4A.3. Results and discussion

Inspired by the biological profile of thiazoles, benzimidazoles, and an extension of previous work on the MCR approach herein, we describe a facile, efficient, and greener protocol for the synthesis of benzimidazole based thiazoles by the reaction of 5-amino-2-mercaptobenzimidazole **1** phenyl isothiocyanate **2**, α-bromo acetophenone **3** in a green solvent medium, PEG 400 at ambient temperature to give 88 % of yield *via* multicomponent approach. To find the optimization condition, we began our investigation for identifying a suitable solvent to obtain the title product **4a** (**Table 4A.1**). Using easily available starting materials 5-amino-2-mercaptobenzimidazole **1** (1.0 equivalent), phenyl isothiocyanate **2** (1.0 equivalent), and α-bromo acetophenone **3** (2.0 equivalents) in different solvents and various bases were employed to improve the yields of reaction (**Table 4A.1, entries 1-13**). But the desired product was not formed with a greater yield. Finally, we tried a reaction with PEG-400 as a reaction solvent. Fortunately, the reaction was smooth in PEG-400 and gave the desired product with good yield within a short time at ambient temperature. Thus, among the solvents tested PEG-400 was found to be the best solvent for the synthesis of title compounds (**4a-s**). Notably, PEG-400 is eco-friendly, cheaper in cost, non-volatile in nature, and a recyclable and reusable solvent. Further, we examined the recyclability of the PEG-400 and it was found that the PEG-400 is recoverable and reusable up to the fourth time in reaction. After isolation of the titled product, water was removed through direct distillation and PEG-400 was washed with diethyl ether (three times, each time 2.0 ml for a single wash). The recovered PEG-400 was used in further runs with a negligible loss of PEG-400 effectiveness.

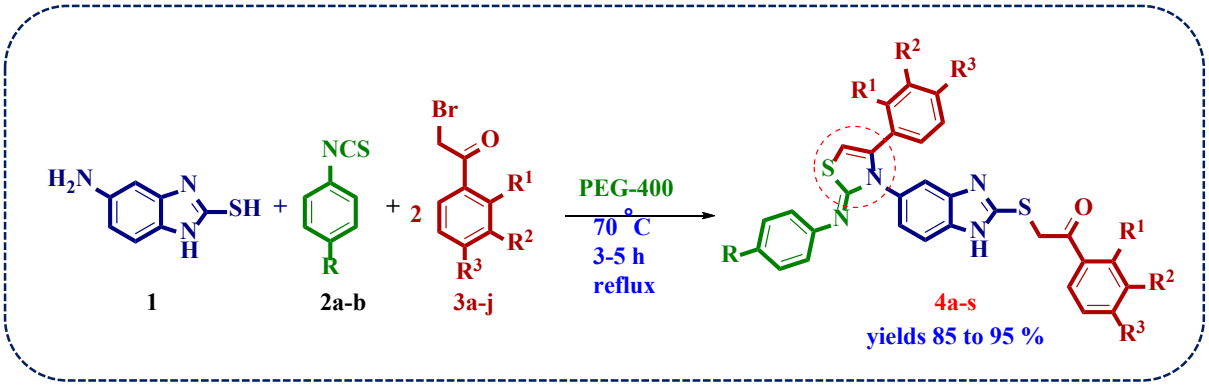

Table 4A.1. Optimized reaction conditions. **4a**[a]

Entry	Solvent	Catalyst (mol%)	Temp (°C)	Time (h)	Yield[b] (%)
1	H_2O	-	60	24	n.r
2	MeOH	-	60	24	25

3	EtOH	-	60	20	30
4	EtOH	AcOH (10)	60	15	41
5	Ethanol	AcOH (20)	60	12	45
6	Ethanol	Na_2CO_3	60	12	30
7	Ethanol	K_2CO_3	60	12	35
8	Ethanol	KOH	60	12	30
9	Ethanol	NaOH	60	12	28
10	Ethanol	DMF (10)	60	12	40
11	Ethanol	DMF (20)	60	10	45
12	DMF	-	60	8	50
13	DMF	-	70	8	65
14	PEG-400	-	60	6	80
15	**PEG-400**	**-**	**70**	**4**	**85**
16	PEG-400	-	reflux	4	60

[a]*Reaction conditions*: 5-amino-2-marcaptobenzimidazole (**1**) (1.0 mmol), phenyl isothiocyanate (**2**) (1.0 mmol), 2-bromoacetophenone (**3**) (2.0 mmol), solvent (2 mL), [b]Isolated yields.

Under these optimized conditions, the substrate scope of the reaction was studied using a series of phenyl isocyanates (**2a-b**) concerning different substituted and α-bromo acetophenones (**3a-j**) derivatives (**Figure 4A. 2**). It is noteworthy that the substituents on the phenyl isothiocyanates and α-bromo acetophenones, regardless of the electron-deficient/ electron-rich nature, did not hamper the efficiency of the reaction, producing the corresponding thiazolines in moderate to excellent yields.

The structure of all the newly synthesized scaffolds was well characterized by IR, ^{1}H, NMR, ^{13}C-NMR, and mass spectral data. For instance, the IR spectrum of compound 4a showed the band at 3391 cm $^{-1}$, 1678 cm $^{-1}$, 1618 cm $^{-1}$, and 1486 cm $^{-1}$ corresponding to the –NH, -C=O, C=N, and C=C stretching vibrations respectively. The ^{1}H-NMR of the spectrum of compound 4a showed peaks at δ 7.99, 6.98, and 3.77 corresponding to the –NH, imidazole C5-proton, and –S-CH_2-aliphatic protons respectively. The ^{13}C-NMR spectrum showed pecks at δ 193.17, 152, 105.0, and 41.25 corresponding to the carbonyl carbon, imine carbon, imidazole C5-carbon, and aliphatic S-CH_2-carbons respectively. The HRMS (ESI) spectra of all the synthesized compounds have shown $[M+H]^+$ ion peck.

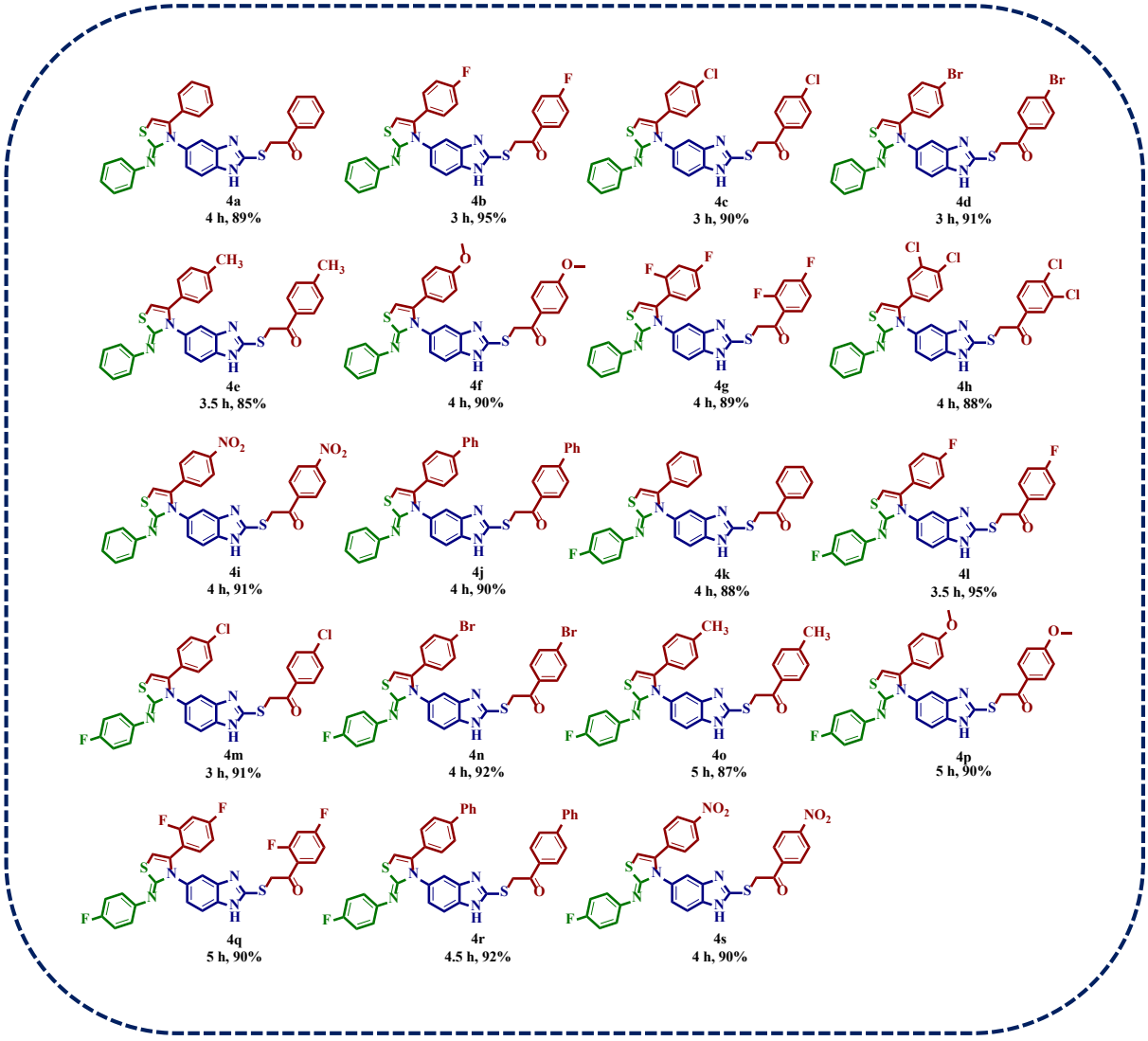

Figure 4A.2. Scope of substrates to synthesize

The plausible reaction mechanism for the formation of title compounds is shown in **Scheme 4A. 2**. Reaction of 5-amino-2-mercaptobenzimidazole, with 1 mmol of phenyl isothiocyanate in presence of PEG-400 to give intermediate 'II' from I. In the next step, the thiol and thiourea groups of 5-amino-2-mercaptobenzimidazole displace the bromine atoms of two equivalents of phenacyl bromides to give intermediate '**III**' with the elimination of two equivalents of hydro bromic acid. The intermediate '**III**' further reacts with PEG-400 to form the intermediate **IV**. Further the intermediate **IV** undergoes elimination of water to give benzimidazole based thiazolidine derivatives **(4a-s) V**.

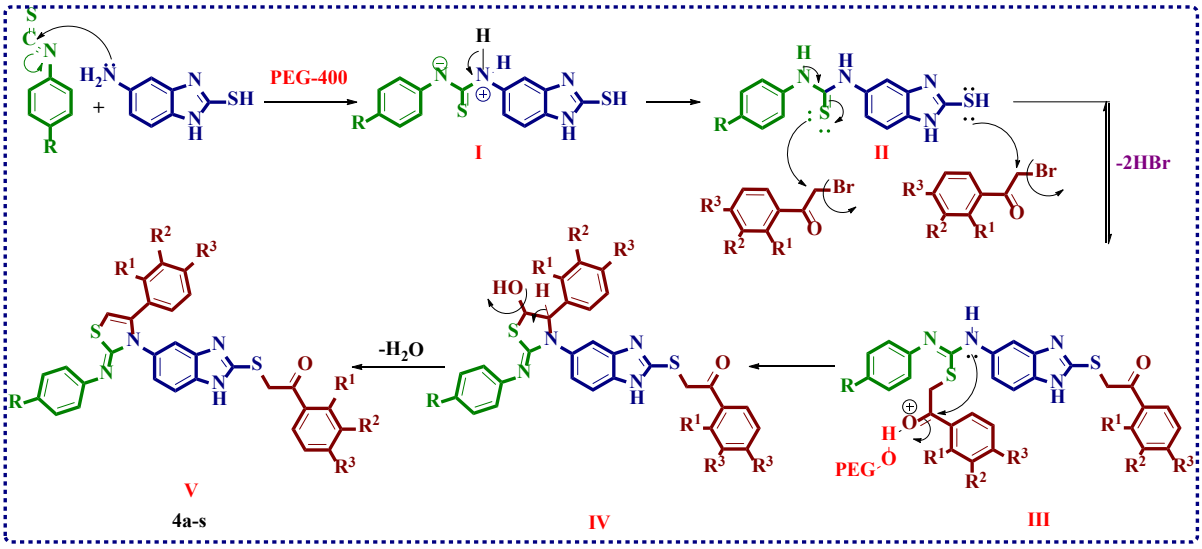

Scheme 4A. 2. Plausible reaction mechanism for the formation of Benzimidazole based thiazlolyl derivatives.

4A.4.Biology

4A.4.1. α-Amylase Inhibitory Activity

The inhibition of *α*-amylase was measured using a modified assay technique were described [27]. The synthesized scaffolds and standard acarbose were prescribed at different concentrations (5-100 µg/mL^{-1}). An aggregate of 50 µL of scaffolds was incubated with 50 µL of porcine α-amylase (0.5 mg/mL in 0.02 M sodium phosphate buffer pH 6.9) at room temperature for 30 minutes. After incubation, each tube was filled with 50 µL of 1%, starch solution in sodium phosphate buffer (pH 6.8) and incubated at room temperature for another 20 minutes. Further,100 µL of DNS (Di-nitro salicylic acid) reagent was added to the reaction mixture and boiled for 10 minutes than cooled to the room temperature. After dilution, the absorbance was measured at 540 nm, and the % of inhibition was calculated using the formula below. The IC_{50} values were found by taking the mean and standard deviation of three measurements, as shown in **Table 4A.2**.

All the synthesized compounds **(4a-s)** were evaluated for *in-vitro* α-amylase activity using Acarbose as a standard positive control. The results with IC_{50} values are represented in **Table 4A.2** and **Figure 4A.3**. All the tested scaffolds showed varying degrees of α-amylase inhibitory activity with the IC_{50} values ranging from 12.02 ± 0.51µg/ml to 44.57 ± 0.47 µg/ml when compared with standard Acarbose has IC_{50} 11.88 ± 0.68 µg/ml. Among the tested scaffolds **4d, 4c, 4h,** and **4b** were found to be excellent inhibitory activity against enzyme with IC_{50} values

found to be 12.02 ± 0.56; 12.25± 0.28; 12.74 ± 0.45; 19.10 ± 0.88 μg/ml respectively. Notably, compounds **4k, 4l,** and **4n** have shown weak inhibitory activity with IC_{50} values are 40.08 ± 0.56; 44.57 ± 0.47, and 39.97 ± 0.64 μg/ml, respectively.

Table 4A.2. α-Amylase activity and molecular docking studies.

S.NO	Compound	IC_{50}(μg/ml)	Molecular Docking Studies			EC Score
		α-Amylase	LF dG	LFV Score	LF Rank Score	
01	4a	36.43 ± 0.65	-8.75	-10.52	-10.42	0.169
02	4b	19.10 ± 0.88	-9.65	-11.38	-9.14	0.21
03	4c	12.25± 0.28	-10.01	-11.45	-10.36	0.226
04	**4d**	**12.02 ± 0.56**	**-11.34**	**-12.39**	**-10.90**	**0.272**
05	4g	15.47 ± 0.51	-9.90	-11.46	-8.59	0.22
06	4h	12.74 ± 0.45	-10.36	-11.89	-10.10	0.224
07	4j	17.83 ± 0.21	-9.02	-12.13	-13.15	0.186
08	4k	40.08 ± 0.56	-7.69	-9.66	-9.41	0.159
09	4l	44.57 ± 0.47	-8.89	-10.79	-7.79	0.2
10	4m	25.34± 0.35	-9.29	-10.93	-9.58	0.223
11	4n	39.97 ± 0.64	-8.96	-11.26	-10.25	0.226
12	4r	16.65 ± 0.91	-9.77	-12.91	-11.34	0.227
13	**Acarbose**	11.88 ± 0.68	-6.73	-16.64	**-10.48**	

LF dG= Lead Finder protein-ligand binding energy; **LFV Score**= Lead Finder Virtual screening (VS) scoring function; **EC Score**= Electrostatic complementarity Score.

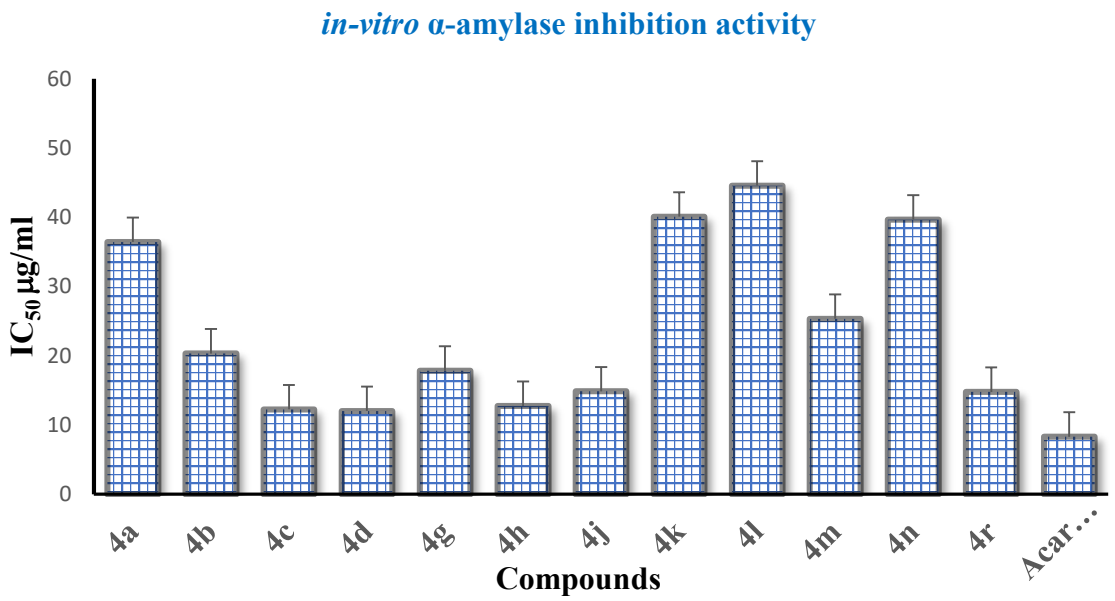

Figure 4A.3. *In vitro* α-amylase inhibition activity of thiazolyl-benzimidazole scaffolds with IC_{50}µg/mL.

Structure-activity relationship: The synthetic scaffolds possess both benzimidazole and thiazole heterocyclic rings. However, different substitutions on these two rings have exhibited variable α-amylase inhibitory activity. The structure activity relationships were evaluated by changing substituents on 2,3,4 position of phenacyl bromides and 4th position of phenyl isothiocyanate as shown in **Table 4A.2**. Notably, among the tested compounds, the compounds with halogen groups (F, Cl, and Br) on the 3rd and 4th position of phenyl ring have showed (**4d, 4c, 4h,** and **4b)** most potent inhibitory activity against the α-amylase enzymes. Furthermore, the electron-donating groups on 4th position of phenyl group such as methyl, methoxy, and scaffolds with no-substituent on the phenyl ring have shown much weaker inhibitory activity (**Table 4A.2**).

4A.5. Molecular docking studies

Molecular docking studies were performed using Cresset Flare Docking software [28,29]. All the synthesized scaffolds were performed for molecular docking studies against the human pancreatic α-amylase in a complex with montbretin A. (PDB ID: 4W93)[30]. The 3D-structures of proteins were retrieved from the protein data bank (PDB). A protein preparation wizard was used to reduce the target protein energies. The receptor grid around their co-crystal ligand was generated using Flare software. The 3D structures of ligands were generated and energies were

minimized using chem3D software. The molecular docking was investigated by normal mode and results were analyzed and protein-ligand interactions were attained. The grid box was defined using the Montbretin A crystal structure within 6 Å around it as binding site for the tested compounds to perform docking studies. After the grid box were generated, docking simulations was subsequently done. Top 10 binding pose were opted for prediction and results were analysed using Discovery studio visualizer.

The cavity was defined using the native ligand of crystal structure 4w93 (a flavonol glycoside called Monotrobtin A) within 6 Å around it. The standard docking protocol in rDOCK was used, including 3 stages of Genetic Algorithm search (GA1, GA2, GA3), followed by low-temperature Monte Carlo (MC) and Simplex minimization (MIN) stages (rDock Reference Guide, August 2015). Three representatives of the synthesized inhibitors (3a, 4f, and 6b) were selected to be docked in the binding pocket of the prepared crystal structure using the empirical score function of rDOCK keeping 20 docking solutions for each inhibitor to be sorted by their binding scores and later visually analyzed for the interactions between the pocket's residues and the inhibitors.

The molecular docking studies of 1-phenyl-2-((5-(4-phenyl-2-(phenylamino) thiazol-3(2*H*)-yl)-1*H*-benzo[*d*]imidazol-2-yl)thio)ethanone (**4a-s)** explored the binding mode and acquire insights into the human pancreatic α-amylase complex with montbretin A (PDB ID: 4W93, (PDB: Protein Data Bank)) binding sites as a probable mechanism.

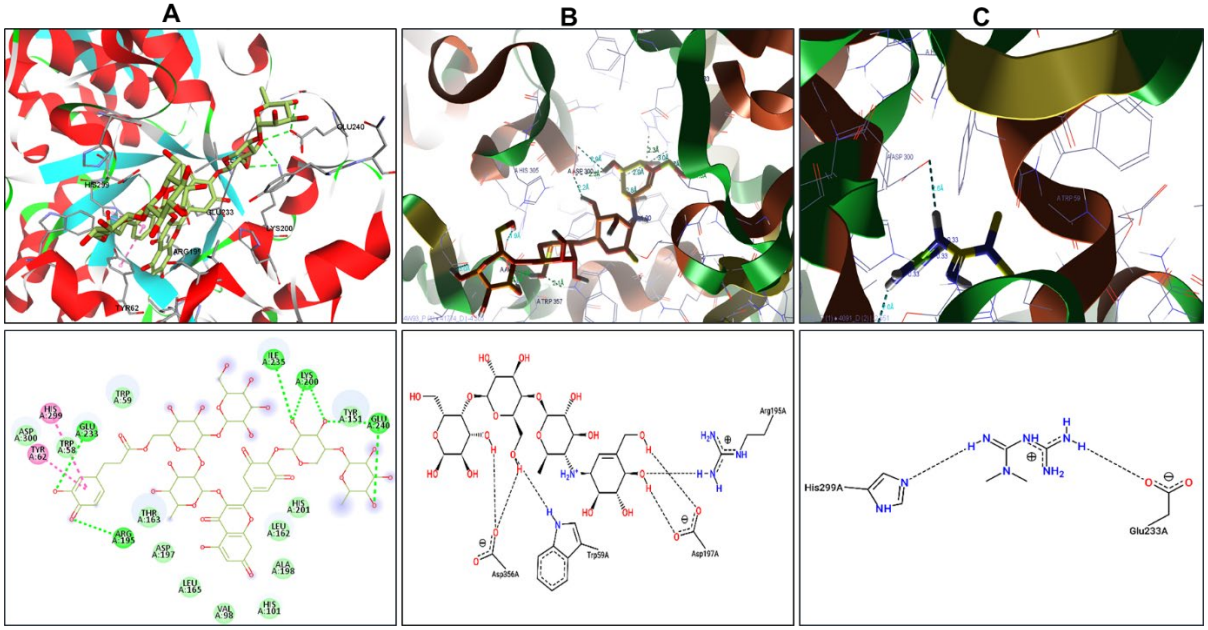

Figure 4A.4. Molecular Docking interactions of ***A) Montbretin A (Co-crystal Ligand) B) Acarbose C) Metformin with Human pancreatic α-amylase*** **(PDB ID: 4W93)**

The Flare Cresset program was used to simulate the molecular docking interactions. The creation of active sites was accomplished according to the earlier published literature[30]. The hypothetical binding mechanism attained between the active site of α-amylase and thiazole-benzimidazole scaffolds is depicted in **Table 4A.2** and **Figures 4A.4-4A.6.**

The docking studies were first confirmed by superimposing the co-crystallized ligand Montbretin A with Montbretin A derived from the crystal structure and redocking into the active binding site of α-amylase enzyme. The co-crystal ligand montbretin A has binding connections in the subsequent manner (**Figure 4A.5**). It forms H-bond interactions with Arg195, Ile235, Lys200, Tyr151, and Glu240 amino acid residues with bond lengths 2.90, 2.94, 3.13, 2.87, and 2.63 A°, respectively. The hydrophobic interactions are exhibited with Trp58 and His299 residues with an LF dG value of -6.73 kcal/mol. The docking studies were also carried out for acarbose and metformin drugs and have shown similar interactions with that of co-crystal ligand. Moreover, the synthesized scaffolds bind to the active site of the α-amylase and exerts similar type of interactions. Based on molecular docking LF dG values ranging between (-11.34 to -6.73 kcal/mol) shown that these analogues possibly display their anti-diabetic activity through collaboration with the active sites of the α-amylase protein.

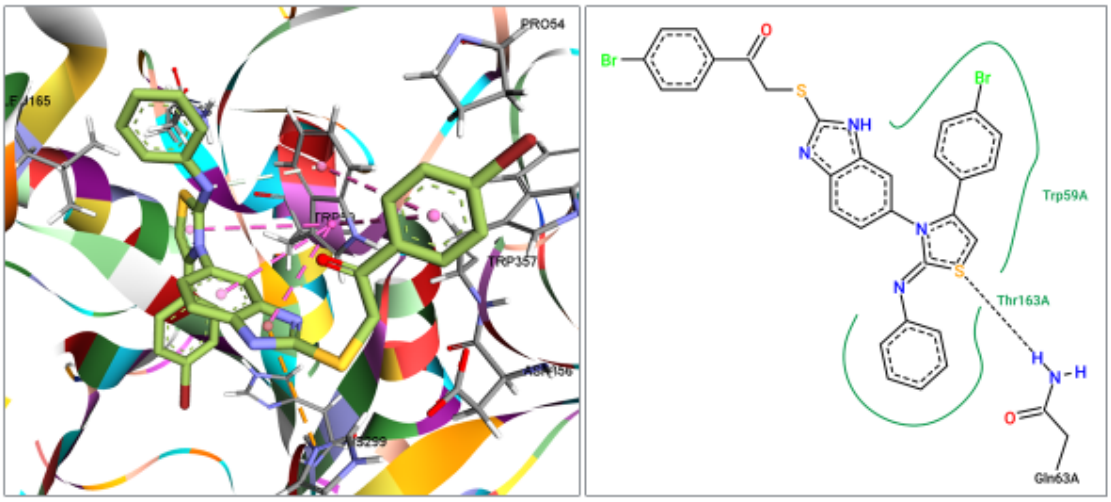

Figure 4A.5. Molecular Docking interactions of compound **4c** with Human pancreatic α-amylase (PDB ID: 4W93).

The *in-vitro* α-amylase activity results exhibited that the **4d** substituted with bromo group showed enhanced enzymatic activity with IC_{50} value 12.02 ± 0.56 µg/mL and exhibited the highest binding energy with LF dG -11.34 kcal/mol. This **4d** showed a hydrogen bond between the amino acid residues Gln63 (Glutamine63) with the sulphur atom of thiazole with a bond length of 2.54 A° (**Figure 4A.6**). It also exhibits hydrophobic interactions with Trp59

(Tryptophan59 amino acid residue) and Thr163 (Threonine163 amino acid residue) of amino acid residues.

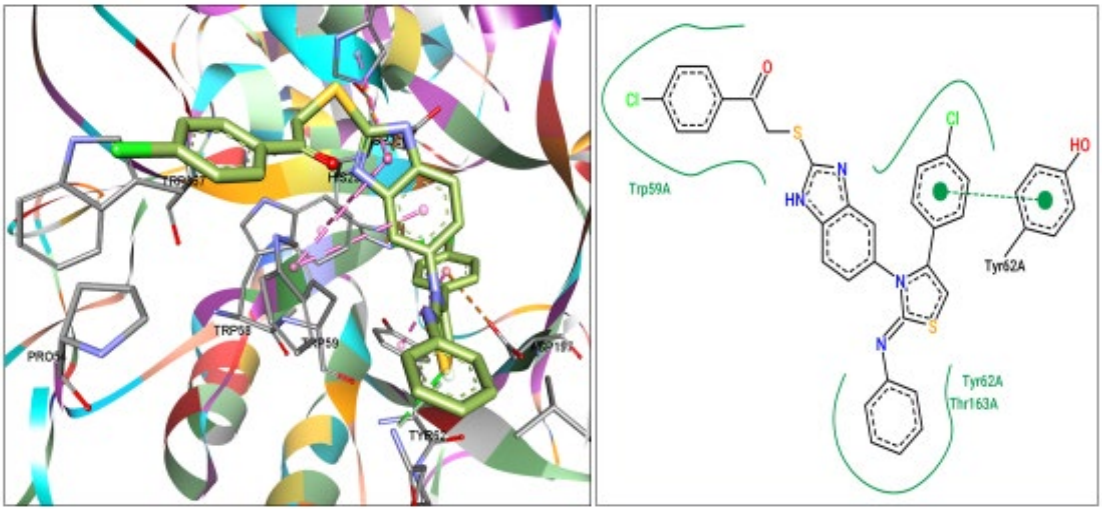

Figure 6. Molecular Docking interactions of compound 4d with Human pancreatic α-amylase (PDB ID: 4W93).

Moreover, **4c** showed the highest binding energy LF dG -10.01 kcal/mol. The ligand forms pi-pi interactions with Tyr62 (Tyrosine62 residue) with chlorophenyl and hydrophobic interactions with Tyr62 and Thr163 amino acid residues.The molecular docking interactions illustrate that the synthesized poly heterocycles have benzimidazole and thiazole rings with diverse group forms as probable bioactive cores and that they form strong binding contacts with active site of amino acid residues. The docking results shown that the docked ligands entered the catalytic reaction centre region of α-amylase. The substrate ligands can form hydrogen bonds with multiple conserved amino acids in α-amylase, especially the core catalytic site Gln63 and Thr163 (Glutamine63 and Threonine163) indicating that the molecular docking model has high confidence.

4A.6. Electrostatic complementarity study

The docked compounds were also studied for Electrostatic complementarity in Flare Software (The electrostatic complementarity colouring and scoring functions within Flare are an extension of the protein interaction potential functions) [31]. Electrostatic interactions between ligands and their protein contribute significantly to the enthalpic aspect of the binding free energy ΔG. Examining the electrostatic match among the docked ligands and active site reveals important information about why ligands bind and what can be done to optimize binding.

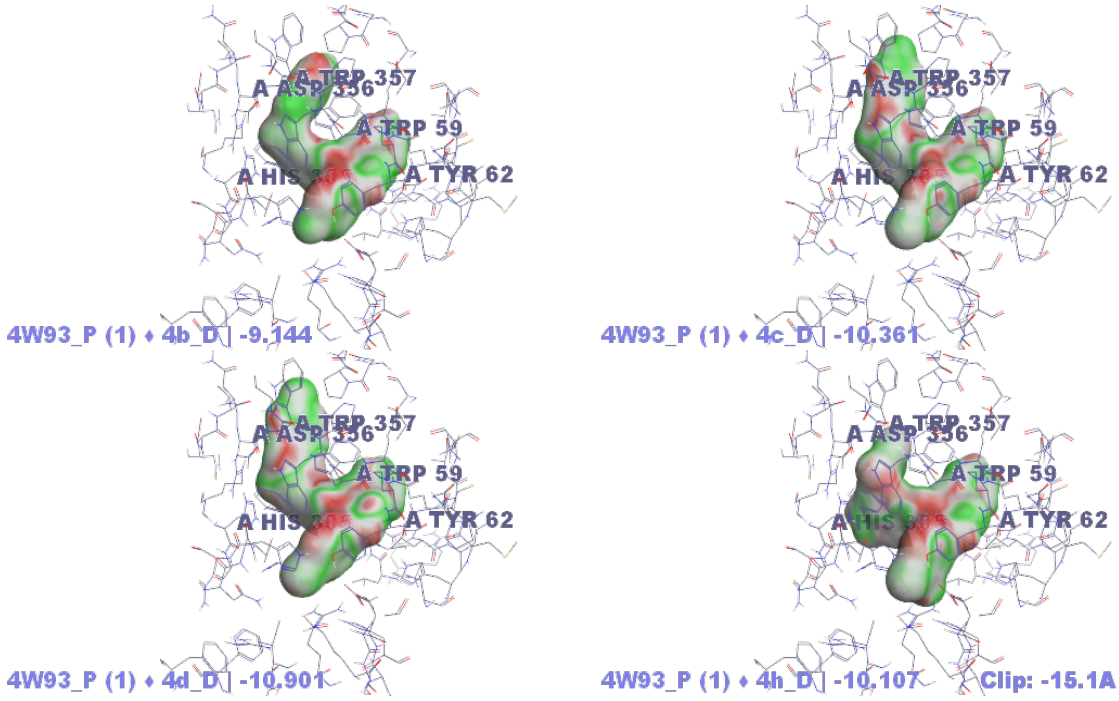

Figure 4A.7. Electrostatic complementarity of the ligand with Human pancreatic α-amylase (PDB ID: 4W93).

By selecting the ligands of interest and selecting Electrostatic complementarity to Protein from the 'Mol' button drop-down menu in the Ligand tab, electrostatic complementarity surfaces for ligands (towards the related protein) can be calculated and displayed. The default colours for minimum and maximum EC vary from green (perfect electrostatic complementarity), white (no electrostatic potential for either the ligand or the protein), and red (electrostatic clash). Each ligand's EC score is calculated against the protein with which it is associated. The score ranges from EC score 1 (perfect complementarity) to EC score -1 (perfect clash). We calculated the EC score of all docked ligand-protein complexes and showed positive values given in **Table 4A.2**. The illustration of Electrostatic Complementarity to Protein-ligand complex was shown in **Figure 4A.7.**

4A.7. Molecular Dynamic Simulations

Gromacs software was used to perform the Molecular Dynamic (MD) simulations [32]. The physical movements of molecules and atoms of the protein-ligand molecular docking complex will be determined *via* MD simulation. The MD simulation is performed on a docked compound **4d** with pancreatic α-amylase complex (PDB ID: 4W93). The structure check wizard tool is used to thoroughly vetted the protein for any missing residues before performing the MD simulations. The AMBER force field was used to minimize the ligand energies, while the AMBER FF14SB force field used to minimize the protein energies. MD simulations were

carried out with default settings of normal calculation method, with the following parameters: simulation length was 10 ns, and the solvent model was explicit. With a 10 A^{o} solvent box, the AM1-BCC charge method is applied. The protein-ligand complexes energy has been minimized to 0.25 kcal/mol, and the system has been equilibrated for 200 ps before the production run begins. After the simulation was done, the trajectory was analyzed for RMSD and RMSF plots and protein-ligand contacts.

To further understand and validate the molecular level interactions binding ability and influence of compound **4d** in complex with α-amylase (PDB ID: 4W93), we have performed MD simulations of 100 nanoseconds. The Gromacs was used for the MD simulations. Periodic boundary conditions were used to determine the specific size and shape of the water box buffered at 10 Å distances and box volume was calculated as ~400000 cubic Ås of simulation box volume respectively. The simulation length is specified as 100 ns and Explicit solvent models with TIP3P (Transferable Intermolecular Potential-3P) water are used for the MD simulation. Ligand is minimized with the AMBER/GAFF (General AMBER Force Field (GAFF)) force field and AMBER FF14SB (FF14SB= force field improved protein secondary structure balance and dynamics from earlier force fields like FF99SB) was used as the protein force field. After completing the MD simulation, the trajectory file was opened from Open Trajectory, and RMSD (Root Mean Square Deviation) plots observed. The RMSD plots of protein-ligand complex and ligand heavy atoms were recorded.

Root mean square fluctuations (RMSF) of individual residues were initially analyzed to understand the impact of compound binding on the protein conformation changes. The RMSD plot for protein-ligand complexes was stable during the simulations. The results were analyzed using the Open Trajectory wizard and observations showed that the RMSD plots were stable during the MD simulations. The study was carried out with 100ns MD simulations for compound **4d-4W93** protein complex. Throughout the MD simulations, the RMSF and RMSD plots of protein were scrutinized, in which the RMSD could measure the protein conformation changes and based on this, identify that the molecular dynamics simulations had reached the equilibrium, while the RMSF plot could identify the local changes of each amino acid residue along the protein chain. The RMSF plot was displayed in **Figure 4A.9**, the plot is obtained for the **4d-4W93** protein complex from the simulation studies. The fluctuations of the majority of amino acid residues were found to be less than 3.5Å, and enormous fluctuations in the residues were comprehended in the plot indicating the protein hoop is high flexibility. A plot of RMSD was generated between the primary frame of the protein and chosen frame. The plots in **Figure 4A.8** illustrate the RMSD plot of the protein-ligand complex of MD simulation.

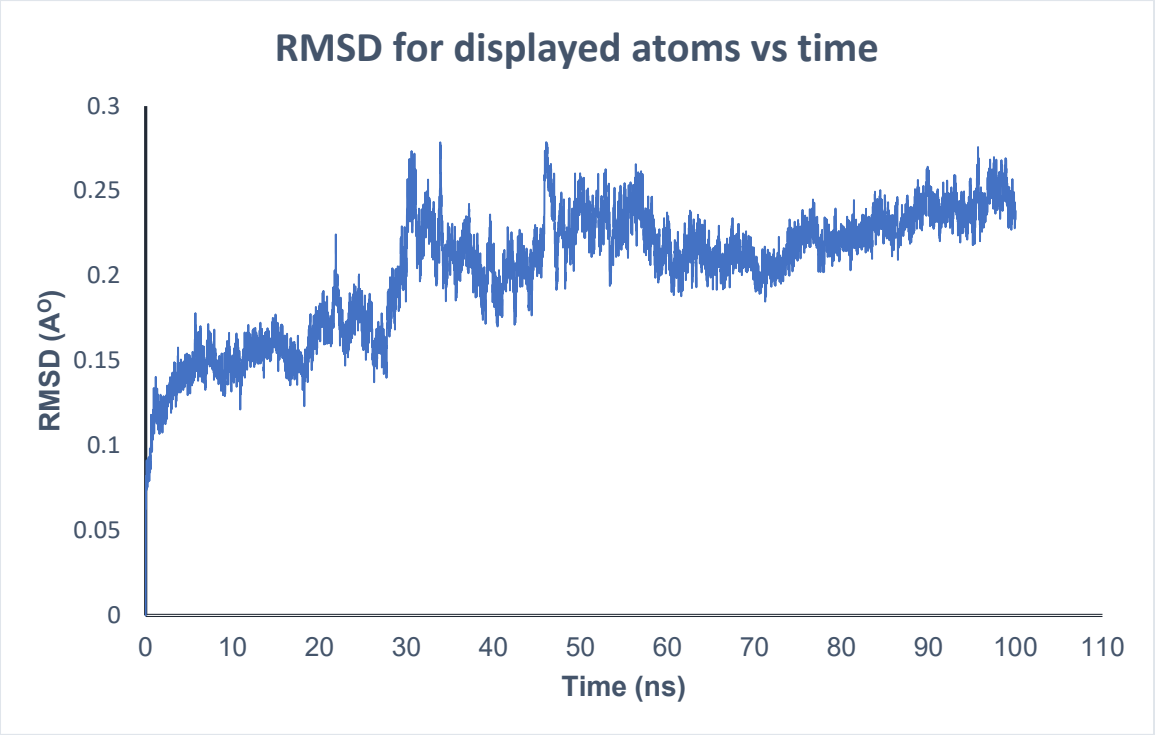

Figure 4A.8. RMSD plot of compound 4d with α-amylase protein complex (PDB ID: 4W93)

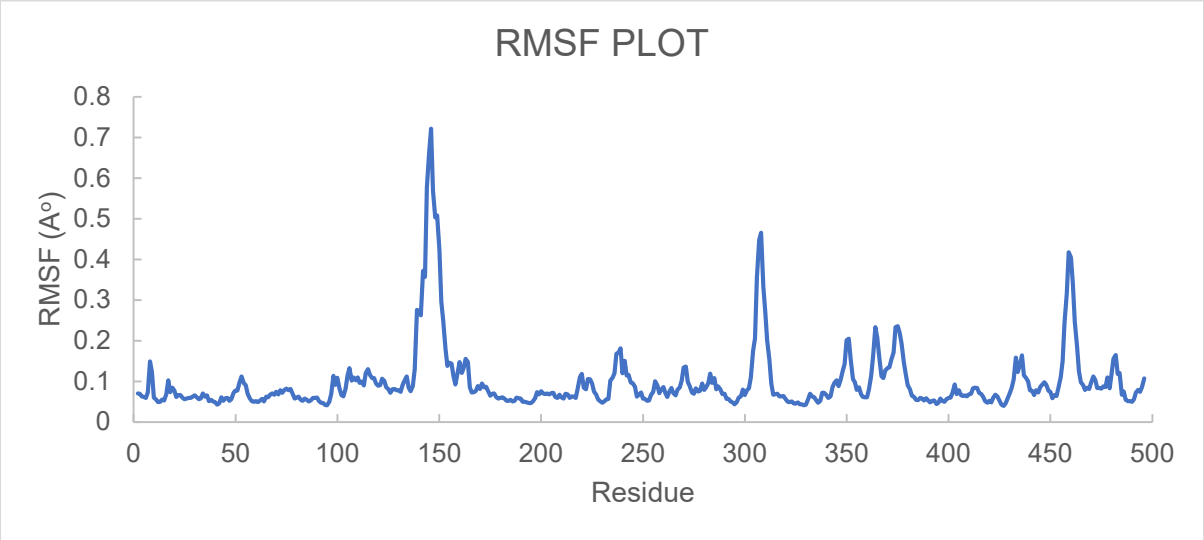

Figure 4A.9. RMSF plot of compound 4d with α-amylase protein complex (PDB ID: 4W93

The reference frame is the molecular docked complex of protein-ligand, and the movement for this original alignment during MD simulation is gauged by aligning all the protein frames in terms of time. The RMSD value of 1-4 A° is agreeable for globular proteins. For our MD simulation of the compound **4d-4W93** protein complex, the value of RMSD did not surpass 1.0

A° showing the stability of the protein conformation. The H-bond analysis of the compound **4d-4W93** complex shows the interactions with the following amino acid residues Trp43, Tyr59, Tyr62, His305, and Asp356 residues.

4A.8. 3D RISM Solvation Studies for 4d-4W93 complex

A three-dimensional reference-site (3D-RISM) algorithm was used to study the stability of the protein in bulk water molecules generated during Flare docking studies at the active site [33]. At the end of 3D-RISM calculations, the high water density at the active site 4W93 was formed. **Figure 4A.9** reveals that the oxygen and hydrogen density of **4d** at the active site of 4W93 protein and is demonstrated in two 3D-RISM colors, one is with green spheres

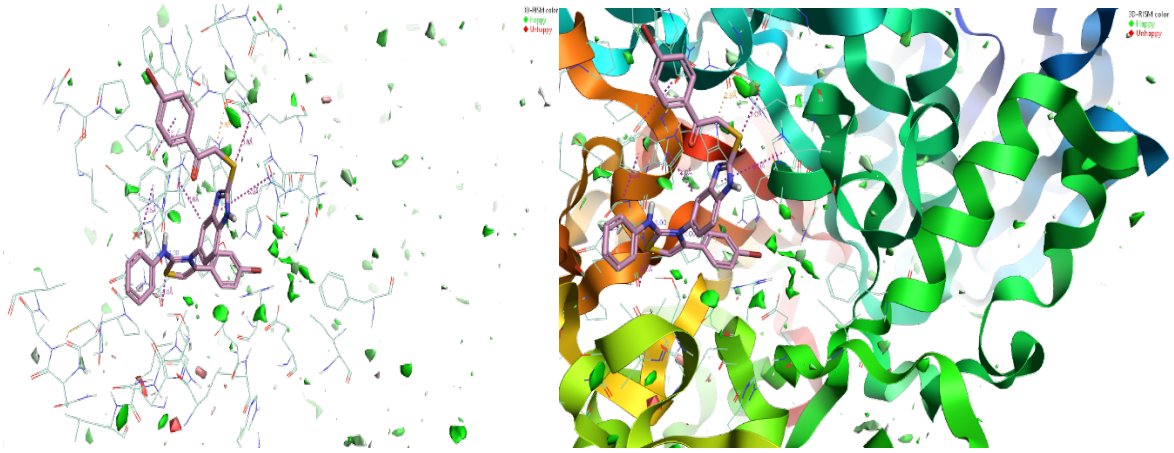

Figure 4A.10. 3D RISM solvation studies for 4d in complex with α-amylase protein complex (PDB ID: 4W93)

indicates as Happy and the red sphere indicates unhappy i.e. favorable and unfavorable regions at the active site. Solvation studies shown that ligand **4d** that bind to the 4W93 active site are stable in bulk water. These studies indicate that the green color sphere (Happy) will favor the interactions between the 4d and 4W93 protein, red color sphere (Unhappy) will not favor interactions **Figure 4A.10.** Thus 3D-RISM will predict the role of water in the active site interactions. 3D-RISM-KH (Three-Dimensional Reference Interaction Site Model (3D-RISM) with Kovalenko−Hirata (KH)) molecular theory of solvation studies explained the mechanism of 4d binding to 4W93 protein.

***In silico* ADME, Toxicity and Pharmacokinetic Studies**

All the tested compounds were evaluated for physicochemical, and ADME descriptors by using galaxy webserver [34]. The toxicity was calculated by using Data warrior software [35]. hERG

toxicity were calculated for tested compounds by using ADMET Prediction Service webserver [36]. The pharmacokinetics studies were carried out in ADMET lab 2.0 [37].

The *in-silico* ADME (absorption, distribution, metabolism and, excretion) properties of 1-phenyl-2-((5-(4-phenyl-2-(phenylamino) thiazol-3(2*H*)-yl)-1*H*-benzo[*d*]imidazol-2-yl) thio)ethanone derivatives was studied by using with RDKit. For evaluating drug-likeliness and oral bioavailability Lipinski's Rule of 5 is often used. According to this criterion, molecular weight must be ≤ 500 Da, logP ≤5, no of H-Acceptors ≤ 10 and, no of H-Donor ≤ 5. The bioavailability of compounds that violate more than two Ro5 will be affected. All the calculated chemical descriptors met the Lipinski rule, which specifies that ligands should not violate more than two Ro5. (**Table 4A.3**). The Quantitative Estimation Drug-Likeliness (QED) is calculated from eight properties i.e. molecular weight (MW), number of hydrogen bond donors (HBD's), octanol-water partition coefficient (ALOGP), number of hydrogen bond acceptors (HBAs), molecular polar surface area (PSA), number of rotatable bonds (ROTBs), number of structural alerts (ALERTS), and number of aromatic rings (AROMs). The value ranges from 0 (unfavorable properties) to 1 (favorable properties). All the synthesized scaffolds do not have drug likeliness properties which indicates the positive value is considered to be Drug likeliness. Data Warrior predicts toxicity qualities for the scaffolds, and all compounds are toxicity-free. The Marvin sketch software is used to predict hERG toxicity for target compounds which exhibited in the range from 6.01 to 6.26 value. All compounds are predicted for toxicity properties by using Data warrior software which predicts organ toxicity Tumorigenic, Reproductive Effective, Irritant, and Mutagenicity. All compounds are free from toxicity and have a high oral bioavailability. All the synthesized compounds were visualized the molecular lipophilicity potential (MLP) in Galaxy 3D visualizer which generates molecular surfaces to see which regions are hydrophobic (blue and violet colors) and hydrophilic (red and orange). MLP is calculated using the same atomic hydrophobicity contributions as the octanol-water partition coefficient (logP). Analysis of 3D molecular surface distribution of hydrophobicity is particularly helpful when explaining differences in observed ADME properties of molecules with the same logP. The calculated logP values of all synthesized compounds are much correlated with the 3D visualized MLP. Among the compounds **4j** and **4r** are highly hydrophobic with blue color and exhibited logP values 10.63 and 10.76 respectively. In addition, all of tested compounds showed acceptable pharmacokinetic properties (**Tables 4A.5-4A.8**).

Table 4A.3. Drug-likeness quantitative estimation (QED) with RDKit and Toxicity with Data Warrior Software

ADME Properties												**Toxicity**				
Entry	MW	ALOGP	HBA	HBD	PSA	ROTB	AROM	ALERTS	LRo5	QED	Drug Likeliness	hERG	Tumorigenic	Reproductive Effective	Irritant	Mutagenicity
4a	518.67	7.29	3	1	63.04	7	6	2	2	0.21	2.28	6.08	None	None	None	None
4b	554.65	7.56	3	1	63.04	7	6	2	2	0.19	0.94	6.07	None	None	None	None
4c	587.56	8.59	3	1	63.04	7	6	2	2	0.16	2.34	6.18	None	None	None	None
4d	676.46	8.81	3	1	63.04	7	6	2	2	0.15	0.49	6.06	None	None	None	None
4g	590.63	7.84	3	1	63.04	7	6	3	2	0.12	0.94	6.01	None	None	None	None
4h	656.45	9.9	3	1	63.04	7	6	2	2	0.14	2.34	6.26	None	None	None	None
4j	670.86	10.63	3	1	63.04	9	8	2	2	0.12	2.28	6.07	None	None	None	None
4k	536.66	7.42	3	1	63.04	7	6	2	2	0.2	0.94	6.1	None	None	low	None
4l	572.64	7.7	3	1	63.04	7	6	2	2	0.18	1	6.16	None	None	low	None
4m	605.55	8.73	3	1	63.04	7	6	2	2	0.16	0.85	6.13	None	None	low	None
4n	694.45	8.95	3	1	63.04	7	6	2	2	0.15	0.84	6.05	None	None	low	None
4r	688.85	10.76	3	1	63.04	9	8	2	2	0.13	0.94	6.04	None	None	low	None

Table 4A.4. Molecular Lipophilicity potential (MLP) of the Tested Compounds

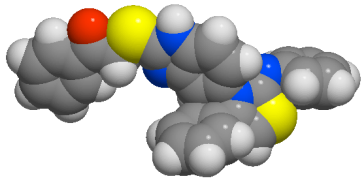 4a	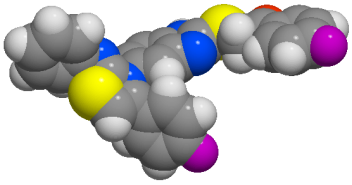 4b	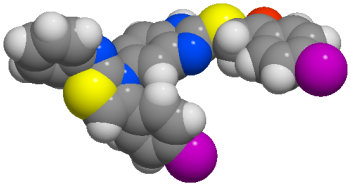 4c
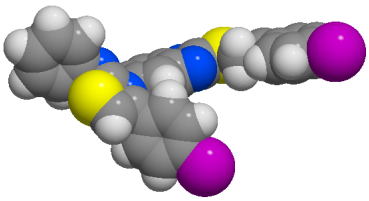 4d	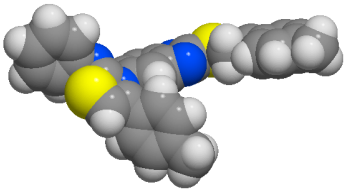 4e	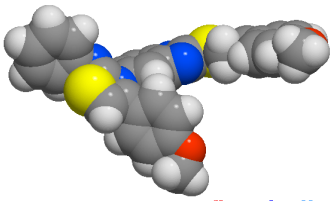 4f
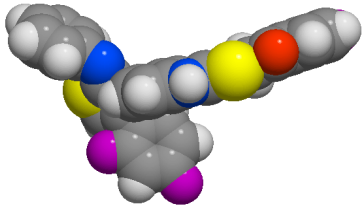 4g	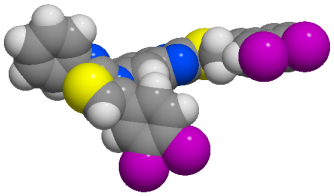 4h	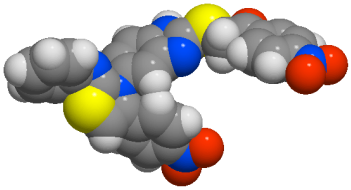 4i
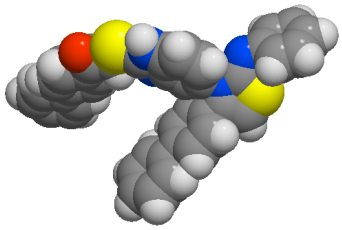 4j	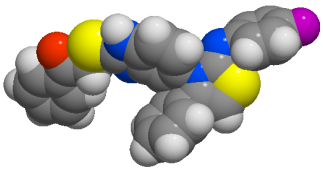 4k	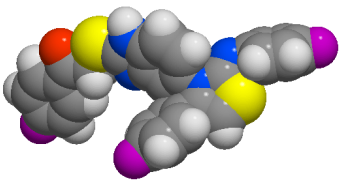 4l
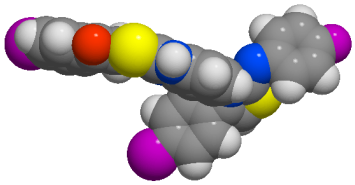 4m	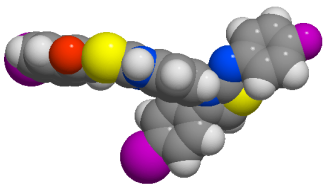 4n	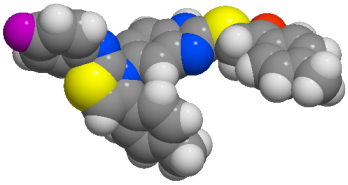 4o
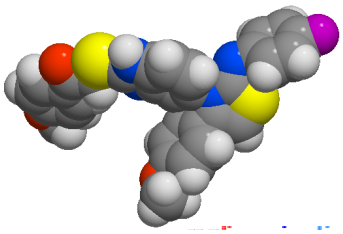 4p	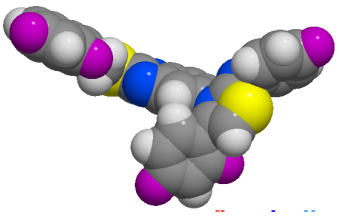 4q	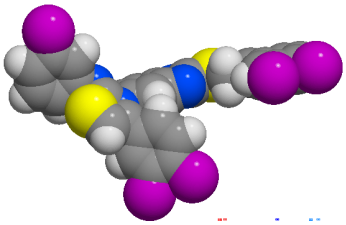 4r

Table 4A.5. Absorption profile for the Tested compounds

Entry	Pgp-inh	Pgp-sub	F(20%)	F(30%)	Caco-2	MDCK
4a	1	0.002	0.661	0.003	-5.464	1.46E-05
4b	1	0.004	0.003	0.003	-5.57	1.32E-05
4c	1	0.004	0.006	0.002	-5.553	8.92E-06
4d	1	0	0.003	0.002	-5.696	1.14E-05
4g	1	0.002	0.002	0.002	-5.959	1.52E-05
4h	1	0.002	0.003	0.011	-5.879	7.38E-06
4j	1	0.055	0.973	0.009	-5.356	1.07E-05
4k	1	0.002	0.017	0.003	-5.489	1.36E-05
4l	1	0.005	0.002	0.003	-5.556	1.29E-05
4m	1	0.01	0.001	0.001	-5.594	9.14E-06
4n	1	0	0.002	0.004	-5.751	1.13E-05
4r	1	0.013	0.654	0.005	-5.466	9.82E-06

Pgp-inhibitor (Category 1: inhibitor); Pgp-substrate (Category 0: non-substrate); F(20%): 20% Bioavailability.Category 1: F20%+ (bioavailability <20%); Category 0: F20%- (bioavailability ≥20%); F(30%): 30% Bioavailability Category 1: F30%+ (bioavailability <30%); Category 0: F30% (bioavailability ≥30%); Caco-2 permeability: Optimal: higher than -5.15 Log unit; MDCK permeability: low: $< 2 \times 10^{-6}$ cm/s medium: 2–20$\times 10^{-6}$ cm/s, high passive: > 20 $\times 10^{-6}$ cm/s

Table 4A.6. Distribution property for the most active compounds

Entry	PPB	VDss	Fu
4a	101.02%	0.183	0.76%
4b	101.66%	0.128	0.74%
4c	102.16%	0.074	0.60%
4d	102.44%	0.231	2.06%
4g	102.00%	0.063	0.54%
4h	103.66%	-0.039	0.71%
4j	104.96%	0.175	0.92%
4k	101.36%	0.167	0.73%
4l	101.97%	0.101	0.69%
4m	102.37%	0.049	0.58%
4n	102.65%	0.184	1.78%
4r	105.52%	0.142	0.92%

PPB: Plasma Protein Binding: Optimal <90%; VDss: Volume Distribution Optimal: 0.04-20L/kg; Fu: The fraction unbound in plasma Low: <5%; Middle: 5~20%; High: >20%

Table 4A.7. Metabolism profile for the Tested compounds

Entry	CYP1 A2-inh	CYP1 A2-sub	CYP2C 19-inh	CYP2C 19-sub	CYP2 C9-inh	CYP2 C9-sub	CYP2 D6-inh	CYP2 D6-sub	CYP3 A4-inh	CYP3 A4-sub
4a	0.90	0.16	0.86	0.05	0.93	0.29	0.13	0.08	0.51	0.74
4b	0.73	0.16	0.61	0.05	0.50	0.72	0.09	0.20	0.33	0.84
4c	0.81	0.16	0.77	0.05	0.52	0.59	0.14	0.12	0.28	0.91
4d	0.75	0.14	0.66	0.05	0.49	0.69	0.07	0.13	0.23	0.85
4g	0.67	0.17	0.78	0.05	0.89	0.91	0.07	0.27	0.41	0.49
4h	0.83	0.16	0.71	0.05	0.77	0.79	0.10	0.20	0.28	0.91
4j	0.59	0.11	0.20	0.04	0.12	0.71	0.00	0.11	0.12	0.86
4k	0.82	0.16	0.80	0.05	0.84	0.53	0.12	0.10	0.45	0.79
4l	0.64	0.16	0.39	0.05	0.22	0.83	0.07	0.44	0.22	0.88
4m	0.74	0.16	0.63	0.05	0.21	0.77	0.11	0.19	0.21	0.91
4n	0.68	0.14	0.57	0.05	0.21	0.82	0.05	0.24	0.20	0.88
4r	0.57	0.12	0.17	0.04	0.08	0.86	0.00	0.23	0.09	0.89

Table 4A.8. Excretion for the Tested compounds

Entry	CL	T12
4a	3.376	0.149
4b	3.41	0.028
4c	3.209	0.052
4d	2.06	0.039
4g	3.602	0.011
4h	3.543	0.029
4j	3.358	0.015
4k	3.442	0.065
4l	3.432	0.013
4m	3.256	0.022
4n	2.153	0.016
4r	3.345	0.007

CL: Clearance, High: >15mL/min/kg, moderate: 5-15 mL/min/kg, low: <5 L/min/kg; T1/2: Category 1: long half-life, Category 0: short half-life, long half-life: >3h; short halflife:<3h.

Table 4A.9. Calculated values of LogBB, HIA and hERG for Tested compounds				
Entry	**LogBB**	**HIA**	**hERG Affinity**	**hERG Activity**
4a	0.31	100	8.08	6.46
4b	0.31	94.3	8.18	6.57
4c	0.31	94.3	8.69	6.78
4d	0.31	94.3	8.18	6.3
4g	1.25	94.3	8.04	5.88
4h	1.13	94.3	8.61	7.03
4j	0.31	94.3	9	7.36
4k	0.31	100	8.13	6.74
4l	0.31	94.3	8.23	6.86
4m	0.31	94.3	8.74	7.06
4n	0.31	94.3	8.23	6.58
4r	0.31	94.3	9	7.62
BB: Blood Brain Barrier; HIA: Human Intestine Absorption				

4A.10. Conclusion

In conclusion, we have synthesized a facile one-pot four-component synthesis of thiazolylbenzimidazole derivatives (**4a-s**) *via a* multi-component approach by using readily available starting materials in green solvent medium PEG-400 as a recyclable and greener solvent in a shorter reaction time without any by-products. All the synthesized compounds (**4a-s**) are well characterized by analytical and spectroscopic techniques. Further, all the synthesized compounds were evaluated for *in vitro* α-amylase activity using acarbose as a standard positive control. Among the tested composites,**4d, 4c, 4h,** and **4b** were found to be excellent inhibitory activity against α-amylase enzyme with IC_{50} values found to be 12.02 ± 0.56; 12.25± 0.28; 12.74 ± 0.45; 19.10 ± 0.88 µg/ml respectively. Structure-activity relationship (SAR) studies indicate compounds substituted with halogen groups on the 3rd and 4th position of the phenyl ring have exhibited (**4d, 4c, 4h,** and **4b)** most potent inhibitory activity against the α-amylase enzyme. The mode of binding connections between the α-amylase enzyme and the composites was studied. The medicine-likeness properties (*in silico* ADME properties) have been prognosticated for the title compounds. The α-amylase inhibition, molecular docking, and drug-likeness properties of the title composite proven that these are promising anti-diabetic active skeletons.

4A.11. Experimental section

4A.11.1. General procedure for the synthesis of compounds (4a-s):

A mixture of 5-amino-2-marcaptobenzimidazole (1.0 mmol), phenyl isothiocyanate (**2a-b)** (1.0 mmol), different substituted α-bromo-acetophenones **3 (a-j**) (2.0 mmol), was taken in a round bottom flask and the reaction mixture was refluxed in PEG-400 (4 ml) at 70 °C for 4 h. After completion of the reaction (checked through TLC, 50:50, n-hexane: EtOAc), the reaction mixture was cooled to room temperature and placed in ice-cold water. The solid separated was filtered, washed with diethyl ether, dried, and recrystallized from ethanol.

4A.12. Characterization data of products

1-Phenyl-2-((5-(4-phenyl-2-(phenylimino)thiazol-3(2*H*)-yl)-1*H*-benzo[*d*]imidazol-2-yl)thio)ethan-1-one (4a).

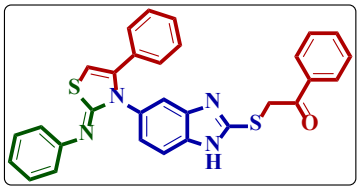

White solid: yield: 89%, mp: 191-193 °C; FT-IR (KBr, cm-1): 3389 (NH), 1680 (C=O), 1623 (C=N); **^{1}H NMR** (400 MHz, DMSO-d_6 δ ppm): 8.09 (d, J = 7.6 Hz, 2H, Ar-H), 7.73 (t, J = 7.2 Hz, 1H, Ar-H), 7.63 – 7.59 (m, 5H, Ar-H), 7.53-7.50 (m, 4H, Ar-H), 7.34 – 7.28 (m, 5H, Ar-H), 7.20 (d, J = 6.8 Hz, 2H, Ar-H), 7.13 (s, 1H, imidazole proton), 5.21 (s, 2H, S-CH_2 protons); **^{13}C-NMR** (100 MHz, DMSO-d_6) δ: 193.17, 152.48, 141.92, 135.52, 134.68, 134.52, 130.91, 130.56, 130.01, 129.71, 129.40, 129.29, 129.00, 128.85, 121.08, 120.49, 115.21, 110.31, 105.00, 41.25; ESI-HRMS: *m/z* Calcd for Chemical Formula: $C_{30}H_{23}N_4OS_2$ 519.1305 $[M+H]^+$ found: 519.1338.

1-(4-Fluorophenyl)-2-((5-(4-(4-fluorophenyl)-2-(phenylimino)thiazol-3(2*H*)-yl)-1*H*-benzo[*d*]imidazol-2-yl)thio)ethan-1-one. (4b):

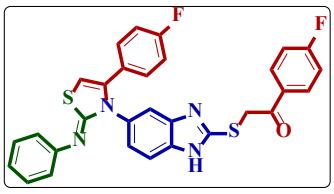

White solid: yield: 95%, mp: 198-200 °C; FT-IR (KBr, cm-1): 3384 (NH), 1678 (C=O), 1593 (C=N); **^{1}H NMR** (400 MHz, DMSO-d_6 δ ppm): 8.18 (dd, J = 9.0, 5.4 Hz, 2H, Ar-H), 7.66 – 7.58 (m, 5H, Ar-H), 7.54-7.51 (m, 3H, Ar-H), 7.44 (t, J = 8.8 Hz, 2H, Ar-H), 7.28-7.24 (m, 3H, Ar-H), 7.18 (s, 1H, imidazole proton), 7.14 (d, J = 8.8 Hz, 2H, Ar-H), 5.21 (s, 2H, S-CH_2-protons); **^{13}C-NMR** (100 MHz, DMSO-d_6) δ: 191.74, 167.21, 164.69, 164.19, 161.72, 152.53, 140.89, 134.47, 132.35, 132.27, 132.18, 132.09, 131.04, 130.62, 129.30, 121.44, 116.61, 116.39, 116.06, 115.84, 115.25, 110.25, 105.56, 41.46; ESI-HRMS: *m/z* Calcd for Chemical Formula: $C_{30}H_{21}F_2N_4OS_2$: 555.1117 $[M+H]^+$ found: 555.1152.

1-(4-Chlorophenyl)-2-((5-(4-(4-chlorophenyl)-2-(phenylimino)thiazol-3(2*H*)-yl)-1*H*-benzo[*d*]imidazol-2-yl)thio)ethan-1-one. 4c

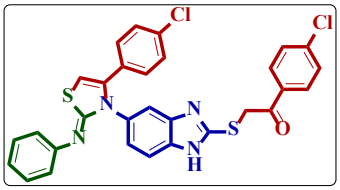

White solid: yield: 90%, mp: 208-210 °C; FT-IR (KBr, cm^{-1}): 3381 (NH), 1677 (C=O), 1622 (C=N); **^{1}H NMR** (400 MHz, DMSO-d_6 δ ppm): 8.09 (d, J = 8.4 Hz, 2H, Ar-H), 7.68 (d, J = 8.8 Hz, 2H, Ar-H), 7.62 – 7.58 (m, 5H, Ar-H), 7.53-7.51 (m, 4H, Ar-H), 7.38 (d, J = 8.8 Hz, 2H), 7.21 (d, J = 8.4 Hz, 2H, Ar-H), 7.13 (s, 1H, imidazole proton), 5.17 (s, 2H, S-CH_2 protons);); **^{13}C-NMR** δ_C (100 MHz, DMSO-d_6) δ: 186.79, 165.34, 141.02, 131.94, 131.39, 131.25, 131.17, 131.04, 129.22, 128.78, 128.52, 107.01, 17.27; ESI-HRMS: *m/z* Calcd for Chemical Formula: $C_{30}H_{21}Cl_2N_4OS_2$: 587.0534 $[M+H]^+$ found: 587.0565.

1-(4-Bromophenyl)-2-((5-(4-(4-bromophenyl)-2-(phenylimino)thiazol-3(2*H*)-yl)-1*H*-benzo[d]imidazol-2-yl)thio)ethan-1-one. 4d

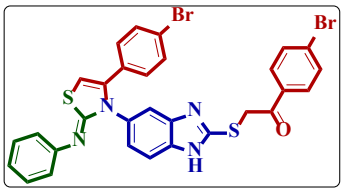

White solid: yield: 91%, mp: 209-211 °C; FT-IR (KBr, cm^{-1}): 3389 (NH), 1677 (C=O), 1621 (C=N); **^{1}H NMR** (400 MHz, $CDCl_3$+DMSO- d_6 δ ppm): 8.07 (d, J = 8.4 Hz, 2H, Ar-H), 7.88 (s, 1H, Ar-H), 7.76 (s, 1H, Ar-H), 7.73-7.70 (m, 3H, Ar -H), 7.54 (unresolvable singlet, 4H, Ar-H), 7.42-7.36 (m, 4H, Ar-H), 7.07 (d, J = 8.4 Hz, 2H, Ar-H), 5.39 (s, 2H, Ar-H), 1.25 (s, 1H, NH proton); **^{13}C-NMR** (100 MHz, DMSO-d_6) δ: 192.59, 152.24, 140.61, 134.63, 132.47, 131.89, 131.71, 130.97, 130.62, 129.29, 128.63, 123.62, 120.79, 115.22, 40.98; ESI-HRMS: *m/z* Calcd for Chemical Formula: $C_{30}H_{21}Br_2N_4OS_2$: 674.9515 $[M+H]^+$ found: 674.9547.

2-((5-(2-(Phenylimino)-4-(p-tolyl)thiazol-3(2*H*)-yl)-1*H*-benzo[*d*]imidazol-2-yl)thio)-1-(p-tolyl)ethan-1-one (4e):.

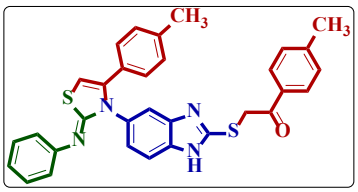

White solid: yield: 85%, mp: 221-223 °C; FT-IR (KBr, cm^{-1}): 3388 (NH), 1676 (C=O), 1602 (C=N); **^{1}H NMR** (400 MHz, DMSO-d_6 δ ppm): 7.99 (d, J = 8.0 Hz, 2H, Ar-H), 7.64 – 7.59 (m, 5H, Ar-H), 7.53 (d, J = 7.6 Hz, 2H, Ar-H), 7.42-7.40 (m, 3H, Ar-H), 7.26 (s, 1H, imidazole proton), 7.11-7.06 (m, 5H, Ar-H), 5.2 (s, 2H, S-CH_2- protons), 2.42 (s, 3H, aliphatic), 2.24 (s, 3H Aliphatic); **^{13}C-NMR** (100 MHz, DMSO) δ: 192.61, 152.61, 145.17, 142.07, 139.77, 134.59, 132.98, 131.00, 130.62, 129.93, 129.57, 129.43, 129.29,

129.13, 126.35, 115.21, 110.35, 104.79, 41.41, 21.75, 21.22; ESI-HRMS: *m/z* Calcd for Chemical Formula: $C_{32}H_{27}N_4OS_2$: 547.1618 $[M+H]^+$ found: 547.1658.

1-(4-Methoxyphenyl)-2-((5-(4-(4-methoxyphenyl)-2-(phenylimino)thiazol-3(2*H*)-yl)-1*H*-benzo[*d*]imidazol-2-yl)thio)ethan-1-one (4f):

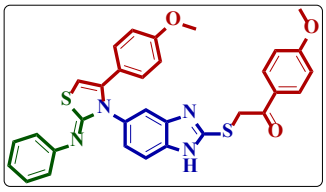

White solid: yield: 90%, mp: 206-208 °C; FT-IR (KBr, cm^{-1}): 3237 (NH), 1662 (C=O), 1597 (C=N); **^{1}H NMR** (400 MHz, DMSO-d_6 δ ppm): 8.26 (d, *J* = 8.8 Hz, 2H), 8.04 (s, 1H, Ar-H), 7.86 (s, 1H, Ar-H), 7.84 (s, 1H, Ar-H), 7.576– 7.54 (m, 4H, Ar-H), 7.34 (dd, *J* = 20.4, 7.2 Hz, 2H, Ar-H), 7.10 (d, *J* = 8.8 Hz, 1H, Ar-H), 6.90 (s, 1H, imidazole proton), 6.79 – 6.75 (m, 2H, Ar-H), 5.52 (s, 2H, S-CH2-protons), 3.90 (s, 3H, aliphatic), 3.77 (s, 3H, aliphatic); (100 MHz, DMSO-d_6) δ: 191.48, 164.29, 160.43, 152.68, 141.93, 134.66, 131.44, 131.22, 130.98, 130.63, 129.31, 128.35, 121.36, 114.64, 114.29, 110.35, 56.22, 55.72, 41.11; ESI-HRMS: *m/z* Calcd for Chemical Formula: $C_{32}H_{27}N_4O_3S_2$: 579.1516 $[M+H]^+$ found: 579.1554.

1-(2,4-Difluorophenyl)-2-((5-(4-(2,4-difluorophenyl)-2-(phenylimino)thiazol-3(2*H*)-yl)-1*H*-benzo[*d*]imidazol-2-yl)thio)ethan-1-one. 4g

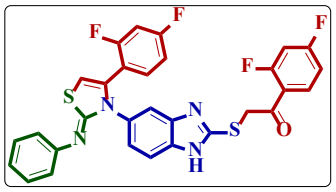

White solid: yield: 89%, mp: 201-203 °C; FT-IR (KBr, cm^{-1}): 3263 (NH), 1687 (C=O), 1608 (C=N); **^{1}H NMR** (400 MHz, DMSO-d_6 δ ppm): 10.50 (s, 1H, Ar-H), 10.30 (s, 1H, Ar-H), 8.07 (d, *J* = 6.8 Hz, 2H, Ar-H), 7.59 (s, 1H, imidazole proton), 7.59-7.52(m, 4H, Ar-H), 7.42 (dd, *J* = 8.8, 2.0 Hz, 1H, Ar-H), 7.36-7.31 (m, 5H, Ar-H), 7.13 (t, *J* = 7.4 Hz, 1H, Ar-H), 5.21 (s, 2H, S-CH_2-protons); **^{13}C-NMR** (100 MHz, DMSO-d_6) δ: 189.09, 179.98, 151.31, 150.26, 139.86, 137.32, 137.04, 133.49, 130.38, 129.75, 128.85, 126.39, 124.87, 123.80, 123.09, 121.53, 113.42, 112.92, 107.31, 105.88, 44.38; ESI-HRMS: *m/z* Calcd for Chemical Formula: $C_{30}H_{19}F_4N_4OS_2$: 591.0928 $[M+H]^+$ found: 591.0958.

1-(3,4-Dichlorophenyl)-2-((5-(4-(3,4-dichlorophenyl)-2-(phenylimino)thiazol-3(2*H*)-yl)-1*H*-benzo[*d*]imidazol-2-yl)thio)ethan-1-one. 4h

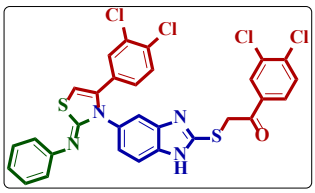

White solid: yield: 88%, mp: 198-200 °C; FT-IR (KBr, cm^{-1}): 3207 (NH), 1691 (C=O), 1581 (C=N); **^{1}H NMR** (400 MHz, DMSO-d_6 δ ppm): 10.36 (s, 1H, Ar-H), 10.19 (s, 1H, Ar-H), 8.03 (s, 1H, Ar-H), 8.00 (s, 1H, Ar-H), 7.80 (d, J = 2.0 Hz, 1H, Ar-H), 7.66 (d, J = 2.4 Hz, 1H, Ar-H), 7.64 (d, J = 2.4 Hz, 1H, Ar-H), 7.56-7.53 (m,3H, Ar-H), 7.46 – 7.32 (m, 5H, Ar-H), 7.13 (t, J = 7.4 Hz, 1H, Ar-H), 5.15 (s, 2H, S-CH2 protons); **^{13}C-NMR** (100 MHz, DMSO-d_6) δ: 194.23, 180.00, 152.56, 150.88, 149.68, 139.89, 137.87, 137.47, 137.06, 135.36, 132.49, 132.20, 130.95, 130.72, 130.38, 129.75, 128.85, 128.10, 128.00, 126.40, 123.81, 123.07, 42.80; ESI-HRMS: *m/z* Calcd for Chemical Formula: $C_{30}H_{19}Cl_4N_4OS_2$: 654.9749 $[M+H]^+$ found: 654.9761.

1-(4-Nitrophenyl)-2-((5-(4-(4-nitrophenyl)-2-(phenylimino)thiazol-3(2H)-yl)-1*H*-benzo[d]imidazol-2-yl)thio)ethan-1-one. 4i

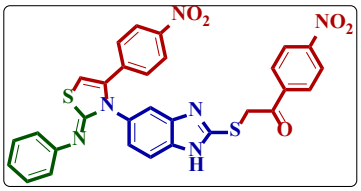

Brown solid: yield: 91%, mp: 218-220 °C; FT-IR (KBr, cm^{-1}): 3390 (NH), 1687 (C=O), 1601 (C=N); **^{1}H NMR** (400 MHz, DMSO-d_6 δ ppm): δ 8.42 (d, J = 8.8 Hz, 2H, Ar-H), 8.31 (d, J = 8.8 Hz, 2H, Ar-H), 8.17 (d, J = 8.8 Hz, 2H), 7.66 (dd, J = 8.6, 5.0 Hz, 2H, Ar-H), 7.62 (s, 1H, Ar-H), 7.59 (s, 1H, Ar-H), 7.48 (d, J = 8.8 Hz, 2H), 7.43-7.34 (m, 4H, Ar-H), 7.21 (s, 1H, Ar-H), 7.14 (d, J = 8.8 Hz, 1H, Ar-H), 5.23 (s, 2H, S-CH_2- protons): **^{13}C-NMR** δ_C (100 MHz, $CDCl_3$+DMSO-d_6) δ: 192.80, 150.73, 147.96, 140.43, 131.28, 130.76, 130.54, 130.40, 129.69, 129.24, 124.43, 123.92, 120.18, 115.22, 41.00; ESI-HRMS: *m/z* Calcd for Chemical Formula: $C_{30}H_{21}N_6O_5S_2$: 609.1007 $[M+H]^+$ found: 609.1047.

1-([1,1'-Biphenyl]-4-yl)-2-((5-(4-([1,1'-biphenyl]-4-yl)-2-(phenylimino)thiazol-3(2*H*)-yl)-1*H*-benzo[d]imidazol-2-yl)thio)ethan-1-one. 4j

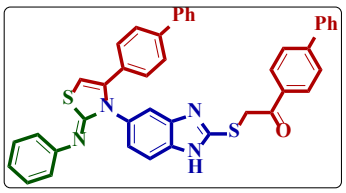

White solid: yield: 90%, mp: 242-244 °C; FT-IR (KBr, cm^{-1}): 3374 (NH), 1669 (C=O), 1600 (C=N); **^{1}H NMR** (400 MHz, DMSO-d_6 δ ppm): 12.34 (s, 1H, NH proton), 9.58 (s, 1H, Ar-H), 8.12 (d, J = 8.4 Hz, 2H, Ar-H), 8.01 (s, 1H, Ar-H), 7.75 (d, J = 8.8 Hz, 2H), 7.67-7.60 (m, 5H, Ar-H), 7.50 – 7.44 (m, 6H, Ar-H), 7.28-7.24 (m, 5H, Ar-H), 7.09 – 7.05 (m, 3H, Ar-H), 6.90 (d, J = 7.2 Hz, 1H, Ar-H), 6.26 (s, 1H, imidazole proton), 4.98 (s, 2H, Ar-H); **^{13}C-NMR** δ_C (100 MHz, DMSO-d_6) δ: 192.70, 152.51, 139.17, 134.56, 134.24, 133.50, 131.95, 131.76, 131.20, 130.84, 130.68, 129.60, 129.46, 128.95, 128.88, 128.29,

123.76, 121.68, 120.55, 119.41, 105.40, 43.11: ESI-HRMS: *m/z* Calcd for Chemical Formula: $C_{42}H_{31}N_4OS_2$: 671.1931 $[M+H]^+$found: 671.1930

2-((5-(2-((4-Fluorophenyl)imino)-4-phenylthiazol-3(2*H*)-yl)-1*H*-benzo[*d*]imidazol-2-yl)thio)-1-phenylethan-1-one. 4k

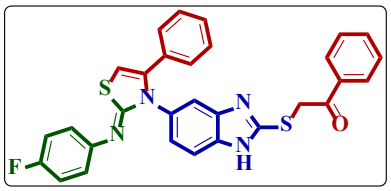

White solid: yield: 88%, mp: 205-207 °C; FT-IR (KBr, cm^{-1}): 3384 (NH), 1680 (C=O), 1595 (C=N); **^{1}H-NMR** (400 MHz, DMSO-d_6 δ ppm): 10.21 (s, 1H, Ar-H), 8.18 – 8.07 (m, 4H, Ar-H), 8.08 (s, 1H, Ar-H), 7.62 (d, *J* = 8.0 Hz, 2H, Ar-H), 7.53 (d, *J*= 7.6 Hz, 2H, Ar-H), 7.48-7.44 (m, 4H, Ar-H), 7.35 (t, *J* = 8.0 Hz, 2H, Ar-H), 7.15 (t, *J*= 7.4 Hz, Ar-H), 7.02 (s, 1H, imidazole proton), 5.35 (s, 2H, S-CH_2-protons); **^{13}C-NMR** (100 MHz, DMSO-d_6) δ: 191.41, 180.16, 167.27, 164.75, 150.61, 139.74, 137.10, 133.70, 132.17, 132.08, 128.95, 125.05, 124.08, 121.80, 116.66, 116.44, 113.53, 107.88, 41.59; ESI-HRMS: *m/z* Calcd for Chemical Formula: $C_{30}H_{22}FN_4OS_2$: 537.1214 $[M+H]^+$ found: 537.1231.

1-(4-Fluorophenyl)-2-((5-(4-(4-fluorophenyl)-2-((4-fluorophenyl)imino)thiazol-3(2*H*)-yl)-1*H*-benzo[*d*]imidazol-2-yl)thio)ethan-1-one. 4l

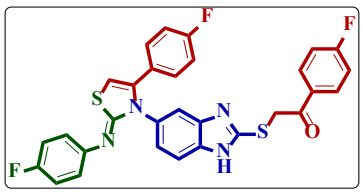

White solid: yield: 95%, mp: 216-218 °C; FT-IR (KBr, cm^{-1}): 3346 (NH), 1677 (C=O), 1594 (C=N); **^{1}H NMR** (400 MHz, $CDCl_3$+DMSO-d_6 δ ppm): 8.27-8.25 (m, 2H, Ar-H), 8.02 (s, 1H, Ar-H), 7.78 (d, *J* = 8.8 Hz, 1H), 7.65 (d, *J* = 8.8 Hz, 1H), 7.58-7.54 (m, 2H, Ar-H), 7.49 (s, 1H, Ar-H), 7.31 (dd, *J* = 9.0, 4.6 Hz, 1H, Ar-H), 7.16 – 7.13 (m, 4H, Ar-H), 6.99-6.91 (m, 4H, Ar-H), 5.54 (s, 2H, S-CH_2- protons); **^{13}C-NMR** (100 MHz, $CDCl_3$+DMSO-d_6); 191.10, 167.32, 164.79, 164.34, 161.86, 152.27, 140.73, 135.61, 133.75, 132.03, 131.94, 131.66, 131.56, 130.62, 125.29, 121.41, 117.55, 117.32, 116.37, 116.15, 115.99, 115.77, 114.98, 109.64, 104.84, 41.79 ; ESI-HRMS: *m/z* Calcd for Chemical Formula: $C_{30}H_{20}F_3N_4OS_2$: 573.1022 $[M+H]^+$ found: 573.1049.

1-(4-Chlorophenyl)-2-((5-(4-(4-chlorophenyl)-2-((4-fluorophenyl)imino)thiazol-3(2*H*)-yl)-1*H*-benzo[*d*]imidazol-2-yl)thio)ethan-1-one. 4m

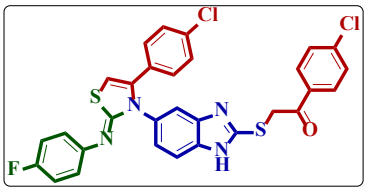

White solid: yield: 91%, mp: 208-210 °C; FT-IR (KBr, cm^{-1}): 3378 (NH), 1676 (C=O), 1588 (C=N); **^{1}H NMR** (400 MHz, DMSO-d_6 δ ppm): 8.09 (d, J = 8.8 Hz, 2H, Ar-H), 7.69-7.67 (m, 4H, Ar-H), 7.62 (d, J = 8.8 Hz, 2H, Ar-H), 7.50 (s, 1H, Ar-H), 7.42– 7.37 (m, 4H, Ar-H), 7.23 (d, J = 8.4 Hz, 2H, Ar-H), 7.18 (s, 1H, Ar-H), 7.12 (s, 1H, Ar-H), 5.17 (s, 2H, S-CH_2- protons); **^{13}C-NMR** (100 MHz, $CDCl_3$+DMSO-d_6) δ; 190.79, 164.54, 162.04, 152.25, 140.94, 140.57, 135.93, 133.09, 132.04, 131.27, 131.18, 130.91, 130.63, 129.96, 129.25, 128.90, 126.98, 122.21, 117.68, 117.45, 114.85, 109.73, 105.42, 43.41; ESI-HRMS: *m/z* Calcd for Chemical Formula: $C_{30}H_{20}Cl_2FN_4OS_2$: 605.0431 $[M+H]^+$ found: 605.0455.

1-(4-Bromophenyl)-2-((5-(4-(4-bromophenyl)-2-((4-fluorophenyl)imino)thiazol-3(2*H*)-yl)-1*H*-benzo[*d*]imidazol-2-yl)thio)ethan-1-one. 4n

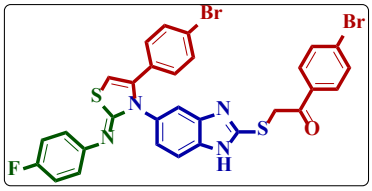

White solid: yield: 92%, mp: 210-212 °C; FT-IR (KBr, cm^{-1}): 3388 (NH), 1676 (C=O), 1620 (C=N); **^{1}H NMR** (400 MHz, $CDCl_3$+DMSO-d_6 δ ppm): 8.17 (s, 1H, Ar-H), 8.00 (d, J = 8.8 Hz, 2H, Ar-H), 7.75 (d, J = 8.0 Hz, 2H, Ar-H), 7.60-7.58 (m, 3H, Ar-H), 7.47-7.45(m, 3H, Ar-H), 7.28 (t, J = 8.2 Hz, 2H), 7.18 (d, J = 8.4 Hz, 1H, Ar-H), 7.11 (d, J = 8.8 Hz, 2H, Ar-H), 6.99 (s, 1H, imidazole proton), 5.16 (s, 2H, S-CH_2-protons); **^{13}C-NMR** (100 MHz, $CDCl_3$+DMSO-d_6) δ; 192.03, 152.03, 140.42, 134.35, 132.31, 131.85, 131.70, 131.60, 131.44, 130.81, 128.80, 128.34, 123.75, 120.98, 117.58, 117.35, 115.02, 109.44, 104.79, 41.35; ESI-HRMS: *m/z* Calcd for Chemical Formula: $C_{30}H_{20}Br_2FN_4OS_2$; 692.9421 $[M+H]^+$ found: 692.9468.

2-((5-(2-((4-Fluorophenyl)imino)-4-(p-tolyl)thiazol-3(2*H*)-yl)-1*H*-benzo[*d*]imidazol-2-yl)thio)-1-(p-tolyl)ethan-1-one.4o

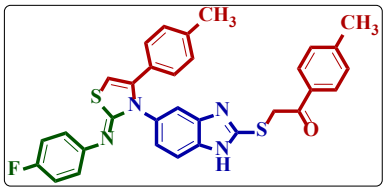

White solid: yield: 87%, mp: 234-236 °C; FT-IR (KBr, cm^{-1}): 3390 (NH), 1676 (C=O), 1602 (C=N); **^{1}H NMR** (400 MHz, DMSO-d_6 δ ppm): 7.98 (d, J = 8.4 Hz, 2H), 7.67 (dd, J = 7.8, 4.2 Hz, 2H), 7.62 (s, 1H, Ar-H), 7.60 (s, 1H, Ar-H), 7.52 (s,

1H, Ar-H), 7.41-7.37 (m, 4H, Ar-H), 7.20 (dd, *J* = 8.4, 2.0 Hz, 1H), 7.15-7.07 (m, 4H, Ar-H) 5.15 (s, 2H, S-CH_2-protons), 2.42 (s, 3H, Aliphatic), 2.25 (s, 3H, Aliphatic); **^{13}C-NMR** (100 MHz, DMSO-*d*$_6$) δ:192.78, 152.45, 145.06, 139.80, 133.11, 131.98, 131.89, 129.92, 129.62, 129.50, 129.10, 126.36, 120.56, 117.70, 117.47, 115.18, 40.89, 21.74, 21.23; ESI-HRMS: *m/z* Calcd for Chemical Formula: $C_{32}H_{26}FN_4OS_2$: 565.1524 $[M+H]^+$ found: 565.1565.

2-((5-(2-((4-Fluorophenyl)imino)-4-(4-methoxyphenyl)thiazol-3(2*H*)-yl)-1*H*-benzo[*d*]imidazol-2-yl)thio)-1-(4-methoxyphenyl)ethan-1-one. 4p

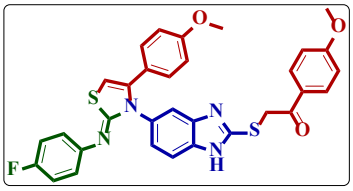

White solid: yield: 90%, mp: 228-230 °C; FT-IR (KBr, cm^{-1}): 3375 (NH), 1669 (C=O), 1598 (C=N);**^{1}H NMR** (400 MHz, DMSO-*d*$_6$ δ ppm): 8.06 (d, *J* = 8.8 Hz, 2H, Ar-H), 7.60 (d, *J* = 8.8 Hz, 1H), 7.48 (s, 1H, Ar-H), 7.38-7.34 (m, 2H, Ar-H), 7.19 – 7.13 (m, 4H, Ar-H), 7.11 (dd, *J* = 6.2, 3.0 Hz, 2H, Ar-H), 6.93 (s, 1H, Ar-H), 6.87 (d, *J* = 8.8 Hz, 2H, Ar-H), 6.82 (d, *J* = 8.8 Hz, 1H, Ar-H), 5.10 (s, 2H, S-CH_2-protons), 3.89 (s, 3H, OCH_3), 3.74 (s, 3H, OCH_3), 3.70 (s, 1H); **^{13}C-NMR** (100 MHz, DMSO-*d*$_6$) δ:191.80, 164.17, 160.40, 131.88, 131.38, 131.19, 128.55, 122.39, 121.44, 119.80, 117.62, 117.42, 114.59, 114.34, 56.17, 55.71, 41.18; ESI-HRMS: *m/z* Calcd for Chemical Formula: $C_{32}H_{26}FN_4O_3S_2$: 597.1422 $[M+H]^+$ found: 597.1463.

1-(2,4-Difluorophenyl)-2-((5-(4-(2,4-difluorophenyl)-2-((4-fluorophenyl)imino)thiazol-3(2*H*)-yl)-1*H*-benzo[*d*]imidazol-2-yl)thio)ethan-1-one. 4q

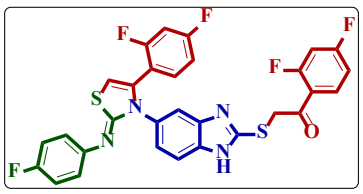

White solid: yield: 90%, mp: 206-208 °C; FT-IR (KBr, cm^{-1}): 3342 (NH), 1686 (C=O), 1608 (C=N); **^{1}H NMR** (400 MHz, DMSO-*d*$_6$ δ ppm): 10.56 (s, 1H, Ar-H), 8.10 – 8.06 (m, 2H, Ar-H), 7.60 – 7.55 (m, 4H, Ar-H), 7.48-7.42 (m, 3H, Ar-H), 7.30 – 7.26 (m, 3H, Ar-H), 7.16 (d, *J* = 8.8 Hz, 2H, Ar-H), 5.21 (s, 2H, S-CH_2-protons); **^{13}C-NMR** (100 MHz, DMSO-*d*$_6$) δ; 189.09, 180.39, 167.32, 164.91, 164.78, 164.06, 163.93, 161.49, 161.36, 160.76, 158.36, 150.33, 137.17, 136.11, 133.58, 133.51, 121.57, 115.61, 115.38, 113.47, 113.20, 112.99, 107.50, 106.15, 105.89, 105.62, 44.35; ESI-HRMS: *m/z* Calcd for Chemical Formula: $C_{30}H_{18}F_5N_4OS_2$: 609.0837 $[M+H]^+$ found: 609.0849

1-([1,1'-Biphenyl]-4-yl)-2-((5-(4-([1,1'-biphenyl]-4-yl)-2-((4-fluorophenyl)imino)thiazol-3(2H)-yl)-1H-benzo[d]imidazol-2-yl)thio)ethan-1-one. 4r

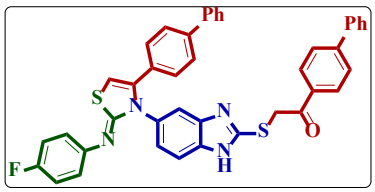

White solid: yield: 92%, mp: 225-227 °C; FT-IR (KBr, cm^{-1}): 3376 (NH), 1668 (C=O), 1621 (C=N); **^{1}H-NMR** (400 MHz, DMSO-d_6 δ ppm): 10.23 (s, 1H, Ar-H), 8.18 – 8.16 (m, 4H, Ar-H), 8.10 (s, 1H, Ar-H), 7.93 (d, *J* = 8.8 Hz, 2H, Ar-H), 7.80 (d, *J*= 7.2 Hz, 2H, Ar-H),7.63 (d, *J*=8.4 Hz, 2H, Ar-H), 7.55-7.52 (m, 5H, Ar-H), 7.48-7.44 (m, 5H, Ar-H), 7.35 (t, *J* = 8.0 Hz, 2H, Ar-H), 7.15 (t, *J*= 7.4 Hz, Ar-H), 7.03 (s, 1H, imidazole proton), 5.40 (s, 2H, S-CH_2-protons); **^{13}C-NMR** (100 MHz, DMSO-d_6) δ: 192.29, 180.16, 150.70, 145.94, 139.75, 139.10, 137.14, 134.06, 129.78, 129.63, 129.14, 128.95, 127.56, 125.05, 124.08, 121.81, 113.53, 107.85, 41.80; ESI-HRMS: *m/z* Calcd for Chemical Formula: $C_{42}H_{30}FN_4OS_2$: 689.184 $[M+H]^+$ found: 689.1868.

2-((5-(2-((4-Fluorophenyl)imino)-4-(4-nitrophenyl)thiazol-3(2*H*)-yl)-1*H*-benzo[*d*]imidazol-2-yl)thio)-1-(4-nitrophenyl)ethan-1-one. 4s

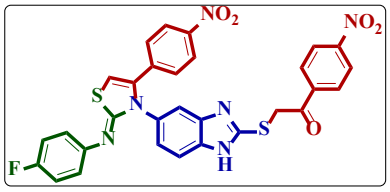

White solid: yield: 90%, mp: 216-218 °C; FT-IR (KBr, cm^{-1}): 3390 (NH), 1688 (C=O), 1600 (C=N), 1522 (NO_2), 1348 (NO_2); **^{1}H NMR** (400 MHz, DMSO-d_6 δ ppm): 8.42 (d, *J* = 8.8 Hz, 2H), 8.31 (d, *J* = 8.8 Hz, 2H), 8.13 (d, *J* = 9.2 Hz, 2H), 7.60-7.56 (m,4H, Ar-H), 7.52-7.45 (m, 5H, Ar-H), 7.21 (s, 1H, Ar-H), 7.12 (s, 1H, Ar-H), 5.22 (s, 2H, S-CH_2- protons); **^{13}C-NMR** (100 MHz, $CDCl_3$+DMSO-d_6) δ; 186.51, 164.60, 150.96, 137.31, 131.28, 131.03, 130.91, 130.76, 128.04, 124.07, 123.69, 123.56, 123.48, 122.79, 107.49; ESI-HRMS: *m/z* Calcd for Chemical Formula: $C_{30}H_{20}FN_6O_5S_2$: 627.0912 $[M+H]^+$ found: 627.0956.

4A.13. Spectra

^{1}H-NMR Spectrum of compound 4a in DMSO-d_6 (400 MHz):

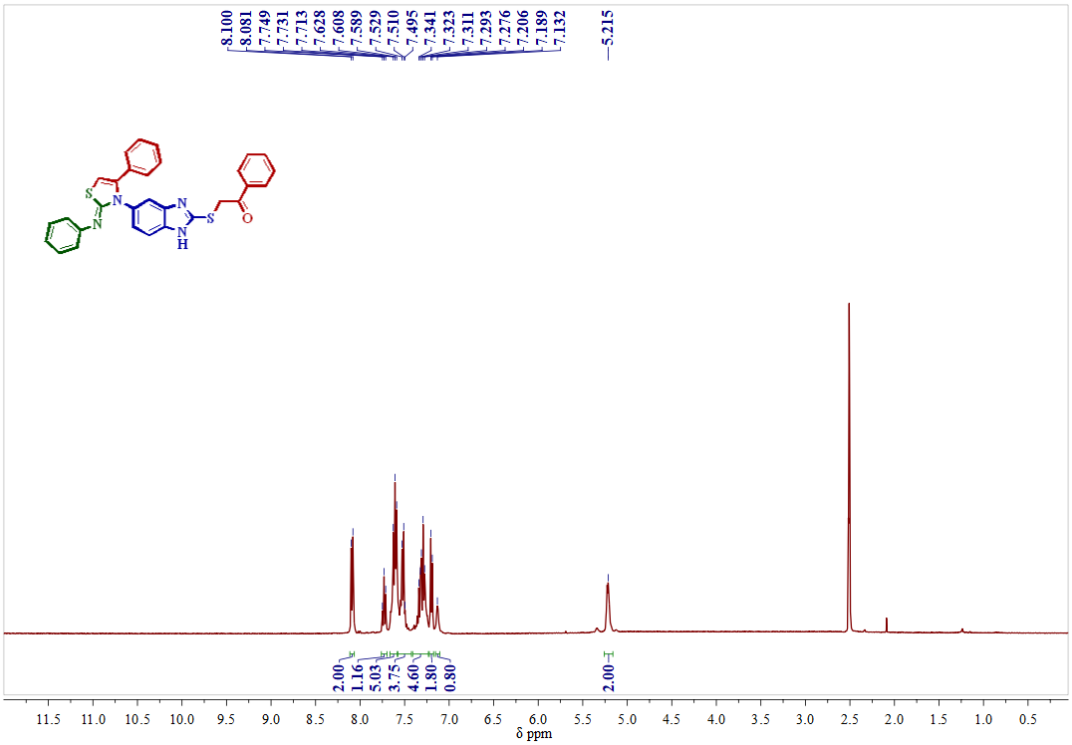

^{13}C-NMR Spectrum of compound 4a in DMSO-d_6 (100 MHz):

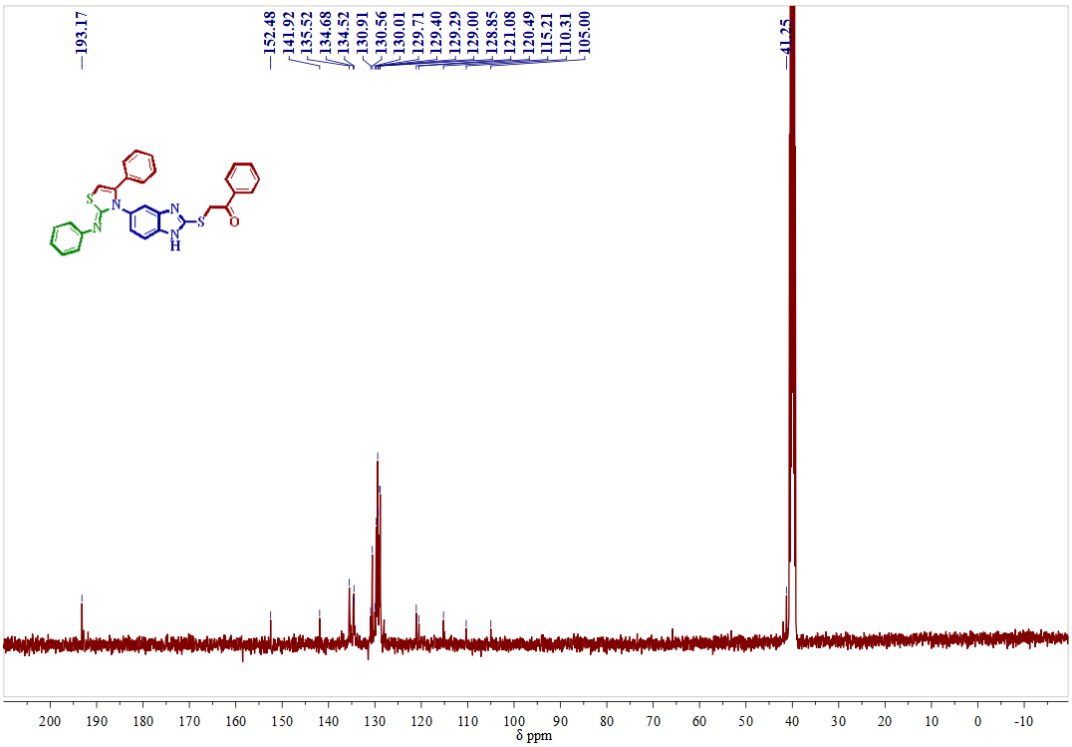

Mass spectrum of compound 4a

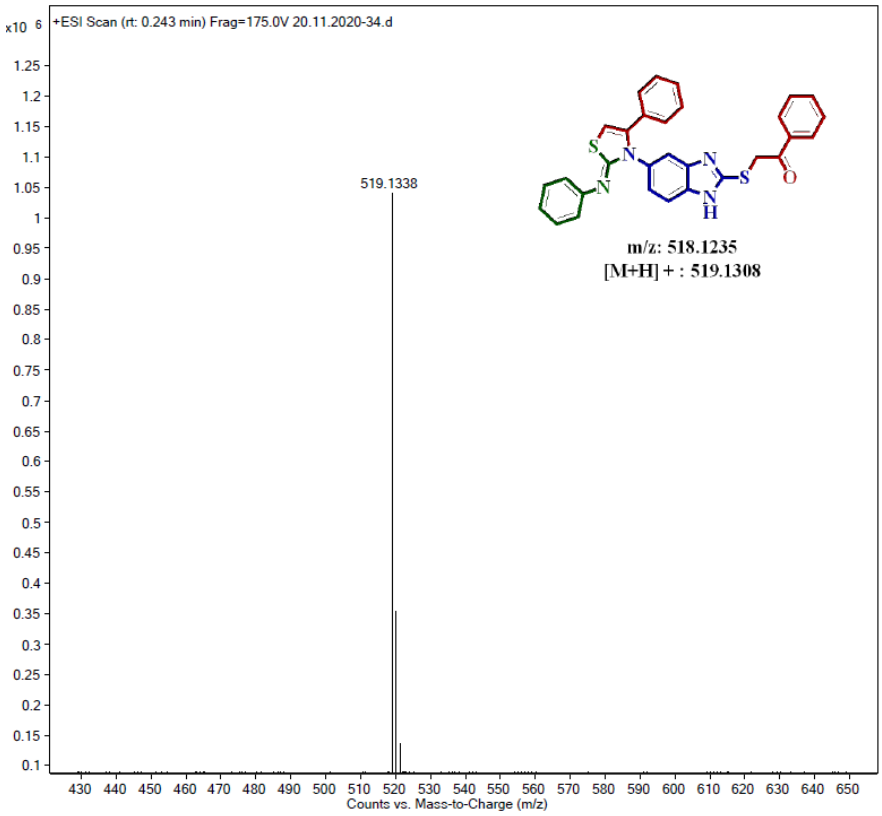

^{1}H-NMR Spectrum of compound 4b in DMSO-d_6 (400MHz):

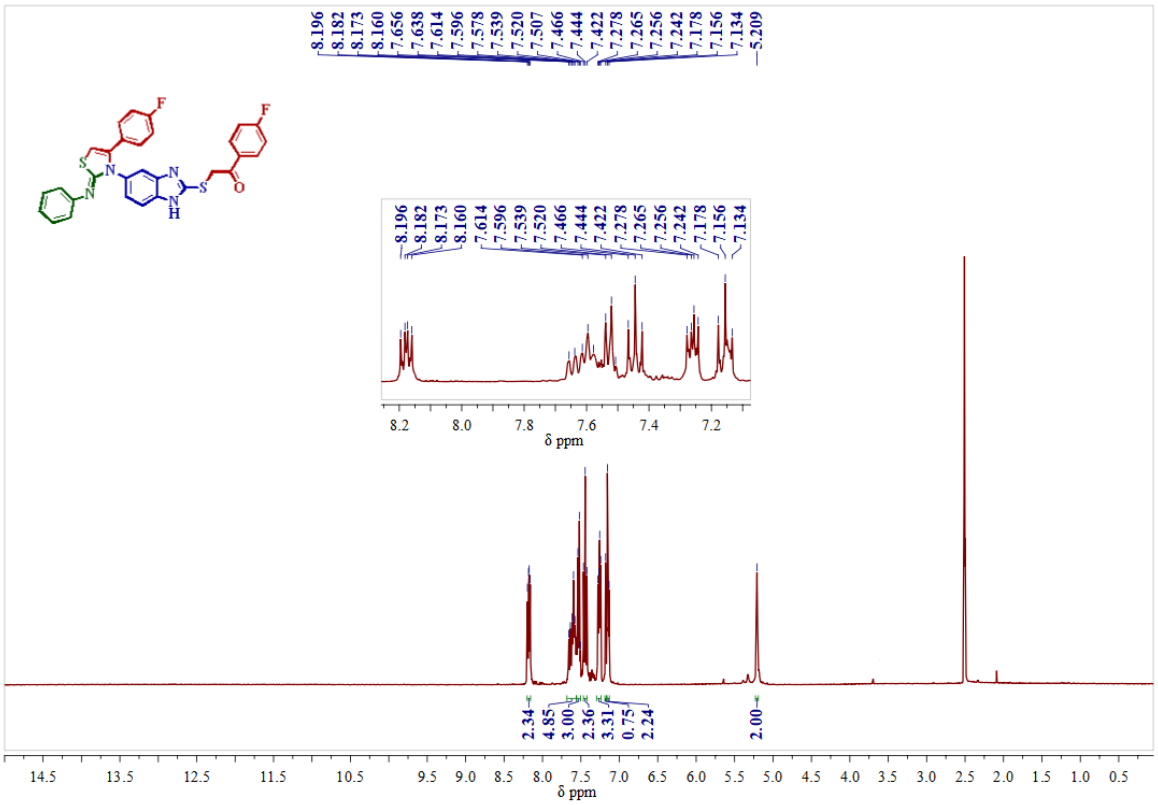

^{13}C-NMR Spectrum of compound 4b in DMSO-d_6 (100MHz):

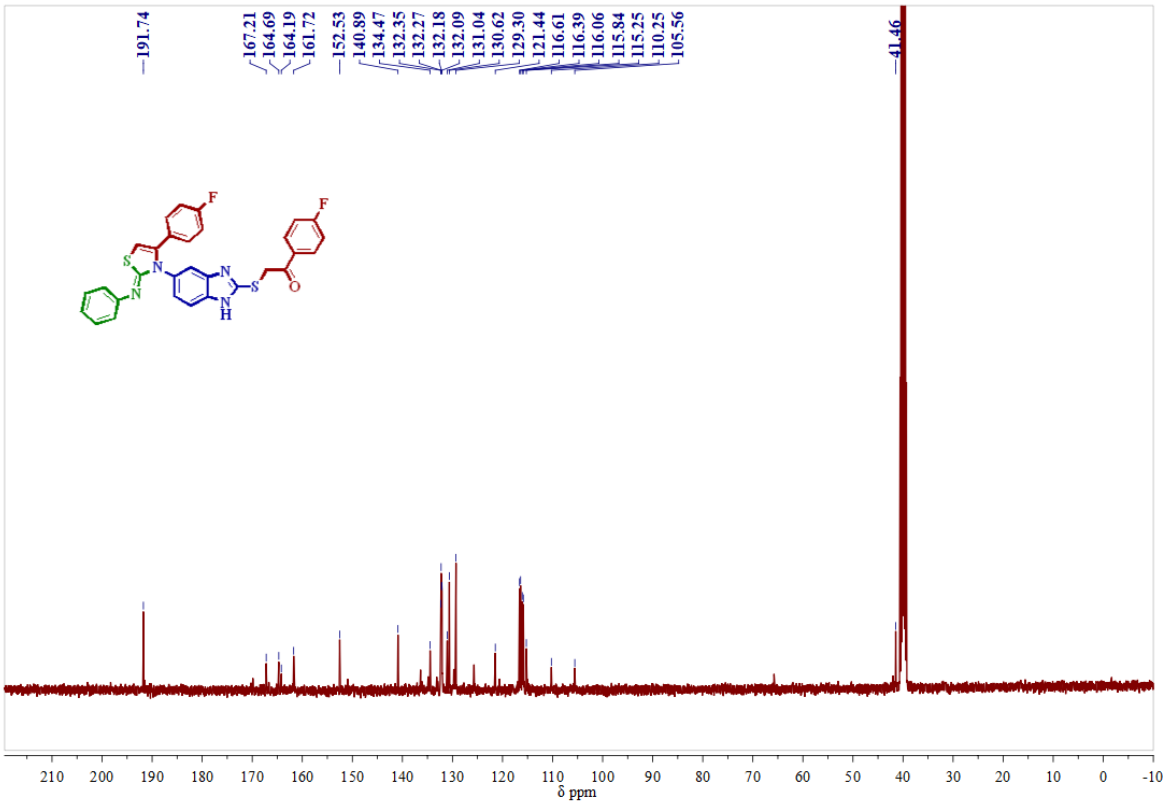

Mass spectrum of compound 4b

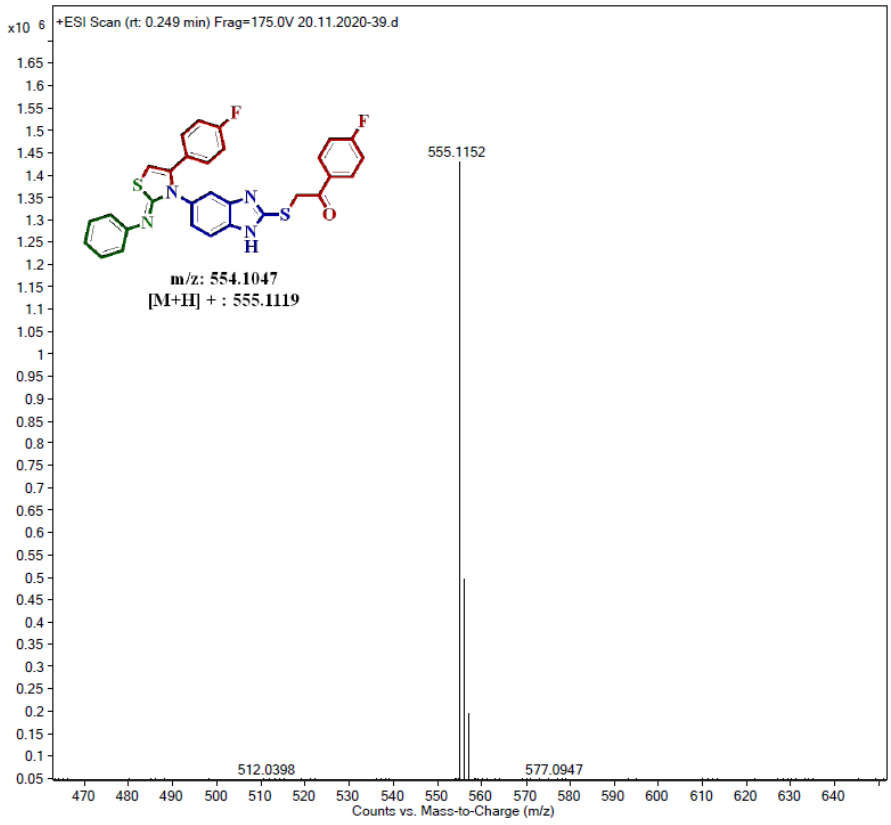

^{1}H-NMR Spectrum of compound 4c in DMSO-d_6 (400MHz):

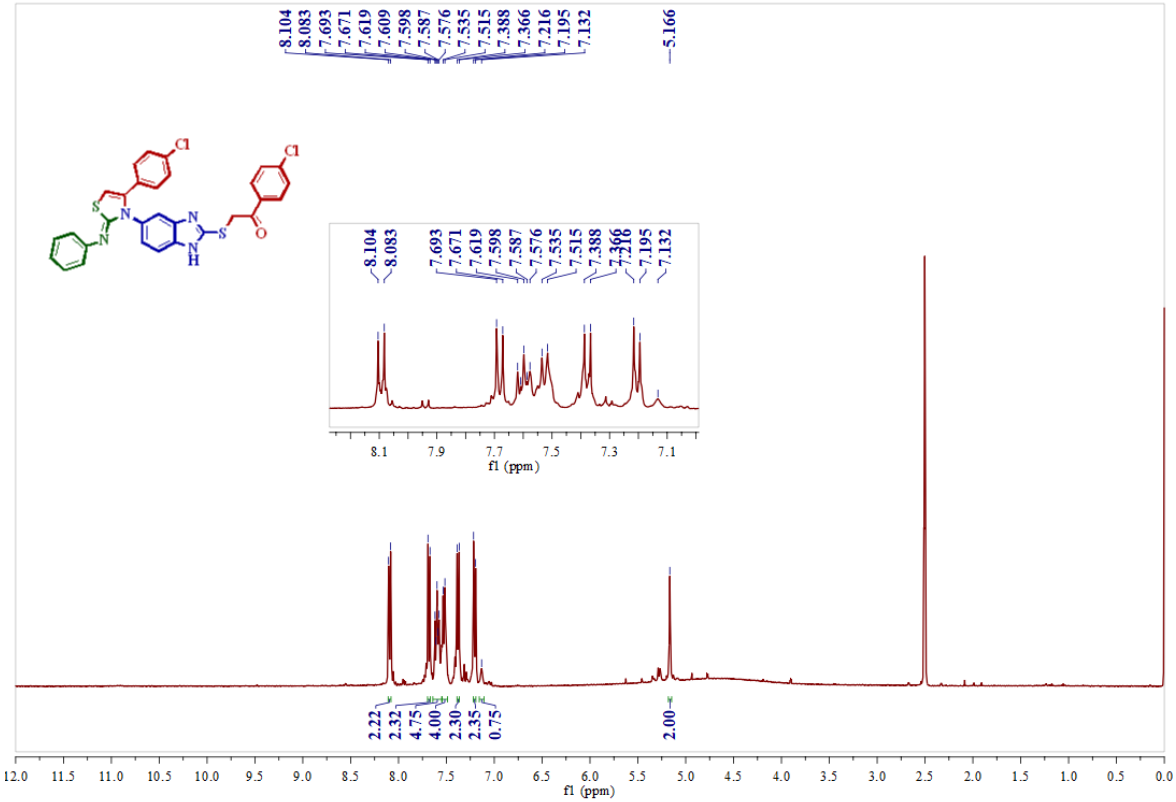

^{13}C-NMR Spectrum of compound 4c in $CDCl_3$-DMSO-d_6 (100 MHz):

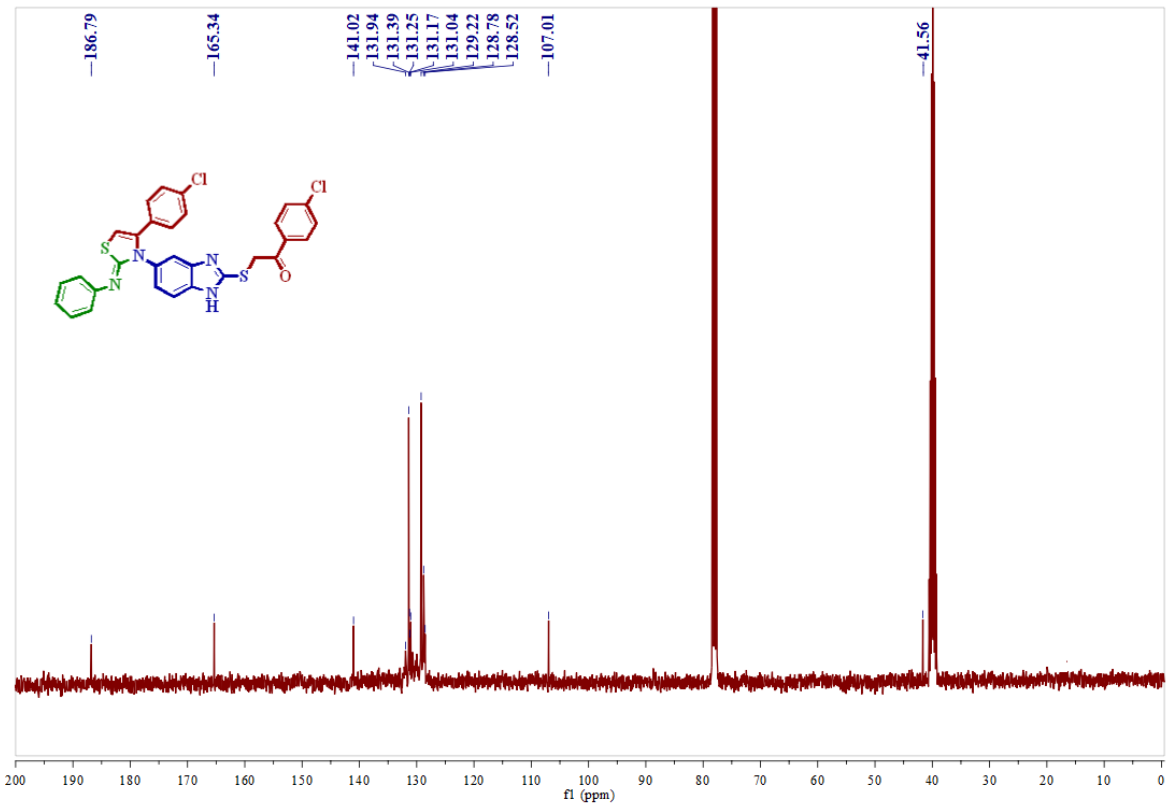

Mass spectrum of compound 4c

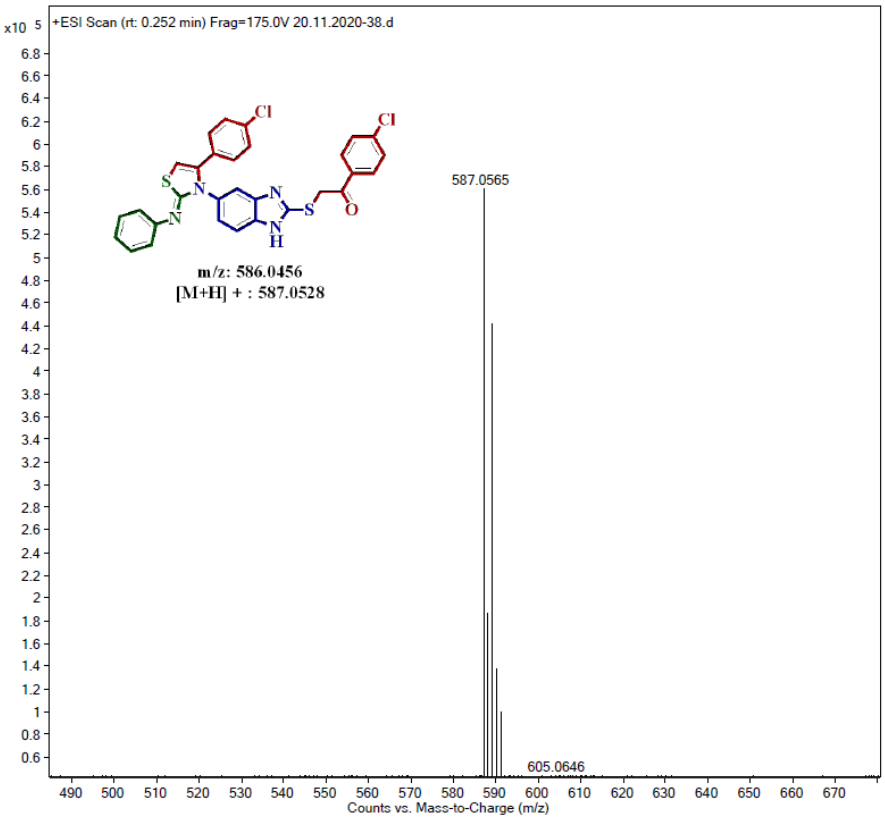

^{1}H-NMR Spectrum of compound 4d in $CDCl_3$-DMSO-d_6 (400MHz):

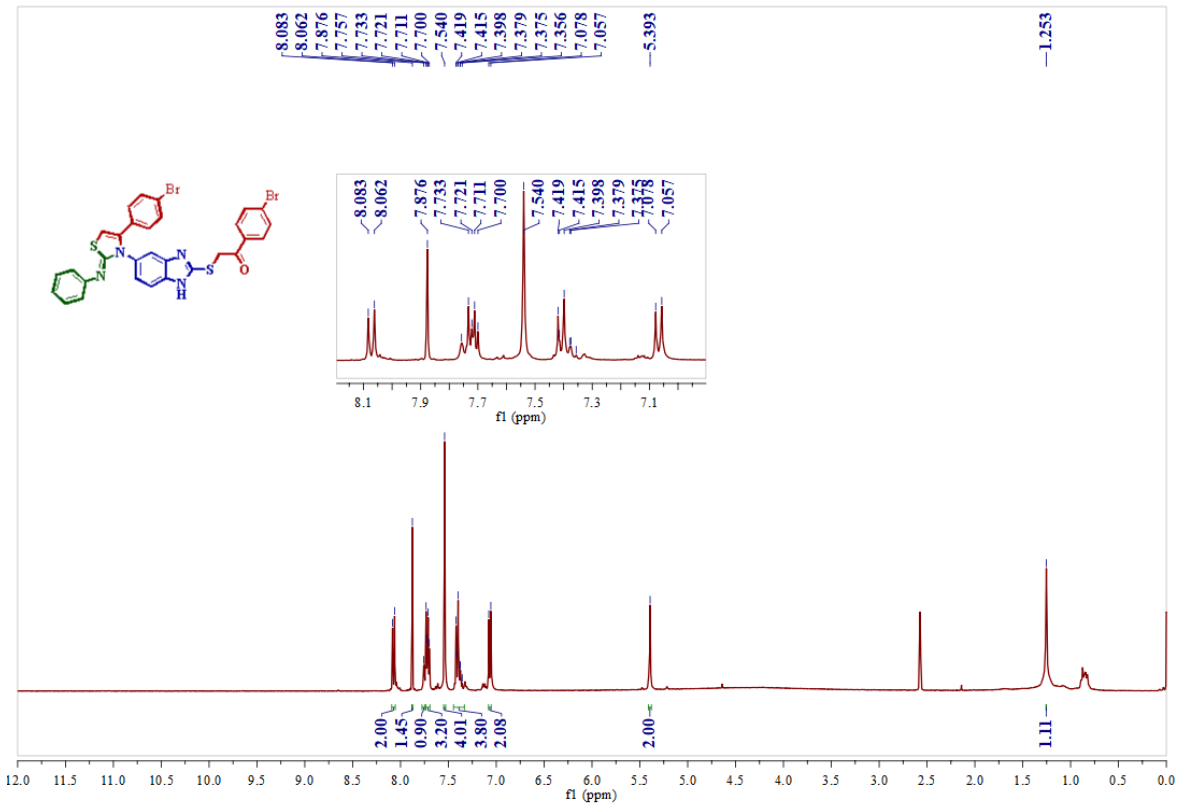

^{13}C-NMR Spectrum of compound 4d in DMSO-d_6 (100MHz):

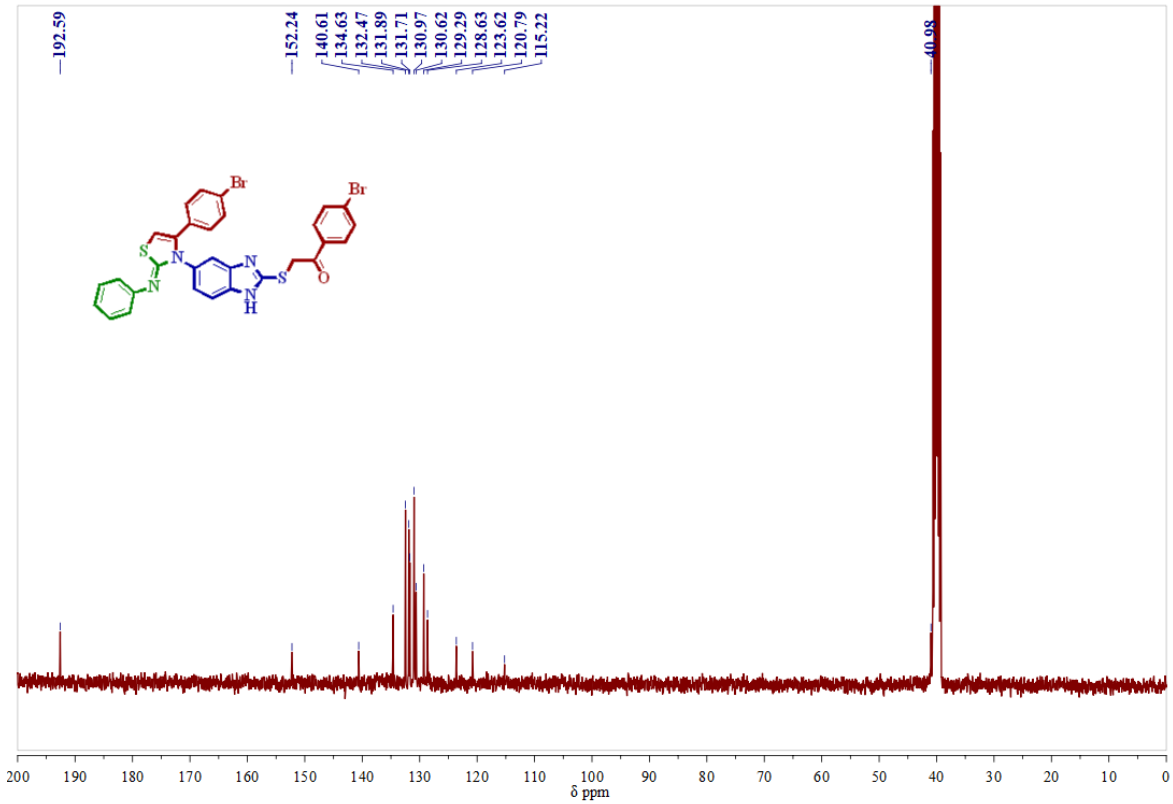

Mass spectrum of compound 4d

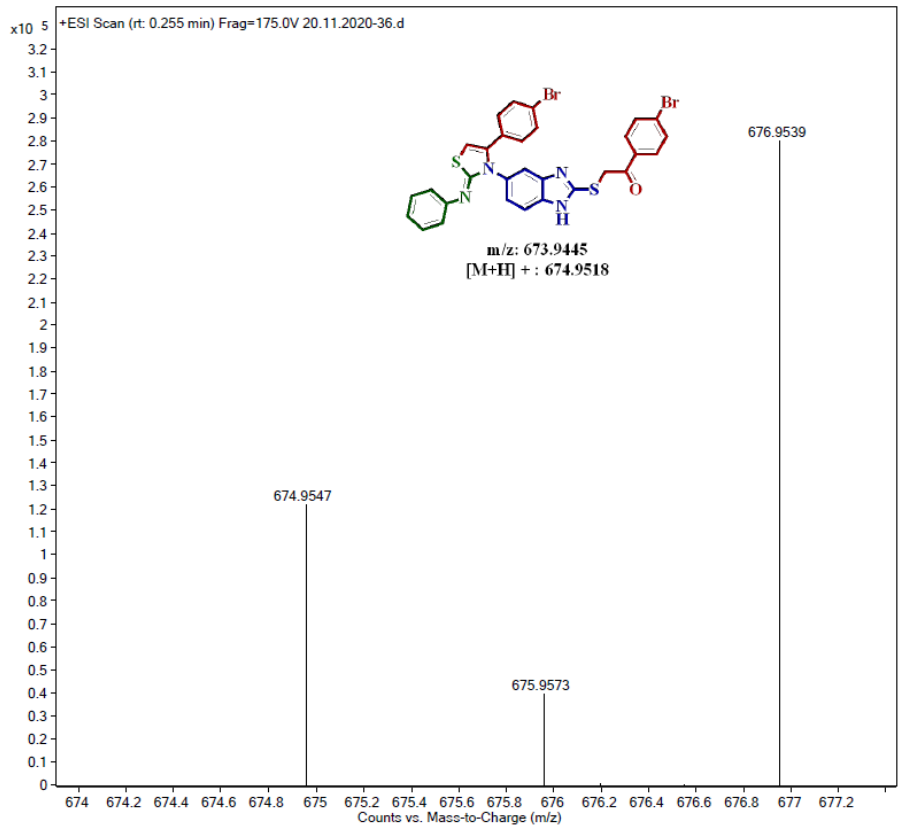

^{1}H-NMR Spectrum of compound 4e in DMSO-d_6 (400 MHz):

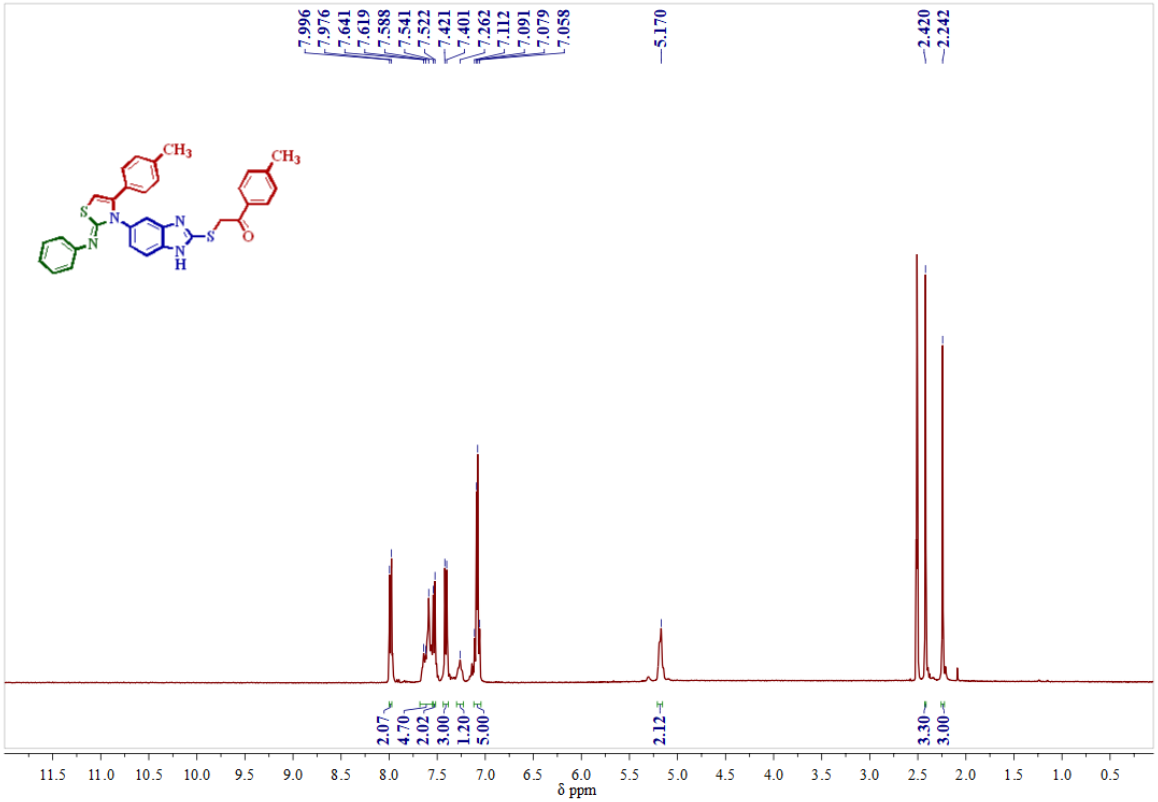

^{13}C-NMR Spectrum of compound 4e in DMSO-d_6 (100 MHz):

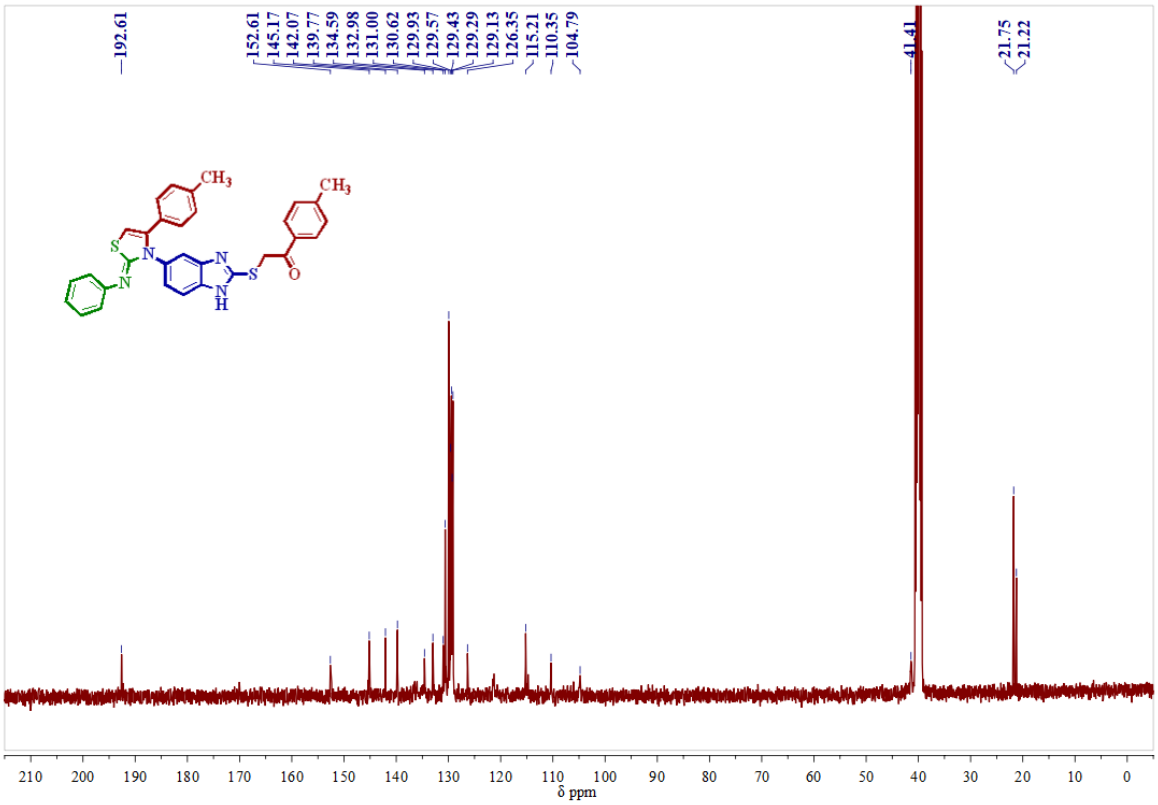

Mass spectrum of compound 4e

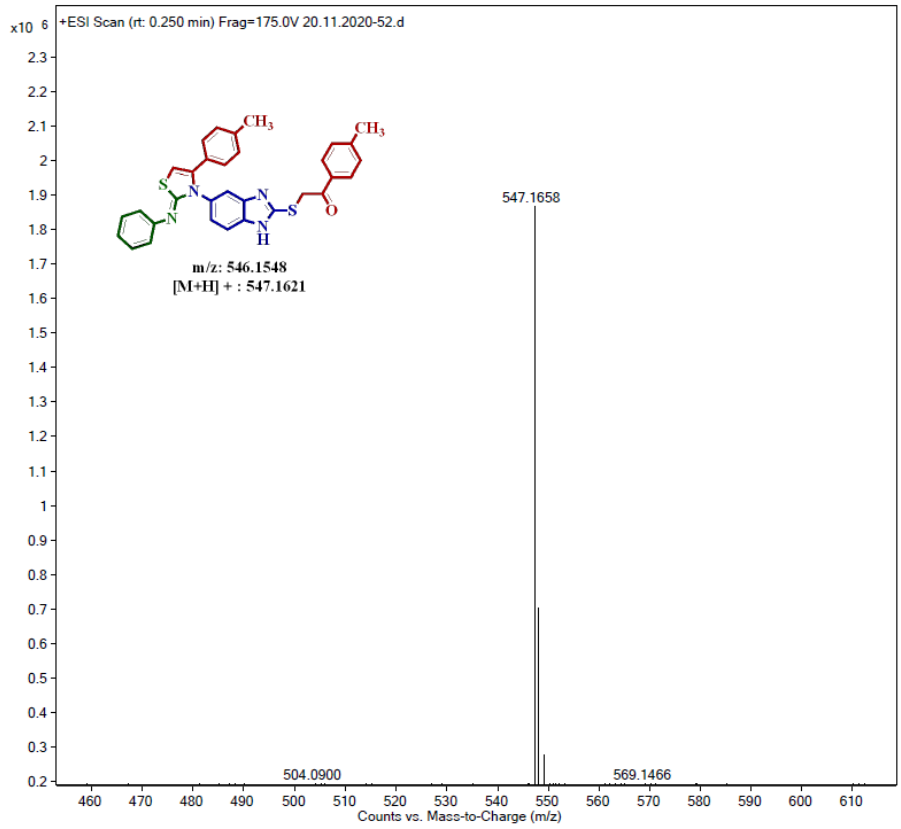

^{1}H-NMR Spectrum of compound 4f in DMSO-d_6 (400 MHz):

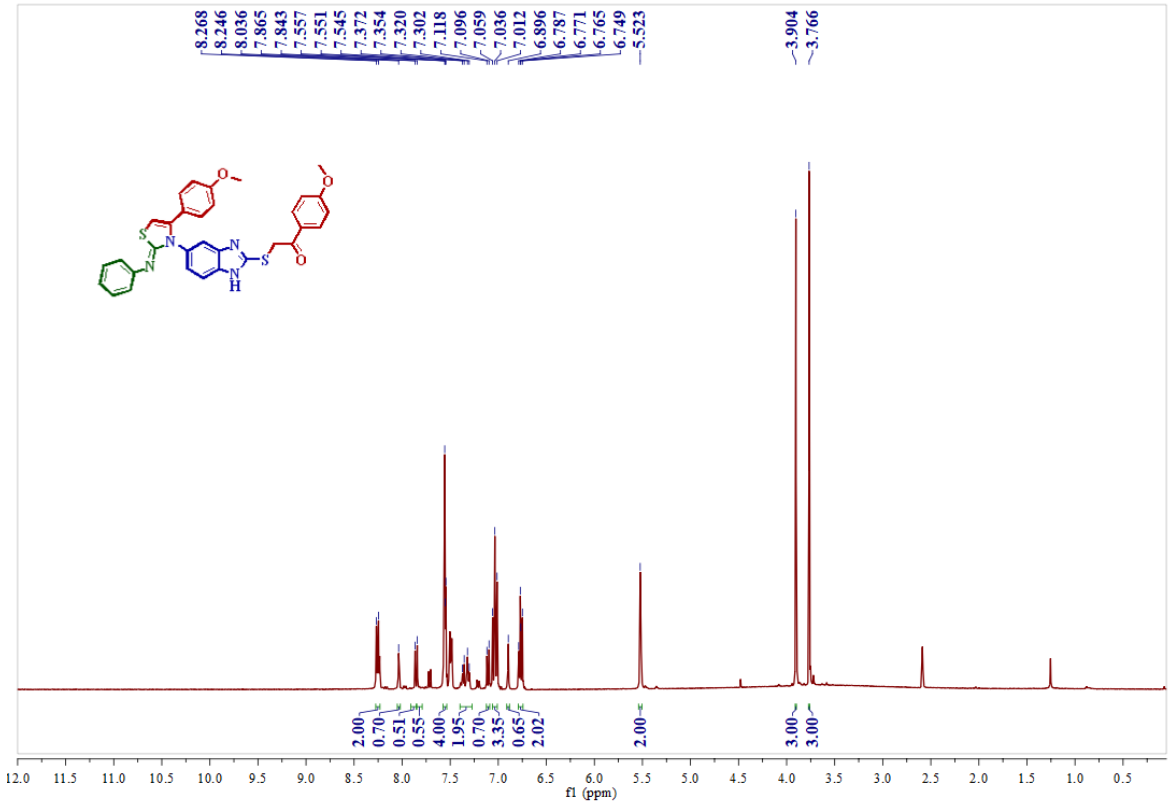

^{13}C-NMR Spectrum of compound 4f in DMSO-d_6 (100 MHz):

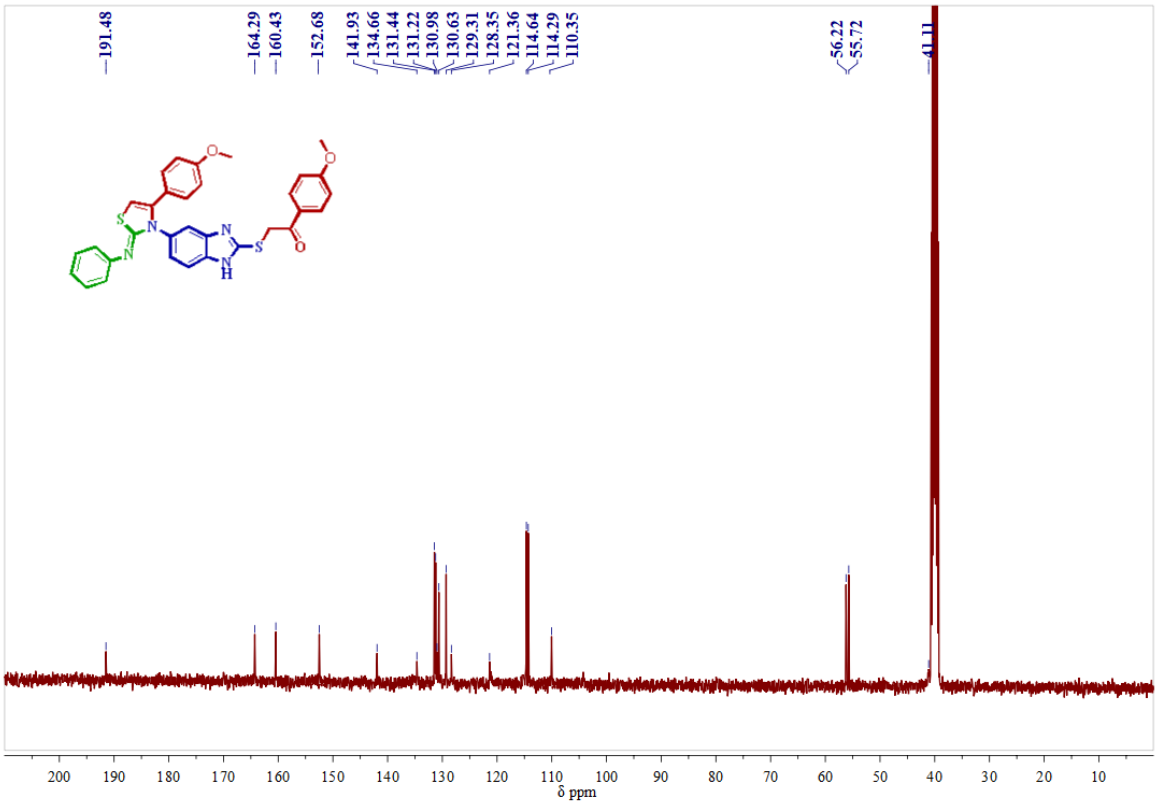

Mass spectrum of compound 4f

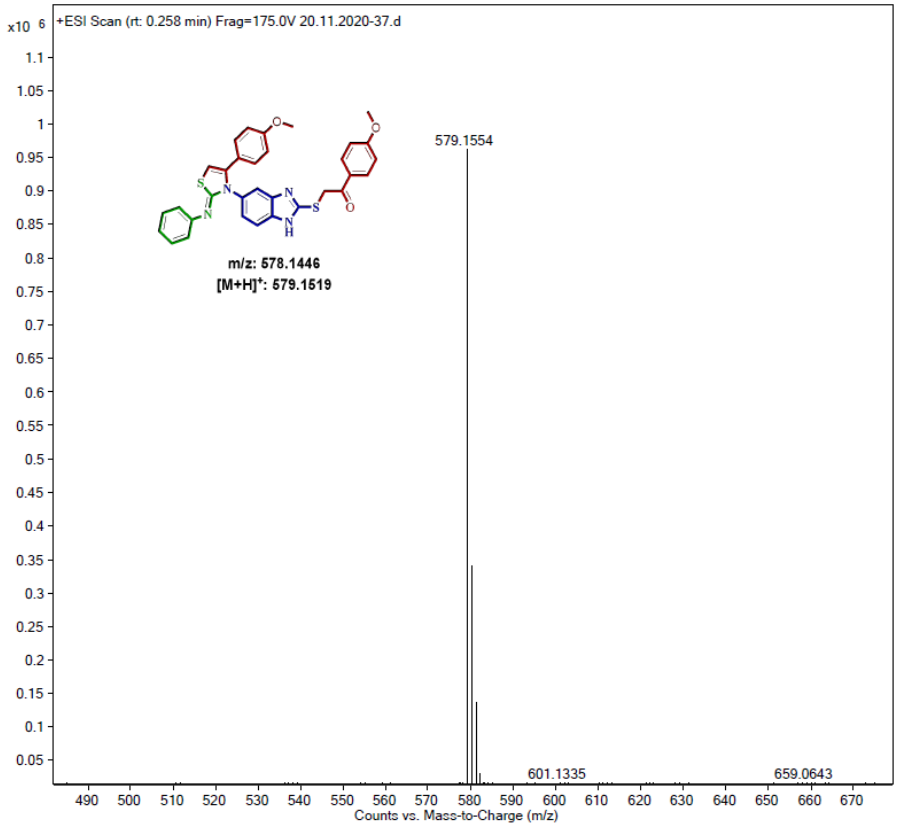

^{1}H-NMR Spectrum of compound 4g in DMSO-d_6 (400MHz):

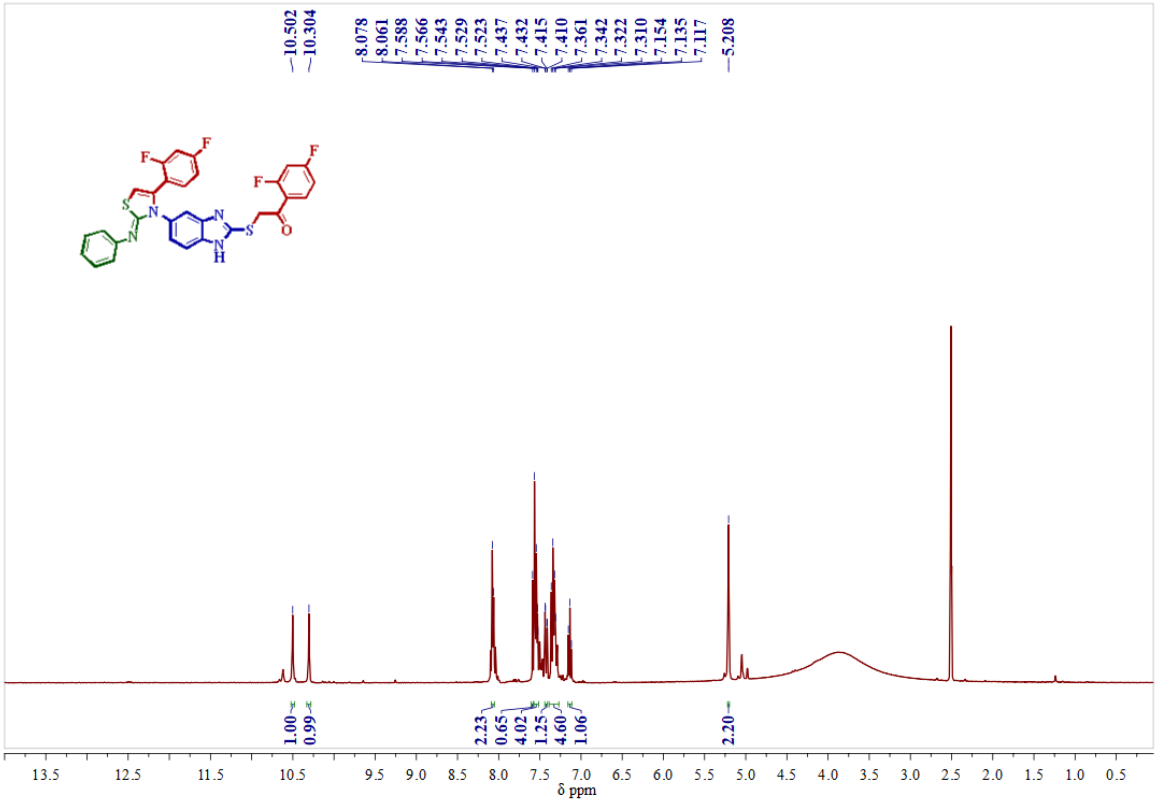

^{13}C-NMR Spectrum of compound 4g in DMSO-d_6 (100MHz):

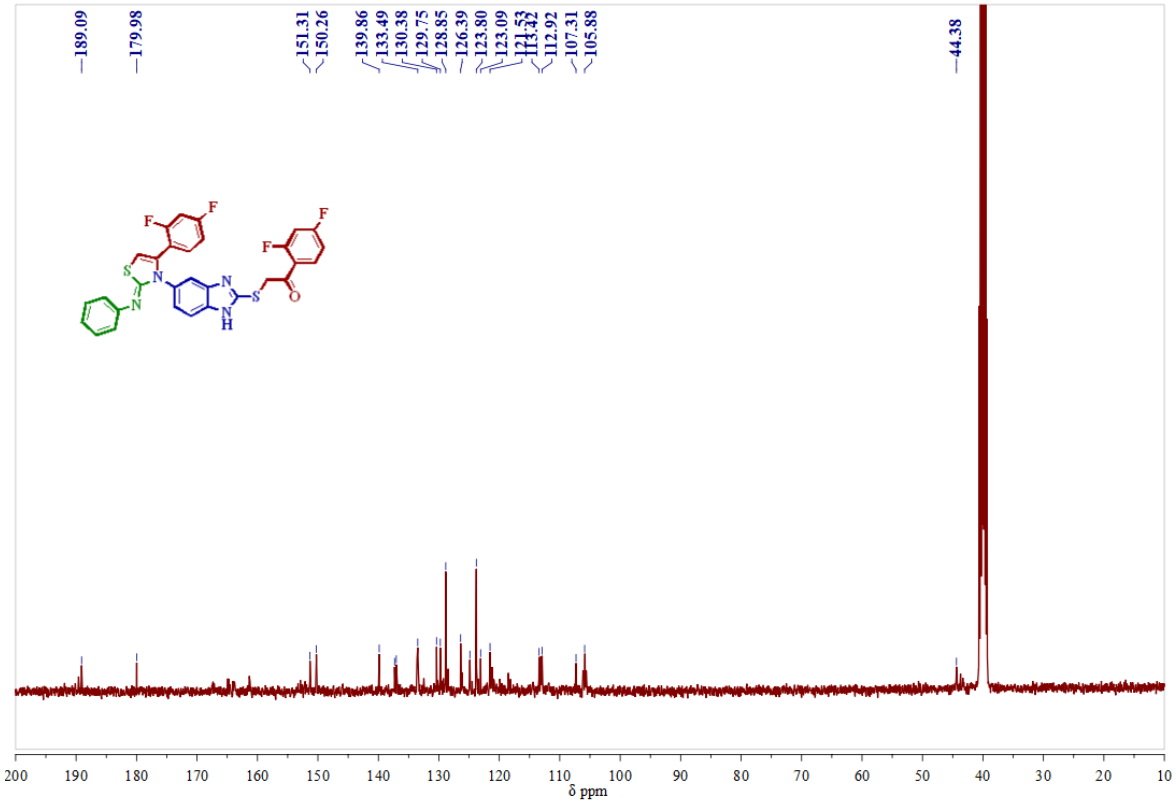

Mass spectrum of compound 4g

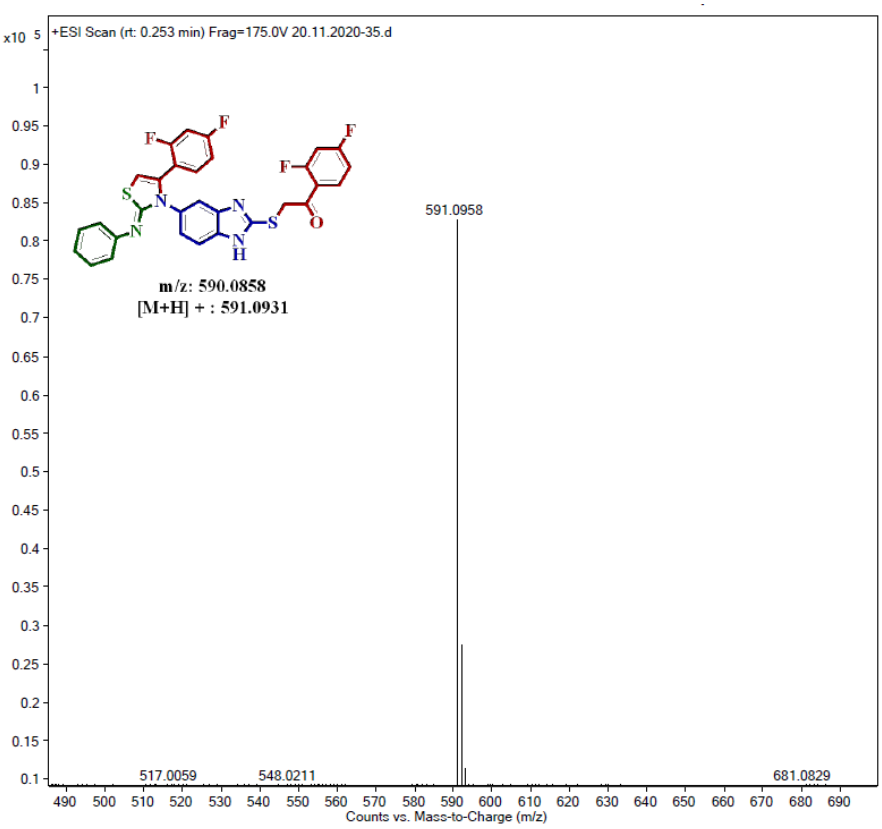

^{1}H-NMR Spectrum of compound 4h in DMSO-d_6 (400MHz):

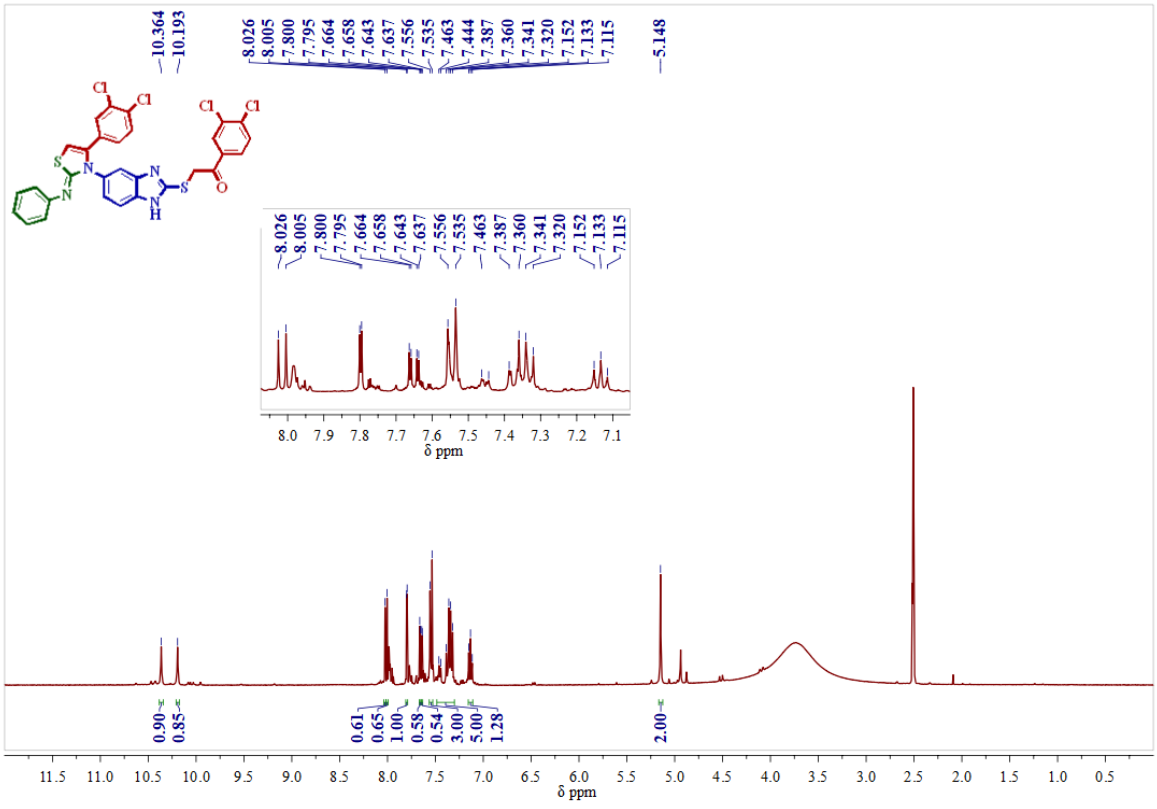

^{13}C-NMR Spectrum of compound 4h in DMSO-d_6 (100MHz):

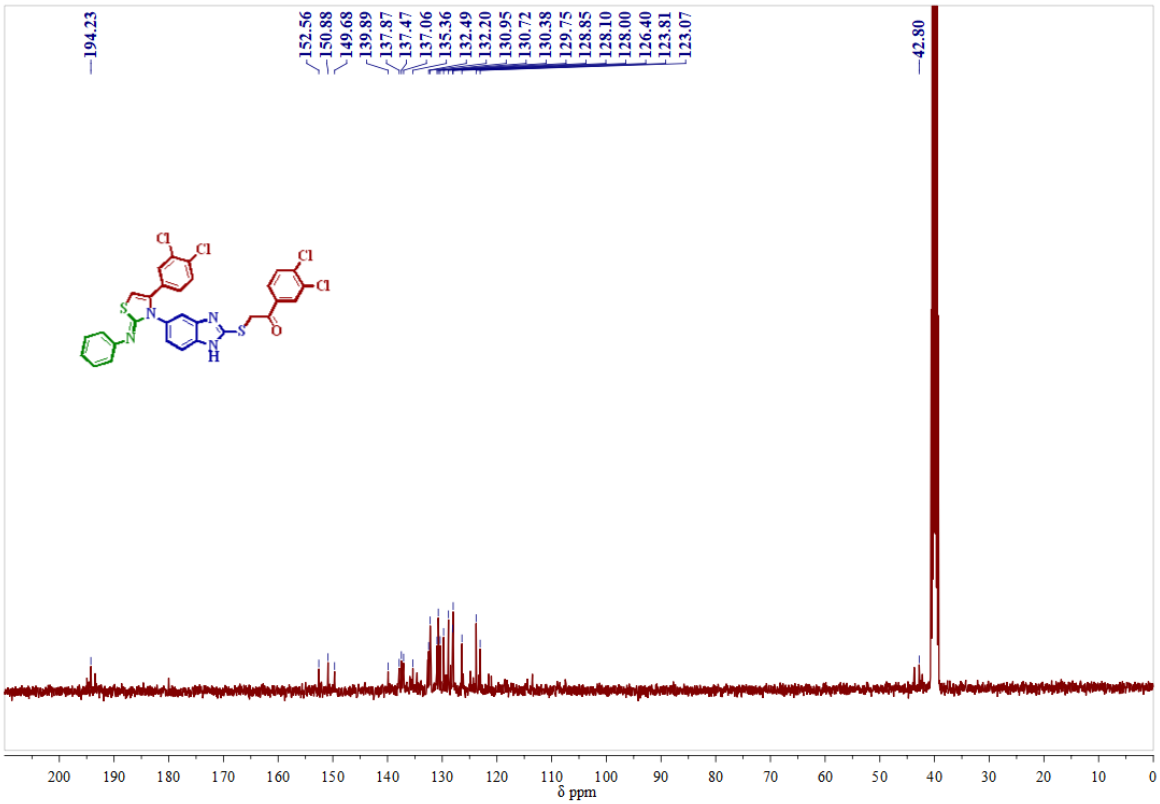

Mass spectrum of compound 4h

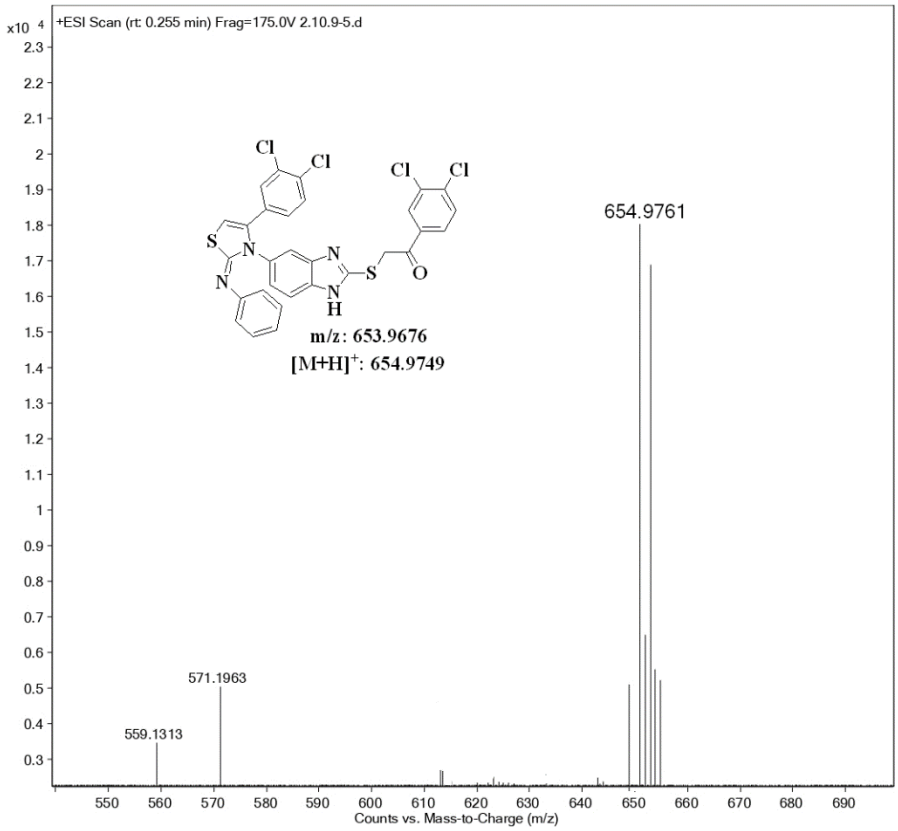

^{1}H-Spectrum of compound 4i in DMSO-d_6 (400MHz):

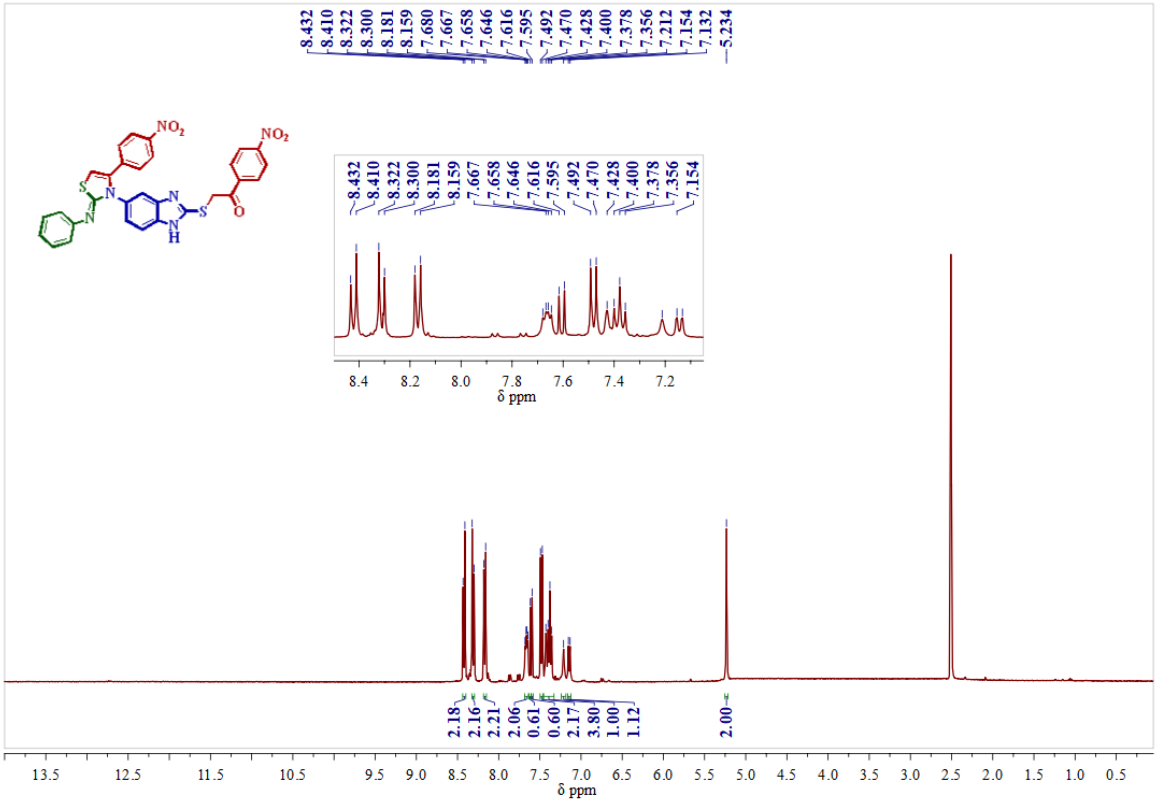

^{13}C-Spectrum of compound 4i in DMSO-d_6 (100MHz):

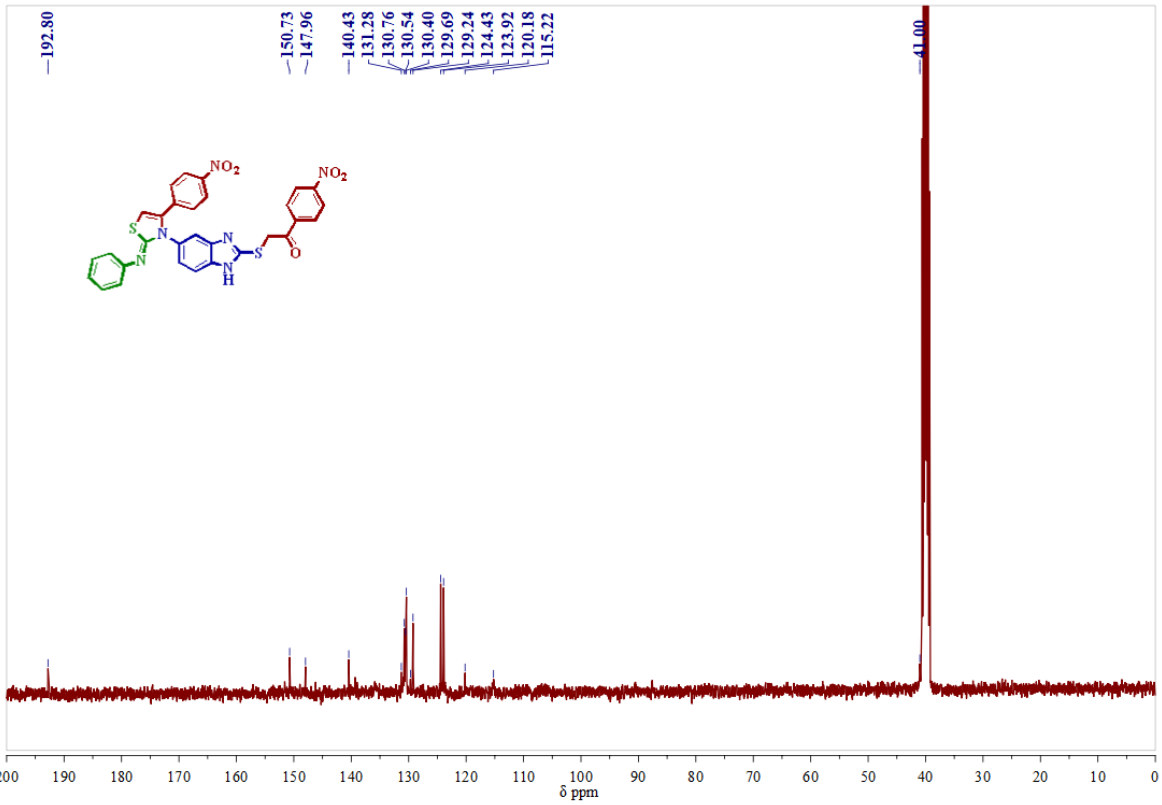

Mass spectrum of compound 4i

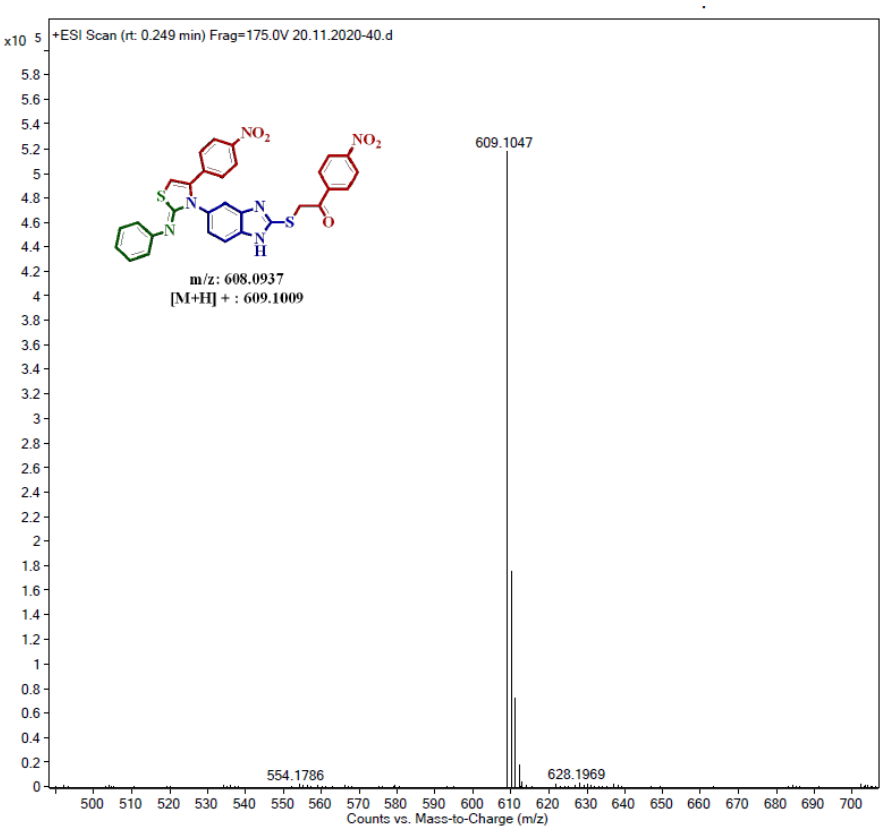

^{1}H-NMR Spectrum of compound 4j in DMSO-d_6 (400MHz):

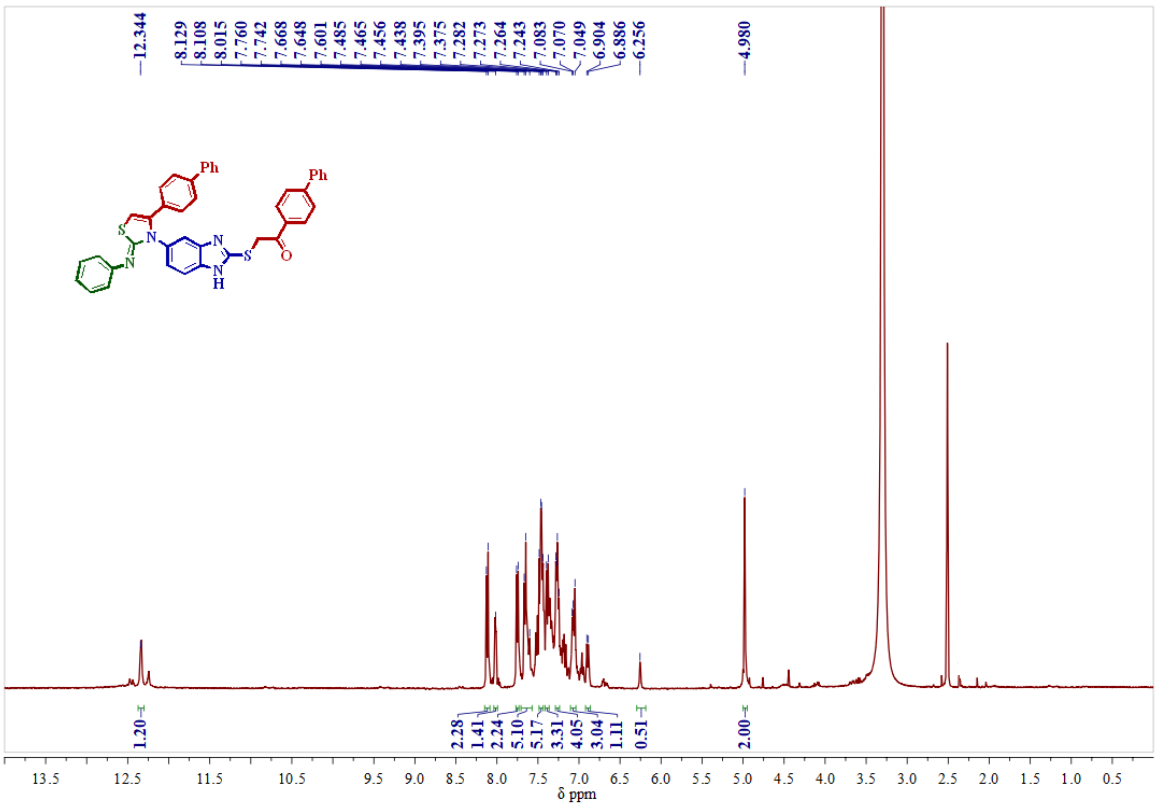

^{13}C-NMR Spectrum of compound 4j in DMSO-d_6 (100MHz):

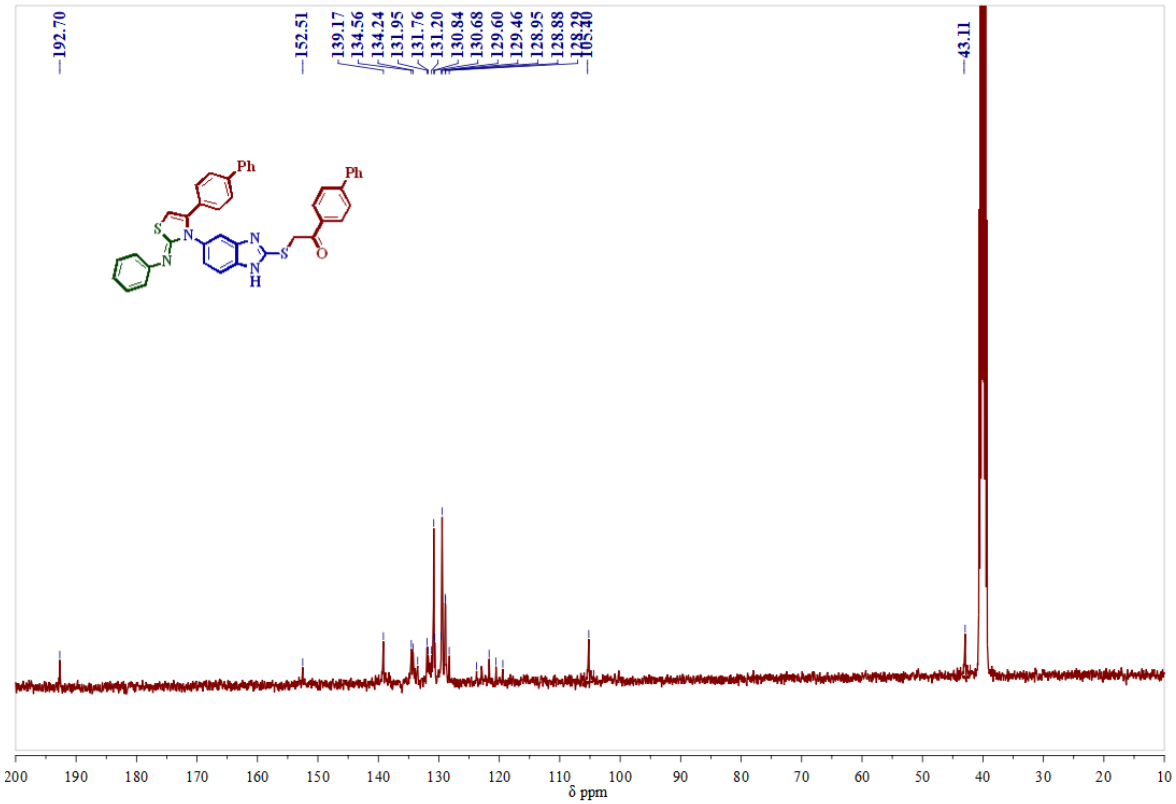

Mass spectrum of compound 4j:

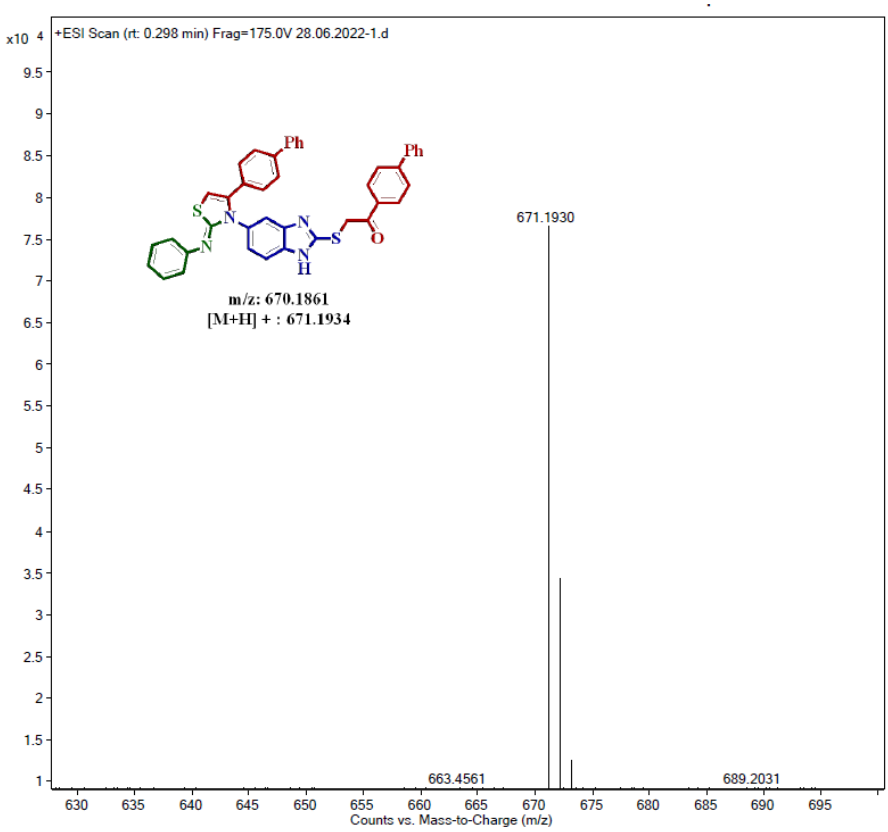

^{1}H-NMR Spectrum of compound 4k in DMSO-d_6 (400MHz):

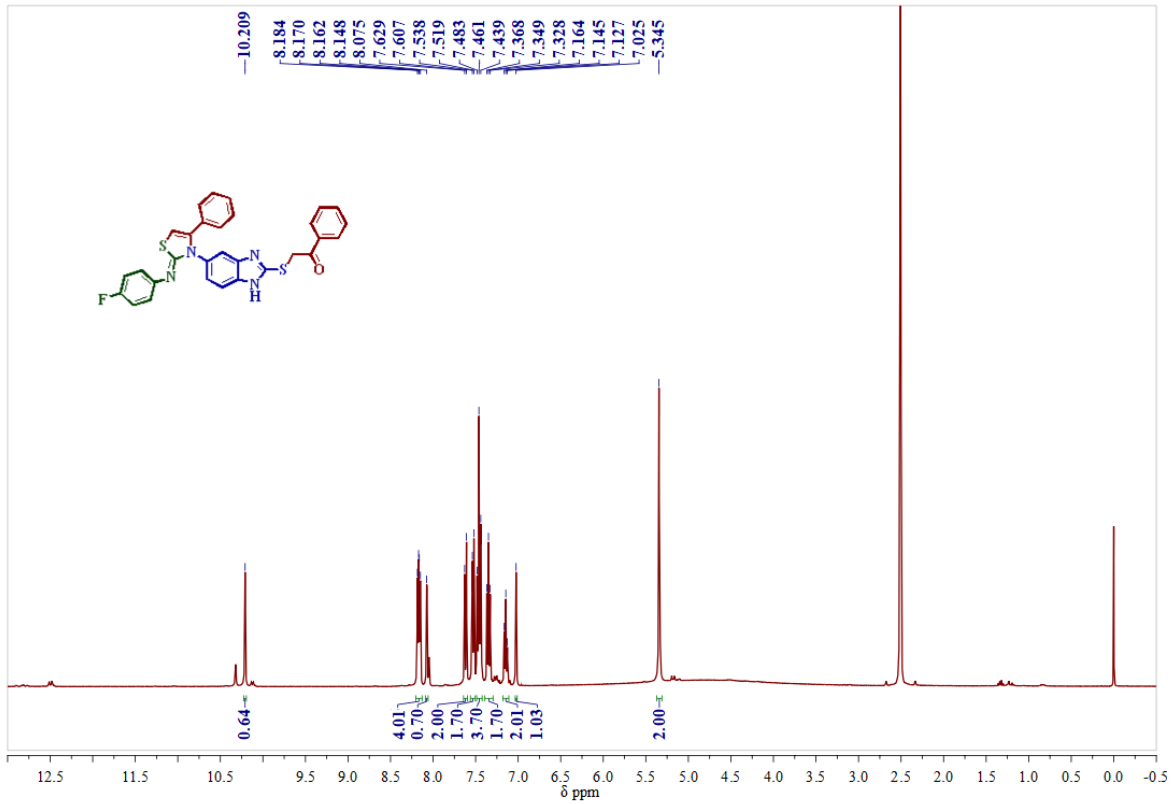

^{13}C-NMR Spectrum of compound 4k in DMSO-d_6 (100MHz):

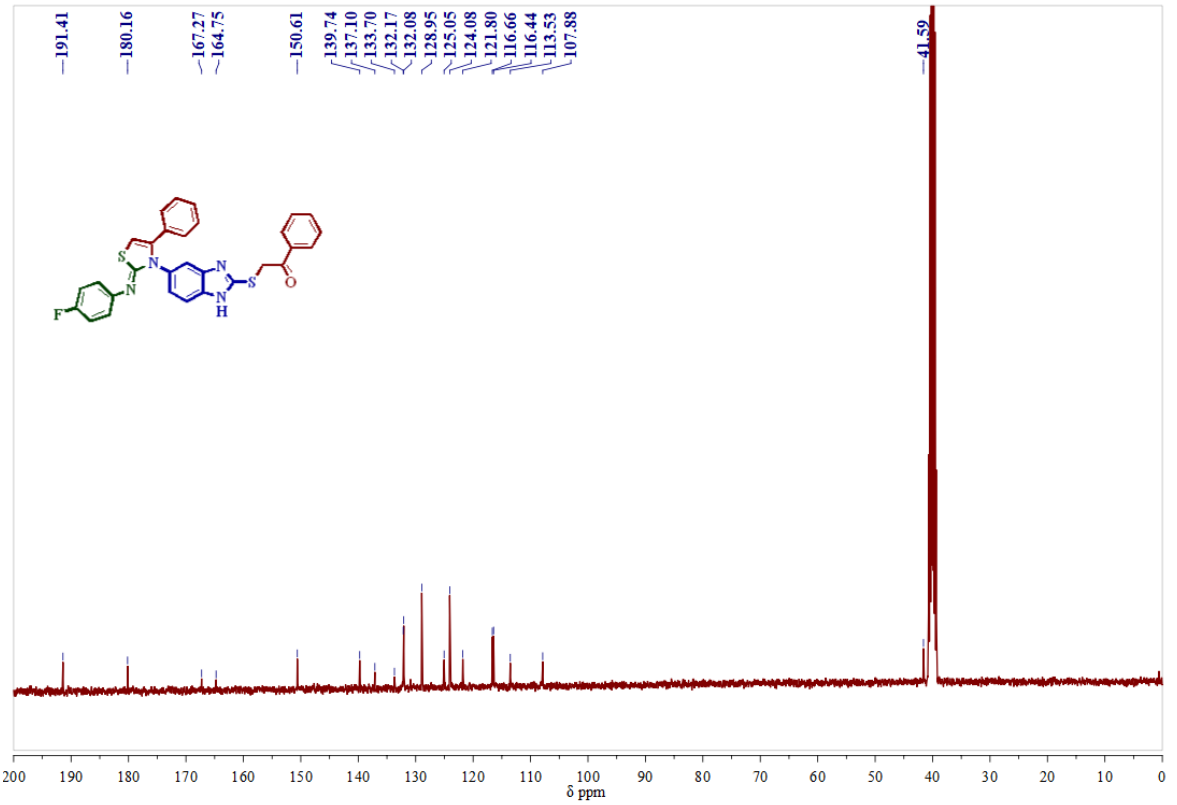

Mass spectrum of compound 4k

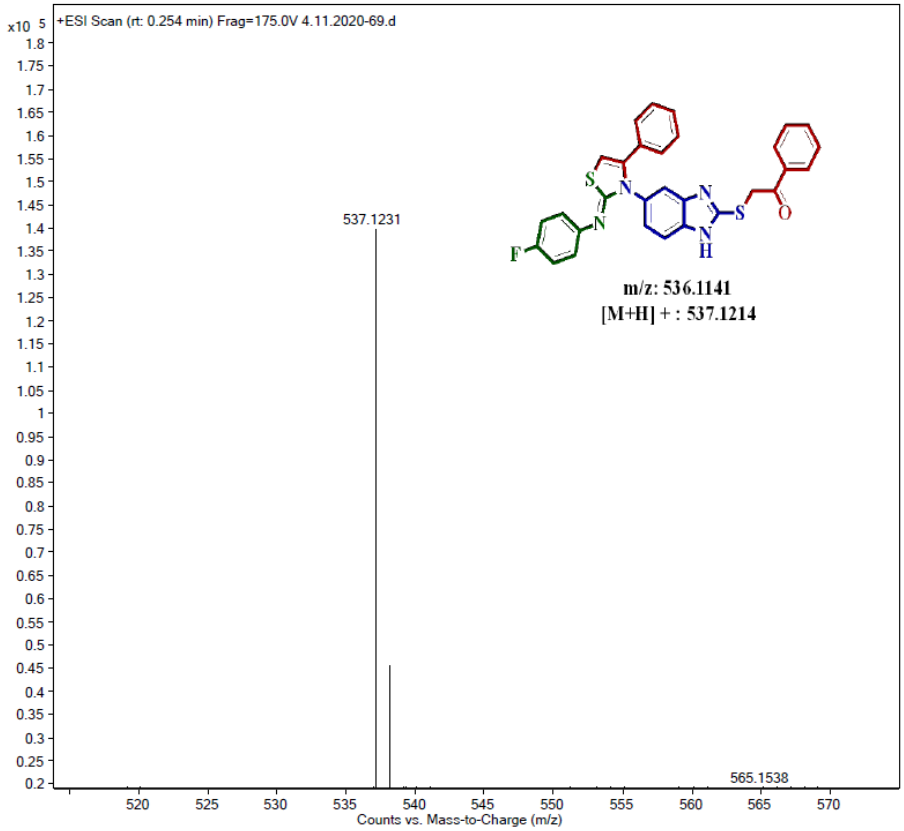

^{1}H-NMR Spectrum of compound 4l in $CDCl_3$-DMSO-d_6 (400MHz):

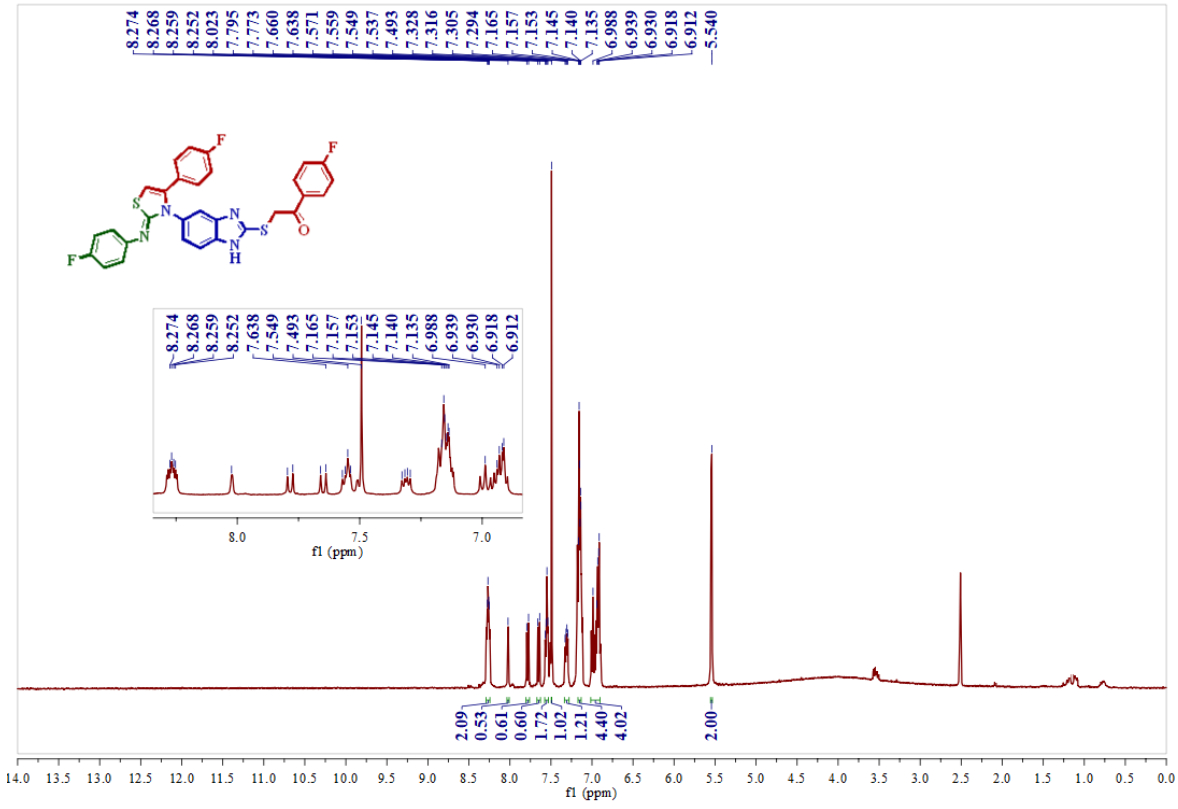

^{13}C-NMR Spectrum of compound 4l in $CDCl_3$-DMSO-d_6 (100MHz):

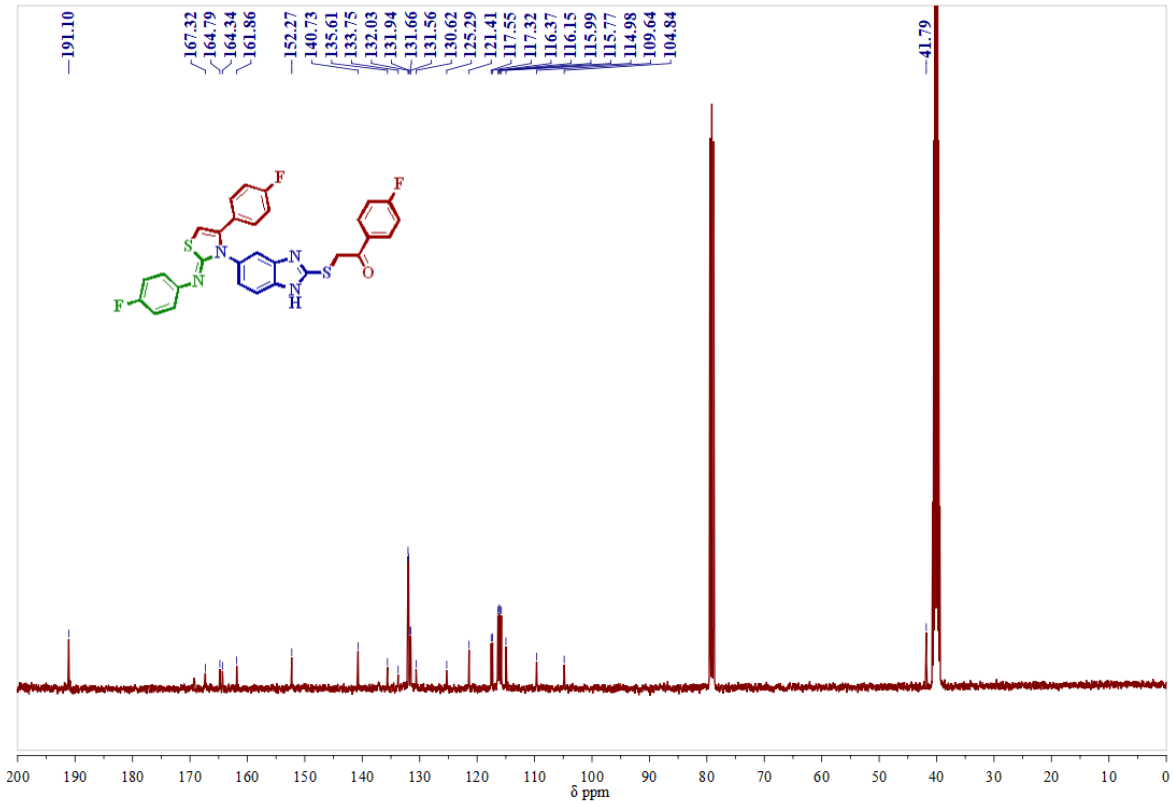

Mass spectrum of compound 4l

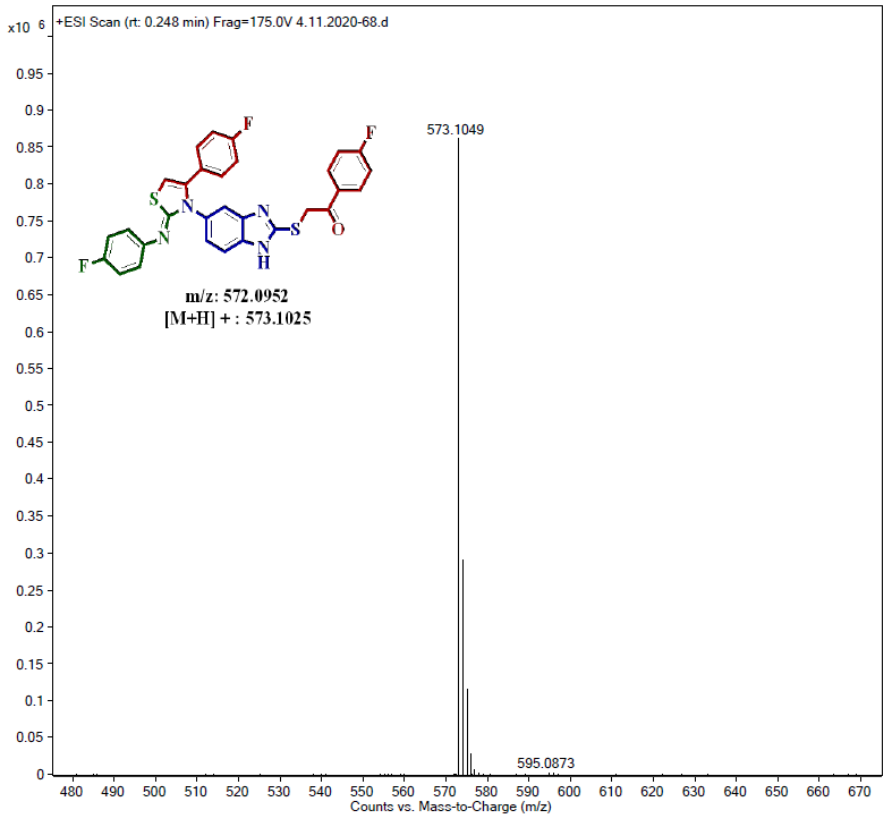

^{1}H-NMR Spectrum of compound 4m in DMSO-d_6 (400MHz):

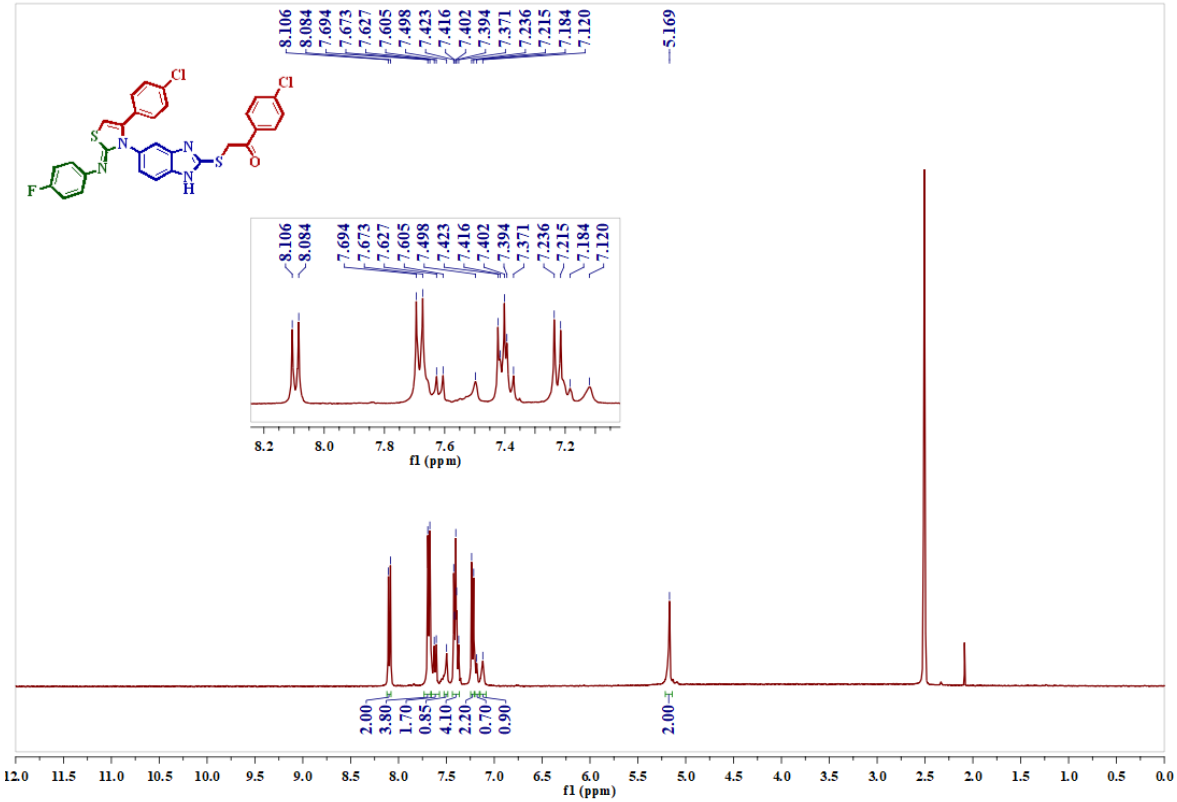

^{13}C-NMR Spectrum of compound 4m in $CDCl_3$-DMSO-d_6 (100MHz):

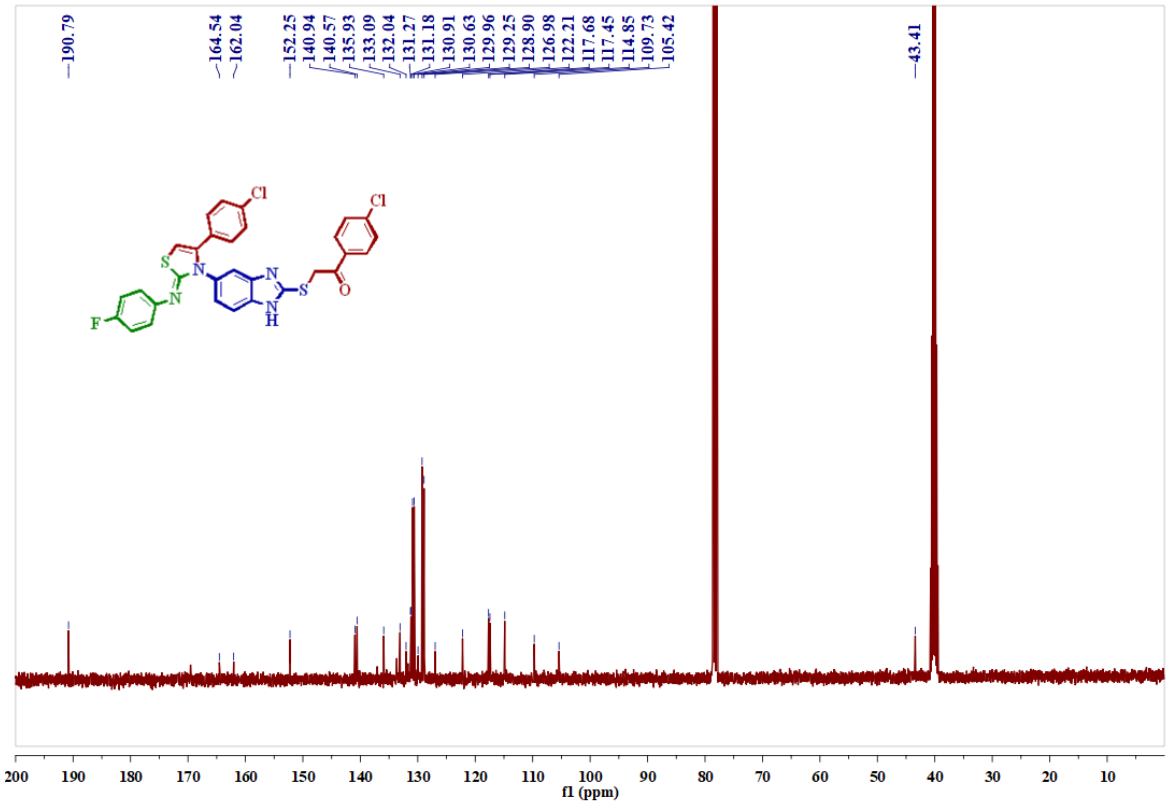

Mass spectrum of compound 4m

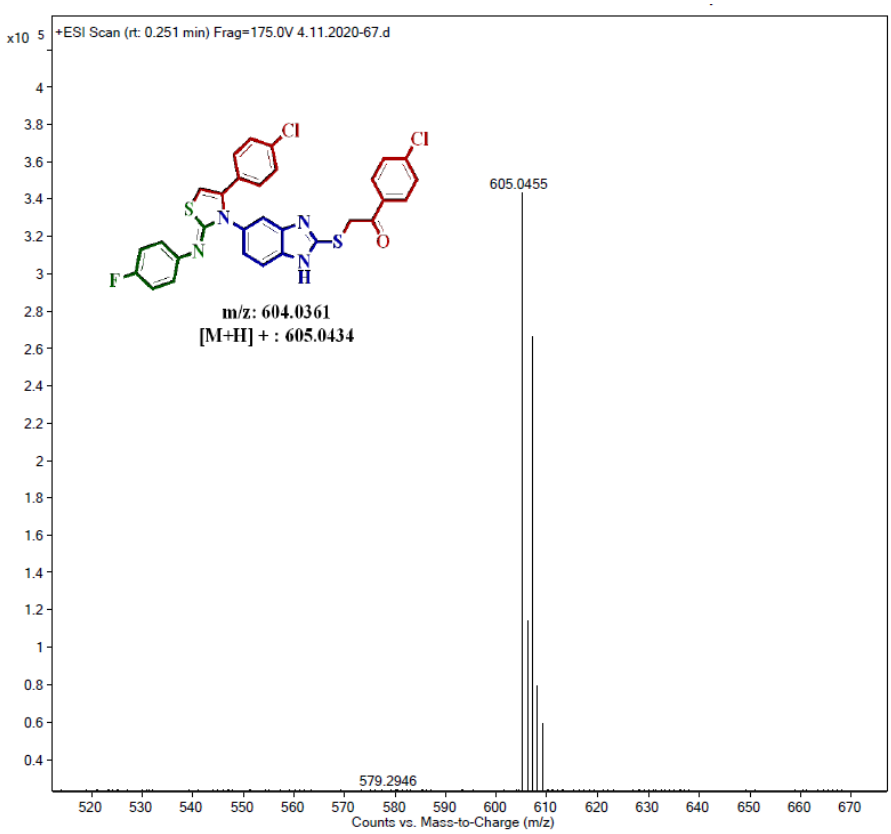

^{1}H-NMR Spectrum of compound 4n in $CDCl_3$-DMSO-d_6 (400MHz):

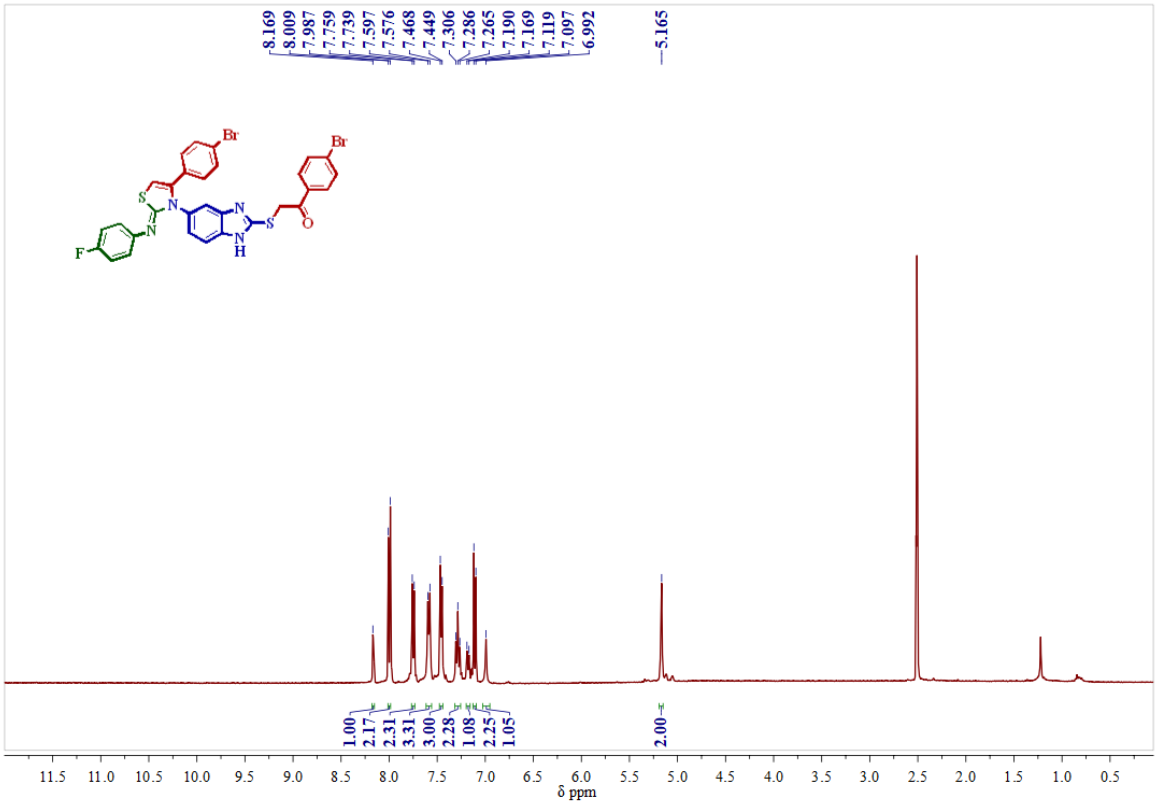

^{13}C-NMR Spectrum of compound 4n in CDCl$_3$-DMSO-*d*$_6$ (100MHz):

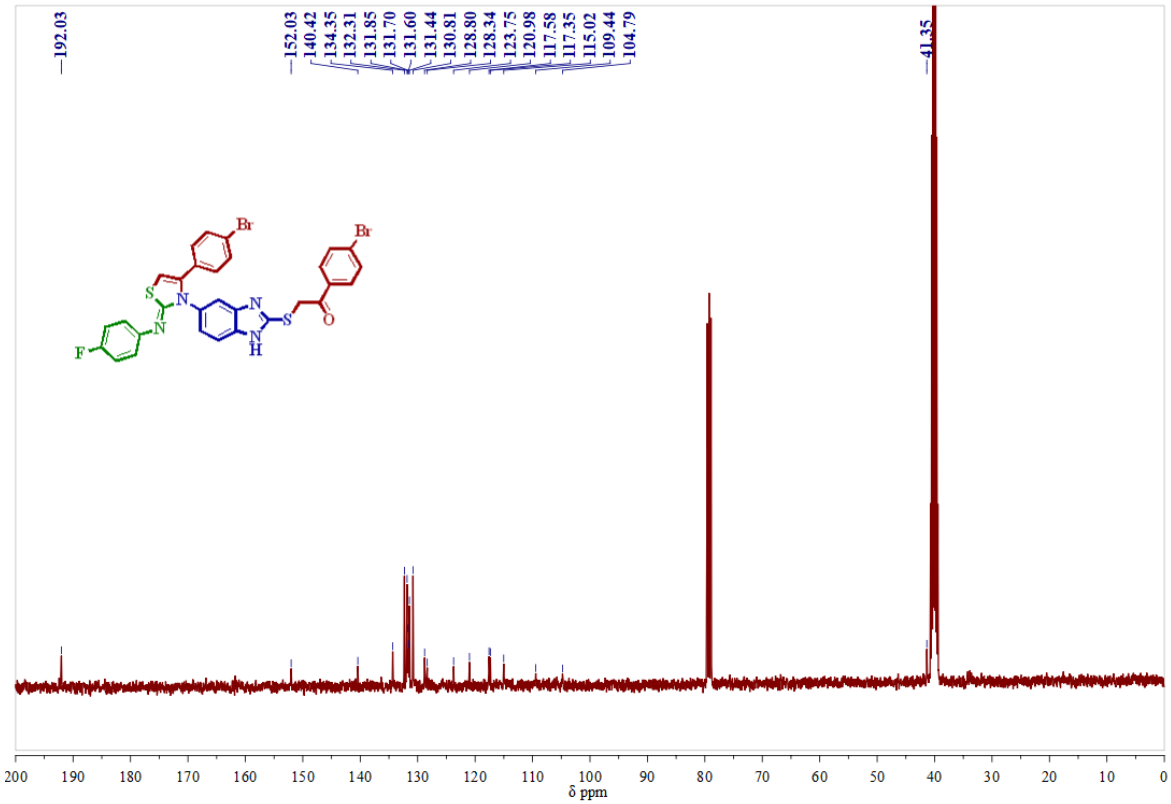

Mass Spectrum of compound 4n

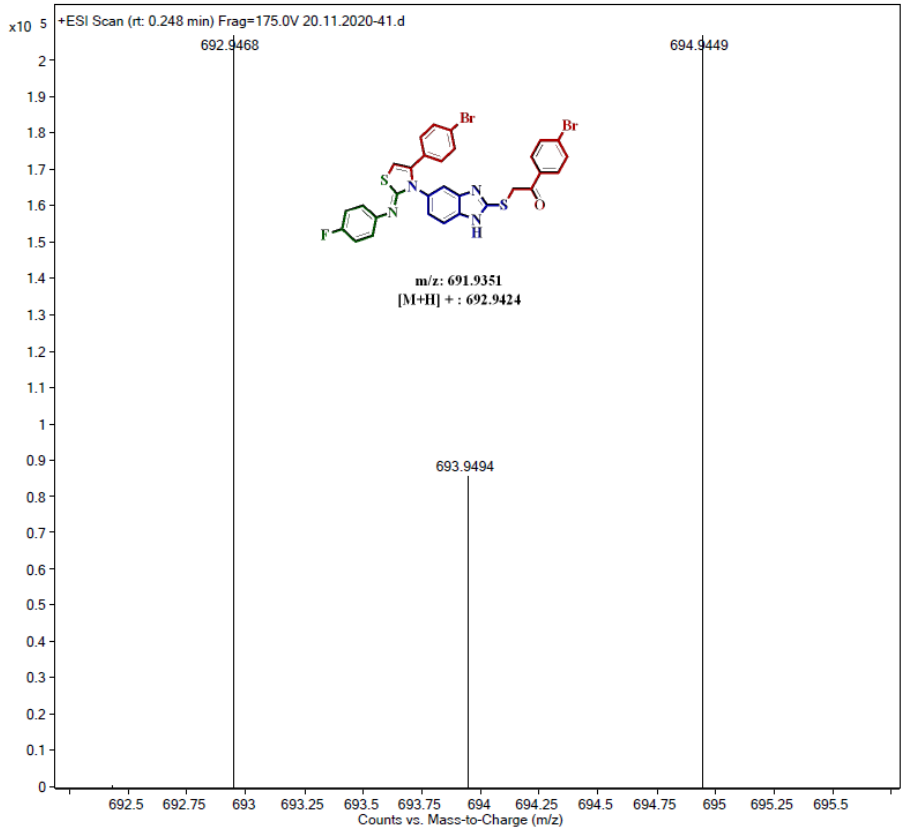

^{1}H-NMR Spectrum of compound 4o in DMSO-d_6 (400MHz):

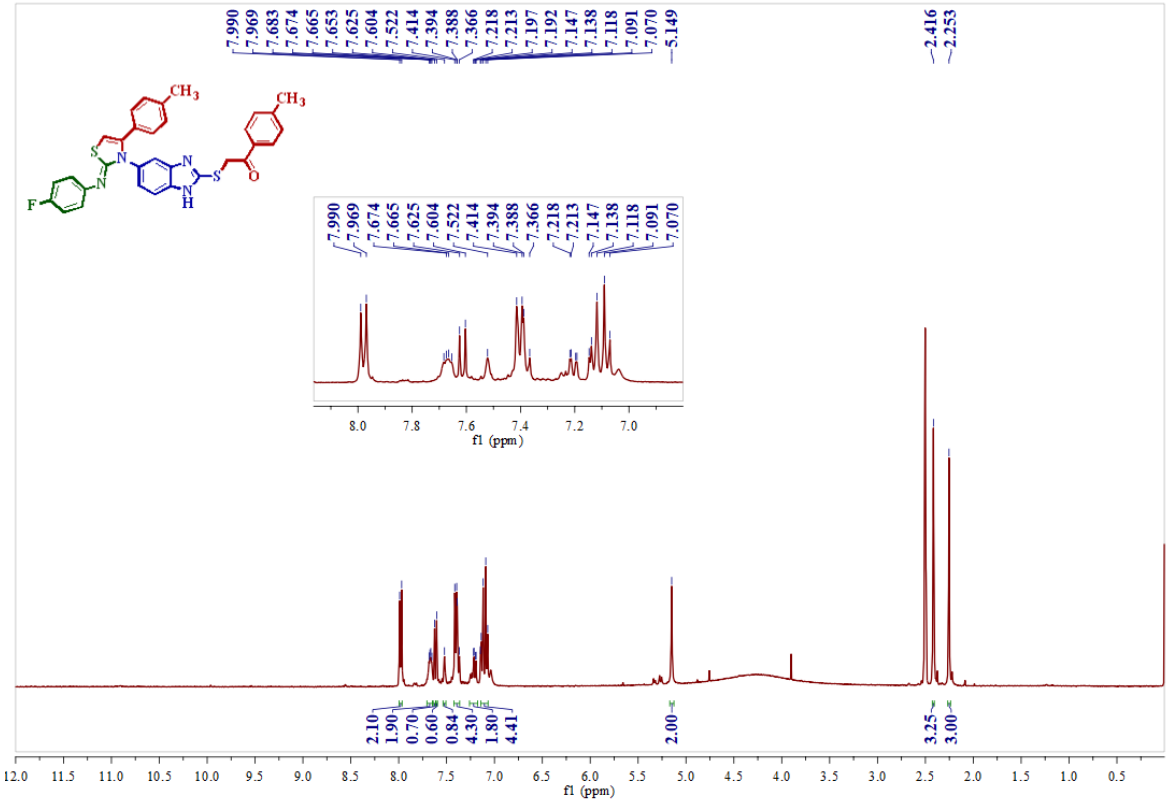

^{13}C-NMR Spectrum of compound 4o in DMSO-d_6 (100MHz):

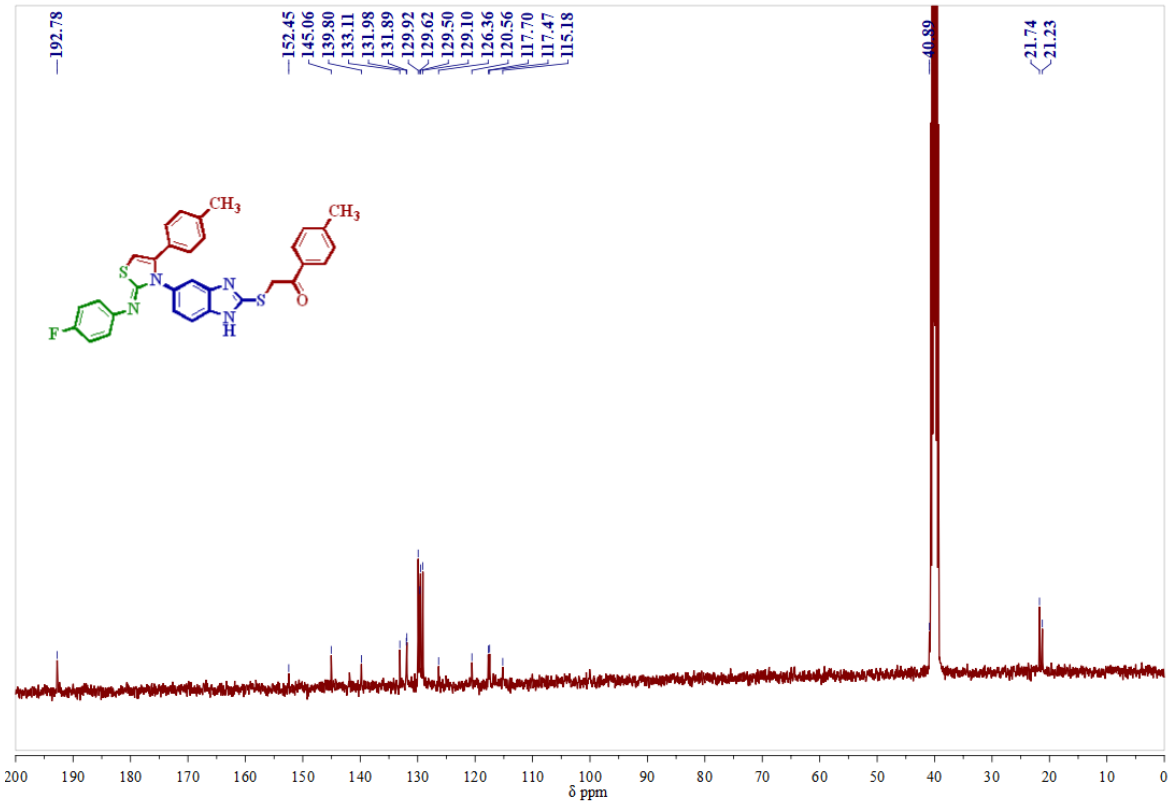

Mass spectrum of compound 4o

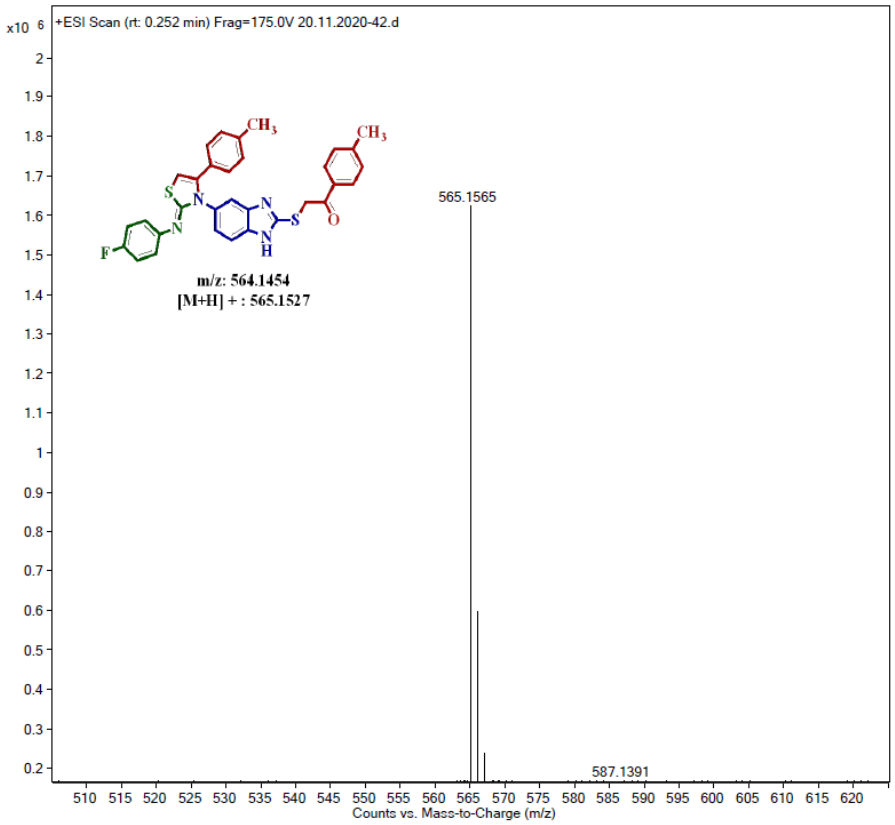

^{1}H-NMR Spectrum of compound 4p in DMSO-d_6 (400MHz):

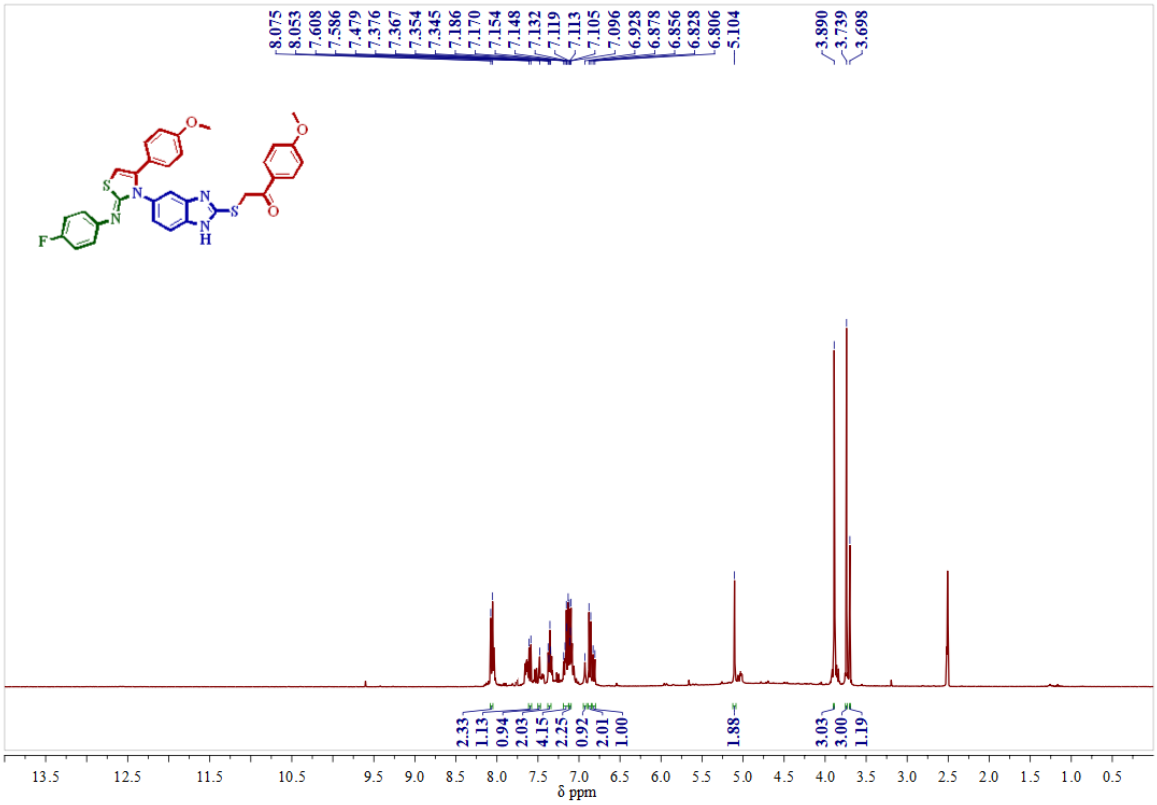

^{13}C-NMR Spectrum of compound 4p in DMSO-d_6 (100MHz):

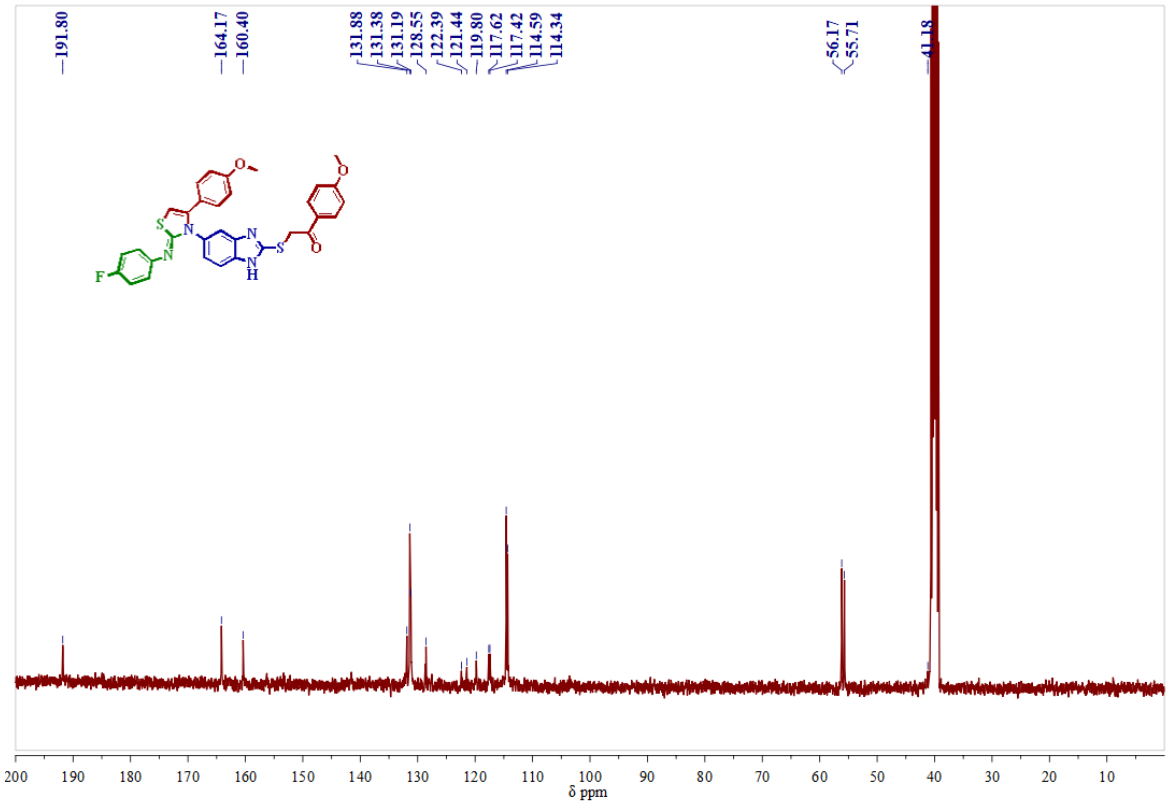

Mass spectrum of compound 4p:

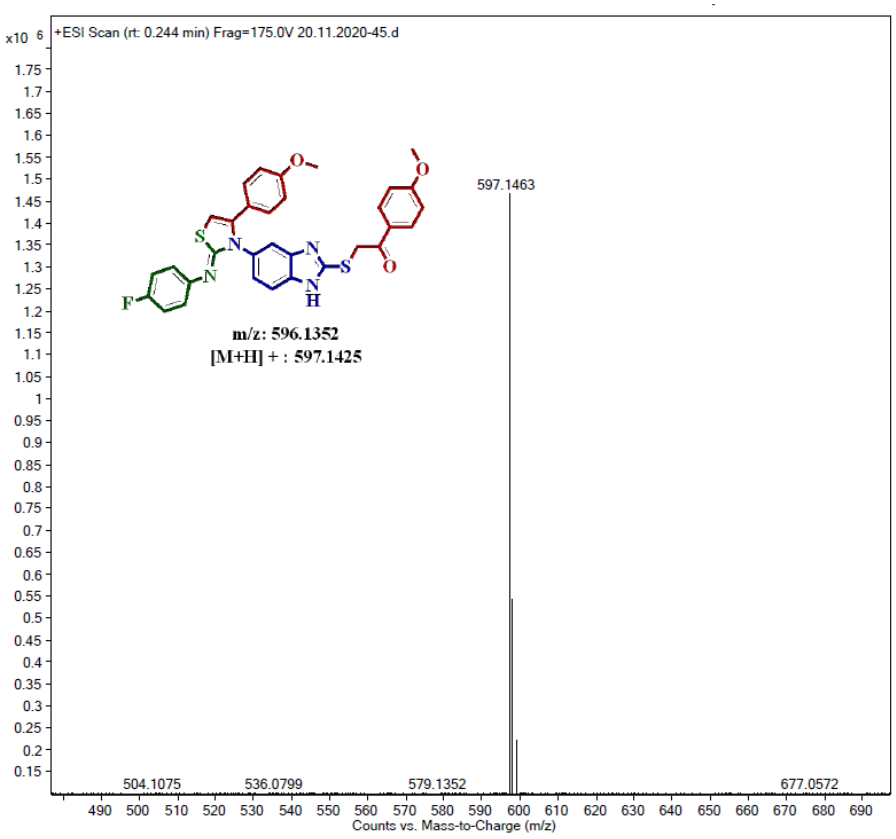

[1]H-NMR Spectrum of compound 4q in DMSO-*d*$_6$ (100MHz):

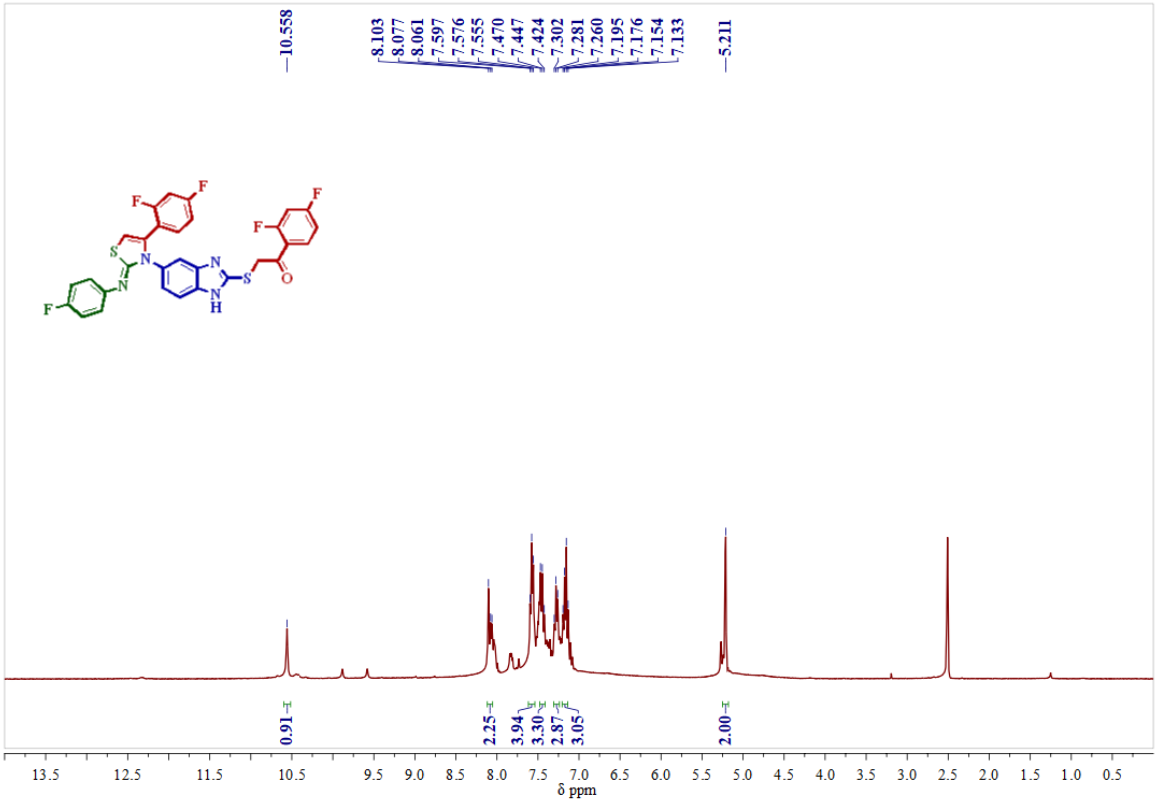

[13]C-NMR Spectrum of compound 4q in DMSO-*d*$_6$ (100MHz):

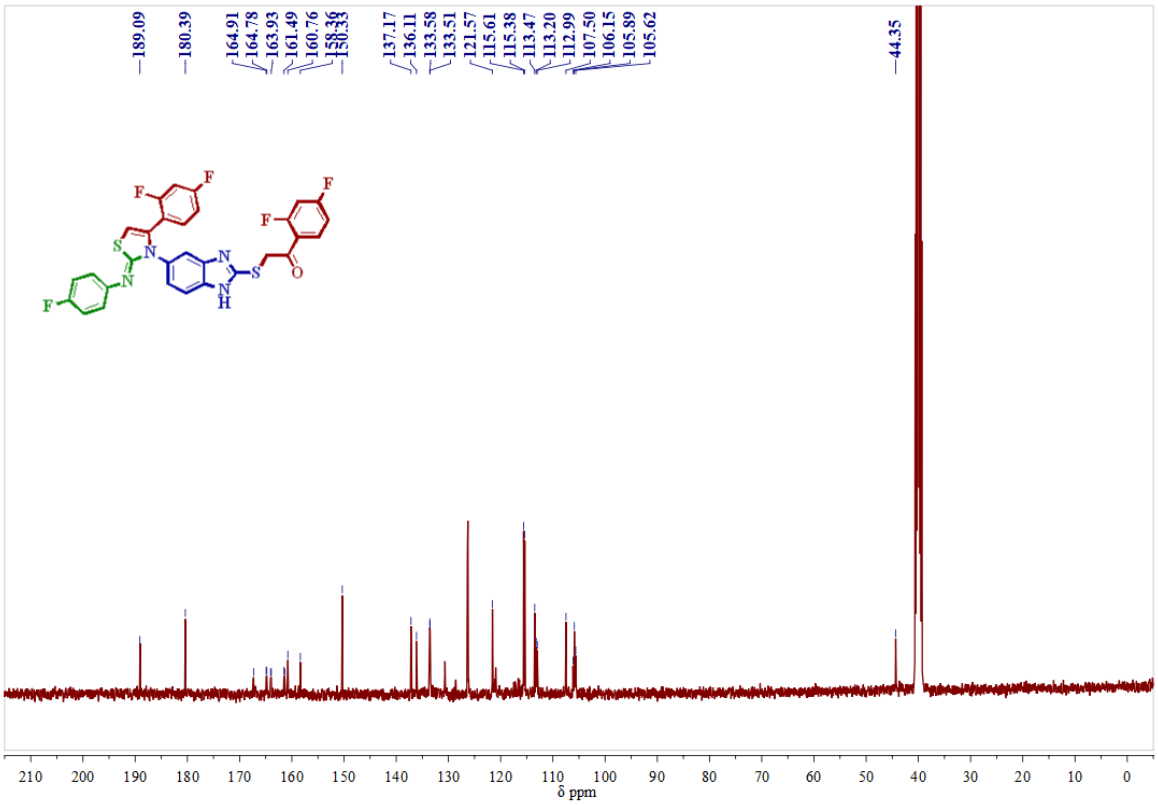

Mass spectrum of compound 4q

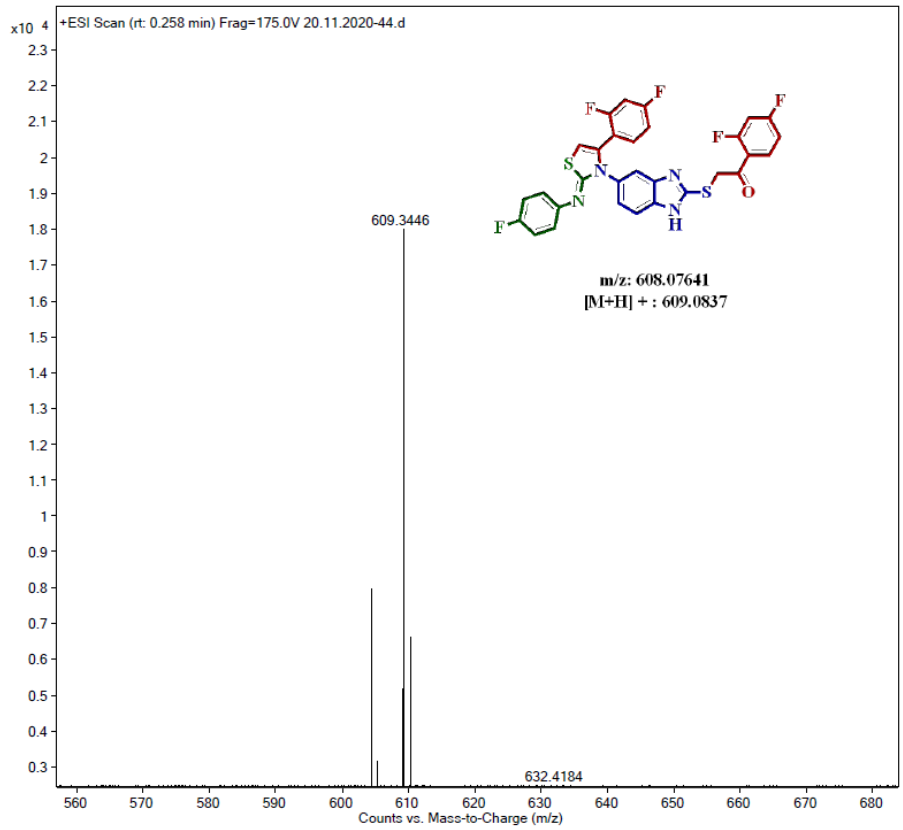

^{1}H-NMR Spectrum of compound 4r in DMSO-d_6 (400MHz):

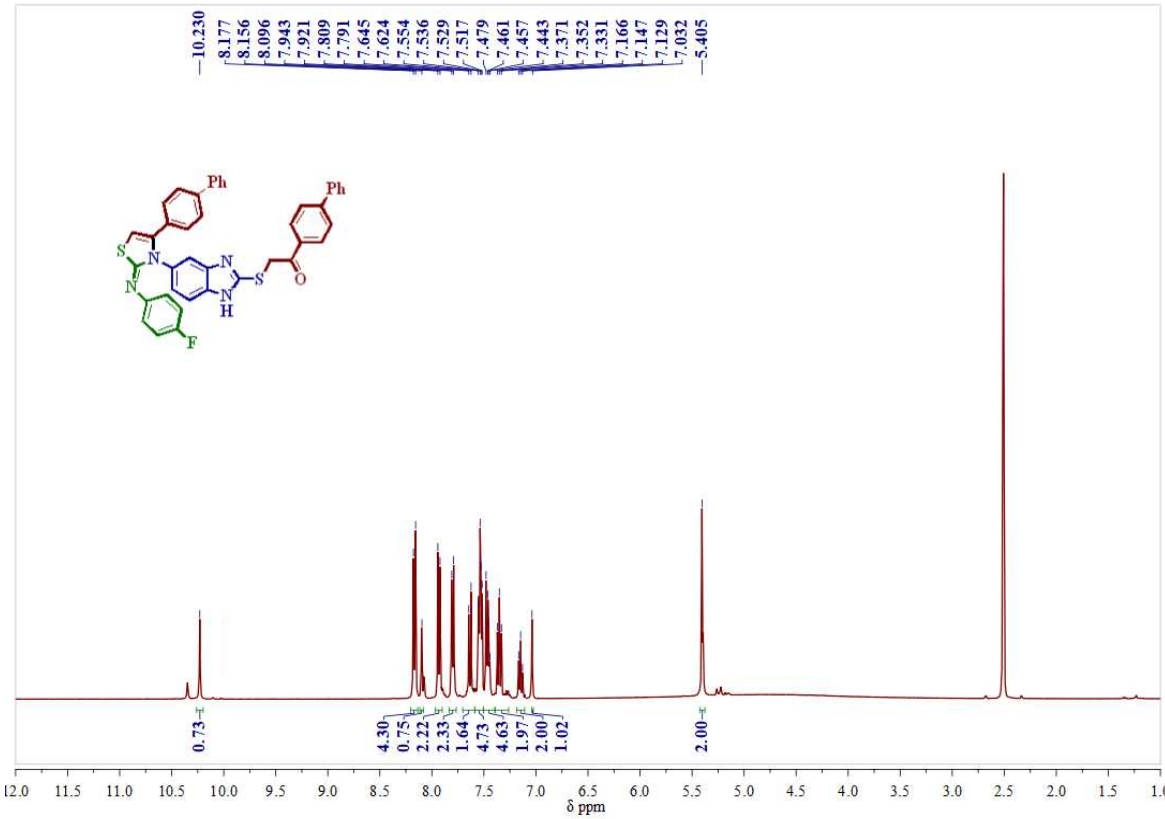

^{13}C-NMR Spectrum of compound 4r in DMSO-d_6 (100MHz):

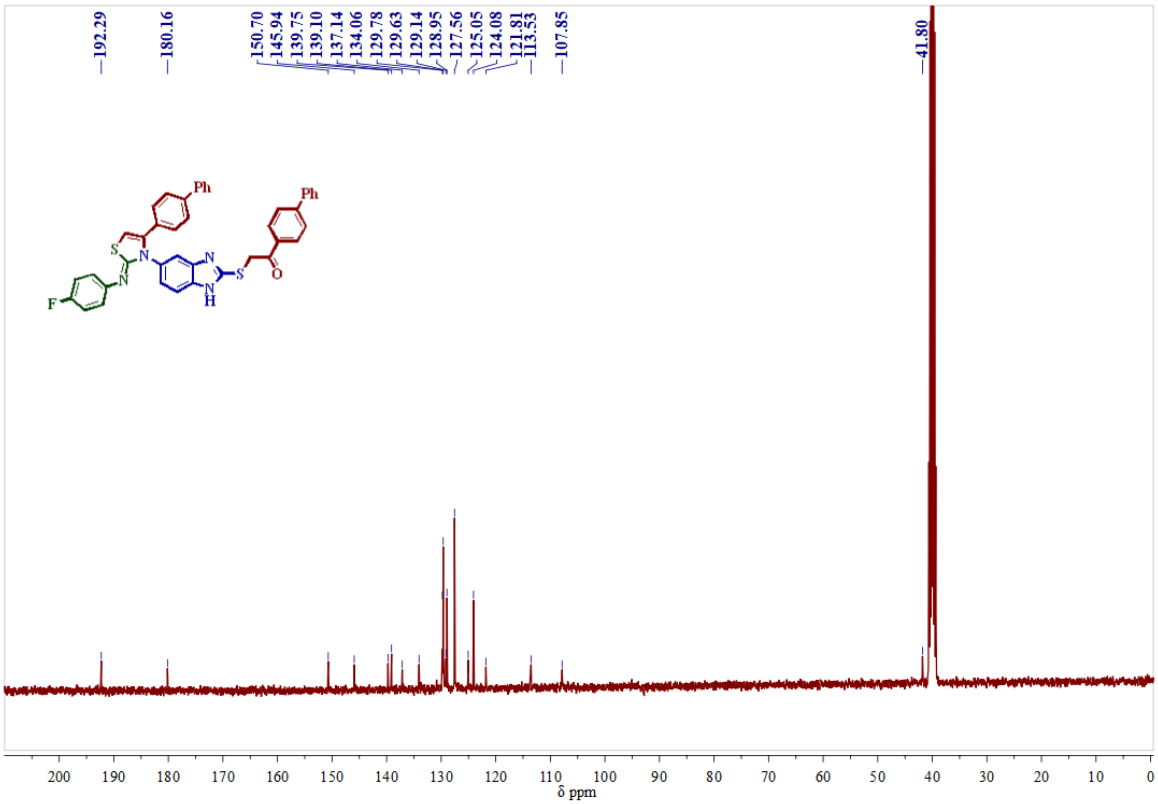

Mass Spectrum of compound 4r

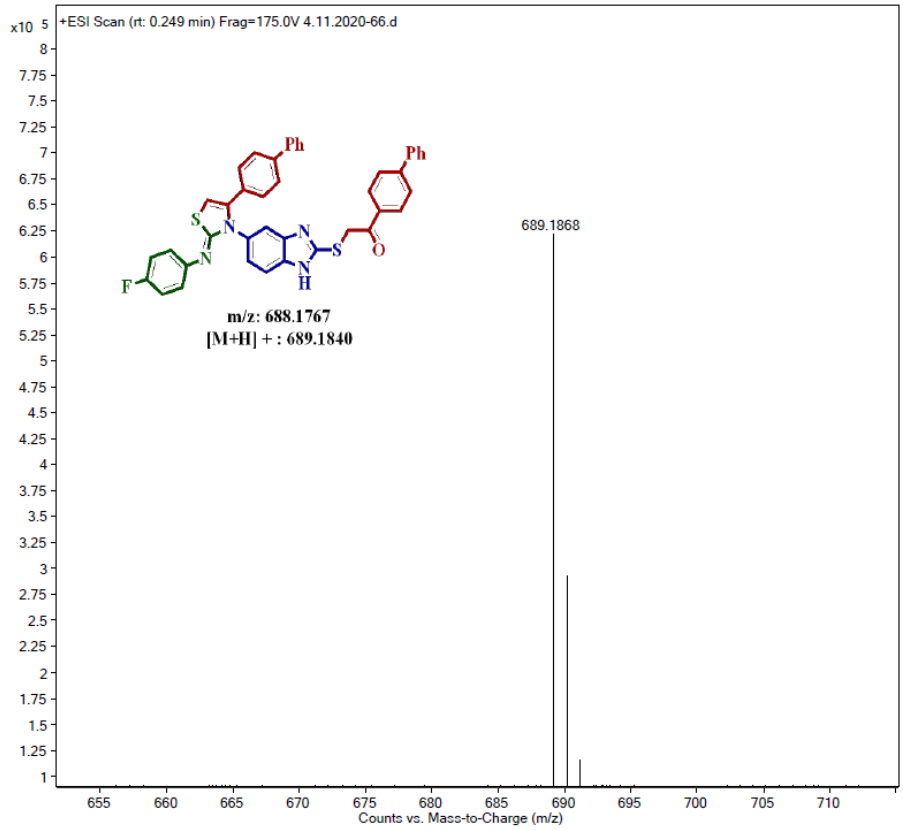

^{1}H-NMR Spectrum of compound 4s in DMSO-d_6 (400MHz):

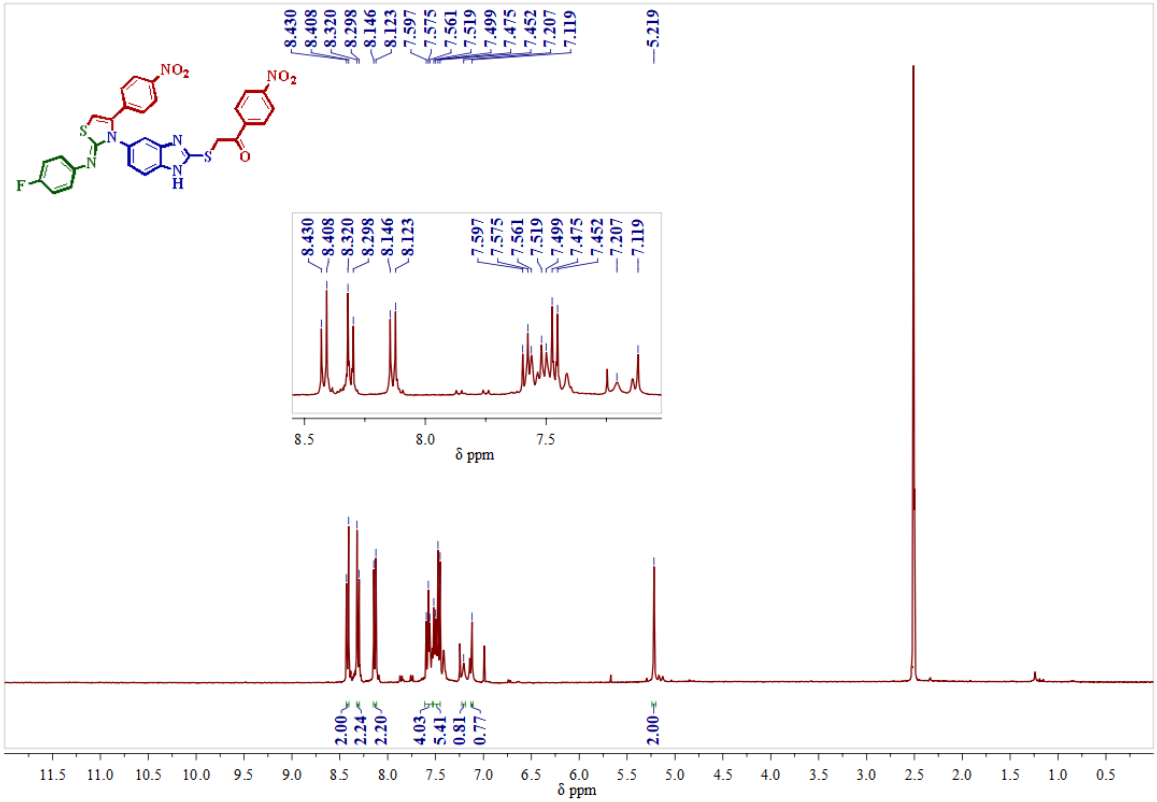

^{13}C-NMR Spectrum of compound 4s in CDCl$_3$-DMSO-d_6 (100MHz):

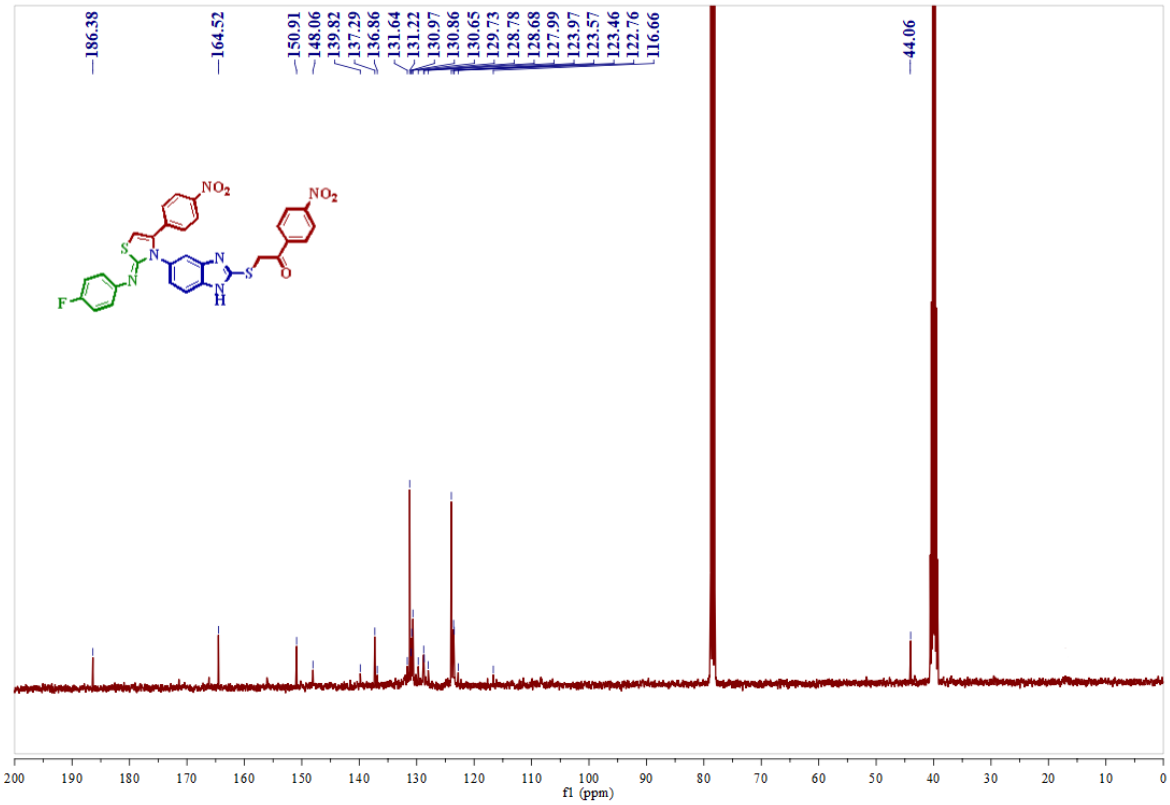

Mass spectrum of compound 4s

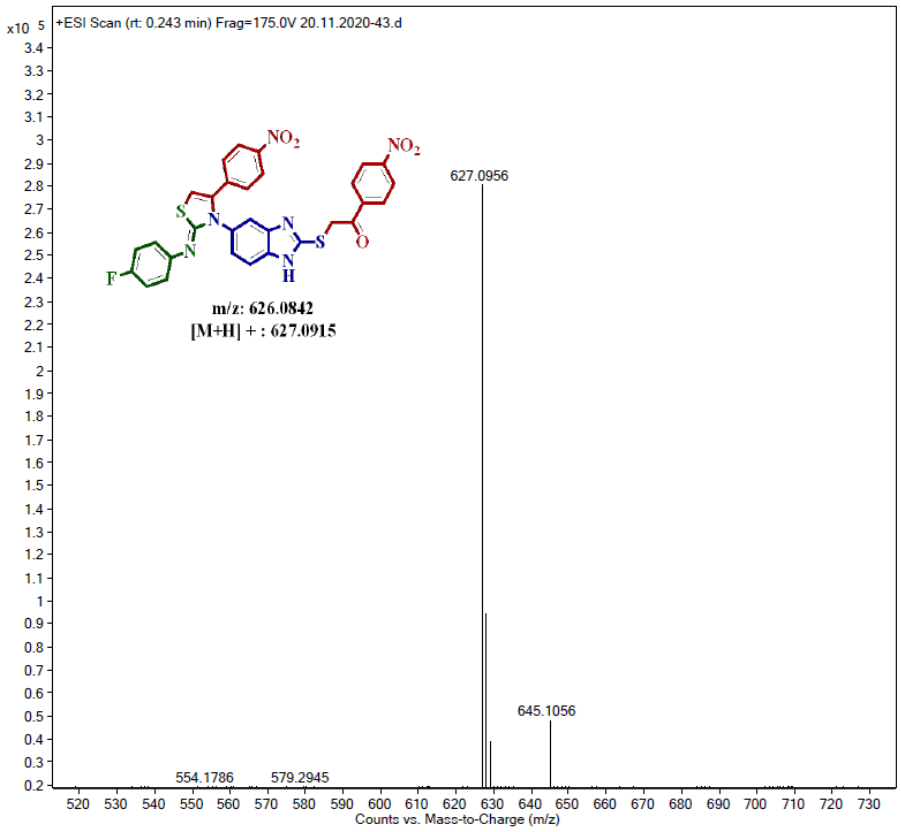

4A. 14. References

1. Aggarwal, T.; Kumar, S.; Verma, A. K. *Org. Biomol. Chem.* **2016**, *14*, 7639–7653.
2. Potewar, T. M.; Ingale, S. A.; Srinivasan, K. V. *Tetrahedron.* **2008**, *64*, 5019–5022.
3. Sever, B.; Altıntop, M.D.; Demir, Y.; Akalın Çiftçi, G.; Beydemir, S.; Özdemir, A. *Bioorg. Chem.* **2020**, *102*, 104110.
4. Hu, Y.; Hu, C.; Pan, G.; Yu, C.; Ansari, M. F.; Yadav Bheemanaboina, R. R.; Cheng, Y.; Zhou, C.; Zhang, J. *Eur. J. Med. Chem.* **2021,** *222*, 113628.
5. Yan, Z.; Liu, A.; Ou, Y.; Li, J.; Yi, H.; Zhang, N.; Liu, M.; Huang, L.; Ren, J.; Liu, W.; Hu, A. *Bioorg. Med. Chem.* **2019**, *27*, 3218–3228.
6. Hassan, A.; Badr, M.; Hassan, H. A.; Abdelhamid, D.; Abuo-Rahma, D. E. A. *Bioorg. Med. Chem.* **2021**, *40*, 116168.
7. Hupfer, M. L.; Kaufmann, M.; Roussille, L.; Preiß, J.; Weiß, D.; Hinrichs, K.; Deckert, V.; Dietzek, B.; Beckert, R.; Presselt, M. *Langmuir.* **2019**, *35*, 2561–2570.
8. Liu, W.; Yu, X.; Kuang, C. *Org. Lett.* **2014**, *16*, 1798–1801.
9. El-Naggar, A. M.; El-Hashash, M. A.; Elkaeed, E. B. *Bioorg. Chem.* **2021**, *108*, 104615.
10. Kiryanov, A. A.; Seed, A. J.; Sampson, P. *Tetrahydron Lett.* **2001**, 42, 8797-8800
11. Hodgetts, K. J.; Kershaw, M. T. *Org. Lett.* **2002,** *4*, 1363–1365.
12. Mamidala, S.; Peddi, S. R.; Aravilli, R. K.; Jilloju, P. C.; Manga, V.; Vedula, R. R. *J. Mol. Struct.* **2021**, *1225*.
13. Sridevi, B.; Tangella, Y.; Babu, K. S.; Nanubolu, J. B.; Sunitha Rani, R.; Ganesh Kumar, C.; Meshram, H. M.; Kamal, A. *New J. Chem.* **2017**, *41*, 3745–3749.
14. Mamidala, S.; Aravilli, R. K.; Vaarla, K.; Vedula, R. R. *ChemistrySelect.* **2019**, *4*, 9878–9881.
15. Gondru, R.; Kanugala, S.; Raj, S.; Ganesh Kumar, C.; Pasupuleti, M.; Banothu, J.; Bavantula, R. *Bioorg. Med. Chem. Lett.* **2021**, *33*, 127746.
16. Sujatha, K.; Vedula, R. R. *Mol. Divers.* **2020**, *24*, 413–421.
17. Titus, S.; Sreejalekshmi, K. G. *Med. Chem. Res.* **2018**, *27*, 23–36.
18. Costa, L. D.; Guieu, S.; Faustino, M. do A. F.; Tomé, A. C. *New J. Chem.* **2022**, *46*, 3602–3615.
19. Mahata, A.; Bhaumick, P.; Panday, A. K.; Yadav, R.; Parvin, T.; Choudhury, L. H. *New J. Chem.* **2020**, *44*, 4798–4811.
20. Saroha, M.; Khurana, J. M. *New J. Chem.* **2019**, *43*, 8644–8650.

21. Peng, X.; Qin, F.; Xu, M.; Zhu, S.; Pan, Y.; Tang, H.; Meng, X.; Wang, H. *Org. Biomol. Chem.* **2019**, *17*, 8403–8407.
22. Dai, T.; Cui, C.; Qi, X.; Cheng, Y.; He, Q.; Zhang, X.; Luo, X.; Yang, C. *Org. Biomol. Chem.* **2020**, *18*, 6162–6170.
23. Ni, P.; Tan, J.; Li, R.; Huang, H.; Zhang, F.; Deng, G. J. *RSC Adv.* **2020**, *10*, 3931–3935.
24. Vaarla, K.; Vishwapathi, V.; Vermeire, K.; Vedula, R. R.; Kulkarni, C. V. *J. Mol. Struct.* **2022**, *1249*, 131662.
25. Ramagiri, R. K.; Vedula, R. R. *Synth. Commun.* **2014**, *44*, 1301–1306.
26. Vaarla, K.; Kesharwani, R. K.; Santosh, K.; Vedula, R. R.; Kotamraju, S.; Toopurani, M. K. *Bioorg. Med. Chem. Lett.* **2015**, *25*, 5797–5803.
27. Ruddarraju, R. R.; Kiran, G.; Murugulla, A. C.; Maroju, R.; Prasad, D. K.; Kumar, B. H.; Bakshi, V.; Reddy, N. S. *Bioorg. Chem.* **2019**, *92*, 103120.
28. Flare, version, Cresset®, Litlington, Cambridgeshire, UK; http://www.cresset-group.com/flare/;
29. Cheeseright, T.; Mackey, M.; Rose, S.; Vinter, A. *J. Chem. Inf. Model.* **2006,** *46*, 665–676.
30. Williams, L. K.; Zhang, X.; Caner, S.; Tysoe, C.; Nguyen, N. T.; Wicki, J.; Williams, D. E.; Coleman, J.; McNeill, J.H.; Yuen, V.; Andersen, R. J.; Withers, S. G.; Brayer, G. D. *Nat. Chem. Biol.* **2015**, *11*, 691–696.
31. Bauer, M. R.; Mackey, M. D. *J. Med. Chem.* **2019,** *62,* 3036–3050.
32. Makarewicz, T.; Kazmierkiewicz, R. *J. Chem. Inf. Model.* **2013**, 53, 1229–1234.
33. Skyner, R. E.; McDonagh, J. L.; Groom, C. R.; Van Mourik, T.; Mitchell, J. B. O. *Phys. Chem. Chem. Phys.* **2015**, *17*, 6174–6191.
34. Bickerton, G.; Paolini, G.; Besnard, J.; Muresan, S.; Hopkin, A. L. *Nature Chem.* **2012,** *4*, 90–98.
35. Sander, T.; Freyss, J.; von Korff, M.; Rufener, C. *J. Chem. Inf. Model*. **2015**, *55*, 460-473.
36. E. V. Radchenko, E. V.; Rulev, Yu. A.; Safanyaev, Ya. A.; Palyulin, V. A.; Zefirov N. S. *Dokl. Biochem. Biophys.* **2017**, *473*, 128-131.
37. Xiong, G.; Wu, Z.; Yi, J.; Fu, L.; Yang, Z.; Hsieh, C.; Cao, D. *Nucleic Acids Res*. **2021**, *49*, W5-W14.

CHAPTER-IV (Section-B)

Facile, One-pot, pseudo four-component synthesis of novel thiazolyl-benzimidazoles *via* multi-component approach and their biological evaluation

CHAPTER-IVB

Facile, pseudo-four-component synthesis of novel thiazolyl-benzimidazoles *via* multi-component approach and their biological evaluation

4B.0. Present Work

4B.0.1. Starting Materials

In this chapter, we describe the synthesis, anti-biotic activity and computational studies of novel thiazolyl-benzimidazole (**4a-p**) compounds as outlined in **Scheme 4B.1**. The title compounds were synthesized by using 5-amino-2-mercaptobenzimidazole **1**, ammonium thiocyanate **2,** substituted α- bromo-acetophenones **3** or aryl alkyl halides. All the starting materials were procured from commercial sources.

4B.1. Synthesis of Thiazoles

The synthesis of target thiazole analogues was carried out as outlined in Scheme 4B.1. The title compounds were synthesized by using 5-amino-2-mercaptobenzimidazole **1**, ammonium thiocyanate **2,** substituted α- bromo-acetophenones **3** or aryl alkyl halides **(1:1:2)** in glacial acetic acid at 70 ºC to give final compounds (**4a-p**) with good to excellent yields in a shorter reaction time.

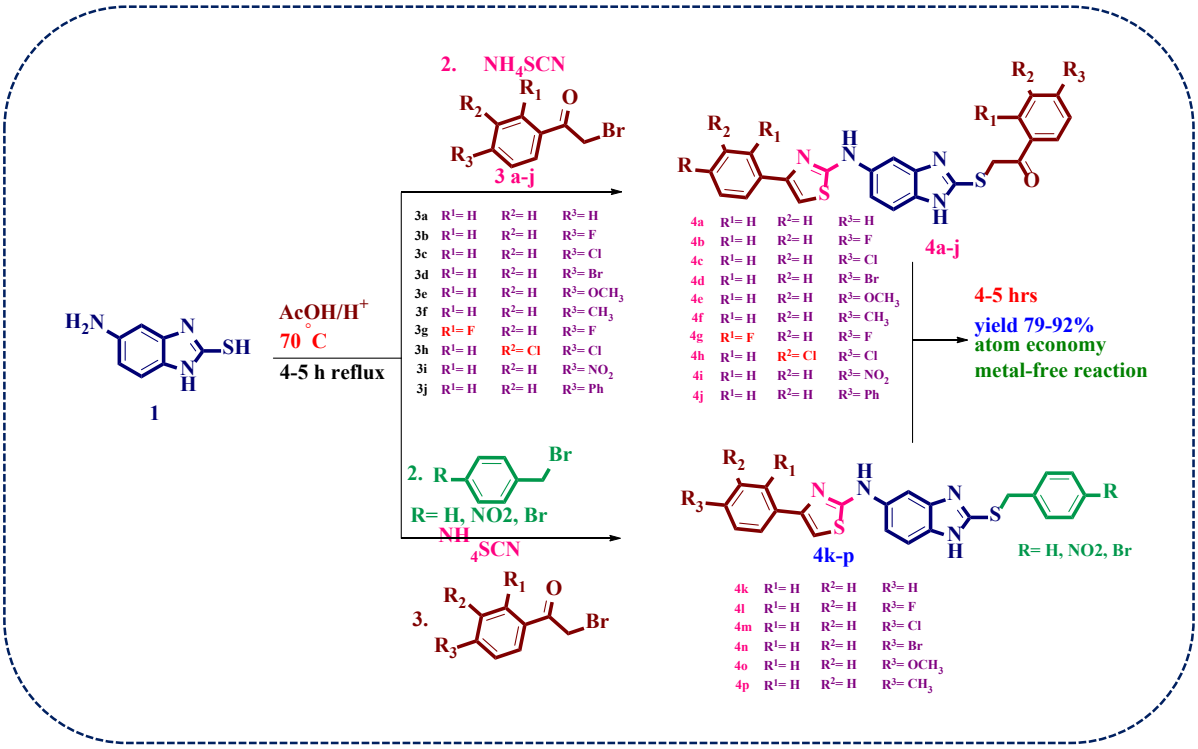

Scheme 4B.1. Synthesis of benzimidazole based thaizoles.

4B.2. Results and discussion

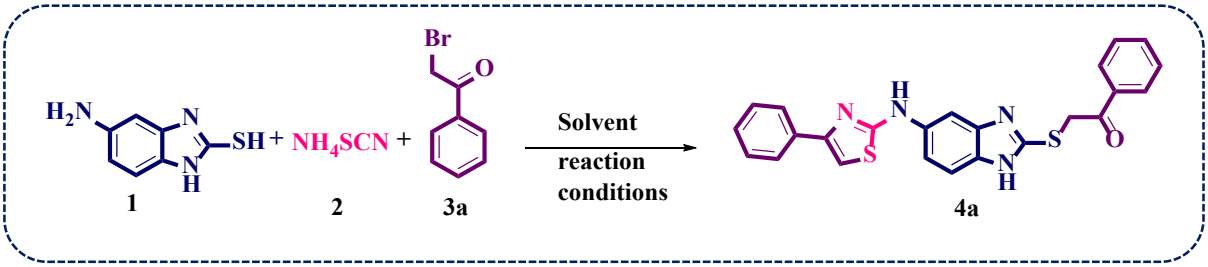

Table 4B.1. Optimized reaction conditions.4a[a]

Entry	Solvent	Catalyst	Temp (°C)	Time (h)	Yield (%)
1	CH_3CN	-	60	24	n.r
2	DMSO	-	60	24	n.r
3	DMF	-	60	20	21
4	Methanol	-	60	15	25
5	Ethanol	-	60	12	38
6	Ethanol	NaOH	60	12	43
7	Ethanol	KOH	60	12	45
8	Ethanol	Na_2CO_3	60	12	35
9	Ethanol	K_2CO_3	60	12	42
10	Ethanol	Et_3N	60	12	41
11	Ethanol	Acetic acid	60	10	52
12	Ethanol	Acetic acid	60	6	60
13	AcOH	-	60	4	65
14	**AcOH**	**AcONa (1.0 mmol)**	**60**	**4**	**70**
15	**AcOH**	**AcONa (2.0 mmol)**	**70**	**4**	**88**
16	AcOH	-	reflux	4	51

[a]*Reaction conditions*: 5-amino-2-marcaptobenzimidazole (**1**) (1.0 mmol), ammonium thiocyanate (**2**) (1.0 mmol), phenacyl bromide (**3**) (2.0 mmol), solvent (2 mL), [b]Isolated yields.

Initially, to find the optimization conditions, we started our investigation to synthesize the title scaffolds starting from 5-amino-2-mercaptobenzimidazole (**1**), ammonium thiocyanate (**2**), and various substituted α-Bromo acetophenones (**3**). To our delight, the desired benzimidazole-based thiazoles obtained 70% of yield in the presence of glacial acetic acid at 70 ºC for about 4 h reflux (**Table 4B.1, entry-14**) and its structure was unambiguously confirmed by IR, ^{1}H-

NMR, ^{13}C-NMR spectra, and HRMS. Other solvents were also screened and it was revealed that DMSO, DMF, CH_3CN, methanol, and ethanol resulted in very poor yields, while DMSO and CH_3CN gave unsuccessful results (**entries-1,2**). Next, we examined the bases to improve the reaction yields, here we screened different organic and inorganic bases, but we did not observe greater yields when inorganic bases were used. Surprisingly, when fused sodium acetate was used as a base there is a sharp increase in reaction yield at 70 ºC within 4 h of time (**Table 4B.1, entry-15**). But, when the reaction temperature increased a significant reduction in the product **4a** yield was noticed (**Table 4B.1, entries-15,16**). From this, we concluded that increasing the reaction temperature did not affect improving the product yield (**Table 4B.1, entries-15,16**). Further, different concentrations of the base were investigated. Finally, two equivalents of fused sodium acetate were found to be in the best condition with 80% yield (**Table 4B.1**, **entry-15**).

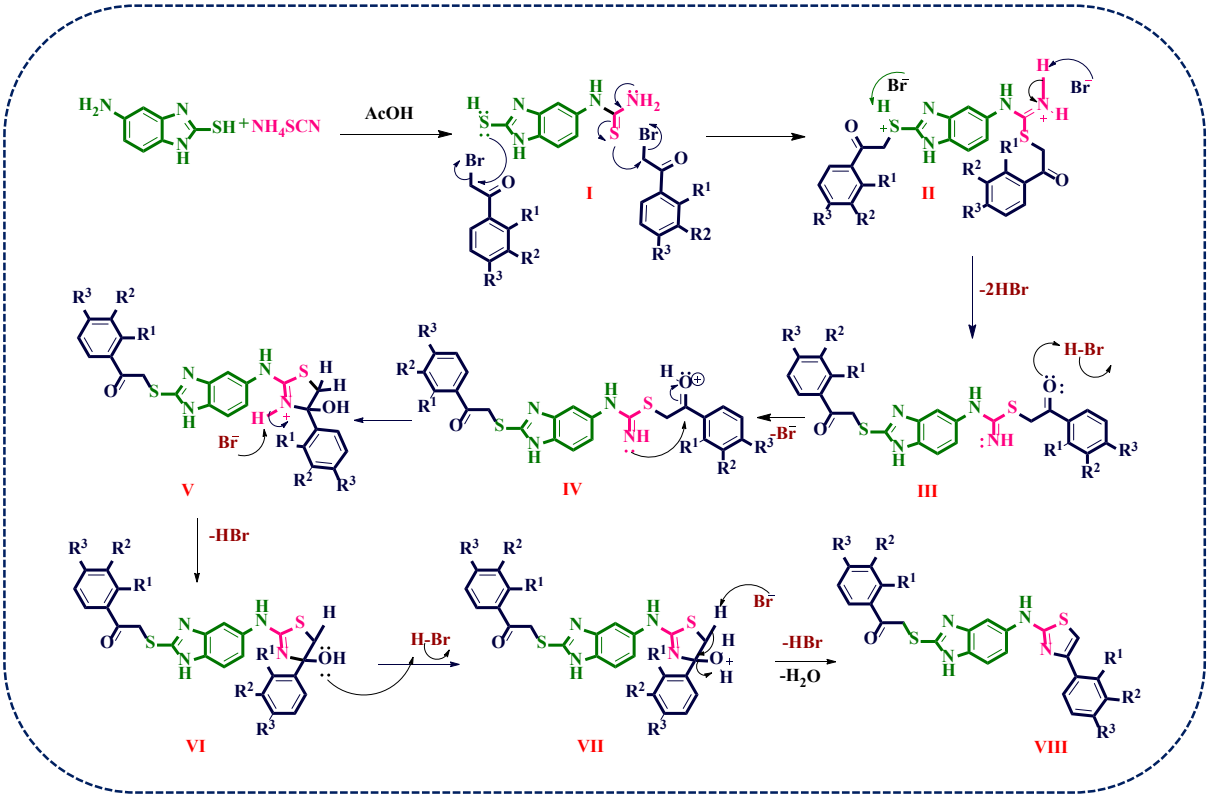

Scheme 4B.1. Plausible reaction mechanism for synthesis of thiazole derivatives.

Under the optimized reaction conditions (**Table 4B.1, entry-15**) the substrate scope of the reaction was studied using a series of α-bromo acetophenones. As shown in (**Figure 4B.2**) different substituted α-bromo acetophenones either electron-withdrawing or electron-donating groups were well tolerated (**4a-j**) and the presence of a strong electron-withdrawing group like the nitro group on the phenyl ring offered the desired product **4i** in excellent yield consequently

the presence of F, Cl, and Br groups on phenyl ring also (**4b,4c,4d**) offered products in good yield.

The final structure of the synthesized compounds (**4a-q**) was subjected to their spectral and analytical data. The ^{1}H-NMR spectrum of compound **4a** as a representative example showed a characteristic two singlet signals at 5.22 and 7.47 δ ppm due to -S-CH_2 and C_5-proton of thiazole respectively.

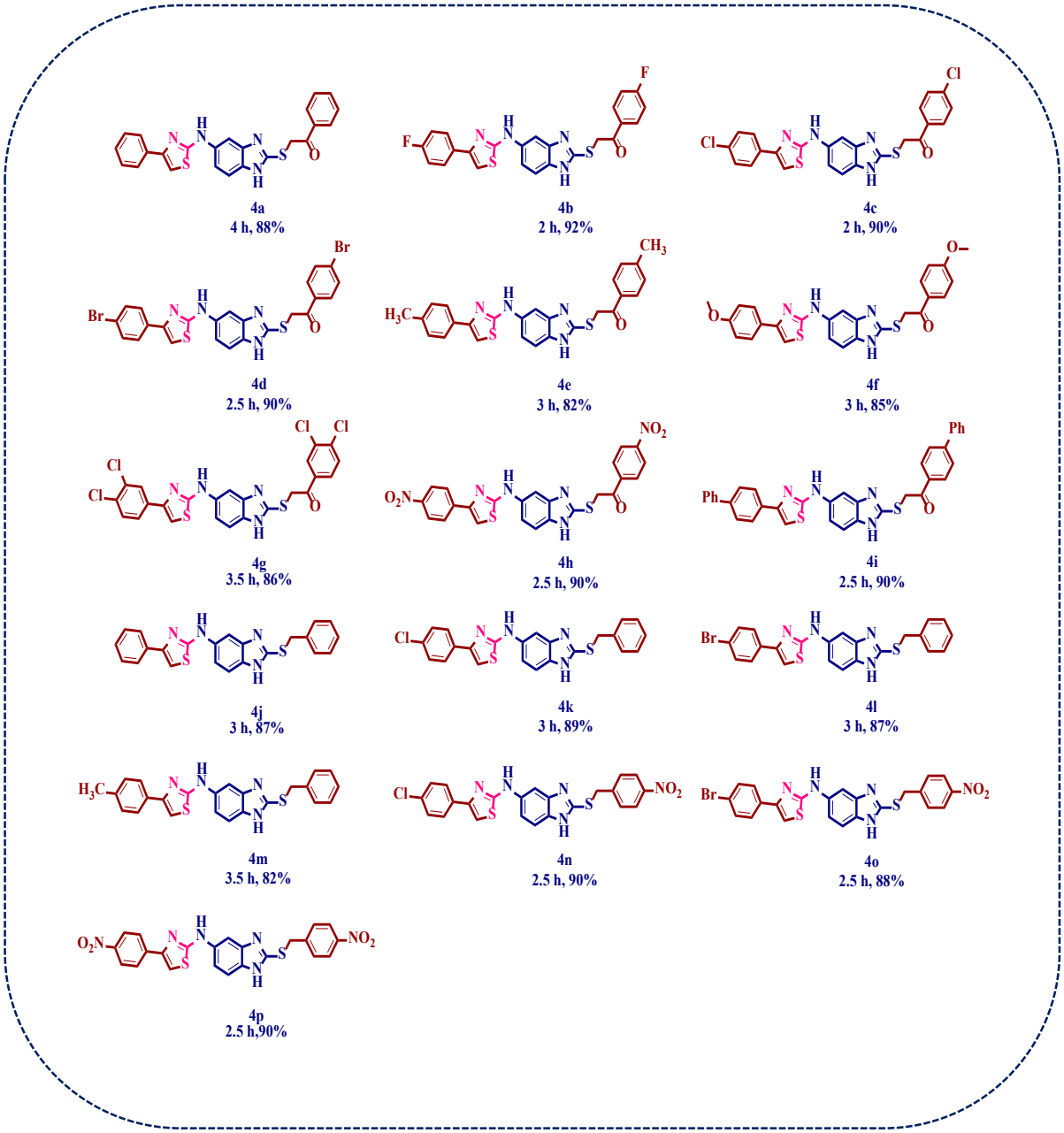

Figure 4B.2. Scope of substrates

The ^{13}C-NMR displayed a significant signal at δ_C 193.06, 172.69, 107.89, and 21.50 δ ppm are assigned for C=O, C=N, C_5 carbon of thiazole, and S-CH_2 carbons respectively. The infrared

spectra of compound **4a** show frequencies at 3404 cm^{-1}, 1685 cm^{-1}, and 1623 cm^{-1} of amine (-NH), carbonyl (-C=O), and imine (C=N) functional groups respectively. The HRMS (ESI) spectra of all the synthesized compounds are shown $[M+H]^+$ as base peck.

4B.3. Biological studies

4B.3.1. Anti-bacterial activity

The assay system used to determine the antibacterial activities of the title compounds was the agar well diffusion method. Two clinical pathogens *Proteus mirabilis* (2081), a gram-negative bacterium, and *Streptococcus Pneumoniae* (2451*)*, a gram-positive bacterium were freshly grown on a Nutrient agar medium. A loop of 48-hour-old pathogens was taken into 10 ml distilled water and added to Nutrient agar medium and poured into sterile Petri plates. After solidification, wells of 0.6 diameters were punctured with a cork borer. Further, 50 µg of sample powder is dissolved in 500µl DMSO solution. 50 µl of the dissolved sample is poured into a well with a micropipette and control with DMSO was maintained and incubated at 37 $^{\circ}C$ for 48 hours. The zone of inhibition was calculated at different time intervals of 48 hours and 96 hours.

4B.3.2. Antibacterial activity results

The *in-vitro* antibacterial activity of synthesized thiazolyl-benzimidazole derivatives **4a, 4b, 4c, 4d, 4e, 4f, 4g, 4h, 4i, 4j, 4k, 4l, 4m, 4o**, and **4p** were analyzed against Gram-positive Bacteria *Streptococcus pneumonia* (ATCC2451) and Gram-negative bacteria *Proteus Mirabilis* (ATCC2081). The *in-vitro* antibacterial activity of synthesized compounds was initially evaluated by determining their minimum inhibition concentration (MIC) values using the agar well diffusion method. Among the tested scaffolds, compound **4f** has shown a maximum value of **3.6** cm of inhibitory activity against Gram Positive *Streptococcus Pneumoniae* (MTCC2451), and compound **4k** has shown a value of **3.3** cm against Gram-negative *Proteus Mirabilis* (MTCC2081).

Table 4B.2. Antibacterial activity of synthesized thiazolyl-benzimidazole scaffolds expressed as MIC against *Proteus mirabilis* (ATCC2081) and *Streptococcus pneumoniae* (ATCC2451).

	Antibiotic activity by Zone of Inhibition (cm)		
S.No	**Compound code**	***Proteus Mirabilis* (2081)**	***Streptococcus Pneumoniae* (2451)**
1	4a	2.1^{+++}	2.1^{+++}
2	**4b**	2.25^{+++}	$\mathbf{2.85}^{++++}$
3	4c	1.35^{++}	2.1^{+++}
4	4d	1.9^{++}	1.8^{++}
5	**4e**	$\mathbf{2.75}^{+++}$	2.55^{+++}
6	**4f**	2.55^{+++}	$\mathbf{3.6}^{++++}$

7	4g	1.45^{++}	1.35^{++}
8	4h	1.5^{++}	2.1^{+++}
9	4i	0.95^{+}	1.2^{++}
10	4j	1.9^{+++}	2.25^{+++}
11	**4k**	$\mathbf{3.3}^{++++}$	2.7^{+++}
12	4l	2.3^{+++}	2.25^{+++}
13	4m	2.3^{+++}	1.95^{+++}
14	4o	2^{+++}	2.25^{+++}
15	4p	1.9^{+++}	2.25^{+++}

(++++ *Maximum* +++: *Medium* ++: *Moderate* + *Minimum* - *Nil)*

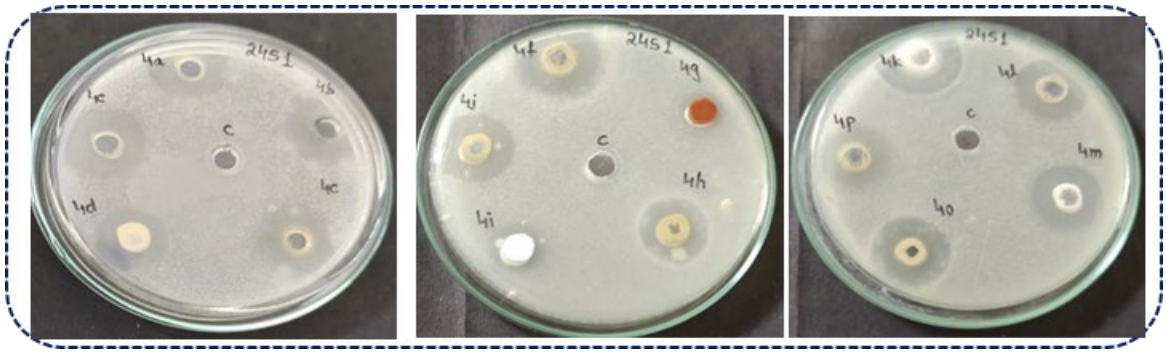

Figure 4B.3. Screening of Antibiotic Activity of compounds against *Streptococcus pneumonia* (ATCC2451) *by* Agar well diffusion method. *C is controlled with 50 µl of DMSO.

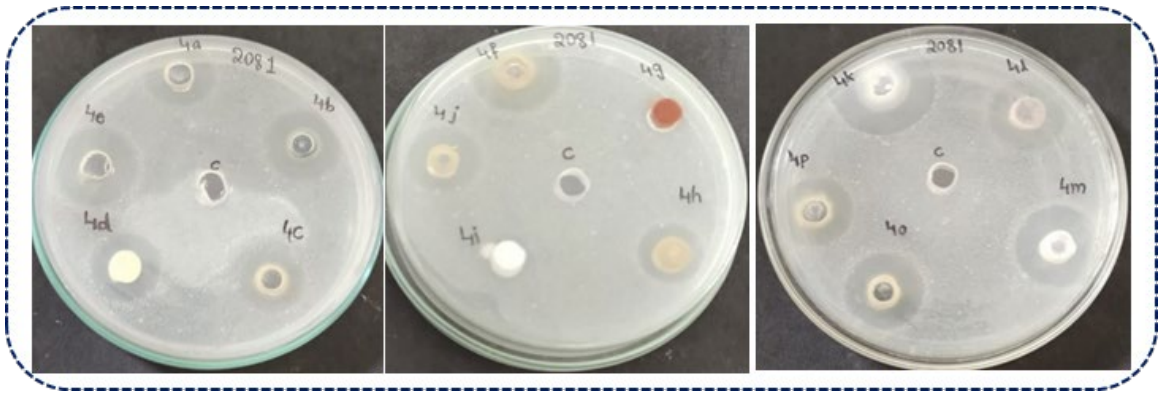

Figure 4B.4. Screening of Antibiotic Activity of compounds against *Proteus mirabilis* (ATCC2081). *C is controlled with 50 µl of DMSO**.**

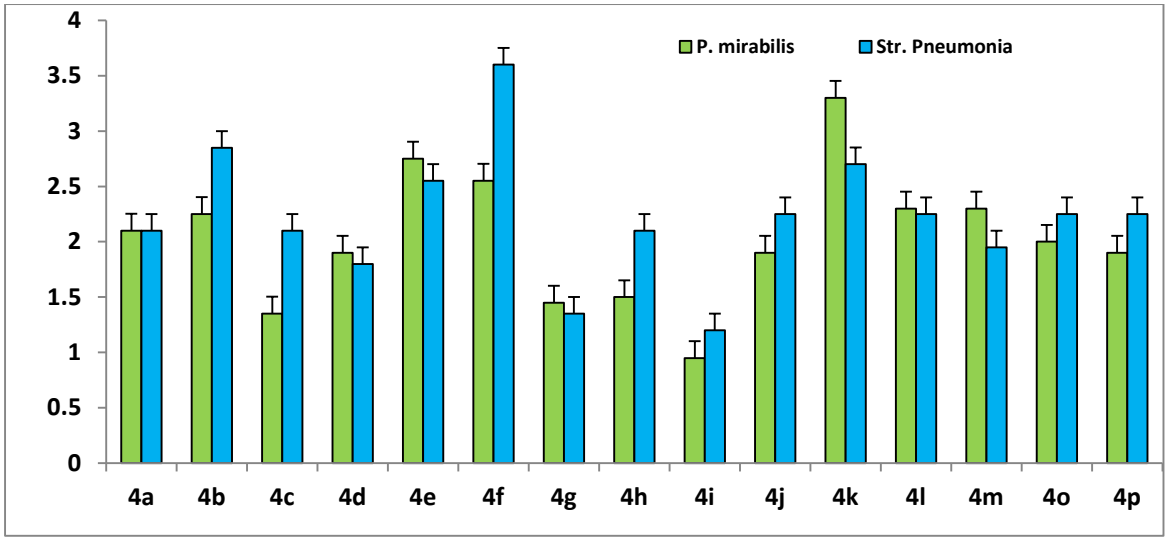

Figure 4B.5. Antibacterial activity of synthesized thiazolyl- benzimidazole scaffolds expressed as MIC against *Proteus mirabilis* (ATCC2081) and *Streptococcus pneumonia* (ATCC2451).

4B.3.3. Structure-activity relationship (SAR)

The SAR studies were evaluated by changing the substituent on the 2,3,4 position of the phenacyl bromide ring as shown in **Table 4B.2** to see the impact of the electronic effects. Among the investigated compounds for their *in-vitro* antibacterial activity when the 4th position of phenacyl bromide ring was substituted with electron-withdrawing groups like F, Cl, Br, and nitro as in **4e**, **4k** showed excellent Gram-negative *in-vitro* antibacterial activity than compound with electron releasing or without any substituents. Further, compound **4f** with electron releasing group (-OCH_3) on phenacyl bromide ring was shown excellent Gram-positive *in-vitro* activity.

4B.4. Molecular Docking and Dynamics Simulations

The demand for structurally and chemically distinct antibiotics with different modes of action is perpetual as the bacteria show the propensity to develop resistance against the therapeutic drugs that have been clinically practiced for a long [1]. The enzyme DNA gyrase B is a specific target that has received enduring interest in the search for novel antibiotics owing to its crucial role in ATP hydrolysis and bacterial DNA synthesis [2,3]. In the present report, attention has also been devoted to scrutinizing the inhibitory activity of the synthesized compounds against the *DNA* gyrase B by analysing the binding affinity and binding mode using molecular docking studies. Further, the molecular dynamics simulation has also been performed to gain insight into the dynamic behaviour, interactions, and stability of the molecule at the active site of the receptor protein.

The X-ray crystallographic structure of gyrase B (receptor protein) complexed with Novobiocin was obtained from the protein data bank (PDB ID: 1KIJ). To facilitate the docking, water and Novobiocin molecule were removed from the receptor protein and polar hydrogens were added. The grid box of sizes 84,78, and 70 were generated at 9.991, 3.548, and 46.044. The Auto Dock Vina software was utilized to perform the *in silico* molecular docking studies [4]. The minimum distance and the interaction of the ligand (synthesized compounds) with the amino acid residues of the proteins were examined with Protein-Ligand Interaction Profiler (PLIP) [5]. The best docking pose of compound **4i** obtained using docking simulation was taken into consideration for the molecular dynamics (MD) simulations. The MD simulations were executed with GROMACS employing OPLS-AA Force Field and SPC/E water model [6, 7]. The Na^+ and Cl^- ions were added to the system to maintain neutral conditions during the simulations in a cubic box. The energy minimization was carried out using the steepest descent algorithm. The system was initially equilibrated with the NVT and NPT ensemble at 300 K temperature and 1.0 bar pressure. The MD simulation was carried out for 10 ns with the time step of 2 fs and the coordinates were saved at an interval of 10 ps.

The calculated binding affinity values of the synthesized compounds at the active site of the gyrase B enzyme range from -9.8 to 12.0 kcal/mol. These values suggest that all the studied compounds show a stronger affinity towards the active site of the receptor protein. Further, the difference in the docking score of the two molecules is not very large which may be attributed due to the significant similarity in their chemical structure. The highest binding affinity value is observed for the compounds **4b**, **4h**, **4i**, **4n**, and **4p**. The binding score is comparatively higher for the Phenyl (-**Ph**) substitution as in **4i** and electron-withdrawing substituents more particularly the nitro group (-$\mathbf{NO_2}$) as in **4h**, **4n**, and **4p**.

The docked pose of the compound **4i** along with 3D and 2D view of the interacting amino acids at the active site of the protein is shown in **Figure 4B.6**. It is apparent from the figure that the binding pose of the studied scaffolds is unique and show a 'dual-arm' U-shaped binding mode on the protein. This U-shaped binding mode is uncommon in the most familiar gyrase inhibitors like quinolones and coumarins, however, it was previously reported for kibdelomycin at the active site of Staphylococcus aureus GyrB.[2] Although, a U-shaped binding mode is observed at the active site of the GyrB, nevertheless, the binding position of the synthesized compounds substantially differs from that of the kibdelomycin. Therefore, the results exclusively emphasize that the synthesized compounds have a distinct binding mode at the active site of

DNA gyrase B and may thus be beneficial to inhibit bacterial proliferation overcoming the cross-resistance for long-practiced drugs.

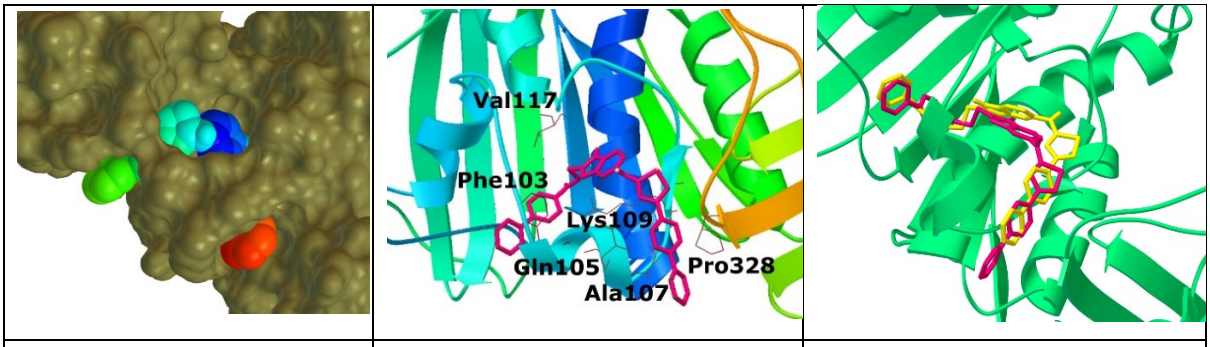

(a)	(b)	(c)

Figure 4B.6. Docked pose of compound **4i** at an active site of the gyrase protein (PDB ID: 1KIJ). (a) Surface view of 4i at an active site, (b) Docked pose of 4i along with the interacting amino acid residue of the protein, (c) overlapping structure of two different docked poses of 4i.

Close analysis of the binding pose revealed that the substituted acetophenyl or benzyl moiety mostly occupies the ATP-binding pocket of the enzyme. The N and -NH of benzimidazole and N of thiazole ring usually establish hydrogen bonding interaction with Asn45, Lys109, Val117, or Gly116 residue of the enzyme. The five-membered ring of benzimidazole or thiazole participates in the cationic interaction with the Lys109 residue while the phenyl ring involves in the pi-stacking interaction with the Phe103 residue. Moreover,

Asp45, Ile77, Phe103, Lys109, Val117, Pro328 are the amino acid residues which shows hydrophobic interactions with most of the synthesized molecules. The details of the binding affinity value and various binding interactions shown by the synthesized compounds with the protein along with the minimum distance from the residues are tabulated in **Table 4B.3**.

Table 4B.3. Binding affinity (kcal/mol), RMSD, interacting amino acid residues and distances between the ligand and interacting residues.

Molecules	Binding affinity (kcal/mol)	RMSD	Interacting amino acid residues along with the distances (Å) from the ligand				
			Hydrophobic	**Hydrogen bonding**	**π stacking**	**π cation**	**Halogen bonding**
4a	-10	1.24	Ile93 (3.58), Phe103 (3.66), Glu104 (3.83), Lys109 (3.81), Pro328 (3.59)	Lys109 (2.77), Val117 (2.85)	Phe103 (4.17)	Lys109 (3.42)	
4b	-10.6	0.725	Asn45 (3.95), Glu49 (3.67), Lys109 (3.50)	Asn45 (2.83), Lys109 (2.45), Val117 (2.45)			
4c	-10.2	1.539	Glu49 (3.78) Ile77 (3.48), Phe103 (3.58), Lys109 (3.69) Val117 (3.75)	Asn45 (2.73), Lys109 (2.78), Gly116 (2.53)		Lys109 (3.98)	
4d	-10.3	2.296	Ile93 (3.56), Phe103 (3.78), Glu104 (3.90), Tyr108 (3.53), Lys109 (3.82)	Lys109 (2.29)	Phe103 (4.15)	Lys109 (3.58)	
4e	-10.3	0.809	Asn45 (3.45), Glu49 (3.48), Ile77 (3.61), Tyr108 (3.78), Lys109 (3.71), Pro328 (3.94)	Asn45 (2.66)			
4f	-9.8	0.657	Lu49 (3.89), Ile77 (3.62), Lys109 (3.66)	Asn45 (2.89), Gly76 (3.01), Lys109 (3.16)			
4g	-10.4	1.94	Ile93 (3.55), Phe103 (3.66), Lys109 (3.59)	Asn45 (3.61), Lys109 (3.00), Val117 (2.70)	Phe103 (4.17)	Lys109 (3.53)	Gln105 (3.31)
4h	-11	0.922	Asn45 (3.55), Ile77 (3.72), Lys109 (3.66)	Asn45 (2.60), Gly113 (2.69)			
4i	**-12**	1.996	Phe103 (3.62), Lys109 (3.80), Pro328 (3.39)	Lys109 (2.30), Val117 (3.50)			

4j	-9.8	1.343	Asn45 (3.28), Glu49 (3.62), Ile77 (3.76), Phe103 (3.74), Lys109 (3.63), Val117 (3.61)	Asn45 (2.71), Lys109 (3.02)	Lys109 (3.89)
4k	-10.1	0.581	Asn45 (3.90), Glu49 (3.55), Ile77 (3.60), Phe103 (3.70), Lys109 (3.67), Val117 (3.58)	Asn45 (2.79), Lys109 (2.99)	Lys109 (3.80)
4l	-10	0.715	Asn45 (3.73), Asp48 (4.00), Ile77 (3.72), Glu104 (3.79), Tyr108 (3.45), Lys109 (3.56), Pro328 (3.49)	Lys109 (3.05)	Lys109 (3.65)
4m	-10.2	1.334	Asn45 (3.90), Glu49 (3.57), Ile77 (3.63), Phe103 (3.71), Lys109 (3.61), Val117 (3.62)	Asn45 (2.74), Lys109 (3.09)	Lys109(3.95)
4n	-10.7	1.276	Glu49 (3.82), Ile77 (3.58), Glu104 (3.88), Tyr108 (3.73), Lys109 (4.00)	Asn45 (3.33), Lys109 (2.20), Val117 (3.65)	Lys109 (3.57)
4o	-10.4	0.919	Ile77 (3.96), Glu104 (3.84), Lys109 (3.84), Pro328 (3.64)	Asn45 (3.33), Lys109 (2.31)	Lys109 (3.63)
4p	-10.7	2.361	Asn45 (3.62), Lys109 (3.46)	Asn45 (2.76), Lys109 (4.04), Gly116 (2.70)	Lys109 (4.10)

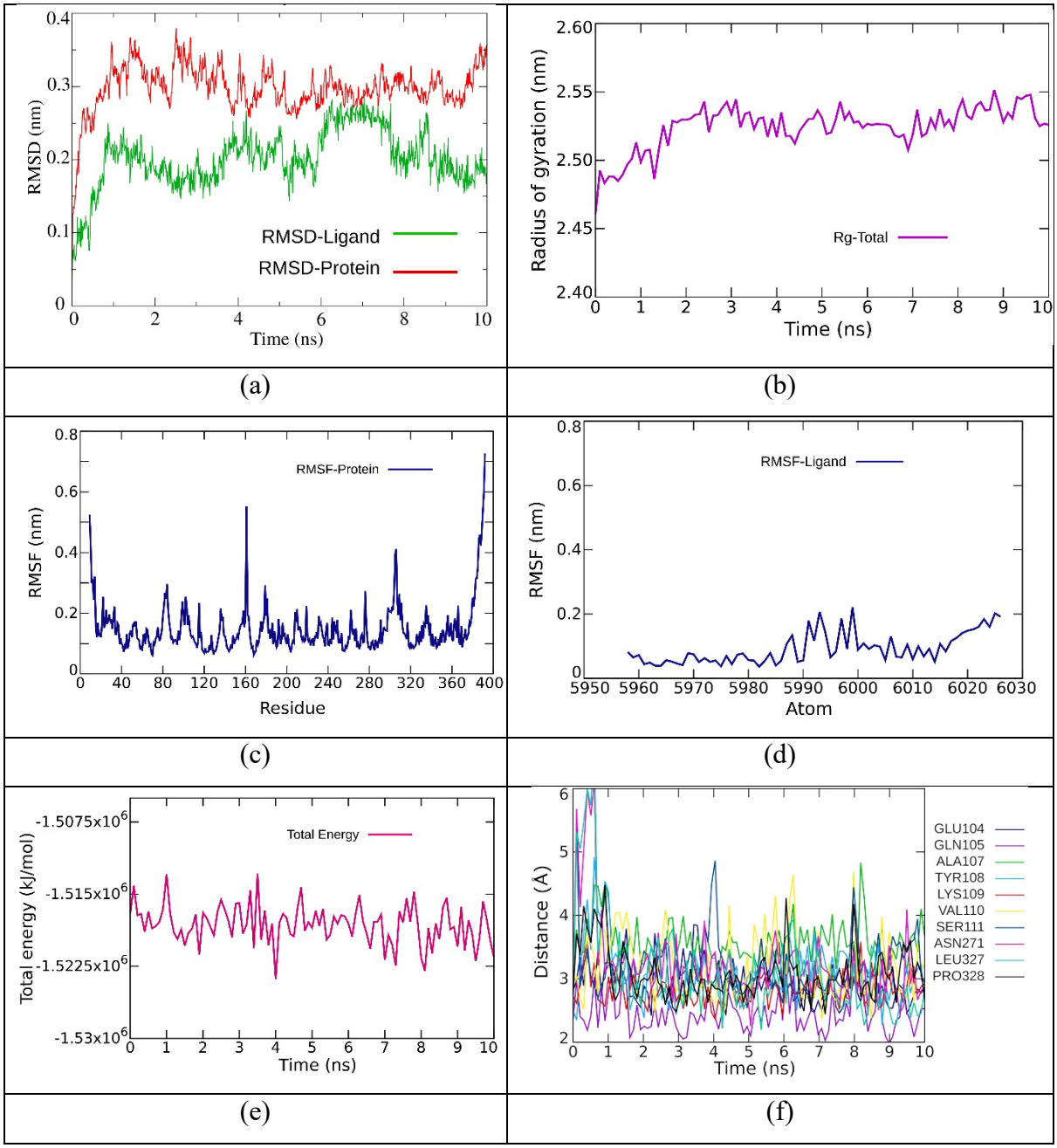

Figure 4B.7. MD analyses of 4i complexed with the gyrase protein. Variation in (a) RMSD of the protein and ligand in their complex, (b) radius of gyration (Rg) of the protein in the complex. (c) RMSF of each residue in the protein, (d) RMSF of an individual atom of the ligand in the complex. Variation in (e) Total energy of the system, and (f) Distance between amino acids residues and the compound 4i.

En route to probing the reproducibility of the binding pose, the root mean square deviation (RMSD) between the two docked conformers has also been estimated at the active site of the receptor protein. The calculated RMSD value for the different compounds is also given in

Table 4B.3 of ESI. It has been noticed that the RMSD values range between 0.581 to 2.361 which explains the reproducibility of the docking pose at the active site of the enzyme. Therefore, the studied compounds could potentially inhibit the functioning of DNA gyrase and serve as a promising antibiotic drug.

Thereafter, attention has been focused to perform molecular dynamics simulations for further insight into the stability of the compound at the active site of the gyrase protein. **Figure 4B.7** displays the plot of the variation in RMSD, the radius of gyration (Rg), total energy, important distances with the amino acid residues during the simulation, and the RMS fluctuation (RMSF) for the protein as well as the ligand.

It can be seen from the figure that the RMSD value of the gyrase protein progressively increased to 0.35 nm within 1.5 ns and stabilized in the range around 2.8–3.5 nm until the simulation time. Likewise, the RMSD value of the ligand is increased to 0.24 in the first 1.5 ns and fluctuates around 1.5–2.5 nm during the simulation. **Figure 4B.7** also reveals that the Rg value only slightly increases from 2.46 to 2.53 nm in the initial 2 ns and then fluctuates within the range of 2.1–2.4 nm till the end of the simulations. Further analysis reveals that the total energy of the system almost remains the same with marginal fluctuations during the simulation. Interestingly, it has been observed that most RMSF of the residues in the protein more particularly the loop 98–118 (active site) is small. The RMSF value for most of the amino acid residues lies below 0.25 nm. Analogous to the protein, the fluctuations in each atom of the ligand are small and do not exceed 0.2 nm. Moreover, the analysis of the variation in the distance unveils that the separation between the ligand and the amino acid residues Glu104, Gln105, Ala107, Tyr108, Lys109, Val110, Ser111, Asn271, Leu327, and Pro328 is maintained below 4 Å. All these shreds of evidence from the MD simulations advocates that the compound **4i** is stable at the active site of the gyrase protein.

The geometries of the protein-ligand (**4i**) complex obtained at an interval of 2 ns are considered to elucidate the interaction of ligand (**4i**) at the active site of the receptor protein. The protein-ligand (**4i**) interaction in these complexes is unraveled using the PLIP and depicted in **Figure 4B.8**. It is evident from the figure that the ligand molecule (**4i**) remains bound at the active site of the protein until the end of the simulation. Further, the unique U-shaped binding mode of the compound (**4i**) is retained during the entire simulations. Close analysis of the figure reveals that the interaction of 4i with Phe103, Lys109, and Pro328 is maintained throughout the simulations.

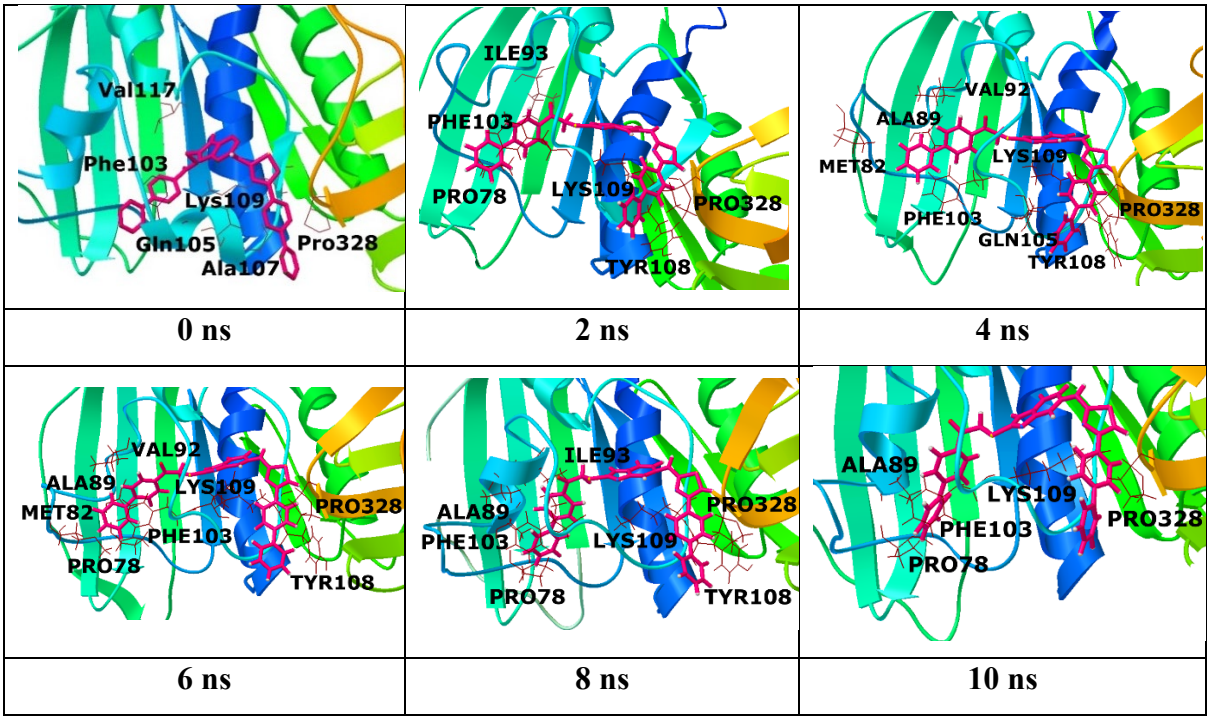

Figure 4B.8. The trajectories of **4i** complexed with gyrase protein along with the interacting amino acid residues obtained during the molecular dynamics simulation.

4B.5. Conclusion

In conclusion, we have synthesized a series of novel thiazolyl-benzimidazole scaffolds *via* the one-pot, four-component reaction by using 5-amino-2-mercaptobenzimidole **1**, aryl alkyl halides **2**, ammonium thiocyanate **3,** and substituted α-bromo-acetophenones **4** in 2 mL of glacial acetic acid to give title compounds (**5a-j**) and (**4a-j**) with good to excellent yields in a shorter time. Further, the synthesized scaffolds were screened for their *in-vitro* antibacterial activity studies using Gram-positive *Streptococcus Pneumonia* (2451) bacteria and Gram-negative *Proteus Mirabilis* (2081) bacteria. Based on the MIC results, it was observed that the most active thiazolyl-benzimidazole derivatives **4f, 4k, 4b**, and **4k** are shown significant anti-bacterial activity with the zone of inhibition values of **2.75** cm and **3.3** cm against Gram-negative *Proteus Mirabilis* bacteria and Gram-positive activity against *Streptococcus Pneumonia* with the zone of inhibition values **2.85** cm and **3.6** cm respectively. Similarly, reaming synthesized compounds exhibited moderate to good antibiotic activity. The *in-vitro* anti-bacterial activity, and molecular docking studies of the title compounds proven that these are promising anti-bacterial active skeletons.

The molecular docking reveals that the synthesized complex bounds as a “dual-arm” U-shaped binding pose at the active site of the receptor protein. The mode of binding exhibited by the synthesized compounds significantly differs from the clinically approved quinolones and

coumarins-based drugs. Further, the outcomes of the molecular dynamics study reinforce the stability of the ligand retaining the binding mode during simulation. Thus, the results exclusively emphasize that the synthesized compounds have the potential to cease bacterial proliferation by inhibiting the activity of the gyrase enzyme responsible for DNA replication. Therefore, the synthesized could act as a promising antibiotic and may be beneficial to overcome the cross-resistance to the other antibacterial agents owing to its different binding modes.

4B.6. Experimental section

General procedure for the synthesis of **1-phenyl-2-((5-((4-phenylthiazol-2-yl)amino)-1*H*-benzo[*d*]imidazol-2-yl)thio)ethan-1-one compounds (4a-i):**

A mixture of 5-amino-2-marcaptobenzimidazole (1.0 mmol), ammonium thiocyanate **2** (1.0 mmol) different substituted α-Bromo-acetophenones **3(a-j**) (2.0 mmol), and fused sodium acetate (2.0 mmol) were taken in a round bottom flask and the reaction mixture was refluxed in acetic acid (2 ml) at 70 ^{0}C for 4 h. After completion of the reaction (checked through TLC, 50:50, n-hexane: EtOAc), the reaction mixture was cooled to room temperature. The solid separated was filtered, washed with water, dried, and recrystallized from ethanol.

General procedure for the synthesis of ***N*-(2-(benzylthio)-1*H*-benzo[*d*]imidazol-5-yl)-4-phenylthiazol-2-amine compounds (4j-p):**

A mixture of 5-amino-2-marcaptobenzimidazole (1.0 mmol), different substituted benzyl bromides (**2a-b**) (1.0 mmol), and fused sodium acetate (1.0 mmol) was taken in a round bottom flask and the reaction mixture was refluxed in acetic acid (2 ml) at 70 ^{0}C for 1 h. To this reaction mixture ammonium thiocyanate 1.0 mmol, fused sodium acetate 1.0 mmol, and α-Bromo-acetophenones **4 (a-j**) were added and refluxed for another 3h. After completion of the reaction (checked through TLC, 50:50, n-hexane: EtOAc), the reaction mixture was cooled to room temperature. The solid separated was filtered, washed with water, dried, and recrystallized from ethanol.

4B.7. Characterization data of products

1-Phenyl-2-((5-((4-phenylthiazol-2-yl)amino)-1*H*-benzo[*d*]imidazol-2-yl)thio)ethan-1-one.4a

White solid: yield: 88% ; m.p: 262-264 ºC FT-IR (KBr, cm^{-1}): 3407 (NH), 1685(C=O), 1623 (C=N); **^{1}H NMR** (400 MHz, DMSO-d_6) δ ppm 8.08-8.07 (m, 5H, Ar-H), 7.74-7.70 (m, 3H, Ar-H), 7.62-7.58 (m, 5H, Ar-H), 7.47 (s, 1H, thiazole proton), 7.18 (s, 1H, NH proton), 5.22 (s, 2H, S-CH_2 protons), 1.91 (s, 1H, NH proton), **^{13}C NMR** (100 MHz, DMSO-d_6) δ: 193.06, 172.69, 152.40, 135.37, 134.77, 134.59, 129.88, 129.64, 129.42, 129.09, 128.95, 118.80, 114.74, 107.89, 21.50; ESI-HRMS: *m/z* Calcd for : $C_{24}H_{19}N_4OS_2$ $[M+H]^+$: 443.0995 found: 443.0996.

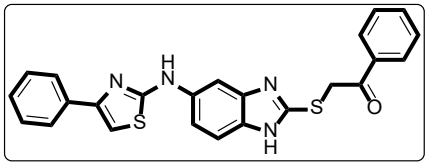

1-(4-Fluorophenyl)-2-((5-((4-(4-fluorophenyl)thiazol-2-yl)amino)-1*H*-benzo[*d*]imidazol-2-yl)thio)ethan-1-one. 4b

White solid: yield: 92% ; m.p. 254-256 ºC FT-IR (KBr, cm^{-1}): 3442 (NH), 1677 (C=O), 1623 (C=N); **^{1}H NMR** (400 MHz, DMSO-d_6 δ ppm): 8.25 (s, 1H, thiazole proton), 8.20 – 8.15 (m, 4H), 7.60 (d, *J* = 8.4 Hz, 1H), 7.54 (s, 1H, NH proton), 7.40-7.36 (m, 4H, Ar-H), 7.23 (d, *J* = 8.4 Hz, 3H), 5.23 (s, 2H, S-CH_2 protons), 1.91 (s, 1H, NH proton), **^{13}C NMR** (100 MHz, DMSO-d_6) δ: 191.41, 167.27, 164.75, 150.61, 139.74, 137.10, 133.70, 132.08, 128.95, 125.05, 124.08, 121.80, 116.66, 116.44, 113.53, 107.88, 41.59; ESI-HRMS: *m/z* Calcd for : $C_{24}H_{17}F_2N_4OS_2$ $[M+H]^+$: 479.0806 found: 479.1784.

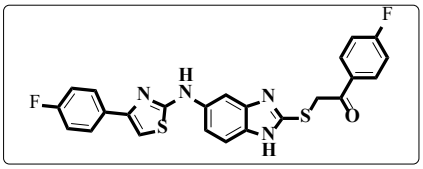

1-(4-Chlorophenyl)-2-((5-((4-(4-chlorophenyl)thiazol-2-yl)amino)-1*H*-benzo[*d*]imidazol-2-yl)thio)ethan-1-one. 4c

White solid: yield: 90% ; mp. 262-264 ºC FT-IR (KBr, cm^{-1}): 3347 (NH), 1675 (C=O), 1624 (C=N); **^{1}H NMR** (400 MHz, DMSO-d_6 δ ppm): 10.55 (s, 1H, NH proton), 8.36 (s, 1H, thiazole proton), 8.08 (d, *J* = 8.8 Hz, 2H, Ar-H), 7.98 (d, *J* = 8.4 Hz, 2H, Ar-H), 7.70 (d, *J* = 8.8 Hz, 2H, Ar-H), 7.57 (s, 1H, NH proton), 7.50 (d, *J* = 8.4 Hz, 2H, Ar-H), 7.46 (s, 1H, Ar-H), 7.41 (dd, *J* = 8.8,1.6 Hz, 2H, Ar-H), 5.25 (s, 2H, S-CH_2 protons). **^{13}C NMR** (100 MHz, DMSO-d_6) δ : 192.11, 163.17, 149.31, 148.95, 139.58, 132.57, 130.92, 129.57, 129.13, 127.94, 114.33, 104.85, 41.72 : ESI-HRMS: *m/z* Calcd for : $C_{24}H_{17}Cl_2N_4OS_2$ $[M+H]^+$: 511.0215 found: 511.1174.

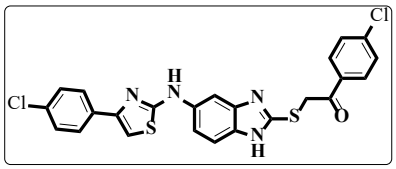

1-(4-Bromophenyl)-2-((5-((4-(4-bromophenyl)thiazol-2-yl)amino)-1*H*-benzo[*d*]imidazol-2-yl)thio)ethan-1-one. 4d

White solid: yield: 90%; mp. 270-272 ºC FT-IR (KBr, cm^{-1}): 3399 (NH), 1672 (C=O), 1631 (C=N); **^{1}H NMR** (400 MHz, DMSO-*d_6* δ ppm); 8.01-7.99 (m, 4H, Ar-H), 7.83-7.81 (m, 4H, Ar-H), 7.56 (s, 1H, thiazole proton), 7.54 (s, 1H, Ar-H), 7.42 (brs, 1H, NH proton), 7.13 (dd, *J* = 8.5, 1.8 Hz, 2H, Ar-H), 5.14 (s, 2H, S-CH_2-protons) **^{13}C NMR** (100 MHz, $CDCl_3$+DMSO-*d_6*) δ: 192.06, 150.57, 139.67, 134.30, 132.51, 130.96, 128.97, 125.14, 124.17, 121.93, 113.53, 107.97, 41.51; ESI-HRMS: *m/z* Calcd for : $C_{24}H_{17}Br_2N_4OS_2$ $[M+H]^+$: 598.9205 found: 598.9166.

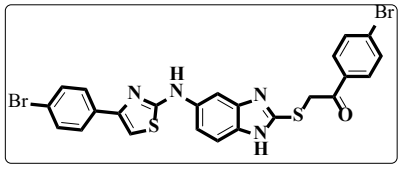

1-(p-Tolyl)-2-((5-((4-(p-tolyl)thiazol-2-yl)amino)-1*H*-benzo[*d*]imidazol-2-yl)thio)ethan-1-one. 4e

White solid: yield: 82% ; m.p. 257-259 ºC FT-IR (KBr, cm^{-1}): 3438 (NH), 1675 (C=O), 1629 (C=N); **^{1}H NMR** (400 MHz, $CDCl_3$+DMSO-*d_6* δ ppm): 10.26 (s, 1H, NH proton), 8.11 (s, 1H, thiazole proton), 7.99 (d, *J* = 8.4 Hz, 2H, Ar-H), 7.66 – 7.62 (m, 2H, Ar-H), 7.62 (s, 1H, Ar-H), 7.40-7.36 (m, 4H, Ar-H), 7.30 (dd, *J* = 8.8 Hz, 2.0Hz 2H, Ar-H), 5.26 (s, 2H, S-CH_2 protons), 2.45 (s, 6H, aliphatic), 2.13 (s, 1H, NH proton). **^{13}C NMR** (100 MHz, $CDCl_3$+DMSO-*d_6*) δ: 191.41, 169.15, 152.72, 149.85, 146.20, 145.30, 137.89, 132.78, 132.55, 129.91, 129.69, 129.19, 129.02, 113.22, 42.27, 21.79; ESI-HRMS: *m/z* Calcd for : $C_{26}H_{23}N_4OS_2$ $[M+H]^+$: 471.1308 found: 471.2280.

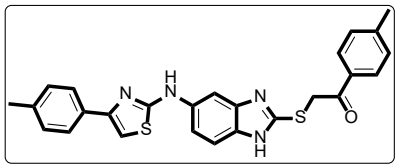

1-(4-Methoxyphenyl)-2-((5-((4-(4-methoxyphenyl)thiazol-2-yl)amino)-1*H*-benzo[*d*]imidazol-2-yl)thio)ethan-1-one. 4f

white solid: yield: 85%; mp. 259-261 ºC, FT-IR (KBr, cm^{-1}):) 3380 (NH), 1667 (C=O), 1629 (C=N);^{1}H NMR (400 MHz, $CDCl_3$+ DMSO-*d_6* δ ppm): 10.25 (s, 1H, Ar-H), 8.61 (s, 1H, Ar-H), 8.12 (s, 1H, Ar-H), 8.12-8.05 (m, 3H, Ar-H), 7.89 (d, *J* = 9.2 Hz, 1H, Ar-H), 7.58 – 7.50 (m, 2H, Ar-H), 7.08 (d, *J* = 8.0 Hz, 2H), 7.03 (s, 1H, Ar-H), 6.97 (d, *J* = 8.8 Hz, 2H, Ar-H), 5.32 (s, 2H, S-CH_2- protons), 3.91 (s, 3H, Aliphatic), 3.83 (s, 3H, aliphatic); **^{13}C NMR** (100 MHz, DMSO-*d_6*) δ; 191.46, 164.28, 152.34, 136.99, 134.89, 131.42, 129.17, 128.22, 118.29, 114.63, 107.56, 56.16: ESI-HRMS: *m/z* Calcd for: $C_{26}H_{23}N_4O_3S_2$ $[M+H]^+$: 503.1206 found: 503.1237**.**

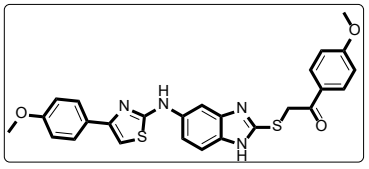

1-(3,4-Dichlorophenyl)-2-((5-((4-(3,4-dichlorophenyl)thiazol-2-yl)amino)-1*H*-benzo[*d*]imidazol-2-yl)thio)ethan-1-one. 4g

Pale yellow solid: yield: 86%; mp. 270-272 ºC FT-IR (KBr, cm^{-1}): 3399 (NH), 1672 (C=O), 1631 (C=N); **^{1}H NMR** (400 MHz, DMSO-d_6 δ ppm); 10.66 (s, 1H, Ar-H), 8.40 (s, 1H, Ar-H), 8.03 (dd, *J* = 8.6, 3.4 Hz, 2H, Ar-H), 7.79 (d, *J* = 2.0 Hz, 1H, Ar-H), 7.73 (d, *J* = 2.4 Hz, 1H, Ar-H), 7.65 (dd, *J* = 8.4, 2.0 Hz, 1H, Ar-H), 7.57 (s, 1H, Ar-H), 7.54 (dd, *J* = 8.4, 2.0 Hz, 2H), 7.45 (s, 1H, Ar-H), 7.39 (d, *J* = 8.8 Hz, 1H), 5.18 (s, 2H, S-CH_2-protons); **^{13}C NMR** (100 MHz, DMSO-d_6) δ; 193.43, 148.25, 145.92, 139.12, 137.89, 134.53, 133.19, 133.01, 132.63, 132.48, 132.31, 132.05, 130.96, 130.25, 128.10, 116.18, 114.18, 109.50, 43.87: ESI-HRMS: *m/z* Calcd for $C_{24}H_{15}Cl_4N_4OS_2$ $[M+H]^+$ 578.9436: found: 578.9432.

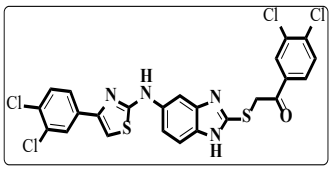

1-(4-Nitrophenyl)-2-((5-((4-(4-nitrophenyl)thiazol-2-yl)amino)-1*H*-benzo[*d*]imidazol-2-yl)thio)ethan-1-one. 4h

Orange solid: yield: 90%; mp. 209-211 ºC FT-IR (KBr, cm^{-1}): 3380 (NH), 1667 (C=O), 1629 (C=N); ^{1}H NMR (400 MHz, DMSO-d_6 δ ppm): 10.70 (s, 1H, Ar-H), 8.44-8.42 (m, 3H, Ar-H), 8.30 (dd, *J* = 9.2, 2.4 Hz, 4H, Ar-H), 8.23 (d, *J* = 8.0Hz, 2H), 7.79 (s, 1H, Ar-H), 7.63 (s, 1H, Ar-H), 7.60 (s, 1H, Ar-H), 7.47 (dd, *J* = 8.8, 2.0 Hz, 1H), 5.36 (s, 2H, S-CH_2-protons); **^{13}C NMR** (100 MHz, DMSO-d_6) δ: 192.11, 169.15, 163.64, 150.83, 148.85, 148.44, 146.75, 140.76, 139.89, 139.12, 137.22, 134.05, 130.47, 127.13, 124.46, 116.34, 114.29, 109.01, 100.33, 42.35: ESI-HRMS: *m/z* Calcd for : $C_{24}H_{17}N_6O_5S_2$ $[M+H]^+$: 533.0696 found: 533.0690.

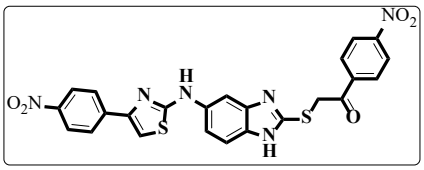

1-([1,1'-Biphenyl]-4-yl)-2-((5-((4-([1,1'-biphenyl]-4-yl)thiazol-2-yl)amino)-1*H*-benzo[*d*]imidazol-2-yl)thio)ethan-1-one. 4i

White solid: yield: 90%; mp. 246-248 ºC, FT-IR (KBr, cm^{-1}): 3407 (NH), 1685(C=O), 1623 (C=N); **^{1}H NMR** (400 MHz, DMSO-d_6 δ ppm); 10.71 (brs, 1H, NH proton), 10.29 (s, 1H, NH proton), 8.17-8.15 (m, 4H), 7.94-7.89 (m, 4H), 7.80-7.77 (m, 5H), 7.56 – 7.52 (m, 5H), 7.48-7.46 (m, 2H, Ar-H), 7.41 (s, 1H, thiazole proton), 7.13 (d, *J* = 6.8, 1H, Ar-H), 5.20 (s, 2H, S-CH_2 protons); **^{13}C NMR** (100 MHz, DMSO-d_6) δ; 192.85, 152.07, 145.72, 139.14, 139.04, 137.94, 134.37, 129.80, 129.73, 129.65, 129.09, 127.53, 127.11, 117.75, 114.71, 107.67, 40.75 :ESI-HRMS: *m/z* Calcd for: $C_{36}H_{27}N_4OS_2$ $[M+H]^+$: 595.1621 found:595.1635.

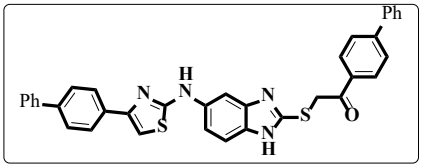

N-(2-(Benzylthio)-1*H*-benzo[*d*]imidazol-5-yl)-4-phenylthiazol-2-amine. 4j

White solid: yield: 87%; mp 170-172 °C; FT-IR (KBr, cm^{-1}): 3348 (NH), 1625 (C=N);**^{1}H NMR** (400 MHz, DMSO-d_6 δ pp.m); 7.58 (s, 1H, Ar-H), 7.56 (s, 1H, Ar-H), 7.43 (d, J = 7.2 Hz, 2H), 7.33 – 7.27 (m, 5H, Ar-H), 7.23 (s, 1H, Ar-H), 7.20 – 7.10 (m, 5H, Ar-H), 7.04 (s, 1H, Ar-H), 4.61 (s, 2H, S-CH_2-protons): **^{13}C NMR** (100 MHz, DMSO-d_6) δ; 159.04, 148.85, 142.93, 131.11, 130.07, 129.75, 129.41, 129.26, 129.11, 128.86, 128.77, 128.49, 128.21, 127.08, 126.88, 106.75, 37.43: ESI-HRMS: *m/z* Calcd for : $C_{23}H_{19}N_4S_2$ Exact Mass: 415.1046 $[M+H]^+$ found: 415.1030.

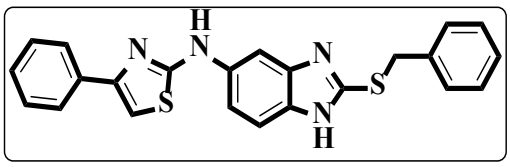

N-(2-(Benzylthio)-1*H*-benzo[*d*]imidazol-5-yl)-4-(4-chlorophenyl)thiazol-2-amine. 4k

White solid: yield: 89%; mp. 150-152 °C; FT-IR (KBr, cm^{-1}): 3379 (NH), 1626 (C=N); **^{1}H NMR** (400 MHz, DMSO-d_6 δ ppm); 7.58 (s, 1H, Ar-H), 7.56 (s, 1H, Ar-H), 7.43 (d, J = 8.8 Hz, 2H), 7.33-7.30 (m, 5H, Ar-H), 7.23 (s, 1H), 7.19 – 7.15 (m, 4H, Ar-H), 7.12 (dd J=8.4, 2.0, Hz, 1H, Ar-H), 4.61 (s, 2H, S-CH2- protons); **^{13}C NMR** (100 MHz, $CDCl_3$+DMSO-d_6) δ: 167.26, 151.50, 135.52, 135.32, 134.75, 131.58, 129.08, 128.90, 128.16, 127.60, 123.76, 122.83, 113.95, 112.56, 105.82, 37.14: ESI-HRMS: *m/z* Calcd for : $C_{23}H_{18}ClN_4S_2$ $[M+H]^+$: 449.0656 found: 449.0650.

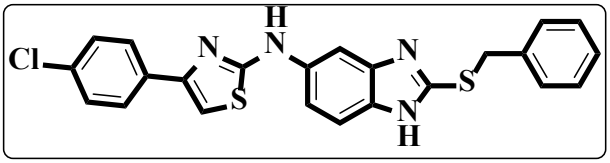

***N*-(2-(Benzylthio)-1*H*-benzo[*d*]imidazol-5-yl)-4-(4-bromophenyl)thiazol-2-amine. 4l**

Pale yellow solid: yield: 87%; mp. 169-171 °C; FT-IR (KBr, cm^{-1}): 3370 (NH), 1633 (C=N); **^{1}H NMR** (400 MHz, DMSO-d_6 δ ppm); 7.99 (d, J = 8.8 Hz, 2H, Ar-H), 7.81 (d, J = 8.8 Hz, 2H, Ar-H), 7.56 (s, 1H, Ar-H), 7.54 (s, 1H, Ar-H), 7.43 (d, J = 2.0 Hz, 1H, Ar-H), 7.31-7.29 (m, 3H, Ar-H), 7.16 – 7.13 (m, 3H, Ar-H), 7.04 (s, 2H, Ar-H), 5.13 (s, 2H, S-CH_2-protons); **^{13}C NMR** (100 MHz, DMSO-d_6) δ; 165.89, 152.55, 132.90, 132.17, 132.01, 131.85, 131.76, 131.11, 130.12, 129.95, 129.77, 129.36, 128.69, 128.51, 127.11, 126.89, 116.57, 108.12, 89.87, 37.42: ESI-HRMS: *m/z* Calcd for : $C_{23}H_{18}BrN_4S_2$ [$M+H]^+$: 493.0151 found: 493.0149.

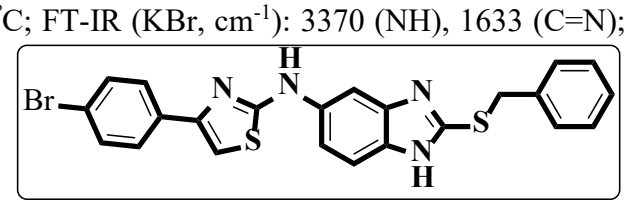

N-(2-(Benzylthio)-1*H*-benzo[*d*]imidazol-5-yl)-4-(p-tolyl)thiazol-2-amine. 4m

White solid: yield: 82%; mp. 174-176 °C; FT-IR (KBr, cm^{-1}): 3370 (NH), 1631 (C=N);**^{1}H NMR** (400 MHz, $CDCl_3$+DMSO-d_6 δ ppm): 12.62 (s, 1H, NH proton), 8.07 (s, 1H, Ar-H), 8.03 (d, J = 9.2 Hz, 2H, Ar-H), 7.54 (d, J = 8.4 Hz, 2H, Ar-H), 7.51 (d, J = 2.0 Hz, 1H, Ar-H), 7.20 – 7.17 (m, 4H, Ar-H), 7.16 (s, 1H, Ar-H),

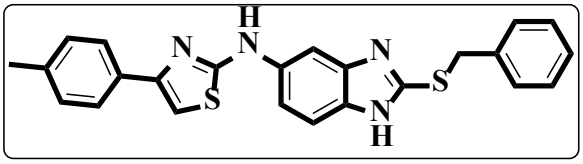

7.10 (d, *J* = 2.0 Hz, 1H, Ar-H), 7.08 (d, *J* = 2.0 Hz, 1H, Ar-H), 7.02 (d, *J* = 9.2 Hz, 2H, Ar-H), 5.15 (s, 2H, S-CH2-protons), 3.86 (s, 3H, aliphatic): ESI-HRMS: *m/z* Calcd for: $C_{24}H_{21}N_4S_2$ $[M+H]^+$: 429.1202 found: 429.1197.

4-(4-Chlorophenyl)-*N*-(2-((4-nitrobenzyl)thio)-1*H*-benzo[*d*]imidazol-5-yl)thiazol-2-amine. 4n

White solid: yield: 90%; mp. 164-166 °C; FT-IR (KBr, cm^{-1}): 3375 (NH), 1625 (C=N); **^{1}H NMR** (400 MHz, DMSO-d_6 δ ppm): 9.25 (s, 1H, Ar-H), 8.18 (d, *J* = 8.8 Hz, 2H, Ar-H), 7.75 (d, *J* = 8.8 Hz, 2H, Ar-H), 7.52 (s, 1H, Ar-H), 7.34 (d, *J* = 8.8 Hz, 2H, Ar-H), 7.26 – 7.23 (m, 4H, Ar-H), 7.18 (d, *J* = 2.0 Hz, 1H, Ar-H), 7.16 (d, *J* = 2.0 Hz, 1H, Ar-H), 4.72 (s, 2H, S-CH_2-protons); **^{13}C NMR** (100 MHz, DMSO-d_6) δ; 170.02, 151.38, 147.20, 146.01, 139.35, 137.15, 134.30, 133.04, 132.48, 130.87, 130.59, 129.50, 126.36, 124.11, 117.81, 114.94, 110.67, 105.05, 34.97: ESI-HRMS: *m/z* Calcd for : $C_{23}H_{17}ClN_5O_2S_2$ [M+H] $^+$: 494.0507 found: 494.0554.

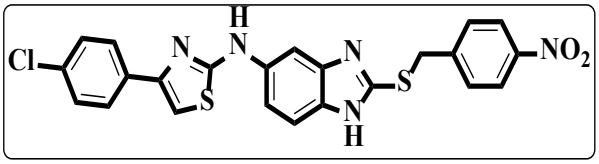

4-(4-Bromophenyl)-*N*-(2-((4-nitrobenzyl)thio)-1*H*-benzo[*d*]imidazol-5-yl)thiazol-2-amine. 4o

White solid: yield: 88%%; mp. 177-179 °C; FT-IR (KBr, cm^{-1}): 3396 (NH), 1628 (C=N);**^{1}H NMR** (400 MHz, DMSO-d_6 δ ppm): 9.24 (s, 1H, Ar-H), 8.18 (d, *J* = 8.8 Hz, 2H), 8.01 (d, *J* = 8.8 Hz, 1H), 7.75 (d, *J* = 8.8 Hz, 2H), 7.73 (d, *J* = 2.0 Hz, 1H), 7.63 (d, *J* = 8.8 Hz, 1H), 7.54 (s, 1H, Ar-H), 7.52 (s, 1H, Ar-H), 7.48 (d, *J* = 8.4 Hz, 2H, Ar-H), 7.23 (s, 1H, Ar-H), 7.17 (d, *J* = 8.8 Hz, 2H, Ar-H), 4.72 (s, 2H, S-CH2-protons); **^{13}C NMR** (100 MHz, DMSO-d_6) δ: 152.16, 151.40, 147.22, 145.93, 134.75, 134.57, 132.46, 130.95, 130.77, 130.60, 128.62, 124.13, 114.95, 114.75, 108.55, 107.99, 35.02 : ESI-HRMS: *m/z* Calcd for : $C_{23}H_{17}BrN_5O_2S_2$ [M+H] $^+$: 538.0002 found: 538.0037.

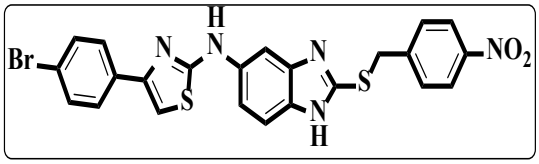

***N*-(2-((4-Nitrobenzyl)thio)-1*H*-benzo[*d*]imidazol-5-yl)-4-(4-nitrophenyl)thiazol-2-amine. 4p**

White solid: yield: 90%; mp. 180-182 °C; FT-IR (KBr, cm^{-1}): 3408 (NH), 1629 (C=N);**^{1}H NMR** (400 MHz, DMSO-d_6 δ ppm): 10.81 (s, 1H, Ar-H), 8.58 (s, 1H, Ar-H), 8.42 (d, *J* = 8.8 Hz, 2H, Ar-H), 8.33 – 8.30 (m, 3H, Ar-H), 8.28 – 8.24 (m, 4H, Ar-H), 7.80 (s, 1H, Ar-H), 7.65 (d, *J* = 8.8 Hz, 1H), 7.51 (dd, *J* = 9.0, 1.8 Hz, 1H), 5.47 (s, 2H, S-CH_2-protons); **^{13}C NMR** (100 MHz, DMSO-d_6) δ:163.56, 150.77, 148.38, 146.66, 140.65, 139.13, 133.89, 130.61, 130.44, 127.06, 124.52, 124.39, 124.00,

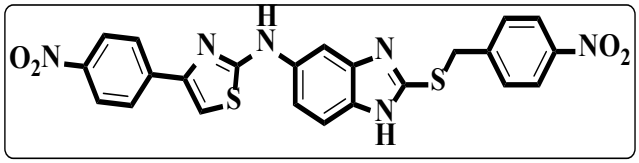

114.16, 108.91, 42.24 : ESI-HRMS: *m/z* Calcd for: $C_{23}H_{17}N_6O_4$ [M+H] $^+$: 505.0747 found: 505.0752.

4B.8. Spectra

^{1}H-NMR Spectrum of compound 4a in DMDO-d_6 (400 MHz):

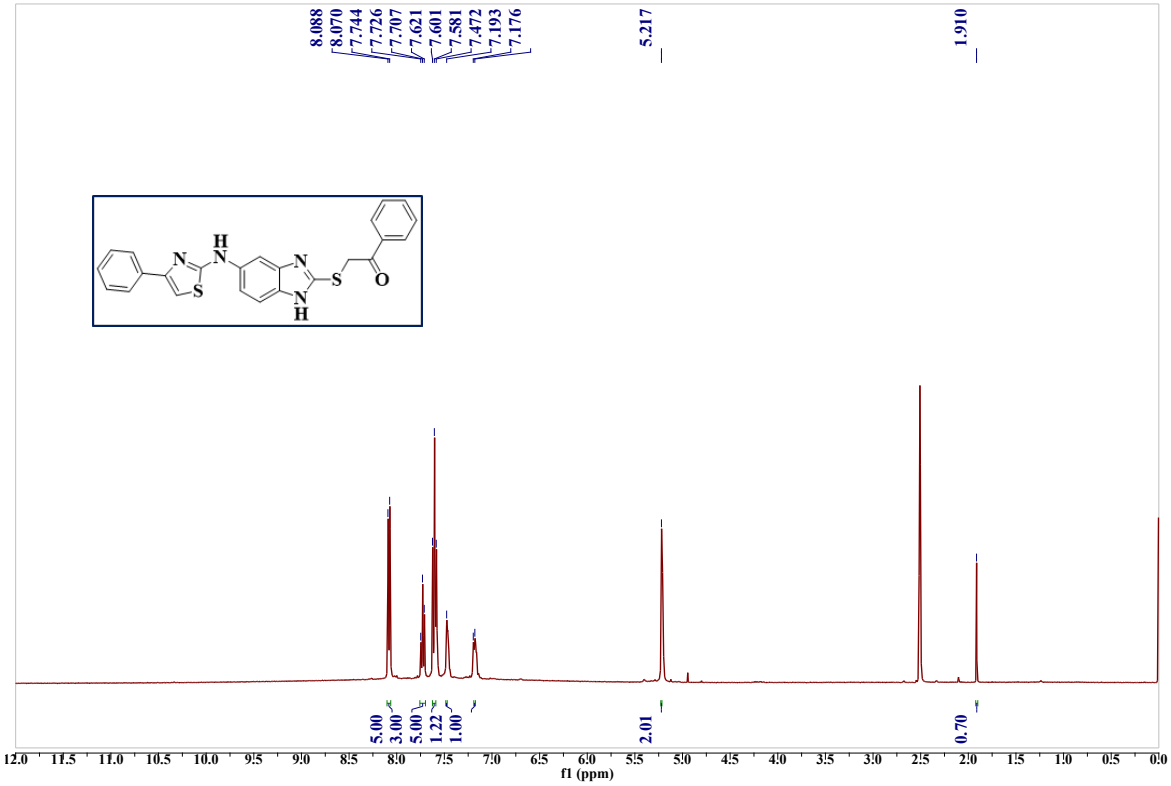

^{13}C-NMR spectrum of compound 4a in DMSO-d_6 (100 MHz):

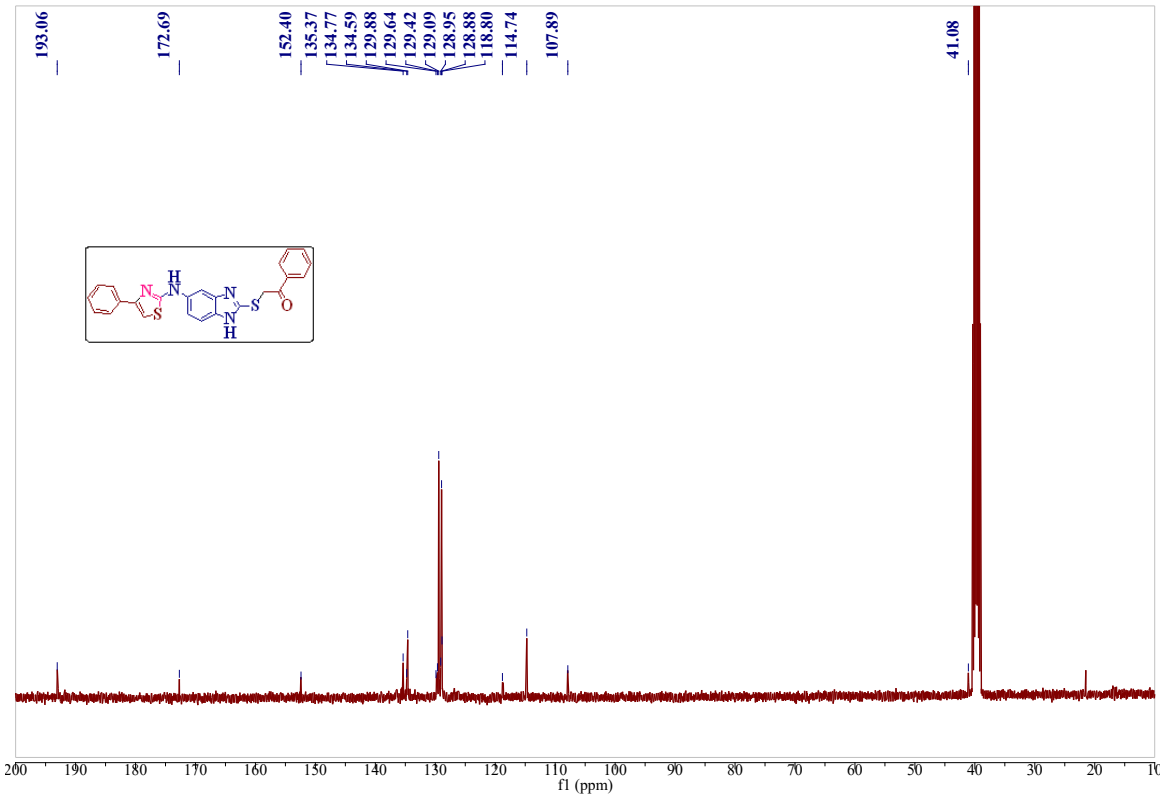

Mass spectrum of compound 4a:

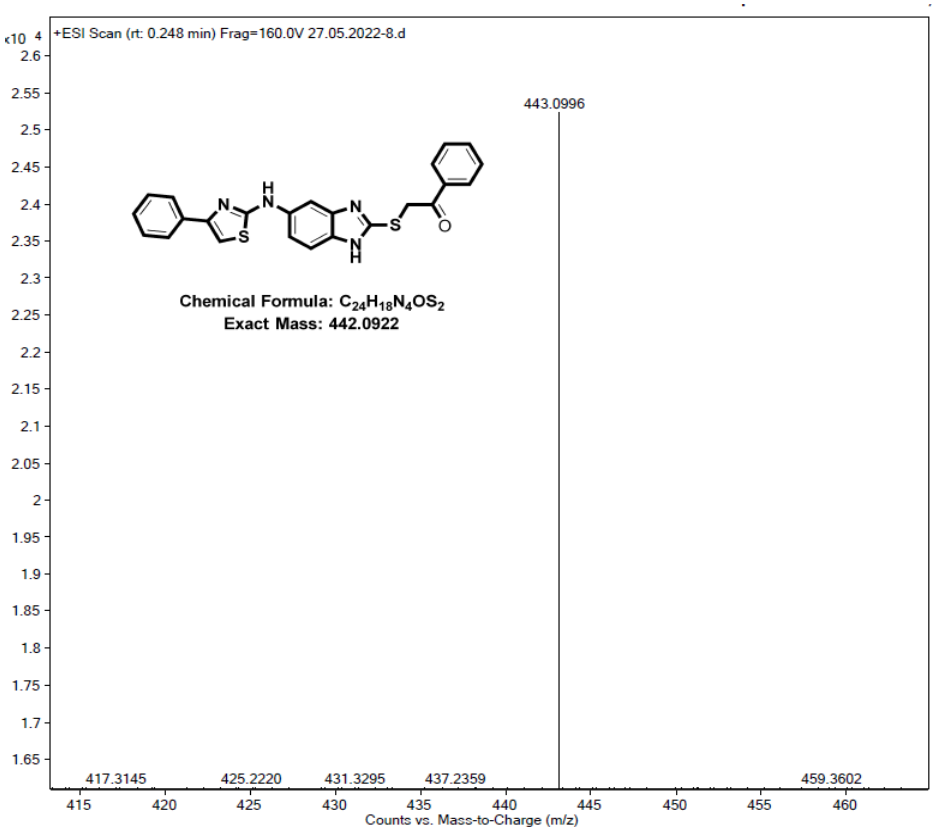

^{1}H-NMR Spectrum of compound 4b in DMSO-d_6 (100 MHz):

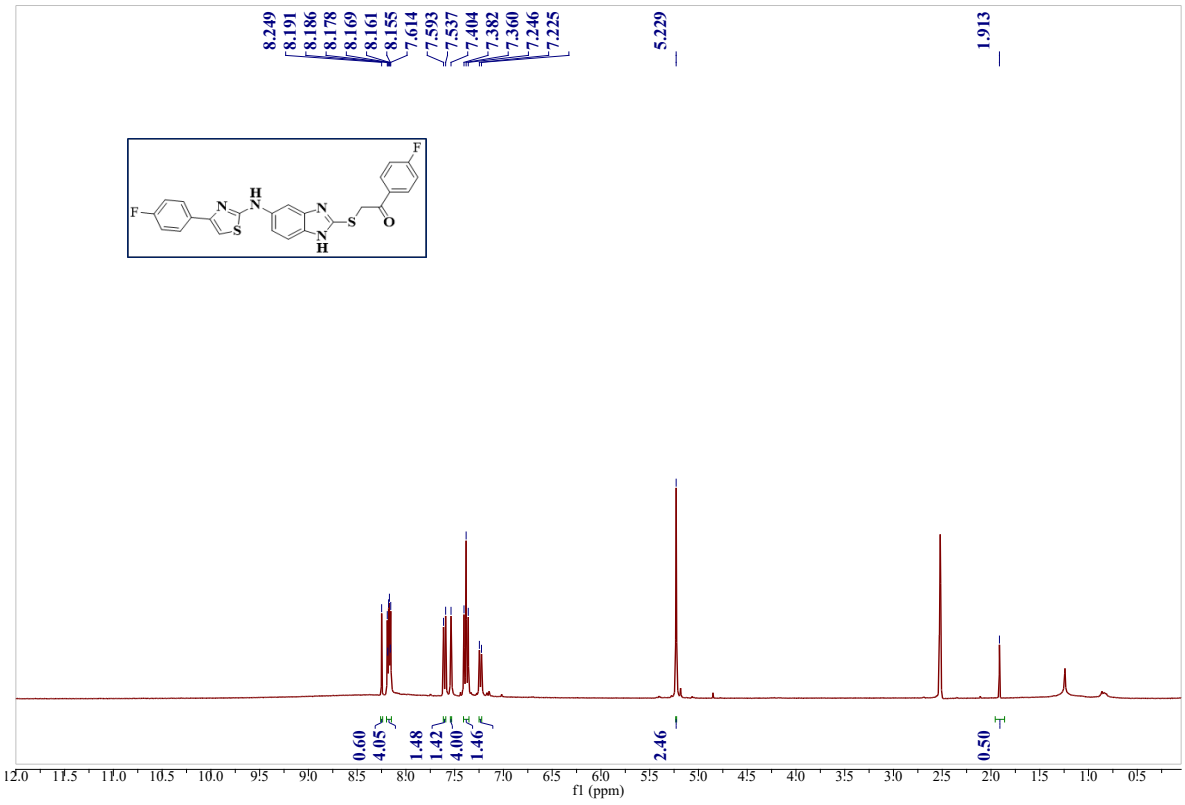

^{13}C-NMR Spectrum of compound 4b in CDCl$_3$-DMSO-d_6 (100 MHz):

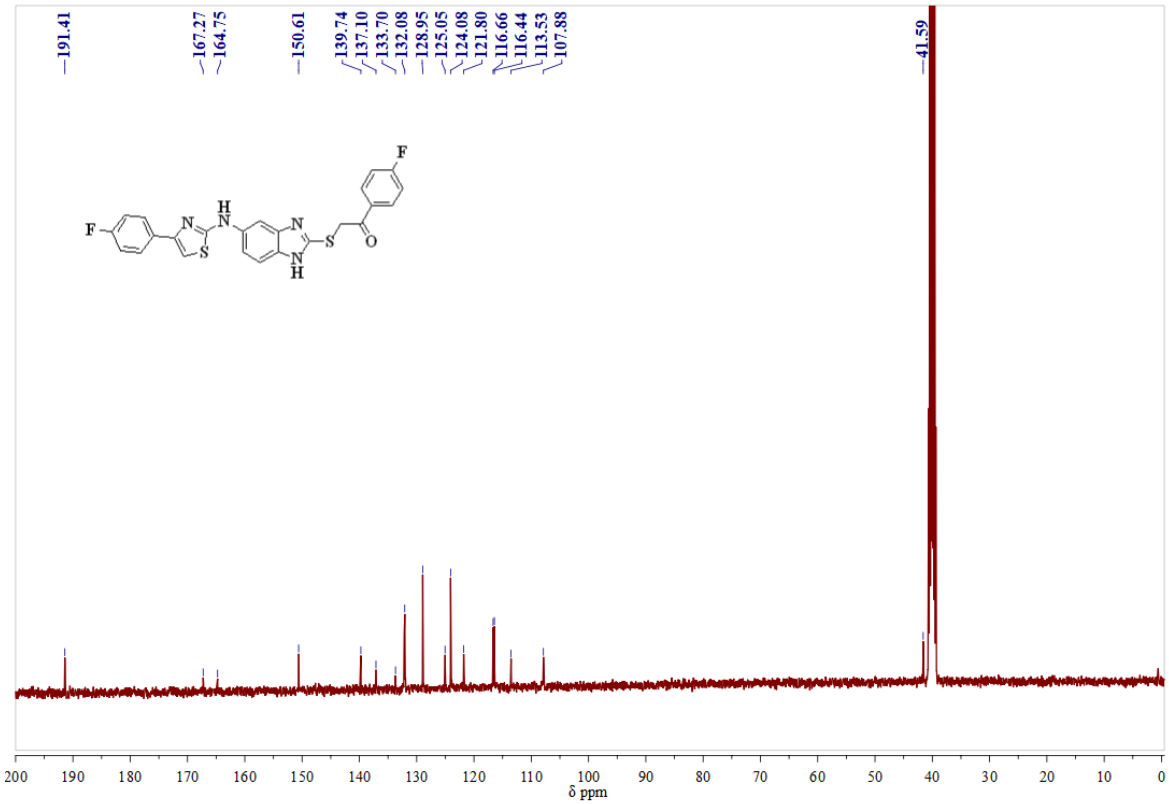

Mass spectrum of compound 4b:

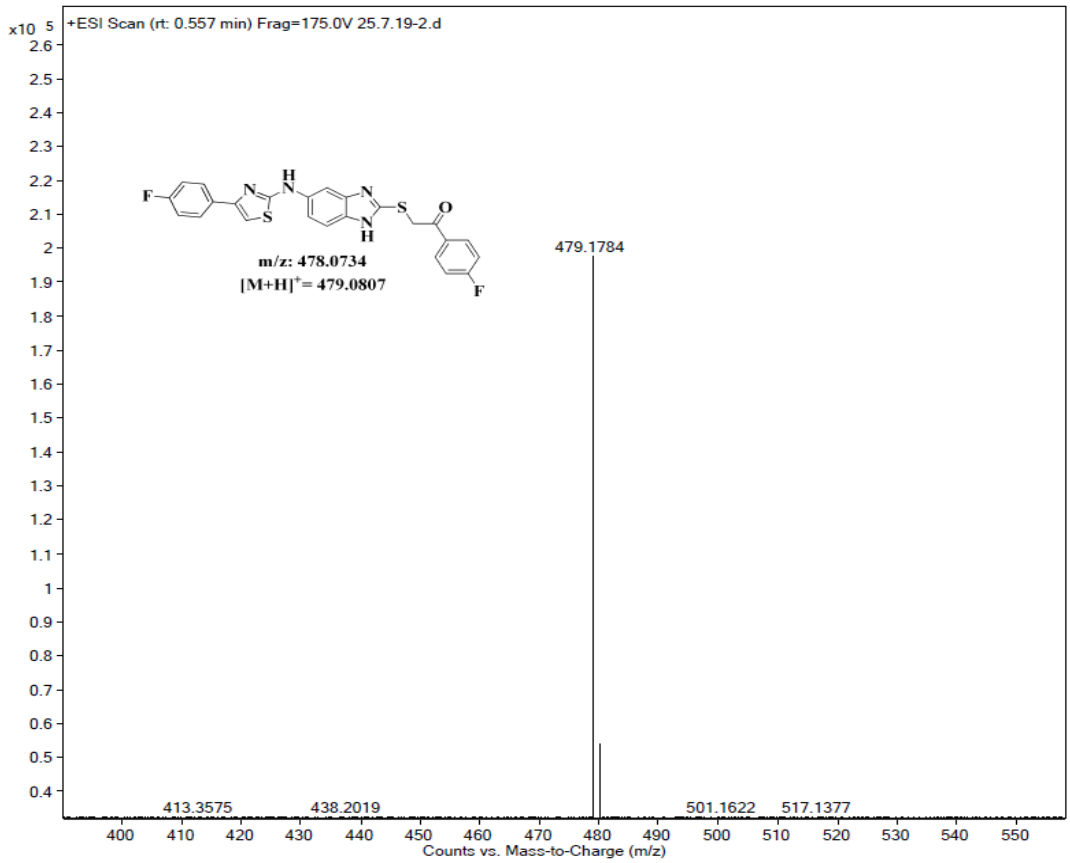

^{1}H-NMR Spectrum of compound 4c in DMSO-d_6 (400 MHz):

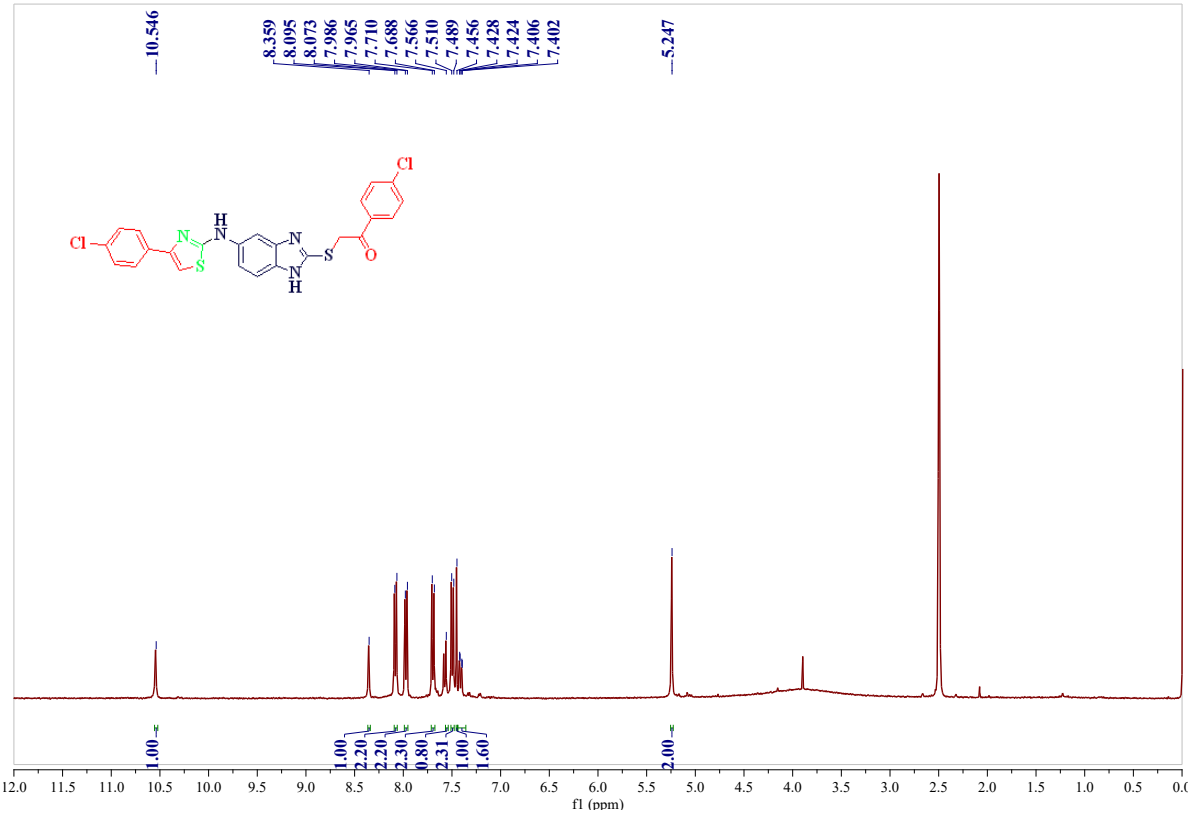

^{13}C-NMR Spectrum of compound 4c in DMSO-d_6 (100 MHz):

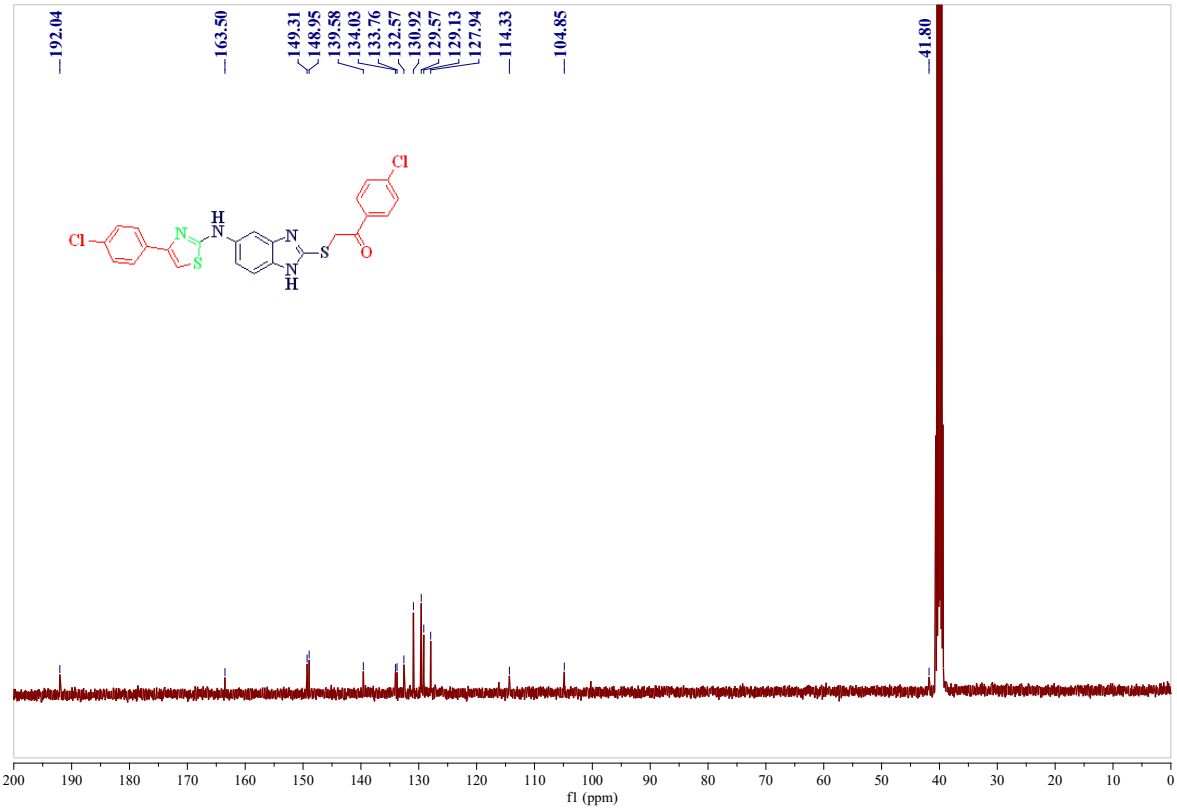

Mass spectrum of compound 4c:

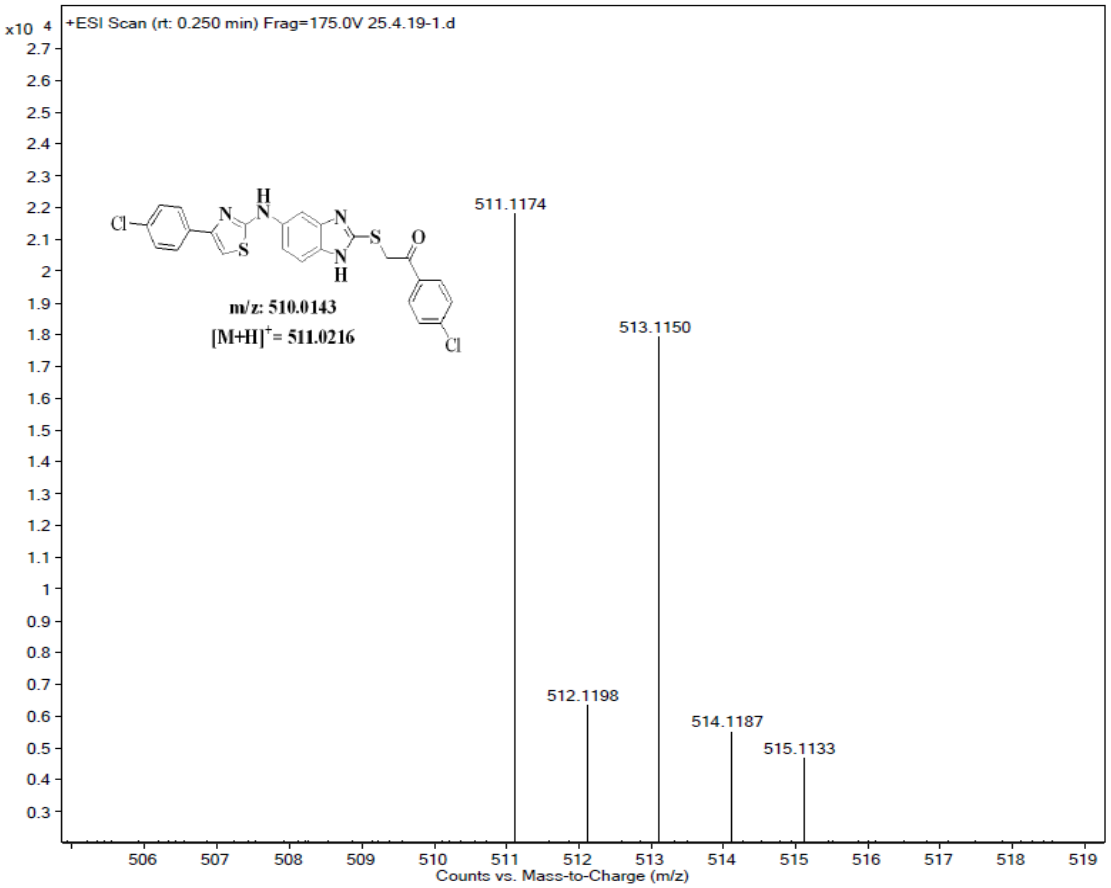

^{1}H-NMR Spectrum of compound 4d in DMSO-d_6 (400 MHz):

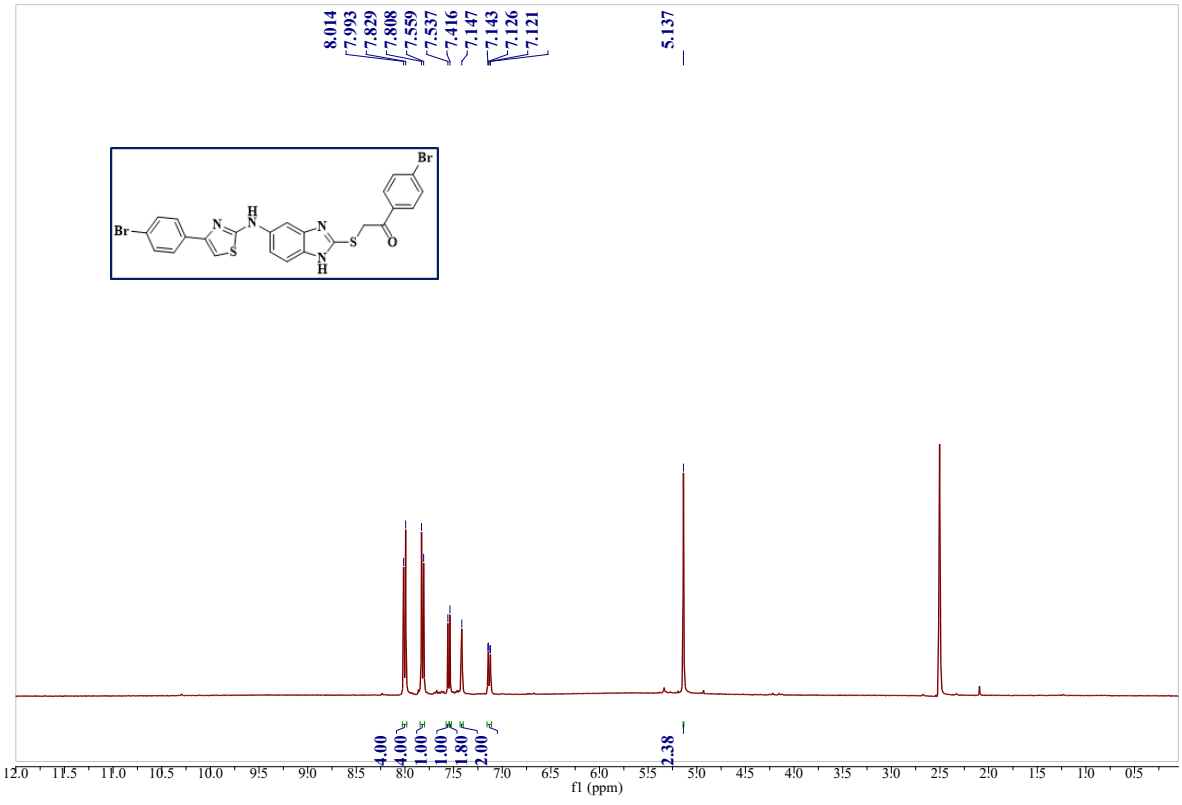

^{13}C-NMR Spectrum of compound 4d in DMSO-d_6 (100 MHz):

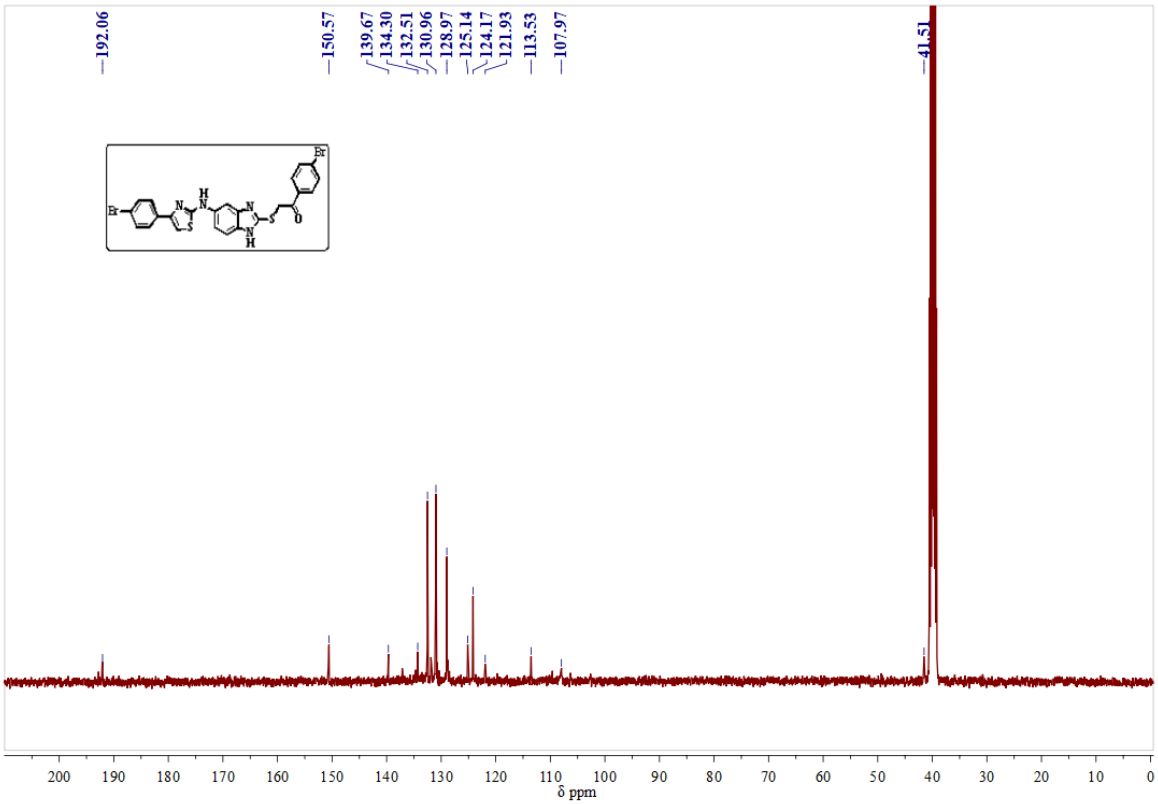

Mass spectrum of compound 4d:

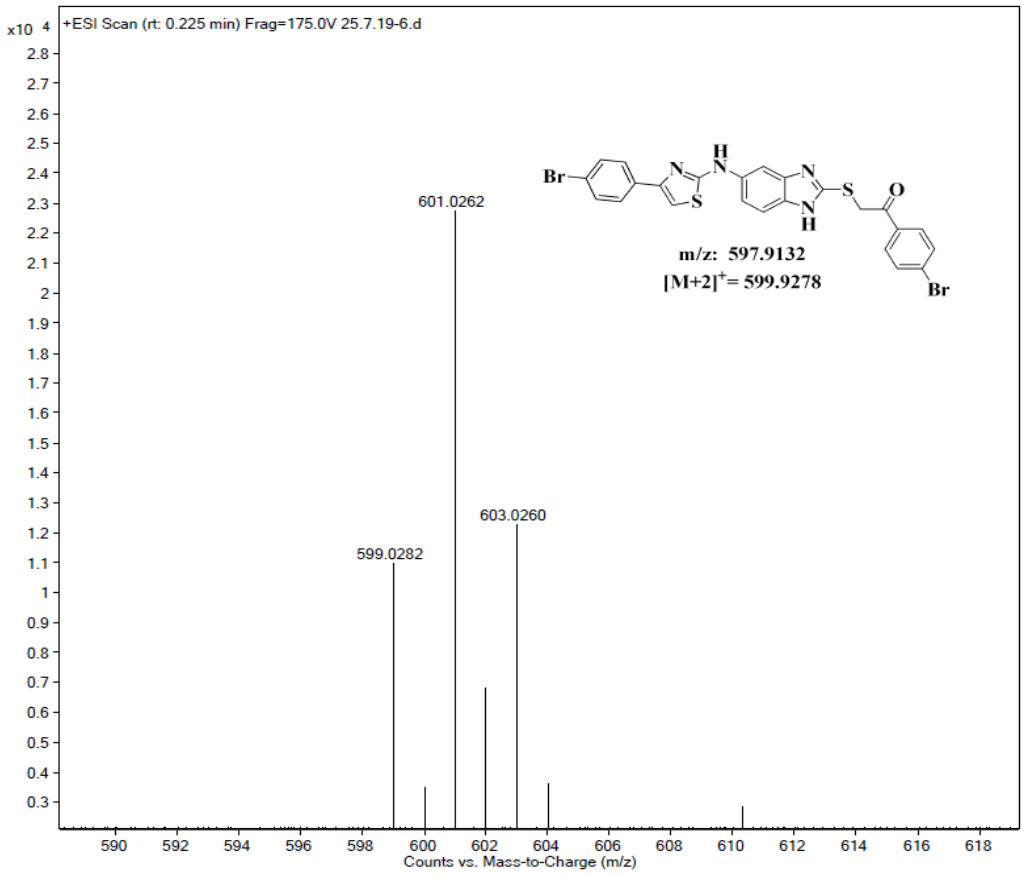

^{1}H-NMR Spectrum of compound 4e in DMSO-d_6 (400 MHz):

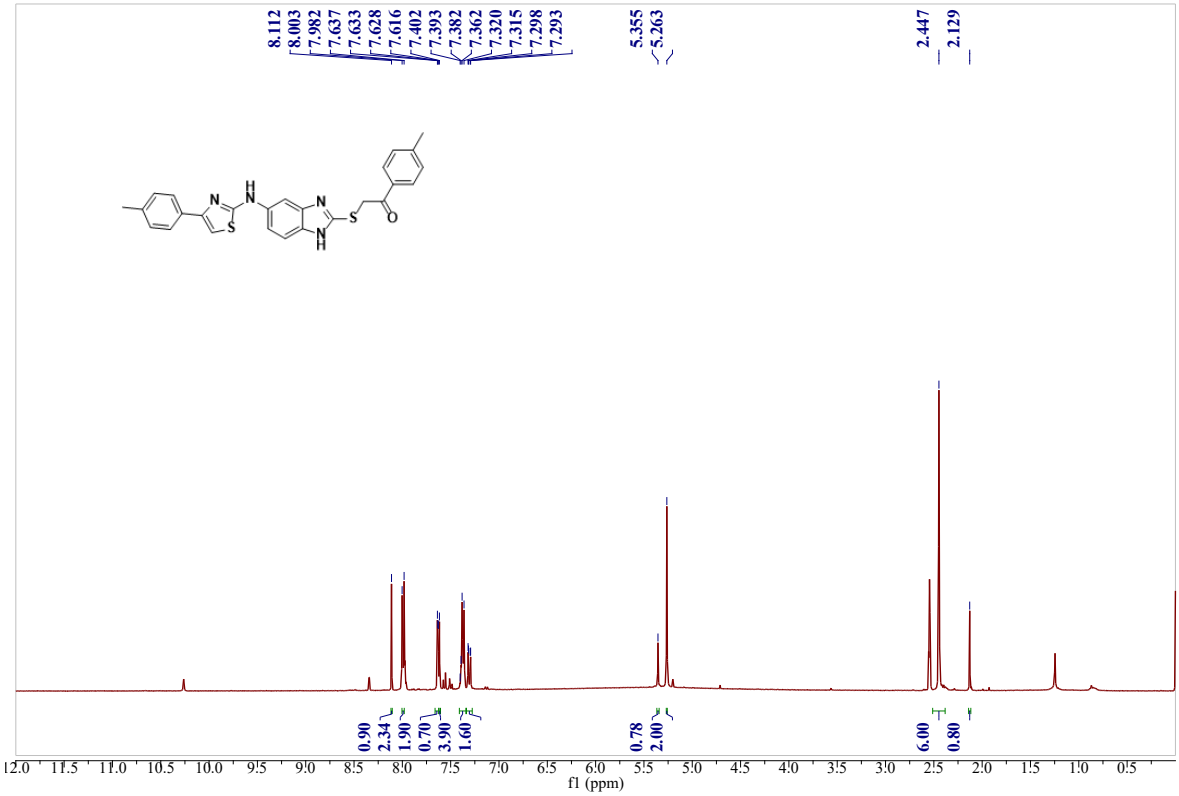

^{13}C-NMR Spectrum of compound 4e inCDCl$_3$-DMSO-d_6 (100 MHz):

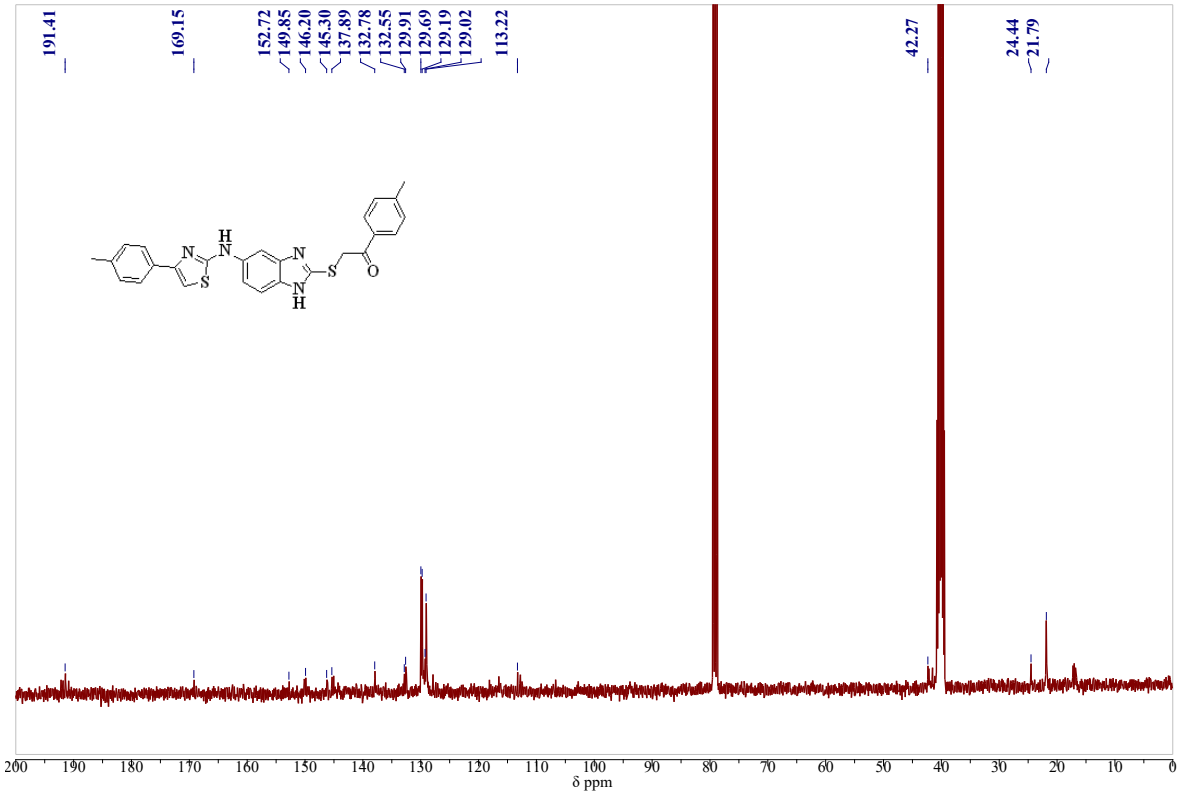

Mass spectrum of compound 4e:

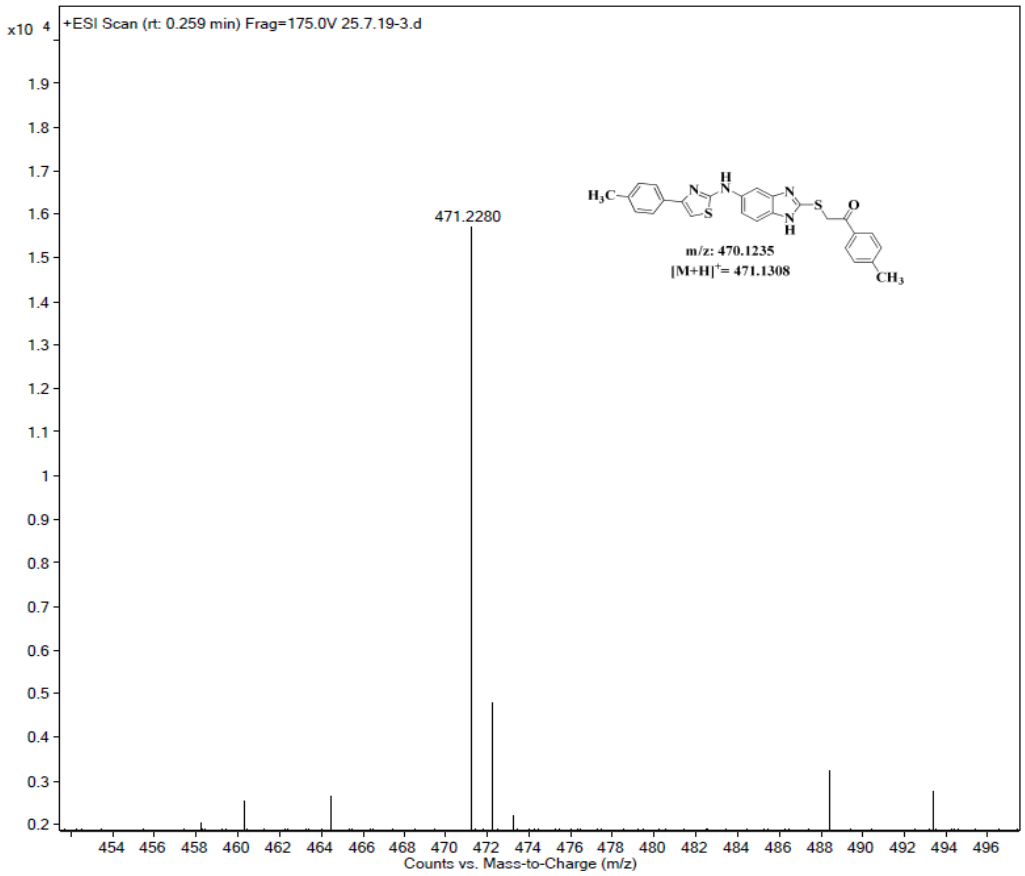

^{1}H-NMR Spectrum of compound 4f in DMSO-d_6 (400 MHz):

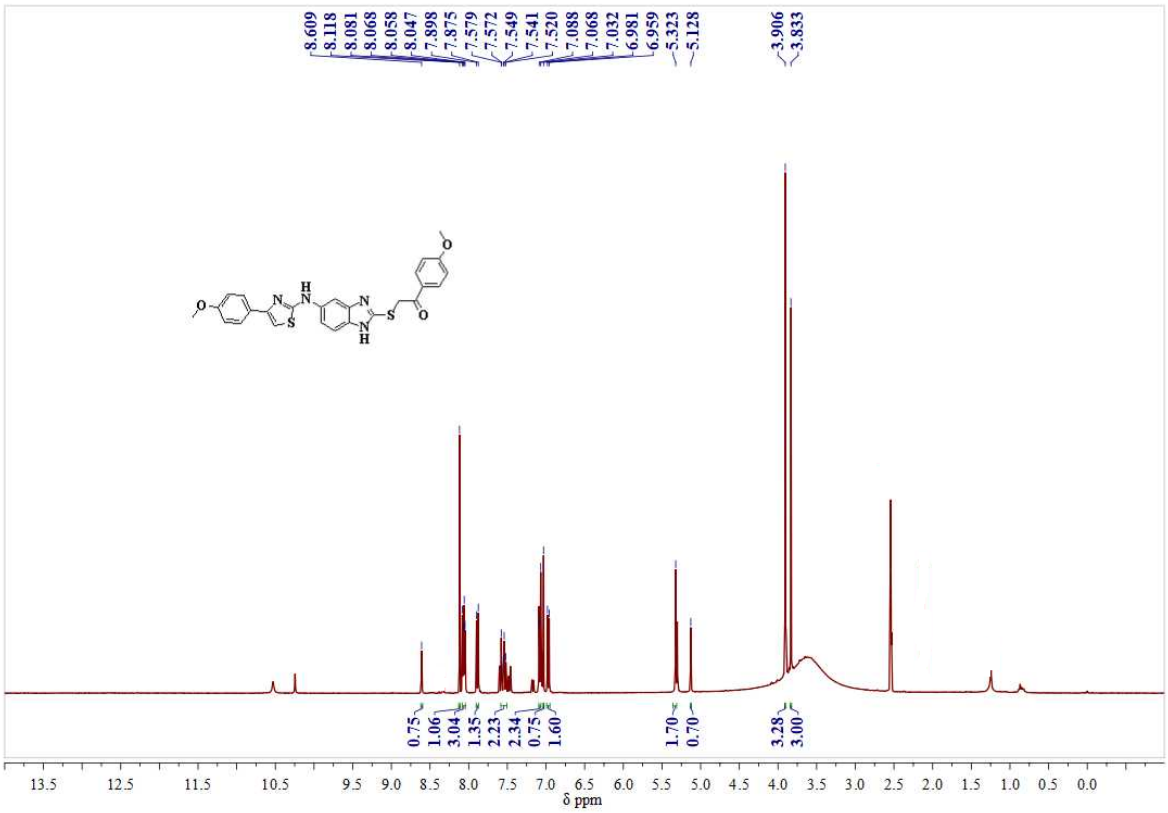

^{13}C-NMR Spectrum of compound 4f inCDCl$_3$-DMSO-*d*$_6$ (100 MHz):

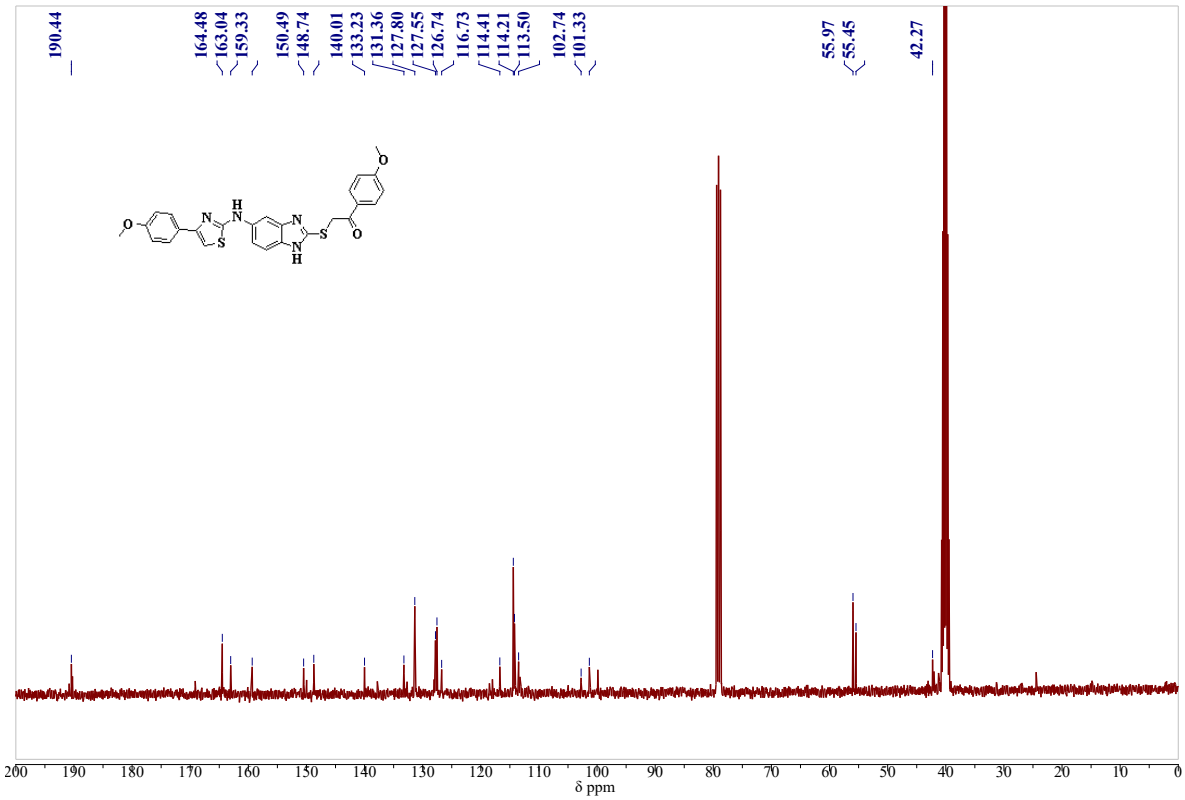

Mass spectrum of compound 4f:

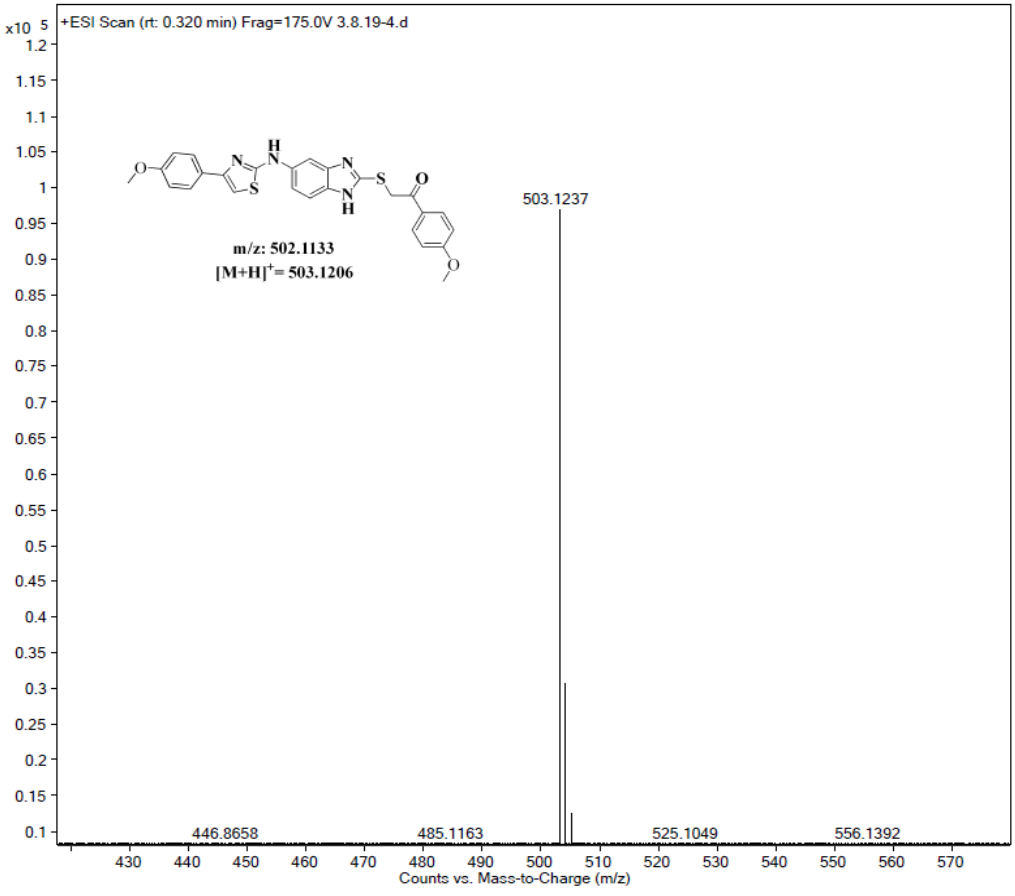

^{1}H-NMR Spectrum of compound 4g in DMSO-d_6 (400 MHz):

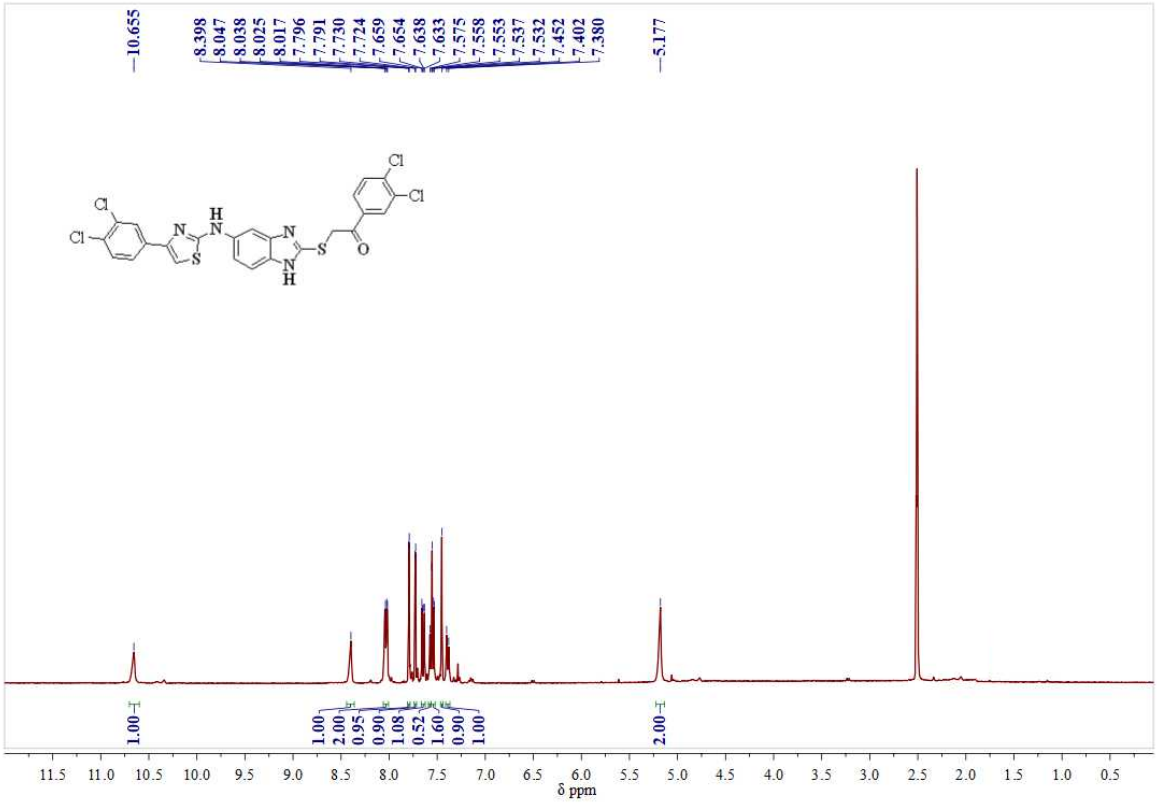

^{13}C-NMR Spectrum of compound 4g inCDCl$_3$-DMSO-d_6 (100 MHz):

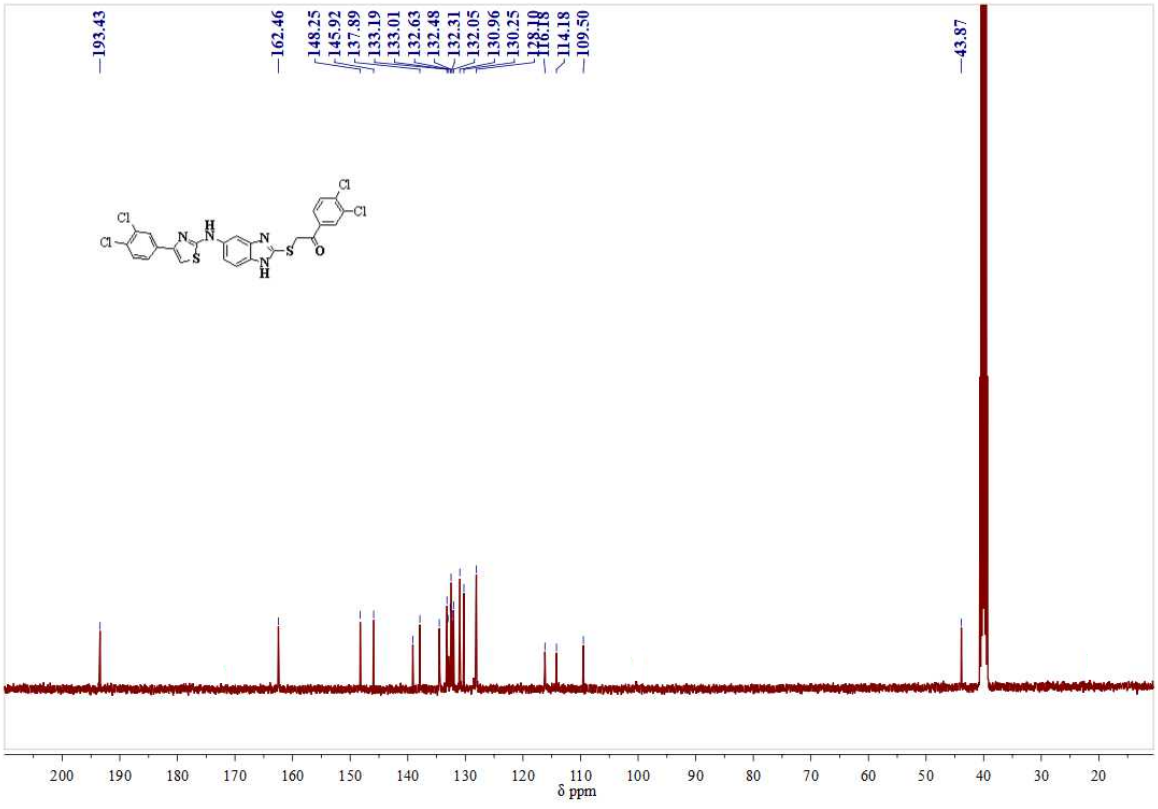

Mass spectrum of compound 4g:

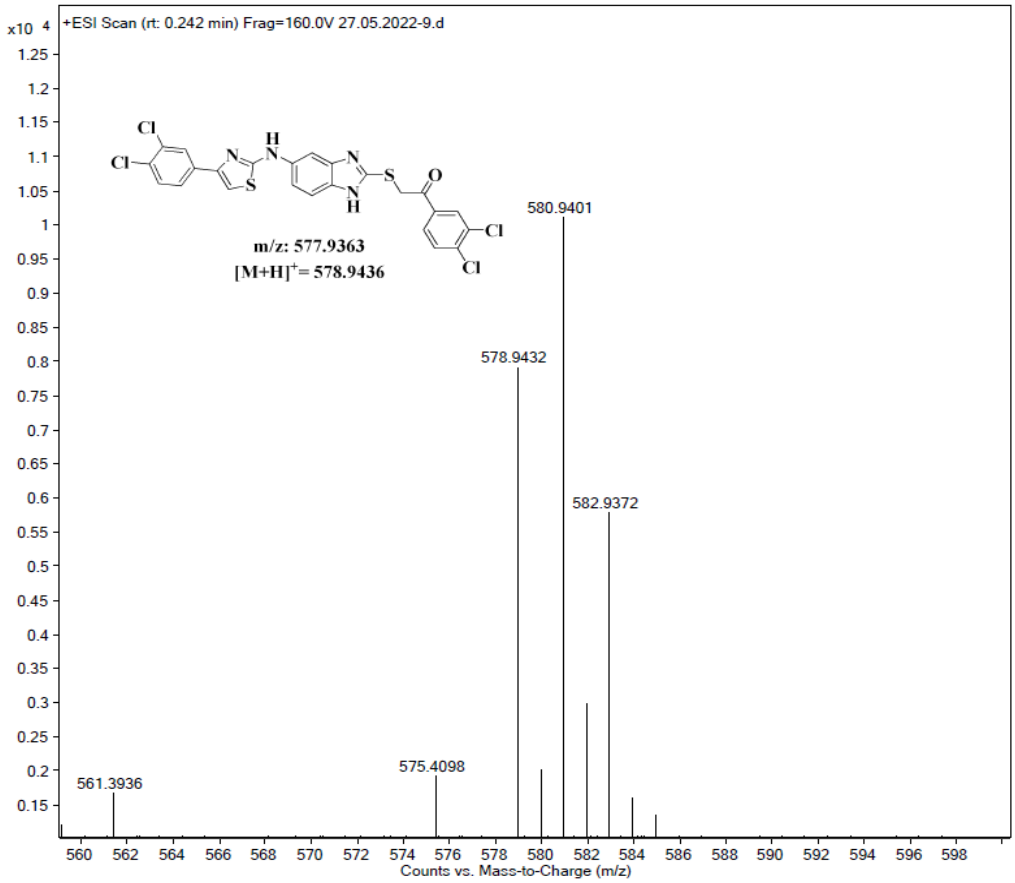

^{1}H-NMR Spectrum of compound 4h in DMSO-d_6 (400 MHz):

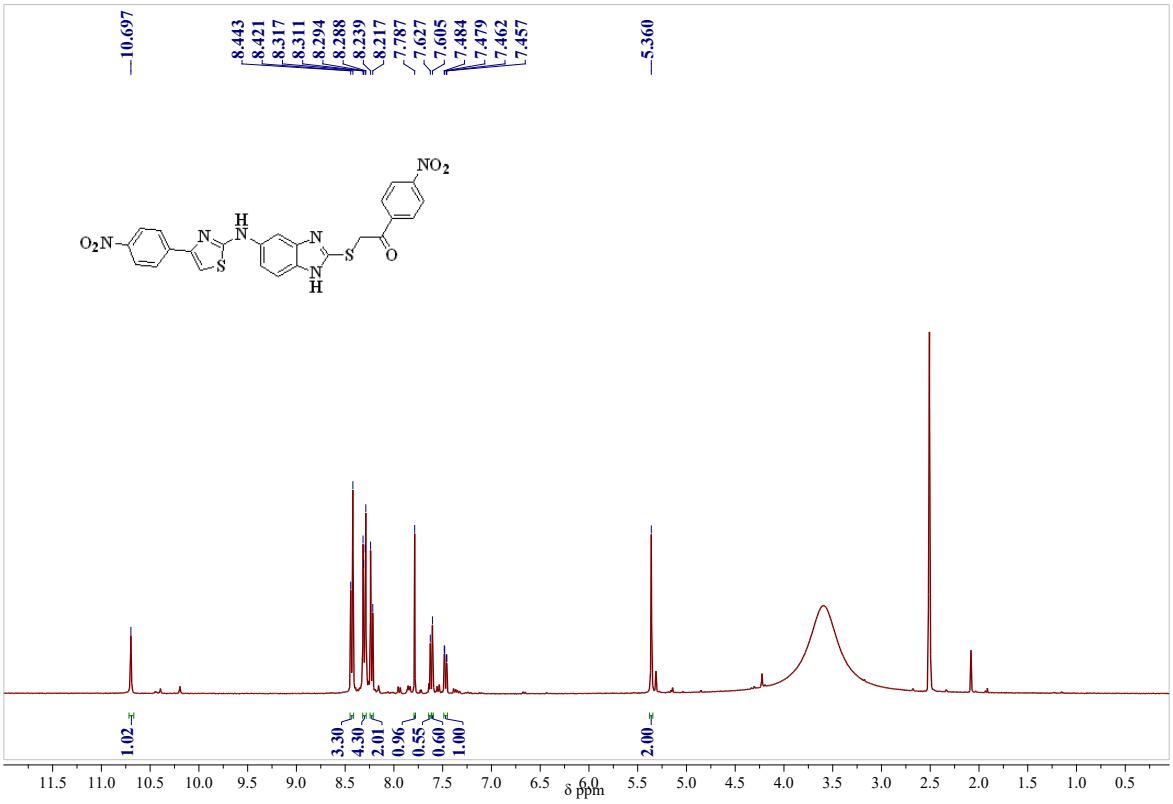

^{13}C-NMR Spectrum of compound 4h in DMSO-d_6 (100 MHz):

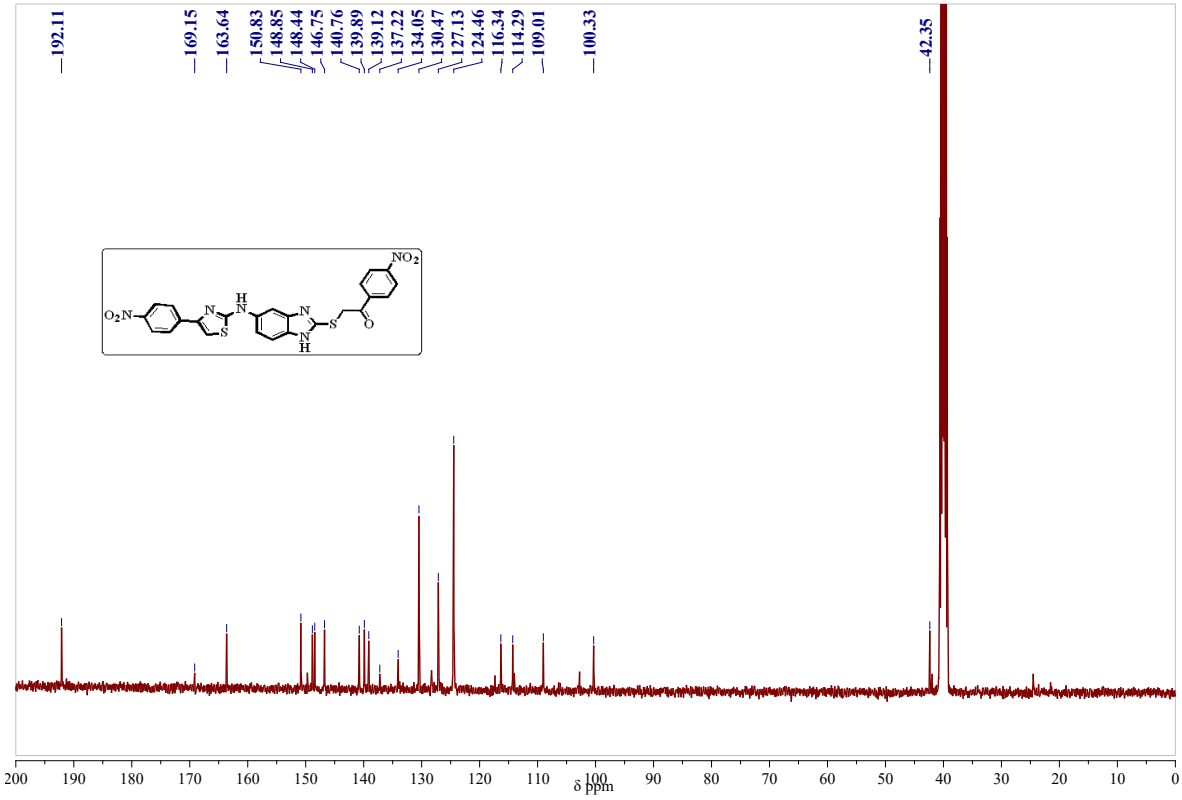

Mass spectrum of compound 4h:

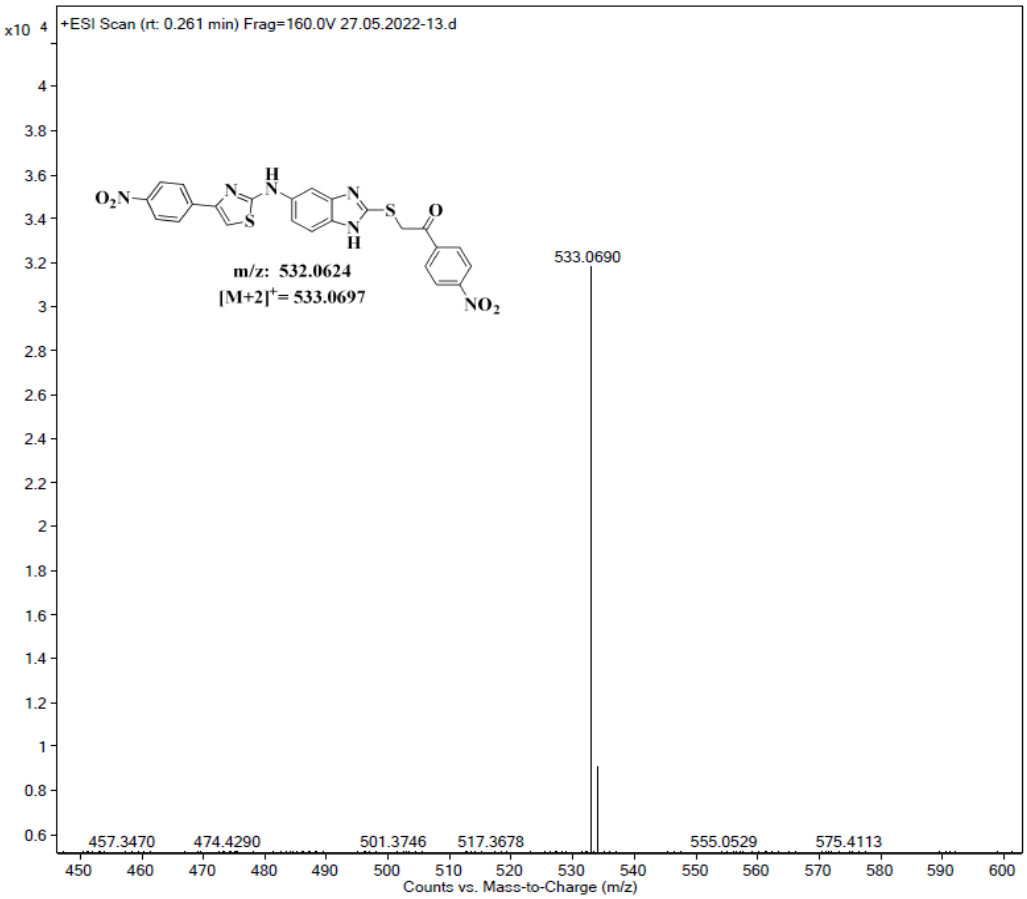

^{1}H-NMR Spectrum of compound 4i in DMSO-d_6 (400 MHz):

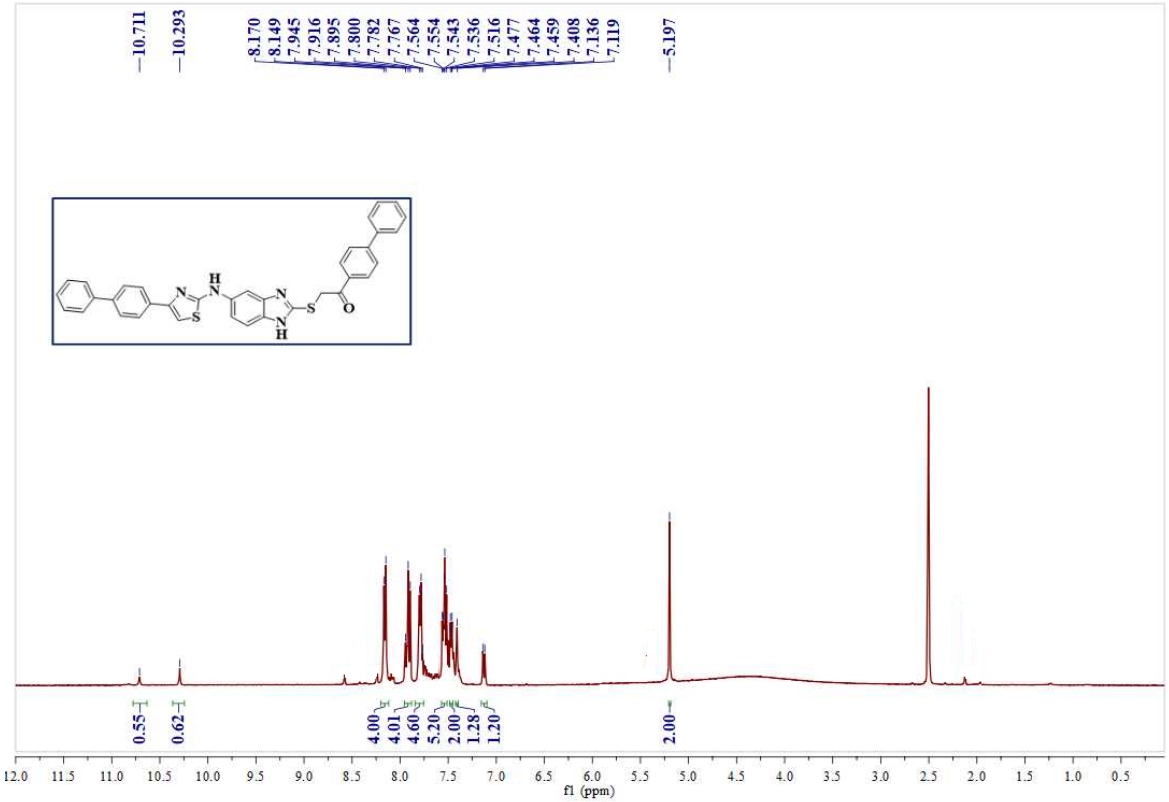

^{13}C-NMR Spectrum of compound 4i in DMSO-d_6 (100 MHz):

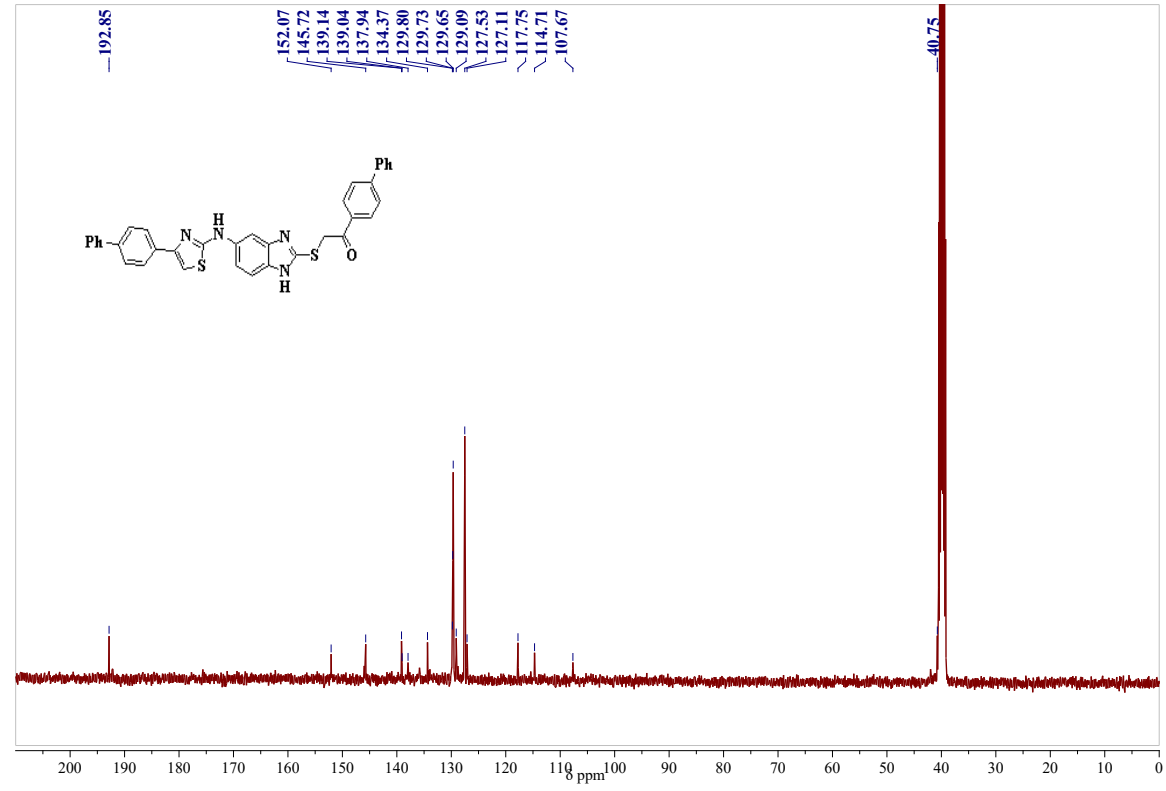

Mass spectrum of compound 4i:

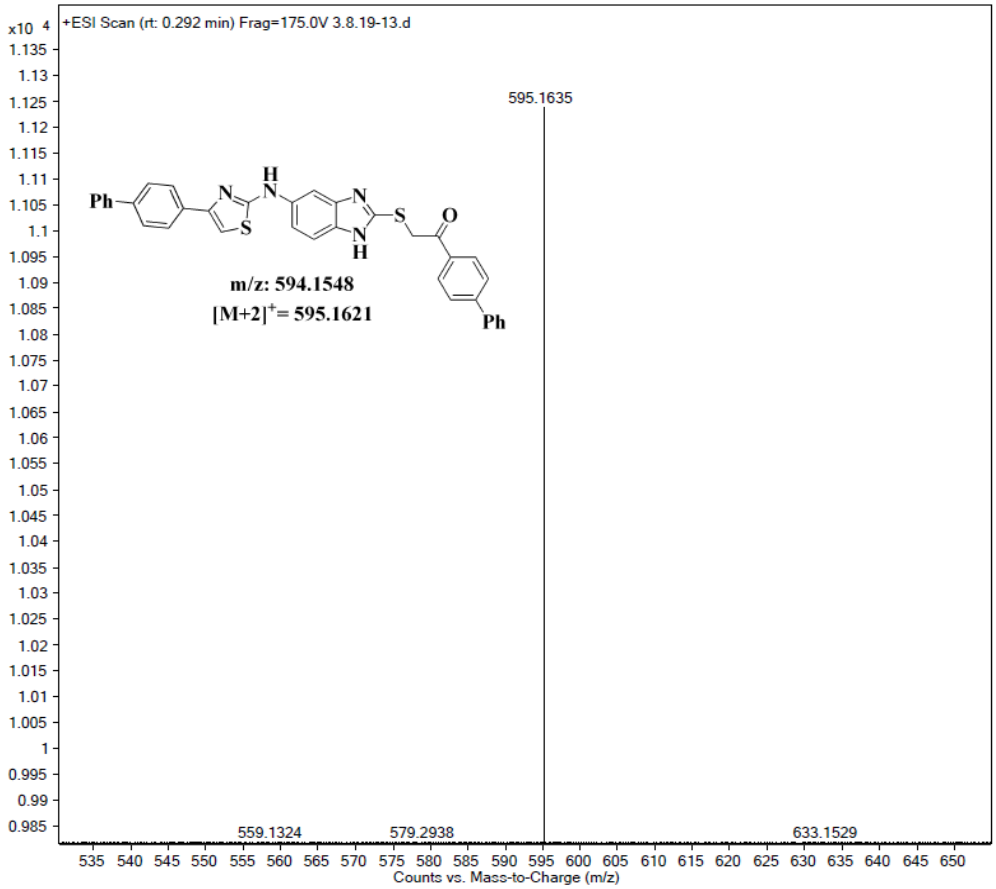

^{1}H-NMR Spectrum of compound 4j in DMSO-d_6 (400 MHz):

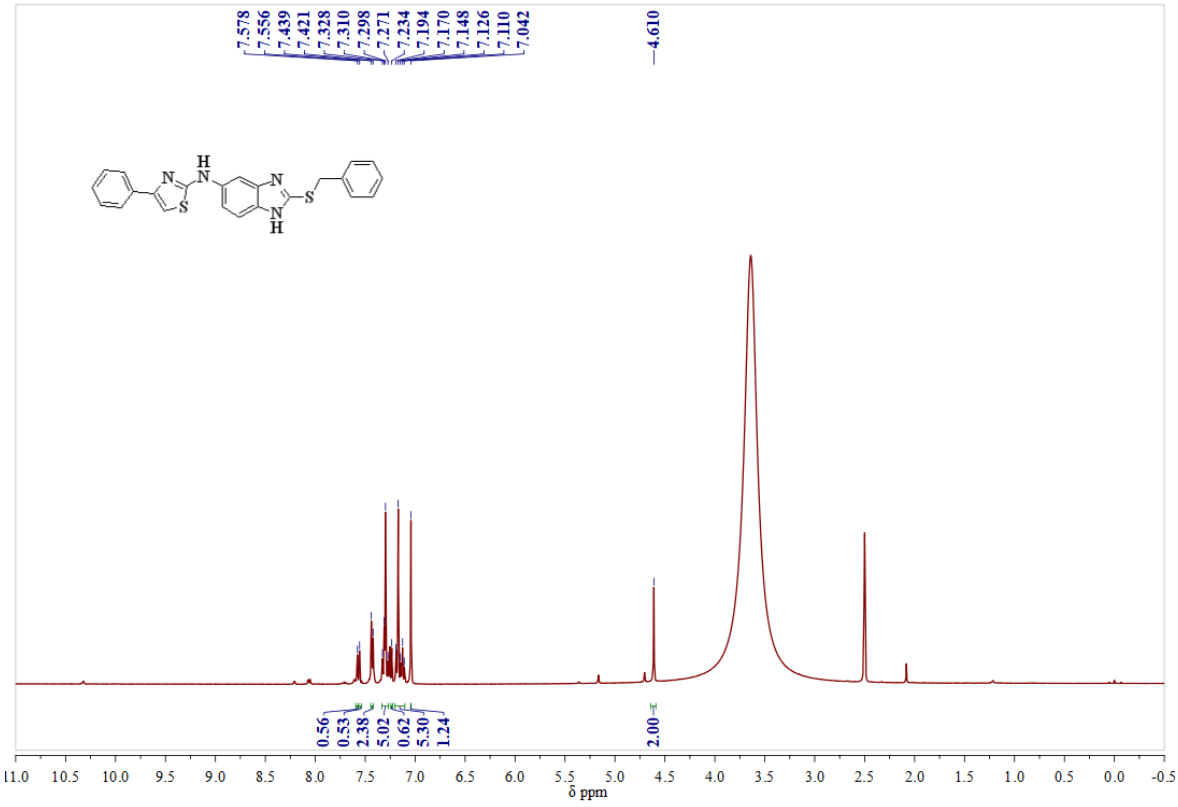

^{13}C-NMR Spectrum of compound 4j in DMSO-d_6 (100 MHz):

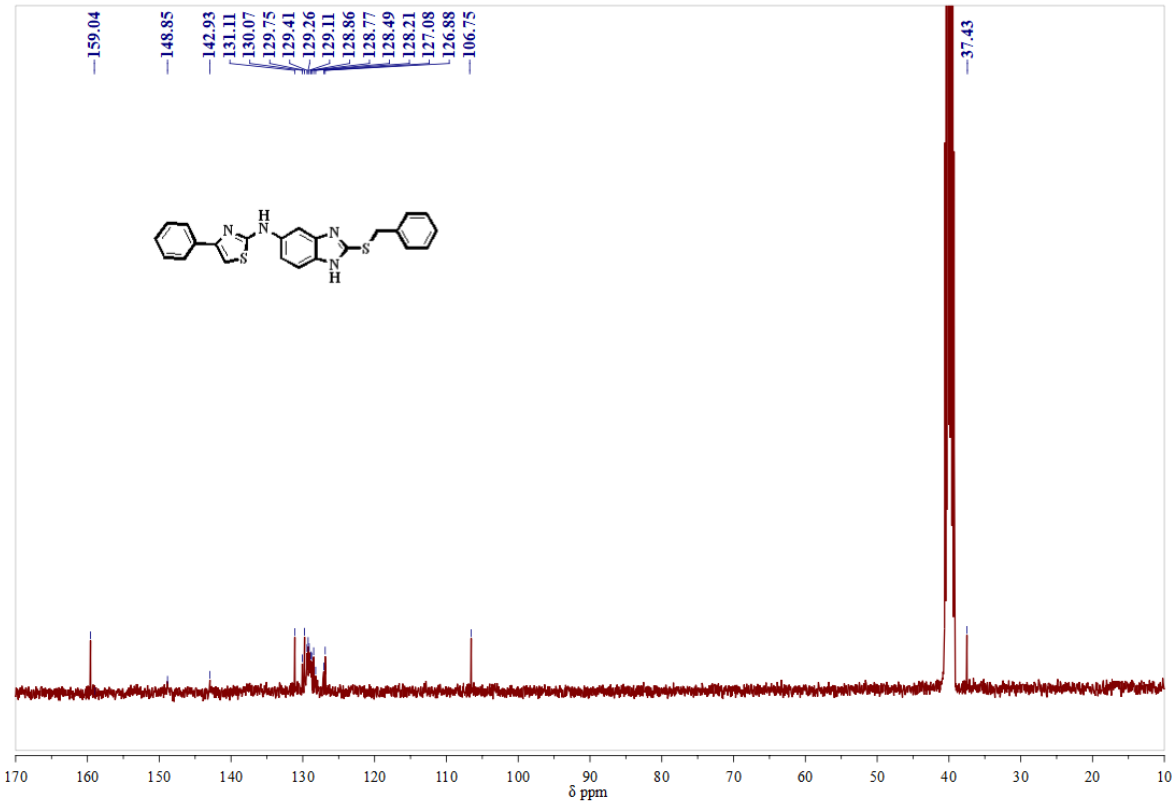

Mass spectrum of compound 4j:

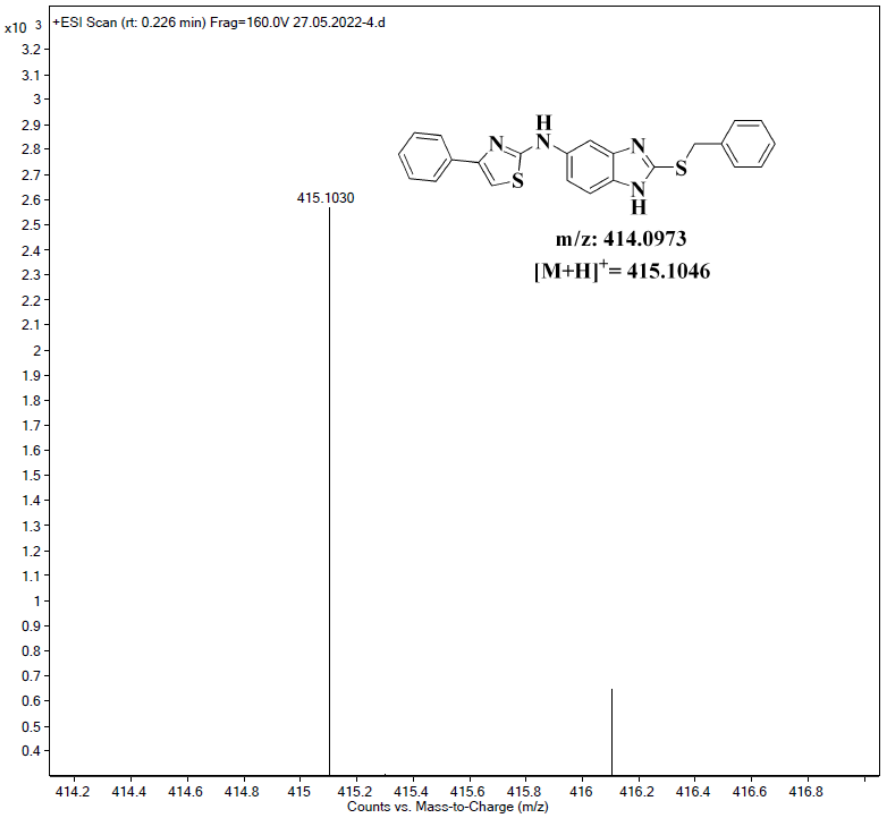

^{1}H-NMR Spectrum of compound 4k in DMSO-d_6 (400 MHz):

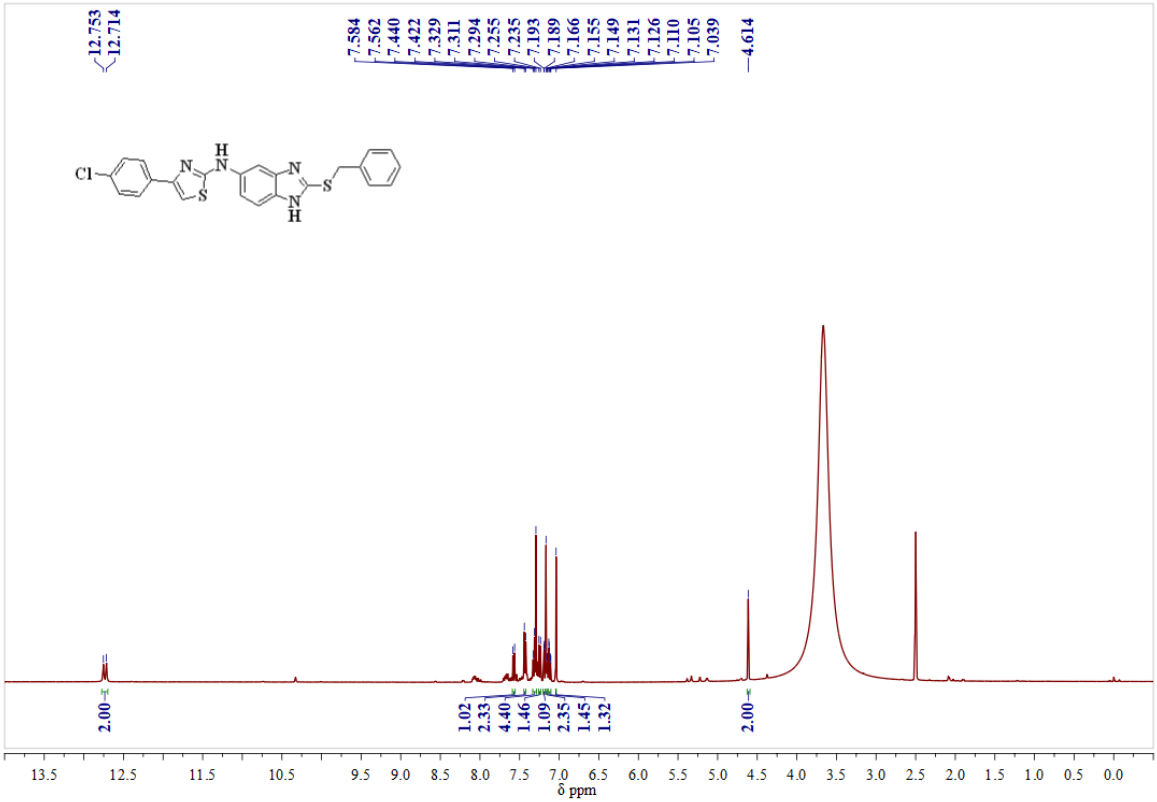

^{13}C-NMR Spectrum of compound 4k in CDCl$_3$-DMSO-d_6 (100 MHz):

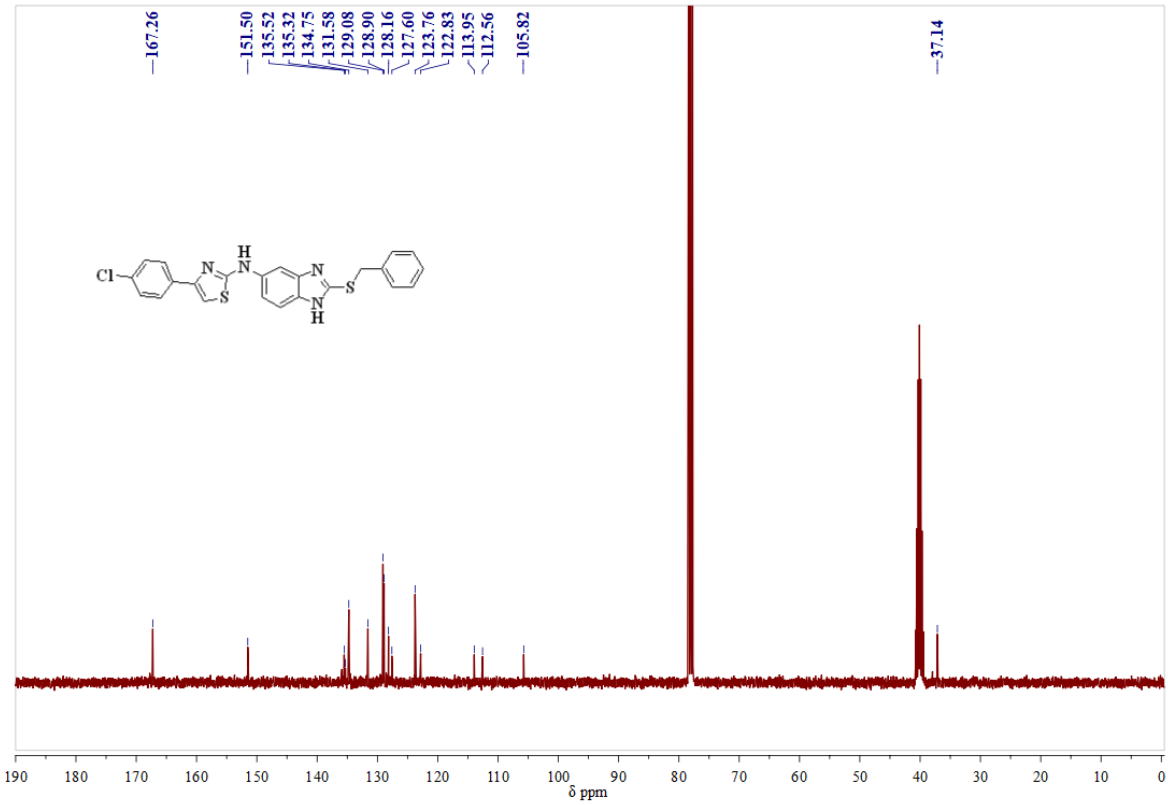

Mass spectrum of compound 4k

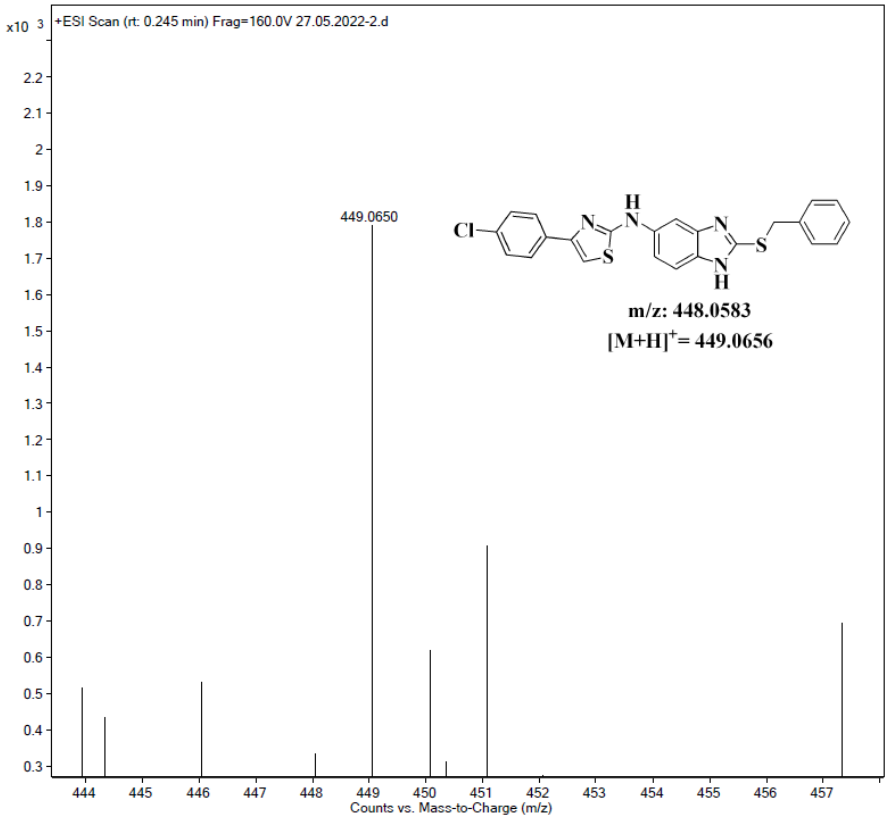

^{1}H-NMR Spectrum of compound 4l in DMSO-d_6 (400 MHz):

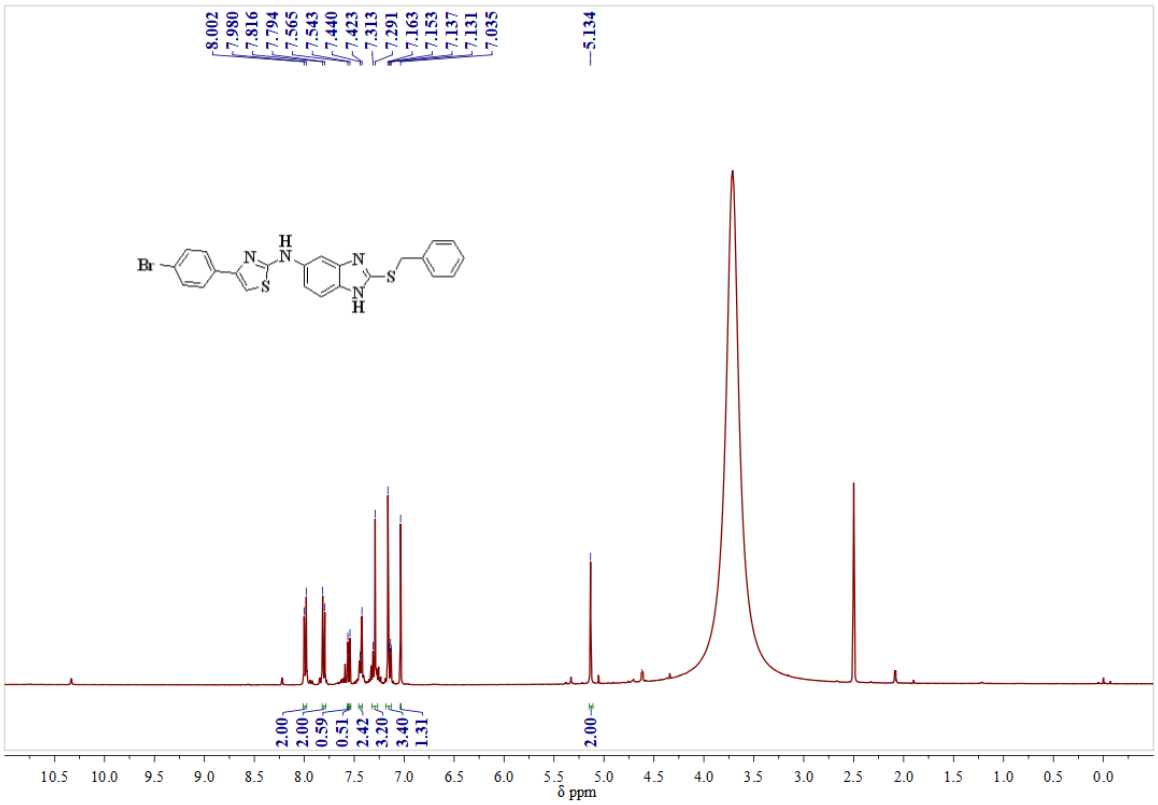

^{13}C-NMR Spectrum of compound 4l in DMSO-d_6 (100 MHz):

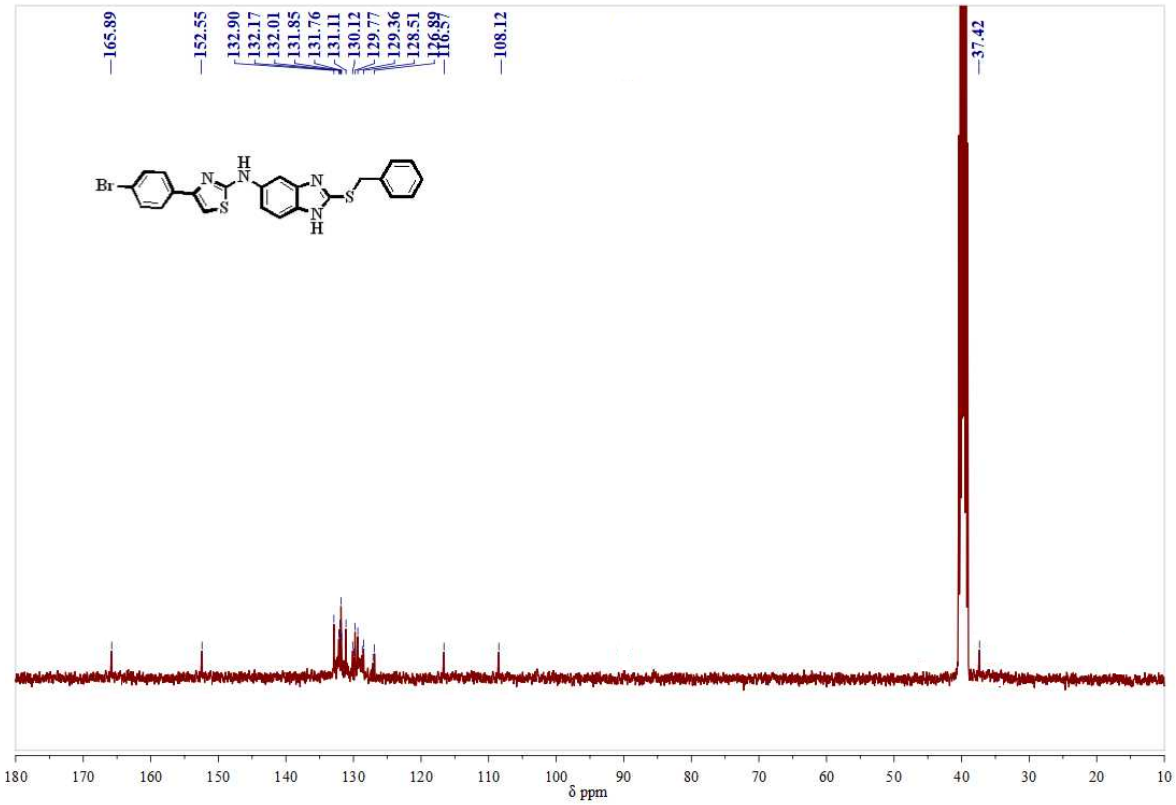

Mass spectrum of compound 4l:

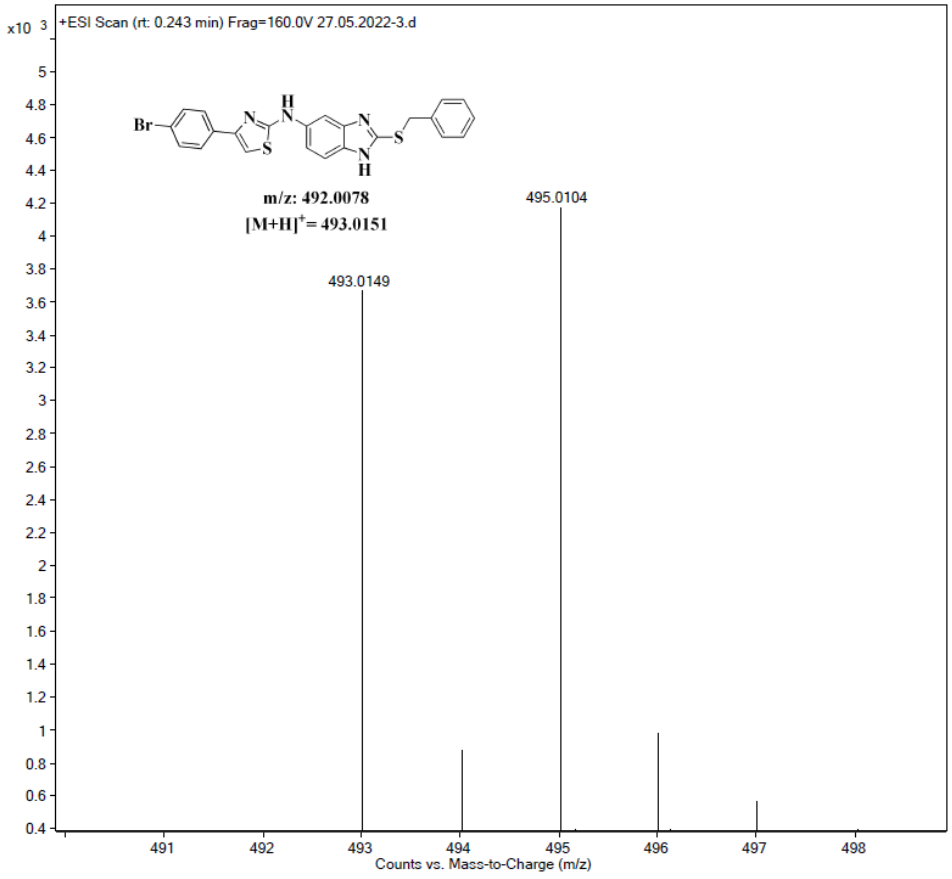

^{1}H-NMR Spectrum of compound 4m in DMSO-d_6 (400 MHz):

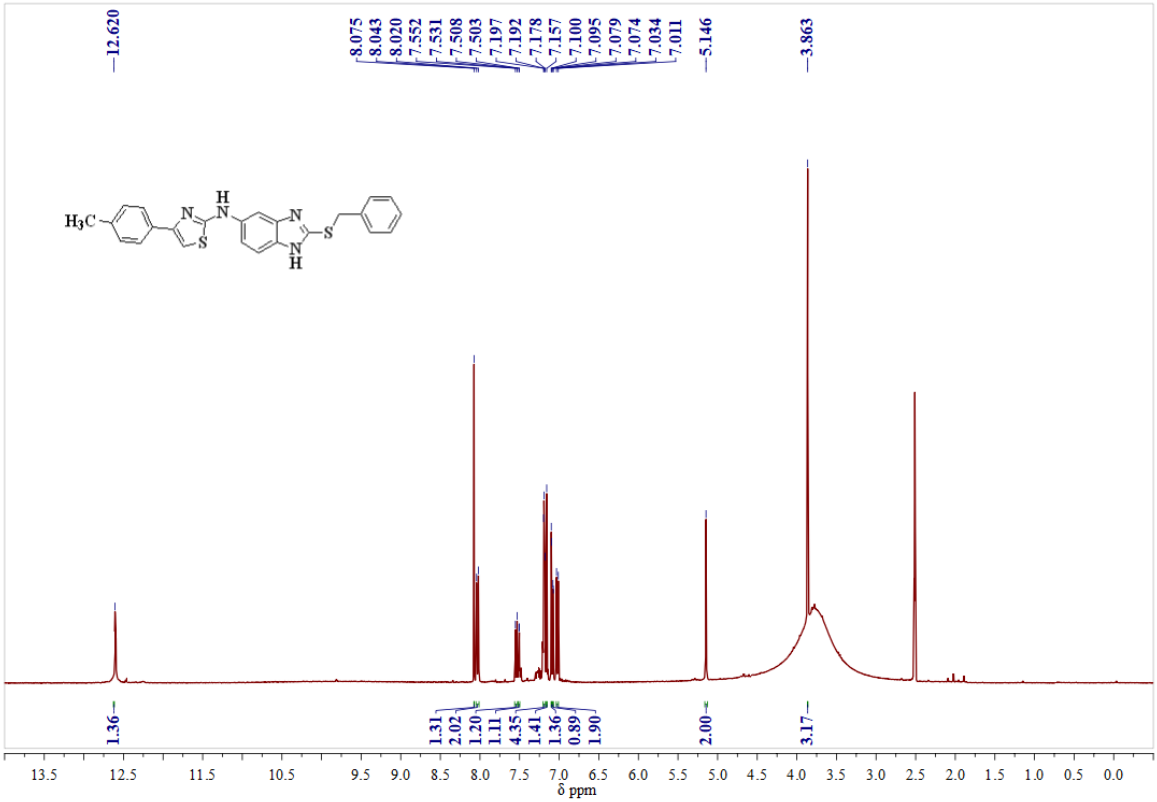

Mass spectrum of compound 4m

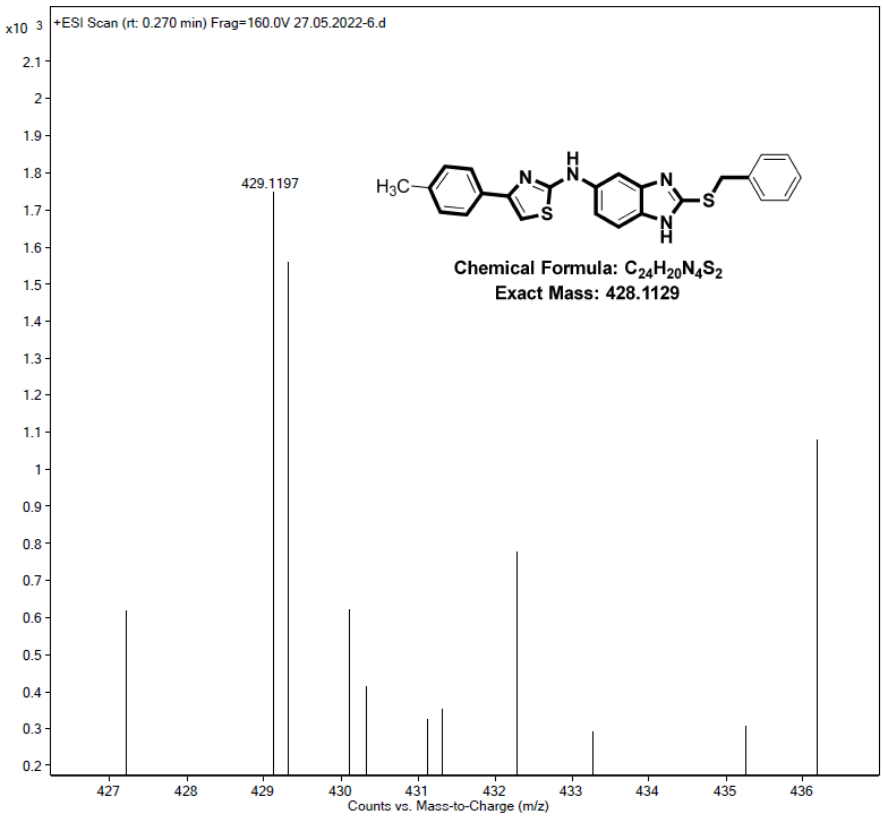

^{1}H-NMR Spectrum of compound 4n in DMSO-d_6 (400 MHz):

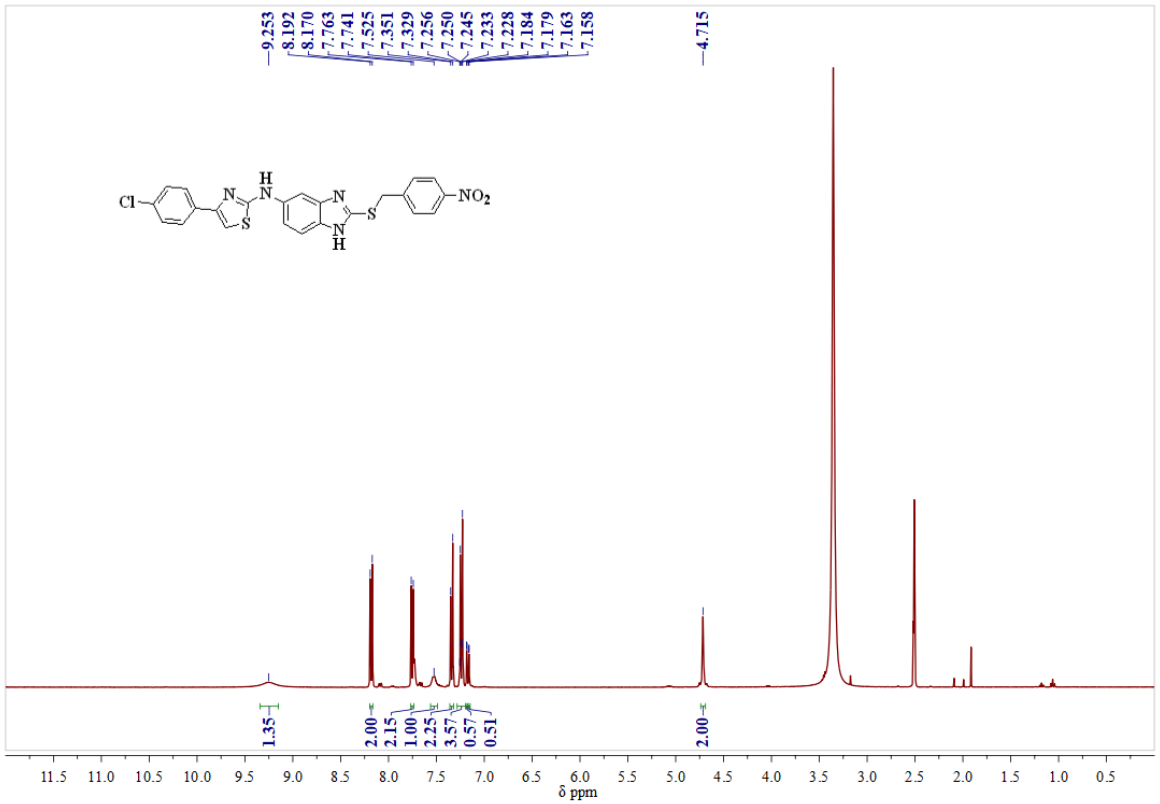

^{13}C-NMR Spectrum of compound 4n in DMSO-d_6 (100 MHz):

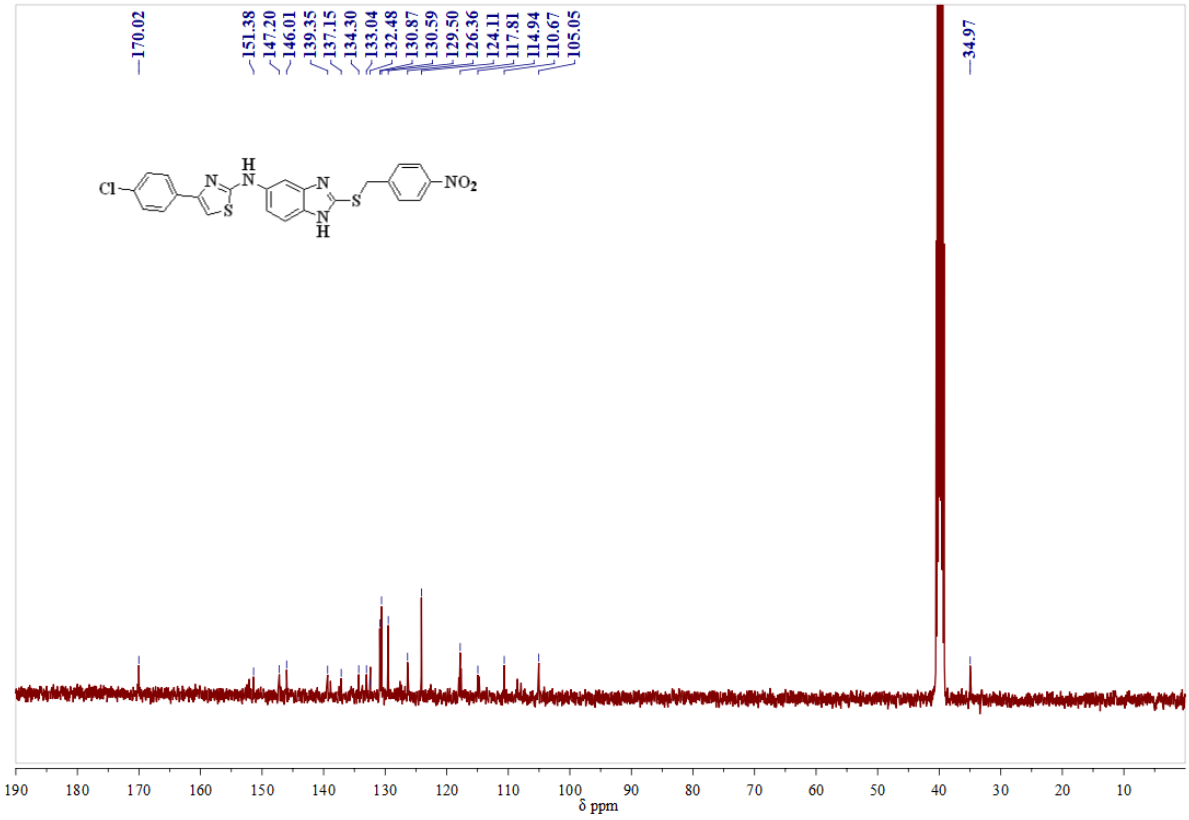

Mass spectrum of compound 4n:

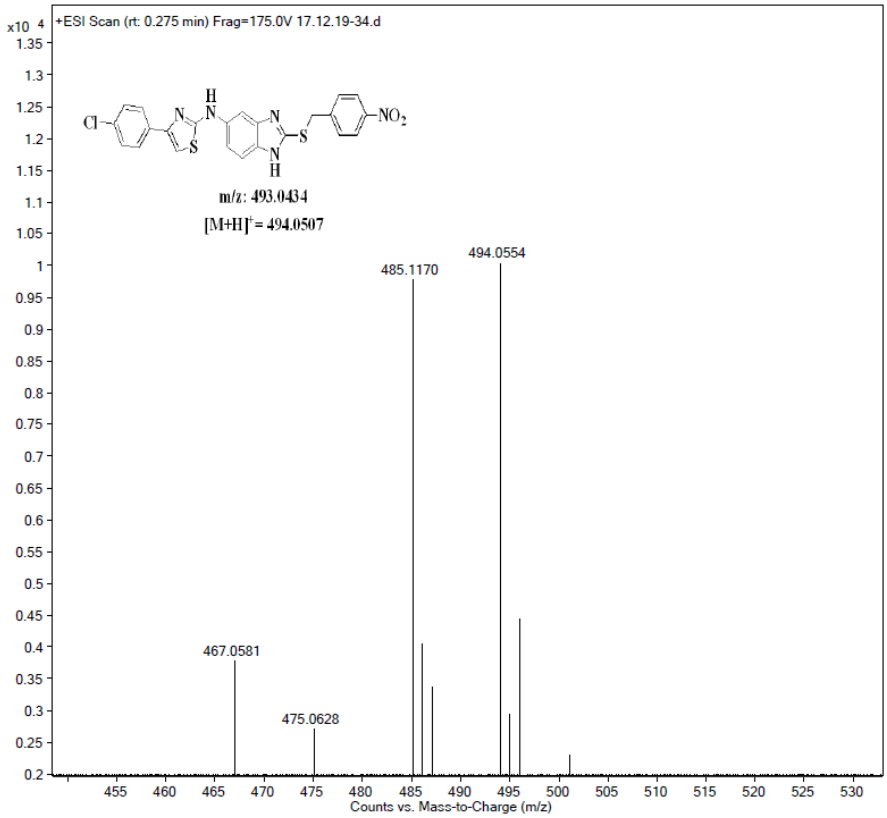

^{1}H-NMR Spectrum of compound 4o in DMSO-d_6 (400 MHz):

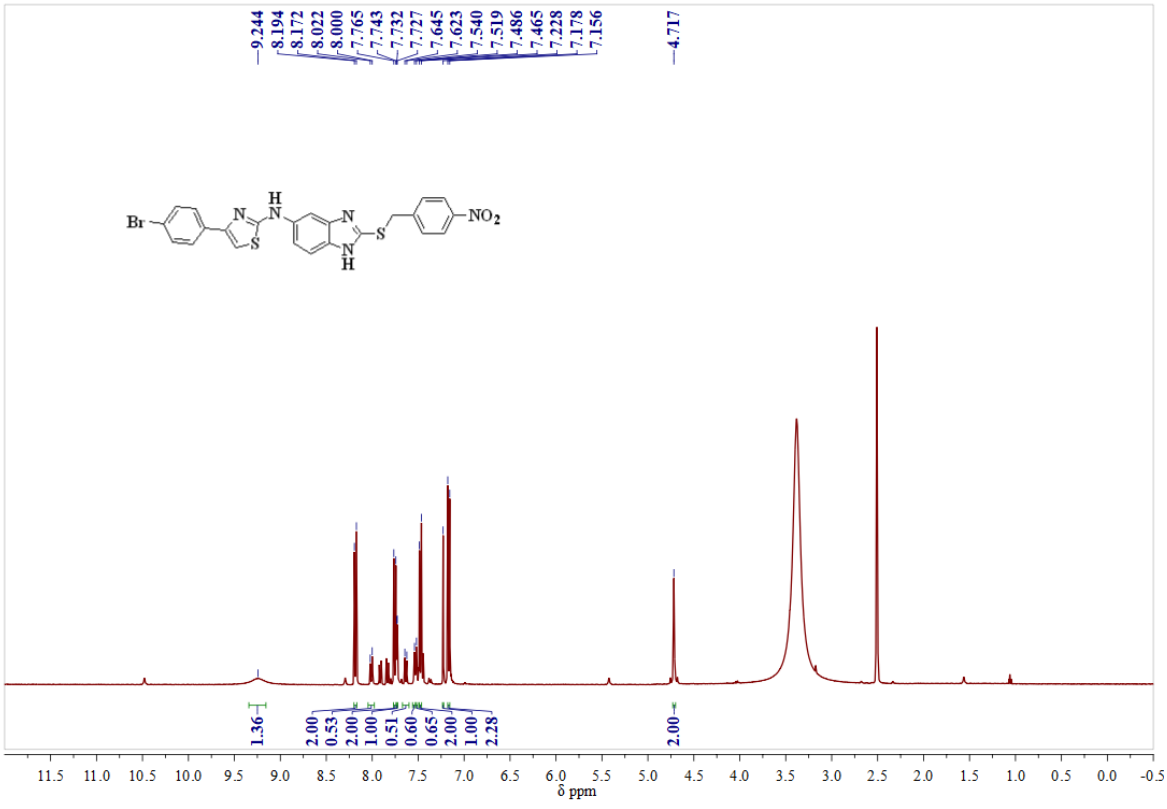

^{13}C-NMR Spectrum of compound 4o in DMSO-d_6 (100 MHz):

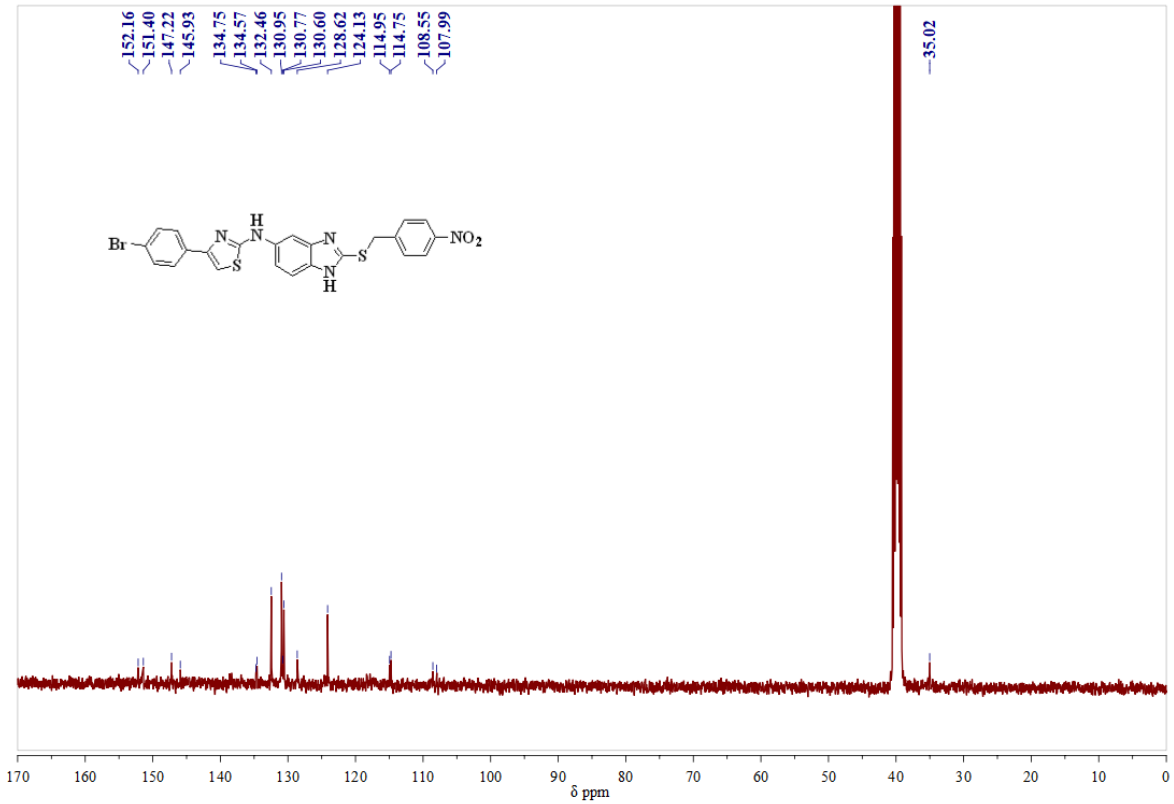

Mass spectrum of compound 4o:

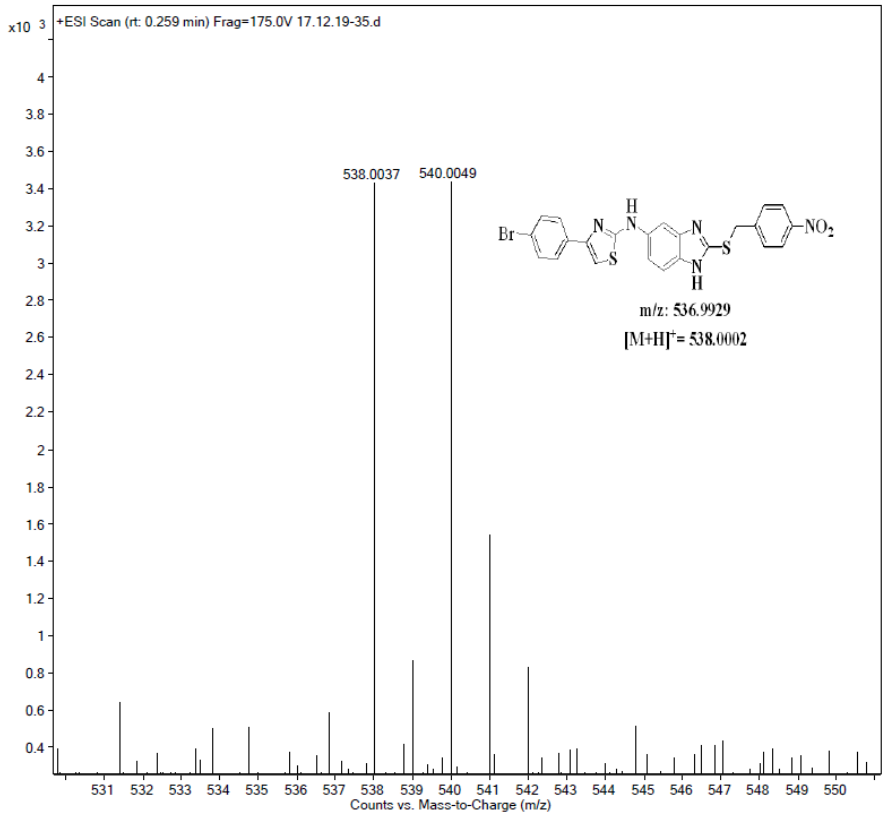

^{1}H-NMR Spectrum of compound 4p in DMSO-d_6 (400 MHz):

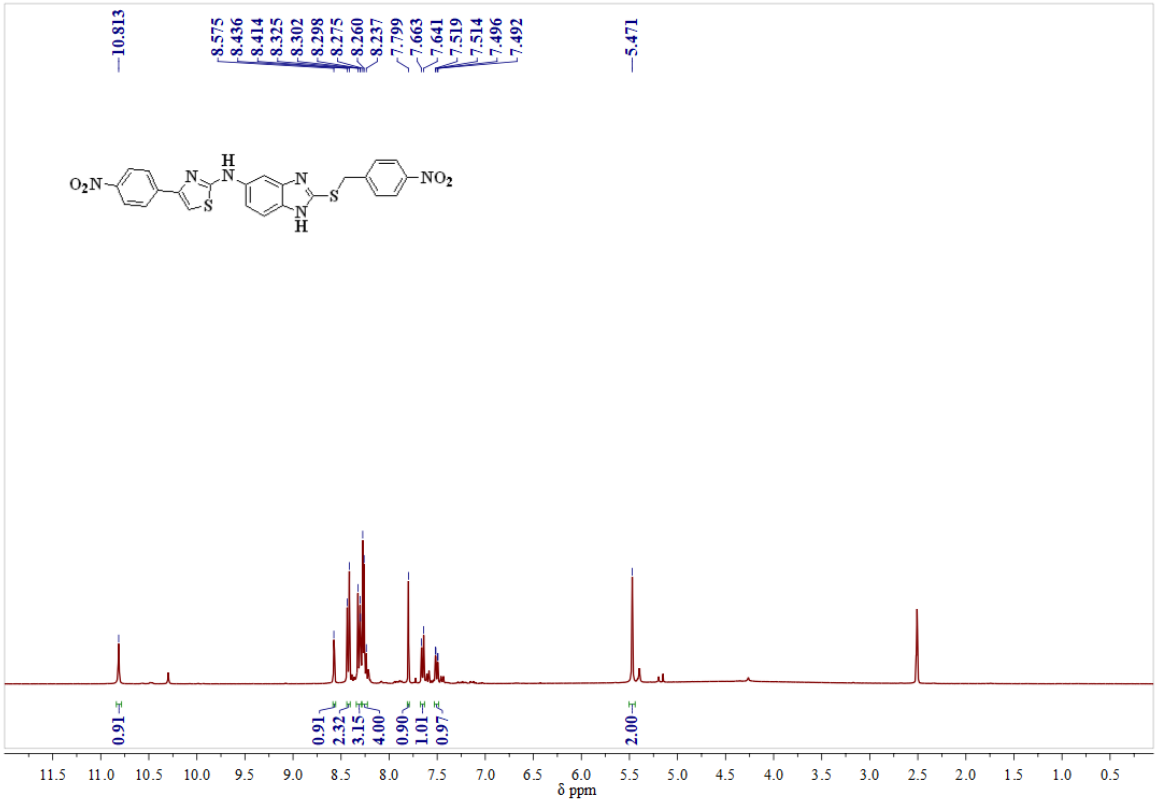

^{13}C-NMR Spectrum of compound 4p in DMSO-d_6 (100 MHz):

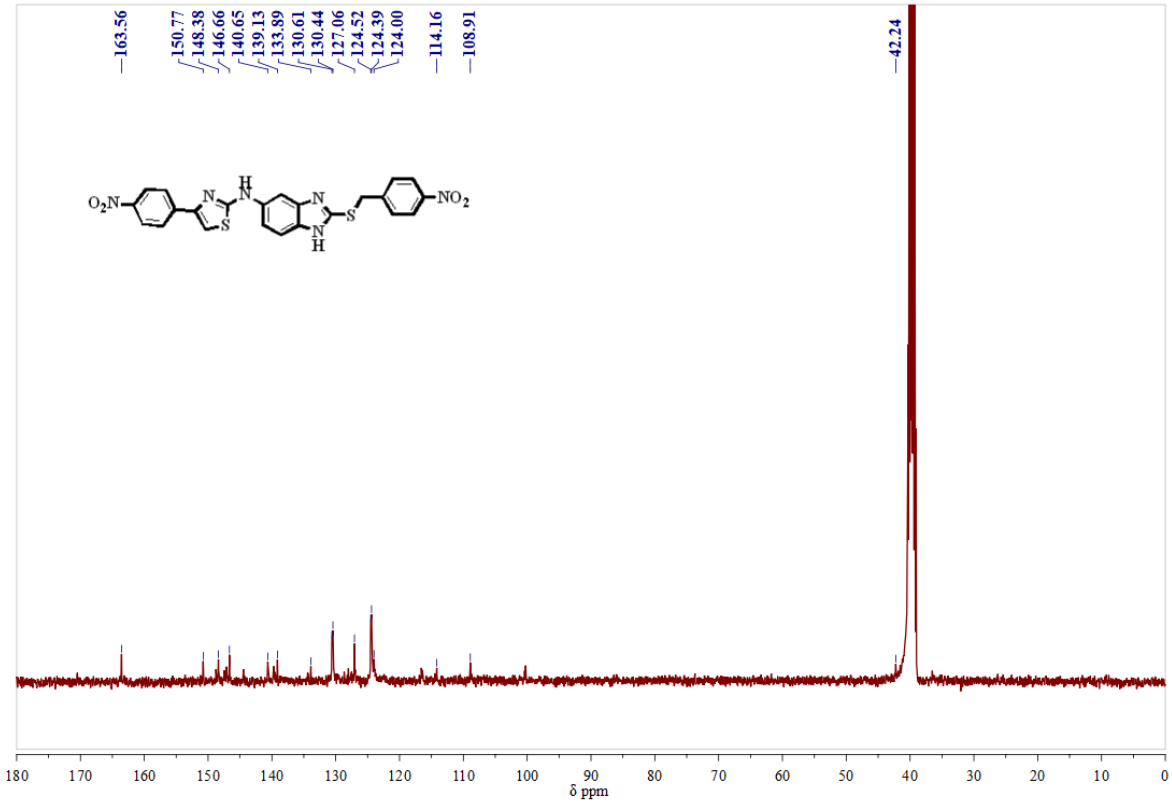

Mass spectrum of compound 4p:

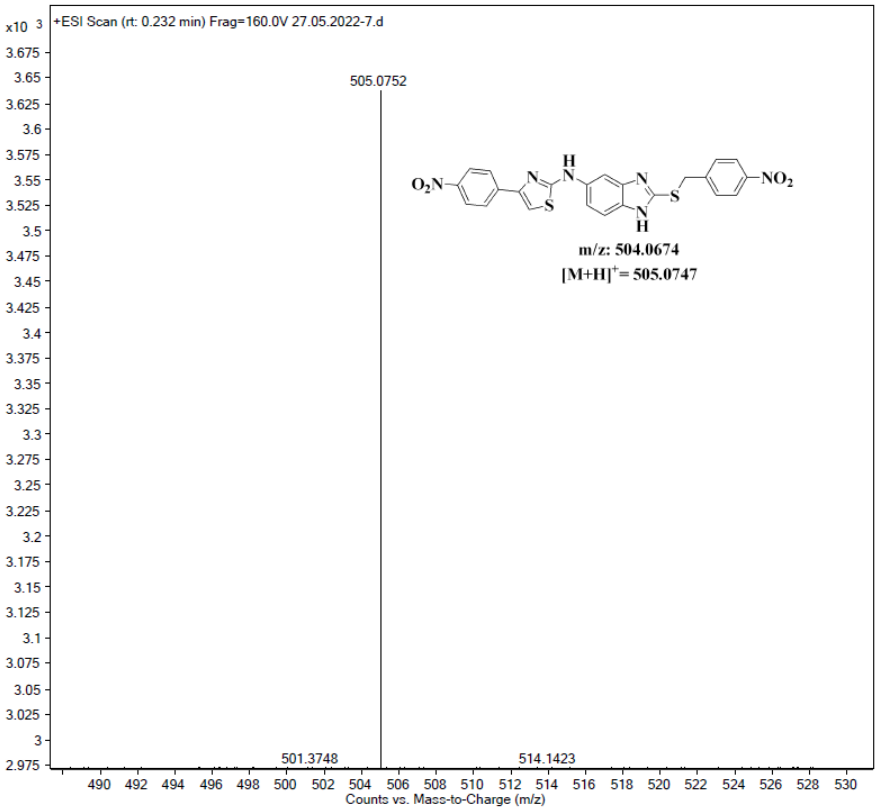

4B.9. References

1. Privalsky, T. M.; Soohoo, A. M.; Wang, J.; Walsh, C. T.; Wright, G. D.; Gordon, E. M.; Gray, N. S.; Khosla, C. *J. Am. Chem. Soc.* **2021**, *143*, 21127–21142.
2. Lu, J.; Patel, S.; Sharma, N.; Soisson, S. M.; Kishii, R.; Takei, M.; Fukuda, Y.; Lumb, K. J.; Singh, S. B. *ACS Chem. Biol.* **2014**, *9*, 2023–2031.
3. Arévalo, J. M. C.; Amorim, J. C. *Sci Rep.* **2022**, *12*, 4742.
4. Trott, O.; Olson, A. J. *J. Comput. Chem.* **2010**, *31*, 455–461.
5. Salentin, S.; Schreiber, S.; Haupt, V. J.; Adasme, M. F.; Schroeder, M. *Nucleic Acids Res.* **2015**, *43*, W443–W447.
6. Van Der Spoel, D.; Lindahl, E.; Hess, B.; Groenhof, G.; Mark, A. E.; Berendsen, H. J. C. *J. Comput. Chem.* **2005**, *26*, 1701–1718.
7. Robertson, M. J.; Tirado-Rives, J.; Jorgensen, W. L. *J. Chem. Theory Comput.* **2015**, *11* , 3499–3509.

CHAPTER-IV (Section-C)

Facile, four-component synthesis of coumarinyl based-thiazoles *via* MCR approach and their anti-cancer activity

CHAPTER-IVC

Facile, one-pot, four-component synthesis of comarinyl-based-thiazole *via* MCR approach and their anti-cancer activity

4C.0. Introduction to 3-heteryl coumarins

Coumarin is a substantial natural product. Also, an oxygen heterocyclic system of benzopyran-2-one derivative. These are the significant metabolics found in extracts of several plant families, such as Euphorbiaceae, Orchidaceae, Asteraceae [1, 2], and microorganism by several extraction methods. Very fistly, coumarin was isolated from Tonka beans by Vogel [3], and first synthesized by Henry perkin in 1868. Moreover, chemically coumarin derivatives can be synthesized by Pechmann [4], Reformatsky [5,6], Knoenengel [7,8], Perkin [9], Hoesch [10], Claisen [11, 12], and Wittig [13] cyclization reaction approaches.

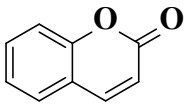

1

5,6-benzo-alpha-pyrone

Coumarin

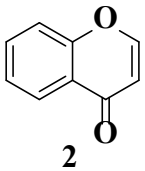

2

benzene-gamma-pyrone

Chromone

Figure 4C.1

4C.1. General characteristics of coumarins:

It is constantly ambiguous regarding the aromatic nature of heterocyclic ring because of its double chemical reaction nature i.e. it displays both the aromatic and aliphatic feature properties. In this moiety, the lactone carbonyl functional (-O=O) group donates the lone pair of electrons to the ring moiety to generate the aromatic structure of 10 π-electrons (Figure 4C.2).

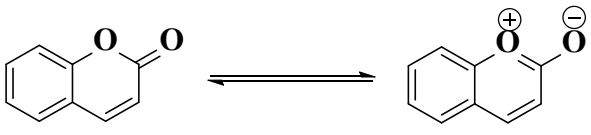

3

Figure 4C.2

From the UV Spectrum of coumarins [14, 15], it's been observed that they displayed funactional absorption values. The outcomes indicated that the introduction of any substituents at various

position of coumarin moiety does not change the nature of the UV spectrum. The λ max and ε values of coumarin are 273 nm (40, 368 M^{-1} cm^{-1}) and 309 nm (37, 449 M^{-1} cm^{-1}) respectively. The IR spectrum [16] of coumarin demonstrates the characteristic stretching frequency for lactone carbonyl functional group at 1705 cm^{-1}, C=C, stretching frequency at 1608, and 1450 cm^{-1} respectively.

Dharmatti [17] *et al.* establishes the proton NMR spectrumof coumarin. The ^{1}H-NMR displays characteric reasonance peaks for C3-H and C4-H at 6.45 and 7.80 δ ppm respectively.

The electron impact mass spectera (EI-Mass) of coumarin was described by Barnes and **Occolowitz [18].** The molecular ion peak and fragmentation peaks shows the transformation of coumarin to benzofuran (Figure 4C.3).

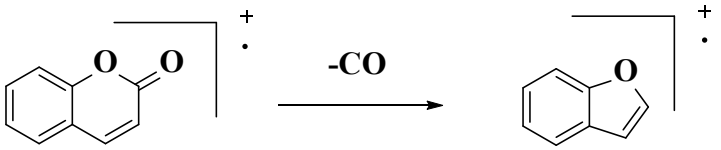

m/z 146 **m/z 118**

4

Figure 4C.3

4C.2. Applications of 3-heteryl coumarins

Nowadays, herbal and synthetic 3-substituted coumarin derivatives have drawn significant attention from the scientific community due to their tremendous appilications inside the area of agrochemicals, dyes, material science, optoelectronics, and therapeutics. Moreover, unique 3-substituted coumarin scaffolds act as privileged heterocyclic analogues with miscellaneous biological activities like antitumor, antioxidant, antimicrobial, anti-aoagulant, anti-tubercular carbonic anhydrase inhibitor, and MAO-B inhibitor activities. Therefore, the development of novel or new artificial and semi-synthetic coumarin heterocyclic derivatives with substantial applications is vital.

Anti-viral activity of 3-substituted coumarins

A novel series of 3-substituted alkyl-4-oxo-coumarinyl ethylidene hydrazono-thiazolidine-5-ylidene **5** analogues were synthesized by **Vedula [19] *et al.*** by using 3-acetyl coumarin, thiosemicarbazide, and dialkyl acetylene dicarboxylate as starting materials and described their

anti-viral activity. These compounds manifested a promising anti-viral activity against various spectrums of human viruses in different cell cultures (**Figure 4C.4**).

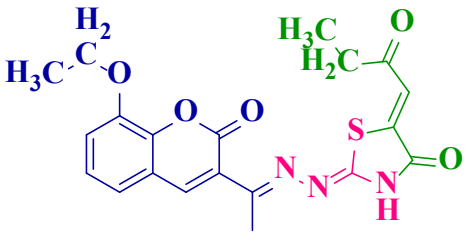

5

Figure 4C.4

Hassan [20] ***et al.*** established a novel series of 3-imidazolylthio methyl-coumarin scaffolds and further screened for their anti-hepatitic C virus activity. Compound 6 has exhibited potent antiviral activity (Figure 4C.5).

6

Figure 4C.5

Anti-malarial activity of 3-substituted coumarins

Sujatha [21] ***et al.*** synthesized a series of new thiazolyl hydrazonothiazolamine derivatives starting from 3-(2-bromoacetyl)coumarins. These compounds were evaluated for their *in vitro* anti-malarial activity. Compounds **7, and 8** exhibited potential activity against malaria **(Figure 4C.6).**

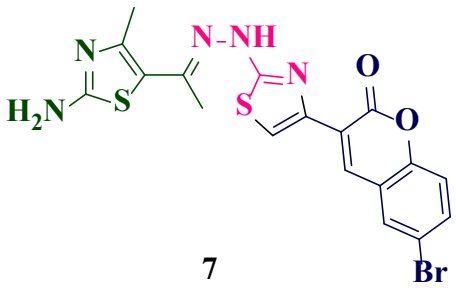

7

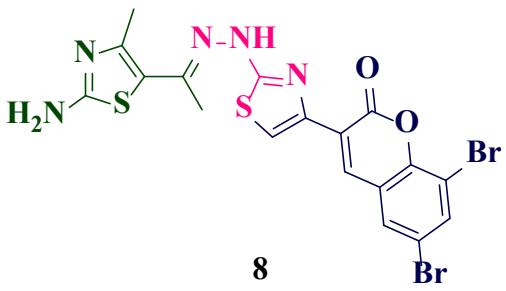

8

Figure 4C.6

Anti-bacterial activity of 3-substituted coumarins

A series of novel coumarin-based thiazoles **9** were synthesized by **Mamidala** [22] ***et al.*** using thiocarbohydrazide, various aldehydes, and substituted 3-(2-bromoacetyl)coumarins. These compounds were further evaluated for their anti-bacterial activity against the Gram-positive bacterium Staphylococcus aureus **(Figure 4C.7).**

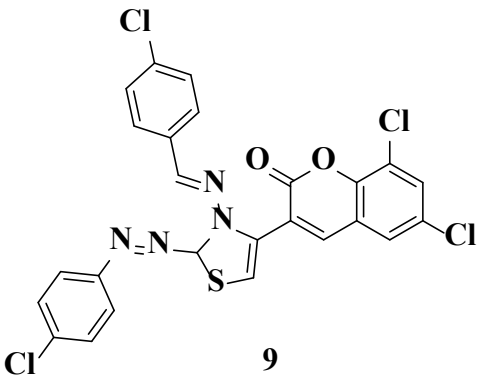

9

Figure 4C.7

A series of coumarin-based α-acyl amino amide derivatives were reported by **Kumar** [23] ***et al.*** *via* a one-pot Knoevengel-Ugi five-component sequential reaction and further described their anti-bacterial activity for Gram-positive and Gram-negative strains. Among the tested compounds, compound **10** have shown good anti-bacterial activity (Figure 4C.8).

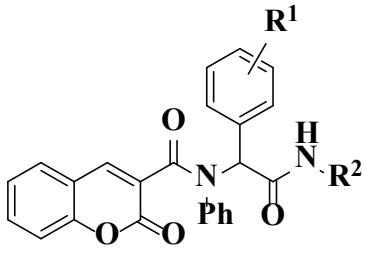

10

Figure 4C.8

Anti-cancer activity of 3-substituted coumarins

Vaarla [24] ***et al.*** has been synthesized a novel series of coumarin based thiazolo-pyrazole **11** derivatives using thiosemicarbazide, 3(2-bromoacetyl)coumarins, and benzoylacetonitriles. These titled compounds were evaluated for their *in-vitro* anti-cancer activity against L1210, CEM, Du145, HeLa, and MCF-7 cell lines and compound **11** shows potent anti-cancer activity (**Figure 4C.9**).

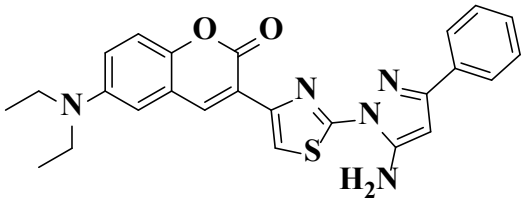

11

Figure 4C.9

Kamath [25] ***et al.*** established a series of new *N*-((2-(2-oxo-2*H*-chromen-3-yl)-1*H*-indol-3-yl)methylene)benzohydrazide **12** derivatives. Further, these derivatives were evaluated for their anticancer activity against human breast adenocarcinoma cells (MCF-7). These derivatives exhibited potential brest cancer activity with apoptosis properties (Figure 4C.10).

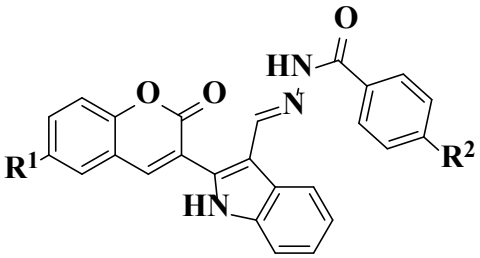

12

Figure 4C.10

Xiang [26] ***et al.*** developed a series of new 3-substituted 4-anilino-coumarin scaffolds and demonstrated *in-vitro* anti-proliferative properties against MCF-7, HepG2, HCT116, and Panc-1 cell lines. Compounds **13**, and **14** have showed good anti-proliferative activity (Figure 4C.11).

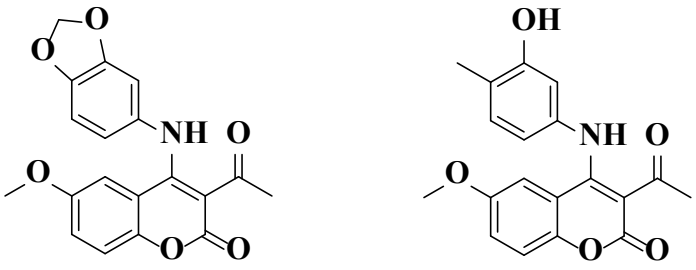

13 **14**

Figure 4C.11

Gali [27] ***et al.*** synthesized indole-incorporated thiazolyl coumarin derivatives and studied in-vitro antibacterial activity against Gram-positive bacteria *bacillus subtilis* and Gram-negative bacteria *Escherichia coli* and also screened for their *in-vitro* anti-cancer activity against the full

panel of 60 human cancer cell lines. Compound **15** shows promising anti-cancer and anti-bacterial activity.

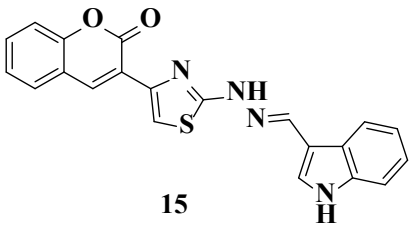

15

Figure 4C.12

Rajitha [28] ***et al***. reported the synthesis of 3-(1-phenyl-4-((2-(4-arylthiazol-2-yl)hydrazono)-methyl)-1*H*-pyrazol-3-*yl*)-2*H*-chromen-2-ones and further evaluated their *in-vitro* anti-microbial activity against Gram-positive bacteria *Staphylococcus aureus*, *Bacillus subtilis*, and Gram-negative bacteria *Escherichia coli, Pseudomonas aeruginosa*, Fungal strains, *Candida albicans*, *Aspergillus niger*, *Candida glabrata*, and *Aspergillus parasiticus*. And anti-oxidant properties.

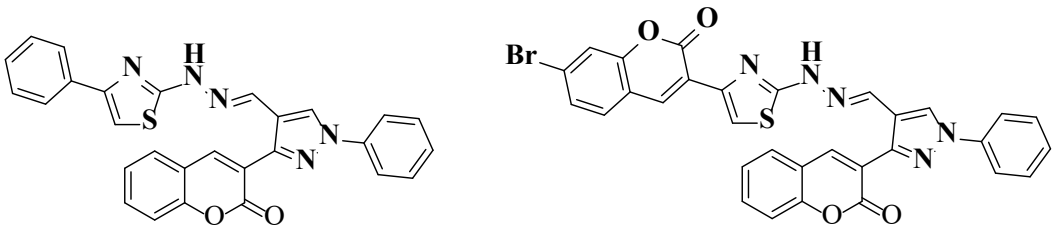

16 **17**

Figure 4C.13

Carbonic anhydrase activity of 3-substituted coumarins

Abdelrahman [29] ***et al.*** synthesized novel 3-substituted coumarin derivatives and described their carbonic anhydrase IX and XII properties. Compounds **18** and **19** exhibit potent carbonic anhydrase properties (Figure 4C.14).

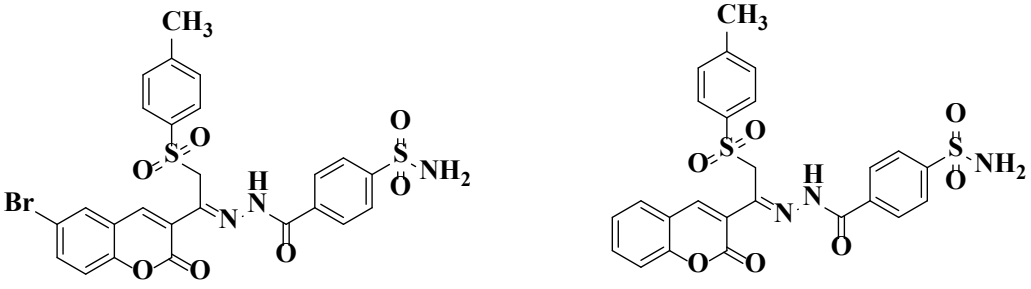

18 **19**

Figure 4C.14

Glucosidase inhibitor activity of 3-substituted coumarins

Salar [30] ***et al.*** established a series of novel 3-thiozolylcoumarin derivatives 20 *via* one-pot approach using 3(2-bromoacetyl)coumarins and 2-benzoyl-*N*-arylhydrazinecarbothioamide in ethanol. Forther these derivatives were evaluated for their *in-vitro* α-glucosidase inhibitory activity. All the synthesized compounds have showed potent inhibitory activity (Figure 4C.15).

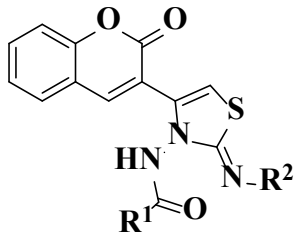

20

Figure 4C.15

Wang [31] ***et al***. developed a series of new thiazolyl coumarin scaffolds using ethyl 4-(2-oxo-2*H*-chromen-3-yl)thiazole-2-carboxylates with substituted aldehydes and hydrazine hydrate. Further, these derivatives were evaluated for their α-glucosidase inhibitory activity. Among the tested compounds, compound **21** have showed remarkable inhibitory activity (Figure 4C.16).

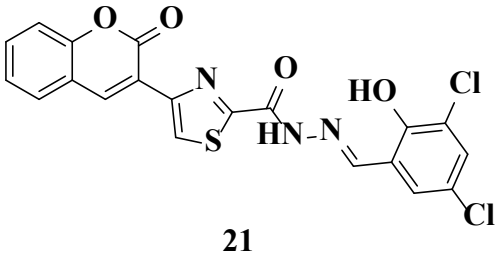

21

Figure 4C.16

Acetylcholinesterase inhibitor activity of 3-substituted coumarins

Yao [32] ***et al***. reported a series of new 2-oxo-N-(4-(2-(piperzine-1-yl)ethylphenyl)-2*H*-chromene-3-carboxamide derivatives strating from 3-chloro-4-((4-ethyl piperazine-1-yl)methyl)aniline with 2-oxo-2*H*-chromene-3-carbonyl chloride. Further, these compounds were evaluated for their acetylcholine esterase inhibition activity. Compound **22** have showed remarkable AChE inhibition activity. Here, Huperzine A used as the reference drug (Figure 4C.17).

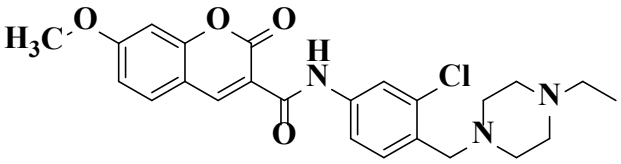

22

Figure 4C.17

Antileishmanial activity of 3-substituted coumarins

Zaheer [33] ***et al.*** reported a series of new 3-substituted amino-4-hydroxycoumarin analogoues. Furthere, these derivatives were screened for their antileishmanial activity against Leishmania donovani promastigotes. Among the tested compounds, compound **23** have showed significant antileishmanial activity (Figure 4C.18). Here, pentamidine and miltefosine are the standard agents.

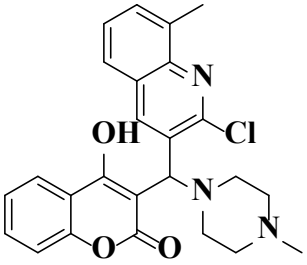

23

Figure 4C.18

Analgesic activity of 3-substituted coumarins

Gupta [34] **et al.** developed and evaluated in-vivo analgesic activity of 2-amino-4-(coumarin-3-yl)-6-aryl pyrimidine derivatives from 3-acetyl coumarin. Here, the diclofenac sodium was used as standard drug. Compound **24** have showed remarkable analgesic activity (Figure 4C.19).

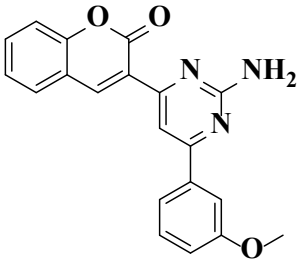

24

Figure 4C.19

Antioxidant activity of 3-substituted coumarins

A series of new 3-(2-oxo-2*H*-chromen-3-yl)-1*H*-pyrazole-5-carboxylic acid 25, 5-(2-oxo-2*H*-chromen-3-yl)-2,3-dihydroisoxazole-3-carboxylic acid derivatives 26 were reported by

Saleem [35] ***et al*** using 4-oxo-4-(2-oxo-2*H*-chromen-3-yl)but-2-enoic acid, hydrazine hydrate or hydroxylamine hydrochloride. Further, these derivatives were screened for their antioxidant activity (Figure 1.20).

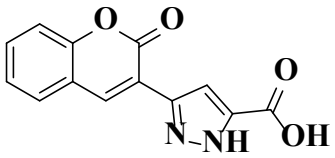

25

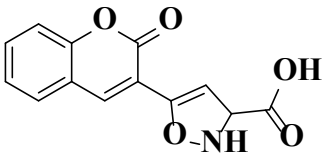

26

Figure 4C.20

Li [36] ***et al.*** reported a series of novel conjugates of hydroxytyrosol-based coumarin scaffolds and described their *in-vitro* anti-oxidant activity. Compound **27** shows promising anti-oxidant activity (Figure 4C.21).

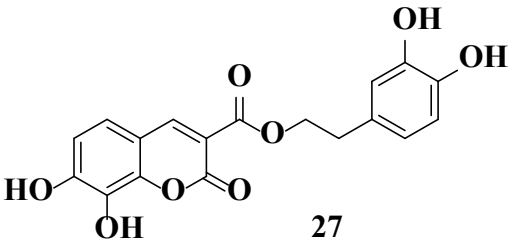

27

Figure 4C.21

4C.3. Present work

In line with our interest, considering the importance of coumarin, and thiazole moieties and prompted by the aforementioned literature, we aimed for an update and extension of its usefulness focusing on the synthesis of coumarin-based thiazole derivatives *via* the MCR approach.

4C.3.1 Starting materials

The present chapter describes the synthesis and anticancer activity of 3- coumarinyl based

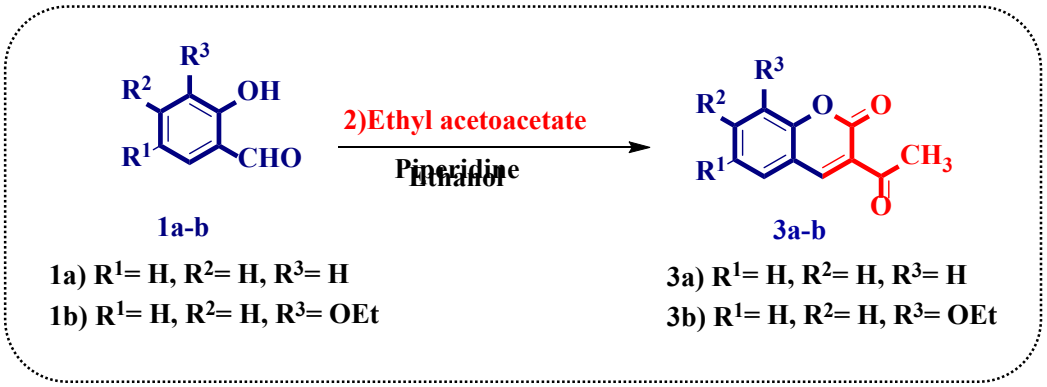

1a-b

1a) R^1= H, R^2= H, R^3= H

1b) R^1= H, R^2= H, R^3= OEt

3a-b

3a) R^1= H, R^2= H, R^3= H

3b) R^1= H, R^2= H, R^3= OEt

Scheme 4C.1. Synthesis of coumarin based thiazoles:

thiazole compounds (**5a-s**) and are outlined in **scheme-4C.1**. The titled compounds were synthesized by reaction of an equimolar ratio of phenyl isothiocyanate (**1**), hydrazine hydrate (**2**), substituted 3-acetyl-coumarins (**3**) and various substituted phenacyl bromides (**4**) (**1:1.2:1:1**) in the catalytic amount of acetic acid and ethanol as solvent at 60 ºC to give titled compounds in good yields.

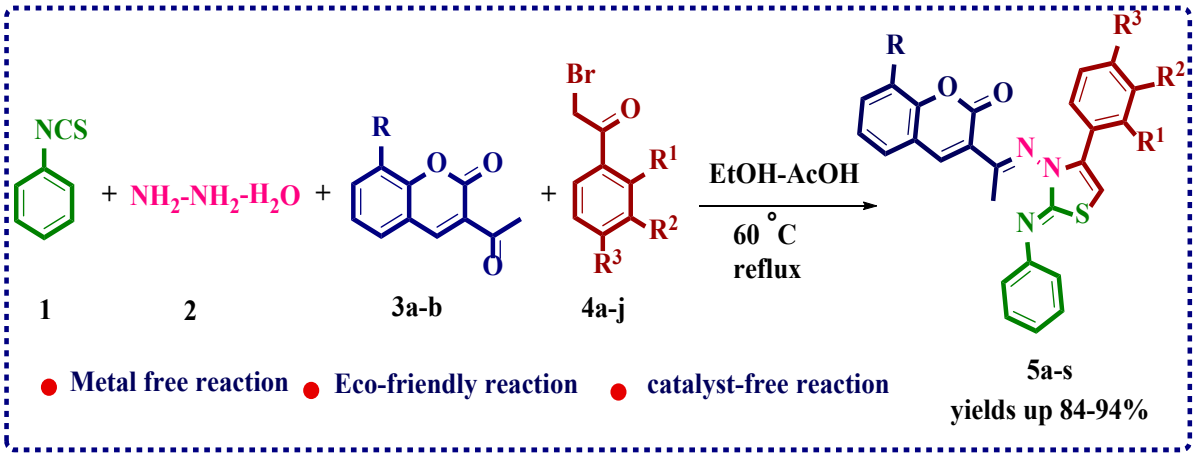

Scheme 4C.2. Synthesis of coumarin-based thiazoles.

4C.4. Results and discussion

The synthetic protocol for the title coumarin-based thiazole derivatives (**5a-s**) has been outlined in **Scheme 4C.2** and was synthesized by the one-pot, four-component condensation of phenyl isothiocyanate **1,** hydrazine hydrate **2**, 3-acetyl coumarin **3,** and phenacyl bromide, in ethanol with a catalytic amount of glacial acetic acid under reflux condition provides good to excellent yields in shorter reaction time. The starting material 3-acetyl coumarins were synthesized by following literature procedures [37,38]. The optimized reaction conditions and physical data of the synthesized compound were presented in **Table 4C.2**.

The starting material phenyl isothiocyanate, hydrazine hydrate and phenacyl bromides were procured from commercial sources and were used as it is. To optimize the reaction condition for the synthesis of the title compounds **5a-t**, a pilot reaction was conducted by taking the trail reactants phenyl isothiocyanate (**1**), hydrazine hydrate (**2**), 3- acetyl coumarin (**3**), and phenacyl bromide (**4**). The optimization of the results of the compound **5a** was summarized in **Table 4C.1.**

Table 4C.1. Optimization reaction conditions of coumarin-based thiazole synthesis.

Entry	Solvent	catalyst	Temp (^{0}C)	Time (h)	Yield[b] (%)
1	H_2O	-	r.t	24	15
2	H_2O	-	60	18	21
3	MeOH	-	r.t	18	28
4	MeOH	-	60	18	40
5	MeOH	KOH	60	15	45
6	MeOH	NaOH	60	15	48
7	MeOH	AcOH (1.0mL)	60	14	50
8	MeOH	Et_3N	60	15	42
9	MeOH	Piperidine (5 drops)	60	15	41
10	EtOH	-	60	15	48
11	EtOH	KOH	60	12	50
12	EtOH	NaOH	60	10	52
13	EtOH	Et_3N	60	10	55
14	EtOH	Piperidine (5 drops)	60	10	58
15	**EtOH**	**AcOH**	**60**	**8**	**85**
16	EtOH	AcOH	70	8	70
17	EtOH	-	reflux	6	60
18	AcOH	-	60	7	72

[a]***Reaction conditions*:** phenylisothiocyanate (1) (1.0 mmol), hydrazine hydrate (2) (1.2 mmol), 3-acetyl-coumarin (3) (1.0 mmol), phenacyl bromide (1.0 mmol) solvent (2 mL), [b]Isolated yields.

A pilot reaction was conducted between phenyl isothiocyanate (**1**), hydrazine hydrate (**2**), 3-acetyl coumarin (**3**), and phenacyl bromide (**4**) in water at room temperature to obtain the desired product **5a** in poor yield (Table 4C.1, entry-1). It is noticed that even methanol also the reaction provided poor yield at room temperature (Table 4C.1, entry-3). Hence, it is well noticed that the room temperature was not effective to get better reaction yields. Further, we focused our attention on to increase the temperature from room temperature to 60 ºC and tried different reaction conditions (Table 4C.1, entries 5-18). Notably, the solvent screening was

continued in polar protic solvents like methanol, ethanol and acetic acid along with the loading of various organic and inorganic bases resulted in moderate reaction yields and took longer reaction time (Table 4C.1, entries 4-14). To our delight, the yield of **5a** was dramatically increased to 85% when the reaction was conducted in ethanol and a catalytic amount of acetic acid at 60 ºC (Table 4C.1, entry-15). Additionally, by variation in temperature and load of catalyst (AcOH) does not increase the product yield (Table 4C.1, entry 15,16). The structure of **5a** was confirmed by ^{1}H and ^{13}C-NMR and ESI-HRMS spectral data.

With these optimized reaction conditions in hand (Table 4C.1, entry-14) then we have focused our attention to explore the scope of this novel one-pot, four-component reaction, with diversely substituted phenacyl bromides and 3-acetyl coumarins. The physical data of the synthesized scaffolds were summarized in Table 4C.2. It is well recognized that electron withdrawing groups like $-NO_2$ substituent on phenacyl bromide at the 4th position has be reacted smoothly and gave the highest yield (96%, Table 4C.2, entry-5i) in a short time. This can also be tolerated with halogen substituents such as F, Cl, and Br and afforded the corresponding coumarin-based substituted thiazole derivatives in 95-96% of yields (Table 4C.2, entries- 5d,5e, and 5f). Further, 3-acetyl coumarin which has variant at the 7th position (-OEt) also well participated in the reaction and gave excellent yields. Further, the final products were purified by simple recrystallization. The uniqueness of this four-component reaction is that 3C-N, 1C-S, bonds are formed at a time, and the reaction does not require any metal catalyst, harsh reaction conditions, and also no column chromatography for the purification of the final compounds.

The structure of newly synthesized scaffolds was well characterized by IR,^{1}H-NMR, ^{13}C-NMR, and HRMS spectral data. For instance, the stretching vibrations of -C=O (lactone), C=N, and C=C were detected in the IR spectrum of compound **4a** at 1735 cm $^{-1}$, 1602 cm $^{-1}$, and 1589 cm $^{-1}$ respectively. The ^{1}H-NMR of the spectrum of compound **4a** revealed peaks at δ 8.09 (C4-proton of coumarin), δ 6.18 corresponding to the C5-proton of thiazole, and δ 2.32 aliphatic protons respectively. The ^{13}C-NMR spectrum showed peaks at δ 170.09, 116.52 and 17.14 corresponding to the carbonyl carbon of lactone, thiazole C5-carbon, and aliphatic methyl carbons respectively. The HRMS (ESI) spectra of all the synthesized compounds have shown $[M+H]^{+}$ ion peak.

Scheme 4C.3. Plausible reaction mechanism for the one-pot, four-component formation of thiazole compounds (**5a-s**)

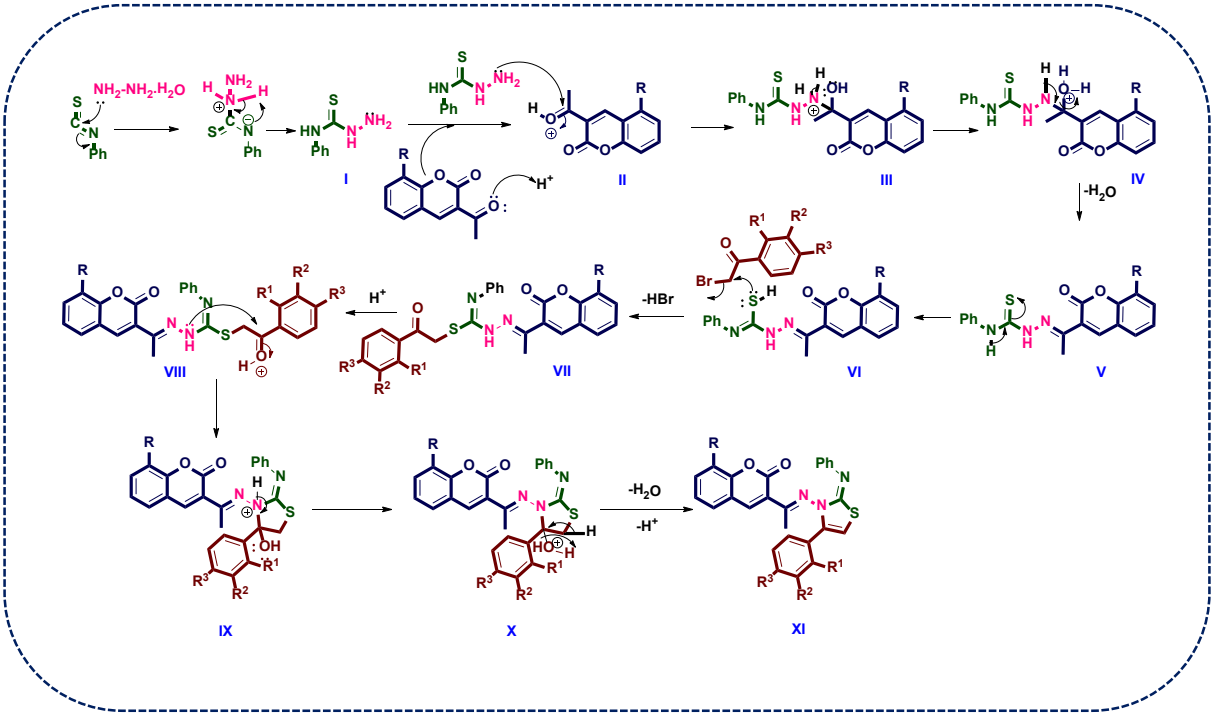

The plausible reaction mechanism of the formation of scaffolds (**5a-s**) was illustrated in Scheme 4C. 3. In this reaction at first 1 equivalent of phenylisothiocyanate reacts with 1.2 equivalent of hydrazine hydrate by acid-catalysed condensation to form intermediate-I phenylthiosemicarbazide. Further, this undergoes condensation with 1 equivalent of protonated carbonyl part of substituted 3-acetyl coumarin to form intermediate-VII. Afterwards, the nucleophilic attack of sulphur on the carbon of C-Br bond of various substituted phenacyl bromides (1 equivalent) gave intermediate IX. This further undergoes acid-catalysed dehydration to form coumarin-based substituted thiazoles (**5a-s**).

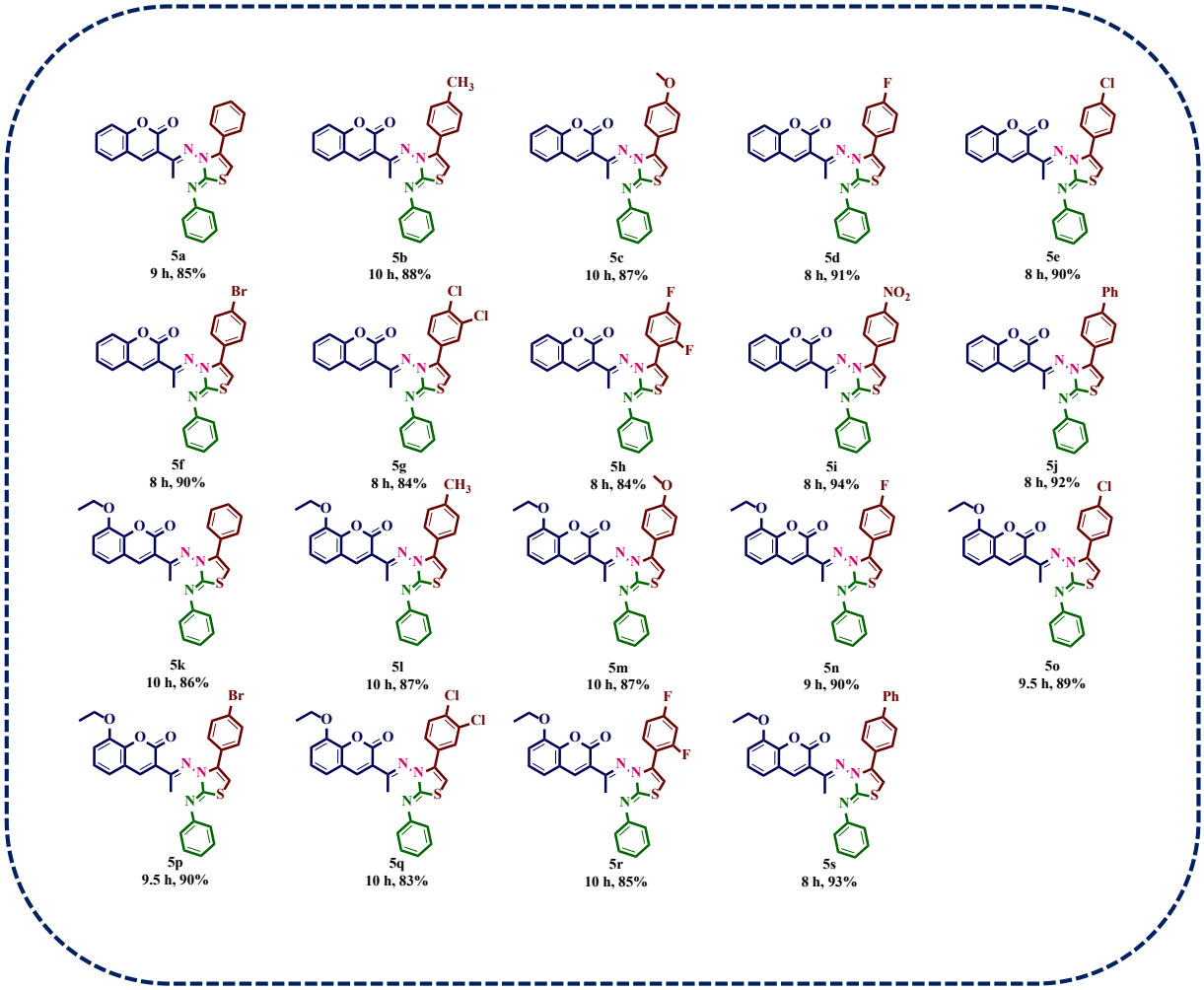

Figure 4C.1 Substrate scope of derivatives.

4C.5. In-vitro anti-cancer activity

The synthesized compounds were checked for their anticancer activities using different cancer cell lines. We used C6 rat glioma and LN18 human glioma cell lines. We also checked the anti-cancer activity in MCF7, the breast cancer cell lines using the MTT assay.

4C.5.1. MTT Cell Viability Assay

A colourimetric assay called MTT is used to measure cellular metabolic activity. Living cells transform the yellow tetrazole MTT into the purple formazan. Tetrazolium salts are transformed into coloured formazan compounds by living (metabolically active) cells but not by dead cells. As a result, only tetrazolium salt-based colourimetric tests can detect live cells. These metabolic activity assays are widely used to assess drug-induced cytotoxicity since a cytotoxic factor, such as a drug or synthetic molecule, would decrease the rate at which a

population of cells cleaves tetrazolium salts. Cells that divide quickly, such as cancer cells, have high rates of MTT decrease.

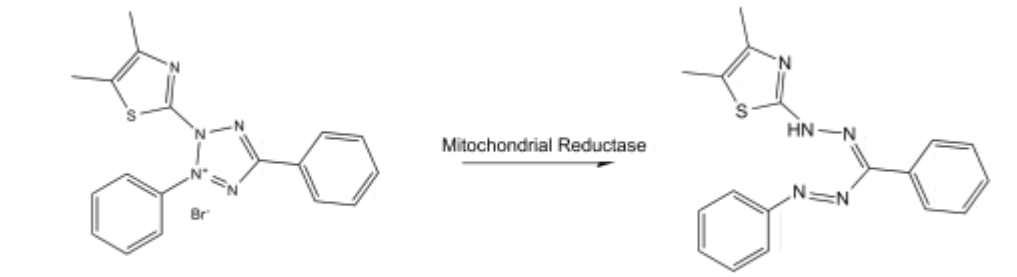

4C.5.2. Principle

Numerous *in vitro* tests of a cell population's reaction to outside influences are based on measurements of cell viability and proliferation. MTT [3-(4,5-dimethylthiazol-2-yl)-2,5-diphenyltetrazolium bromide] assay, was first described by Mosmann [39] in 1983 and is based on the ability of a mitochondrial dehydrogenase enzyme from viable cells to cleave the tetrazolium rings of the pale yellow MTT to form dark blue formazan crystals. The formazan is impermeable to cell membranes and thus results in its accumulation within healthy cells. By using spectrophotometric techniques, the resulting intracellular purple formazan can be solubilized and measured. The insoluble purple formazan product is converted into a coloured solution by adding a solubilization solution, which is typically either dimethyl sulfoxide, an acidified ethanol solution, or a solution of the detergent sodium dodecyl sulphate in diluted hydrochloric acid. After that, the colour can be measured using a simple colorimetric assay. The absorbance of this coloured solution can be measured using a spectrophotometer at a certain wavelength (often between 500 and 600 nm). The results can be read on a multiwell scanning spectrophotometer (ELISA reader). The MTT Cell Proliferation assay measures the cell proliferation rate and conversely when metabolic events lead to a reduction in cell viability (**Further MTT assay studies was going in laboratories**).

4C.5.3. Results

Preliminary investigations were done by screening the compounds for anti-cancer activity on C6 glioma cell lines. The synthesized compounds were screened for cytotoxicity in C6 rat glioma cell lines by MTT assay. Based on the reduction of the tetrazolium bromide salt MTT [3-(4,5-dimethylthiazol-2-yl)-2,5-diphenyl-tetrazolium bromide], this assay gives a

quantitative measurement of the number of cells with metabolically active mitochondria. All treatments were performed in triplicate. As depicted in the table, all compounds showed well. Analysis of data showed that the compounds significantly diminished the cell viability over time in a dose-dependent manner and showed a good inhibitory effect against the growth of C6 glioma cell proliferation. **5a-s** exhibited a good anti-proliferative effect and **5m** displayed the highest inhibition of cell proliferation with the IC_{50} value of 0.617 micromoles.

Table 4C.2. IC_{50} values in μM for the compounds **5a–s** against human cancer cell lines through Cell Viability (MTT) Assay

Code	LN18	MCF7
5a	12.91	2.9
5b	31.39	
5c	32.48	17.51
5d	47.73	20.82
5e	15.37	4.7
5f	2.55	619
5g	Above 100	Above 100
5h	29.6	5.05
5i	Above 60	4.81
5j	9779	2.28
5k	67.4	12.89
5l	14.25	3.21
5m	0.617	4.61
5n	266.9	73.72
5o	51.27	24.3
5p	21.46	76.97
5q	22.41	55.56
5r	21.53	14.4
5s	14.82	10.3

Structure-activity relationship

To explore and understand the structure-activity relationship (SAR) of new thiazole derivatives, the synthesized compounds were screened against cancer cell lines. The new thiazole derivatives were synthesized by incorporating various electron-donating groups (methoxy and hydroxyl) and electron-withdrawing groups (Fluorine, Chlorine, Bromine and Nitro) at R position of 3-acetyl coumarin, R_1, R_2 and R_3 positions on phenacyl bromides. Among the newly synthesized compounds, compound **5m** which is having methoxy group at R_3 and ethoxy at R positions has shown potent activity against all cancer cell lines (Table **5.5**).

Notably, compound **5f** possessing bromine at the 'R_3' position showed comparatively moderate activity against all cancer cell lines when compared with the remaining compounds in the series. It indicates that the presence of strong electron-withdrawing groups at the 'R_3' position may not be beneficial for activity instead small electron-withdrawing groups may favour the activity. Compounds which possessed electron-withdrawing groups at R_1, R_2 and R_3 positions could not show any significant effect on activity. Therefore, it was evident from the anti-cancer data that electron-donating groups at R and R_3 positions will be beneficial for activity.

4C.6. Conclusion

In summary, we have developed a potential protocol for the synthesis of new coumarin-based thiazole derivatives by a one-pot MCR approach. Further, we have screened the title compounds (5a-t) for their in-vitro anticancer activity against MCF7 and LN18 cancer cell lines. Among tested compounds, compound **5m** was showed excellent anticancer activity. Here, temozolomide was used as reference-positive control drug.

4C.7. Experimental section

4C.7.1. General procedure for the synthesis of **4-phenyl-2-(phenylimino)thiazol-3(2H)-yl)imino)ethyl)-2H-chromen-2-ones** (**5a-s**).

A mixture of phenyl isothiocyanate (1 mmol), hydrazine hydrate (1.2 mmol), substituted 3-acetyl coumarin (1 mmol) and various phenacyl bromide (1 mmol) along with the catalytic amount of acetic acid and ethanol was taken in a round bottom flask. The reaction mixture was refluxed for 8-10 h. Progress of the reaction was monitored by thin-layer chromatography. After completion of the reaction, the product was filtered and separated, washed with ethanol, dried and recrystallized from ethanol.

4C.8. Characterization data of products

4-Phenyl-2-(phenylimino)thiazol-3(2*H*)-yl)imino)ethyl)-2*H*-chromen-2-one. 5a

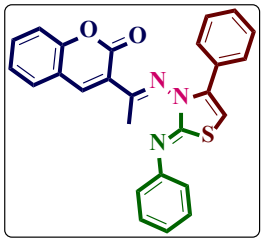

Yellow solid: yield: 85% ; mp. 207-209 °C; FT-IR (KBr, cm^{-1}): 1735 (lactone –C=O), 1602 (C=N), 1589 (C=C); ^{1}H NMR (400 MHz, $CDCl_3$ δ ppm): 8.09 (s, 1H, C_4-coumarin proton), 7.57 (d, *J* = 7.6 Hz, 2H, Ar-H), 7.50 (t, *J*= 7.0 Hz, 1H, Ar-H), 7.33-7.30 (m, 3H, Ar-H), 7.27-7.24 (m, 5H, Ar-H), 7.21 (d, *J* = 7.6 Hz, 2H, Ar-H), 7.12 (dd, *J* = 7.8, 1.8 Hz, 2H, Ar-H), 6.18 (s, 1H, thiazole C_5-ptoton), 2.32 (s, 3H, CH_3-protons). ^{13}C NMR (100 MHz, $CDCl_3$) δ: 170.09, 160.29, 156.04, 154.16, 140.76, 140.59, 137.97, 131.75, 131.36, 128.85, 128.78, 128.59, 128.50, 128.41, 127.84, 127.71, 124.55, 119.72, 116.52, 101.63, 17.14; ESI-HRMS: *m/z* Calcd for Chemical Formula: $C_{26}H_{20}N_3O_2S$: 438.1271 $[M+H]^+$ found: 438.1270.

2-(Phenylimino)-4-(p-tolyl)thiazol-3(2*H*)-yl)imino)ethyl)-2*H*-chromen-2-one. 5b

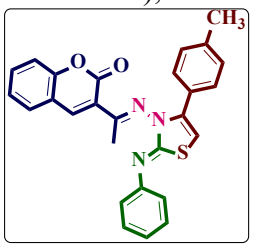

Yellow solid: yield: 87% ; mp. 226-228 °C; FT-IR (KBr, cm^{-1}): 1722 (lactone –C=O), 1603 (C=N), 1572 (C=C); ^{1}H NMR (400 MHz, $CDCl_3$ δc): 8.08 (s, 1H, C_4-coumarin proton), 7.57 (dd, *J* = 7.8, 1.4 Hz, 1H, Ar-H), 7.50 (t, *J*= 7.0 Hz, 1H, Ar-H), 7.34– 7.31 (m, 3H, Ar-H), 7.27 – 7.24 (m, 4H, Ar-H), 7.00 (unresolvable singlet, 4H, Ar-H), 6.13 (s, 1H, thiazole C_5-ptoton), 2.31 (s, 3H, CH_3 protons), 2.28 (s, 3H, CH_3 protons). ^{13}C NMR (100 MHz, $CDCl_3$) δ: 170.00, 160.13, 155.72, 153.97, 140.55, 138.40, 137.88, 131.54, 128.99, 128.65, 128.37, 128.11, 127.68, 127.48, 124.36, 119.56, 116.34, 100.81, 21.24, 16.94; ESI-HRMS: *m/z* Calcd for Chemical Formula: $C_{27}H_{22}N_3O_2S$: 452.1427 $[M+H]^+$ found: 452.1447.

4-(4-Methoxyphenyl)-2-(phenylimino)thiazol-3(2*H*)-yl)imino)ethyl)-2*H*-chromen-2-one. 5c

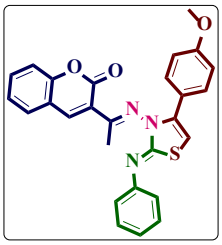

Yellow solid: yield: 89% ; mp. 205-207 °C; FT-IR (KBr, cm^{-1}): 1721 (lactone –C=O), 1603 (C=N), 1570 (C=C); ^{1}H NMR (400 MHz, $CDCl_3$ δ ppm): 8.08 (s, 1H, C_4-coumarin proton), 7.57 (dd, *J* = 7.6, 1.6 Hz, 1H, Ar-H), 7.50 (t, *J*= 7.0 Hz, 1H, Ar-H), 7.32 (d, *J* = 8.0 Hz, 3H, Ar-H), 7.27-7.24 (m, 4H, Ar-H), 7.04 (d, *J* = 9.2 Hz, 2H, Ar-H), 6.72 (d, *J* = 8.8 Hz, 2H, Ar-H), 6.09 (s, 1H, thiazole C_5-ptoton), 3.75 (s, 3H, -OCH_3 protons), 2.31 (s, 3H, CH_3 protons). ^{13}C NMR (100 MHz, $CDCl_3$) δ: 169.99, 160.13, 159.58, 155.66, 153.97, 140.53, 140.19, 137.86, 131.54, 129.61, 128.67, 128.59, 128.42, 127.68, 127.50, 124.36, 123.61, 119.56, 116.33, 113.70, 100.18, 55.23, 16.93; ESI-HRMS: *m/z* Calcd for Chemical Formula: $C_{27}H_{22}N_3O_3S$: 468.1376 $[M+H]^+$ found: 468.1375.

(4-Fluorophenyl)-2-(phenylimino)thiazol-3(2*H*)-yl)imino)ethyl)-2*H*-chromen-2-one. 5d

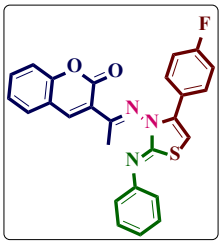

Yellow solid: yield: 90% ; mp. 212-214 °C; FT-IR (KBr, cm^{-1}): 1734 (lactone –C=O), 1599 (C=N), 1582 (C=C);^{1}H NMR (400 MHz, $CDCl_3$ δ ppm): 8.08 (s, 1H, C_4-coumarin proton), 7.57 (dd, *J* = 7.6, 1.6 Hz, 1H, Ar-H), 7.51 (t, *J*= 7.2 Hz, 1H, Ar-H), 7.32 (d, *J* = 6.0 Hz, 2H, Ar-H), 7.29 – 7.23 (m, 5H, Ar-H), 7.10 (dd, *J* = 9.2, 4.6 Hz, 2H, Ar-H), 6.90 (t, *J* = 8.8 Hz, 2H, Ar-H), 6.15 (s, 1H, thiazole C_5-ptoton), 2.31 (s, 3H, CH_3 protons). ^{13}C NMR (100 MHz, $CDCl_3$) δ: 169.70, 163.77, 161.30, 160.09, 156.04, 153.98, 140.62, 139.31, 137.60, 131.61, 130.14, 130.06, 128.79, 128.60, 128.34, 127.69, 127.62, 127.29, 124.38, 119.51, 116.36, 115.56, 115.34, 101.41, 16.96; ESI-HRMS: *m/z* Calcd for Chemical Formula: $C_{26}H_{19}FN_3O_2S$: 456.1177 $[M+H]^+$ found: 456.1176.

4-Chlorophenyl)-2-(phenylimino)thiazol-3(2*H*)-yl)imino)ethyl)-2*H*-chromen-2-one. 5e

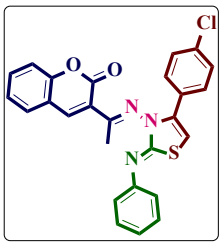

Yellow solid: yield: 91% ; mp. 234-236 °C; FT-IR (KBr, cm^{-1}): 1735 (lactone –C=O), 1601 (C=N), 1586 (C=C); ^{1}H NMR (400 MHz, $CDCl_3$ δ ppm): 8.08 (s, 1H, C_4-coumarin proton), 7.57 (dd, *J* = 7.6, 1.4 Hz, 1H, Ar-H), 7.51 (t, *J*=7.2 Hz, 1H, Ar-H), 7.33 (d, *J* = 7.6 Hz, 2H, Ar-H), 7.30 – 7.23 (m, 5H, Ar-H), 7.18 (d, *J* = 8.8 Hz, 2H, Ar-H), 7.05 (d, *J* = 8.4 Hz, 2H, Ar-H), 6.19 (s, 1H, thiazole C_5-ptoton), 2.31 (s, 3H, CH_3 protons). ^{13}C NMR (100 MHz, $CDCl_3$) δ: 169.82, 160.26, 156.36, 154.17, 140.83, 139.38, 137.74, 134.61, 131.81, 129.80, 129.57, 129.03, 128.79, 128.45, 127.92, 127.78, 124.58, 119.68, 116.55, 102.21, 17.17; ESI-HRMS: *m/z* Calcd for Chemical Formula: $C_{26}H_{19}ClN_3O_2S$: 472.0881 $[M+H]^+$ found: 472.0881.

4-(4-Bromophenyl)-2-(phenylimino)thiazol-3(2*H*)-yl)imino)ethyl)-2*H*-chromen-2-one. 5f

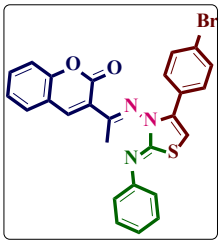

Yellow solid: yield: 92% ; mp. 226-228 °C; FT-IR (KBr, cm^{-1}): 1735 (lactone –C=O), 1600 (C=N), 1582 (C=C); ^{1}H NMR (400 MHz, $CDCl_3$ δ ppm): 8.07 (s, 1H, C_4-coumarin proton), 7.57 (dd, *J* = 7.8, 1.4 Hz, 1H, Ar-H), 7.51 (t, *J*=7.0 Hz, 1H, Ar-H), 7.33 (dd, *J* = 8.2, 1.4 Hz, 4H, Ar-H), 7.30 – 7.23 (m, 5H, Ar-H), 6.99 (d, *J* = 8.4 Hz, 2H, Ar-H), 6.20 (s, 1H, thiazole C_5-ptoton), 2.31 (s, 3H, CH_3 protons). ^{13}C NMR (100 MHz, $CDCl_3$) δ: 169.63, 160.07, 156.20, 153.98, 140.66, 139.22, 137.55, 131.64, 131.56, 130.07, 129.62, 128.87, 128.61, 128.25, 127.75, 127.58, 124.40, 122.65, 119.49, 116.36, 102.11, 17.00; ESI-HRMS: *m/z* Calcd for Chemical Formula: $C_{26}H_{19}BrN_3O_2S$: 516.0376 $[M+H]^+$ found: 516.0379.

4-(3,4-Dichlorophenyl)-2-(phenylimino)thiazol-3(2*H*)-yl)imino)ethyl)-2*H*-chromen-2-one. 5g

Pale yellow solid: yield: 82% ; mp. 184-186 °C; FT-IR (KBr, cm^{-1}): 1718 (lactone –C=O), 1610 (C=N), 1594 (C=C);^{1}H NMR (400 MHz, $CDCl_3$ δ ppm): 9.44 (s, 1H, Ar-H), 8.87 (s, 1H, Ar-H), 7.99 (s, 1H, C_4-coumarin proton), 7.69 (d, *J* = 7.6 Hz, 2H, Ar-H), 7.60 (d, *J* = 7.2 Hz, 2H, Ar-H), 7.40 – 7.31 (m, 5H, Ar-H), 7.23 (t, *J* = 7.4 Hz, 1H, Ar-H), 2.33 (s, 3H, CH_3 protons). ^{13}C NMR (100 MHz, $CDCl_3$) δ: 176.31, 159.31, 154.01, 144.59, 141.56, 137.79, 132.71, 128.81, 128.72, 126.21, 125.90, 124.90, 124.12, 118.81, 116.64, 15.02; ESI-HRMS: *m/z* Calcd for Chemical Formula: $C_{26}H_{18}Cl_2N_3O_2S$: 506.0491 $[M+H]^+$ found: 506.0499.

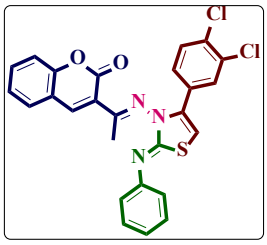

4-(2,4-Difluorophenyl)-2-(phenylimino)thiazol-3(2*H*)-yl)imino)ethyl)-2*H*-chromen-2-one. 5g

Pale yellow solid: yield: 83% ; mp. 172-174 °C; FT-IR (KBr, cm^{-1}): 1719 (lactone –C=O), 1604 (C=N), 1560 (C=C);^{1}H NMR (400 MHz, $CDCl_3$ δ ppm): 8.08 (s, 1H, C_4-coumarin proton), 7.57 (dd, *J* = 8.0, 1.6 Hz, 1H, Ar-H), 7.53 – 7.48 (m, 1H, Ar-H), 7.33 – 7.29 (m, 4H, Ar-H), 7.25-7.22 (m, 3H, Ar-H), 7.17 (d, *J* = 6.4 Hz, 1H, Ar-H), 6.80-6.75 (m, 1H, Ar-H), 6.71 – 6.66 (m, 1H, Ar-H), 6.23 (s, 1H, thiazole C_5-ptoton), 2.30 (s, 3H, CH_3 protons). ^{13}C NMR (100 MHz, $CDCl_3$) δ: 169.20, 160.08, 156.03, 153.98, 140.63, 137.18, 133.31, 132.72, 132.23, 132.10, 131.61, 128.64, 127.97, 127.61, 126.27, 124.39, 124.18, 119.51, 116.68, 116.36, 111.63, 111.38, 104.36, 103.63, 16.94; ESI-HRMS: *m/z* Calcd for Chemical Formula: $C_{26}H_{18}F_2N_3O_2S$: 474.1082 $[M+H]^+$ found: 474.1088.

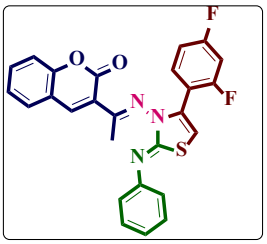

4-(4-Nitrophenyl)-2-(phenylimino)thiazol-3(2*H*)-yl)imino)ethyl)-2*H*-chromen-2-one. 5i

White solid: yield: 94% ; mp. 162-164 °C; FT-IR (KBr, cm^{-1}): 1714 (lactone –C=O), 1605 (C=N), 1561 (C=C); ^{1}H NMR (400 MHz, $CDCl_3$+DMSO-d_6 δ ppm): 8.11 (d, *J* = 5.6 Hz, 2H, Ar-H), 7.89 (s, 1H, C_4-coumarin proton), 7.81 (d, *J* = 9.2 Hz, 2H, Ar-H), 7.76 (s, 1H, thiazole C_5-ptoton), 7.69 (dd, *J* = 8.0, 1.6 Hz, 1H, Ar-H), 7.61 – 7.57 (m, 1H, Ar-H), 7.39-7.33 (m, 4H, Ar-H), 7.19 (t, *J* = 7.8 Hz, 2H, Ar-H), 7.07 (t, *J* = 7.4 Hz, 1H, Ar-H), 2.20 (s, 3H, CH_3 protons); ^{13}C NMR (100 MHz, $CDCl_3$+DMSO-d_6) δ: 168.02, 159.70, 156.94, 153.85, 149.17, 147.34, 141.02, 138.84, 132.19, 129.01, 128.23, 127.66, 127.29, 126.24, 124.80, 123.27, 119.20, 116.21, 94.88, 17.07; ESI-HRMS: *m/z* Calcd for Chemical Formula: $C_{26}H_{19}N_4O_4S$: 483.1122 $[M+H]^+$ found: 483.1120.

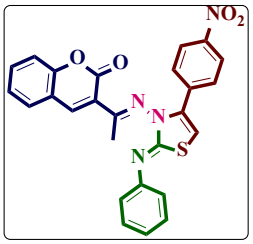

4-([1,1'-Biphenyl]-4-yl)-2-(phenylimino)thiazol-3(2*H*)-yl)imino)ethyl)-2*H*-chromen-2-one. 5j

Orange solid: yield: 92% ; mp. 208-210 °C; FT-IR (KBr, cm^{-1}): 1721 (lactone –C=O), 1601 (C=N), 1587 (C=C); ^{1}H NMR (400 MHz, $CDCl_3$ δ ppm): 8.09 (s, 1H, C_4-coumarin proton), 7.57 (dd, *J* = 7.6, 1.6 Hz, 1H, Ar-H), 7.53 (d, *J* = 7.2 Hz, 2H, Ar-H), 7.45-7.40 (m, 5H, Ar-H), 7.35 – 7.27 (m, 8H, Ar-H), 7.18 (d, *J* = 8.4 Hz, 2H, Ar-H), 6.23 (s, 1H, thiazole C_5-ptoton), 2.33 (s, 3H, CH_3 protons). ^{13}C NMR (100 MHz, $CDCl_3$) δ: 170.09, 160.29, 156.10, 154.16, 142.58, 141.20, 140.78, 140.19, 138.01, 131.75, 130.19, 129.02, 128.93, 128.78, 128.69, 128.52, 128.39, 127.86, 127.77, 127.11, 127.07, 124.55, 119.71, 116.52, 101.76, 17.16; ESI-HRMS: *m/z* Calcd for Chemical Formula: $C_{32}H_{24}N_3O_2S$: 514.1584 $[M+H]^+$ found: 514.1588.

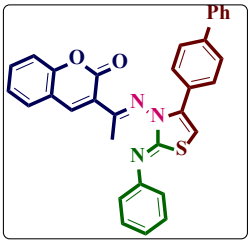

8-Ethoxy-4-phenyl-2-(phenylimino)thiazol-3(2*H*)-yl)imino)ethyl)-2*H*-chromen-2-one. 5k

Yellow solid: yield: 88% ; mp. 204-206 °C; FT-IR (KBr, cm^{-1}): 1713 (lactone –C=O), 1601 (C=N), 1590 (C=C);^{1}H NMR (400 MHz, $CDCl_3$ δ ppm): 8.06 (s, 1H, C_4-coumarin proton), 7.31 (d, *J* = 6.8 Hz, 2H, Ar-H), 7.25 – 7.21 (m, 5H, Ar-H), 7.18 – 7.11 (m, 5H, Ar-H), 7.05 (dd, *J* = 7.6, 2.0 Hz, 1H, Ar-H), 6.18 (s, 1H, thiazole C_5-ptoton), 4.19 (q, *J* = 7.2 Hz, 2H, -CH_2-protons), 2.31 (s, 3H, CH_3 protons), 1.50 (t, *J* = 7.0 Hz, 3H, CH_3 protons). ^{13}C NMR (101 MHz, $CDCl_3$) δ: 169.82, 159.70, 155.99, 146.26, 143.94, 140.78, 140.39, 137.81, 131.20, 128.65, 128.39, 128.28, 128.23, 127.76, 127.51, 124.17, 120.29, 120.09, 114.95, 101.44, 65.07, 16.96, 14.79; ESI-HRMS: *m/z* Calcd for Chemical Formula: $C_{28}H_{24}N_3O_3S$: 482.1533 $[M+H]^+$ found: 482.1541.

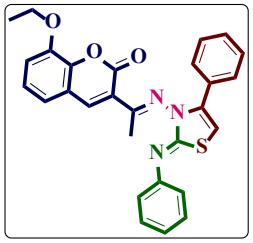

8-Ethoxy-2-(phenylimino)-4-(p-tolyl)thiazol-3(2*H*)-yl)imino)ethyl)-2*H*-chromen-2-one. 5l

Yellow solid: yield: 89% ; mp. 198-200 °C; FT-IR (KBr, cm^{-1}): 1714 (lactone –C=O), 1599 (C=N), 1588 (C=C); ^{1}H NMR (400 MHz, $CDCl_3$ δ ppm): 8.05 (s, 1H, C_4-coumarin proton), 7.31 (d, *J* = 7.2 Hz, 1H, Ar-H), 7.27 – 7.24 (m, 4H, Ar-H), 7.16 (d, *J* = 7.6 Hz, 1H, Ar-H), 7.13 (dd, *J* = 7.8, 1.8 Hz, 1H, Ar-H), 7.05 (dd, *J* = 7.6, 1.6 Hz, 1H, Ar-H), 7.00 (unresolvable singlet, 4H, Ar-H), 6.13 (s, 1H, thiazole C_5-ptoton), 4.18 (q, *J* = 7.2 Hz, 2H, -CH_2-protons), 2.31 (s, 3H, CH_3 protons), 2.28 (s, 3H, CH_3 protons), 1.50 (t, *J* = 7.0 Hz, 3H, CH_3 protons). ^{13}C NMR (100 MHz, $CDCl_3$) δ: 169.92, 159.72, 155.85, 146.25, 143.92, 140.76, 140.45, 138.38, 137.88, 128.98, 128.64, 128.37, 128.10, 127.78, 127.46, 124.16, 120.08, 114.91, 100.79, 65.05, 21.23, 16.94, 14.79; ESI-HRMS: *m/z* Calcd for Chemical Formula: $C_{29}H_{26}N_3O_3S$: 496.1689 $[M+H]^+$ found: 496.1687.

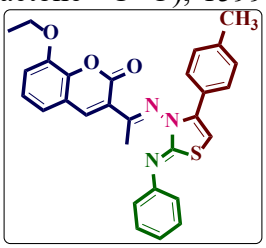

8-4-(4-Methoxyphenyl)-2-(phenylimino)thiazol-3(2*H*)-yl)imino)ethyl)-2*H*-chromen-2-one. 5m

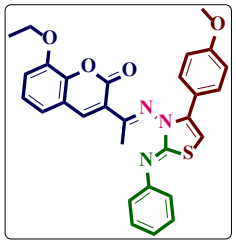

Orange solid: yield: 88% ; mp. 175-177 °C; FT-IR (KBr, cm^{-1}): 1731 (lactone –C=O), 1589 (C=N), 1574 (C=C); ^{1}H NMR (400 MHz, $CDCl_3$ δ ppm): 8.05 (s, 1H, C_4-coumarin proton), 7.31 (d, *J* = 6.8 Hz, 2H, Ar-H), 7.28 – 7.23 (m, 4H, Ar-H), 7.20 – 7.12 (m, 2H, Ar-H), 7.05 – 7.02 (m, 2H, Ar-H), 6.72 (d, *J* = 8.8 Hz, 2H, Ar-H), 6.09 (s, 1H, thiazole C_5-ptoton), 4.18 (q, *J* = 6.8 Hz, 2H, -CH_2-protons), 3.75 (s, 3H, -OCH3 protons), 2.30 (s, 3H, CH_3 protons), 1.50 (t, *J* = 7.0 Hz, 3H, CH_3 protons). ^{13}C NMR (100 MHz, $CDCl_3$) δ: 169.90, 159.56, 155.80, 146.25, 143.92, 140.73, 140.16, 137.87, 129.61, 128.66, 128.41, 127.47, 124.16, 123.63, 120.08, 114.90, 113.69, 100.16, 65.05, 55.23, 16.93, 14.80; ESI-HRMS: *m/z* Calcd for Chemical Formula: $C_{29}H_{26}N_3O_4S$: 512.1639 $[M+H]^+$ found: 512.1631.

8-Mthoxy-4-(4-fluorophenyl)-2-(phenylimino)thiazol-3(2*H*)-yl)imino)ethyl)-2*H*-chromen-2-one. 5n

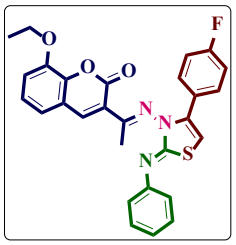

Yellow solid: yield: 91% ; mp. 226-228 °C; FT-IR (KBr, cm^{-1}): 1714 (lactone –C=O), 1599 (C=N), 1583 (C=C);^{1}H NMR (400 MHz, $CDCl_3$ δ ppm): 8.05 (s, 1H, C_4-coumarin proton), 7.32 (d, *J* = 7.6 Hz, 2H, Ar-H), 7.23 (d, *J* = 7.2 Hz, 2H, Ar-H), 7.19 (d, *J* = 7.6 Hz, 1H, Ar-H), 7.15 (d, *J* = 5.2 Hz, 1H, Ar-H), 7.12 (m, 1H, Ar-H), 7.09 (d, *J* = 5.6 Hz, 1H, Ar-H), 7.05 (dd, *J* = 7.8, 1.8 Hz, 1H, Ar-H), 6.90 (t, *J* = 8.8 Hz, 2H, Ar-H), 6.15 (s, 1H, thiazole C_5-ptoton), 4.19 (q, *J* = 7.2 Hz, 2H, -CH_2-protons), 2.31 (s, 3H, CH_3 protons), 1.50 (t, *J* = 7.0 Hz, 3H, CH_3 protons). ^{13}C NMR (100 MHz, $CDCl_3$) δ: 169.61, 161.29, 159.69, 156.17, 146.27, 143.93, 140.82, 139.29, 137.61, 130.14, 130.06, 128.78, 128.34, 127.67, 127.34, 124.18, 120.07, 115.55, 115.33, 114.94, 101.41, 65.06, 16.97, 14.79; ESI-HRMS: *m/z* Calcd for Chemical Formula: $C_{28}H_{23}FN_3O_3S$: 500.1439 $[M+H]^+$ found: 500.1433.

3-4-(4-Chlorophenyl)-2-(phenylimino)thiazol-3(2*H*)-yl)imino)ethyl)-8-ethoxy-2*H*-chromen-2-one. 5o

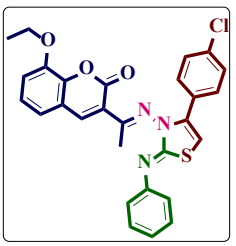

Yellow solid: yield: 93% ; mp. 214-216 °C; FT-IR (KBr, cm^{-1}): 1715 (lactone –C=O), 1600 (C=N), 1585 (C=C);^{1}H NMR (400 MHz, $CDCl_3$ δ ppm): 8.05 (s, 1H, C_4-coumarin proton), 7.33 (d, *J* = 7.6 Hz, 2H, Ar-H), 7.30 – 7.23 (m, 4H, Ar-H), 7.19 – 7.11 (m, 4H, Ar-H), 7.05 (d, *J* = 8.4 Hz, 2H, Ar-H), 6.18 (s, 1H, thiazole C_5-ptoton), 4.19 (q, *J* = 7.2 Hz, 2H, -CH_2-protons), 2.31 (s, 3H, CH_3 protons), 1.50 (t, *J* = 7.0 Hz, 3H, CH_3 protons). ^{13}C NMR (100 MHz, $CDCl_3$) δ: 169.55, 159.67, 156.30, 146.27, 143.93, 140.85, 139.16, 137.57, 134.40,

129.38, 128.84, 128.60, 128.26, 127.70, 124.19, 120.07, 114.96, 102.03, 65.05, 16.99, 14.79; ESI-HRMS: *m/z* Calcd for Chemical Formula: $C_{28}H_{23}ClN_3O_3S$: 516.1143 $[M+H]^+$ found: 516.1141.

3-4-(4-Bromophenyl)-2-(phenylimino)thiazol-3(2*H*)-yl)imino)ethyl)-8-ethoxy-2*H*-chromen-2-one. 5p

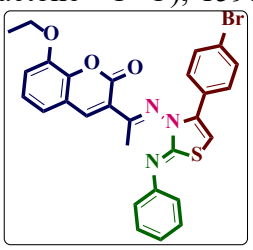

Yellow solid: yield: 93% ; mp. 197-199 °C; FT-IR (KBr, cm^{-1}): 1727 (lactone –C=O), 1598 (C=N), 1581 (C=C);^{1}H NMR (400 MHz, $CDCl_3$ δ ppm): 8.04 (s, 1H, C_4-coumarin proton), 7.33 (d, *J* = 8.4 Hz, 4H, Ar-H), 7.28 (d, *J* = 7.2 Hz, 1H, Ar-H), 7.23 (d, *J* = 7.2 Hz, 2H, Ar-H), 7.17 (d, *J* = 8.0 Hz, 1H, Ar-H), 7.13 (dd, *J* = 7.6, 1.6 Hz, 1H, Ar-H), 7.05 (dd, *J* = 8.0, 1.6 Hz, 1H, Ar-H), 6.99 (d, *J* = 8.4 Hz, 2H, Ar-H), 6.19 (s, 1H, thiazole C_5-ptoton), 4.19 (q, *J* = 6.8 Hz, 2H, -CH_2-protons), 2.31 (s, 3H, CH_3 protons), 1.50 (t, *J* = 7.0 Hz, 3H, CH_3 protons). ^{13}C NMR (100 MHz, $CDCl_3$) δ: 169.54, 159.67, 156.33, 146.27, 143.94, 140.86, 139.20, 137.56, 131.55, 129.61, 128.85, 128.25, 127.73, 124.19, 122.62, 120.07, 114.96, 102.10, 65.06, 17.00, 14.80; ESI-HRMS: *m/z* Calcd for Chemical Formula: $C_{28}H_{23}BrN_3O_3S$: 560.0638 $[M+H]^+$ found: 560.0638.

3-4-(3,4-Dichlorophenyl)-2-(phenylimino)thiazol-3(2*H*)-yl)imino)ethyl)-8-ethoxy-2*H*-chromen-2-one. 5q

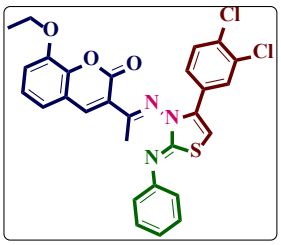

White solid: yield: 83% ; mp. 186-188 °C; FT-IR (KBr, cm^{-1}): 1716 (lactone –C=O), 1618 (C=N), 1591 (C=C);^{1}H NMR (400 MHz, $CDCl_3$ δ ppm): 9.45 (s, 1H, C_4-coumarin proton), 8.87 (s, 1H, Ar-H), 7.96 (s, 1H, Ar-H), 7.69 (d, *J* = 7.6 Hz, 2H, Ar-H), 7.39 (t, *J* = 8.0 Hz, 2H, Ar-H), 7.24 (dd, *J* = 7.6, 2.2 Hz, 2H, Ar-H), 7.21 (d, *J* = 3.2 Hz, 1H, Ar-H), 7.15 – 7.12 (m, 2H, Ar-H), 7.11 (d, *J* = 1.2 Hz, 1H, Ar-H), 4.20 (q, *J* = 7.2 Hz, 2H, -CH_2-protons), 2.33 (s, 3H, CH_3 protons), 1.51 (t, *J* = 7.0 Hz, 3H, CH_3 protons). ^{13}C NMR (100 MHz, $CDCl_3$) δc: 176.32, 158.95, 146.44, 144.64, 143.88, 141.80, 137.80, 128.79, 126.19, 124.74, 124.14, 119.91, 119.45, 115.62, 65.07, 14.98, 14.74; ESI-HRMS: *m/z* Calcd for Chemical Formula: $C_{28}H_{22}Cl_2N_3O_3S$: 550.0753[M+H]$^+$ found: 550.0760.

3-4-(2,4-Difluorophenyl)-2-(phenylimino)thiazol-3(2*H*)-yl)imino)ethyl)-8-ethoxy-2*H*-chromen-2-one. 5r

White solid: yield: 84% ; mp. 188-190°C; FT-IR (KBr, cm^{-1}): 1731 (lactone –C=O), 1619 (C=N), 1591 (C=C); ^{1}H NMR (400 MHz, $CDCl_3$ δ ppm) : 9.44 (s, 1H, Ar-H), 8.87 (s, 1H, Ar-H), 7.96 (s, 1H, C_4-coumarin proton), 7.68 (d, *J* = 7.6 Hz, 2H, Ar-H), 7.38 (t, *J* = 8.0 Hz, 2H, Ar-H), 7.25-720 (m, 2H, Ar-H), 7.15-7.10 (m, 2H, Ar-H), 4.19 (q, *J* = 7.2 Hz, 2H, -CH_2-protons), 2.32 (s, 3H, CH_3 protons), 1.50 (t, *J* = 7.0 Hz, 3H, CH_3 protons); ^{13}C NMR (100 MHz, $CDCl_3$) δ: 176.32, 158.96, 146.44, 144.64, 143.88, 141.80, 137.80, 128.80, 126.20, 125.99, 124.75, 124.15, 119.91, 119.45, 115.62, 65.07, 14.99, 14.74; ESI-HRMS: *m/z* Calcd for Chemical Formula: $C_{28}H_{22}F_2N_3O_3S$: 518.1344[M+H] $^+$ found: 518.1354.

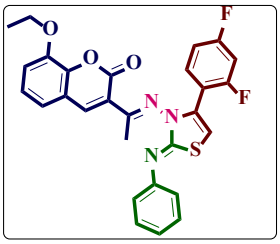

3-4-([1,1'-Biphenyl]-4-yl)-2-(phenylimino)thiazol-3(2*H*)-yl)imino)ethyl)-8-ethoxy-2*H*-chromen-2-one. 5s

Yellow solid: yield: 93% ; mp. 198-200 °C; FT-IR (KBr, cm^{-1}): 1718 (lactone –C=O), 1600 (C=N), 1587 (C=C);^{1}H NMR (400 MHz, $CDCl_3$ δ ppm): 8.06 (s, 1H, C_4-coumarin proton), 7.53 (d, *J* = 6.8 Hz, 2H, Ar-H), 7.45-7.39 (m, 4H, Ar-H), 7.36 – 7.28 (m, 6H, Ar-H), 7.19 – 7.12 (m, 4H, Ar-H), 7.05 (dd, *J* = 7.6, 1.6 Hz, 1H, Ar-H), 6.23 (s, 1H, thiazole C_5-ptoton), 4.18 (q, *J* = 7.2 Hz, 2H, -CH_2-protons), 2.32 (s, 3H, CH_3 protons), 1.50 (t, *J* = 7.0 Hz, 3H, CH_3 protons). ^{13}C NMR (100 MHz, $CDCl_3$) δc: 169.82, 159.70, 156.06, 146.27, 143.96, 141.01, 140.79, 140.03, 137.86, 130.05, 128.84, 128.74, 128.52, 128.35, 127.57, 124.17, 120.09, 114.96, 101.58, 65.07, 16.98, 14.80; ESI-HRMS: *m/z* Calcd for Chemical Formula: $C_{34}H_{28}N_3O_3S$: 558.1846 [M+H] $^+$ found: 558.1854.

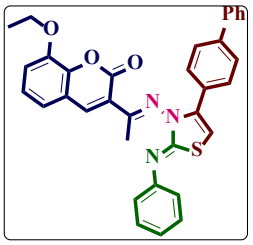

4C.9. Spectra

^{1}H-NMR Spectrum of compound 5a in $CDCl_3$ (400 MHz):

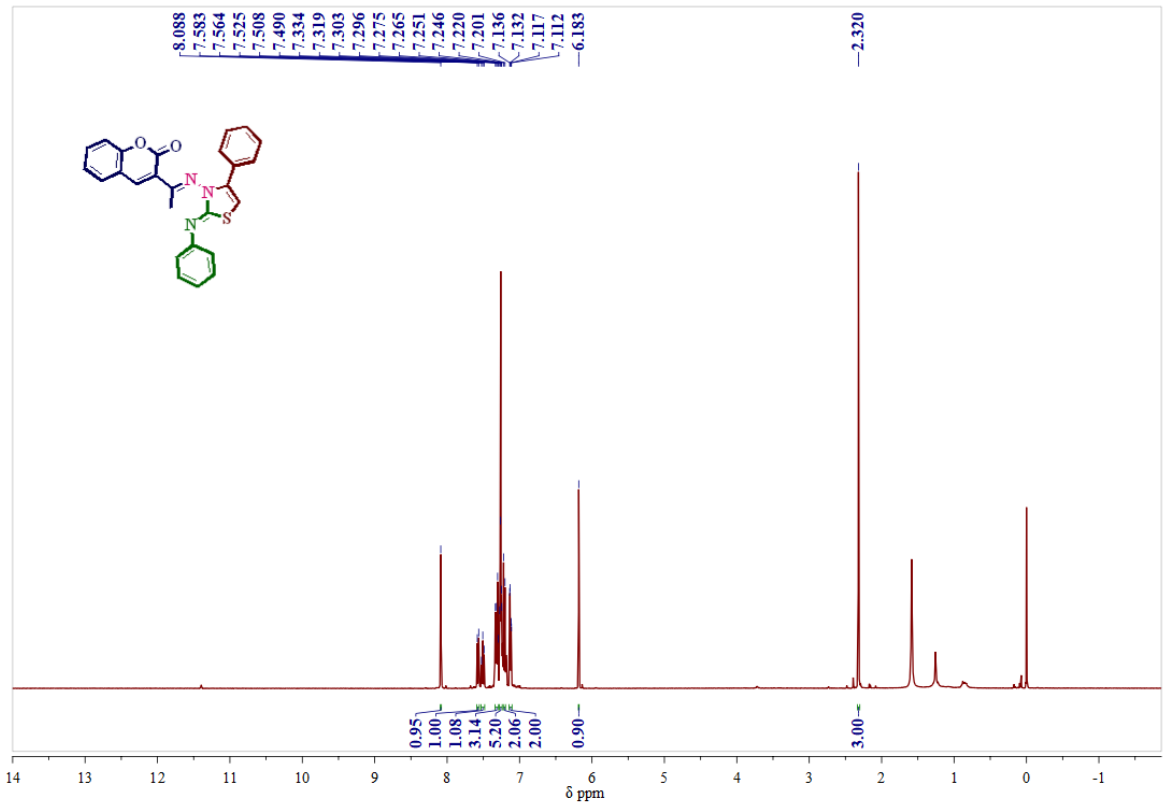

^{13}C-NMR Spectrum of compound 5a in $CDCl_3$ (100 MHz):

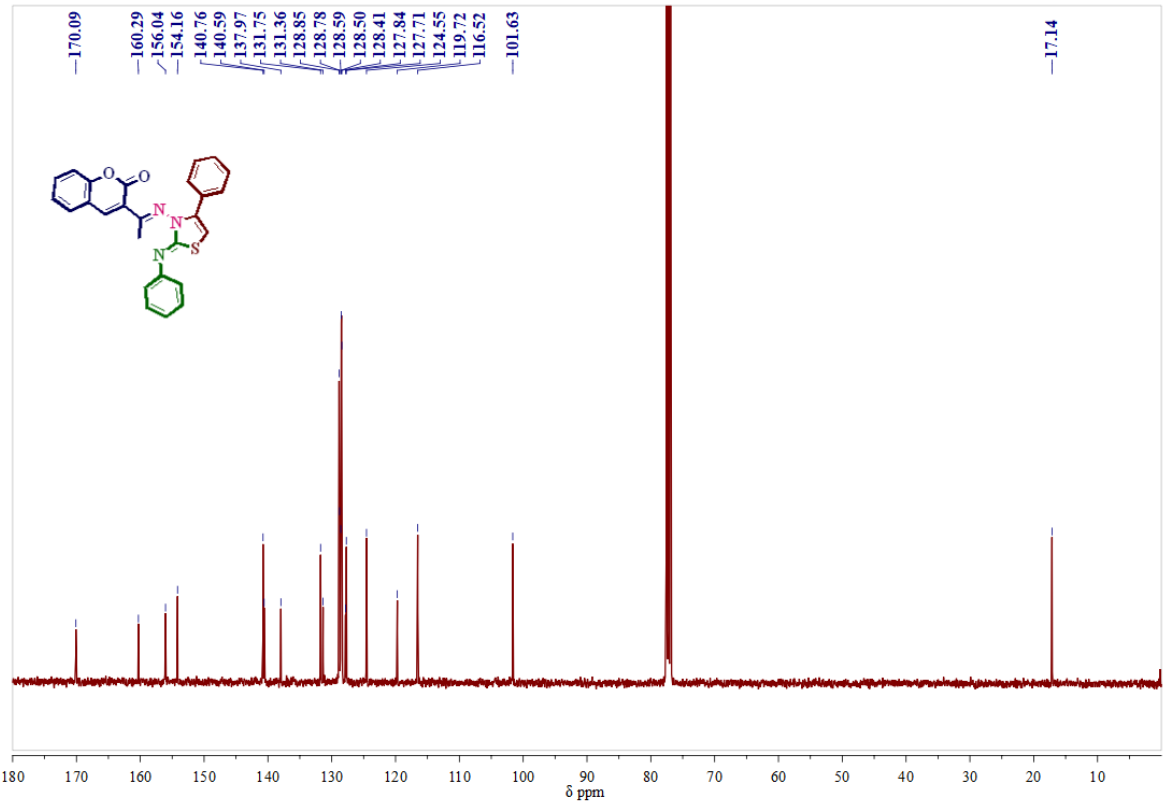

Mass spectrum of compound 5a

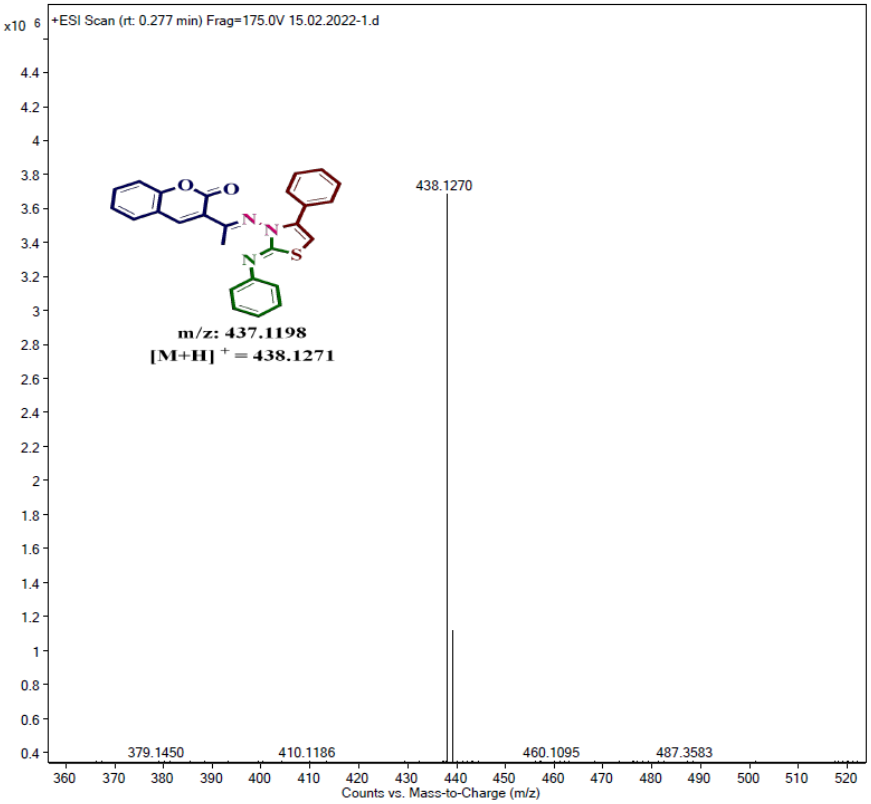

^{1}H-NMR Spectrum of compound 5b in $CDCl_3$ (400 MHz):

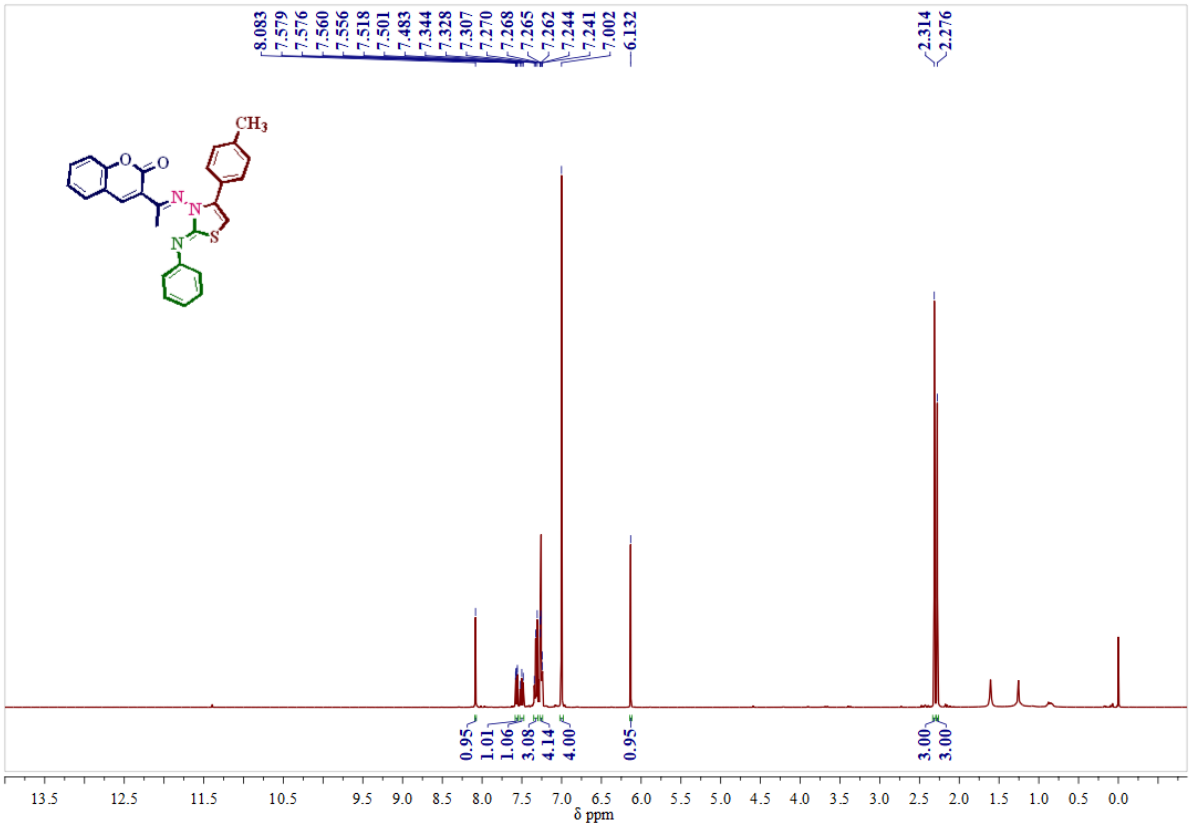

^{13}C-NMR Spectrum of compound 5b in $CDCl_3$ (100 MHz):

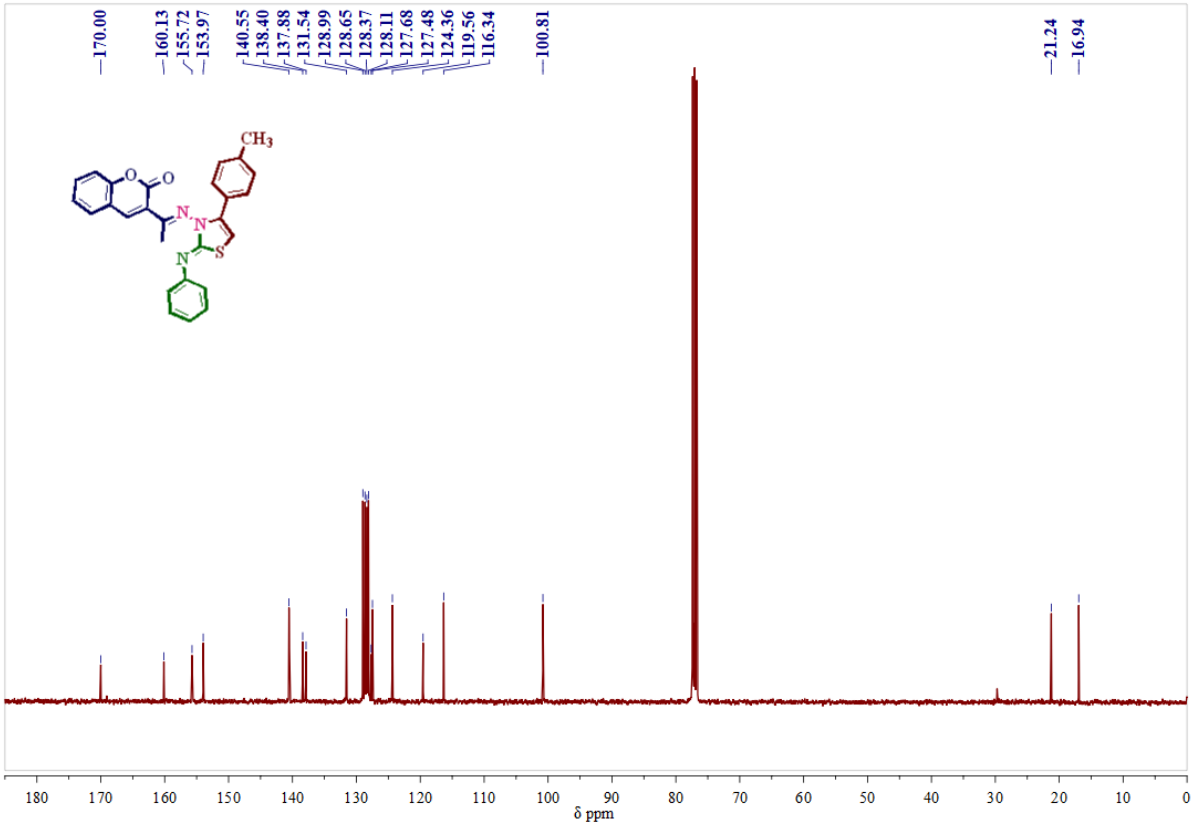

Mass spectrum of compound 5b

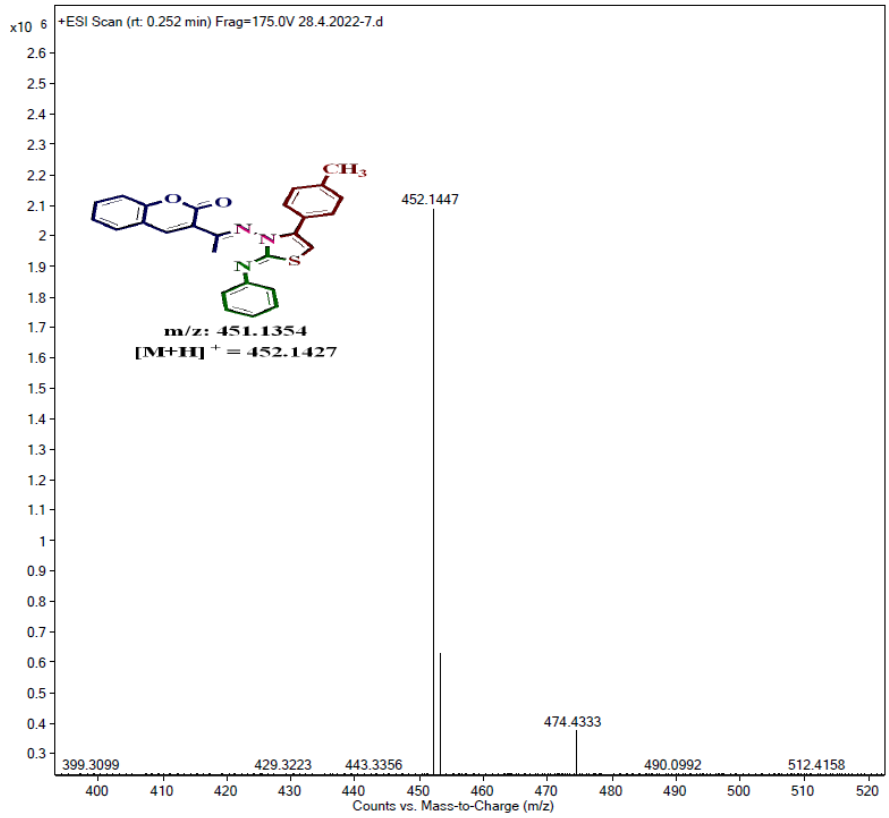

^{1}H-NMR Spectrum of compound 5c in $CDCl_3$ (400 MHz):

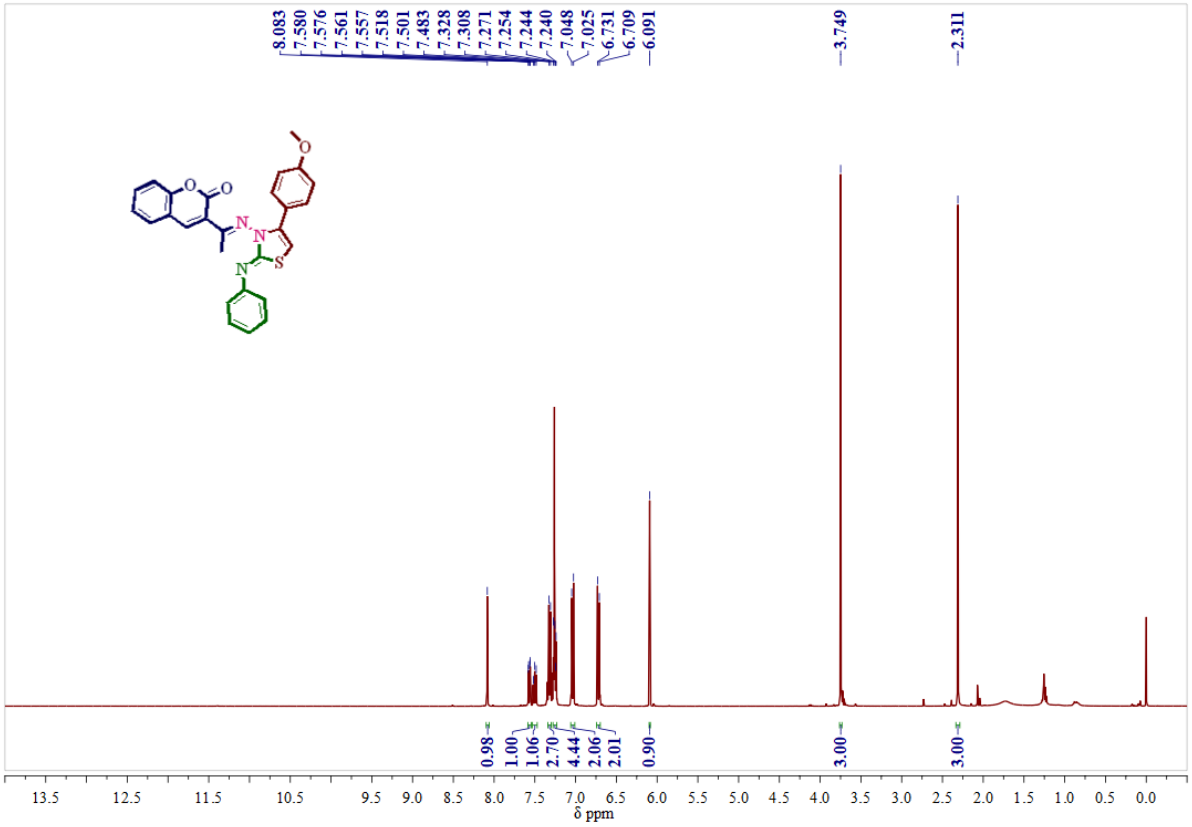

^{13}C-NMR Spectrum of compound 5c in $CDCl_3$ (100 MHz):

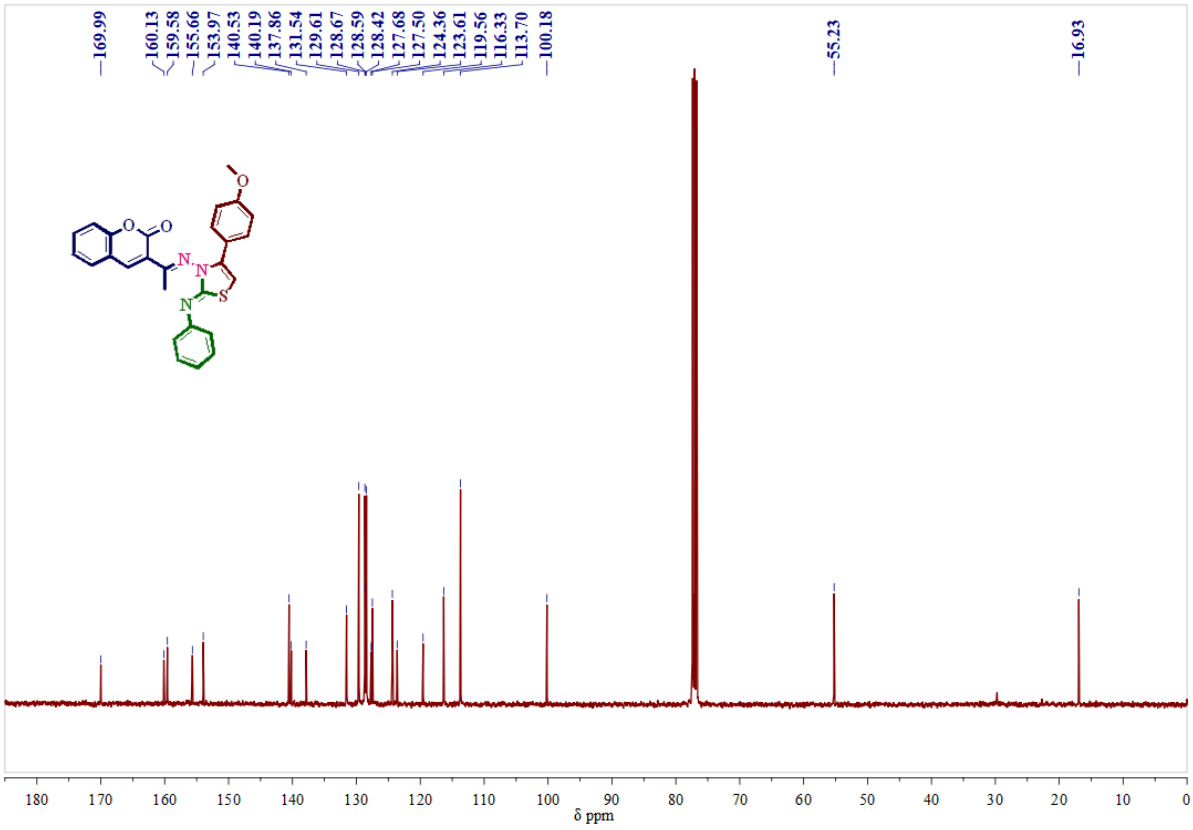

Mass spectrum of compound 5c

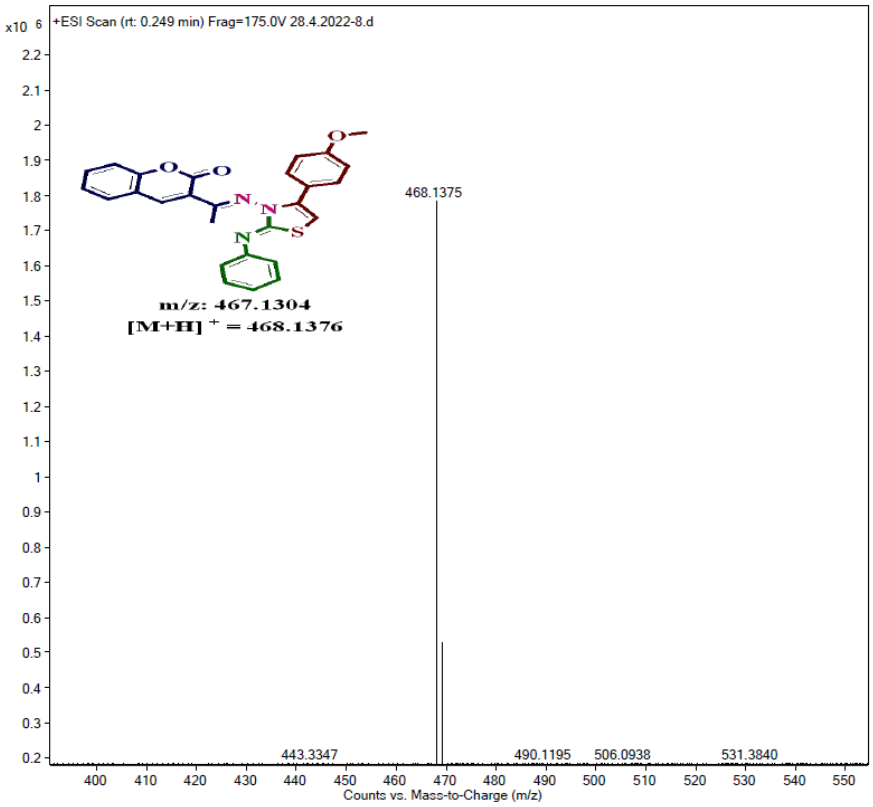

^{1}H-NMR Spectrum of compound 5d in $CDCl_3$ (400 MHz):

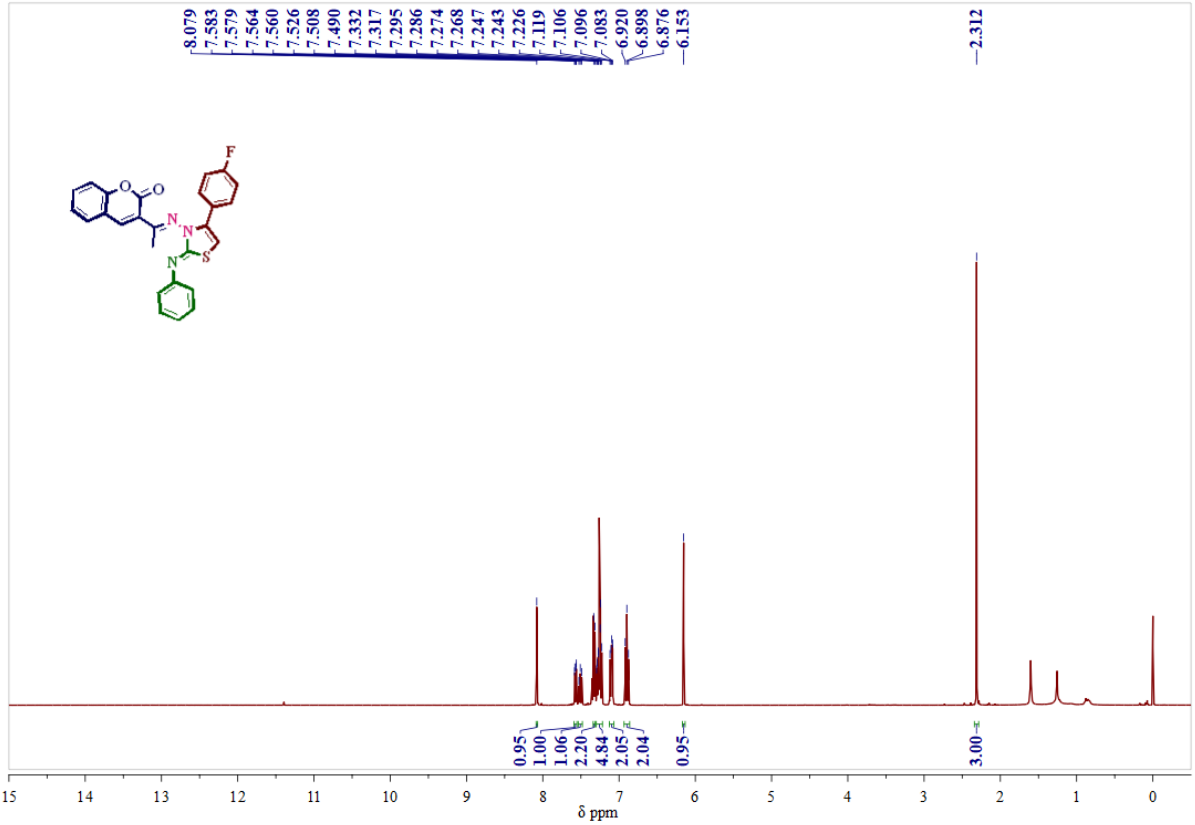

^{13}C-NMR Spectrum of compound 5d in $CDCl_3$ (100 MHz):

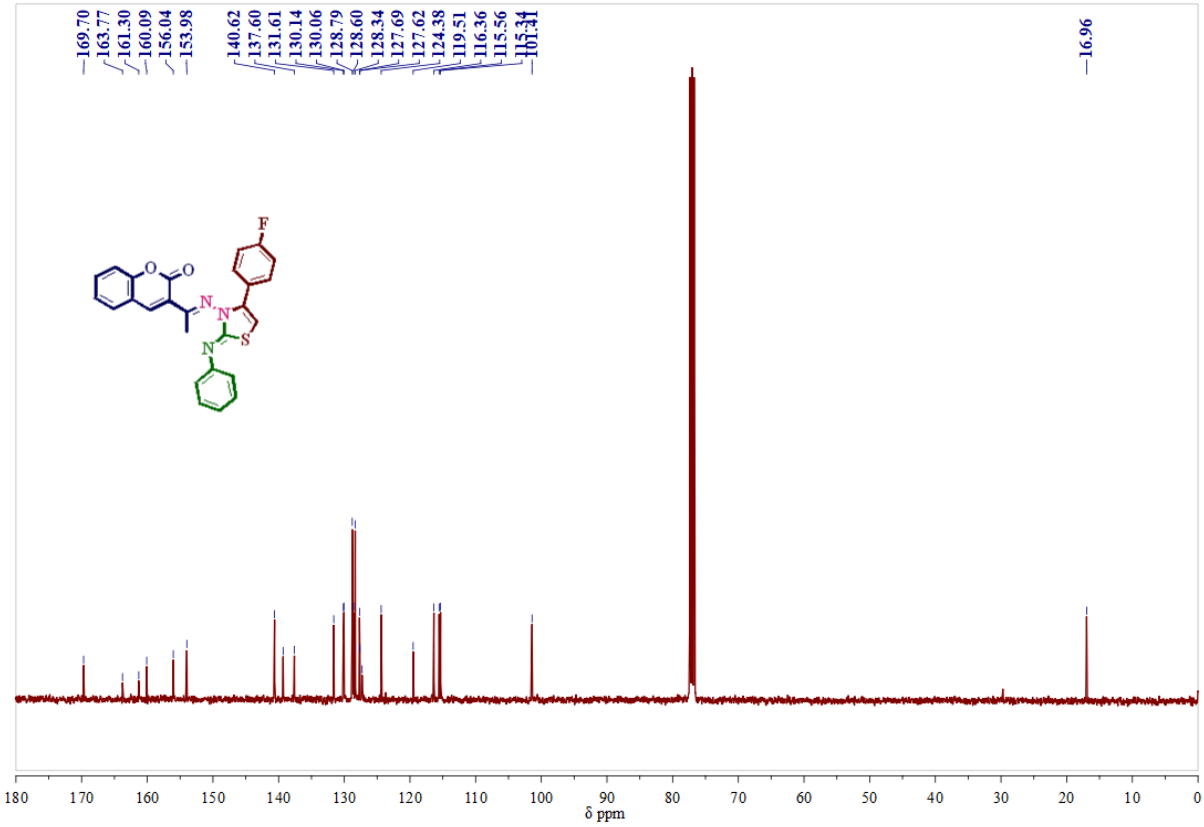

Mass spectrum of compound 5d

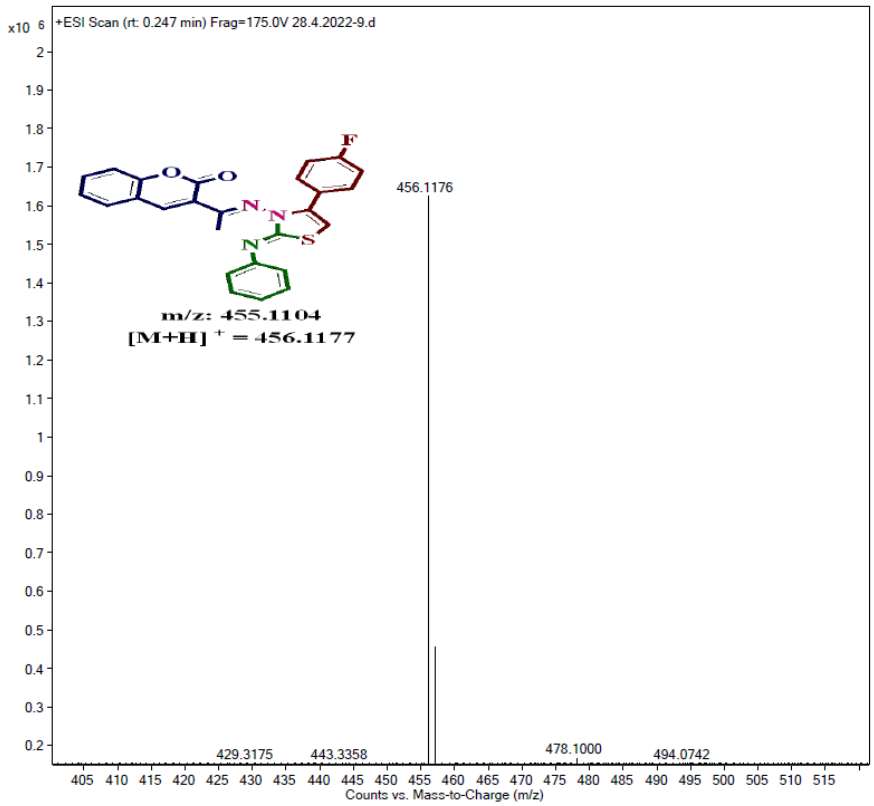

^{1}H-NMR Spectrum of compound 5e in $CDCl_3$ (400 MHz):

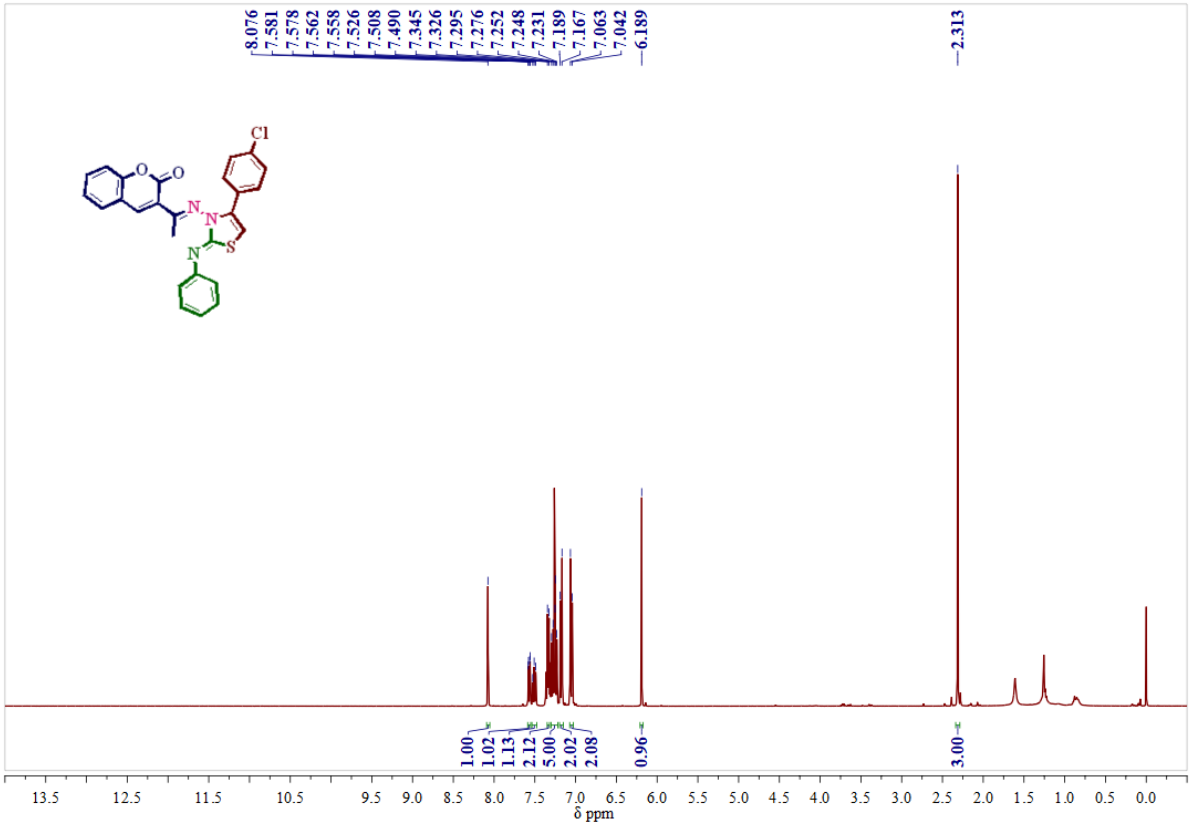

^{13}C-NMR Spectrum of compound 5e in $CDCl_3$ (100 MHz):

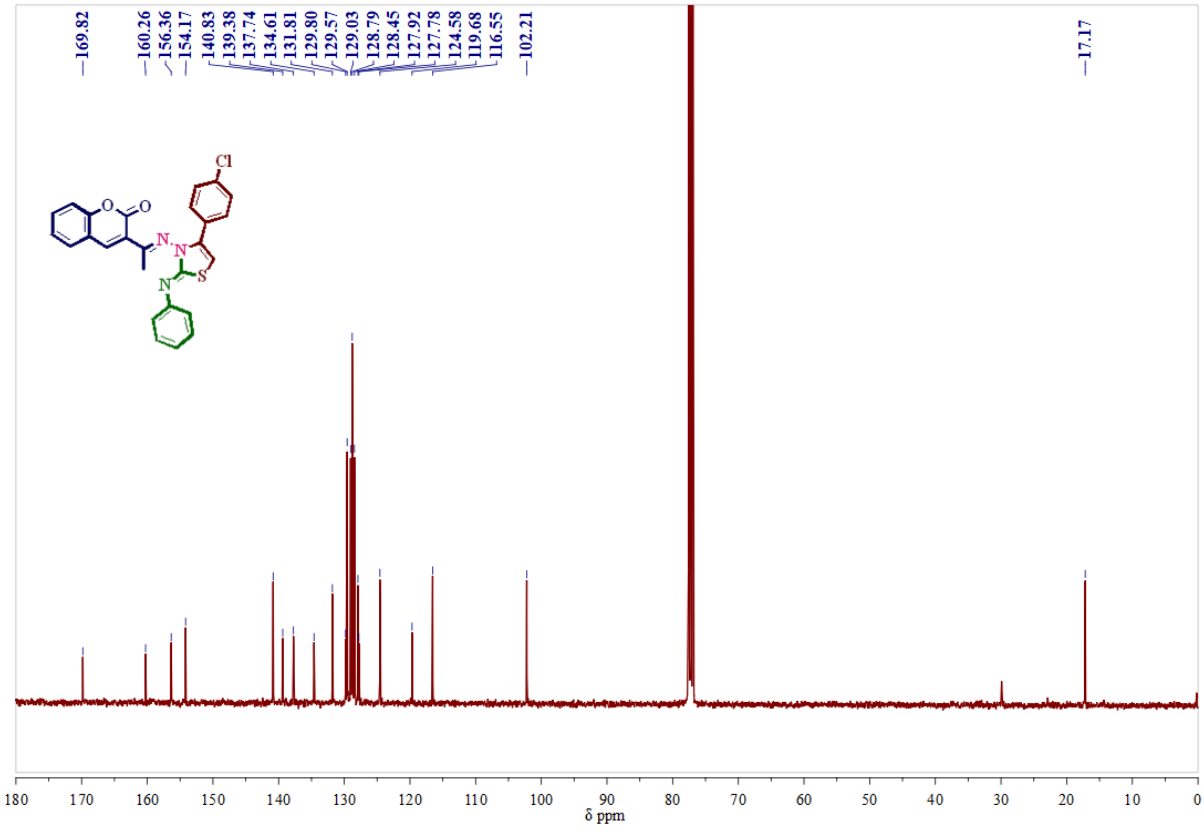

Mass spectrum of compound 5e

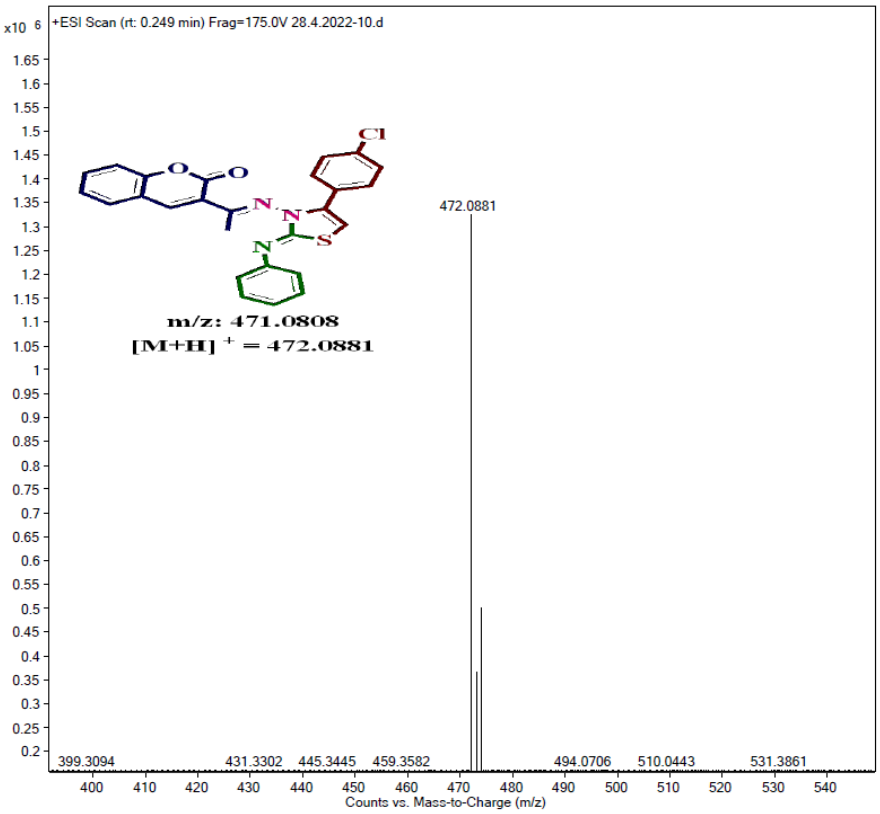

^{1}H-NMR Spectrum of compound 5f in $CDCl_3$ (400 MHz):

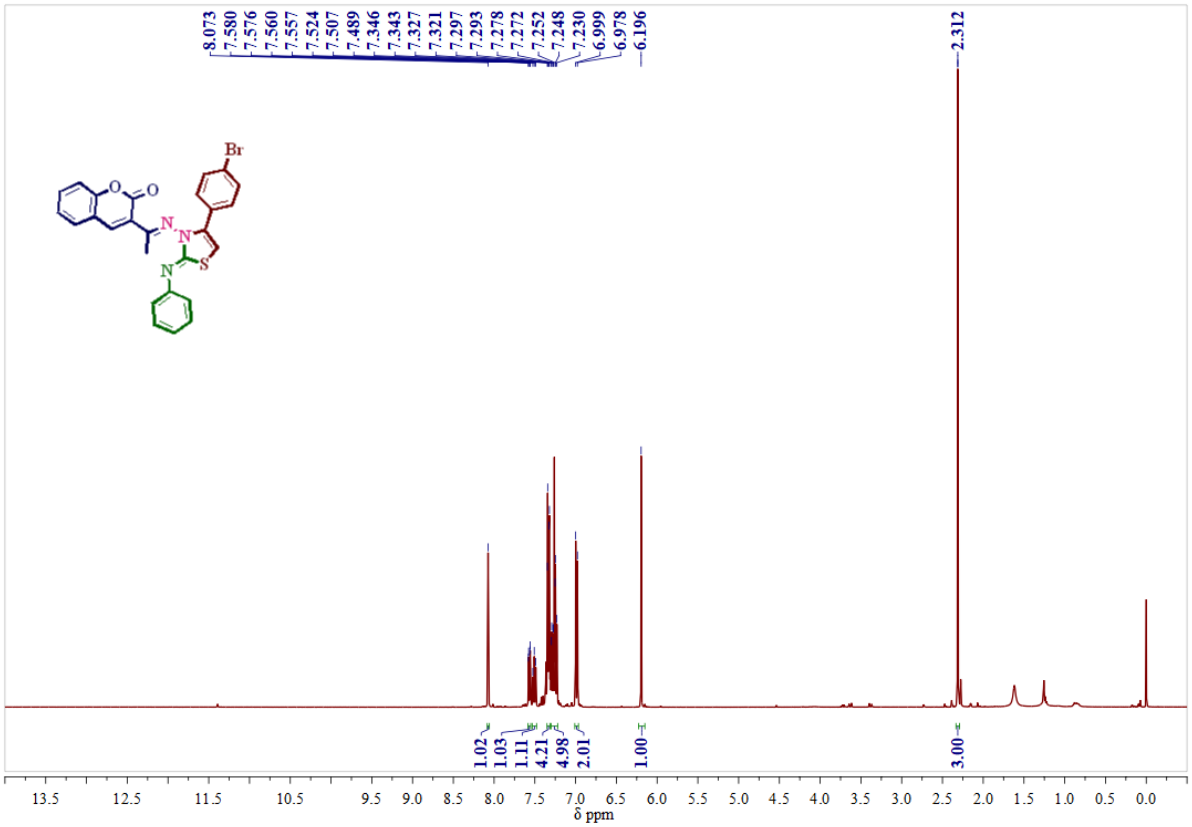

^{13}C-NMR Spectrum of compound 5f in $CDCl_3$ (100 MHz):

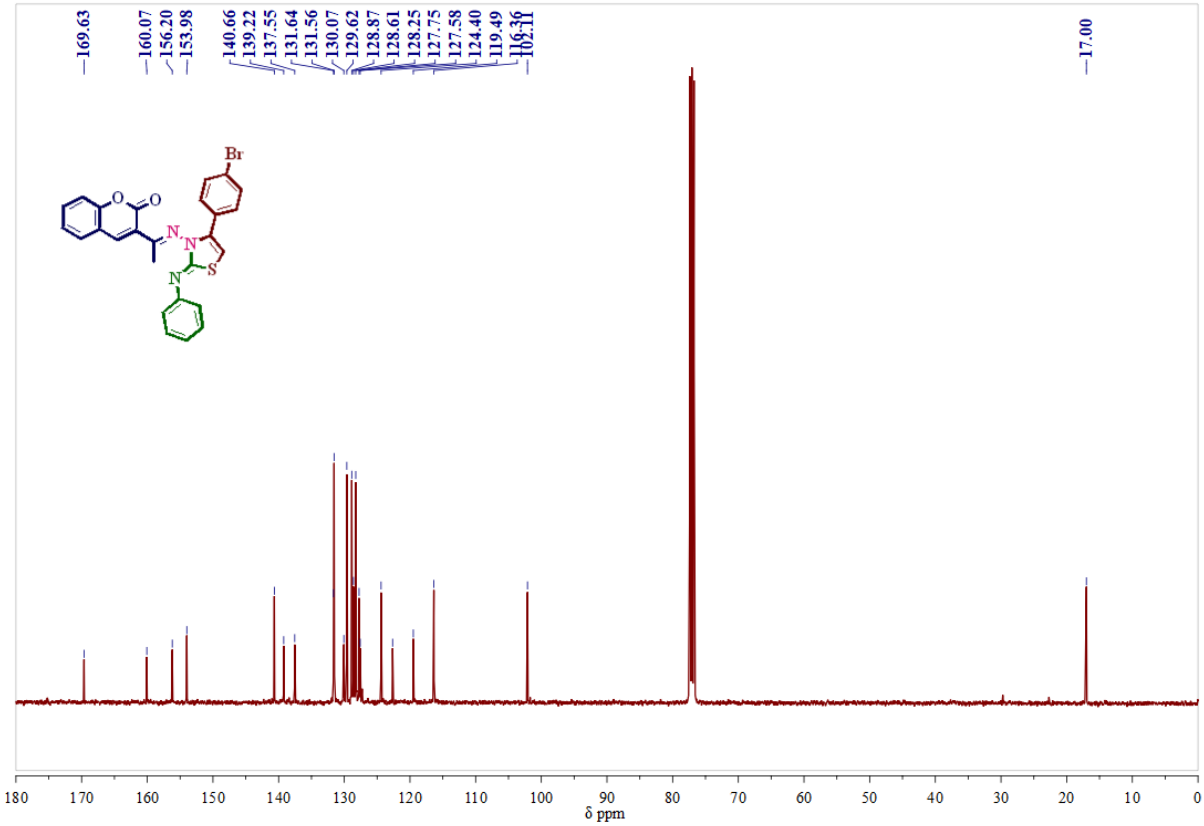

Mass spectrum of compound 5f

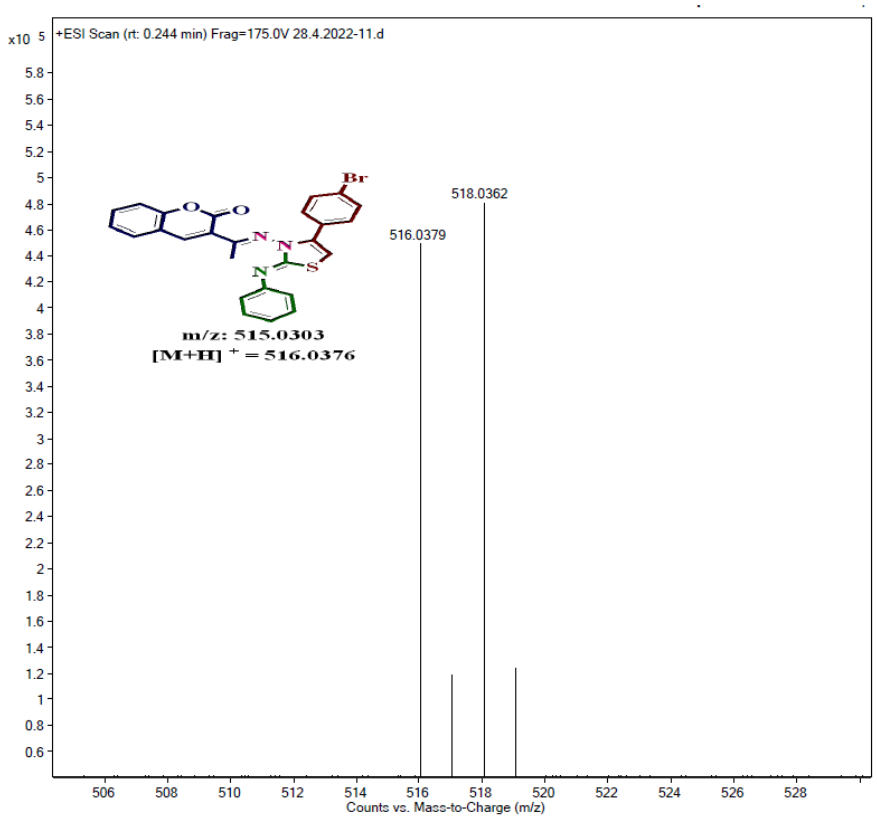

^{1}H-NMR Spectrum of compound 5g in $CDCl_3$ (400 MHz):

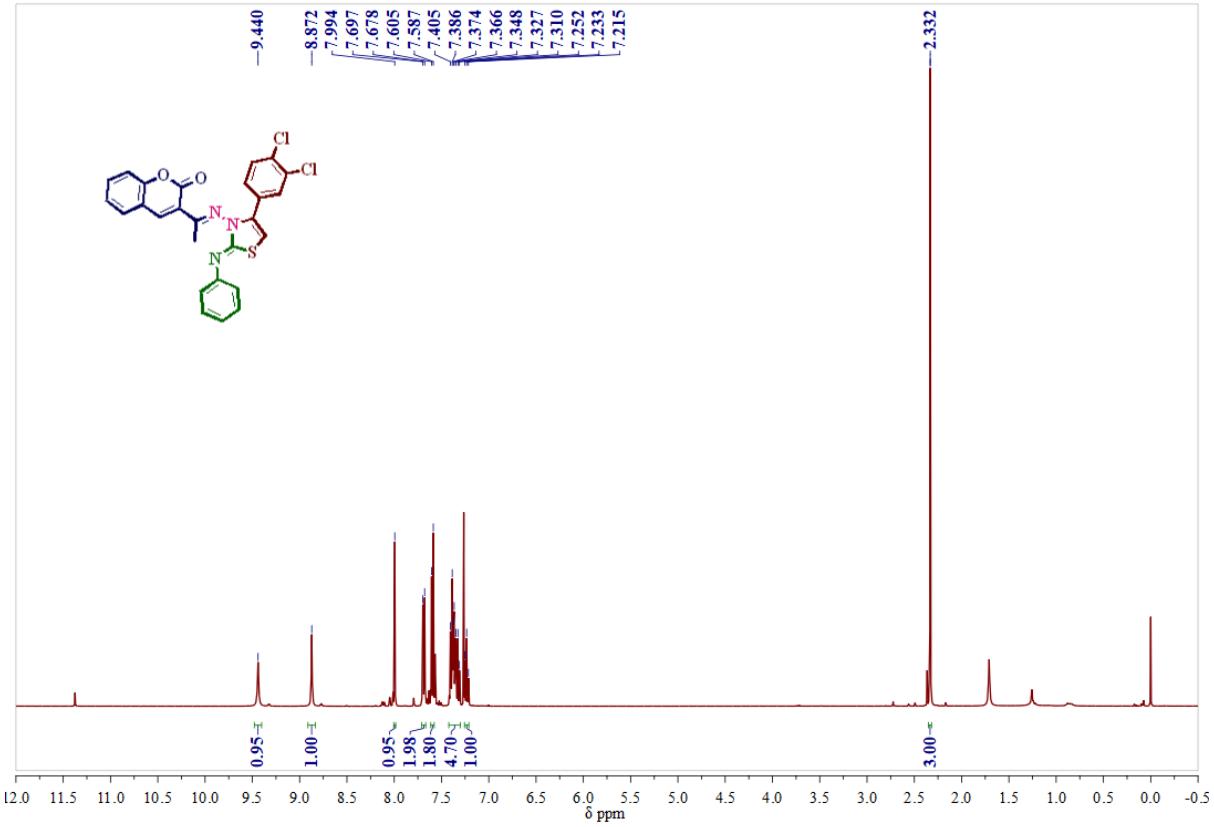

^{13}C-NMR Spectrum of compound 5g in $CDCl_3$ (100 MHz):

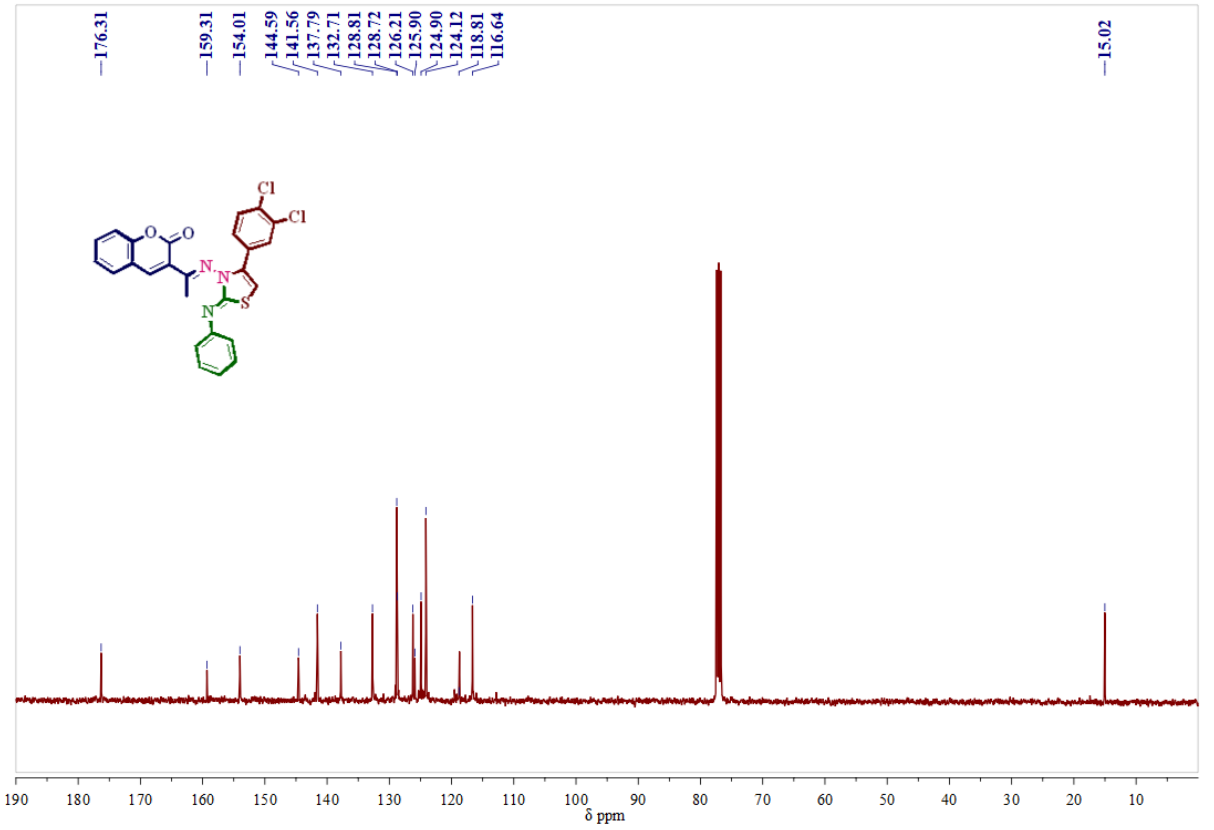

Mass spectrum of compound 5g

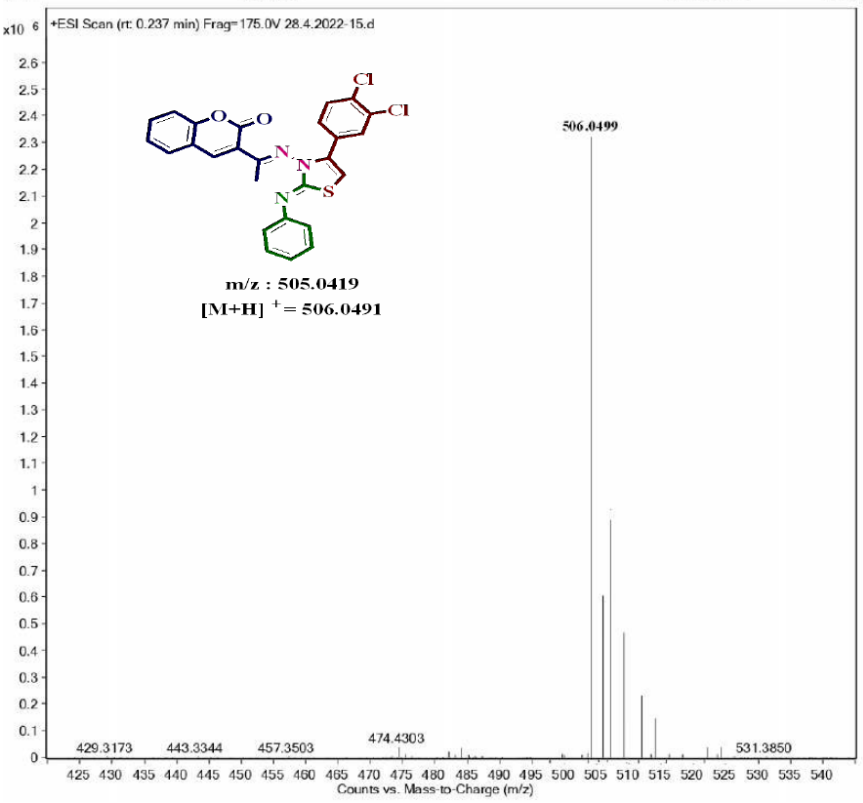

^{1}H-NMR Spectrum of compound 5h in $CDCl_3$ (400 MHz):

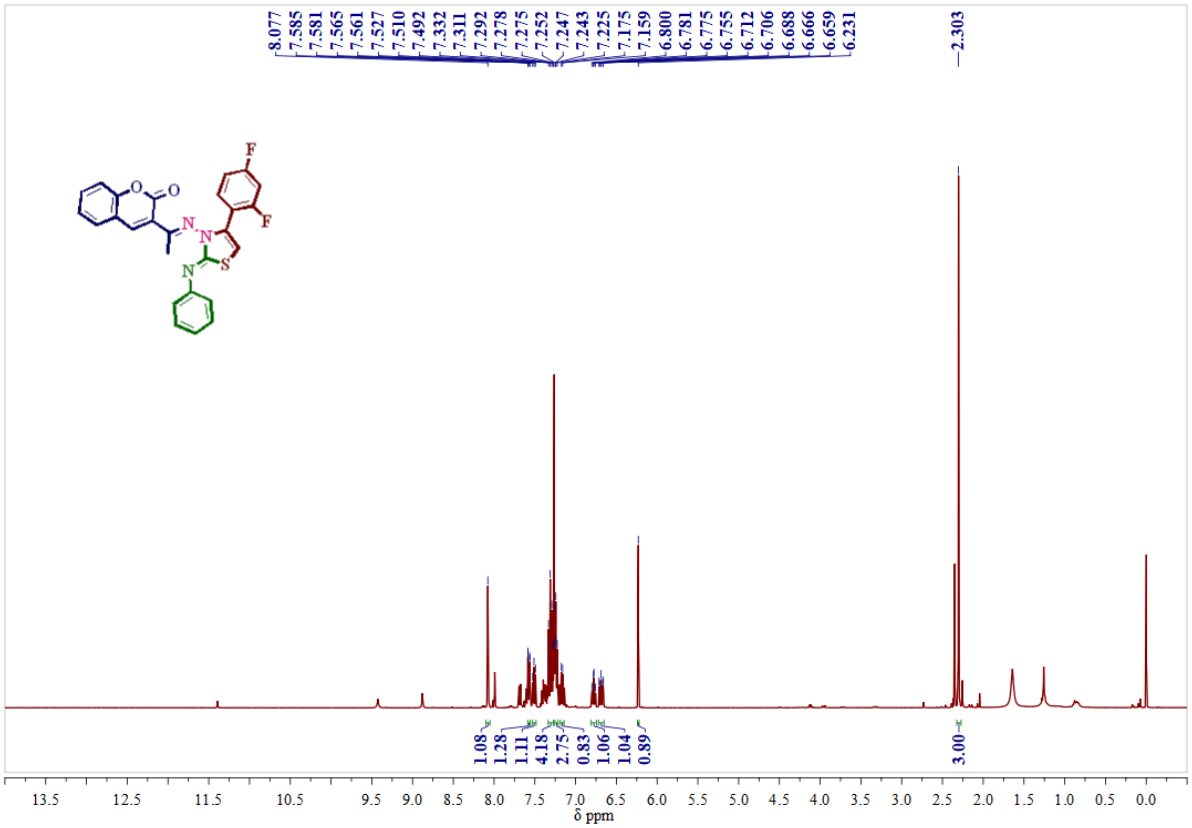

^{13}C-NMR Spectrum of compound 5h in $CDCl_3$ (100 MHz):

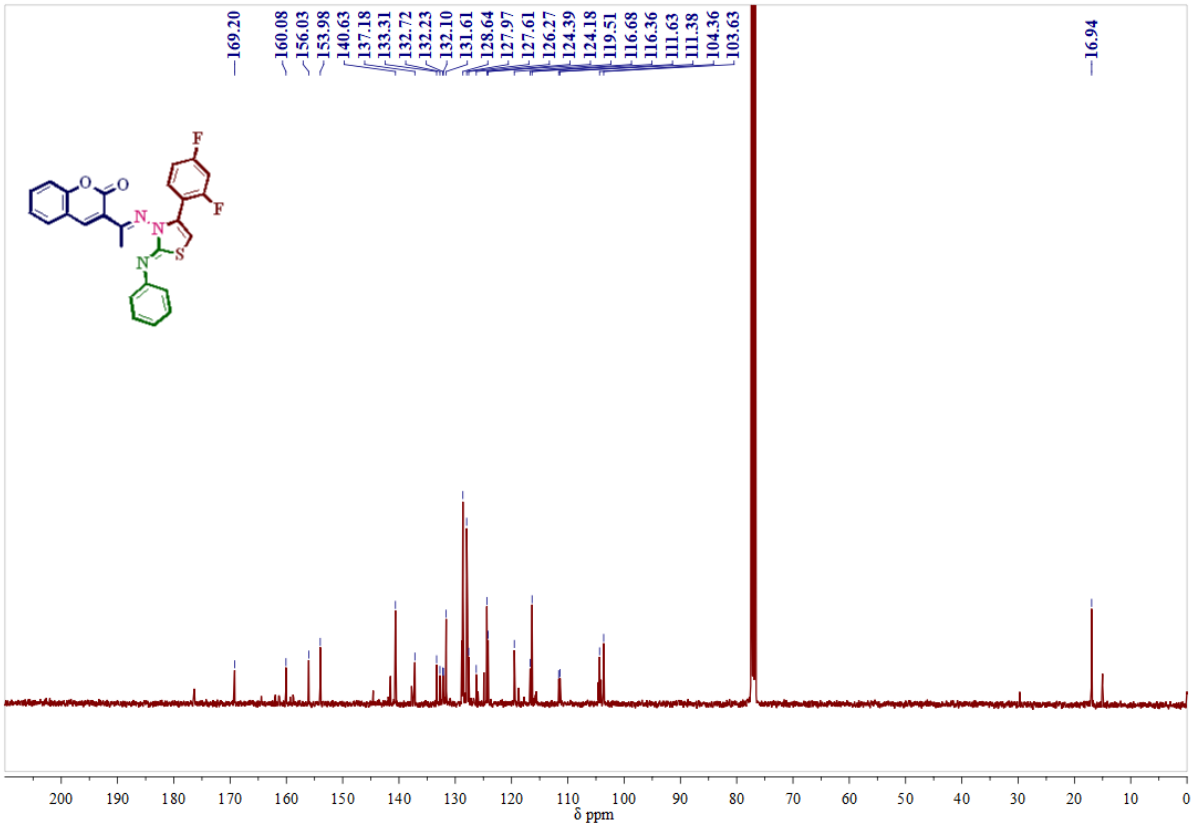

Mass spectrum of compound 5h

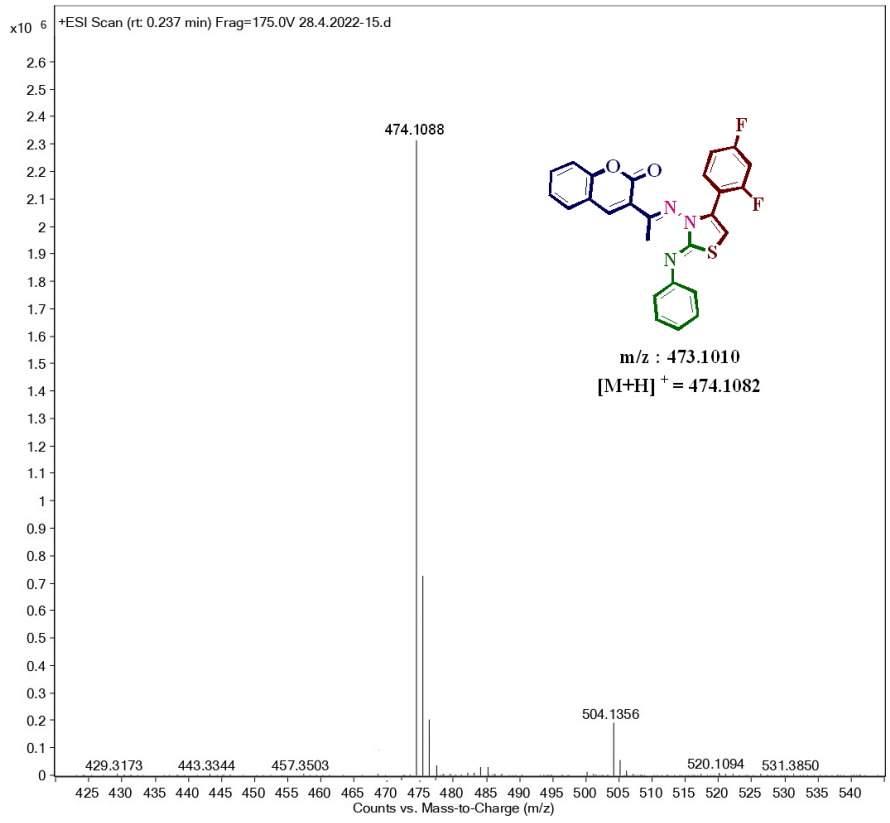

[1]H-NMR Spectrum of compound 5i in $CDCl_3$ (400 MHz):

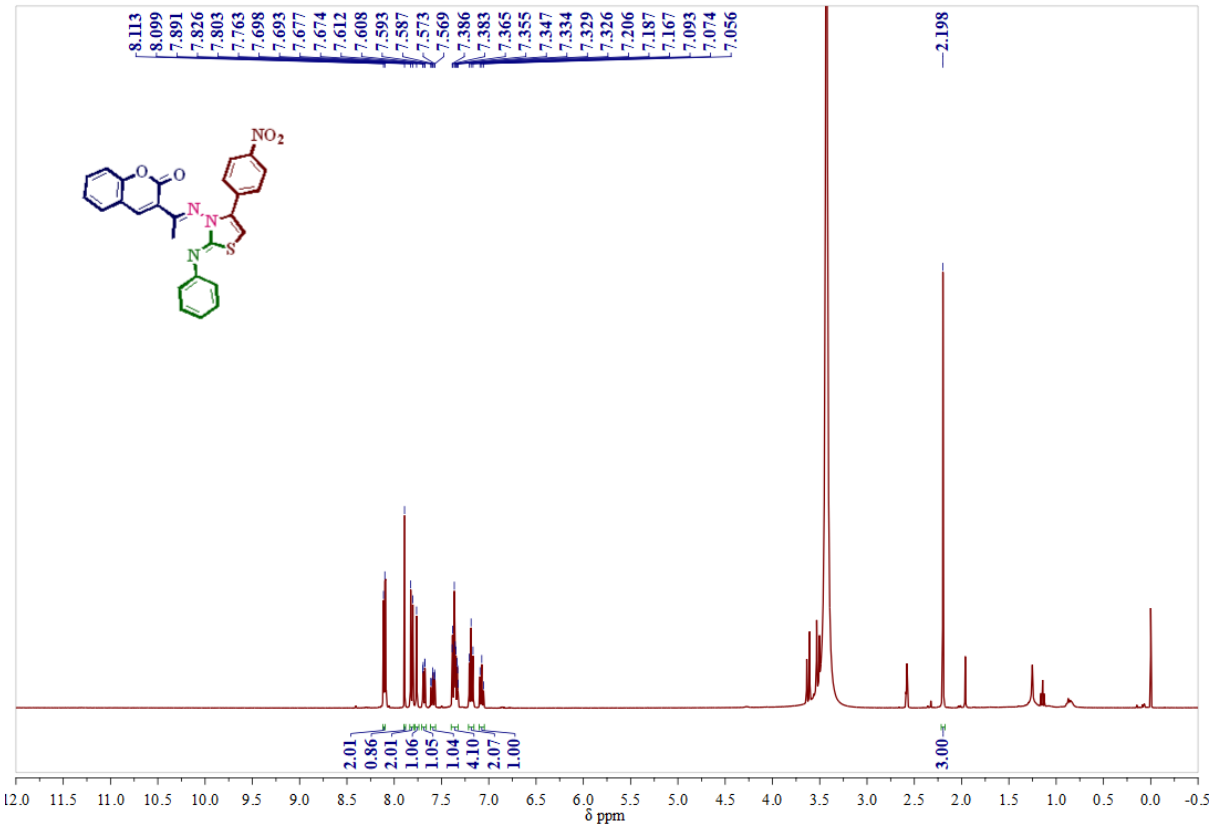

[13]C-NMR Spectrum of compound 5i in $CDCl_3$ (100 MHz):

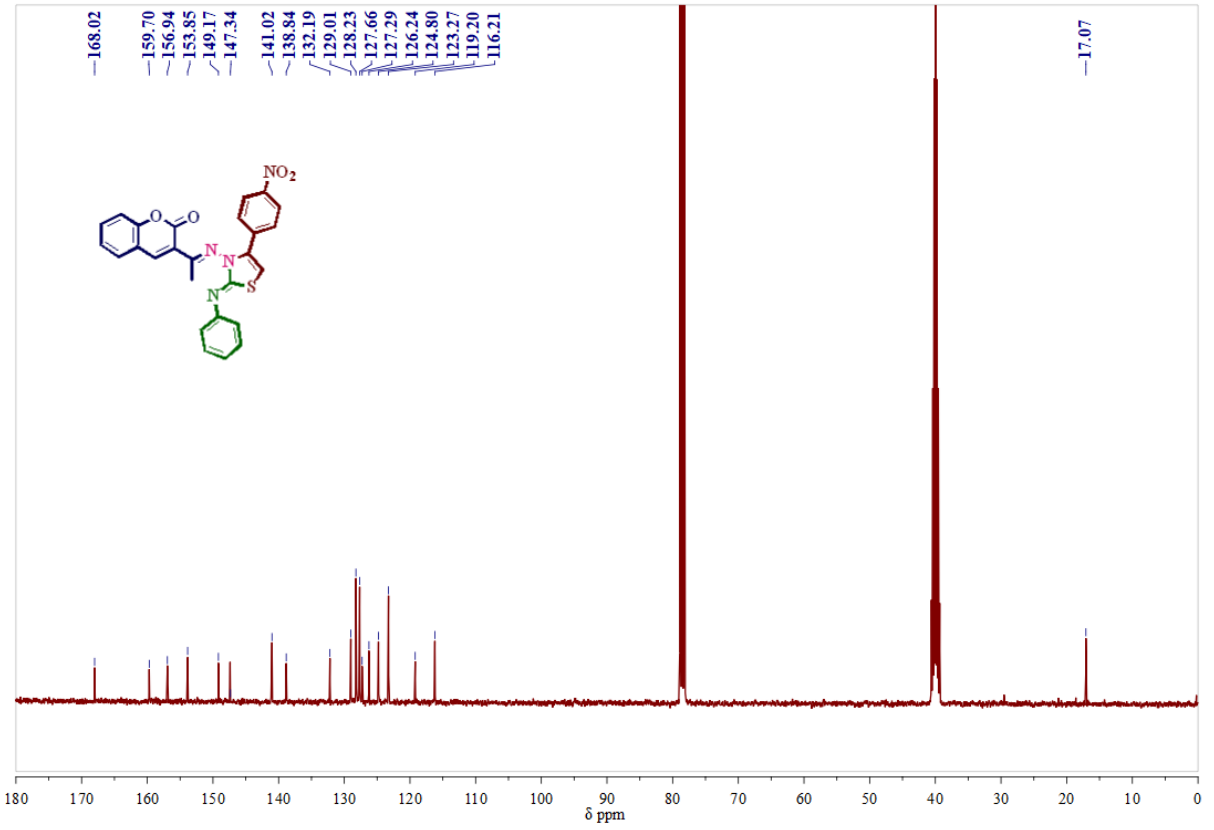

Mass spectrum of compound 5i

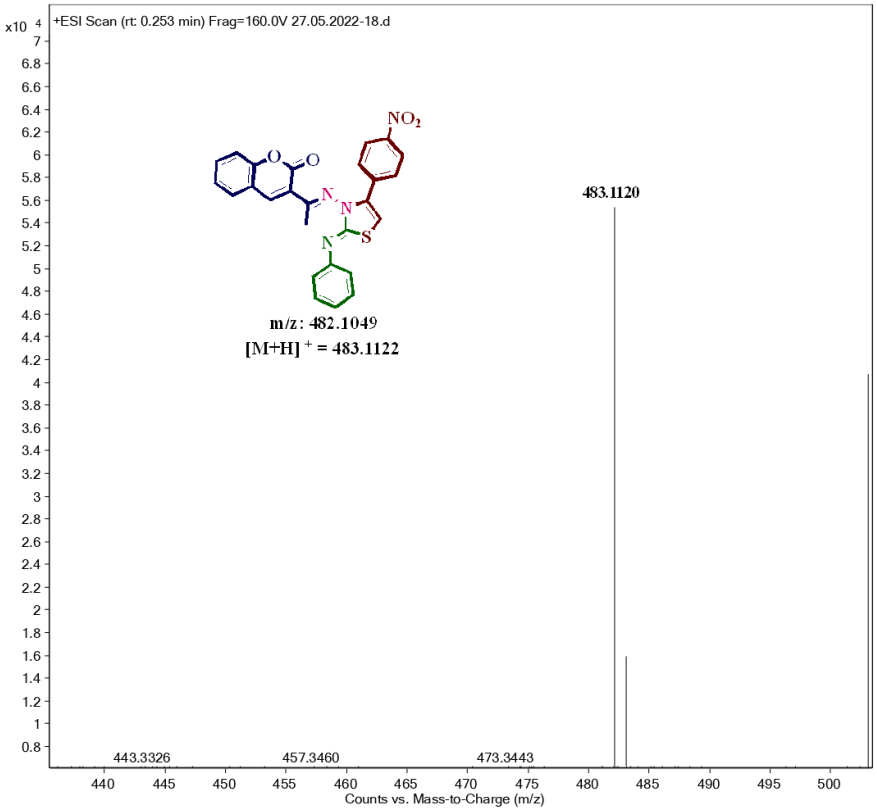

^{1}H-NMR Spectrum of compound 5j in $CDCl_3$ (400 MHz):

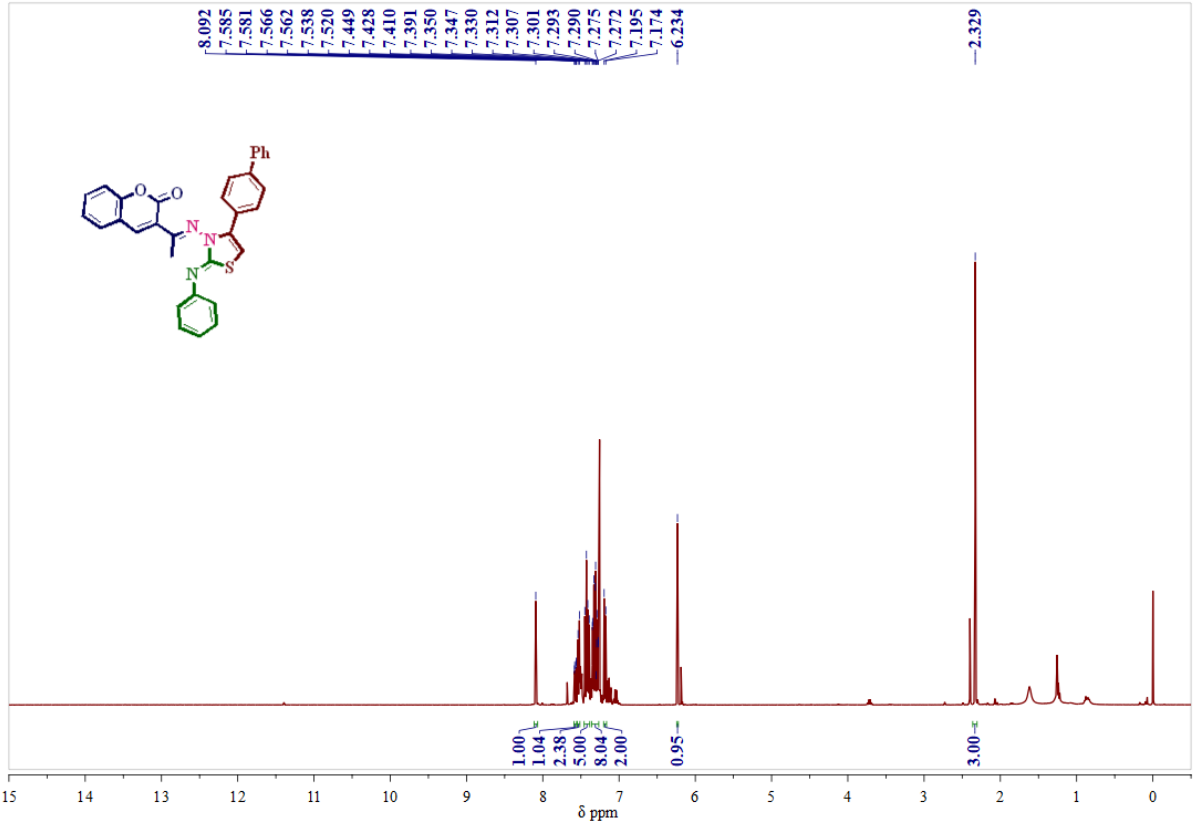

^{13}C-NMR Spectrum of compound 5j in $CDCl_3$ (100 MHz):

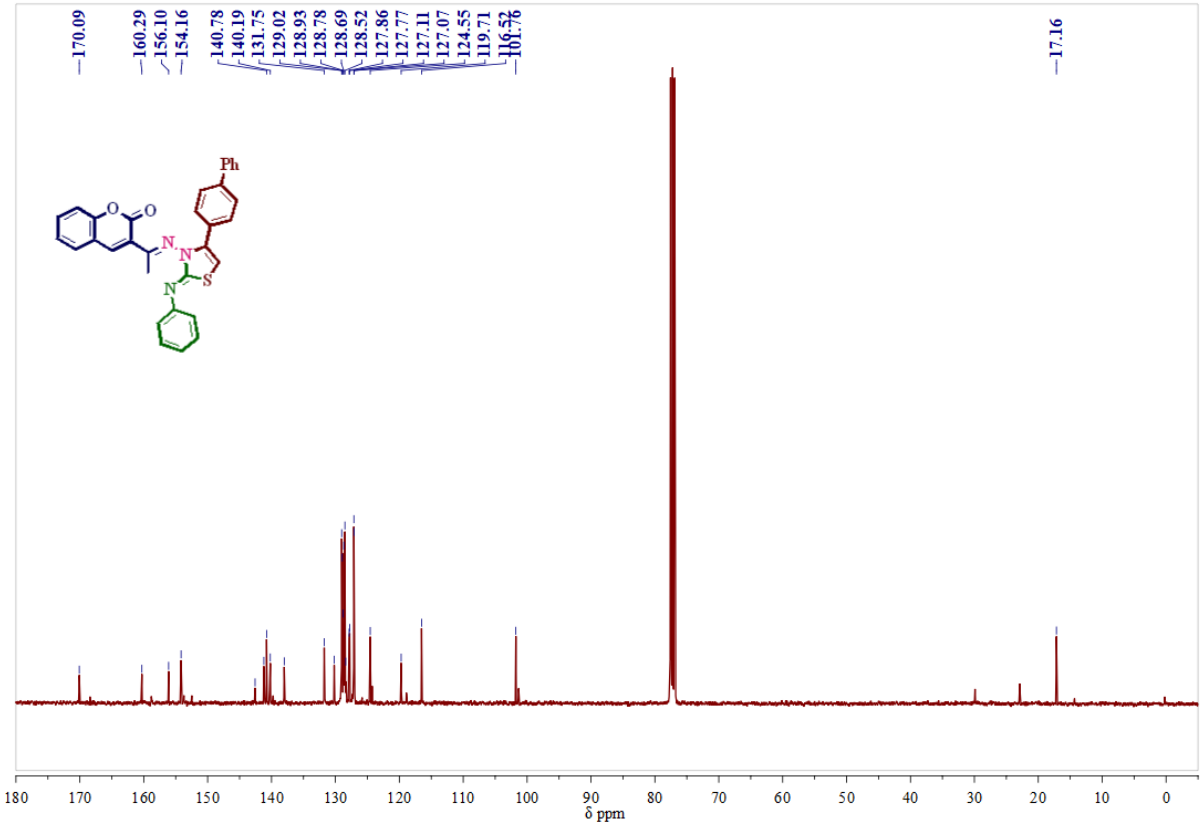

Mass spectrum of compound 5j

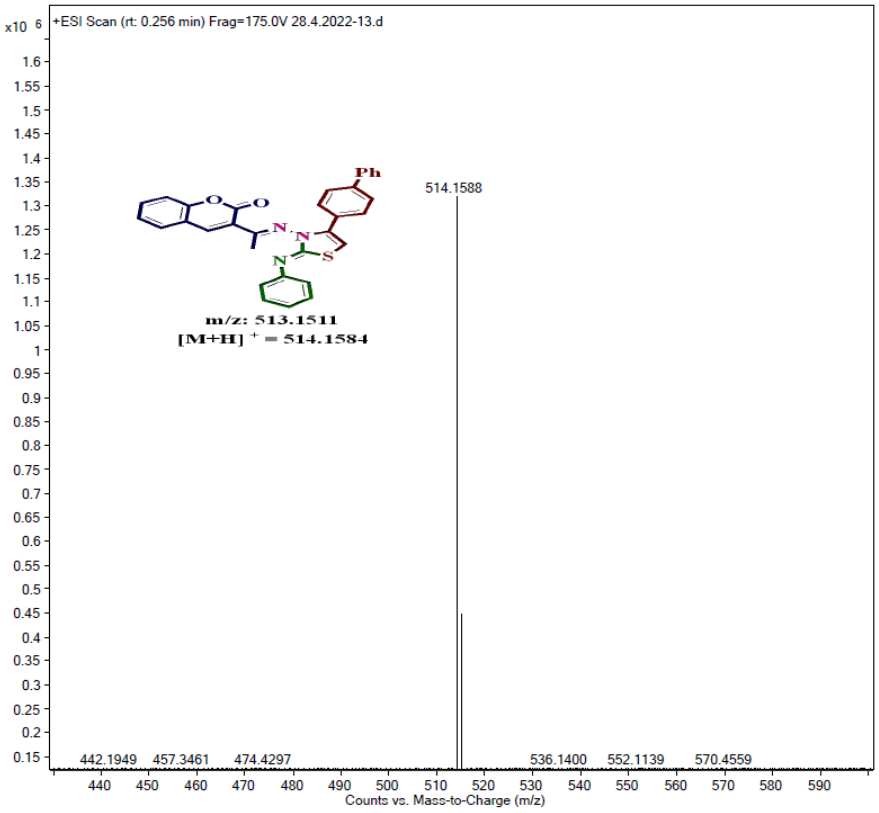

^{1}H-NMR Spectrum of compound 5k in $CDCl_3$ (400 MHz):

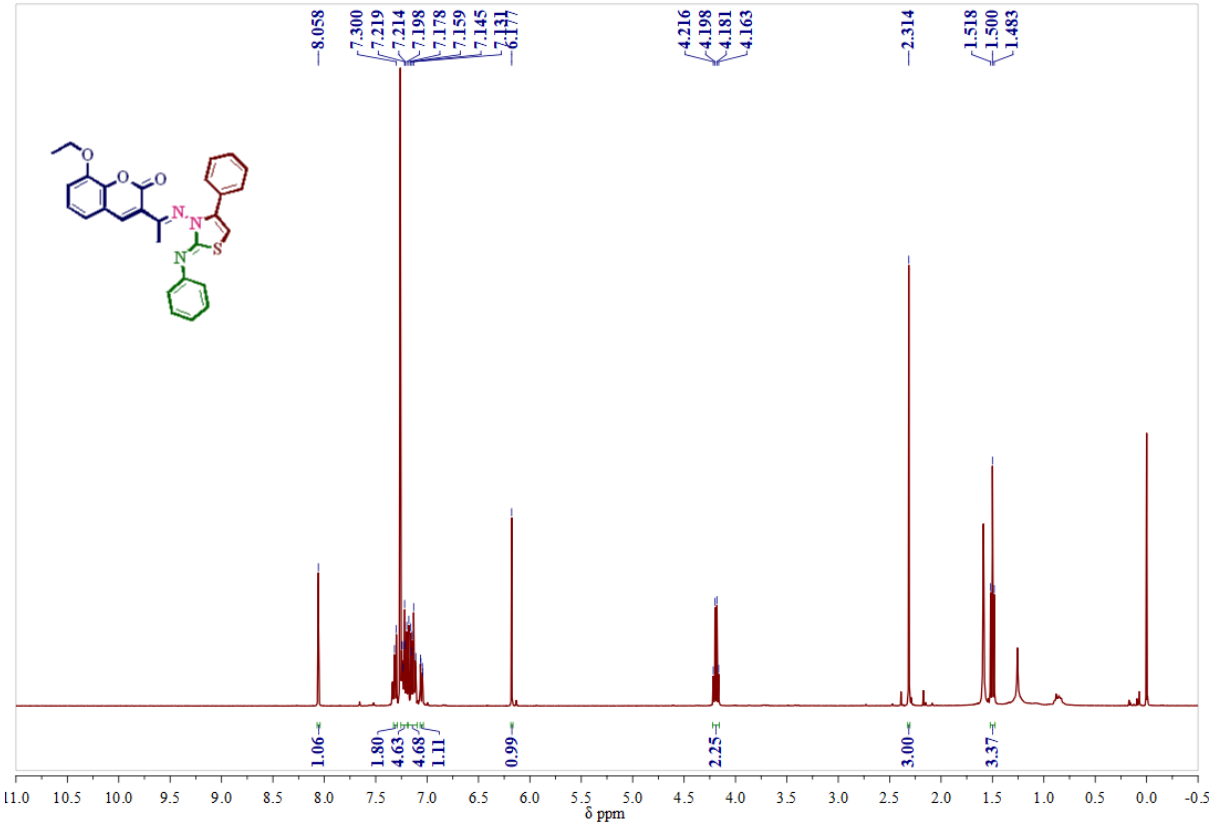

^{13}C-NMR Spectrum of compound 5k in $CDCl_3$ (100 MHz):

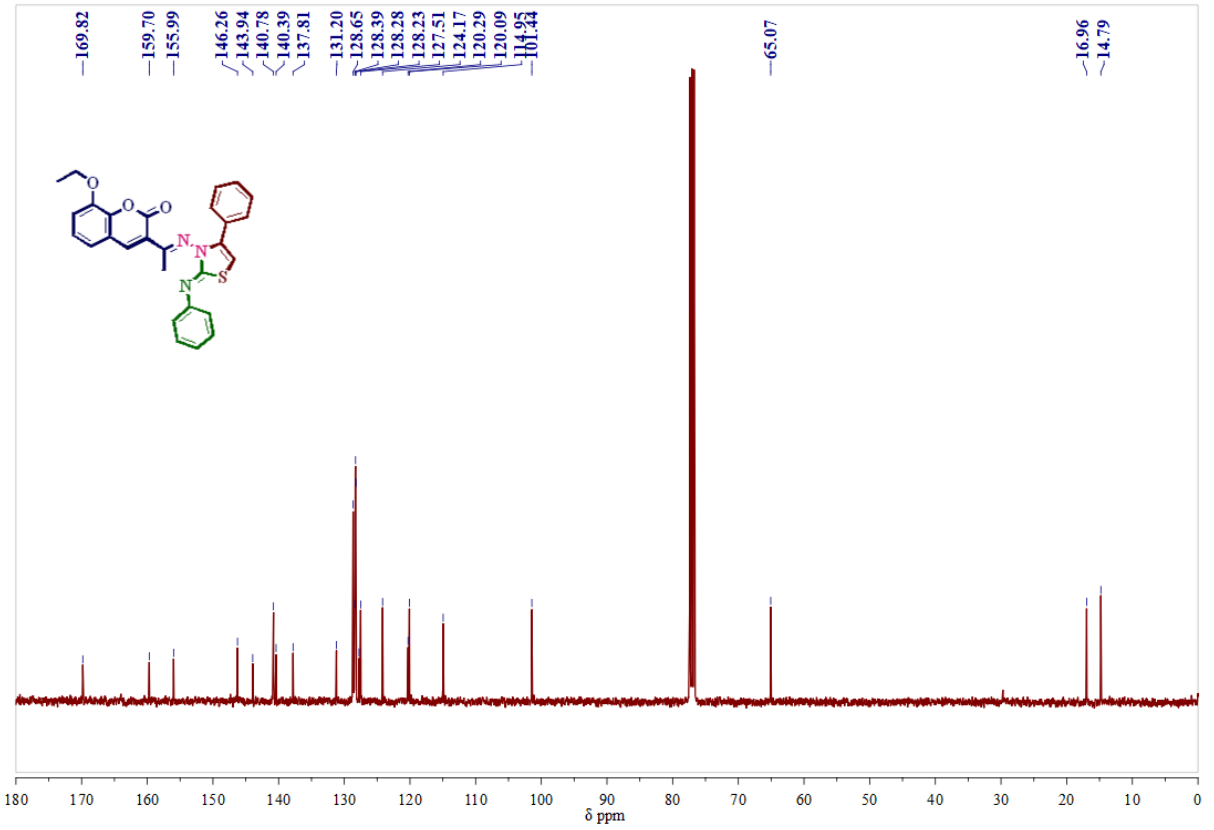

Mass spectrum of compound 5k

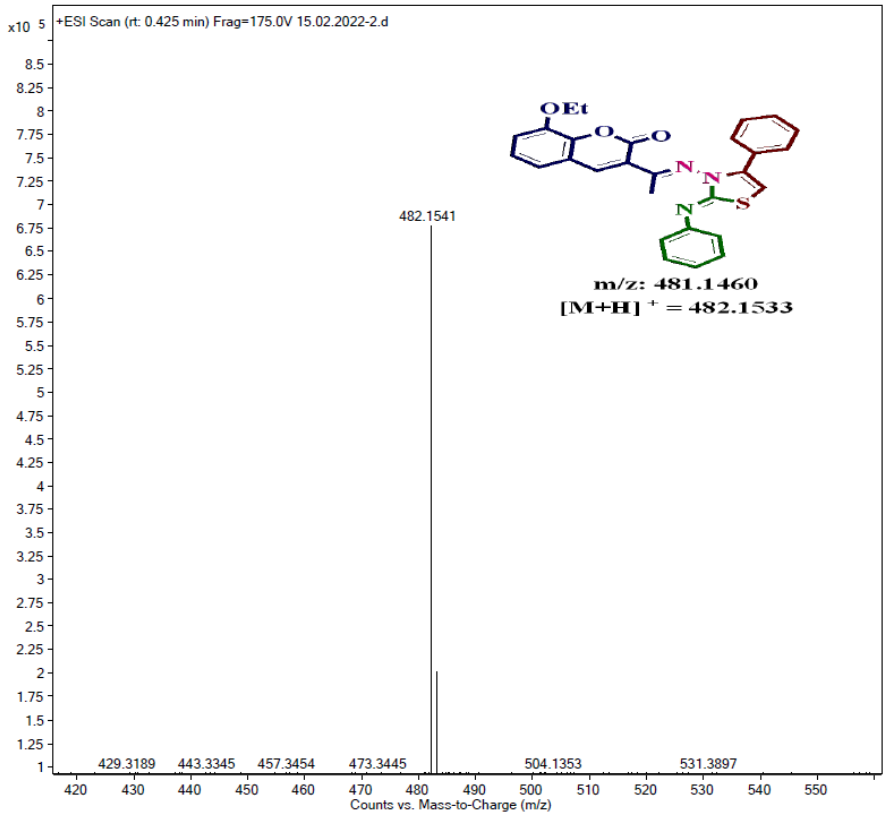

^{1}H-NMR Spectrum of compound 5l in $CDCl_3$ (400 MHz):

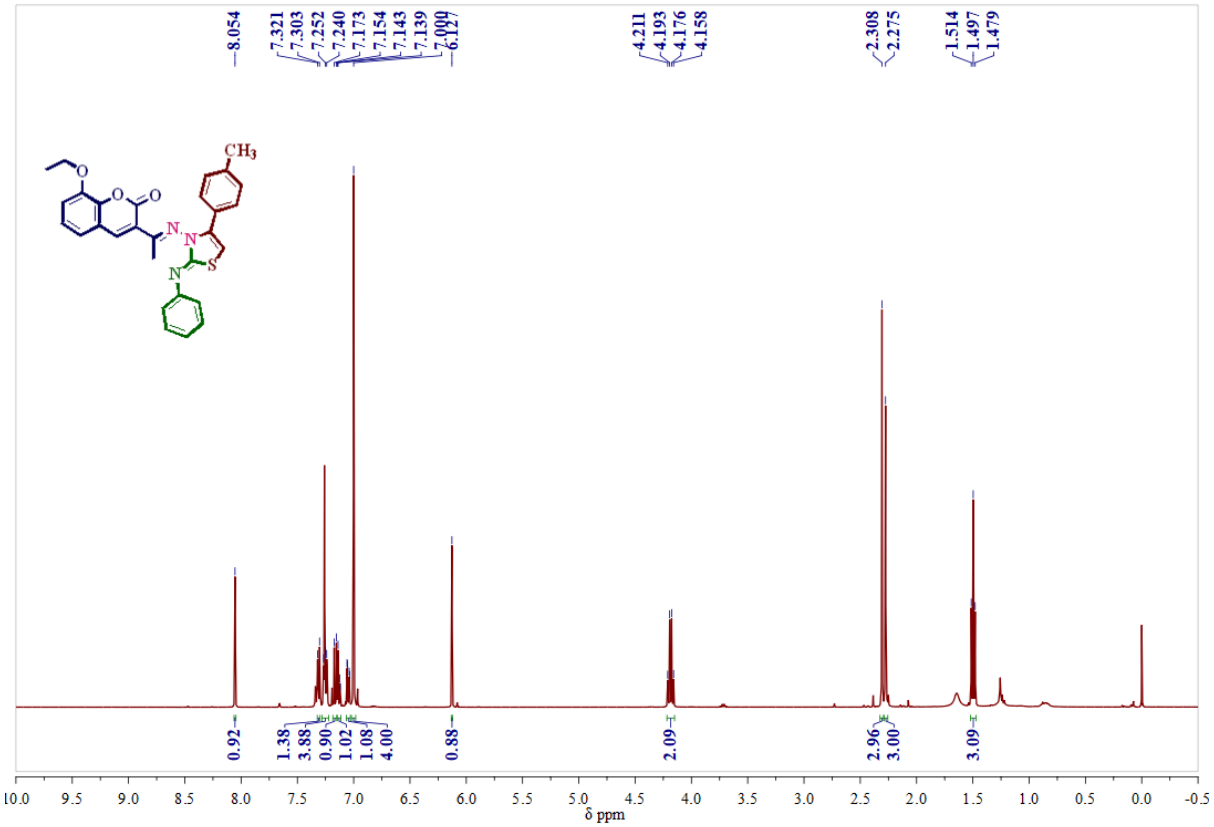

^{13}C-NMR Spectrum of compound 5l in $CDCl_3$ (100 MHz):

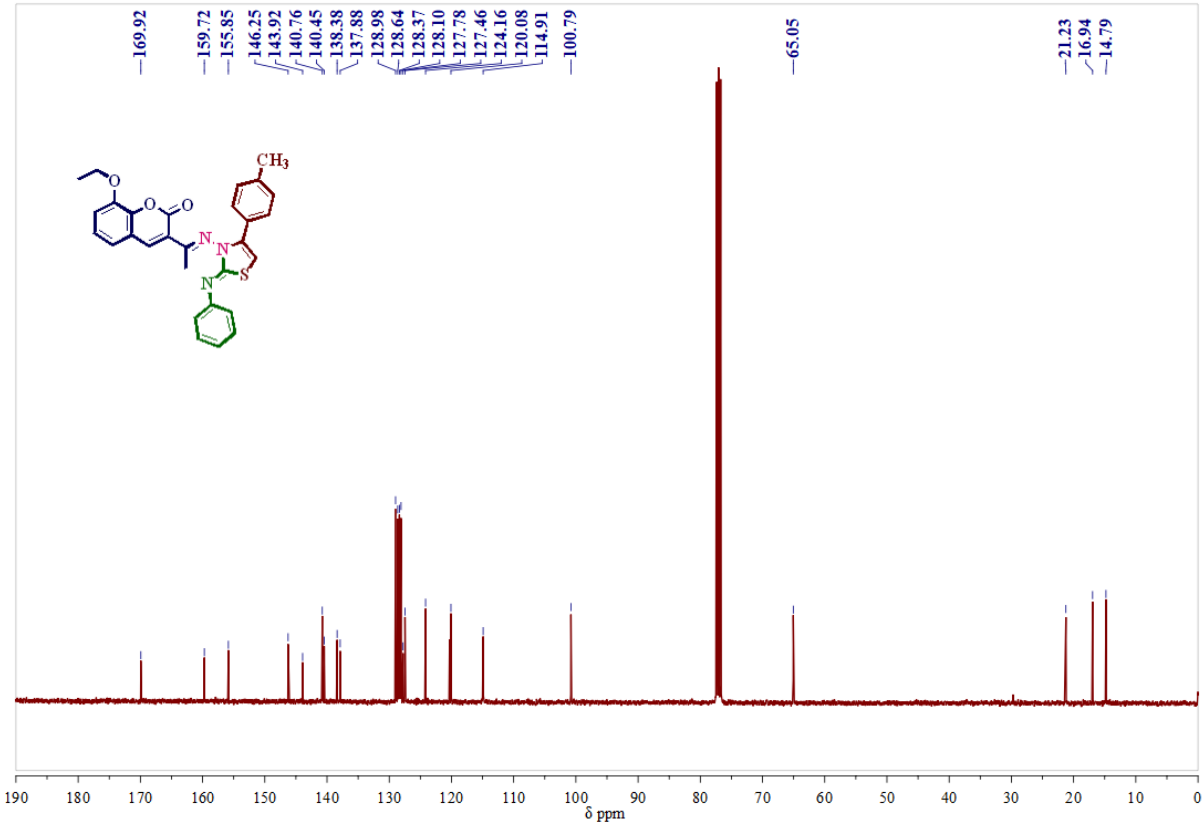

Mass spectrum of compound 5l

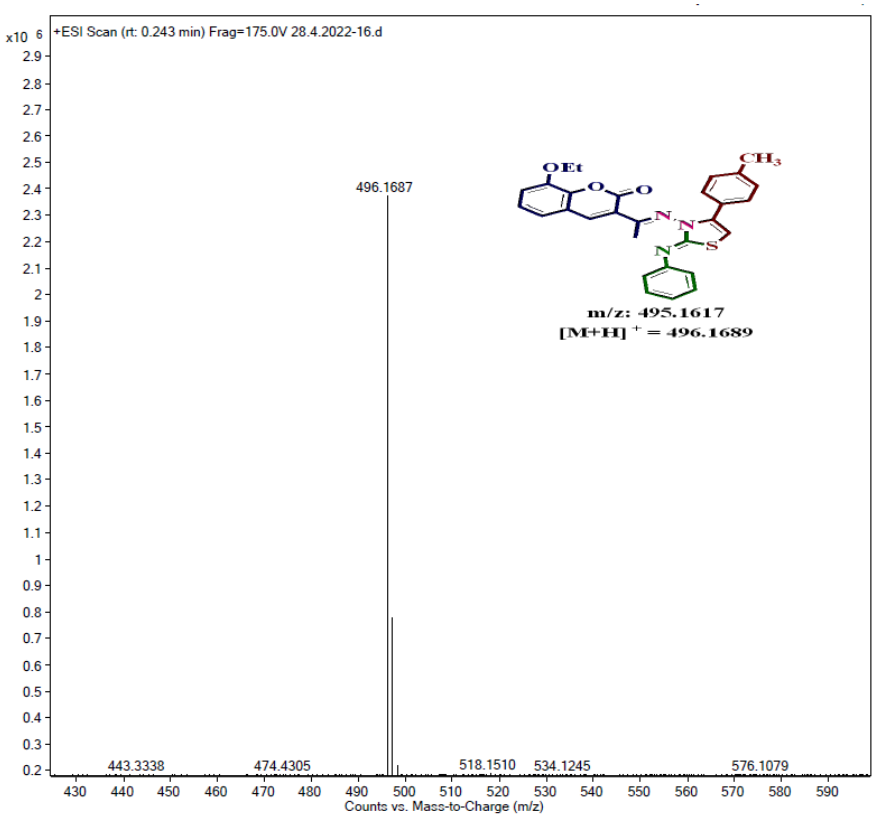

^{1}H-NMR Spectrum of compound 5m in $CDCl_3$ (400 MHz):

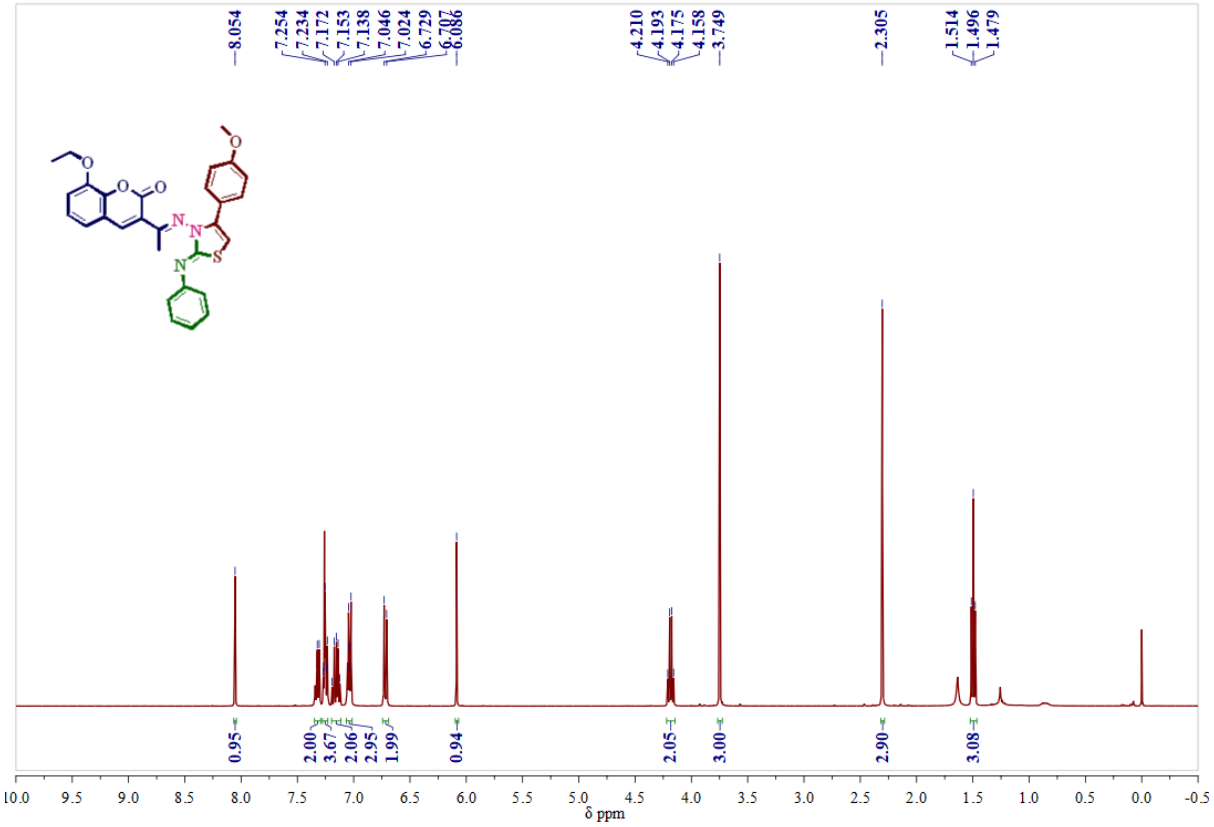

^{13}C-NMR Spectrum of compound 5m in $CDCl_3$ (100 MHz):

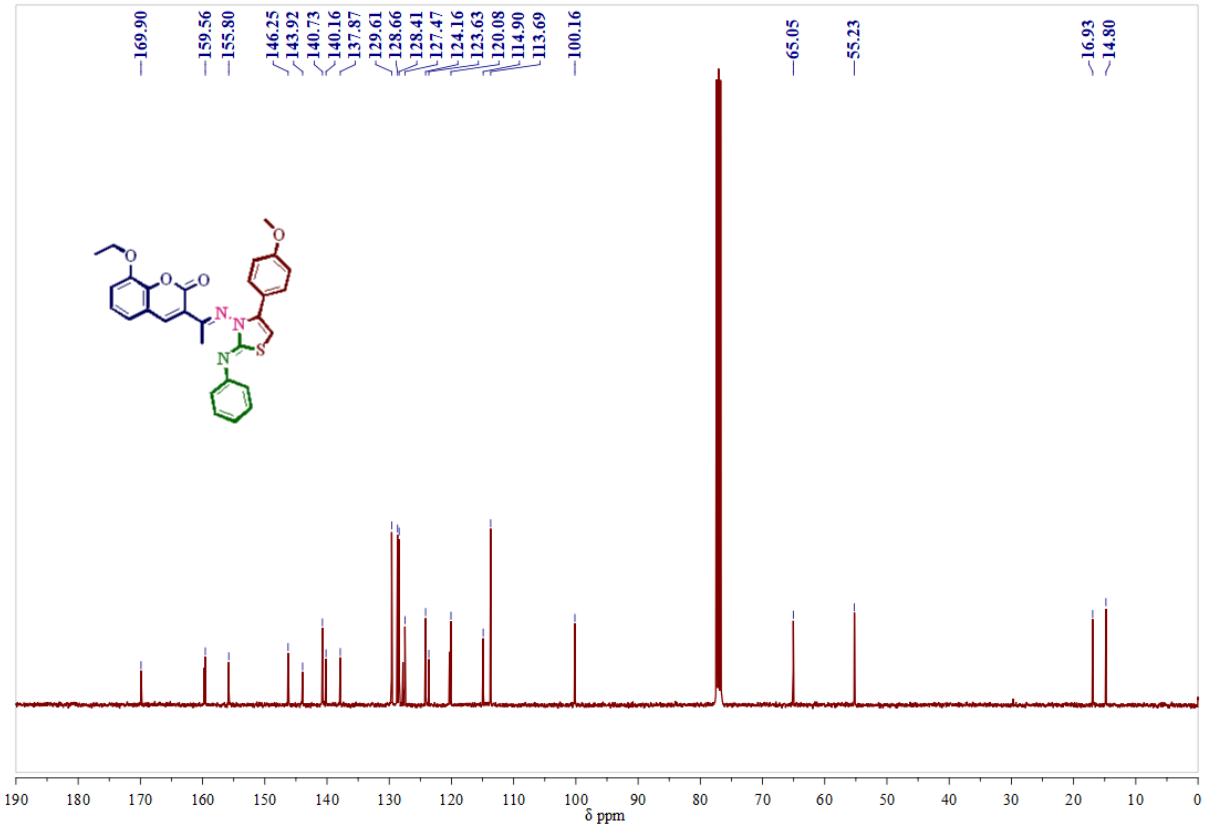

Mass spectrum of compound 5m

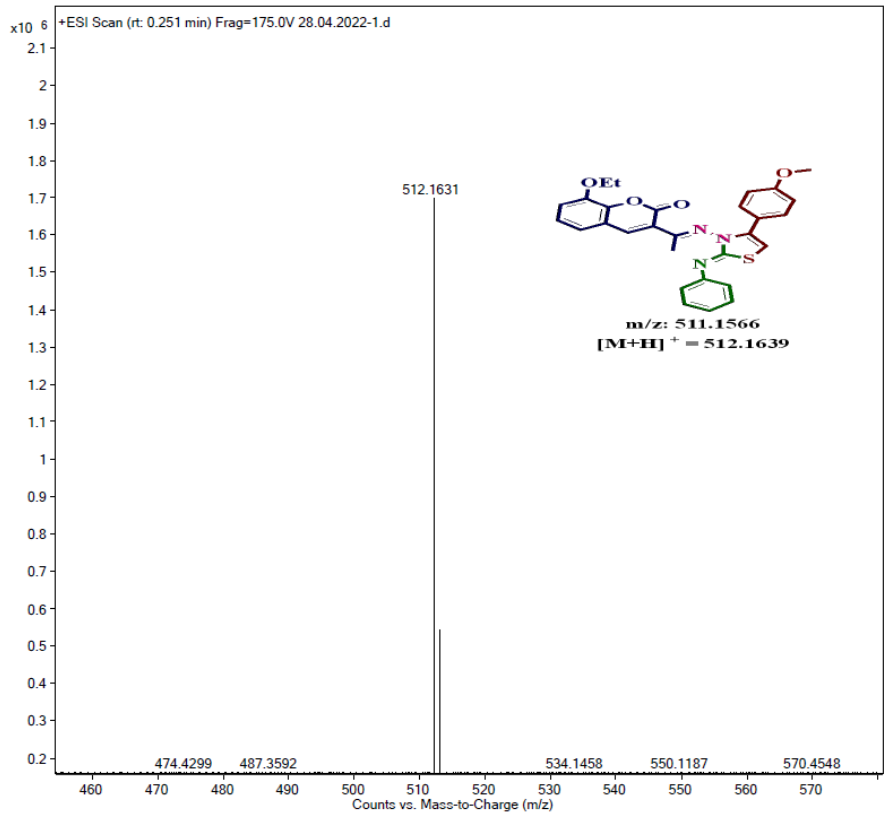

^{1}H-NMR Spectrum of compound 5n in $CDCl_3$ (400 MHz):

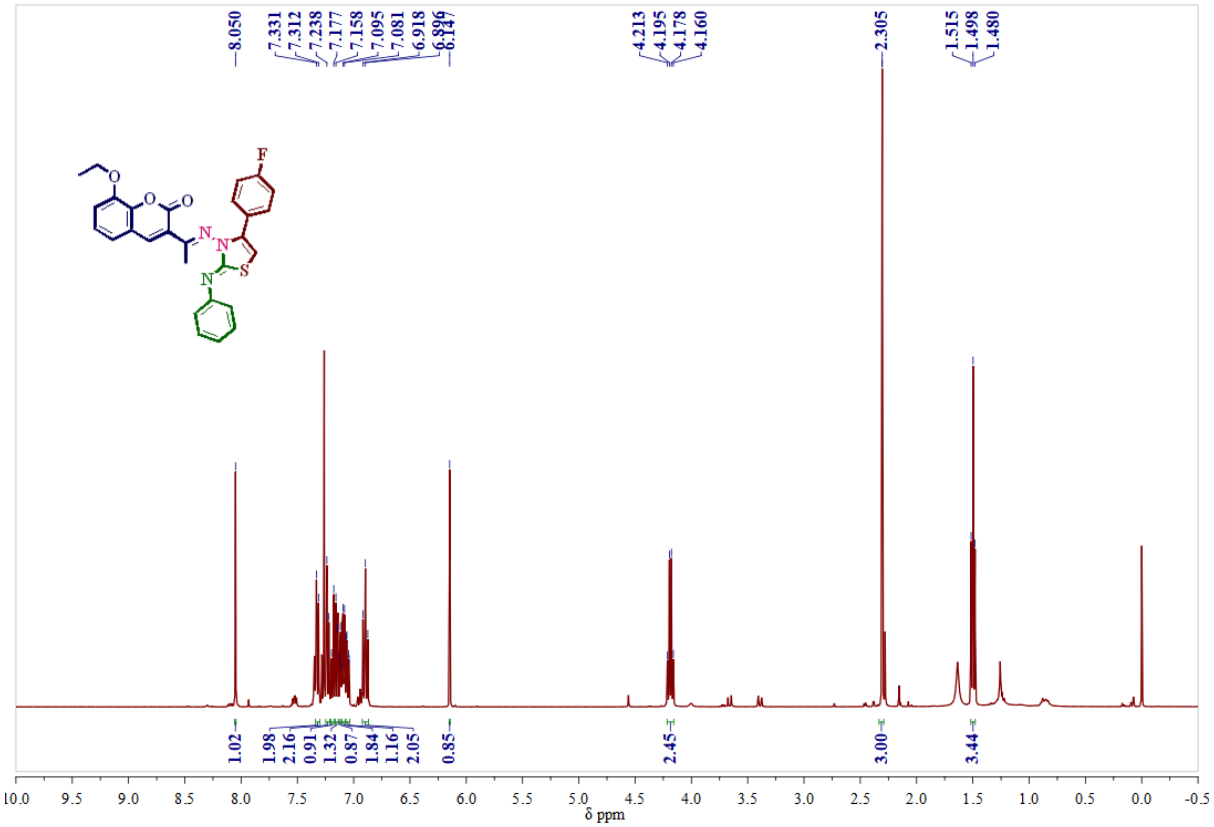

^{13}C-NMR Spectrum of compound 5n in $CDCl_3$ (100 MHz):

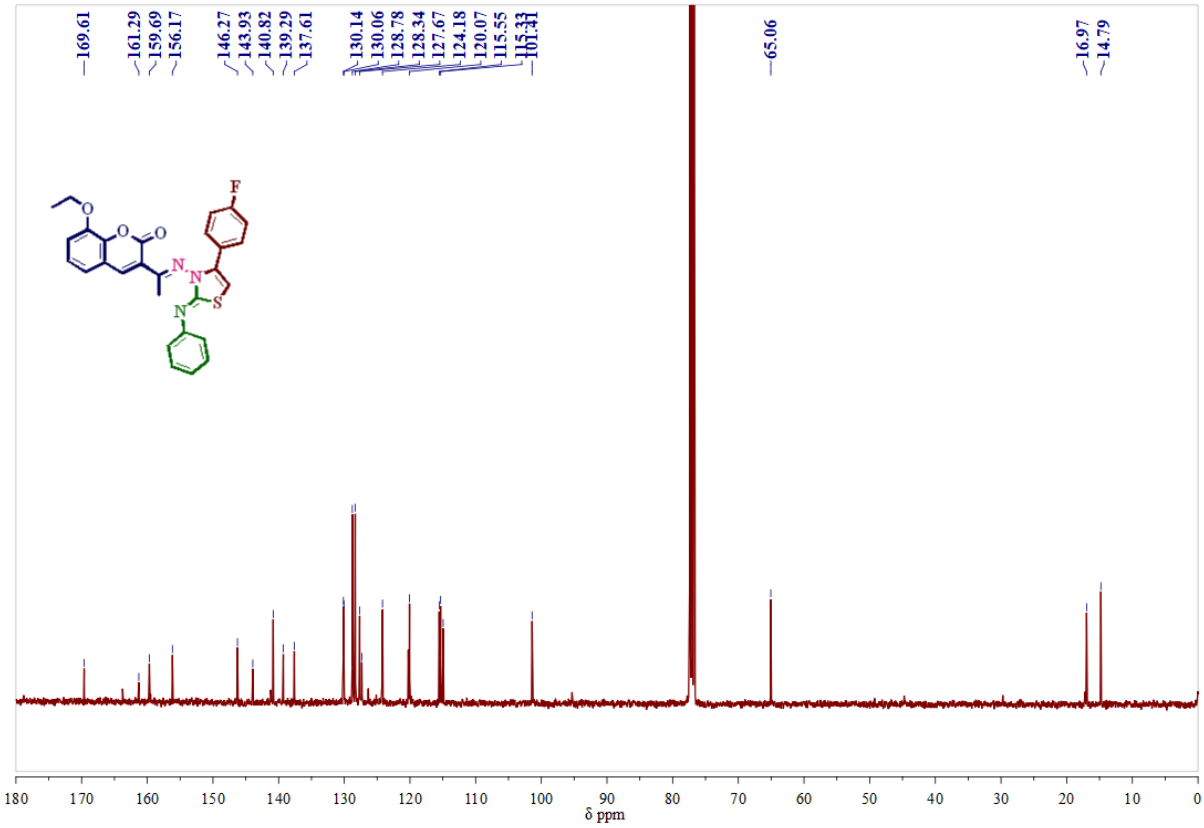

Mass spectrum of compound 5n

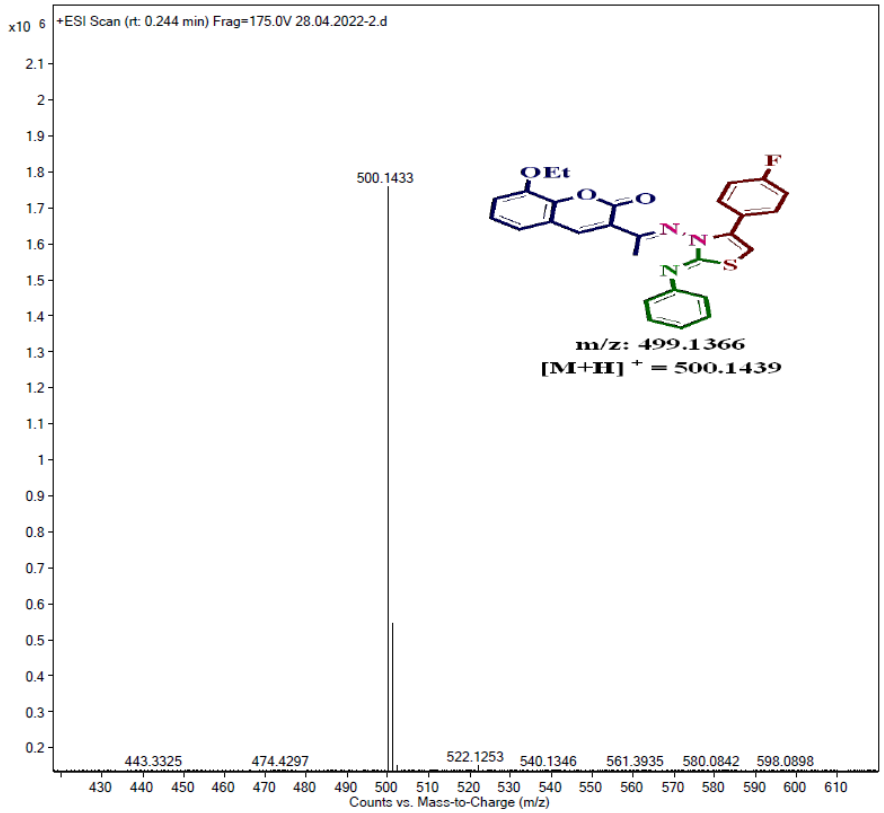

[1]H-NMR Spectrum of compound 5o in $CDCl_3$ (400 MHz):

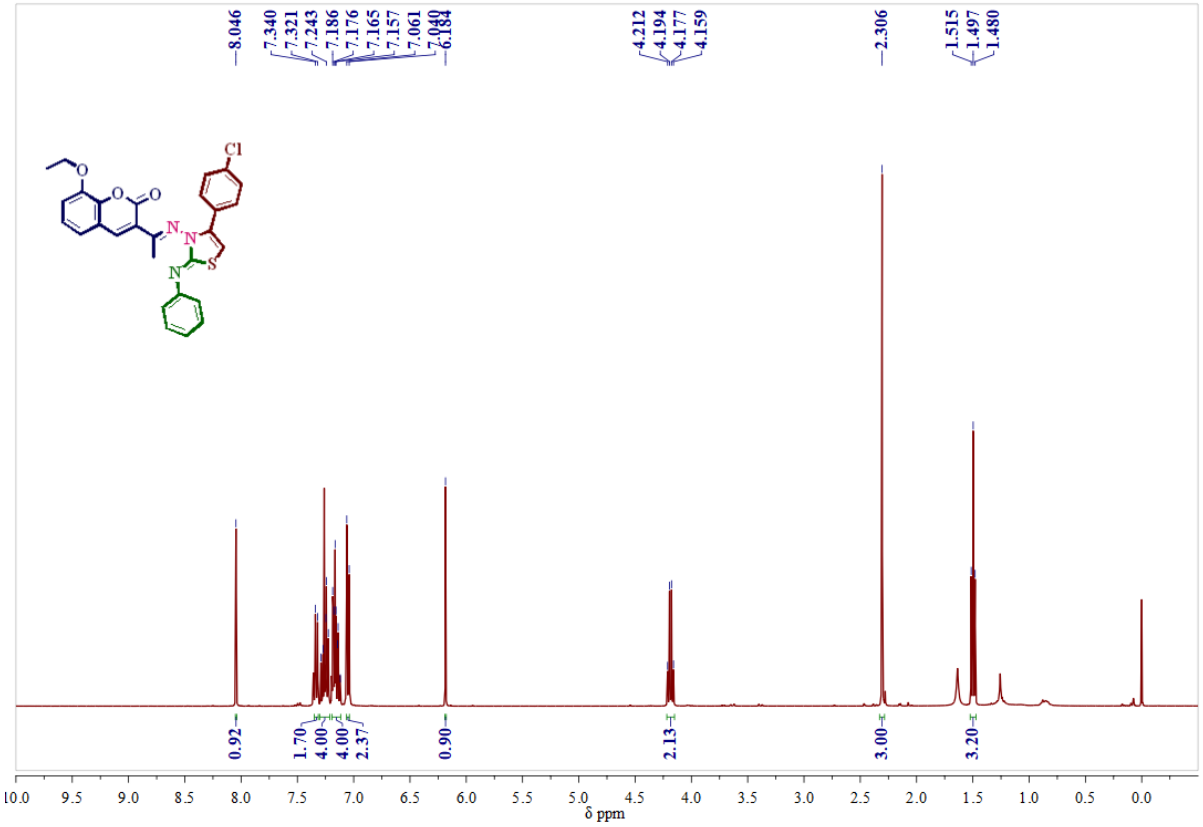

[13]C-NMR Spectrum of compound 5o in $CDCl_3$ (100 MHz):

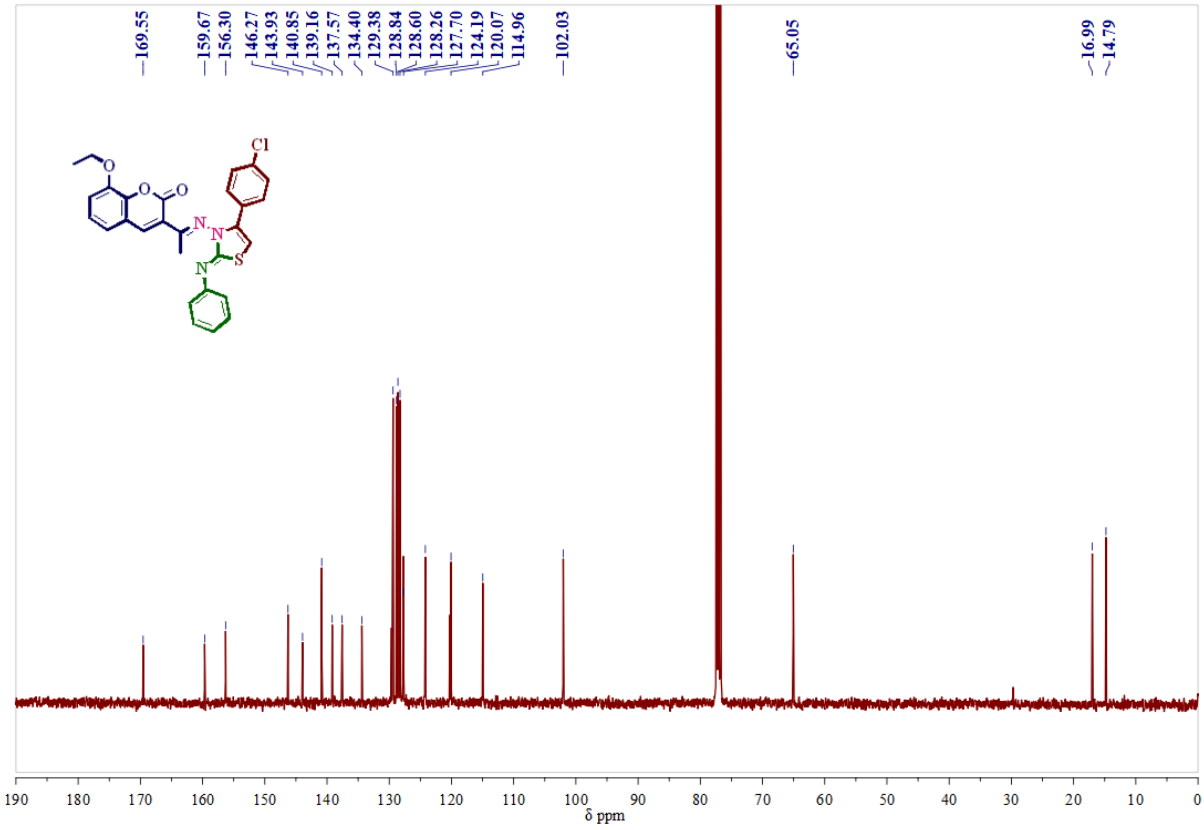

Mass spectrum of compound 5o

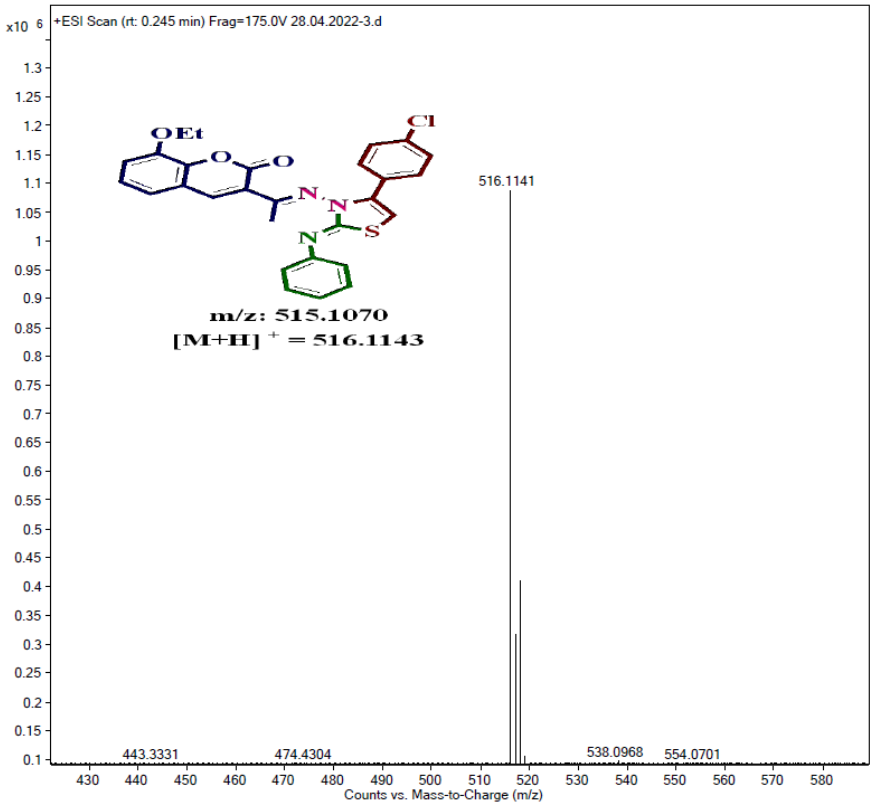

^{1}H-NMR Spectrum of compound 5p in $CDCl_3$ (400 MHz):

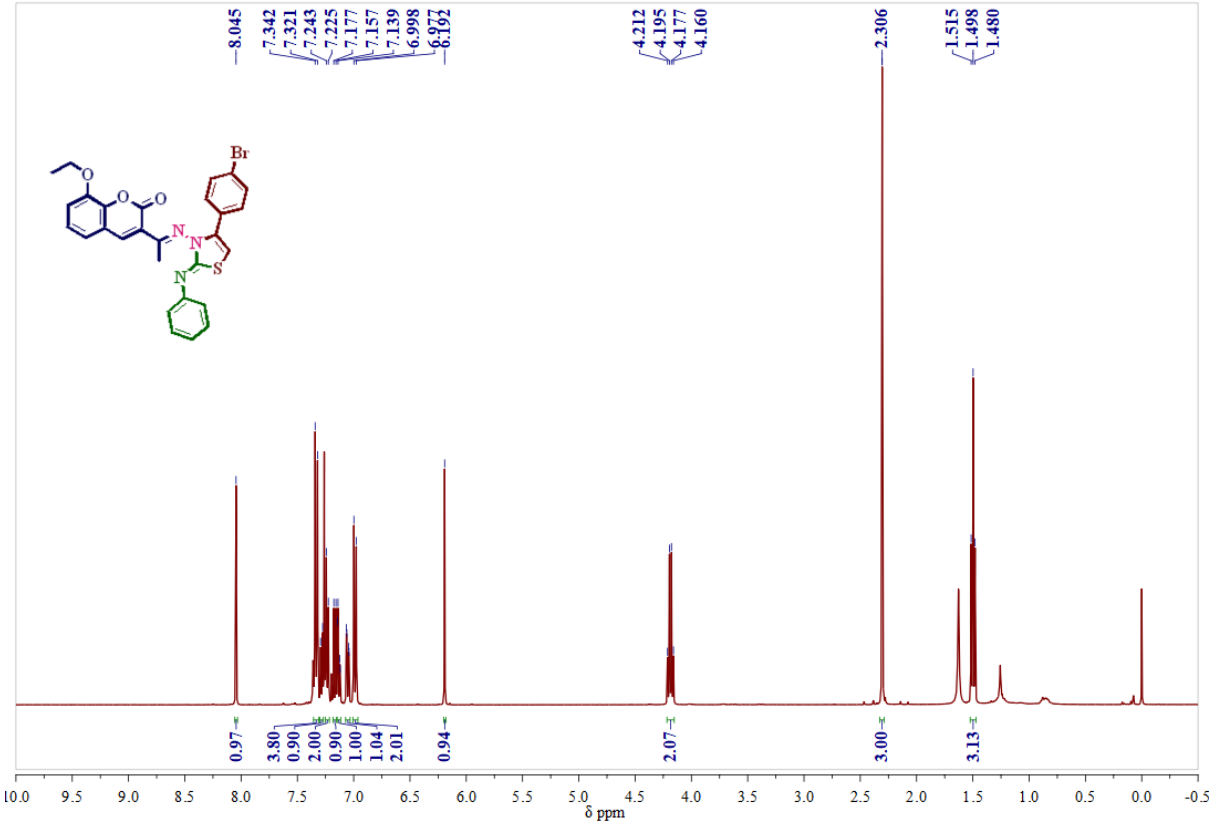

^{13}C-NMR Spectrum of compound 5p in $CDCl_3$ (100 MHz):

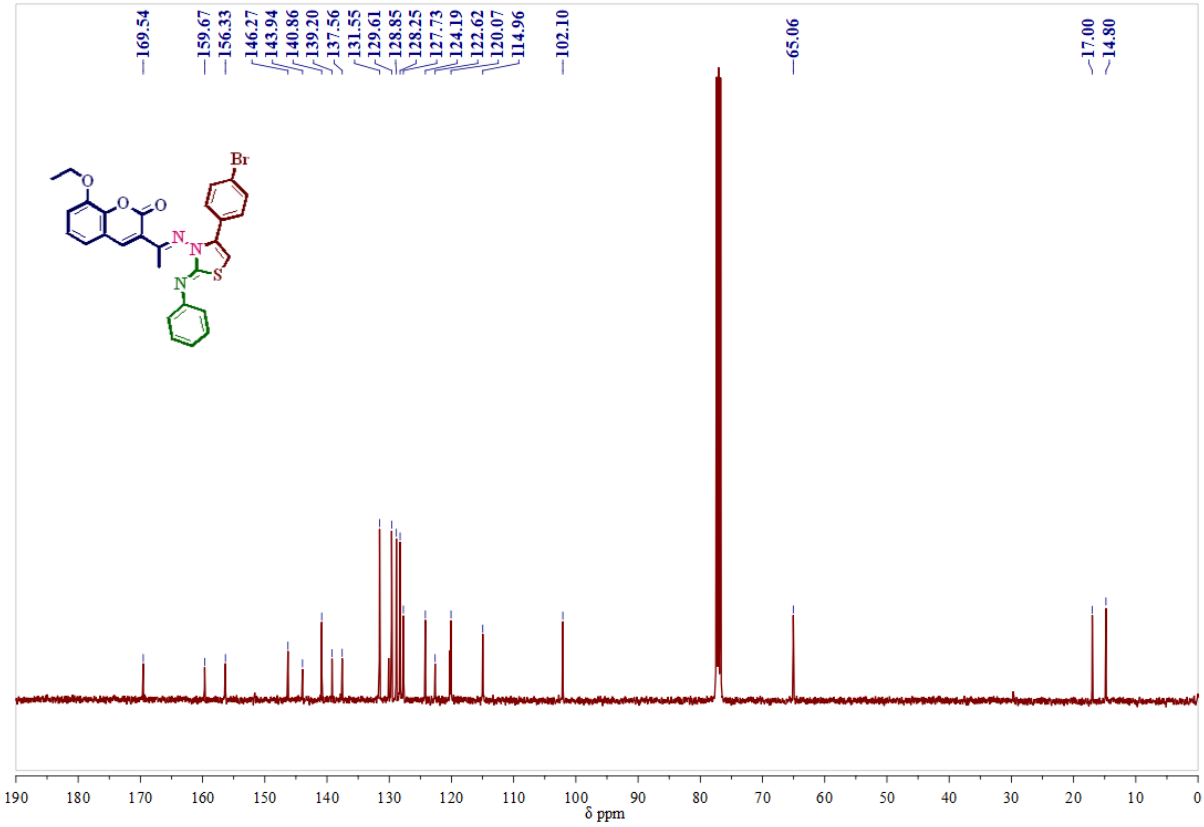

Mass spectrum of compound 5p

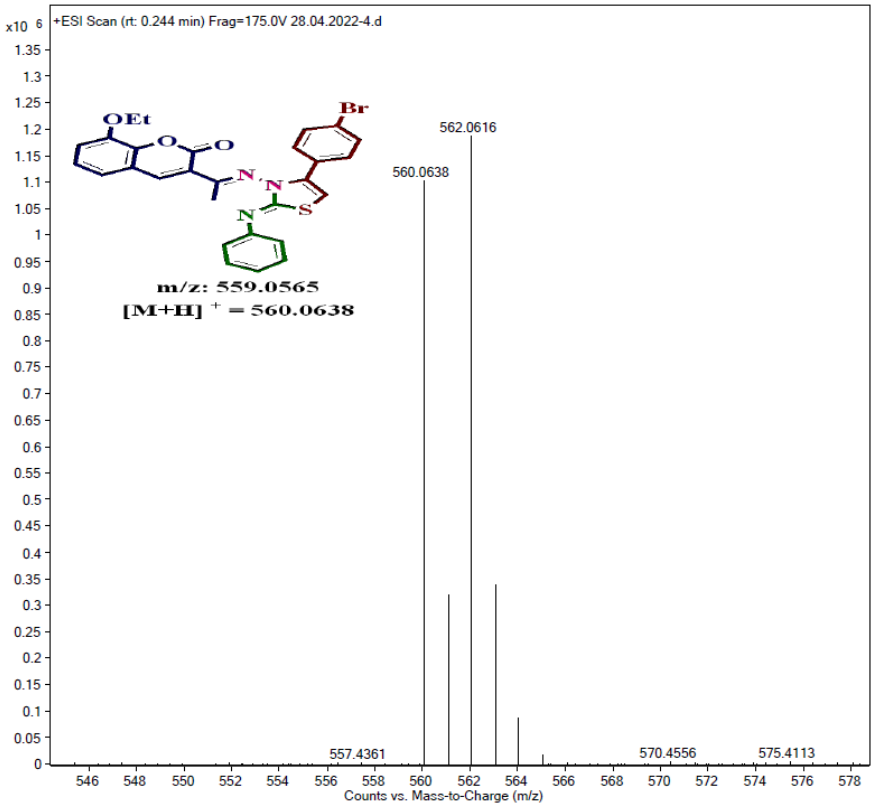

^{1}H-NMR Spectrum of compound 5q in $CDCl_3$ (400 MHz):

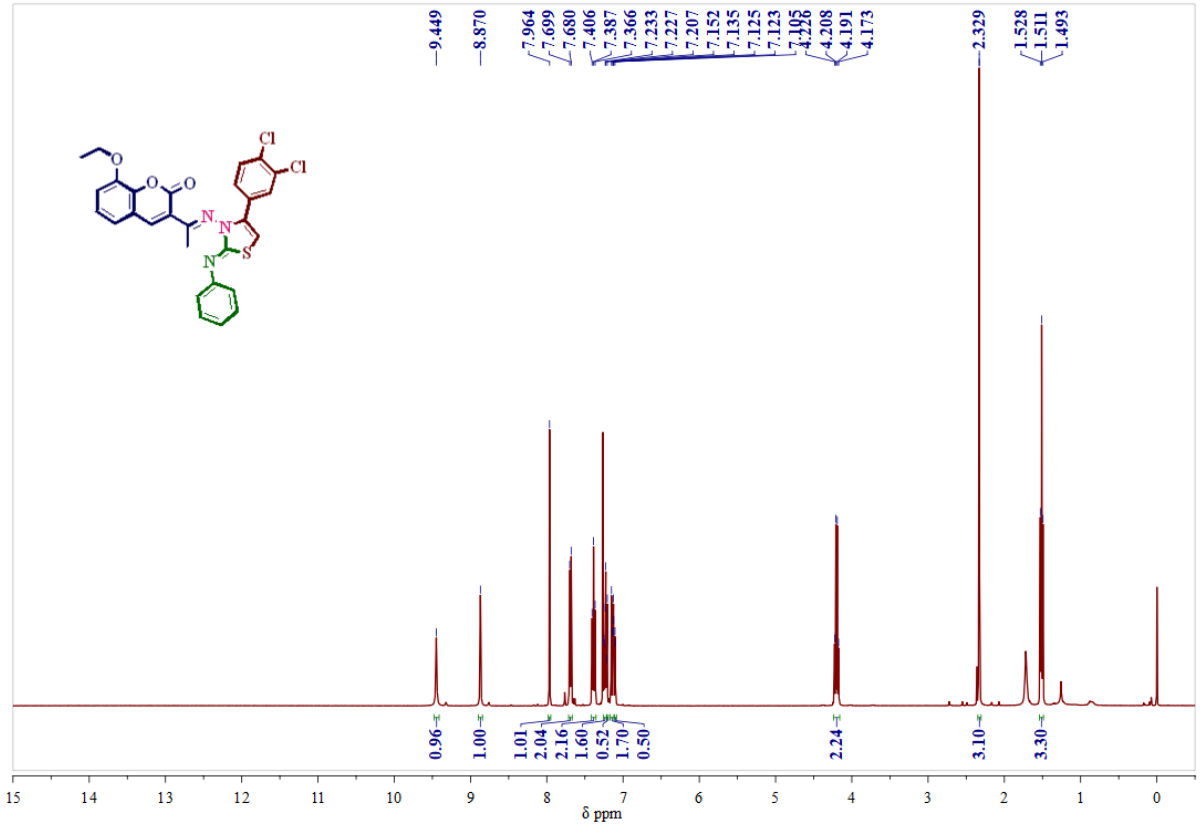

^{13}C-NMR Spectrum of compound 5q in $CDCl_3$ (100 MHz):

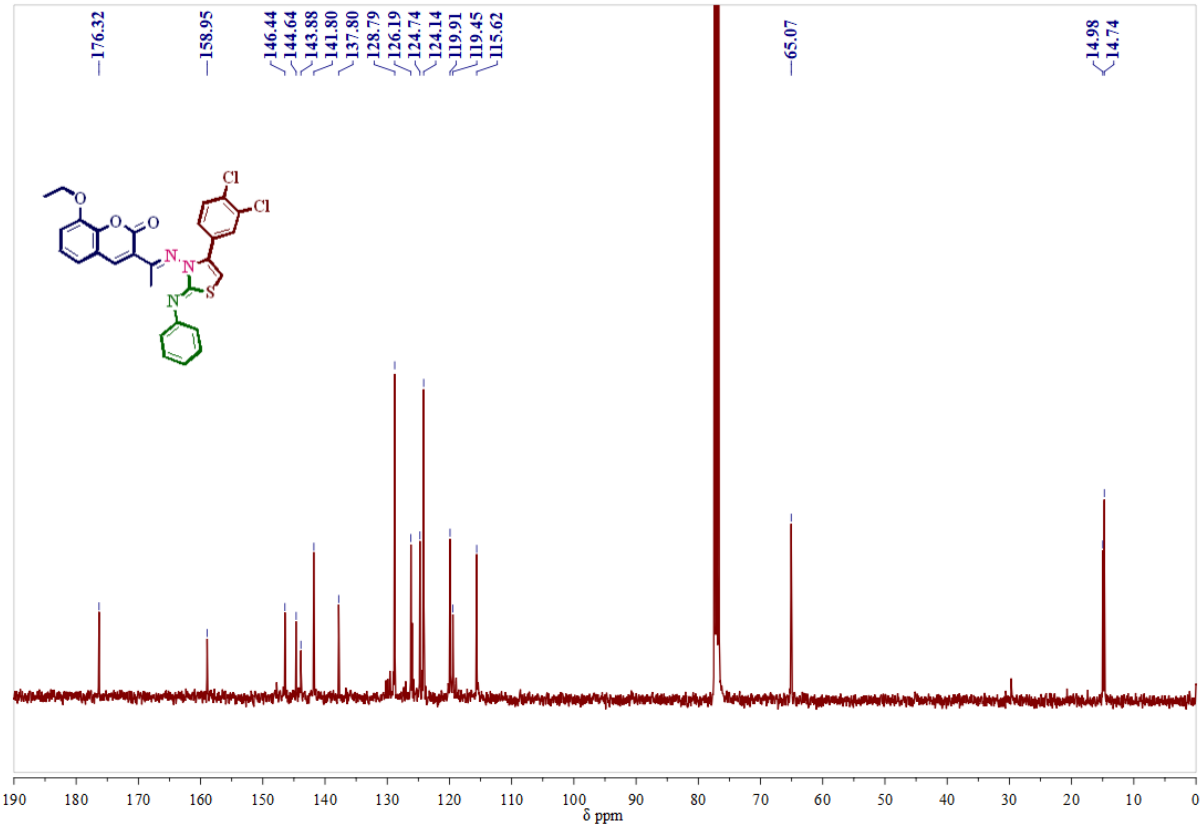

Mass spectrum of compound 5q

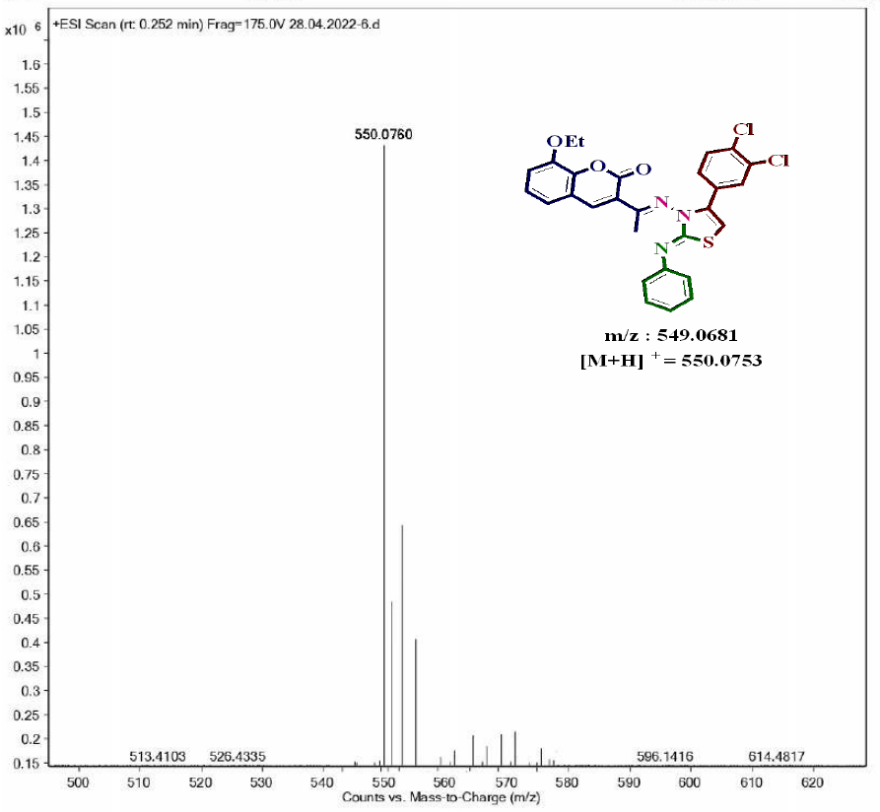

^{1}H-NMR Spectrum of compound 5r in $CDCl_3$ (400 MHz):

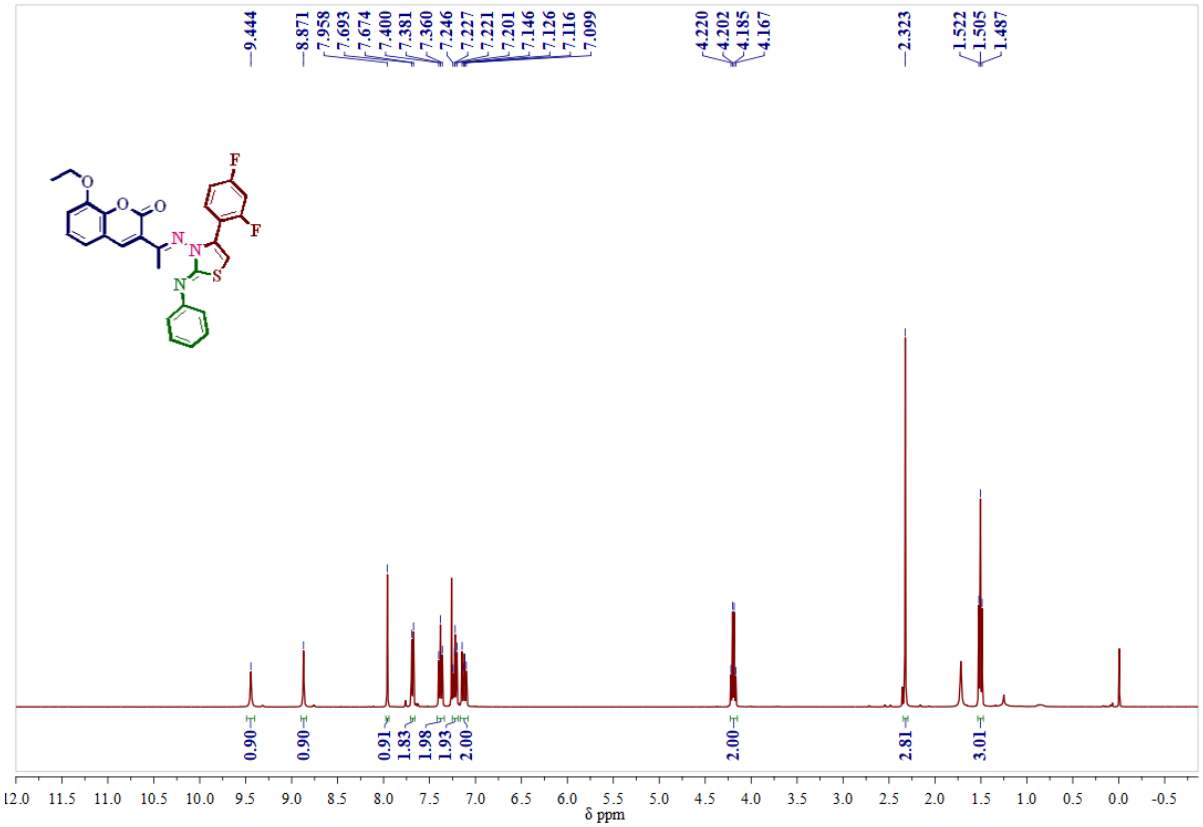

^{13}C-NMR Spectrum of compound 5r in $CDCl_3$ (100 MHz):

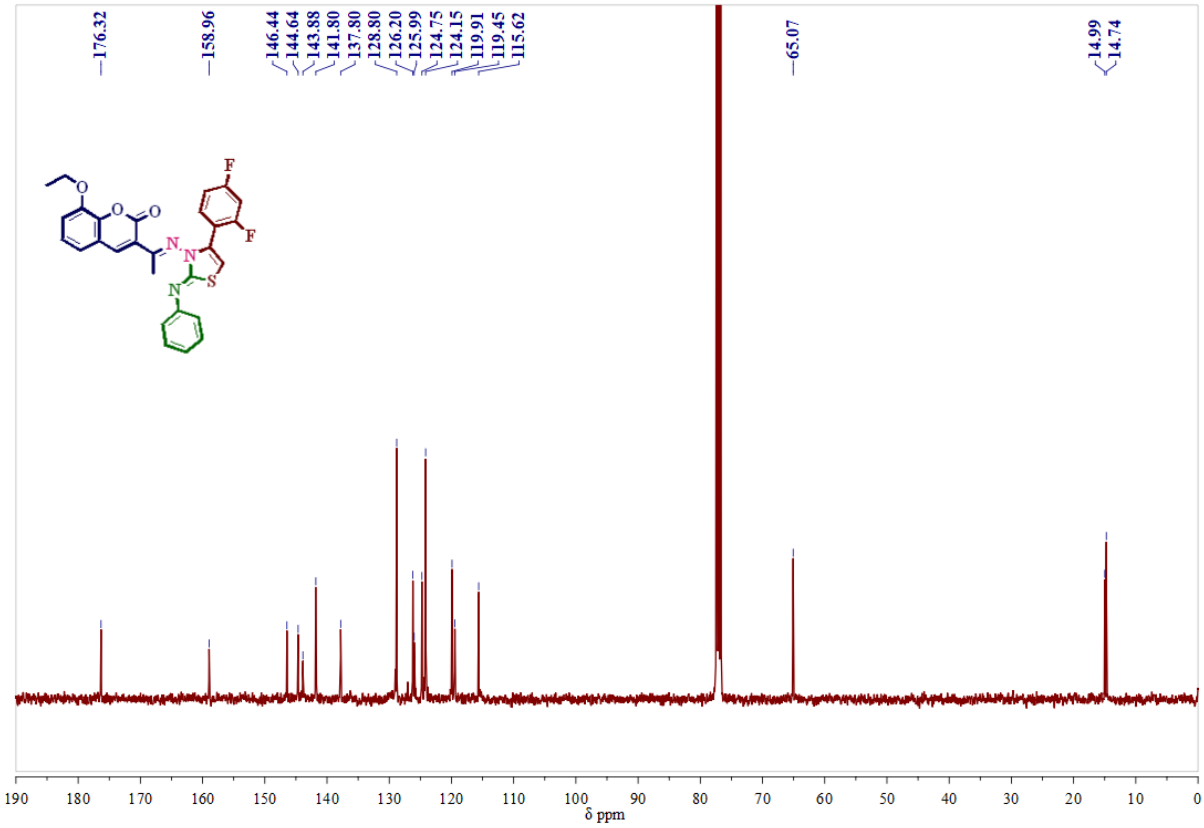

Mass spectrum of compound 5r

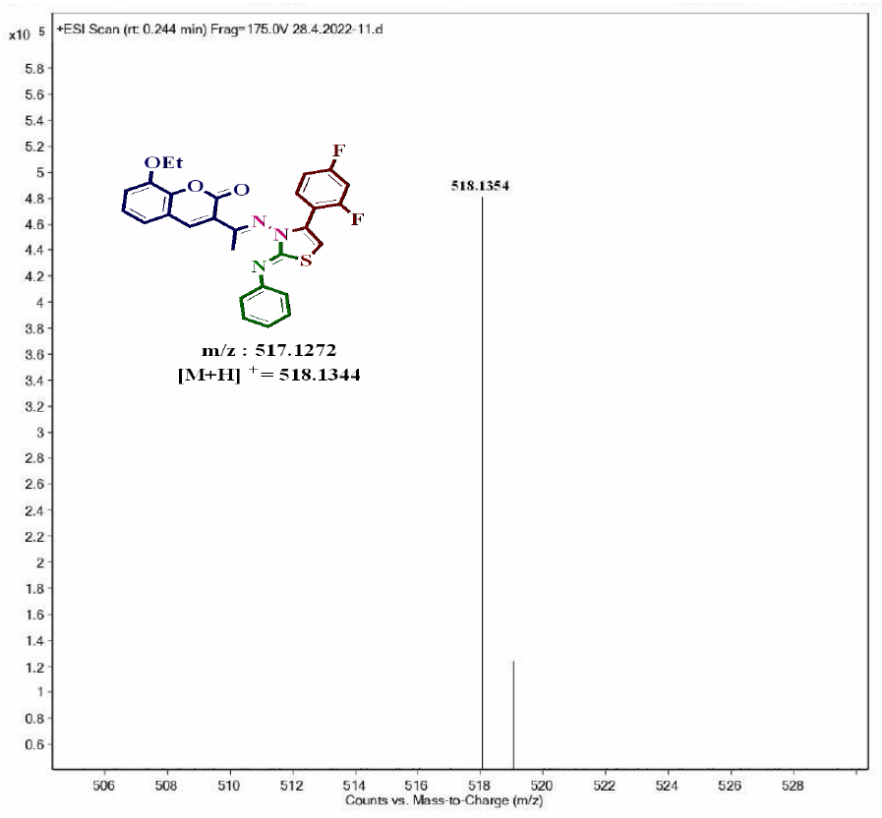

^{1}H-NMR Spectrum of compound 5s in $CDCl_3$ (400 MHz):

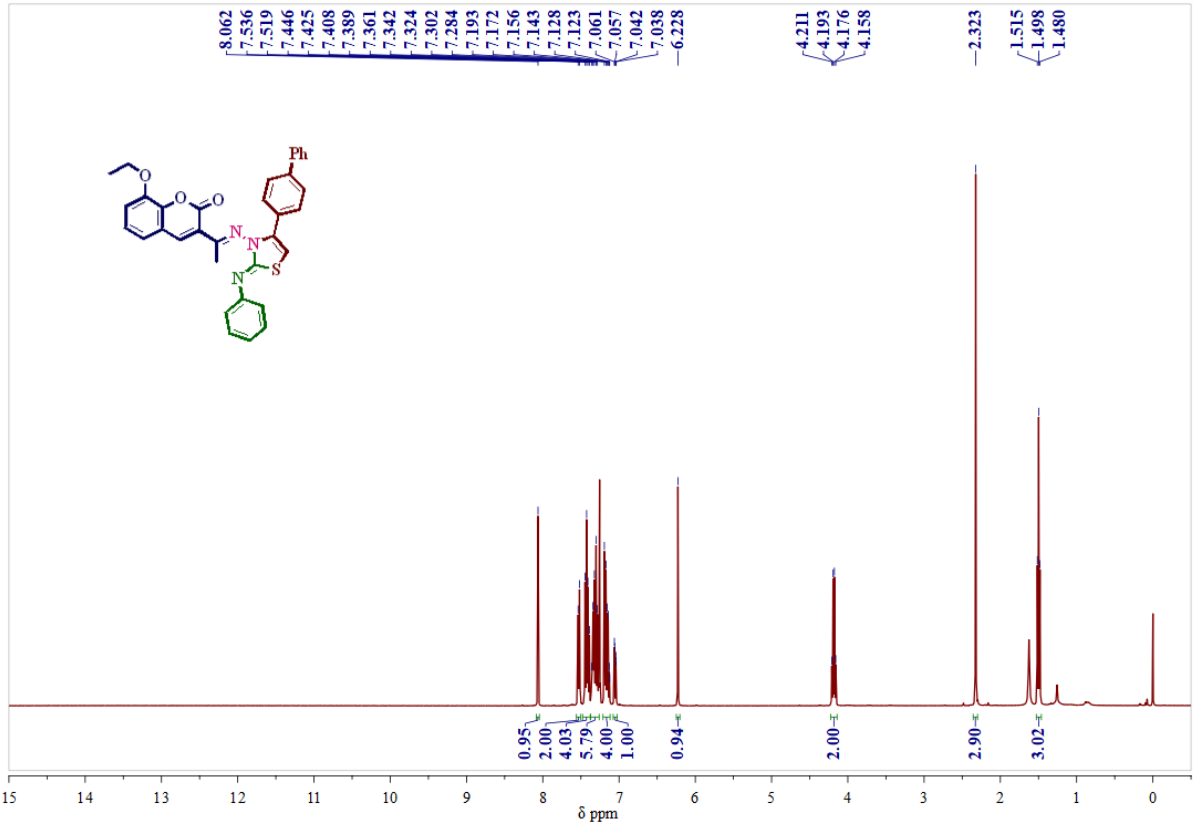

^{13}C-NMR Spectrum of compound 5s in $CDCl_3$ (100 MHz):

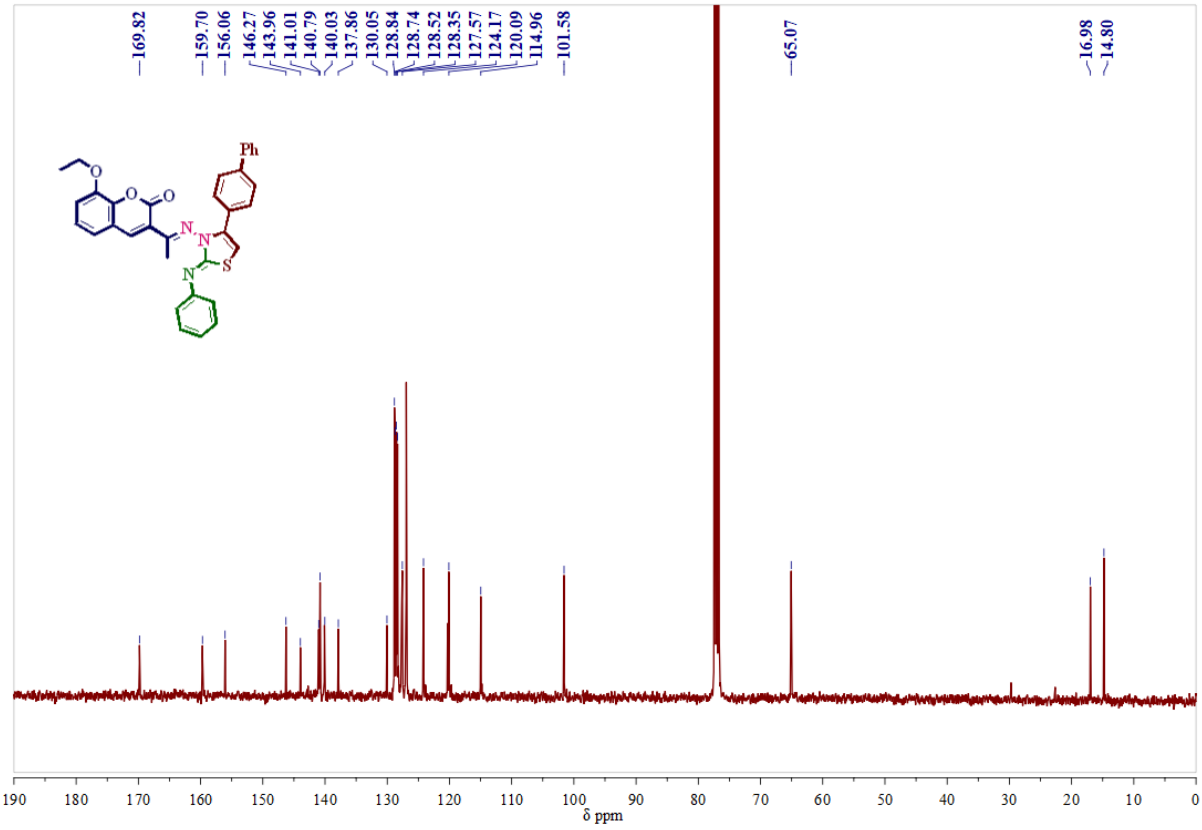

Mass spectrum of compound 5s

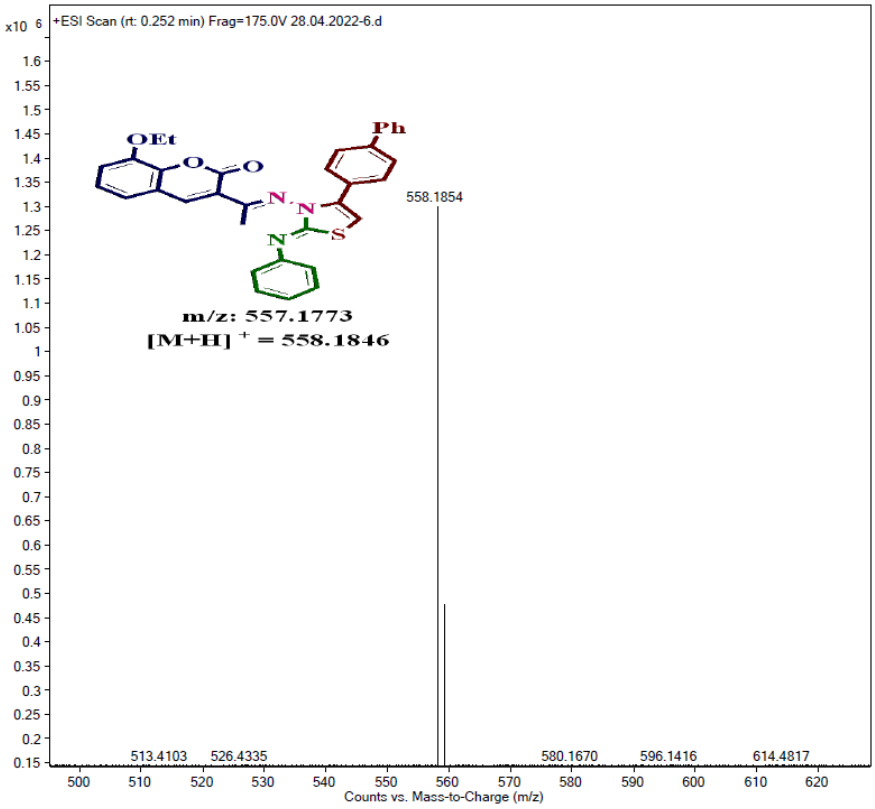

4C.10. References

1. Nazari, Z. E.; Iranshahi, M. *Phyther. Res.* **2010**, n/a-n/a.
2. Rosselli, S.; Maggio, A. M.; Faraone, N.; Spadaro, V.; Morris-Natschke, S. L.; Bastow, K. F.; Lee, K.-H.; Bruno, H. *Nat. Prod. Commun.* **2009**, *4*, 1934578X0900401.
3. Vogel, A. *Ann. der Phys. und der Phys. Chemie* **1820**, *64*, 161–166.
4. Von Pechmann, H.; Duisberg, C. *Berichte der Dtsch. Chem. Gesellschaft* **1883**, *16*, 2119–2128.
5. Fall, Y.; Terán, C.; Teijeira, M.; Santana, L.; Uriarte, E. *Synthesis (Stuttg).* **2000**, *2000*, 643–645.
6. Reformatsky, S. *Berichte der Dtsch. Chem. Gesellschaft* **1887**, *20*, 1210–1211.
7. Knoevenagel, E. *Berichte der Dtsch. Chem. Gesellschaft* **1898**, *31*, 730–737.
8. Valizadeh, H.; Vaghefi, S. *Synth. Commun.* **2009**, *39*, 1666–1678.
9. Perkin, W. H. *J. Chem. Soc.* **1875**, *28*, 10–15.
10. Hoesch, K. *Berichte der Dtsch. Chem. Gesellschaft* **1915**, *48*, 1122–1133.
11. Claisen, L.; Claparède, A. *Berichte der Dtsch. Chem. Gesellschaft* **1881**, *14*, 2460–2468.
12. Cairns, N.; Harwood, L. M.; Astles, D. P. *J. Chem. Soc., Perkin Trans. 1* **1994**, 3101–3107.
13. Wittig, G.; Haag, W. *Chem. Ber.* **1955**, *88*, 1654–1666.
14. Goodwin, R. H.; Pollock, B. M. *Am. J. Bot.* **1954**, *41*, 516.
15. Sen, K.; Bagchi, P. *J. Org. Chem.* **1959**, *24*, 316–319.
16. Lee, K.-H.; Soine, T. O. *J. Pharm. Sci.* **1969**, *58*, 681–683.
17. Dharmatti, Y. P. V. S. S.; Govil,G.; Kanekar, C. R.; Khetrapal, C. L. *Proc. Indian Acad. Sci.* **1962**, 71–85.
18. Barnes, C.; Occolowitz, J. *Aust. J. Chem.* **1964**, *17*, 975.
19. Vaarla, K.; Vishwapathi, K.V.; Vermeire, K.; Vedula, R. R. *J. Mol. Struct.* **2022**, 1249, 131662.
20. Hassan, M. Z.; Osman, H.; Ali, M. A.; Ahsan, M. J. *Eur. J. Med. Chem.* **2016**, *123*, 236–255.
21. Sujatha, K.; Ommi, N. B.; Mudiraj, A.; Babu, P. P.; Vedula, R. R. *Arch. Pharm. (Weinheim).* **2019**, *352*, 1900079.

22. Mamidala, S.; Peddi, S. R.; Aravilli, R. K.; Jilloju, P. C.; Manga, V.; Vedula. R. R. *J. Mol. Struct.* **2021**, 1225, 129114.
23. Kumar, S.; Mukesh, K.; Harjai, K.; Singh, V. *Tetrahedron Lett.* **2019**, *60*, 8–12.
24. Vaarla, K.; Karnewar, S.; Panuganti, D.; Peddi, S. R.; Vedula, R. R.; Manga, V.; Kotamraju, S. *Chemistry Select* **2019**, *4*, 4324 –4330.
25. Kamath, P. R.; Sunil, D.; Ajees, A. A.; Pai, K. S. R.; Biswas, S. *Eur. J. Med. Chem.* **2016**, *120*, 134–147.
26. Luo, G.; Muyaba, M.; Lyu, W.; Tang, Z.; Zhao, R.; Xu, Q.; You, Q.; Xiang, H. *Bioorg. Med. Chem. Lett.* **2017**, *27*, 867–874.
27. [Gali, R.; Banoth, J.; Gondru, R.; Banvantula, R.; Velivela, Y.; Crooks, P. A. *Bioorg. Med. Chem. Lett.* 25, 2015, 106-112.
28. Gondru, R.; Banothu, J.; Thatipamula, R. K.; Althaf Hussain, SK.; Bavantula, R. *RSC Adv*., **2015**, 5, 33562.
29. Abdelrehamann, M. A.; Ibrahim, H. S.; Nocentini, A.; Eldehna,W. M.; Bonardi, A.; Abdel-Aziz, H. A.; Gratteri, P.; Abou-seri, S. M.; Supuran, C. T. *Eur. J. Med. Chem*. **2021**, 209, 112897.
30. Salar, U.; Taha, M.; Khan, K. M.; Ismail, N. H.; Imran, S.; Perveen, S.; Gul, S.; Wadood, A. *Eur. J. Med. Chem.* **2016**, *122*, 196–204.
31. Wang, G.; He, D.; Li, X.; Li, J.; Peng, Z. *Bioorg. Chem.* **2016**, *65*, 167–174.
32. Yao, D.; Wang, J.; Wang, G.; Jiang, Y.; Shang, L.; Zhao,Y.; Huang, J.; Yang, S.; Wang, J.; Yu, Y. *Bioorg. Chem.* **2016**, *68*, 112–123.
33. Zaheer, Z.; Khan, F. A. K; Sangshetti, J. N.; Patil, R. H. *Chinese Chem. Lett.* **2016**, *27*, 287–294.
34. Gupta, J. K.; Sharma, P. K.; Dudhe, R.; Chaudhary, A.; Singh, A.; Verma, P. K.; Mondal, S. C.; Yadav, R. K.; Kashyap, S. *Med. Chem. Res.* **2012**, *21*, 1625–1632.
35. Salem, M.; Marzouk, M.; El-Kazak, A. *Molecules* **2016**, *21*, 249.
36. Li, W.-B.; Qiao, X-P.; Wang, Z-X.; Wang, S.; Chen,S-W. *Bio.org. Chem.* **2020**, 105, 104427.
37. Aggarwal, R.; Kumar, S.; Kaushik, P.; Kaushik, D.; Gupta, G. K. *Eur. J. Med. Chem.* **2013**, *62*, 508–514.
38. Arshad, A.; Osman, H.; Bagley, M. C.; Lam, C. K.; Mohamad, S.; Zahariluddin, A. S. M. *Eur. J. Med. Chem.* **2011**, *46*, 3788–3794.
39. Mosmann, T. *J. Immunol. Methods.* **1983,** *65*, 55–63.

CHAPTER-V

Synthesis and antibacterial activity of novel benzimidazole based isoindoline-1,3-diones and benzo[4,5]imidazol[2,1-*b*]thiazoles

CHAPTER-V

Synthesis and antibacterial activity of novel benzimidazole based isoindoline-1,3-dione compounds and benzo[4,5]imidazol[2,1-*b*]thiazoles

Introduction 5.0

The main objective of green chemistry [1,2] is to minimize the production of toxic and hazardous substances during the synthesis and design of synthetic protocols in the path of low risk to nature. This demand the need of exploring green and novel perspectives towards the synthesis of biologically active polyheterocyclic analogues.

Hence, the development of novel heterocyclic compounds from simple and easily available starting components is of significant importance in medicinal and Pharmaceutical chemistry. Out of the heterocyclic compounds *N*-fused heterocyclic derivatives are considered an important therapeutic agent with diversified applications in agrochemical, pharmaceutical and materials. Imidazol[2,1-*b*]thiazole are pivotal aromatic bicyclic five-membered heterocyclic compound containing one sulphur and one nitrogen atom in a cyclic ring. Moreover, imidazol[2,1-*b*]thiazole rings are quotient motifs exemplifying an interest in heterocyclic compounds establishing a plethora of pharmacological activities such as anti-inflammatory [3], anti-tumour agents [4,5], anti-tubercular agents [6], CDC25 phosphatase inhibitor activity [7], calcium channel antagonistic activity [8], anti-diabetic agents [9,10], anti-cardiovascular agents [11], anti-neurodegenerative [12] and mGluRs antagonist activity [13], anti-microbial [14] and so on [15]. Some of the pharmaceutically active compounds containing fused thiazole core units were depicted in **Figure 5.1.**

On the other hand, the amide bond (-NH-(CO)-R peptide linkage) communicates the backbone of proteins, which is not only responsible for the evaluation of the mysterious process of life on the earth but also encountered in the number of pharmaceutical active drugs, dyes, polymers, and agrochemicals [16-24]. Some of the pharmacologically important drugs consisting of amide moiety are depicted in **Figure 5.1.** Given the aforementioned importance and pharmaceutical applications of fused thiazole and indoline 1,3-dione derivatives, we have made an unswerving interest to synthesize the fused thiazolyl derivatives, hoping these may exhibit and enhance pivotal biological activity.

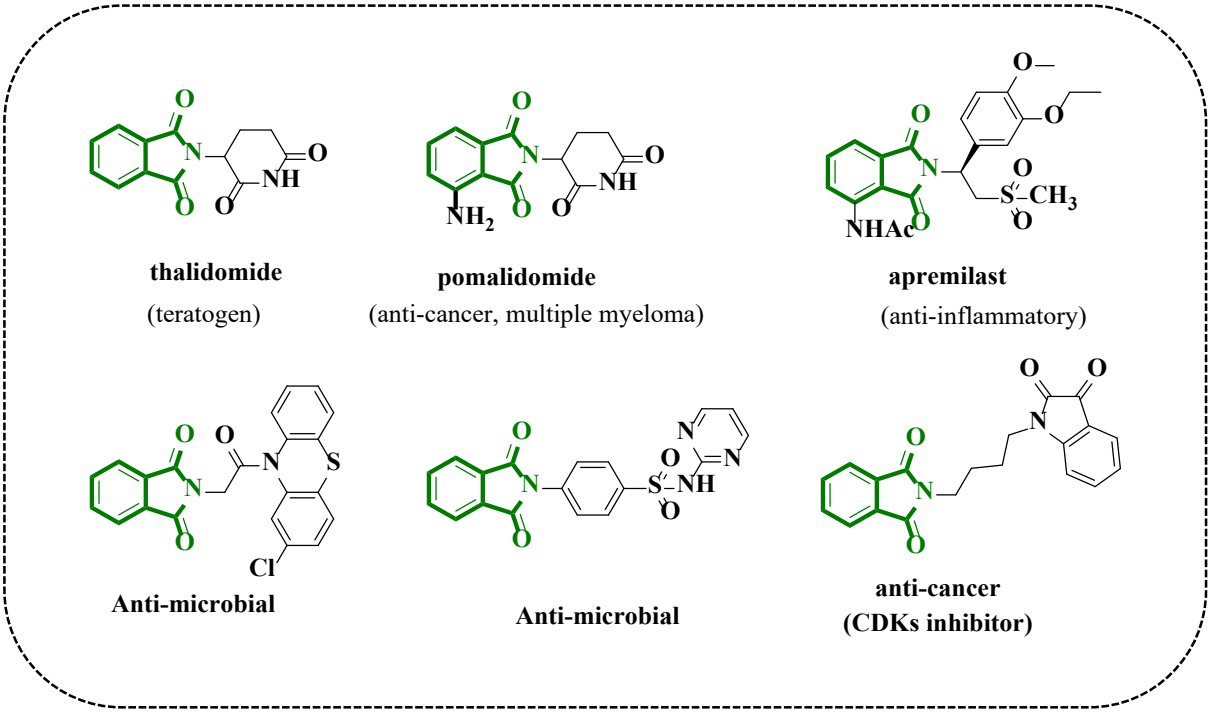

Figure 5.1. Biologically active compounds

The following is a brief literature review on the synthesis of isoindoline1,3-diones and benzimidazolyl thiazoles.

Wang [25] ***et al.*** have reported a one-pot novel synthetic strategy for the cuprous oxide catalysed oxidative C-C bond cleavage of ketones for the cyclic imides. For this reaction, various substituted 1-indanone and substituted primary amines like aniline, benzylamine, aliphatic and heteroaromatic amines provide good to excellent yields in presence of DMSO.

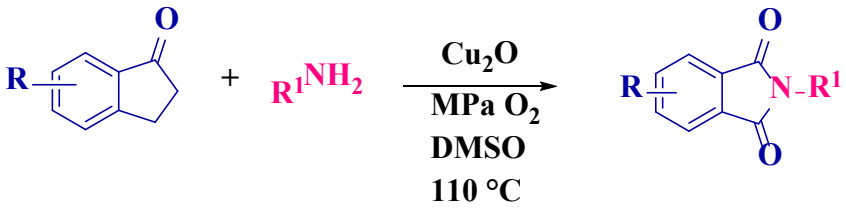

Scheme 5.1. One-pot synthesis of cyclic imide

Jayaprakash [26] ***et al.*** have developed a series of 4-(1,3-dioxo-2,3-dihydro-1*H*-isoindol-2-yl)benzene-1-sulphonamide scaffolds. For this reaction, a mixture of aniline and phthalic anhydride in presence of glacial acetic acid gave good to excellent yields. This intermediate further reacts with chlorosulphonic acid and phosphorous pentachloride in presence of DCM to give sulphonyl chloride isoindoline compound, again this isolated compound reacts with

various amines/anilines in presence of pyridine base and di-chloromethane solvent providing titled compounds in good to excellent yields. Furthermore, these compounds were evaluated for their in-vitro anti-viral activity against DENV2 NS2B-NS3 protease inhibitory activity.

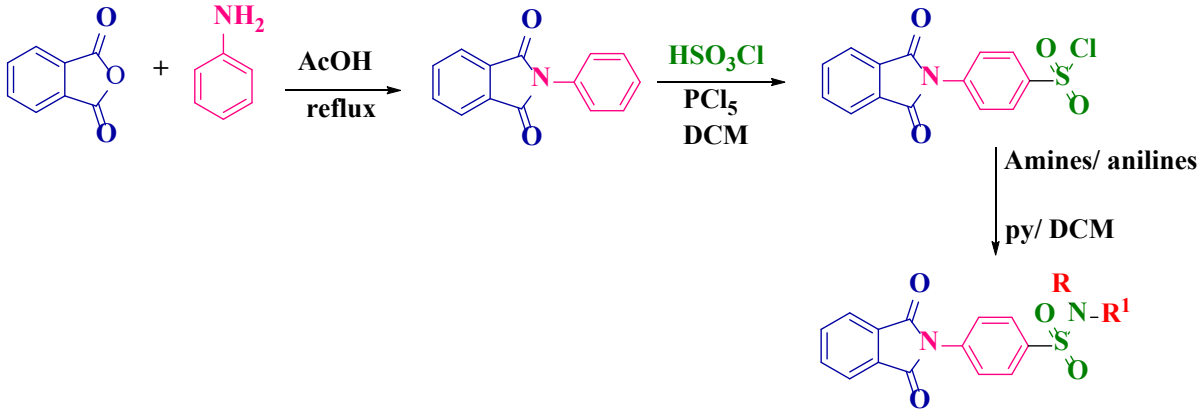

Scheme 5.2. Synthesis of isoindoline-based sulphonamide derivatives

Patil [27] ***et al.*** have reported, an efficient, one-pot, eco-friendly, inexpensive graphene oxide (GO) promoted cyclic amides from transamidation reaction. For this reaction, carboxamides/ phthalimide/ urea/ thioamide/ substituted urea with aliphatic/aromatic amine in presence of 20 wt.% of graphene oxide provides good to excellent yields.

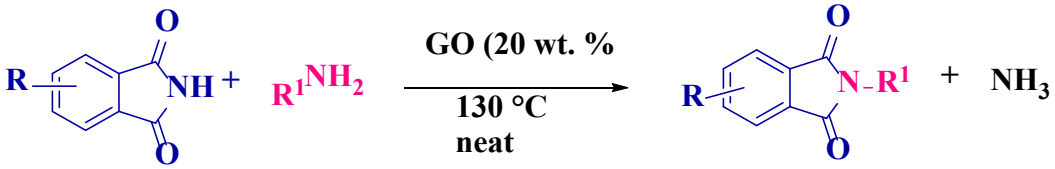

Scheme 5.3. One-pot synthesis of cyclic imides *via* transamidation

Chen[28] ***et al.*** have reported an efficient, one-pot, green reaction method for the synthesis of N-arylphthalimide in presence of an easily accessible and inexpensive ionic liquid. For this reaction, a mixture of phthalic anhydride and various aromatic amines in [Bmim][BF_4] was used and yields are good to excellent.

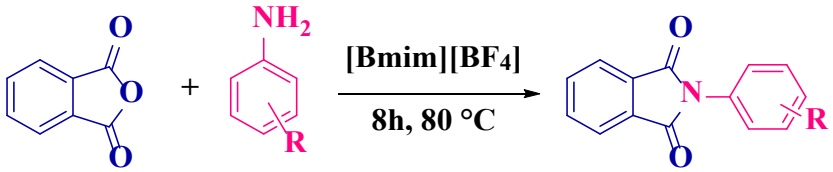

Scheme 5.4. Ionic liquid catalysed one-pot synthesis of isoindoline scaffolds

Dos Santos [29] ***et al.*** have developed a series of novel phthalimide derivatives which contain furoxanyl nitric oxide as a subunit donor molecule. In this reaction, a mixture of phthalic anhydride reacts with 4-(2-aminoethoxy)-3- (phenylsulfonyl)-1,2,5-oxadiazole 2-oxide in presence of glacial acetic acid gave titled compounds in good to excellent yields. Further, these derivatives were evaluated for their *in vitro* and in vivo activity against Sickle cell disease symptoms. Among the tested, compound **3b** showed promising activity.

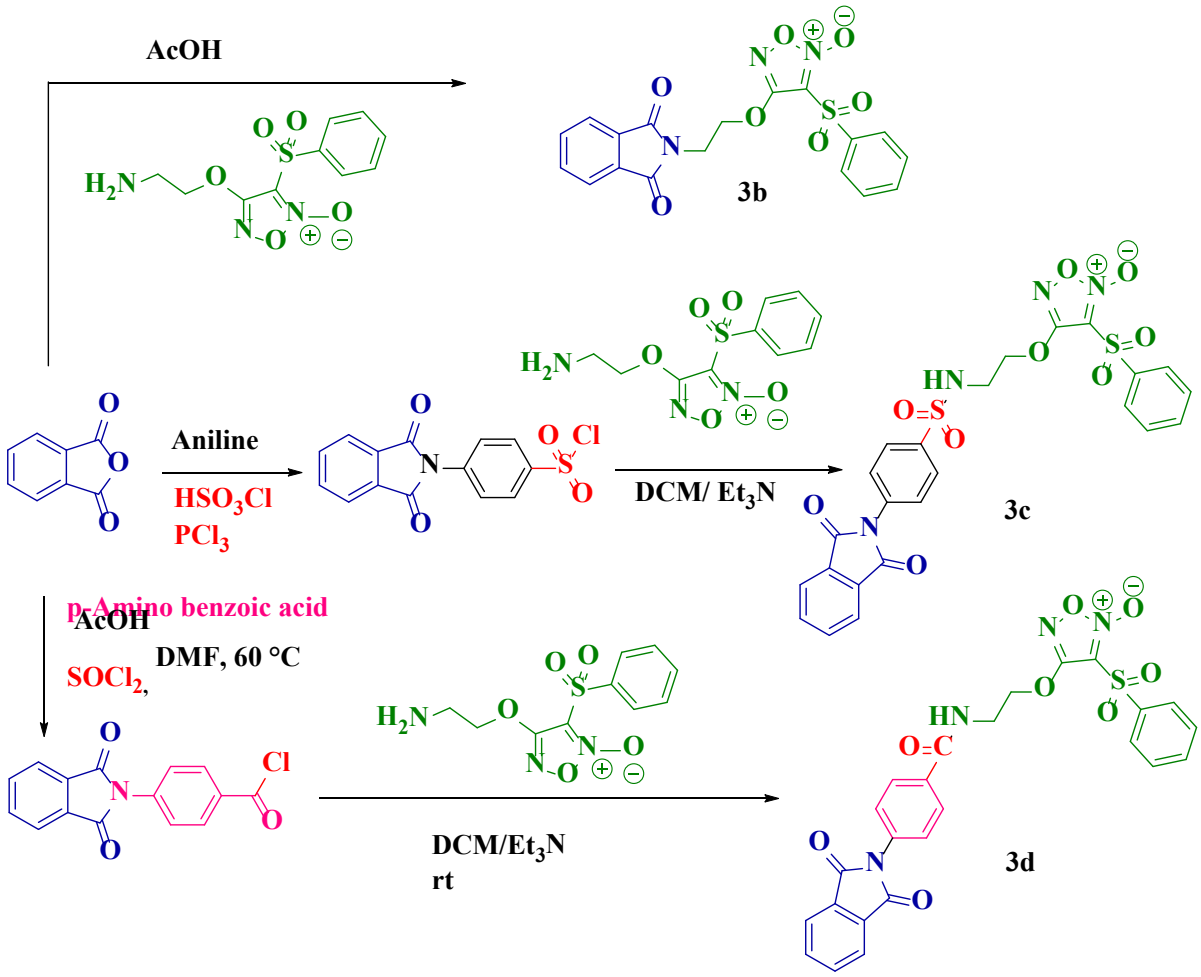

Scheme 5.5. Synthesis of phthalimide derivatives containing furoxanyl nitric oxide as donor

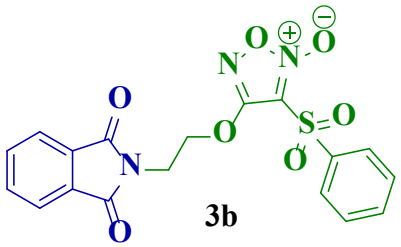

Figure 5.2. Biologically potent molecule

Le [30] ***et al.*** have developed an efficient, eco-friendly, one-pot synthesis for N-alky and N-aryl phthalimide derivatives in presence of ionic liquid. For this reaction, a mixture of phthalic

anhydride and various substituted aromatic primary amines in [Bmim][PF_6] was used as a solvent and the yields are good to excellent.

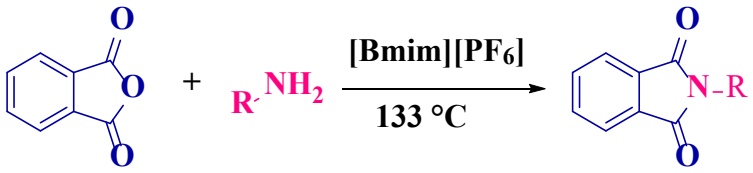

Scheme 5.6. Synthesis of N-alkyl and N-aryl phthalimide derivatives

Kuribara [31] ***et al.*** have reported a visible light-mediated, one-pot, metal-free and photo-catalyst-free synthesis of N-aryl phthalimide derivatives *via* intramolecular C-H bond imidation. For this reaction, a mixture of various substituted arenes and phthalimide with di-acetoxy iodo benzene and molecular iodine provides good to excellent yields at ambient reaction conditions.

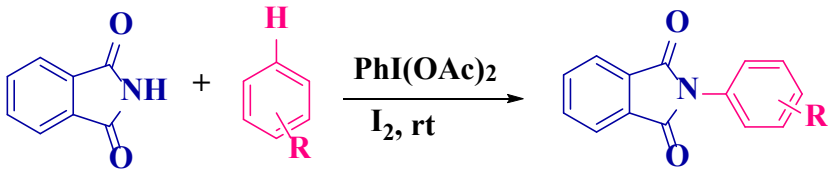

Scheme 5.7. One-pot, visible light-mediated synthesis of phthalimide derivatives

Bhatt [32] ***et al.*** have developed a series of novel azo-linked hybrids of 1,3,4-thia-/ oxadiazolo cyclic imides. The title compounds were synthesized by using phthalic anhydride / maleic anhydride with various aromatic amines in presence of glacial acetic acid gave *N*-substituted cyclic imides. Further, these N-substituted cyclic imides coupling with diazonium salt of 1,3,4-thia-/ oxadiazolo compound gave titled compounds with good to excellent yields. Further, these compounds were screened for their *in-vitro* anticancer activity against MCF-7 and HT-29 cell lines. Among the tested compounds, compound **C14** showed promising activity against two cell lines with IC_{50} values of 0.09 ± 0.02 µM and 0.11 ± 0.03 µM respectively.

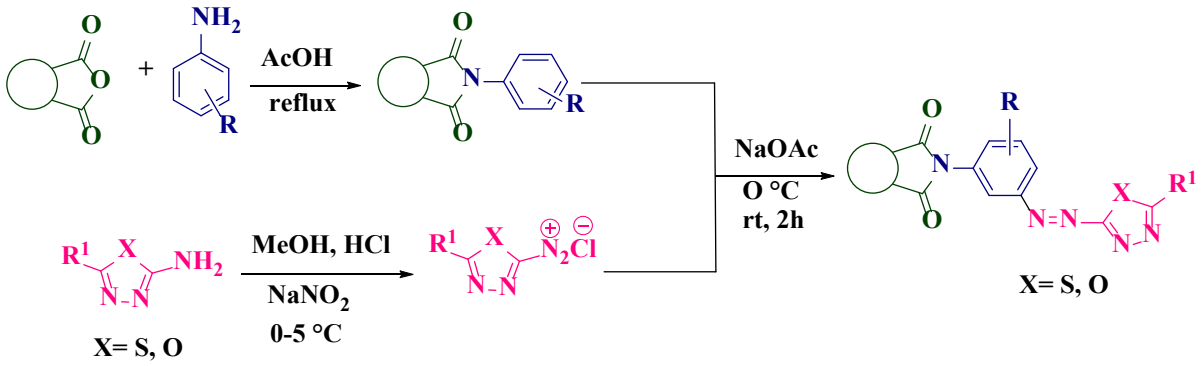

Scheme 5.8. Azo-linked 1,3,4-thia/oxadiazolo-cyclic imide scaffolds

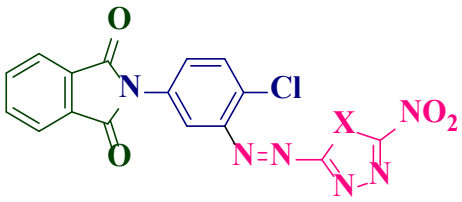

compound-14

Figure 5.3 Biologically active compound

Bhange [33] ***et al.*** have reported synthetically an efficient, solvent-free, one-pot, facile synthesis of N-aryl phthalimide derivatives *via* metal oxide (MnO_2) catalysed amine formylation and transamidation of primary and secondary amides by amines under reflux condition gave good to excellent yields.

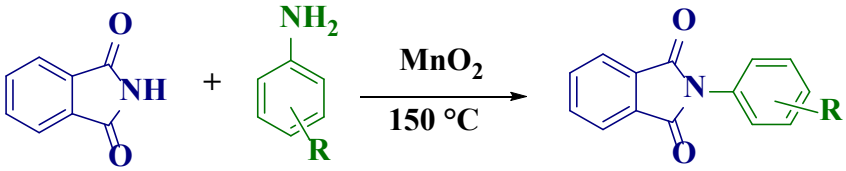

Scheme 5.9. Metal oxide catalysed N-substituted phthalimide derivatives

Liang [34] ***et al.*** have reported an efficient, one-pot, synthesis of N-alkyl and N-arylphthalimide derivatives in presence of an eco-friendly and nontoxic solvent medium. For the synthesis of title compounds, a mixture of various primary amines and different substituted cyclic anhydrides in presence of PEG-400 gave good to excellent yields.

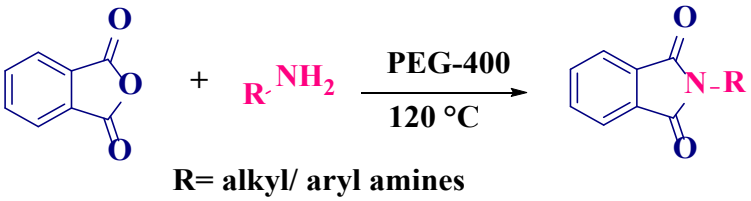

R= alkyl/ aryl amines

Scheme 5.10. PEG-400 catalysed N-substituted phthalimide scaffolds

Srinivas [35] **et al.** established a one-pot, efficient, and eco-friendly protocol for the synthesis of *N*-substituted phthalimide derivatives *via* microwave irradiation method in presence of an aqueous medium. For this synthesis, various amides react with substituted amines in presence of $K_2S_2O_8$ under transamidation of microwave irradiation conditions giving good yields.

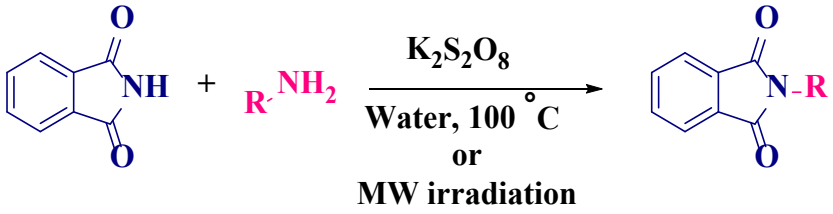

Scheme 5.11. One-pot synthesis of N-substituted phthalimide derivatives

Upadhyay [36] ***et al.*** explored an efficient, one-pot, and microwave-irradiated synthesis of cyclic imide derivatives. In this reaction, different substituted cyclic anhydrides and amines react in presence of DMF under reflux conditions giving good to excellent yields.

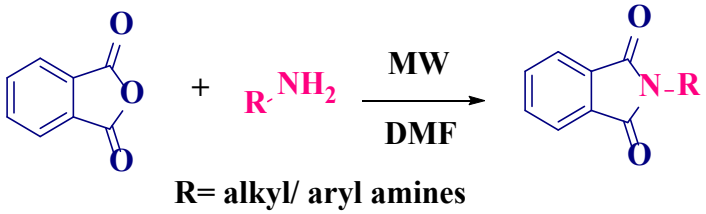

Scheme 5.12. One-pot synthesis of cyclic imides

Nocentini [37] ***et al.*** developed a novel, one-pot synthesis of isoindoline-1,3-dione-based oximes and benzenesulfonamide hydrazone derivatives. For this reaction, various cyclic anhydrides, hydroxyl amines and 4(hydrazine carbonyl) benzene sulphonamides gave title compounds with good to excellent yields in presence of methanol and a catalytic amount of glacial acetic acid. Further, the titled compounds were evaluated for their carbonic anhydrase inhibition and all the compounds were shown remarkable activity against hCA-IX, hCA -I, hCA -II, and hCA -IV.

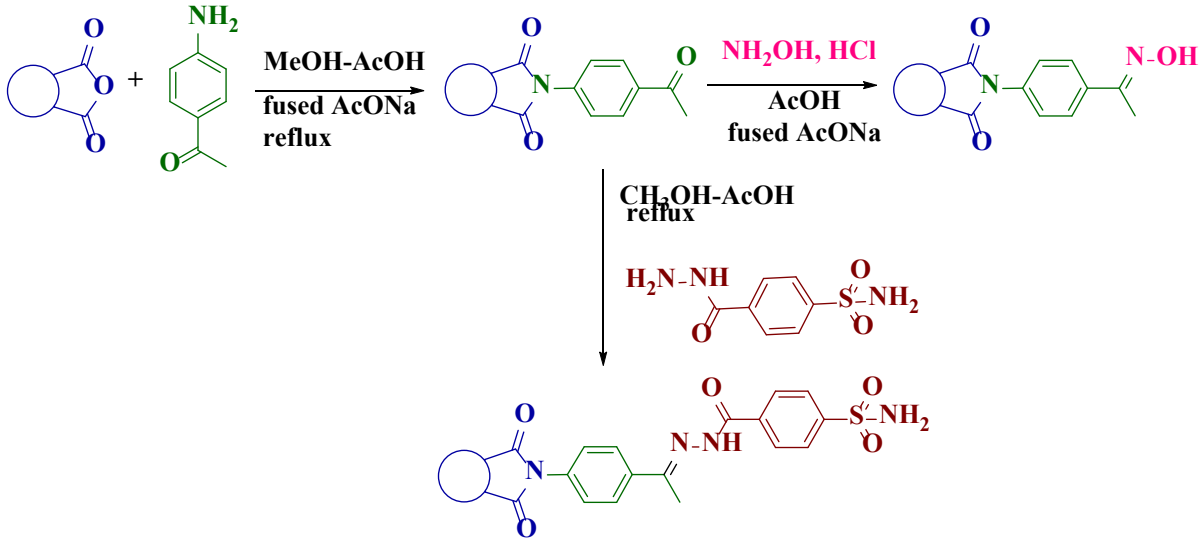

Scheme 5.13. One-pot synthesis of isoindoline-1,3-dione-based oximes and benzenesulfonamide scaffolds

Wu [38] ***et al.*** reported a novel series of isoindoline-1,3-dione containing 1,2,4-traizole derivatives *via* a one-pot reaction. For this conversion, 4-amino-5-substituted-4*H*-1,2,4 traizole-3-thiol, various cyclic anhydrides, Zinc bromide and tri-ethyl amine in presence of dry toluene at room temperature gave good to excellent yields. Further, these compounds were screened for their *in-vitro* anti-fungal and anti-cancer activity against *C. musae, F. oxysporum* f. sp. *Niveum, C. gloeosporioides penz, B. theobromae, F. Oxysporum,* f. sp. cubense and *P. Oryzae Cav.* and anti-cancer activity against HepG2, A549, PC-3M, and MKN45 cell lines. Among the tested compounds, compound **37** showed promising activity.

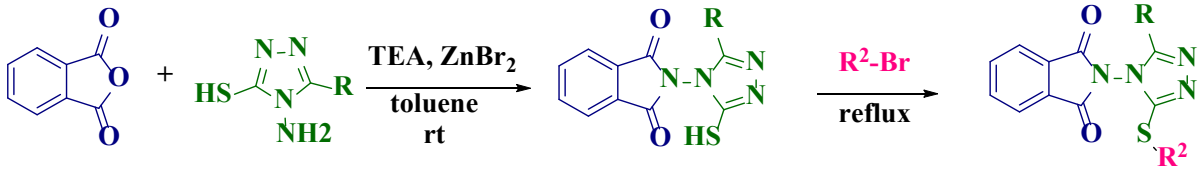

Scheme 5.14. One-pot synthesis of 1,2,4-triazolo-isoindoline-1,3-dione derivatives

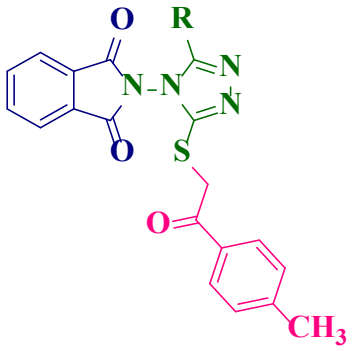

Figure 5.4. Biologically potent molecule

Kok [39] ***et al.*** have reported an efficient, novel, one-pot synthesis of benzothiazole-containing phthalimide derivatives. For this conversion, a mixture of phthalic anhydrides reacts with different substituted benzothiazoles in presence of toluene and triethyl amine giving good to excellent yields. Further, these compounds were screened for their anti-cancer activity against CA46, K562, and SKHeP1 cell lines. All the synthesized compounds were shown remarkable activity.

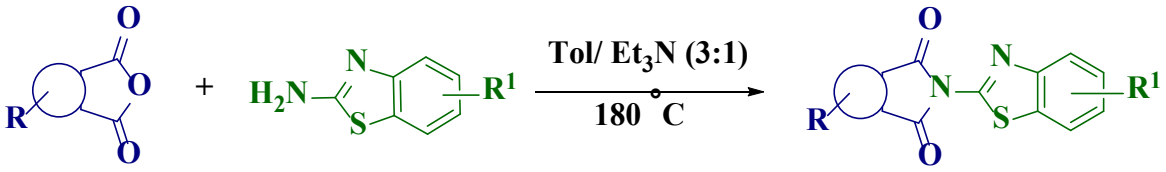

Scheme 5.15. Condensation of phthalic anhydride with benzothiazoles

Mei [40] ***et al.*** have reported an efficient, Brønsted acid catalysed, one-pot, three-component synthesis of imidazole [2,1-*b*] thiazole derivatives. For this synthesis, various benzimidazole, aryl nitro alkenes and elemental sulphur in presence of DMSO and salicylic acid gave titled compounds in good to excellent yields. This reaction follows aza-Michael addition followed by nucleophilic sulfuration with deamination aromatization.

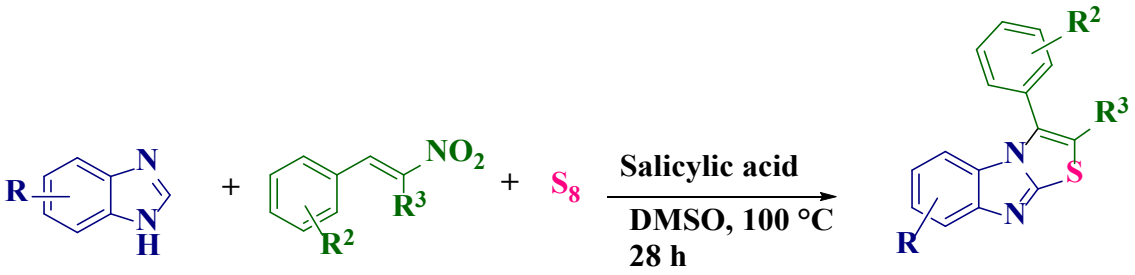

Scheme 5.16. One-thee component synthesis of N-fused thiazoles

Jana [41] ***et al.*** synthesized copper and catalysed an efficient, one-pot synthesis of benzo[4,5]imidazo[2,1-*b*]thiazole derivatives by using a catalytic amount of $Cu(OAc)_2$. For this synthesis *β*-nitro alkenes, and 2-mercaptobenzimidazole in presence of DMF gave good to excellent yields.

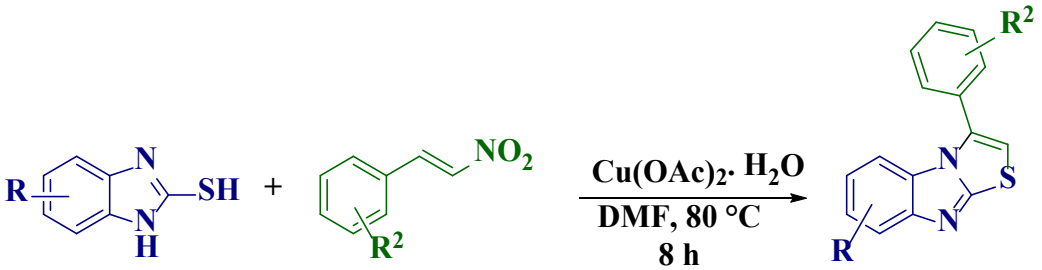

Scheme 5.17. Copper catalysed synthesis of benzo[4,5]imidazo[2,1-*b*]thiazole derivatives

Zhao [42] ***et al.*** reported a facile one-pot metal-free oxidative cyclization reaction for the synthesis of imidazole[2,1-*b*]thiazoles. For this reaction, 2-mercaptobenzimidazoles, and ketones undergo oxidative cyclization in presence of methane sulfonic acid combined with acetic anhydride, selectfluor as reaction mediator in sulfolane solvent giving good to excellent

yields.

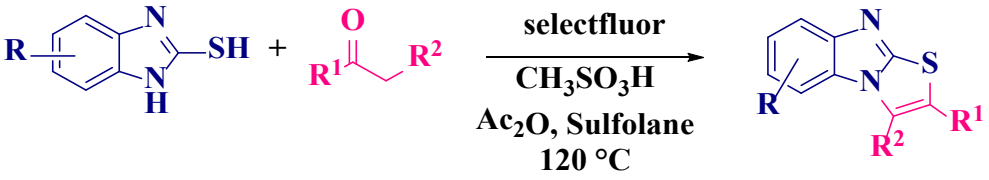

Scheme 5.18. One-pot oxidative synthesis of imidazole[2,1-*b*]thiazoles

Shen [43] ***et al.*** have explored an efficient, one-pot cross-coupling reaction for the synthesis of 3-substituted and 2,3-disubstituted benzo[4,5]imidazo[2,1-*b*]thiazole derivatives. For this synthesis, trans-1,2-diiodoalkenes, 2-mercaptobenzimidazole and various haloarenes in presence of the catalytic amount of copper catalyst combines with K_2CO_3 in presence of DMF solvent gave benzo[4,5]imidazo[2,1-*b*] thiazoles. Further, these compounds undergo cross-coupling reaction using a catalytic amount of palladium catalyst in presence of p-xylene solvent combined with Cs_2CO_3 gave 2,3-disubstituted benzo[4,5]imidazo[2,1-*b*]thiazole compounds in good to excellent yields.

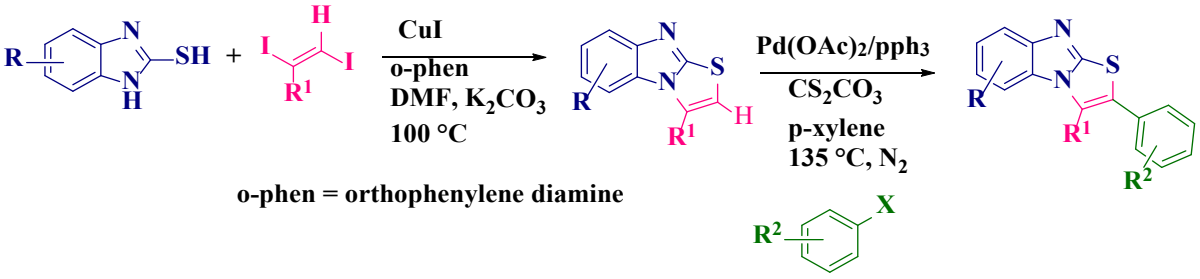

Scheme 5.19. Cross-coupling synthesis of 2,3-disubstituted benzo[4,5]imidazo[2,1-*b*]thiazole

Chen [44] ***et al.*** developed a series of copper-catalysed synthesis of *N*-fused benzo[4,5]imidazo[2,1-*b*]thiazole derivatives using 2-mercaptobenzimidazole, 1,1-dibromoalkenes in presence of a catalytic amount of CuI in presence of DMF gave good to excellent yields.

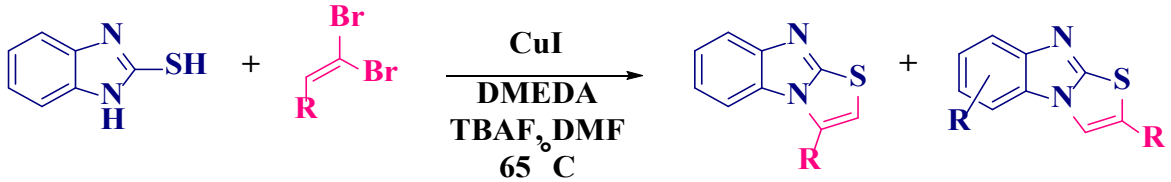

Scheme 5.20. One-pot copper catalysed synthesis benzo[4,5]imidazo[2,1-*b*]thiazoles

Li [45] ***et al.*** synthesized an efficient, one-pot copper-mediated synthesis of N-fused benzo[2,3]imidazo[2,1-*b*]thiazoles by using 2-mercaptobenzimidazole and various substituted terminal alkynes in presence of toluene and a catalytic amount of CuCl and ICy.HCl.

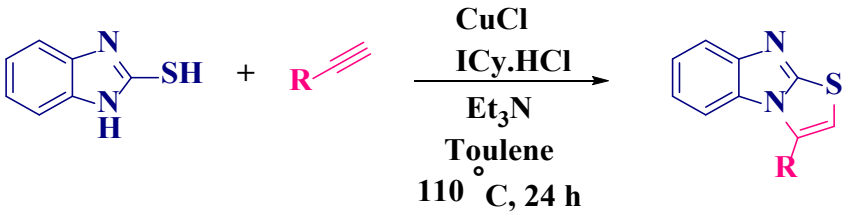

Scheme 5.21. One-pot synthesis of *N*-fused Benzo[2,3]imidazo[2,1-*b*]thiazole scaffolds

5.1. Present work

5.1.1. Starting Materials

In this chapter, we describe the synthesis, antibacterial activity and molecular docking studies of benzimidazole-based isoindoline-1,3-dione compounds and benzo[4,5]imidazol[2,1-*b*]thiazoles (4a-w) and (5a-h) compounds as outlined in **Scheme 5.1.** The title compounds were synthesized by using 5-amino-2-mercaptobenzimidazole **1**, various cyclic anhydrides **2**, and different alkyl/ aralkyl halides **3**. All the starting materials were procured from commercial sources.

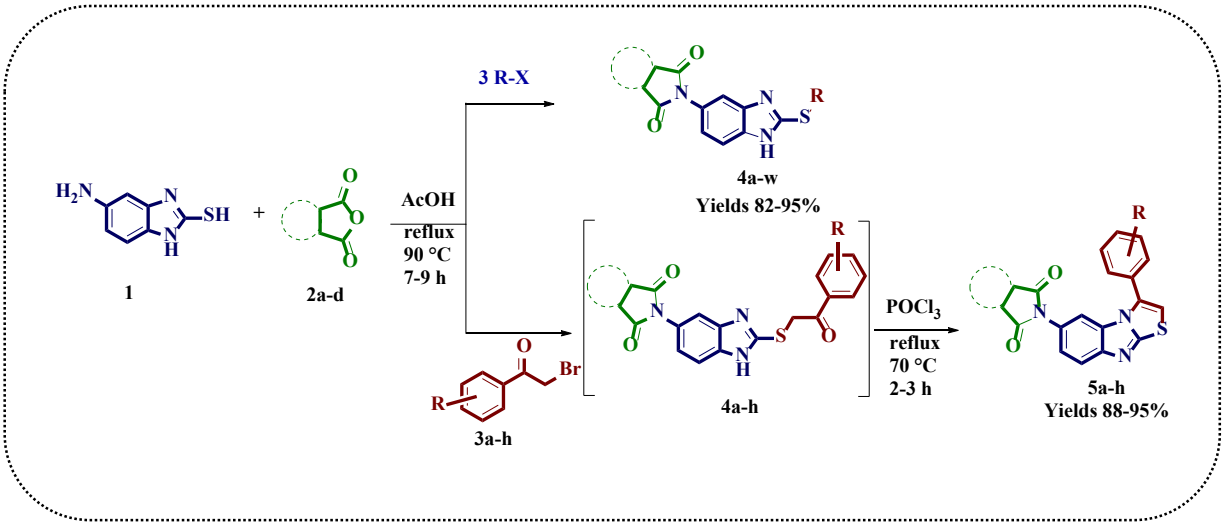

Scheme 5.1 Benzimidazole based isoindoline-1,3-dione and benzo[4,5]imidazo[2,1-*b*]thiazol derivatives.

5.1.2. Synthesis of title compounds

The synthesis of target compounds was carried out as outlined in **Scheme 5.1**. The title compounds were synthesized by using 5-amino-2-mercaptobenzimidazole **1**, various cyclic anhydrides **2,** alkyl or substituted aralkyl halides **3** or **(1:1:1)** in glacial acetic acid using fused sodium acetate at 70 ºC to give final compounds (**4a-w**) with good to excellent yields in a shorter reaction time.

5.3. Results and discussion

Given the aforementioned importance and pharmaceutical applications of fused thiazole and indoline 1,3-dione derivatives, we have made an unswerving interest to synthesize the fused thiazolyl derivatives, hoping that these compounds may exhibit and enhance pivotal biological activity.

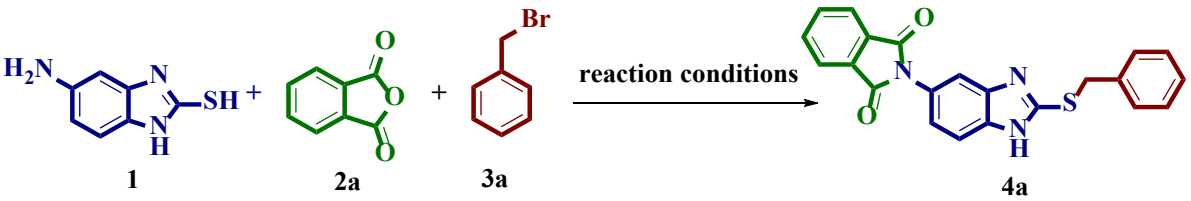

Scheme 5.1: **Synthesis of 2-(2-(benzylthio)-1*H*-benzo[*d*]imidazol-5-yl)isoindoline-1,3-dione**

Table 5.1. Optimization of reaction conditions 4a.

S.NO	Solvent	Base	Temp(°C)	Time (h)	Yields[b] (%)
1	DMF	-	RT	24	Trace
2	DMF	-	60	18	17
3	Methanol	-	60	18	19
4	Ethanol	-	60	18	22
5	**AcOH**	**-**	**60**	**15**	**60**
6	AcOH	NaOH (1.0 mmol)	60	12	43
7	AcOH	Na_2CO_3(1.0 mmol)	60	12	40
8	AcOH	K_2CO_3 (1.0 mmol)	60	15	35
9	ACOH	Piperidine (5 mol%)	60	12	55

10	AcOH	Pyridine (5 mol%)	60	12	50
11	**AcOH**	**AcONa (1.0 mmol)**	**60**	**10**	**70**
12	AcOH	AcONa (1.0 mmol)	70	10	84
13	AcOH	AcONa (1.0 mmol)	80	10	90
14	**AcOH**	**AcONa (1.0 mmol)**	**90**	**9**	**95**
15	AcOH	AcONa (2.0 mmol)	90	8	87
16	AcOH	-	90	12	85
17	AcOH	-	100	10	80
18	AcOH	AcONa (1.0 mmol)	reflux	8	80

Reaction conditions: 5-amino-2-mercaptobenzimidazole (1.0 mmol), phthalic anhydride (1.0 mmol), benzyl bromide (1.2 mmol), fused sodium acetate (1.0 mmol), Acetic acid (2.0 mL) 90 ºC. [b]Isolated yields.

The initial experiment was focused on identifying the suitable reaction parameters (solvent, base, temperature) to obtain the **4a** (**Table 5.1**) using the readily available 5-amino-2-mercaptobenzimidazole **1**, phthalic anhydride **2a**, and benzyl bromide **3a** in DMF solvent, we found that the reaction takes longer time and provides lower the reaction yield (**Table 5.1, entry-1**). Then the same reaction mixture was attempted under the thermal condition at 60 ºC, the reaction yielded little improved product with 17% (**Table 5.1, entry-2**).

Further, we demonstrated the same reaction in various polar solvents such as methanol, ethanol and glacial acetic acid to find the effect of solvent on reaction yield timings as shown in **Table 5.1**. These findings suggest that the reaction proceeds much better in glacial acetic acid (**Table 5.1, entry-5**). Further, we examine the amount of base to improve the reaction yield. Therefore, we demonstrated various organic and inorganic bases such as NaOH, Na_2CO_3, K_2CO_3, Piperidine, pyridine, and fused sodium acetate (**Table 5.1, entries 6-11**). Among the tested, sodium acetate was found to be a better base to improve the reaction yields and reduce the reaction timings (**Table 5.1, entry-14**). Next, we examine the temperature study demonstrated that the reaction requires a high temperature (90 ºC) for the formation of **4a** in good yields as shown in **Table 5.1, Entry-14 Vs 1-13**. In addition, we have also carried out the reaction at more than 90 ºC and lesser than 90 ºC without base and we found lower yields (**Table 5.1, entries-16,17**). **Table 5.1** indicates the best results were obtained when the reaction was

performed using 1.0 mmol of fused sodium acetate as a base at 90 °C in acetic acid (**Table 5.1, entry 14**).

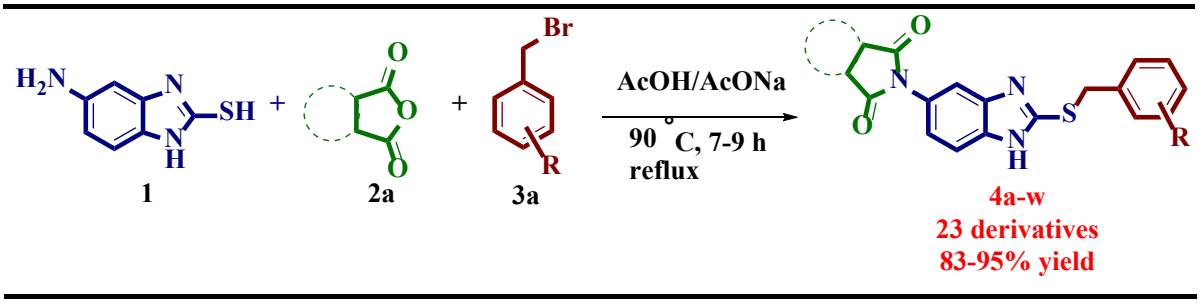

In order, to explore the scope of this new three-component reaction, we examined the effectiveness and tolerance of the product yields when both benzyl and phenacyl bromides contain various functional groups on the phenyl ring. The developed optimized conditions were

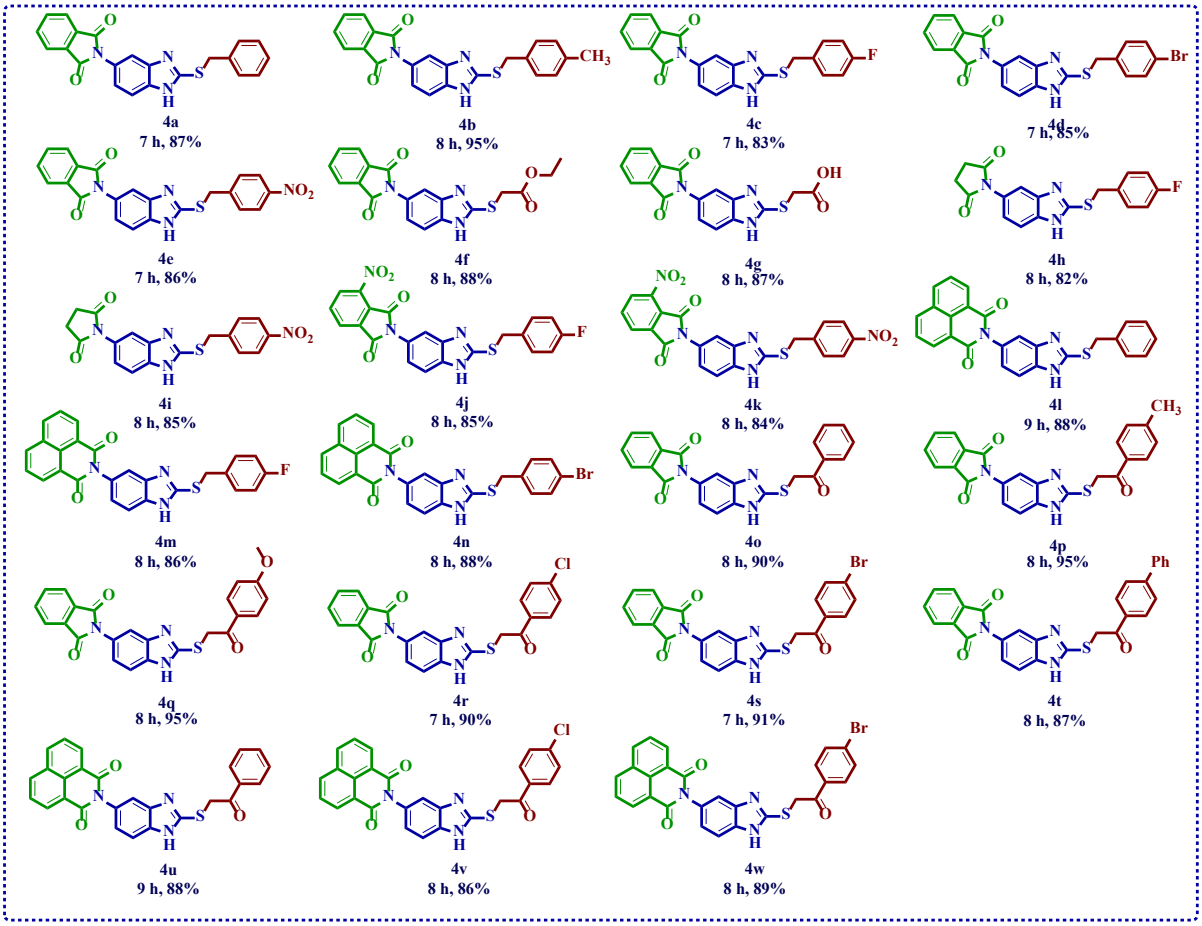

Figure 5.2. The scope of substrates.

applied for both diversely substituted benzyl bromide and phenacyl bromide compounds, and we observed that the benzyl and phenacyl bromides with electron-donating substituents (4-methyl benzyl bromide,4-methyl phenacyl bromides) gave excellent yields 95% and 93%

respectively as shown in **Figure 5.1, entries-4b, 4q and 4r**. When the same reaction conditions were performed to electron withdrawing halo, nitro-substituted benzyl bromides and phenacyl bromides will reduce the product's yields (**Figure 5.1**).

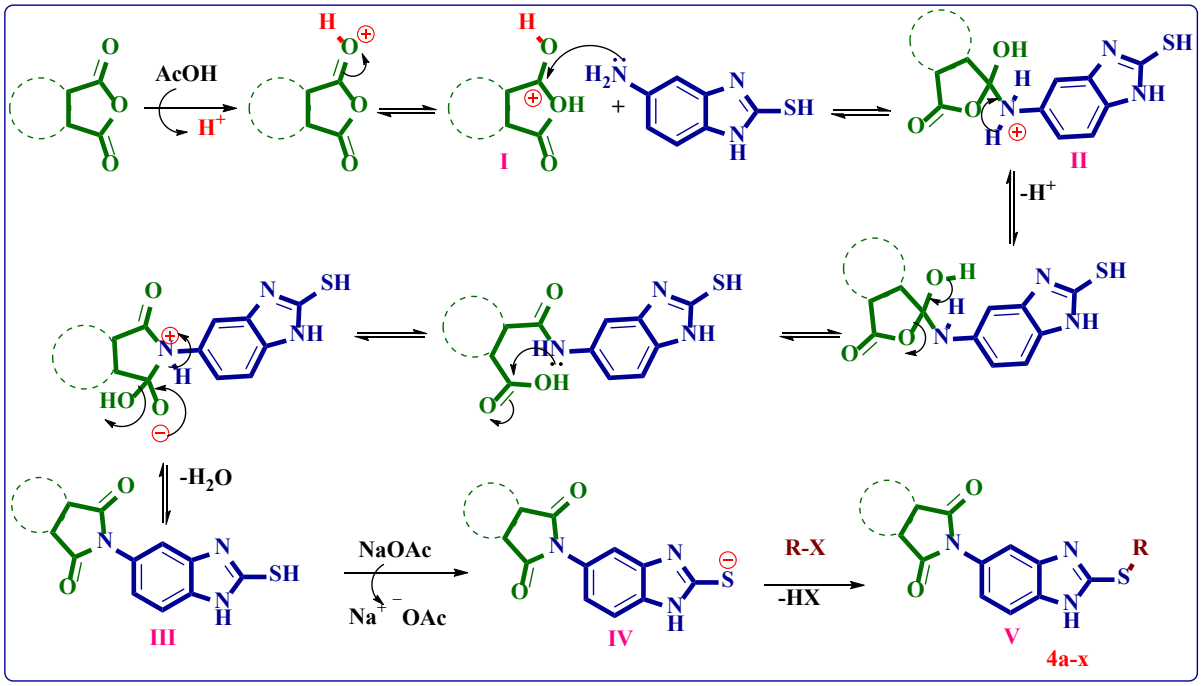

Scheme 5.2. Plausible reaction mechanism

Initially, the condensation between phthalic anhydride and 5-amino-2-mercaptobenzimidazoles takes place by an acid-catalysed reaction. At first, the ester carbonyl oxygen was pronated to give intermediate I. Further this intermediate I was attacked by the amino group of 5-amino-2- mercaptobenzimidazole to yield protonated amine intermediate II. Next, this intermediate undergoes deprotonated followed by ring opening and leads to the formation of elimination of water molecule gave 2-(2-mercapto-1*H*-benzo[*d*]imidazol-5-yl) isoindoline-1,3-dione intermediate III. Further, the thiol hydrogen of intermediate III was attacked by fused sodium acetate to give intermediate IV. Finally, the mercaptide ion displaces the bromine atom of alkyl/aralkyl/phenacyl bromide to give final compounds **4a-w**.

5.3. Anti-microbial evaluation

Assay of in vitro antibacterial activity, bacterial strains were purchased from the National Collection of industrial microorganisms, Pune, India. Antibacterial activity was tested against *E. coli, S. typhi, and S. aureus, Micrococcus luteus* by agar well diffusion method. The zone of inhibition was measured after 24hrs incubation at 37^0C. The sterilized nutrient agar medium was distributed 100 mL each in two 250 mL conical flasks and allowed to cool to room

temperature. To these media, 18-24 h grown bacterial sub-cultures were added and shaken thoroughly to ensure uniform distribution of organisms throughout the medium.

Then, the agar medium was distributed in equal portions, in sterilized Petri dishes, ensuring that each petri dish contains about 900 µg/ml of the medium. The medium was then allowed for solidification. The cups were made with the help of a sterile cork borer (6 mm diameter) punching into the set of agar media. The solutions of required concentrations (100 µg/ml) of test compounds were prepared by dissolving the compounds in DMSO and were filled into the cups with 1 mL of respective solution. Then, the Petri dishes were kept for incubation in an inverted position for 24 - 48 h at 37 °C in an incubator. When growth inhibition zones were developed surrounding each cup, their diameter in mm was measured and compared with that of the standard drugs. Each experiment was made in triplicate using DMSO as a control.

5.4.1. Results

All the newly synthesized compounds (**4a – w**) were investigated for antibacterial activity. Compounds **4a, 4g, 4j, 4q, 4s,** and **4t** showed good activity against *Gram-positive*, Gram-positive bacteria had a thick cell wall, containing a high amount of peptidoglycan and Gram-negative bacteria had two layers of cell membrane: the inner membrane contains peptidoglycan and the outer membrane contains lipopolysaccharides (**Table 5.2**).

Table 5.2. Antibacterial activity

Compounds	**Conc.**	**Minimum Inhibitory Concentration**			
	µg/ml	*Escherichia coli*	*Salmonella typhi*	*Staphylococcus aureus*	*Micrococcus luteus*
4a	900	450	200	200	150
4b	900	400	300	200	450
4c	900	400	450	600	200
4d	900	700	600	170	300
4e	900	160	260	550	500
4f	900	00	00	00	00
4g	900	510	430	260	125
4h	900	700	650	600	640
4i	900	500	420	500	550
4j	900	700	290	210	450

4k	900	00	00	560	700
4l	900	700	500	400	440
4m	900	00	00	00	500
4n	900	00	400	00	00
4o	900	00	00	700	00
4p	900	00	700	00	120
4q	900	285	220	190	180
4r	900	390	400	600	500
4s	900	400	530	300	210
4t	900	515	320	200	330
4u	900	800	750	600	480
4v	900	300	620	510	600
4w	900	600	500	600	720
Standard (streptomycin)	900	08	15	10	12

5.4. Molecular docking studies

In silico docking studies are very useful to examine and to gain a wise reflection in the way of binding interactions of each ligand molecule (**4a-z**) with receptor structure. All the synthesized structures were drawn by using Chem Draw Ultra 13.0, Molecular energy was minimized using the Energy Minimization module of Maestro Tool (Schrodinger software). The three-dimensional structure of the receptor structure was retrieved from the RCSB database (PDB ID: 1BNA). Similar synthesized chemical compounds have shown cancer-like activity in the previous literature and the active site of the structure of a B-DNA dodecamer will have a similar binding potentiality to inhibit the DNA binding event. The target receptor was prepared by removing the structural water molecule, hetero atoms and co-factors by leaving only the residues associated with the receptor structure. Further, the grid was prepared and molecular docking was performed using the Glide docking module the results obtained were scrutinized based on the highest dock score and number of H-bonds by visualizing in Pymol.

Molecular docking results were identified basis on the ideal interacted ligands were scrutinized based on the greatest ligand binding poses were identified using the low binding energy, high docking score and the number of H-bonding, hydrophobic interactions at receptor site i.e., 4s,

4j, 4a, 4q, 4t, 4g (**Figure 5.3**). **Table 5.3** represents the docking score, Hydrogen bond distance and interacting atoms. All the compounds were found to be buried.

Table 5.3. Molecular interactions with ligands against B-DNA (PDB ID: 1BNA).

Receptor	Ligands	Receptor Interaction Atoms	Ligand Atoms	Distance (A°)	Docking Affinity (kcal/mol)
1BNA	4g	NH	O	2.02	-7.26
		NH	O	2.06	
		NH	O	2.07	
	4a	NH	O	1.55	-8.90
	4j	O	NH	1.53	-8.94
	4q	O	NH	1.74	-8.60
	4q	NH	O	1.80	-9.50
	4s	O	NH	1.44	-9.94
	4t	O	NH	1.73	-8.55
		NH	O	1.80	

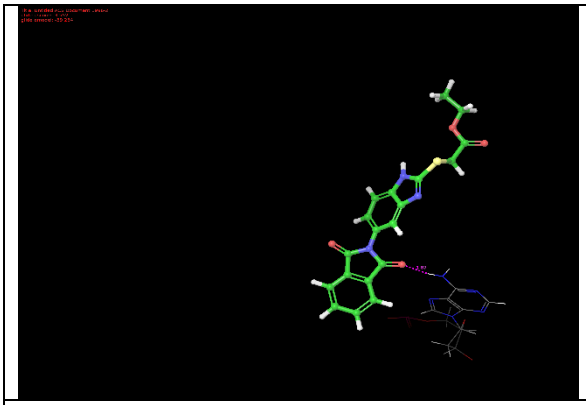

Compound 4g

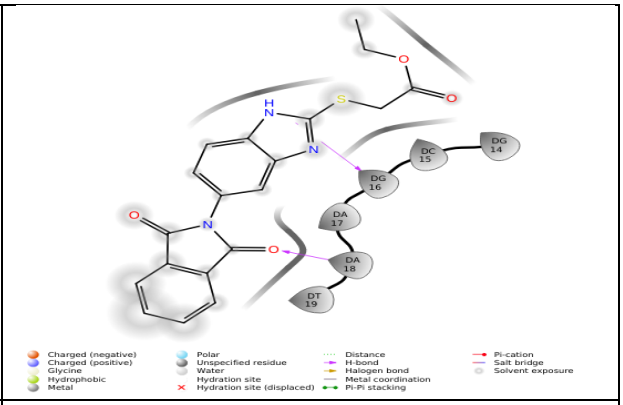

Compound 4g

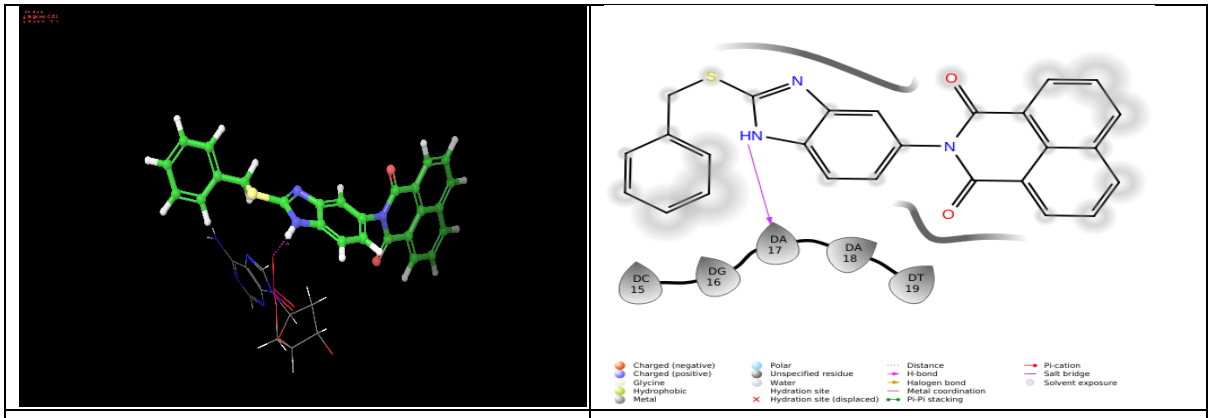

Compound 4j | Compound 4j

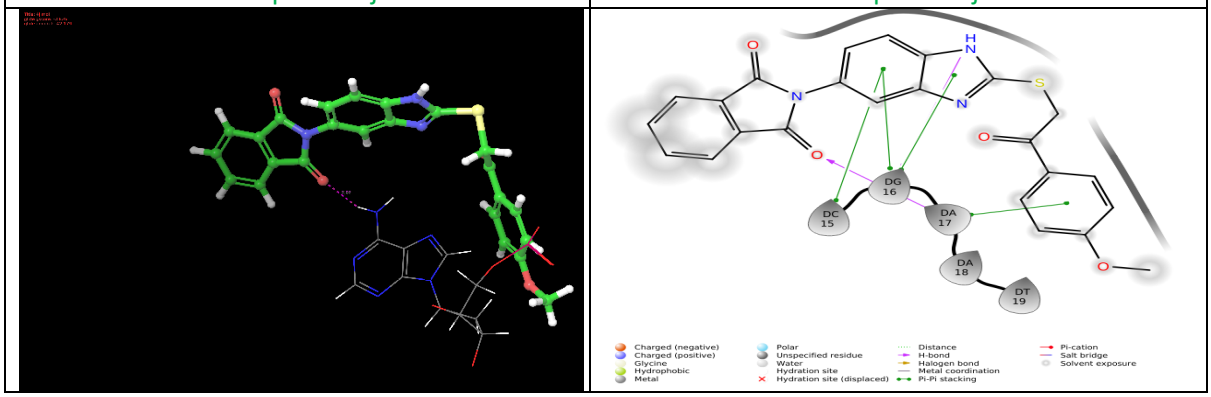

Compound 4q 3d and 2d structures

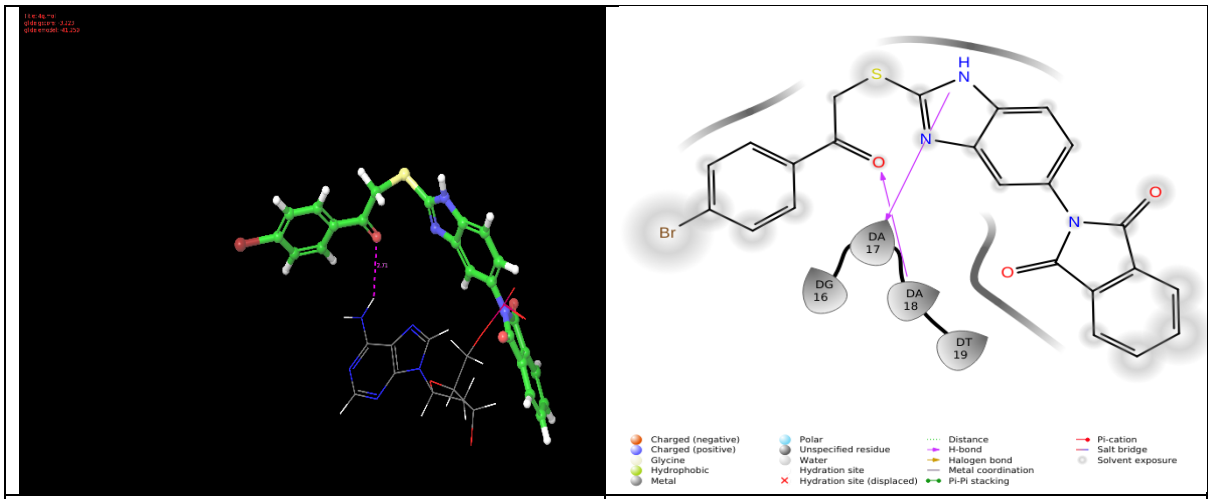

Compound 4s | Compound 4s

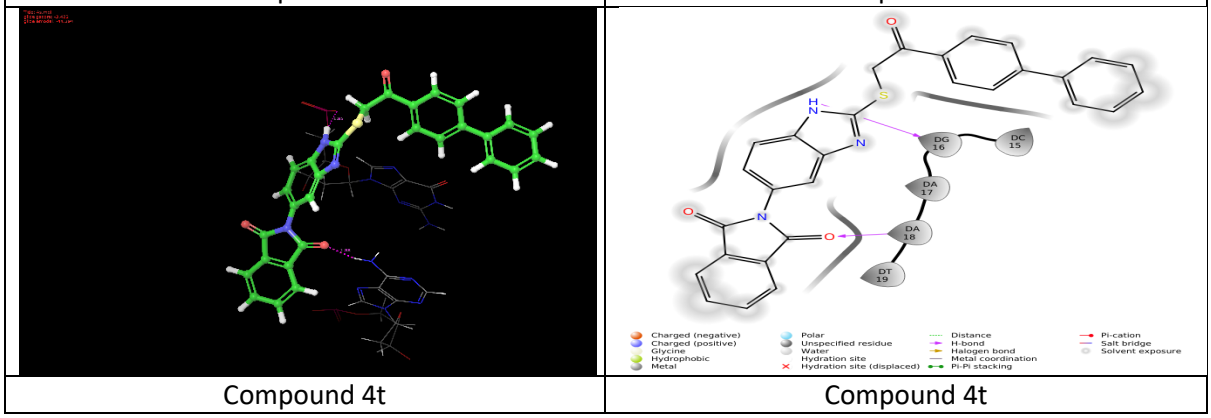

Compound 4t | Compound 4t

Figure 5.3. Molecular docking interaction with PDB ID: 1BNA.

Next, we turned our attention to investigating the suitable solvent for the conversion of 2-(2-((2-oxo-2-phenylethyl)thio)-1*H*-benzo[d]imidazol-5-yl)isoindoline-1,3-dione derivatives to 2-(3- phenylbenzo[4,5]imidazo[2,1-*b*]thiazol-7-yl)isoindoline-1,3-dione derivatives **5a-f**. Therefore, we examine different solvents and acid catalysts (**Table 5.2, entries 1-7**) to find the better yields a model reaction was demonstrated by using a combination of AcOH: HCl, AcOH:H_2SO_4 and phosphorous oxychloride ($POCl_3$) (**Table 5.2, entries 1-7**). The findings suggest that the reaction proceeds better in $POCl_3$ and provides good reaction yields (**Table 5.2, entry-5**). The temperature study indicates that this conversion requires a high temperature (90 ºC).

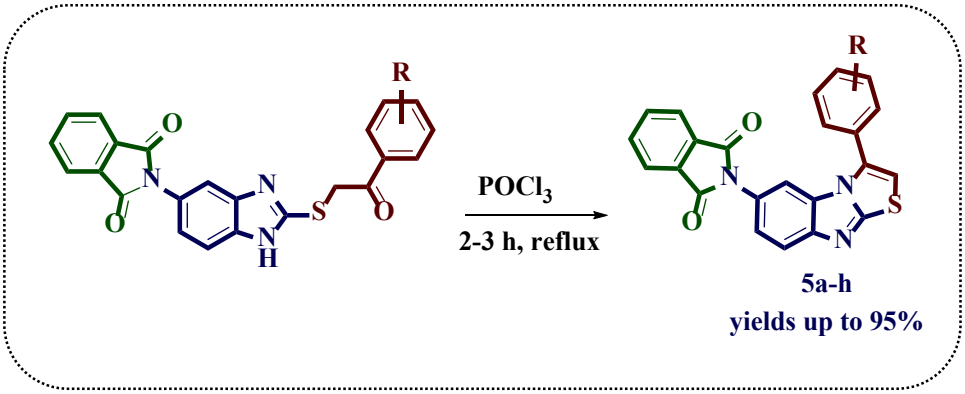

Scheme 5.1. Synthesis of benzo[4,5]imidazo[2,1-*b*]thiazol derivatives.

Table 5.4. Optimization of reaction conditions 5a.

S.NO	Solvent	Catalyst	Temp(°C)	Time(h)	Yield[b]
1	AcOH	HCl (5 mol%)	90	18	50
2	AcOH	HCl (10 mol%)	90	18	55
3	AcOH	H_2SO_4 (5 mol%)	90	15	58
4	AcOH	H_2SO_4 (10 mol%)	90	15	62
5	$POCl_3$	-	90	10	88
6	$POCl_3$	-	100	8	65
7	$POCl_3$	-	110	8	51

Reaction conditions: 2-(2-((2-oxo-2-phenylethyl)thio)-1*H*-benzo[*d*]imidazol-5-yl)isoindoline-1,3-dione (1 mmol), solvent 2 mL. 90 ºC. [b]Isolated yields

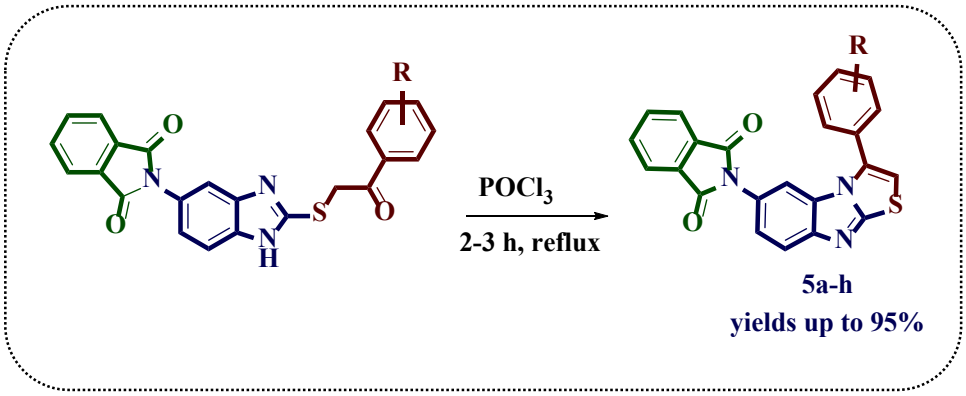

Scheme 5.2. 2-(2-((2-Oxo-2-phenylethyl)thio)-1*H*-benzo[d]imidazol-5-yl)isoindoline-1,3-dione

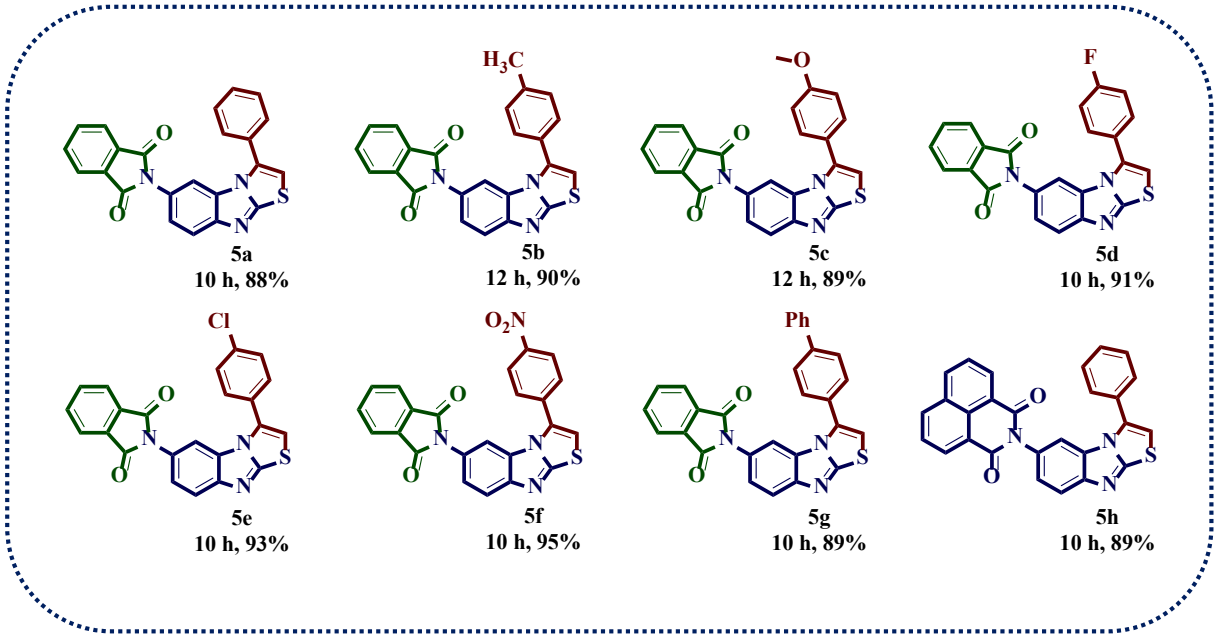

Figure 5.3. The substrate scope of derivatives.

5.5. Conclusion

In conclusion, we have synthesized thioalkylated benzimidazole-based isoindoline-1,3-dione and *N*-fused 4,5-benzo[4,5]imidaz[2,1-*b*]thiazole derivatives *via* a novel, one-pot three/ four-component approach using acetic acid and fused sodium acetate as a reaction medium with good to excellent yields. The usefulness of this reaction is that it involves easy workup, shorter reaction time, broad substrate scope, and column-free purification of the products. Further, the synthesized compounds (4a-w) were evaluated for their *in-vitro* anti-microbial activity. Compounds **4a, 4g, 4j, 4q, 4s,** and **4t** showed good activity against *Gram-positive* and *Gram-negative bacteria.*

5.6. Experimental section

5.6.1. General procedure for the synthesis of **benzo[3,4]imidazo[2,1-*b*]thiazole (5a-f):**

An equimolar mixture of 5-amino-2-mercaptobenzimidazole (1 mmol) and various substituted cyclic anhydrides (1mmol) in 2 mL of glacial acetic acid and fused sodium acetate (1.0 mmol) was added, then various alkyl aryl halides/ phenacyl bromides (1.2 mmol) were added after the disappearance of all starting compounds by TLC and continued the stirring under reflux condition for 3-4 h. After completion of the reaction (ensured by TLC), the solvent from the reaction mixture was removed under reduced pressure. Then the reaction mixture was cooled in an ice bath and treated with an ice-cold solution of $POCl_3$ (1 mL) was added and allowed to stir at 0-5 ºC for 10-15 minutes followed by at room temperature for another 15 minutes. Then, the reaction mixture was serried at 70 ºC for 2-3 h. After completion of the reaction, the reaction mixture was poured into crushed ice and the precipitated product was neutralized with 10 mol% of K_2CO_3 solution, filtered the precipitated solid, and washed several times with ice-cold water the crude product was recrystallized from ethanol and yields of the products are 88-95%.

5.7. Characterization data of products

2-(2-(Benzylthio)-1*H*-benzo[*d*]imidazol-5-yl)isoindoline-1,3-dione. 4a

White solid: yield: 87%, mp 244-246 °C; FT-IR (KBr, cm^{-1}): 3390 (-NH), 1735 (imide –C=O), 1602 (C=N), ^{1}H NMR (400 MHz, DMSO-d_6 δ ppm): 10.43 (s, 1H, Ar-H), 8.0-7.95 (m, 2H, Ar-H), 7.86 (s, 1H, Ar-H), 7.68 – 7.61 (m, 1H, Ar-H), 7.57-7.54 (m, 3H, Ar-H), 7.43 (t, J = 7.0 Hz, 2H, Ar-H), 7.32 (t, J = 7.2 Hz, 2H, Ar-H), 4.65 (s, 2H, S-CH_2); ^{13}C NMR (100 MHz, DMSO-d_6 δ ppm): 167.90, 167.72, 155.96, 151.74, 136.76, 135.19, 135.03, 132.12, 130.18, 129.99, 129.39, 129.23, 128.34, 127.97, 125.01, 123.91, 123.76, 120.63, 114.08, 113.64, 108.71, 36.44; ESI-HRMS: *m/z* Calcd for Chemical Formula: $C_{22}H_{16}N_3O_2S$: 386.0958 $[M+H]^+$ found: 386.0956.

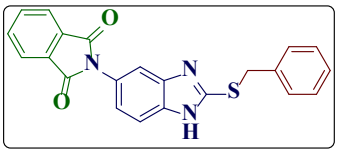

2-(2-((4-Methylbenzyl)thio)-1*H*-benzo[*d*]imidazol-5-yl)isoindoline-1,3-dione. 4b

White solid: Yield: 95%, mp 220-222 ºC; FT-IR (KBr, cm^{-1}): 3355 (-NH), 1735 (imide –C=O), 1629 (C=N); ^{1}H NMR (400 MHz, DMSO-d_6 δ ppm): 8.0-7.98 (m, 2H, Ar-H), 7.94-7.92 (m, 2H, Ar-H), 7.68 (d, J = 8.0 Hz, 2H), 7.35 (d, J = 8.0 Hz, 2H), 7.15 (d, J = 7.6 Hz, 2H), 4.64 (s, 2H, S-CH_2-protons), 2.27 (s, 3H, CH_3-protons), 2.09 (s, 1H, NH proton); ^{13}C NMR (100 MHz, DMSO-d_6 δ ppm): 167.74, 151.80, 137.73, 135.92, 135.44, 135.23, 133.48, 132.03,

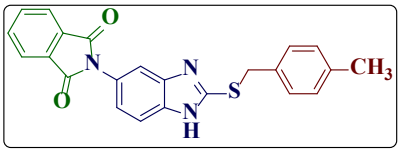

129.79, 129.30, 128.00, 123.92, 114.02, 113.55, 110.31, 36.36, 21.16; ESI-HRMS: *m/z* Calcd for Chemical Formula: $C_{23}H_{18}N_3O_2S$: 400.1114 $[M+H]^+$ found:400.1117.

2-(2-((4-Fluorobenzyl)thio)-1*H*-benzo[*d*]imidazol-5-yl)isoindoline-1,3-dione. 4c

White solid: Yield: 83% ; mp. 236-238 ºC; FT-IR (KBr, cm^{-1}): 3392 (NH), 1764 (imide –C=O), 1619 (C=N); ^{1}H NMR (400 MHz, DMSO) δ 7.99-7.97 (m, 2H, Ar-H), 7.94-7.92 (m, 2H, Ar-H), 7.68 (s, 1H, Ar-H, NH proton), 7.66-7.65 (m, 2H, Ar-H), 7.54 (d, *J* = 8.4 Hz, 2H), 7.43 (d, *J* = 8.4 Hz, 2H), 7.34 (dd, *J* = 8.4, 2.0 Hz, 2H), 4.65 (s, 2H, S-CH_2 protons); ^{13}C NMR (100 MHz, DMSO-*d*$_6$) δ: 167.58, 151.03, 147.30, 145.39, 136.88, 136.36, 135.23, 131.94, 130.58, 127. 61, 124.20, 123.90, 123.61, 114.14, 11.77, 35.36; ESI-HRMS: *m/z* Cacld for Chemical Formula: $C_{22}H_{15}FN_3O_2S$: 404.0864 $[M+H]^+$ found: 404.0870.

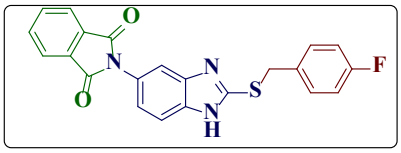

2-(2-((4-Bromobenzyl)thio)-1*H*-benzo[*d*]imidazol-5-yl)isoindoline-1,3-dione. 4d

White solid: Yield: 85%; mp. 240-242 ºC; FT-IR (KBr, cm^{-1}): 3390 (NH), 1726 (imide –C=O), 1601 (C=N); ^{1}H NMR (400 MHz, $CDCl_3$+DMSO-*d*$_6$ ppm) δ 7.91-7.89 (m, 2H, Ar-H), 7.83-7.81 (m, 2H, Ar-H), 7.78 (s, 1H, Ar-H), 7.69 (s, 1H, Ar-H, NH proton), 7.67 (d, *J* = 2.0 Hz, Ar-H, 2H), 7.41 (d, *J* = 8.4 Hz, 2H, Ar-H), 7.33 (d, *J* = 8.4 Hz, 2H, Ar-H), 4.65 (s, 2H, S-CH_2 protons); ^{13}C NMR (100 MHz, $CDCl_3$+DMSO-*d*$_6$) δ: 167.15, 151.00, 134.89, 134.68, 134.56, 133.88, 132.42, 131.99, 131.59, 131.08, 128.47, 123.80, 122.06, 113.92, 112.53, 36.39: ESI-HRMS: *m/z* Calcld for Chemical Formula: $C_{22}H_{15}BrN_3O_2S$: 464.0063 $[M+H]^+$ found: 464.0068.

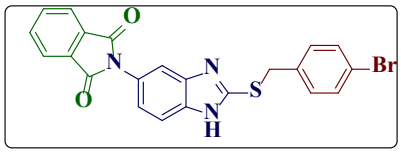

2-(2-((4-Nitrobenzyl)thio)-1*H*-benzo[*d*]imidazol-5-yl)isoindoline-1,3-dione. 4e

White solid: Yield: 86% ; mp. 287-289 ºC; FT-IR (KBr, cm^{-1}): 3427 (NH), 1732 (imide –C=O), 1613 (C=N); ^{1}H NMR (400 MHz, DMSO-*d*$_6$ δ ppm): 8.17 (d, *J* = 8.8 Hz, 2H, Ar-H), 7.97-7.95 (m, 2H, Ar-H), 7.92 – 7.89 (m, 2H, Ar-H), 7.73 (d, *J* = 8.8 Hz, 2H, Ar-H), 7.68 (s, 1H, Ar-H), 7.65-7.64, m, 2H, Ar-H), 7.33 (dd, *J* = 8.4, 2.0 Hz, 1H, Ar-H), 4.77 (s, 2H, S-CH_2 protons); ^{13}C NMR (100 MHz, DMSO-*d*$_6$) δ: 167.84, 151.05, 147.28, 145. 52, 137.23, 136.71, 135.23, 131.95, 130.57, 127.44, 124.19, 123.90, 123.43, 114.17, 113.83, 35.28; ESI-HRMS: *m/z* Cacld for Chemical Formula: $C_{22}H_{15}N_4O_4S$: 431.0809 $[M+H]^+$ found: 431.0805.

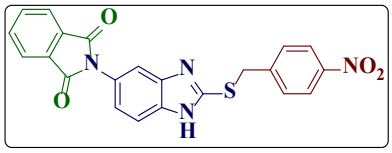

Ethyl 2-((5-(1,3-dioxoisoindolin-2-yl)-1H-benzo[d]imidazol-2-yl)thio)acetate. 4f

White solid: Yield: 88%; mp. 188-190 ºC; FT-IR (KBr, cm^{-1}): 3385 (-NH), 1725 (imide –C=O), 1710 (O-C=O), 1625 (C=N) ^{1}H NMR (400 MHz, $CDCl_3$) δ 8.34 (s, 1H, Ar-H), 7.27 (d, *J* = 8.8 Hz, 2H, Ar-H), 6.99 (d, *J* = 9.2 Hz, 2H, Ar-H), 6.78 (s, 2H, Ar-H), 6.06 (s, 2H, Ar-H), 5.72-5.66 (m, 2H, aliphatic protons), 3.68 (s, 2H, S-CH_2 Protons), 1.50 (t, *J* = 7.2 Hz, 3H, CH_3 Protons); ^{13}C NMR (100 MHz, $CDCl_3$+DMSO-d_6) δ: 167.72, 167.24, 151.18, 134.95, 131.76, 123.80, 113.88, 112.77, 62.23, 34.65, 14.28: ESI-HRMS: *m/z* Cacld for Chemical Formula: $C_{19}H_{16}N_3O_4S$: 382.0856 $[M+H]^+$ found: 382.0857.

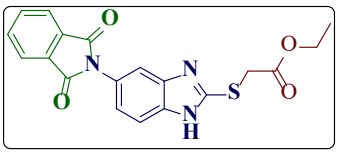

2-((5-(1,3-Dioxoisoindolin-2-yl)-1*H*-benzo[*d*]imidazol-2-yl)thio)acetic acid. 4g

White solid: Yield: 87%; mp. 243-245 ºC; FT-IR (KBr, cm^{-1}): 3465 (-COOH), 3390 (-NH), 1719 (imide –C=O), 1613 (C=N); ^{1}H NMR (400 MHz, $CDCl_3$+ DMSO-d_6 ppm) δ: 7.99-7.97 (m, 2H, Ar-H), 7.89-7.87 (m, 2H, Ar-H), 7.79 (s, 1H, Ar-H, NH proton), 7.77-7.76 (m, 2H, Ar-H), 7.71 (s, 1H, Ar-H), 7.52 (dd, *J* = 8.4, 1.6 Hz, 1H), 4.46 (s, 2H, S-CH_2 protons); ^{13}C NMR ^{13}C NMR (100 MHz, $CDCl_3$+DMSO-d_6) δ: 167.59, 167.16, 151.07, 134.93, 131.70, 123.81, 113.85, 112.62, 34.67; ESI-HRMS: *m/z* Cacld for Chemical Formula: $C_{17}H_{12}N_3O_4S$: 354.0543 $[M+H]^+$ found: 354.0540.

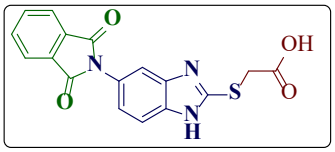

1-(2-((4-Fluorobenzyl)thio)-1*H*-benzo[*d*]imidazol-5-yl)pyrrolidine-2,5-dione. 4h

White solid: Yield: 82%; mp. 185-187 ºC; FT-IR (KBr, cm^{-1}): 3425 (-NH), 1718 (imide –C=O), 1623 (-C=N); ^{1}H NMR (400 MHz, $CDCl_3$+DMSO-d_6 δ ppm): 10.21 (s, 1H, Ar-H, NH proton), 7.90 (s, 1H, Ar-H), 7.53 – 7.51 (m, 2H, Ar-H), 7.45 (dd, *J* = 8.6, 5.4 Hz, 2H, Ar-H), 7.05 (t, *J* = 8.6 Hz, 2H, Ar-H), 4.72 (s, 2H, S-CH_2 prptons), 2.16 (s, 4H, aliphatic protons); ^{13}C NMR (100 MHz, $CDCl_3$+DMSO-d_6) δ: 169.55, 163.63, 161.17, 148.05, 137.79, 132.69, 131.22, 131.14, 128.20, 118.57, 116.07, 115.85, 113.36, 103.15, 36.90, 24.36; ESI-HRMS: *m/z* Cacld for Chemical Formula: $C_{18}H_{15}FN_3O_2S$: 356.0864 $[M+H]^+$ found: 356.0865.

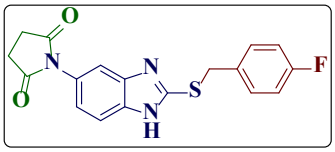

1-(2-((4-Nitrobenzyl)thio)-1*H*-benzo[*d*]imidazol-5-yl)pyrrolidine-2,5-dione. 4i

White solid: Yield: 85%; mp. 193-195 ºC; FT-IR (KBr, cm^{-1}): 3427 (-NH), 1735 (imide –C=O), 1626 (C=N); ^{1}H NMR (400 MHz, $CDCl_3$+DMSO-d_6 δ ppm): 10.15 (s, 1H, Ar-H, NH proton), 8.26 (s, 1H, Ar-H), 8.08 (d, *J* = 8.4 Hz, 2H, Ar-H), 7.66 (d, *J* = 8.8 Hz, 2H, Ar-H), 7.49 – 7.44 (m, 2H, Ar-H), 4.82 (s, 2H, S-CH_2 protons), 2.09 (s, 4H, aliphatic protons); ^{13}C NMR (100 MHz, $CDCl_3$+DMSO-d_6) δ: 169.38, 147.56, 147.23, 142.98, 137.87, 132.94,

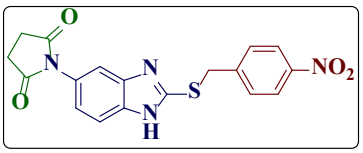

130.33, 128.47, 124.02, 118.53, 113.43, 103.15, 36.54, 24.39; ESI-HRMS: *m/z* Cacld for Chemical Formula: $C_{18}H_{15}N_4O_4S$: 383.0809 $[M+H]^+$ found: 383.0424.

2-(2-((4-Fluorobenzyl)thio)-1*H*-benzo[*d*]imidazol-5-yl)-4-nitroisoindoline-1,3-dione. 4j

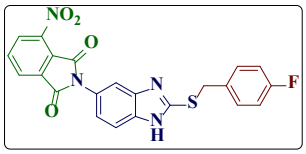

Orange solid: Yield: 85%; mp. 226-228 ºC; FT-IR (KBr, cm^{-1}): 3426 (-NH), 1731 (imide – C=O), 1612 (C=N) ; ^{1}H NMR (400 MHz, $CDCl_3$+DMSO-d_6 δ ppm): 8.27 (d, *J* = 8.0 Hz, 1H, Ar-H), 8.22 (d, *J* = 6.8 Hz, 1H, Ar-H), 8.10 (t, *J* = 7.8 Hz, 2H, Ar-H), 7.64 (s, 1H, Ar-H, NH proton), 7.62 – 7.61 (m, 1H, Ar-H), 7.45 (d, *J* = 8.8 Hz, 2H, Ar-H), 7.38 (d, *J* = 8.4 Hz, 2H, Ar-H), 7.30 (dd, *J* = 8.6, 1.8 Hz, 1H, Ar-H), 4.61 (s, 2H, S-CH_2 protons); ^{13}C NMR (100 MHz, DMSO-d_6) δ: 166.02, 163.45, 160.80, 151.89, 144.95, 137.07, 136.87, 131.46, 131.38, 128.80, 127.49, 123.41, 123.01, 116.02, 115.81, 114.20, 114.04, 35.19; ESI-HRMS: *m/z* Cacld for Chemical Formula: $C_{22}H_{14}FN_4O_4S$: 449.0714 $[M+H]^+$ found: 449.0710.

4-Nitro-2-(2-((4-nitrobenzyl)thio)-1*H*-benzo[*d*]imidazol-5-yl)isoindoline-1,3-dione. 4k

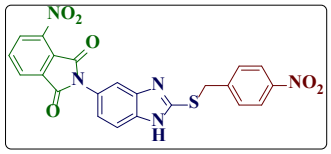

Orange solid: Yield: 84%; mp. 230-232 ºC; FT-IR (KBr, cm^{-1}): 3408 (-NH), 1729 (imide – C=O), 1623 (C=N) ^{1}H NMR (400 MHz, DMSO-d_6 δ ppm): 10. 34 (s, 1H, Ar-H, NH proton), 8.34 (d, *J* = 8.0 Hz, 1H, Ar-H), 8.27 – 8.23 (m, 1H, Ar-H), 8.13 (t, *J* = 7.8 Hz, 1H, Ar-H), 7.73 – 7.69 (m, 1H, Ar-H), 7.62 (d, *J* = 8.8 Hz, 1H, Ar-H), 7.47-7.41 (m, 2H, Ar-H), 7.35-7.27 (m, 3H, Ar-H), 4.71 (s, 2H, S-CH_2-protons); ^{13}C NMR (100 MHz, $CDCl_3$+ DMSO-d_6) δ: 167.26, 151.50, 135.52, 134.75, 131.58, 129.08, 128.90, 128.16, 127.60, 123.76, 122.83, 113.95, 112.56, 37.14; ESI-HRMS: *m/z* Cacld for Chemical Formula: $C_{22}H_{14}N_5O_6S$: 476.0659 $[M+H]^+$ found: 476.0653.

2-(2-(Benzylthio)-1*H*-benzo[*d*]imidazol-5-yl)-1*H*-benzo[*de*]isoquinoline-1,3(2*H*)-dione. 4l

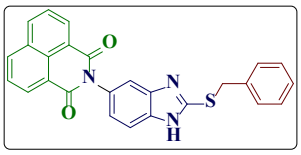

White solid: Yield: 88%; mp. 268-270 ºC; IR FT-IR (KBr, cm^{-1}): 3377 (-NH), 1737 (imide – C=O), 1622 (C=N) ; ^{1}H NMR (400 MHz, DMSO-d_6 δ ppm): 8.54-8.51 (m, 5H, Ar-H), 7.92 (t, *J* = 7.8 Hz, 1H, Ar-H), 7.77 (d, *J* = 8.0 Hz, 2H), 7.50 (d, *J* = 7.2 Hz, 2H), 7.43 – 7.31 (m, 4H, Ar-H), 4.76 (s, 2H, S-CH_2 Protons); ^{13}C NMR (100 MHz, DMSO-d_6) δ: 164.45, 151.30, 136.50, 134.98, 131.93, 131.23, 129.39, 129.29, 128.45, 128.35, 127.73, 123.12, 114.97, 114.00, 36.70; ESI-HRMS: *m/z:* Cacld for Chemical Formula: $C_{26}H_{18}N_3O_2S$: 436.1114 $[M+H]^+$ found: 436.1121.

2-(2-((4-Fluorobenzyl)thio)-1H-benzo[*d*]imidazol-5-yl)-1*H*-benzo[de]isoquinoline-1,3(2H)-dione. 4m

White solid: Yield: 86%; mp. 268-270 ºC; FT-IR (KBr, cm^{-1}): 3398 (-NH), 1736 (imide –C=O), 1623 (C=N); ^{1}H NMR (400 MHz, DMSO-d_6) δ: 8.53-8.51 (m, 5H, Ar-H), 7.92 (t, *J* = 7.8 Hz, 2H, Ar-H), 7.71 (d, *J* = 8.8 Hz, 2H, Ar-H), 7.54 (t, J = 6.8 Hz, 2H, Ar-H), 7.34 (d, *J* = 8.0 Hz, 1H, Ar-H), 7.19 (t, *J* = 8.6 Hz, 2H, Ar-H), 4.71 (s, 2H, S-CH_2 Protons); ^{13}C NMR (100 MHz, DMSO-d_6) δ: 164.47, 151.17, 134.93, 133.44, 131.93, 131.49, 131.41, 131.21, 128.35, 127.72, 125.12, 123.17, 116.12, 115.91, 115.09, 114.04, 35.53; ESI-HRMS: *m/z*: Cacld for Chemical Formula: $C_{26}H_{17}FN_3O_2S$: 454.1020 $[M+H]^+$ found: 454.1022.

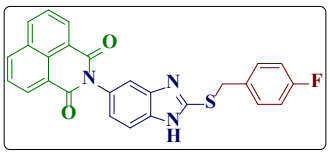

2-(2-((4-Bromobenzyl)thio)-1*H*-benzo[*d*]imidazol-5-yl)-1*H*-benzo[*de*]isoquinoline-1,3(2*H*)-dione. 4n

White solid: Yield: 88%; mp. 268-270 ºC; FT-IR (KBr, cm^{-1}): 3366 (-NH), 1711 (imide –C=O), 1623 (C=N); ^{1}H NMR (400 MHz, DMSO-d_6 δ ppm): 8.54 – 8.51 (m, 5H, Ar-H), 7.92 (t, *J* = 7.8 Hz, 2H, Ar-H), 7.77 – 7.75 (m, 2H, Ar-H), 7.56 (d, *J* = 8.4 Hz, 2H, Ar-H), 7.46 (d, *J* = 8.4 Hz, 2H, Ar-H), 7.41 (dd, *J* = 8.6, 2.4 Hz, 1H, Ar-H), 4.73 (s, 2H, S-CH_2 protons); ^{13}C NMR (100 MHz, DMSO-d_6) δ: 164.44, 151.00, 136.46, 134.95, 132.69, 132.16, 131.95, 131.57, 131.20, 128.38, 127.73, 125.82, 123.20, 121.58, 115.04, 114.04, 35.86; ESI-HRMS: *m/z* Cacld for Chemical Formula: $C_{26}H_{17}BrN_3O_2S$: 514.0219 [M+H] + found: 514.0217

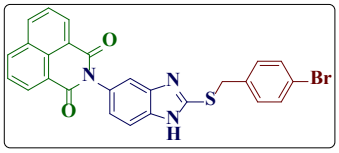

2-(2-((2-Oxo-2-phenylethyl)thio)-1*H*-benzo[*d*]imidazol-5-yl)isoindoline-1,3-dione. 4o

White solid: Yield: 95%; mp. 226-228 ºC; FT-IR (KBr, cm^{-1}): 3326 (-NH), 1735 (carbonyl –C=O), 1690 (imide –C=O), 1626 (C=N); ^{1}H NMR (400 MHz, DMSO-d_6 δ ppm): 8.07 (d, *J* = 7.2 Hz, 2H), 7.97-7.94 (m, 2H, Ar-H), 7.91-7.89 (m, 2H, Ar-H), 7.70 (t, *J* = 7.4 Hz, 1H, Ar-H), 7.64-7.56 (m, 5H, Ar-H), 7.30 (d, *J* = 8.4 Hz, 1H, Ar-H), 5.20 (s, 2H, S-CH_2 Protons); ^{13}C NMR (100 MHz, DMSO-d_6 δ) δ: 193.33, 167.81, 152.06, 137.29, 136.79, 135.58, 135.18, 134.45, 132.03, 129.39, 128.94, 127.24, 123.87, 123.14, 113.94, 113.64, 40.74; ESI-HRMS: *m/z* Cacld for Chemical Formula: $C_{23}H_{16}N_3O_3S$: 414.0907 $[M+H]^+$ found: 414.0905.

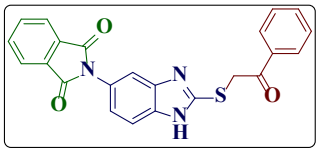

2-(2-((2-Oxo-2-(p-tolyl)ethyl)thio)-1*H*-benzo[*d*]imidazol-5-yl)isoindoline-1,3-dione. 4p

Yellow solid: yield: 95%; mp. 226-228 ºC; FT-IR (KBr, cm^{-1}): 3260 (-NH), 1727 (carbonyl –C=O), 1685 (imide –C=O), 1613 (C=N); ^{1}H NMR (400 MHz, DMSO) δ 8.10 (s, 1H, Ar-H), 7.97-7.91 (m, 2H, Ar-H), 7.87-7.85 (m, 2H, Ar-H), 7.62 (d, *J* = 8.4 Hz, 1H), 7.58 (s, 1H, Ar-H), 7.34 (d, *J* = 8.0 Hz, 2H, Ar-H), 7.29 (dd, *J* = 8.6, 1.8 Hz, 1H, Ar-H), 5.14 (s, 2H, S-CH_2 Protons), 2.40 (s, 3H, -CH_3 Protons); ^{13}C NMR (100 MHz, DMSO-*d*$_6$) δ: 192.37, 167.49, 152.05, 144.93, 134.96, 132.93, 131.86, 129.73, 128.94, 127.29, 123.78, 122.85, 113.83, 113.12, 40.81, 21.77; ESI-HRMS: *m/z* Cacld for Chemical Formula: $C_{24}H_{18}N_3O_3S$: 428.1063 $[M+H]^+$ found: 428.1067.

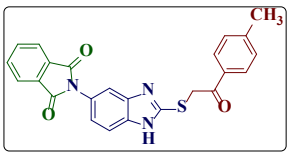

2-(2-((2-(4-Methoxyphenyl)-2-oxoethyl)thio)-1*H*-benzo[*d*]imidazol-5-yl)isoindoline-1,3-dione. 4q

Yellow solid: yield: 95%; mp. 226-228 ºC; FT-IR (KBr, cm^{-1}): 3426 (-NH), 1733 (carbonyl –C=O), 1695 (imide –C=O), 1625 (C=N); ^{1}H NMR (400 MHz, DMSO-*d*$_6$ δ ppm): 8.04 (d, *J* = 8.8 Hz, 2H, Ar-H), 7.95-7.93 (m, 2H, Ar-H), 7.90-7.87 (m, 2H, Ar-H), 7.58 (s, 1H, Ar-H), 7.55 – 7.54 (m, 2H, Ar-H), 7.22 (dd, *J* = 8.4, 2.0 Hz, 1H), 7.08 (d, *J* = 8.8 Hz, 2H, Ar-H), 5.07 (s, 2H, S-CH_2- protons), 3.85 (s, 3H, OCH_3 protons); ^{13}C NMR (100 MHz, DMSO-*d*$_6$) δ: 191.94, 167.90, 164.10, 152.01, 138.79, 135.12, 132.04, 131.35, 128.56, 126.48, 123.83, 122.33, 114.55, 113.87, 56.11, 40.92; ESI-HRMS: *m/z* Cacld for Chemical Formula: $C_{24}H_{18}N_3O_4S$: 444.1013 $[M+H]^+$ found: 444.1009.

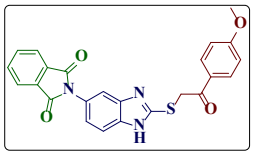

2-(2-((2-(4-Chlorophenyl)-2-oxoethyl)thio)-1*H*-benzo[*d*]imidazol-5-yl)isoindoline-1,3-dione. 4r

Yellow solid: yield: 95%; mp. 226-228 ºC; FT-IR (KBr, cm^{-1}): 3327 (-NH), 1735 (carbonyl –C=O), 1692 (imide –C=O), 1619 (C=N); ^{1}H NMR (400 MHz, $CDCl_3$+DMSO-*d*$_6$ δ ppm): 8.08 (d, *J* = 8.4 Hz, 2H), 7.98-7.96 (m, 2H, Ar-H), 7.92-7.90 (m, 2H, Ar-H), 7.68 – 7.64 (m, 4H, Ar-H), 7.35 (dd, *J* = 8.6, 1.8 Hz, 1H), 5.30 (s, 1H, -NH Proton), 5.21 (s, 2H, S-CH_2 Protons); ^{13}C NMR (100 MHz, DMSO-*d*$_6$) δ: 192.32, 167.76, 152.02, 139.40, 135.20, 134.26, 132.04, 130.88, 129.52, 123.90, 113.92, 113.56, 40.82; ESI-HRMS: *m/z* Cacld for Chemical Formula: $C_{23}H_{15}ClN_3O_3S$: 448.0517 $[M+H]^+$ found: 448.0519.

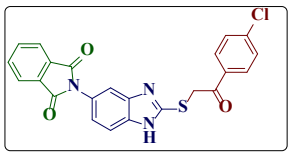

2-(2-((2-(4-Bromophenyl)-2-oxoethyl)thio)-1*H*-benzo[*d*]imidazol-5-yl)isoindoline-1,3-dione. 4s

White solid: yield: 91%; mp. 285-287 ºC; FT-IR (KBr, cm^{-1}): 3297 (-NH), 1721 (carbonyl –C=O), 1677 (imide –C=O), 1620 (C=N); ^{1}H NMR (400 MHz, $CDCl_3$+ DMSO- d_6 δ ppm): 8.10 (s, 1H, Ar-H), 7.99 (d, J = 8.4 Hz, 2H, Ar-H), 7.93-7.85 (m, 3H, Ar-H), 7.71 (d, J = 8.8 Hz, 2H, Ar-H), 7.55 – 7.50 (m, 2H, Ar-H), 7.19 (d, J = 8.4 Hz, 1H), 5.18 (s, 1H, Ar-H), 5.05 (s, 2H, S-CH_2 Protons): ^{13}C NMR (100 MHz, DMSO-d_6) δ: 192.61, 170.03, 152.61, 145.17, 142.07, 139.77, 134.59, 132.98, 131.00, 130.62, 129.93, 129.57, 129.43, 129.29, 129.13, 126.35, 115.21, 110.35, 104.79, 41.34; ESI-HRMS: *m/z* Cacld for Chemical Formula: $C_{23}H_{15}BrN_3O_3S$: 492.0012 $[M+H]^+$ found: 492.0024.

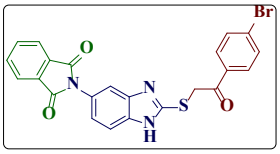

2-(2-((2-([1,1'-Biphenyl]-4-yl)-2-oxoethyl)thio)-1*H*-benzo[*d*]imidazol-5-yl)isoindoline-1,3-dione. 4t

White solid: yield: 87%, mp. 199-201 ºC; FT-IR (KBr, cm^{-1}): 3336 (-NH), 1738 (carbonyl –C=O), 1696 (imide –C=O), 1628 (C=N); ^{1}H NMR (400 MHz, DMSO-d_6 δ ppm): 12.89 (s, 1H, Ar-H, NH Proton), 8.15 (d, J = 8.4 Hz, 2H, Ar-H), 7.93-7.85 (m, 6H, Ar-H), 7.75 (d, J = 7.2 Hz, 2H, Ar-H), 7.52-7.48 (m, 4H, Ar-H), 7.42 (t, J = 7.4 Hz, 1H, Ar-H), 7.16 (t, J = 7.4 Hz, 1H, Ar-H), 5.09 (s, 2H, S-CH_2 protons); ^{13}C NMR (100 MHz, DMSO-d_6) δ: 193.39, 167.97, 151.75, 145.52, 139.23, 135.09, 134.66, 132.05, 129.68, 129.62, 129.01, 127.50, 123.80, 121.97, 117.37, 110.54, 41.15; ESI-HRMS: *m/z* Cacld for Chemical Formula: $C_{29}H_{20}N_3O_3S$: 490.1220 $[M+H]^+$ found: 490.1220.

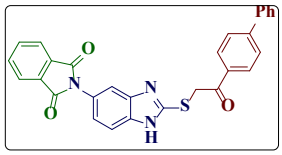

2-(2-((2-Oxo-2-phenylethyl)thio)-1*H*-benzo[*d*]imidazol-5-yl)-1*H*-benzo[*de*]isoquinoline-1,3(2*H*)-dione. 4u

White solid: yield: 88%; mp. 246-248 ºC; FT-IR (KBr, cm^{-1}): 3320 (-NH), 1729 (carbonyl –C=O), 1698 (imide –C=O), 1626 (C=N); ^{1}H NMR (400 MHz, DMSO-d_6 δ ppm): 10.38 (s, 1H, Ar-H), 8.52 (t, J = 6.6 Hz 3H, Ar-H), 8.26 (d, J = 1.6 Hz, 1H, Ar-H), 8.10 (t, J = 7.8 Hz, 2H, Ar-H), 7.91 (t, J = 7.8 Hz, 1H, Ar-H), 7.79-7.77 (m, 1H, Ar-H), 7.75-7.74 (m, 1H, Ar-H), 7.67-7.60 (m, 3H, Ar-H), 7.52 (dd, J = 8.8, 2.0 Hz, 1H, Ar-H), 7.47-7.45 (m, 1H, Ar-H), 5.43 (s, 2H, S-CH_2 Protons); ^{13}C NMR (100 MHz, DMSO-d_6) δ: 192.56, 169.26, 164.42, 152.02, 150.19, 137.61, 135.89, 135.30, 134.97, 132.94, 131.93, 131.19, 129.44, 129.05, 127.72, 123.17, 117.73, 114.76, 113.81, 102.55, 42.23; ESI-HRMS: *m/z* Cacld for Chemical Formula: $C_{27}H_{18}N_3O_3S$: 464.1063 $[M+H]^+$ found: 464.1070.

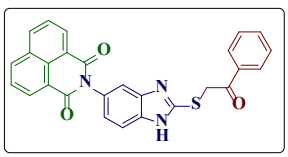

2-(2-((2-(4-Chlorophenyl)-2-oxoethyl)thio)-1*H*-benzo[*d*]imidazol-5-yl)-1*H*-benzo[*de*]isoquinoline-1,3(2*H*)-dione. 4v

White solid: yield: 86%, mp. 270-272 ºC; FT-IR (KBr, cm^{-1}): 3348 (-NH), 1738 (carbonyl –C=O), 1707 (imide –C=O), 1630 (C=N); ^{1}H NMR (400 MHz, $CDCl_3$+DMSO-d_6 δ ppm): 10.24 (s, 1H, Ar-H, NH Proton), 8.55 (dd, *J* = 7.2, 1.2 Hz, 1H), 8.46 (d, *J* = 8.0 Hz, 1H, Ar-H), 8.33 (d, *J* = 1.6 Hz, 1H, Ar-H), 8.10 (t, *J* = 9.0 Hz, 2H, Ar-H), 7.88 (t, *J*=7.8 Hz, 1H, Ar-H), 7.75 (d, *J* = 8.4 Hz, 1H, Ar-H), 7.69 (s, 1H, Ar-H), 7.61 (dd, *J* = 8.6, 1.8 Hz, 2H, Ar-H), 7.55 (d, *J* = 8.8 Hz, 1H, Ar-H), 7.47 (dd, *J* = 8.8, 1.6 Hz, 1H), 7.39 (dd, *J* = 8.6, 1.8 Hz, 1H, Ar-H), 5.32 (s, 2H, S-CH_2 Protons); ^{13}C NMR (100 MHz, DMSO-d_6) δ: 192.16, 169.42, 164.48, 151.72, 150.02, 139.48, 137.22, 135.00, 133.88, 133.47, 132.43, 131.27, 130.89, 129.52, 127.73, 125.60, 123.03, 117.61, 114.86, 113.90, 41.63; ESI-HRMS: *m/z* Cacld for Chemical Formula: $C_{27}H_{17}ClN_3O_3S$: 498.0674 $[M+H]^+$ found: 498.0675.

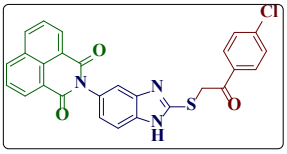

2-(2-((2-(4-Bromophenyl)-2-oxoethyl)thio)-1*H*-benzo[*d*]imidazol-5-yl)-1*H*-benzo[*de*]isoquinoline-1,3(2*H*)-dione. 4w

White solid: yield: 89%; mp. 261-263 ºC; FT-IR (KBr, cm^{-1}): 3352 (-NH), 1731 (carbonyl –C=O), 1687 (imide –C=O), 1622 (C=N); ^{1}H NMR (400 MHz, DMSO-d_6 δ ppm): 10.34 (s, 1H, Ar-H, NH Proton), 8.57-8.50 (m, 3H, Ar-H), 8.24 (s, 1H, Ar-H), 8.01 (t, *J*= 9.2, 2H, Ar-H), 7.92 (t, *J* = 7.8 Hz, 1H, Ar-H), 7.85 (dd, *J* = 8.8, 3.2 Hz, 2H), 7.76 – 7.74 (m, 1H, Ar-H), 7.62 (d, *J* = 8.8 Hz, 1H, Ar-H), 7.49 (dd, *J* = 8.8, 1.6 Hz, 1H, Ar-H), 7.42 (dd, *J* = 8.6, 1.4 Hz, 1H, Ar-H), 5.36 (s, 2H, S-CH_2 Protons); ^{13}C NMR (100 MHz, DMSO-d_6) δ: 192.24, 169.24, 164.42, 151.79, 150.00, 137.53, 135.89, 134.96, 132.94, 132.51, 131.20, 130.98, 128.76, 128.04, 127.72, 123.18, 113.87, 41.93: ESI-HRMS: *m/z* Cacld for Chemical Formula: $C_{27}H_{17}BrN_3O_3S$: 542.0169 $[M+H]^+$ found: 542.0170.

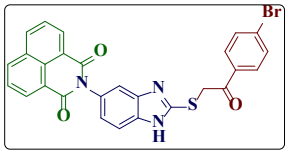

2-(3-Phenylbenzo[4,5]imidazo[2,1-*b*]thiazol-6-yl)isoindoline-1,3-dione. 5a

White solid: yield: 88%; mp. 216-218 ºC; FT-IR (KBr, cm^{-1}): 1747 (imide –C=O); ^{1}H NMR (400 MHz, DMSO-d_6 δ ppm): 7.97-7.89 (m, Ar-H, 5H), 7.83-7.80 (m, Ar-H, 2H), 7.67 – 7.66 (m, 2H, Ar-H), 7.60-7.59 (m, 2H, Ar-H), 7.42 (dd, *J* = 8.8, 1.6 Hz, 1H, Ar-H), 7.36 (s, 1H, Ar-H); ^{13}C NMR (100 MHz, DMSO-d_6) δ: 166.93, 150.87, 136.79, 135.23, 134.71, 129.45, 129.01, 121.94, 113.57, 108.23; ESI-HRMS: *m/z* Cacld for Chemical Formula: $C_{23}H_{14}N_3O_2S$: 396.0801 $[M+H]^+$ found: 396.0802.

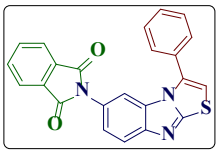

2-(3-(p-Tolyl)benzo[4,5]imidazo[2,1-*b*]thiazol-6-yl)isoindoline-1,3-dione. 5b

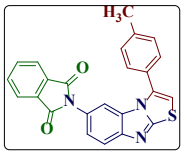

White solid: yield: 90%; mp. 233-235 ºC; FT-IR (KBr, cm^{-1}): 1742 (imide –C=O); ^{1}H NMR (400 MHz, $CDCl_3$+DMSO-d_6 δ ppm): 8.09 (s, 1H, Ar-H), 7.96-7.85 (m, 6H, Ar-H), 7.48-7.43 (m, 2H, Ar-H), 7.32 (d, *J* = 7.6 Hz, 2H, Ar-H), 7.10 (s, 1H, Ar-H), 2.40 (s, 3H, CH_3 Protons); ^{13}C NMR (100 MHz, DMSO-d_6 δ ppm): 167.33, 150.81, 145.40, 139.66, 132.72, 129.98, 129.12, 128.98, 125.16, 124.20, 121.96, 113.50, 108.06, 21.74; ESI-HRMS: *m/z* Cacld for Chemical Formula: $C_{24}H_{16}N_3O_2S$: 410.0958 $[M+H]^+$ found: 410.0956.

2-(3-(4-Methoxyphenyl)benzo[4,5]imidazo[2,1-*b*]thiazol-6-yl)isoindoline-1,3-dione. 5c

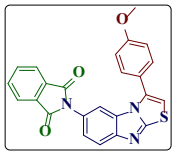

White solid: yield: 89%; mp. 218-220 ºC; FT-IR (KBr, cm^{-1}): 1723 (imide –C=O); ^{1}H NMR (400 MHz, DMSO-d_6 δ ppm): 7.94-7.90 (m, 4H, Ar-H), 7.74-7.68 (m, 3H, Ar-H), 7.40 (s, 1H, Ar-H), 7.18 (d, *J* = 8.4 Hz, 2H, Ar-H), 7.13 (d, *J* = 8.4 Hz, 2H, Ar-H), 3.82 (s, 3H, OCH_3 Protons); ^{13}C NMR (100 MHz, $CDCl_3$+ DMSO-d_6) δ: 164.44, 150.53, 139.42, 137.44, 131.29, 128.69, 127.81, 125.04, 124.15, 114.37, 113.16, 107.76, 55.93; ESI-HRMS: *m/z* Cacld for Chemical Formula: $C_{24}H_{16}N_3O_3S$: 426.0907 $[M+H]^+$ found: 426.0913.

2-(3-(4-Fluorophenyl)benzo[4,5]imidazo[2,1-*b*]thiazol-6-yl)isoindoline-1,3-dione. 5d

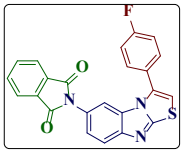

White solid: yield: 91%; mp. 232-234 ºC; FT-IR (KBr, cm^{-1}): 1747 (imide –C=O); ^{1}H NMR (400 MHz, DMSO-d_6 δ ppm): 8.17 (dd, *J* = 8.4, 5.6 Hz, 2H, Ar-H), 8.08 (s, 1H, Ar-H), 7.62 (d, *J* = 8.8 Hz, 1H, Ar-H), 7.53 (d, *J* = 7.6 Hz, 2H, Ar-H), 7.46 (t, *J* = 8.8 Hz, 3H, Ar-H), 7.35 (t, *J* = 8.0 Hz, 2H, Ar-H), 7.15 (s, 1H, Ar-H); ^{13}C NMR (100 MHz, DMSO-d_6 δ) δ: 167.27, 164.75, 152.57, 132.10, 132.01, 129.04, 119.65, 116.95, 116.83, 116.49, 116.27, 114.67, 112.80, 108.28; ESI-HRMS: *m/z* Cacld for Chemical Formula: $C_{23}H_{13}FN_3O_2S$: 414.0707 $[M+H]^+$ found: 414.0707.

2-(3-(4-Chlorophenyl)benzo[4,5]imidazo[2,1-*b*]thiazol-6-yl)isoindoline-1,3-dione. 5e

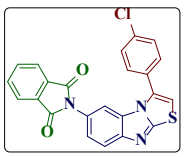

White solid: yield: 93%; mp. 270-272 ºC; FT-IR (KBr, cm^{-1}): 1746 (imide –C=O); ^{1}H NMR (400 MHz, DMSO-d_6 δ ppm): 7.93-7.91 (m, 3H, Ar-H), 7.84-7.78 (m, 2H, Ar-H), 7.71 (d, *J* = 8.4 Hz, 2H, Ar-H), 7.64 (d, *J* = 8.4 Hz, 2H, Ar-H), 7.39 (s, 1H, Ar-H), 7.30-7.27 (m, 2H, Ar-H), 7.20 (dd, *J* = 8.4, 1.6 Hz, 1H, Ar-H); ^{13}C NMR (100 MHz, DMSO-d_6) δ: 165.10, 150.57, 139.67, 139.58, 133.98, 130.90, 129.56, 128.97, 125.15, 124.20, 121.89, 113.54, 108.15; ESI-HRMS: *m/z* Cacld for Chemical Formula: $C_{23}H_{13}ClN_3O_2S$: 430.0412 $[M+H]^+$ found: 430.0420.

2-(3-(4-Nitrophenyl)benzo[4,5]imidazo[2,1-*b*]thiazol-6-yl)isoindoline-1,3-dione. 5f

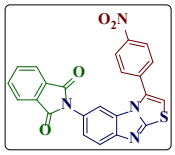

Yellow solid: yield: 95%, mp. 263-265 ºC; FT-IR (KBr, cm^{-1}): 1748 (imide –C=O), (NO_2) 1525, 1341; ^{1}H NMR (400 MHz, DMSO-d_6 δ ppm): 8.36 (d, *J* = 9.2 Hz, 2H, Ar-H), 8.30 (d, *J* = 9.2 Hz, 2H, Ar-H), 7.96-7.91 (m, 4H, Ar-H), 7.53 (s, 1H, Ar-H), 7.51 – 7.50 (m, 2H, Ar-H), 7.18 (dd, *J* = 845, 2.0 Hz, 1H, Ar-H); ^{13}C NMR (100 MHz, DMSO-d_6) δ: 166.11, 157.31, 153.82, 135.92, 132.47, 132.32, 131.66, 131.60, 128.83, 128.69, 127.03, 124.58, 123.70, 112.38, 109.77; ESI-HRMS: *m/z* Cacld for Chemical Formula: $C_{23}H_{13}N_4O_4S$: 441.0652 $[M+H]^+$ found: 441.0652.

2-(3-([1,1'-Biphenyl]-4-yl)benzo[4,5]imidazo[2,1-*b*]thiazol-6-yl)isoindoline-1,3-dione. 5g

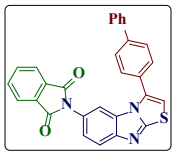

White solid: yield: 89%, mp. 198-200 ºC; FT-IR (KBr, cm^{-1}): 1745 (imide –C=O); ^{1}H NMR (400 MHz, DMSO)-d_6 δ ppm): 8.17 (d, *J* = 8.4 Hz, 2H, Ar-H), 8.10 (s, 1H, Ar-H), 7.93 (d, *J* = 8.8 Hz, 2H, Ar-H), 7.80 (d, *J* = 7.2 Hz, 2H, Ar-H), 7.63 (d, *J* = 8.4 Hz, 2H, Ar-H), 7.55-7.53 (m, 3H, Ar-H), 7.48-7.44 (m, 2H, Ar-H), 7.35 (t, *J* = 8.0 Hz, 2H, Ar-H), 7.15 (s, 1H, Ar-H); ^{13}C NMR (100 MHz, DMSO-d_6 δ) δ: 167.35, 150.70, 145.94, 139.75, 139.10, 137.14, 134.06, 129.78, 129.63, 129.14, 128.95, 127.56, 125.05, 124.08, 121.81, 113.53, 107.85; ESI-HRMS: *m/z* Cacld for Chemical Formula: $C_{29}H_{18}N_3O_2S$: 472.1114 $[M+H]^+$ found: 472.1117.

2-(3-Phenylbenzo[4,5]imidazo[2,1-*b*]thiazol-6-yl)-1*H*-benzo[*de*]isoquinoline-1,3(2*H*)-dione. 5h

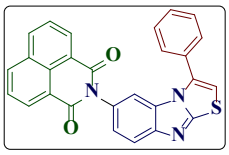

White solid: yield: 89%; mp. 276-278 ºC; FT-IR (KBr, cm^{-1}): 1745 (imide –C=O); ^{1}H NMR (400 MHz, DMSO-d_6 δ ppm): 7.94 – 7.92 (m, 2H, Ar-H), 7.86 – 7.83 (m, 2H, Ar-H), 7.78 (d, *J* = 6.4 Hz, 2H, Ar-H), 7.73 (d, *J* = 8.4 Hz, 2H, Ar-H), 7.66 (s, 1H, Ar-H), 7.43 – 7.41 (m, 2H, Ar-H), 7.35-7.32 (m, 2H, Ar-H), 7.30 (s, 1H, Ar-H), 7.21 (dd, *J* = 8.8, 1.6 Hz, 1H, Ar-H); ^{13}C NMR (100 MHz, DMSO-d_6) δ: 166.37, 157.29, 153.45, 141.82, 139.47, 136.02, 132.14, 131.42, 129.53, 128.50, 127.62, 127.33, 127.19, 126.61, 124.69, 111.81, 109.20, 105.42, 79.54; ESI-HRMS: *m/z* Cacld for Chemical Formula: $C_{27}H_{16}N_3O_2S$: 446.0958 $[M+H]^+$ found: 446.0995.

5.8. Spectra

^{1}H-NMR Spectrum of compound 4a in DMSO-d_6 (400MHz):

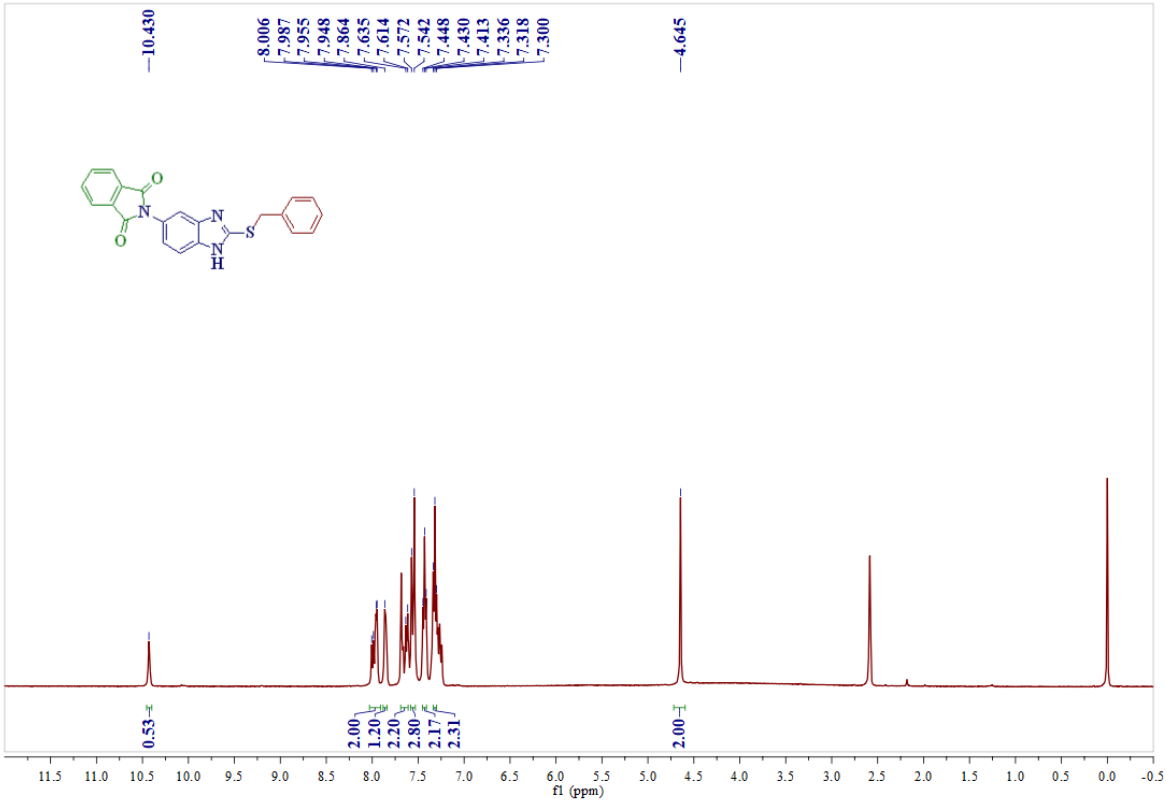

^{13}C-NMR Spectrum of compound 4a in DMSO-d_6 (100MHz):

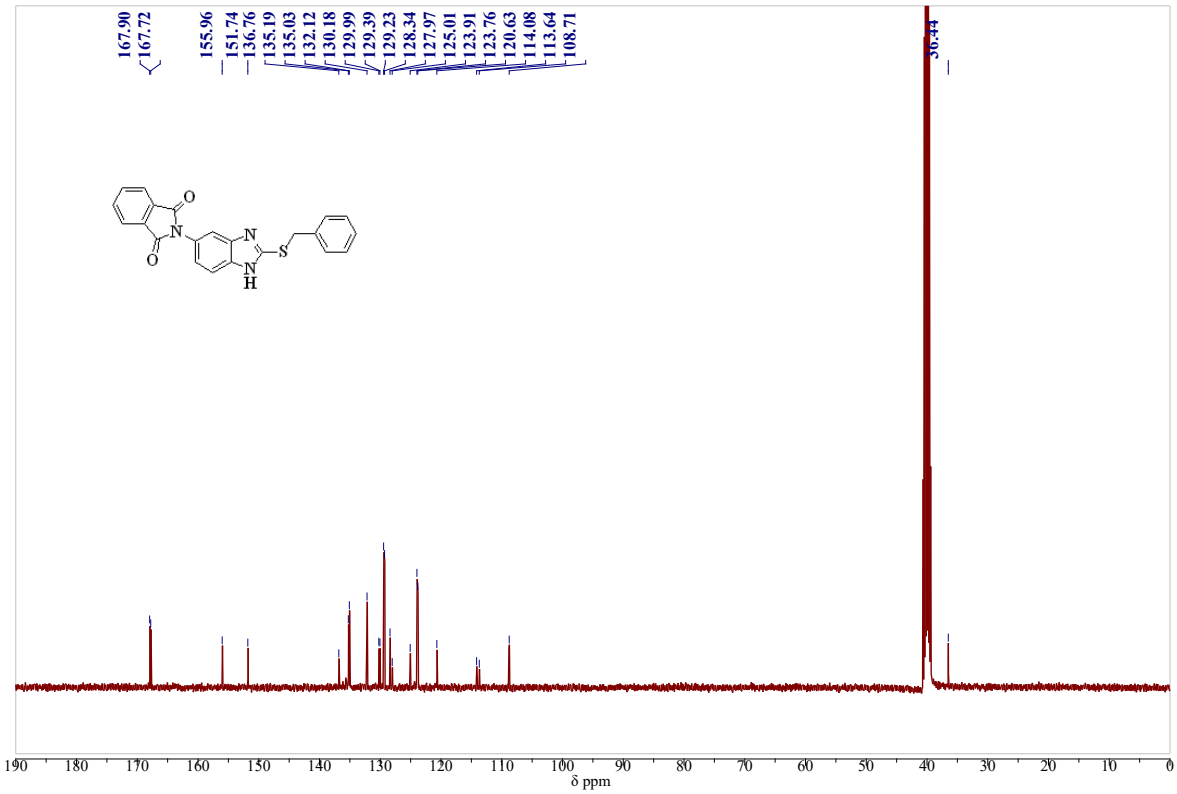

Mass spectrum of compound 4a:

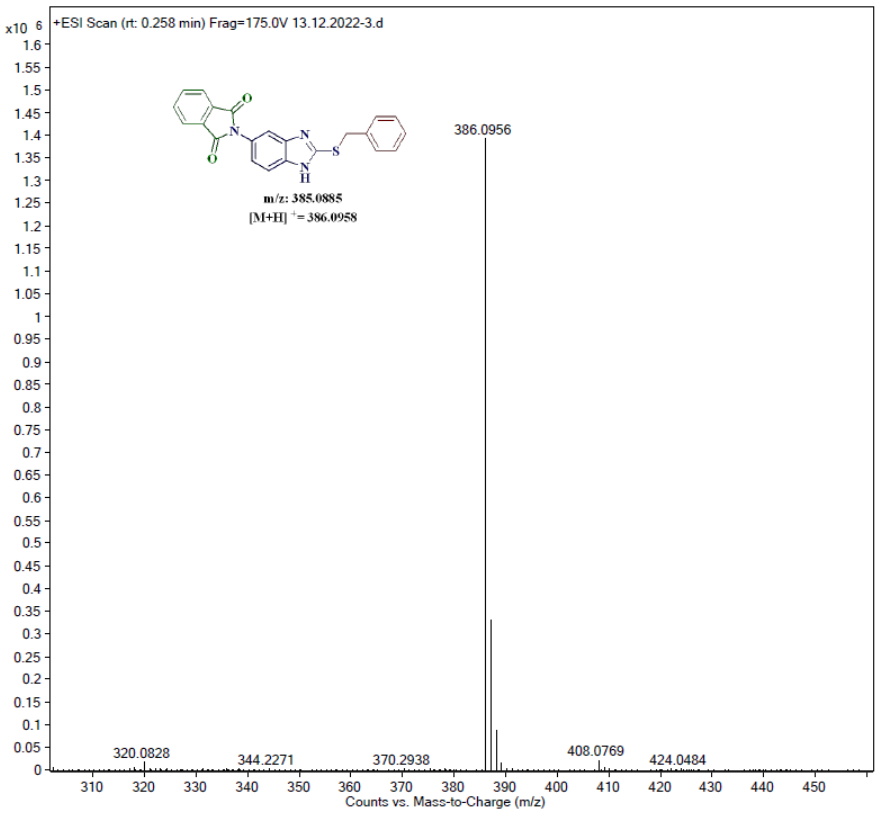

^{1}H-NMR Spectrum of compound 4b in DMSO-d_6 (400MHz):

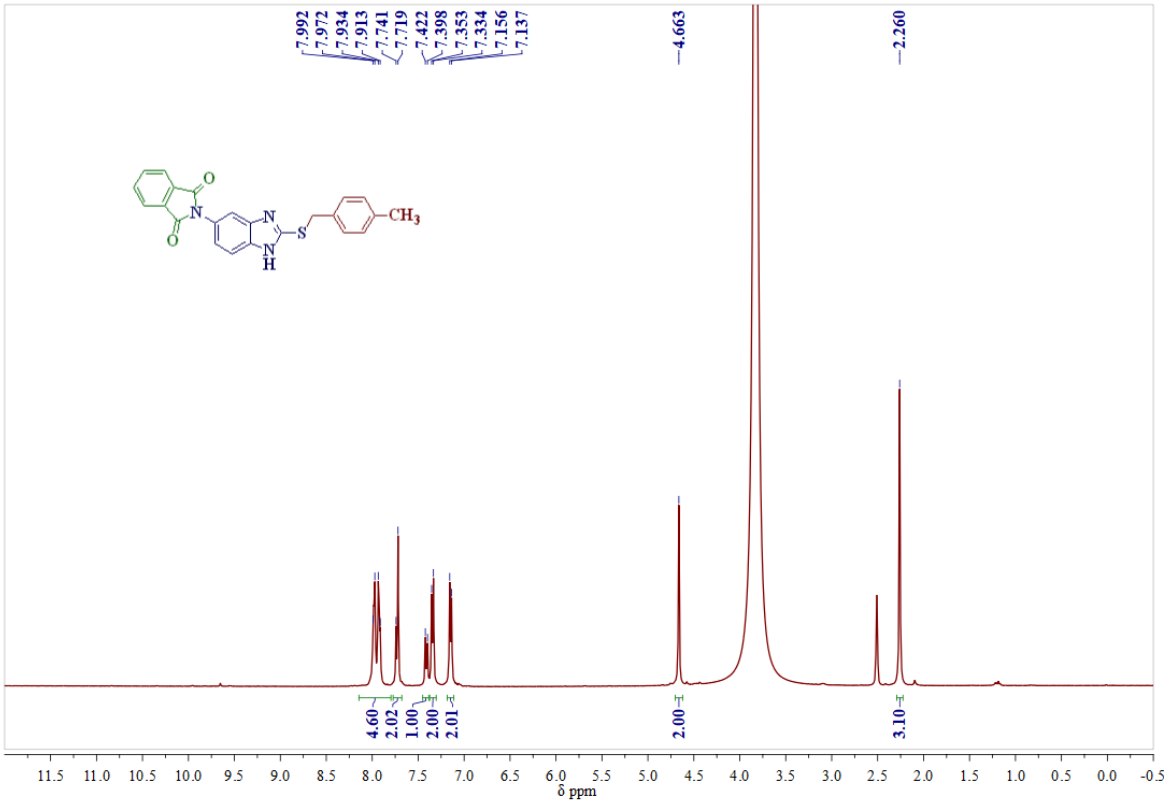

^{13}C-NMR Spectrum of compound 4b in DMSO-d_6 (100MHz):

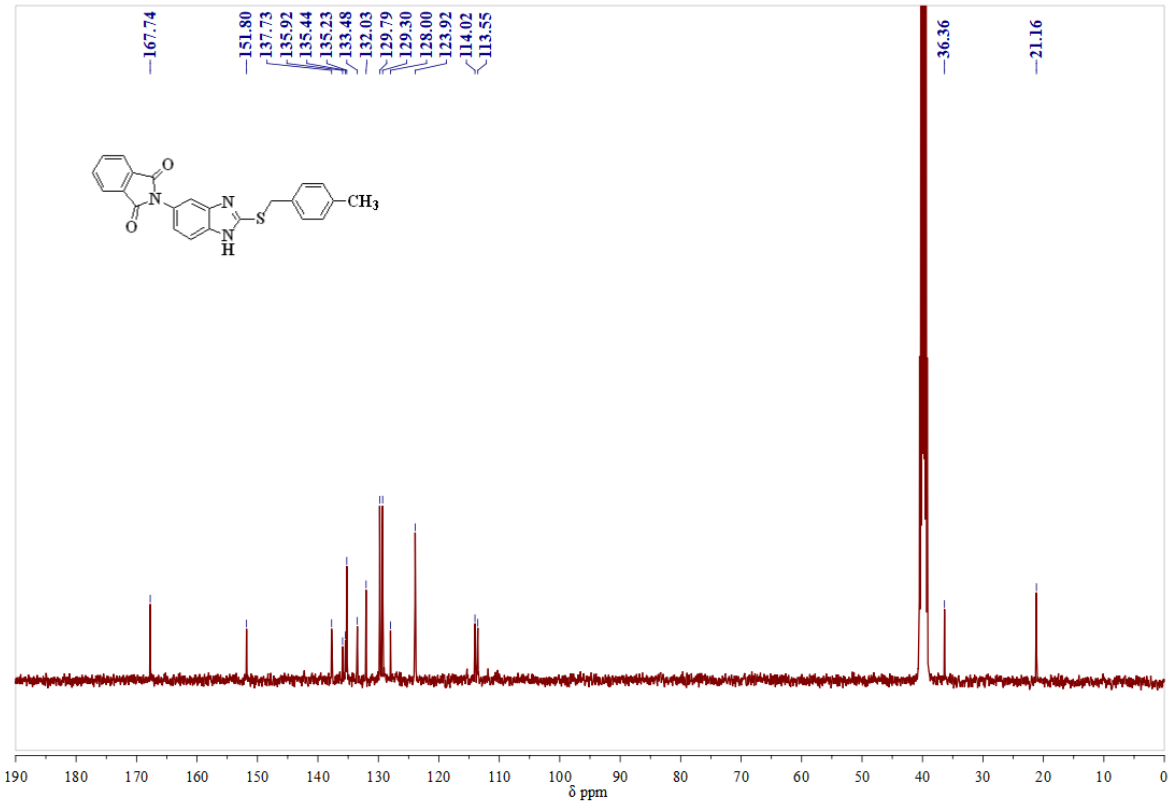

Mass spectrum of compound 4b:

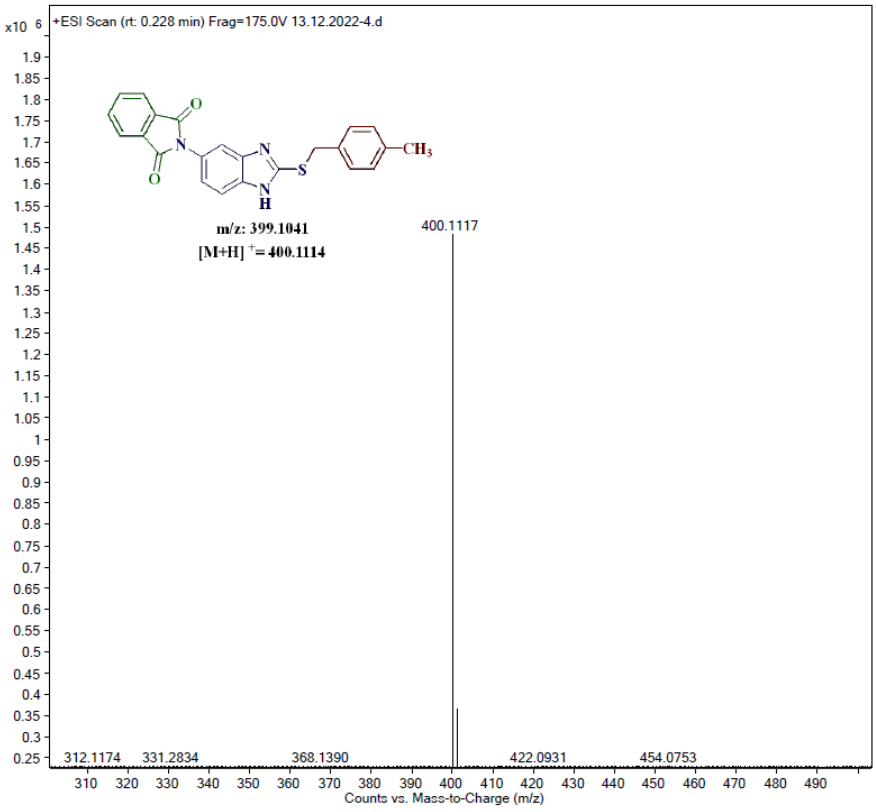

^{1}H-NMR Spectrum of compound 4c in DMSO-d_6 (400MHz):

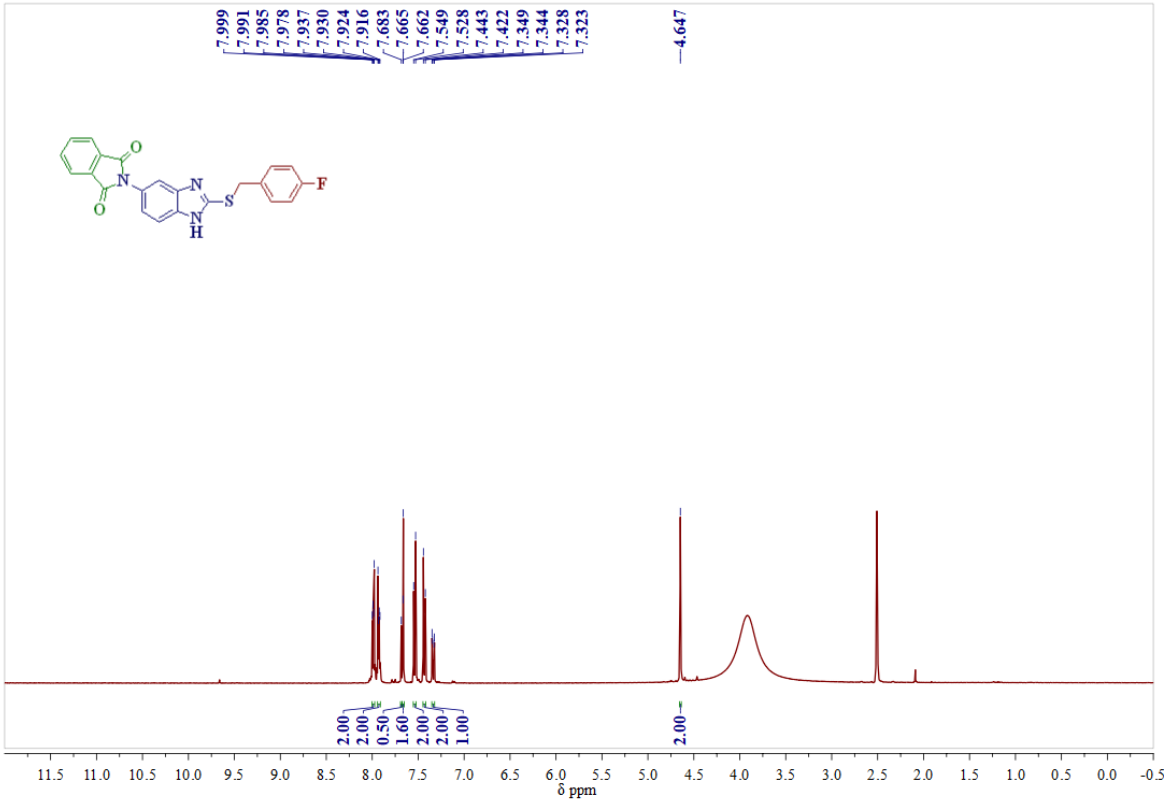

^{13}C-NMR Spectrum of compound 4c in DMSO-d_6 (100MHz):

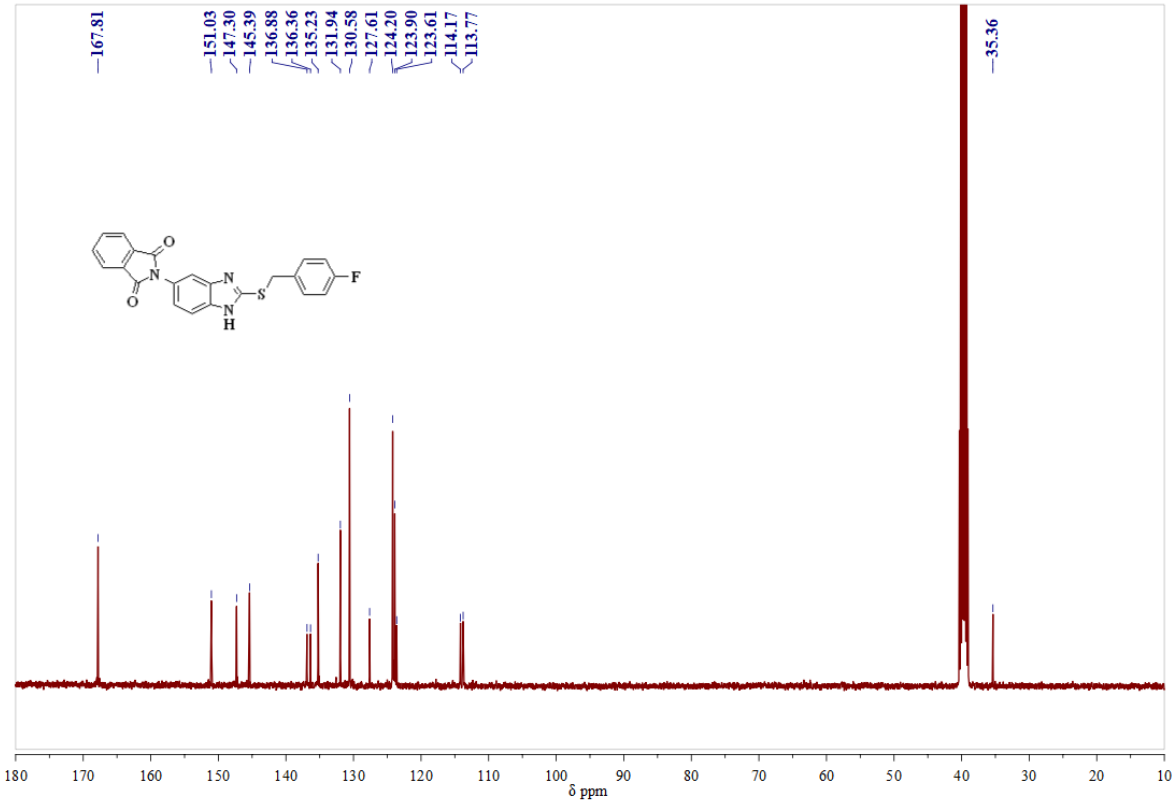

Mass spectrum of compound 4c:

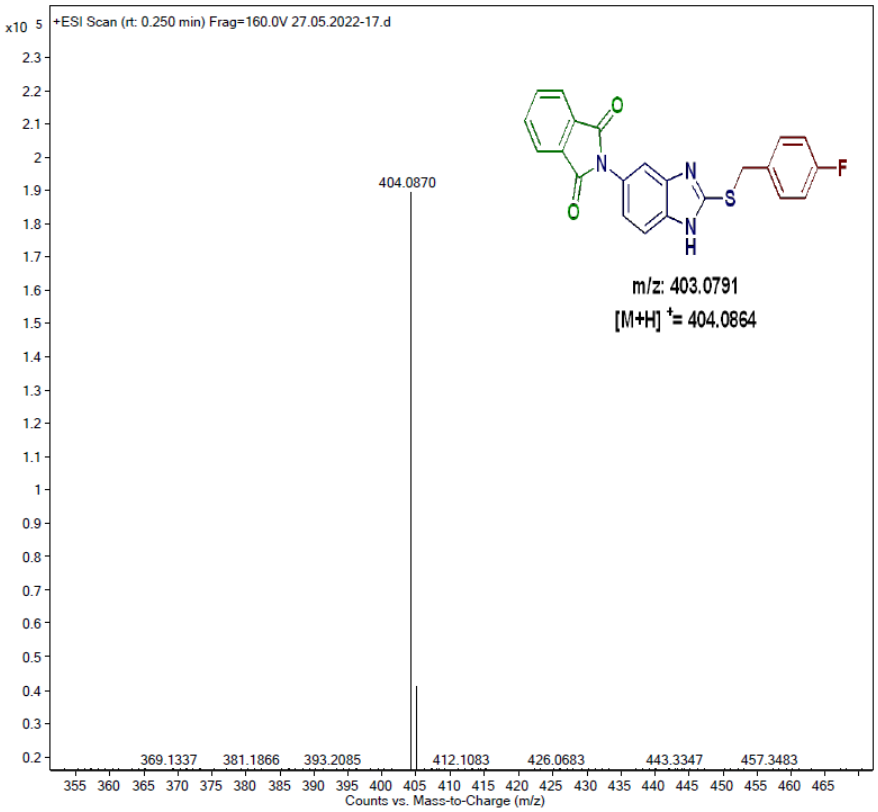

^{1}H-NMR Spectrum of compound 4d in DMSO-d_6 (400MHz):

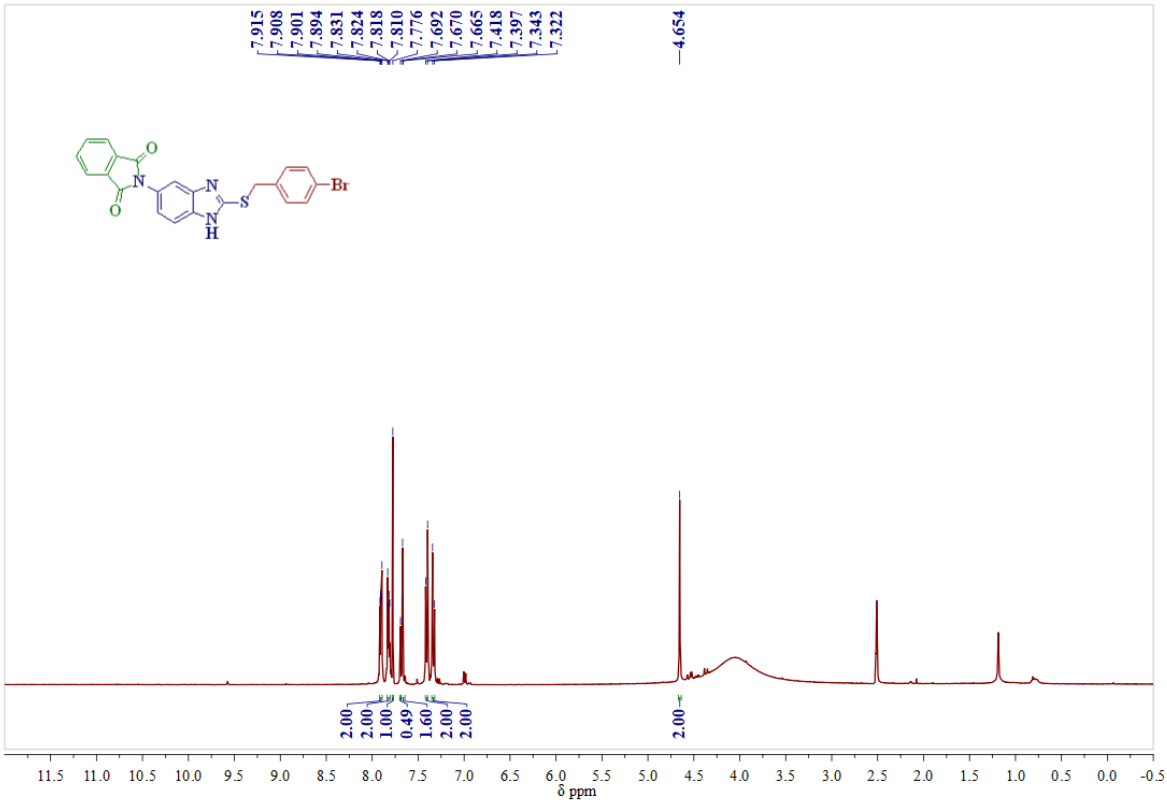

^{13}C-NMR Spectrum of compound 4d in CDCl$_3$-DMSO-*d*$_6$ (100MHz):

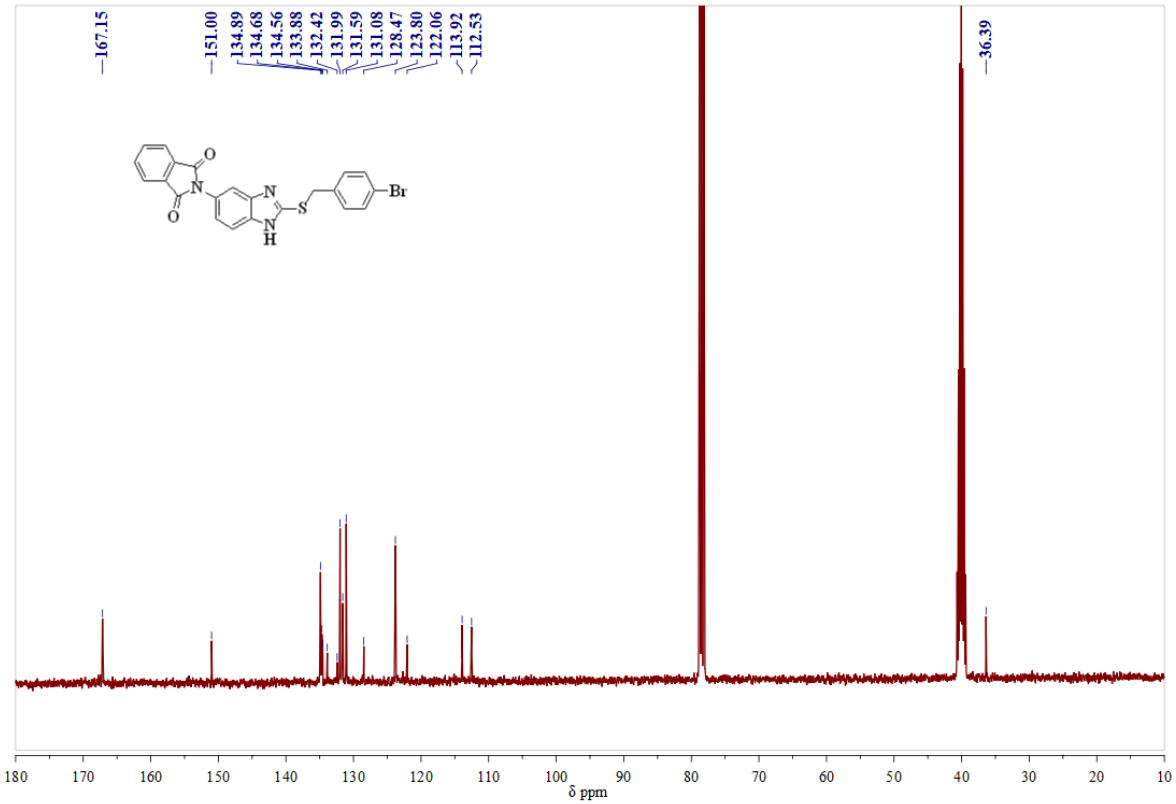

Mass spectrum of compound 4d:

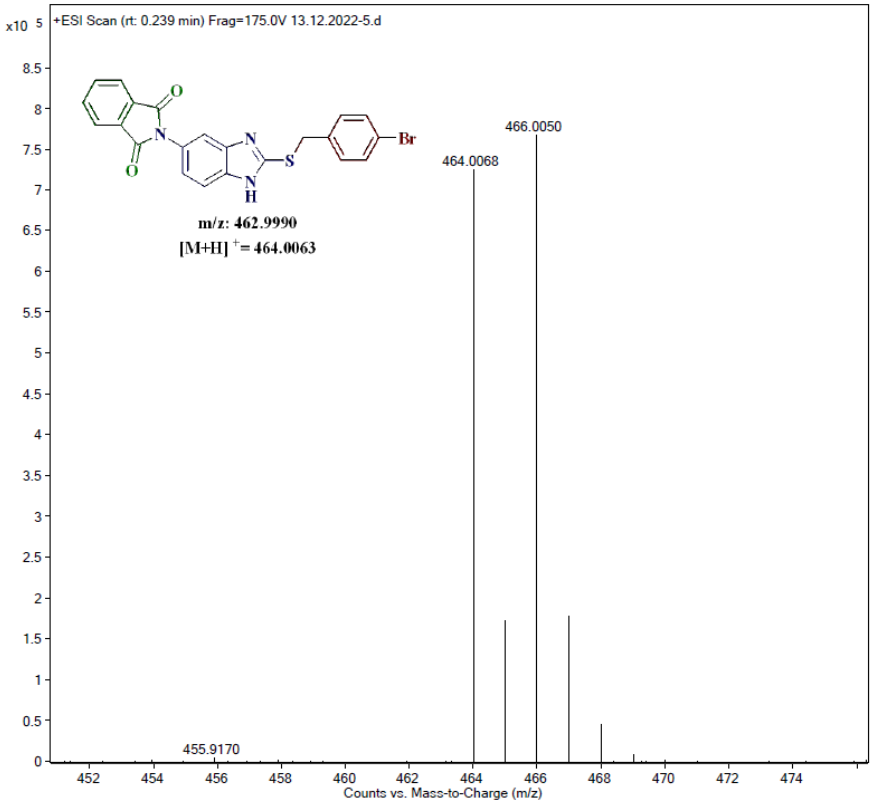

^{1}H-NMR Spectrum of compound 4e in DMSO-d_6 (400MHz):

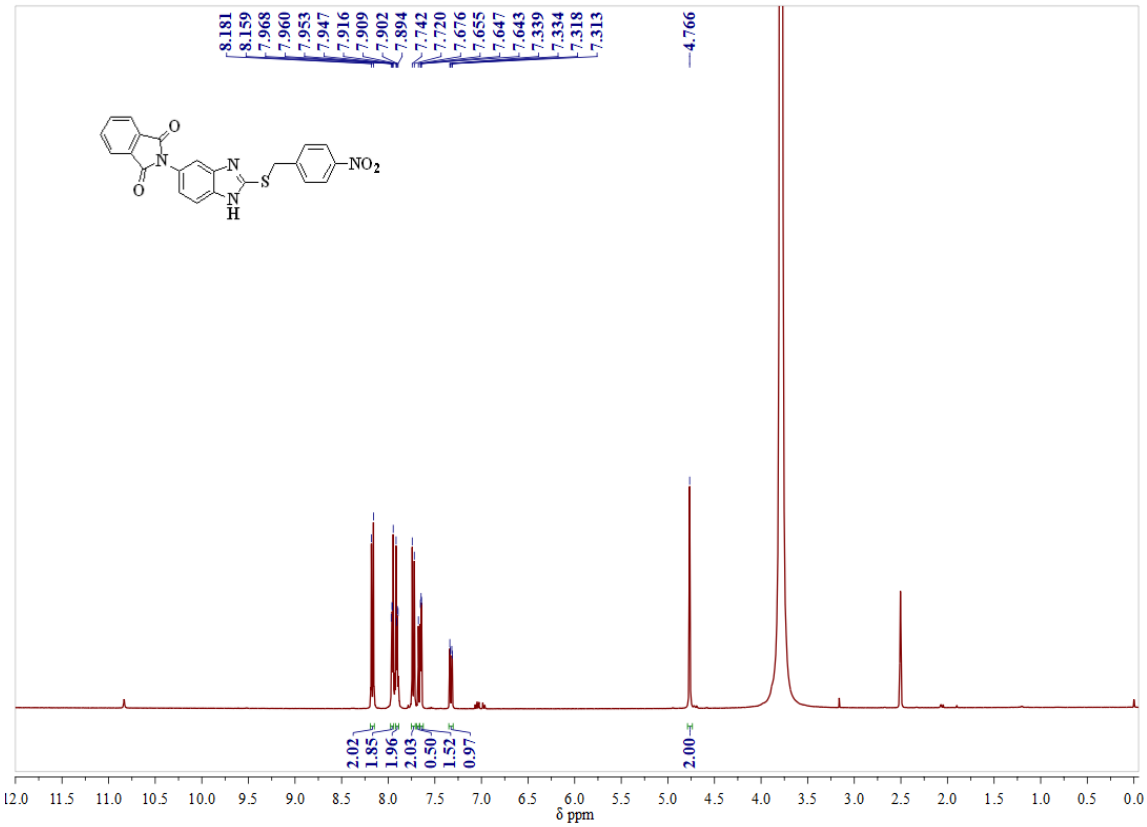

^{13}C-NMR Spectrum of compound 4e in DMSO-d_6 (100MHz):

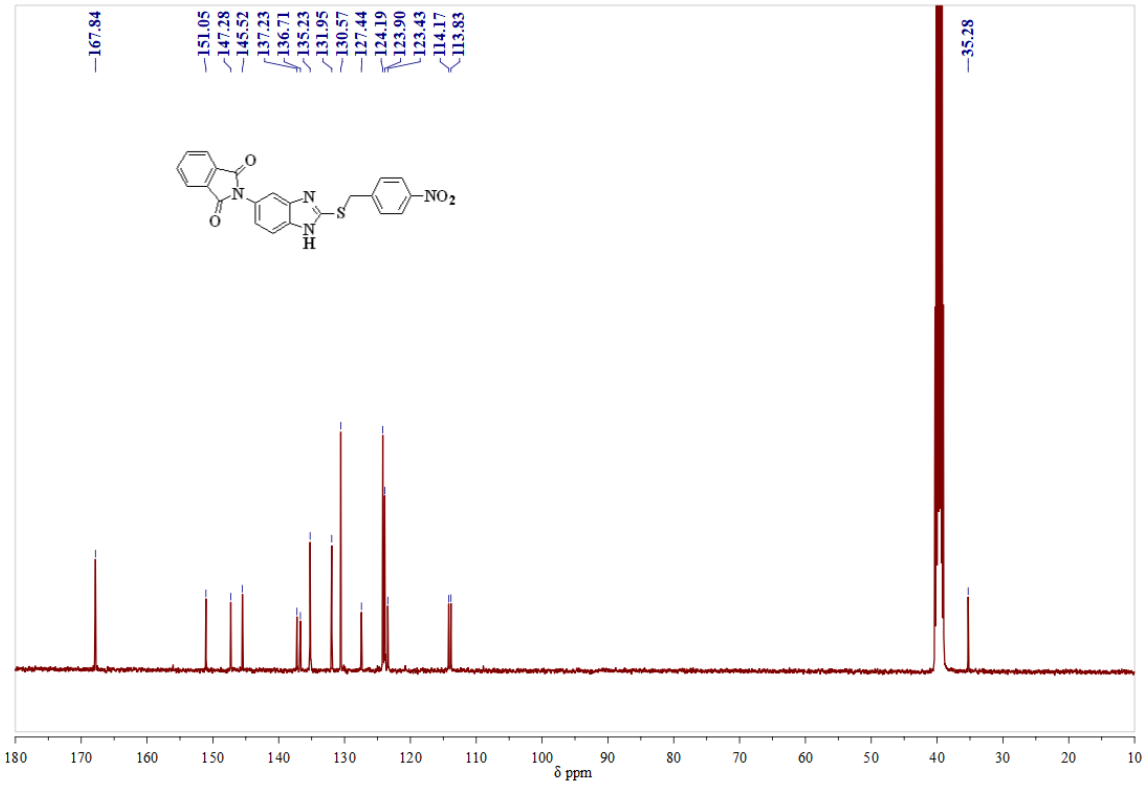

Mass spectrum of compound 4e:

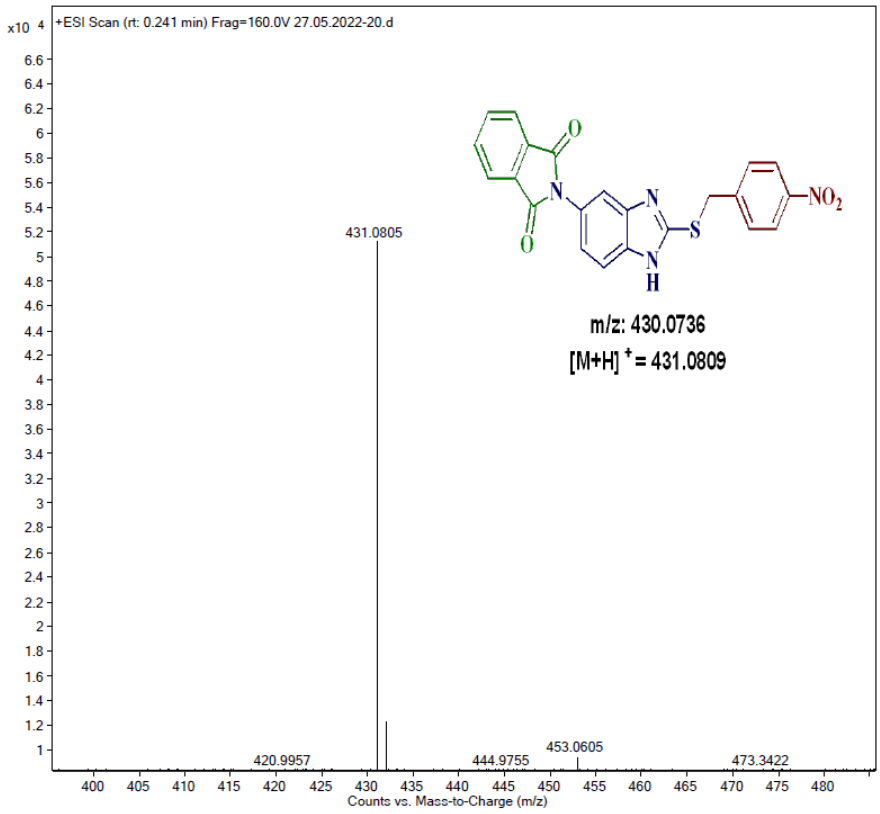

^{1}H-NMR Spectrum of compound 4f in DMSO-d_6 (400 MHz):

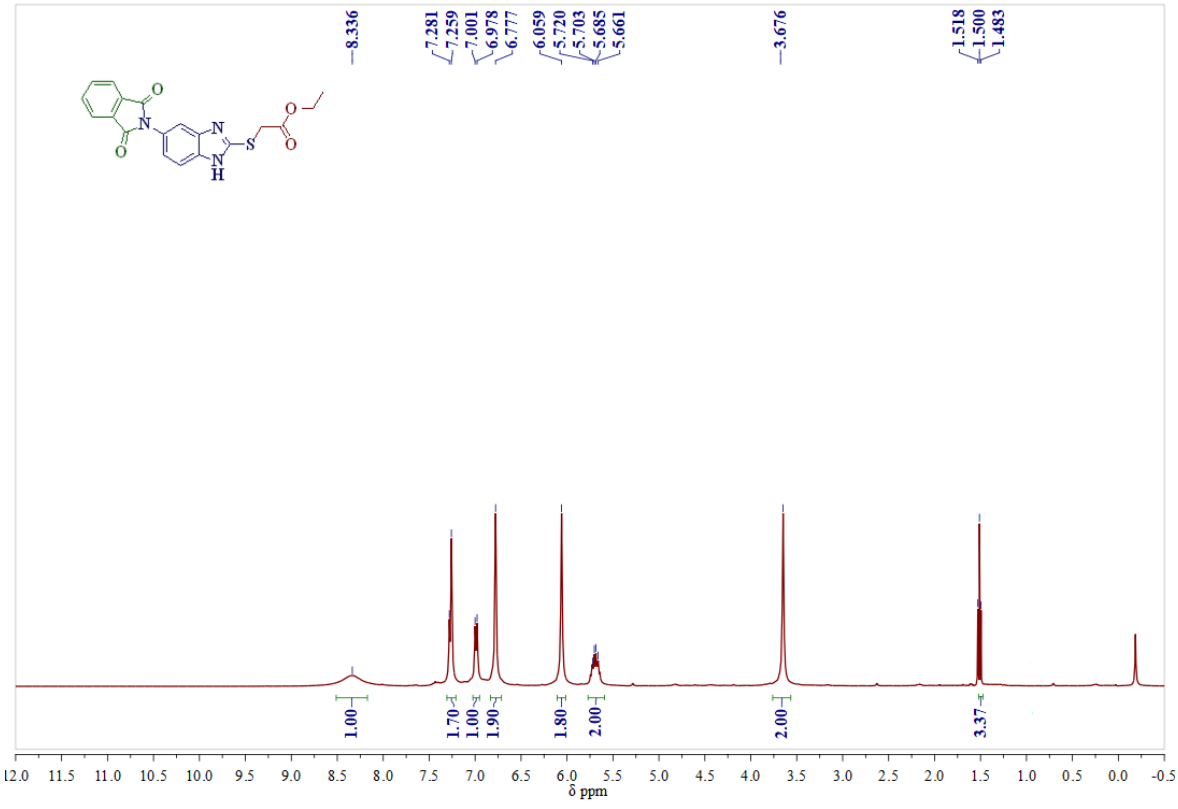

^{13}C-NMR Spectrum of compound 4f in CDCl$_3$-DMSO-d_6 (100MHz):

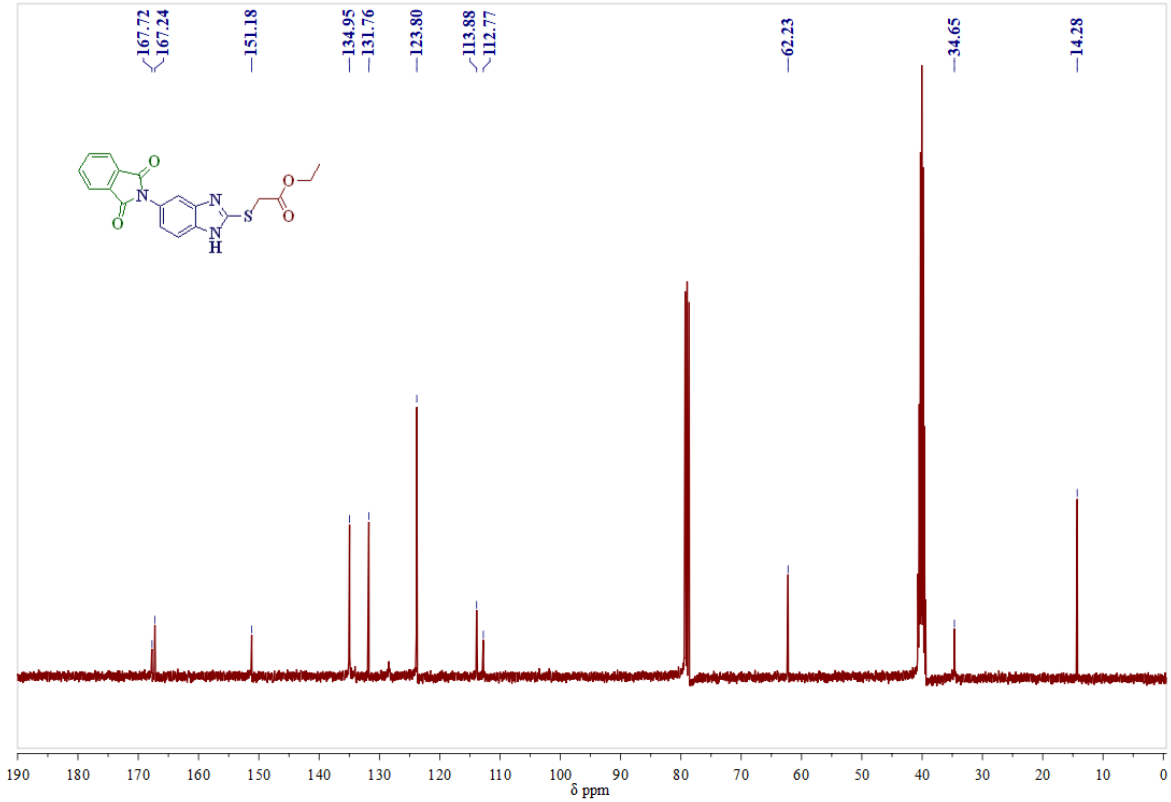

Mass spectrum of compound 4f

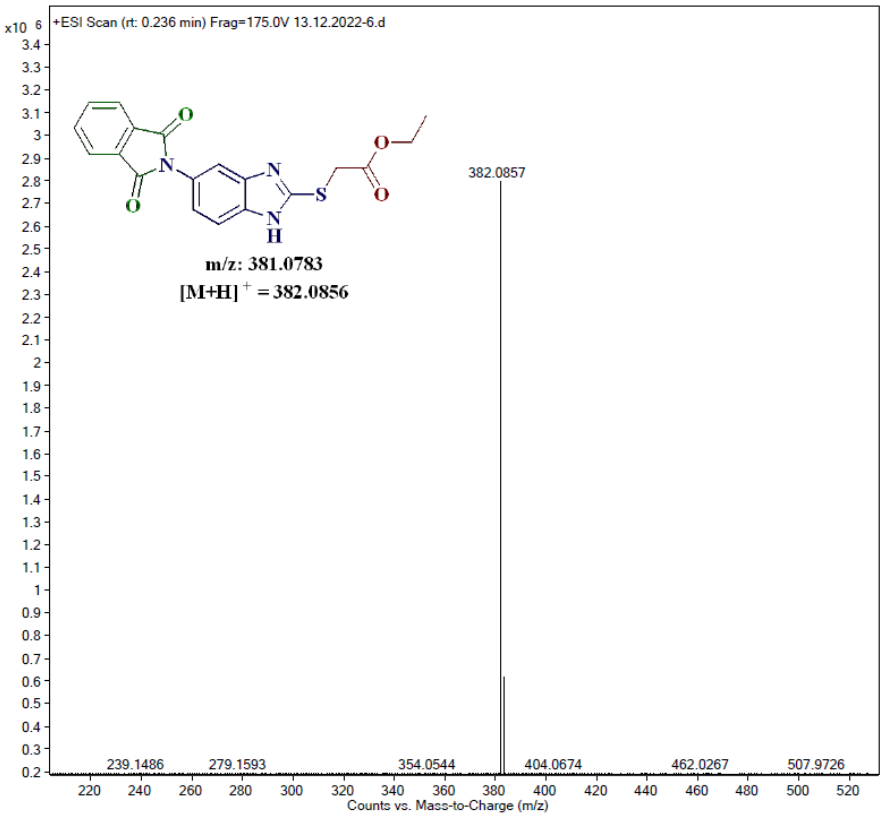

^{1}H-NMR Spectrum of compound 4g in DMSO-d_6 (400MHz):

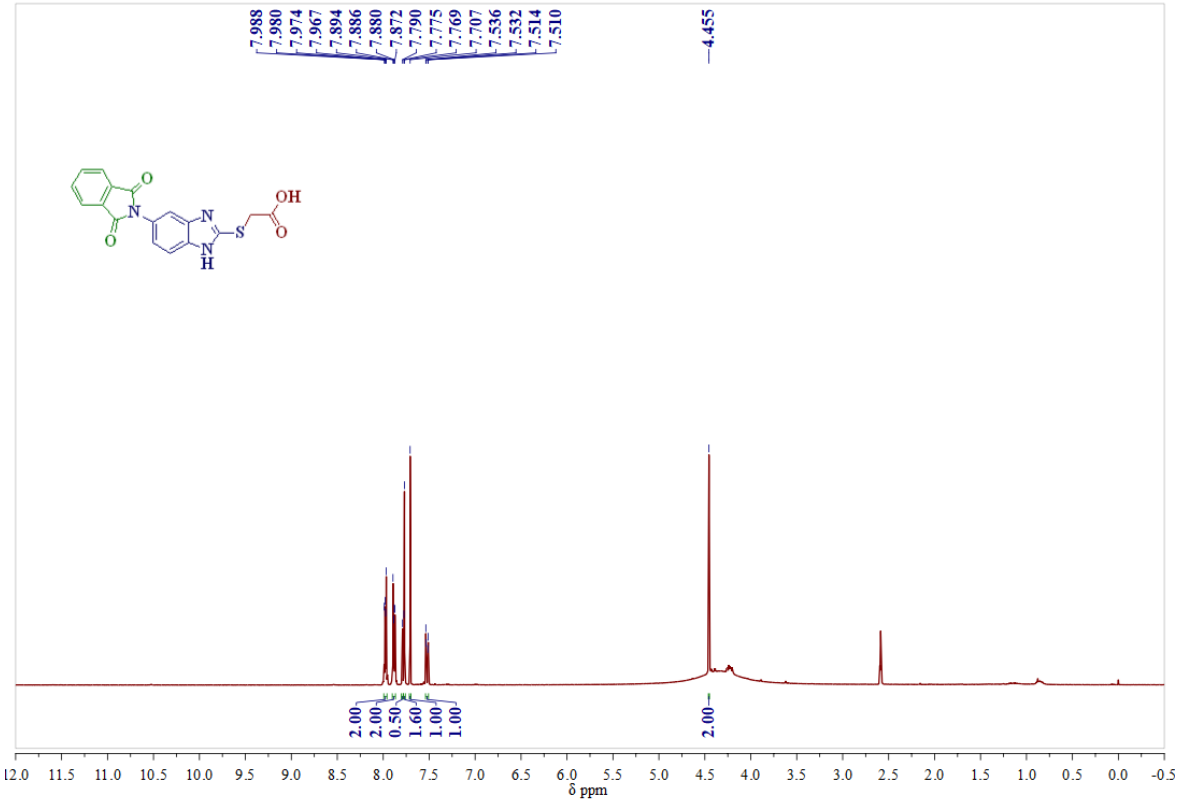

^{13}C-NMR Spectrum of compound 4g in $CDCl_3$-DMSO-d_6 (100MHz):

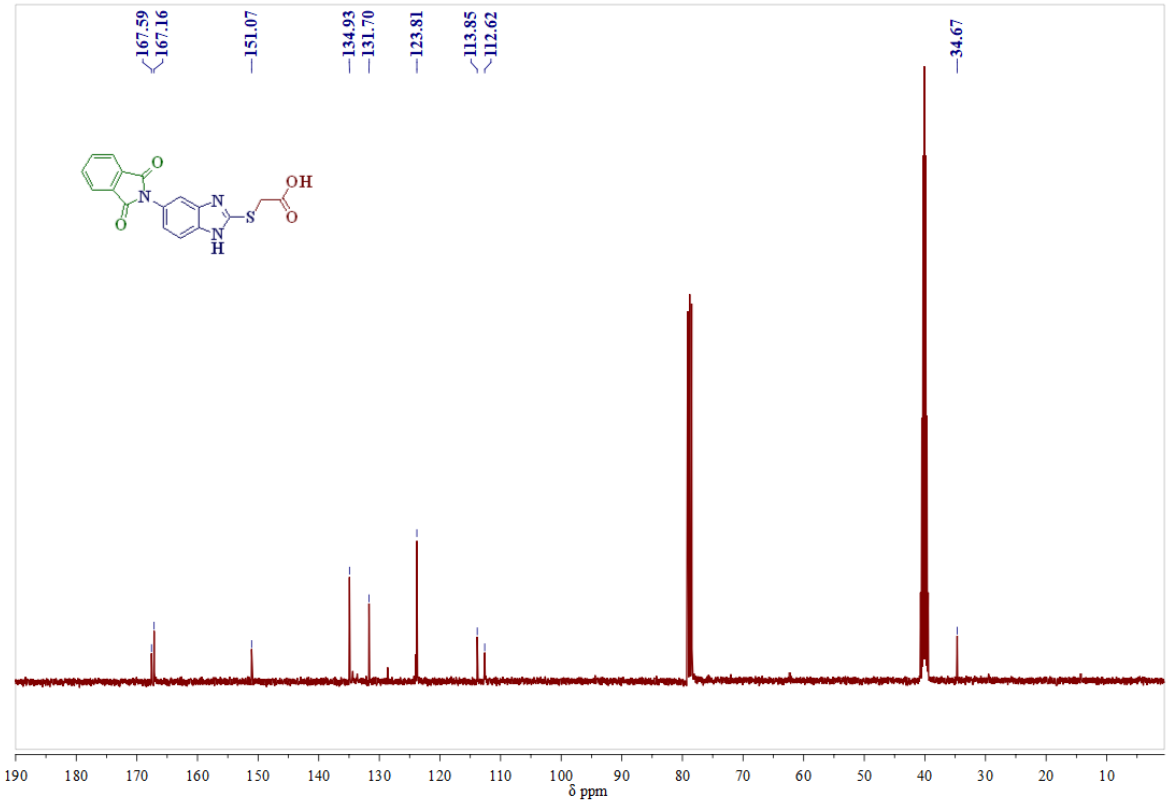

Mass spectrum of compound 4g:

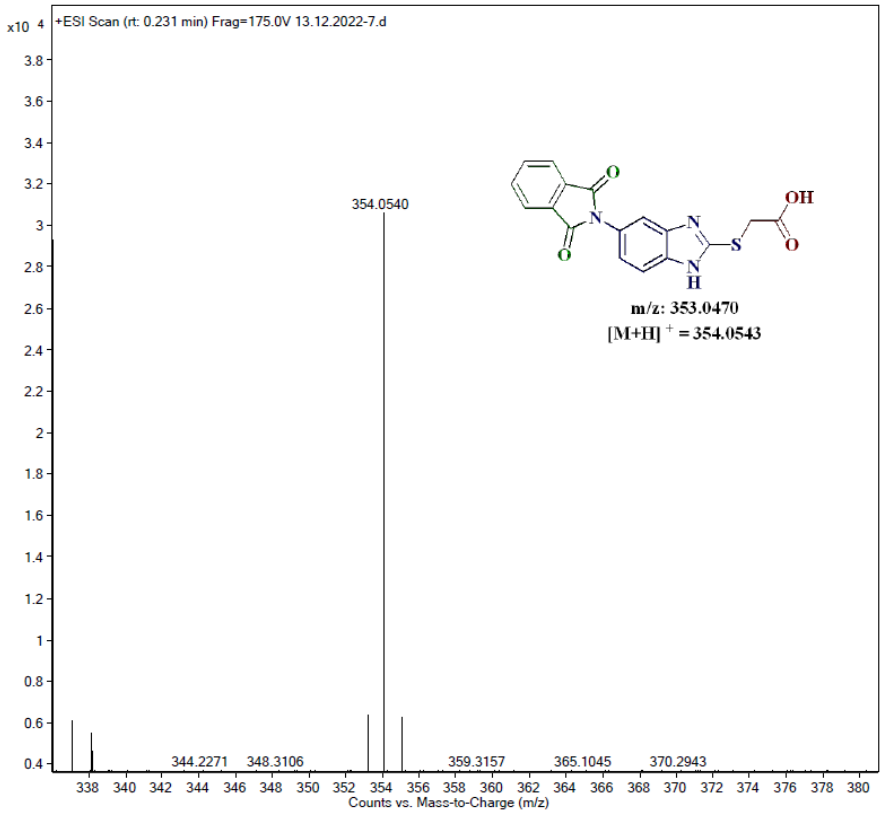

^{1}H-NMR Spectrum of compound 4h in DMSO-d_6 (400MHz):

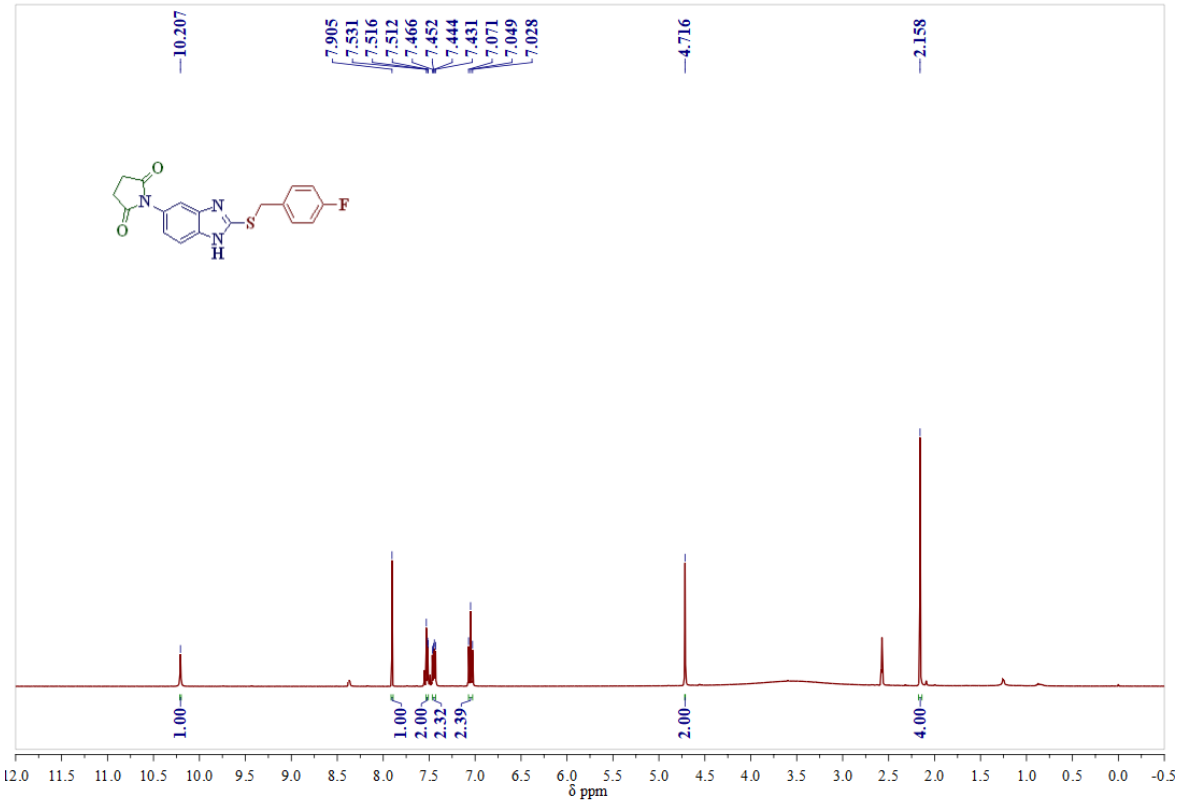

^{13}C-NMR Spectrum of compound 4h in CDCl$_3$-DMSO-d_6 (100MHz):

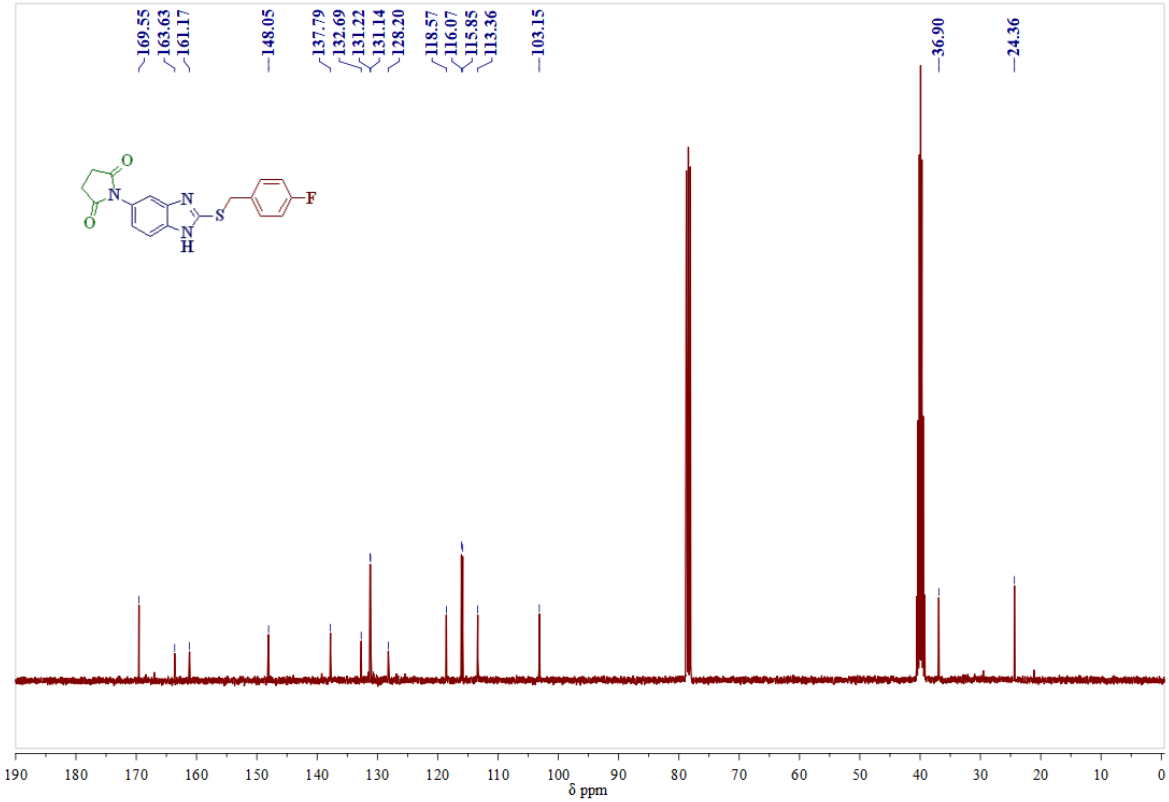

Mass spectrum of compound 4h

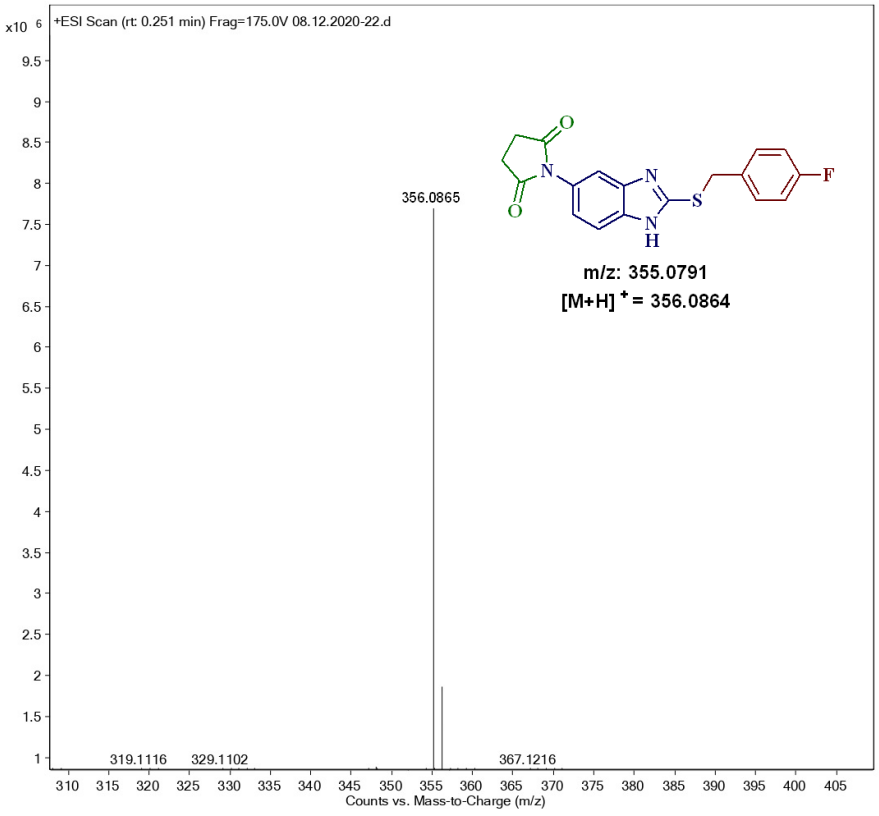

^{1}H-NMR Spectrum of compound 4i in DMSO-d_6 (400 MHz):

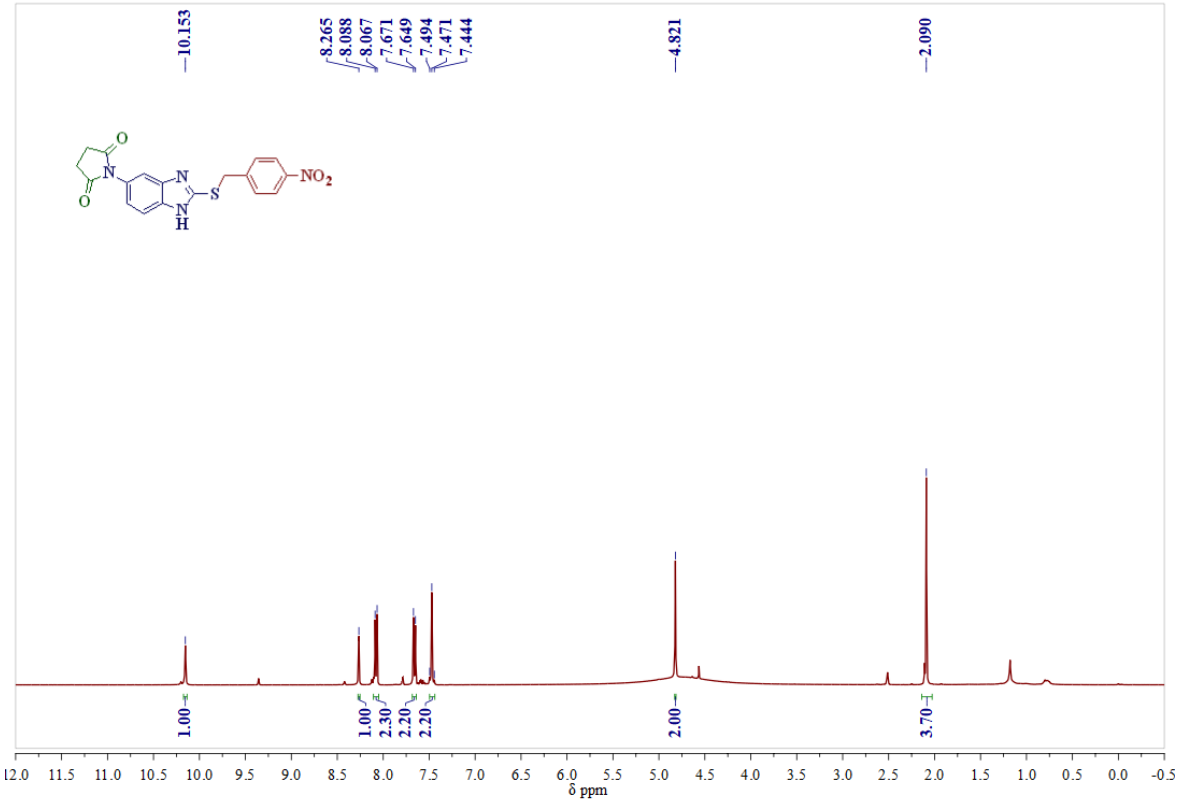

^{13}C-NMR Spectrum of compound 4i in DMSO-d_6 (100MHz):

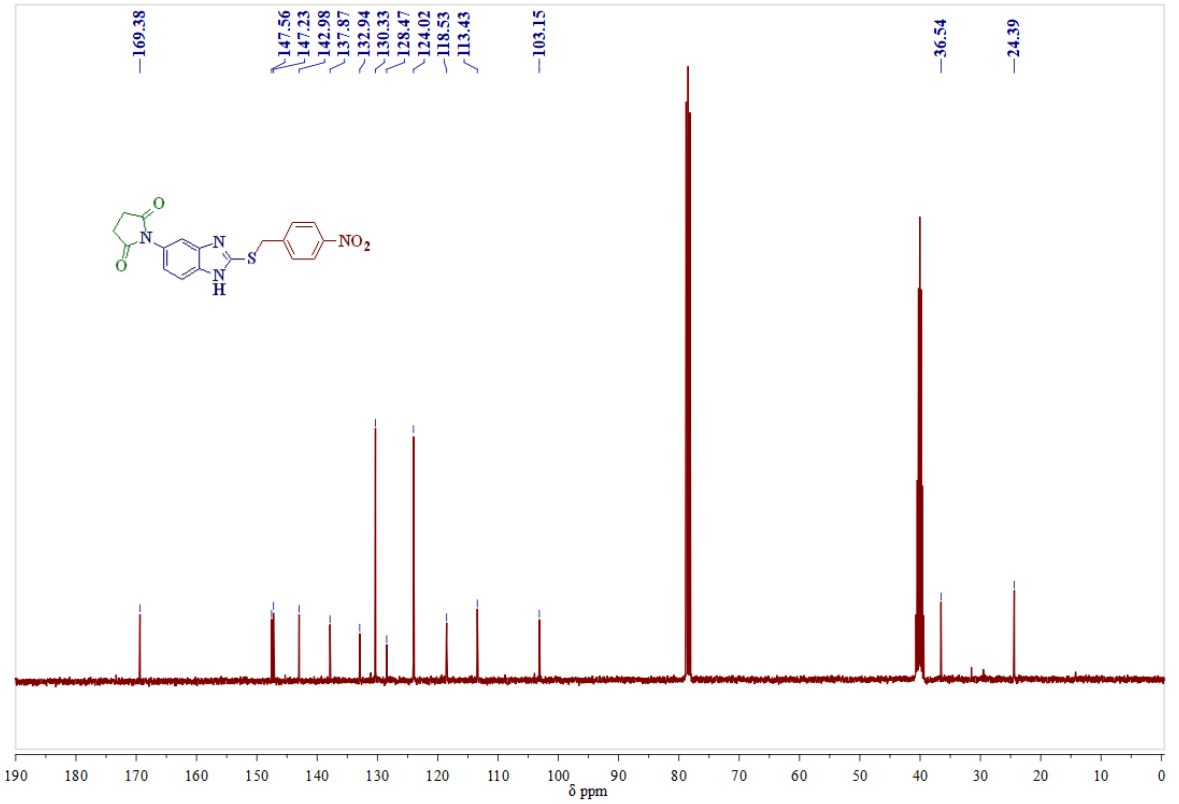

Mass spectrum of compound 4i

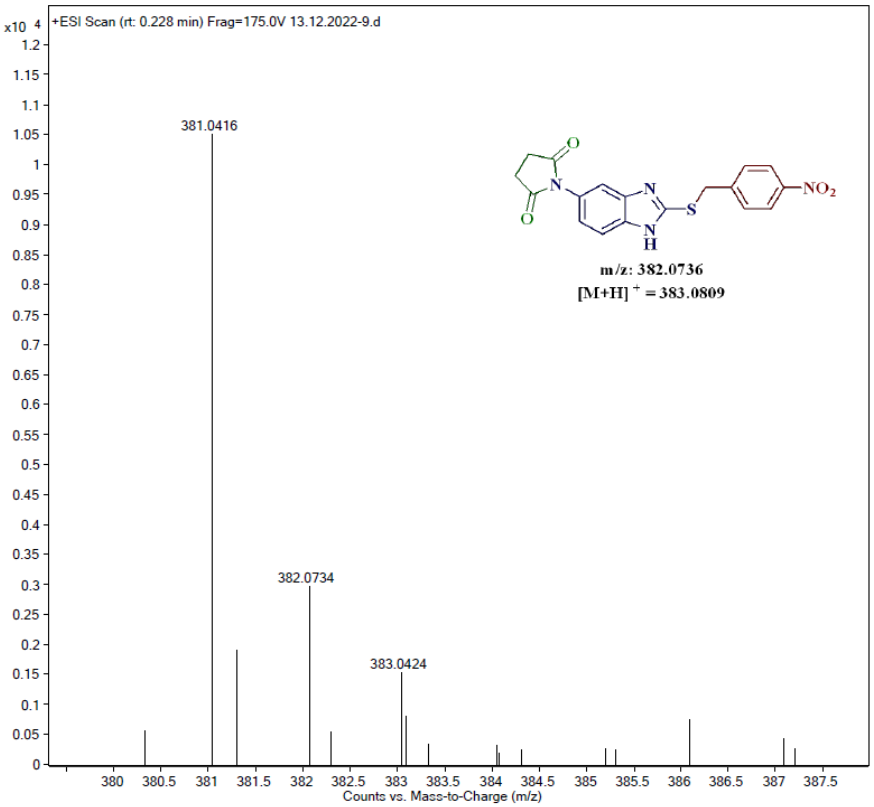

^{1}H-NMR Spectrum of compound 4j in DMSO-d_6 (400MHz):

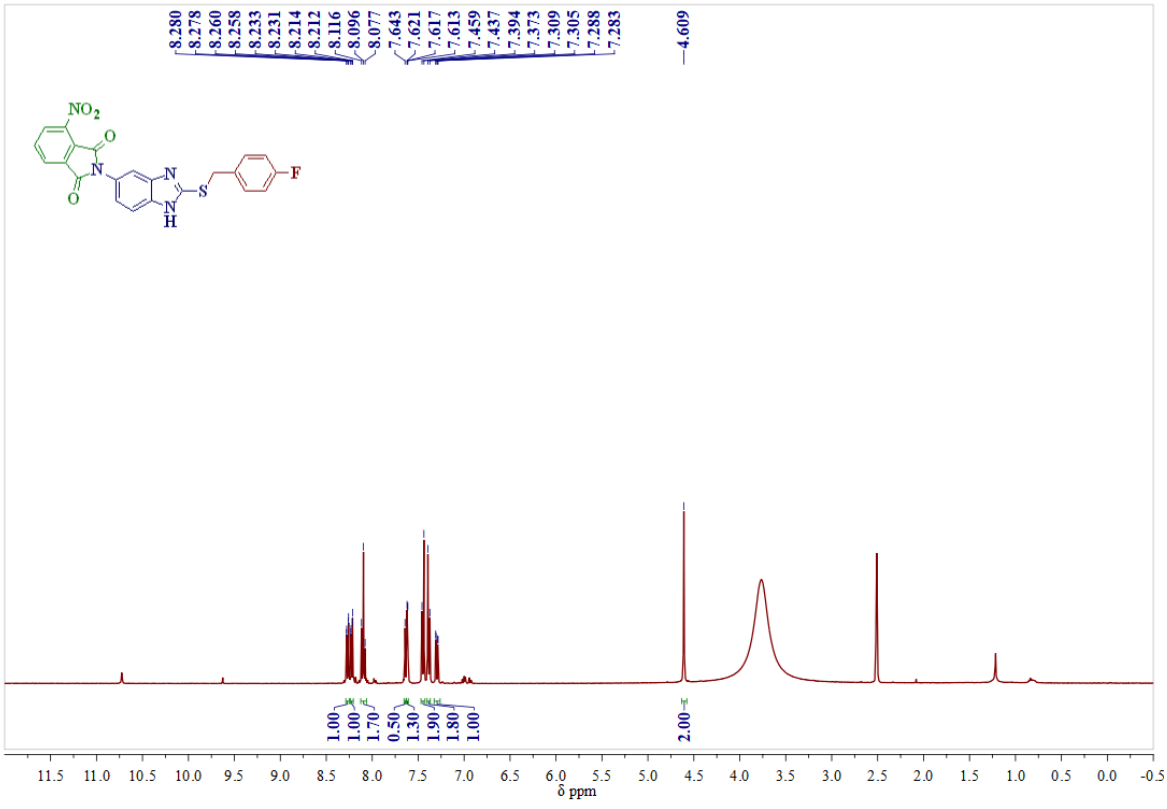

^{13}C-NMR Spectrum of compound 4j in DMSO-d_6 (100MHz):

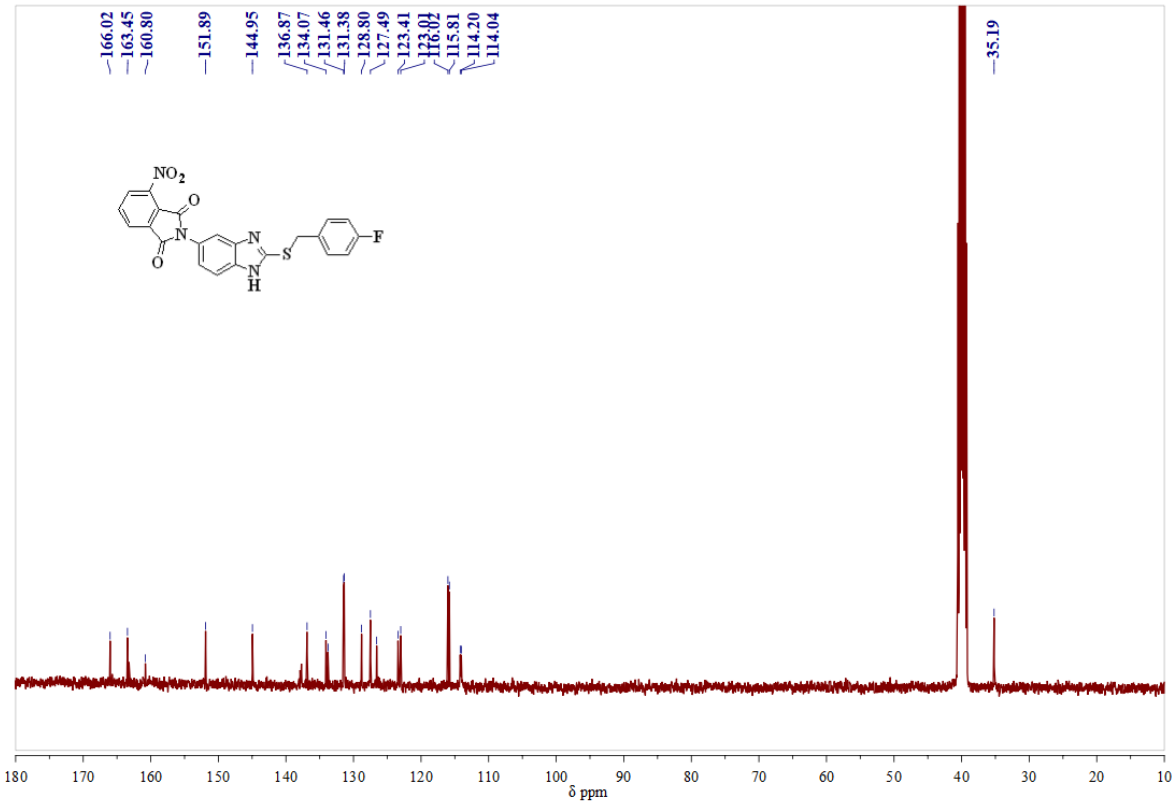

Mass spectrum of compound 4j:

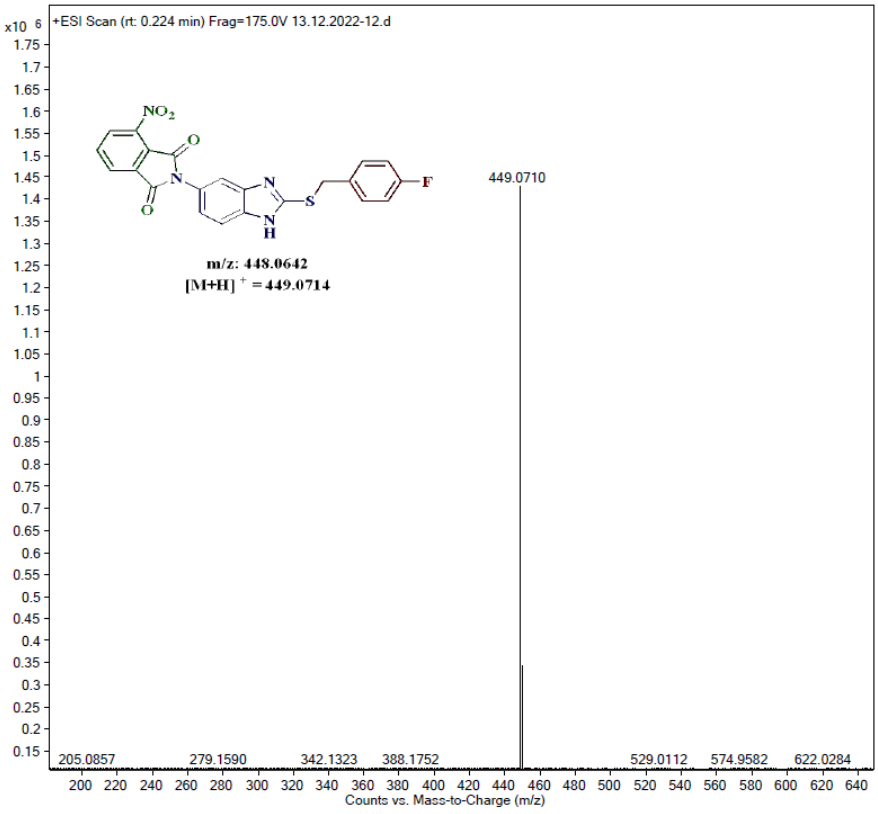

^{1}H-NMR Spectrum of compound 4k in DMSO-d_6 (400MHz):

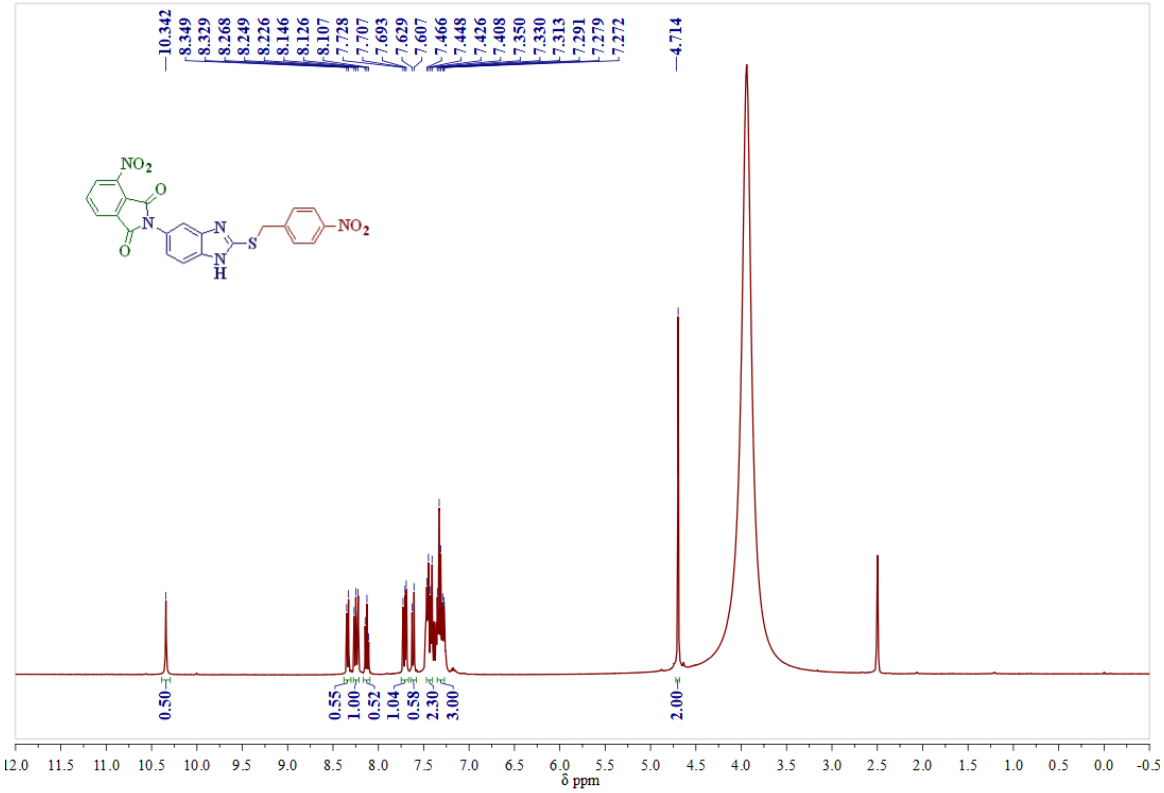

^{13}C-NMR Spectrum of compound 4k in CDCl$_3$-DMSO-d_6 (100MHz):

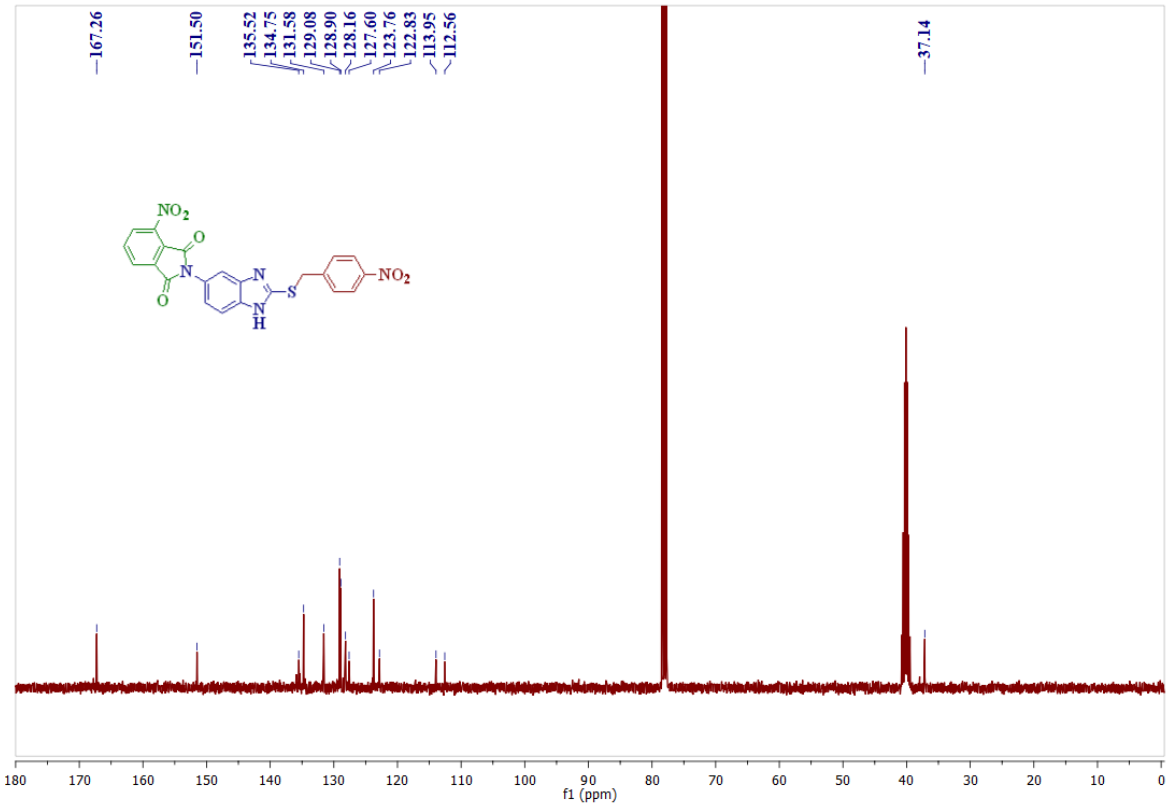

Mass spectrum of compound 4k

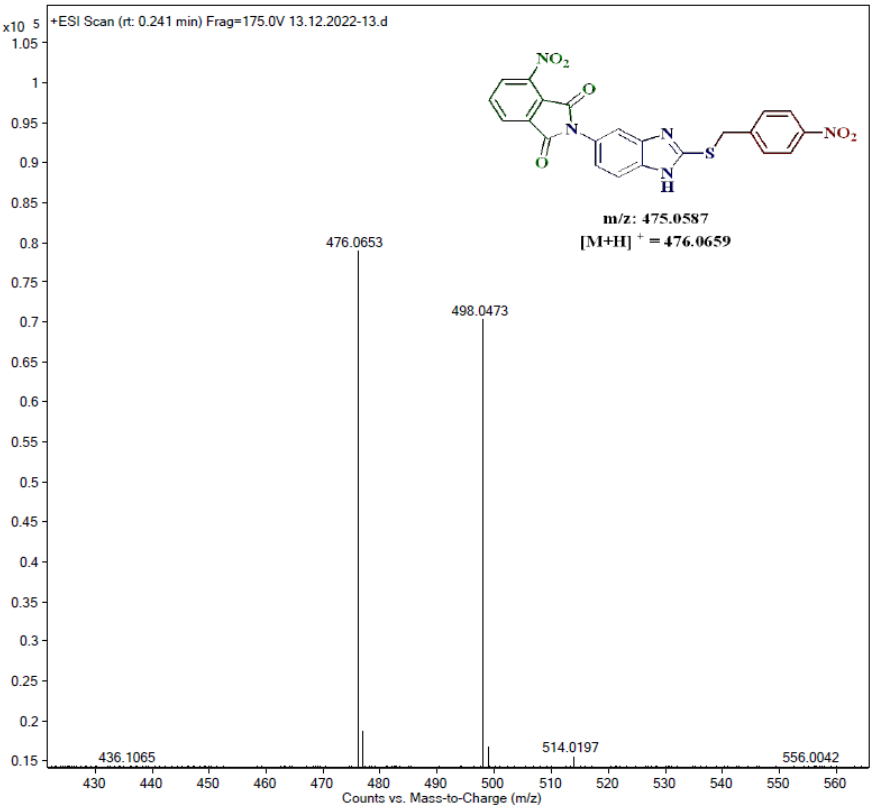

^{1}H-NMR Spectrum of compound 4l in DMSO-d_6 (400MHz):

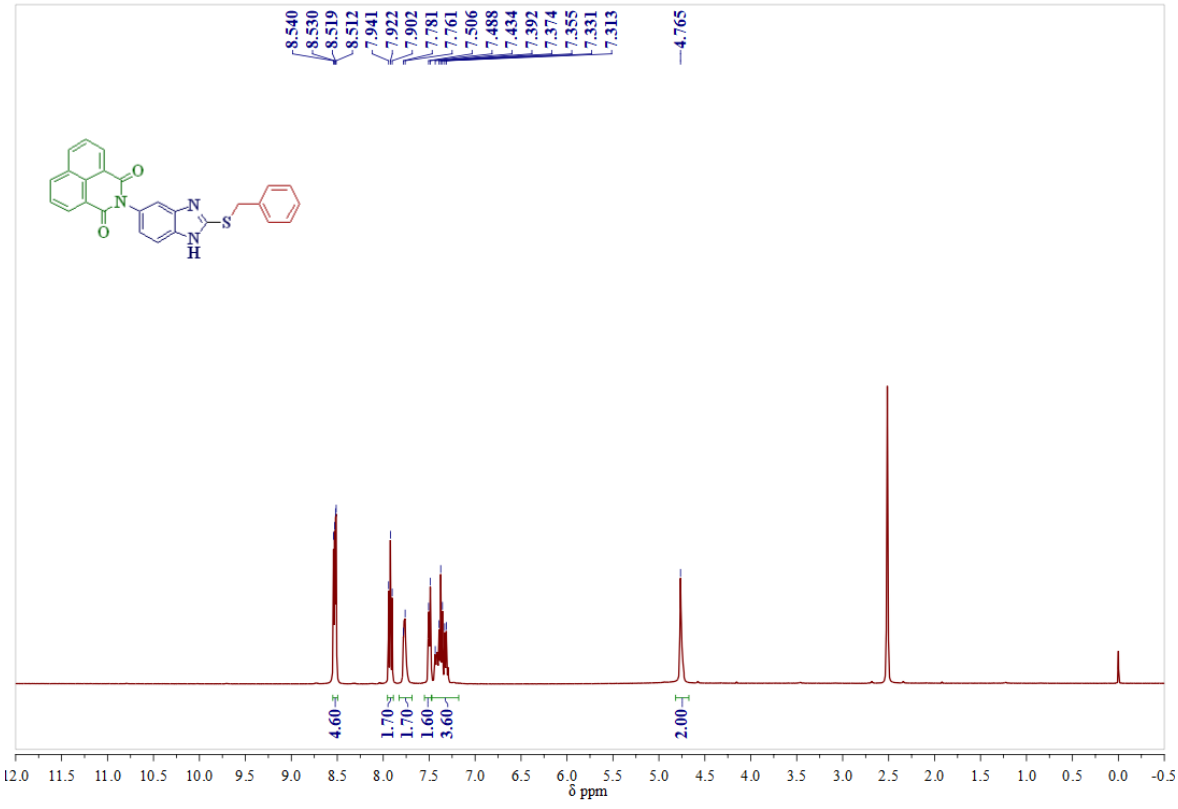

^{13}C-NMR Spectrum of compound 4l in DMSO-d_6 (100MHz):

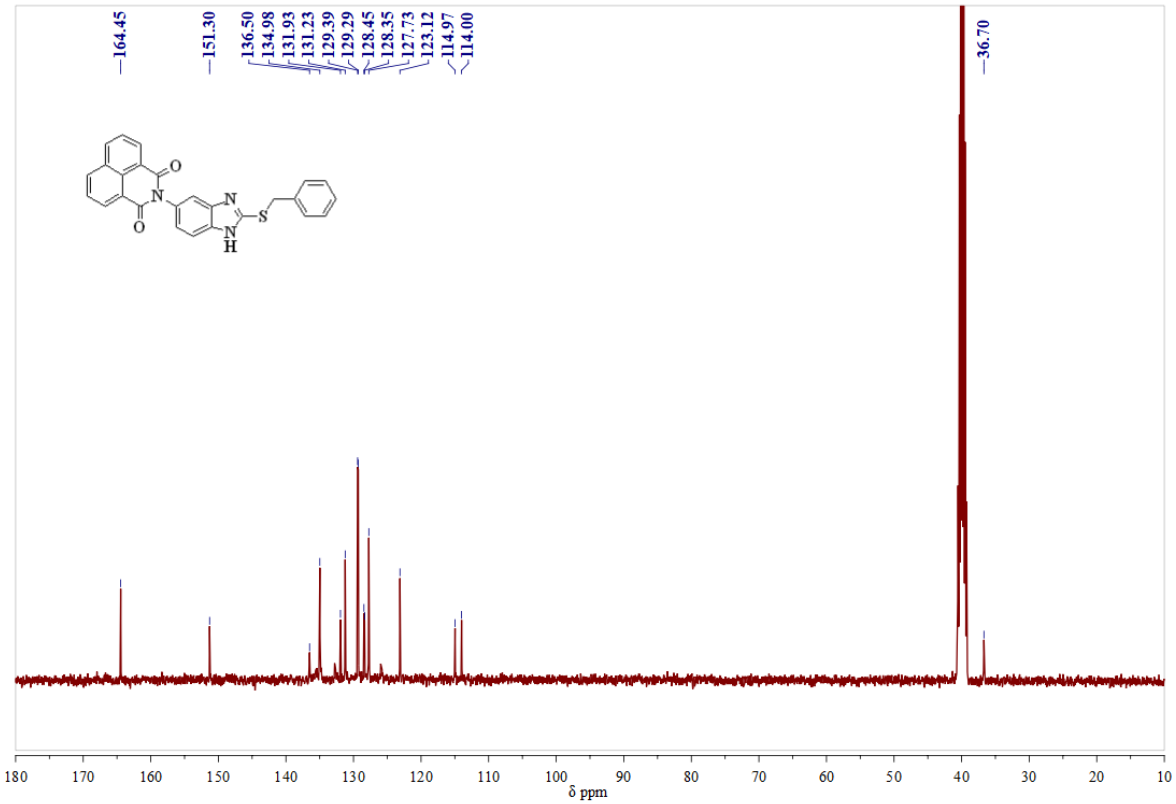

Mass spectrum of compound 4l

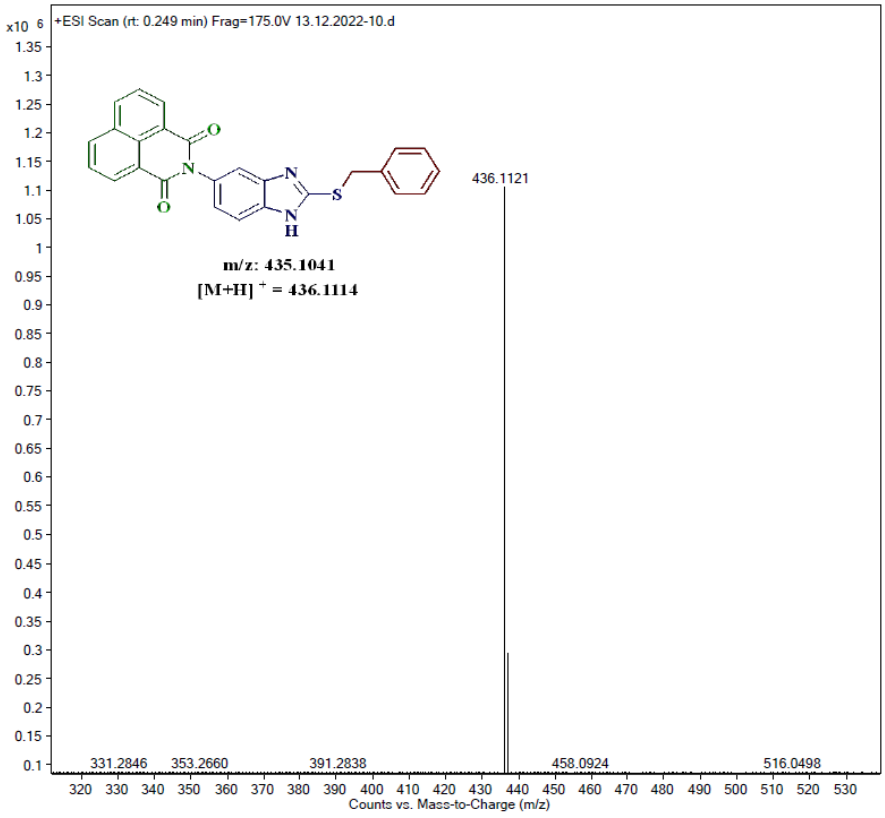

^{1}H-NMR Spectrum of compound 4m in DMSO-d_6 (400MHz):

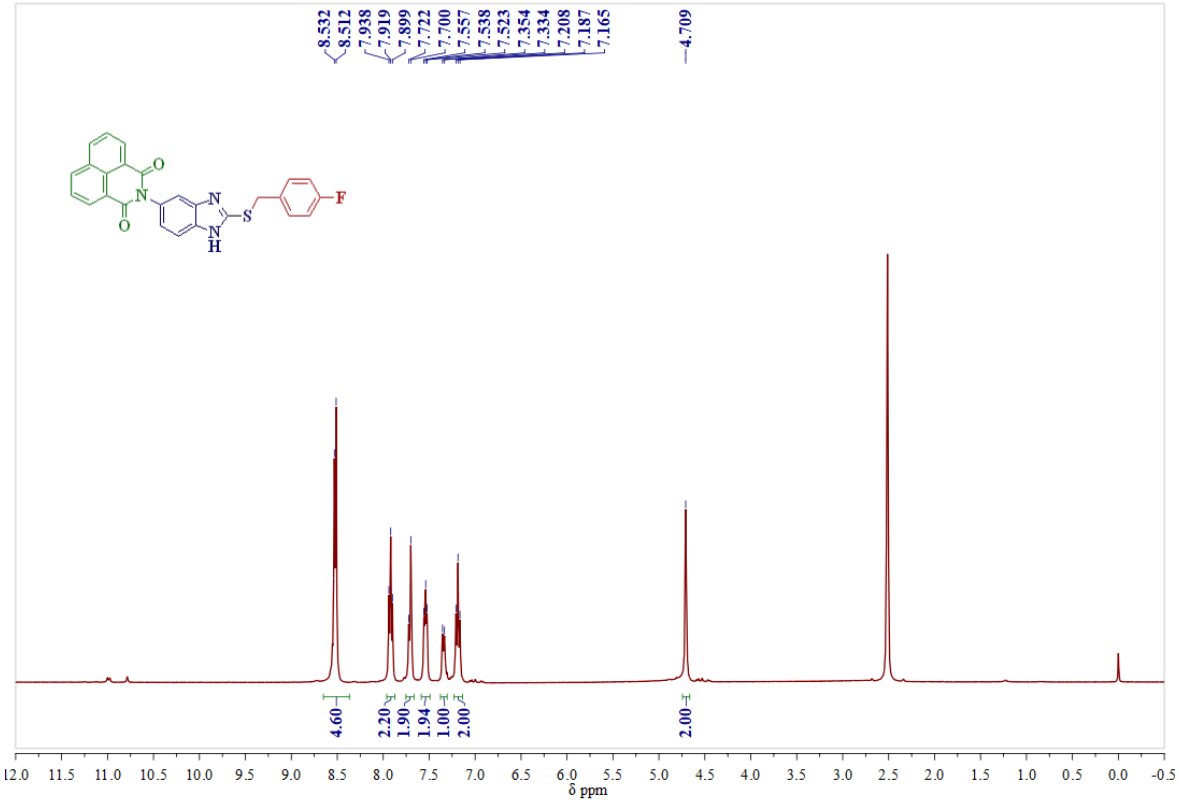

^{13}C-NMR Spectrum of compound 4m in DMSO-d_6 (100MHz):

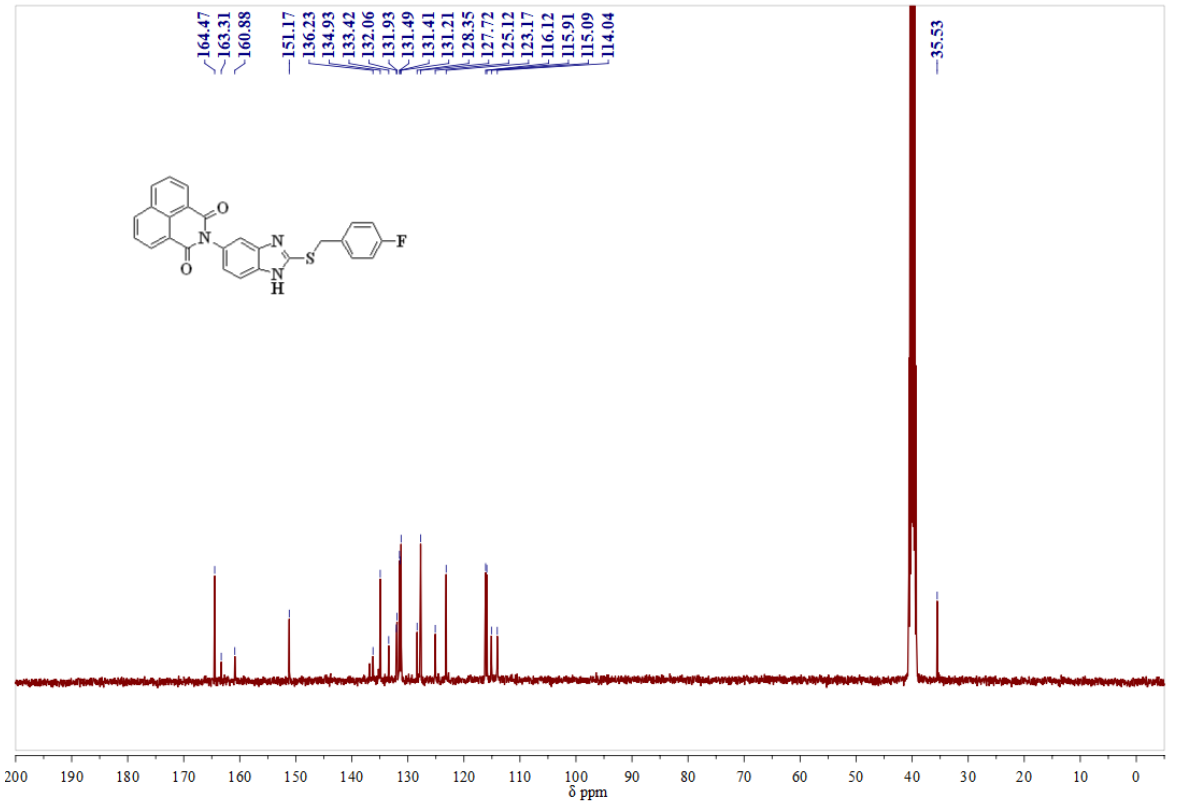

Mass spectrum of compound 4m

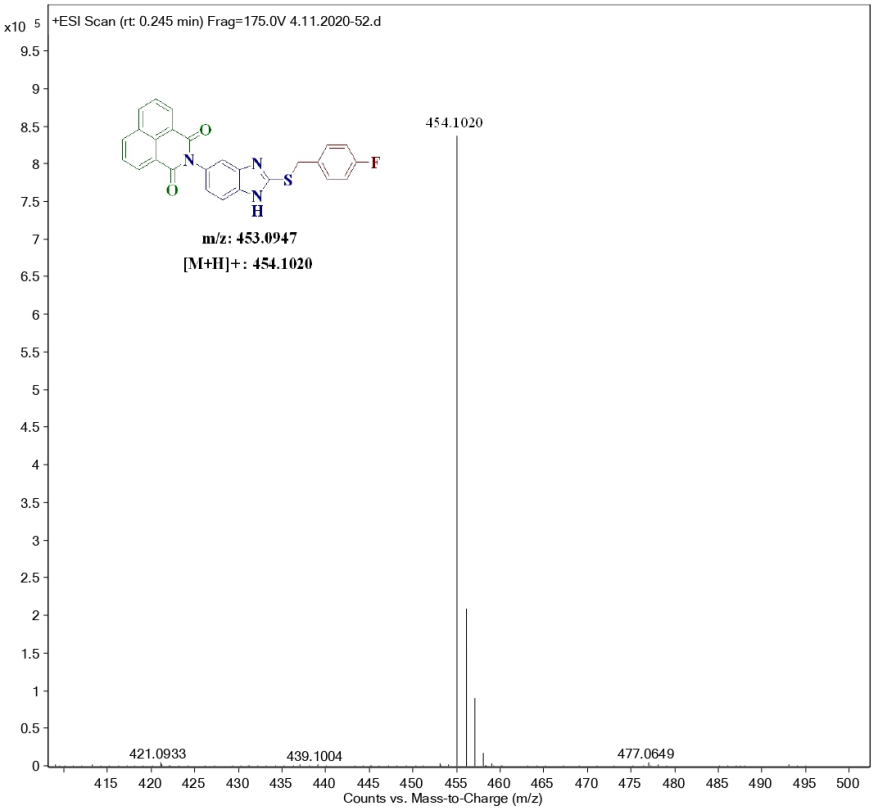

^{1}H-NMR Spectrum of compound 4n in DMSO-d_6 (400MHz):

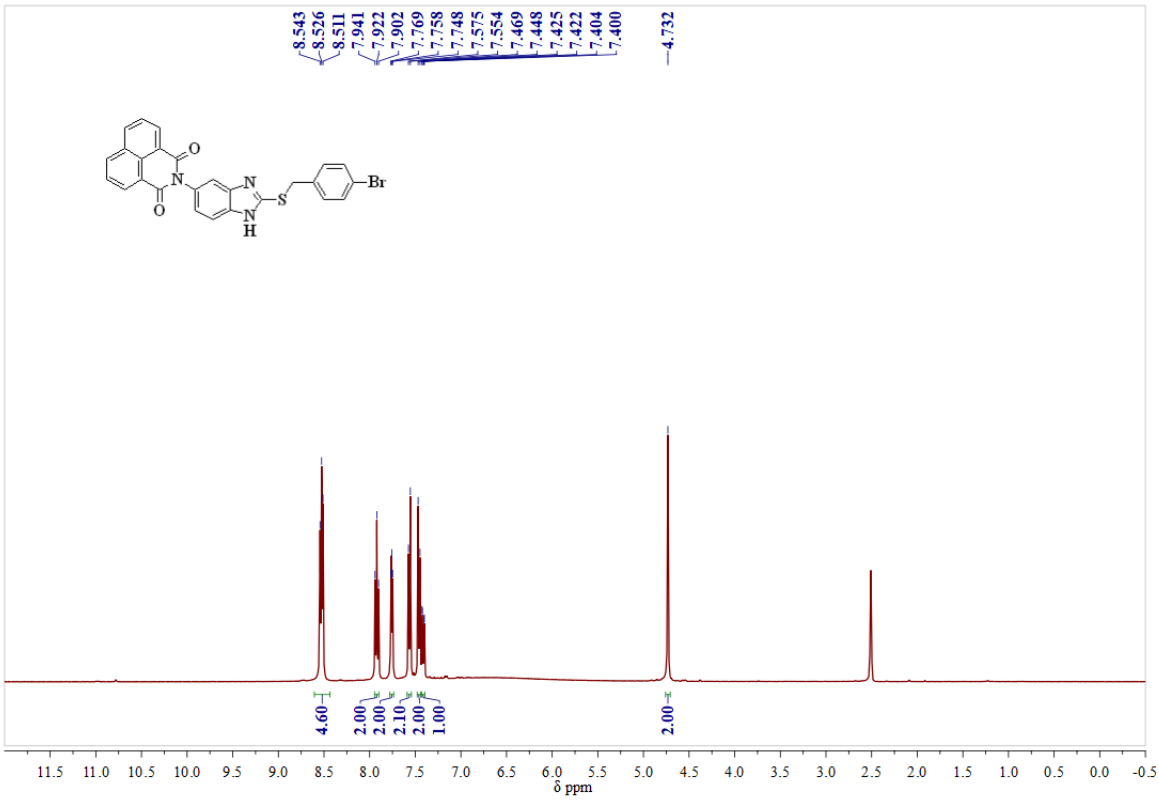

^{13}C-NMR Spectrum of compound 4n in DMSO-d_6 (100MHz):

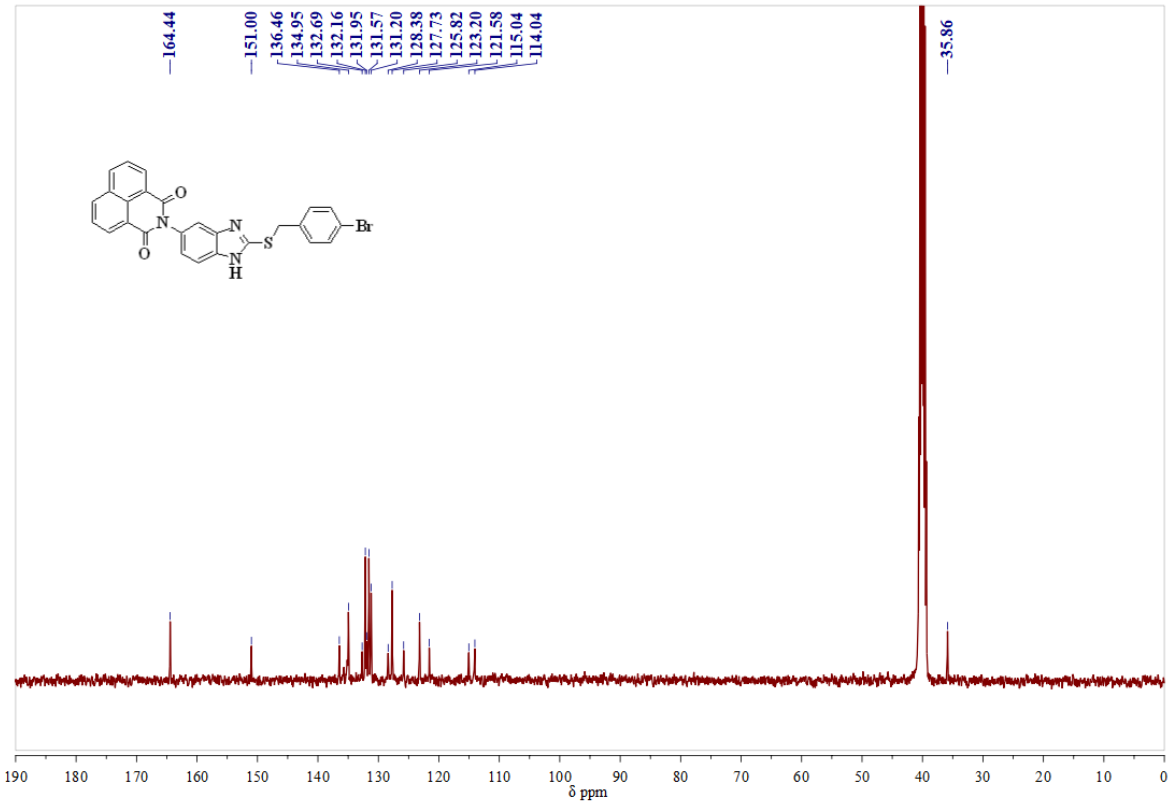

Mass spectrum of compound 4n

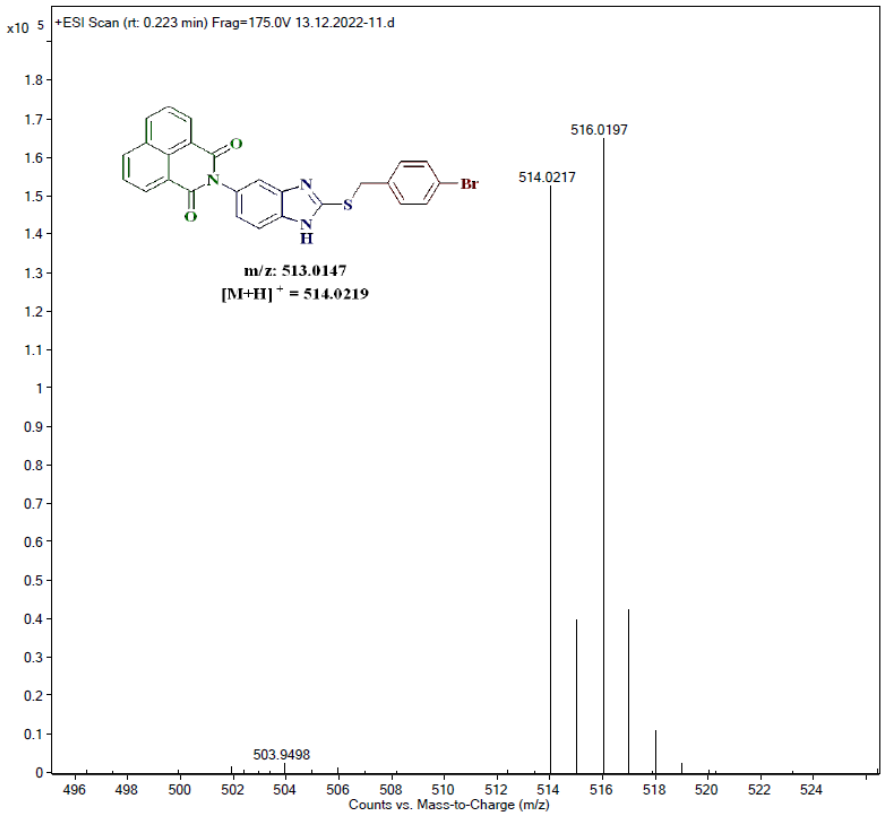

^{1}H-NMR Spectrum of compound 4o in DMSO-d_6 (400MHz):

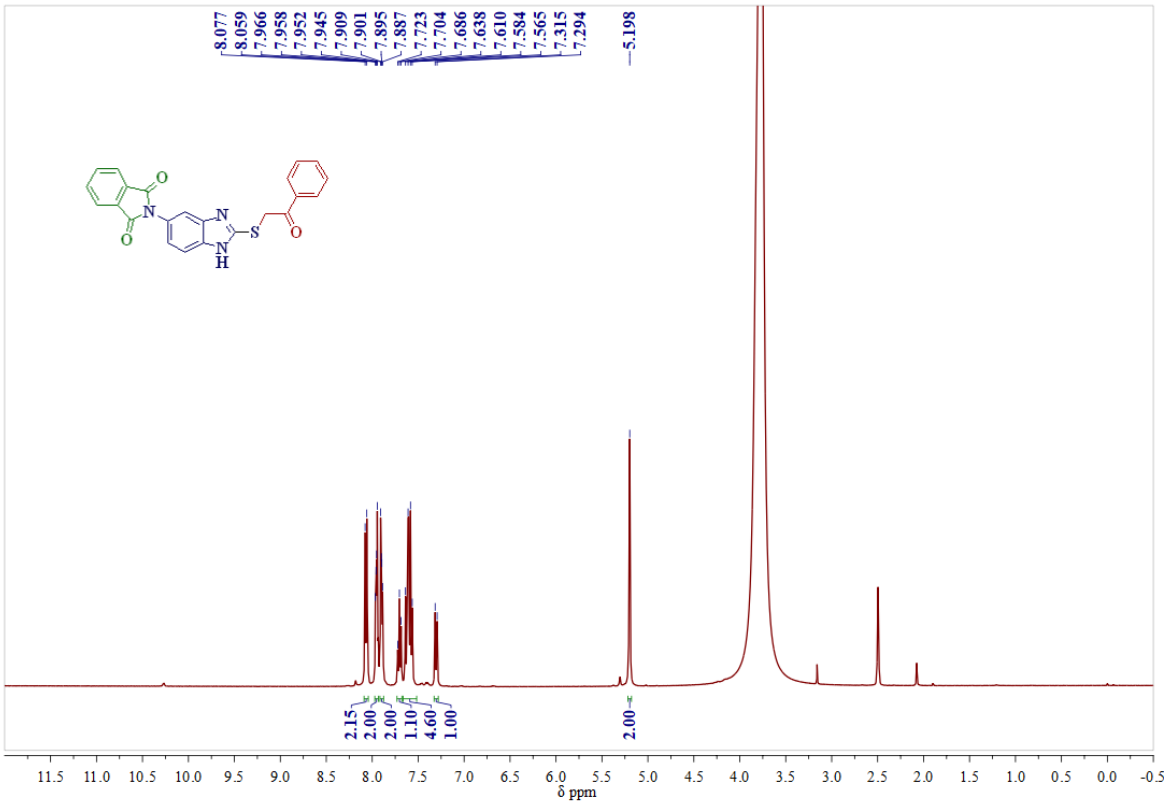

^{13}C-NMR Spectrum of compound 4o in DMSO-d_6 (100MHz):

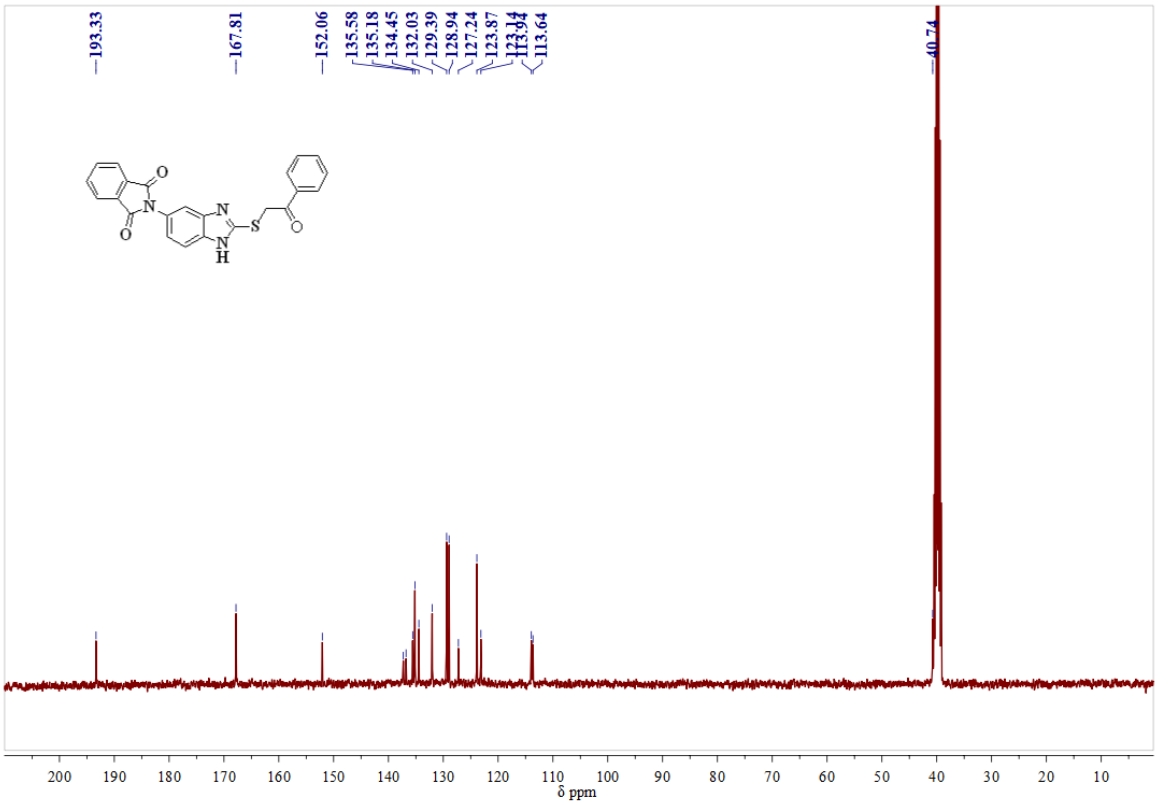

Mass spectrum of compound 4o

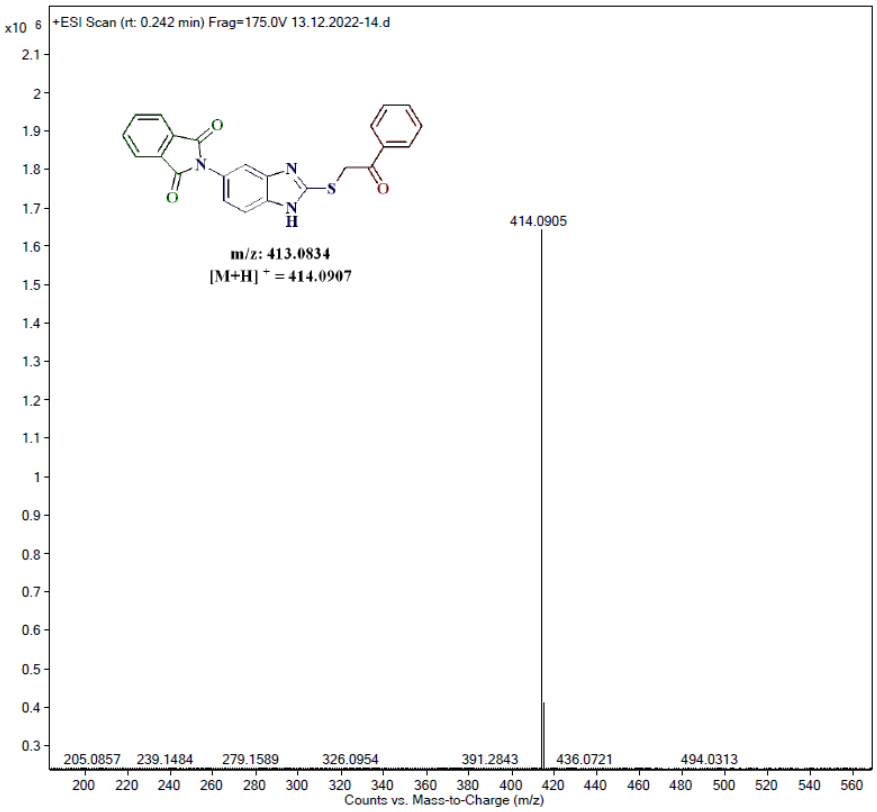

^{1}H-NMR Spectrum of compound 4p in DMSO-d_6 (400MHz):

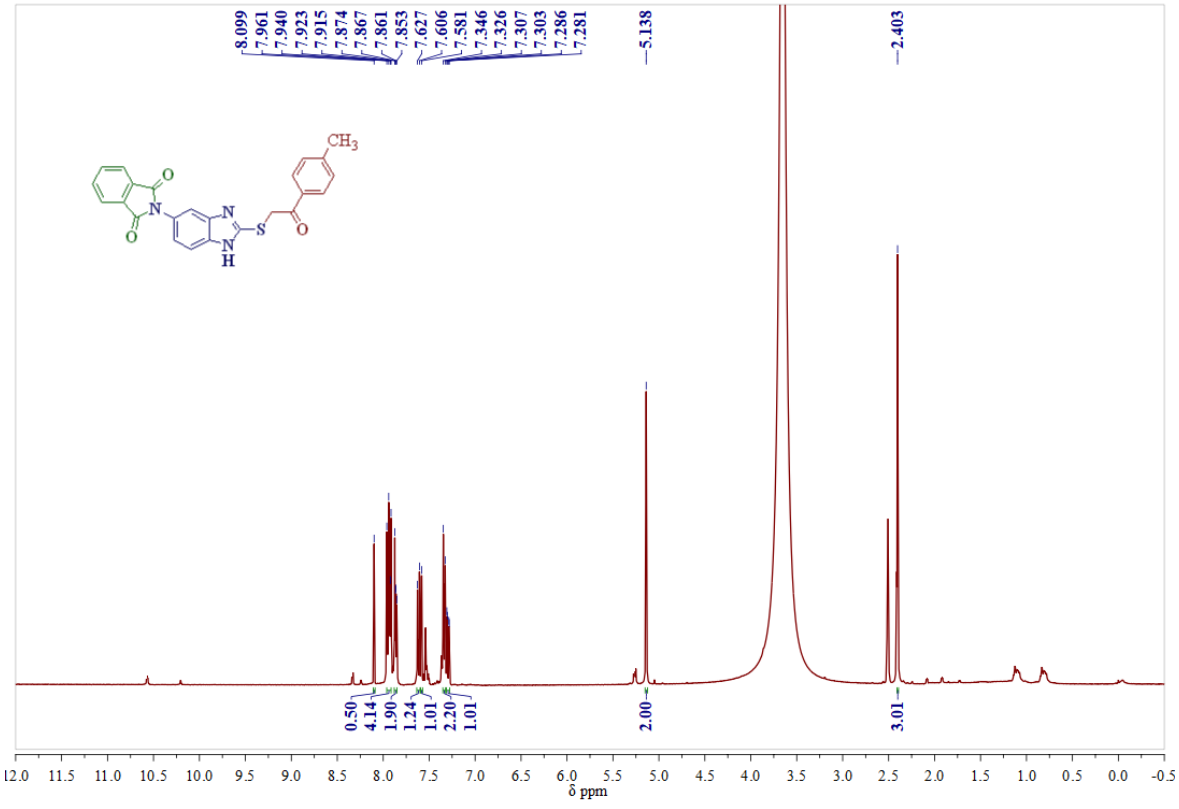

^{13}C-NMR Spectrum of compound 4p in $CDCl_3$- DMSO-*d_6* (100MHz):

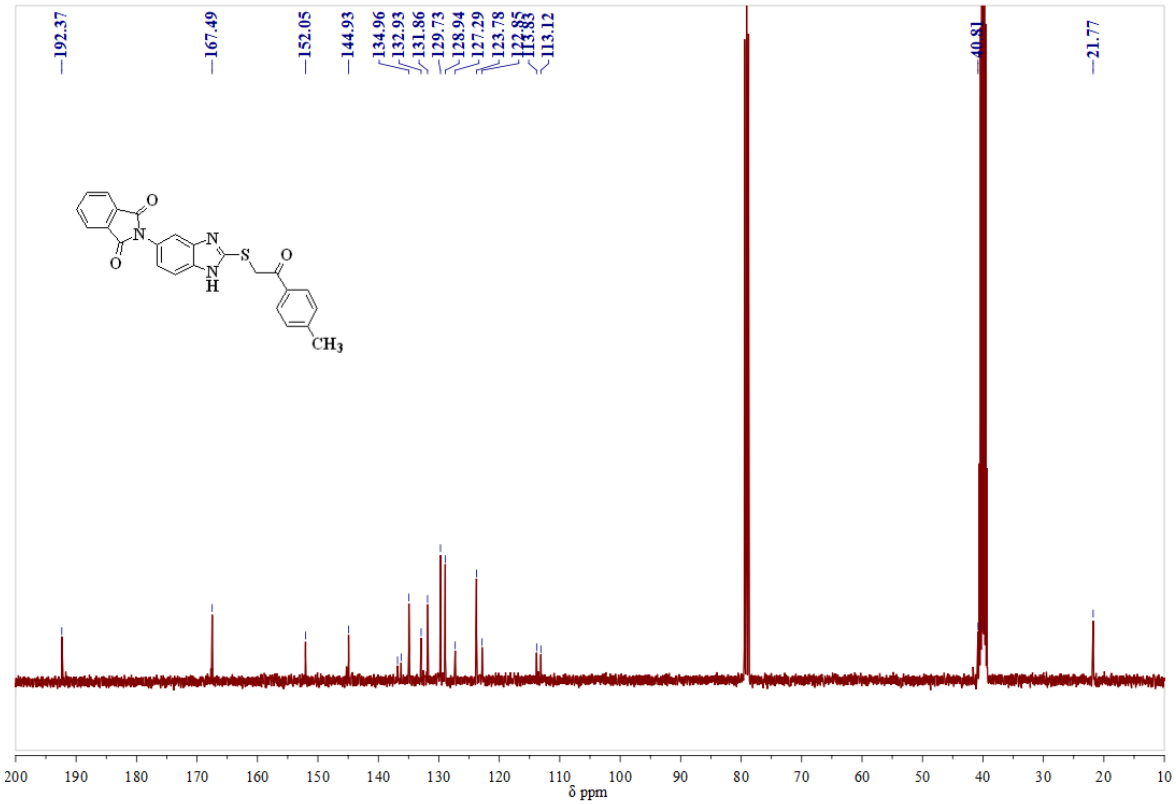

Mass spectrum of compound 4p

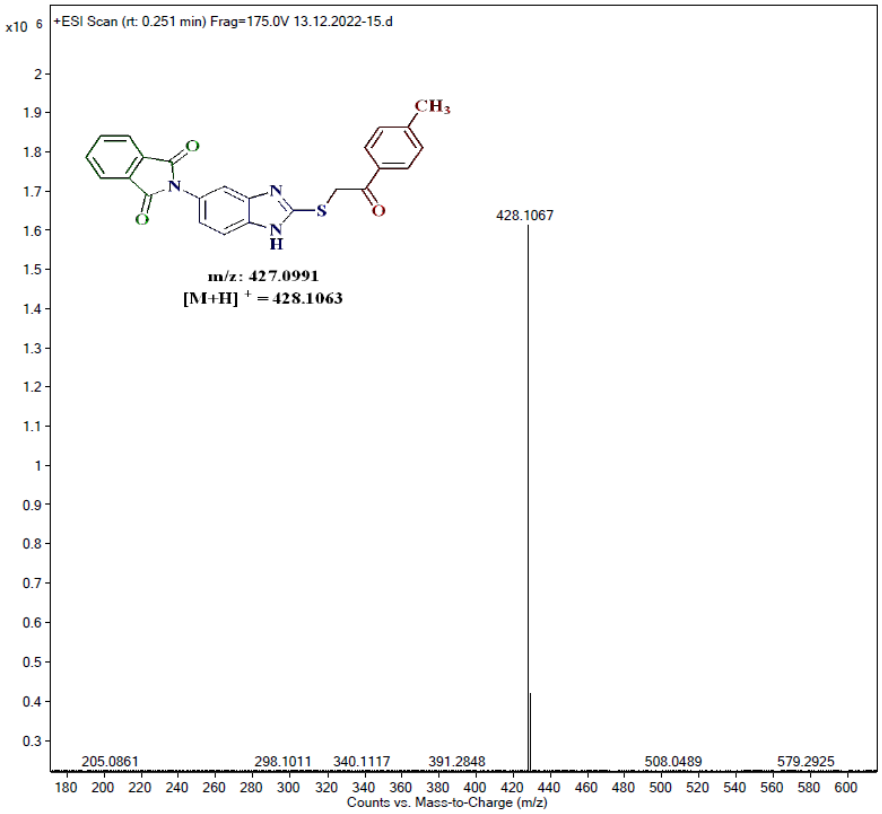

^{1}H-NMR Spectrum of compound 4q in DMSO-d_6 (400MHz):

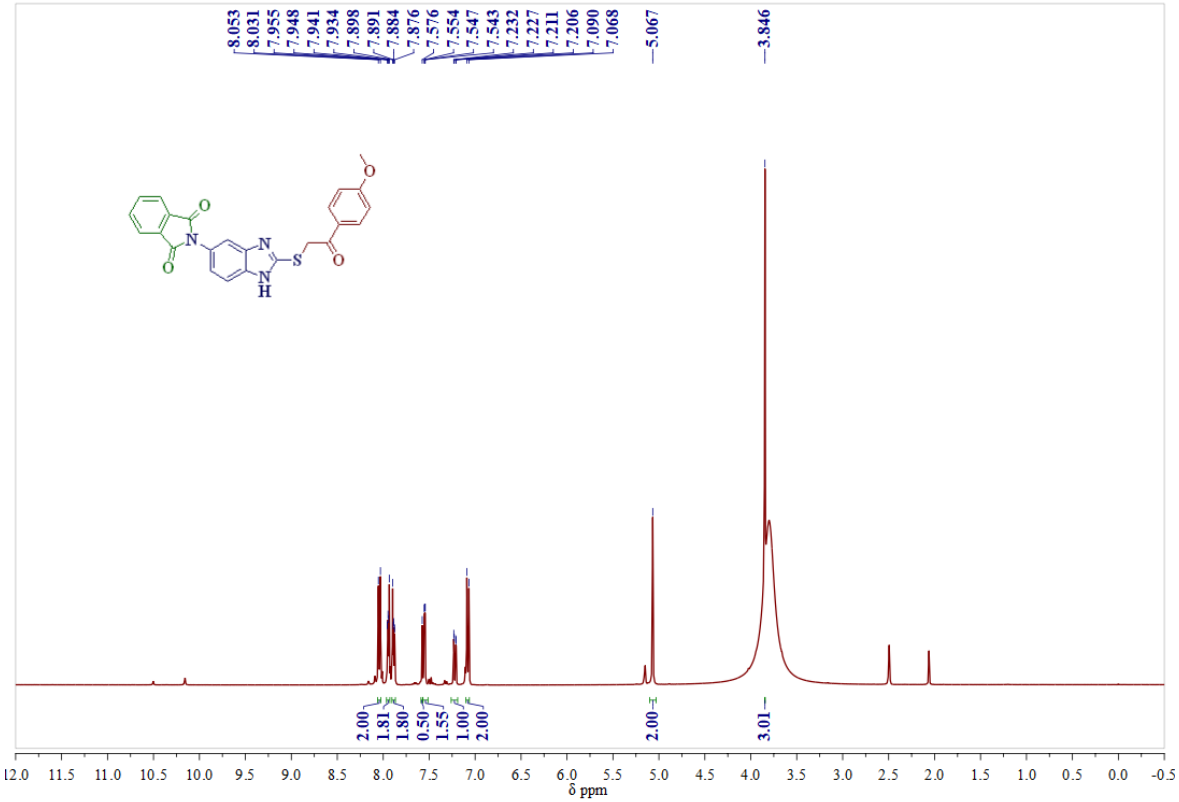

^{13}C-NMR Spectrum of compound 4q in DMSO-d_6 (100MHz):

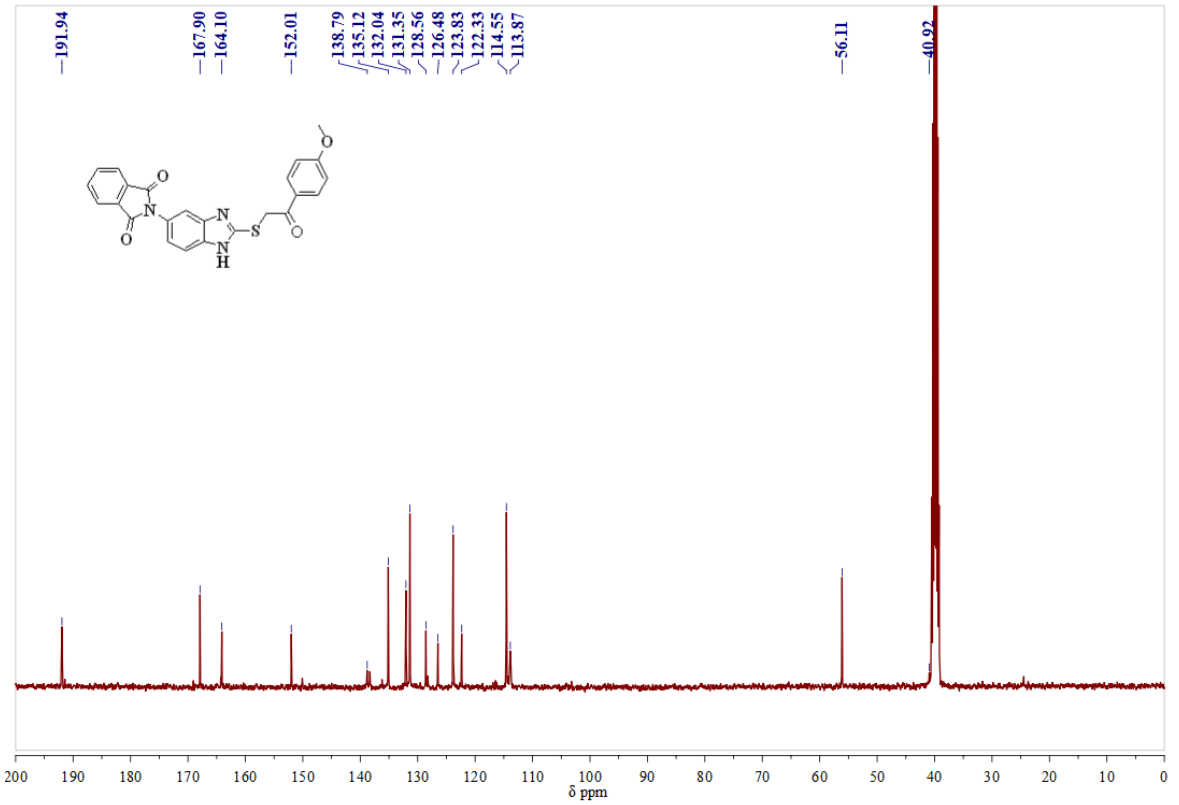

Mass spectrum of compound 4q

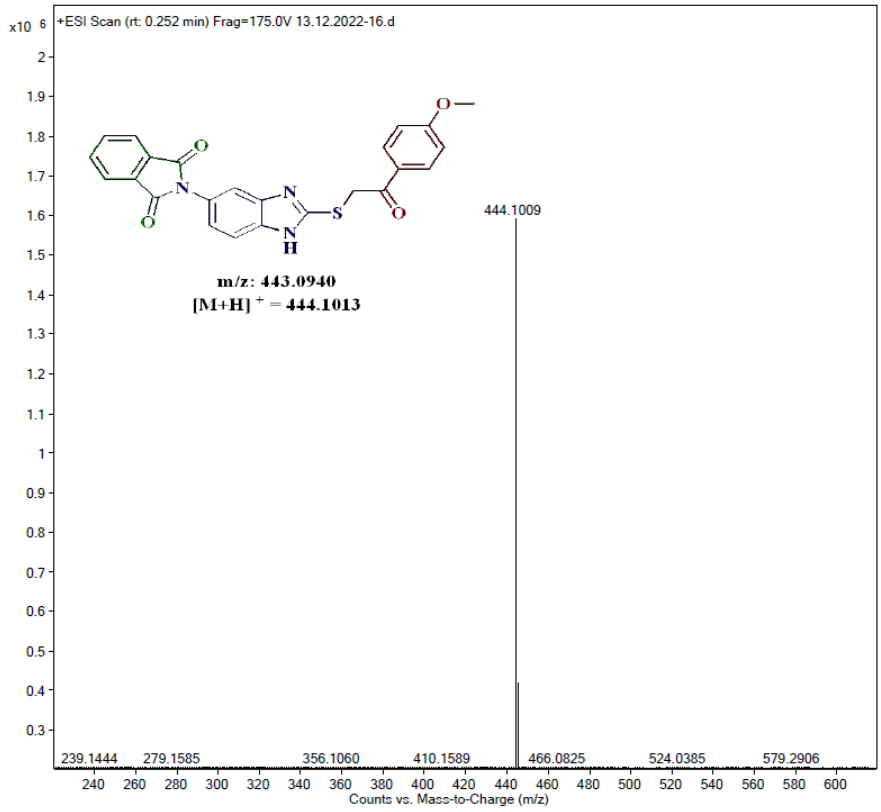

^{1}H-NMR Spectrum of compound 4r in DMSO-d_6 (400MHz):

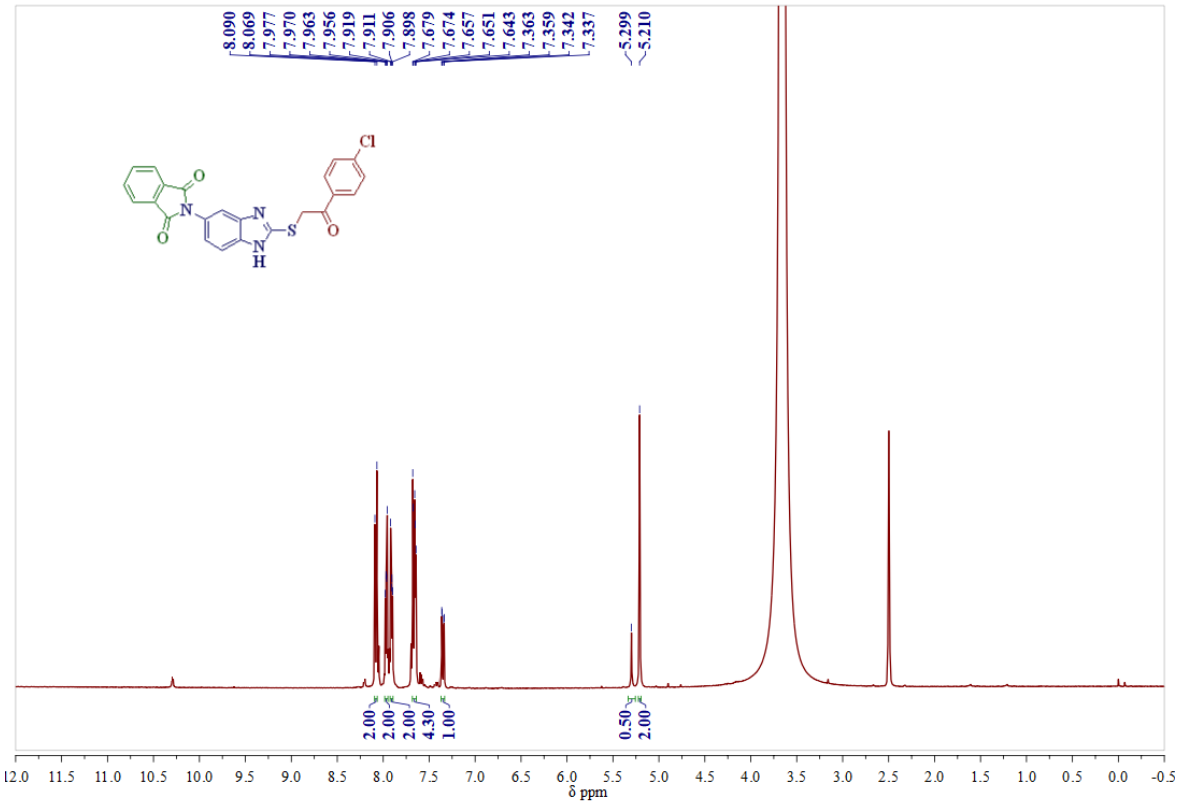

^{13}C-NMR Spectrum of compound 4r in CDCl$_3$- DMSO-d_6 (100MHz):

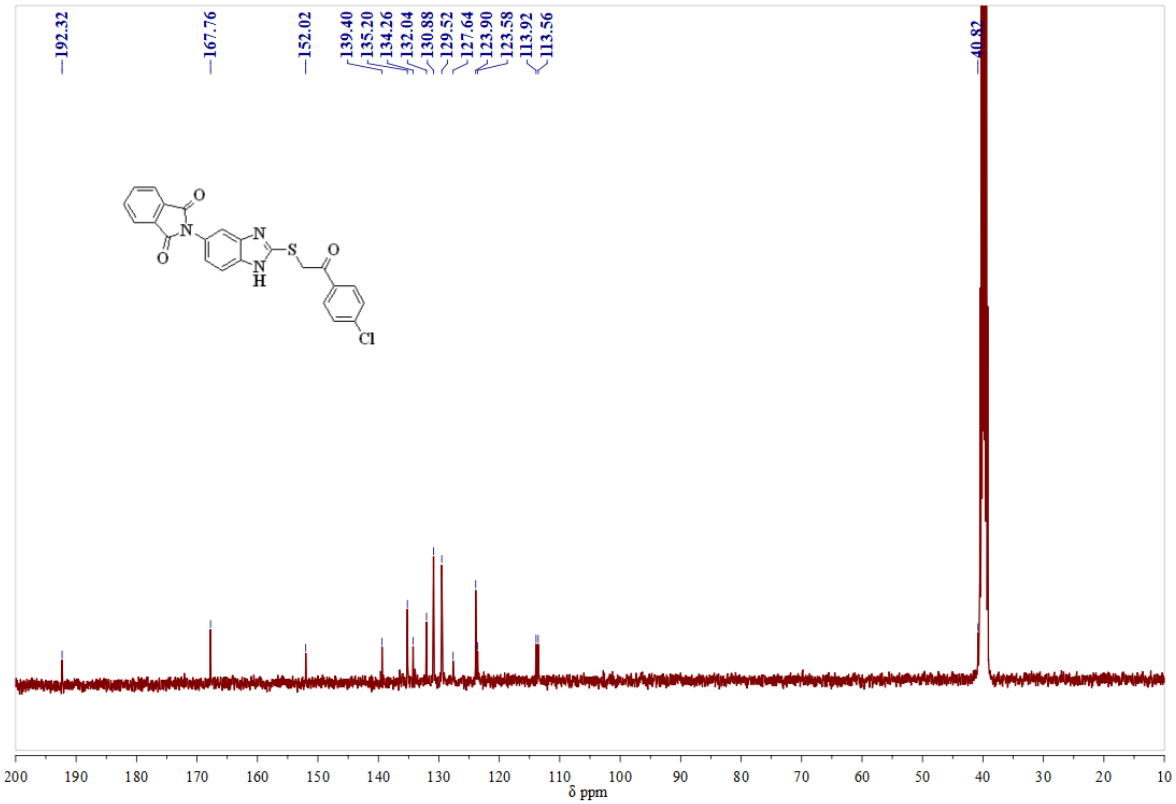

Mass spectrum of compound 4r

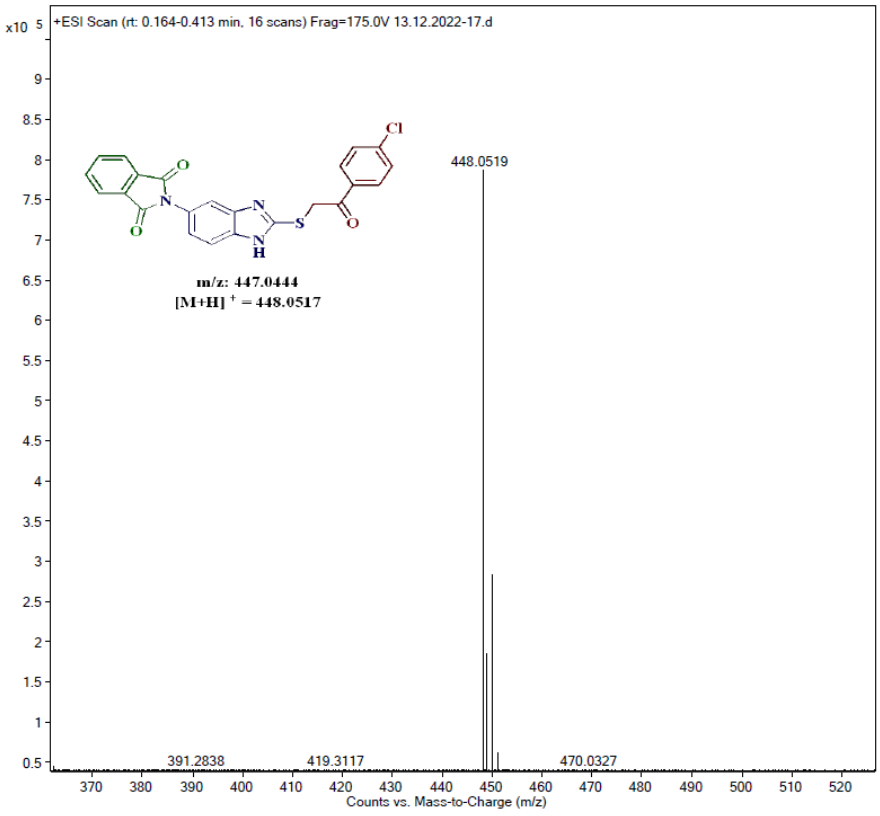

[1]H-NMR Spectrum of compound 4s in DMSO-d_6 (400MHz):

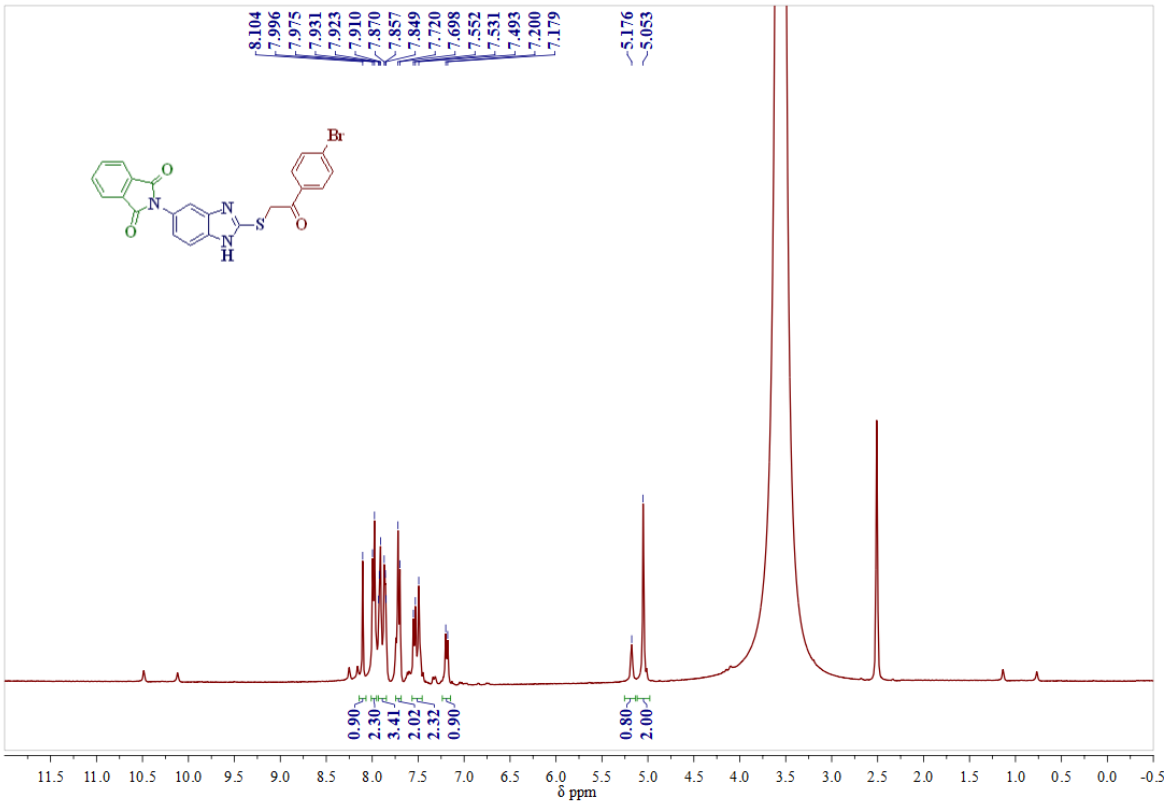

[13]C-NMR Spectrum of compound 4s in DMSO-d_6 (100MHz):

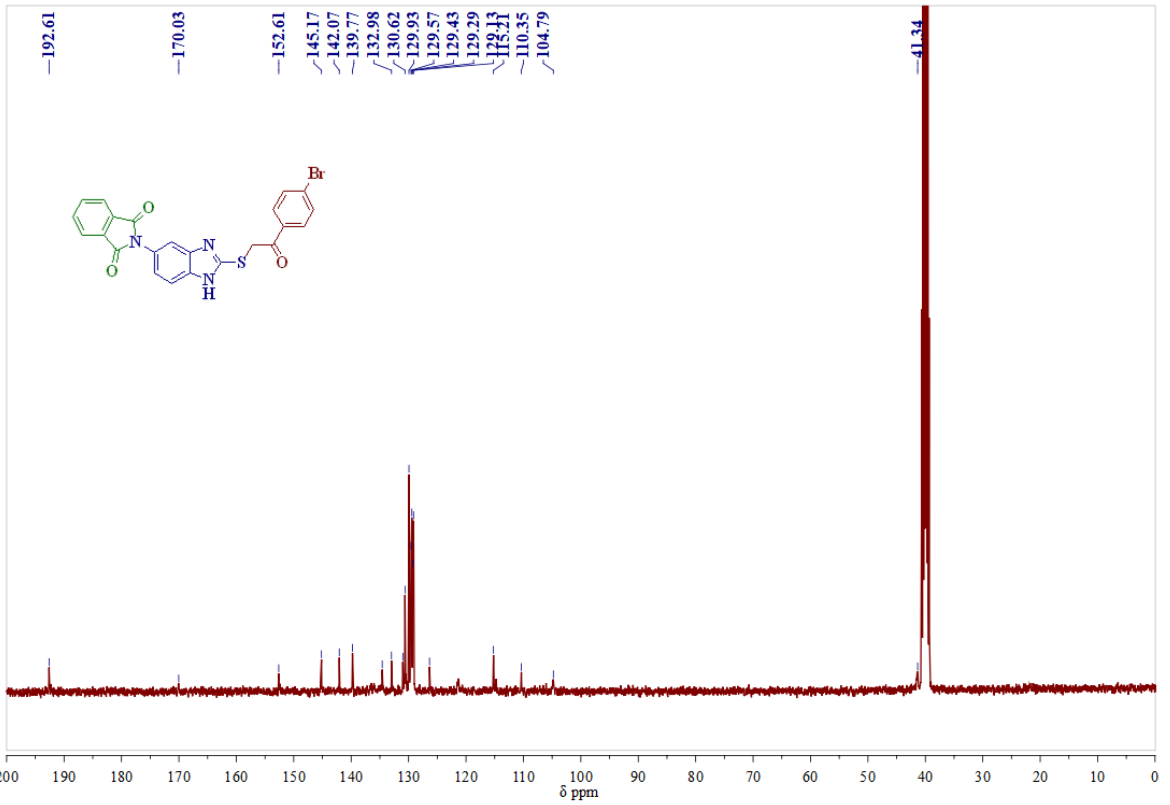

Mass spectrum of compound 4s

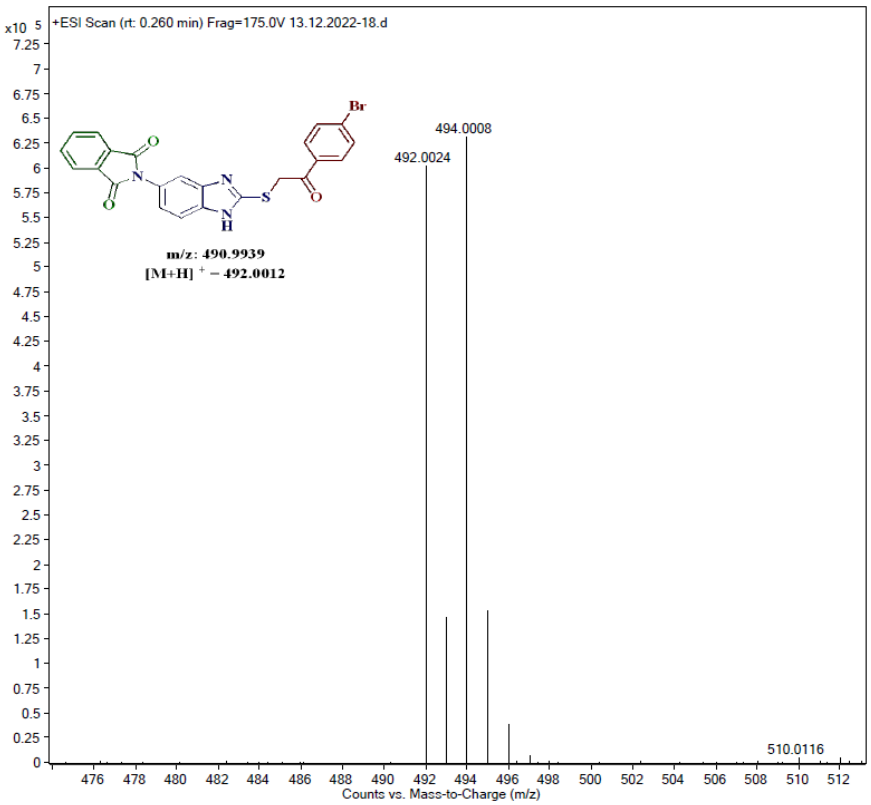

^{1}H-NMR Spectrum of compound 4t in DMSO-d_6 (400MHz):

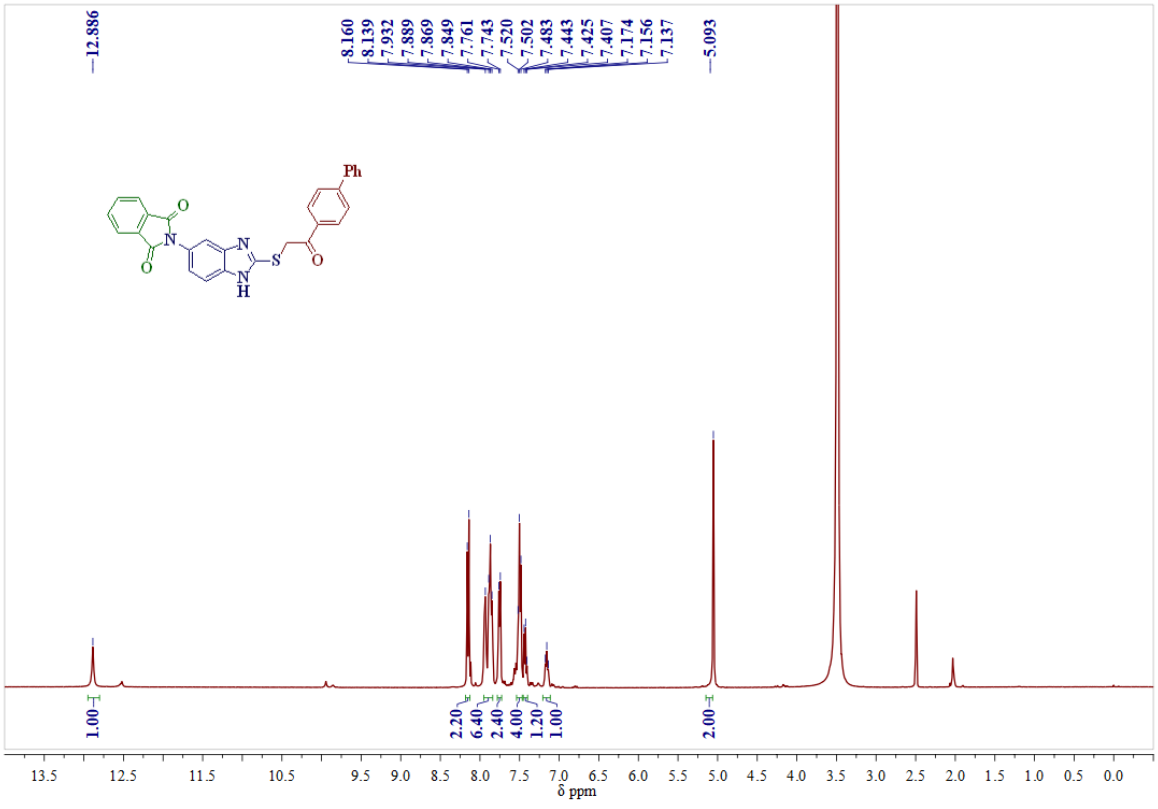

^{13}C-NMR Spectrum of compound 4t in $CDCl_3$- DMSO-d_6 (100MHz):

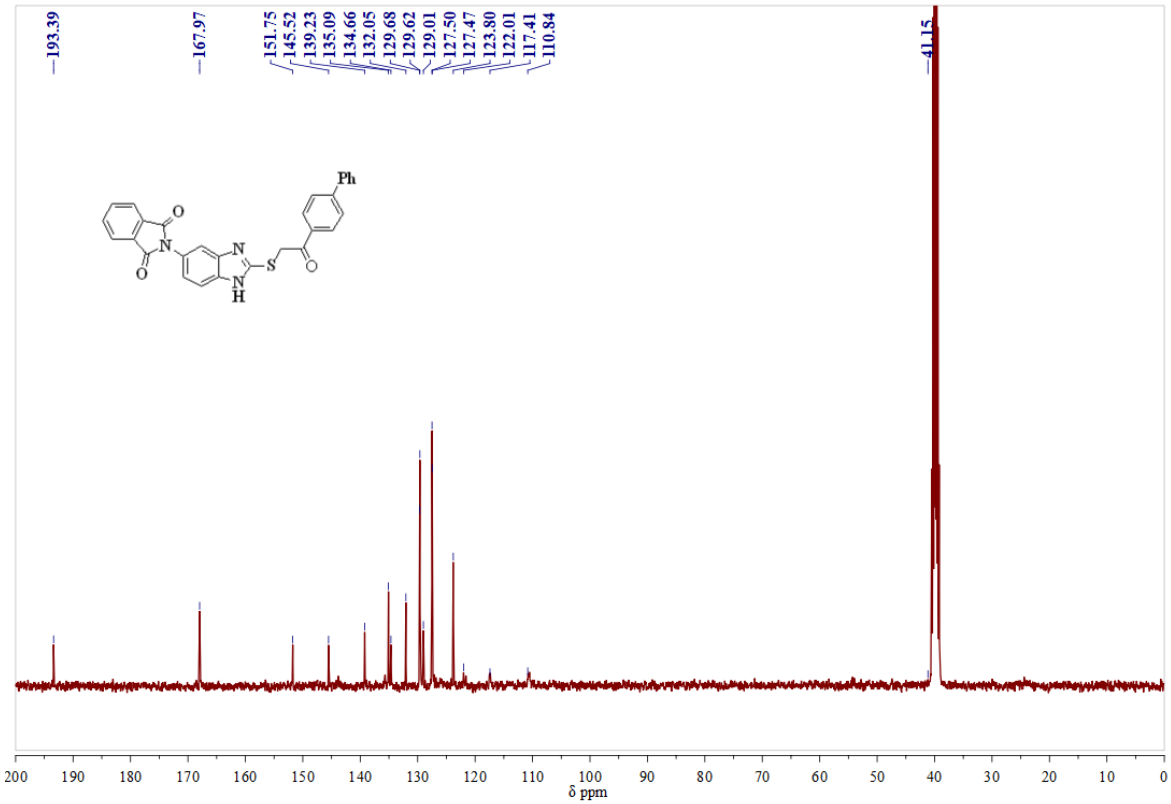

Mass spectrum of compound 4t

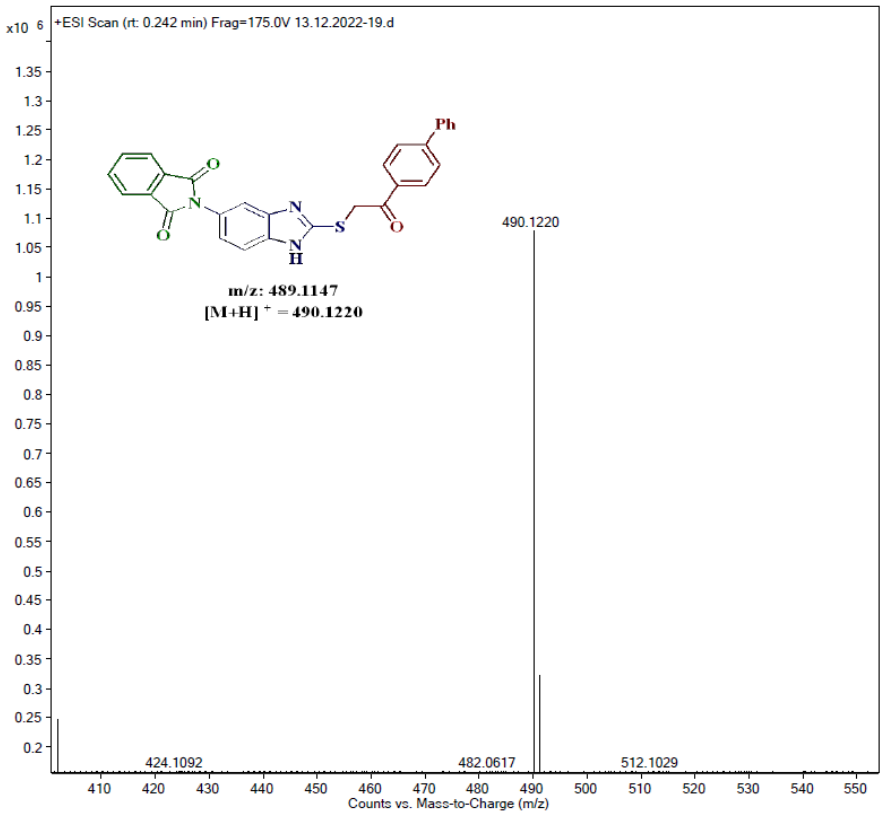

^{1}H-NMR Spectrum of compound 4u in DMSO-d_6 (400MHz):

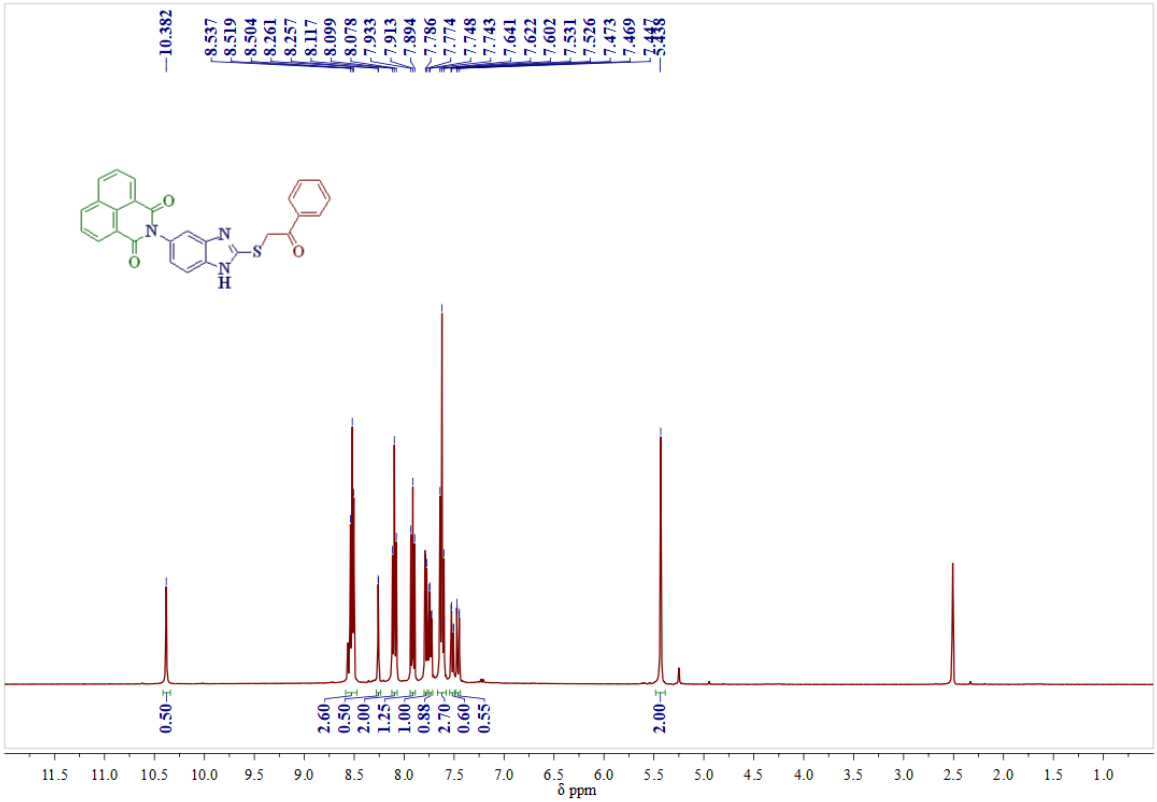

^{13}C-NMR Spectrum of compound 4u in $CDCl_3$- DMSO-d_6 (100 MHz):

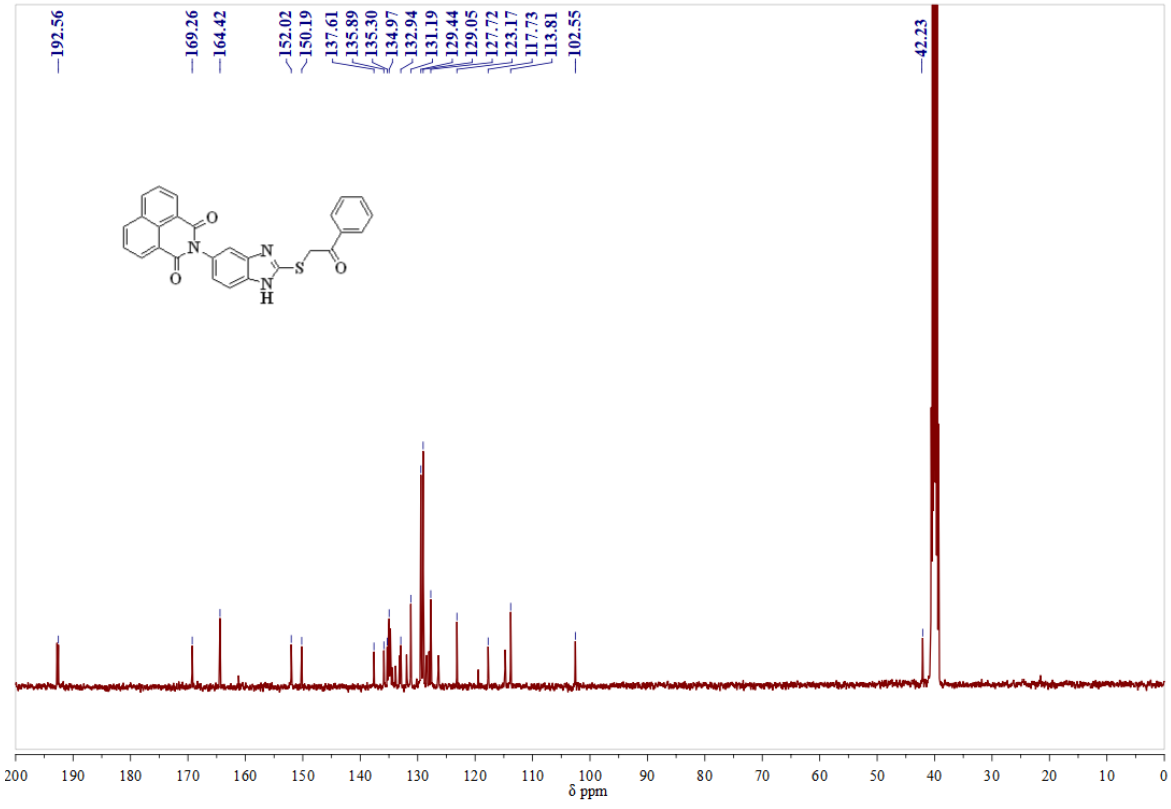

Mass spectrum of compound 4u

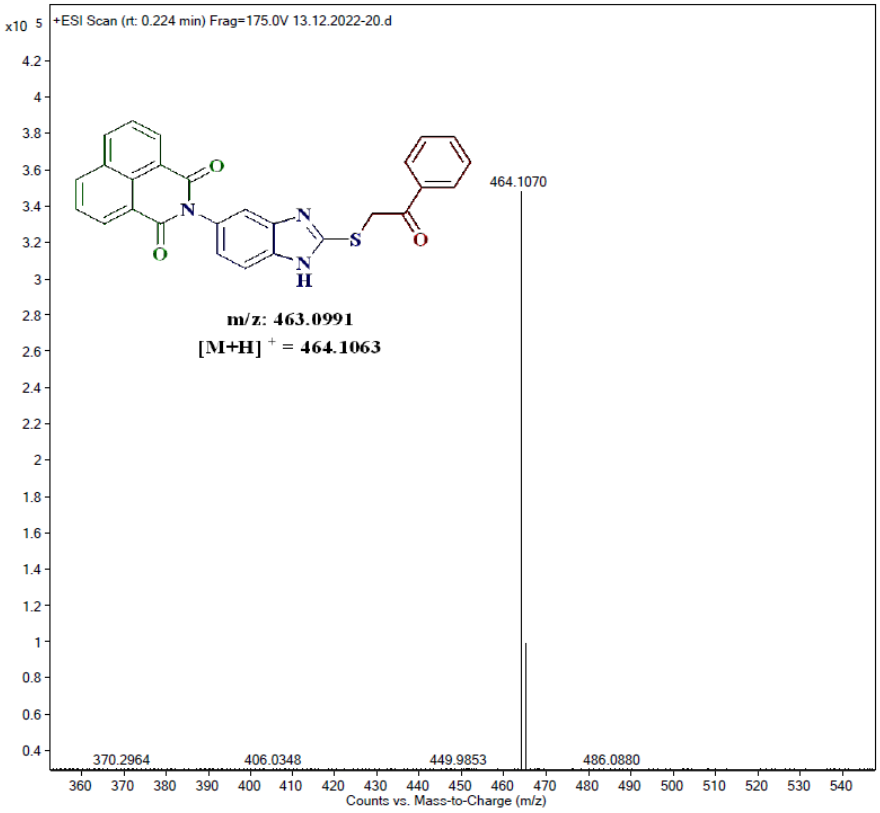

^{1}H-NMR Spectrum of compound 4v in DMSO-d_6 (400 MHz):

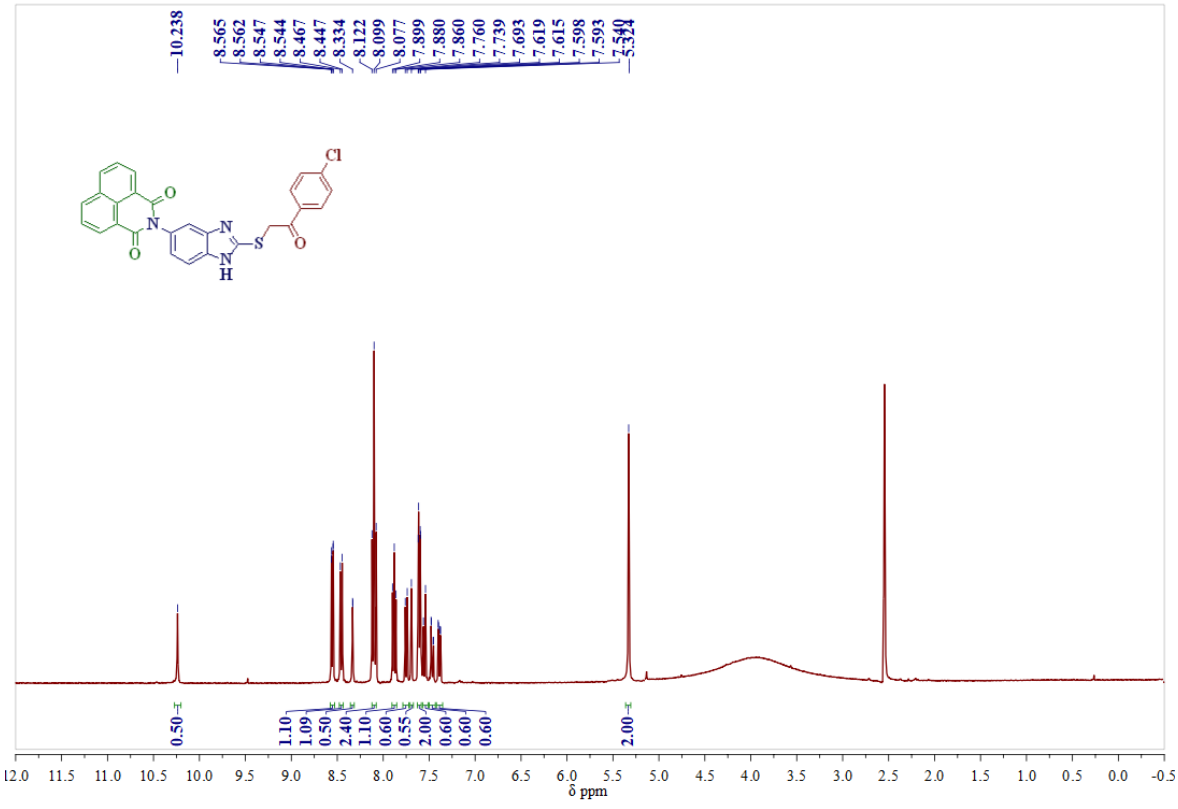

^{13}C-NMR Spectrum of compound 4v in $CDCl_3$- DMSO-d_6 (100 MHz):

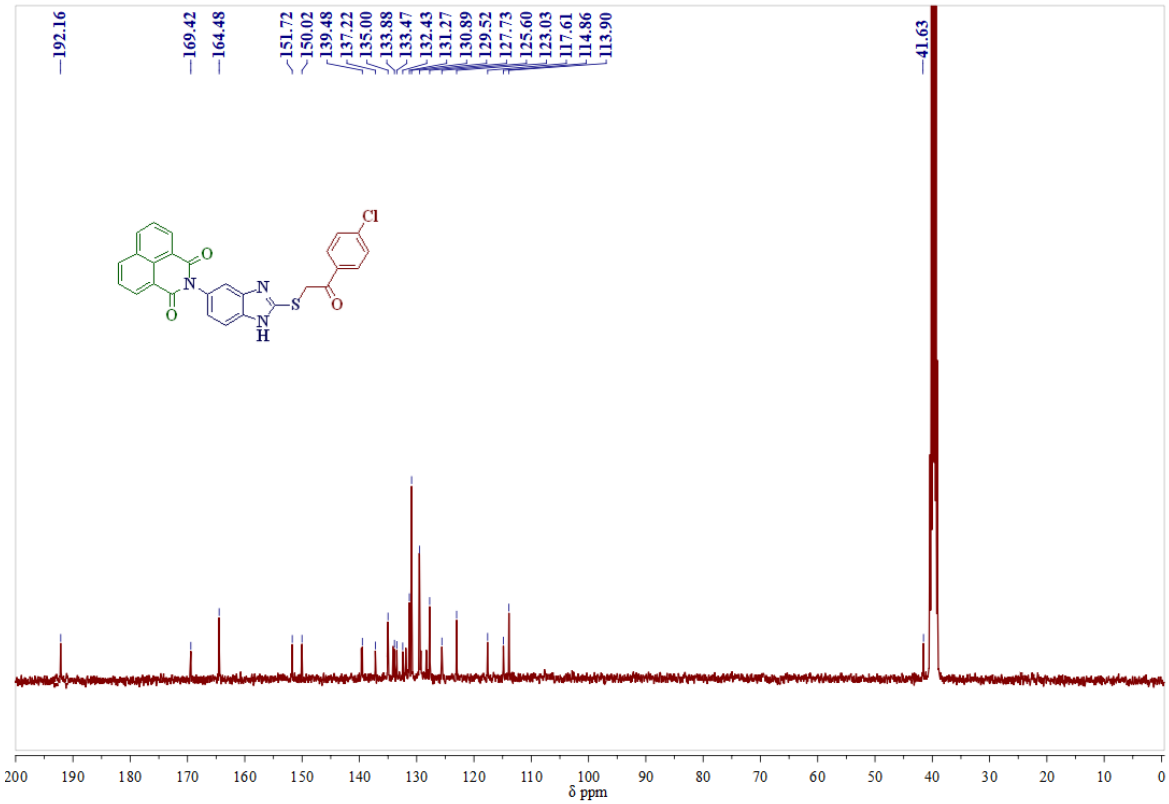

Mass spectrum of compound 4v

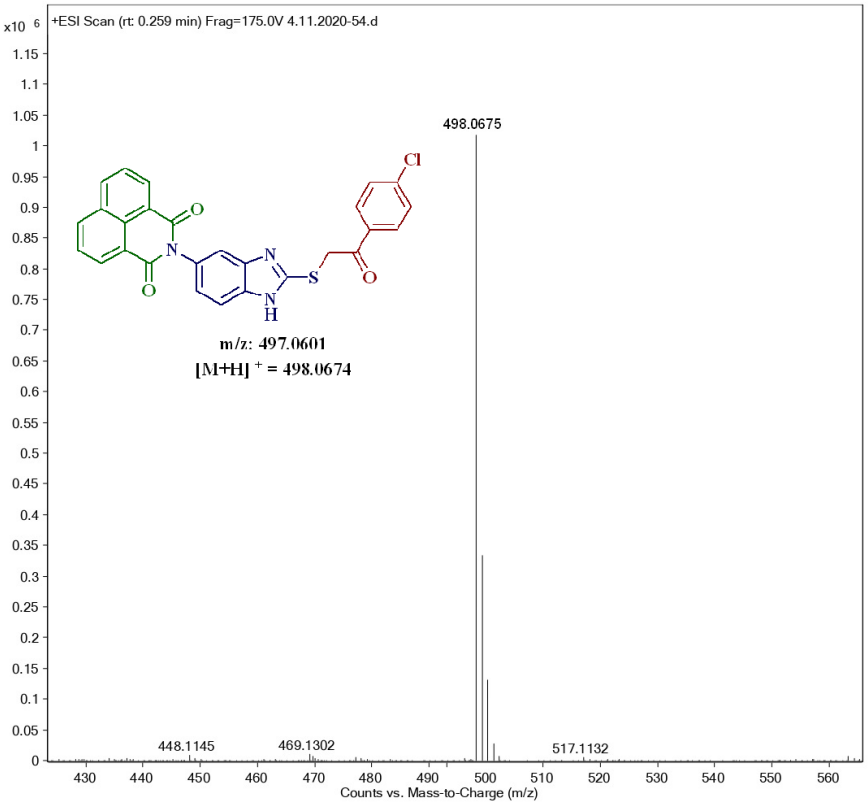

^{1}H-NMR Spectrum of compound 4w in DMSO-d_6 (400 MHz):

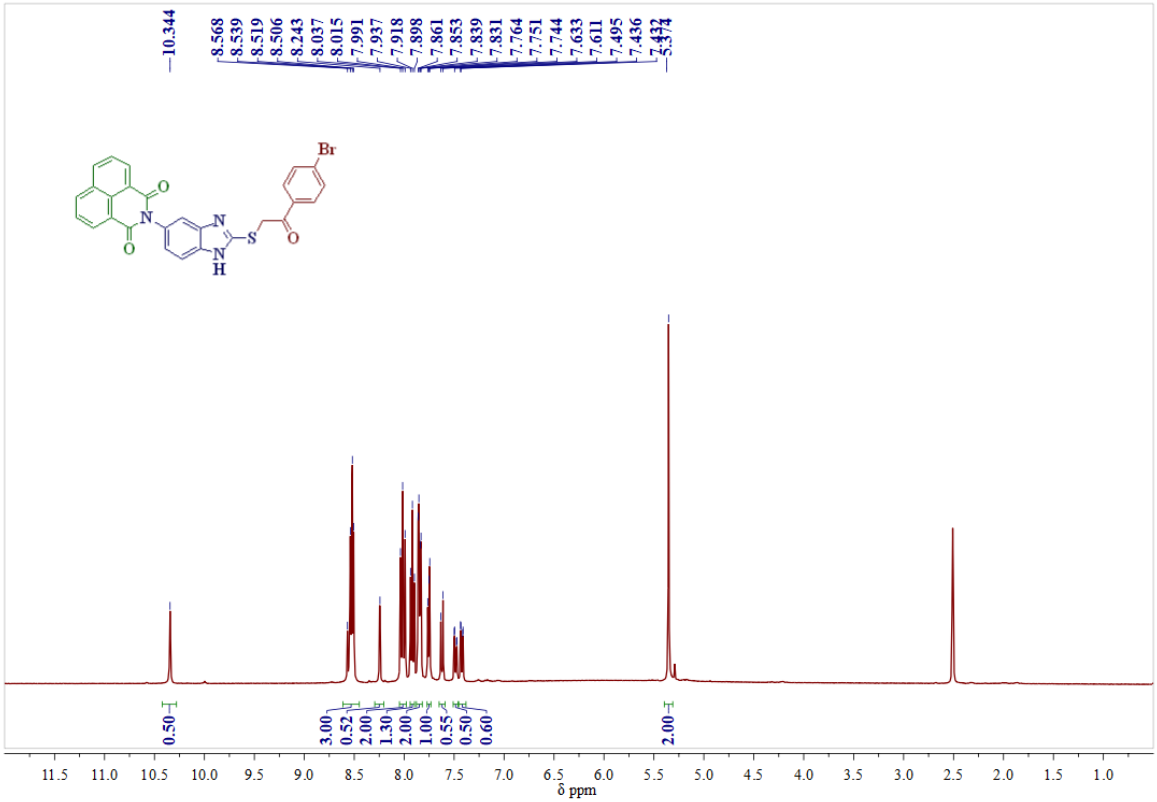

^{13}C-NMR Spectrum of compound 4w in DMSO-d_6 (100 MHz):

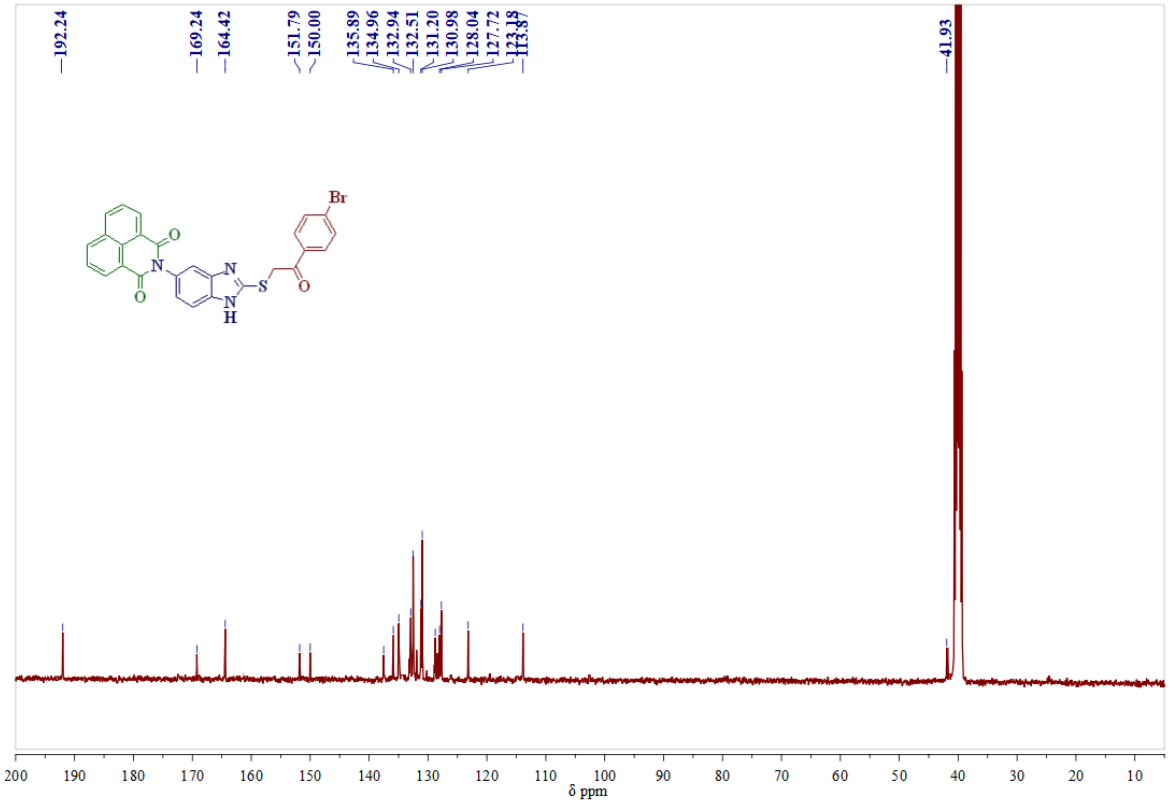

Mass spectrum of compound 4w

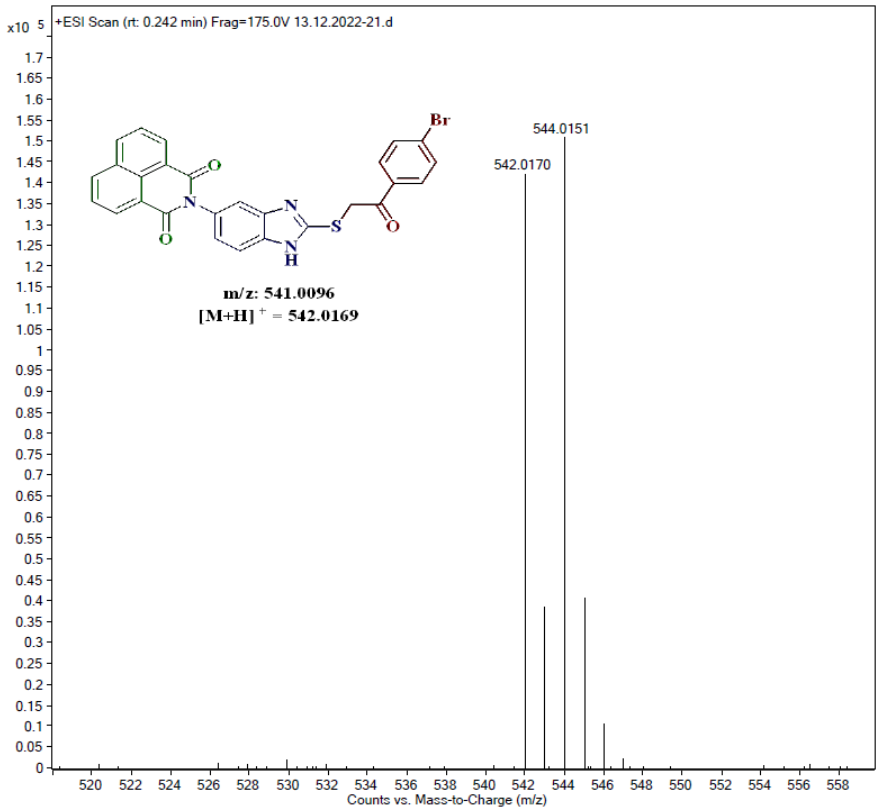

^{1}H-NMR Spectrum of compound 5a in DMSO-d_6 (400MHz):

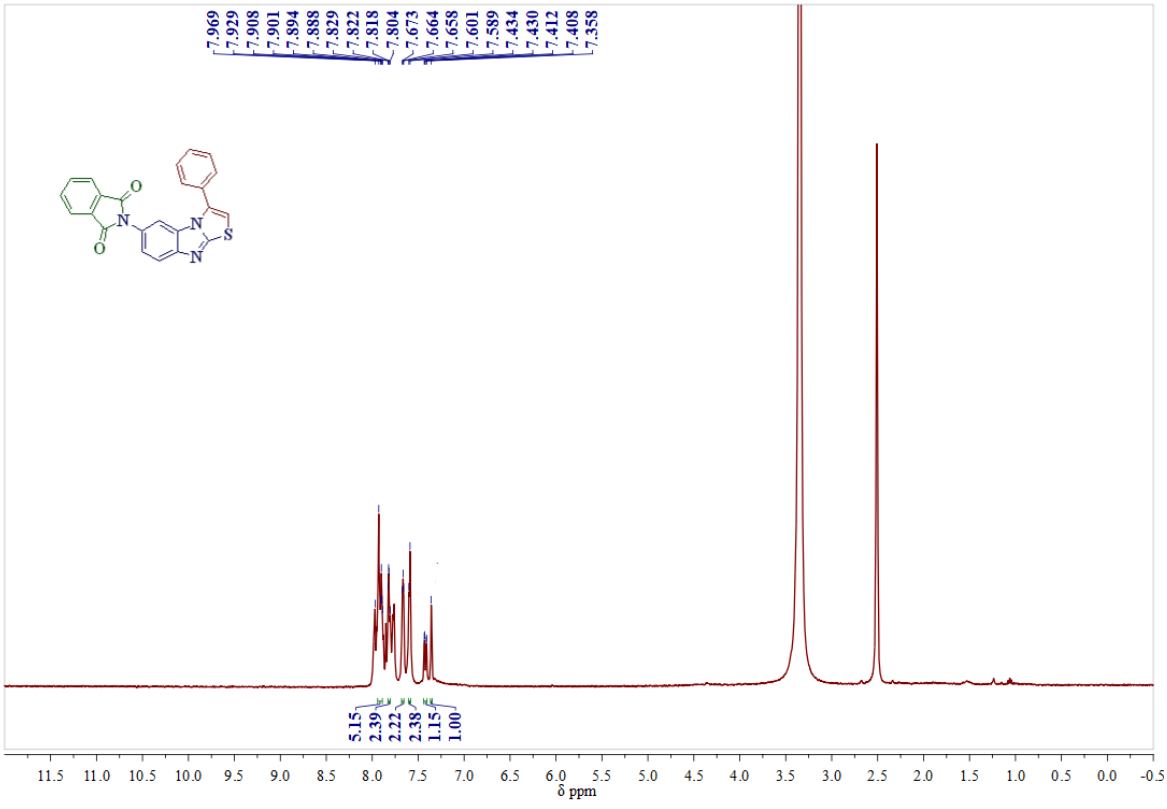

^{13}C-NMR Spectrum of compound 5a in DMSO-d_6 (100MHz):

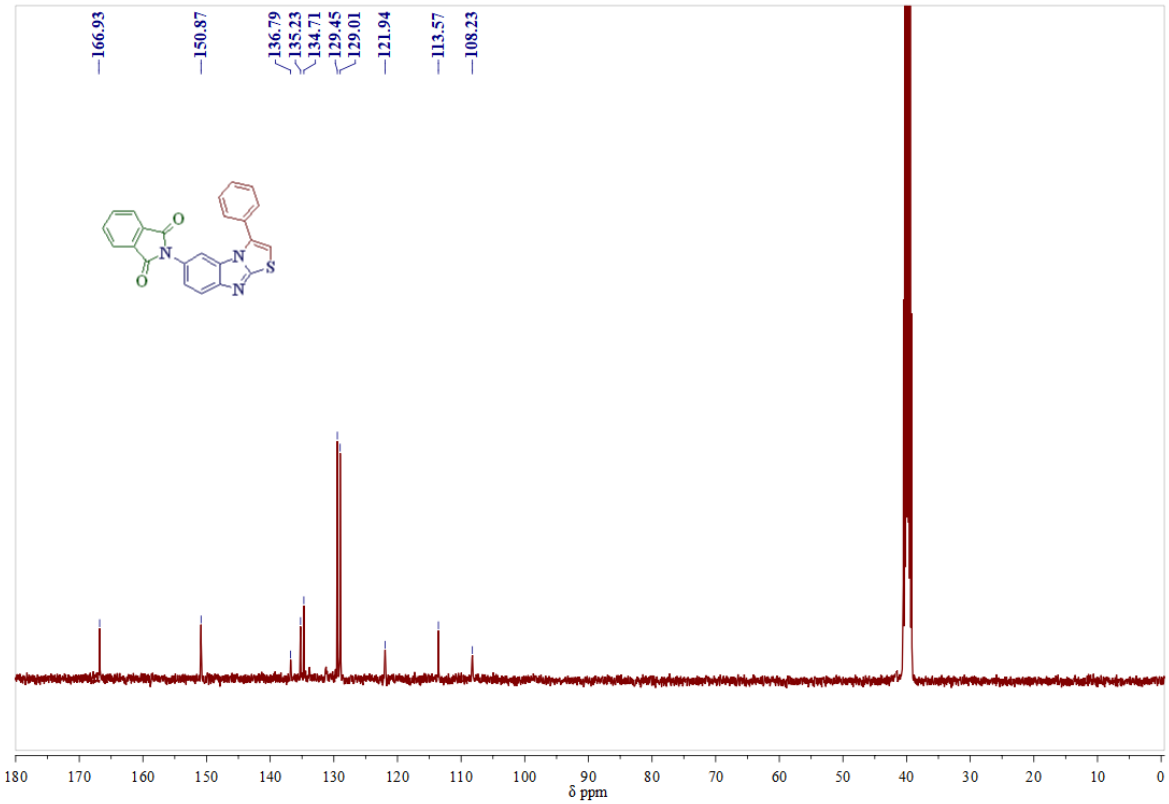

Mass spectrum of compound 5a

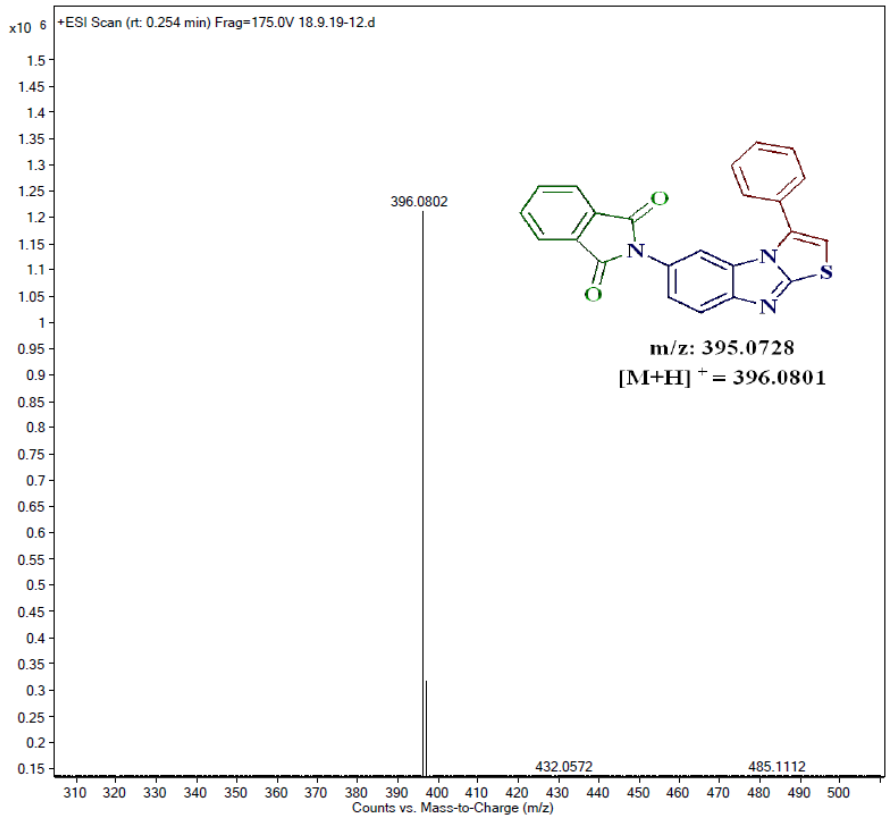

[1]H-NMR Spectrum of compound 5b in DMSO-*d*$_6$ (400MHz):

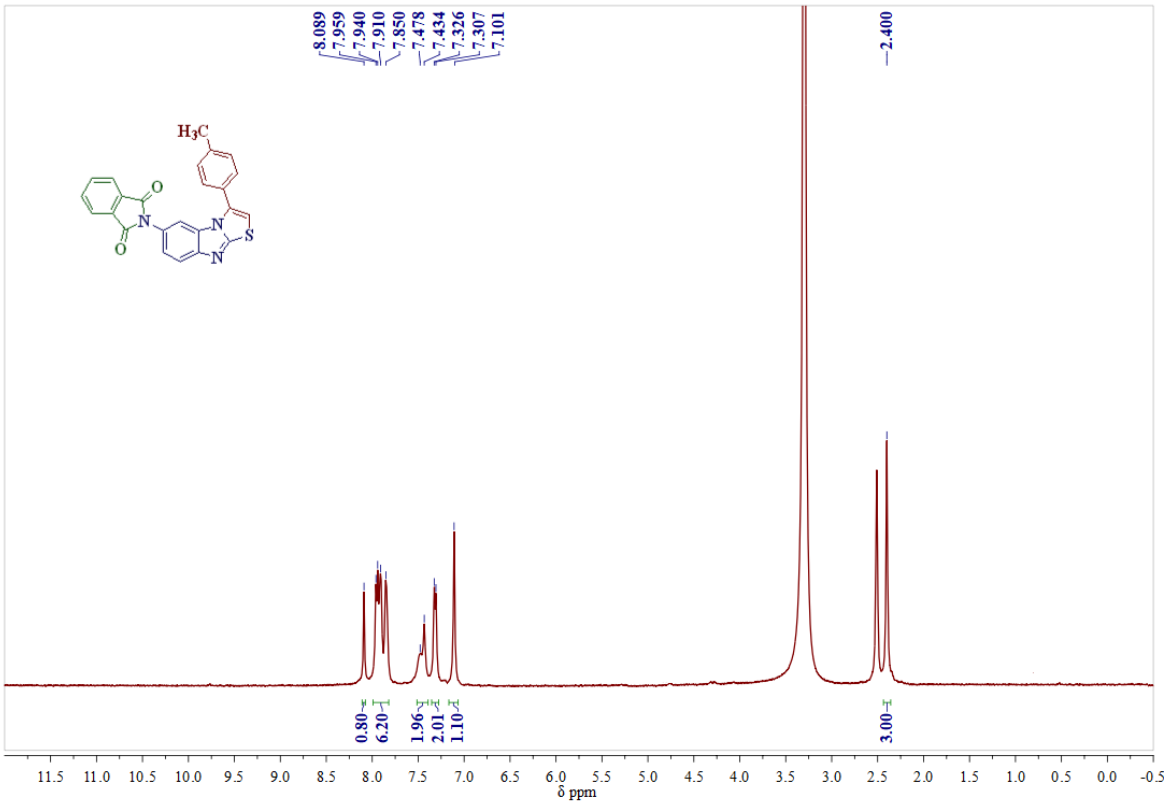

[13]C-NMR Spectrum of compound 5b in DMSO-*d*$_6$ (100MHz):

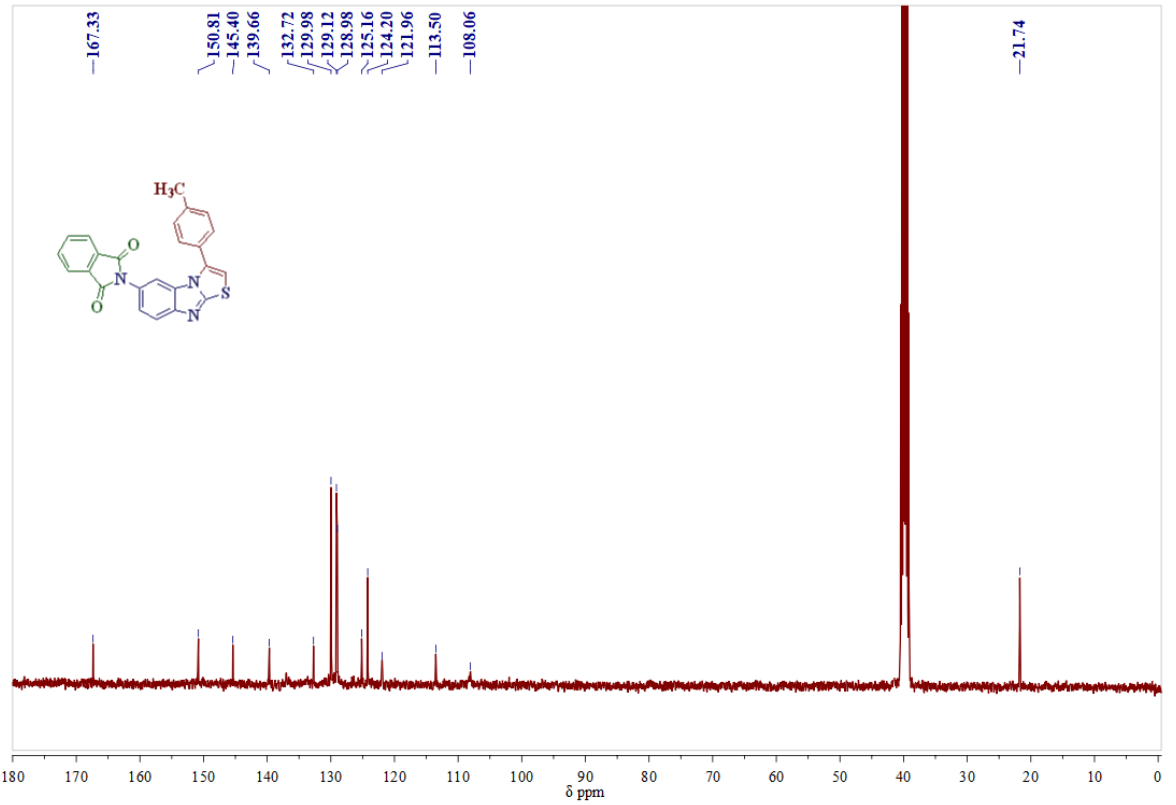

Mass spectrum of compound 5b

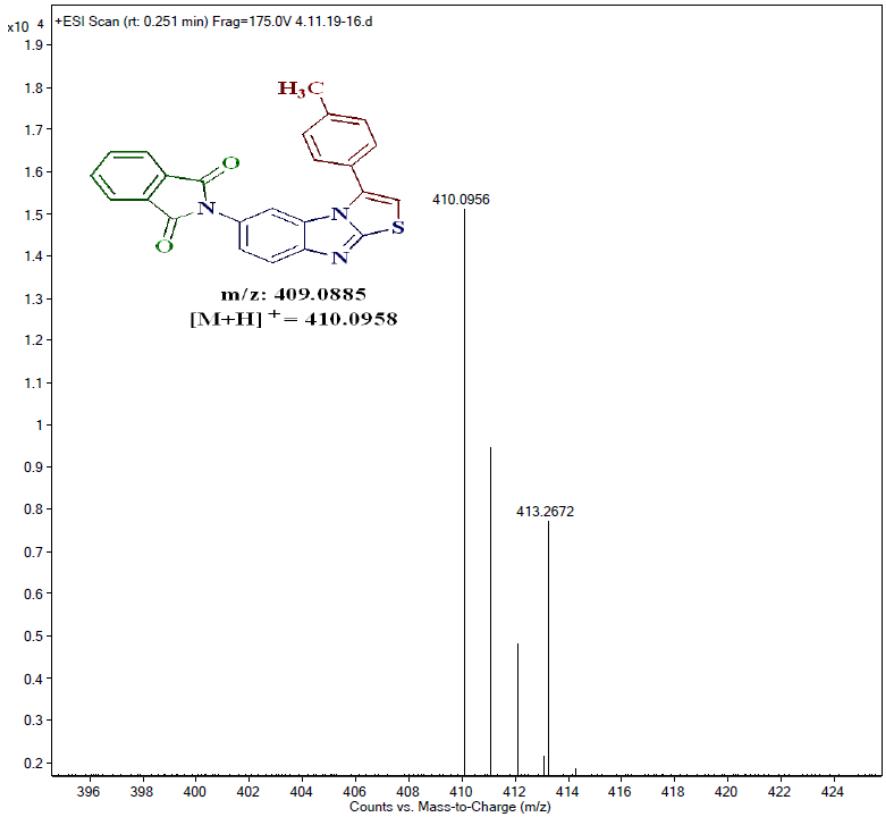

^{1}H-NMR Spectrum of compound 5c in DMSO-d_6 (400MHz):

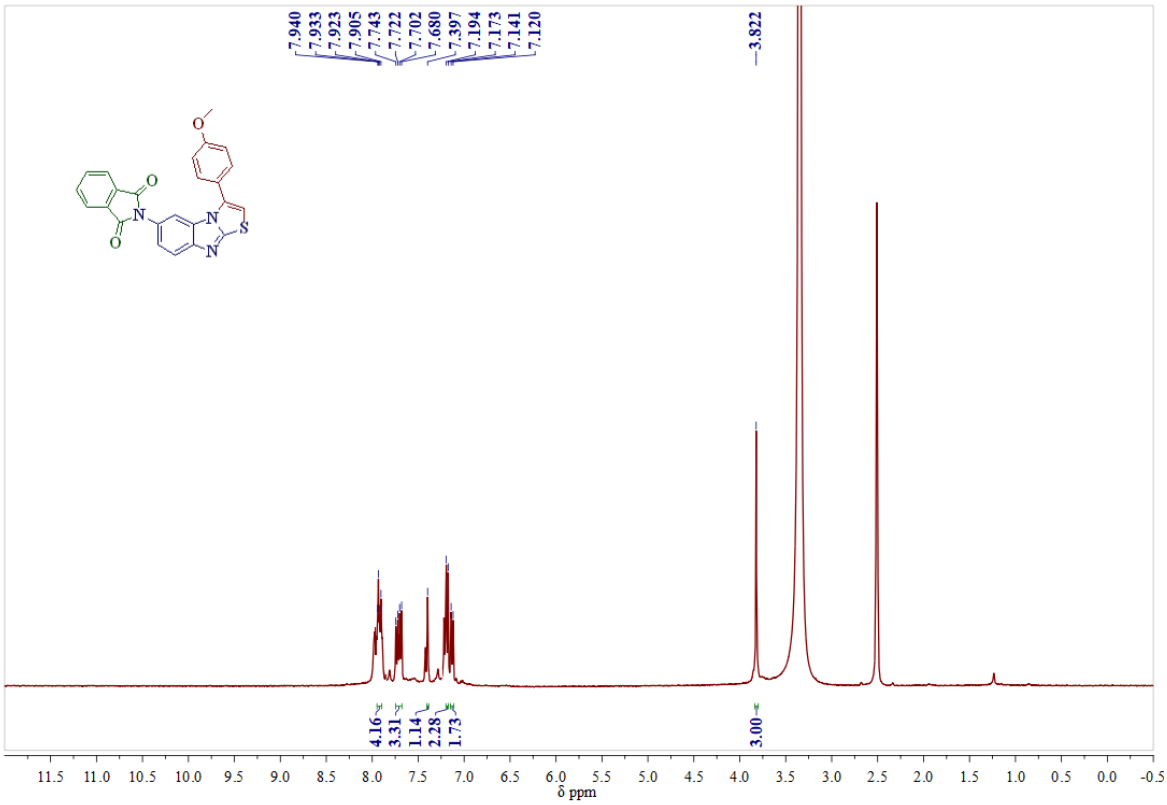

^{13}C-NMR Spectrum of compound 5c in CDCl$_3$-DMSO-d_6 (100MHz):

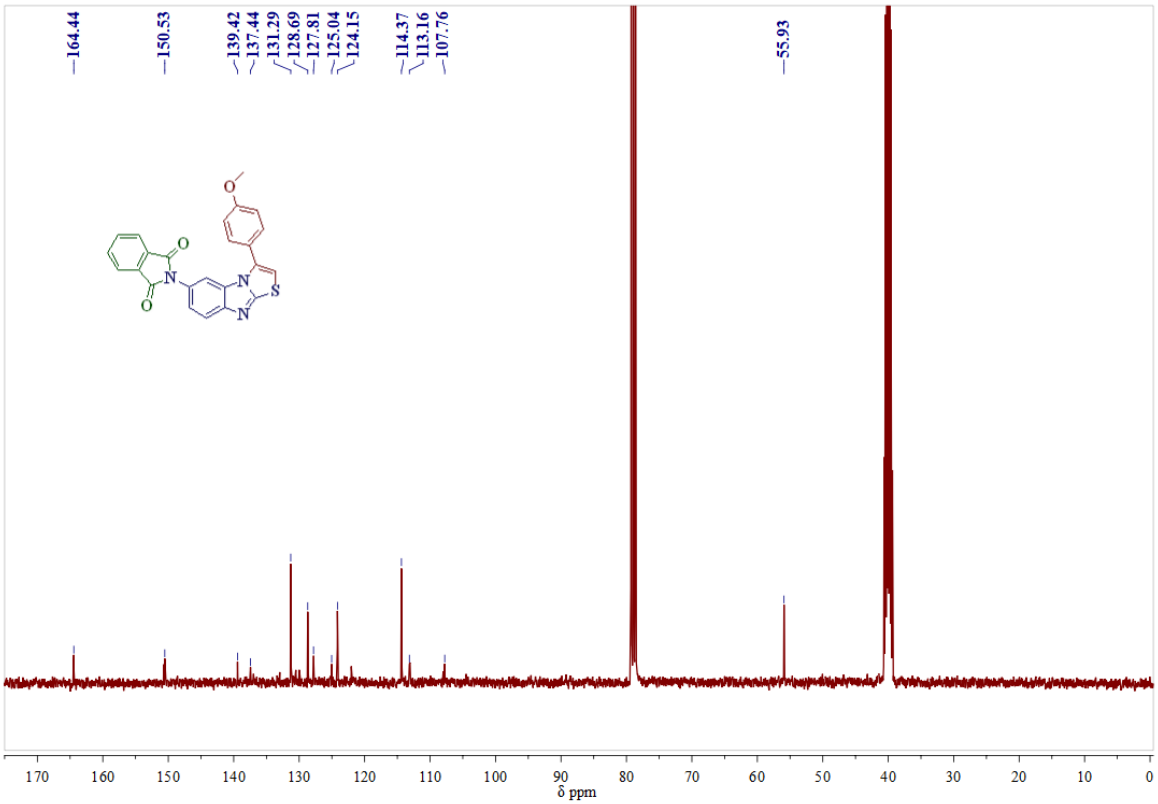

Mass spectrum of compound 5c

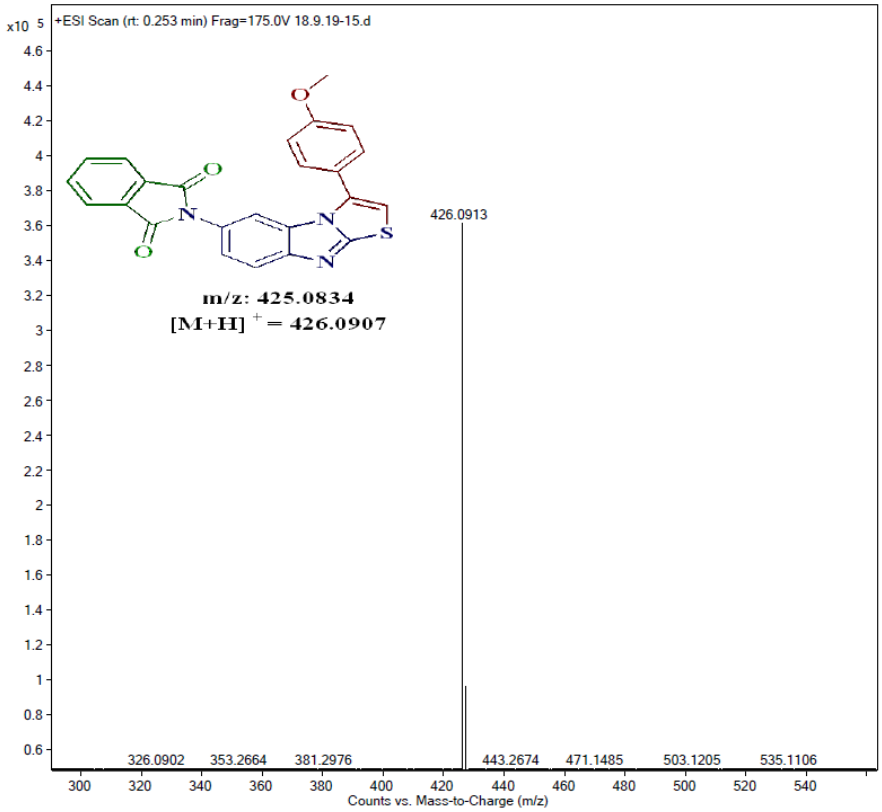

[1]H-NMR Spectrum of compound 5d in DMSO-*d*$_6$ (400MHz):

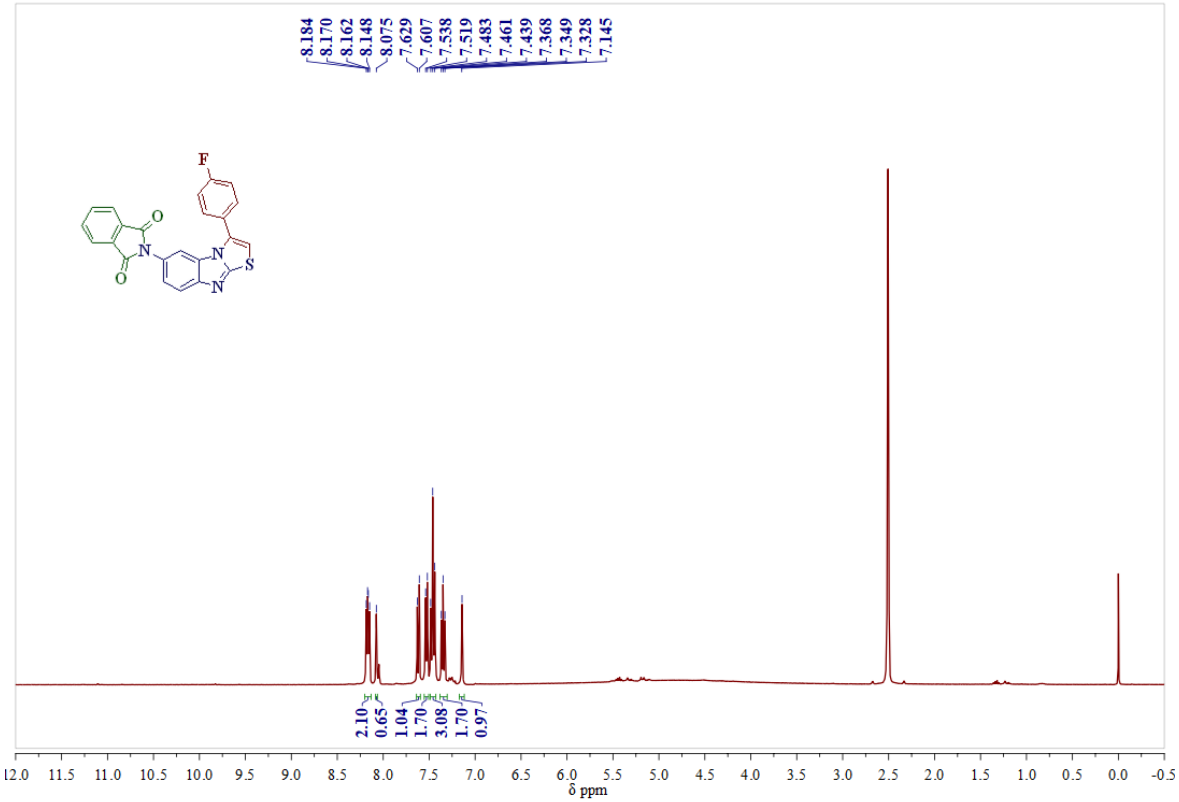

[13]C-NMR Spectrum of compound 5d in CDCl$_3$-DMSO-*d*$_6$ (100MHz):

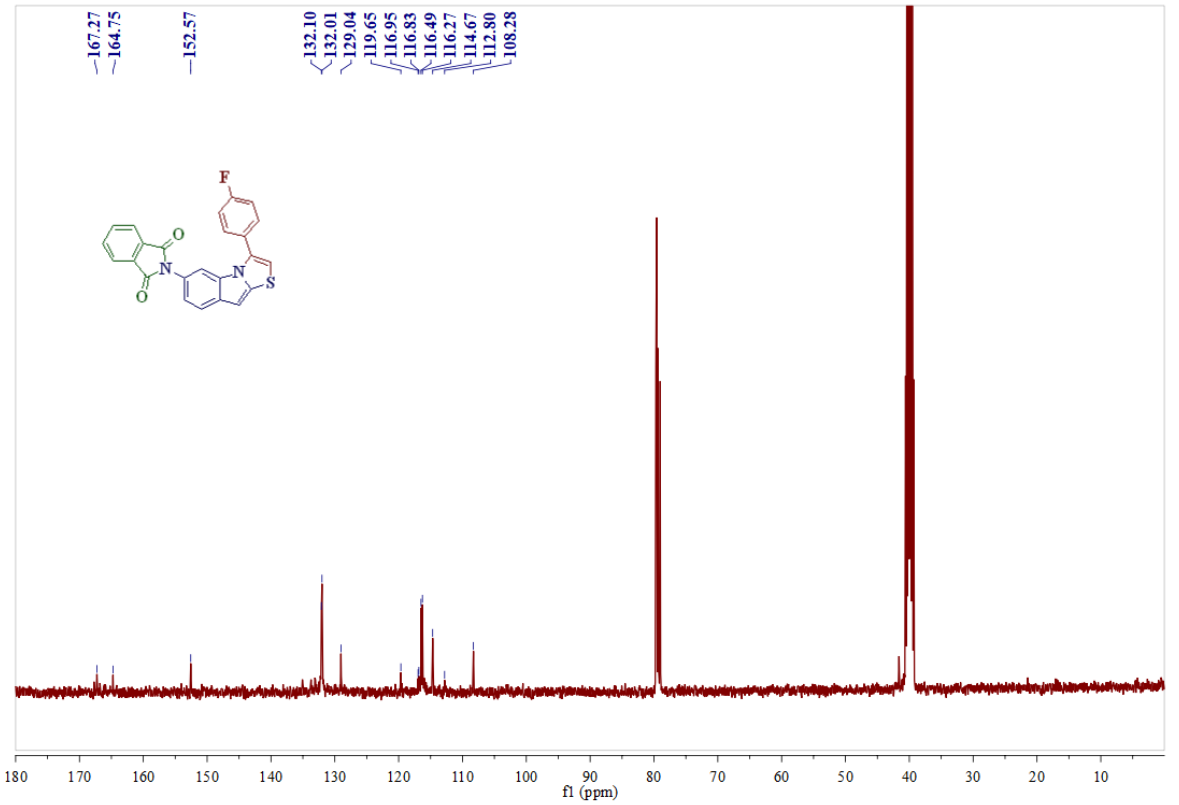

Mass spectrum of compound 5d

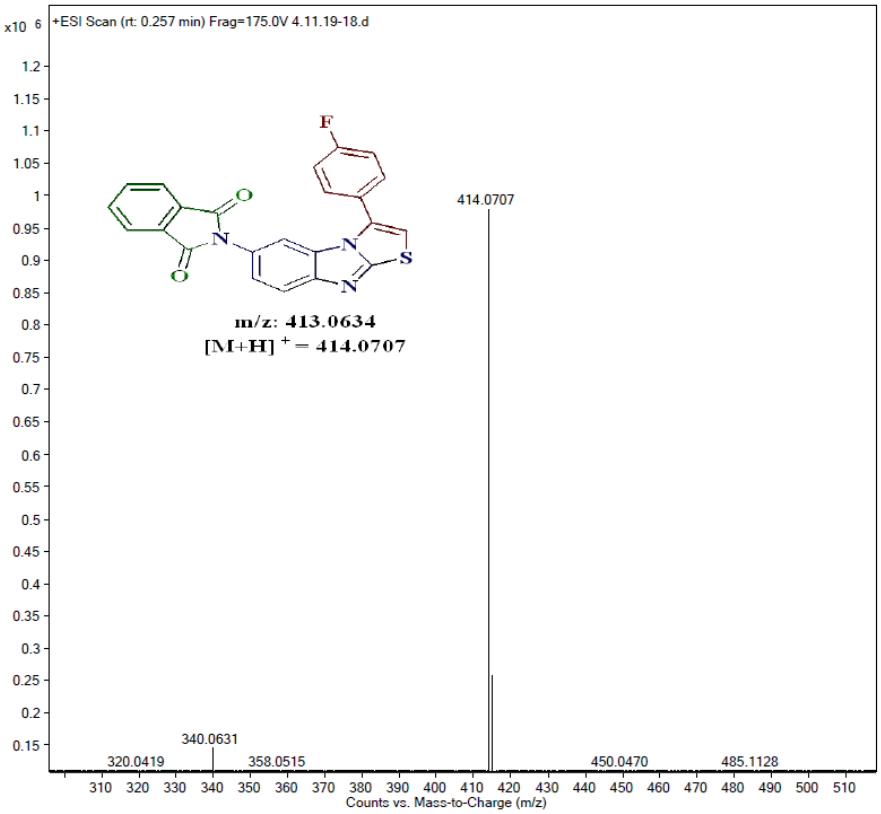

^{1}H-NMR Spectrum of compound 5e in DMSO-d_6 (400MHz):

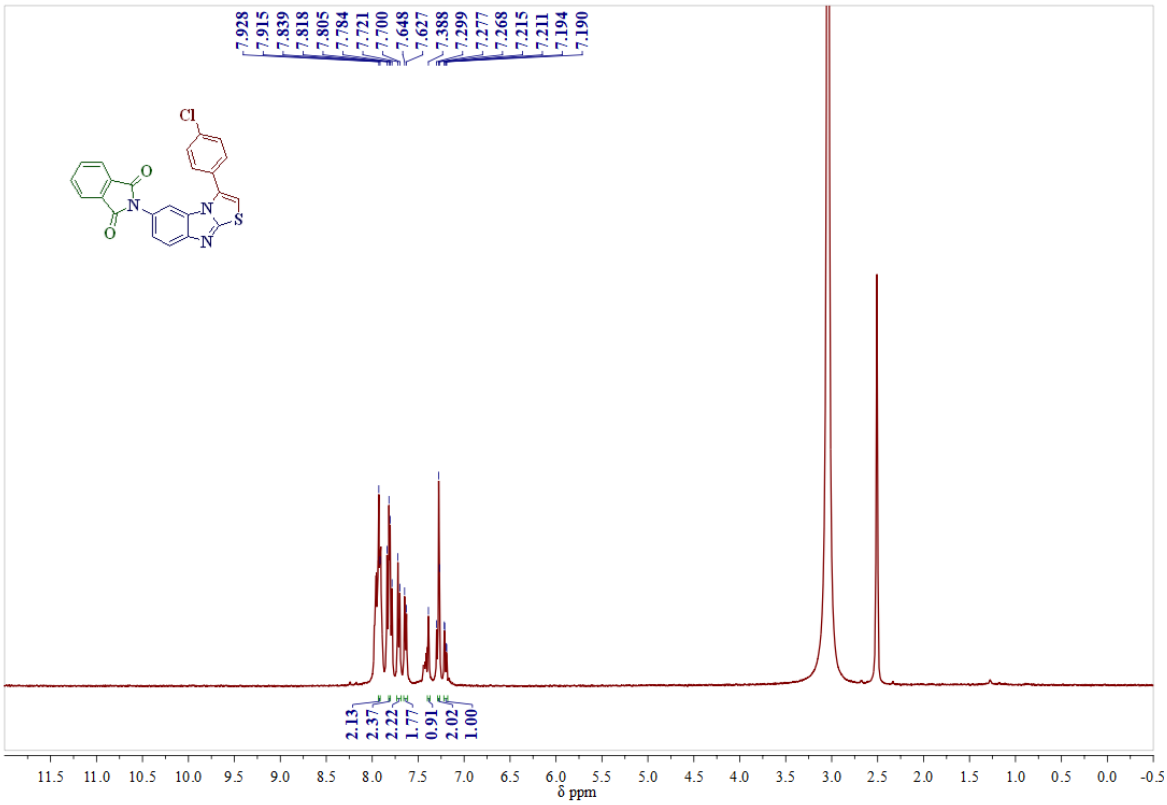

^{13}C-NMR Spectrum of compound 5e in DMSO-d_6 (100MHz):

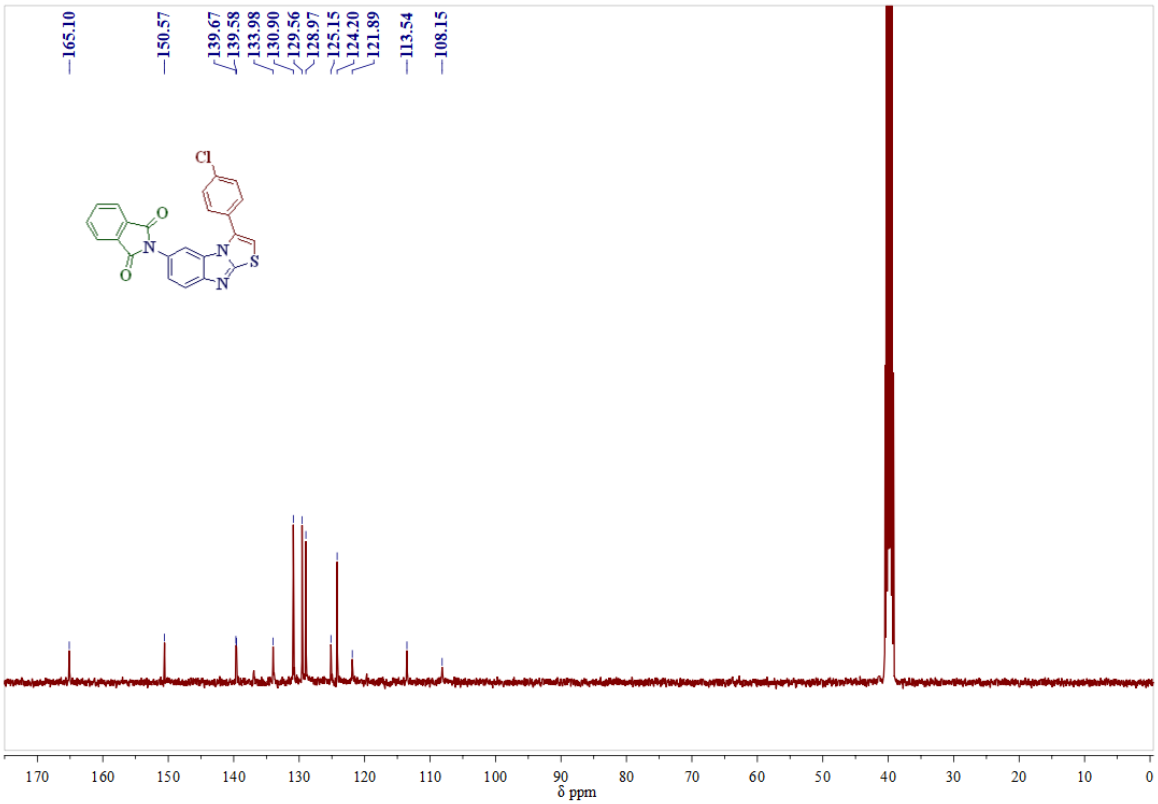

Mass spectrum of compound 5e

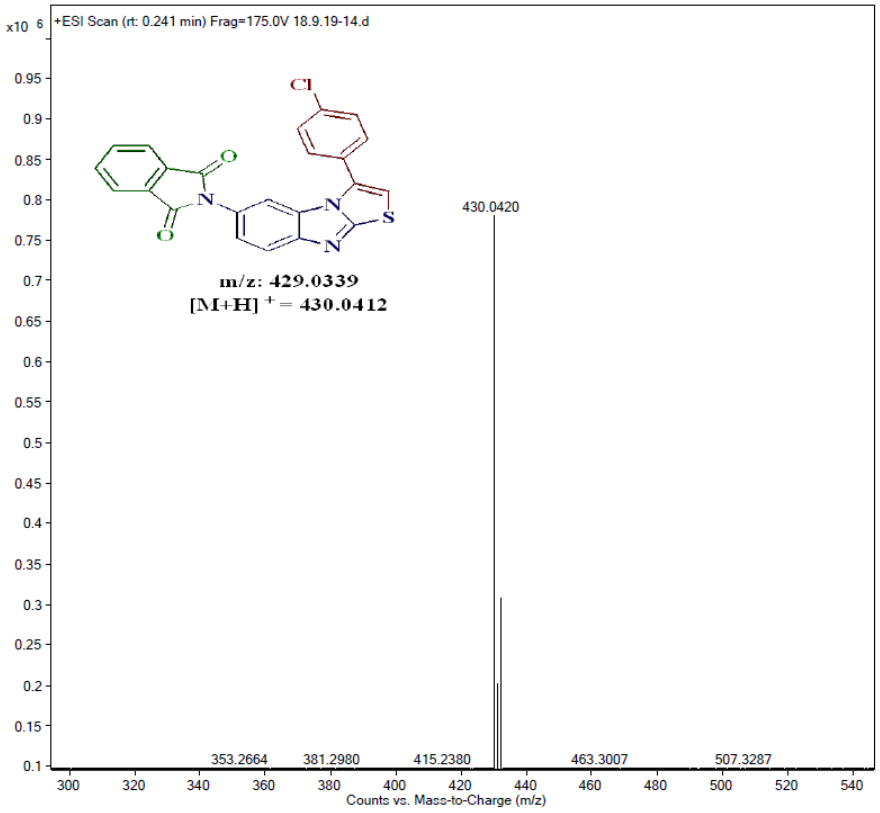

[1]H-NMR Spectrum of compound 5f in DMSO-d_6 (400MHz):

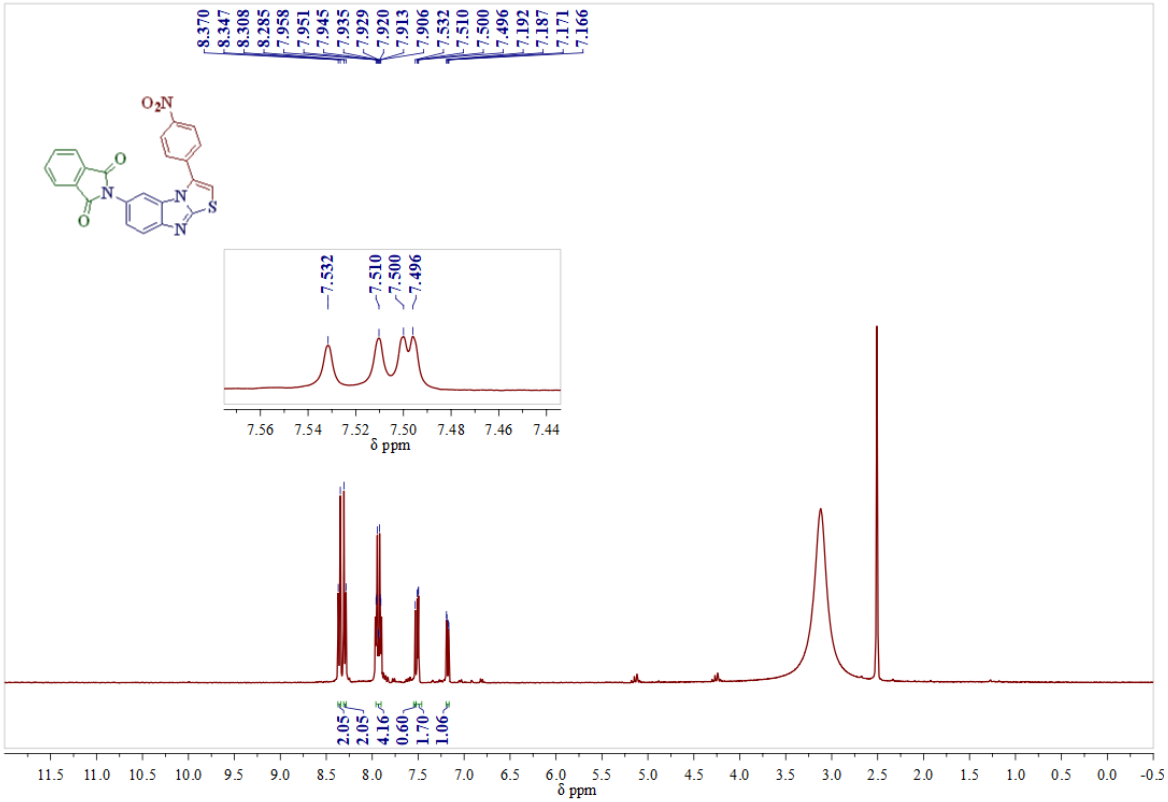

[13]C-NMR Spectrum of compound 5f in DMSO-d_6 (100MHz):

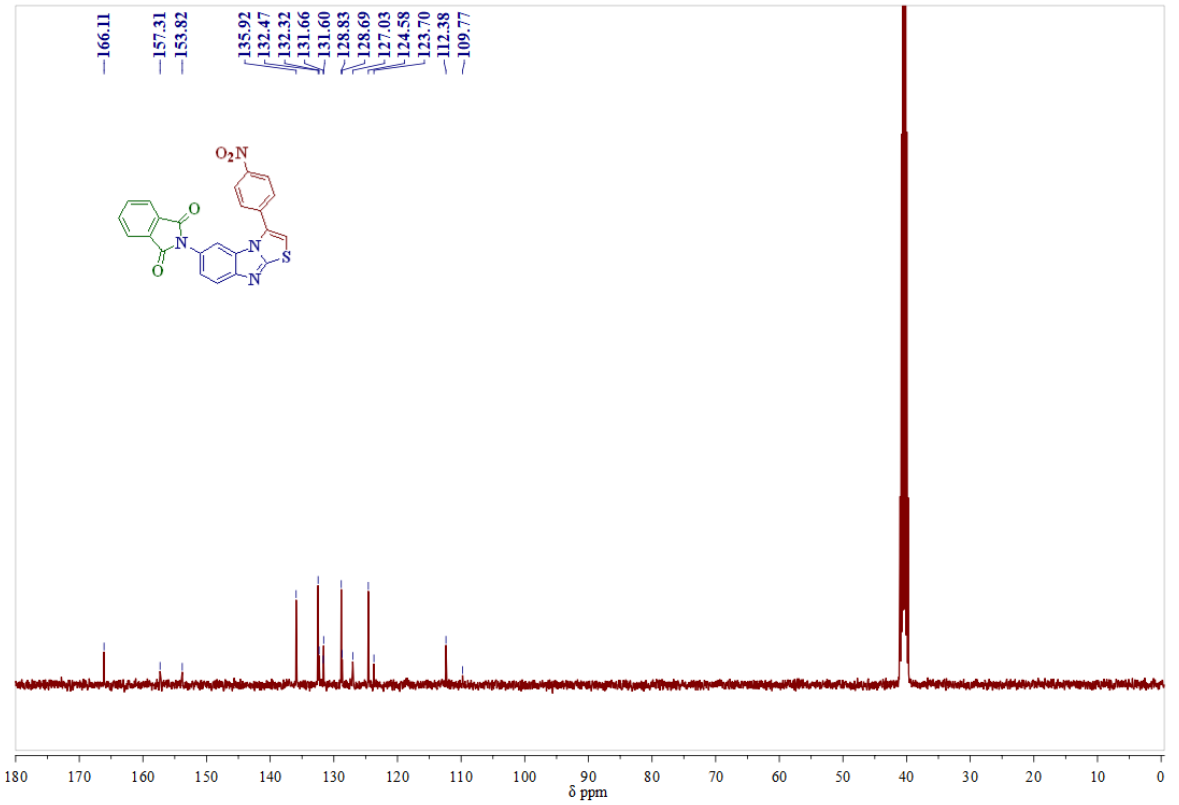

Mass Spectrum of compound 5f

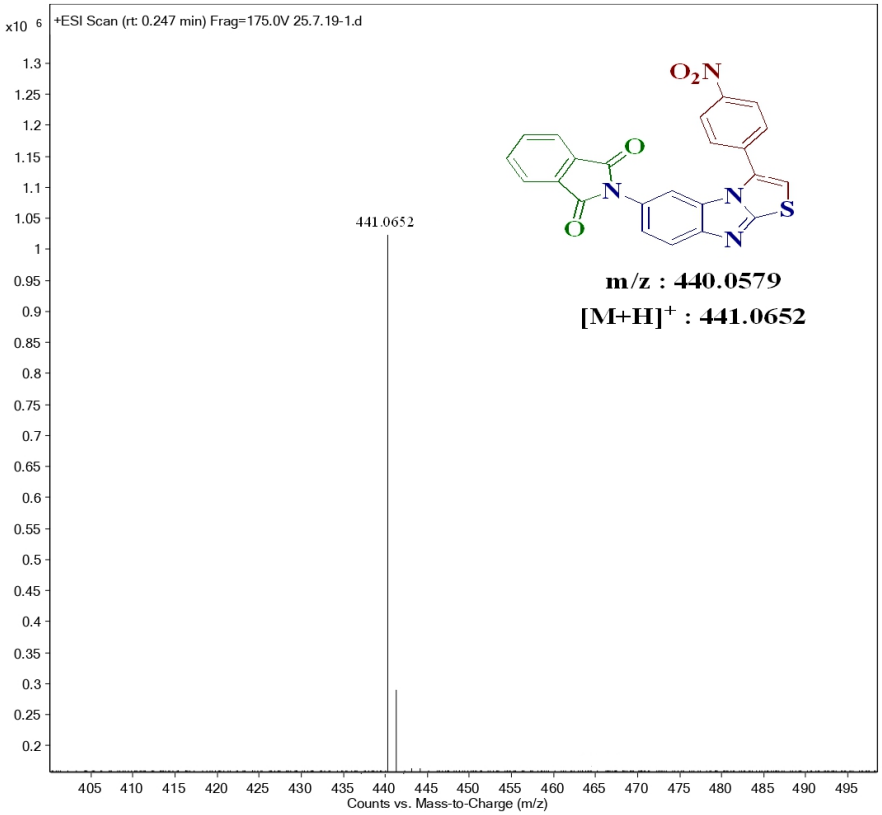

^{1}H-NMR Spectrum of compound 5g in DMSO-d_6 (400MHz):

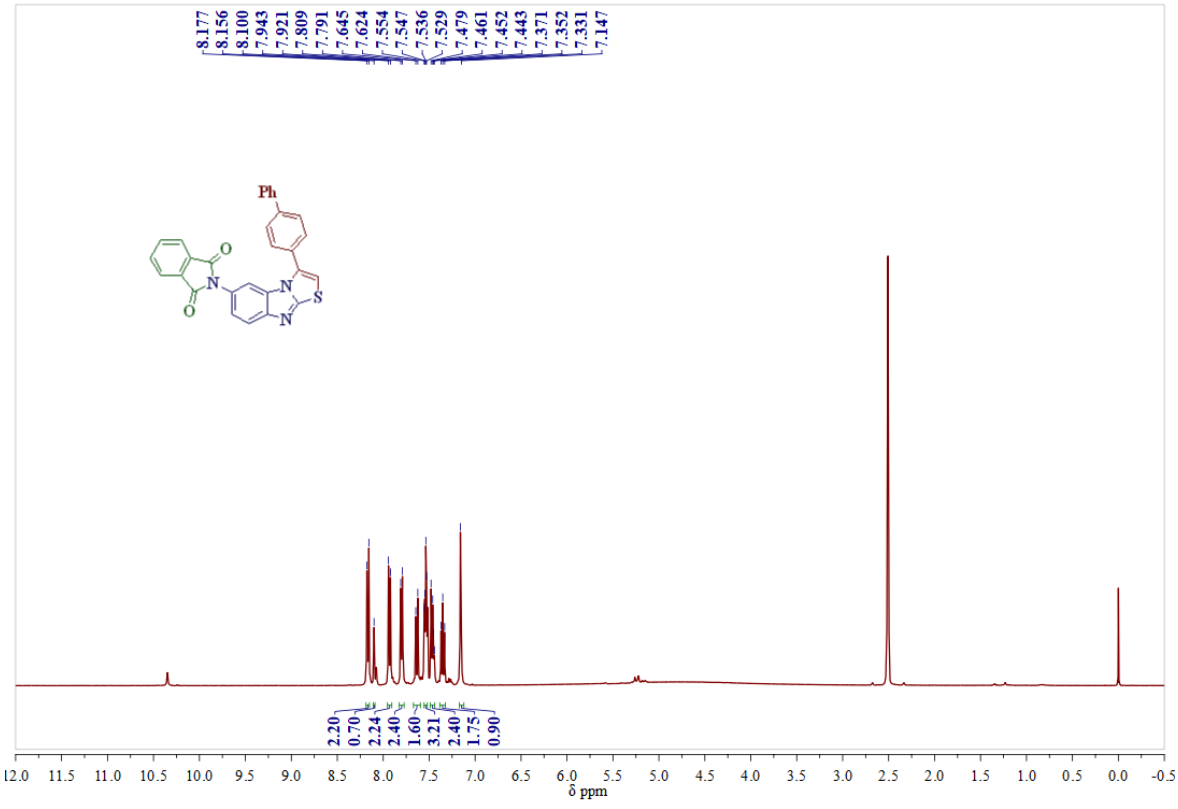

^{13}C-NMR Spectrum of compound 5g in DMSO-d_6 (100MHz):

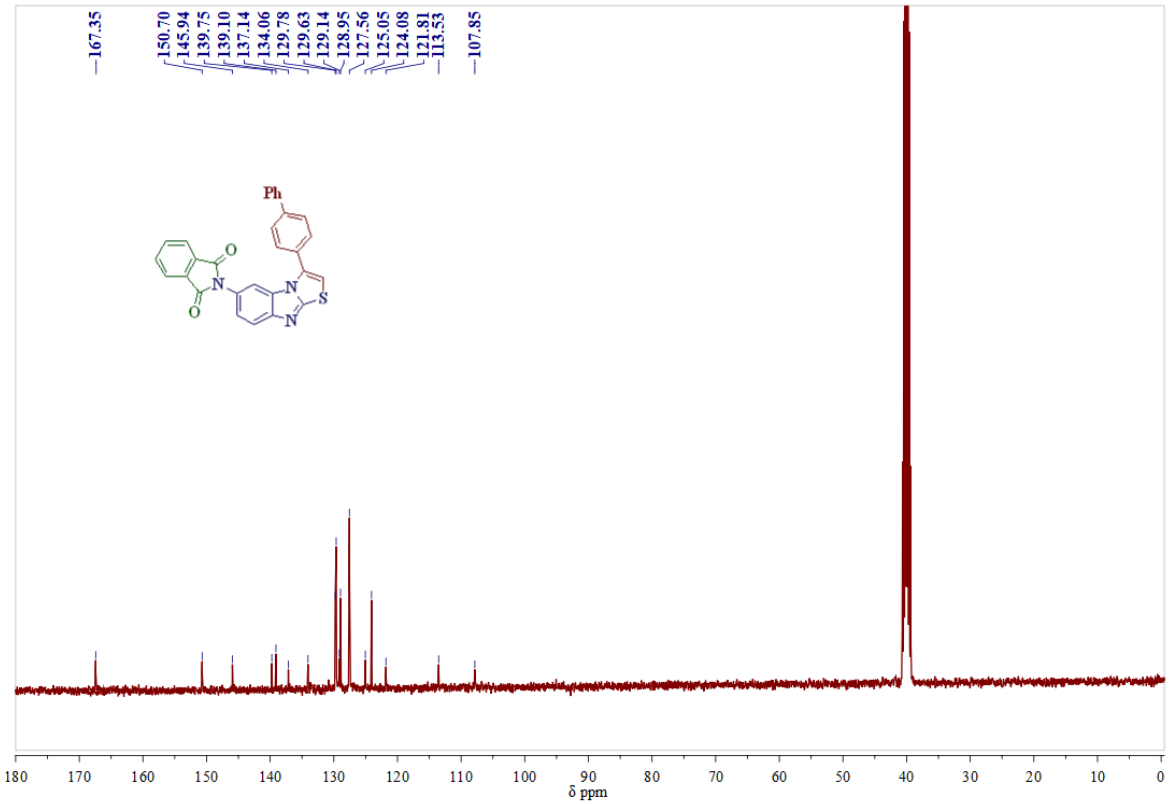

Mass spectrum of compound 5g

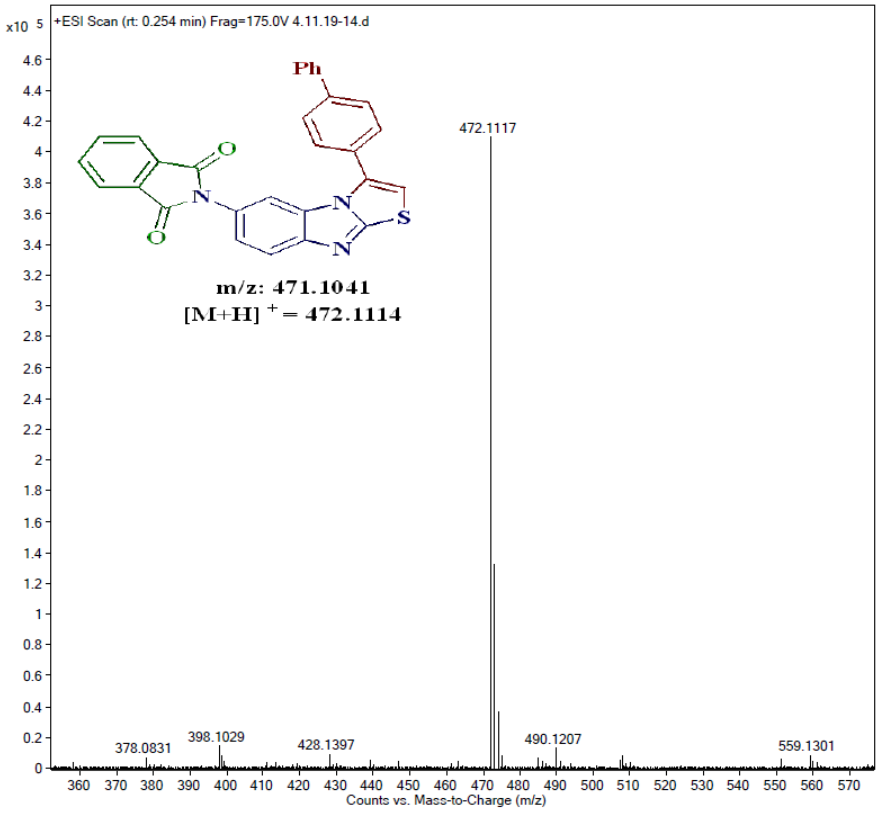

^{1}H-NMR Spectrum of compound 5h in DMSO-d_6 (400MHz):

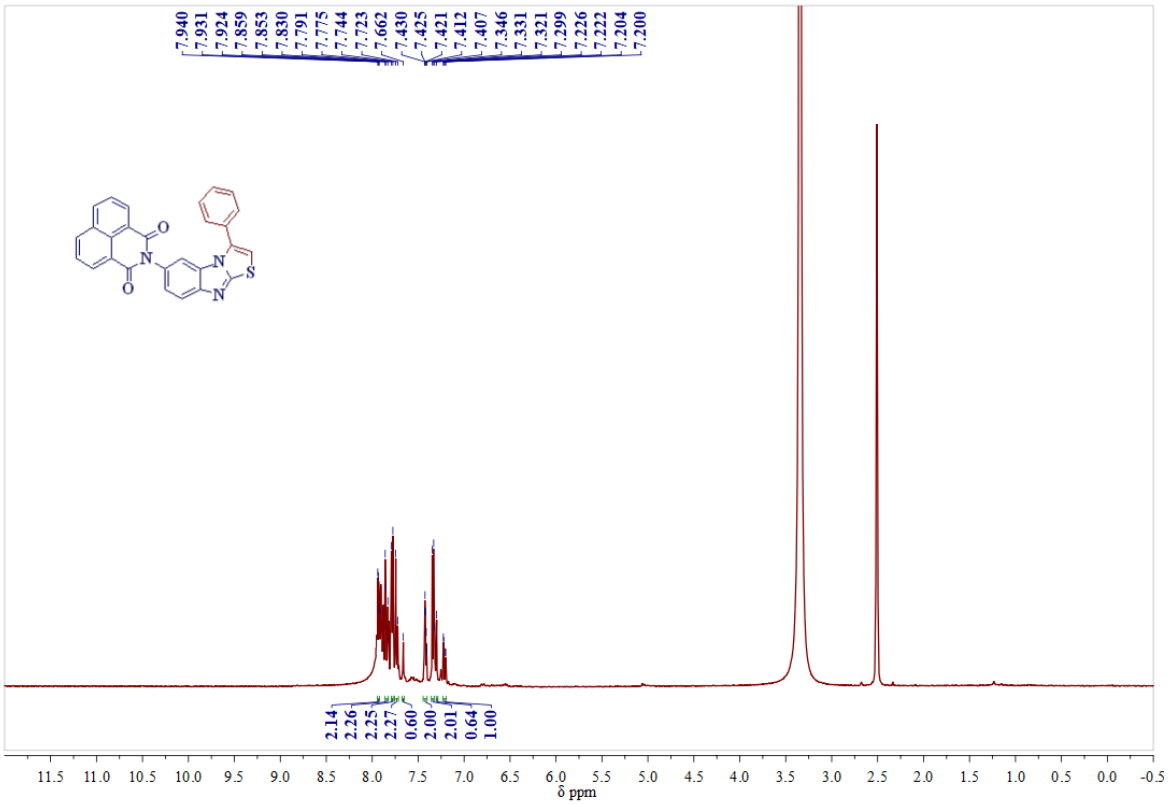

^{13}C-NMR Spectrum of compound 5h in DMSO-d_6 (100MHz):

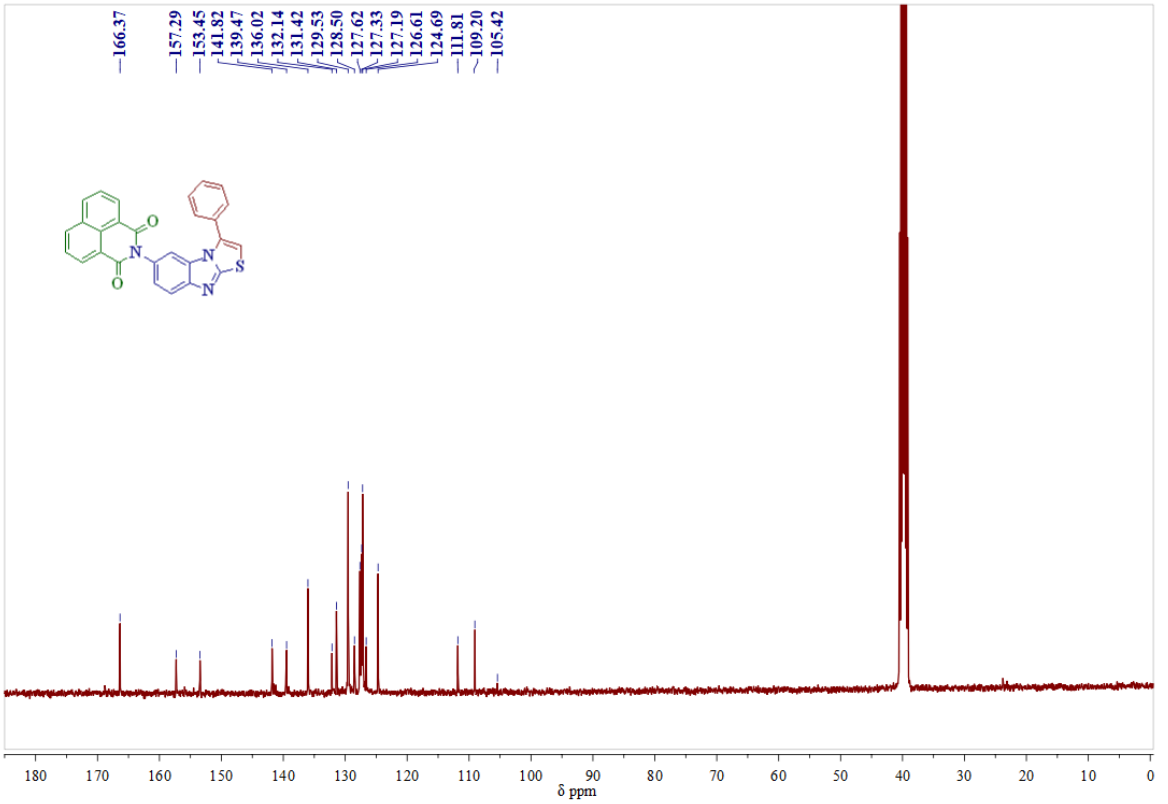

Mass spectrum of compound 5h

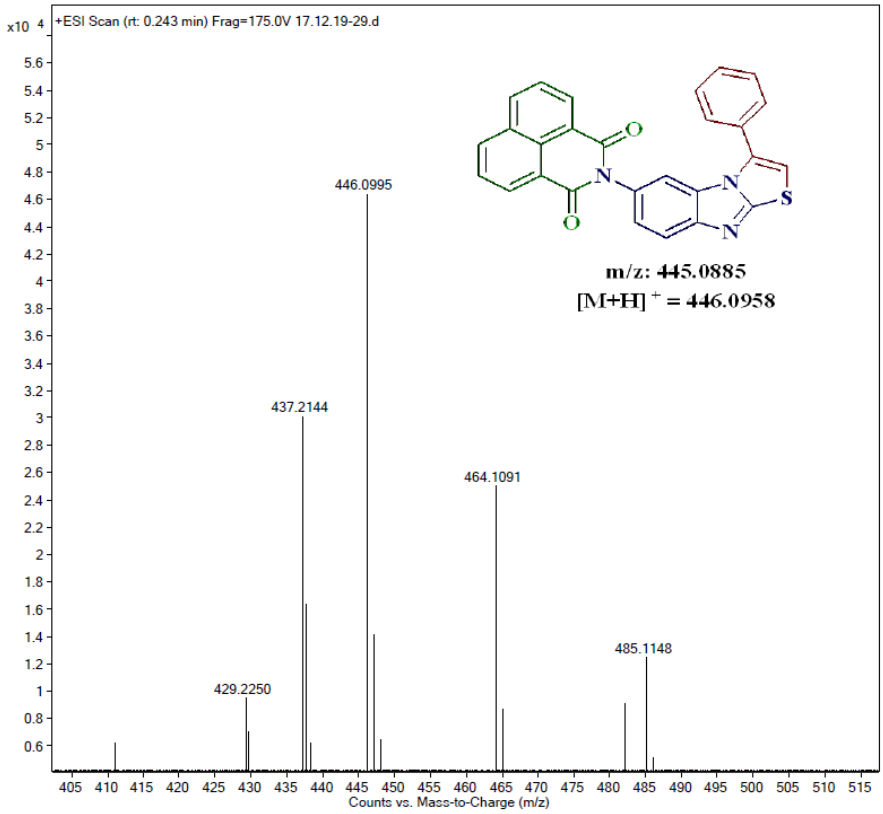

5.9. References

1. Anastas, P. T.; Kirchhoff, M. M. *Acc. Chem. Res.* **2002**, *35,* 686-694.
2. de Marco, B.A.; Rechelo, B. S.; Totoli, E. G.; Kogawa, A. C.; Salgado, H. R. N. *Saudi Pharm. J.* **2019**, *27*, 1–8.
3. Tozkoparan, B.; Ertan, M.; Kelicen, P.; Demirdamar, R. *Farmaco.* **1999,** *30*, 54(9), 588-593.
4. Ali, A. R.; El-Bendary, E. R.; Ghaly, M. A.; Shehata, I. A. *Eur. J. Med. Chem.* **2014**, *75*, 492–500.
5. Park, J. H.; El-Gamal, M. I.; Lee, Y. S.; Oh, C-.H. *Eur. J. Med. Chem.* **2011**, *46,* 5769–5777.
6. Moraski, G. C.; Markley, L. D.; Chang, M. et al. *Bioorganic. Med. Chem.* **2012,** *20*, 2214–2220.
7. Romain, D.; Ste´phanie, K.; Emmanuelle, B.; David, G.; Christiane, G. *J. Comb. Chem.* **2009,** *11,* 947–950.
8. Balkan, A.; Uma, S.; Ertan, M.; Wiegrebe, W. *Pharmazie.* **1992**, *47*, 687-688.
9. Vu, C. B.; Bemis, J. E.; Disch, J. S. *et al. J. Med. Chem.* **2009**, *52*, 1275–1283.
10. Milne, J. C.; Lambert, P. D.; Schenk, S. *et al. Nature.* **2007,** *450*, 712-716.
11. Budriesi, R.; Ioan, P.; Locatelli. A. *et al.* J. Med. Chem. **2008,** *51,* 1592–1600.
12. Locatelli, A.; Cosconati, S.; Micucci, M. *et al. J Med Chem.* **2013,** *56,* 3866–3877.
13. Wichmann, J.; Adam, G.; Kolczewski, S. *et al*. *Bioorg. Med. Chem. Lett.* **1999**, *9*, 1573–1576.
14. Ghorab, M. M.; Hassan, A. Y. *Phosphorus, Sulfur Silicon Relat. Elem.* **1998,** *141*, 251–261. https://doi.org/10.1080/10426509808033737
15. Pietrancosta, N.; Moumen, A.; Dono, R. *et al*. J. Med. Chem. **2006,** *49,* 3645–3652.
16. Humphrey, J. M.; Chamberlin, A. R. *Chem. Rev.* **1997**, *97*, 2243–2266.
17. Norman, M. H.; Minick, D. J.; Rigdon, G. C. *J. Med. Chem.* **1996,** *39,* 149–157.
18. Hardcastle, I. R.; Ahmed, S. U.; Atkins, H. *et al. Bioorg. Med. Chem. Lett.* **2005,** 15, 1515–1520.
19. Szadowski, J.; Niewiadomski, Z. *Dyes Pigm.* **1993,** *21,* 123–133.
20. Lee, S.; Shinji, C.; Ogura, K. *et al. Bioorg. Med. Chem. Lett.* **2007,** *17,* 4895–4900.
21. Letizia, J. A.; Salata, M. R.; Tribout, C. M, *et al. J. Am. Chem. Soc.* **2008,** *130,* 9679–9694.
22. Hardcastle, I. R.; Ahmed, S. U.; Atkins, H. *et al. J. Med. Chem.* **2006**, *49*, 6209–6221.

23. Andrew, H. F.; Bradsher, C. K. *J. Heterocycl. Chem.* **1967**, *4*, 577.
24. Narayan, S. A. T.; Kumar, V.; Pujari, H. K.; *Indian J. Chem. Sec B: Org. Chem. Incl. Med. Chem.* **1986**, *25B* (3), 267.
25. Wang, M.; Lu, J.; Ma, J.; Zhang, Z.; Wang, F. *Angew. Chemie - Int. Ed.* **2015**, *54*, 14061–14065.
26. Timiri, A. K.; Selvarasu, S.; Kesherwani, M.; Vijayan, V.; Sinha, B. N.; Devadasan, V.; Jayaprakash, V. *Bioorg. Chem.* **2015**, *62*, 74–82.
27. Khushbu, K.P.; Gayakwad, E.M.; Vilas V. Patil V.V.; Ganapati S.; Shankarling, G.S. *Adv.Syn. Catal.* **2018**, 10.1002/adsc.201801673.
28. Chen, D. C.; Ye, H. Q.; Wu, H. *Catal. Commun.* **2007**, *8*, 1527–1530.
29. Dos Santos, J. L.; Lanaro, C.; Chelucci, R. C.; Gambero, S.; Bosquesi, P. L.; Reis, J. S.; Lima, L. M.; Cerecetto, H.; González, M.; Costa, F. F.; Chung, M. C. *J. Med. Chem.* **2012**, *55*, 7583–7592.
30. Le, Z. G.; Chen, Z. C.; Hu, Y.; Zheng, Q. G. *Chinese Chem. Lett.* **2005**, *16*, 201–204.
31. Kuribara, T.; Nakajima, M.; Nemoto, T. *Org. Lett.* **2020**, *22*, 2235–2239.
32. Bhatt, P.; Kumar, M.; Jha, A. *Mol. Divers.* **2018**, *22*, 827–840.
33. Yedage, S. L.; D'Silva, D. S.; Bhanage, B. M. *RSC Adv.* **2015**, *5*, 80441–80449.
34. Liang, J.; Lv, J.; Fan, J. C.; Shang, Z. C. *Synth. Commun.* **2009**, *39*, 2822–2828.
35. Srinivas, M.; Hudwekar, A. D.; Venkateswarlu, V.; Reddy, G. L.; Kumar, K. A. A.; Vishwakarma, R. A.; Sawant, S. D. *Tetrahedron Lett.* **2015**, *56*, 4775–4779.
36. Upadhyay, S. K.; Pingali, S. R. K.; Jursic, B. S. *Tetrahedron Lett.* **2010**, *51*, 2215–2217.
37. Abdel-Aziz, A. A.-M.; El-Azab, A. S.; Abu El-Enin, M. A.; Almehizia, A. A.; Supuran, C. T.; Nocentini, A. *Bioorg. Chem.* **2018**, *80*, 706–713.
38. Zhao, P.-L.; Ma, W.-F.; Duan, A.-N.; Zou, M.; Yan, Y.-C.; You, W.-W.; Wu, S.-G. *Eur. J. Med. Chem.* **2012**, *54*, 813–822. https://doi.org/10.1016/j.ejmech.2012.06.041.
39. Kok, S. H. L.; Gambari, R.; Chui, C. H.; Yuen, M. C. W.; Lin, E.; Wong, R. S. M.; Lau, F. Y.; Cheng, G. Y. M.; Lam, W. S.; Chan, S. H. *Bioorg. Med. Chem.* **2008**, *16*, 3626–3631.
40. Mei, R.; Xiong, F.; Yang, C.; Zhao, J. *Adv. Synth. Catal.* **2021**, *363*, 1861–1866.
41. Jana, S.; Chakraborty, A.; Shirinian, V. Z.; Hajra, A. *Adv. Synth. Catal.* **2018**, *360*, 2402–2408.
42. Zhao, J.; Xiao, Q.; Chen, J.; Xu, J. *European J. Org. Chem.* **2020**, *2020*, 5201–5206.
43. Shen, G.; Yang, B.; Huang, X.; Hou, Y.; Gao, H.; Cui, J.; Cui, C.; Zhang, T. *J. Org. Chem.* **2017**, *82*, 3798–3805.

44. Xu, H.; Zhang, Y.; Huang, J.; Chen, W. *Org. Lett.* **2010**, *12*, 3704–3707.

45. Xiao, D.; Han, L.; Sun, Q.; Chen, Q.; Gong, N.; Lv, Y.; Suzenet, F.; Guillaumet, G.; Cheng, T.; Li, R. *RSC Adv.* **2012**, *2*, 5054–5057.

Summary

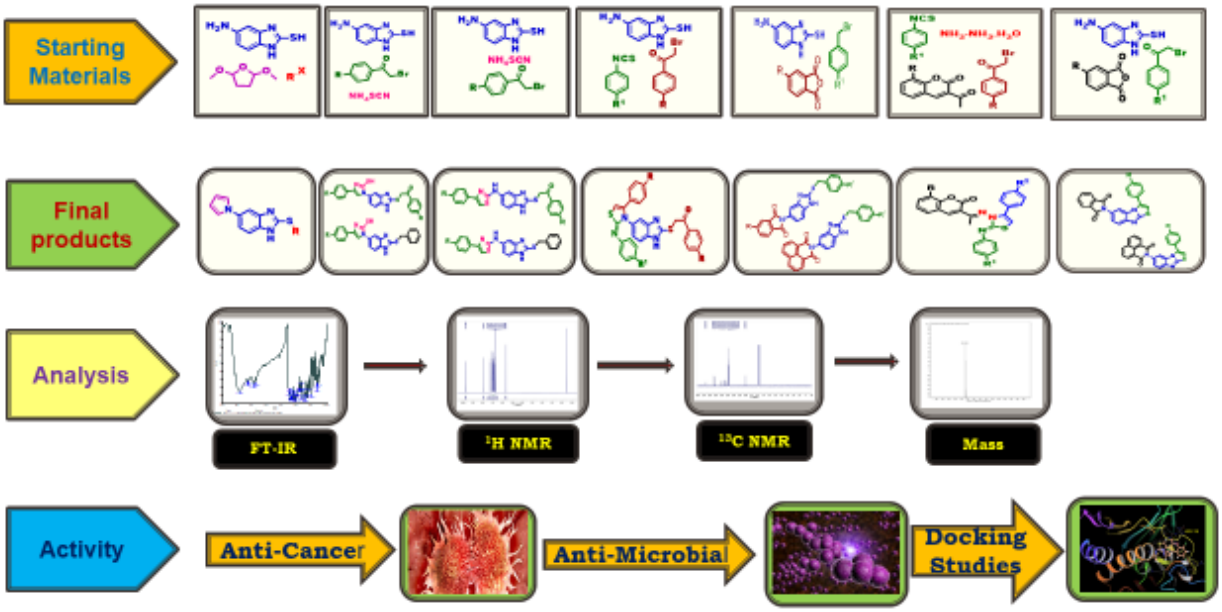
Starting Materials
Final products
Analysis
FT-IR
^{1}H NMR
^{13}C NMR
Mass
Activity
Anti-Cancer
Anti-Microbial
Docking Studies

The title of the thesis is "**Multicomponent Synthesis of New Heterocyclic Compounds and their Biological Evaluation"** and it consists of five chapters**,** out of which four chapters (II/III/IVA/IVB/IVC/V) deal with the synthesis of various heterocyclic compounds containing nitrogen and sulphur relying on the multi-component approach as a common theme. The introduction part (**Chapter-**I) gives a brief overview of multi-component reactions showing their various applications in modern organic synthesis and their uses in the synthesis of biologically active compounds.

CHAPTER-I

A brief review of multi-component reactions and their applications in the synthesis of biologically active compounds

This Chapter describes the history and importance of multi-component reactions (MCRs) and reactions on 5-amino-2-mercapto-benzimidazoles. In the present study, different heterocyclic compounds were synthesized through a multi-component approach involving green chemistry principles. In recent years, modern organic chemists have paid attention to environmentally-benign synthetic strategies both in industry and academia. Also, hazardous, impulsive, and poisonous organic solvents are constantly replaced by either the use of solvent-free [1], water-medium [2], microwave irradiated [3], or multicomponent reactions [4-7] (MCRs), etc. Nonetheless, the aforementioned MCRs received considerable interest in the area of green synthesis. In general, MCRs are defined as the components consisting of three or more reactants in a single reaction vessel to give products containing virtually all the number of reactants. Due to its featured applications like using shorter reaction time, lower energy consumption, high yield, facile synthesis, atom proficiency, and straightforward reactions became more popular. Hence, in recent years the multicomponent strategy has become an increasingly active area of modern organic synthesis [8], medicinal chemistry [9], natural product synthesis [10], polymer chemistry [11], agro chemistry [12], and combinatorial chemistry [13]. Thus, we have selected the development of new methodologies by ensuring a multi-component strategy as our research program.

The main objectives of the present work are revealed and outlines of the present work carried out are given.

The objectives of the work

- To establish facile, efficient, and eco-friendly methods for the synthesis of biologically active molecules.
- To establish the structures of newly synthesized compounds by analytical and spectral methods.
- To study and screen the biological activities and to carry out computational studies of the newly synthesized compounds.

3-Acetyl coumarins [14,15] phenacyl bromides [16,17] and 5-amino-2-mercaptobenzimidazole [18] are the key intermediates in the synthesis of heterocyclic compounds. The reactivity of these intermediates is also discussed.

CHAPTER-II

Synthesis of benzimidazole linked pyrrole derivatives by MCR approach and their molecular docking studies.

This chapter describes the synthesis of S-alkylated/aralkylated benzimidazole–linked pyrrole **(4a-p)** derivatives as outlined in **Scheme 2.1**. The title compounds **4a-p** were synthesized by using 5-amino-2-mercaptobenzimidazole, 2,5-dimethoxytetrahydrafuran, and various alkyl/aralkyl halides (**1:1:1**) in acetic acid in presence of fused sodium acetate *via* multi-component reaction with good yields.

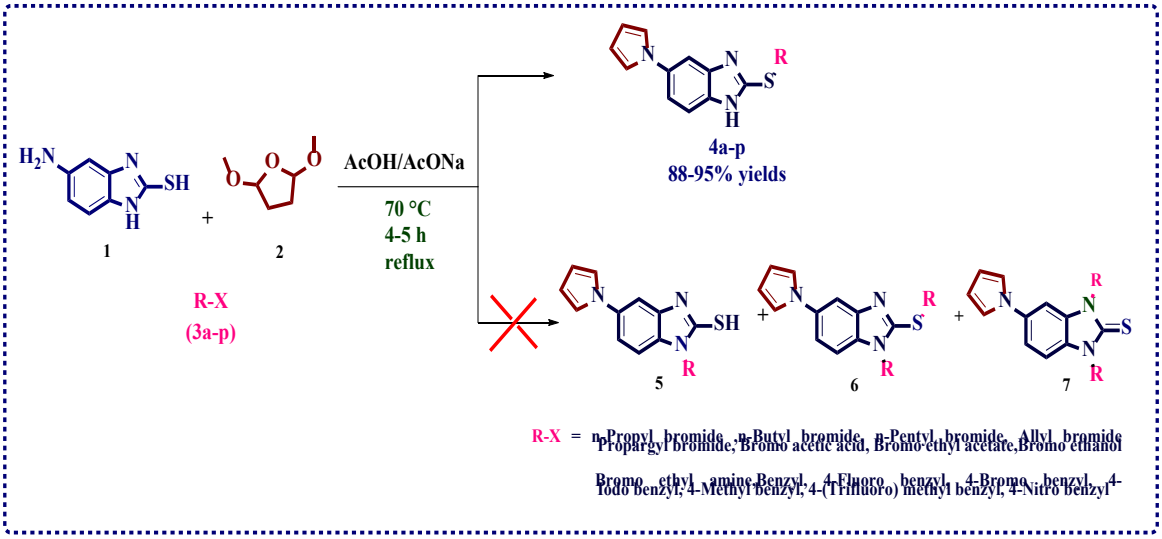

Scheme 2.1. Synthesis of benzimidazole-based pyrroles

The alternative possible condensed products 5,6 and 7 from 1,2 and 3 can be rejected based on their analytical and spectral data.

For the optimization of the reaction, we screened the reaction with various solvents, at different temperatures, and with different amounts of catalysts. High yields of the products were obtained when one equivalent of fused sodium acetate and one equivalent of alkyl/aralkyl halides were used in glacial acetic acid at 70 ºC.

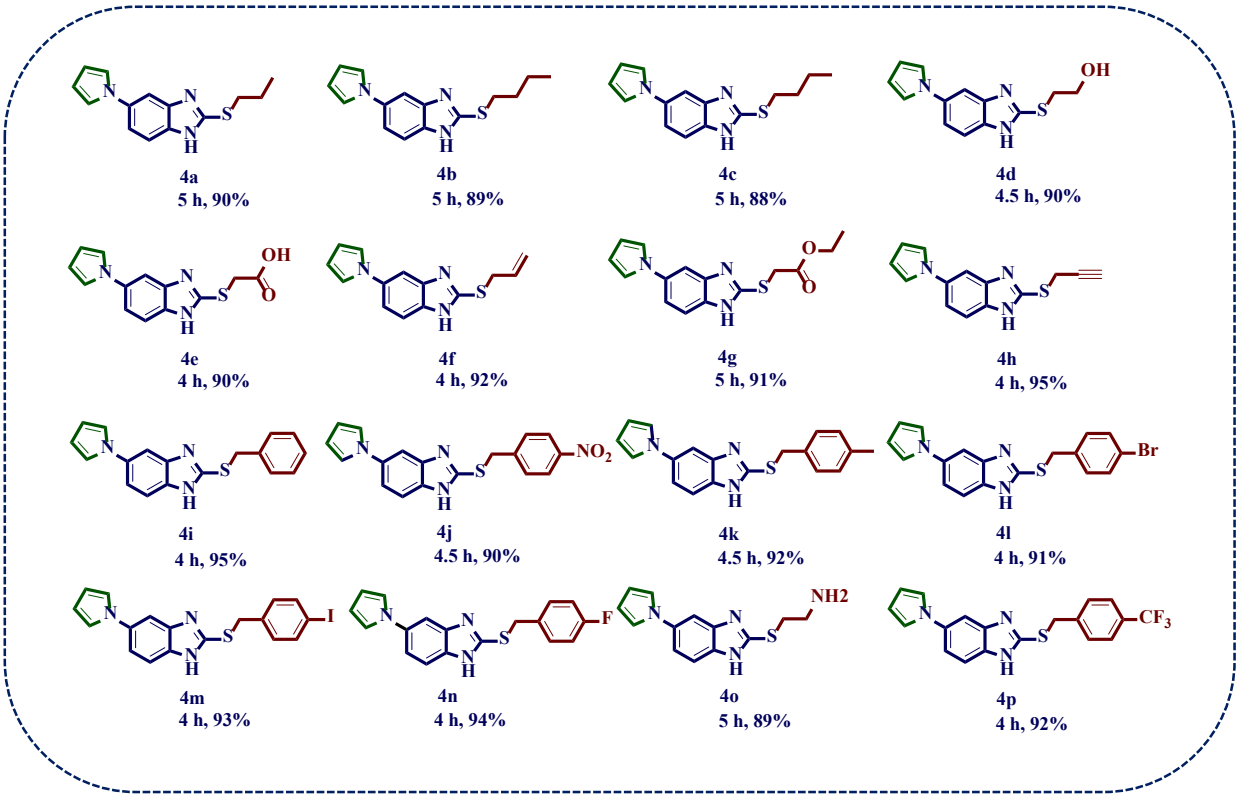

Figure 2.1. Different substitutions of benzimidazole-based pyrrole hybrids (**4a-p)**

Molecular Docking Studies

The in-silico molecular docking simulation was performed to scrutinize the *anti-tubulin* properties of the synthesized compounds (**4a-p**). The *anti-tubulin* properties of the molecules are predicted based on their binding affinity values at the active site of the receptor protein (1SA0). The lower binding affinity value indicates the better affinity of the molecule towards the protein. The compounds **4j** and **4p** showed the least binding affinity -8.3 kcal/mol and -8.9 kcal/mol respectively towards the active site of the receptor protein (1SA0).

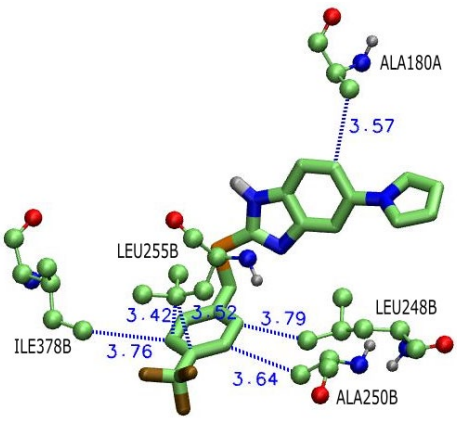

(**4p**)

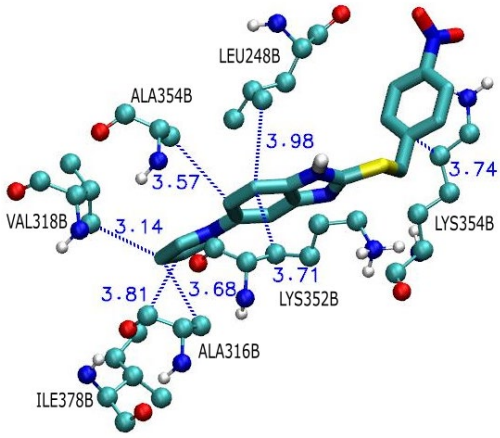

(**4j**)

Figure 2.2. Interacting amino acids at the active site of the protein with the compounds

The amino acid residues are involved in H-bonding, salt bridge, and π-cationic interactions. The compound **4p** showed hydrophobic interactions at the active site of the receptor protein. The interacting amino acids are ALA180A (3.57), LEU248B (3.79), ALA250B (3.64), LEU255B (3.52), LEU255B (3.42), and ILE378B (3.76). The compound **4j** is found to interact at the active site involving both hydrophobic and π-cationic interactions. LEU248B (3.98), LYS254B (3.74), ALA316B (3.68), VAL318B (3.14), LYS352B (3.71), ALA354B (3.57), and ILE378B (3.81) shows hydrophobic interactions while LYS254B (3.91) shows π-cationic interactions.

In conclusion, we have developed a potential green approach for the synthesis of novel benzimidazole-based pyrrole derivatives *via a* multi-component method. Further, the synthesized compounds were also subjected to molecular docking studies. The specialty of the reaction is that it is a transition-metal-free, column-free, catalyst-free reaction. And two N-C and one C-S bond are formed at a time.

CHAPTER-III

One-pot synthesis of thioalkylated benzimidazole-based 4-substituted mercaptoimidazole molecular hybrids *via a* multi-component approach

This chapter includes the synthesis of new mercaptoimidazoles and their benzyl hybrids (**4a-j**) and (**5a-f**). The starting materials required for the synthesis of the target compounds are, 5-amino-2-mercapto-benzimidazole, various substituted phenacyl bromides, aralkyl halides, and ammonium thiocyanate. The synthesis of title scaffolds was carried out as outlined in **Scheme 3.1**

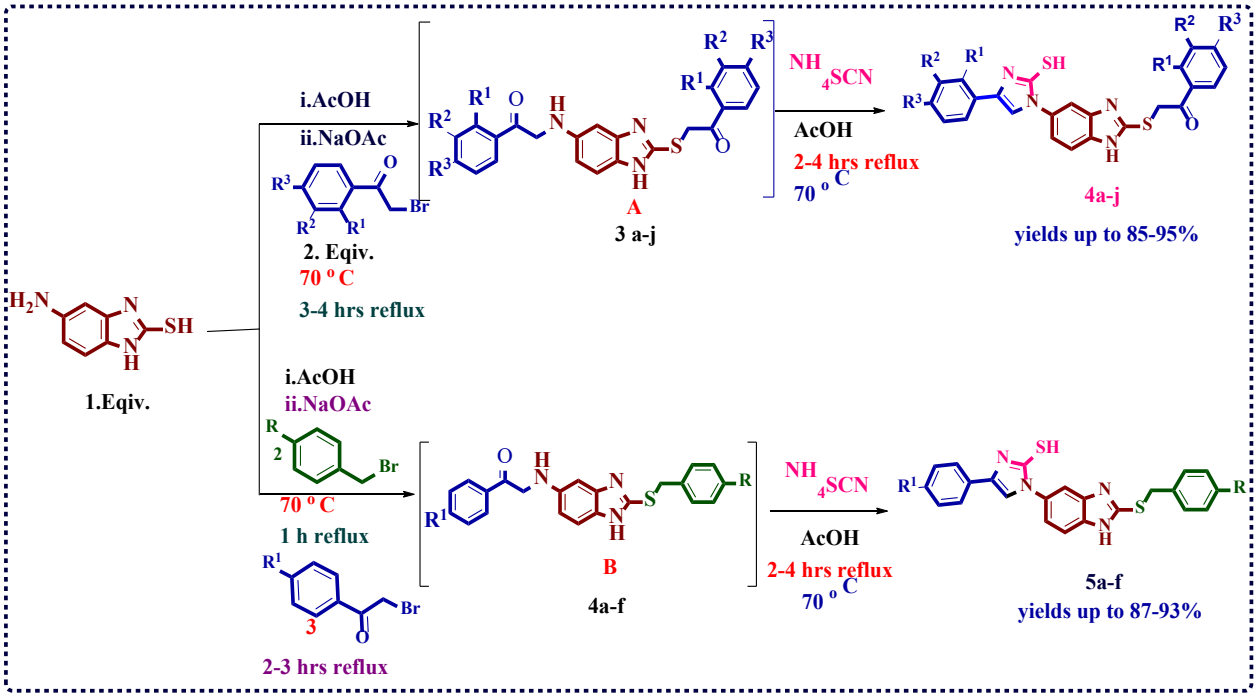

Scheme 3.1. Synthesis of mercaptoimidazoles

For the optimization of the reaction, we screened the reaction with various solvents, temperatures, and different amounts of catalyst. High yields of the products were observed when the reactions were carried with two equivalents of fused sodium acetate and two equivalents of phenacyl bromides or one equivalent of aralkyl halide and one equivalent of phenacyl bromides in glacial acetic acid at 70 ºC. All the synthesized compounds (**4a-j**) and (**5a-f**) structures were confirmed by their spectral and analytical studies.

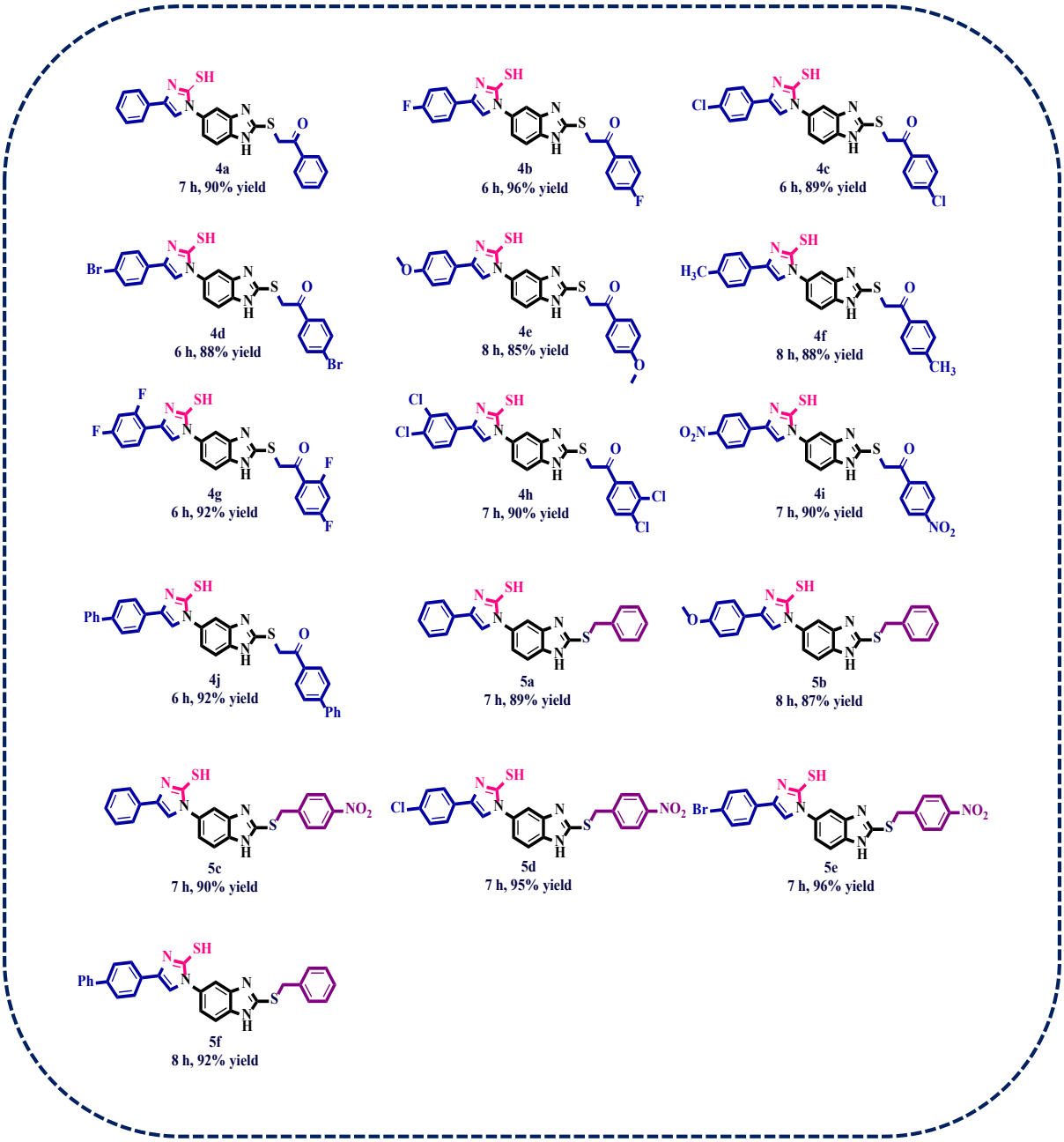

Figure 3.1. Scope of substrates.

3.4. Density Functional Theory (DFT) Calculations

The mechanistic insight into the formation of the final products has been provided based on their DFT calculation. Overall, the reaction is exothermic and the initiation of the reaction is barrier-less.

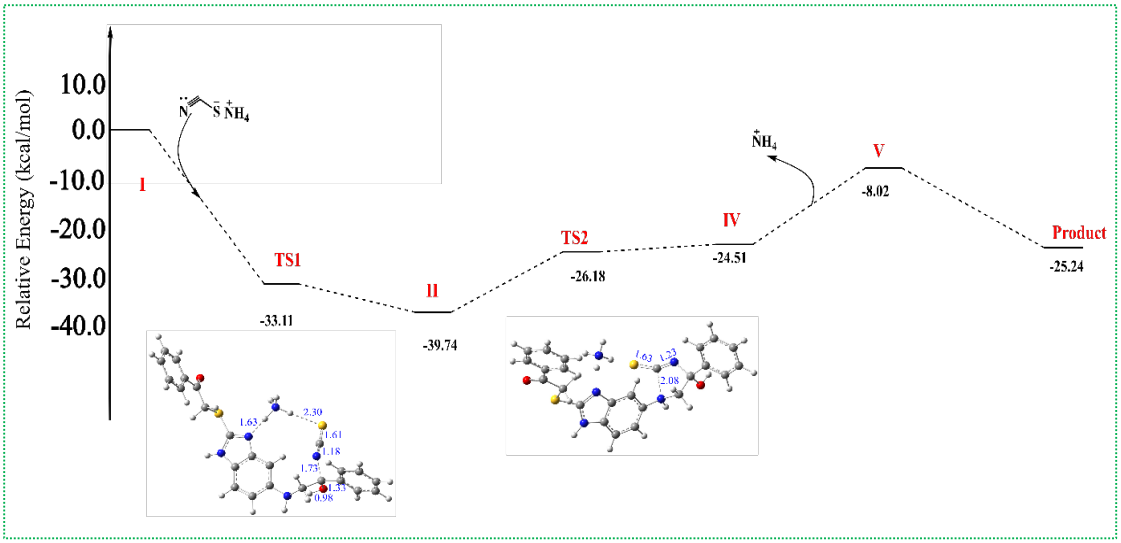

Figure 3.2. Relative energy profile for the synthesis of substituted imidazole.

In conclusion, we have synthesized thioalkylated benzimidazole-tethered 4-substituted mercaptoimidazole molecular hybrids *via* a novel, facile, one-pot three/ four-component approach using acetic acid and fused sodium acetate as a reaction medium with good to excellent yields. Further DFT calculations were performed to gain insight into the reaction mechanism.

CHAPTER-IV

Chapter IV consists of, **Polyethylene glycol mediated, three-component synthesis of thiazolyl-benzimidazoles as potent α-glucosidase inhibitors: Design, synthesis, molecular modeling, and ADME studies, facile, pseudo-four-component synthesis of novel thiazolyl-benzimidazoles *via* multi-component approach and their biological evaluation and facile, four-component synthesis of 3-coumarinyl based-thiazoles *via* MCR approach and their anti-cancer activity**

The chapter is divided into three sections, 4A, 4B, and 4C

Section-4A

Polyethylene glycol mediated, three-component synthesis of thiazolyl-benzimidazoles as potent α-glucosidase inhibitors: Design, synthesis, molecular modeling, and ADME studies

This chapter deals with the three-component synthesis, anti-diabetic activity, and computational studies of thiazolyl-benzimidazole (**4a-s**) derivatives as shown in **scheme 4A.1**. The title scaffolds (**4a-s**) were synthesized by using 5-amino-2-mercaptobenzimidazole, phenyl isothiocyanates, and

substituted phenacyl bromides (**1:1:2**) using PEG-400 as a recyclable and greener solvent in a shorter reaction time.

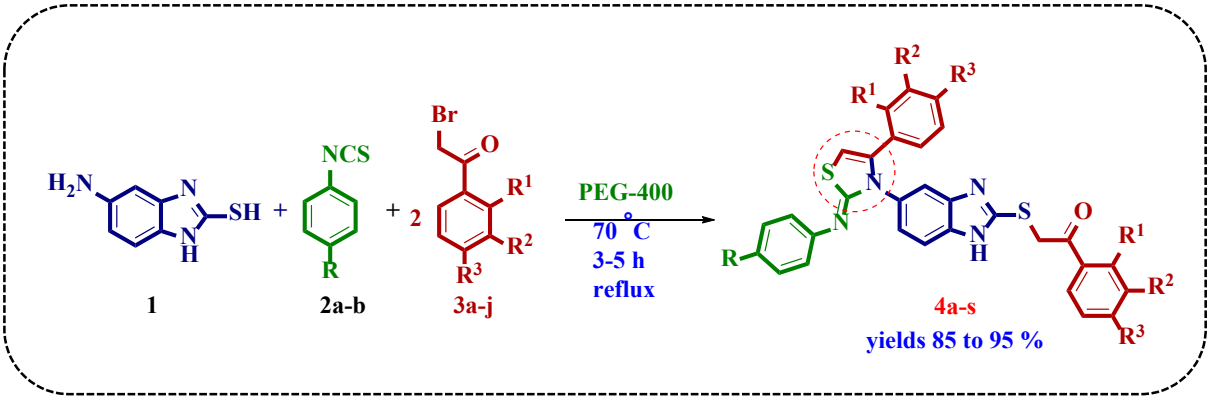

Scheme 4A.1. Benzimidazole-based thiazoles

For the optimization of the reaction, we screened the reaction with various solvents, temperatures, and different amounts of catalyst. High yields of the products were observed in PEG-400 at 70 ºC without any base and two equivalents of phenacyl bromides under a multi-component approach. All the synthesized compounds (**4a-s**) structures were confirmed by their spectral and analytical studies.

Anti-diabetic activity: *α-Amylase Inhibitory Activity*

Further, the synthesized compounds **(4a-s)** were evaluated for their *in-vitro* inhibition of α-amylase activity using Acarbose as a standard positive control. All the tested scaffolds showed varying degrees of α-amylase inhibitory activity with the IC_{50} values ranging from 12.02 ± 0.51µg/mL to 44.57 ± 0.47 µg/mL when compared with standard Acarbose has IC_{50} 11.88 ± 0.68 µg/mL. Among the tested scaffolds **4d, 4c, 4h,** and **4b** were found to be excellent inhibitory activity against enzyme with IC_{50} values found to be 12.02 ± 0.56; 12.25± 0.28; 12.74 ± 0.45; 19.10 ± 0.88 µg/mL respectively.

Molecular Docking Studies

The *in-silico* molecular docking studies of 1-phenyl-2-((5-(4-phenyl-2-(phenylamino) thiazol-3(2*H*)-yl)-1*H*-benzo[*d*]imidazol-2-yl)thio)ethanone derivatives (**4a-s)** explored the binding mode and acquire insights into the human pancreatic α-amylase complex with montbretia A (PDB ID: 4W93). Molecular docking studies revealed that compounds **4c** and **4d** have stable binding patterns to the human pancreatic α–amylase (PDB ID: 4W93).

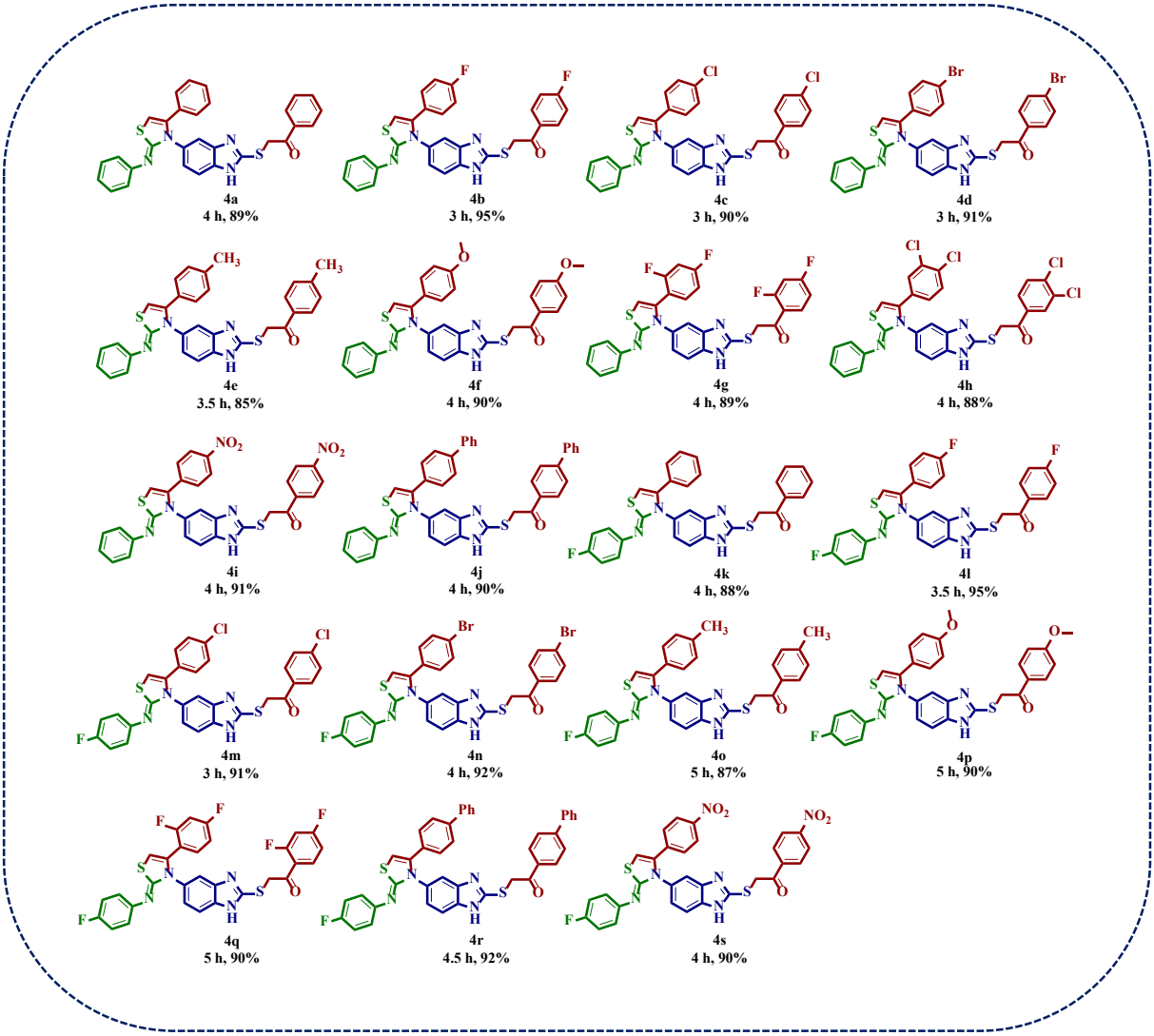

Figure 4A.1. Scope of substrates.

The *in-vitro* α-amylase activity results exhibited that the **4d** substituted with bromo group enhanced enzymatic activity with IC_{50} value 12.02 ± 0.56 µg/mL and exhibited the highest binding energy with LF dG -11.34 kcal/mol. This **4d** showed a hydrogen bond between the amino acid residues Gln63 (Glutamine63) with the sulphur atom of thiazole with a bond length of 2.54 A^{o} (**Figure 4A.2**). It also exhibits hydrophobic interactions with Trp59 (Tryptophan59 amino acid residue) and Thr163 (Threonine163 amino acid residue) of amino acid residue.

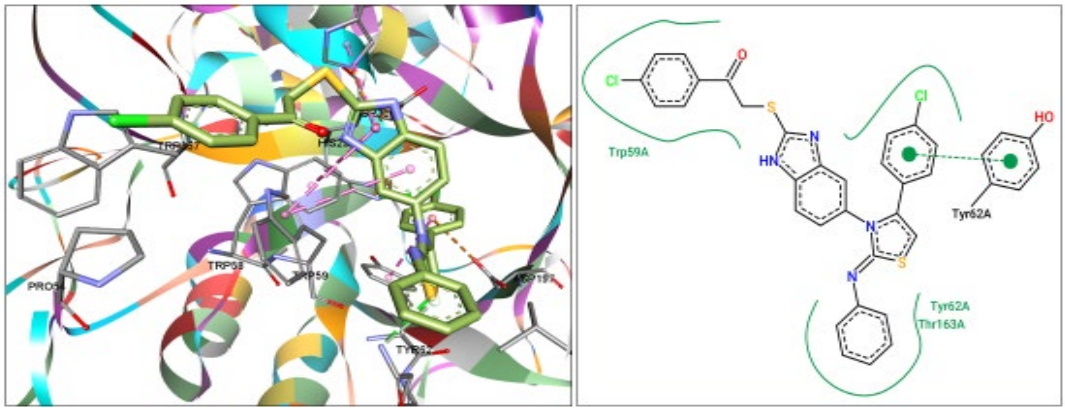

Figure 4A.2. Molecular Docking interactions of compound **4d** with Human pancreatic α-amylase (PDB ID: 4W93).

Moreover, **4c** showed the highest binding energy LF dG -10.01 kcal/mol. The ligand forms π-π interactions with Tyr62 (Tyrosine62 residue) with chlorophenyl and hydrophobic interactions with Tyr62 and Thr163 amino acid residues. The molecular docking interactions illustrate that the synthesized poly heterocycles have benzimidazole and thiazole rings with diverse group forms as probable bioactive cores and that they form strong binding contacts with the active site of amino acid residues. The docking results have shown that the docked ligands entered the catalytic reaction center region of α-amylase.

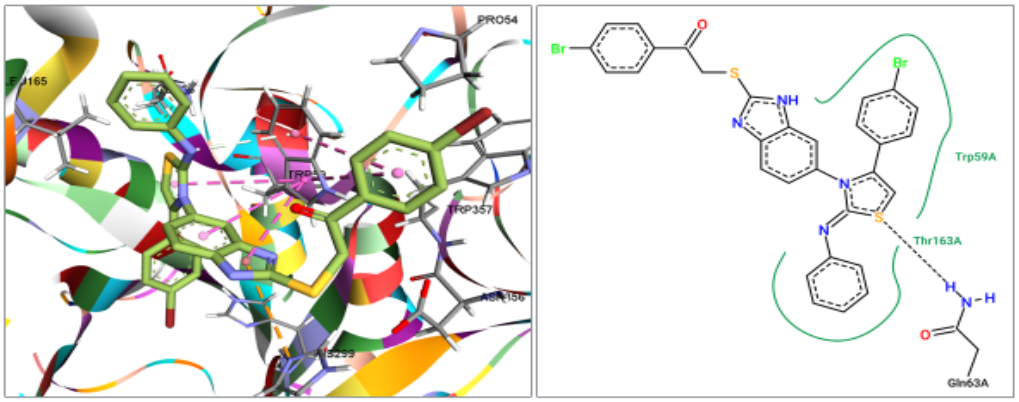

Figure 4A.3. Molecular Docking interactions of compound **4c** with Human pancreatic α-amylase (PDB ID: 4W93).

In summary, we have developed an efficient, one-pot, three-component synthesis of benzimidazolyl-thiazole scaffolds (**4a-s**) using green solvent *via* a multi-component approach. Further, we screened the title compounds for their *in-vitro* anti-diabetic activity, and also

performed computational studies i.*e*., molecular docking, dynamic studies, and drug-like ADME properties.

CHAPTER-IVB

Facile, pseudo-four-component synthesis of novel thiazolyl-benzimidazoles *via* multi-component approach and their biological evaluation

In this chapter, we describe the synthesis, anti-bacterial activity, and computational studies of novel thiazolyl-benzimidazole (**4a-p**) scaffolds as outlined in **scheme 4B.1**. The title compounds were synthesized by using 5-amino-2-mercaptobenzimidazole **1**, ammonium thiocyanate **2,** substituted α- bromo-acetophenones **3** or aralkyl halides **(1:1:2)** in glacial acetic acid at 70 ºC to give final compounds (**4a-p**) with good to excellent yields in a shorter reaction time *via* MCR approach.

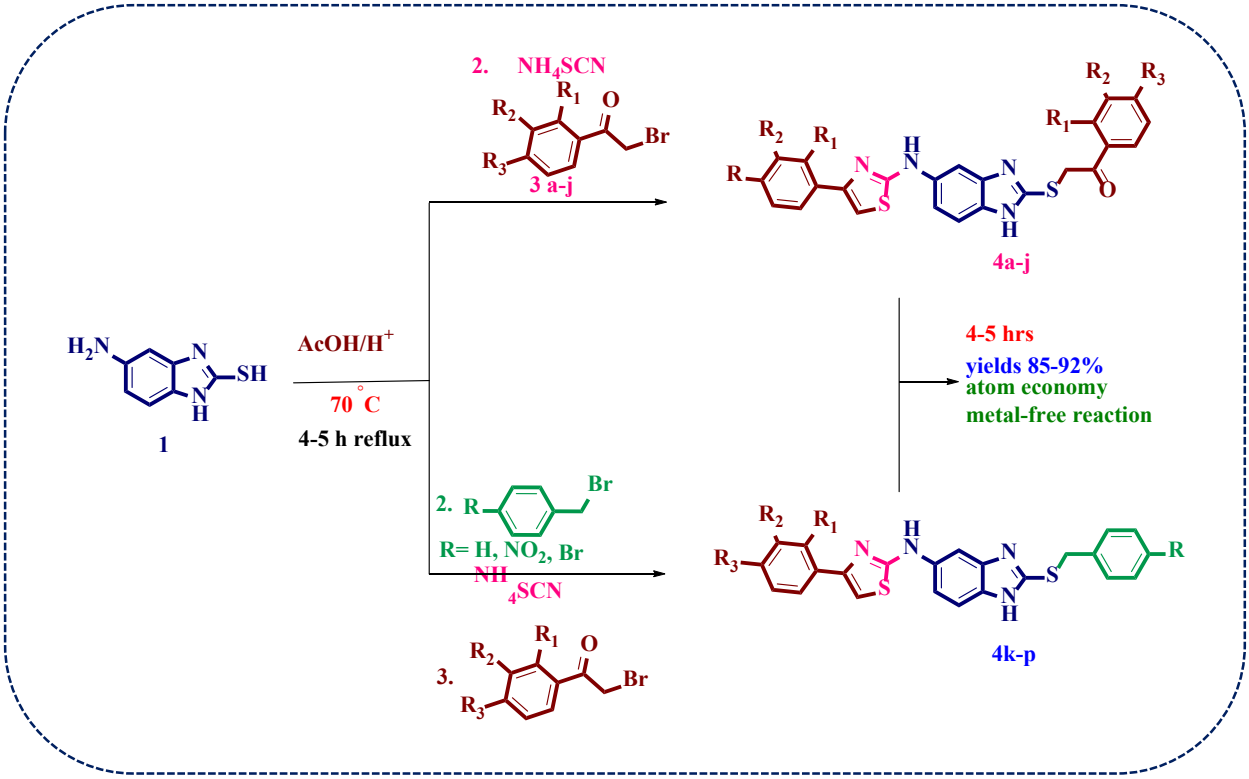

Scheme 4B.1. Synthesis of benzimidazole-based thiazoles.

For the optimization of the reactions, we screened the reaction with various solvents, temperatures, and different amounts of catalyst. High yields were observed in glacial AcOH at 70 ºC using two equivalents of phenacyl bromides or one equivalent of aralkyl halides and one equivalent of

phenacyl bromides. All the synthesized compounds (**4a-p**) structures were confirmed by their spectral and analytical studies.

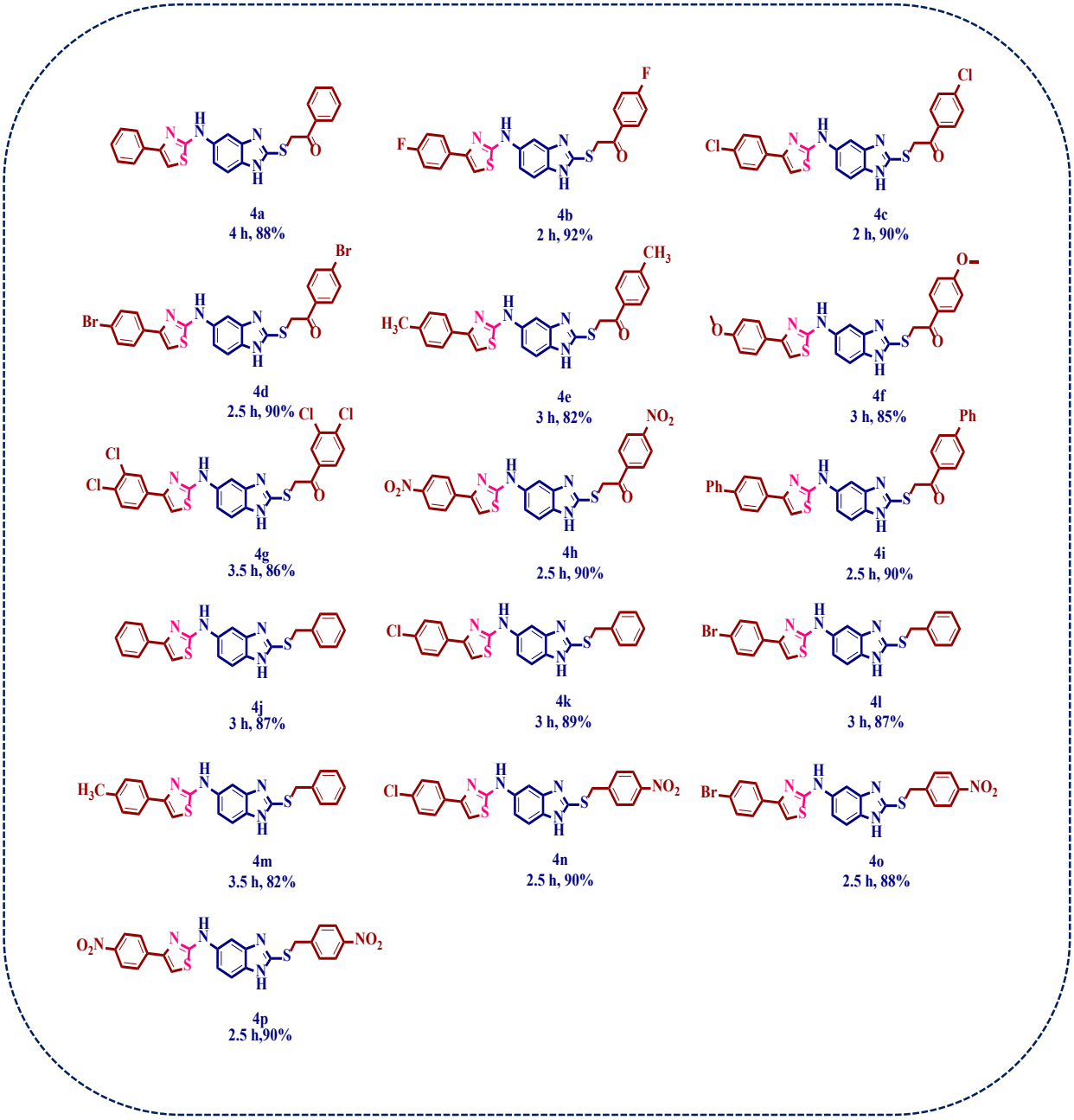

Figure IVB.1. Scope of substrates.

Anti-bacterial activity

The *in-vitro* antibacterial activity of the synthesized benzimidazolyl based thiazole compounds (**4a-p**) was analyzed for their antibiotic activity against Gram-positive bacteria *Streptococcus*

pneumonia (ATCC2451) and Gram-negative bacteria *Proteus Mirabilis* (ATCC2081). The *in-vitro* antibacterial activity of synthesized compounds was initially evaluated by determining their minimum inhibition concentration (MIC) values using the Agar well diffusion method. Among tested compounds, **4b, 4f,** and **4k** were shown significant anti-bacterial activity.

Molecular Docking Simulations

To gain further insights into the interactions, the title compounds were subjected to their molecular docking studies using PDB ID: 1KIJ. The molecular docking results showed that compound **4i** showed the highest binding affinity at -12 kcal/mol. The N and -NH of benzimidazole and N of thiazole ring usually establish hydrogen bonding interaction with Asn45, Lys109, Val117, or Gly116 residue of the enzyme. The five-membered ring of benzimidazole or thiazole participates in the cationic interaction with the Lys109 residue while the phenyl ring involves in the pi-stacking interaction with the Phe103 residue. Moreover, Asp45, Ile77, Phe103, Lys109, Val117, and Pro328 are the amino acid residues that show hydrophobic interactions with most of the synthesized molecules.

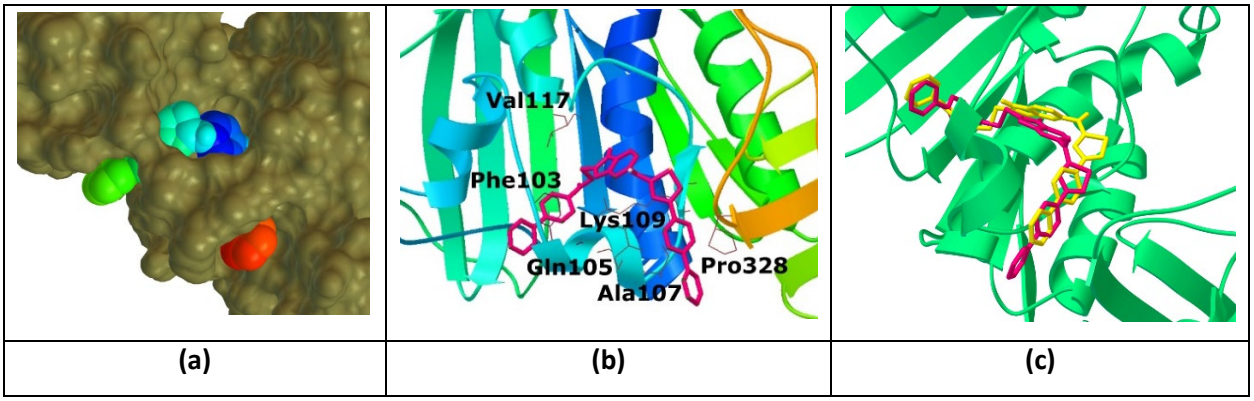

Figure IVB.2. Docked pose of compound **4i** at an active site of the gyrase protein (PDB ID: 1KIJ). (a) Surface view of **4i** at an active site, (b) Docked pose of **4i** along with the interacting amino acid residue of the protein, (c) overlapping structure of two different docked poses of **4i**.

In conclusion, we have synthesized benzimidazolyl-thiazoles *via* the MCR approach. Further, the synthesized compounds were screened for their anti-bacterial activity against Gram-positive *Streptococcus Pneumoniae* (2451) and Gram-negative bacteria *Porteous Mirabilis* (2081). Compounds **4b, 4f,** and **4k,** and have shown excellent activity. And also performed molecular docking studies.

CHAPTER-IVC

Facile, four-component synthesis of 3-comarinyl based-thiazoles *via* MCR approach and their anti-cancer activity

The present chapter describes the synthesis and anticancer activity of 3-coumarinyl-based thiazoles (**5a-s**) which is indicated in **scheme 4C.1**. The title compounds were synthesized by reaction of an equimolar ratio of phenyl isothiocyanate (**1**), hydrazine hydrate (**2**), substituted 3-acetyl-coumarins (**3**) and substituted phenacyl bromides (**4**) (**1:1.2:1:1**) in the catalytic amount of acetic acid and ethanol at 60 ºC in good yields.

For the optimization of the reaction, we have screened the reactions with various solvents, at different temperatures and various loads of catalysts. By screening the reaction in ethanol along with the catalytic amount of acetic acid, we got the best results in terms of reaction yields. Then the reaction was carried out with different temperatures and different amounts of acetic acid. It was observed that with 10 mol% of an acetic acid catalyst, using ethanol as solvent under reflux conditions gave good results in terms of time and reaction yields. All the synthesized scaffolds (**5a-s**) structures were confirmed by their analytical and spectral data.

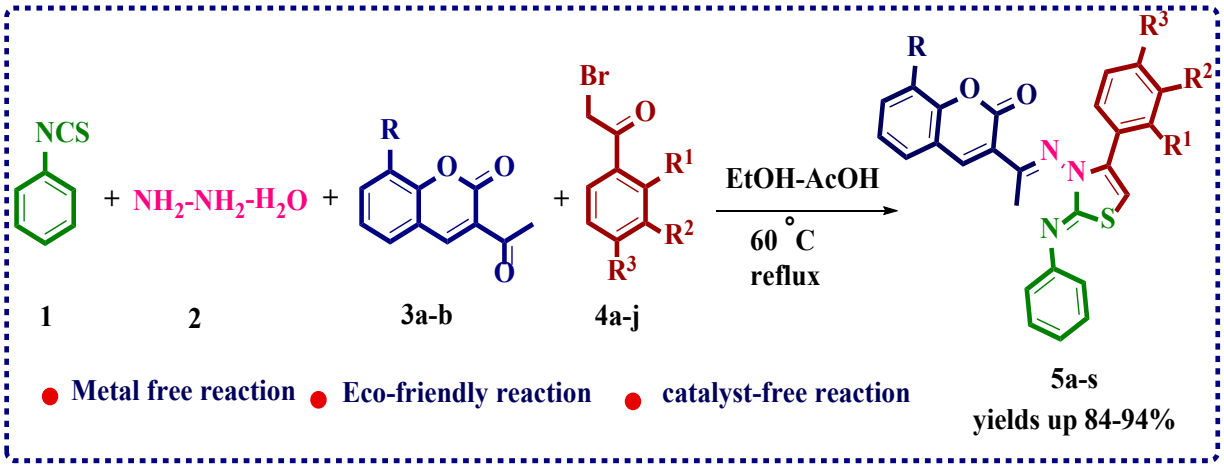

Scheme 4C.1. Synthesis of coumarin-based thiazoles.

Anti-cancer activity

The *in-vitro* anti-cancer activity of synthesized coumarinyl-based thiazole derivatives (**5a-s**) was screened against different human cancer cell lines **LN18** and breast cancer **MCF7.** Preliminary investigations were done by screening the compounds for anti-cancer activity on C6 glioma cell lines. The synthesized compounds were screened for their cytotoxicity in C6 rat glioma cell lines

by MTT assay. From the *in-vitro* results, it was found that compound **5e** (IC_{50} = 0.5 μM) showed excellent anti-cancer activity against LN18 and MCF7 cell lines.

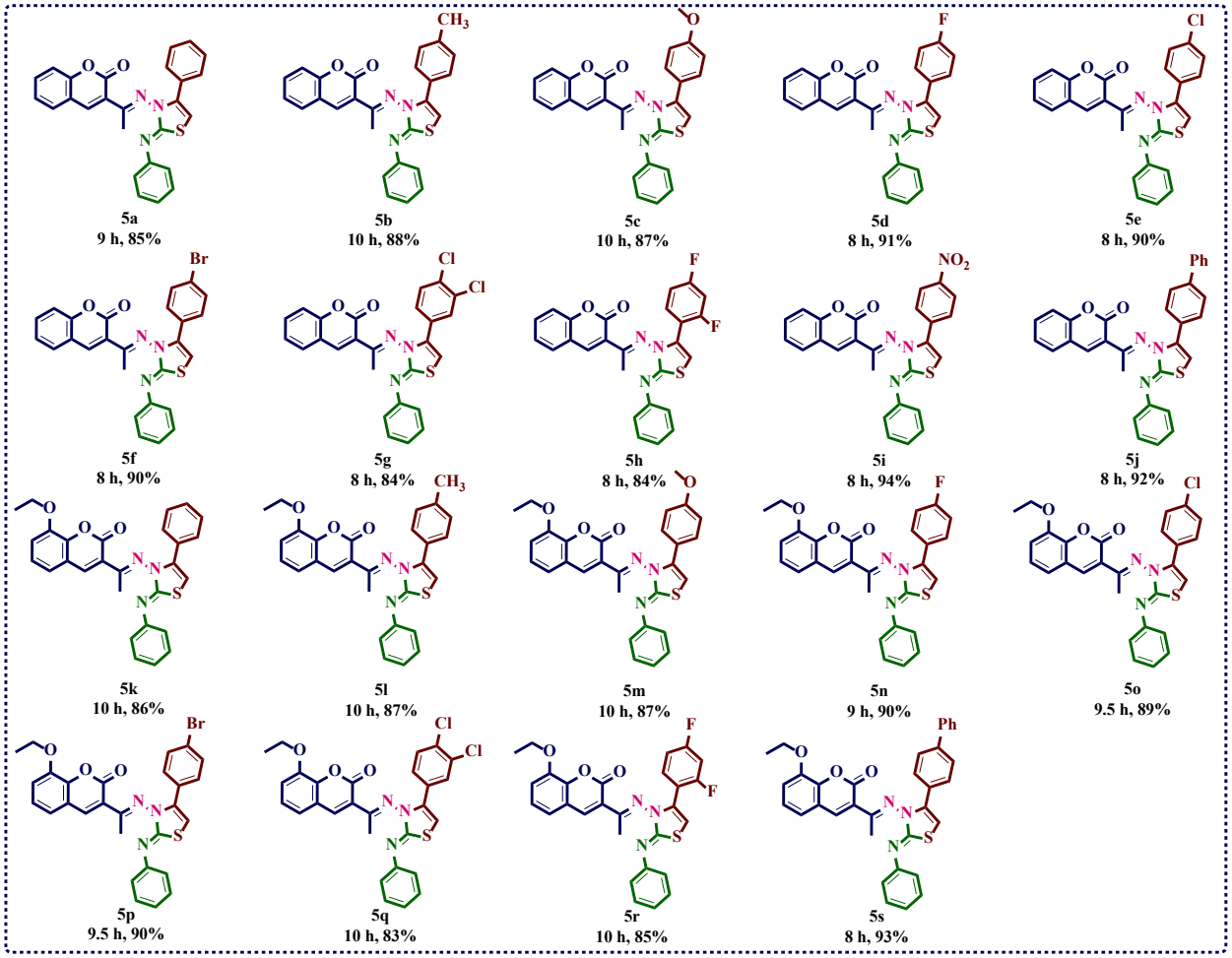

Figure 4C.1. Substrate scope of thiazole hybrids.

In summary, we have developed a potential green protocol for the synthesis of new coumarinyl thiazole derivatives by the multi-component reaction. Further, these compounds were screened for their *in-vitro* anti-cancer activity.

CHAPTER-V

Synthesis and anti-bacterial activity of novel benzimidazole based isoindoline-1,3-diones and benzo[4,5]imidazol[2,1-*b*]thiazoles

This chapter deals with the synthesis of benzimidazole-based isoindoline-1,3-dione and benzo[4,5]imidazo[2,1-*b*]thiazol (**4a-w)** and (**5a-h)** derivatives as outlined in **Scheme 5.1**. The

title compounds were synthesized by using 5-amino-2-mercaptobenzimidazole, various cyclic anhydrides, and different substituted aralkyl halides/phenacyl bromides (**1:1:1**) using glacial acetic

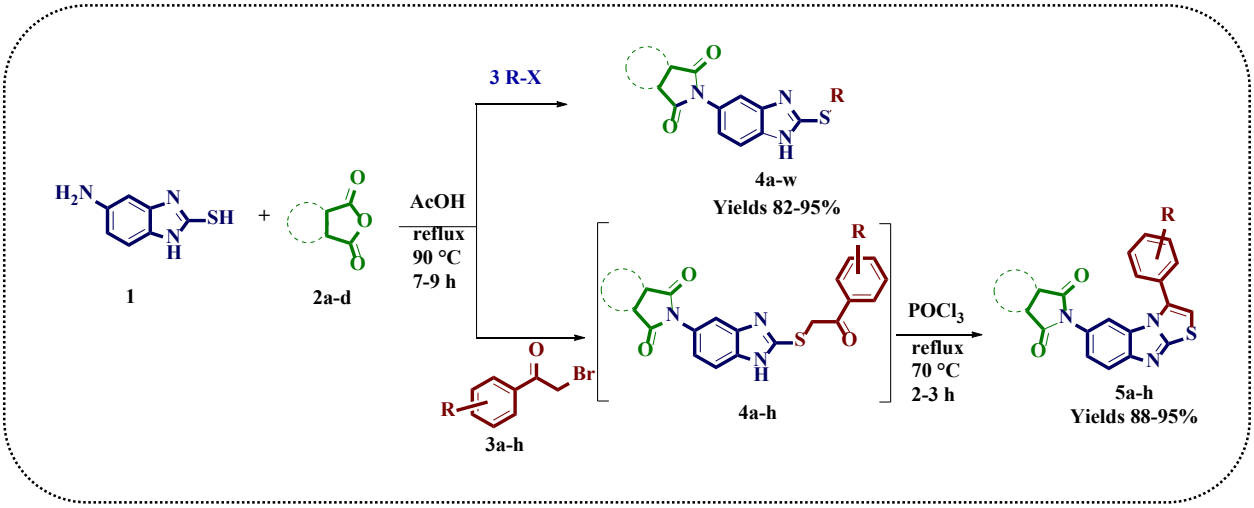

Scheme 5.1. Benzimidazole based isoindoline-1,3-dione and benzo[4,5]imidazo[2,1-*b*]thiazol derivatives.

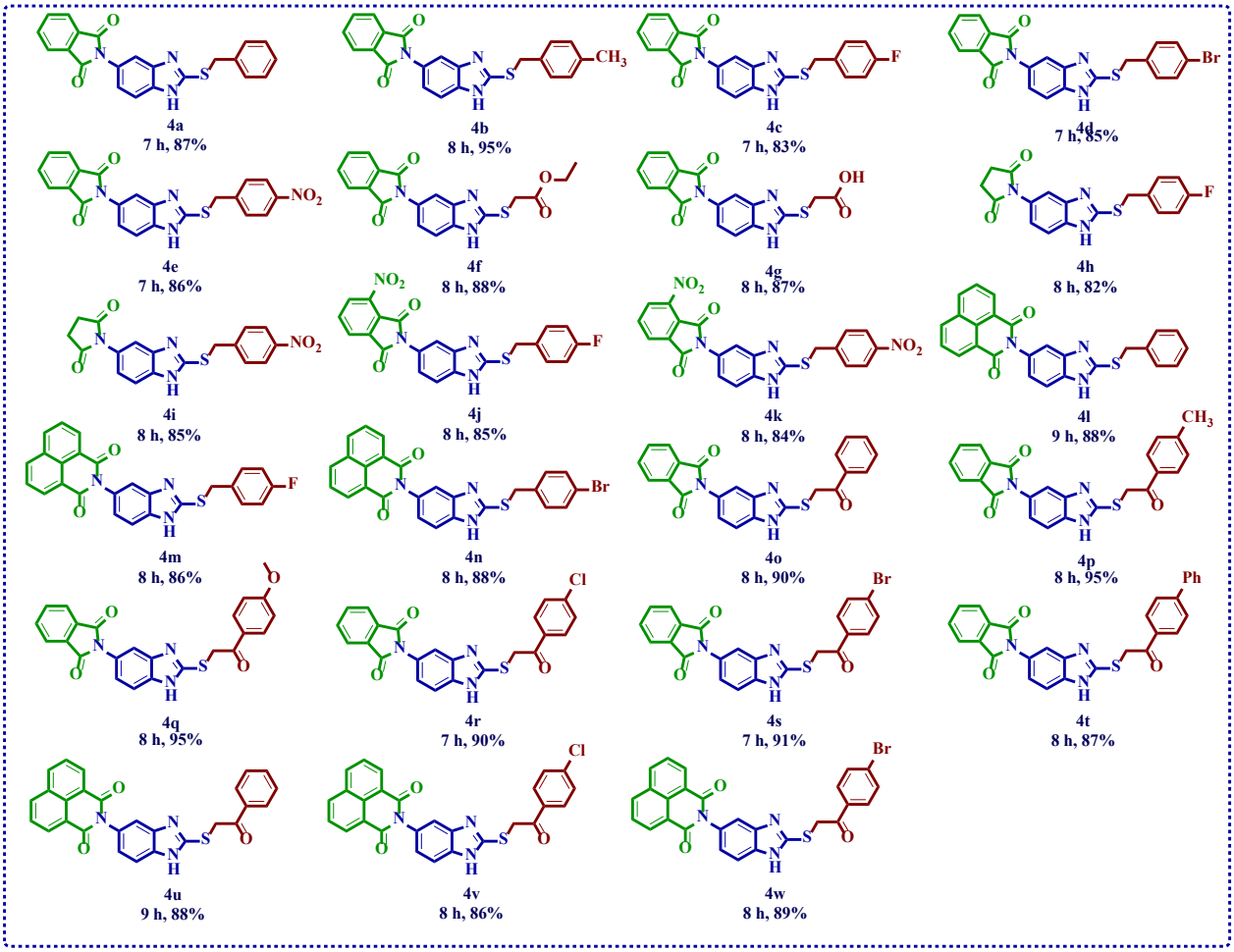

Figure 5.1. Scope of substrates.

acid solvent at 70 ºC. Further, these derivatives with thiophenacyl moiety undergo cyclo dehydration in presence of strong acid $POCl_3$ to give (**5a-h**) good yields in a shorter reaction time. For the optimization of the reaction, we screened the reaction with various solvents, at different temperatures and loads of catalysts. It has been found that acetic acid was the best solvent in terms of time and yield. All the synthesized scaffolds (**4a-w**) structures were confirmed by their analytical and spectral data.

Anti-bacterial activity

The *in-vitro* antibacterial activity of the synthesized benzimidazole-based isoindoline-1,3-diones and benzo[4,5]imidazo[2,1-*b*]thiazoles were carried out against Gram-negative *Escherichia coli*, *Salmonella typhi*, and Gram-positive bacteria *Staphylococcus aureus*, *Micrococcus luteus* by Agar well diffusion method. Compounds **4a, 4g, 4j, 4q, 4s,** and **4t** showed significant activity against the standard drug Streptomycin.

Molecular docking studies

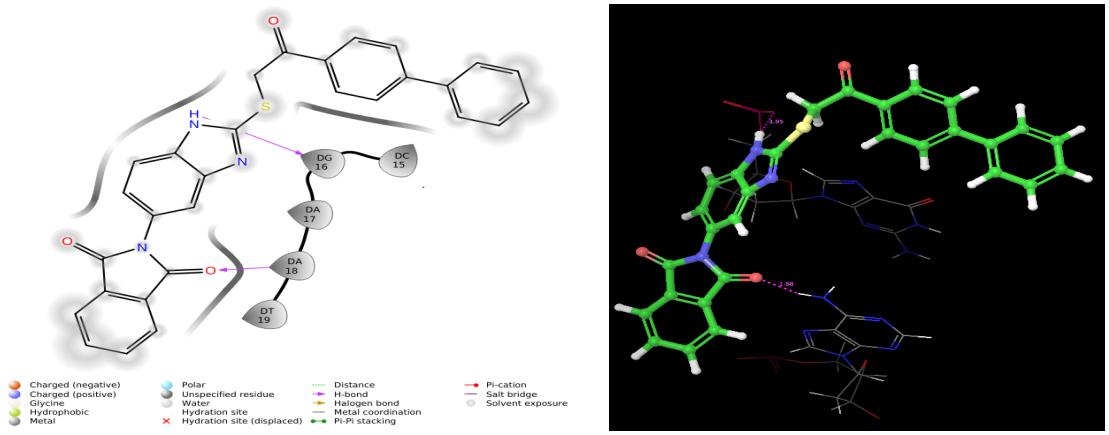

Figure 5.3. Molecular docking interaction of compound **4t** with the active site.

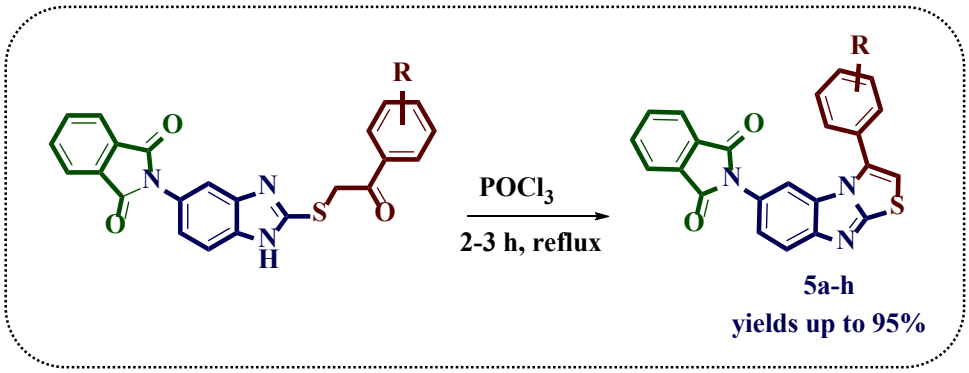

Scheme 5.1. Synthesis of benzo[4,5]imidazo[2,1-*b*]thiazol derivatives.

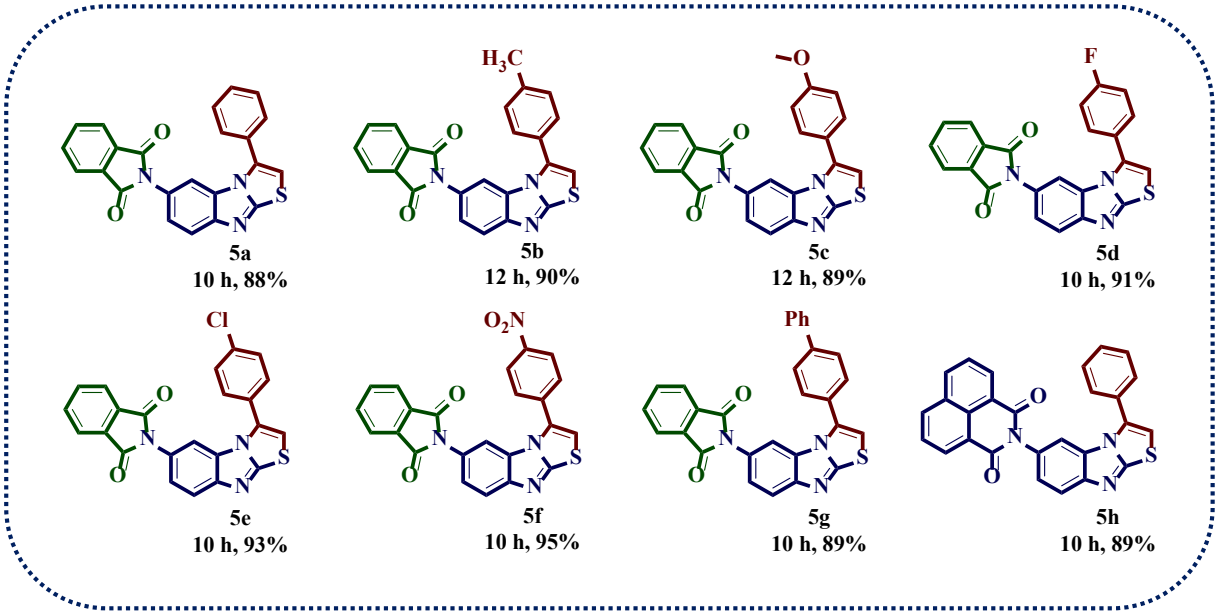

Figure 5.2. The scope of substrates.

References:

1. Walsh, P. J.; Li, H.; C. Anaya de Parrodi, C. *Chem. Rev.* **2007**, 107, 2503–2545.
2. Maya, V.; Raj, M.; Singh, V. K. *Org. Lett.* **2007**, 9, 2593–2595.
3. Mamidala, S.; Peddi, S. R.; Aravilli, R. K.; Jilloju, P. C.; Manga, V.; Vedula, R. R. *J. Mol. Struct.* **2021**, 1225.
4. Vila, C.; Rueping, M. *Green Chem.* **2013,** 15, 2056–2059.
5. Xin, X.; Wang, Y.; Kumar, S.; Lu, X.; Lin, Y.; Dong, D. *Org. & Biomol. Chem.* **2010**, *8,* 3078-3082.
6. Dömling, A.; Wang, W.; Wang, K. *Chem. Rev.* **2012***, 112*, 3083-135.
7. Valizadeh, H.; Fakhari, A. *Mol. Divers.* **2011**, *15*, 233-237.
8. Gu, Y. *Green Chem.* **2012**, *14*, 2091.
9. Ruijter, E.; Orru, R. V. A. *Drug Discov. Today Technol.* **2013**, *10*, e15–e20.
10. Touré, B. B.; Hall, D. G. *Chem. Rev.* **2009**, *109*, 4439–4486.
11. Dong, R.; Chen, Q.; Cai, X.; Zhang, Q.; Liu, Z. *Polym. Chem.* **2020**, *11*, 5200–5206.
12. Gonzalez, M. A.; Gorman, D. B.; Hamilton, C. T.; Roth, G. A. *Org. Process Res. Dev.* **2008**, *12*, 301–303.

13. Sumesh, R. V.; Muthu, M.; Almansour, A. I.; Suresh Kumar, R.; Arumugam, N.; Athimoolam, S.; Jeya Yasmi Prabha, E. A.; Kumar, R. R. *ACS Comb. Sci.* **2016**, *18*, 262–270.
14. Aggarwal, R.; Kumar, S.; Kaushik, P.; Kaushik, D.; Gupta, G. K. *Eur. J. Med. Chem.* **2013**, *62*, 508–514.
15. Arshad, A.; Osman, H.; Bagley, M. C.; Lam, C. K.; Mohamad, S.; Zahariluddin, A. S. M. *Eur. J. Med. Chem.* **2011**, *46*, 3788–3794.
16. Sket, B.; Zupan, M. *Synth. Commun.* **1989**, *19*, 2481-2487.
17. Jiang, Q.; Sheng, W.; Guo, C. *Green chem.* **2013,** *15*, 2175-2179.
18. Samanta, S.; Lim, T. L.; Lam, Y. *Chem. Med. Chem.* **2013**, *8*, 994-1001.

List of publications

1. **A Facile One-Pot Synthesis of Benzimidazole-Linked Pyrrole Structural Motifs *via* Multicomponent Approach: Design, Synthesis, and Molecular Docking Studies. Raju Chedupaka, Papisetti Venkatesham, Akanksha Ashok Sangolkar, Rajeswar Rao Vedula***

   Polycyclic aromatic compounds. https://doi.org/10.1080/10406638.2021.1995010

2. **Synthesis, characterization and Density Functional Theory of novel one-pot thioalkylated benzimidazole-linked 4-substituted mercaptoimidazole molecular hybrids via multicomponent approach. Raju Chedupaka, Ravinder Pawar, Papisetti Venkatesham, and Rajeswar Rao Vedula. Synthetic communications. 2022, *52,* 1111-1121. https://doi.org/10.1080/00397911.2022.2072745**

3. **Polyethylene glycol mediated, novel, one-pot three-component synthesis of thiazolyl-benzimidazoles as potent α- glucosidase inhibitors: Design, synthesis, molecular modelling, ADME studies**

   (under review in Journal of Molecular Structure).

   Raju Chedupaka[a], Kiran Gangarapu[b], Srikanth Mamidala[a], Papisetti Venkatesham[a], Rajeswar Rao Vedula*[a]

4. **Facile, pseudo four component synthesis of novel thiazolyl-benzimidazoles *via* multi-component approach and their biological evaluation**

   (ready to submit).

   Raju chedupaka [a], Amrutha V Audipudi [b], Srikanth Mamidala [a], Rajeswar Rao Vedula [a] *

5. **Facile, four-component synthesis of 3-comarinyl based-thiazoles *via* MCR approach and their anti-cancer activity (Manuscript under preparation).**

6. **Synthesis and anti-bacterial activity of novel benzimidazole based isoindoline-1,3-diones and benzo[4,5]imidazol[2,1-*b*]thiazoles.**

   (ready to submit).

   Raju chedupaka [a], shyam perugu [b], Srikanth Mamidala [a], Rajeswar Rao Vedula [a] *

7. **An Efficient One-Pot Synthesis of 6-Phenyl-3-(1H-Pyrazol-1-yl)- [1,2,4]Triazolo[3,4-b][1,3,4]Thiadiazole Derivatives and Their Antimicrobial Evaluation and Molecular Docking Studies. Parameshwara Chary Jilloju , Perugu Shyam , Chedupaka Raju,**

and Rajeswar Rao Vedula. Polycyclic aromatic compounds, 2022, *42*, 4240-4254. https://doi.org/10.1080/10406638.2021.1886127.

8. **Facile One-Pot Multi-Component Synthesis, Characterization, Molecular Docking Studies, Biological Evaluation of 1,2,4-Triazolo Isoindoline-1,3-Diones and Their DFT Calculations. Papisetti Venkatesham, Perugu Shyam, Pooja, Raju Chedupaka & Rajeswar Rao Vedula*. *Polycyclic aromatic compounds*. https://doi.org/10.1080/10406638.2022.2042333**

9. **A facile one-pot, three-component synthesis of a new series of thiazolyl pyrazole carbaldehydes: In vitro anticancer evaluation, in silico ADME/T, and molecular docking studies. Srikanth Mamidala, R Kowshik Aravilli, Gondru Ramesh, Shaik Khajavali, Raju Chedupaka, Vijjulatha Manga, Rajeswar Rao Vedula.**
Journal of molecular structure, **2021, *1236,* 130356. https://doi.org/10.1016/j.molstruc.2021.130356.**

10. **A facile one-pot, three component synthesis of a new series of 1,3,4-thiadiazines: Anticancer evaluation and molecular docking studies. Srikanth Mamidala, Venugopal Vangala, Saikiran Reddy Peddi, Raju Chedupaka, Vijjulatha Manga, Rajeswar Rao Vedula. Journal of Molecular Structure, 2021, *1233,* 130111. https://doi.org/10.1016/j.molstruc.2021.130111.**

POLYCYCLIC AROMATIC COMPOUNDS
https://doi.org/10.1080/10406638.2021.1995010

A Facile One-Pot Synthesis of Benzimidazole-Linked Pyrrole Structural Motifs *via* Multicomponent Approach: Design, Synthesis, and Molecular Docking Studies

Raju Chedupaka, Venkatesham Papisetti, Akanksha Ashok Sangolkar, and Rajeswar Rao Vedula

Department of Chemistry, National Institute of Technology, Warangal, Telangana, India

ABSTRACT

Novel, a series of pyrrolyl-thio alkylated/aryl alkylated benzimidazole derivatives were synthesized *via* one-pot, the three-component reaction of 5-amino-2-mercaptobenzimidazole, 2,5-dimethoxytetrahydrofuran, and different substituted alkyl/aryl alkyl halides in acetic acid and sodium acetate is described. The newly synthesized scaffolds were purified and confirmed by their spectroscopic (IR, ^{1}H-NMR, ^{13}C-NMR, Mass) and elemental analysis. Further, *in silico* molecular docking studies were carried out for the synthesized compounds against the colchicine binding site of $\alpha\beta$-tubulin (PDB ID: 1SA0). Among all the synthesized compounds **4j**, **4p** was shown good binding affinity with colchicine binding site of $\alpha\beta$-tubulin.

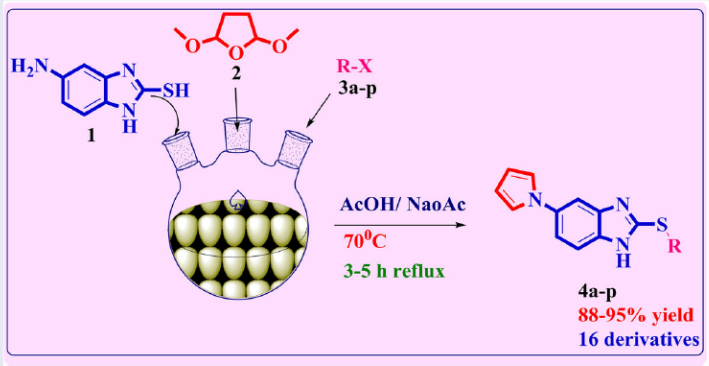

ARTICLE HISTORY
Received 11 August 2021
Accepted 13 October 2021

KEYWORDS
5-Amino-2-marcaptobenzimidazole; molecular docking studies; pyrrole; three-component reaction

Introduction

In the conventional method, the synthesis of complex molecules involves a huge number of synthetic operations as well as purification techniques such as recrystallization, solvent extraction, and also column chromatographic techniques are involved in each step. And also, uses high energy consumption and a longer reaction time.

CONTACT Rajeswar Rao Vedula rajeswarnitw@gmail.com; vrajesw@nitw.ac.in Department of chemistry, National Institute of Technology, Warangal, Telangana 506004, India.

Supplemental data for this article can be accessed online at https://doi.org/10.1080/10406638.2021.1995010.

SYNTHETIC COMMUNICATIONS®
https://doi.org/10.1080/00397911.2022.2072745

Synthesis, characterization and Density Functional Theory of novel one-pot thioalkylated benzimidazole-linked 4-substituted mercaptoimidazole molecular hybrids *via* multi-component approach

Raju Chedupaka, Ravinder Pawar, Papisetti Venkatesham, and Rajeswar Rao Vedula

Department of chemistry, National Institute of Technology Warangal, Warangal, India

ABSTRACT

A series of novel, one-pot, four components synthetic procedure has been developed for the synthesis of thioalkylated benzimidazole-linked 4-substituted mercaptoimidazole molecular hybrids and their benzyl derivatives (**4a–j**) and (**5a–f**) were synthesized by the reaction of 5-amino-2-mercaptobenzimidazole, with different substituted phenacyl bromides/aryl alkyl halides in the presence of glacial acetic acid and fused sodium acetate under reflux condition to give corresponding intermediates. These compounds on further reaction with ammonium thiocyanate *via* multi-component reaction to give the title compounds (**4a–j**) and (**5a–f**)**.** All the newly synthesized compounds were well characterized by their spectral and analytical studies. This procedure includes several advantages such as transition metal-free, catalyst-free, mild reaction temperature, shorter reaction time, and gives good to excellent yields without any column purification techniques. Further, mechanistic insight into the formation of the final products has also been provided based on their density functional theory (DFT) studies.

GRAPHICAL ABSTRACT

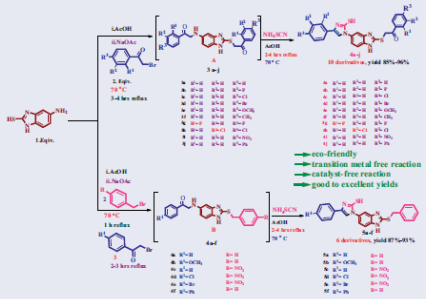

ARTICLE HISTORY
Received 9 December 2021

KEYWORDS
DFT studies; 5-amino-2-mercaptobenzimidazole; phenacyl bromides; imidazole; multi-component component approach

CONTACT Rajeswar Rao Vedula rajeswarnitw@gmail.com Department of chemistry, National Institute of Technology Warangal, Warangal, India.

Supplemental data for this article can be accessed on the publisher's website.

POLYCYCLIC AROMATIC COMPOUNDS
https://doi.org/10.1080/10406638.2021.1886127

An Efficient One-Pot Synthesis of 6-Phenyl-3-(1*H*-Pyrazol-1-yl)-[1,2,4]Triazolo[3,4-*b*][1,3,4]Thiadiazole Derivatives and Their Antimicrobial Evaluation and Molecular Docking Studies

Parameshwara Chary Jilloju[a], Perugu Shyam[b], Chedupaka Raju[a], and Rajeswar Rao Vedula[a]

[a]Department of Chemistry, National Institute of Technology, Warangal, Telangana 506004, India; [b]Department of Biotechnology, National Institute of Technology, Warangal, Telangana 506004, India

ABSTRACT

An efficient rapid synthesis of a new class of diversely functionalized 6-phenyl-3-(1H-pyrazol-1-yl)-[1,2,4]triazolo[3,4-b][1,3,4]thiadiazole derivatives (**4a–q**) is described via a facile one-pot, three-component cascade reaction with high yields. It is a multi-functional cyclization reaction to form two new heterocycles. The structures of newly formed compounds were confirmed by using spectral and analytical studies. Simple reaction conditions, the good isolated yield of the product, and no column chromatographic purification are attractive features of the present protocol. Further, the newly synthesized compounds were screened for anti-microbial activity and molecular docking interactions.

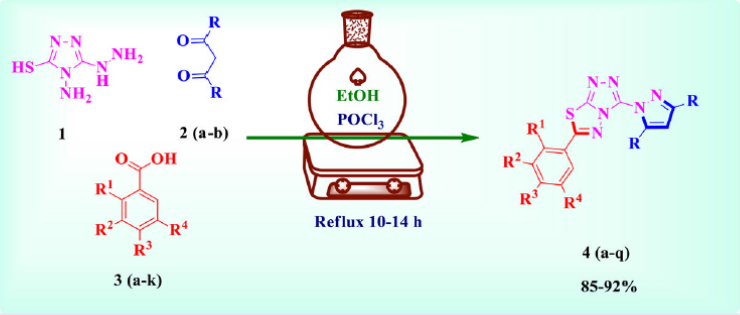

ARTICLE HISTORY
Received 21 December 2020
Accepted 30 January 2021

KEYWORDS
Triazole; pyrazole; thiadiazole; multi-component reaction; docking studies; anti-microbial

Introduction

In the multi-component reactions, three or more reactants combine closely in a single reaction pot to yield the final desire products. Currently, most of the researchers are interested in multi-component reactions (MCRs) to synthesize the different types of heterocyclic compounds.[1,2] Strategy for the synthesis of complex compound and generation of C–C bond, C–heteroatom bond and ring with high atom economy, high selectivity, simple protocol in a unique synthetic operation without isolation of intermediate *via* a multi-component reaction.[3–8]

CONTACT Rajeswar Rao Vedula rajeswarnitw@gmail.com Department of Chemistry, National Institute of Technology, Warangal Telangana 506004, India.

Supplemental data for this article is available online at https://doi.org/10.1080/10406638.2021.1886127.

Journal of Molecular Structure 1233 (2021) 130111

Contents lists available at ScienceDirect

Journal of Molecular Structure

journal homepage: www.elsevier.com/locate/molstr

A facile one-pot, three component synthesis of a new series of 1,3,4-thiadiazines: Anticancer evaluation and molecular docking studies

Srikanth Mamidala[a], Venugopal Vangala[b], Saikiran Reddy Peddi[c], Raju Chedupaka[a], Vijjulatha Manga[c], Rajeswar Rao Vedula[a,*]

[a] Department of Chemistry, National Institute of Technology, Warangal 506004, Telangana State, India
[b] Council of Scientific and Industrial Research–Indian Institute of Chemical Technology (CSIR-IICT), Uppal Rd, IICT Colony, Tamaka, Hyderabad 500007, Telangana, India
[c] Molecular Modeling and Medicinal Chemistry Group, Department of Chemistry, University College of Science, Osmania University, Hyderabad 500007, Telangana, India

ARTICLE INFO

Article history:
Received 15 January 2021
Revised 7 February 2021
Accepted 8 February 2021
Available online 16 February 2021

Keywords:
1,3,4-Thiadiazines
Anti-cancer
Molecular docking

ABSTRACT

A series of new 1,3,4-thiadiazines were synthesized by the conventional method of dehydroacetic acid, thiocarbohydrazide and substituted phenacyl bromides or substituted 3-(2-bromoacetyl) coumarins. Structures of all the synthesized compounds were confirmed by spectral (^{1}H &^{13}C NMR, FTIR, Mass) and analytical data. The target compounds were screened for their in vitro anticancer activity, From the in vitro anticancer results, it was found that the compound 6a has shown significant activity with the standard. Furthermore, the synthesized 1,3,4-thiadiazines were inflicted to molecular docking simulations for gaining insights into their mechanism of action and possible mode of binding against STAT3. The docking results were consistent with the experimental data.

1. Introduction

Green chemistry is described by Environmental Protection Agency as adapt of chemical procedures and products that minimize or eradicate the use or generation of hazardous chemicals. The Green chemistry or sustainable chemistry has initiated to save the environment, in which E factor, process mass intensity and atom economy in the chemical procedures are the major focusing areas [1,2].

Moreover, in the green chemistry process for instance Multi Component Reaction [3–5] (MCR), aqueous medium reactions [6], solvent free reactions [7,8], ultra-sonication reactions [9,10], solid phase synthesis [11,12], microwave irradiation [13,14], photochemical synthesis [15] etc. among these green chemistry processes multi component reaction has gained preference on top of conventional and multi-step reaction. Furthermore, it is a powerful chemical tool for the synthesis of complex molecules, in this reaction without isolation of intermediates, minimization of cost, time and waste and also diversified, high atom economy process. In consequence it is a powerful robust tool to synthesize the biological active compounds in pharmaceutical industry [16,17]. Subsequently multi component reaction process is extremely effective to synthesize a wide variety of heterocyclic compounds [18,19].

Among this hetero cyclic compounds 1,3,4-thiadiazines and their derivatives are a prominent class of medicinally relevant compounds on account of their anticancer [20], anti-viral [21], antimicrobial [22], antifungal [23], antibacterial [24], antioxidant [25]. Moreover, thiadiazines and its analogues manifest inhibitory activities like STAT3 inhibitor [26], matrix metalloproteinase inhibitor [27], cyclic AMP phosphodiesterase inhibitor [28], Hepatitis C virus polymerase inhibitor [29], cholinesterase inhibitor [30], cyclindependent kinase inhibitor [31], PDE4 inhibitor [32]. Subsequently coumarin based derivatives are one of the prime class of biologically active compounds due to their antioxidant [33,34], anti-inflammatory [35], antimicrobial [36–38], antiviral [39], antituberculosis [40], anticancer [41,42], anticoagulant [43], anticholinesterase [44,45], antidepressant agent [46] (Fig. 1).

Considering the enormous medicinal and biological importance of 1,3,4-thiadiazines and coumarin motifs and in continu-

* Corresponding author.
E-mail address: rajeswarnitw@gmail.com (R.R. Vedula).

https://doi.org/10.1016/j.molstruc.2021.130111
0022-2860/

Journal of Molecular Structure 1236 (2021) 130356

Contents lists available at ScienceDirect

Journal of Molecular Structure

journal homepage: www.elsevier.com/locate/molstr

A facile one-pot, three-component synthesis of a new series of thiazolyl pyrazole carbaldehydes: In vitro anticancer evaluation, in silico ADME/T, and molecular docking studies

Srikanth Mamidala[a], R Kowshik Aravilli[b], Gondru Ramesh[c], Shaik Khajavali[d], Raju Chedupaka[a], Vijjulatha Manga[d], Rajeswar Rao Vedula[a,*]

[a] Department of Chemistry, National Institute of Technology, Warangal, 506004, Telangana, India
[b] Department of Biotechnology, National Institute of Technology, Warangal, 506004, Telangana, India
[c] Environmental Monitoring & Exposure Assessment (Air) Laboratory, ICMR–NIREH, Bhopal, 462030, Madhya Pradesh, India
[d] Molecular Modeling and Medicinal Chemistry Group, Department of Chemistry, University College of Science, Osmania University, Hyderabad, 500007, Telangana, India

ARTICLE INFO

Article history:
Received 26 January 2021
Revised 11 March 2021
Accepted 19 March 2021
Available online 26 March 2021

Keywords:
thiazolyl pyrazole carbaldehydes
Anti-cancer
ADME/T
Molecular Docking

ABSTRACT

A series of thiazolyl pyrazole carbaldehydes (**4a-n**) were synthesized by conventional method using thiosemicarbazide, substituted phenacyl bromides, substituted 3-acetylcoumarins, and Vilsmeyer-Hack reagent. Structures of all the synthesized compounds were confirmed by spectral (^{1}H & ^{13}C NMR, FTIR, Mass) and analytical data. The target compounds were screened for their in vitro anticancer activity. From the results, it was found that the compound **4m** has shown significant antiproliferative activity against all tested cell-lines. Furthermore, in silico ADME/T profiles were also carried out to set effective lead candidates for the future anticancer drug discovery initiatives. Molecular docking studies were carried out against colchicine binding site of β-tubulin and the results were in concordance with the in vitro anticancer data.

1. Introduction

With the increasing consciousness over environmental problems, there is a growing demand for usage of less or non-hazardous chemicals in industrial and medicinal research on account of their impact and the subsequent problems on the environment and human health. Nowadays green chemistry has become an interesting domain of chemical research to design eco-friendly chemical methodologies and synthetic approaches towards eliminating the harmful chemicals at any stage of production [1–3].

Furthermore, eco-friendly methodologies includes aqueous medium [4], solvent free [5,6], multi-component reactions (MCR) [7-9], solid-phase synthesis [10,11], ultra-sonication [12,13] and microwave irradiation [14,15] etc. Among the above mentioned green methodologies, MCR provides a fascinating method to attain structurally diversified analogs of medicinal and organic interest. Also, MCR becomes a powerful chemical tool for the preparation of complex compounds on account of step and atom economy, avoiding protecting group strategies and less time purification process. Nevertheless, MCR method is a notably effective to synthesize a variety of heterocyclic compounds [16].

Out of the various heterocyclic compounds, coumarin ring has wide range of biological activities such as antiviral [17], antioxidant [18,19], anticancer [20,21], antidepressant [22], antituberculosis [23], anti-inflammatory [24], anticholinesterase [25–27], antimicrobial [28–30], anticoagulant agent [31,32] etc. Also, pyrazole, thiazole scaffolds have attained great interest from the scientific community due to their broad spectrum of biological potency like antitumor [33–35], antituberculosis [36,37], antiviral [38,39], anti-inflammatory [40–42], antimicrobial activity [43–46] etc. Some of the biologically potent compounds embedding the above discussed scaffolds are shown in Fig. 1. Impressed, due to the importance of coumarin, pyrazole, and thiazole rings in the area of medicinal chemistry, we have been fascinated to synthesize a new structural unit that consists of all three moieties. We further assessed for their in vitro anticancer activity, and in silico ADME/T profiles.

Furthermore, the mode of action of these thiazolyl pyrazole carbaldehyde derivatives with the colchicine binding site of β-tubulin through their interactions was explored through molecular docking studies.

* Corresponding author.
E-mail address: rajeswarnitw@gmail.com (R.R. Vedula).

https://doi.org/10.1016/j.molstruc.2021.130356
0022-2860/

POLYCYCLIC AROMATIC COMPOUNDS
https://doi.org/10.1080/10406638.2022.2042333

Facile One-Pot Multi-Component Synthesis, Characterization, Molecular Docking Studies, Biological Evaluation of 1,2,4-Triazolo Isoindoline-1,3-Diones and Their DFT Calculations

Papisetti Venkatesham[a], Perugu Shyam[b], Pooja[a], Raju Chedupaka[a], and Rajeswar Rao Vedula[a]

[a]Department of Chemistry, National Institute of Technology, Warangal, Telangana, India; [b]Department of Biotechnology, National Institute of Technology, Warangal, Telangana, India

ABSTRACT

Alkyl/aralkyl/phenacyl thiotriazolyl isoindoline-1,3-diones were synthesized by the reaction of dipotassium cyanodithioimidocarbonate salt with hydrazine hydrate, phthalic anhydride and alkyl/aralkyl/phenacyl bromides using acetic acid and sodium acetate *via* a one-pot four-component synthesis. Alternatively, the same final products were also synthesized by the reaction of dipotassium cyanodithioimidocarbonate salt with hydrazine hydrate in presence of acetic acid to give intermediate 5-amino-4*H*-1,2,4-triazole-3-thiol [**I**]. This compound was further reacted with phthalic anhydride, followed by a reaction with alkyl/aralkyl/phenacyl bromides to give the title compounds in a two-step process. In this method, the yields are less compared to one-pot four-component synthesis. All the newly synthesized compounds were characterized by their spectral studies (FTIR, ^{1}H-NMR, ^{13}C-NMR, Mass). Further, the synthesized compounds were screened for their *in-vitro* anticancer activity. Compounds **5 m**, **5p**, **5r** showed good cytotoxic assay against *Hela* cancer cell lines. Furthermore, compounds **5(a-t)** were subjected to their docking analysis and DFT calculations.

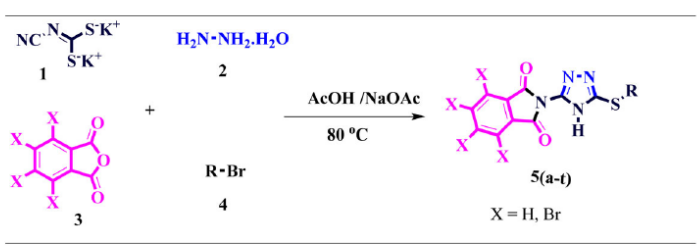

ARTICLE HISTORY
Received 10 October 2021
Accepted 9 February 2022

KEYWORDS
Isoindoline; Sulfone; Anti-cancer activity; Docking; DFT calculations

Introduction

Ailments of human beings were mostly caused by genetic disorders. Few diseases like Diabetes, Obesity, Cancer, T.B etc, are genealogically transformed diseases from generation to generations.[1] Across the globe cancer is highly dangerous and it is the second main leading cause of death in human beings[2] due to multiple uncontrolled development of cells. There are numerous therapeutic and literature reports on cancer. The available anti-cancer agents are not effectively (100%)

CONTACT Rajeswar Rao Vedula rajeswarnitw@gmail.com Department of Chemistry, National Institute of Technology, Warangal-506004, Telangana, India

Supplemental data for this article can be accessed online at https://doi.org/10.1080/10406638.2022.2042333

Bioorg. Med. Chem. Lett. 80 (2023) 129103

Contents lists available at ScienceDirect

Bioorganic & Medicinal Chemistry Letters

journal homepage: www.elsevier.com/locate/bmcl

New class of fused [3,2-b][1,2,4]triazolothiazoles for targeting glioma *in vitro*

Papisetti Venkatesham [a], Nikhil Ranjan [b], Anwita Mudiraj [b], Vinutha Kuchana [c], Raju Chedupaka [a], Vijjulatha Manga [c], Phanithi Prakash Babu [b,*], Rajeswar Rao Vedula [a,*]

[a] Department of Chemistry National Institute of Technology, Warangal, Telangana 506004, India
[b] Department of Biotechnology and Bioinformatics, School of Life Sciences, University of Hyderabad, Hyderabad 500046, India
[c] Molecular Modeling and Medicinal Chemistry Group, Department of Chemistry, University College of Science, Osmania University, 500007 Hyderabad, Telangana, India

ARTICLE INFO

Keywords:
Fused heterocycles
Apoptosis
MAP kinase pathway
X-ray crystal data

ABSTRACT

Glioma is aggressive malignant tumor with limited therapeutic interventions. Herein we report the synthesis of fused bicyclic 1,2,4-triazolothiazoles by a one-pot multi-component approach and their activity against C6 rat and LN18 human glioma cell lines. The target compounds 2-(6-phenylthiazolo[3,2–b][1,2,4]triazol-2-yl) isoindoline-1,3-diones and (E)-1-phenyl-N-(6-phenylthiazolo[3,2–b][1,2,4]triazol-2-yl) methanimines were obtained by the reaction of 5-amino-4H-1,2,4-triazole-3-thiol with substituted phenacyl bromide, phthalic anhydride, and different aromatic aldehydes in EtOH/HCl under reflux conditions. In C6 rat glioma cell lines, compounds 4g and 6i showed good cytotoxic activity with IC_{50} values of 8.09 and 8.74 μM, respectively, resulting in G1 and G2-M phase arrest of the cell cycle and activation of apoptosis by modulating phosphorylation of ERK and AKT pathway.

Glioma is the most aggressive primary brain tumor with few treatment options and dismal prognosis. While standard treatment includes complete surgical resection followed by chemo-radiotherapy, recent scientific advances have led to the consideration of novel approaches like immunotherapy, gene therapy, altered signal transduction, and angiogenesis.[1] Despite all the available treatments, recurrence of GBM and drug resistance are its limitations and the reason for small median survival rate.[2] Hence, comprehensive analysis is required for a better understanding of this fatal disease. Genomic profiling of various tumors has revealed aberrant mutations in Mitogen-activated protein-kinase (MAPK) and associated pathways. such as AKT/mTOR pathway.[3,4] Overactivation of MAPK/ERK pathway promotes cell proliferation and subsequent phosphorylation of downstream substrates which can be related to tumor formation.[5] Elevated ERK expression has been detected in some of the common human cancers like ovarian, breast, brain and lung. But inhibition of ERK/MAPK path can significantly decrease the survival of tumor-forming cells and promote apoptosis.[6] MAPK and associated signaling pathways can lead to a response through ER stress signaling pathway.[7] Therefore, in this study we evaluated the *in vitro* activity of the synthesized triazolothiazoles against glioma cell lines as well as their mode of action.

The *N*-substituted imines and isoindolines have been identified as one of the most important scaffolds with R-CH = *N*-R, –CO-N(R)–CO– structures. The isoindoline unit makes them hydrophobic, neutral and can easily cross biological membranes.[8–10]

Because of their good biological activity, fused heterocyclic compounds with N and S have attracted a lot of interest in the field of medicinal chemistry.[11–16] The antitumor properties of the 2-amino-1,3,4-thiadiazole skeleton are well recognized, and its fused systems with the imidazo [3,2–b][1,2,4] triazole ring system are likewise known to possess remarkable anticancer activities.[17,18] Hybrid molecules created by combining distinct pharmacophores could lead to compounds with interesting biological characteristics. Fig. 1 shows similar reported anticancer moieties.[19–22]

Motivated by these findings and in continuation of our research in the synthesis of various bioactive heterocyclic units[23,24] we have synthesized a series of fused triazolothiazole scaffolds bearing isoindoline and schiff base moieties and evaluated their activity against C6 rat and LN18 human glioma cell lines.

The target compounds were synthesized by a multi-component

* Corresponding authors.
E-mail addresses: prakash@uohyd.ac.in (P.P. Babu), vrajesw@nitw.ac.in (R.R. Vedula).

https://doi.org/10.1016/j.bmcl.2022.129103
Received 17 August 2022; Received in revised form 28 November 2022; Accepted 3 December 2022
Available online 6 December 2022
0960-894X/

Presentation & participation in symposia

1. International Conference on "Advanced Functional Material and Sciences (ICAFM), 2017 in IIIT Basar.
2. International Conference on Advances in Chemical Sciences and Technologies (ACST 2019) held on 23-25th September 2019, organized by NIT Warangal.
3. International Conference On "Emerging Trends in Catalysis (ETC-2020) in Vellore (VIT).
4. National Seminar on "Recent Trends and Challenges in Chemical Science "2017, Kakathiya University, Warangal.
5. Participated in Telangana State Science Congress (TSSC-2018) ,2018 in NIT Warangal.
6. National Work Shop on "Research Methodology & Scholarly Writing Skills" (RMSWS-2019) in NIT Warangal.
7. National Conference on Emerging Trends in Instrumental Methods of Chemical Analysis (ETIMCA- 2019) organized by NIT Warangal.
8. National Conference on "Emerging Trends in Instrumental Methods of Chemical Analysis" (ETIMCA-2019) in NIT-Warangal.

BRIEF BIOGRAPHY OF THE AUTHOR

Mr. Chedupaka Raju was born in Nainala, Mahabubabad district of Telangana state, India. He completed his secondary school education at Government High School Nellikuduru, his Intermediate at Government Junior College Nellikuduru, and his B. Sc. from the University of Arts & Science College affiliated with Kakathiya University Warangal. After completing his M.Sc. (Organic Chemistry) from the National Institute of Technology Warangal, he joined the Ph.D., program in July 2016 under the guidance of **Dr. Rajeswar Rao** (Professor) Department of chemistry, National Institute of Technology Warangal with financial assistance from the NITW. He has published seven research articles in peer-reviewed international journals and presented papers in National/International conferences. His research interest lies in the development of new methodologies for the synthesis of bio-active molecules by employing an efficient and green methodology.